



JRC CONFERENCE AND WORKSHOP REPORTS

# ESARDA 41<sup>st</sup> Annual Meeting Symposium on Safeguards and Nuclear Material Management

*14-16 May, 2019  
Regina Palace Hotel  
Stresa (VB), Italy*

De Luca Andrea  
Veronique Berthou

2019

**ESARDA**  
European Safeguards Research & Development Association

1969 ~ 2019

**50**  
years

Joint  
Research  
Centre

EUR 29786

This publication is a Conference and Workshop report by the Joint Research Centre (JRC), the European Commission's science and knowledge service. It aims to provide evidence-based scientific support to the European policymaking process. The scientific output expressed does not imply a policy position of the European Commission. Neither the European Commission nor any person acting on behalf of the Commission is responsible for the use that might be made of this publication.

#### **Contact information**

Name: Veronique BERTHOU

Address: DG Joint Research Centre, Directorate G - Nuclear Safety and Security, Department G.II - Nuclear Security and Safeguards, Unit G.II.7 – Nuclear Security, T.P. 800, Via E Fermi 2749, 21027 Ispra, Italy

Email: Veronique.BERTHOU@ec.europa.eu

Tel.: +39 0332-786740

#### **EU Science Hub**

<https://ec.europa.eu/jrc>

JRC116881

EUR 29786

PDF ISBN 978-92-76-08679-6 ISSN 1831-9424 doi:10.2760/159550

Luxembourg: Publications Office of the European Union, 2019

© European Atomic Energy Community, 2019

The reuse policy of the European Commission is implemented by Commission Decision 2011/833/EU of 12 December 2011 on the reuse of Commission documents (OJ L 330, 14.12.2011, p. 39). Reuse is authorised, provided the source of the document is acknowledged and its original meaning or message is not distorted. The European Commission shall not be liable for any consequence stemming from the reuse. For any use or reproduction of photos or other material that is not owned by the EU, permission must be sought directly from the copyright holders.

All content © European Atomic Energy Community, 2019, except:

-front cover page, artist's name: EleSi, image #: 140807681. Source: Adobe Stock

-pages 486-491, author's name: Jennifer Schofield, Year 2019. Source: British Crown Owned Copyright 2019/AWE

-pages 679-683, authors' name: Ian Hayes and Keir Allen, Year 2019. Source: British Crown Owned Copyright 2019/AWE

How to cite this report: Author(s), *Title*, EUR 29786, Publisher, Publisher City, Year of Publication, ISBN 978-92-76-08679-6, doi:10.2760/159550, JRC116881.

## **Foreword**

The 41st ESARDA Annual Meeting Symposium on Safeguards and Nuclear Material Management, was held at the Regina Palace Hotel in Stresa, Italy from 14-16 May, 2019. The Symposium was preceded by meetings of the ESARDA Steering Committee and the Working Groups on Monday 13 May 2019.

The 2019 Symposium marks the 50th anniversary of ESARDA, which provided a unique opportunity for research organisations, safeguards authorities and nuclear plant operators to exchange information on new aspects of international safeguards and non-proliferation, as well as recent developments in nuclear safeguards and non-proliferation related research activities and their implications for the safeguards community.

## Table of Content

### Session 1: Implementation of Safeguards at State Level

Fifty Years On, Time for a New NPT Standard? (20) <i>J. Larrimore</i>	1
The Evolution of State-level Safeguards Implementation by the IAEA (134) <i>T. Renis, J. Whitlock and Z. Radecki</i>	12

### Session 2: Spent Fuel I

Parametrizing the differential die-away self-interrogation early die-away time for PWR assemblies as a function of fuel parameters (22) <i>L. Caldeira Balkeståhl, Z. Elter and S. Grape</i>	18
Passive Neutron Albedo Reactivity (PNAR) Prototype for Spent Nuclear Fuel Verification (51) <i>T. Tupasela, T. Honkamaa, M. Moring and A. Turunen</i>	29
Verifying PWR assemblies with control rod cluster inserts using a DCVD (27) <i>E. Branger, S. Grape and P. Jansson</i>	36
Determination of <sup>239</sup> Pu content in spent fuel with the SINRD technique by using artificial and natural neural networks (5) <i>A. Borella, R. Rossa and H. Zaïoun</i>	43

### Session 3: Nuclear Forensics

Nuclear Archaeology: Reconstructing Reactor Histories From Reprocessing Waste (87) <i>A. Figueroa Caceres and M. Goettsche</i>	53
Determining the production date of Cf-252 sources (130) <i>J. Zsigrai, J-M. Crochemore, A. Apostol, A. Rozite, J. Bagi, K. Abbas and K. Mayer</i>	63
Nuclear Forensics via the Electronic Properties of Particulate and Samples (1) <i>R. Hayes, R. O'Mara and F. Abdelrahman</i>	67
Analysis of light elements in U bearing materials for safeguards purposes (40) <i>S. Morel, K. Casteleyn, E. Zuleger, M. Rosenzweig and U. Repinc</i>	76

### Session 4: Environmental Sampling - Particle Measurements

NUSIMEP-9 Inter-Laboratory Comparison on uranium isotope amount ratios and uranium mass in uranium micro-particles (7) <i>C. Venchiarutti, S. Richter, R. Middendorp and Y. Aregbe</i>	89
Production of Uranium Oxide Microparticles as Certified Reference Materials for Analytical Measurements (94) <i>S. Neumeier, P. Kegler, M. Klinkenberg, F. Kreft, D. Bosbach, I. Niemeyer, C. Venchiarutti, J. Truyens, S. Richter, Y. Aregbe, L. Sangely, N. Dzigal, T. Tanpraphan, S. Konegger-Kappel, Z. Macsik, G. Stadelmann and S. Vogt</i>	101

Production of Particle Reference and Quality Control Materials (82) 105  
*C. Barrett, T. Pope, M. Wellons, B. Arey and M. Zimmer*

Characterization of the nuclear material at the particle scale at CEA DAM Ile de France : a powerful tool for Safeguards (119) 117  
*A-L. Fauré, C. Rodriguez and T. Dalger*

### **Session 5: Muon and Antineutrino-based methods**

The AIT-WATCHMAN Project for Remote Monitoring of Nuclear Reactors (34) 126  
*Y-J. Schnellbach*

Liquid Argon - Based Antineutrino Detection Techniques for Nuclear Waste Verification (56) 132  
*M. Wittel, A. Stahl and M. Götsche*

Modelling of safeguards verification of spent fuel dry storage containers using muon trackers (59) 142  
*D. Ancius, K. Aymanns, P. Checchia, F. Gonella, A. Jussofie, F. Montecassiano, M. Murtezi, P. Schwalbach, K. Schoop, S. Vaccaro, S. Vanini and G. Zumerle*

### **Session 6: Spent Fuel II**

Use of machine learning models for the detection of fuel pin replacement in spent fuel assemblies (2) 150  
*R. Rossa and A. Borella*

Investigating the gamma and neutron radiation around quivers for verification purposes (131) 165  
*Z. Elter, V. Mishra, S. Grape, E. Branger, P. Jansson and L. Caldeira Balkeståhl*

Validating the reported irradiation history of spent fuel assemblies using high-resolution gamma spectrometry and the Origen 2.2 burnup code (96) 176  
*P. Kirchknopf, I. Almási, A. Kocsonya, C. Tam Nguyen, L. Lakosi, Z. H. and P. Völgyesi*

### **Session 7: Destructive Analysis**

Optimising the use of reference materials for destructive analysis in nuclear safeguards (61) 188  
*A.M. Sánchez Hernández, C-I. Andor, R. Buda, L. Commin, F. D'Amati, J. Horta Domenech, S. Morel, A. Nicholl, C. Nourry, G. Suurkuust, M. Vargas Zuñiga, D. Wojnowski and E. Zuleger*

EQRAIN U and EQRAIN Pu interlaboratory comparisons from 1997 to 2016 – Comparison to ITVs-2010 (12) 200  
*M. Crozet, D. Roudil, C. Rigaux, C. Bertorello, S. Picart and C. Maillard*

International certification process of the ABACC-Cristallini method for UF<sub>6</sub> sampling – current status (30) 211  
*L.C. Machado Da Silva, A. Bonino and S. Fernandez Moreno*

## Session 8: Geological Disposal

Aspects on declared accountancy data for the Final Spent Fuel Disposal in Sweden (55) <i>G. Af Ekenstam, S. Lindgren, R. Fagerholm, L. Hildingson, A. Sjöland and J-O. Stål</i>	218
Identification and authentication of copper canisters for spent nuclear fuel: the ultrasonic method (26) <i>C. Clementi, L. Capineri and F. Littmann</i>	225
National Safeguards Concept for Encapsulation Plant and Geological Repository (50) <i>T. Honkamaa, M. Hämäläinen, E. Martikka, M. Moring, O. Okko and T. Tupasela</i>	235
Potential SG equipment infrastructure for the Geological Repository in Finland (44) <i>K. Khrustalev, M. Murtezi, E. Martikka, M. Lahti, I. Tsvetkov, W-S. Park and K. Baird</i>	240
Verification of Spent Fuel in Dry Storage Casks Using Fast Neutrons (139) <i>Y. Ham, S. Sitaraman and P. Kerr</i>	247

## Session 9: Nuclear Security Detection

Development of active non-destructive analysis technologies for nuclear nonproliferation and security of JAEA (110) <i>M. Koizumi</i>	260
Investigation of an alternative RPM concept design for special nuclear material detection (105) <i>D. Trombetta, B. Cederwall and K. Axell</i>	268
Testing of a Radiation Portal Monitor on the Detection Thresholds (19) <i>A. Rozite</i>	275
Capacity building in EU MS for the testing and assessment of detection equipment in nuclear security within ITRAP+10 Phase II (76) <i>F. Raiola, A. Rozite and H. Tagziria</i>	287

## Session 10: Sealing/Dry Storage

Spent fuel cask reverification: technology survey for an integrated multi-method toolkit (62) <i>S. Vaccaro, H. Tagziria, D. Ancius, K. Abbas, B. Pedersen, A. Tomanin, M. Murtezi, P. Schwalbach and K. Aymanns</i>	315
Aspects of Safeguarding On-Site Dry Storage Facilities (48) <i>K. Aymanns, D. Ancius, M. Hahn, A. Jussofie, T. Krieger, L. Matloch, M. Murtezi, I. Niemeyer, A. Rezniczek, J. Pekkarinen, K. Schoop and P. Schwalbach</i>	323
Laser Scanning for Safeguarding Spent Fuel Storage Facilities (13) <i>E. Wolfart, G. Boström and V. Sequeira</i>	331
Mechanical Design of the Operator Applied & Removed Sealing Bolt (8) <i>F. Littmann</i>	338

## Session 11: NDA Neutrons

Nuclear and Atomic Data Needs for Safeguards (120) <i>C. Pickett, C. Ramos, F. Tovesson and K. Ventura</i>	348
New developments in neutron counting chains for nuclear safeguards (112) <i>G. Varasano, M. Abousahl, T. Bogucarska and B. Pedersen</i>	357
High rate approximation for extendable dead time corrections in allabote settings (16) <i>C. Dubi and R. Atar</i>	368
Sample shape effect on nuclear material quantification with neutron resonance transmission analysis (21) <i>H. Tsuchiya, F. Ma, F. Kitatani, C. Paradela, J. Heyse, S. Kopecky and P. Schillebeeckx</i>	374
Inter-Comparison Exercise for the Safeguards Verification of PWR Fresh Fuel Assemblies using Fast and Thermal Neutron Coincidence Collars (63) <i>A. Tomanin, L. Bourva, J. Beaumont, P. de Baere, A. Terrasi, V. De Pooter, M. Arias Arenas, P. Marion, P. de Lavarène and P. Turbiault</i>	378

## Session 12: Statistics

Statistical Design of Experiments: A Powerful Tool in Your Nonproliferation Toolbox (4) <i>R. Brigantic, A. Trevino Gavito, N. Betzsold, C. Perkins and G. Mckinney</i>	390
Modelers meet practitioners: On 20% selection probability and random physical inventory verifications (39) <i>T. Krieger, R. Avenhaus and T.L. Burr</i>	400
Improve a weighing scale with operator concerns (102) <i>V. Bruel</i>	410
Unaccounted for uncertainties in radioaerosol assays as used in plume reconstruction or treaty verification (23) <i>R. Hayes</i>	433

## Session 13: Containment & Surveillance

JRC Embedded Universal Seal Reader (46) <i>G. Boström, V. Sequeira, D. Puig, C. Bergonzi and A. Fassi</i>	444
Use of commercial components for a future Surveillance Camera (45) <i>G. Boström, F. Ghiringhelli and V. Sequeira</i>	452
Tamper-Indicating Enclosures with Visually Obvious Tamper Response (11) <i>H. Smartt, C. Corbin, N. Myllenbeck, P. Feng, A. Benin, J. Custer and A. Jones</i>	461
Light Field Cameras Offer Surveillance a New Dimension (104) <i>J. Garner</i>	468

## Session 14: Arms Control Verification

Arms Control Verification Research and Development Activities (124) <i>E. Padilla</i>	479
Understanding the inverse problem in nuclear arms control scenarios (36) <i>J. Schofield</i>	486

## Session 15: Process Monitoring

Developing a new safeguards sensor control platform and its application in EURATOM safeguards IMAP, the Integrated Monitoring and Acquisition Platform, Challenges and techniques (37) <i>A. Smejkal, R. Linnebach and L. Holzleitner</i>	493
Pre-NRTA Systems: Opportunities and Challenges (114) <i>J.-B. Darphin, F. Bonino and J. Oddou</i>	503

## Session 16: NDA Gamma

International testing platform for Uranium & Plutonium gamma-ray isotopic analysis codes: achievements and prospects (74) <i>A.-L. Weber, P. Funk, B. Mcginnis, D. Vo, H. Nordquist, J. Dreyer, R. Venkataraman and R. Haddal</i>	512
Application of Delayed Gamma-Ray Spectrometry in Nuclear Safeguards and Non-Proliferation (129) <i>K. Abbas, D.C. Rodriguez, J.-M. Crochemore, F. Rossi, T. Bogucarska, T. Takahashi, B. Pedersen, M. Seya, S. Nonneman and M. Koizumi</i>	522
Performance of FRAM isotopic analysis of shielded plutonium with electrically cooled gamma-spectrometers (53) <i>J. Zsigrai, A. Berlizov, D. van Eerten, A. Muehleisen and J. Bagi</i>	533
Optimization and Uncertainty Estimation of the Enrichment Meter Measurement Technique for UF <sub>6</sub> Cylinder (54) <i>J.-L. Dufour, C. Deyglun, N. Pepin and A.-L. Weber</i>	547

## Poster Session 1: Focus on NDA

Spectroscopic SiPM based Fast Neutron Detector for Safeguard Applications (73) <i>M. Meshkian, U. Gendotti, G. Davatz, R. Chandra, C. Philipp, M. P. and J. Nowakowski</i>	561
Evaluation of advanced deadtime correction algorithms for neutron correlated counting (81) <i>D. Henzlova, V. Henzl and L. Holzleitner</i>	567
Calibration of a combined PNCC / HRGS non-destructive assay system for measurement of Plutonium and MOX packages to verify declared inventory (83) <i>A. Cormack, N. Bain, J. Mason, K. Burke, A. Towner, P. Mullarkey, D. Paton, C. McIntosh, R. Gunn and D. Ancius</i>	578
Research on Uranium Enrichment Determination Using 143-1001 keV Region of HPGe Uranium Spectrum (14) <i>Y. Tian, G. Liu and H. Zhou</i>	598

Extended verification of fresh fuel assembly using LaBr <sub>3</sub> scintillation detectors at the Paks Nuclear Power Plant (106) <i>G. Dosa, P. Volgyesi and I. Almasi</i>	603
C-BORD high-level equipment to enhance freight inspection in support to customs (101) <i>G. Sannie, B. Pilorget and H. Tagziria</i>	611
Application of Gamma Tomography for Nuclear Waste Characterization (127) <i>E. Roesgen, S. Vanzo, F. Raiola, G. Bostroem, P. Hubert and K. Abbas</i>	615
INS3L – a new NDA laboratory for the European safeguards R&D community (117) <i>B. Pedersen, T. Bogucarska, K. Abbas, J-M. Crochemore, F. Raiola, E. Roesgen, A. Rozite, H. Tagziria, G. Varasano, I. Maschio, S. Nonneman and W. Janssens</i>	627
An SNM detection method based on fission signatures induced by a low-energy neutron source (98) <i>B. Pedersen, A. Ocherashvili, G. Varasano, T. Bogucarska, D. Mikhaeli, G. Heger and V. Mayorov</i>	633
<b>Poster Session 2</b>	
Evolving Technologies for Future Deep Geological Repositories: A Closer Look (70) <i>T. Le and C. Vestergaard</i>	647
Synergy of robotized nondestructive testing methods: a key for safe, secure and reliable operation (89) <i>D. Sednev, A. Lider, I. Bolotina and D. Koneva</i>	654
Imaging of a nuclear waste storage facility (126) <i>A. Rozite, K. Abbas, F. Raiola, G. Boström and P. Hubert</i>	663
Characteristics of Site boundary monitoring systems for verifying future nuclear weapon arms control agreements (35) <i>I. Hayes and K. Allen</i>	679
Opportunities for a graded approach in air sample assay and triage (24) <i>R. Hayes and S.J. Cope</i>	684
On site evaluation of safeguards technical data in multi-cameras surveillance systems (31) <i>A. Bonino, L.C. Machado Da Silva and S. Fernandez Moreno</i>	697
Applying knowledge retention to preserve a core safeguards technical area (77) <i>N. Peter-Stein, H. Smartt and W. Corbin</i>	702
3D image recognition of nuclear fuel waste using tree-based classifiers (65) <i>S. Puydarrieux, M. Picq, J-J. Dupont and A. Delahaye</i>	710
Results of DataMatrix Barcode Testing for Field Applications (103) <i>J. Garner, J. White-Horton and M. Whitaker</i>	721
Hafnium Isotope Ratio Method for Enhanced Safeguards at Research Reactors (123) <i>J. Johns, B. Reid, S. Shen, D. Reilly and E. Krogstad</i>	731
Application of the revised Small Quantities Protocol in French territories part of the Nuclear-Weapon-Free Zone in Latin America and the Caribbean (72) <i>L. Olivier</i>	744

The algorithm for State-level concept software educational simulator (92) 749  
*D. Koneva and D. Sednev*

Latest Improvement on FNCL for IAEA Safeguards (141) 760  
*M. Corbo, M. Morichi, C. Raffo, F. Pepe and G. Cerretani*

Data science in safeguards – opportunities and challenges (67) 766  
*I. Niemeyer*

## **Panel 1: Regional Safeguards Systems**

Comparing regional proliferation risks and safeguards systems (84) 771  
*M. Gerlini and M. Ikegami*

Euratom safeguards: sixty years of implementation in France (29) 784  
*F. Bonino*

Bringing IAEA Safeguards in the United States into the 21st Century (10) 791  
*E. Sastre and D. Hanks*

Experience with maintaining the SSAC in the Czech Republic (57) 797  
*A. Pavlik, K. Janatkova and O. Stastny*

Web-Portals complementing the NMAC centralised accountancy : The French experience (28) 805  
*F. Lanave*

Nuclear Material Measurements at ABACC: Status Update and Future Steps (32) 809  
*L.C. Machado Da Silva, A. Bonino, S. Fernandez M. and F. Dias*

Back-end to the Future: Considering Safeguards Criteria for Multinational Geological Repositories (15) 816  
*C. Vestergaard*

The CWC and its verification regime, a tool against the non-proliferation and reemergence of chemical weapons: a parallel with the nuclear treaty (66) 822  
*N. Balistreri*

## **Panel 2: Safeguards by Design**

Progress in SBD for Pyroprocessing Facilities by KAERI (17) 834  
*H-D. Kim, S-H. Park, S-K. Ahn, B-H. Won, C-H. Lee, D-Y. Song and H-S. Shin*

15 Years of Safeguards-by-Design in Finland (42) 842  
*M. Hämäläinen, T. Honkamaa, E. Martikka, M. Moring and O. Okko*

Safeguards Regulatory Review for Small Modular Reactor Designs in Canada (78) 848  
*H. Gao, M. Kent, S. Herstead, M. de Vos and D. Moroz*

Safeguards Information Assurance by Design (80) 858  
*D. Blair and F. McCrory*

The GIF Proliferation Resistance and Physical Protection METHodology Applied to GEN IV System Designs: an update (132) 867  
*G.G.M Cojazzi, G. Renda, L-Y. Cheng, B.D. Boyer, B. Cipiti, G. Edwards, E. Hervieu, K. Hori and H. Kim*

Regulatory Experience with the Safeguards By Design Project of Planned New Nuclear Power Reactors in Hungary (86) <i>A. Jezeri, Á. Vincze and E. Földesi</i>	879
-----------------------------------------------------------------------------------------------------------------------------------------------------------------	-----

### Panel 3: Education and Training

Collaboration for Development of Comprehensive NDA Course in SSAC Training (43) <i>M. Sekine, Y. Kawakubo, P. Rodriguez, N. Noro, F. Raiola, J-M. Crochemore, A. Rozite and K. Abbas</i>	886
Strengthening of the French training and qualification activities on nuclear safeguards (47) <i>C. Decroocq and M. Humbert-Brun</i>	894
EURATOM safeguards inspector training capabilities of the JRC-Ispra (125) <i>F. Raiola, J-M. Crochemore, T. Bogucarska, A. Rozite, B. Pedersen and K. Abbas</i>	901
Current training activities at IRSN and ENSTTI on Safeguards (64) <i>P. Funk and D. Louvat</i>	911
The Need to Establish Certified Professional Development Programmes for Safeguards (100) <i>D. Johnson, R. Evans, J. Chapman and C. Crawford</i>	915
Evolution of ESARDA Course: Outreach Contribution of ESARDA Course on Nuclear Safeguards and Non-Proliferation (128) <i>K. Abbas, W. Janssens, F. Raiola, G. Cojazzi and P. Richir</i>	927

### Panel 4: Digital Transformation

The Role of Maps in Site Knowledge and Wayfinding: A Human Performance Evaluation for International Nuclear Safeguards Inspections (6) <i>Z. Gastelum, M. Stites and L. Matzen</i>	936
Digital Declaration Site Maps of Additional Protocol are Digitalization at State Level (60) <i>T. Honkamaa, T. Ansaranta, M. Hämäläinen, J. Heinonen, T. Ilander, E. Martikka and M. Moring</i>	946
Trusting Embedded Hardware and Software in Treaty Verification Equipment (71) <i>J. Brotz</i>	950
ICPIA Modeling and Red Teaming (79) <i>L. Dawson and F. McCrory</i>	957
Defense Nuclear Nonproliferation Research and Development Initiatives in Data Science for Safeguards (121) <i>C. Ramos and Ch. Pickett</i>	963

### Panel 5: Strategic Trade Control

Export control and nuclear safeguards (33) <i>F. Sevinci, W. Janssens, G. Renda, X. Arnes N., C. Charatsis, E. Stringa, C. Versino and S. Cagno</i>	970
--------------------------------------------------------------------------------------------------------------------------------------------------------	-----

Export controls and safeguards: inseparable elements of the non-proliferation regime (93) <i>I. Stewart</i>	979
The NSG Part 1 Guidelines and the mutually reinforcing role of nuclear safeguards and export controls in the non-proliferation regime (91) <i>D. Cándano</i>	986
Nuclear Export Control System of the Czech Republic (52) <i>A. Tichy, O. Stastny and M. Kafka</i>	991
Export control and Additional Protocol working in synergy to strengthen nuclear non- proliferation: implementation in France (69) <i>E. Vial and L. Olivier</i>	996
Development and Examination of a Proliferation Trade Risk Metric (122) <i>P. Heine, T. Blackburn and A. Attarian</i>	1001

# **Session 1:**

# **Implementation of**

# **Safeguards at State Level**

## Fifty Years On, Time for a New NPT Standard?

**James Larrimore**

Former IAEA Senior Staff and Consultant to the Department of Safeguards, IAEA  
Del Mar, California, U.S.A.  
Email: [jameslarrimore11@gmail.com](mailto:jameslarrimore11@gmail.com)

### ABSTRACT

This presentation will present a proposal that a new standard for NPT safeguards be established. This proposal is based on a review of the evolution of safeguards over the fifty years of ESARDA's existence, starting with specific facility safeguards and developing into facility-based NPT safeguards. Then came the challenge of the undeclared nuclear weapons program in Iraq, which led to recognition of the need to strengthen safeguards with more information and greater access, and to the adoption of the Model Additional Protocol. The result, 'strengthened' safeguards evolved into so-called 'integrated' safeguards. The safeguards conclusions drawn by the IAEA expanded from '*no indications of diversion of declared nuclear material from peaceful activities*' to include '*no indications of undeclared nuclear material or activities*'.

The capabilities of IAEA to carry out NPT safeguards have developed both through technological advances and through experience with special situations in some countries. These latter were North Korea, South Africa, Iraq, Libya and most recently Iran. Taken all together, IAEA safeguards in 2019 are mature and tested.

This presentation asks whether it would be timely to adopt a new NPT Safeguards Standard, codifying the evolution of safeguards implementation that has taken place in the past five decades, and in particular the necessary contribution of the Additional Protocol. A preliminary proposal is presented for how that standard could incorporate the objectives of NPT safeguards under INFCIRC/153 and the Model Additional Protocol, the state-level concept and approach, timely detection, evaluation and safeguards conclusions. Also, a potential role for ESARDA in developing a new NPT standard is addressed.

Keywords: NPT safeguards; Additional Protocol; State-level concept; state-level approach; integrated safeguards

### 1. Introduction

The evolution of IAEA safeguards in the fifty years of ESARDA's existence is an impressive story. When ESARDA was founded in 1969, safeguards at IAEA was in its beginnings. Safeguards were being applied under INFCIRC/66, the legal framework established in 1965, to a specific designated nuclear facility in a State, usually as a requirement of the supplier of the facility.

When **ESARDA was 10 years old in 1979**, the Nonproliferation Treaty (NPT) had been developed; it entered into force in 1970. To provide a standard basis for safeguards implementation by IAEA in accordance with Article III.1 of the NPT, INFCIRC/153 had been prepared and approved from 1972. In contrast to INFCIRC/66, which applied to nuclear material in specific facilities, INFCIRC/153 applied to all the nuclear material in a State.

### **NPT ARTICLE III.1**

*Each Non-nuclear-weapon State Party to the Treaty undertakes to accept safeguards, as set forth in an agreement to be negotiated and concluded with the International Atomic Energy Agency ..., for the exclusive purpose of verification of the fulfilment of its obligations assumed under this Treaty with a view to preventing diversion of nuclear energy from peaceful uses to nuclear weapons or other nuclear explosive devices.*

When **ESARDA was 20 years old in 1989**, IAEA was in the process of documenting what today might be termed 'best practices' for safeguards verification under the NPT; that is, under a safeguards agreement based on INFCIRC/153. IAEA completed the work in 1991 with the name 'IAEA Safeguards Criteria', initially titled '1991-1995'. Those Safeguards Criteria codified existing 'good' verification practice for the NPT 'standard' – which was that an NPT state had an INFCIRC153 safeguards agreement in force. The Safeguards Criteria did not break new ground; it just set on paper – some would say in concrete – existing verification practice. An important feature of safeguards implementation under the Safeguards Criteria was that so-called 'inspection goal' attainment was independently evaluated and the results reported to States in the annual Safeguards Implementation Report (SIR).

When **ESARDA was 30 years old in 1999**, the uncovering of the clandestine nuclear weapon program in NPT State Iraq had led to the development and adoption in 1997 of the Model Additional Protocol to safeguards agreements, INFCIRC/540. IAEA Director General Amano recently said [1]: "*The Additional Protocol significantly increases the Agency's ability to verify the peaceful use of all nuclear material in a country.*" The IAEA Board of Governors decided that it was to be adopted on a voluntary basis by States. The rationale for the Additional Protocol was stated in the second paragraph of the Preamble to INFCIRC/540.

### **INFCIRC/540, Preamble, Second paragraph**

*The desire of the international community to further enhance nuclear non-proliferation by strengthening the effectiveness and improving the efficiency of the Agency's safeguards system.*

In 1999, the IAEA was in the process of evolving its safeguards implementation to incorporate the additional information and access provided by States that put an Additional Protocol into force.

When **ESARDA was 40 years old in 2009**, more and more states were adopting the Additional Protocol to their NPT safeguards agreement, and the focus of IAEA safeguards was moving from facilities towards safeguards at the state level. IAEA was starting to draw on an annual basis a so-called 'broader' conclusion for States, after an exhaustive evaluation that supported the conclusion that, at that point in time, IAEA had no credible evidence of undeclared nuclear material or activities in the State. For such States so-called 'integrated safeguards' had been introduced. By 2017, integrated safeguards were applied in 65 NPT states.

The adoption of the Additional Protocol in 1997 and the introduction of 'integrated' safeguards around 2000 did break new ground. The evolution was underway to applying the 'state level concept', the 'state level approach', and 'integrated safeguards' under INFCIRC/153 and the Additional Protocol for states with a 'broader' safeguards conclusion. John Carlson [2] recently wrote that, "The State Level Concept ... is perhaps the most important single innovation in the development of the IAEA safeguards system."

Now with **ESARDA at 50 years in 2019**, where does NPT safeguards implementation stand? Currently 128 States are implementing an Additional Protocol to their NPT safeguards agreement. (In addition, Additional Protocols have been adopted by the five nuclear-weapon states and by India.) For the year 2017, IAEA drew the broader conclusion for 70 NPT states with Additional Protocols. And those numbers continue to move upwards, year by year. The 'state-level concept' has continued to be developed, and implemented through 'state-level approaches' and 'annual implementation plans'.

For States with the evaluation for a broader conclusion in progress, and for States which have not put an Additional Protocol in force, NPT safeguards continues to be performed pretty much as defined in the Safeguards Criteria.

In addition to the procedural evolution, during these 50 years the capabilities of IAEA have developed significantly both through technological advances and through experience with special situations in some countries. These latter were North Korea, South Africa, Iraq, Libya and most recently Iran.

Taking these developments all together, NPT safeguards implemented by IAEA in 2019 are mature and tested. However, as recently stated by John Carlson [2], *“It is essential for states to be fully informed on how the safeguards system works, and to have a realistic understanding of its strengths and weaknesses. The IAEA itself has a responsibility here to ensure it is communicating effectively with states on these matters. The IAEA needs to do more to explain its methods to member states.”* *“The challenge is to develop methodologies, quality assurance systems, and safeguards cultures that are clearly understood and supported and that ensure objective and valid outcomes.”*

With that challenge in mind, this paper raises the question whether it would be timely for another step in safeguards implementation to be taken, and makes a modest proposal of what that step could be – to adopt a new NPT Safeguards Standard.

What is the standard for NPT safeguards in non-nuclear weapon states today, and what are the principal elements of the structure for implementing it?

### **What is a Standard?**

*The type, model or example commonly or generally accepted or adhered to; criterion set for usages or practices; a level of excellence, attainment, etc. regarded as a measure of adequacy. [Webster’s New World Dictionary, 2<sup>nd</sup> College Edition]*

When INFCIRC/153 was issued in 1972, it became the standard for implementation of the safeguards accepted by non-nuclear-weapon States that signed on to the NPT. The safeguards agreement between that State and the IAEA, based on INFCIRC/153, came to be called a ‘comprehensive safeguards agreement’, often abbreviated as CSA. In that sense, the CSA is the NPT standard. The procedures for implementing a CSA have evolved, as described above.

In 1997 the Additional Protocol (AP) was introduced. This led the IAEA to introduce distinctions between: States with a CSA; States with a CSA and an AP; States with a CSA and an AP and a ‘broader conclusion’ drawn. For the many NPT States with minor nuclear activities, the NPT standard initially was the Small Quantities Protocol (SQP). A strengthened, Modified SQP was introduced in 2005. What the safeguards agreement of a State should be in any of those situations is not judged. In that sense, a new NPT standard has not been proclaimed; the formally recognized standard remains a CSA, or a CSA with original SQP.

A new standard and implementation structure have not yet been developed and adopted for IAEA NPT safeguards in the 21<sup>st</sup> century. It could be. Such a standard and structure would clarify for the IAEA itself, for governments, and for the interested public how NPT safeguards verification and evaluation now should be carried out for NPT non-nuclear-weapon States, as the culmination of the evolution which began some fifty years ago.

## **2. NPT safeguards today**

Let’s recall where safeguards in NPT States with sizeable nuclear activities are today. The basis is INFCIRC/153. Some principal provisions of INFCIRC/153 that must be met are as follows.

- *The Objective of Safeguards: the timely detection of diversion of significant quantities of nuclear material from peaceful nuclear activities to the manufacture of nuclear*

*weapons or of other nuclear explosive devices or for purposes unknown, and deterrence of such diversion by the risk of early detection. [paragraph 28]*

- *The concentration of verification procedures on those stages in the nuclear fuel cycle involving the production, processing, use or storage of nuclear material from which nuclear weapons or other nuclear explosive devices could readily be made, and minimization of verification procedures in respect of other nuclear material. [Paragraph 6(c)]*
- *The use of material accountancy as a safeguards measure of fundamental importance. [paragraph 29]*
- *The technical conclusion of the Agency's verification activities shall be a statement, in respect of each material balance area, of the amount of material unaccounted for over a specific period. [paragraph 30]*
- *The Agency and the State shall cooperate to facilitate the implementation of the safeguards. [paragraph 3]*
- 

The principal features of safeguards are:

For States with INFCIRC/153 agreement in force

- State-level concept and State-level approach;
- Facility safeguards based on Safeguards Criteria with modifications;
- Cooperation with State and regional safeguards authorities;
- Safeguards conclusion: *'no indications of diversion of declared nuclear material from peaceful activities.'*

For States with INFCIRC/153 agreement and an Additional Protocol in force, in addition:

- Application of INFCIRC/540 to support a 'broader conclusion' regarding the absence of undeclared nuclear material and activities;
- Addition to safeguards conclusion, with a broader conclusion: *'no indications of undeclared nuclear material or activities.'*

### 3. A new NPT Safeguards Standard.

It is proposed that the NPT Safeguards Standard should become an INFCIRC153 comprehensive safeguards agreement (CSA) and Additional Protocol (AP) in force, and a broader safeguards conclusion (absence of undeclared nuclear activities and material) drawn for the State on an annual basis. That should be presented as the 'standard' for NPT safeguards implementation – the accepted model for implementation in order to provide the level of confidence in IAEA safeguards conclusions desired by States.

Secondarily, IAEA should state that it also applies safeguards under other conditions, in States:

- with a CSA,
- with a CSA and AP,
- with a CSA with Small Quantity Protocol [SQP],
- with a CSA with modified SQP,
- with a CSA with modified SQP and AP,
- with a Voluntary Offer agreement (nuclear weapon states),
- with INFCIRC/66 safeguards agreements in non-NPT states, and
- under special mandates from the UN Security Council and the IAEA Board of Governors.

Safeguards in each of those cases should reflect a state-level approach in defined ways. How that is done will need attention, but is beyond the scope of this paper.

This proposal may seem to be a minor change. It is not. To quote IAEA Director General Amano's recent statement [1]: *"The combination of comprehensive safeguards agreement and AP needs to become universal. Efforts to make it universal must continue and the cooperation of Member States is crucial."*

It would be best to have it accepted or approved by the IAEA Board of Governors. Opposition is likely to come from a variety of directions. In particular, while adoption of the Additional

Protocol would remain voluntary, there would be increased pressure on the remaining States to put an Additional Protocol in force to meet the NPT Safeguards Standard. That pressure would be appropriate and good, in my view.

#### 4. Justification for new NPT Safeguards Standard: Status of Additional Protocols

Where do things stand regarding Additional Protocols in force? Remarkably good. The following record is taken from the IAEA website (as of March 2019):

- Additional Protocols are in force for 134 States and Euratom;
- There are now 14 States that have signed their additional protocol but it has not entered in force. Table 1 shows these States;
- Iran began to provisionally implement its additional protocol on January 16, 2016, and under the JCPOA is committed to have it enter permanently into force in a few years – if the JCPOA still exists;
- Of 98 States that have Small Quantity Protocols to their NPT safeguards agreement in force, while sixty-five States have signed an Additional Protocol, thirty-three States have not. Table 2 shows these States. They have minimal nuclear activities.

Algeria	Belarus	Benin
Cabo Verde	Guinea	Guinea-Bissau
Iran	Kiribati	Lao P.D.R.
Malaysia	Myanmar	Timor-Leste
Tunisia	Zambia	

**Table 1: States that have signed an Additional Protocol but not put it in force**

Bahamas	Barbados	Belize
Bhutan	Bolivia	Brunei Darussalam
Dominica	Equatorial Guinea	Ethiopia
Grenada	Guyana	Lebanon
Maldives	Micronesia	Nauru
Nepal	Oman	Papua New Guinea
Qatar	Saint Lucia	St Vincent & Grenadines
Samoa	San Marino	Saudi Arabia
Sierra Leone	Solomon Islands	Sudan
Suriname	Tonga	Trinidad & Tobago
Tuvalu	Yemen	Zimbabwe

**Table 2: States with Small Quantity Protocols that have not signed an Additional Protocol**

Only five NPT States with a CSA (plus DPRK and two States with INFCIRC/66 agreements) have not signed an Additional Protocol (Table 3). These NPT States might be called outliers. Twenty-two years after its introduction, their decisions not to adopt an Additional Protocol should not impede the adoption of a new NPT standard including the AP.

Argentina	Brazil	Egypt
Sri Lanka	Syria Arab Republic	

**Table 3: NPT States that have not signed an additional protocol**

#### 5. New NPT safeguards

What might IAEA safeguards under a new NPT standard, and the principal elements of the structure for implementing it, look like?

First of all, why not call it 'NPT Safeguards', or just 'Safeguards'? Let's drop those evolutionary terms, 'integrated' and 'state-level' -- just NPT Safeguards.

Here is a top-level description.

NPT States with INFCIRC/153 Safeguards Agreement and Additional Protocol in force and broader conclusion drawn

- State-level concept and State-level approach, defining State-level technical objectives based on acquisition path analysis;
- Safeguards Procedures for Facility Safeguards [*including performance targets*];
- Safeguards-relevant information evaluation;
- IAEA cooperation with State and regional safeguards authorities;
  - [*Regional applies to Euratom. Once Argentina and Brazil adopt the NPT standard, i.e., have an Additional Protocol in force, it can apply to them.*]
- Safeguards conclusion: *no indications of diversion of declared nuclear material from peaceful activities and no indications of undeclared nuclear material or activities.*

For NPT States with minor nuclear activities:

- Implementation of a Modified Small Quantity Protocol and an Additional Protocol.

## 6. Implementing the new NPT Safeguards

How would safeguards implementation be modified for the new NPT Safeguards? Here are some proposals for main elements.

**Objective of Safeguards.** Under INFCIRC/153 safeguards, the objective of safeguards is defined in paragraph 28:

*The objective of safeguards is the timely detection of diversion of significant quantities of nuclear material from peaceful nuclear activities to the manufacture of nuclear weapons or of other nuclear explosive devices or for purposes unknown, and deterrence of such diversion by the risk of early detection.*

The IAEA in its Annual Report (2017) states the objective of Nuclear Verification differently, indicating that a transition has begun. It states:

*To deter the proliferation of nuclear weapons by detecting early the misuse of nuclear material or technology, and by providing credible assurances that States are honouring their safeguards obligations.*

What is significant here is 'early' in place of 'timely', and 'credible assurances', meaning credible to Member States. Also, 'honouring their safeguards obligations' encompasses that there have been no safeguards violations.

Under the new NPT Safeguards Standard, the transition from INFCIRC/153 paragraph 28 should be completed, with the objective of NPT safeguards encompassing the broader commitment of non-nuclear-weapon States under the NPT. To this end, the objective of NPT safeguards under the new standard might be expanded to read:

*The objective of safeguards is the early detection of diversion of significant quantities of nuclear material from peaceful nuclear activities to the manufacture of nuclear weapons or of other nuclear explosive devices or for purposes unknown, and of undeclared nuclear material or activities, and deterrence of such diversion or activities by the risk of early detection.*

**Safeguards Conclusions and Statement.** The result of IAEA safeguards implementation in a State is a 'safeguards conclusion', drawn annually. The safeguards conclusion currently drawn by the IAEA for NPT States with a broader conclusion is stated as: "*all nuclear material*

remained in peaceful activities,” which appears more fully in the Safeguards Statement for the year as:

*The Secretariat found no indication of the diversion of declared nuclear material from peaceful nuclear activities and no indication of undeclared nuclear material or activities. On this basis, the Secretariat concluded that, for these States, all nuclear material remained in peaceful activities.*

Under the new NPT Safeguards Standard, in line with the broader objective, the last sentence of the Safeguards Statement might be restated as:

*On this basis, the Secretariat concluded that these States are honouring their safeguards obligations; all nuclear material remained in peaceful activities and there was no indication of undeclared nuclear material or activities.*

The change to this conclusion – including undeclared nuclear material and activities - would be significant. John Carlson [2] has described this well: “For the IAEA’s conclusions on the absence of undeclared nuclear activities to be credible, a number of conditions must be satisfied:

- States must understand the process for looking for indicators of undeclared activities and accept that these are appropriate;
- States must be satisfied that the process is applied consistently and at the requisite standard;
- States must be satisfied that judgments are exercised and conclusions drawn in a suitably disciplined way.

This calls for a substantial level of transparency into the workings of the safeguards system. The IAEA needs to ensure it is explaining its processes adequately to states, and must be responsive to states’ suggestions and concerns.”

**Early Detection.** Since the introduction of INFCIRC/153 in the 1970s ‘*timely detection*’ was based on ‘*the maximum time that may elapse between diversion of a given amount of nuclear material and detection of that diversion by IAEA safeguards activities*’. Before the Additional Protocol and the broader conclusion, it was assumed “(a) that all facilities needed to clandestinely convert the diverted material into components of a nuclear explosive device exist in a State; (b) that processes have been tested; and (c) that non-nuclear components of the device have been manufactured, assembled and tested. Under these circumstances, detection time should correspond approximately to estimated conversion times, i.e., the time required to convert different forms of nuclear material to the metallic components of a nuclear explosive device.” [IAEA Safeguards Glossary, 2001 Edition, 3.15, 3.13] Under state level safeguards and with the conclusion drawn of “*no indication of undeclared nuclear material or activities*,” those generalized assumptions need to be replaced with state-specific assumptions based on estimated times for such activities.

How the transition from ‘*timely detection of diversion of significant quantities of nuclear material*’ to ‘*early detection of manufacture or acquisition of nuclear weapons or other nuclear explosive devices*’ will be implemented needs to be explained and justified. This involves moving away from the timeliness detection goals in the Safeguards Criteria. That will be a challenge. State-level safeguards are based on the acquisition paths applicable to the state. Implementation must be carried out sufficient for ‘early’ detection of diversion or of an undeclared activity at any step in an acquisition path. Implementing ‘*early detection of undeclared nuclear material or activities*’ presents questions to be decided; one example illustrating the difficulty would be, how often should satellite imagery be obtained of a suspect site.

Just to be clear, ‘*timely detection*’ and timeliness goals of 1 month for unirradiated direct-use material, 3 months for irradiated direct-use material and 1 year for indirect-use material should remain for other cases of safeguards implementation, in particular for INFCIRC/66-type agreements, Voluntary Offer Agreements, and comprehensive safeguards agreements without an AP in force or a broader conclusion drawn.

**State-Level Concept.** The transition from ‘facility level’ safeguards, as represented by the Safeguards Criteria of 1991, to State-level safeguards needs to be documented in a way understandable for States and others, and for use by the IAEA Operations Divisions in planning and implementing safeguards. This should start with the State-level concept, then

present the development of the acquisition paths judged to be credible in a State and the deriving of State-level technical objectives there from. Then comes development of the State-level approach defining the safeguards measures in and external to the State (including performance targets for the safeguards measures). Based on that, an Annual Implementation Plan is established, specifying the verification measures and their frequency to be carried out during a current year.

**Evaluation.** The other key pillar of safeguards implementation is evaluation. This has two related but largely independent parts. Of primary importance is the evaluation leading to the drawing of safeguards conclusions for each State on an annual basis. This involves the assessment of all information available to the IAEA on the nuclear activities in the State – that provided by the State, that obtained through verification activities, and that obtained from other sources, including open-source material and information provided by third parties. This evaluation relates to potential action by the IAEA Director General under INFCIRC/153 paragraph 18, reporting to the IAEA Board of Governors that “*an action by the State is essential and urgent*” or a finding that “*IAEA is not able to verify that there has been no diversion of nuclear material.*” This continues to be a critical element of NPT Safeguards.

The second part is the evaluation of how well performance targets for safeguards measures including verification activities are being met. This activity was called ‘safeguards effectiveness evaluation’ (IAEA Safeguards Glossary, 2001 Edition, 12.23). This is carried out to support the reliability of safeguards conclusions, and to identify specific measures of safeguards implementation for the ‘continual improvement program’. In carrying this out, there has been a transition from using IAEA ‘inspection goals’ (IAEA Safeguards Glossary, 2001 Edition, 3.22) to ‘performance targets’, and that needs to be explained and documented.

**System of Accounting for and Control of Nuclear Materials.** Finally, recognizing that this anniversary symposium is organized by the European Safeguards Research and Development Association – ESARDA – within the European Union, the home of EURATOM, let me address how the Regional System might – or should – fit into safeguards implementation under a new NPT Safeguards Standard.

Since the introduction of INFCIRC/153 in 1972, the interpretation and implementation of paragraph 7 has been a continuing matter of negotiation. To recall, it states that “*safeguards should be applied in such a manner as to enable the [IAEA] to verify ... findings of the State’s system. The [IAEA’s] verification shall include, inter alia, independent measurements and observations... The [IAEA], in its verification, shall take due account of the technical effectiveness of the State’s system.*”

In that framework, in 1992 the New Partnership Approach was agreed between the IAEA and Euratom for implementing safeguards in the non-nuclear-weapon States members of Euratom. [IAEA Safeguards Glossary, 2001 Edition, 3.35] Since that time, there has been continuing development of IAEA-Euratom cooperation in safeguards implementation. That should be featured as an element of the new NPT Safeguards Standard, and incorporated in the state-level approaches for the member States of Euratom. And development of further cooperation should be encouraged.

## 7. Documenting the new NPT Safeguards Standard

The IAEA Department of Safeguards will have the role of documenting the new NPT Safeguards Standard.

One documentation need is to prepare a revision of the IAEA Safeguards Glossary (2001 Edition). As indication of what needs to be done, Chapters 1-3 [*Legal instruments; Purposes, Objectives, Scope; Safeguards Approaches, Concepts and Measures; Safeguards Approaches, Concepts and Measures*] need substantial revision. Here are some examples:

- Paragraph 1.19 (CSA) should be followed by Paragraph 1.22 (AP);

- In Chapter 2, Paragraph 2.1, Objectives of IAEA Safeguards, should be revised to reflect the new NPT Safeguards Standard;
- Paragraph 3.4, State-level safeguards approach, should come before Paragraph 3.3, Facility safeguards approach;
- Paragraphs 3.5, Integrated safeguards, 3.8, Acquisition strategy (acquisition path), and 3.12, Acquisition path analysis, should be modified to present the current application of acquisition path analysis leading to the State-level approach.

Regarding the structure of documentation for NPT Safeguards, here are suggestions.

### **NPT Safeguards**

NPT safeguards are implemented at the level of a State in order to meet the Agency's requirements in INFCIRC/153 safeguards agreements and in the Model Additional Protocol, and to provide the data and information to support the drawing of safeguards conclusions, which is normally done on an annual basis.

#### **State-Level Safeguards**

- State-level concept
- State-level information file
- State-level safeguards approach  
*The state-level approach is based on acquisition path analysis for the state.*
- Annual implementation Plan  
*The annual implementation plan for a State is based on the State-level technical objectives specific to the state-level approach.*
- Safeguards evaluation and follow-up actions

#### **Procedures for Safeguards at Facilities**

*Procedures are specified for carrying out the specific safeguards measures necessary to meet the safeguards objectives at facilities, when those measures are specified in the State-level approach and annual implementation plan for a State. These procedures can be based on, and replace, the Safeguards Criteria. The procedures address:*

- Material balance evaluation and MUF;
- Application of containment and surveillance, and monitoring;
- Early detection of diversion; and
- Early detection of facility misuse and undeclared nuclear material and activities.

#### **Safeguards Evaluation and Performance Targets**

- State-level information report
- Documentation of results of safeguards measures
- Evaluation leading to safeguards conclusions  
*An annual evaluation and recommendations for the safeguards conclusion for a State are done by the responsible Operations Division, with independent review. The decisions on safeguards conclusions are made by a designated departmental committee.*
- Assessment of meeting performance targets for safeguards measures  
*An independent departmental review is performed to assess how well performance targets specified in the Procedures for Safeguards at Facilities and for other safeguards measures are met, and to develop recommendations for continuing improvement actions*
- Continuing improvement actions

## 8. Conclusion

IAEA has written, in an article by Claude Norman et al in the December 2018 issue No. 57 of the ESARDA Bulletin (p 40), that the '*most demanding challenge is the need to evolve facility-based evaluation concepts to innovative, consolidated concepts that can integrate different kinds of information and support credible State-level safeguards conclusions*'.

With that end in mind, it is proposed that a new NPT Safeguards Standard be developed, documented and adopted, codifying the evolution of IAEA safeguards implementation that has taken place in the past five decades.

Member States can make important contributions to the development of this NPT Safeguards Standard. This can contribute to improving the transparency of today's IAEA safeguards and thereby the acceptance and credibility of IAEA safeguards conclusions by Member States. This is an important objective in introducing a new NPT Safeguards Standard.

IAEA Director General Amano has recently called for such Member State contributions, stating [1]: "*Impartial, independent and objective nuclear verification ... is at the heart of the credibility which the IAEA enjoys. Credibility ... is a shared responsibility. Member States need to play their part. I am confident that Member States will provide the active practical and moral support that will enable the IAEA to continue to make a unique and valuable contribution to international security through nuclear verification.*"

To bring this new standard into being will be challenging. A ground swell could start here today, perhaps making the 50<sup>th</sup> anniversary ESARDA Symposium a milestone in creating more effective and efficient safeguards for the 21<sup>st</sup> century, through the introduction of a new NPT Safeguards Standard!

## Acknowledgements

The author would like to acknowledge John Carlson for his review and contributions to this paper.

## References

[1] Yukiya Amano; *Challenges in Nuclear Verification*, Center for Strategic and International Studies (CSIS), Washington D.C. USA, April 5, 2019

[2] John Carlson; *Future Directions in IAEA Safeguards*; Managing the Atom Project, Harvard Belfer Center, November 2018

# The Evolution of State-level Safeguards Implementation by the IAEA

Therese Renis, Jeremy Whitlock, Zbigniew Radecki

International Atomic Energy Agency  
Department of Safeguards  
PO Box 100  
1400 Vienna, Austria  
J.Whitlock@iaea.org

## **Abstract:**

*Under comprehensive safeguards agreements (CSAs), the International Atomic Energy Agency (IAEA) has the right and obligation to verify the correctness and completeness of States' declarations so that there is credible assurance of the non-diversion of nuclear material from declared activities and the absence of undeclared nuclear material and activities. However, for many years after the IAEA started implementing safeguards, its safeguards activities and conclusions for a State focused primarily on the State's declared nuclear material and facilities. The shortcomings of this approach were recognized in the 1990s by the IAEA's inability to detect Iraq's clandestine nuclear weapons programme. The IAEA recognized the need to give greater consideration to the State as a whole and to strengthen its ability to exercise its full rights and obligations. In addition to strengthening the implementation of safeguards under the existing legal authority, in 1997 the IAEA Board of Governors approved the Model Additional Protocol as a standard for concluding additional protocols with States. The additional protocol provides the complementary legal authority needed to draw the broader conclusion that all nuclear material remains in peaceful activities in the State. This paved the way for developing State-specific safeguards approaches, taking into account State-specific features and characteristics. Early State-level approaches, referred to as integrated safeguards, were largely based on model facility-level approaches, but the means of taking into account State-specific features has evolved over the years. The use of analytical processes and the consideration and use of State-specific factors in the development of State-level approaches has been refined and documented in clearly defined procedures. It is foreseen that these processes and factors will be used to develop safeguards approaches for all States, within the scope of their safeguards agreement. This paper outlines the evolution of State-level safeguards by the IAEA and the current status of its implementation.*

**Keywords:** safeguards, IAEA, State-level, SLA

## **1. Introduction**

Safeguards implementation by the International Atomic Energy Agency (IAEA) has evolved over the past 60 years, and has continually strengthened through the introduction of new methods and techniques. This evolution resulted from the need to meet emerging challenges, while adhering to the general principles of IAEA safeguards:

- governance under State-specific safeguards agreements;
- reliance upon nuclear accountancy;
- non-discrimination;
- technical basis;
- cost-effectiveness; and
- conclusions based upon objective and independent analysis.

Every non-nuclear-weapons State (NNWS) party to the Treaty on the Non-Proliferation of Nuclear Weapons (NPT) is required to conclude a comprehensive safeguards agreement (CSA) with the IAEA. All existing nuclear weapon-free zone treaties also obligate the parties to them to conclude CSAs with the IAEA. Under a CSA the IAEA has the right and obligation to verify the correctness and completeness of the State's nuclear material declarations, so that there is credible assurance of both the non-diversion of nuclear material and the absence of undeclared nuclear material and activities. However, despite the implication of State-level considerations inherent in the "comprehensive" nature of CSAs, for many years the IAEA's implementation of safeguards focussed on nuclear materials and facilities declared by the State. This paper describes the evolution of State-level safeguards by the IAEA, which give greater consideration to the State as a whole and strengthen the ability of the IAEA to meet the three generic State-level objectives under CSAs:

- to detect any diversion of declared nuclear material at facilities and locations-outside-facilities (LOFs);
- to detect any undeclared production or processing of nuclear material at declared facilities or LOFs; and
- to detect any undeclared nuclear material or activities in the State as a whole.

## 2. Origin of IAEA Comprehensive Safeguards (1957 to mid-1990s)

Following the establishment of the IAEA in 1957, existing bilateral supplier-receiver agreements were gradually replaced by an international verification regime under the IAEA. Initially this verification was "item-specific" and focussed solely upon the specific material, facilities, or equipment listed in the respective State agreements (concluded based upon [1] and [2]). A fundamental change in IAEA safeguards was introduced by the Treaty on the Non-Proliferation of Nuclear Weapons (NPT) that entered into force in 1970. The NPT included a commitment by non-nuclear-weapons States (NNWS) to accept IAEA safeguards on *all* their holdings of nuclear material (not just supplied items), by concluding a comprehensive safeguards agreement (CSA) [3]. Thus, IAEA safeguards went from being "item-specific" to "full-scope", and introduced the following new notions:

- detection of diversion of significant quantities (SQ) of nuclear material (defined as the approximate amount of nuclear material for which the possibility of manufacturing a nuclear explosive device cannot be excluded);
- nuclear material flow;
- nuclear material accountancy based on the establishment of material balance areas (MBAs), uniformly applied by national and/or regional systems of accounting and control (SSAC); and
- safeguards implementation criteria, ensuring the uniform application of safeguards in each State.

Under comprehensive safeguards agreements the IAEA formulated safeguards verification activities mainly at the facility level, and drew safeguards conclusions on the correctness of States' declarations based upon the evaluation of results of verification activities carried out primarily at the facility level. The IAEA's obligation to apply safeguards to all nuclear material in a State implied an additional assurance of *completeness* in addition to correctness, but the legal scope of the CSA limited the IAEA's ability to fulfil this obligation.

Beginning in the late 1980s this verification effort at declared facilities was based on the Safeguards Criteria, which specified the frequency and intensity of safeguards activities for each type of facility or LOF, taking into account the quantity and type of nuclear material. The *frequency* was determined by the "timeliness" goals for detecting the abrupt diversion of a significant quantity (SQ) or more of nuclear material, which were developed under the assumption that the State's technical capability to process diverted nuclear material into weapons usable material could not be ruled out (the IAEA having little technical ability at the time to determine otherwise). The *intensity* was determined by the specified detection probabilities, which were categorized as low (20%), medium (50%), or high (90%) depending upon the type of nuclear material and the inspection purpose.

### 3. Enhancement of IAEA Safeguards (mid-1990s to mid-2000s)

The discovery of undeclared nuclear material and facilities in Iraq after the 1991 Gulf War, as well as later problems associated with the IAEA's verification in the Democratic People's Republic of Korea (DPRK), clearly demonstrated that the IAEA's traditional safeguards system was neither robust nor comprehensive. These events highlighted the need for IAEA safeguards to provide credible assurances not only regarding declared nuclear material and activities, but also regarding the absence of undeclared nuclear activities – that is, assurances of *completeness* as well as correctness.

This recognition prompted a major program by the IAEA, with Member State involvement and support, to strengthen IAEA safeguards and establish the technical capabilities and legal authority necessary for the detection of undeclared activities. In 1993 the IAEA launched its "Programme 93+2", aimed at enhancing the effectiveness and efficiency of IAEA safeguards. The Programme was implemented in two parts:

- Part I comprised safeguards measures which the IAEA had the legal authority to implement within the framework of existing CSAs (i.e. early provision of facility design information, environmental sampling inside facilities, remote monitoring of facilities under safeguards, and unannounced inspections);
- Part II comprised safeguards measures which the IAEA required additional legal authority to implement (i.e. extended State declarations covering all aspects of its nuclear fuel cycle and activities, and complementary access to additional locations in the State). The additional legal authority that enabled these enhanced measures was the Model Additional Protocol (AP), approved by the IAEA Board of Directors in 1997 [4].

In parallel with the introduction of these enhancements to safeguards measures, the IAEA introduced enhanced information analysis integrating a wider range of information sources. State evaluation meant assessing the consistency of all safeguards-relevant information regarding a State's nuclear fuel cycle (NFC) and related capabilities. These sources include:

- information provided by the State itself (e.g. declarations and reports, including clarifications and amplifications at the IAEA's request, and voluntarily-provided information);
- information from safeguards activities conducted by the IAEA in the field and at Headquarters (e.g. inspections, design information verification, material balance evaluations); and
- other relevant information (e.g. from open sources or provided by third parties).

The first two categories of information comprise the great majority of information used for safeguards implementation by the IAEA. All safeguards relevant information collected by the IAEA is validated through internal consistency review by staff with relevant technical expertise. Evaluation of safeguards-relevant information is a continuous task, summarized on an annual basis.

The results of Programme 93+2 enabled the IAEA to verify the completeness of State declarations, with the goal of providing assurance of the absence of undeclared nuclear material and activities in the *State as a whole*. Thus, although the lexicon and concept of State-level safeguards was yet to mature within the IAEA, by the mid-1990s we see the explicit addition of State-level considerations in the implementation of IAEA safeguards.

In order to provide the most efficient means for realizing the effectiveness of strengthened safeguards, the IAEA introduced the concept of Integrated Safeguards (IS) – defined as the optimum combination of all safeguards measures available to the IAEA under CSAs and APs, which achieves the enhanced effectiveness within available resources in fulfilling the IAEA's right and obligation to apply safeguards to *all* nuclear material within a State. [5]

In 2001, the IAEA began implementing Integrated Safeguards through the following process:

1. The IAEA implements the procedures of a CSA and AP in the State, drawing a safeguards conclusion that all nuclear material has remained in peaceful activities. This conclusion is based on the IAEA's finding that there are no indications of both (a) diversion of declared nuclear material from peaceful activities, and (b) undeclared nuclear material or activities in the State as a whole;

2. Once the above assurances are achieved, it becomes possible for the IAEA to draw a broader conclusion that all nuclear material in the State has remained in peaceful activities; and
3. Once the broader conclusion is drawn, the IAEA develops a State-level Integrated Safeguards Approach (ISA) for the State, in which the inspection activities at facilities and LOFs can in some cases be applied at reduced levels, based upon model IS facility-based approaches, as compared with the Safeguards Criteria for States with CSAs alone.

The reduction in verification effort is justified since the Safeguards Criteria for States with CSAs alone were developed, as noted in Section 2, under the assumption that contributing steps in an acquisition path (e.g. undeclared reprocessing or enrichments plants) may exist undetected. For IS States the IAEA now had the necessary tools to provide assurances obviating the need for such assumptions.

The basic principles which govern the development of Integrated Safeguards are [5]:

- they should be non-discriminatory; i.e. the same technical objectives should be pursued in all States with comparable safeguards obligations, although the measures actually used in individual States may differ;
- they should be based on State-wide considerations; more specifically: (a) comprehensive information evaluation for the State as a whole; and (b) integrated safeguards approaches should provide coverage of all technically available acquisition paths; and
- nuclear material accountancy should remain a safeguards measure of fundamental importance.

#### **4. Development of Full State-level Safeguards (mid-2000s to present)**

While Integrated Safeguards represented a significant shift of focus to State-level considerations within IAEA safeguards, there was room for improvement. Although some considerations relating to the State-as-a-whole were reflected in the Integrated Safeguards Approaches, the primary basis for determining safeguards activities at declared facilities in these States remained the facility-based Safeguards Criteria (albeit their application adjusted to take into account the broader conclusion). True integration of approaches would be a challenge without further conceptual development, since safeguards verification activities under a CSA are primarily formulated at the facility level, while safeguards activities related to an AP are formulated at the State level.

Another limitation of Integrated Safeguards was its applicability to a limited subset of States, while it was becoming increasingly clear that certain benefits of State-level safeguards could be realized in all States (within the constraints of their respective safeguards agreements). The benefits include the ability to apply a consistent, non-discriminatory safeguards conceptual framework to all States, with activities tailored to individual States' nuclear fuel cycles and other State-specific factors.

The term "State-level concept" was first introduced in the IAEA's Safeguards Implementation Report (SIR) for 2004. Its implementation marked a shift in emphasis from a traditional, facility-based approach to a holistic, State-level approach, with the flexibility to take account of differences between States' nuclear fuel cycles. In 2013 and 2014 the IAEA reported to its Board of Governors on the development of the State-level concept to date and on its future plans to implement the concept in all States [6],[7].

Under a CSA the State-level concept can be characterized by the following elements (some newly introduced; some brought forward from Integrated Safeguards):

- establishment of safeguards objectives at the State level (i.e. generic objectives that are based on a State's safeguards agreement, and related technical objectives that are based on an acquisition path analysis);
- development of a customized (i.e. tailor-made) safeguards approach for a State (i.e. an SLA), and its execution through an annual implementation plan (AIP);
- consideration and use of State-specific factors (including nuclear fuel cycle and related capabilities) in the implementation of safeguards;
- evaluation of all safeguards relevant information available to the IAEA about a State; and

- drawing and reporting of a safeguards conclusion for a State in an annual State evaluation report (SER).

## 5. Current status and future plans

To date (May 2019) the IAEA has developed 131 State-level approaches (out of 181 States with IAEA safeguards agreements) covering 97% of the nuclear material under comprehensive safeguards agreements. The IAEA will continue to develop and implement State-level approaches for all States, while also updating existing SLAs as lessons are learned from implementation. Guidance continues to be developed where more consistency of implementation among State Evaluation Groups is needed (e.g. establishing State-level verification requirements, characterizing undeclared acquisition path steps, replacement of facility-based implementation Safeguards Criteria with State-level standards), drawing upon the expertise of the IAEA's Standing Advisory Group on Safeguards Implementation (SAGSI) and Member State Support Programmes as necessary. Software tools will also be developed that will help to ensure consistent and efficient implementation.

IAEA safeguards will continue to evolve as necessary to meet emerging challenges. The IAEA will continue to engage in open dialogue on safeguards matters with States, and keep the Board of Governors informed of progress. The State-level concept provides a flexible framework for safeguards implementation, allowing adaptation to a changing environment while maintaining non-discriminatory, effective, and efficient implementation across all States.

## 6. References

- [1] International Atomic Energy Agency, *Agency Safeguards Relating to Large Reactor Facilities*, INFCIRC/26/Add.1, 1964.
- [2] International Atomic Energy Agency, *The Agency's Safeguards System*, INFCIRC/66/Rev.1, 1968.
- [3] International Atomic Energy Agency, *The Structure and Content of Agreements Between the Agency and States Required in Connection with the Treaty on the Non-Proliferation of Nuclear Weapons*, INFCIRC/153 (Corrected), 1972.
- [4] International Atomic Energy Agency, *Model Protocol Additional to the Agreement(s) Between State(s) and the International Atomic Energy Agency for the Application of Safeguards*, INFCIRC/540 (Corrected), 1997.
- [5] International Atomic Energy Agency Board of Governors, *The Development of Integrated Safeguards*, Report by the Director General, GOV/INF/2000/26, November 2000.
- [6] International Atomic Energy Agency Board of Governors, *The Conceptualization and Development of Safeguards Implementation at the State Level*, Report by the Director General, GOV/2013/38, August 2013.
- [7] International Atomic Energy Agency Board of Governors, *Supplementary Document to the Report on the Conceptualization and Development of Safeguards Implementation at the State Level (GOV/2013/38)*, Report by the Director General, GOV/2014/41, August 2014.

# **Session 2:**

# **Spent Fuel I**

# Parametrization of the differential die-away self-interrogation early die-away time for PWR spent fuel assemblies

L. Caldeira Balkeståhl, Zs. Elter, S. Grape

Uppsala University, Division of Applied Nuclear Physics, Uppsala, Sweden

## Abstract:

*The differential die-away self-interrogation (DDSI) instrument developed and built in Los Alamos National Laboratory (LANL) is being considered for verification before final disposal. One of the signals from this instrument, the early die-away time, has been shown to be proportional to the multiplication of the spent fuel assembly. Full-scale simulations of the instrument response using MCNP are time consuming. This may become a problem in cases when the instrument response to a large number of fuel assemblies is required, such as in the case of training machine learning models.*

*In this paper, we propose a parametrization of the early die-away time as a function of initial enrichment (IE), burn-up (BU) and cooling time (CT), for intact PWR spent fuel assemblies. The parametrization is calculated from a dataset of 1040 simulated PWR spent fuel assemblies with fuel parameters in the range of IE=2-5%, BU=15-60 GWd/tU and CT=5-70 years. The simulations are done using Serpent2 for the depletion calculation and MCNP6 for the neutron transport and detection in the DDSI.*

*It was found that the CT dependence can be decoupled from the BU and IE dependence, and that it follows an exponential decay. The BU and IE dependences have been fitted with several different functions, and the best fit was chosen based on the chi-square value. The determination of the die-away time using the parametrization has been tested on a separate dataset, resulting in a root mean square error (RMSE) of 0.6  $\mu$ s (the early die-away time ranges from 28  $\mu$ s to 84  $\mu$ s). A description of this work is given in the paper together with details on the choice of parametrizing function, and qualitative arguments for that choice.*

**Keywords:** DDSI; die-away time; parametrization; modelling; PWR

## 1. Introduction

The differential die-away self-interrogation (DDSI) technique has been studied by Los Alamos National Laboratory (LANL) [1] as part of the Next Generation Safeguards Initiative - Spent Fuel [2]. A prototype instrument has been manufactured and recently tested on spent nuclear fuel at Clab [3]; the technique may also be considered for future use at encapsulation facilities.

As has been shown in [4] for simulation space, and in [3] and [5] for experimental data, the DDSI early die-away time,  $\tau$ , is proportional to the multiplication of a fuel assembly. The early die-away time is defined as the decay constant in an exponential fit to the real coincidence Rossi-alpha distribution for neutrons, in the time domain of 4 to 52  $\mu$ s. The proportionality to the multiplication makes  $\tau$  an interesting instrument response to study, especially in the context of nuclear safeguards verification where the fuel assembly parameters initial enrichment (IE), burnup (BU) and cooling time (IE) as well as fissile mass are central concepts. The reason is that assembly multiplication reflects the balance between the fissile content and neutron absorbers such as fission products and minor actinides in the assembly. This balance, in turn, varies with the fuel parameters IE, BU, and CT.

Full-scale simulations of the DDSI instrument response using Monte Carlo techniques are however time consuming, especially if many such simulations are needed. For this reason, we here present a

parametrization of the early die-away time, as a function of fuel parameters CT, IE and BU, which can be used as an approximation of the instrument response in place of the full simulations.

Section 2 of this paper describes the simulation methods used to obtain the instrument response, section 3 explains how the parametrization was derived and section 4 shows the results of the parametrization for a separate data set.

## 2. Simulation methods

The simulations of the response of the DDSI instrument to spent nuclear fuel are done in two steps. In the first step, a depletion calculation is performed with Serpent2 [6] to get the isotopic content of the spent fuel. In the second step, the neutron transport and detection is simulated in MCNP6 [7].

Simulations have been performed for 1040 PWR spent fuel assemblies, covering a range of values of IE, BU and CT. IE ranges from 2-5 % atomic weight in steps of 0.25 % (corresponding to a range of 1.98 to 4.94 % in mass weight), and BU ranges between 15-60 GWd/tU in steps of 5 GWd/tU up to 40 GWd/tU and then in two more steps of 10 GWd/tU. CT ranges between 5-70 y, with smaller steps for shorter cooling times (5 y, 7.5 y, 10 y, 12.5 y, 15 y, 20 y, 30 y, 40 y, 55 y and 70 y). The choice of a grid with an uneven sampling of BU and CT space is made to more accurately capture the variation of  $\tau$  with these variables, with a smaller grid spacing where  $\tau$  changes more rapidly.

### 2.1. Burnup calculation

The burnup, or depletion, calculation is performed in Serpent2 in criticality source mode, in an infinite 2D lattice. The geometry consists of one pin surrounded by water, with reflective boundary conditions. The pin radius is 0.41 cm, the inner cladding radius 0.42 cm, the outer cladding radius 0.48 cm and the pitch 1.26 cm.

The fuel cycles are defined as cycles of 365 days of irradiation at constant power density, resulting in a burnup of 10 GWd/tU per cycle, followed by a down-time of 30 days. The length of the last cycle is adjusted to give the desired burnup, and the desired cooling time is then calculated with the radioactive decay of the spent fuel.

The simulated spent fuel assemblies resulting from this depletion calculation are ideal in several respects: the assembly is uniform, all pins have identical properties; and all assemblies follow idealized cycles (while commercial assemblies might e.g. spend a cycle outside the reactor).

### 2.2. DDSI physics and modelling

The DDSI instrument consists of 56  $^3\text{He}$  tubes in four detector pods surrounding the fuel assembly, as described in [1]. The instrument detects neutrons emitted from the spent nuclear fuel, and can be used to calculate the early die-away time  $\tau$ .

The detected neutrons follow the Rossi-alpha distribution (shown in figure 1). This distribution describes the time difference between detected neutrons, and the non-flat distribution can be explained by the correlation between detected neutrons from the same fission or fission chain. There are in fact two components that describe the neutron correlation, a fast and a slow component, and both are exponential in nature. The fast component corresponds to neutrons from the same fission event or from a fast fission chain, but since the instrument is not capable of resolving this time scale, the decay time of this component instead depends on the instrument geometry and the thermalization of the neutrons before detection. The slow component corresponds to neutrons from a thermal fission chain, i.e. where the neutron thermalizes before inducing a new fission.

The early die-away time results from an interplay between the two components, and has been shown [3-5] to be proportional to the multiplication of the fuel assembly.  $\tau$  measures how long the neutron population survives in the spent fuel and a larger  $\tau$ -value shows that the neutrons die-away more slowly. Fissile material therefore increases  $\tau$ , while neutron poisons decrease it, and the value for each spent fuel assembly is a result of the interplay between these two types of materials.

In MCNP6, the DDSI instrument is modelled surrounding PWR 17x17 spent fuel assemblies, all submerged in water. The fuel pins in the assembly have the geometry described earlier, and the material composition is taken from the output of the Serpent2 simulation. The source term is defined as a spontaneous fission source, and it is distributed evenly in all the fuel rods. The source is restricted to 145 cm of axial length, centred on the DDSI instrument, as a means to speed up the simulation while retaining most of the signal (for details see [8]). The F8 coincidence capture tallies are used to calculate the Rossi-alpha distribution of real coincidences, similarly as in [1]. The Rossi-alpha distribution is simulated from 0 to 200  $\mu\text{s}$ , and  $\tau$  is calculated from an exponential fit over the range 4-52  $\mu\text{s}$  (including statistical errors).

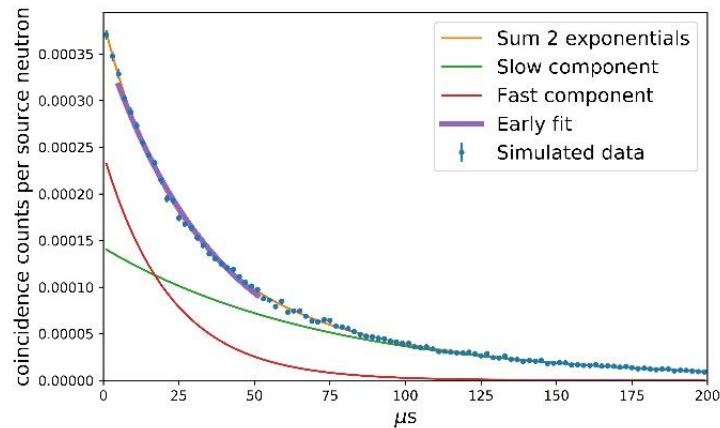


**Figure 1:** Rossi-alpha distribution for real coincident neutrons as simulated with MCNP6. The simulated spent fuel assembly has IE=3.5 %, BU=43 GWd/tU and CT=59 y, and  $\tau = 37.0 \pm 0.4 \mu\text{s}$ .

### 3. Parametrization of $\tau$

Intuitively, since the early die-away time is proportional to multiplication, we expect it to decrease with BU (less fissile material and more neutron absorbers are present) and to increase with IE (more fissile material is present). The CT dependence is not so intuitive, most of the fissile material will not depend on CT, although  $^{241}\text{Pu}$  does. Figures 2-4 show how  $\tau$  depends on IE, BU and CT for a part of the data. The dependence for the whole dataset is smooth, and an interpolation between the shown data points can be made.

As can be seen from figures 2a-2d, there is a strong dependence of  $\tau$  on IE. As expected,  $\tau$  increases with increasing IE. Figures 2a-2b show that the IE dependence does not depend on CT, since the data sets corresponding to different CT are only separated by a constant offset depending on CT. Figures 2c-2d however show a noticeable effect of BU on the IE dependence, with an increasing slope for lower BU-values.

Similar conclusions can be drawn from figure 3. Figures 3a-3b show a similar shape of the  $\tau$ -dependence on BU independent of CT (only the constant offset is different), while figures 3c-3d show a dependence on IE where different IE-values give different slopes to the  $\tau$ -dependence on BU.

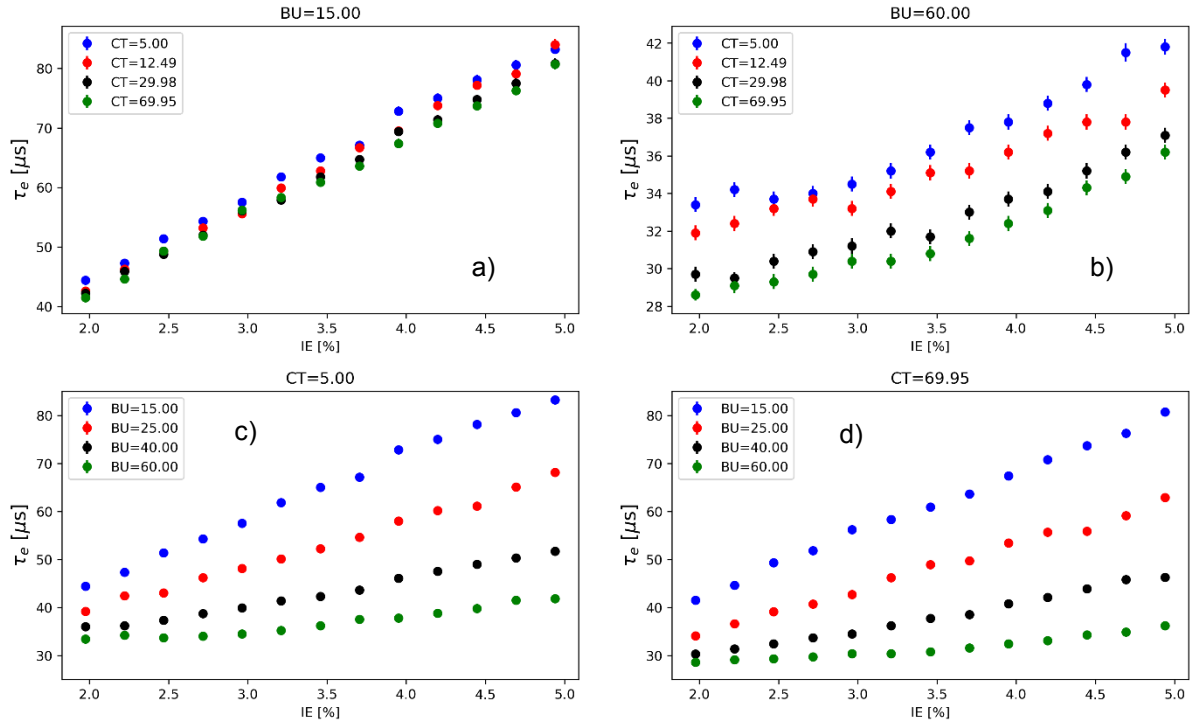


**Figure 2:** The  $\tau$  dependence on IE, for low BU (a), high BU (b), low CT (c) and high CT (d). In the top figures, the colors indicate different CT, for the bottom figures it indicates different BU. For a more understandable figure, all simulated data points are not shown.

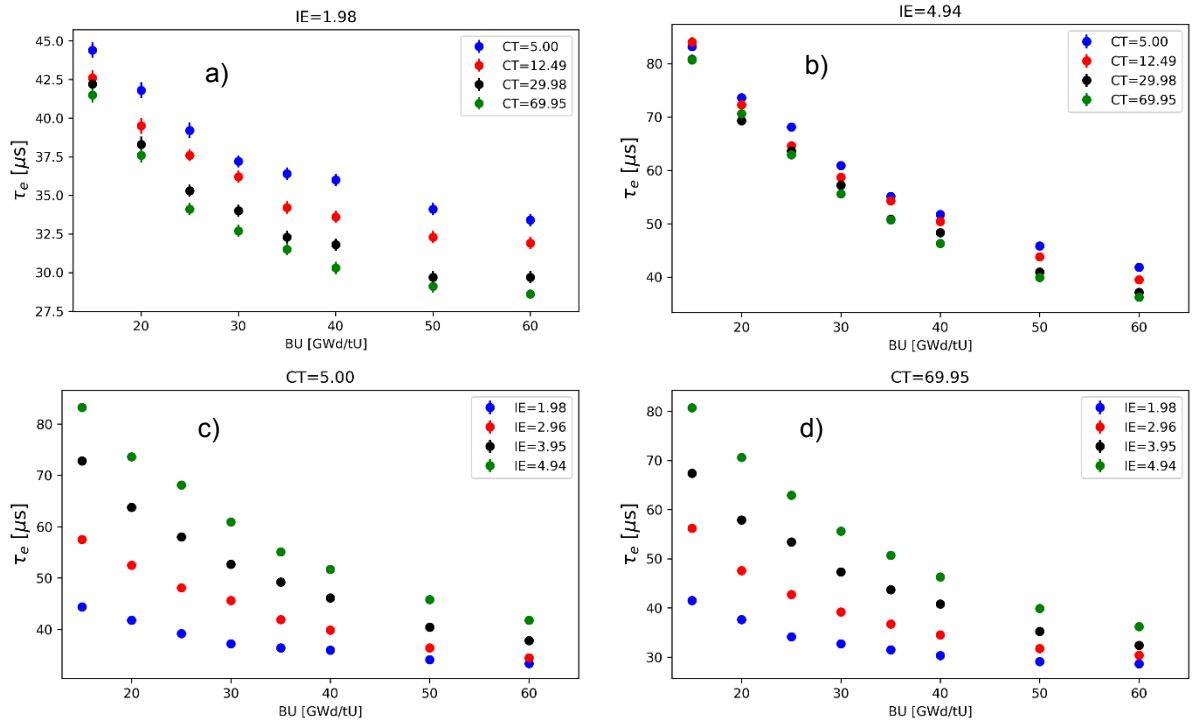


**Figure 3:** The  $\tau$  dependence on BU, for low IE (a), high IE (b), low CT (c) and high CT (d). For the top figures, the colors indicate different CT, for the bottom figure it indicates different IE. For a more understandable figure, all simulated data points are not shown.

Figure 4 shows that the CT-dependence can be described with an exponentially decreasing function, with figures 4a-4b showing that IE only affects a constant offset and not the exponential itself, and figures 4c-4d show the same but for BU. The different scales of the y-axis make it difficult to compare different subplots with each other, but one can note this effect also by comparing the different colors in each subfigure (they colored data sets only vary by a constant offset). This implies that the CT dependence, described by an exponential function, is independent of IE and BU except for a constant offset. Since the IE and BU dependencies are interconnected, it is more difficult to assess what functional form to use in order to describe them. However, the figures qualitatively tell us that  $\tau$  increases with IE, with a steeper slope for low BU (e.g. figure 2c); and  $\tau$  decreases with BU, with a slope that increases with higher IE and flattens out with BU (eg figure 3c).

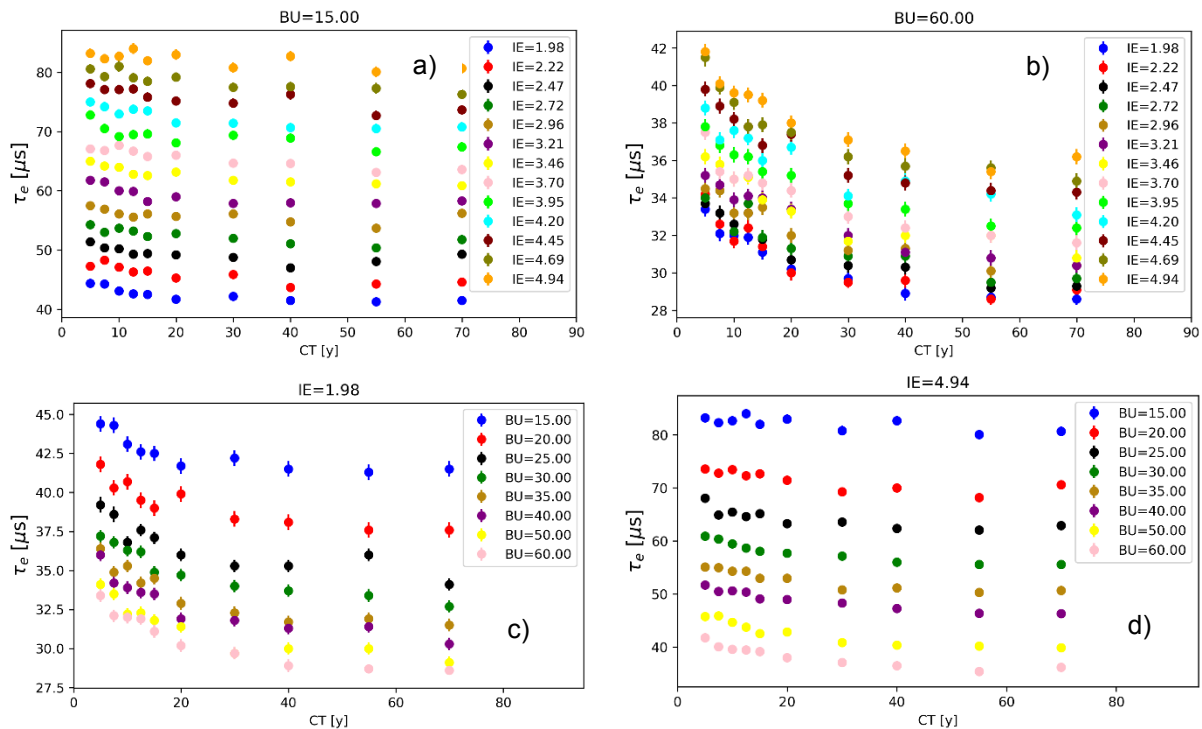


**Figure 4:** The  $\tau$  dependence on CT, for low BU (a), high BU (b), low IE (c) and high IE (d). For the top figures, the colors indicate different IE, for the bottom figure the colors indicates different BU.

### 3.1 Physical considerations

As mentioned above, the early die-away time depends on the quantity of fissile material and neutron absorbers (such as some fission products) in the fuel. To understand which isotopes that are most important when determining  $\tau$ , we have investigated three quantities in eight example fuels: i) the neutron absorption rate, ii) the neutron induced fission rate and iii) the rate of neutrons produced from fission. The eight example fuels have low and high CT, low and high BU and low and high IE. The respective rates were calculated using the MCNP6 F4 neutron flux tally score, multiplied with the relevant cross-sections. The isotopes were then ranked according to the absolute value of their net neutron emission rate, defined as the difference between the neutron emission rate from fission and the total neutron absorption, where total neutron absorption also includes neutrons lost to fission.

Looking at the top six isotopes for each of the eight example fuels, we find that the sixth isotope always has a net neutron emission which is at least one order of magnitude smaller than the first isotope. Table 1 shows the six top ranked isotopes for one of the eight fuels.

Isotope	Net neutron emission [au]
<sup>239</sup> Pu	7.8
<sup>235</sup> U	4.4
<sup>238</sup> U	-4.2
<sup>241</sup> Pu	2.4
<sup>240</sup> Pu	-2.0
<sup>143</sup> Nd	-0.51

**Table 1:** Net neutron emissions for an example fuel with IE=4.9%, BU=60 GWd/tU and CT=5y.

To reach a reduction in net neutron emission of two orders of magnitude, it was sometimes necessary to consider 30 ranked isotopes. In qualitatively understanding the impact of the different isotopes on  $\tau$ , we focus here on eight isotopes that appear at least once in the top five list for the eight fuels: <sup>239</sup>Pu, <sup>240</sup>Pu, <sup>241</sup>Pu, <sup>241</sup>Am, <sup>235</sup>U, <sup>238</sup>U, <sup>155</sup>Gd and <sup>149</sup>Sm. The top 3 list is often consisting of <sup>239</sup>Pu, <sup>235</sup>U and <sup>238</sup>U. The following subsections give some insight into the mechanism governing  $\tau$  and its dependence on IE, BU and CT. A more quantitative understanding is beyond the scope of this paper.

### 3.1.1. CT dependence of $\tau$

From the list of isotopes above, the one isotope with a half-life likely to have a visible effect in the range of CT=5-70 y is <sup>241</sup>Pu ( $t_{1/2} = 14.3$  y). This isotope mainly  $\beta^-$ -decays to <sup>241</sup>Am. While <sup>241</sup>Pu is fissile and has a positive contribution to the early die-away time (more <sup>241</sup>Pu gives a larger  $\tau$ ), <sup>241</sup>Am absorbs neutrons and has a low probability of fissioning, and thus has a negative contribution to  $\tau$ . From these considerations, one would expect  $\tau$  to follow an exponential decay law with CT, with a mean lifetime (the inverse of the exponential decay constant  $\lambda$ ) smaller than that of <sup>241</sup>Pu, since the decay of <sup>241</sup>Pu creates <sup>241</sup>Am which lowers  $\tau$  even more. This is indeed the result found in the study; the mean lifetime of <sup>241</sup>Pu is 20.6 y, and the mean lifetime obtained for  $\tau$  in the fit in section 3.2.1 is 15.8 y (parameter  $b$  in table 3).

### 3.1.2. BU and IE dependence of $\tau$

Since higher BU means that more fissile <sup>235</sup>U nuclei have been split,  $\tau$  is expected to decrease with BU. The buildup of other fissile isotopes should offset this and slow down the decrease, while production of neutron poisons would speed up the decrease. Studying how the <sup>235</sup>U concentration changes as a function of burnup, we note that the rate of decrease of the <sup>235</sup>U concentration depends on the IE, with higher IE resulting in a sharper decrease of the <sup>235</sup>U concentration with increasing BU.

Figure 5 shows how the total fissile concentration (i.e. <sup>235</sup>U, <sup>239</sup>Pu and <sup>241</sup>Pu) changes with BU and IE. This dependence is very similar to the dependences observed for only <sup>235</sup>U, and this isotope is hence assumed to dominate the dependence. The dependences in figure 5 are qualitatively very similar to the  $\tau$ -dependence on these variables, so the contribution from <sup>235</sup>U seems to be the most important one. Higher IE, meaning more <sup>235</sup>U and less <sup>238</sup>U, is expected to give larger values of  $\tau$ , as is also seen in figure 2. As BU increases, the fuel composition becomes more complex and varied and the increase of  $\tau$  with IE slows down.

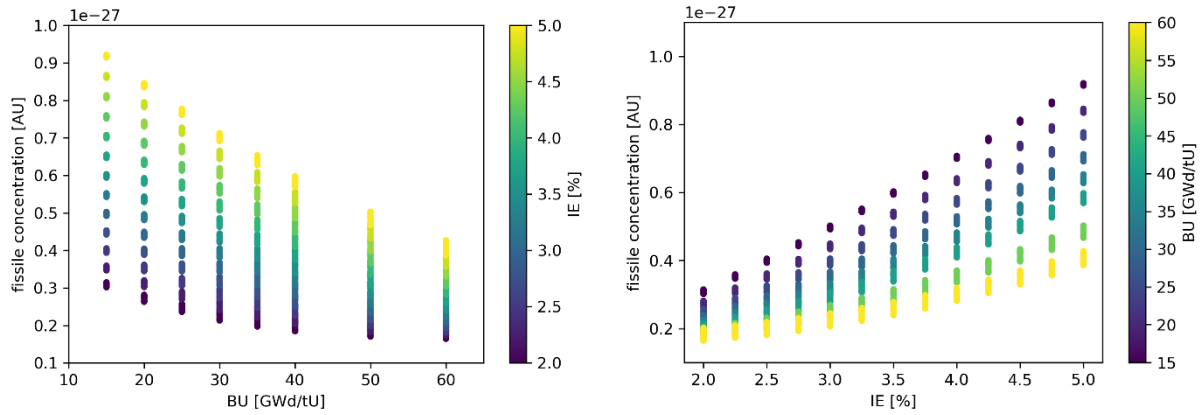


Figure 5: The concentration of fissile isotopes vs BU (left) and IE (right), colored with the IE (left) and BU (right).

### 3.2 Fitting functions

Since the  $\tau$ -dependence on CT seems to be independent of BU and IE, this was investigated first. The function describing the dependence of  $\tau$  on CT was chosen to be an exponential function of the form

$$\tau = a \cdot e^{-\frac{CT}{b}} + c \tag{1}$$

where  $a$ ,  $b$  and  $c$  are the fitting parameters. The choice of the exponential function is explained in section 3.1.1. One exponential function (each generating unique  $a$ ,  $b$  and  $c$  parameter values) was fitted to each group of data points with one combination of IE and BU, e.g. each group with the same color in one subplot of figure 4. The fit parameters  $a$ ,  $b$  and  $c$  are then analyzed with respect to their dependence on IE and BU. The dependences of the  $a$  and  $c$  parameters on BU and IE can be seen in figure 6; the dependence of the  $b$  parameter looks similar to the  $a$  dependence and is hence not shown.

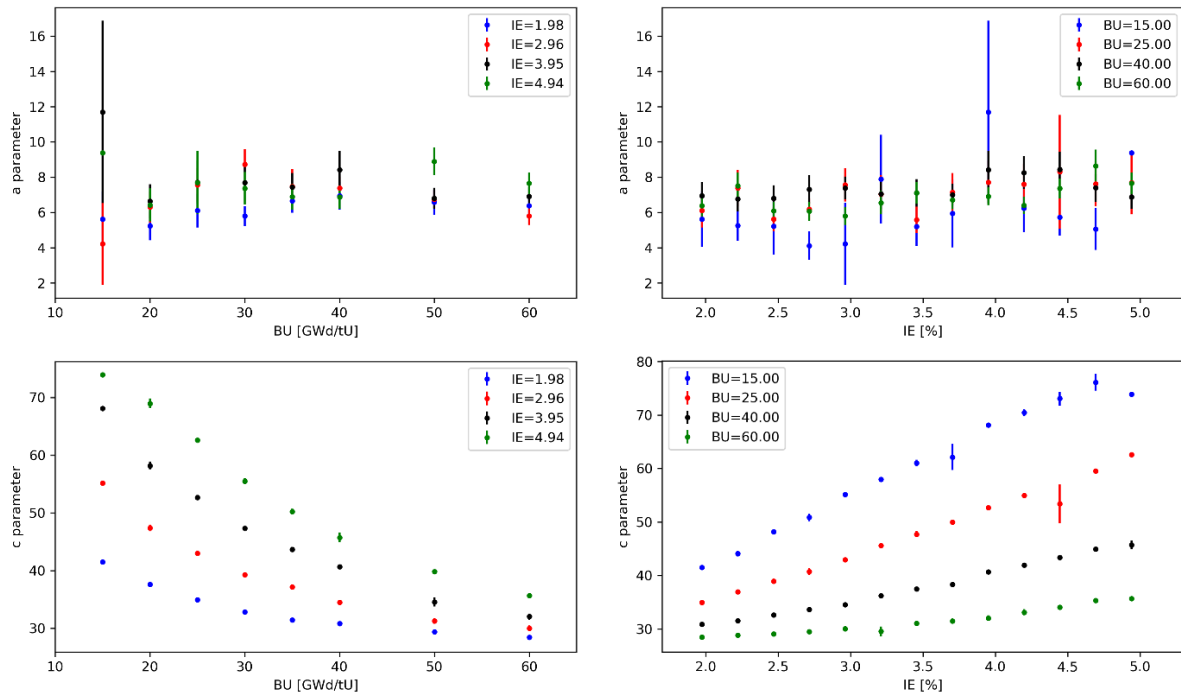


Figure 6: The  $a$  (upper row) and  $c$  (lower row) parameters resulting from an exponential fit of  $\tau$  to CT, shown as a function of BU (left) and IE (right). The data points corresponding to BU=15 GWd/tU and IE=4,94% are plotted without error bars, since the error associated these points is so large that they obscure all other trends. For a more understandable figure, all simulated data points are not shown.

Despite rather large statistical fluctuations in figure 6 (the error bars represent the statistical uncertainties in the fit), both the  $a$  and  $b$  parameters have been found to be consistent with a constant value. This means that these two parameters can be considered to be independent of IE and BU. The  $c$  parameter however displays the same trend as  $\tau$  does for a fixed CT, also indicating that the BU and IE dependence of  $\tau$  is captured by the  $c$ -parameter and not by the  $a$  or  $b$  parameters. With the ultimate goal of finding a function that describes how  $\tau$  varies with IE, BU and CT, equation 1 was accordingly chosen with the  $a$  and  $b$  parameters constant for the whole range of IE and BU values, but with the  $c$  parameter replaced by a function that better captures the IE and BU dependences.

In the determination of the second function (capturing the dependence of the  $c$  parameter on BU and IE), a fit of equation 1 was performed to fix the  $a$  and  $b$  constants while allowing the  $c$  parameter to vary with BU and IE. Accordingly, a different  $c$  parameter value was obtained for each value of IE and BU.

Determining then the BU dependence first, and to avoid an unphysical increase of  $\tau$  with BU values outside the fitting range, an exponential fit (Equation 2) was tried

$$c = a_1 \cdot e^{-\frac{BU}{b_1}} + c_1 \tag{2}$$

where  $a_1$ ,  $b_1$  and  $c_1$  are the fit parameters that vary with IE. Since each fit, corresponding to one IE value, is associated with a unique determination of the parameters  $a_1$ ,  $b_1$  and  $c_1$ , a function can be used to describe how each parameter varies with IE. This function can be described by either a linear, quadratic or constant polynomial of IE. Figure 7 shows the variation of the parameter values with IE, together with a linear fit.

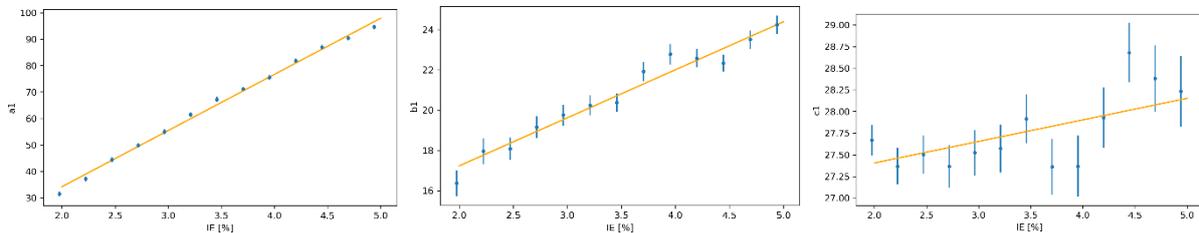


**Figure 7:** The dependence of the parameters  $a_1$ ,  $b_1$  and  $c_1$  of the BU fit (equation 2) on IE. The fitted function is linear in all three cases, although table 3 shows that this does not always give the best fit.

Table 3 shows the resulting  $\chi^2$  and  $\chi^2$  probability values for different functions describing the variation of the  $a_1$ ,  $b_1$  and  $c_1$  parameters with IE. Table 2 tells us that the  $a_1$  parameter is best described by a function that depends quadratically on IE, the  $b_1$ -parameter is best described by a linear function of IE (although the quadratic function is almost equally good), and that the  $c_1$  parameter is best described by a quadratic function (but a linear function is still relevant to try in a global fit).

Parameter	Fit type	$\chi^2$	$\chi^2$ probability
$a_1$	Linear	25.7	0.007
	Quadratic	5.2	0.88
$b_1$	Linear	10.7	0.45
	Quadratic	8.6	0.57
$c_1$	Linear	12.6	0.32
	Quadratic	8.0	0.62
	Constant	21.3	0.04

**Table 2:** Fit statistics for the BU parameters  $a_1$ ,  $b_1$  and  $c_1$  as functions of IE.

### 3.2.1. Global fit

Following the considerations above, several functions were tried in order to find a suitable function for a global fit, that simultaneously describes the dependence of  $\tau$  on CT, BU and IE. All the functions which were tried, make use of equation 1 but with parameter  $c$  replaced by a function  $C$ , as shown in equation 3:

$$\tau = a \cdot e^{-\frac{CT}{b}} + C \tag{3}$$

Many different functions  $C$  were tried and assessed, the best function as determined by the resulting  $\chi^2$  value is shown in equations 4-7

$$C = c' \cdot e^{-\frac{BU}{d}} + e \tag{4}$$

$$c' = (c_2 \cdot IE^2 + c_1 \cdot IE + c_0) \tag{5}$$

$$d = (d_2 \cdot IE^2 + d_1 \cdot IE + d_0) \tag{6}$$

$$e = (e_2 \cdot IE^2 + e_1 \cdot IE + e_0) \tag{7}$$

The resulting parameter values are shown in table 3. This fit has  $\chi^2 = 1245$  and  $\chi^2$  probability  $3.9 \cdot 10^{-6}$ . The errors are probably underestimated, leading to this large value of  $\chi^2$ , and a better error estimate is under consideration.

Figure 8 shows the  $\tau$  value determined using the parametrization versus the  $\tau$  value determined using the MCNP simulations, together with the line representing a perfect fit. As can be understood, the global parametrization function seems to work quite well.

Parameter	Value
a	6.87(8)
b	15.8(4)
c0	-28(3)
c1	33(2)
c2	-1.8(2)
d0	11(1)
d1	3.3(7)
d2	-0.14(10)
e0	28.2(6)
e1	-0.7(4)
e2	0.14(7)

**Table 3:** Fit parameters determined for the best global fit.

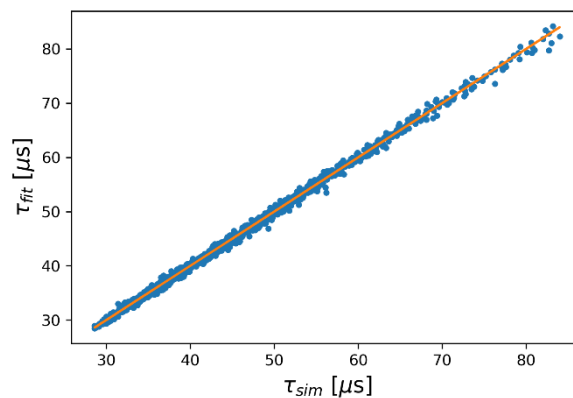


**Figure 8:** The  $\tau$  values determined from the parametrization versus those obtained from a full-scale MCNP6 modelling together with a line indicating a perfect match.

## 4. Test of parametrization

The parametrization has been tested on a separate set of modelled data. The data set comprises 980 simulated PWR fuels, with depletion calculations done using Serpent2 as described in section 2. However, the ranges of IE, BU and CT were slightly different from the fuels described earlier. IE ranged from 2-5% atomic weight in steps of 0.5%, while BU and CT were randomly selected with a uniform probability in the intervals 15-50 GWd/tU and 5-70 y, respectively. Figure 9 shows the early die-away time  $\tau$  determined using the parametrization versus determination using MCNP, as well as the normalized residuals  $r_n = \frac{\tau_{fit} - \tau_{sim}}{\sigma_{\tau_{sim}}}$ , centered around zero.

The root mean squared error (RMSE) is 0.57  $\mu\text{s}$ ,  $\chi^2 = 1131$  and the  $\chi^2$  probability  $5.4 \cdot 10^{-4}$ . As previously mentioned, the errors are probably underestimated, leading to a larger value of  $\chi^2$  than is to be expected, but this remains to be investigated.

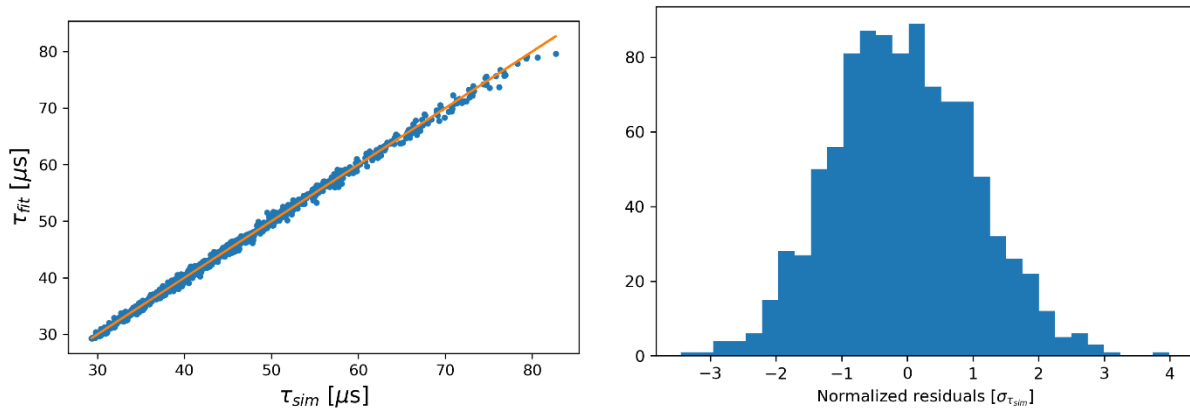


**Figure 9:** The simulated and calculated values of  $\tau$  for the test data fall close to the line indicating a perfect match (left). The normalized residuals are shown in the right figure.

## 5. Conclusion and Outlook

This paper describes a way to estimate the early die-away time  $\tau$  from the DDSI prototype instrument, as a way to avoid the computationally demanding MCNP simulations that are usually performed. This can be specifically useful when die-away times for large number of fuel assemblies are required, such as in the case of training machine learning models.

Our work shows that in the case of modelled PWR 17x17 fuel assemblies, the CT dependence of the early die-away time can be decoupled from the BU and IE dependencies. The research also suggested that the CT dependence of  $\tau$  follows an exponential decay. In this work it was decided to, in the second step, describe the BU dependence and thirdly the IE dependence. The reverse order was tried, although the results are not shown in this paper, and the results were similar to those obtained here but not as good. The BU dependence could be best described using another exponential decay, although other functions with a similar fall-off were found to also work well. The IE-dependence was finally captured using functions with a quadratic dependence on this parameter.

The die-away times estimated using the resulting parametrization function were compared to the accurate estimations using MCNP6 modelling and a fit to the Rossi-alpha distribution, and the agreement was shown to be very good, also for the case of a new data set of modelled fuel assemblies with a slightly different set of fuel parameters (within the same range as the first one). As an important next step, an experimental validation of this parametrization is planned, since the ability of the parametrizing function to estimate the DDSI die-away time for commercial reactor fuel might be significantly influenced by a deviation of burnup, initial enrichment and cooling time from the assumed ideal case. Furthermore, it is important to study to what extent the parametrization function also correctly estimates the die-away time for other fuel types or designs.

## 6. Acknowledgements

We would like to acknowledge the financial support from the Swedish Radiation Safety Authority under contracts SSM2016-661, SSM2015-4125 and SSM2016-4600.

The authors would also like to thank Dr. Alexis Trahan at Los Alamos National Laboratory for her kind assistance with respect to DDSI modelling.

The work presented in this contribution has been accepted for publication in the ESARDA Bulletin n. 58 (June 2019), ISSN 0392-3029

## 7. References

- [1] A. Trahan. "Utilization of the Differential Die-Away Self-Interrogation Technique for Characterization and Verification of Spent Nuclear Fuel". PhD thesis. University of Michigan, 2016.
- [2] M. A. Humphrey, S. T. Tobin, and K. D. Veal. "The Next Generation Safeguards Initiative's Spent Fuel Nondestructive Assay Project". In: *Journal of Nuclear Material Management* 40 (2012), pp. 6-11.
- [3] A. Trahan, G. McMath, P. Mendoza, H. Trelle, U. Backstrom, and A. Sjöland. "Preliminary Results from the Spent Nuclear Fuel Assembly Field Trials with the Differential Die-Away Self-Interrogation Instrument". In: *Proceedings of the Institute of Nuclear Materials Management 59th Annual Meeting, July 22-26, Baltimore, Maryland*. Institute of Nuclear Materials Management. 2018.
- [4] A. C. Kaplan, V. Henzl, H. O. Menlove, M. T. Swinhoe, A. P. Belian, M. Flaska, and S. A. Pozzi. "Determination of spent nuclear fuel assembly multiplication with the differential die-away self-interrogation instrument". In: *Nuclear Instruments and Methods in Physics Research Section A: Accelerators, Spectrometers, Detectors and Associated Equipment* 757 (2014), pp. 20-27.
- [5] A. C. Trahan, A. P. Belian, M. T. Swinhoe, H. O. Menlove, M. Flaska, and S. A. Pozzi. "Fresh Fuel Measurements with the Differential Die-Away Self-Interrogation Instrument". In: *IEEE Transactions on Nuclear Science* 64.7 (2017), pp. 1664-1669.
- [6] J. Leppänen, M. Pusa, T. Viitanen, V. Valtavirta, and T. Kaltiaisenaho. "The Serpent Monte Carlo code: Status, development and applications in 2013". In: *Annals of Nuclear Energy* 82 (2015), pp. 142-150.
- [7] T. Goorley et al. "Initial MCNP6 Release Overview". In: *Nuclear Technology* 180.3 (2012), pp. 298-315.
- [8] L. Caldeira Balkeståhl, Z. Elter, S. Grape, and C. Hellesen. "MCNP simulations of prototype DDSI detector". In: *Proceedings of the International Workshop on Numerical Modelling of NDA Instrumentation and Methods for Nuclear Safeguards (NM-NDA-IMNS18)*. ESARDA. 2018.

# Passive Neutron Albedo Reactivity (PNAR) Prototype for Spent Nuclear Fuel Verification

Topi Tupasela<sup>1</sup>  
Tapani Honkamaa<sup>1</sup>  
Mikael Moring<sup>1</sup>  
Asko Turunen<sup>2</sup>

<sup>1</sup>STUK – Radiation and Nuclear Safety Authority, FI-00881 Helsinki, Finland

<sup>2</sup>Provedos Oy, FI-00881 Helsinki, Finland

## **Abstract:**

*The Finnish safeguards concept for encapsulation plant and geological repository includes verification of all fuel items before encapsulation and disposal. The verification process is carried out according to IAEA Group of Experts ASTOR (Application of Safeguards TO Repositories) recommendations. One of the non-destructive assay (NDA) instruments featured in the concept is Passive Neutron Albedo Reactivity (PNAR). The PNAR device will be used to verify the presence of fissile material in spent nuclear fuel assemblies.*

*The PNAR instrument makes two relative neutron flux measurements. One in a neutron albedo maximizing and one in a neutron albedo minimizing configuration. From the ratio of the two measurements, a measure of the presence of fissile material can be calculated. The albedo minimizing configuration is achieved by surrounding the fuel assembly with cadmium.*

*A prototype of the PNAR device is being built by STUK. The prototype is designed for underwater measurements of BWR fuel used in Olkiluoto nuclear power plants. This article presents the final design of the prototype device and presents the upcoming measurement plans with the detector. A mock-up PNAR detector pod was assembled and tested under laboratory conditions to quantify the detector signals and find potential sources of errors in the design.*

**Keywords:** non-destructive assay; PNAR; encapsulation safeguards

## **1. Introduction**

Disposal of spent nuclear fuel in Finland is anticipated to begin in mid-2020's. A national safeguards concept has been developed by STUK, the radiation and nuclear safety authority, to prepare for the possible safeguards related challenges of the disposal process. One aspect of the safeguards concept is verification of all fuel items before disposal. The verification is expected to be performed at the wet spent fuel storage, before transportation to the encapsulation facility. Additionally an optional verification location is expected to be integrated into the encapsulation process at the encapsulation facility in case of loss of CoK (Continuity of Knowledge).

The verification concept has been developed according to the IAEA Group of Experts ASTOR (Application of Safeguards TO Repositories) recommendations [1]. The concept suggests a combined measurement with three instruments: PGET (Passive Gamma-Emission Tomography), PNAR (Passive Neutron Albedo Reactivity), and a load cell. PGET can detect individual fuel pins, PNAR can verify the fissile material content inside a fuel assembly, and a load cell is used to measure the weight of an assembly. [2]

A prototype of a PNAR instrument is currently being built by STUK. In this article, the final design of the instrument is presented, followed by a view to the current status of the project. A mock-up PNAR detector pod was tested in laboratory conditions to quantify detector responses to different neutron flux intensities. The upcoming spent fuel measurement plans are described and at the end, the NDA

(non-destructive assay) measurements, that are expected to take place prior fuel disposal, are discussed.

## 2. Theory

PNAR utilizes the neutron radiation of the spent nuclear fuel itself to probe the neutron multiplication by the fissile materials still present in the fuel. The main source of neutrons is spontaneous fission of  $^{244}\text{Cm}$ , which accumulates in nuclear fuel during burn. After a neutron is emitted from a fuel assembly, it has a chance to reflect back inside by neutron albedo through a series of inelastic scatterings in the surrounding coolant. These albedo neutrons can cause new fission events, further increasing the flux of neutrons – provided that fissile material is present.

A PNAR instrument makes two relative measurements; one that minimizes neutron albedo and one that maximizes it. The minimizing configuration is achieved by surrounding the fuel assembly with cadmium. Neutrons lose a portion of their energy in each scattering event and thus, albedo neutrons are concentrated in the thermal energy range. Cadmium, particularly  $^{113}\text{Cd}$ , has a very high absorption cross section for low energy (<0.5 eV) neutrons. The neutron albedo maximizing configuration is achieved by ensuring that the fuel assembly is surrounded by neutron reflecting materials, e.g water or polyethylene.

Neutron detectors in the PNAR device measure the flux of fast neutrons radiating from the nuclear fuel. Fast neutrons are created both in spontaneous and induced fission reactions. If all other measurement conditions except the presence or absence of the cadmium envelope are kept identical between the two measurement configurations, the increase in fission events, caused by albedo neutrons, shows as an increased detector response.

The design of a PNAR is like that of a FORK detector, as will become evident in Chapter 3. An automated data verification module, based on SCALE/ORIGEN, has been integrated into the FORK detector data analysis software developed by EURATOM and IAEA. The software verifies the declared fuel item usage history by comparing the detector responses to a pre-calculated database of simulated responses to different fuel histories. Adding gamma detectors to the PNAR instrument enables it to measure identical signals that are currently measured using a FORK detector. Thus, PNAR can also be used as a fuel history verification tool. [3]

## 3. PNAR design

To improve measurement efficiency, neutron albedo preventing cadmium needs to be placed as close to the fuel as possible. Thus, PNAR detector designs vary between fuel types. The STUK's PNAR prototype is designed for the BWR fuel assemblies from Olkiluoto 1 and 2 units in Finland. This is also the fuel that the disposal is planned to start with. The instrument is designed to be used in the spent fuel storage pool at the Olkiluoto NPP. The conceptual design was published by Tobin et al. in 2017 [4].

The design includes a 3.6 m tall support quadropod for both PNAR and PGET instruments positioned around a common central fuel guide. Either of the instruments can be used individually or simultaneously. The quadropod will be positioned on the bottom of the fuel storage pool. The system height is designed to allow for measuring at almost any axial height of a fuel assembly. The design of the quadropod, together with both measurement instruments can be found in Figure 1.

A movable cadmium liner is positioned between the central fuel guide and the PNAR detector to allow for the two relative measurements without moving the fuel assembly. The liner slides along the fuel guide, and is moved manually, through a series of pulleys, from poolside. The liner is highlighted in Figure 1 in its lowest position (i.e. in the albedo maximizing configuration).

A cross sectional image of the PNAR detector is shown in Figure 1. The PNAR optimized for BWR fuel consists of four identical and independent rectangular measurement pods assembled into a square, with an opening in the middle. Each pod houses one fast neutron detector and one gamma detector. The fast neutron detectors are  $^3\text{He}$  chambers, surrounded by polyethylene and cadmium. Surrounding

the neutron detectors, is lead for gamma shielding, and the outer pod is polyethylene (PE). The design is optimized for long cooled fuel assemblies (CT > 20 y). For example, it can be expected that gamma-radiation will not provide any notable response to  $^3\text{He}$  chambers if CT exceeds 20 y [4]. The gamma detector is positioned in the outer PE, near the top of the pod. The placement of the gamma detector can be seen in Figure 2. At one end of each pod, empty space is reserved for making necessary electrical connections.

One source of uncertainty in the FORK data verification is caused by positional uncertainty raising from the positioning of the detector and inspected fuel item [5]. Having detectors on all sides of the measured fuel assembly and averaging over all the responses, decreases this positioning uncertainty.

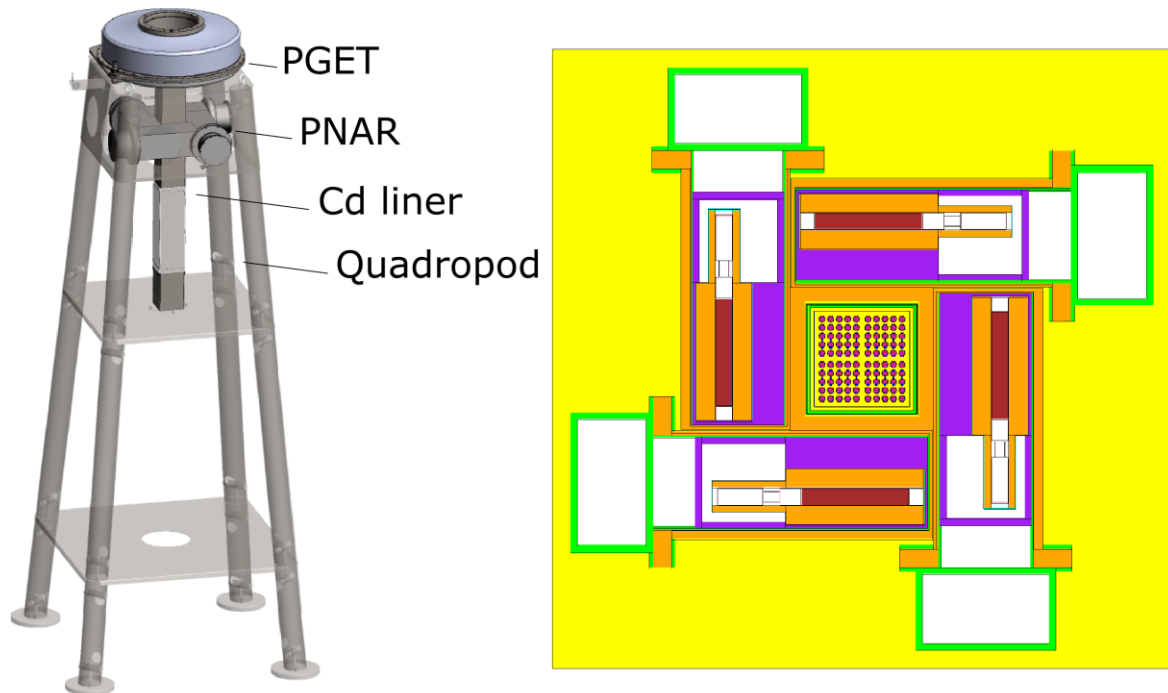


**Figure 1:** Left: Combined PNAR-PGET measurement station on a common support quadropod. Right: Neutron detector level cross section of the PNAR device;  $^3\text{He}$  chambers (dark red), polyethylene (orange), lead (purple). The fuel assembly and the central steel tube with cadmium lining can be seen in the middle.

#### 4. Preliminary measurements

Preliminary dry tests with a mock-up PNAR pod were performed at the STUK laboratories. The mock-up pod has the same polyethylene and lead component geometries around the  $^3\text{He}$  detectors as the real pods. To study detector responses to different neutron energy distributions, a californium source was measured in four configurations – bare, and surrounded with 2,3, and 4 cm polyethylene moderators. Additionally, the gamma shielding, and dead time of the detectors were studied. Pictures of the measurement setup and the mock-up PNAR pod are shown in Figure 2.

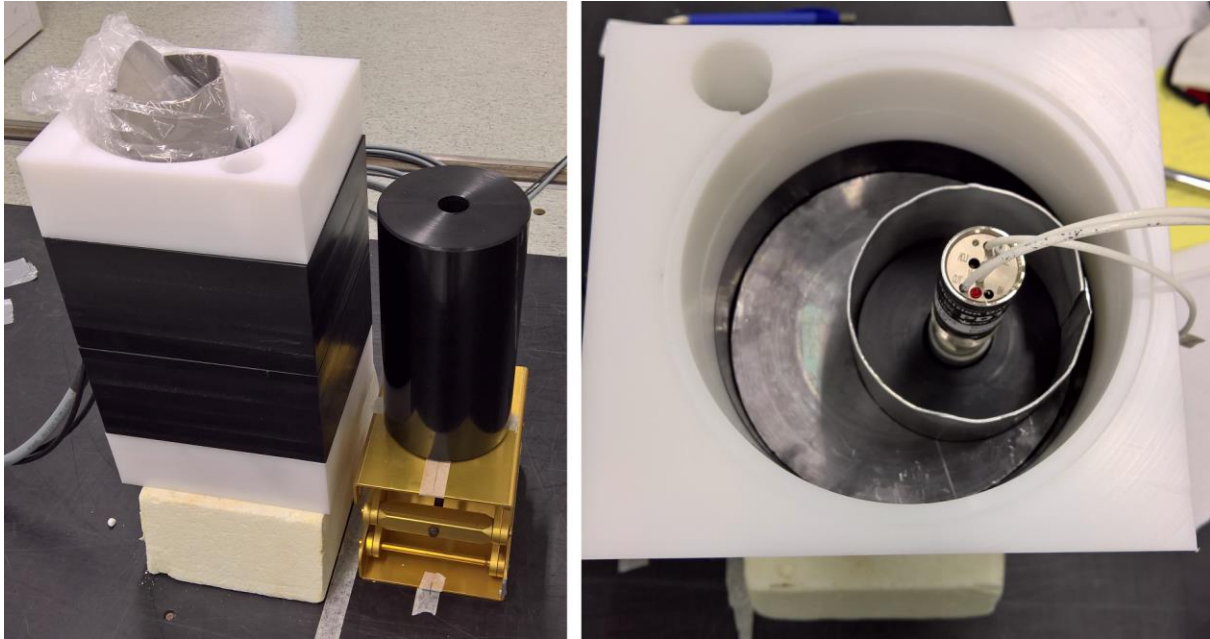


**Figure 2:** Mock-up PNAR pod measurements. Left: Measurement setup. Neutron source is positioned inside the cylindrical polyethylene (PE) moderator. Right: Close-up of the detector inside. Materials from out to in: PE, lead, cadmium, PE, detector. The left face is positioned towards the source. The hole in the upper-left corner is for the gamma detector.

#### 4.1. Detector response to fast neutrons

For all measurements the same 240 MBq californium source was placed inside PE moderators of various thickness. The distance between the source and the detector was kept constant. The moderator thickness affects the energy spectrum of the neutron flux while the total amount of neutrons stays approximately the same between measurements. As only fast neutrons are meant to be detected a thicker moderator should yield a lower count rate.

All measurement configurations were also simulated with MCNP6.2 to quantify the ratio of fast neutrons entering the PNAR pod. What was quantified from the simulations, was the energy of neutrons entering the PNAR pod through the source facing facet. The energy cut-off for fast neutrons was set at 10 keV. The detected count rate as a function of the simulated fast neutron flux is presented in Figure 3. The response grows linearly with the Monte-Carlo calculated flux.

All of the measurements were repeated with and without a cadmium sheet between the PE moderator and the PNAR pod to simulate measurements in albedo minimizing and maximizing configurations. This measurement corresponds to a PNAR measurement of a non-multiplying object. According to theory, in such measurement both responses are the same. In all of the measurements, the responses were within the numerical error margin from each other.

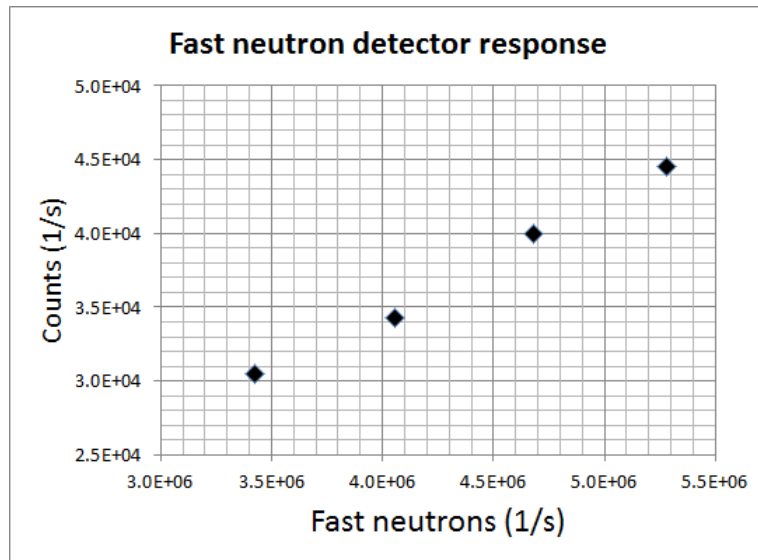


**Figure 3:** The measured detector response vs MCNP calculated fast neutron flux (>10 keV) was linear. The total neutron generation rate was the same in each measurement.

#### 4.2. Gamma shielding

The effectiveness of the gamma shielding was tested by directing a cone of radiation towards the fuel facing face of the PNAR mock-up pod. A <sup>137</sup>Cs source was used, which had a dose rate of 136 mSv/h at the measurement distance. The detected signal was indistinguishable from the background level - even though the mock-up pod lacked the lead shielding around the detector preamplifier which will be part of the final design. The shielding appears to be thick enough to prevent gammas from causing false signals in the <sup>3</sup>He detectors. Although, it should be noted, that the shape of the gamma flux did not accurately represent that of a spent nuclear fuel element measured underwater.

#### 4.3. Detector dead time

Dead time of the neutron detectors was tested with two neutron sources. Detector responses to a 240 MBq Cf source and a 170 MBq AmBe source were measured together and separately. The measured signals with one standard deviation uncertainties are presented in Table 1. The detector dead time based on these measurements is 1.2±0.2 µs.

Neutron source	Background	Cf	AmBe	Combined
Detector response (cps)	0	44510±210	26540±160	68250±260

**Table 1:** Detector responses to dead time measurements

### 5. Upcoming measurement campaign

A testing campaign for combined PNAR-PGET measurements is planned to be held later this year. The campaign will be the proof-of-concept for the PNAR detector, but it will also yield much needed data for PGET image reconstruction software development. To characterize the PNAR responses to different fuel compositions, the plan is to measure fuel assemblies with various initial enrichments, burnups, cooling times, and multiplication. Additionally, fuel assemblies will be measured for the whole axial length. This will allow for studying how the axial burnup profile affects the measurements. Furthermore, partial length pins should be identifiable from the PGET measurements. The availability of partial length pins can also be utilized to simulate pin removal.

## 6. Verification before encapsulation

According to the national safeguards concept for fuel disposal, NDA-measurements (consisting of a combined PNAR-PGET measurement) will be performed on every fuel assembly prior disposal. This measurement step must be seamlessly integrated into the encapsulation process not to interfere with the operator's process. One option is to have the NDA measurement step immediately before moving a fuel assembly into the transportation cask. This requires the NDA equipment to be able to reliably perform the measurements in the given time window as any complications would directly affect the encapsulation process. Another option is to move measured assemblies into a buffer storage kept under strict dual C/S, from which the assemblies are transported into the encapsulation facility. This option is less vulnerable to unpredicted complications in the measurement process but requires additional storage area and causes more movements per fuel assembly. Currently, the measurements are expected to take five minutes in total.

However the fuel handling will be organized, the NDA verification process should be automated and remotely controlled under video surveillance. The data-analysis should also be automated and give an easily interpretable signal while also saving the raw measurement data. The current concept is to use a traffic lights signal to tell the operator how to proceed.

- Green: The assembly can proceed in the encapsulation process.
- Orange: Measure the assembly again. If orange signal repeats N times, it will be interpreted as red. Orange signal could be caused, for example, by faults in the measurement system or insufficient counting statistics.
- Red: The assembly declaration does not match the measurement data. The assembly can not proceed into encapsulation until additional actions.

As stated, the measurement station needs to be reliable, automated, and provide fast data analysis when the disposal begins. This requires solving both computational and logistical challenges. First of all, the utility of the PNAR system will be verified in the upcoming measurement campaign. The measurement software is expected to be able to independently compare the measurement responses, from both PNAR and PGET measurements, to the declared fuel parameters, and to draw conclusions about the results. Yearly PNAR and PGET measurement campaigns are planned to collect data for development of data analysis software. Logistical challenges include the placement of the NDA measurement station and the possible buffer storage area.

Additionally, an optional NDA measurement station will be located in the encapsulation plant. If required e.g. by the loss of CoK during transport, any assembly can be re-verified just before encapsulation. This measurement station will be located below the fuel handling cell. Unlike in the fuel shipping facility, these measurements must be done in dry conditions. Neither PNAR nor PGET have been tested in dry conditions yet. Especially for PNAR, the dry measurement setup must be different compared to wet measurements, where water is utilized to allow for neutron albedo. It is foreseen that water can be substituted by plastic compounds like polyethylene.

## 7. Conclusions

Spent fuel disposal in Finland is expected to start in mid-2020's. The national safeguard concept requires NDA of all fuel items prior disposal. Currently the plan is to use a combined PNAR-PGET measurement. PGET is a relatively new technology, while PNAR is still in a prototype phase. Practical testing and data collection using both instruments will be done to support the development. When disposal into the geological repository begins, a fully automated and remotely controllable measurement station will be utilized.

A PNAR prototype is being built by STUK. Preliminary laboratory testing of a mock-up PNAR pod showed that the detector behaves as expected. Additionally, gamma radiation was found not to affect the neutron detectors and an estimate for the dead time was found. The PNAR prototype is expected to be tested in the Olkiluoto spent fuel storage facility later this year.

## 8. References

- [1] International Atomic Energy Agency, *Technologies potentially useful for safeguarding geological repositories*, July 2017.
- [2] Tobin, S. J., Peura, P., Bélanger-Champagne, C., Moring, M., Dendooven, P., and Honkamaa, T., *Utility of including passive neutron albedo reactivity in an integrated nda system for encapsulation safeguards*, ESARDA BULLETIN 56 (June 2018), 12–18.
- [3] Gauld, I.C., Bowman, S.M., Murphy, B.D., Schwalbach, P., *Applications of ORIGEN to spent fuel safeguards and non-proliferation*, in: Proc. of INMM 47th Annual Meeting, July 16–20, 2006, Nashville, Tennessee.
- [4] Tobin, S. J., Peura, P., Honkamaa, T., Dendooven, P., Moring, M., and Belanger-Champagne, C. *Passive neutron albedo reactivity in the Finnish encapsulation context*. Säteilyturvakeskus, 2017. Available online: <http://www.julkari.fi/handle/10024/135811>.
- [5] Vaccaro, S., Gauld, I., Hu, J., Baere, P. D., Peterson, J., Schwalbach, P., Smejkal, A., Tomanin, A., Sjolund, A., Tobin, S., and Wiarda, D., *Advancing the fork detector for quantitative spent nuclear fuel verification*, Nuclear Instruments and Methods in Physics Research Section A: Accelerators, Spectrometers, Detectors and Associated Equipment 888 (2018), 202 – 217.

# Verifying PWR assemblies with rod cluster control assembly inserts using a DCVD

**Erik Branger, Sophie Grape, Peter Jansson,**

Uppsala University, Uppsala, Sweden  
E-mail: erik.branger@physics.uu.se

## **Abstract:**

*One of the instruments available to authority inspectors to measure and characterize the Cherenkov light emissions from irradiated nuclear fuel assemblies in wet storage is the Digital Cherenkov Viewing Device (DCVD). Based on the presence, characteristics and intensity of the Cherenkov light, the inspectors can verify that an assembly under study is not a dummy object, as well as perform partial defect verification of the assembly.*

*PWR assemblies are sometimes stored with a rod cluster control assembly (RCCA) inserted, which affects the Cherenkov light production and transport in the assembly. Such an insert will also block light from exiting the top of the fuel assembly, which will affect the light distribution and intensity of the Cherenkov light emissions. Whether or not this constitutes a problem when verifying the assemblies for gross or partial defects with a DCVD has not previously been investigated thoroughly.*

*In this work, the Cherenkov light intensity of a PWR 17x17 assembly with two different RCCA inserts were simulated and analysed, and compared to the Cherenkov light intensity from an assembly without an insert. For the studied assembly and insert types, the DCVD was found to be able to detect partial defects on the level of 50% in all studied cases with similar performance, though with a higher measurement uncertainty due to the reduced intensity when an RCCA insert is present. Consequently, for the studied assembly and insert types, assemblies with inserts can be verified with the same methodology as used for assemblies without inserts, with similar partial defect detection performance.*

*The simulation approach used also made it possible to investigate the minimum Cherenkov light intensity reduction resulting from partial defects of other levels than 50%, in the PWR 17x17 fuel assembly with and without RCCA inserts. The results for the simulations without an insert were in agreement with previous results, despite differences in substitution patterns, substitution materials, modeling software and analysis approach.*

**Keywords:** DCVD; partial defect verification; Rod cluster control assembly, Cherenkov light; Geant4

## **1. Introduction**

One of the many safeguards inspection tasks undertaken by authority inspectors is to measure irradiated nuclear fuel assemblies to verify that all nuclear material is present and accounted for. To aid the inspectors, a multitude of instruments has been developed. One of the instruments available is the Digital Cherenkov Viewing Device (DCVD), which measures the Cherenkov light produced in the water surrounding an assembly. The characteristics and quality of the Cherenkov light can be used to perform *gross defect verification*, verifying that the assembly under study is a spent nuclear fuel and not a dummy object. The DCVD is more frequently used for *partial defect verification*, verifying that 50% or more of the rods in an assembly have not been diverted. In such a verification, the Cherenkov light intensity emitted by the assembly is integrated to provide a value corresponding to the total light intensity of the assembly. Based on earlier simulations, it is estimated that a 50% substitution of irradiated fuel rods in an assembly with non-radioactive steel rods will decrease the total Cherenkov light intensity of the assembly by at least 30% [1]. Hence, by comparing the measured intensities to predicted ones, assembly intensities deviating more than 30% can be identified. Recent prediction

methods account for the irradiation history of the assembly, i.e. its cycle-wise burnup and cooling time, as well as the physical design of the assembly [2]. Any assembly having an intensity deviating more than 30% from expected is flagged as an outlier, and further investigations and measurements are called for to confirm whether the assembly is subject to a partial defect, or if the deviation is caused by something else such as erroneous declarations.

PWR assemblies in wet storage are in some cases stored with inserts, such as a rod cluster control assembly (RCCA) insert. For such storage cases, the neutron absorber rods of the RCCA are stored inserted into the guide tubes of PWR fuels. This can help save storage space, since no additional space is needed to store the RCCA. In addition, when inserted into a fuel assembly, the RCCA helps ensure sufficient limits to criticality. Before placing spent nuclear fuel in a difficult-to-access storage, the assemblies must be verified for partial defects [3]. It is reasonable to assume that the fuel assemblies will be verified in their current state, with any RCCA inserts still present during the verification measurements.

The presence of an RCCA is believed to affect the Cherenkov light in such fuel assemblies in two ways. Firstly, it prevents Cherenkov light from being created in the guide tubes, as the water inside the guide tubes is substituted by absorber material. Secondly, the RCCA will partly cover the top of the assembly, preventing a significant fraction of Cherenkov light from exiting the assembly to be detected.

Against this background, the objectives with this work is to i) verify the 30% intensity reduction limits of [1] for a 50% partial defect using different simulations codes and partial defect scenarios, since the limit in [1] is an estimate based on 30% rod substitutions. And ii) investigate how RCCA inserts affect the 30% intensity reduction limit assumed for a 50% partial defect level. As a consequence of the methodology chosen to investigate this, it becomes possible to also to study the minimum Cherenkov light reduction resulting from other partial defect levels, ranging from 0-100% substitution of the irradiated rods in an assembly.

## 2. Simulating the effect of top plates and inserts

To simulate DCVD images of PWR 17x17 assemblies, the three-step method of [4] has been used. These three steps are:

1. In the first step, the gamma emission spectrum of the assembly is simulated using ORIGEN-ARP [5]. In principle, beta decays may contribute, but their contribution has been shown in [2] to be minor and they were therefore neglected here.
2. In the second step, the gamma transport and interaction in a fuel assembly geometry is simulated using Geant4 [6], using a simulation toolkit based on [7]. In this process, Cherenkov light is created and transported to the top of the assembly. Once a Cherenkov photon reaches the top of the assembly, its position and direction is saved. The simulation model considers the full 3-D geometry and axial burnup distribution of the assembly.
3. In the third step, the saved photons are projected onto an imaging plane, using a pinhole camera model, to simulate a DCVD image.

Note that in the second step, the top plate, lifting handle and other structures at the assembly top are not included. The effect of these structures are instead included in the third step. This allows for the computationally expensive second step to be run only once, and different top plates and other structures at the assembly top can quickly be simulated in the third step. The effects of the top structures are studied by applying a mask, detailing where structure material is preventing the Cherenkov light from exiting the fuel assembly, and where light can pass through to be detected.

It was found in [4] that the burnup and cooling time of an assembly will not strongly influence the light distribution in a simulated image. For burnups of 10-40 MWd/kgU and cooling times of 1-40 years the total intensity of the simulated image will change at most 1% due to the changing light distribution. Consequently, in this work one PWR 17x17 assembly with a burnup of 40 MWd/kgU and a cooling time of 10 years was chosen, which is expected to be representative for assemblies with other burnups and cooling times. Using ORIGEN-ARP, the gamma spectrum of the assembly was simulated in the first step, and in the second step the gamma emissions from the fission products were simulated in a fuel geometry. Two different geometries were simulated: one where all guide tubes were filled with

water, corresponding to the absence of an insert, and one where all guide tubes were filled with In-Ag-Cd, corresponding to control rod material. Depending on the design of the RCCA, some or all guide tubes will contain absorber material. By applying the top plate mask to the simulations without control rods and with control rods, the extreme values are found for the Cherenkov light intensity in the simulated images. The case of some guide tubes containing control rods are expected to fall between these extreme values.

In the simulations of the second step, the light contribution from each rod in the assembly was stored separately. Thus, it was easy to include only the light contributions from selected rods in the final image. This facilitates studies of partial defect verification, where irradiated fuel rods are substituted by non-irradiated rods with similar density containing natural uranium, depleted uranium or low enriched uranium. Using this approach, it is thus possible to investigate the resulting total Cherenkov light intensity as a function of various rod substitution patterns, and to assess the DCVD capability to detect such substitutions.

### 2.1. Masks used

To obtain a mask representing the regions of the assembly covered by the top plate, a photograph of a PWR assembly top plate was used. Using the photograph, the covered regions could be manually identified and traced, and converted into a binary mask. The photograph and the resulting mask obtained is shown in Figure 1.

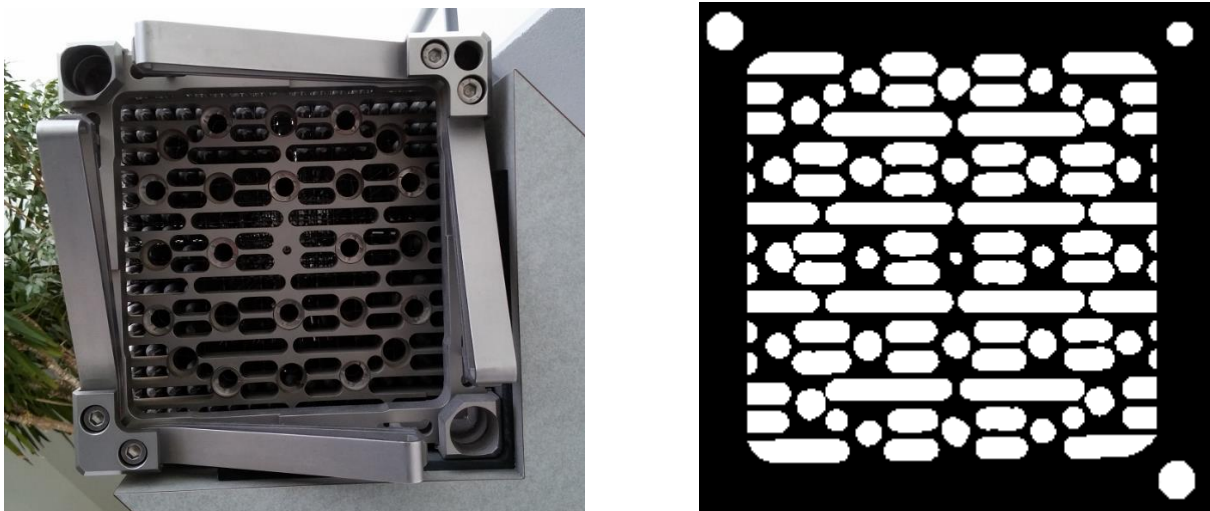


**Figure 1** Left: a photograph of the top structure of an assembly model. Right: the mask created based on the photograph, to indicate which regions are covered by the top plate and lifting handle.

Two different RCCA inserts were studied in this work. For the two RCCA inserts, DCVD images of assemblies with inserts were used to identify which additional regions were covered. This information was used to manually design a mask for assemblies with such inserts. One of the studied inserts had a comparatively large frame for holding the control rods, and consequently covered a substantial fraction of the assembly top, as seen to the left in Figure 2. This RCCA will be referred to as the “thick insert” in this work. The other studied insert had much finer features, and was relatively more open, as can be seen to the right in Figure 2. This insert will be referred to as the “thin insert” in this work. The thin insert is likely the insert described in [8].

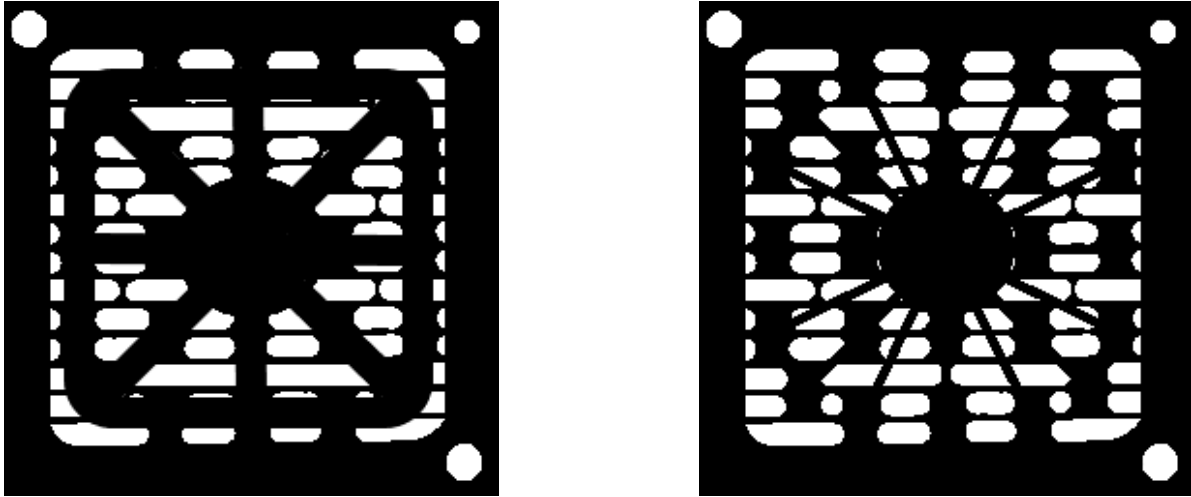


**Figure 2** Left: The top plate mask with the addition of the thick RCCA insert, covering a substantial part of the assembly top. Right: the top plate mask with the addition of a second, thin type of RCCA insert, having smaller features and covering relatively less compared to the mask on the left. A picture of this insert can be found in [8].

### 3. Sensitivity of DCVD verification of partial defect in assemblies with inserts

The effect on the total Cherenkov light intensity of substituting irradiated rods with non-radioactive rods is shown in

**Figure 3.** These values show the minimum Cherenkov light intensity reduction for partial defects of a given magnitude. In order to find the most challenging partial defect case to detect, the rods were substituted in an order reflecting their contribution to the total light intensity, starting with replacement of the least significant rod. The rod substitution pattern was estimated individually for the studied cases based on the identification of the fuel rods contributing the least to the total intensity, and the patterns thus differ between the cases. Hence,

Figure 1

Figure 3 shows the minimum intensity reduction in the total Cherenkov light intensity for various levels of partial defects, with replacement rods having similar gamma attenuation as the original rod and otherwise identical properties. Thus, for all other substitution scenarios, the intensity reduction will be larger and should be easier to detect.

As mentioned, there are different RCCA designs. In some cases, fuel assemblies with RCCA inserts may have control rods inserted into all guide tubes, while in other cases only some of the guide tubes have control rods while others are water-filled. To investigate the impact of this variability on the light intensity, the masks from Figure 2 were applied to the simulated fuel assembly with all control rods present, and to the fuel assembly with only water-filled rods in the guide tube positions. The results for an assembly with an RCCA insert having control rods at only some of the available positions are expected to fall between the results of these two cases. The results show that as the control rods are removed, the light reduction due to a partial defect increases slightly. For both types of RCCA inserts, the light reduction could be up to 1 percent unit higher if the control rods are missing, as compared to if all control rods are present, shown in figure Figure 3. Hence, the case of an RCCA with a full complement of control rods is the most challenging one, and can conservatively be used to estimate the minimum light intensity reduction that a partial defect in an assembly with a RCCA causes.

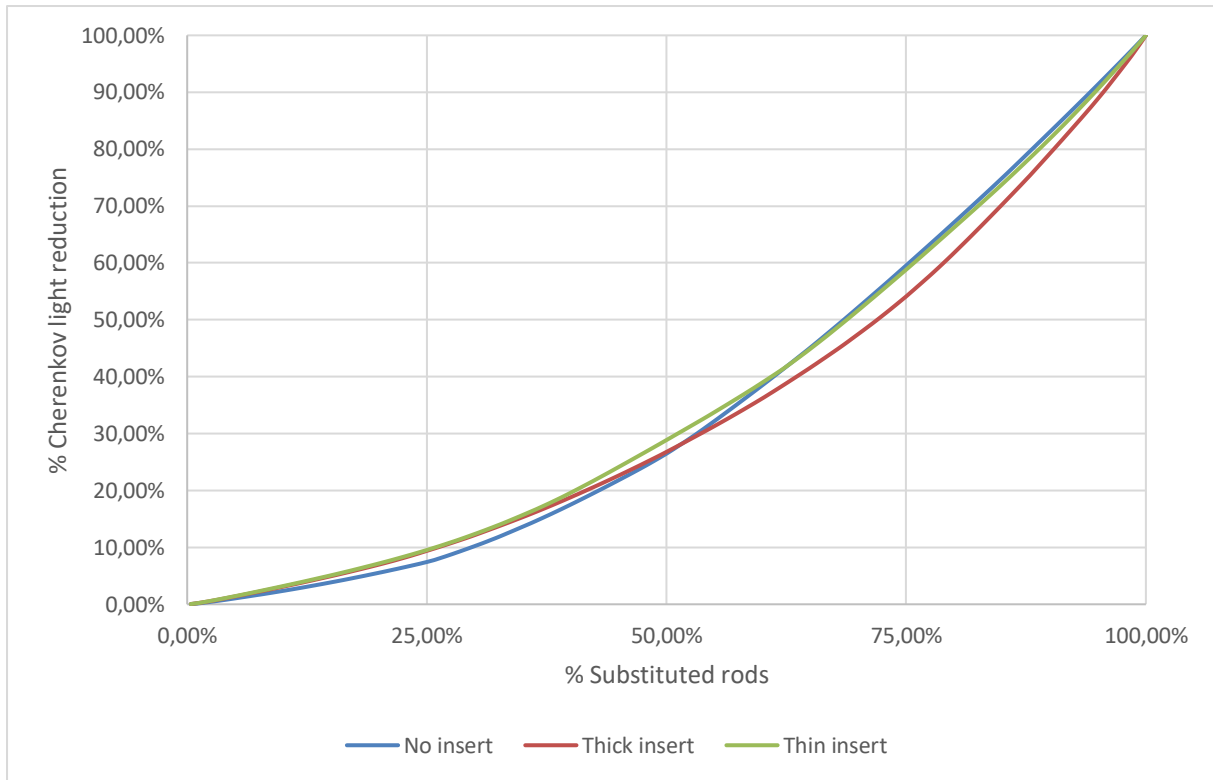


**Figure 3** Reduction in Cherenkov light intensity as a function of the fraction of rods replaced with non-radioactive substitutes. Rods contributing the least to the total intensity were removed first, and accordingly the rod substitution pattern differs in all three cases.

	No insert	Thick insert	Thin insert
Intensity reduction	27%	27%	29%

**Table 1** Cherenkov light intensity reduction at a 50% partial defect level for the studied partial defect cases.

In [1], partial defect detection using the DCVD was studied using simulations. Partial defect levels of 30% (where fuel rods were substituted with stainless steel rods) were studied, with resulting reductions in total Cherenkov light ranging from 15% to 40% depending on the diversion pattern. In [1], it was also estimated that a 50% partial defect would result in at least a 30% intensity reduction. For the case studied here, where partial defects on the level of 30% (where fuel rods are substituted with natural uranium, depleted uranium or low-enriched uranium) are modelled, it is found that the Cherenkov light intensity will be reduced by at least 10%. Partial defects on the level of 50% gives a Cherenkov light intensity reduction of at least 27%, as seen in Table 2 . Both studies hence give rather similar results, despite using different substitution patterns, substitution materials, modeling software and analysis approach.

For the cases of RCCA inserts, the DCVD verification methodology is found to actually be slightly more sensitive to a 50% partial defect, compared to the case of no insert, since the total Cherenkov light reduction is slightly higher. For the thick insert ( Figure 2 left), the intensity reduction is at least 27%, and for the thin insert ( Figure 2 right) the intensity reduction is at least 29%. Hence, for partial defects at the 50% level, the same partial defect detection criteria in terms of required light intensity reduction can be used for both the insert case as in the non-insert case.

The reason for the higher sensitivity in the RCCA case has to do with the light distribution in a DCVD image. Since the light emitted by the assembly is highly collimated, the central region vertically below the DCVD will be the brightest, and regions further away will appear dimmer. Consequently, in an image without an insert, a rod in the central region will contribute more, in relative terms, to the total

Cherenkov light intensity, as compared to a rod near the edge. In addition, since the lifting handle covers the edges, the intensity contribution from a rod at the edge is further suppressed. When an RCCA is present, it will cover large parts of the central region, and consequently suppress the intensity from the otherwise brightest regions at the center. As a result, the distribution of light over the measurement image will be more even, and the relative intensity contributions from the rods will vary less when an RCCA is present.

For the studied cases with and without an RCCA insert, the DCVD verification methodology is least sensitive to substitution of rods near the assembly edge. As noted above, this is a combined effect of the collimation and of the lifting handle obstructing the view. For the more centrally located rods, the contribution per rod to the total intensity varies significantly, depending on which parts that are covered by the RCCA insert. Thus, for partial defect on the order of 50%, the rod substitution pattern that is most challenging to detect using the DCVD, will differ depending on the presence or absence of an RCCA insert, and will be different for RCCA of different designs.

While the inserts do not significantly change the intensity reduction limits, they do change the total Cherenkov light intensity of the image. The simulated total intensity reduction for the two RCCA cases is compared to the non-insert case in

Table 2. As can be seen, the insert will significantly reduce the intensity of the Cherenkov light reaching the DCVD detector, and consequently the measurement uncertainties in the RCCA insert case will be higher, for otherwise identical assemblies. Thus, care must be taken when verifying low-intensity assemblies with inserts. Without inserts such assemblies may have a sufficiently high Cherenkov light intensity to be verified for a 50% partial defect level, but with an RCCA present, the intensity may be too low to allow for an accurate measurement, and thus an accurate verification. For the case of a RCCA insert with only a few control rods, the relative intensity is slightly higher, and can increase up to 40% for the thick insert and up to 50% for the thin insert (an increase with 3 percentage points in both cases). These values are similar enough that the assemblies can be readily compared, even if their RCCA inserts contain a different number of control rods, as long as the physical design of the top of the RCCA is the same. The main cause of the change in Cherenkov light intensity in the RCCA case is that more parts of the top of the assembly are covered, the effect of having RCCA inserts with differing number of control rods is less significant.

	No insert	Thick insert	Thin insert
Relative intensity	100%	37%	47%

**Table 2** Relative measured Cherenkov light intensity for an assembly without an RCCA insert and for the same assembly with a thick respectively a thin insert present. The values are scaled so that the intensity of the no-insert case is 100%.

#### 4. Conclusions and outlook

PWR assemblies in wet storage can be stored with an RCCA inserted, which will alter the characteristics and detected total intensity of the Cherenkov light produced inside the assembly. This work has investigated the partial defect detection capability of the DCVD for one PWR 17x17 fuel assembly. A regular fuel assembly has been modelled, as well as the same fuel assembly with two different kinds of RCCA inserts. The minimum expected reduction in total Cherenkov light has then been modelled for partial defects ranging from 0% to 100% for the fuel assembly without as well as with RCCA inserts. The substitution scenario considered is that the irradiated rods are replaced by non-irradiated rods, having identical gamma attenuation properties. Such replacement rods could for example be made of low-enriched uranium, natural uranium or depleted uranium.

The simulation results indicate that the studied partial defect scenarios affects assemblies with and without RCCA inserts in a similar way. Consequently, the currently adopted partial defect verification method using the DCVD can be used also to verify partial defects also in the case of assemblies with inserts, with similar partial defect detection performance. Furthermore, the previously established detection requirement of a 30% reduction in the measured Cherenkov light intensity (for a partial defect level of 50%) compared to the predicted one, can be applied also to the RCCA insert cases.

Some RCCA inserts do not have control rods in all available positions, but the simulation results show that this has a comparatively small effect on the total Cherenkov light intensity, and does not pose any additional problems to the verification methodology.

For the studied PWR 17x17 assembly, the rods closest to the edges contribute the least to the detected Cherenkov light intensity. This is due to the collimation of the Cherenkov light, coupled with the positioning of the DCVD during a measurement, and due to the lifting handle covering rod positions around the edges of the fuel assembly. It may be possible to compensate for the collimation by performing measurements with the DCVD aligned over the edges of the assembly. Alternatively, it may be possible to model the effect of the collimation on the light distribution in an image, and use that information to compensate for the collimation effect. Both these procedures could potentially increase the DCVD verification methodology sensitivity to rod substitution near the assembly edges. However, care must be taken to consider Cherenkov light produced in an assembly due to radiation originating in neighbouring assemblies, since such radiation will not travel far to reach a neighbouring assembly, and will hence predominately create Cherenkov light near the edges of an assembly.

In addition to RCCA inserts, assemblies may be stored with other inserts, such as a flow stoppers. The methodology developed here could be applied to assess how such an insert affects the partial defect sensitivity of the DCVD verification methodology. Ideally, all types of inserts that frequently occur should be investigated in this way, to ensure that the standard DCVD verification procedure will accurately verify such assemblies.

## 5. Acknowledgements

The work presented in this contribution has been accepted for publication in the ESARDA Bulletin n. 58 (June 2019), ISSN 0392-3029. This work was supported by the Swedish Radiation Safety Authority (SSM), under contract SSM2012-2750, and SSM2017-5979. The computations were performed on resources provided by SNIC through Uppsala Multidisciplinary Centre for Advanced Computational Science (UPPMAX) under project p2007011.

## 6. References

- [1] J.D. Chen et al., "Partial defect detection in LWR spent fuel using a Digital Cherenkov Viewing," *Institute of Nuclear Materials Management 50th annual meeting*, 2009.
- [2] E. Branger, S. Grape, S. Jacobsson Svärd and P. Jansson, "Comparison of prediction models for Cherenkov light emissions from nuclear fuel assemblies," *Journal of instrumentation*, 2017.
- [3] International Atomic Energy Agency, "Special Criteria for Difficult-to-Access Fuel Items. SG-GC-Annex-04," Vienna, Austria, 2009.
- [4] E. Branger, S. Grape, P. Jansson and S. Jacobsson Svärd, "On the inclusion of light transport in prediction tools for Cherenkov light intensity assessment of irradiated nuclear fuel assemblies," *Journal of Instrumentation*, vol. 14, 2019.
- [5] S. Bowman, L. Leal, O. Hermann and C. Parks, "ORIGEN-ARP, a fast and easy to use source term generation tool," *Journal of Nuclear Science and Technology*, vol. 37, pp. 575-579, 2000.
- [6] Agostinelli, S, et al (the Geant4 collaboration), "Geant4 - a simulation toolkit," *Nuclear Inst. and Meth. in Physics Research Section A: Accelerators, Spectrometers, Detectors and Associated Equipment*, Volume 506, Issue 3, 1 July 2003, Pages 250-303.
- [7] S. Grape, S. Jacobsson Svärd and B. Lindberg, "Verifying nuclear fuel assemblies in wet storage on a partial defect level: A software simulation tool for evaluating the capabilities of the Digital Cherenkov Viewing Device," *Nuclear inst. and Meth. A*, Volume 698, 11 January 2013, Pages 66-71, ISSN 0168-9002, 10.1016/j.nima.2012.09.048.
- [8] Westinghouse Nuclear, "Enhanced Performance – Rod Cluster Control Assemblies (EP-RCCAs). Data sheet," 10 2014. [Online]. Available: <http://www.westinghousenuclear.com/Portals/0/flysheets/NF-FE-0047%20Enhanced%20Performance%20RCCAs.pdf>. [Accessed 04 04 2019].

# Determination of $^{239}\text{Pu}$ content in spent fuel with the SINRD technique by using artificial and natural neural networks

**Alessandro Borella<sup>1</sup>, Riccardo Rossa<sup>1</sup>, Hugo Zaioun<sup>1,2</sup>**

<sup>1</sup>SCK•CEN, Boeretang 200, B2400 Mol, Belgium

<sup>2</sup>IMT Atlantique, Campus de Nantes, rue Alfred Kastler 4, 44307 Nantes, France

Email: aborella@sckcen.be

## **Abstract:**

*In the last years, a database of simulated spent fuel observables was developed at SCK•CEN by combining the results of depletion-evolution codes and the responses of several detectors obtained by Monte Carlo models. Given the large amount of generated data we propose an approach based on Artificial Neural Networks, by using the MATLAB toolbox.*

*In this paper we first describe an analysis tool that was developed to easily handle the large number of options and data sets that are available. The tool was then applied to the simulated Self-Interrogation Neutron Resonance Densitometry observables with the aim to quantify the  $^{239}\text{Pu}$  content in spent fuel. In view of a realistic application of the method, the number of data in the training and validation sets was limited to 20 spent fuel assemblies; the obtained performance when using randomly selected spent fuel assembly was compared with the one obtained when the spent fuel assemblies were selected by expert judgement. The  $^{239}\text{Pu}$  in the testing data set was in very good agreement with the nominal value; the average deviation between the nominal  $^{239}\text{Pu}$  content and the calculated one was 0.2% with a standard deviation of 3.5% and a maximum deviation of 10%.*

*It was found that the selection of spent fuel assemblies based on expert judgement results in better performances and therefore speeds up the data analysis when compared to a pure random selection of the data; hence the term natural is present in the title of the paper.*

**Keywords:** Spent Fuel; Non Destructive Analysis observables; Artificial neural networks; Self-Interrogation Neutron Resonance Densitometry; Large Data sets

## **1. Introduction**

Non-destructive assay (NDA) of spent fuel assemblies (SFA), either for safeguards verification purposes or for safety aspects related to nuclear fuel cycle, relies often on the detection of neutron and gamma radiation spontaneously emitted by the spent fuel [1]. Gamma radiation is mainly emitted by fission products and therefore its measurement does not represent a direct assay of the quantity of fissile material present in the SFA. Neutron radiation is originating mainly from spontaneous fission decay and  $\alpha$ -decay via ( $\alpha$ ,n) reactions on oxygen isotopes. The decay of actinides such as Cm isotopes represents the main source of such neutron radiation which can then undergo subsequent multiplication in the fissile material of the fuel. Therefore, also the observables associated to neutron measurements on SFA do not represent a direct assay of the quantity of fissile material present in the SFA, unless one is able to determine the multiplication and relate that to the residual fissile mass [2].

In this framework, and in relation to increased verification needs associated to the imminent start of operation of geological repositories[3,4], R&D on NDA intensified in the last decade [5,6,7,8,9]. One of the techniques that were studied is the Self-Interrogation Neutron Resonance Densitometry (SINRD) [10,11]. The observables associated to this technique are directly related to the quantity of  $^{239}\text{Pu}$  in the fuel and therefore have the potential to provide means for a direct quantification of the residual amount  $^{239}\text{Pu}$  in a SFA.

The use of the SINRD technique and the data analysis of the associated observables by means of artificial neural network (ANN) [12,13] is described in the paper.

## 2. Self-Interrogation Neutron Resonance Densitometry observables

The SINRD technique [10] is a NDA technique for the direct quantification of  $^{239}\text{Pu}$ . The total neutron cross-section of  $^{239}\text{Pu}$  shows a strong resonance around 0.3 eV and the attenuation of the neutron flux around the 0.3 eV energy region is used to directly quantify the  $^{239}\text{Pu}$  mass. The passive neutron emission from spent fuel is measured with fission chambers bare or wrapped with different absorbers as follows:

- Cd wrapped  $^{235}\text{U}$  fission chamber, mainly sensitive to thermal neutrons
- Bare  $^{238}\text{U}$  fission chamber, mainly sensitive to fast neutrons
- $^{239}\text{Pu}$  fission chamber covered by Gd foil, sensitive to neutrons with energy > 0.1 eV
- $^{239}\text{Pu}$  fission chamber covered by Cd foil, sensitive to neutrons with energy > 1 eV

The observables of interest are the SINRD signature  $R_{\text{SI}}$ , defined as the ratio between the neutron count by the  $^{238}\text{U}$  fission chamber ( $C_{\text{fast}}$ ) and the count differences in the Gd and Cd wrapped  $^{239}\text{Pu}$  loaded fission chamber ( $C_{\text{Gd}} - C_{\text{Cd}}$ ); the ratio between  $C_{\text{fast}}$  and a  $^{235}\text{U}$  Cd wrapped fission chamber ( $C_{\text{th}}$ ). The use of  $^{239}\text{Pu}$  fission chambers enhances the sensitivity of the technique to  $^{239}\text{Pu}$  content [11].

The two observables were determined by means of Monte Carlo simulations with the code MCNPX 2.7.0 [14], the radionuclide composition of the fuel was taken from the spent fuel library developed at SCK•CEN [15,16,17]. Two observables,  $R_{\text{SI}}$  and  $C_{\text{fast}}/C_{\text{th}}$ , were determined for a total of 2940 cases of the spent fuel library [18].

The obtained results [7] for 17x17 PWR SFA indicated that SINRD can only be applied in dry conditions and that calibration curves can be determined that allow the quantification of  $^{239}\text{Pu}$  provided that initial enrichment (IE) is known.

Figure 1 shows the  $R_{\text{SI}}$  observable as a function of  $^{239}\text{Pu}$  content for different values of IE and BU. If the burnup (BU) is above 30 GWd/t<sub>HM</sub> the data cluster around an almost straight line and there is a strong correlation between  $R_{\text{SI}}$  and  $^{239}\text{Pu}$  content irrespective of the IE. This is due to the fact that at lower BU values the presence of  $^{235}\text{U}$  interferes due to the presence of a weak resonance at about the same energy as the one of  $^{239}\text{Pu}$ .

The ratio  $C_{\text{fast}}/C_{\text{th}}$ , shown in Fig. 2, can be used to determine the IE if the BU is known and to account for this interference. The ratio  $R_{\text{SI}}$  is almost independent from the cooling time (CT) up to CT of 300 years, while the ratio  $C_{\text{fast}}/C_{\text{th}}$  starts to decrease from not less than 10 years (Fig. 3).

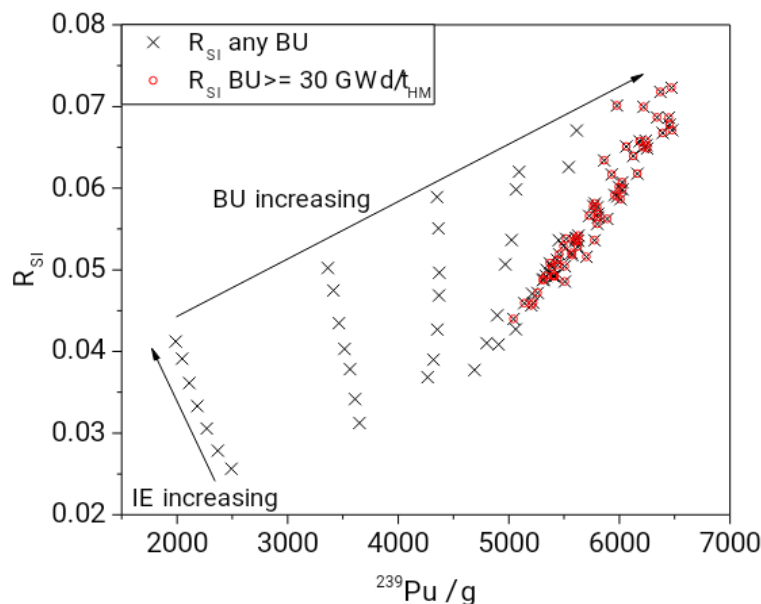


**Figure 1:**  $R_{\text{SI}}$  as function of  $^{239}\text{Pu}$  amount for any BU values and for BU values of at least 30 GWd/t<sub>HM</sub>. CT was 5 years and IE between 2% and 5%.

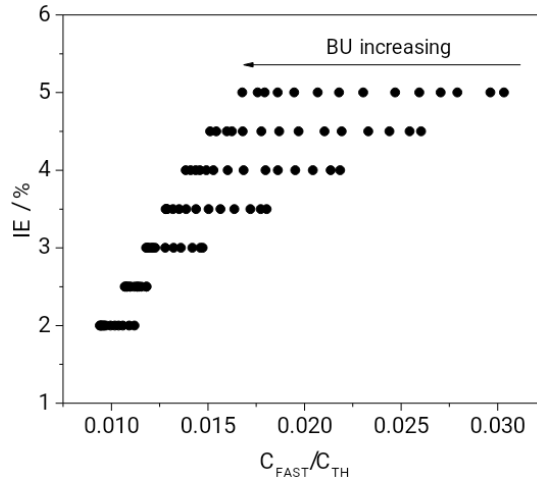


Figure 2: IE as function of  $C_{fast}/C_{th}$   $^{239}\text{Pu}$  amount for any BU values and a CT of 5 years.

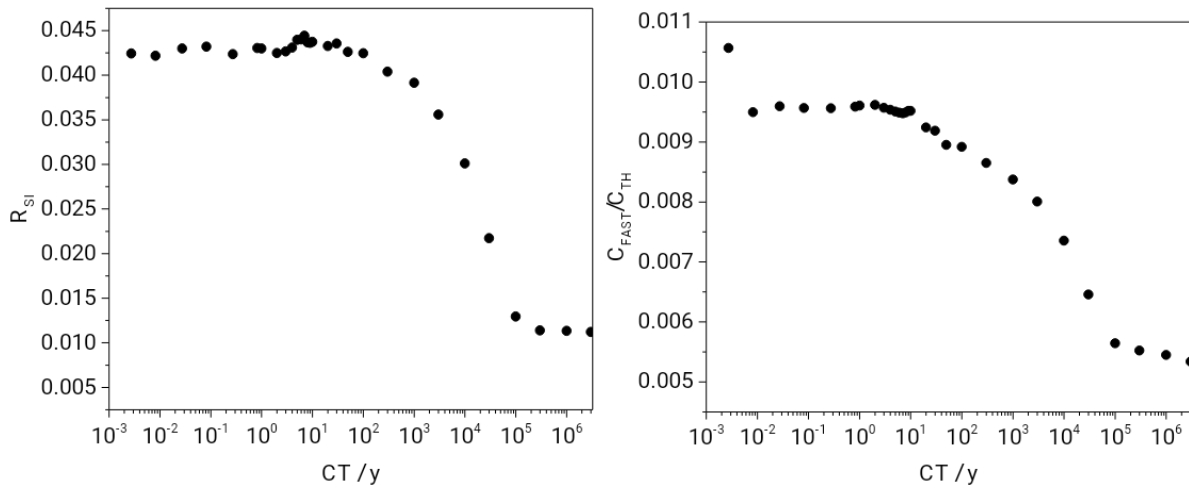


Figure 3:  $R_{SI}$  and  $C_{fast}/C_{th}$  as a function of CT. The data are for an IE of 2% and BU of 30 GWd/t<sub>HM</sub>.

### 3. Data analysis with artificial neural networks

#### 3.1. Artificial Neural Networks

Given the fact that we could not determine a satisfactory approach with standard means of analysis, we decided to investigate the use of artificial neural network [12] as mean to determine the residual  $^{239}\text{Pu}$  quantity given the two observables  $R_{SI}$  and  $C_{fast}/C_{th}$ .

An ANN can be described as a network in which each node  $i$  processes the  $n$  input units it is connected to through a transfer (or activation) function  $f_i$ :

$$y_i = f_i\left(\sum_{j=1}^n (w_{ij} \cdot x_j - \theta_i)\right) \quad (1)$$

where  $y_i$  is the output of neuron  $i$ ,  $x_j$  is the  $j$ -th input to node  $i$ ,  $w_{ij}$  is the weight of the connection between input  $j$  and node  $i$ , and  $\theta_i$  is the threshold (or bias) of the node. While each neuron  $i$  can have its own transfer function in our implementation [13,19] the same transfer function was used for all the neurons in a given layer.

The database of simulated observables and spent fuel characteristics is divided in three sets, corresponding to training, validation and testing. The training set is used by the training algorithm to adapt the weights and biases according to it, therefore it is the most impactful set. The weights and biases are then fine-tuned with the validation set. The testing set is used to determine the accuracy of the trained ANN and to evaluate its capability to predict results from data it was not trained with.

### 3.2. Data analysis of SINRD signatures

We considered only SINRD observables for cases with CT of 5 years, given the weak dependence on the CT and the fact that the CT is usually a well-known parameter. The dataset is therefore reduced to 98 entries associated to 14 values of BU and 7 IE.

The size of the data set is relatively small when compared to the large data sets that are usually used when training an ANN; however, this is in line with the fact that, in view of a deployment of the ANN with experimental data, the data set would also not be large when considering realistic combinations of IE and BU values.

Starting from Eq. (1) we estimated the number of parameters of the ANN that need to be estimated during the training procedure as a function of the network structure. The results are shown in Table 1 and indicate the number  $n$  of parameters as a function of the number of nodes  $I$  in the input layer, the number of nodes  $H_k$  in the hidden layer number  $k$ , and the number of nodes  $O$  in the output layer. Different configurations with  $k$  between one and three were considered with a minimum level of complexity, in view of the limited availability of training data.

In this work we use an architecture where the two observables enter the input layer, and the  $^{239}\text{Pu}$  amount is the only quantity in the output layer. Therefore for our case  $I=2$ , representing the two SINRD observables, and  $O=1$ , representing the  $^{239}\text{Pu}$  amount.

In practice, the data processing with ANN consists in identifying a ANN configuration that describes the dependence of  $^{239}\text{Pu}$  varies in the space of the variable  $C_{\text{fast}}/C_{\text{th}}$  and  $R_{\text{SI}}$ .

I	H <sub>1</sub>	H <sub>2</sub>	H <sub>3</sub>	O	N
2	3			1	13
2	2	2		1	15
2	2	2	2	1	21

**Table 1:** Number  $n$  of the ANN parameters to be determined as a function of the network architecture.

For a given ANN configuration, there is a level of arbitrariness when choosing the size of training, testing and validation. In our case, given the limited size of the whole database and the limited possibilities to carry out actual measurement we decided to limit the size of the training and validation set to 10 entries each; the rest of the database was used for testing.

Since the number  $n$  of the network parameters should not exceed the size of the training and validation data set we opted for a network two hidden layers with two nodes each where considered. The choice of two layers stems from previous experience where we learned that better performance can be achieved when the number of layers is increased [13,19].

The analysis of the data was carried with a tool developed in MATLAB [20,21]; the tool allows to carry out the analysis through a graphical user interface (GUI); through this GUI the user can import data from a text file, filter the data based on certain criteria, define the network architecture and several optimization options such as internal processing functions, performance function and training function [19]. The results and network configuration can be exported. The tool allows training with random or fixed initial values for weights and offset. Also the entries of the database to be used for training, validation can be chosen randomly by the programme or by the user via flags associated to entries in the database.

Our analysis was carried out with the following configuration with which we observed better results:

- The function *mapminmax*, which maps all the values of a column linearly between -1 and 1, was applied for internal processing on input and output variables.
- the optimization of the ANN through the quantity *mse*

$$mse = \frac{1}{N} \sum_{k=1}^N (A_{k,calc} - A_k)^2 \quad (2)$$

Where  $A_{k,calc}$  is the value of the parameter as determined by the ANN in the output layer,  $A_k$  is the nominal value of the parameter.

- The maximum number of epochs was set to  $10^5$  and the maximum execution time to 1,000 seconds.  
An epoch is one run of the training algorithm: after each epoch, all the weights and biases of all the neurons are modified (if needed) according to the training algorithm.

### 3.3. Results

Initially we kept random initial values for weights and offset as well as the entries of the database to be used for training, testing and validation. We observed large variation in terms of *mse* as well as number of epochs before the timing was stopped. In addition, the obtained *mse* and the corresponding deviations between the predicted  $^{239}\text{Pu}$  mass and the value in the data base were not satisfactory.

We observed that the choice of initial values for weights and offset can affect significantly the final *mse* as well as the choice of the entries for training and testing; the changes can be several orders of magnitude in the *mse*. Since weights and offset define the ANN to be trained, we focussed on the determination of the initial entries for training and testing that gave the best results. The training was repeated several times to try different initial values for weights and offset.

Assuming that the assignment of an entry to the validation or training data set does not matter, with 20 entries in 98 this would correspond to

$$\binom{n}{k} = \frac{n!}{k!(n-k)!} = \frac{98!}{20!(78)!} \sim 3 \times 10^{20}$$

combinations.

It is evidently impossible to identify the configuration with the minimum *mse* based on a random or sequential selection of the combinations. In this work, we then tried to identify the entries of the database based on how the  $^{239}\text{Pu}$  varies in the space of the variable  $C_{\text{fast}}/C_{\text{th}}$  and  $R_{\text{SI}}$ . This is shown in Fig. 4.

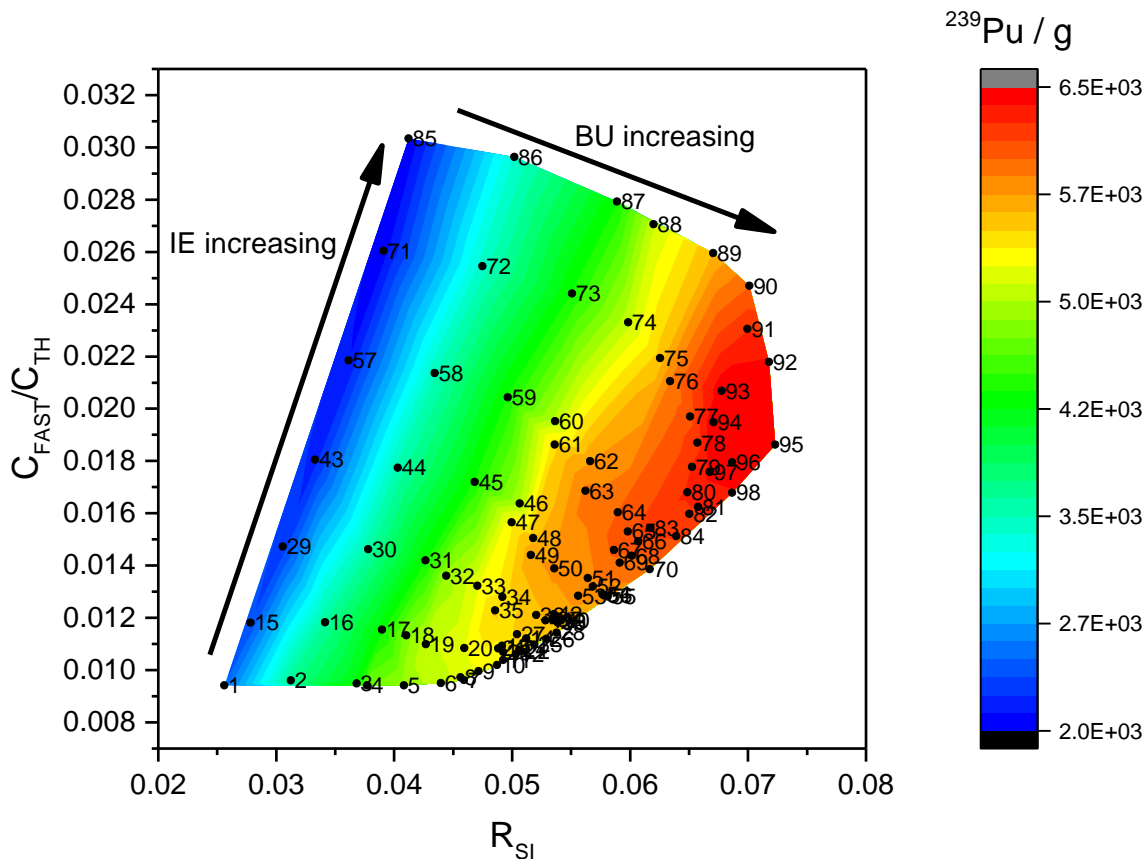


**Figure 4:**  $^{239}\text{Pu}$  amount as a function of  $R_{\text{SI}}$  and  $C_{\text{fast}}/C_{\text{th}}$ . The number indicate the corresponding entry in the considered data set.

The data in Fig. 4 reveal that  $C_{fast}/C_{th}$  and RSI lie in specific domain. As explained before, we are looking for a ANN configuration that describes the dependence of  $^{239}\text{Pu}$  in the space of the variables  $C_{fast}/C_{th}$  and RSI. Given the results in Fig. 4, it was logical to assume that entries to use in the training and validation data set should lie at the boundary of the domain of  $C_{fast}/C_{th}$  and SINRD can have values. In addition, it seemed logical that a sufficient number of them should lie inside the area in order to allow to describe the shape over the domain of  $C_{fast}/C_{th}$  and RSI.

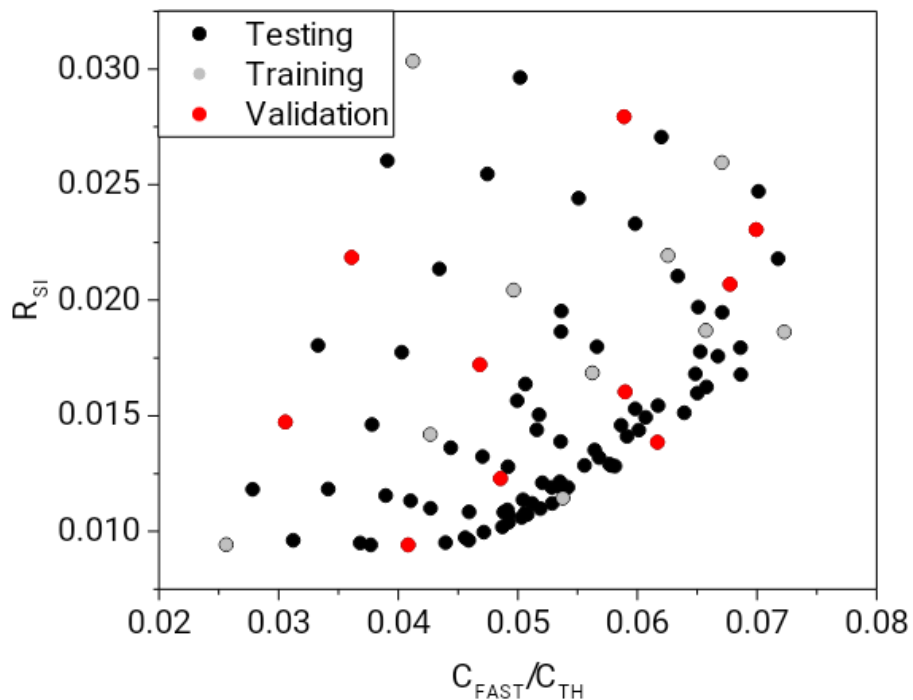
Based on these criteria, we defined the following entries for the training validation data set as indicated in the Table 2 and Fig. 5. It is worth to comment that the entries indicated in italic, although present in the spent fuel library, are not realistic since the BU is too high for the chosen IE.

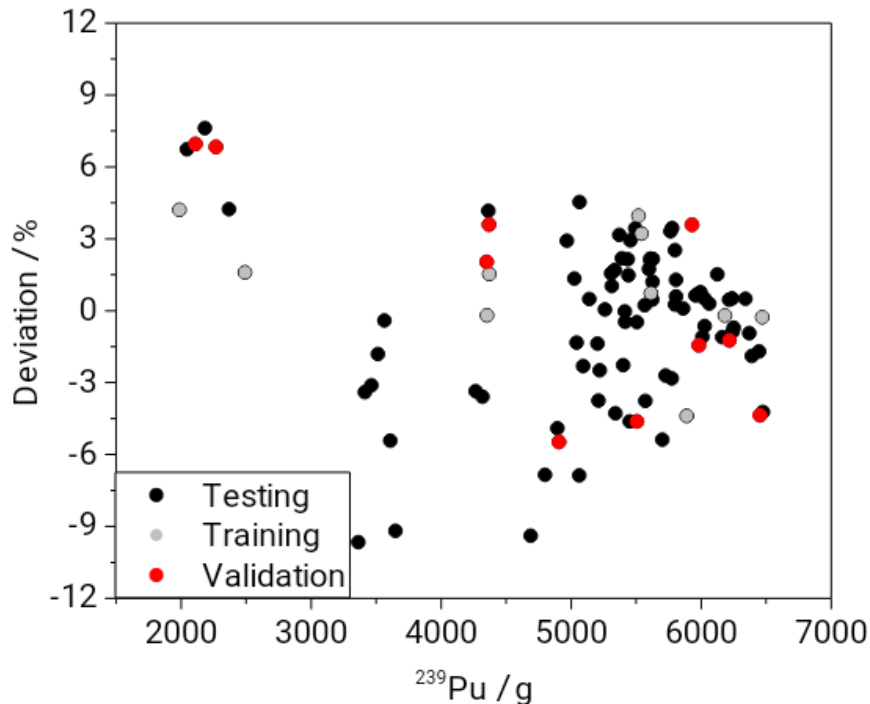
For these entries we obtained a value of  $mse$  that was  $2.3 \times 10^4$  with a square root corresponding to a deviation between declared and predicted of  $^{239}\text{Pu}$  about 150 g. Changing the training function between *trainlm* and *trainbr* did not seem to affect the results. *trainlm* and *trainbr* differ in the way they optimize the weight and bias [21].

The deviation between the predicted  $^{239}\text{Pu}$  mass and the value in the data base is shown in Fig. 6, where the entries used for training, validation and testing are shown with different colours.

ID	Flag	BU	IE	CT	ID	Flag	BU	IE	CT
1	T	5	2	5	5	V	25	2	5
28	T	70	2.5	5	29	V	5	3	5
31	T	15	3	5	35	V	35	3	5
59	T	15	4	5	45	V	15	3.5	5
63	T	35	4	5	57	V	5	4	5
75	T	25	4.5	5	64	V	40	4	5
78	T	40	4.5	5	70	V	70	4	5
85	T	5	5	5	87	V	15	5	5
89	T	25	5	5	91	V	35	5	5
95	T	55	5	5	93	V	45	5	5

Table 2: Selected entries for training (T) and validation (V) data sets.



**Figure 5:** Training, validation and testing data sets.**Figure 6:** Percentage deviation between predicted and nominal  $^{239}\text{Pu}$  amount for training, validation and testing data sets.

The  $^{239}\text{Pu}$  in the testing data set was in very good agreement with the nominal value; the average deviation between the nominal  $^{239}\text{Pu}$  content and the calculated one was 0.2% with a standard deviation of 3.5% and a maximum deviation of -10%.

#### 4. Conclusions

We described a data analysis approach based on artificial neural networks (ANN) to process the observables associated to the SINRD technique. The SINRD observables were obtained with Monte Carlo based simulations using fuel composition from a spent fuel library and represent a data set of nearly 3,000 entries.

Given the fact that the SINRD observables are not depending on cooling time, we restricted the analysis to the 98 entries with a cooling time of 5 years. The obtained results reveal that very good performances could be achieved by using 20 human selected entries for training and validation of the ANN. The average deviation between the nominal  $^{239}\text{Pu}$  content and the calculated one was 0.2% with a standard deviation of 3.5% and a maximum deviation of 10%.

The selection of spent fuel assemblies based on expert judgement is not necessarily the best, in terms of ANN precision, but allowed to resolve quickly a problem that would have not been possible to solve by selecting on a randomly the database entries for training and validation.

Future work will focus on possibly reducing even further the size of the data base for training and validation and limiting only on realistic cases of the library of observables. In addition, we would like to study a different form of the performance function for example accounting for the relative deviations rather than absolute deviations.

## Acknowledgements

The authors would like to acknowledge that this manuscript has been published in the ESARDA Bulletin number 58.

## References

- [1] D. Reilly, N. Ensslin, H. Smith Jr. and S. Kreiner, *Passive Nondestructive Assay of Nuclear Materials*, NUREG/CR-5550, LA-UR-90-732, 1991
- [2] H. Würz, *A Simple Non-Destructive Measurement System For Spent Fuel Management*, Nuclear Technology 95 (1991) pp 193-206
- [3] Park W. S., et al., 2014. "Safeguards by design at the encapsulation plant in Finland". Proceedings of the 2014 IAEA safeguards symposium.
- [4] European Council Decision 2006/976/Euratom of 19 December 2006
- [5] *Coordinated Technical Research Meeting on Spent Fuel Verification Methods*, IAEA March 3-6 2003
- [6] A. Borella, et al., *Advances in the Development of a Spent Fuel Measurement Device in Belgian Nuclear Power Plants.*- In: Symposium on International Safeguards, Linking Strategy, Implementation and People, Book of Abstracts, Presentations and Papers, 2014, IAEA, Vienna, Austria, p. 272
- [7] R. Rossa, *Advanced non-destructive methods for criticality safety and safeguards of used nuclear fuel*, PhD thesis at Université libre de Bruxelles, September 2016.
- [8] S. Tobin, H. Menlove, M. Swinhoe, M. Schear, *Next Generation Safeguards Initiative research to determine the Pu mass in spent fuel assemblies: Purpose, approach, constraints, implementation, and calibration*, Nuclear Instruments & Methods In Physics Research Section A, 2011, doi 10.1016/j.nima.2010.09.064
- [9] T. White, et al., 2018. "Application of Passive Gamma Emission Tomography (PGET) to the inspection of spent nuclear fuel". Proceedings of the 2018 INMM annual meeting.
- [10] H. Menlove, C. Tesche, M. Thorpe and B. Walton, *A Resonance Self-Indication Technique for Isotopic Assay of Fissile Materials*, Nuclear application Vol. 6 April 1969 pp 401-408
- [11] Rossa, R., Borella, A. & van der Meer, K. *Investigation of the Self-Interrogation Neutron Resonance Densitometry applied to spent fuel using Monte Carlo simulations* Jan 2015 In : Annals of Nuclear Energy. 75, p. 176-183
- [12] Leshno, M., Lin, V. Y., Pinkus, A., & Schocken, S., *Multilayer feedforward networks with a nonpolynomial activation function can approximate any function*, Neural networks, 6(6):861-867, 1993.
- [13] Borella, A., Rossa, R. & Turcanu, C, *Signatures from the spent fuel: simulations and interpretation of the data with neural network analysis*, 1 Dec 2017 In : ESARDA Bulletin. p. 29-38 10 p.
- [14] D.B. Pelowitz, Ed., "MCNPX Users Manual Version 2.7.0"LA-CP-11-00438 (2011).
- [15] R. Rossa., et al., *Development of a reference spent fuel library of 17x17 PWR fuel assemblies*, ESARDA BULLETIN, No. 50, December 2013
- [16] A. Borella, et al., *Extension of the SCK•CEN spent fuel inventory library*, 37th ESARDA Annual Meeting, 2015

[17] A. Borella, M. Gad, R. Rossa, K. van der Meer, *Sensitivity Studies on the Neutron Emission of Spent Nuclear Fuel by Means of the Origen-ARP Code*, In: Proceeding of the 55th INMM Annual Meeting, Atlanta, Georgia, United States, July 2014.

[18] Borella, A., Rossa, R. & van der Meer, K. *Simulated observables for spent fuel non-destructive assay* 22 Jul 2018 Proceedings of the 2018 INMM annual meeting

[19] Zaïoun, H. *Analysis and interpretation of spent fuel signatures with an artificial neural network: Improvement of the network, based on the previous work, and development of a graphical user interface* 30 Mar 2018 Studiecentrum voor Kernenergie. 25 p. (SCK•CEN Reports; no. I-0687)

[20] <https://www.mathworks.com/help/matlab/>

[21] Matlab, Neural Network Toolbox Documentation, <https://www.mathworks.com/help/deeplearning/>

# **Session 3:**

# **Nuclear Forensics**

# Nuclear Archaeology: Reconstructing Reactor Histories From Reprocessing Waste

Antonio Figueroa, Malte Göttsche

Aachen Institute for Advanced Study in Computational Engineering Science  
Physikalisches Institut III B  
RWTH Aachen, Germany  
Schinkelstr. 2a, 52062 Aachen, Germany  
E-mail: [figueroa@ices.rwth-aachen.de](mailto:figueroa@ices.rwth-aachen.de), [goettsche@ices.rwth-aachen.de](mailto:goettsche@ices.rwth-aachen.de)

## **Abstract:**

Nuclear archaeology is a field dedicated to the reconstruction and quantification of the past production of weapons-usable fissile materials. As part of related research efforts, we examine the possibilities and limitations of exploiting measurements of high level waste to deduce parameters related to the operational history of reactors such as burnup. For the first stage of this project, we use high fidelity forward calculations to estimate spent fuel compositions, and develop a surrogate model which can be used as a computationally less expensive way to map combinations of input parameters to fuel compositions. This model will give us a better understanding of the challenges involved in solving the inverse problem of deducing the reactor history from waste. A promising method to solve this inverse problem may be Bayesian inference, where prior existing information (e.g. a declaration by a state) can be taken into account, and waste measurements would be used to update this knowledge. This way, measurements may confirm the existing information, make it more accurate, or identify inconsistencies which may indicate cheating. For a proof of concept of the methodology, we examine simple scenarios and try to determine a few reactor parameters, given a hypothetical incomplete declaration by a state and a simulated measurement of the waste isotopics.

**Keywords:** Disarmament, Forensics, Verification, Bayesian Inference, Nuclear Archaeology

## **1. Introduction**

While there is extensive experience in verifying both the correctness and completeness of nuclear material declarations issued by non-weapon states that are members of the Non-Proliferation Treaty, there is a lack of methods to verify nuclear material “baseline” declarations, i.e. the first verified declaration a state makes upon entering an agreement. A solid understanding of fissile-material holdings is needed to achieve a meaningful degree of predictability and irreversibility of future arms-control initiatives. Speculations about unaccounted fissile-material stockpiles, possibly equivalent to hundreds of nuclear weapons, could make progress in this area very difficult [1].

Most large-scale fissile-material production programs were driven by a sense of urgency and typically shrouded in secrecy. It is generally believed that accounting for these military operations was poor. The fissile material production uncertainty is very large, and even states themselves have had difficulty reconciling production records with physical inventories. In the United States, for example, estimated plutonium acquisitions exceeded the actual inventory by 2.4 tons, but it is not clear if this material ever existed [2].

In addition to direct data on produced fissile materials, such records would contain operational information of the nuclear facilities. For reactors, in addition to reactor and fuel designs, this would include data on reactor power, fuel burnup, and cooling time (which refer to the time passed since a specific campaign). We call these data operational parameters.

In order to obtain more accurate plutonium estimates, a first approach in reconstructing the production history is performing reactor simulations with more accurate codes than those used decades ago. One

such code is SERPENT 2 [3]. Such codes would take the operational parameters as input, and produce the isotopic composition of the discharged fuel – including plutonium, but also fission products and minor actinides – as output.

In addition, measurements in shut-down facilities can be taken to obtain complementary data. For example, research has been done on taking moderator or structural material samples in reactors to independently deduce the amount of plutonium produced there [4] [5]. This approach is called nuclear archaeology.

What is lacking is a systematic and integrated approach that ties together all available information –not only from measurements, but also from available records about the past fissile material production. Such an approach could be used to identify inconsistencies (for example between records and today's measurements), reconstruct missing data from records using measurements, and quantify and reduce the uncertainties on the amount of produced fissile materials.

Here, we propose to use Bayesian inference for this purpose. To demonstrate the approach, we present a first and preliminary proof-of-concept study using a very simple scenario. Besides nuclear archaeology, it would be directly relevant for nuclear forensics purposes.

It is based on measuring high-level waste from reprocessing using mass spectrometry, as has been proposed for nuclear archaeology [6]. The high-level reprocessing waste contains nearly all fission products and minor actinides after dissolving the spent fuel. Accordingly, it contains a rich isotopic signature of past fuel cycle activities. Radioactive waste could be used to estimate operational parameters such as fuel burnup or cooling times.

In addition to states applying such a method to better understand their own programme history, it could be used as a verification tool. If a state declared that a reactor was used for civilian purposes with high burnup, this method could prove that low burnup campaign for possibly military purposes were run. Similarly, a reactor may have run for more time than declared, which could be detected by examining the cooling times. While it is not clear whether the proposed approach can be applied to complex programmes, it may be feasible for use in small programmes of a complexity similar to the North Korean case.

Section 2 provides an overview to the theoretical background and methodology used on the paper. In Section 3, the implementation is described. In Section 4, test scenarios and the practical application of the Bayesian framework are presented. Section 5 contains the results of the test scenarios evaluated and their discussion, followed by conclusions and research outlook in Section 6.

## 2. Theoretical Background

Our task is to solve an inverse problem. The isotopic composition of high-level waste ( $\vec{y}_{obs}$ ), which would be measured, is the output of reactor simulations. We seek, however, the input to those simulations – which we call forward-simulations – the operational parameters ( $\vec{x}$ ). Our forward-simulations can then be thought of a model that can compute  $\vec{y} = f(\vec{x})$ . Reactor simulations couple a Monte Carlo neutron transport routine with a fuel depletion routine. Therefore,  $f(\vec{x})$  cannot be described in a simple function, which could perhaps be inverted analytically. In the following, we explain how it can be inverted using a numerical method.

### 2.1 Bayesian Inference

Bayesian inference can solve the inverse problem, by treating it statistically. It is in particular suited for inverting intractable and complex models, as is the case here. It calculates the *posterior*, which is the distribution of the probabilities  $p(\vec{x}|\vec{y}_{obs})$  that specific reactor parameter combinations  $\vec{x}$  could have produced to measured isotopic composition  $\vec{y}_{obs}$ , using Bayes' theorem

$$p(\vec{x}|\vec{y}_{obs}) \propto p(\vec{y}_{obs}|\vec{x}) \cdot p(\vec{x}) \quad (1)$$

$p(\vec{y}_{obs}|\vec{x})$  is the *likelihood*, which is the distribution of probabilities that the measured isotopic composition would have been obtained by a specific combination of operational parameters. It is obtained by running a large number of forward-simulations to explore the reactor parameter space. The output of each forward-simulation  $\vec{y}$  is compared to the measured isotopic composition  $\vec{y}_{obs}$ . We assume that  $\vec{y}$  is normally distributed, hence

$$p(\vec{y}_{obs}|\vec{x}) = \prod_{i=1}^N \exp\left(-\frac{|y_{obs}^i - f_i(\vec{x})|^2}{\sqrt{2}\sigma}\right)$$

where the index  $i$  represents an isotope under consideration, and  $\sigma_i$  is the corresponding uncertainty, which must be chosen. It must include all sources of uncertainties: measurement uncertainties, model uncertainties, etc. The equation holds if the isotopes chosen are independent of each other.

The particular benefit of this approach is that *prior* knowledge can be included, which is given by manually formulating  $p(\vec{x})$ . This could, for instance, be information from records of the production history. It does not have to be taken at face value, as an uncertainty can be associated with the information. According to the Bayes' theorem, this prior information is then combined with the measurement to produce the posterior. Another advantage of this approach is that, due to its probabilistic nature, it allows for the propagation of uncertainties, so that we obtain the uncertainty of the reactor parameter estimates.

## 2.2. Markov Chain Monte Carlo (MCMC) and Gaussian Process Regression (GPR)

To numerically obtain the posterior by exploring the reactor parameter space by evaluating different reactor parameter combinations  $\vec{x}$ , we use Markov Chain Monte Carlo. It is a method to choose the vectors  $\vec{x}$  to be evaluated. A Markov chain is a sequence of events constructed in such a way that any given event  $\vec{x}$  is only affected by the immediate previous event [7]. MCMC is a class of algorithms that combine traditional Monte Carlo methods together with Markov chains to sample from a given probability distribution, the posterior. In the present work, we have chosen to use the MCMC NUTS algorithm which, a standard algorithm in the context of Bayesian inference.

Using a high-fidelity model – such a detailed reactor simulation – can be computationally prohibitive, as – depending on the number of parameters to be reconstructed – usually thousands of simulations would be required for MCMC. Therefore, instead of directly running reactor simulations, we develop a surrogate model that accurately represents the high-fidelity model but is computationally feasible to evaluate. Specifically, we generate a surrogate model which approximates the results from the simulations using Gaussian Process Regression (GPR).

GPR belongs to a class of interpolation methods with important applications on response surface approximation for complicated functions, in particular those of 'black-box' type for which no closed form expression exists. This is our case. Unlike other regression methods using a particular function type or polynomial decomposition, GPR performs a regression using a distribution over functions which share basic assumptions such as smoothness and differentiability [8]. These assumptions are codified through the use of covariance information of a set of parameter vectors ( $\vec{x}$ ) with which the interpolation model is created. This information being used under the hypothesis that parameter vectors close to each other would map to not too distant output isotopic vectors ( $\vec{y}$ ). GPR allows to predict the value of the underlying function  $\vec{y} = f(\vec{x})$  at non-simulated values  $\vec{x}$  [9].

We create our surrogate model by running SERPENT 2 simulations using different  $\vec{x}$ . The choices of  $\vec{x}$  have been obtained using quasi-Monte Carlo sampling. We use the Halton sequence, through which input parameter vectors can be generated from a deterministic sequence with low discrepancy [10].

## 3. Model and Surrogate Model Implementation

As a proof of concept, we create an infinite lattice model of the Savannah River Reactor K's inner core using data from [11], [12], [13], [14], [15]. This reactor was designed for the production of weapons-grade plutonium as well as tritium. It consists of a high power heavy water reactor operated almost continuously for a period of approximately 5 decades, along with 4 other similar reactors in the Savannah River Site with maximum operational power rate of 2400 MWth. During the operation of this reactor several fuel element designs were tested, the design implemented in this work is that of the Mark 15 uniform lattice fuel element which uses an enrichment of 1.1%. This design was chosen due to the data availability as well as the fact that it was the most efficient design ever tested.

Figure 1 shows the SRS-K Reactor implementation in SERPENT 2. As information on spent fuel concentrations do not appear to be published that could serve to validate the model, we have successfully examined the general quality of our model by checking that the evolution of the infinite multiplication factor as a function of irradiation time is plausible, and that the energy-integrated reactor flux  $\phi$  and the fuel load that can be calculated based on SERPENT output agree with the literature.

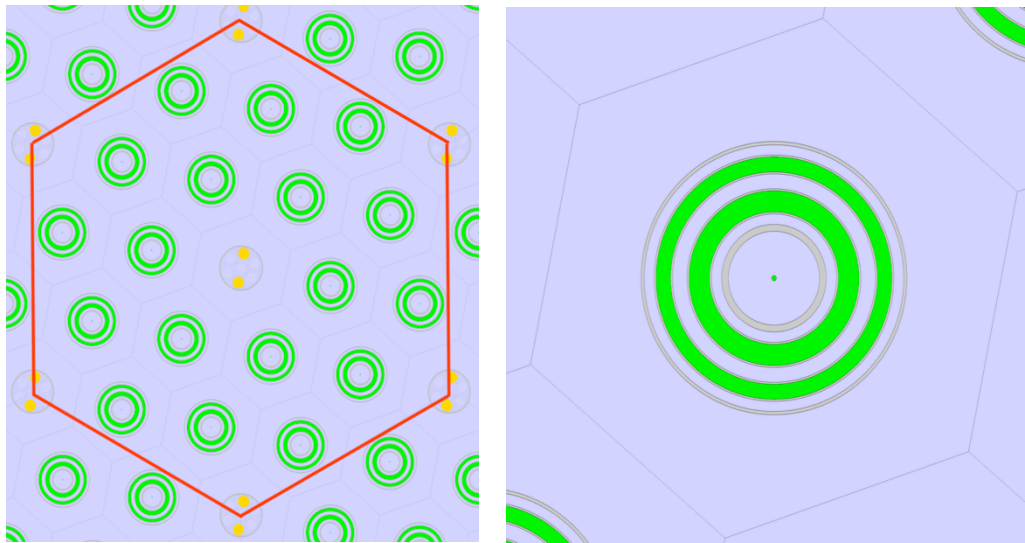


**Figure 1:** Mark 15, 2D – Infinite Lattice Implementation (left). Detail of Mark 15 fuel element (right)

The operational parameters  $\vec{x}$  considered for the surrogate model are mostly fuel burnup ( $B$ ), cooling time ( $Ct$ ), and power. In addition, enrichment values are sampled around 1.1% within a range consistent with criticality considerations. To create the surrogate model, we run 1000 SERPENT 2 simulations. The ranges of sampled parameters are shown in Table 1. The parameters obey operational limitations due to the reactor design and historical constrains. For each output isotope, we build a GPR model using the Scikit-learn library in Python.

To evaluate the accuracy of the interpolation model, we have conducted a self-determination analysis which involves the estimation of Pearson's coefficient ( $R^2$ ). We conduct 6000 additional SERPENT 2 simulations, based on the subsequent entries of the Halton sequences following the initial 1000, and compare the isotopic concentrations to those given by the surrogate model. The value obtained is  $R^2 = 0.9995$ , which indicates a good model performance.

Power (MW)	Burnup (MWd/kg)	Cooling Time (a)
600 – 2400	0 – 3	0 – 50

**Table 1:** Range of input parameters used in the SRS K reactor model. These values also describe the limiting values for the reliable reconstruction of these parameters

Our study aims at examining whether fuel burnup and cooling time can be reconstructed using  $^{137}\text{Cs}$ ,  $^{154}\text{Eu}$ ,  $^{95}\text{Mo}$ ,  $^{142}\text{Nd}$  and  $^{90}\text{Sr}$ , assuming power and enrichment to be known. We choose these for their good sensitivity on the two parameters, which has been quantified by a variance-based sensitivity analysis calculating Sobol indices [16]. Simulations results are presented in Figure 2. In an actual application, one would study ratios of isotopes. If the proof-of-concept can be demonstrated with individual isotopic concentrations, it should also be feasible with isotopic ratios, as the underlying mathematical principles would remain the same.

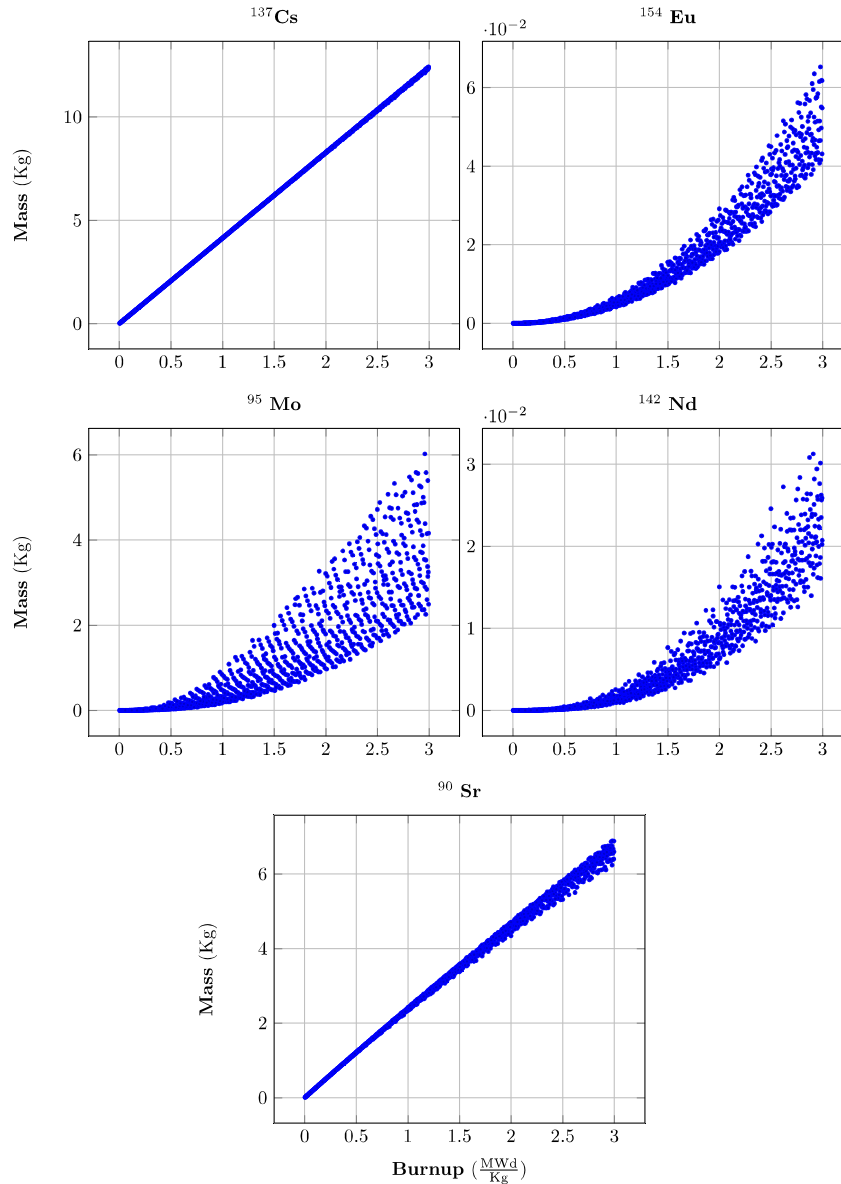


**Figure 2:** Scatterplots of selected isotopes as a function of burnup. The values serve as the basis for calculating sensitivity indices. These plots are one-dimensional projections of simulation results using SERPENT 2 for different parameter combinations of power, burnup and enrichment.

#### 4. Proof of Principle – Scenarios

We consider a very limited plutonium production scenario with a state having a single reactor and discharging and reprocessing fuel only once or twice. The high-level waste is stored in a single tank. Conceptually, this very roughly corresponds to the situation in North Korea, when IAEA inspectors conducted on-site-inspections after the state joining the Non-Proliferation Treaty, including reprocessing waste samples [17].

To solve the inverse problem, first,  $\vec{y}_{obs}$  must be calculated. We do this by choosing specific values of  $\vec{x}$  we use as input to SERPENT 2 to produce  $\vec{y}_{obs}$ . We then use the software package PyMC3 [18] calculate the posterior. The algorithm has no knowledge of the chosen values, but reconstructs them based on  $\vec{y}_{obs}$ . For each case study, we have used 10,000 posterior evaluations. The implementation works if maximum probability of the posterior distribution is close to the chosen values.

Three scenarios are studied:

1. A single fuel batch has been reprocessed, the burnup and cooling time are unknown, the power is known (1018 MW). Uniform probability distributions of the two parameters are used as a prior, i.e. giving equal probability for the parameters within a range defined by minimum and maximum values,  $U[min, max]$ , see Table 2. A vector  $y_{obs}$  for the isotopes  $^{137}\text{Cs}$ ,  $^{154}\text{Eu}$  and  $^{95}\text{Mo}$  is calculated. We assume that all isotopic concentrations carry an uncertainty of 10% ( $\sigma_i$ ). This is a very conservative estimate.
2. The same scenario as above, but assuming more precise prior information, e.g. from authenticated records, resulting in narrower ranges of the uniform prior, see Table 2.
3. Two batches ( $\vec{y}_i^{obs}$ ) with different burnup values are assumed, with their waste of composition  $\vec{y}_{mix}$  being stored in the same tank. In this case also uniform priors are considered for both B urnups covering the span of possible model values. The mass ratio  $\alpha$  of the two batches must also be reconstructed:  $\vec{y}_{mix} = \alpha \vec{y}_1^{obs} + (1 - \alpha) \vec{y}_2^{obs}$ . Here, the power is again 1018 MW, the cooling time is known to be 29.6 years. A vector  $y_{obs}$  for the isotopes  $^{137}\text{Cs}$ ,  $^{154}\text{Eu}$ ,  $^{95}\text{Mo}$ ,  $^{142}\text{Nd}$  and  $^{90}\text{Sr}$  is calculated, the assumed uncertainties of isotopic concentrations are 5%.

Scenario	Burnup (MWd/Kg)	Cooling Time (Years)
Scenario 1	$U[0,3]$	$U[0,50]$
Scenario 2	$U[1.7,1.9]$	$U[27,31]$

Table 2: Comparison of priors for scenarios 1 and 2

## 5. Results & Discussion

### 5.1. Scenario 1: Reconstruction of burnup and cooling time with uninformative prior

The results for scenario 1 are shown in Table 3 and Figure 3. One observes a well-defined posterior distribution both joint and marginal. By examining Table 2, it can be assessed that the burnup and cooling time parameters are reconstructed with reported uncertainties of 5% and 6%, respectively. Quantifying uncertainties of the estimates is an important advantage of using the Bayesian approach. The estimated mean values lie within 0.1% of the true values used to compute the measurements vector.

Parameter	True Value	Posterior Mean	Posterior Std.
Burnup (MWd/Kg)	1.793	1.790	0.091
Cooling Time (Years)	29.6	29.7	1.8

Table 3: Scenario 1, Summary. True values refer to the values used to obtain the vector of simulated measurements  $y_{obs}$ .

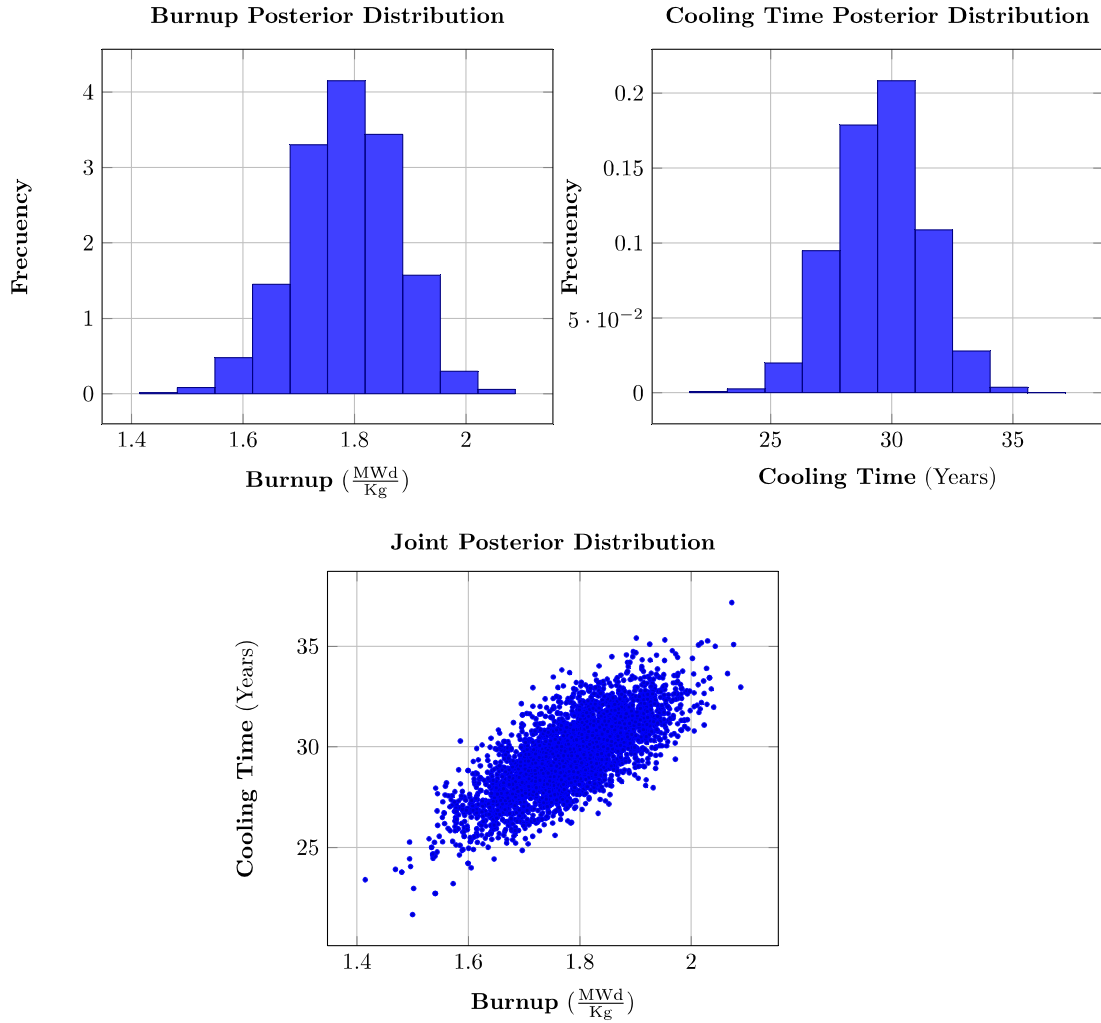


**Figure 3:** Posterior distribution for scenario 1. Each data point in the scatterplot refers to one evaluation.

### 5.2. Scenario 2: Reconstruction of burnup and cooling Time with a constrained prior

The results for scenario 2 are shown in Table 4 and Figure 4. One sees that the constrained prior is able to reduce the spread of the posterior distribution: The uncertainties of the reconstructed burnup and cooling time are 2.8% and 3.3%, respectively. This demonstrates the important role of the Bayesian approach to reduce uncertainties.

Parameter	True Value	Posterior Mean	Posterior Std.
Burnup (MWd/Kg)	1.793	1.799	0.050
Cooling Time (Years)	29.6	29.8	1.0

**Table 4:** Scenario 2, summary. True values refer to the values used to obtain the vector of simulated measurements  $y_{obs}$ .

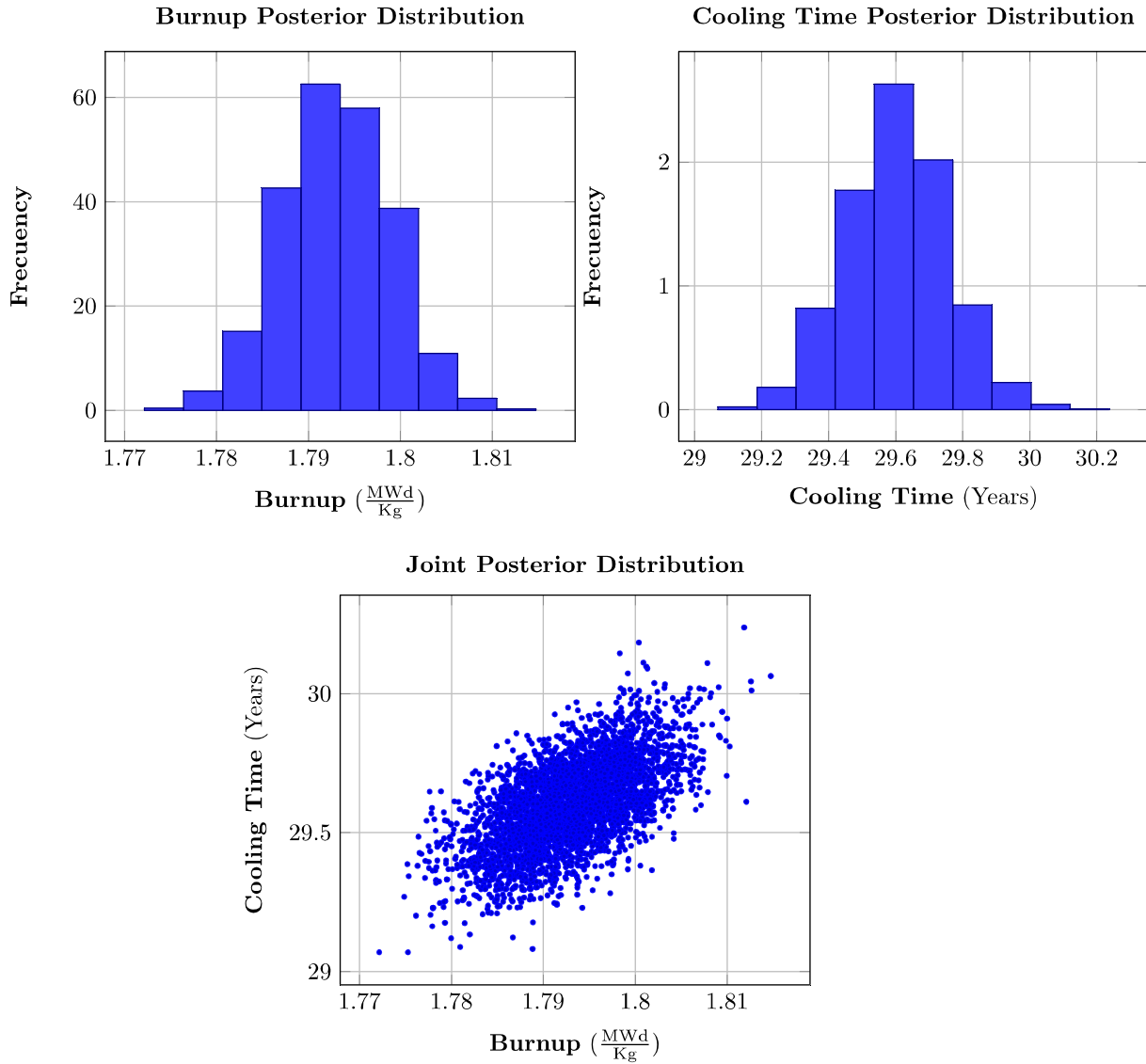


**Figure 4:** Posterior distribution for scenario 2. Each data point in the scatterplot refers to one evaluation.

### 5.3. Scenario 3: Reconstruction of burnup values of a mix of two batches

The results for scenario 3 are shown in Table 5 and Figure 5. In a similar way as in the previous scenarios, it can be observed that the reconstructed posterior is well-defined. Although the burnup values are close, they can be distinguished. The estimated uncertainty for *Burnup 1* is 2.5%. For *Burnup 2* and the *Mixing Ratio*, the estimated uncertainties are 4.9% and 4.6%, respectively.

Parameter	True Value	Posterior Mean	Posterior Std.
<b>Burnup 1 (MWd/Kg)</b>	0.802	0.800	0.020
<b>Burnup 2 (MWd/Kg)</b>	0.930	0.942	0.096
<b>Mixing Ratio</b>	0.64	0.64	0.03

**Table 5:** Scenario 2, summary. True values refer to the values used to obtain the vector of simulated measurements  $y_{obs}$ .

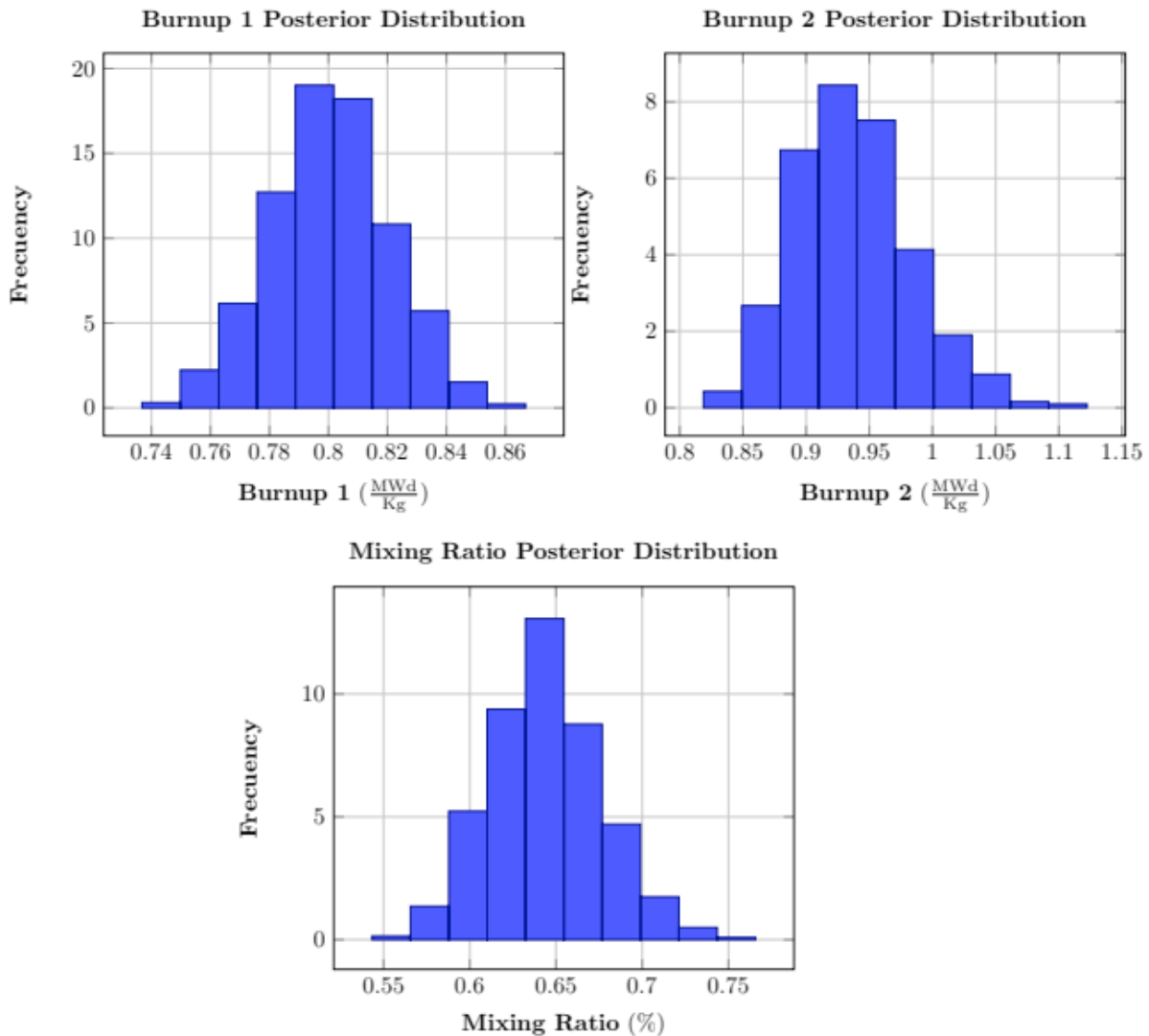


**Figure 5:** Marginal Posterior distributions for scenario 3. The resulting means and deviations of the distributions describe very closely the simulated parameters.

## 6. Conclusions and Outlook

With this study, we successfully demonstrate the proof-of-concept of the approach using GPR, MCMC, and Bayesian inference. Deducing operational parameters is possible, and their uncertainties can be quantified. All three scenarios produce well-defined posteriors with uncertainties smaller or around 5%. These uncertainties are obtained assuming that uncertainties of the measured isotopic concentrations are 10%, in one case 5%. The actual uncertainties are most likely smaller, which would further reduce the uncertainties of the posteriors. Further works must include looking at full-core simulations, and conducting a systematic study of isotopic ratios to be used.

Any real nuclear programme would be more complex than these scenarios. In particular the number of reprocessed batches, each with varying operational parameters, would be larger. For small nuclear programmes such as North Korea, perhaps this larger list of parameters could still be reconstructed as a much larger set of isotopes could be considered in the analysis than those presented here. However, this would clearly not work for large programmes such as in the U.S. or Russia. In such cases, strategies must be found to reduce the amount of parameters to be reconstructed. This is called model reduction, a classical topic in computational science.

In any case, using Bayesian inference appears to be the best implementation of the numerical challenge. Especially in more complex programmes, the problem can only be solved by taking into

account prior information. For instance, it should be studied how some missing information can be reconstructed, if other parts of a programme are well-documented. This could be implemented by taking this into account in specifying parameter uncertainties in the prior. Another topic is to examine how the method behaves when information is inconsistent, e.g. when a civilian programme with high burnup has been declared, but low burnup campaigns were run, or when the declared history is incomplete, for instance when a programme is older than declared.

## 7. Acknowledgements

We thank Martin Frank (KIT) and Florian Wellmann (RWTH) for their expertise in Bayesian inference, GPR and inverse problems. This work has been funded by the Volkswagen Foundation.

## 8. References

- [1] Podvig P., *Verifiable Declarations of Fissile Material Stocks: Challenges and Solutions*, UNIDIR, 2016.
- [2] U.S.Department of Energy, "The United States Plutonium Balance, 1944-2009," 2012.
- [3] Serpent, A Continuous-energy Monte Carlo Reactor Physics Burnup Calculation Code. <http://MonteCarlo.vtt.fi/index.htm>
- [4] C. Gesh, "A Graphite Isotope Ratio Method Primer -A Method for Estimating Plutonium Production in Graphite Moderated Reactors," Richland, Washington, USA, 2004.
- [5] Julien de Troullioud de Lanversin, Malte Göttsche and Alexander Glaser, Nuclear Archaeology to Distinguish Plutonium and Tritium Production Modes in Heavy Water Reactors, *Science and Global Security* 26, 2018, pp. 70-90.
- [6] Malte Göttsche, Julien de Troullioud de Lanversin, Holger Tietze-Jaensch, Examining Reprocessing Waste to Help Estimate Past Plutonium Production, 58th Annual INMM Meeting, July 16-20, 2017, Indian Wells, California, United States.
- [7] Gaugnic P.A., *Markov Chains: From Theory to Implementation and Experimentation*, John Wiley & Sons, 2017.
- [8] Rasmussen C.E. & Williams C.K.I., *Gaussian Processes for Machine Learning*, Massachusetts Institute of Technology, 2006.
- [9] Jones D.R., *A taxonomy of global optimization methods based on response surfaces*, *Journal of Global Optimization*, vol. 21, 2001, pp. 345-383.
- [10] Loyola. D. et al, *Smart sampling and incremental function learning for very large high dimensional data*, *Neural Networks*, vol. 78, 2016, pp. 75-87.
- [11] Cochran T. & Arkin W., *Nuclear Weapons Databook*, vol. III, Ballinger Publishing Company, 1984.
- [12] Cozzuol J.M. & Griggs D.P., *TRAC L Reactor Model: Geometry Review and Benchmarking*, Savannah River Laboratory, 1990.
- [13] *The Savannah River Site at Fifty*, Savannah River Laboratory, 2000.
- [14] White A.M, *MCNP photon transport benchmarking calculations performed at SRP*, in 1989 Annual Meeting of the American Nuclear Society at Atlanta, GA, E. I. du Pont de Nemours and Co., 1989.
- [15] Hamm J.L.L. & Mcallister J.E., *Uncertainties affecting BOSFN for the Mark 15 assembly*, Savannah River Laboratory, 1983.
- [16] A. Saltelli, M. Ratto, T. Andres, F. Campolongo, J. Cariboni, D. Gatelli, M. Saisana and S. Tarantola, *Global Sensitivity Analysis. The Primer* John Wiley & Sons, 2008.
- [17] Albright D., *Plutonium and Highly Enriched Uranium 1996*, Oxford University Press, 1997.
- [18] Salvatier J., Wiecki T.V., Fonnesbeck C. (2016) Probabilistic programming in Python using PyMC3. *PeerJ Computer Science* 2:e55 DOI: 10.7717/peerj-cs.55.

## Determining the production date of $^{252}\text{Cf}$ sources

J. Zsigrai<sup>1</sup>, J. M. Crochemore<sup>2</sup>, A. Apostol<sup>1, 3</sup>, A. Rozite<sup>2</sup>, J. Bagi<sup>1</sup>, K. Abbas<sup>2</sup>, K. Mayer<sup>1</sup>

<sup>1</sup>European Commission, Joint Research Centre, Directorate G, Karlsruhe, Germany

<sup>2</sup>European Commission, Joint Research Centre, Ispra, Italy

<sup>3</sup>Horia Hulubei National Institute for R&D in Physics and Nuclear Engineering (IFIN-HH), Bucharest-Magurele, Romania

Abstract:

Gamma-ray spectra of several sealed  $^{252}\text{Cf}$  sources were recorded by the Joint Research Centre laboratories in both Karlsruhe and Ispra to identify signatures relevant to nuclear forensic characterization of the sources. High-resolution gamma-ray spectra were acquired in well-defined geometry, for which an efficiency calibration was made using Monte-Carlo modelling and reference point sources. This allowed accurate activity determination of the different measurable radionuclides present in the source. This paper reports on the calculation of the date of the last chemical separation of  $^{252}\text{Cf}$  from its daughter products ("age" of the source). The age of the sources was calculated from the ratio of the activities of the fission products  $^{137}\text{Cs}$  and  $^{132}\text{I}$  and compared to the values obtained from the certificates of the sources

**Keywords:** gamma spectrometry, nuclear forensics,  $^{252}\text{Cf}$ , neutron source, age determination

### 1. Introduction

The purpose of this work was to test the method for determining the age (the time passed since the chemical separation of Cf) of  $^{252}\text{Cf}$  neutron sources using a wide range of sources available at JRC-Karlsruhe and JRC-Ispra. If  $^{252}\text{Cf}$  neutron sources get out of regulatory control, they pose a safety and security risk, which triggers nuclear forensic investigations. The age of the sources is a very important parameter for tracing back the sources to their origin.

In this work the performance of the gamma-spectrometric method described in [1], [2] and [3] was studied using reference  $^{252}\text{Cf}$  sources. The tests were done in order to establish more confidence in the applicability of this method. Although the certificates of the Cf reference sources do not always contain the date of chemical separation, the date of the certificates gives an indication about the age of the sources, confirming the plausibility of the measured ages. It was shown that gamma spectrometry can be successfully used for age determination of  $^{252}\text{Cf}$  neutron sources for nuclear-forensic purposes.

### 2. Equipment

Spectra of ten  $^{252}\text{Cf}$  reference neutron sources were recorded by coaxial high-purity germanium detectors. An Ortec Detective-EX portable gamma spectrometer was used to record spectra in Karlsruhe, while a Canberra GC4518 coaxial detector was used to record spectra in Ispra. Both spectrometers were electrically cooled. The Detective-EX had a declared 40% efficiency relative to a 2x2 inch NaI(Tl), crystal diameter 64.4 mm and crystal length 52.4 mm. Its energy resolution (FWHM) was 1.6 keV at 122 keV and 2.3 keV at 1.33 MeV. The Canberra GC4518 had a measured relative efficiency of 50.1% and energy resolution of 1.0 keV at 122 keV and 1.8 keV at 1.33 MeV. Depending on source activity, spectrum collection lasted from about 5 minutes to about 24 hours.

The declared activities of the Cf sources and certificate dates are shown in Table 1.

**Table 1.** Declared data of the investigated neutron sources

Nr.	Source ID	<sup>252</sup> Cf activity [kBq]	Date of <sup>252</sup> Cf activity certification	Date of Cf chemical purification
1	D2-401	425.5	1 Apr 06	unknown
2	D2-402	425.5	1 Apr 06	unknown
3	M5-028	481	15 Apr 15	15 Aug 13
4	M5-029	518	15 Apr 15	15 Aug 13
5	J4-240	37000	15 Jul 12	26 Sep 11
6	0905NC	unknown*	18 Mar 1979	unknown
7	2859 NC	unknown*	18 Mar 1979	unknown
8	5987 NC	4800	17 Dec 1997	unknown
9	6001 NC	45600	17 Dec 1997	unknown
10	J4-238	3700	29 Jul 2012	assumed to be the same as for J-240

\*Only the neutron output is certified for these two sources.

Spectra of the sources 1-5 have been recorded at JRC-Karlsruhe in 2017, and spectra of the rest at JRC-Ispra in 2018.

### 3. Method

<sup>252</sup>Cf has two decay modes: alpha-decay with a branching ratio of 0.96908 and spontaneous fission with branching ratio 0.03092 [4]. To determine the time which has passed since <sup>252</sup>Cf has been separated from its decay products, one has to measure the activity ratio of <sup>252</sup>Cf to a decay product which is not in radioactive equilibrium with <sup>252</sup>Cf. Neither <sup>252</sup>Cf, nor the decay products from alpha decay have any measurable gamma lines for determining their activity. However, gamma lines from the fission products are abundantly present in the <sup>252</sup>Cf spectra.

The method for gamma spectrometric age determination of <sup>252</sup>Cf relies on measuring the activity ratio of a long-lived and of a short-lived fission product of <sup>252</sup>Cf. The short-lived fission product is in radioactive equilibrium with <sup>252</sup>Cf, so its activity is the same as that of <sup>252</sup>Cf, while the activity of the long-lived fission product increases with time. Short-lived products, having visible gamma line(s) in the spectra of Cf sources include <sup>131</sup>I, <sup>132</sup>I, <sup>140</sup>La and <sup>138</sup>Cs. A long-lived fission product, having the most prominent peak in the spectra, is <sup>137</sup>Cs.

In most situations a convenient isotope pair for determining the <sup>252</sup>Cf age is <sup>137</sup>Cs/<sup>132</sup>I, because they have gamma lines very close to each other (662 and 668 keV), and the efficiency of the detector can be considered constant in this very narrow energy range. The activity ratio <sup>137</sup>Cs/<sup>132</sup>I is equal to the activity ratio <sup>137</sup>Cs/<sup>252</sup>Cf and can be used as a "chronometer".

If other short-lived isotopes are used instead of <sup>132</sup>I to determine the <sup>137</sup>Cs/<sup>252</sup>Cf activity ratio then a careful efficiency calibration, spanning the energy range from about 300 to 2000 keV, has to be done [3].

The activity of a fission product (FP) produced by spontaneous fission of a heavy nucleus (HN) is given by the equation

$$A_{FP} = A_{HN} \times \frac{\lambda_{FP}}{\lambda_{FP} - \lambda_{HN}} \times (e^{-\lambda_{HN} \times t} - e^{-\lambda_{FP} \times t}) \times B_{HN} \times Y_{FP_{HN}},$$

where

$A_{FP}$  - activity of the formed fission product

$A_{HN}$  - activity of the fissioning heavy nucleus

$t$  - time since last chemical separation

$\lambda_{HN}$  - decay constant of the heavy fissioning nucleus

$\lambda_{FP}$  - decay constant of the fission product

$B_{HN}$  - decay branching ratio of the heavy nucleus

$Y_{FP_{HN}}$  - cumulative fission yield of the fission product FP resulting from the heavy nucleus HN.

In Cf neutron sources fission products come both from  $^{252}\text{Cf}$  and  $^{250}\text{Cf}$ . The activity,  $A_{FP}$ , of a fission product coming from spontaneous fission of  $^{250}\text{Cf}$  and  $^{252}\text{Cf}$  can be written as

$$A_{FP} = A_{FP252} + A_{FP250},$$

where  $A_{FP252}$  and  $A_{FP250}$  are the contributions to the activity of the fission product coming from  $^{252}\text{Cf}$  and  $^{250}\text{Cf}$ , respectively. As the source gets older, the contribution of  $^{250}\text{Cf}$  increases relative to  $^{252}\text{Cf}$ . For sources of unknown origin and age the mass ratio of  $^{250}\text{Cf}$  to  $^{252}\text{Cf}$  is also not known. However, its average value is usually around 0.025 and it normally does not go above 0.05, as discussed in [3]. Therefore, as it has been shown in [3], the uncertainty coming from the incomplete knowledge of this ratio is usually smaller than, or comparable to, other sources of uncertainty.

The exact equation containing the contributions from both  $^{252}\text{Cf}$  and  $^{250}\text{Cf}$  is discussed in [3]. Here we constrain the calculations to the simplified case when the contribution of  $^{250}\text{Cf}$  can be neglected. In such case the age of the sources,  $t$ , is obtained by solving the following equation:

$$\frac{A_{Cs137}}{A_{I132}} = \frac{\frac{\lambda_{Cs137}}{\lambda_{Cs137} - \lambda_{Cf252}} \times (e^{-\lambda_{Cf252} \times t} - e^{-\lambda_{Cs137} \times t}) \times Y_{Cs137Cf252}}{\frac{\lambda_{I132}}{\lambda_{I132} - \lambda_{Cf252}} \times (e^{-\lambda_{Cf252} \times t} - e^{-\lambda_{I132} \times t}) \times Y_{I132Cf252}},$$

where the activity ratio  $A_{Cs137}/A_{I132}$  is obtained from the gamma measurement. Note that  $\lambda_{I132} \gg \lambda_{Cf252}$ , which greatly simplifies the above equation. Thus we get

$$t = \frac{1}{\lambda_{Cf252} - \lambda_{Cs137}} \times \ln \left( 1 - \frac{A_{Cs137}}{A_{I132}} \times \frac{\lambda_{Cs137} - \lambda_{Cf252}}{\lambda_{Cs137}} \times \frac{Y_{I132Cf252}}{Y_{Cs137Cf252}} \right).$$

#### 4. Results

For sources D2-401 and D2-402 the age measurement has shown that the  $^{252}\text{Cf}$  was separated about 10 years before issuing the certificate. The bias between the measured and the assumed age for the other sources is show in Figure 1. The assumed age was obtained either from the known date of chemical separation or, if this was not available, it was calculated from the date of the certificate.

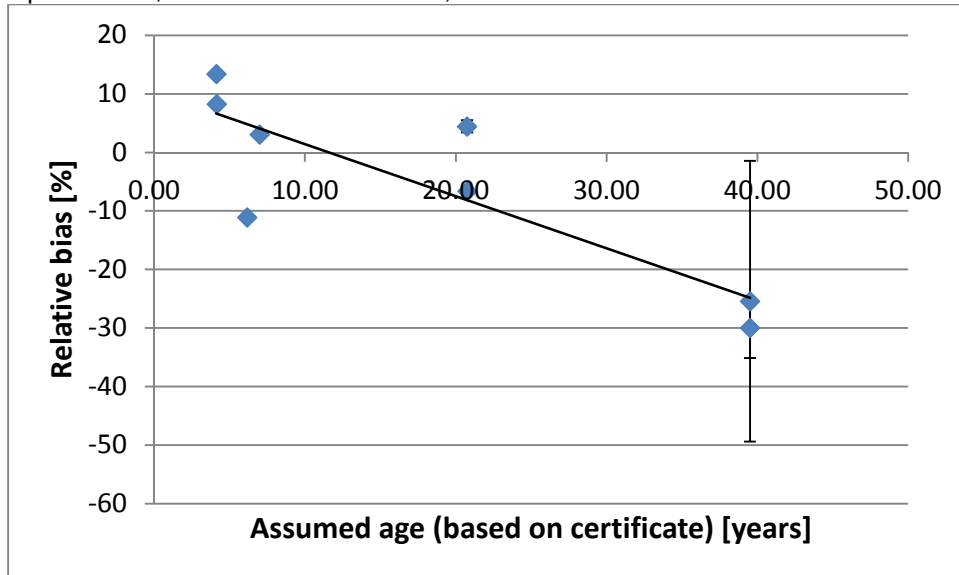


**Figure 1.** Relative bias of the measured age with respect to the assumed age, as a function of assumed age

It can be seen from Figure 1 that the measured age of the 5 to 20 years old sources age agrees with the assumed age within 15%. The high negative bias in the case of the almost 40 years old sources is

mainly due to the difficulties in evaluating the area of the very small 668 keV peak of  $^{132}\text{I}$  in the spectra of such sources, but partially also due to the influence of  $^{250}\text{Cf}$ . In order to be able to better assess the performance of the method, more accurate details about the chemical separation date would be needed.

## 5. Conclusion

High-resolution gamma spectrometry can be used to estimate the production date of unknown Cf neutron sources for nuclear-forensic purposes. The method is based on measuring the activity ratio of long-lived to short-lived fission products of  $^{252}\text{Cf}$ . In this work the activity ratio  $^{137}\text{Cs}/^{132}\text{I}$  was used for this purpose, as  $^{132}\text{I}$  is in equilibrium with  $^{252}\text{Cf}$  and  $^{137}\text{Cs}$  grows in with time. In most cases the influence of the contribution of  $^{250}\text{Cf}$  to the creation of fission products can be neglected in Cf age calculations, though it becomes noticeable for older sources.

The method was tested using spectra of neutron sources recorded at JRC-Karlsruhe in 2017 and at JRC-Ispra in 2018 by two different coaxial high-purity germanium detectors. Most of the sources at JRC-Karlsruhe had known chemical separation date (considered to be the production date), while for the sources at JRC-Ispra only the date of activity certification was available. This information was used to check the plausibility of the measured ages.

This study confirms that the gamma-spectrometric method presented here can be universally applied for determining the age of Cf sources for nuclear forensic purposes. Further studies are ongoing to better assess and improve the accuracy of the method.

## 6. References

- [1] R. J. Gehrke, R. Aryaeinejad, J. K. Hartwell, W. Y. Yoon, E. Reber and J. R. Davidson, "The  $\gamma$ -ray spectrum of  $^{252}\text{Cf}$  and the information contained within it" *Nuclear Instruments and Methods in Physics Research B*, vol. 2013, pp. 10-21, 2004.
- [2] J. Gregor, J. Kesten, E. A. Kroeger, M. Baron and J.-T. Eischeh, "Nuclear forensics information obtained from the  $\gamma$ -ray spectra of  $^{252}\text{Cf}$  sources of differing provenance," *Nuclear Instruments and Methods in Physics Research B*, vol. 437, p. 13–19, 2018.
- [3] A. I. Apostol, J. Zsigrai, J. Bagi, M. Brandis, J. Nikolov and K. Mayer, "Characterization of californium sources by gamma spectrometry: relevance for nuclear forensics," *submitted to Journal of Radioanalytical and Nuclear Chemistry*, 2019.
- [4] "Nucleonica Nuclear Science Portal (www.nucleonica.com), Version 3.0.65," 2017. [Online].

# Nuclear Forensics via the Electronic Properties of Particulate and Samples

Robert B. Hayes, Ryan P. O'Mara, Fatma Abdelrahman

North Carolina State University, Nuclear Engineering Department  
2500 Stinson Dr, Raleigh NC, 27695-7909  
rbhayes@ncsu.edu

## Abstract:

*Recent research has shown how solid state dosimetry techniques can be used as a powerful tool in nuclear treaty verification. Using thermoluminescence, it has been shown that common bricks can serve as gamma ray spectrometers with 10% energy resolution for  $^{241}\text{Am}$  [1]. Using optically stimulated luminescence (OSL), it has been shown that  $^{137}\text{Cs}$  and  $^{60}\text{Co}$  can be identified and imaged again using common bricks [2]. Likewise, surface mount resistors (such as in portable memory flash drives, credit cards or other electronics) are capable of recording dose approaching common background levels using these techniques [3]. Even imaging of weapons grade plutonium has now been accomplished using OSL, the extent to which this can be accomplished using the mineral particulate from smears and air filters is yet to be explored. Now that the theory has been worked out to use this science to carry out retrospective assay of uranium enrichment, the various applications for treaty verification are almost unbounded including retrospective assay of historical uranium enrichment [4]. Applications using electron paramagnetic resonance (EPR) have shown great promise [5] but new options will be explored here. This technology effectively puts low resolution imaging gamma ray spectrometers in every inhabited location on the planet throughout all time as insulator samples are ubiquitous in building materials, personal items and electrical circuit peripherals.*

**Keywords:** Solid state dosimetry; Nuclear Forensics; Nuclear Safeguards; Luminescence; Magnetic resonance

## 1. Introduction

The main goal in nuclear forensics is to characterize radiological material with regards to its isotopic composition, provenance, age and/or history. The conventional tools applied within this field of study generally require direct access to the source material of interest, or remnants of that material. However, the ability to perform forensic analysis at a distance, whether spatially or temporally, would provide an attractive toolset for both nuclear nonproliferation and emergency response. The purpose of this work is to illustrate how solid state dosimetry (SSD) of small samples may soon allow for retrospective nuclear forensics analysis using commonly disregarded mineral material.

The principle mechanism in SSD is charge trapping by lattice defects in crystalline insulator materials. During irradiation, electrons liberated from atomic bonds may become trapped at lattice defect sites such that the population of trapped charges is proportional to the radiation dose received. Once trapped and in the absence of additional stimulation, the populations of trapped charges will be stable over very long periods of time. To the extent that the populations of trapped charges can be quantified and the dose response for the crystalline material can be characterized, then the dose to the material can be reconstructed. The ability to determine the doses received by crystalline materials allows for the possibility to characterize historical radiation environments. The two main methods used, in this work, to quantify material dose are luminescence dosimetry and electron paramagnetic resonance (EPR).

Luminescence dosimetry uses the light emitted by materials upon optical or thermal stimulation to determine the population of trapped charges in a previously irradiated material. Additionally, these methods are best suited to determining the doses to inorganic insulator materials, such as silicate or

aluminum oxide ceramics. The utility of luminescence dosimetry for assaying radiological sources using ubiquitous materials has been well documented in the literature. [1-3] For example, using thermoluminescence (TL), it has been shown that common bricks can serve as gamma ray spectrometers with 10% energy resolution for  $^{241}\text{Am}$  [1]. Using optically stimulated luminescence (OSL), it has been shown that  $^{137}\text{Cs}$  and  $^{60}\text{Co}$  can be identified and imaged again using common bricks [2]. Likewise, surface mount resistors (such as in portable memory flash drives, credit cards or other electronics) are capable of recording dose approaching common background levels using these techniques [3].

Electron paramagnetic resonance dosimetry uses resonant absorption of precisely tuned microwaves under an applied magnetic field to quantify the number of radiation-induced trapped charges. Unlike luminescence dosimetry methods, EPR is generally best suited for organic insulating materials. EPR is also recognized as the gold standard for epidemiological dose reconstruction for populations exposed to anthropogenic external radiological sources [4]. Previous work with sucrose crystals has demonstrated detection limits ranging from 500 mGy [5,6] up to 1.5 Gy [7,8] to list a short sample from multiple studies.

By utilizing a combination of EPR and thermoluminescence dosimetry, it should be possible to characterize historic radiation environments in nearly every corner of the developed world. Additionally, extending these techniques to small sample sizes would allow for forensics analysis using particulate material fortuitously collected during routine air and smear sampling. For example, plume modelling can be used to reconstruct historical releases by distant nuclear facilities [10]. If the aerosols incorporated in this release have nonconducting components integrated into the distribution, these can in principle be used as dosimeters using solid state techniques such as luminescence and EPR. While current techniques focus only on chemical and isotopic signatures in such samples with the added potential to conduct morphological analysis, dosimetric analyses could be performed on the particulate matter that is generally discarded. Recent work has explored this potential to use ubiquitous dust particulate from smears and air filters as common dosimeters via luminescent techniques [11].

In the case of luminescence dosimetry, it has been shown in the literature that using specialized instrumentation and measurement protocols accurate dosimetric reconstructions can be performed on particulate matter the size of a single grain of sand. [12] Such sample sizes are what one might expect to collect on an air filter or environmental smear. Similarly, using sophisticated sample measurements protocols our technique allows precision of a few percent with tooth enamel [13] or alanine [14] which has been shown to improve detection limits by an order of magnitude over traditional techniques [15].

## 1.1 Complementary Techniques

As with any detector modality, the minimum detection limit depends on background signal amplitudes. When using EPR and luminescent techniques, the background typically depends on sample age and its inherent solid state chemistry. This latter component will affect sensitivity, signal stability and even native interfering signals, which can include sample preparation effects.

While luminescence dosimetry has proven useful for dosimetric measurements, the ability to perform single grain EPR measurements remains to be demonstrated. For EPR, the decision limit for any dose reconstruction is dependent on the minimum detectable spin density of the spectrometer system [16] among other parameters. Under ideal conditions, the minimum detectable number of spins for a commercial X-band spectrometer is approximately  $10^{12}$  [16]. Since the spin density in the sample is proportional to the radiation dose received, it is likely that EPR dosimetry on small particulate samples would be relegated to only those samples with large doses. However, since many organic insulating materials tend to have very large saturation doses small aliquot EPR dosimetry may still be a viable option [17].

Most luminescence materials have a drastic light attenuation property such that exposure to ambient sources will cause the signal to decay drastically (having half-lives on the order of hours) [18]. Consequently, for luminescence dosimetry analysis, environmental samples would ideally be collected from locations shielded from ambient light sources, such as underneath painted surfaces. Organic insulators often are not subject to the same light sensitivity and so may offer a more robust approach to scavenging dosimetric information from air samples and smears.

Despite the potential challenges inherent to luminescence dosimetry or EPR dosimetry, it is proposed here that having access to both will allow for robust characterization of historical radiation environments using scavenged materials.

## 2. Example Results

Given the intractable number of materials which are insulators to any extent, the literature reviews on common examples should be consulted for specific types if they have been evaluated [13,14]. A few new examples of potential interest in nuclear forensics carried out in our lab will be offered here but the full range of possibilities is expectedly yet to be explored.

The typical approach in solid state dosimetry techniques is to measure the initial dosimetric signal and then via subsequent irradiation to determine the sample sensitivity to radiation and so back extrapolate to the initial dose obtained by the sample prior to laboratory measurement. If the initial signal is measured as  $S_i$  and then the sensitivity is signal intensity per dose given by the symbol  $S/pD$ , then the sample dose estimate is easily obtained by the ratio  $S_i / S/pD$ . More generally this is done by additive irradiations where the subsequent measurements follow a linear trend, which is least squares fit, to back extrapolate to the initial dose.

### 2.1. Combined TL/OSL and EPR

Typical experimental configurations have been given elsewhere for luminescent and EPR parameters [18,19]. An example of the luminescent and EPR results from diatomaceous earth are shown in Figures 1 and 2 respectively [20]. The fit parameters from Figure 1 are given in Table 1. Note that when dose values become large (which is materially dependent), then the dose response is no longer linear but follows a saturating exponential profile as seen in figure 3. Here, the results were shown to be fairly insensitive to luminescence methods but offered the hope of new EPR properties very different from geological quartz samples.

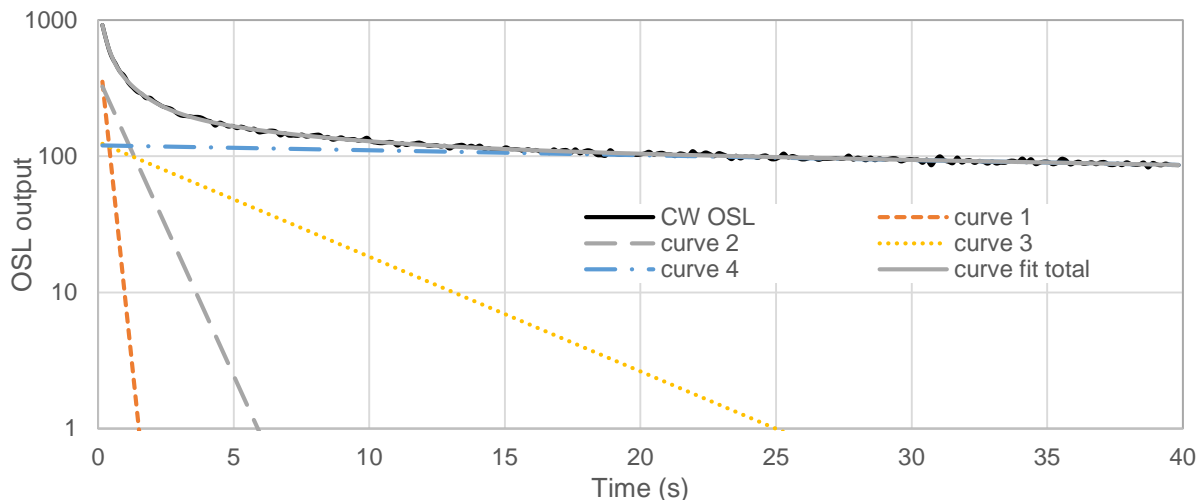


**Figure 1:** Deconvoluted OSL spectrum from diatomaceous earth [20] where the measured signal is the continuous wave OSL (CW OSL) with fit parameters provided in Table 1. Note that the ordinate axis is logarithmic so all the fits are simple exponential decay curves.

**Table 1:** Curve fit parameters from Figure 1 using the exponential model for each fit parameter being given by the functional form of  $f(t) = Ae^{-\lambda t}$ . where  $A$  is the amplitude parameter and  $\lambda$  is the decay parameter.

Curve #	A amplitude parameter	A amplitude uncertainty	$\lambda$ decay parameter	$\lambda$ decay uncertainty
1	709	29	4.36	0.23
2	382	20	1.01	0.071
3	127.1	8.5	0.194	0.016
4	120.2	2.7	0.00834	0.00068

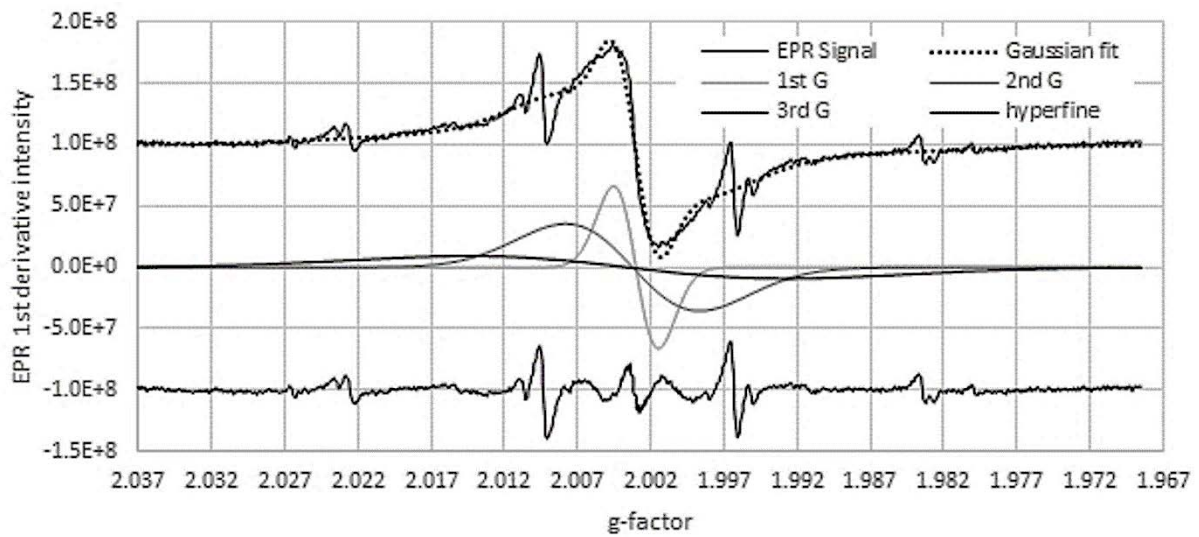


**Figure 2:** Deconvoluted EPR spectrum from diatomaceous earth [20]. Various Gaussian components are deconvoluted and shown in the central set being listed as 1<sup>st</sup> G, 2<sup>nd</sup> G and 3<sup>rd</sup> G respectively. The residual unresolved spectral components are shown at the bottom as the hyperfine portion of the signal.

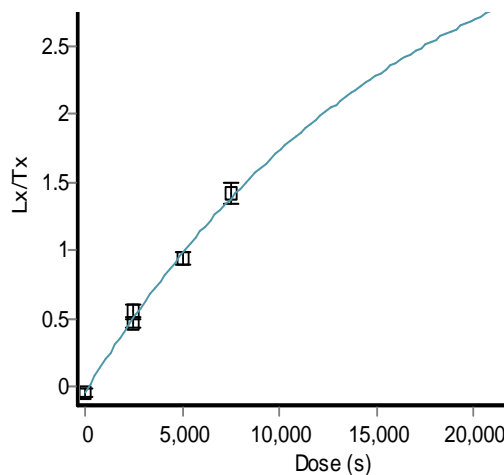


**Figure 3:** Example saturating exponential dose response shown as a function of additional exposure time in seconds. The functional form when trap centers are approaching maximum population results in a dose response following the functional  $f(s) = k(1 - e^{-(s-E)/D})$  where  $E$  is the resultant dose estimate,  $k$  is the maximum signal amplitude at infinite dose and  $D$  is the saturation dose.

## 2.2. EPR

Sucrose is known to be an excellent EPR dosimeter having high sensitivity, low detection limits and long signal stability [8]. Using the same techniques previously shown to have drastically reduced the detection limits for alanine dosimetry using EPR [15], the results from Figure 4 were obtained using 0.5 g aliquots. Here, although a goniometer was not utilized the results are still quite impressive showing an 80 mGy standard deviation of the residuals. The rest of the curve fit parameters are shown given in the inset of the figure.

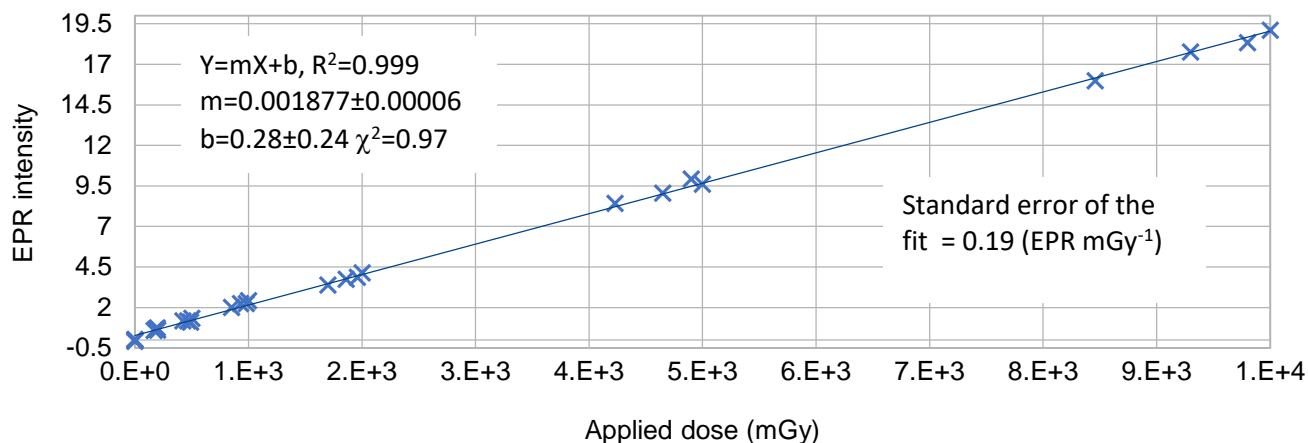


**Figure 4:** Dose response of commercial sugar granules using techniques initially developed for alanine EPR [13]. EPR values are shown in terms of peak to peak counts.

A measured dose response, such as that shown in Figure 4, is still in the linear range; therefore, the sample sensitivity can be taken to be the slope of the least squares fit. Coupling such a dose response function with an initial signal intensity allows the equivalent initial dose to be determined. Although these results were not obtained using single sucrose granules, the linearity of the dose response out to 10 Gy is promising.

The intercept in Figure 4 represents the combined native organic signal and accumulated background radiation. If the signal were purely background accumulation, this would be equivalent to approximately 180 mGy, which would be approximately 2 years worth of exposure to natural background. This value of 0.16 EPR counts per mGy represents the  $1\sigma$  level for a 0.5 g sample. Taking a single grain of sugar to be approximately 0.6 mg, then the EPR response for a single grain would be expected to be near  $0.16 \times 0.6 / 500 = 0.19 \times 10^{-3}$  EPR mGy<sup>-1</sup>. To then just approach the variation seen in Figure 4 would require around a full Gy of radiation dose. Taking into account all combined errors otherwise ignored in this estimate and going to the 95% CL, the detection limit should approach many Gy. Even if difficulties prevent detection below 10's of Gy, this would still be within the needed to linear range of the dose response to accommodate single grain dosimetry by EPR as the linear range extends to the kGy range [21].

## 2.3. TL/OSL

A recent development of forensic interest is the potential to use common electronic components as dosimeters at the natural background level [3] similar to that done with sugar in section 2.2. The ability to discriminate doses at the level of environmental exposures has the potential to literally implement ubiquitous sensing. As an example, it was shown in [3] that simply using multiple electrical elements in a cell phone is sufficient to carry out energy spectroscopy sufficient to discriminate low energy gamma emitters from industrial or medical source typically having higher energies.

The concept for using differential attenuation in ubiquitous materials is effectively equivalent to that already used in radiation worker dosimetry. In both TL and OSL dosimetry, 4 separate luminescent elements are used with each being able to individually measure dose. These are placed behind distinct

attenuating materials such as tin, Mylar, copper and polyethylene (with the element behind the polyethylene being enriched in a neutron absorbing isotope). Using the resulting differential response of the 4 elements along with functional relationships among the same, algorithms can then discriminate between high energy gamma, x-ray, beta and neutron exposures allowing accurate worker dosimetry to be ascribed.

### 3. Analysis

The utility for developing technologies to determine historical doses to ubiquitous materials is exemplified in Figure 5. This generic bunker configuration would expectedly be under international treaty control requiring that the warheads remain in-place between successive International Atomic Energy Agency (IAEA) inspections. If the entry controls are in any way spoofed, then the owner of these items could have deployed them intermediate to the IAEA inspections. Utilizing these solid state dosimetry techniques, the dust particulate on the very walls of the bunker could determine if the ambient dose rate was consistent with the long-term placement of the warheads between successive inspections. Likewise, the bricks can provide age estimates as to whether any were new or replaced in any kind of spoofing attempt.



**Figure 5:** Nuclear weapons storage (creative commons license image).

The application in forensics as proposed here is not a panacea of detection solutions. The measurement is only a single long-term acquisition. This means that a large dose rate source in motion (such as a spent fuel bundle) would appear as a distributed source along the path of the movement. If any imaging approach were attempted [2], then multiple samples would be required from well-defined locations.

In general, the method only provides some form of the product between dose rate and integration time (hence dose). If the time is known, then a dose rate or activity could be estimated. Conversely, if the source activity were known, then an integration time could be obtained. This in turn assumes intervening materials were known to account for shielding and scatter. Depending on operational knowledge, an upper bound may only be possible on a time window; this would then offer a lower bound on the source activity or dose rate giving rise to the resultant dose. All this of course assumes a single known, or assumed, source.

### 3.1. Caveats, limitations and considerations

As with any detector, SSD approaches have limitations although these vary greatly from those of electrically powered detector systems. Most detectors have a 1 second or less temporal resolution between successive spectra with the potential to acquire for many days in some cases. An SSD material would offer only a single measurement with an integration window typically being the lifetime of that material. The quartz in brick would provide the accumulated dose to that material all the way back to the time it was fired. Ambient quartz or feldspar from smears or air samples would give an OSL dose estimate back to the time it was zeroed based on exposure to sunlight or any other sufficiently intense optical photon source.

Depending on the material, chemical properties may generate a native signal, which is not radiogenic and would have to be subtracted from the resultant measurements. Sample preparation can likewise generate interfering signals, which require identification and mitigation. To further complicate the approach, internal radioactivity, signal decay and variable sensitivity all have to likewise be properly addressed.

Perhaps the largest drawback to using SSD as a forensics technique is the overall throughput for obtaining results. Typical dose estimates from opportunistic materials such as brick, wallboard (sheetrock or plasterboard) and confectionary range from days to weeks. In this sense, the time commitment to obtaining quality results is comparable to modern radiochemistry and so does not allow rapid analysis unless quality is commensurately poor.

Other groups have proposed portable OSL systems [22] but without TL, they are of limited value in determining sensitivity, which severely limits their overall utility. Similarly, portable EPR systems have likewise been proposed but have also been shown to have very low sensitivity [23]. Currently, laboratory based SSD systems are required to obtain meaningful results which are now able to start approaching background levels.

### 3.2. Spoofing

As with any detector, surrogate sources could be envisaged, designed and constructed. Similarly, this detector could be annealed or made impotent. If an evasive actor were to heat all the walls around a source up to 500° C, then the TL/OSL/EPR signals would all be zeroed back as though it had just been created in the kiln. Alternatively, an actor could construct their walls out of conducting metal and keep dust meticulously clean so as not to leave ambient dosimeters about. Even then, the lighting would require some form of insulation to enable workers to be productive without requiring miner's lamps to conduct operations.

Even an annealed wall will retain tell-tale SSD signatures if they are not uniformly heated to 500° C. Assuming this can be done, it would have to occur in such a way that heating the room itself did not leave evidence such as requiring all new wood, plastic and rubber peripherals as these would all combust or melt under such a kiln treatment. Still, removing a full brick may be reasonably rejected due to building integrity if reparative measures are not properly implemented.

Given the requirements inherent to spoof an SSD forensics approach, it would be prohibitively difficult to fully erase all evidence of noncompliant actions on the part of any nuclear state.

## 4. Discussion

The utility of measuring the electronic properties of nonconducting materials enables these to become effective dosimeters. Utilizing differential attenuation in multiple samples then provides means by which the energy of the radiation field can then be obtained (albeit at a low effective resolution). Using multiple samples over a grid offers the potential to reconstruct the location of the nuclear material (via inverse square and any shielding considerations) such that the technique can serve as a gamma camera [2].

Additionally, combining SSD with plume reconstruction techniques may allow for forensic analysis at large standoff distances. To the extent that the atmospheric transport of nonconductive particulate matter mirrors the transport of other materials released by nuclear facilities, one can envision performing

dosimetric analysis on particles released by such facilities. In this way, it may be possible to gather information about the activities being performed within. Realization of this capability would allow verification of nuclear operations from a distance, without the need to even step foot inside the facility itself.

By combining the applications of EPR with TL and OSL, all insulator materials can be utilized. One drawback with common environmental materials is the potential for a large geological dose background. This can be partially mitigated using various techniques presented by others [24] although at the cost of decreased quality in the resulting dose estimate. However, given the variety in materials that this combination of techniques may utilize there is some likelihood that in any given sample some useful material could be scavenged.

## 5. Conclusions

The potential applicability for SSD in nuclear forensics is effectively in its infancy. The realization that imaging gamma ray spectrometers (with spectral capability) are ubiquitous has implications, which are lightly explored in this work. If the success of prior studies could be extended to particulate matter from environmental smears or air samples, then it would be possible to perform dosimetric assay for treaty verification without direct access to the facility. This would mark a significant improvement in the current suite of tools currently employed for treaty verification and nonproliferation.

## 6. Acknowledgements

This material is based upon work supported by the Department of Energy National Nuclear Security Administration under Award Number DE-NA0002576. This work partially paid for by the Nuclear Regulatory Commission grant NRC-HQ-84-14-G-0059. Additional support of this work was through a joint faculty appointment between North Carolina State University and Oak Ridge National Laboratory in coordination with the Office of Defense Nuclear Nonproliferation R&D of the National Nuclear Security Administration sponsored Consortium for Nonproliferation Enabling Capabilities.

## 7. References

- [1] O'Mara RP, Hayes RB: Dose deposition profiles in untreated brick material. *Health Phys.* **114**(4), 414-420, 2018.
- [2] Hayes RB, Sholom SV; Retrospective imaging and characterization of nuclear material. *Health Phys.* **113**(2), 91-101, 2017.
- [3] Hayes RB, O'Mara RP; Retrospective dosimetry at the natural background level with commercial surface mount resistors. *Radiat. Meas.* **121**, 42-48, 2019.
- [4] Hayes RB. Retrospective uranium enrichment potential using solid state dosimetry techniques on ubiquitous building materials *J Nuc Mat Mgmt.* **47**(2), 4-12, 2019.
- [5] Alexander GA, Swartz HM, Amundson SA, Blakely WF, Buddemeier B, Gallez B, Dainiak N, Goans RE, Hayes RB, Lowry PC, Noska MA, Okunieff P, Salner AL, Schauer DA, Trompier F, Turteltaub KW, Voisin P, Wiley AL, Wilkins R. BiodosEPR-2006 Meeting: Acute dosimetry consensus committee recommendations on biodosimetry applications in events involving uses of radiation by terrorists and radiation accidents. *Radiat. Meas.* **42**, 972-996, 2007.
- [6] Wieser A, Goksu HY, Regulla DF, Vogenauer A; Limits of retrospective accident dosimetry by EPR and TL with natural materials. *Radiat. Meas.* **23**(2/3) 509-514, 1994.
- [7] Ding Y, Jiao L, Zhang W, Zhou L, Zhang X, Zhang L. Research on EPR measurement methods of sucrose used in radiation accident dose reconstruction. *Radiat. Prot. Dosim.* **138**(4), 393-396, 2010.

- [8] Belahmar A, Mikou M, Mamadou Saidou A, Bougteb M; EPR analysis of dosimetry properties of various organic materials for radiotherapy applications. *Physica Medica* **32**, 246, 2016.
- [9] Belahmar A, Mikou M, Mamadou Saidou A, Baydaoui RE; EPR spectroscopy investigations of some organic materials irradiated by electrons, in prospect of their use in radiotherapy. *Physica Medica* **44**, 14-15, 2017.
- [10] Hayes RB; Reconstruction of a radiological release using aerosol sampling *Health Phys.* **112**(4), 326-337. 2017.
- [11] Hayes RB, O'Mara RP; Enabling Nuclear Forensics Applications from the Mineral Particulate in Contamination Surveys. *Advances in Nonproliferation Technology and Policy Conference*, Orlando FL, Nov 12-15, 200-204, 2018.
- [12] Duller GAT, Bøtter-Jensen L, Murray AS and Truscott AJ. Single Grain Laser Luminescence (SGLL) Measurements Using A Novel Automated Reader. *Nucl. Instr. Meth. In Phys. Res. B.* **155**, 506-514. 199.
- [13] Hayes RB, Haskell EH, Barrus JK, Kenner GH and Romanyukha AA; Accurate EPR radiosensitivity calibration using small sample masses. *Nucl. Instr. Meth. A.* **441**, 535-550. 2000.
- [14] Hayes RB, Haskell EH, Wieser A, Romanyukha AA, Hardy BL and Barrus JK; Assessment of an alanine EPR dosimetry technique with enhanced precision and accuracy. *Nucl. Instr. Meth. A.* **440**, 453-461. 2000.
- [15] Haskell EH, Hayes RB and Kenner GH; Native signal subtraction, g-factor normalization and constant rotation goniometry are valid methods in EPR dosimetry. *Health Phys.* **77**, 472-475. 1999.
- [16] Rieger PH. *Electron Spin Resonance – Analysis and Interpretation*. Royal Society of Chemistry, Retrieved from <https://app.knovel.com/hotlink/toc/id:kpESRAI001/electron-spin-resonance/electron-spin-resonance>
- [17] Rank WJ and Schwarcz HP. Dose Response of ESR Signals in Tooth Enamel. *Rad. Meas.* **23**, 481-484. 1994.
- [18] Yukihiro EG, McKeever SWS; *Optically Stimulated Luminescence: Fundamentals and Applications 1st Edition*. John Wiley & Sons, West Sussex, UK, 2011.
- [19] Ikeya M; *New Applications Of Electron Spin Resonance: Dating, Dosimetry And Microscopy*. World Scientific, Singapore, 1993.
- [20] Hayes RB, O'Mara RP and Hooper DA. Initial TL/OSL/EPR Considerations for Commercial Diatomaceous Earth in Retrospective Dosimetry and Dating. *Rad. Prot. Dosim.* 1-10, doi:10.1093/rpd/ncz013, 2019
- [21] Karakirova Y, Yordanov ND Sucrose as a dosimetric material for photon and heavy particle radiation: A review. *Radiat. Phys. Chem.* **110**, 42-50, 2015
- [22] Thomsen KJ, Bøtter-Jensen L, Jain M, Denby PM and Murray AS. Recent Instrumental Developments for Trapped Electron Dosimetry. *Rad. Meas.* **43**, 414-421, 2008.
- [23] Williams BB et al. A deployable *in vivo* EPR tooth dosimeter for triage after a radiation event involving large populations. *Rad. Meas.* **46**(9), 772-777, 2011.
- [24] Ikeya M. *New Applications of Electron Spin Resonance Dating, Dosimetry and Microscopy*. World Scientific Publishers, Singapore, 1993.

## Analysis of Light Elements in Uranium-Bearing Materials for Safeguards Purposes

Morel Sylvain<sup>1</sup>, Casteleyn Karin<sup>1</sup>, Zuleger Evelyn<sup>1</sup>  
Repinc Urska<sup>2</sup>, Rosenzweig Mathieu<sup>2</sup>

<sup>1</sup>EC-JRC.G.II.6  
P.O. Box 2340, DE-76125 Karlsruhe  
<sup>2</sup>IAEA-SGAS NML  
VIC, P.O. Box 100, A-1400 Vienna  
E-mail: sylvain.morel@ec.europa.eu

### Abstract:

*Some uranium bearing materials utilized in the early stages of the nuclear fuel cycle are relatively pure and hence subject to safeguards agreements with International Atomic Energy Agency (IAEA), specifically paragraph 34(c) of INFCIRC/153 (Corrected). For determination of which uranium materials meet the conditions of paragraph 34(c) of INFCIRC/153 (Corrected), technical standards are referred to that were established by industry to define the purity of uranium dioxide powder intended for fuel fabrication for nuclear power reactors. The uranium materials in question, and the related impurities and concentration limits, are described in IAEA Policy Paper 21 (SG-PL-12684). Among the elements listed in Policy Paper 21 are carbon, chlorine, fluorine and nitrogen. As these light-element impurities are difficult to measure by common techniques such as ICP-MS, other analytical methods have been adapted from industry. Carbon concentration is assayed by fusion-extraction/infrared absorption (IAEA-SGAS NML & EC-JRC.G.II.6), nitrogen concentration is determined by fusion extraction/thermal conductivity (IAEA-SGAS NML & EC-JRC.G.II.6), and chlorine and fluorine contents are determined by combustion ion chromatography (IAEA-SGAS NML). An incomplete understanding of these methods in depth, a lack of appropriate certified reference materials for calibration and measurement control, and the need for more robustness studies for uranium matrices, are the main challenges in the further development of these analytical methods. A working group meeting, with mainly European actors in the nuclear area, was recently convened by CEA/CETAMA to develop synergies and to exchange practises in order to tackle these common analytical issues. Finally, these types of measurements are not only relevant to Safeguards authorities and for dual-use control purposes, but are also of interest to nuclear forensics practitioners*

**Keywords:** nuclear material measurements, chemical analysis, nuclear forensics, Strategic dual-use trade control

### 1. Introduction

Due to technological advances, concentration plants usually located in the vicinity of mining sites can produce uranium bearing materials, mainly uranium ore concentrates (UOC), with levels of impurities below the requirements stated by industry standards for uranium dioxide fuel fabrication in ASTM C753-04 (2009) [1]. These materials can clearly be considered as suitable for fuel fabrication, without further processing, within the meaning of paragraph 34(c) of INFCIRC/153 (Corrected) [2] and are candidates to international safeguards.

Among the impurities of interest are the light elements carbon, chlorine, fluorine, and nitrogen. The concentration thresholds, set in the IAEA Policy Paper 21 (SG-PL-12684), are listed in Table 1. Because these maximum concentration limits are defined as µg of element per g of U, the assay of uranium is required and is usually performed either using modified Davies and Gray potentiometric titration or Isotope Dilution Thermal Ionisation Mass Spectrometry (ID-TIMS).

Element	Maximum Concentration Limit of Uranium ( $\mu\text{g/gU}$ )
Carbon	100
Chlorine	100
Fluorine	100
Nitrogen	200

**Table 1: maximum concentration limits**

Most multi-element analytical methods for impurities at trace and ultra-trace level used in the nuclear field (such as Inductively Coupled Plasma Mass Spectrometry ICP-MS) are not suitable for the measurement of the light elements C, Cl, F or N. Alternative analytical techniques must be used for which specific methods suitable for uranium bearing matrices are applicable. Depending on the element, the development of an appropriate method for the matrices and the range of interest of the analyte is not straightforward and may require experimental investigations.

The technique selected by IAEA-SGAS NML (Department of Safeguards Nuclear Material laboratory) for the measurement of halogens is combustion ion chromatography, which is also widely used in industry applications (petrochemicals, pharmaceutical) but is not commonly used for nuclear safeguards applications. The technique selected by the EC-JRC.G.II.6 Nuclear Safeguards and Forensic unit and IAEA-SGAS NML for the measurement of carbon is the direct combustion / infrared absorption, and for the measurement of nitrogen, direct combustion / thermal conductivity is used. These two techniques are commonly used in the industry (steel, inorganic materials) and several suppliers produce commercially available instruments since several decades. However, most of the developed applications concern measurements of quantities higher than 100  $\mu\text{g/g}$  in non-nuclear matrices (steel, cement...) for process control, which do not require low uncertainties. Moreover, the techniques for carbon and nitrogen assay are subject to matrix effects and total extraction rates are only possible under specific conditions. Further developments and investigations are necessary to set up a robust method for the quantification of these elements in the range of interest and to determine that matrix effects do not significantly bias the results.

Typical safeguards inspection samples subject to impurity analysis are UOC (uranium ore concentrate also called yellowcake) in the form of a mixture of  $\text{U}_3\text{O}_8$ ,  $\text{UO}_2$  and  $\text{UO}_3$ , or samples of ammonium diuranate powder (ADU), or of ammonium uranyl carbonate (AUC) which are in certain cases also requested for carbon and nitrogen determination.

## 2. Measurement of carbon

### 2.1. Principle of the analytical technique

A known mass (between 0.01 to 1 g to the nearest 0.1 mg) of solid sample is combusted, using an induction furnace at high temperature (above 3000 °C), in a ceramic crucible under a stream of highly pure oxygen. The carbon present in the sample is extracted as a mixture of carbon dioxide ( $\text{CO}_2$ ) and carbon monoxide (CO). A catalyst converts the CO into  $\text{CO}_2$  which is then measured in an infrared cell.

The measurement is based on the absorption by  $\text{CO}_2$  of the infrared radiation at the specific wavelength of  $4.27 \mu\text{m} / 2343 \text{ cm}^{-1}$  [3]. The rate of absorption as the gas flows through the  $\text{CO}_2$  cell at a constant rate is proportional to the carbon concentration of the gas. Figure 1 gives a schematic representation of the analytical principle.

Note: most of the commercially available instruments measuring carbon also allow the simultaneous measurement of sulphur: during the combustion, the sulphur contained in the sample is extracted as  $\text{SO}_2$  which is directly measured by infrared absorption. It is then oxidized in  $\text{SO}_3$  and filtered with a cellulose trap before the measurement of  $\text{CO}_2$  to avoid interferences.

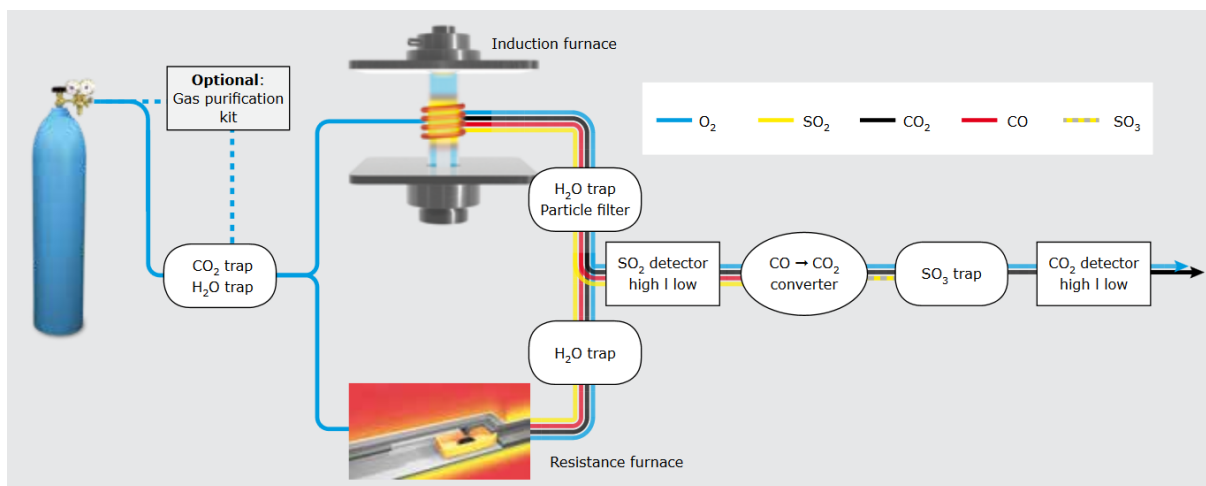


Figure 1: Schematic representation of carbon and sulphur determination – Copyright ELTRA®

The output signal is a peak (detector output voltage as function of time) whose area is integrated and converted into carbon mass. This conversion requires a calibration step, done by means of certified reference materials. Most instruments are equipped with two infrared cells of different path lengths to accommodate both low and high content of carbon. The analysis time is less than a minute. IAEA-SGAS NML operates a LECO CS-844, and EC-JRC.G.II.6 operates an ELTRA CS-800 that has been nuclearized (furnace separated from the rest of the instrument and fitted into a glovebox).

Reaching a complete combustion is required to obtain a bias-free (total extraction of the carbon) and repeatable measurement result. A sufficiently high temperature must therefore be reached and maintained, and is only possible in an induction furnace if there is enough coupling material in the crucible. Therefore a coupling material, also called accelerator, is systematically added to the sample. The accelerator generates the heat and transmits it directly to the sample. Depending on the sample type, a combination of accelerators may be required. The most commonly used accelerators are:

- Tungsten alone or in combination with tin, for steel alloys, nickel and cobalt base alloys
- Copper, generally used when low power is required (cannot be used to measure sulphur)
- Iron, for samples that contain little or no inductive elements

## 2.2. Validation of the method for uranium bearing materials

The norm ASTM C1408-16 [4] provides useful general guidelines for the measurement of carbon in uranium oxide powders but lacks references and does not assess the full recovery of carbon in uranium oxides, and thus the absence of bias. The absence of suitable certified reference materials (CRM) doesn't allow for a straightforward validation, so other means must be used to quantify the recovery of carbon.

The accurate measurement of low concentrations ( $<100 \mu\text{g/g}$ ) of carbon in uranium matrices requires particular attention to:

- The reduction and control of the blank value, see 2.2.1
- The quantification of the recovery rate (bias) in the absence of an appropriate CRM, See 2.2.2

### 2.2.1. Blank determination

The preferred approach for reducing the influence of the blank is to analyse a large sample mass. A sample with a mass of carbon greater than  $150 - 200 \mu\text{g}$  is normally outside of the range of influence of the blank (under normal conditions). Small samples require that great care be given to two parameters having a high influence on the value of the blank: the crucible and the accelerator. The crucible must be properly pre-treated and the accelerator must be carefully selected.

#### Pre-treatment of the crucible:

Ceramic crucibles contain a significant amount of carbon trapped in the interstices, which has to be removed. ASTM C1408-16 [4] recommends pre-igniting the crucibles in a muffle furnace at  $1000^\circ\text{C}$ , in

order to remove the carbon and reduce the blank value. The heating time used by IAEA-SGAS NML and EC-JRC.G.II.6 ranges from 45 min to 2 h. This pre-heating step reduces the amount of carbon trapped in the crucible by 80% (see Figure 2) and reduces also the variation of the blank value by a factor 10.

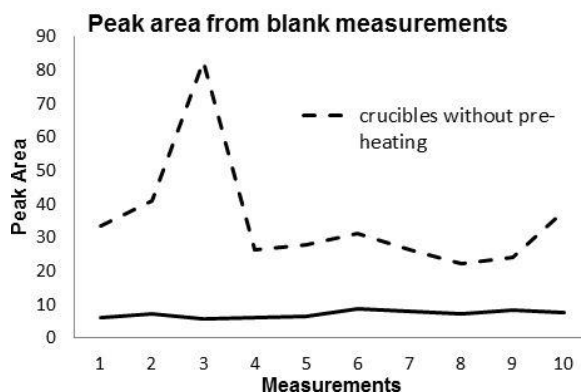


Figure 2: Blank area with 1g of W-Sn accelerator

Shortly after pre-ignition of the crucibles, the carbon present in the airborne dust is slowly absorbed in the crucible. The crucible must therefore be immediately (once it has cooled down to a safe temperature for manipulation) stored under vacuum or inert atmosphere to prevent absorption of carbon. Tests have shown that crucibles have already recaptured a measurable amount of carbon within 24 hours (see Figure 3).

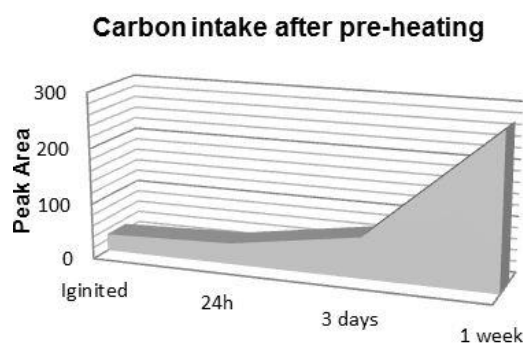


Figure 3: Evolution of the carbon intake with time

#### Selection of the accelerator:

It is known from the analytical protocols provided by the manufacturers that the recovery rate may not be complete for all matrices depending on the accelerator used for the measurement. Ores and oxides may have little to no coupling with the magnetic field induced by the induction furnace. Consequently without an accelerator, no sufficient heat will be produced during the 40 to 60 s necessary to fully extract the carbon in the sample. The quantity and the type of accelerator (or a combination of two accelerators) to be added to the sample must be chosen with great attention as they strongly impact the combustion and the extraction of the carbon.

It should also be kept in mind that accelerators contain carbon in unequal amount and homogeneity. Best performances are obtained with high purity products which should be systematically checked as the quality from one batch to another can be uneven.

For ores and oxides, a mixture of 1 g of W+Sn (to bring enough heat) and 0.5 g of Fe (to ensure that enough coupling material is in the crucible) was found to be effective.

## 2.2.2. Assessment of the recovery rate in uranium bearing materials

As stated above, the recovery rate of carbon is not always guaranteed. The use of a certified reference material with a matched matrix and carbon content can be used to confirm total extraction, or in the opposite case, to correct a bias.

Only two suitable CRM with a uranium matrix certified for carbon content are available on the market, both from CEA/CETAMA: OPERA 103 (uranium-vanadium alloy certified at  $226 \text{ mg.kg}^{-1}$ ) and OPERA 104 (uranium metal certified at  $58 \text{ mg.kg}^{-1}$ ). For the other uranium matrices of interest (UC,  $\text{UO}_2$ ...), no reference materials certified for carbon are available.

To guarantee a complete extraction of the carbon, two conditions must be fulfilled:

- the sample must be melted to ensure optimised contact between the carbon in the sample and the oxygen from the carrier gas
- The bonds of the carbon with the other elements must be broken

The carbon is present in the sample in two forms: (1) free carbon or  $\text{CO}_x$ , trapped in the lattices of the sample, and (2) carbon bonded in molecules (carbides, carbonates).

The free carbon, or  $\text{CO}_x$ , trapped in the interstices is usually extracted immediately as the samples are heated, providing the carbon does not preferentially react with uranium and convert to a carbide in the crucible.

The most stable uranium compounds that contain carbon are UC and  $\text{UO}_2$  (which may contain free carbon). Their melting points (see Table 2) are below the temperature reached in the furnace (above  $3000 \text{ }^\circ\text{C}$ ) which guarantees that the sample will melt. This ensures an optimum contact with oxygen gas, which is the first condition for a total extraction of the carbon.

Compound	Melting point
UC	$2780 \text{ }^\circ\text{C}$
$\text{UO}_2$	$2865 \text{ }^\circ\text{C}$

Table 2: melting points of uranium compound

To predict the behaviour of UC in the furnace, and to know if it will decompose, a thermodynamic simulation [5] on the system  $\text{UC} + \text{O}_2$  was made assuming conservative (i.e. less favourable to the decomposition of UC) conditions.

The simulation shows (see Figure 4) that UC is already fully decomposed in a mixture of  $\text{CO}_2$  and CO at a temperature below  $3000 \text{ }^\circ\text{C}$ .

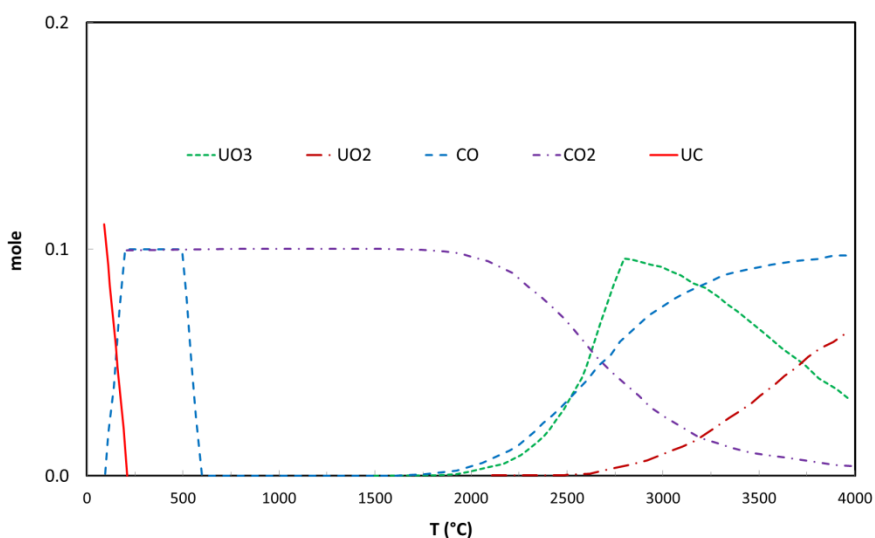


Figure 4: UC + O<sub>2</sub>

With a guaranteed fusion of the sample and a total decomposition of the uranium carbide, the total extraction of the carbon is confirmed and the method can be considered fit for purpose for uranium bearing materials.

This prediction has been empirically corroborated by experiences on different  $UC_x$  compositions [6].

### 2.3. Analytical performances for safeguards samples

Typically, two cases are considered for quantifying the analytical performance, especially the uncertainty, of this type of measurement:

- The case of samples with low amount of carbon, where results are subject, among others, to the influence of the blank and to the limited availability of CRM
- The case of samples with high amount of carbon

The performance of this method for high carbon concentration is illustrated with the measurement of ammonium uranyl carbonate, AUC (Figure 5).

The error bars represent the expanded uncertainty of the individual measurement ( $k=2$ ).

Thanks to the availability of accurately certified reference materials for the calibration of the instrument for such amount of carbon, it is possible to reach a relative expanded uncertainty of 2 to 3% with an interval of confidence of 95%.

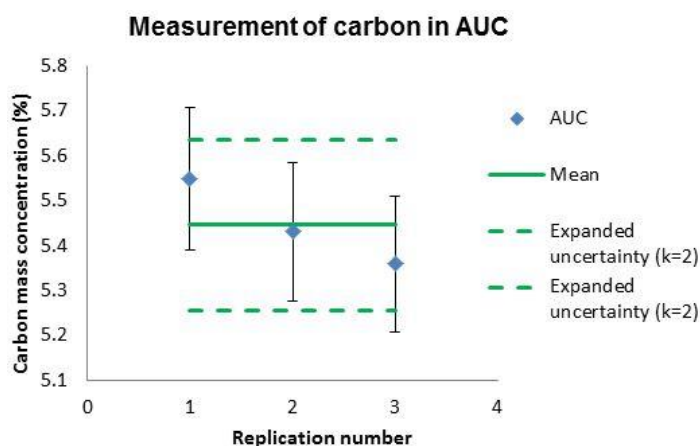


**Figure 5: measurement of 30 mg of AUC with 1 g W + 0.5 g Fe**

The performance of this method for low carbon concentrations is illustrated with the measurement of a uranium ore concentrate, UOC (Figure 6).

The error bars represent the expanded uncertainty of the individual measurement ( $k=2$ ).

Because available certified reference materials for the calibration of the instrument for such amounts of carbon are less precisely quantified, and because the variation of the blank is influencing the results, it is not possible to reach a relative expanded uncertainty lower than 20% with an interval of confidence of 95%.

It is interesting to note in this example that the total uncertainty (represented by the dashed lines) is greater than the individual uncertainties. This highlights a heterogeneous distribution of the carbon in the samples of 150 mg size.

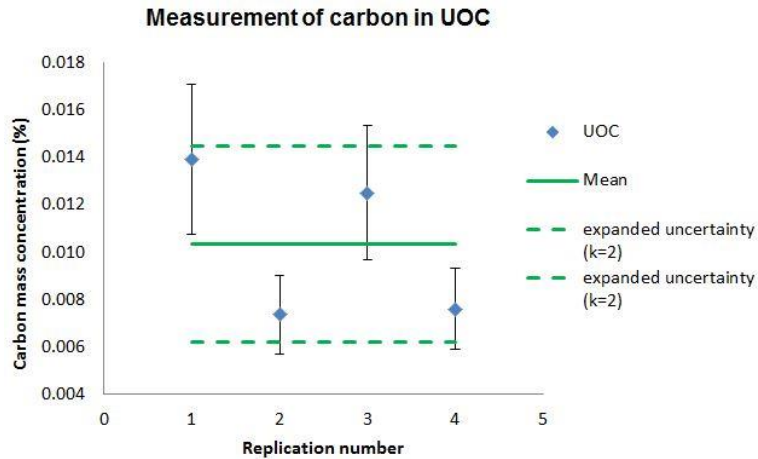


Figure 6: measurement of 150 mg of UOC with 1 g W + 0.5 g Fe

### 3. Measurement of nitrogen

#### 3.1. Description of the analytical technique

A known mass of solid sample is combusted in a graphite crucible under a stream of helium in a resistance furnace at a set temperature (max. 2500 °C). The nitrogen present in the sample is extracted as N<sub>2</sub> which is measured in a thermal conductivity detector (TCD) shown in Figure 7.

The measurement is based on the change of thermal conductivity that modifies electrical current in a Wheatstone bridge. The variation of current from the reference cell (measuring pure helium) as the gas flows through the measuring cell at a constant rate is proportional to the nitrogen concentration of the gas.

EC-JRC.G.II.6 operates an ELTRA ONH-200 which has been nuclearized (furnace separated from the rest of the instrument and fitted into a glovebox).

Note: most of the commercially available instruments measuring nitrogen also allow the simultaneous measurement of oxygen following a similar analytical principle as described previously for the carbon measurement: during the combustion the oxygen contained in the sample reacts with the carbon of the graphite crucible and is extracted as a mixture of CO and CO<sub>2</sub> which is then directly measured by infrared absorption after oxidation into CO<sub>2</sub>. It is to be noted that a high amount of oxygen in the sample can induce a signal in the TCD thus positively biasing the measurement of nitrogen. This important point will be discussed later.

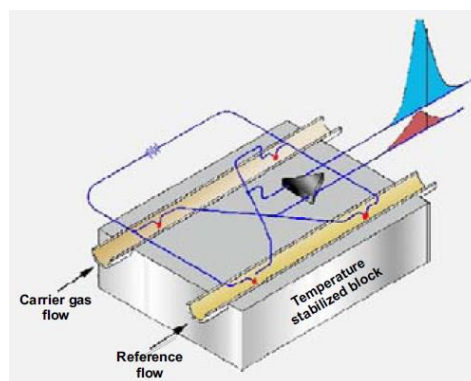


Figure 7: Schematic of a TCD – copyright ELTRA®

### 3.2. Validation of the method for uranium bearing materials

The main difficulty with the extraction of nitrogen from uranium matrices by direct combustion lies in the furnace: the maximum temperature reachable with a resistance furnace, of about 2500 °C, is not enough to melt all uranium compounds (see Table 2) which hinders the total extraction of the nitrogen. In addition, at such temperature N<sub>2</sub> easily interacts with reactive and refractory metals to form nitride, leading to even more negatively biased results. This is the case for uranium, as uranium nitride already forms at low temperature in the presence of N<sub>2</sub> [7]. Some uranium ores, such as uraninite, are mixed oxides of uranium and other refractory metals (Ti for uraninite), which also easily combine with nitrogen to form nitride. This phenomenon has been observed by a producer of certified reference materials in steel matrices containing around 0.1-0.2% of Ti and of Zr: the obtained recovery rate was at most 66% [8].

Little information is available in the literature regarding the measurement of nitrogen in uranium matrices. Only one study [9] has been released on the measurement in U-Pu mixed oxide fuels which does not address the formation of nitride and the impact on the recovery rate. The study however mentions a crucial point for the measurement of nitrogen in uranium matrices which is the addition of metal flux to the sample.

This metal flux, mainly in the form of a nickel basket, has a double utility: it creates a eutectic with the sample, thus allowing melting the sample at the temperature of operation, and it favours the formation of alloy over nitride, thus allowing more nitrogen to leave the crucible.

In the absence of reference material, it is difficult to assess if the use of a metal flux is sufficient to obtain a total recovery of the nitrogen.

Furthermore manufacturers recommend a ratio nickel:sample of 10:1, ranging between 7:1 to 17:1, which deviates from the study of Hiyama and Al. [9] that was done with a ratio of only 5:1.

Another issue with the measurement of nitrogen is inherent to the design of the instruments measuring oxygen at the same time: when the sample contains a lot of oxygen, a lot of CO<sub>2</sub> will be released in the system. As the CO<sub>2</sub> is quickly trapped after quantification in the infrared absorption cell, the pressure and thus the gas flow suddenly changes, triggering a false-positive signal in the TCD, leading to a positive bias in the measurement of nitrogen. A few instruments do have a flow compensator installed after the CO<sub>2</sub> trap but for the others the operator must find a way to correct for this effect. UOC samples contain copious amounts of oxygen and are therefore susceptible to this effect.

At the present time, further studies are needed to define the analytical protocol that will reliably allow the total extraction of nitrogen in uranium matrices.

In the absence of proper CRMs, this could be done by means of spiking with reagent grade chemicals with known composition.

## 4. Measurement of fluorine and chlorine

### 4.1. Description of the technique

Combustion ion chromatography is very effective in reducing the time and effort for the analysis of halogens. The advantages of this methodology are: simple sample preparation, matrix removal, highly sensitive on-line detection and the possibility of automatization. A Mitsubishi AQF-2100 furnace in combination with a Dionex ICS-2100H ion-chromatography system is used at the IAEA-SGAS NML for analysis of halogens in uranium bearing samples. The AQF-2100H consists of an ABC-210 Automatic boat controller, a HF-210 Horizontal Furnace and a GA-210 Absorption Unit, connected to Dionex ICS-2100 ion chromatograph. For combustion ion-chromatography, several subsamples, each containing 50-100 mg, are taken by weight into prebaked sample boats. In order to limit the amount of the impurities added to the sample, no accelerator is used. The sample boat is inserted into the injection port of the ABC-210 boat controller, which transfers the sample into the pyrolysis tube of the HF-210 horizontal furnace. The sample is combusted in an oxidizing atmosphere at 900-1100 °C (process flowchart in Figure 8) The resultant vapours (volatile HX and X<sub>2</sub>) are absorbed in a solution of the GA-absorption unit, while uranium and its decay products remain in the sample combustion boat. This limits the possible radioactive contamination to the combustion system. Before automatic injection of sample through a 100 µL sample loop into the ICS-2100 system, the volume of the absorption solution can be adjusted automatically by the use of an optical sensor. The sample preparation

procedure is actually a combination of matrix removal followed by substantial dilution, and the automatic system is processing the sample through those intermediate steps without user intervention.

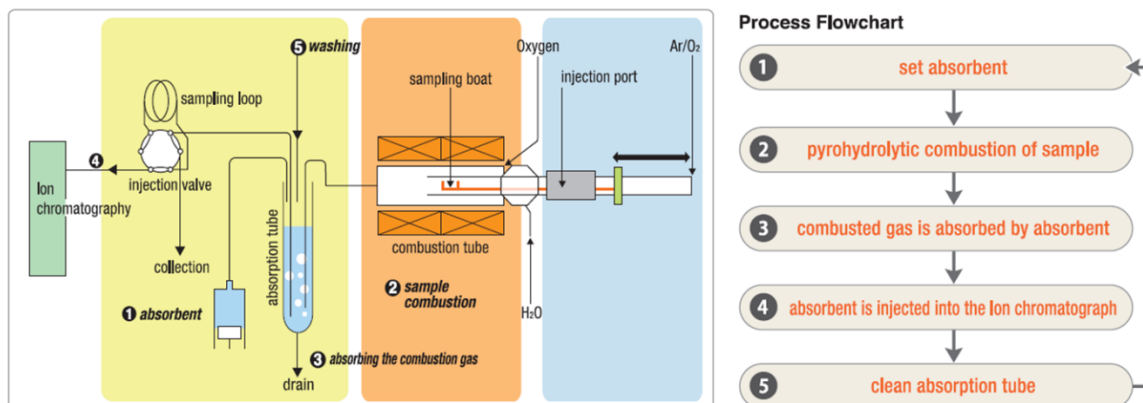


**Figure 8: Process flowchart of combustion ion-chromatography system**

The concentration of halogens in the absorption solution in comparison to the original sample is lowered due to dilution (a 50 mg sample is pre-concentrated in 14 mL absorption solution), therefore sensitive detection by ion chromatography can cover a wide concentration range, from 0.001 to 10  $\mu\text{g/g}$ . Very impure UOC samples may contain high concentrations of chlorine or very high levels of sulphate. Pure uranium oxide powders contain very low amounts of halogens, often just above the detection limit of the instrument. The ion chromatography system itself can also be used for analysis of anions, like fluoride, chloride, bromide, phosphate, nitrate, nitrite, and sulphate in aqueous samples. IAEA-SGAS NML therefore regularly participates in the EQRAIN IONS inter-comparison exercises organized by CEA/CETAMA, in order to test the performance of the detection system. The ion chromatography ICS-2100 system is calibrated yearly using commercially available multi-anion standards being able to cover anion concentrations from 0.001  $\mu\text{g/g}$  to 10  $\mu\text{g/g}$ , by preparing four calibration curves each covering one concentration range.

#### 4.2. Validation of the method for uranium bearing materials

A relevant certified reference material, ideally matrix-matched and at a concentration range of  $\sim 100$   $\mu\text{g/g}$ , is preferred in order to estimate bias of the method when applied to uranium bearing samples. No suitable matrix-matched reference material for U was available when the method was validated. Likewise, other reference materials with certified fluorine and chlorine content around 100  $\mu\text{g/g}$  were rare, since these levels are in general considered to be quite low for industrial applications. Therefore reference materials MRC No.880-1 (Blast furnace dust), BCR-038 (Fly ash from pulverized coal), BCR-109 (Zinc ore concentrate), BCR461 (Clay) and ERM-EC680k (Low density polyethylene) were used. BCR-109 material contains enormous amount of carbon that saturates the IC column, therefore it is unsuitable for the purpose, while ERM-EC680k is unsuitable from the perspective of matrix reactivity (requiring a different combustion program as uranium samples). The reference materials that were most suitable for quality control purposes, to be used as associated samples when analysing safeguards inspection uranium bearing samples, were BCR-038 (536.7  $\mu\text{g F/g}$ , 323  $\mu\text{g Cl/g Cl}$ ), MCR 880-1 (340  $\mu\text{g F/g}$ , 860  $\mu\text{g Cl/g}$ ) and BCR-461 (568  $\mu\text{g F/g}$ ). In those reference materials, the concentration levels of fluorine and chlorine were still much higher than the levels measured in inspection samples. The following reference materials were used for determination of the bias of the method, which relies on the analysis of the reference material and comparison of the measured mean with a suitable reference value. In normal conditions, the recovery of the combustion ion-chromatography method is expected to be 100%, with some variability that should not exceed the range of 80-120%.

In 2016 IAEA-SGAS NML acquired CEA/CETAMA Viognier  $\text{UO}_2$ , which is a uranium oxide powder (0.25% U-235, 100 g of the material per bottle) and certified for fluorine ( $32.7 \pm 1.1$   $\mu\text{g F/g}$ ) and chlorine ( $17.9 \pm 1.0$   $\mu\text{g Cl/g}$ ). The IAEA-SGAS NML has used this CRM as a quality control material for the analysis of the uranium samples since 2017. The results obtained during the last few years have

confirmed the certified values for both fluorine and chlorine, using variable sample amounts from around 50 mg to 200 mg. IAEA-SGAS NML was able to prove that the recovery of the halogen trapping and analysis using combustion ion-chromatography system can be considered quantitative. For combustion ion-chromatography, a general approach to estimate LOD (limit of detection) and LOQ (and limit of quantification), are based on the standard deviation of results at concentrations near zero and obtained under intermediate precision conditions (since values vary from day-to-day). The obtained estimates of LOD (0.2  $\mu\text{g/g}$  for F and 0.056  $\mu\text{g/g}$  for Cl) and LOQ (0.4  $\mu\text{g/g}$  F and 0.11  $\mu\text{g/g}$  Cl) should be taken as indicative values. They demonstrate that the concentrations of halogens in inspection samples at the decision level of 100  $\mu\text{g/g}$  F or Cl are well above the LOD and LOQ. Therefore no blank correction is normally required, and when required it is applied only for samples where measured levels of fluorine and chlorine are close to detection limits.

### 4.3. Analysis of halogens in safeguards samples

Before each batch of inspection samples one or more combustion blanks (empty boat) are analysed in order to prove that blank levels are acceptably low. Each sample set (usually 4 subsamples from the same inspection sample) is accompanied by at least one quality control sample (Viognier  $\text{UO}_2$ ). Inspection samples are kept under weight control and precisely weighed subsamples are taken using a five digit analytical balance (Mettler Toledo XP205).

Over the past few years more than 60 inspection samples have been analysed for halogens. The F and Cl concentration levels were mostly well below the 100  $\mu\text{g/g}$  U limit. Only approximately 10% of the samples contained higher concentration levels of halogens (Figure 9). For some inspection samples, usually UOC, the concentrations of halogens were so high that quantification by ion chromatography system was possible only after additional dilution of the absorption solution and subsequent manual injection of the solution in the ion chromatography system. This user-friendly feature allow collection of the absorption solution after combustion and IC measurement, therefore allowing the user to repeat injection in a manual mode, either using direct injection of the collected absorption solution or injection of the solution after dilution (to target the calibration curve of the instrument).

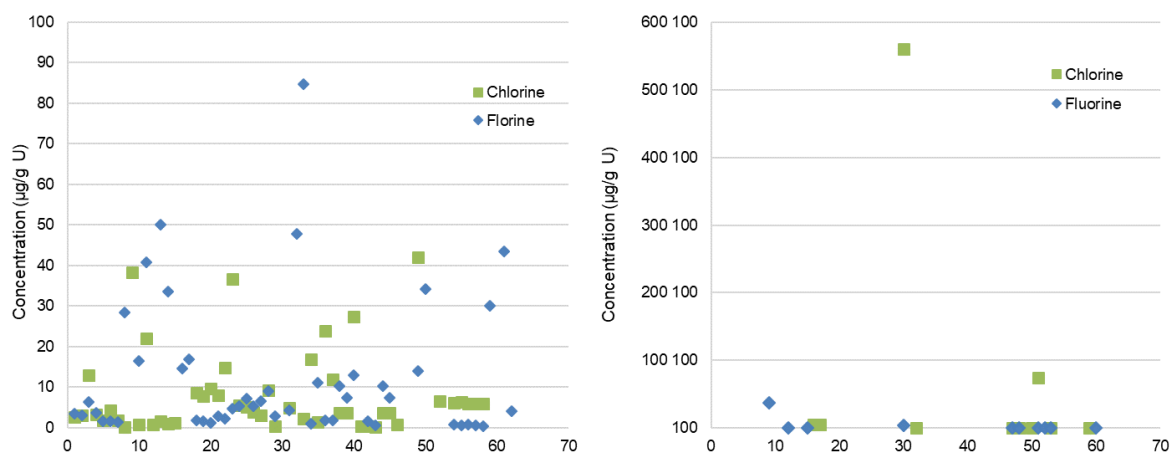


**Figure 9: Measured concentration levels of halogens in safeguards inspection samples analysed for characterization purposes**

The system is very reliable and robust, and therefore well suited for analysis of uranium samples. Approximately 200 mg of sample is sufficient to obtain four reliable results. The combined measurement uncertainty is mostly dominated by the homogeneity of the sample and the uncertainty of detection (uncertainty in volume adjustment, peak evaluations and statistical uncertainty of conductivity detection). The system is installed on an open work bench in the uranium laboratory in NML. The combustion part is running in automatic mode using a previously defined combustion program and is well controlled in both temperature and gas flows. The U-shaped glass tube is placed on the outlet of the pyrolysis tube to retain any particulates in case of incomplete combustion or

emission of particulates. The combustion gas from the pyrolysis tube passes through the U-tube to the absorption tube where halogens are absorbed in gas form. After the combustion, the boat is automatically transferred back to the injection port of the ABC-210, where the sample is cooled and collected for disposal.

## 5. Nuclearisation

The handling of nuclear materials is challenging and the requirements are different from laboratory to laboratory. The handling of uranium containing materials in glove boxes also requires modifications of the instrumental set-up. Most manufacturers can provide modified instruments with a furnace separated from the electronics and the detection part (measurement cells), therefore only the furnace is fitted in the glovebox. The contamination is fully contained in the particle metal filter fitted after the furnace. Additional filters must nevertheless be added for safety at the exit of the glovebox. To reduce the dispersion of the contamination in the furnace, crucible lids can be used. This has the advantage of better containing the generated dust, thus lowering the maintenance on the metal filter.

A few users have reported technical issues during the process of nuclearisation such as high frequency interference with the induction furnace [10], heat propagation to the wall of the glovebox with a resistance furnace [11]. These issues have been mentioned during meetings of the CEA/CETAMA sub-working group 06 (see below).

On the other hand, the combustion ion chromatography system used for halogen analysis at the IAEA-SGAS NML has been installed on a laboratory workbench and has been used safely and reliably for several years for analyses of uranium samples.

## 6. CEA/CETAMA sub-working 06

At the end of 2016, a new CEA/CETAMA sub-working group focusing on the analysis of light elements (C, H, O, N, S) has been created. It brings together a diverse audience from international and national nuclear institutions, suppliers of laboratory equipment and nuclear companies. The group meets several times per year (for plenary or thematic sessions) to share knowledge and feedback. The following themes are addressed:

- Sharing of knowledge, expertise and issues on measurement and equipment implementation (for instance: nuclearisation)
- Organisation of proficiency testing focusing on the participants needs
- Redaction of a detailed technical guide on the measurement of light elements in solid matrices

## 7. Conclusion

The measurement of carbon and of halogens respectively by direct combustion / infrared absorption and by combustion ion chromatography has been validated and can be reliably applied to analysis of safeguards samples. The measurement of nitrogen in uranium matrices needs to be further investigated as the robustness of the method is still not confirmed for all the uranium matrices as described in chapter 3.2.

## 8. Acknowledgements

The authors would like to acknowledge Steven Balsley (IAEA-SGAS NML) who has reviewed this paper and contributed to its completion.

## 9. Legal matters

### 9.1. Privacy regulations and protection of personal data

The authors agree that ESARDA may print my name/contact/data/article in the ESARDA Bulletin/Symposium proceedings or any other ESARDA publications and when necessary for any other purposes connected with ESARDA activities.

### 9.2. Copyright

The authors agree that submission of an article automatically authorises ESARDA to publish the work/article in whole or in part in all ESARDA publications – the bulletin, meeting proceedings, and on the website.

Once the article has been accepted for publication the copyright is reserved, but part of the publication may be reproduced, stored in a retrieval system, or transmitted in any form or by any means, mechanical, photocopy, recording, or otherwise, provided that the source is properly acknowledged.

The authors declare that their work/article is original and not a violation or infringement of any existing copyright.

## 10. References

- [1] ASTM C753-04(2009), *Standard Specification for Nuclear-Grade, Sinterable Uranium Dioxide Powder*, ASTM International, West Conshohocken, PA, 2009, [www.astm.org](http://www.astm.org)
- [2] IAEA, *INFCIRC/153/Corr The Structure and Content of Agreements Between the Agency and States Required in Connection with the Treaty on the Non-Proliferation of Nuclear Weapons*; 1972.
- [3] NIST Standard Reference Database 69: *NIST Chemistry WebBook*.
- [4] ASTM C1408-16, *Standard Test Method for Carbon (Total) in Uranium Oxide Powders and Pellets By Direct Combustion-Infrared Detection Method*, ASTM International, West Conshohocken, PA, 2016, [www.astm.org](http://www.astm.org)
- [5] Morel S, Benes O; *Validation report - measurement of carbon and oxygen in (U,Pu)<sub>x</sub>(C,O)<sub>y</sub> matrices*; JRC109884; 2018
- [6] Manara D., Boboridis K., Morel S., De Bruycker F.; *The UC<sub>2-x</sub> – Carbon eutectic: A laser heating study*; *Journal of Nuclear Materials*; Volume 466; 2015; Pages 393-401
- [7] Zhehao Q., Bangyue Y., Jinru R., Xuan W.; *Low temperature synthesis of uranium mononitride powder*; *Journal of Nuclear Materials*; Volume 496; 2017; Pages 193-196
- [8] CEA/CETAMA; *DO 15 CR sous-Groupe de travail 6 – Analyse des éléments légers*; 2018
- [9] Toshiaki Hiyama, Toshio Takahashi, Katsuichiro Kamimura; *Determination of nitrogen in uranium-plutonium mixed oxide fuel by gas chromatography after fusion in an inert gas atmosphere*; *Analytica Chimica Acta*; Volume 345, Issues 1–3; 1997; Pages 131-137
- [10] CEA/CETAMA; *DO 196 CR sous-Groupe de travail 6 – Analyse des éléments légers*; 2017
- [11] CEA/CETAMA; *DO 99 CR sous-Groupe de travail 6 – Analyse des éléments légers*; 2018

# **Session 4:**

# **Environmental Sampling - Particle Measurements**

# NUSIMEP-9 Inter-Laboratory Comparison on Uranium Isotope Amount Ratios and Uranium Mass in Uranium Micro-Particles

**Vencharutti Célia<sup>1</sup>, Richter Stephan<sup>1</sup>, Middendorp Ronald<sup>1</sup>, Aregbe Yetunde<sup>1</sup>**

<sup>1</sup>European Commission - Joint Research Centre, Directorate G – Nuclear Safety and Security, Unit G.2 for Standards for Nuclear Safety, Security and Safeguards

## **Abstract:**

*NUSIMEP (Nuclear Signatures Inter-laboratory Measurement Evaluation Programme) is an external quality control programme organised by the European Commission - Joint Research Centre, Directorate G – Nuclear Safety and Security, Unit G.2 for Standards for Nuclear Safety, Security and Safeguards (JRC-Geel, former IRMM), which aims at providing materials for measurements of trace amounts of nuclear materials in environmental matrices.*

*Measurements of the uranium and plutonium isotopic ratios in small amounts, such as typically found in environmental samples, are required for nuclear safeguards, for the control of environmental contamination and for the detection of nuclear proliferation.*

*The JRC-Geel, the Forschungszentrum Jülich (Germany) and the IAEA-SGAS (Seibersdorf, Vienna) joined forces to produce and characterise micrometre-sized uranium oxide particles, which can be used for Safeguards purposes as Reference Materials (RM).*

*In this context, JRC-Geel decided to organise a new NUSIMEP, targeting more particularly the IAEA-NWAL, a worldwide network of analytical laboratories. However, NUSIMEP-9 was opened to all laboratories in various scientific fields. Finally, 30 laboratories worldwide registered for it.*

*Participants in NUSIMEP-9 received one certified test item, a carbon planchet on which were deposited some thousands U<sub>3</sub>O<sub>8</sub> particles of about 1 µm diameter-size and of single isotopic composition.*

*They were asked to measure, using their routine analytical procedures, and report the  $n(^{234}\text{U})/n(^{238}\text{U})$ ,  $n(^{235}\text{U})/n(^{238}\text{U})$  and  $n(^{236}\text{U})/n(^{238}\text{U})$  isotope amount ratios of ten particles, which belong to the main particle population. Moreover, participants were also encouraged to measure and report the uranium mass per particle by measuring at least ten particles.*

*The participants' measurement results were evaluated against the certified reference values in accordance to ISO 17043 and ISO 13528, while guaranteeing full confidentiality with respect to the link between measurement results and the participants' identity.*

*The organisation of the NUSIMEP-9 exercise according to ISO 17043 and the preliminary evaluation of the results of this exercise according to ISO 13528 will be presented here.*

**Keywords:** Uranium; micro-particles; NUSIMEP; inter-laboratory comparison; Nuclear Safeguards

## **1. Introduction**

During the past decades, the European Commission Joint Research Centre (EC-JRC) has developed a significant experience in the implementation of nuclear safeguards in support to the International Atomic Energy Agency (IAEA) and more specifically to the Euratom inspectorate. With the implementation of the Additional Protocol (INFCIRC/540), the analysis of environmental samples (such as particles, swipes, etc.) has become one of the most important way of strengthening international nuclear safeguards in order to detect undeclared operations as well as inconsistent or non-conformed data to official declarations [1].

In this context, the IAEA network of analytical laboratories (NWAL) for environmental sampling must apply validated measurement methods for the safeguards analyses since conclusions drawn from their measurements might be used in a court of law and therefore might have political and legal consequences on the international scale. As a consequence, to respond to the importance of precisely verifying nuclear treaty compliances and detecting undeclared nuclear activities, new safeguards technologies and methods were developed, such as the determination of isotopic abundances of

uranium in microscopic single particles, collected from the swipe samples taken by safeguards inspectors in the different nuclear facilities during nuclear safeguards inspections. These analytical techniques require the development of new and more complex reference materials (RMs), such as RMs for particle analysis in nuclear materials in order to determine for instance the origin of the material or its processing history [2].

Such RMs play a key role in analytical quality assurance as they are widely used for the calibration of instruments and measurement systems, for method development and validation, or as quality control samples. They are indispensable to provide reliable measurement results of high quality in order to draw conclusions on the origin, history, purpose and intended use of the material or sample under investigation. However, to this date, there is no (certified) reference material (CRM) for the uranium isotopic composition in micrometre-sized particles, which would be an essential tool for laboratories carrying out particle analysis while meeting the needs of a quality assurance system, improving their analytical performances [3].

For these reasons, the European Commission - Joint Research Centre, Directorate G – Nuclear Safety and Security, Unit G.2 for Standards for Nuclear Safety, Security and Safeguards (JRC-Geel, former IRMM), the Forschungszentrum Jülich (FZJ, Germany) and the IAEA-Safeguards Analytical Service laboratories in Seibersdorf (SGAS, Austria) joined forces to produce and characterise micrometre-sized uranium oxide particles, which can be used as RMs for Safeguards purposes [4,5]. One of these produced uranium microparticle materials is currently being certified at JRC-Geel G.2 in compliance with the ISO 17034 [6], not only for the uranium isotopic composition of the particle, but as well for the uranium content and mass per particle. Such CRM will be of great importance for the IAEA-NWAL in order to optimise the overall transmission efficiency in Large Geometry Secondary Ion Mass Spectrometry (LG-SIMS) [7], but will be as well beneficial for the analysis with (Fission-Track) Thermal Ionisation Mass Spectrometry (TIMS) [8,9] and Laser Ablation Inductively Coupled Mass Spectrometry (LA-ICP-MS) [10], both instrumental techniques being used in particle analysis.

## 2. General context

The JRC-Geel has a long experience in providing the Safeguards community with (certified) reference materials, reference measurements and conformity assessment tools (i.e. inter-laboratory comparisons, proficiency tests).

### 2.1 Previous NUSIMEP campaigns

The Nuclear Signatures Inter-laboratory Measurement Evaluation Programme (NUSIMEP) was established in 1996 as an external quality control programme organised by the JRC-Geel G.2 unit, for nuclear safeguards and environmental laboratories which are involved in the analysis of uranium and plutonium containing materials from the nuclear fuel cycle and nuclear signatures in the environment. During NUSIMEP inter-laboratory comparisons (ILCs), participating laboratories receive materials (known as test items) for the measurements of the amounts and of the isotopic abundances of uranium and plutonium present as traces in environmental samples. This gives the opportunity to participating laboratories to demonstrate their measurement capabilities to customers, accreditation bodies and safeguards authorities.

In this context, JRC-Geel G.2 unit developed uranium particles from certified  $UF_6$  reference materials that were similar to the particles possibly collected on swipe samples by the safeguards inspectors in nuclear facilities. These materials, which were thus "certified" for uranium isotopic abundances of the sub-micrometre-sized particles, were used in the ILCs, NUSIMEP-6, which was completed in 2008 [11] and in NUSIMEP-7, which took place in 2011 [12]. Both NUSIMEP ILCs mainly addressed the IAEA-NWAL, although they were also open to all laboratories carrying out particle analysis in various application fields. Participating laboratories in these two NUSIMEP ILCs were asked to measure, using their standard/routine analytical methods, the uranium isotopic compositions in hydrolysed  $UF_6$  particles with various isotopic compositions.

NUSIMEP-6 and NUSIMEP-7 were of great use to investigate the performances of the different analytical techniques used in particle analysis. But they were as well a good opportunity to collect feedback from the participants on future improvements and needs, which highlighted the need for a mono-disperse uranium oxide microparticle reference materials and material with a lower population density of particles.

## 2.2 Uranium particle reference material as test item for NUSIMEP-9

In the framework of a collaborative project between the JRC-Geel G.2, FZJ and IAEA-SGAS micrometre-sized uranium oxide ( $U_3O_8$ ) particle materials were produced in compliance with ISO 17034 [6] from uranium (mother) solutions certified by JRC-Geel for the uranium isotopic compositions [4,5]. Following IAEA's recommendations for such reference material, the particles had to be produced as a Low Enriched Uranium (LEU) with  $^{235}U$  abundance in the 3 -5 % range and a  $^{236}U$  isotopic abundance of 20 -100 ppm, to be detectable by most of the commonly applied techniques.

These produced uranium particles were then considered as a candidate reference material for certification according to ISO 17034 [6] and selected as well as test item for the inter-laboratory comparison/proficiency test NUSIMEP-9 according to ISO 17043 prior to the release of the CRM [13].

The solution, used for the production of the uranium particles, was prepared by mixing the certified uranium solutions IRMM-023 and IRMM-029 [14,15]. Then, based on a special processing set-up designed at the Forschungszentrum Jülich, using a vibrating orifice aerosol generator (VOAG) to generate droplets and a respective procedure to stabilize and homogenize the particles [16], the produced uranium particles were distributed onto 25 mm diameter glass-like carbon disks.

Process control measurements (verifications) were carried out at the IAEA-SGAS, in compliance with ISO 17025 [17], to guarantee the integrity of the uranium isotope amount ratio values from the solutions to the produced particles. For this purpose, some planchets were leached and the dissolved particles from the uranium nitrate leaching solutions were measured by MC-ICP-MS. The measurement results from the leaching solutions were then compared to the uranium isotopic composition measured in the original (mother) solutions by MC-ICP-MS. These process control measurements showed that during the production of the uranium particles the isotopic composition of the original uranium solutions was not altered when producing the particles.

In addition to the determination of the uranium isotopic composition of the particles, the uranium amount content (mass of uranium) per particle was also determined at JRC-Geel G.2 using Isotope Dilution TIMS (ID-TIMS). Verification measurements of the uranium mass per particle using MC-ICP-MS were carried out at IAEA-SGAS and confirmed the uranium mass per particle value that had been previously determined by ID-TIMS.

A full uncertainty budget of the respective uncertainties for the uranium isotope amount ratios and uranium mass per particle was established in accordance with the "Guide to the Expression of Uncertainty in Measurement" [18].

Scanning Electron Microscopy (SEM) of the uranium particles gave insights on the particle morphology characteristics, confirming their spherical shapes, the absence of significant voids and that the main population of particles was of ca. 1.4  $\mu m$  diameter-sized particles. Following recommendations from the previous NUSIMEP exercises, NUSIMEP-9 test items had also a lower density of particles with roughly 15 000 particles per glass-like carbon disk (carbon planchet).

## 2.3 Homogeneity and stability

According to ISO 17034 and ISO Guide 35 [19], the between-unit homogeneity was evaluated in the candidate test items certification to ensure that the reference values of the test items (certification values for the uranium isotope amount ratios and the uranium amount per particle) are applicable to all produced units of the material, within the stated uncertainties [20]. The homogeneity assessment showed that both the isotopic composition of the particles and the uranium amount per particle are homogeneous throughout the whole batch.

A minimum sample intake of 10 particles was determined for the determination of the uranium mass per particle [20] and corresponds to the minimum size of sample that is representative for the whole unit and guarantees the certified value within its stated uncertainty.

The short-term stability of the uranium particle material was also assessed according to ISO 17034 and ISO Guide 35 to check that the conditions for dispatch of the material to the customers/ILC participants did not change the property/certified values of the material [20]. This study showed that the material is stable within its stated uncertainty and can be dispatched under ambient conditions without further precautions.

## 3. NUSIMEP-9

### 3.1 Scope

Several recommendations were made by the IAEA, during the recent IAEA Technical Meetings on particles, asking for "*future tests using well-characterized materials, to provide a fair assessment of accuracy and precision and encouraging the use of methods to characterize a particle's combined morphology, isotopic, and elemental composition (such as SEM+SIMS/TIMS or LA-ICP-MS)*".

The NUSIMEP-9 inter-laboratory comparison on "Uranium isotope amount ratios and uranium mass in uranium micro-particles" was open to all laboratories performing particle analysis in various application fields. It was, however, more specifically designed for the participation of the IAEA-NWAL, as recommended by the IAEA during the recent IAEA Technical Meetings on particles, giving these laboratories the opportunity to evaluate their performances and analytical methods for the analysis of uranium particles.

Participating laboratories in NUSIMEP-9 received one certified test item of mono-dispersed  $U_3O_8$  particles with an approximate diameter of 1  $\mu m$  deposited on a carbon planchet of 2.5 cm diameter. These certified test items contain some thousands of micro-particles of a single isotopic composition, i.e. with a significantly lower density (lower number) of particles than those of the previous NUSIMEP-6 and NUSIMEP-7 test items, following recommendations of the IAEA and participants in the previous NUSIMEP.

The laboratories participating in NUSIMEP-9 were asked to measure and report the  $n(^{234}U)/n(^{238}U)$ ,  $n(^{235}U)/n(^{238}U)$  and  $n(^{236}U)/n(^{238}U)$  isotope amount ratios of ten particles, which belong to the main particle population. In addition, they were asked to report the average value and its associated expanded uncertainty for each of the isotope amount ratios. The average values of the isotope amount ratios were then compared to the reference values for the test item, as defined during the certification of the candidate uranium particle reference material. The measurements of the three isotope amount ratios were obligatory. Participants were encouraged to use their routine methods for the analysis of the measurands per particle, hence a range of mass spectrometric techniques were expected; from the state of the art LG-SIMS, increasingly used nowadays to analyse particles collected on swipe samples, to Fission-Track TIMS, as well as to the developing LA-ICP-MS [7,21, 22, 23].

Additionally, the participating laboratories were strongly encouraged to measure and report the uranium mass per particle by measuring at least ten particles of the main population. Such measurements are not as commonly carried out for the particle analysis in safeguards environmental sampling but are of particular interest for the optimisation of the overall transmission efficiency for LG-SIMS and uranium mass per particle measurement, which is also relevant for TIMS [24] and LA-ICP-MS.

### 3.2 Organisation

NUSIMEP-9 inter-laboratory comparison was organised according to ISO 17043 [13] and announced for participation beginning of September 2018. The registration for this ILC was open till 19<sup>th</sup> October 2018. At this date, thirty participants from all over the world had registered for NUSIMEP-9. Fourteen out of the participating laboratories are members of the IAEA-NWAL. Some laboratories registered several times in order to carry out particle analysis using different instrumental techniques (TIMS, SIMS, ICP-MS).

Beginning of November 2018, most of the certified test items were sent to the participants within 2 to 5 working days (Figure 1). Together with the test item, participants received an accompanying letter with the instructions for the measurements and their unique participation key, guidelines to guide them through the reporting of the results using the JRC ILC online reporting tool and a confirmation of receipt to be returned by participants in order to confirm the good receipt and attest that the material was in good state, without damages. A unique sample code was attributed to each test item, and linked to the participation key, so as to guarantee both traceability and confidentiality throughout the ILC and the results reporting process.

Participants in NUSIMEP-9 were initially invited to report their results for the uranium isotope amount ratios (compulsory) and uranium mass per particle (optional) for February 19<sup>th</sup>, 2019 the latest. However, this reporting deadline was later extended till March 1<sup>st</sup>, 2019.



**Figure 1: Examples of NUSIMEP-9 test samples and of the accompanying documents for shipment**

### 3.3 Participants in the ILC

For NUSIMEP-9, 28 participants worldwide had registered, and two of them registered twice to be able to use different techniques. Finally, at the end of the reporting period, 23 results had been reported for the uranium isotopic amount ratios and 5 results for the uranium mass per particle (Table 1). Among the participating countries, the five Non-Proliferation Treaty designated nuclear weapon states reported results (see Table 1).

Most of the participants, who could not report in time, experienced some technical/instrumentation issues preventing them from performing the analysis of the test item. Two participants informed that they could not report because they were unable to analyse the sample using their routine and validated analytical method as the uranium concentration of the test item was lower than expected. Another participant could not measure using gamma-ray spectrometry as planned, due to the lower concentration than expected.

Country	Number of participants
Australia	1
Canada	1
China	1
Czech Republic	1
France	2
Republic of Korea	1
Russian Federation	1
Sweden	1
United Kingdom	1
United Nations	1
United States	13

**Table 1** List of participants per country

## 4. Measurement results and preliminary evaluation

### 4.1 Preliminary results

The participants' measurement results were evaluated against the certified reference values as defined during the certification process of the candidate uranium particle reference material in compliance with ISO 17043 and ISO 13528 [25]. Since the candidate particle CRM has not been released yet at the time of this publication, the reference values for the uranium isotope amount ratios and the uranium mass per particle cannot yet be disclosed. Therefore all reported results will be

presented here as deviations in % from the respective reference values. Moreover, full confidentiality is guaranteed with respect to the link between measurement results and the participants' identity. Participants are represented by their respective lab code.

In general, NUSIMEP-9 participants performed well in the reporting of the three uranium isotope amount ratios as measured in the LEU particles and averaged for 10 measured particles. Participants reported most of the major  $n(^{235}\text{U})/n(^{238}\text{U})$  ratios with deviations from the reference value of less than 0.5% (Figure 2), while most of the  $n(^{234}\text{U})/n(^{238}\text{U})$  ratios were reported within 3% of the reference value (Figure 3).

Most of the minor  $n(^{236}\text{U})/n(^{238}\text{U})$  amount ratios were reported with deviations of less than 5% from the reference value (Figure 4). Also, it is interesting to note that a majority of them showed positive deviations, i.e. reported higher ratio values than the reference value.

Finally, although the measurement of the uranium mass per particle was not compulsory and was likely to be challenging for most of the participating laboratories, since not commonly measured as routine analyses of environmental samples. Nevertheless, five laboratories reported this measurand (Figure 5). The spread among these five reported values is quite large, with one participant reporting a uranium mass per particle largely overestimated and one with a reported value with only -0.6 % deviation to the reference value for the uranium mass per particle.

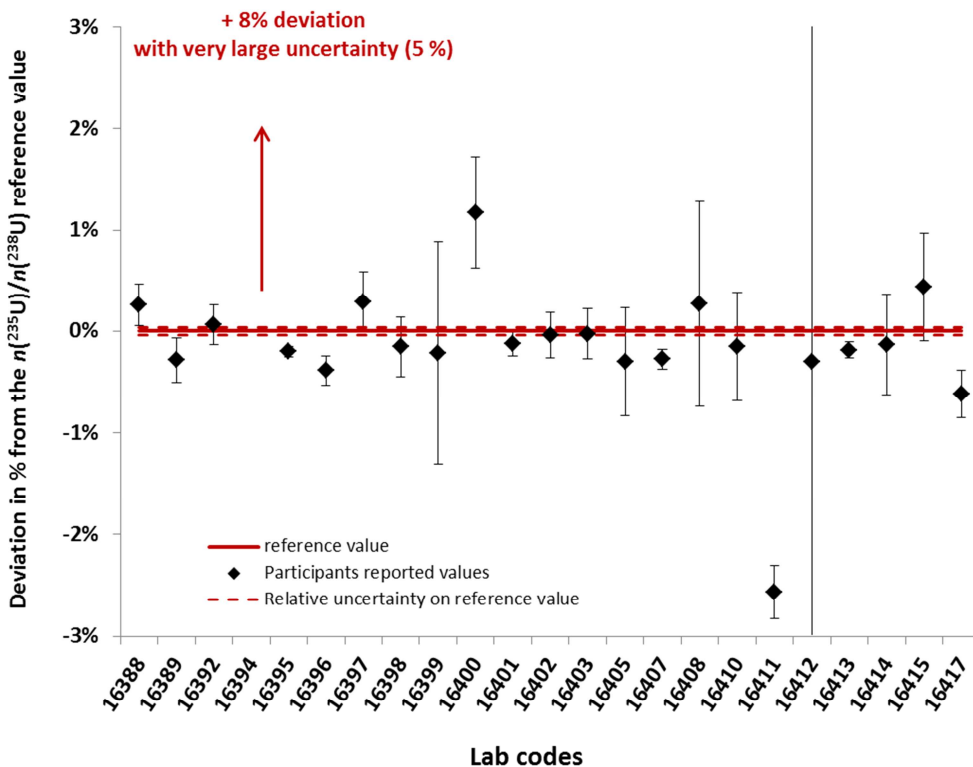


**Figure 2:** Deviation in % of participant reported results (with relative expanded uncertainties, as reported by participants) from the reference value for the isotope amount ratio  $n(^{235}\text{U})/n(^{238}\text{U})$  and its extended relative uncertainty ( $k=2$ ). Note that for lab code 16394, the value is not represented in the graph since deviation to reference value was too large (ca. +8 %).

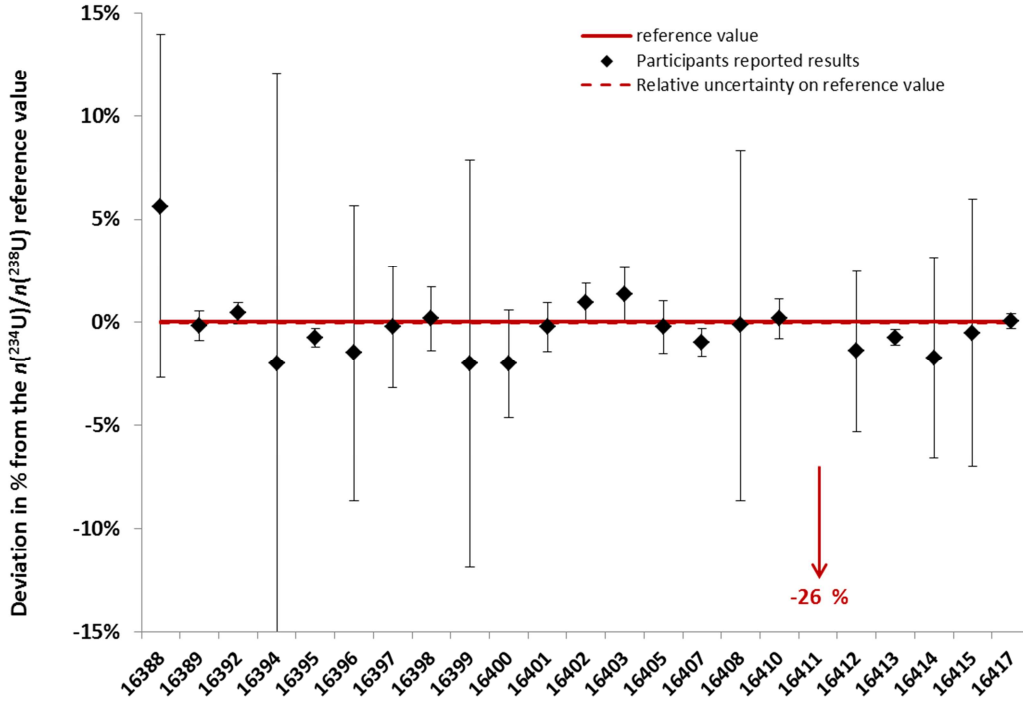


**Figure 3:** Deviation in % of participant reported results (with relative expanded uncertainties, as reported by participants) from the reference value for the isotope amount ratio  $n(^{234}\text{U})/n(^{238}\text{U})$  and its extended relative uncertainty ( $k=2$ ). Note that for lab code 16411, the value is not represented in the graph since deviation to reference value was too large.

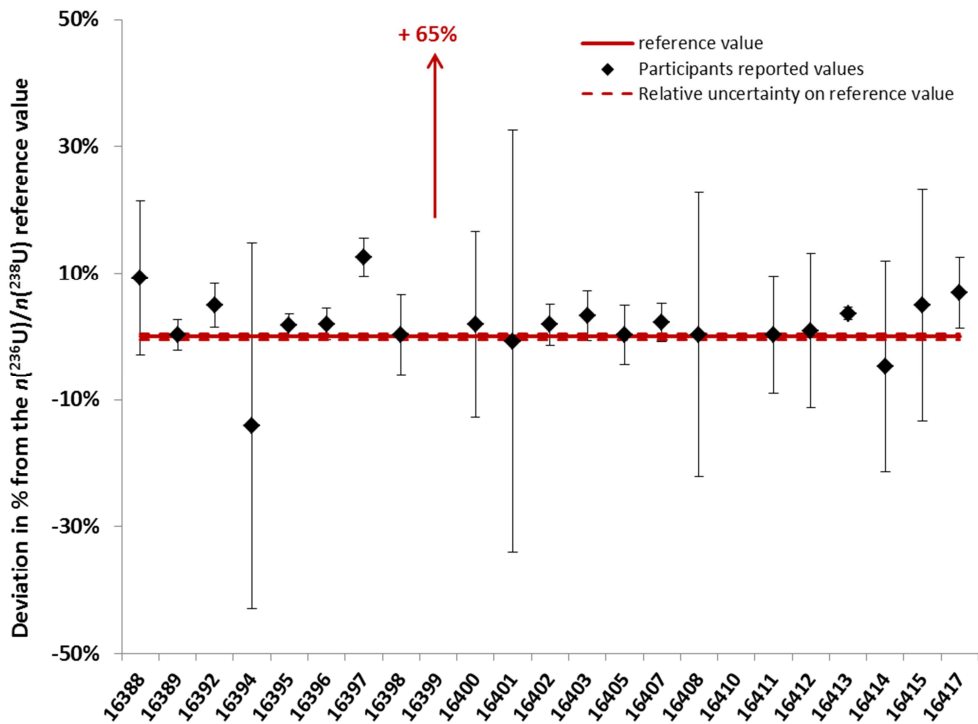


**Figure 4:** Deviation in % of participant reported results (with relative expanded uncertainties, as reported by participants) from the reference value for the isotope amount ratio  $n(^{236}\text{U})/n(^{238}\text{U})$  and its extended relative uncertainty ( $k=2$ ). Note that for lab code 16399, the value is not represented in the graph since deviation to reference value was too large.

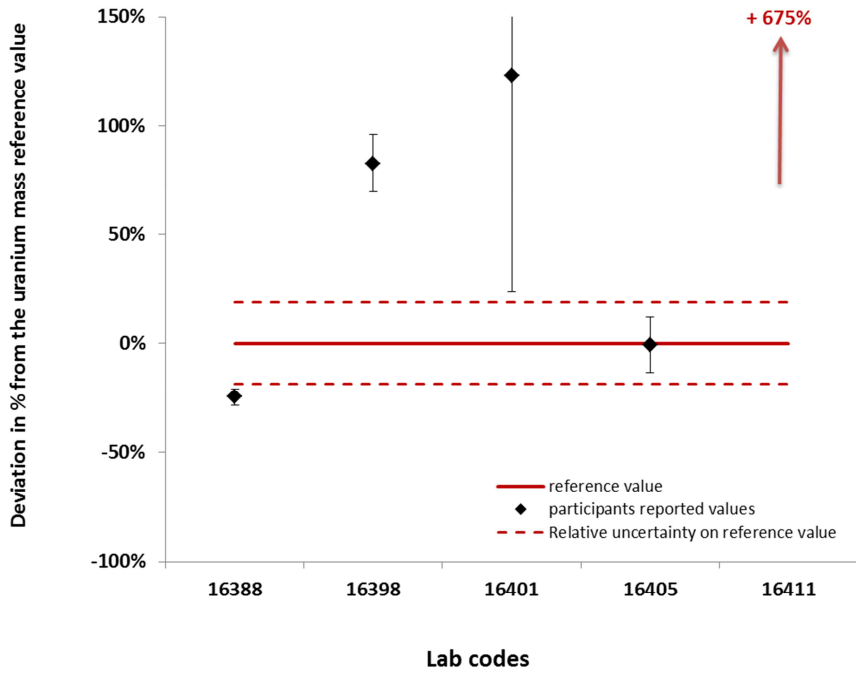


**Figure 5:** Deviation in % of participant reported results (with relative expanded uncertainties, as reported by participants) from the reference value for the uranium mass per particle and its extended relative uncertainty ( $k=2$ ). Note that for lab code 16411 the value is not represented in the graph since the deviation from reference value was too large.

#### 4.2 Evaluation: by means of zeta-scores

The individual laboratory performances for the uranium isotope amount ratios, as done for previous NUSIMEP exercises were expressed by means of zeta scores, as well as performances for the analysis of uranium mass per particle, in compliance with ISO 13528 (see Equation 1).

$$zeta = \frac{X_{lab} - X_{ref}}{\sqrt{u_{ref}^2 + u_{lab}^2}} \quad \text{Equation 1}$$

Where

$X_{lab}$  is the measurement result reported by a participant

$X_{ref}$  is the certified reference value (assigned value)

$u_{ref}$  is the standard uncertainty of the reference value

$u_{lab}$  is the standard uncertainty reported by a participant

The zeta score gives an indication of whether the uncertainty reported by a laboratory is consistent with the laboratory deviation from the reference value. An unsatisfactory zeta score may then depict an underestimation of the uncertainty reported by the laboratory or a large deviation to the reference value. For the zeta scores, the standard uncertainty of the laboratory ( $u_{lab}$ ) was calculated as the reported uncertainty divided by the coverage factor ( $k$ ) provided by participants. The zeta scores can be interpreted according to ISO 13528 as:

- satisfactory performance for  $|score| \leq 2$ ,
- questionable performance for  $2 < |score| \leq 3$ ,
- unsatisfactory performance for  $|score| > 3$ .

Overall, the participants' performances in reporting the three uranium isotope amount ratios as measured in NUSIMEP-9 test items were satisfactory (Figure 6, Figure 7 and Figure 8), indicating that whatever technique was chosen (FT-TIMS, LG- or Nano-SIMS, SIMS or various ICP-MS), participants

managed to successfully measure the major and minor uranium isotope amount ratios, while reporting as well uncertainties in the range of those expected based on the uncertainties for such measurements and the expanded uncertainty on the reference value. It is interesting that participants' performances are even more satisfactory for the minor isotope ratios than for the major  $n(^{235}\text{U})/n(^{238}\text{U})$  isotope amount ratio.

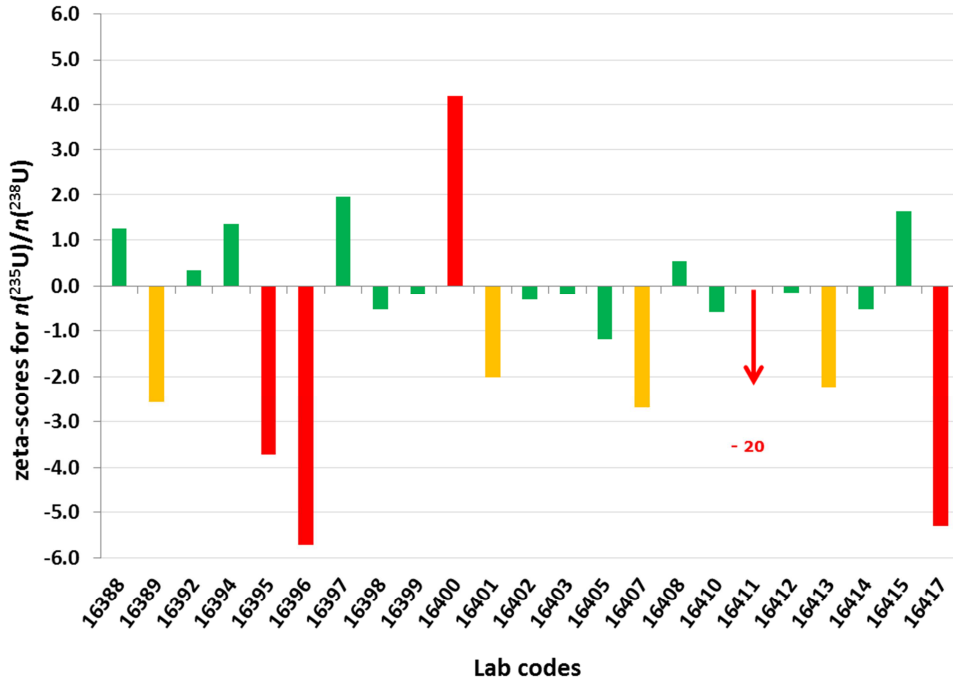


**Figure 6:** Participants' zeta scores for the major isotope amount ratio  $n(^{235}\text{U})/n(^{238}\text{U})$ , where satisfactory performances are represented in green, questionable in yellow and unsatisfactory in red. The zeta-score for lab code 16411 is not represented in the graph since out of scale.

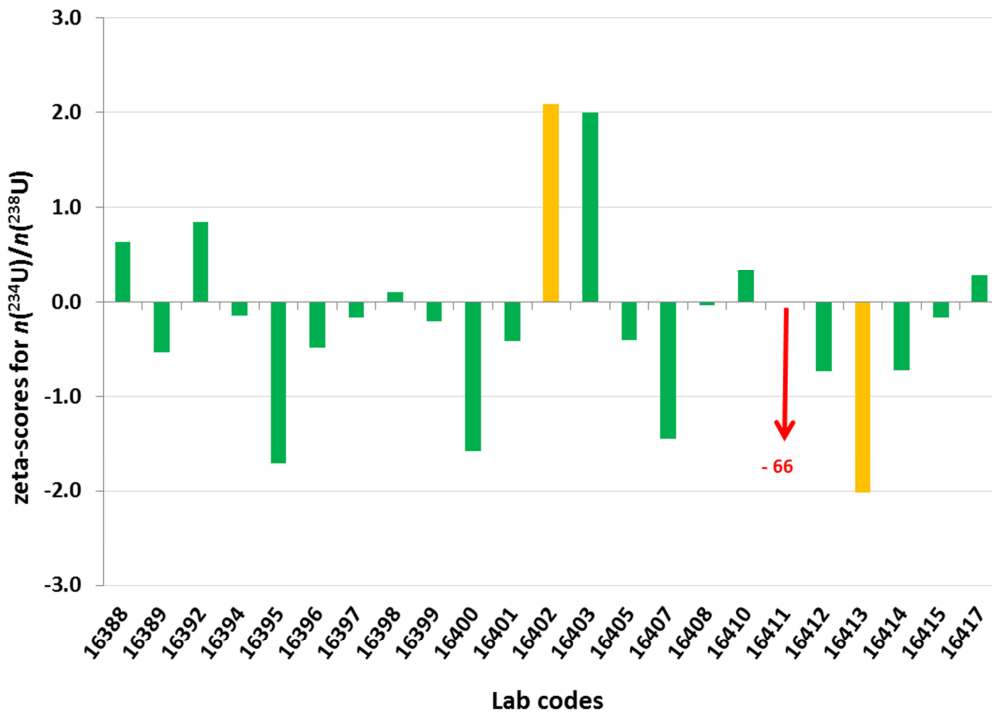


**Figure 7:** Participants' zeta scores for the minor isotope amount ratio  $n(^{234}\text{U})/n(^{238}\text{U})$ . The zeta-score for lab code 16411 is not represented in the graph since out of scale.

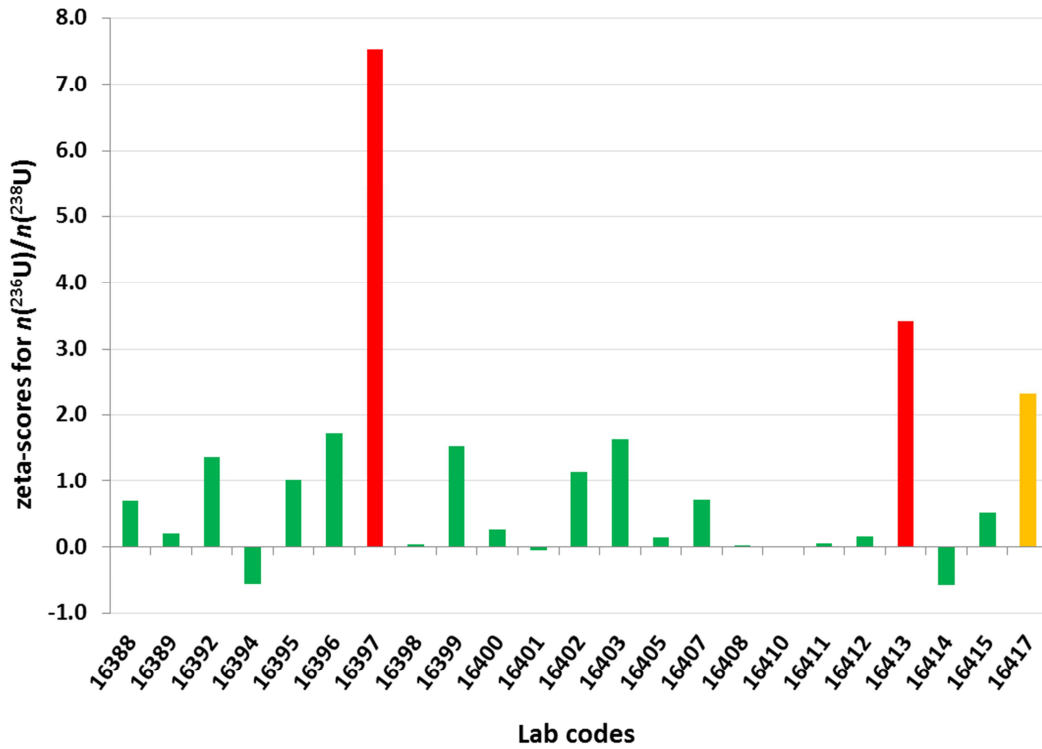


**Figure 8:** Participants' zeta scores for the minor isotope amount ratio  $n(^{236}\text{U})/n(^{238}\text{U})$ . The zeta-score for lab code 16410 is not represented in the graph since the participant did not report any result for this measurand.

For the determination of the uranium mass per particle, the participants' performances are acceptable (Figure 9), especially considering the challenge that this measurement represents for the laboratories, since it is not usually a routine lab procedure and analysis.

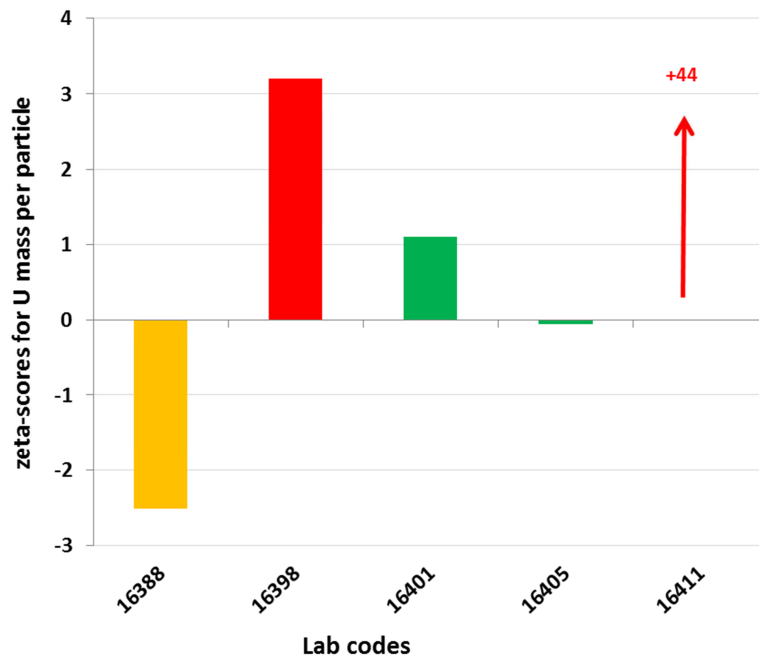


**Figure 9:** Participants' zeta scores for the uranium mass per particle. Lab 16411's performance is not represented in this graph since its zeta-score is too large for the scale of this graph.

## 5. Conclusions

Seven years after NUSIMEP-7, which had been the last ILC organised by JRC-Geel G.2 on uranium particle test items, NUSIMEP-9 gave an opportunity to expert laboratories in the field of particle analysis to evaluate their performance capabilities in the analysis of uranium isotope amount ratios in test items with a low density of mono-disperse particles of LEU isotopic composition. The laboratories' performances using various mass spectrometric techniques for the measurement of uranium isotope amount ratios in NUSIMEP-9 were overall satisfactory. This confirms that, independently of the technique used (LG-SIMS, ICP-MS, FT-TIMS), the uranium test items for NUSIMEP-9 were fit-for-purpose.

Additionally, NUSIMEP-9 offered for the first time to the participants the possibility to determine the uranium mass per particle using their technique of choice. A few participants undertook this challenging analysis and despite the large spread in participants' results, overall performances are satisfactory, with one expert lab even confirming the reference value for the uranium mass per particle in NUSIMEP-9.

The full analysis and evaluation of the results, as well as the analysis of the participants' feedback in NUSIMEP-9 are still on-going, so further insight is expected on the outcomes of this NUSIMEP-9 exercise shortly.

## 6. Acknowledgements

The authors are particularly grateful to the colleagues at Forschungszentrum Jülich for the production of the particles and to the colleagues at the IAEA-SGAS for their support and collaboration on this project.

We would like to thank all the participants in NUSIMEP-9 for their great professionalism and their contribution to this NUSIMEP-9 exercise.

The authors would also like to acknowledge all those who have contributed to the successful completion of NUSIMEP-9 and who have reviewed this publication.

## 7. Legal matters

### 7.1 Privacy regulations and protection of personal data

"I agree that ESARDA may print my name/contact data/photograph/article in the ESARDA Bulletin/Symposium proceedings or any other ESARDA publications and when necessary for any other purposes connected with ESARDA activities."

### 7.2 Copyright

The authors agree that submission of an article automatically authorises ESARDA to publish the work/article in whole or in part in all ESARDA publications – the bulletin, meeting proceedings, and on the website.

The authors declare that their work/article is original and not a violation or infringement of any existing copyright.

## 8. References

- [1] International Atomic Energy Agency. Model Protocol Additional to the Agreement(s) between State(s) and the International Atomic Energy Agency for the Application of Safeguards, September 1997
- [2] General IAEA-TECDOC-1663, *Radioactive Particles in the Environment: Sources, Particle Characterization and Analytical Techniques*, 2011, ISBN 978-92-0-119010-9
- [3] Boulyga et al., *Mass spectrometric analysis for nuclear safeguards*, *J. Anal. At. Spectrom.* 30, 215, 1469-1489.

- [4] Neumeier et al., *Microparticle production as reference materials for particle analysis methods in safeguards*, *Scientific Basis for Nuclear Waste Management XLI*, Volume 3, Issue 19, 2018, 1005-1012, <https://doi.org/10.1557/adv.2018.166>
- [5] R. Middendorp, M. Dürr, I. Niemeyer, and D. Bosbach. *Micro Particle Suspensions for Preparation of Reference Materials for Particle Analysis Methods in Safeguards*. *ESARDA Bulletin*, 54:23-30 (2017).
- [6] ISO 17034:2016 *General requirements for the competence of reference material producers*.
- [7] L. Sangely, et al. *Implementation of Large-Geometry SIMS for Safeguards: 4 years later*. *ESARDA 37th Annual Meeting Proceedings*, 2015, 66:873–883.
- [8] Iguchi et al., *Study on the etching conditions of polycarbonate detectors for particle analysis of safeguards environmental samples*. *Radiation Measurements* 40, 2005, 363 – 366
- [9] M. Kraiem, et al., *Investigation of Uranium Isotopic Signatures in Real-Life particles from a Nuclear Facility by Thermal Ionization Mass Spectrometry*, *Analytical Chemistry* 83, 2011, 3011-3016.
- [10] Lloyd et al. *Precise and accurate isotopic analysis of microscopic uranium-oxide grains using LA-MC-ICP-MS*, *J. Anal. At. Spectrom*, 2009, 24, 752–758
- [11] Aregbe, Y., et al., *NUSIMEP-6: Uranium Isotope Amount Ratios in Uranium Particles*, EUR 23702 EN, 2008.
- [12] J. Truyens, et al., *NUSIMEP-7: Uranium isotope amount ratios in uranium particles*. *Journal of Environmental Radioactivity* 125, 2013, 50-55
- [13] ISO 17043:2010 *Conformity assessment- General requirements for Proficiency Testing*.
- [14] S. Mialle, et al., *Certification of the uranium hexafluoride (UF<sub>6</sub>) isotopic composition: The IRMM-019 to IRMM-029 series*, 2014.
- [15] S. Richter, et al., *Preparation and certification of the uranium nitrate solution reference materials series IRMM-2019 to IRMM-2029 for the isotopic composition*, *Journal of Radioanalytical and Nuclear Chemistry*, 2018 318:1359–1368.
- [16] R. Middendorp, et al., *Characterization of the Aerosol-Based Synthesis of Uranium Particles as a Potential Reference Material for Microanalytical Methods*. *Analytical Chemistry* 89, 2017, 4721-4728
- [17] ISO 17025:2017 *General requirements for the competence testing and calibration laboratories*.
- [18] ISO/IEC Guide 98-3:2008 *Uncertainty of measurement - Part 3: Guide to the expression of uncertainty in measurement (GUM:1995)*.
- [19] ISO Guide 35:2006 *Reference materials – General and statistical principles for certification*.
- [20] Truyens J et al., *Production and certification of of the Uranium Oxide Microparticles IRMM-2329P Certification for Isotope Ratios and Uranium amount per Particle*. *EU Bookshop report, in preparation*.
- [21] Pointurier F., Marie O., *Identification of the chemical forms of uranium compounds in micrometer-size particles by means of micro-Raman spectrometry and scanning electron microscope*. *Spectrochimica Acta Part B* 65, 2010, 797–804
- [22] Stebelkov et al., *Occurrence of Particles with Morphology Characteristics Which Are Typical for Certain Kinds of Nuclear Activity*. IAEA-CN-184/82
- [23] Esaka et al., *Dependence of the precision of uranium isotope ratio on particle diameter in individual particle analysis with SIMS*. *Applied Surface Science* 255, 2008, 1512–1515
- [24] Kraiem et al., *Characterizing uranium oxide reference particles for isotopic abundances and uranium mass by single particle isotope dilution mass spectrometry*, *Analytica Chimica Acta* 748, 2012, 37– 44
- [25] ISO 13528:2015 *Statistical methods for use in proficiency testing by inter-laboratory comparison*.

## Production of Uranium Oxide Microparticles as Certified Reference Materials for Analytical Measurements

**Stefan Neumeier<sup>1</sup>, Philip Kegler<sup>1</sup>, Martina Klinkenberg<sup>1</sup>, Fabian Kreft<sup>1</sup>, Irmgard Niemeyer<sup>1</sup>, Dirk Bosbach<sup>1</sup>, Celia Venchiarutti<sup>2</sup>, Jan Truyens<sup>2</sup>, Stephan Richter<sup>2</sup>, Yetunde Aregbe<sup>2</sup>, Laure Sangely<sup>3</sup>, Naida Dzical<sup>3</sup>, Thippatai Tanpraphan<sup>3</sup>, Stefanie Konegger-Kappel<sup>3</sup>, Zsuzsanna Macsik<sup>3</sup>, Guillaume Stadelmann<sup>3</sup>, Stephan Vogt<sup>3</sup>**

<sup>1</sup> Forschungszentrum Jülich GmbH  
IEK-6: Nuclear Waste Management and Reactor Safety,  
Jülich, Germany

<sup>2</sup> European Commission – Joint Research Centre, Directorate G (Nuclear Safety and Security), Unit G.2 (Standards for Nuclear Safety, Security and Safeguards), 2440 Geel, Belgium

<sup>3</sup> International Atomic Energy Agency, Safeguards Analytical Services, 2444 Vienna/Seibersdorf, Austria

### **Abstract:**

*Quality Assurance and Control (QC) of analytical measurements on nuclear safeguards samples are of utmost importance to maintain the International Atomic Energy Agency's (IAEA's) credibility with its Member States. To implement a robust QC system for measurements of individual particles collected by inspectors on swipe samples during inspections, reference materials in microparticulate form are needed.*

*For this purpose, a reliable process was developed and established at Forschungszentrum Jülich (FZJ), capable of producing uranium oxide microparticles with well-defined properties, such as monodisperse particle size distribution and consistent isotopic composition. The produced particles are intended to be used as QC materials and selected batches will be certified as reference materials (CRM) for particle analysis methods in Safeguards.*

*A batch of uranium oxide microparticles samples was successfully produced, characterised by the IAEA and the Joint Research Centre (JRC) in Geel and finally certified for the amount of U per particle and the uranium isotope ratios by JRC-Geel G.2 according to ISO 17034. Some of these uranium particles samples have been used in a current interlaboratory comparison exercise in the framework of Nuclear Signatures Interlaboratory Measurement Evaluation Program (NUSIMEP) organised by the JRC-Geel G.2. Future research activities will focus on the production and characterisation of microparticles with well-defined mixed elemental compositions, such as Ln/U, Th/U and Pu/U microparticles. First neodymium doped uranium oxide microparticles with monodisperse size distribution were recently produced with the procedure established in Jülich.*

**Keywords:** Reference materials; Uranium oxide microparticles, Quality Assurance and Control

## 1 Introduction

In the implementation of safeguards, to detect undeclared nuclear material and activities, environmental swipe samples may be collected during in-field verification activities. These samples are screened, anonymised and shipped to the IAEA's Network of Analytical Laboratories (NWAL). The NWAL applies sensitive analytical methods for the analysis of elemental and isotopic composition of nuclear fuel cycle related signatures collected on swipe samples.

Over the last few years highly sensitive methods such as Large Geometry – Secondary Ion Mass Spectrometry (LG-SIMS), Thermal Ionisation Mass Spectrometry (TIMS) and Multi Collector Inductively Coupled Plasma Mass Spectrometry (MC-ICP-MS) have been developed and improved to analyse individual microparticles present on the environmental samples [1]. However, dedicated and well-defined reference materials are needed for quality control measurements, including proficiency testing, method development, optimisation and validation as well as instrument calibration.

Since 2012 FZJ cooperates with the IAEA's Office of Safeguards Analytical Services (IAEA-SGAS) and the JRC-Geel G.2 to develop and establish a process in Jülich laboratories for the production of micrometer-sized uranium oxide particles that can be used as Reference Materials for QC applications.

## 2 Production & characterisation of uranium oxide based microspheres

### 2.1 Production of pure uranium-oxide microparticles

In Jülich, a two-step process for the production of uranium oxide microspheres was developed and established within two doctoral theses [1,2]. The first step is the production and collection of microspheres using a commercially available vibrating orifice aerosol generator (VOAG). The details of the aerosol-based production procedure are explained elsewhere [3-5], but are described briefly herein. A vibrating orifice is fed slowly and homogeneously with a well-defined uranyl-nitrate starting solution forming micro-sized uranyl-nitrate droplets. While passing a connected drying column these droplets solidify to uranyl-nitrate particles by solvent evaporation. Subsequently, these particles decompose through thermal treatment at 500°C forming uranium oxide particles. Finally, solid uranium oxide particles are collected on solid substrates such as quartz discs in an inert vacuum impactor. In Figure 1 the VOAG set-up installed in the FZJ laboratory for the production and collection of microparticles (left) is shown together with a high resolution (SEM) image of a single particle (right).

The particles were thoroughly characterised regarding the morphology, size distribution and elemental composition using Scanning Electron Microscopy with Energy Dispersive X-ray spectroscopy (SEM/EDX), as well as the crystal structure by  $\mu$ -Raman,  $\mu$ -XRD (X-ray Diffractometry) and  $\mu$ -XANES (X-ray Absorption Near Edge Structure spectroscopy). It turns out that monodisperse, orthorhombic  $U_3O_8$  microspheres with a diameter between 0.9  $\mu m$  and 1.4  $\mu m$  (depending on the applied process parameters) are produced using the aerosol-based particle production process [1, 5, 6]. The isotopic composition of the produced microparticles was verified to be consistent with the starting feed solution by advanced mass spectrometry methods performed at IAEA-SGAS (Multi-Collector Inductively Coupled Plasma Mass Spectrometry (MC-ICP-MS)) and JRC-Geel G.2 (Thermal Ionization Mass Spectrometry (TIMS)).

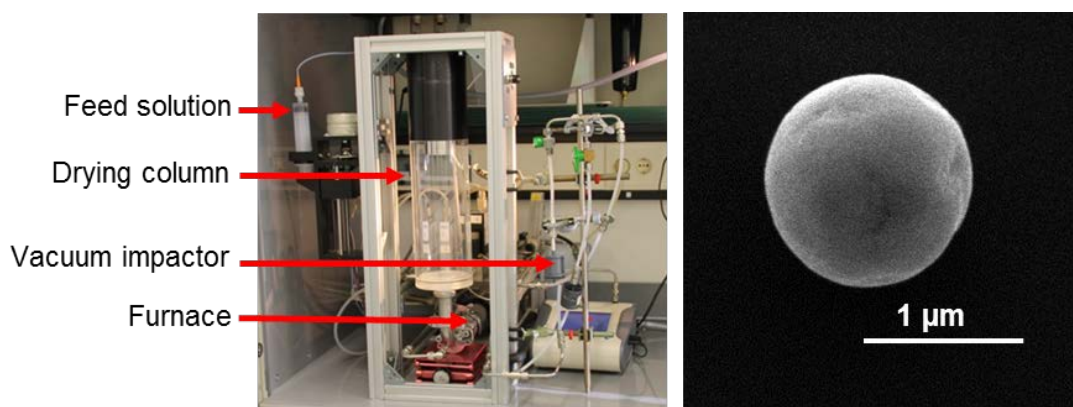


Figure 1: Left: VOAG set-up for production and collection of microparticles at FZJ's laboratory. Right: High resolution SEM image of an individual uranium oxide microparticle.

The second “particles-in-suspension” step aims at the controlled microparticle distribution of uranium oxide microspheres on substrates. In order to prepare the suspension the particles which are collected on quartz discs, for instance, by the aerosol based particle production step are transferred into an ethanol suspension by ultrasonification [7]. Subsequently, the suspension was pipetted onto glass-like carbon discs or even on cotton swipes and carefully dried at 50°C. The chemical stability of the microparticles in ethanol as suspension media was successfully demonstrated by SEM and ICP-MS measurements on samples stored in ethanol over several hundred days [1, 6, 7].

After successfully demonstrating the reproducible production of monodisperse microparticle applying the two-step process developed in FZJ’s laboratory a joint project between the IAEA-SGAS, JRC-Geel G.2 and FZJ was dedicated for the production of microparticles intended to be certified as reference materials for the U amount per particle and the isotopic composition [8].

The initial uranyl-nitrate solution was prepared and analysed by JRC-Geel G.2 and IAEA-SGAS using advanced mass spectrometry methods and finally certified by JRC-Geel G.2.

In the next step, the certified initial solution was used for the production and homogeneously distribution of  $U_3O_8$  particles on glass-like carbon discs using the two-step process established at FZJ. After characterisation of the number and morphology of the microparticles as well as of the particle size distribution by SEM at FZJ, the isotopic composition and the total uranium amount per particle were determined by MC-ICP-MS and IDMS (Isotope Dilution Mass Spectrometry) / TIMS measurements at IAEA-SGAS and JRC-Geel G.2, respectively. Finally, the samples were certified for the uranium amount per individual microparticle and their isotopic composition by JRC-Geel G.2 according to ISO 17034 and successfully used as test sample in an interlaboratory comparison exercise in the framework of Nuclear Signatures Interlaboratory Measurement Evaluation Program (NUSIMEP-9).

## 2.2 Production of Nd-doped uranium-oxide compound microparticles

Besides the pure uranium-oxide microparticles with defined uranium isotopic composition, reference compound microparticles with mixed elemental composition are of high interest for the IAEA’s QC system of analytical measurements. To this purpose, the first Nd-doped uranium oxide microparticles were produced and collected using the VOAG process at FZJ. An initial uranyl-nitrate solution was prepared by dissolving  $U_{Nat}$  oxide CRM from New Brunswick Laboratory (NBL-129A) in suprapur nitric acid and subsequently mixed with 15 mol% Nd-nitrate solution. The VOAG was fed with the mixed solution for the production of compound microparticles adopting the same process parameters from the previous production of the pure uranium-oxide microparticles, such as mass flow, frequency and furnace temperature. Figure 2 is presenting results of the SEM/EDX investigations of the produced compound particles. As expected, the particles produced are well-separated on the surface of the substrate while applying the aerosol-based process. From the SEM measurements a narrow particle size distribution between 1.2  $\mu m$  and 1.3  $\mu m$  very similar to the pure uranium-oxide particles were determined. Finally, the expected Nd-content per particle (16%) was confirmed by EDX measurements.

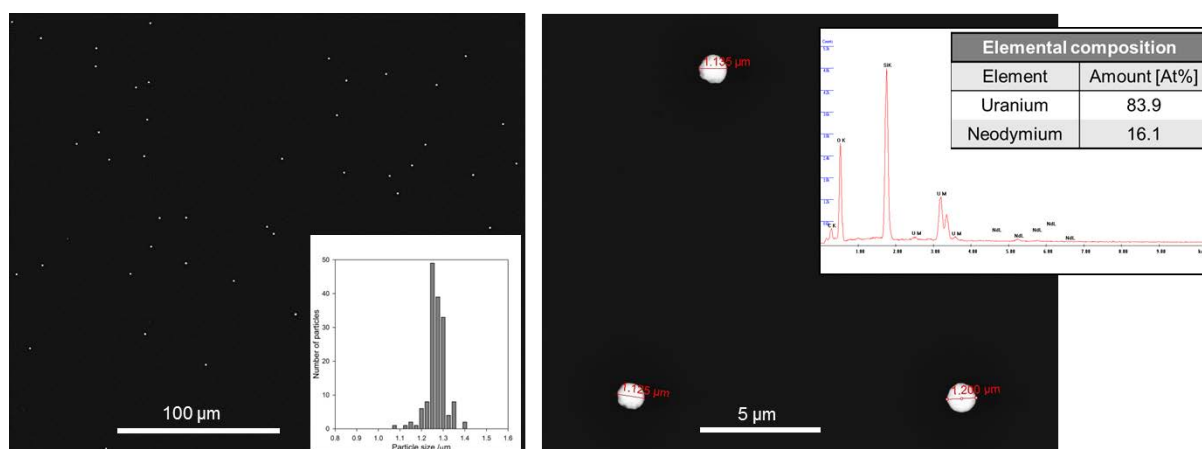


Figure 2. Left: Representative SEM image of the distribution of compound (U/Nd)-oxide microparticles produced by the process established in FZJ’s laboratory. The inset presents the particle size

distribution of produced compound particles. Right: Particle size determination and Nd-content per particle of selected (U/Nd)-oxide microparticles by combined SEM/EDX measurements.

### 3 Conclusion and Outlook

In Jülich a reliable two-step process for the reproducible production of monodisperse pure U-oxide and their distribution on substrates like solid discs was established. The first batch of samples produced in Jülich is certified for the uranium content per individual particles and their isotopic composition. The first production of mixed (U/Nd)-oxide compound microparticles was successfully demonstrated. The compound microparticles are currently subjected to structural investigations by  $\mu$ -Raman and X-ray absorption spectroscopy measurements. These results and ongoing investigations are the first promising steps towards the production of thorium and plutonium-doped uranium-oxide compound microparticles.

### 4 Acknowledgments

This paper benefits from the support of ESARDA, Working Group on techniques and standards for Destructive Analysis (WG DA)". It was prepared as an account of work sponsored by the Government of the Federal Republic of Germany within the Joint Programme on the Technical Development and Further Improvement of IAEA Safeguards between the Federal Republic of Germany and the IAEA. Neither the authors of this paper, nor the organization or industrial company they are affiliated with, nor the Federal Government assume any liability whatsoever for any use of this paper or parts of it. Furthermore, the content of this paper does not reflect any policy of the Federal Government.

### 5 References

- [1] R. Middendorp, "Synthesis and stability assessment of uranium microparticles: Providing reference materials for nuclear verification purposes", *Schriften des Forschungszentrums Jülich, Reihe Energie & Umwelt / Energy & Environment*, Vol. 424, 2018.
- [2] A. Knott, "Production and characterization of monodisperse uranium particles for nuclear safeguards application", *Schriften des Forschungszentrums Jülich, Reihe Energie & Umwelt / Energy & Environment*, Vol. 336, 2016.
- [3] R.N. Berglund, B.H.Y. Liu, "Generation of monodisperse aerosol standards", *Environmental Science & Technology* 7, 147-153, 1973.
- [4] N. Erdmann, M. Betti, O. Stetzer, G. Tamborini, J.V. Kratz, N. Trautmann, J. van Geel, "Production of monodisperse uranium oxide particles and their characterization by scanning electron microscopy and secondary ion mass spectrometry", *Spectrochimica Acta Part B*, 55, 1565-1575 2000.
- [5] R. Middendorp, M. Dürr, A. Knott, F. Pointurier, D. Ferreira Sanchez, V. Samson, D. Grolimund, "Characterization of the aerosol-based synthesis of uranium particles as a potential reference material for microanalytical methods", *Analytical Chemistry* 89(8), 4721-4728, 2017.
- [6] S. Neumeier, R. Middendorp, A. Knott, M. Dürr, M. Klinkenberg, F. Pointurier, D.F. Sanchez, V.-A. Samson, D. Grolimund, I. Niemeyer, D. Bosbach, "Microparticle production as reference materials for particle analysis methods in safeguards", *MRS Advances* 3(199), 1005-1012, 2018.
- [7] R. Middendorp, M. Klinkenberg, M. Dürr, "Uranium oxide microparticle suspensions for the production of reference materials for microanalytical methods", *Journal of Radioanalytical and Nuclear Chemistry*, 318(2), 907-914, 2018.
- [8] S. Neumeier, Ph. Kegler, M. Klinkenberg, D. Bosbach, I. Niemeyer, C. Venchiarutti, J. Truyens, S. Richter, Y. Aregbe, L. Sangely, N. Dzigal, S. Konegger-Kappel, Z. Macsik, G. Stadelmann, T. Tanpraphan, S. Vogt, "Establishing production and provision of microparticle reference materials for particle analysis through collaboration." *IAEA Symposium on International Safeguards: Building Future Safeguards Capabilities - Proceedings, Vienna, CN-267*, 2018.

## Production of Particle Reference and Quality Control Materials

CA Barrett<sup>1</sup>, TR Pope<sup>1</sup>, BW Arey<sup>1</sup>, MM Zimmer<sup>1</sup>, C Padilla-Cintron<sup>1</sup>, NC Anheier<sup>1</sup>,  
MG Warner<sup>1</sup>, AT Baldwin<sup>2</sup>, MG Bronikowski<sup>2</sup>, M DeVore II<sup>2</sup>, W Kuhne<sup>2</sup>, and MS  
Wellons<sup>2</sup>

<sup>1</sup>Pacific Northwest National Laboratory, Richland, WA 99354, USA

<sup>2</sup>Savannah River National Laboratory, Aiken, SC 29808, USA

E-mail: Chris.Barrett@pnnl.gov

### **Abstract:**

*Maintaining the superior performance of new analytical instrumentation and pushing the boundaries of ever-smaller particle analysis by methods such as secondary ion mass spectrometry (SIMS) has become limited by the availability of certified particle standards for calibration, quality control, and validation. To meet this growing demand for a reliable and universal approach to the generation of uranium particle reference material, the Pacific Northwest National Laboratory (PNNL) and Savannah River National Laboratory (SRNL) are collaborating on a joint venture that establishes a number of chemical pathways to the fabrication, purification, and stabilization of uranium particle material to within a fixed particle size range, and well-characterized isotopics. PNNL particle standards are designed and tailored to meet the criteria essential to the calibration and benchmarking of instruments used in both the non-destructive and destructive assay of particulate material, typically collected from environmental swipe sampling. Previous testing and optimization of this colloidal approach to particulate material has centred on tight size distributions, singular composition and density, uniform morphology, and tailored isotopic abundances. Extensive validation of this material has since been performed, both at the National Institute of Standards and Technology (NIST) and the International Atomic Energy Agency (IAEA), demonstrating its suitability for quality control needs of large geometry (LG)-SIMS analysis. Building on this momentum, the production of low-enriched uranium particle reference material, with specially tailored isotopics, has moved from development to full operation. Herein, various aspects of the production cycle will be discussed, including detailed accounts of the technical methodologies being employed, as well as insights into the sample characterization and acceptance testing requirements.*

**Keywords:** particle; standards; uranium; safeguards, synthesis

### **1. Introduction**

Trace analysis of particulate material collected on environmental swipe samples has long been a cornerstone in the IAEA's process of verifying member state compliancy as part of the Non-Proliferation Treaty (NPT).<sup>1</sup> The swipe samples collected by inspectors are taken from the surrounding environment within a nuclear site and then subjected to two primary forms of measurement, namely bulk and discrete analysis. In the first case, the entire cotton swipe is digested and analysed with respect to U, Pu, and other elements present at ultra-low concentration levels. The latter approach takes aim at the precise isotopic analysis of individual U- or Pu-containing particles, with sizes ranging from 1-10  $\mu\text{m}$  typically observed. Discrete analysis of individual particles generally entails the use of both scanning electron microscopy (SEM) and SIMS, both of which are regarded as non-destructive in nature, as the swipe is not destroyed as part of the sample preparation process. By contrast, a swipe is completely consumed by bulk analysis using a combination of high-temperature ashing and acid digestion. While many different isotopic standards, commonly referred to as certified reference material (CRM), are available for destructive forms of assay, notably thermal ionization mass spectrometry (TIMS) and inductively coupled plasma mass spectrometry (ICP-MS), particle standards for SIMS analysis are far less common and more difficult to produce.<sup>2</sup>

In recent years, the IAEA has had limited success in maintaining a steady supply of particle-based standards from the Joint Research Centre's Institute for Reference Materials and Measurements (IRMM), mainly due to the fact that certified particle standards are atypical products for both IRMM, and the New Brunswick Laboratory (NBL) in the US. Because the IAEA requires a longer-term strategy for particle standards supply, production methods have been pursued at the Institute for Transuranium Elements (ITU),<sup>3</sup> as well as by several other member states partnered to the Network of Analytical Laboratories (NWAL).<sup>4-6</sup> While many different technical approaches are being developed, all are constrained by the same stringent requirements necessary for useful particle standards for SIMS analysis. As an example, techniques for the generation of uranium-bearing particles should provide uniform particle morphology and density, narrow particle size distributions (~1  $\mu\text{m}$ ), singular chemical composition (oxides preferable), tailorable isotopic profiles, and a demonstrated shelf-life of 1 year or more. Additional factors to be considered range from the relative structural integrity of the particles subjected to mechanical forces such as sonication or micro-manipulation, to estimates on the rate of U leaching in different storage media.<sup>7</sup> Of paramount importance is the ability of any proposed technique to continually produce unbiased, isotopic uniformity in each batch of material. By their very nature, particles can easily migrate through an environment and deposit across surfaces, which is the premise behind environmental swipe sampling. Consequently, steps to mitigate particle cross-talk must be fully integrated with the design of any production process.

To this end, a method and system of producing  $\text{UO}_2$  particle reference material of a prescribed isotopic profile is introduced. This work is the culmination of collaborative efforts between PNNL and SRNL, under the support of the National Nuclear Security Association and the United States Support Program to the IAEA. The systematic approach laid out in this paper begins with the detailed formulation and blending of CRM to generate uranium material of a desired isotopic composition, followed by chemically transforming it into a suitable precursor form for colloidal synthesis. A tailored synthesis protocol for the generation of  $\text{UO}_2$  particulate is then introduced, including parameters to optimize the technique for specific IAEA requirements. Finally, a thorough characterization of particle properties, including crystallinity, size, shape, and density, is reported. Further, an isotopic evaluation is performed by LG-SIMS, the mass spectrometry technique for which the particles were originally designed. It is hoped that the combined efforts of PNNL and SRNL reported herein demonstrate the viability of this new production process and its potential for delivering uranium oxide particles sourced from current CRM and tailored to the stringent criteria necessary for particle reference materials.

## 2. Uranium Feedstock Formulation

### 2.1. Isotopic Mixing

New QA/QC particulate reference materials may require the formulation of a unique uranium isotopic composition with a specific composition of the four stable U isotopes (i.e.  $^{234}\text{U}$ ,  $^{235}\text{U}$ ,  $^{236}\text{U}$ , and  $^{238}\text{U}$ ). For example, new reference materials may be designed to validate specific environmental sampling scenarios representative of typical nuclear operations, such as uranium enrichment and spent fuel reprocessing, among others. Manufacture of the desired uranium isotopic composition requires the mixing of uranium starting material with precisely known isotopic content, such as CRMs. CRMs are available commercially from multiple international organizations, both in Europe and the US, and have well-documented and published values for each uranium isotope. Development of the specific mixing recipe for a new QA/QC material involves the reconciliation of available CRM feedstock, their respective expense of procurement, and a desire to minimize the number of CRMs used in a formulation.

Choosing a combination of isotopic standards to incorporate under the specified constraints can be categorized as a convex optimization problem,<sup>8</sup> which can be solved in a variety of ways. In the optimization of isotopic standard mixing, we seek the best way to combine a set of  $n$  reference materials to meet a set of conditions set by the QA/QC material end user (i.e. the IAEA). These constraints are concerned with the content of  $^{234}\text{U}$ ,  $^{235}\text{U}$ , and  $^{236}\text{U}$  and the balance of  $^{238}\text{U}$ . Note that minimizing the computational power necessary to solve the problem is an important consideration, as well as reducing the number of standards used within the mix. Additionally, a range of ratios must be considered for all possible CRM combinations. To date, several methods have been used to generate permutations of all possible mixes of uranium certified reference materials. Described below is the method utilized by initial work in this topic.

The primary method used was a brute force R-based program that created arrays to represent each standard. These were combined into matrices that were multiplied by a content matrix. The content matrix contained four columns that matched an isotopic composition value to each standard in the array. This multiplication generated a list of possible solutions, and such multiplications were performed over the entire problem space. Certain constraints were applied to the problem to generate a set of solutions. Figure 1 provides a visual representation of the possible combinations of all US commercially available uranium CRMs limited to combinations of  $\leq 3$ . For convenience, this plot is labelled in terms of the  $^{235}\text{U}$  enrichment, the  $^{236}\text{U}$  concentration, and the  $^{235}\text{U}/^{234}\text{U}$  ratio. The data points represent  $>10^6$  individual CRM combinations varied in both CRM selection and their ratios. In practice, we have found the 3D representation to be valuable in rapidly determining potentially impossible U isotopic composition targets. The solutions were manually screened, and  $<10$  viable recipe candidates were selected based on factors mentioned previously. This method did not take advantage of programmatic methods to reduce problem complexity and improve computational efficiency. The selected CRM mixing recipes were always checked against two separate independent review calculations to verify the numerical accuracy. We found that a subsequent iterative discussion between the various stakeholders was invaluable to validate and down select the proposed recipes (plus their respective isotopic composition) to a single mixture.

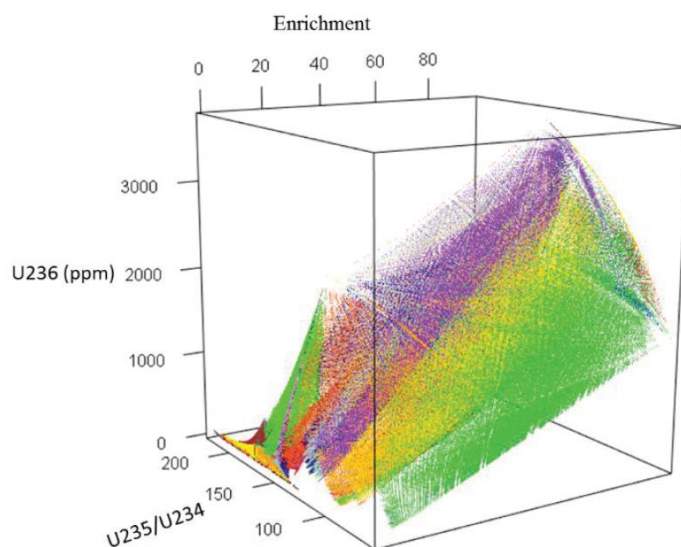


**Figure 1:** 3D plot of approximately  $10^6$  data points representing potential combinations of  $\leq 3$  CRM mixture isotopic compositions in terms of  $^{235}\text{U}$  enrichment,  $^{236}\text{U}$  concentration in ppm, and the  $^{235}\text{U}/^{234}\text{U}$  ratio. Colours are for 3D illustrative purposes only.

Note that due to the proprietary nature of new QA/QC specimens for nuclear safeguards proficiency testing, feedstock and micrometre particle syntheses are discussed in a manner agnostic to specific isotopic compositions.

## 2.2. Chemical Manipulation

CRMs were obtained from the US Department of Energy, NBL Program Office. The mixing ratio and identity of specific CRM combinations was determined by the calculation method detailed earlier in this publication. The overall synthesis scheme is shown in Figure 2, which demonstrates the generic formulation of metal and/or oxide CRM feedstocks into a uranyl acetate product with tailored uranium isotopic content. Mixing of CRMs and subsequent synthesis of uranyl acetate were typically done on the gram scale to ease physical laboratory manipulations and minimize routine sources of measurement errors, such as with balances, pipettes, etc.

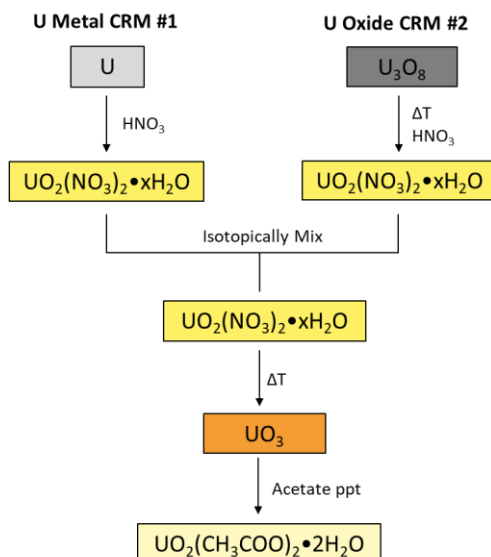


**Figure 2:** Prototypical chemical reaction and manipulation pathway for the dissolution of various CRMs, their mixing, and subsequent synthesis of uranyl acetate with predefined isotopic composition.

A typical uranyl acetate feedstock preparation starts with the dissolution of the CRMs, which are either uranium oxide or metal. Uranium metal rods are broken into pieces and placed in 8 M HNO<sub>3</sub> to remove the oxide layer. After 30 minutes, the pieces are removed, rinsed with water and acetone, dried, and weighed.<sup>9</sup> The pieces are then put into a fresh solution of 8 M HNO<sub>3</sub> to dissolve and form uranyl nitrate (UO<sub>2</sub>(NO<sub>3</sub>)<sub>2</sub>·xH<sub>2</sub>O). The U<sub>3</sub>O<sub>8</sub> CRMs are heated at 400°C for 2 hours to drive off water in accordance with recommended practices. After cooling, the U<sub>3</sub>O<sub>8</sub> was weighed and dissolved in 8 M HNO<sub>3</sub> with heating at 60°C to generate a second uranyl nitrate solution.

Portions of the two uranyl nitrate solutions were mixed based on a previously calculated recipe to generate a uranyl nitrate solution with the desired isotopic composition. The product was subsampled and analysed by TIMS to verify the isotopic composition. The uranyl nitrate solution was heated at between 80°C and 100°C until dryness to form a nitrate solid salt of the isotopically mixed crystalline hydrate. Next, uranyl nitrate was heated at first at 120°C to remove water and then at 400°C for 2.5 hours to generate the gamma phase of UO<sub>3</sub>.<sup>10</sup> The UO<sub>3</sub> was allowed to cool before being weighed and then a solution of dilute acetic acid was added and heated to 50°C. The material dissolves and upon evaporation precipitates as uranyl acetate, which was filtered and washed first with cold dilute acetic acid and then with water.<sup>11</sup>

The isotopically mixed uranyl acetate product was characterized by Raman spectroscopy, fluorescence spectroscopy, and powder X-ray diffraction (PXRD) to verify the material phase and identify any other potentially undesirable chemical phases (e.g. schoepite, uranyl carbonate, etc.). Once the acetate material phase was confirmed, the product was subsampled again and analysed with TIMS to confirm isotopic content. Uranyl acetate slowly degrades in ambient conditions by reaction with atmospheric moisture, and therefore, all product was stored in nitrogen-purged containers within double mylar containers that included desiccating capsules. All laboratory workspaces were rigorously cleaned between before and after synthesis of the CRM mixed uranyl acetate product to avoid contamination between batches.

### 3. Production & Processing of UO<sub>2</sub> Particle Standards

#### 3.1. Reaction Procedure

A facile hydrothermal route for the phase-controlled synthesis of highly crystalline UO<sub>2</sub> particles was developed and tailored to meet the desired characteristics needed for the milligram synthesis of particle standards. The technique can be described as a scalable batch reaction, which offers greater batch-to-batch repeatability and can be easily tuned to vary the material yield within the order of a few milligrams,

all the way up to 200 mg. Hydrothermal synthesis is a well-established method of synthesizing colloid particles using a combination of high temperature and pressure.<sup>12</sup> In this way, reaction mechanisms not achievable at standard temperature and pressure can be performed within the confinement of a Teflon-lined pressure vessel, as shown in Figure 3. The specific method described herein uses organic amines as both reducing agents and structure-directing ligands, further simplifying the synthetic procedure. In its acetate form, uranyl ions are found to readily complex with ethylenediamine, which then undergo a thermolysis reaction that triggers the nucleation and growth of  $\text{UO}_2$  crystals. In using a sealed reaction vessel during heating and synthesis, considerations for safe operation and handling of radioactive material are streamlined, adding multiple layers of containment and providing a simple means of mitigating any batch-to-batch “cross-talk” between particles of different isotopic profiles.

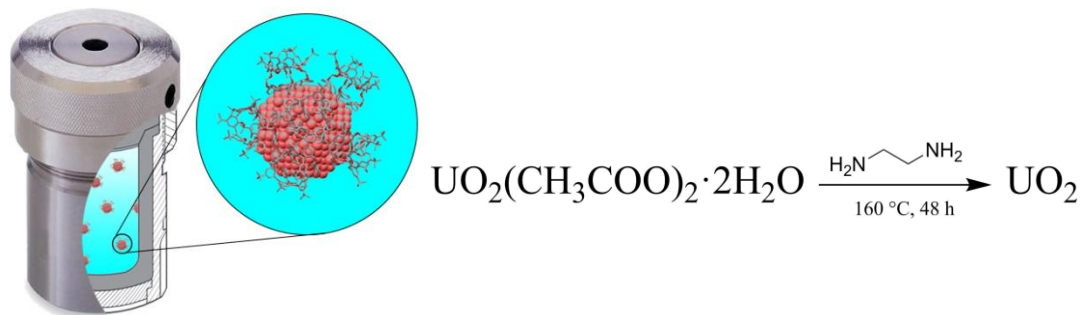


**Figure 3:** Hydrothermal reaction vessel comprised of a Teflon insert encased in a stainless-steel housing and the prototypical chemical reaction scheme for the synthesis of  $\text{UO}_2$  particles.

For this study,  $\text{UO}_2$  particles were synthesized by the following protocol: 0.05 mmol (20 mg) of uranyl acetate ( $\text{UO}_2(\text{CH}_3\text{COO})_2 \cdot 2\text{H}_2\text{O}$ ) and deionized water (15 mL, 0.833 mol) are mixed to form a homogeneous solution under vigorous stirring. Once the uranyl acetate is completely dissolved, 8.5 mL of glacial acetic acid ( $\text{CH}_3\text{CO}_2\text{H}$ , 0.15 mol) is added and stirred for 20 minutes. To this yellow solution, 5 mL of ethylenediamine ( $\text{C}_2\text{H}_4(\text{NH}_2)_2$ , 75 mmol) is added dropwise under continuous stirring for 20 minutes. After the potential of hydrogen (pH) equilibrates, a surfactant can be added to the solution as an additional growth-directing agent. The resulting solution is then sealed in a 25 mL Teflon-lined, stainless-steel autoclave and heated at 160°C for 48 hours. After the heating step, the reaction vessel is cooled to ambient temperature, and the final product is washed with deionized water and isopropanol several times using bath sonication and centrifugation (4,250 rpm) before being stored over isopropanol. A minimum of 5-7 washing steps are required to remove trace amounts of organic residue on the surface of the particles. Prior to washing with isopropanol, a 15-minute dilute acetic acid (0.1 M) wash under bath sonication is performed to ensure the removal of any trace amounts of schoepite (discussed below).

### 3.2. Hydrothermal Synthesis

Under ordinary circumstances,  $\text{UO}_2$  production for nuclear fuel comprises a series of chemical modifications followed by high-temperature annealing (>700°C) of  $\text{UO}_3$  under hydrogen atmosphere. While efficient, the process takes considerable effort and no small degree of risk when dealing with explosive gases. A hydrothermal synthesis, on the other hand, is a simple water-based approach that exploits the reduced nucleation threshold of crystalline  $\text{UO}_2$  material when under pressurized conditions. By carefully controlling the starting conditions of the hydrothermal synthesis, it is possible to optimize the reaction further. One such optimization involves the reduction of schoepite, a hydroxide species that typically forms under basic conditions, in a range of pH 8-12. Schoepite has a characteristic two-dimensional morphology—distinct from the spherical shape of  $\text{UO}_2$  particles—which is correlated to its layered crystal structure that is comprised of alternating layers of uranium oxide and a hydrated hydroxide species of uranyl oxide. This phase of uranium has an undesired geometry, poor stability in ambient conditions, and a lower density than pure oxides of uranium (e.g.  $\text{UO}_2$ ). While schoepite can be removed by bath sonicating dispersions in dilute acetic acid, the  $\text{UO}_2$  fraction is inadvertently damaged by surface etching. In a less-invasive attempt of mitigating schoepite, the pH of the starting solution can be systematically reduced by controlling the amount of acetic acid added to the initial solution. In this

way, the production of  $\text{UO}_2$  spheres increases to near 100% as the pH decreases to 7.5. Conversely, observations of any schoepite crystals rapidly diminished, with only trace amounts detected on rare occasion. It should also be noted that the schoepite reduces in size as the pH is decreased, visually indicating the unfavourable schoepite growth conditions in the lower, close to neutral, pH range. As the pH is adjusted to neutral and further to the acidic range (pH 6), neither schoepite nor  $\text{UO}_2$  is produced, which is expected, as these phases are both oxide-based and are not stable under acidic conditions.

### 3.3. Crystal Growth & Post-Processing

During synthesis development, batches of  $\text{UO}_2$  particles are screened using transmission electron microscopy (TEM) to evaluate the size, shape, and crystallinity of individual particles. Figure 4(A) and 4(B) show representative images of particles synthesized from a large-batch (200 mg), hydrothermal reaction. Most particles were found to have a spherical morphology, with size distributions shifting to larger diameters (1-3  $\mu\text{m}$ ) for reactions on the scale of hundreds of milligrams to lower diameters (0.5-1.5  $\mu\text{m}$ ) for smaller batches of material (10-20 mg). This level of size control was demonstrated by simply changing the starting precursor concentration while keeping reactor, solution, and reagent volumes constant. In this way, monomer supply to evolving nuclei is far less abundant, which slows the crystal growth and reduces the average diameter of the resulting  $\text{UO}_2$  particles. The corresponding selected area electron diffraction (SAED) pattern shown in Figure 4(B) seems to indicate that the particles are close to single crystal. However, as the diffraction spots are slightly skewed along a specific d-spacing, it is more likely that the particles are pseudo-polycrystalline. Such characteristic would suggest an orientated-attachment mechanism for crystal growth, which would follow that smaller nanosized crystals are first nucleated during the reaction and then agglomerate to further crystallize into larger micrometre-sized particles. In such an instance, nanocrystalline grains assume a preferred orientation that energetically favours attachment. Under tighter ligand and precursor control, it would be possible to synthesize single-crystal  $\text{UO}_2$  particles with ideal density characteristics.

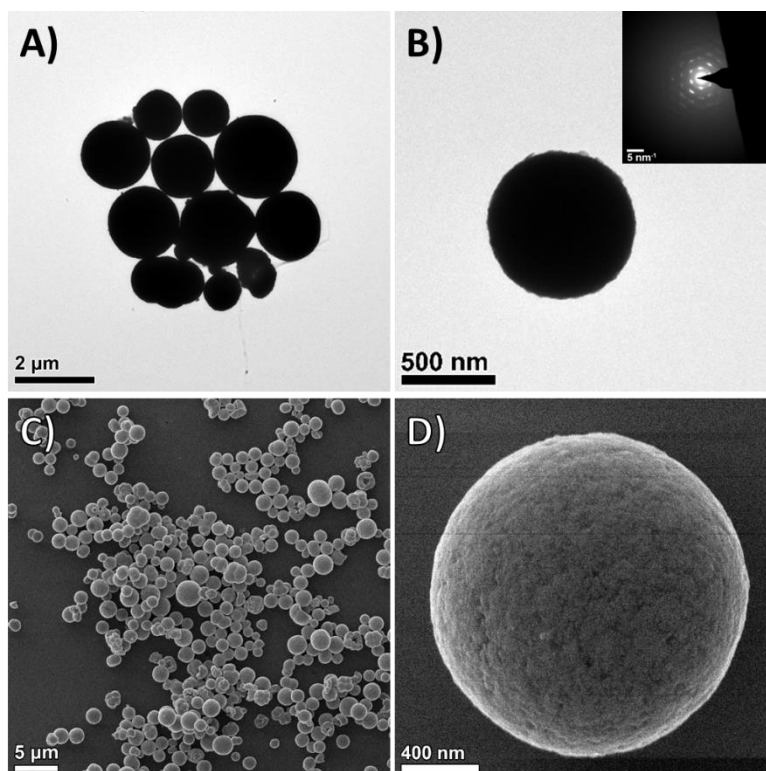


**Figure 4:** (A, B) TEM and (C, D) HeIM images of  $\text{UO}_2$  particles post-processed with solvent washing.

Given that the primary end use for these materials is directed towards particle standards for LG-SIMS, removal of all organic residue from as-synthesized  $\text{UO}_2$  particles was another primary focus of this work.

Many colloidal approaches use high concentrations of surfactant ligands and structure-directing agents, all of which lead to heavy deposits of carbon contamination and poor mass spectrometry measurements. While TEM has proved to be the workhorse instrument for particle screening, helium ion microscopy (HeIM) can be employed for its surface-sensitive imaging capability and capacity to identify any residual organic material. TEM is a transmission-based technique, and so lighter element materials are transparent when imaged by this approach. Electron-based microscopy, both the scanning and transmission variants, typically suffers from what is referred to as a high-interaction volume. This phenomenon arises because of the elevated accelerating voltage and current used to image a sample with electrons, which can reach up to 300 keV in the case of transmission systems. Consequently, the volume of sample releasing secondary electrons increases, and the resulting image can appear transparent and less representative of the surface topography. In the case of high-Z contrast material, the effect is suppressed; however, the low-Z organic residue, often encountered with colloidal synthesis, can be difficult if not impossible to fully observe. To gauge the level of “cleanliness” of our  $\text{UO}_2$  particles, HeIM is used to thoroughly evaluate samples washed with repeated amounts of isopropyl alcohol and deionized water. The end result, as portrayed in Figure 4(C) and 4(D), is well-defined particles in which the surface topography is clearly resolved, with no trace of organic residue detected.

## 4. Material Characterization & Validation

### 4.1. Particle Crystallinity and Size Distribution

Pure oxide of uranium, including  $\text{UO}_2$ ,  $\text{UO}_3$ , and  $\text{U}_3\text{O}_8$ , have extend storage times in both solution and powder form such that particulate materials meet the requirement to maintain a shelf-life of 1 year or more. PXRD analysis is employed to evaluate the chemical composition and crystal structure from the bulk product of each hydrothermal synthesis. In all cases, peak analysis of collected data matched to that of a fluorite crystal structure, indicative of  $\text{UO}_2$  material. Over the course of many different variations of hydrothermal synthesis, only  $\text{UO}_2$  and schoepite were observed from the reaction of uranyl acetate and ethylenediamine. As can be seen in Figure 5(A), precisely tuning the pH of the starting mixture to 7.5 gives a single composition of  $\text{UO}_2$  material. The sharp peak intensities of the observed diffraction pattern are typical of highly crystalline material and provide a useful means of estimating the average density of the particles.

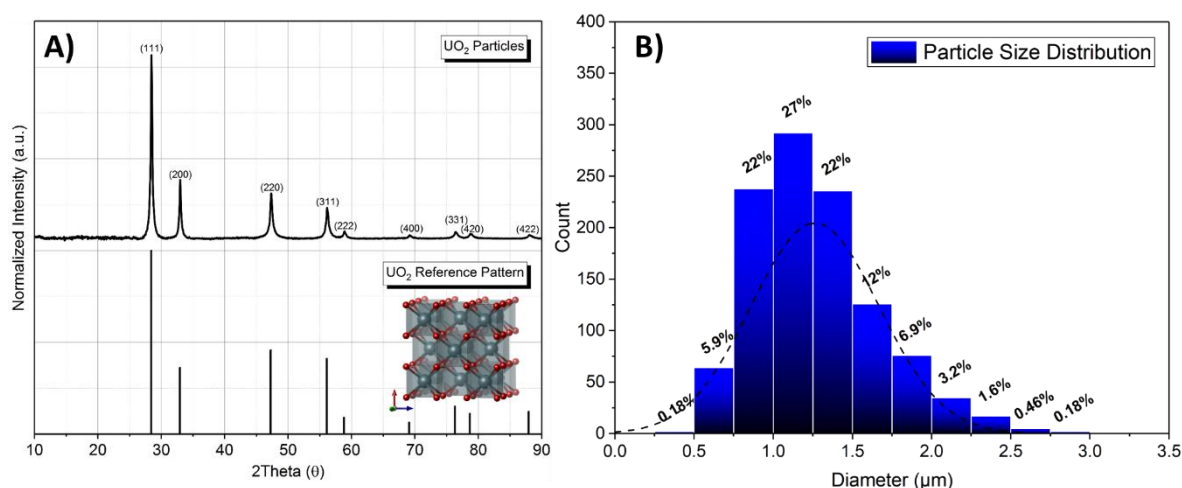


**Figure 5:** (A) PXRD data of the as-synthesized material, including the matching reference pattern of  $\text{UO}_2$  (cubic/fluorite crystal structure, black droplines). (B) Size distribution of all U-containing particles.

Aliquots taken from milligram-sized (~20 mg) reactions of as-synthesized  $\text{UO}_2$  particles are used to prepare a silicon planchet with concentrated areas of particles for imaging and size analysis. Multiple images are then collected at a consistent field of view (100 μm) so that a large population of particles can be measured for a representative estimate of the size distribution. Figure 5(B) summarizes the results from this analysis; however, it should be noted that a circularity filter was used during image

processing to isolate particle agglomerations and instead focus on the measurement of discrete, individual particles. This commonly employed practice of size analysis mitigates the addition of spurious measurements to the overall distribution that might otherwise skew the results in one direction or the other. As can be seen from the plotted size distribution, the largest fraction of  $\text{UO}_2$  particles (27%) are found to have a diameter in the range of 1-1.25  $\mu\text{m}$ . In addition, approximately 55% of particles analysed fell within a size range of 0.5-1.25  $\mu\text{m}$ , a metric mandated by the IAEA in their request for QC particle materials. Roughly 77% of the sample falls within the size range of 0.5-1.5  $\mu\text{m}$ , which gives a corresponding mean diameter of 1.26  $\mu\text{m}$ . However, the median diameter, measured at 1.19  $\mu\text{m}$ , is likely a better reflection of the sample, given the slight downshift in the mean diameter due to a few larger particles in the 2.5-3  $\mu\text{m}$  range, which constitute less than 1% of the total sample.

## 4.2. Microstructure and Density

While estimation of particle density can be qualitatively calculated from bulk PXRD, microstructural analysis of individual  $\text{UO}_2$  particles is a more accurate means of quantifying density and other influencing factors such as porosity and void fraction. For this analysis, a method of particle encapsulation and focused-ion beam (FIB) milling is used to generate cross-sections for internal micro/nanostructural imaging. This process is accomplished by first depositing a thick layer of carbon via electron beam-induced deposition (EBID) that encompasses the entire particle. The surrounding layer of carbon encapsulates the particle, providing support during the FIB milling process and manipulation of the thin particle cross-section. Cross-sections are extracted from individual  $\text{UO}_2$  particles and then mounted such that the inner surface of the particle can be imaged from a side-on perspective using SEM and STEM (Figure 6).

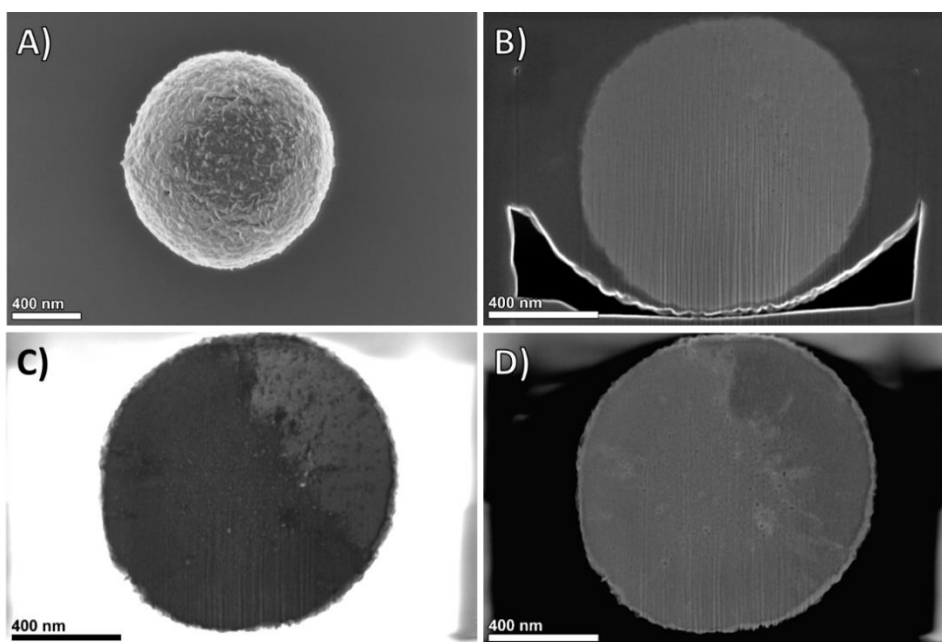


**Figure 6:** SEM images of (A) a 1  $\mu\text{m}$  particle and (B) a FIB-milled cross-section of a carbon encapsulated  $\text{UO}_2$  particle. (C) Annular bright-field and (D) annular dark-field images of the same cross-section.

A representative set of images taken of a 1  $\mu\text{m}$  particle is given in Figure 6. The results highlight near-uniform density expected for crystalline particles, with small amounts of porosity on the order of 4-6%. Cross-sectional images in Figure 6, captured with several different imaging modes, resolved only a minute number of nanosized pores, likely arising from the postulated crystal growth mechanism of orientated-attachment. Estimates for the measured particle void fraction and density were calculated using the theoretical density of single-crystal  $\text{UO}_2$  (10.97  $\text{g}/\text{cm}^3$ ) and the volume of a particle calculated from the diameter observed during SEM imaging. Calculations for the particle shown in Figure 6 were based on a measured diameter of 1.1  $\mu\text{m}$  and a relative porosity of 4.5%, giving an estimated density of 9.23  $\text{g}$  of  $\text{U}/\text{cm}^3$  ( $1.8 \times 10^{10}$  U atoms). A lack of severe porosity of the synthesized particles is an

important result, as the theoretical density of the particles presented in this work is higher than that of other forms of uranium oxide, providing more uranium atoms per particle volume for mass spectroscopy applications.

### 4.3. Isotopic Profile

To facilitate end-user analysis and develop a capability for the selection of specific particles of interest, a technique akin to fission track TIMS can be used to prepare  $\text{UO}_2$  particles on a specialized substrate.<sup>13</sup> As a means of expediting the search routine normally employed to find uranium-bearing particles, a  $500 \times 500 \mu\text{m}$  grid (with letter and number reference markings) is etched into the surface of a vitreous-carbon planchet for particle placement at marked locations. Under SEM imaging, shown in Figure 7A, a nanomanipulator is then used to pick and place particles of interest to the patterned grid. The manipulator, housing a FIB-sharpened tungsten needle, can extract particles from the surface using localized carbon adhesion focused at a point of contact and then places them onto designated regions of a secondary substrate. Once deposited, the particle is held to the substrate via weak forces and can be analysed immediately or, alternatively, held in place via a small amount of deposited platinum (Figure 7B) for long-term storage or shipment. The patterned, vitreous-carbon planchet provides a referenceable grid location (Figure 7C) of each particle placed on the substrate, negating the need to run Automatic Particle Measurement software and expediting the overall measurement time. Additionally, this method provides the opportunity to directly image particles prior to and directly after SIMS analysis. Figure 7D shows a representative sample prepared on a laser-etched carbon planchet.

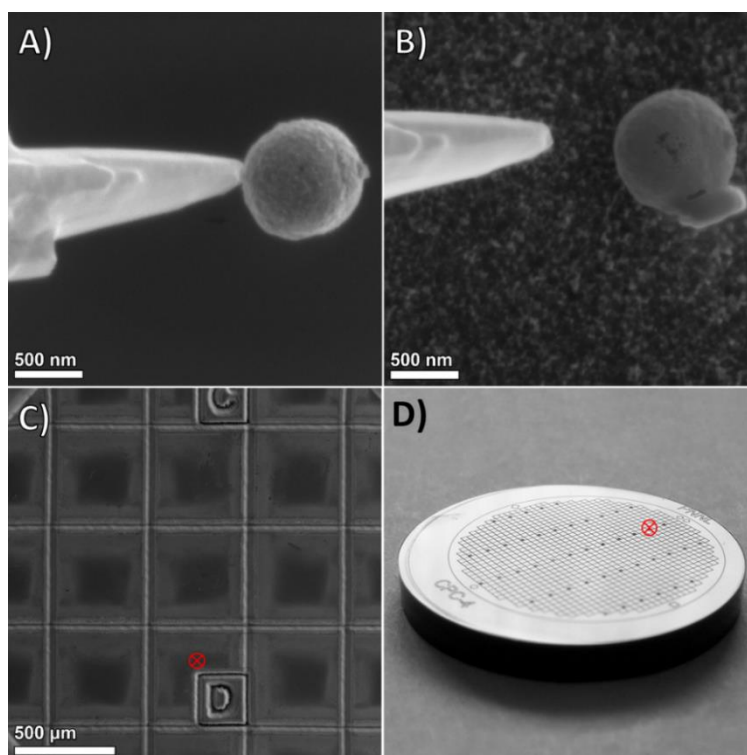


**Figure 7:** SEM images showing (A) the removal of a particle from a silicon wafer, followed by (B) placement on a carbon planchet at a (C) known marked location. (D) Optical image of the laser-patterned planchet.

To test the suitability of the particles to serve as standards in the environmental sampling program for IAEA Safeguards, prepared planchets are evaluated using a Cameca IMS-1280 Large Geometry SIMS. This is the same model that is used for particle measurements by most of the members of the IAEA NWAL. Analyses are performed with a focused primary ion beam of  $\text{O}^{2+}$  at an impact energy of 8 keV. The species detected are positive uranium ions at an energy of 10 keV. The primary beam current and raster-scanned area are adjusted depending on the specific analysis. Uranium-bearing particles are located by real-time scanning ion imaging over a  $500 \times 500 \mu\text{m}$  area with the mass spectrometer tuned

to  $^{238}\text{U}$ . Bright particle images are easily visible against a uniform uranium background after a period of pre-sputtering. A selected target particle is centred on the ion optical axis by translation of the sample stage, and the raster size and beam current are adjusted to  $10 \times 10 \mu\text{m}$  and 200 pA, respectively, for isotopic analysis. In this manner, isotopic measurements of all six particles picked and placed to a patterned substrate can be made, and the results processed to account for signal trending, detector dead time, isotopic mass bias, and hydride correction for  $^{236}\text{U}$ . The results of these isotopic composition measurements are given in Table 1, along with the weighted averages and standard deviations. The measured isotopic variation among the particles is consistent with the internal measurement uncertainty for each particle, and is in good agreement with the bulk analysis of the same material analysed by multi-collector ICP-MS.

Sample	$^{234}\text{U}$	$^{235}\text{U}$	$^{236}\text{U}$	$^{238}\text{U}$	$\phi$ ( $\mu\text{m}$ )
E	0.00088	0.20330	0.00287	99.79295	0.675
ED	0.00062	0.20370	0.00300	99.79268	0.525
DE	0.00067	0.20339	0.00297	99.79296	0.725
D	0.00070	0.20405	0.00295	99.79229	0.850
DC	0.00068	0.20178	0.00309	99.79444	0.600
C	0.00073	0.20099	0.00275	99.79553	0.500
SIMS Average	0.00071	0.20287	0.00294	99.79348	0.645
$1\sigma$	0.00006	0.00121	0.00015	0.00122	
ICP-MS Average	0.000695	0.1984	0.00278	99.798	
$1\sigma$	0.000043	0.0004	0.00009	0.0003	

**Table 1:** Uranium isotopic composition of PNNL particles in atom percent.

Several individual particles were subjected to depth profile measurements by SIMS. Particles were selected in a similar manner to that described above for isotopic measurements, but they were analysed by monitoring the  $^{238}\text{U}$  signal continuously as a function of time until the signal fell to about 1% of its maximum value, and then the integrated number of  $^{238}\text{U}$  ion counts was determined. Two different types of profiles shapes (count rate vs. sputter time) are observed, as illustrated in Figure 8. One type, depicted by particles D and DE, shows a short increase in signal, followed by a gradual signal fall-off, with the entire profile lasting 300-400 seconds. Based on the previous analysis, this behaviour is characteristic of particles at or near a micrometre in size. The other type of profile, illustrated by particles DC and ED, shows an almost immediate onset of a roughly exponential signal decay, and the signal persists for a little less than 200 seconds. This behaviour is characteristic of much smaller particles or of a thin film of uranium. The first profile type contains much higher  $^{238}\text{U}$  counts than the second profile, which is consistent with the smaller particle size measured by SEM. Following SIMS analysis, particles were re-imaged by SEM, where it was found that the depth profile analysis completely consumes the  $\text{UO}_2$ , leaving behind only a small amount of platinum (from EBID) and a sputtered region of about  $12 \mu\text{m}$  in diameter.

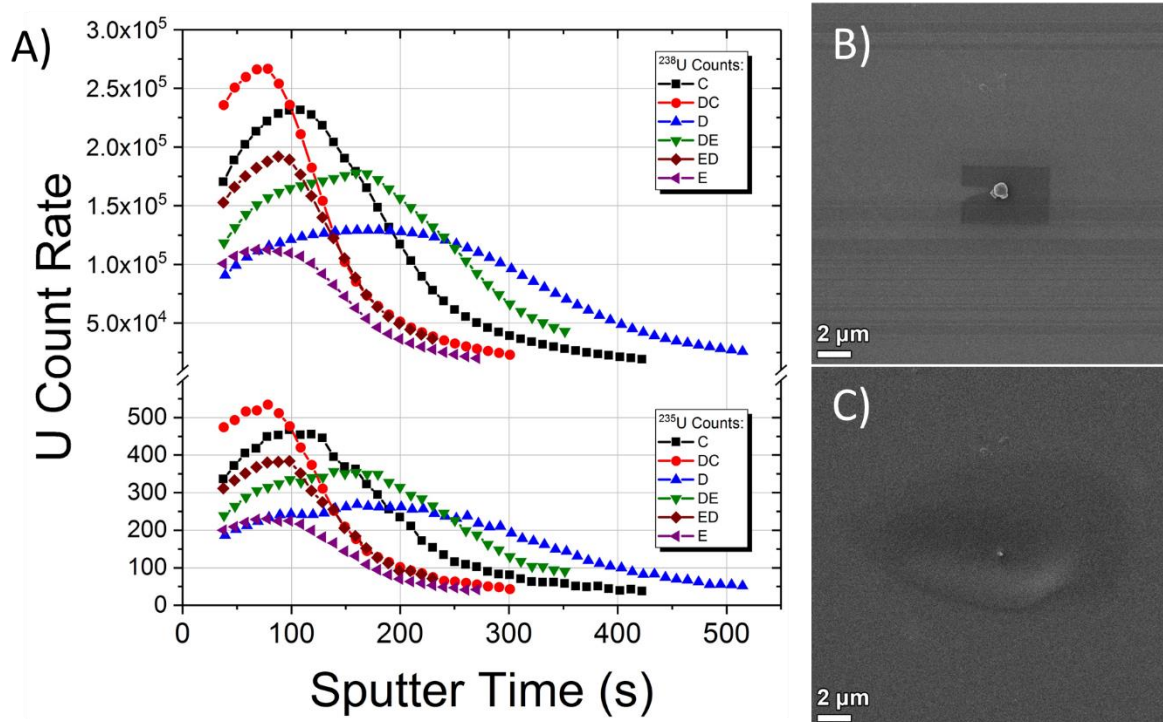


**Figure 8:** (A) The measured trends for count rate over sputtering time, and (B,C) SEM images of  $\text{UO}_2$  particle (designated “DE”) before and after depth profile analysis by LG-SIMS.

## 6. Summary

To tackle the shortfall in particle reference material for nuclear safeguards activities, PNNL and SRNL have devised a multi-step production process to meet the stringent requirements mandated for uranium particle standards. SRNL have developed a unique means of generating tailored isotopic profiles derived from a computational matrix of different blending options available from current CRM inventories. It was also shown that a method of re-crystallising blended material into different chemical forms, more conducive to particle synthesis, could be used following the CRM mixing process. In this way, precursor material of a desired isotopic profile could be prepared at SRNL and shipped in a form compatible with a given synthetic procedure. In the case of this study, uranyl acetate precursor was outlined for PNNL’s synthesis of uranium oxide ( $\text{UO}_2$ ) particle standards, realised by a hydrothermal reaction technique. The colloidal chemistry approach developed at PNNL is tailored for the primary production of  $\text{UO}_2$ , and the minimization of other uranium products—namely, schoepite—and other morphologies. Optimization was accomplished through acid-base equilibrium chemistry (pH control), and control of reactant stoichiometry.

The bulk composition of the produced particles was examined by PXRD and SAED, with both analytical techniques confirming the particles to be highly crystalline and of a single fluorite structural phase. Additionally, particle size analysis from TEM, SEM, and HeIM images showed that the isolated spherical particles had a size range of  $0.5\text{-}1.25 \mu\text{m}$  for a typical synthesis of  $20 \text{ mg}$  batches. If particles could also be produced with much tighter control of particle size and in different size ranges, they could be suitable for other applications such as interlaboratory comparisons and improvement of mass spectrometry measurement techniques. Using FIB and STEM analysis, observations were made of the internal structure of individual  $\text{UO}_2$  particles, with measurements for the void fraction confirming low-levels of porosity ( $4\text{-}6\%$ ), and densities reaching near theoretical levels for  $\text{UO}_2$  ( $9.23 \text{ g of U/cm}^3$ ).  $\text{UO}_2$  particle standards generated by hydrothermal synthesis afford much greater uranium densities compared with other oxide compositions, making them ideal candidates for particle standards analysis. Throughout each phase of the production process, a rigorous handling and cleaning protocol was continually maintained to ensure that batches of particles remained free of cross-contaminants.

Finally, a technique to select particles of specific size and morphology and place them on a laser-patterned grid of a vitreous carbon planchet for SIMS analysis was reported. This approach was then

used in conjunction with a SIMS analysis to assess particle proficiency. Findings from the evaluation study of UO<sub>2</sub> particles suggests that in their present form they could be quite useful as QC samples that the IAEA could introduce to the NWAL as blind samples on cloth. The micrometre size range is typical of the samples that the IAEA collects, and for this purpose, they do not need to be monodispersed. To be useful on a continuing basis, they would need to be produced in batches of various enrichment levels with avoidance of cross-contamination and validation of the isotopic composition after production. It is advantageous that they are not bound to a medium during production and instead can be supplied in a vial for the IAEA to use as it sees fit.

## 7. Acknowledgements

The authors wish to thank the team at the IAEA Safeguards Analytical Laboratory for their expert advice and critical feedback throughout this work. The Pacific Northwest National Laboratory is operated for the U.S. Department of Energy by Battelle Memorial Institute under Contract No. DE-AC05-76RL01830. This work was sponsored by the U.S. Department of Energy, National Nuclear Security Administration, Office of Nonproliferation and Arms Control, International Nuclear Safeguards program.

## 8. References

- [1] Boulyga, S.; Konegger-Kappel, S.; Richter, S.; Sangely, L. *J. Anal. At. Spectrom.* 2015, 30, 1469-1489.
- [2] Mathew, K. J.; Stanley, F. E.; Thomas, M. R.; Spencer, K. J.; Colletti L. P.; Tandon, L. *Anal. Methods*, 2016,8, 7289-7305
- [3] Middendorp, R.; Dürr, M.; Knott, A.; Pointurier, F.; Ferreira Sanchez, D.; Samson, V.; Grolimund D. *Anal. Chem.* 2017 89 (8), 4721-4728.
- [4] Stoffel, J. J.; Briant, J. K.; Simons, D. S. *J. Am. Soc. Mass Spectrom.* 1994, 5, 852-858.
- [5] Erdmann, N.; Betti, M.; Stetzer, O.; Tamborini, G.; Kratz, J. et al. *J. Spectrochim. Acta, Part B* 2000, 55, 1565-1575.
- [6] Kips, R.; Pidduck, A. J.; Houlton, M. R.; Leenaers, A.; Mace, J. D.; Marie, O.; et al. *Spectrochim. Acta, Part B* 2009, 64, 199– 207.
- [7] Middendorp, R.; Dürr, M.; Niemeyer, I.; Bosbach D. *ESARDA BULLETIN*, No. 54, June 2017
- [8] Boyd, S.; Boyd, S. P.; Vandenberghe, L.; Press, C. U., *Convex Optimization. Cambridge University Press*: 2004.
- [9] Lacher, J. R.; Salzman, J. D.; Park, J. D., *Dissolving Uranium in Nitric Acid. Industrial & Engineering Chemistry*. 1961, 53, 282-284.
- [10] Herrmann, W. A., *Synthetic Methods of Organometallic and Inorganic Chemistry Georg Thieme Verlag*: 1996.
- [11] Bagnall, K. W., *The actinide elements. Elsevier Publishing Company*: 1973.
- [12] Nkou Bouala, G. I.; Clavier, N.; Podor, R.; Cambedouzou, J.; Mesbah, A.; Brau, H. P.; Léchelle J.; Dacheux N. *CrystEngComm*, 2014, 16, 6944-6954.
- [13] Admon, U.; Donohue, D.; Aigner, H.; Tamborini, G.; Bildstein, O.; Betti M. *Microsc. Microanal.* 2005, 11, 354–362.

# Characterization of the nuclear material at the particle scale at CEA DAM Ile de France: a powerful tool for Safeguards

Anne-Laure Fauré, Celine Rodriguez and Thomas Dalger

CEA DAM DIF  
91297 Arpajon Cedex, France  
E-mail: anne-laure.faure@cea.fr

## **Abstract:**

*The development of new methodologies for particle analysis is an important challenge for a more comprehensive characterization of the nuclear material operated in a nuclear facility. Every nuclear industrial facility releases particles whose isotopic and elementary composition can be considered as fingerprints of the processes involved. These particles can be easily collected by wiping surfaces inside or in the vicinity of the facility. The analytical methods initially developed focused on the measurement of the isotopic composition of individual particle. Latest developments carried out by the Laboratories dedicated to Safeguards activities have enlarged the range of the particle analysis to identify more precisely the industrial origin of nuclear material.*

*Since 2001 the CEA DAM Ile de France Laboratories are involved in the analysis of actinide traces for Safeguards and are members of the IAEA Network of Analytical Laboratories for environmental samples. After presenting briefly the methodology of isotopic analysis at the particle scale, some recent developments carried out on Secondary Ion Mass Spectrometer will be described. The first one concerns the detection of fluorine in uranium particle which is considered as a fingerprint of the conversion and enrichment activities. The second one is related to the determination of the age of the nuclear material which refers to the last purification step. This characterization at the particle scale constitutes an important step to access to the history of nuclear activities of an inspected facility.*

**Keywords:** Particle analysis, secondary ion mass spectrometry, Uranium, Safeguards

## **1. Introduction**

A challenge of international nuclear safeguards is to detect any undeclared nuclear activities. For that purposes, it has become increasingly important to develop analytical techniques applicable to particulate matter collected at both established nuclear facilities and locations suspected of clandestine nuclear material handling [1]. When nuclear materials are processed, such aerosol particles are released in the immediate environment of the nuclear facility. They can be easily collected by wiping smooth surfaces at various locations inside the facility using square pieces of cotton cloths, referred to as "swipe samples". Because particle isotopic and elementary compositions are representative of the original material, these particles can be considered as fingerprints of specific nuclear processes [2]. The initial goal of the analyses of such samples is to detect the presence of any particles of nuclear materials (mainly uranium) and to determine their isotopic composition. These analyses are predominantly performed by Secondary Ion Mass Spectrometry [3, 4] and Fission Track-Thermal Ionization Mass Spectrometry [5, 6]. Nevertheless isotopic measurements alone are not sufficient to fully characterize a facility or a nuclear process. For instance, the initial steps of the nuclear fuel cycle, from the uranium mining to the conversion activity, may involve only natural uranium. Therefore the isotopic measurement cannot reveal some crucial nuclear operations, like uranium conversion, carried out just before enrichment. In another field, isotopic measurements cannot give access to the history of nuclear activities of an inspected facility: to access this information, the determination of the age, referred to the date of the latest purification, is required.

Therefore latest developments on particle analysis aim to identify more precisely the industrial origin of nuclear material.

Since 2001 the CEA DAM Ile de France Laboratories are involved in the analysis of actinide traces for Safeguards and are members of the IAEA Network of Analytical Laboratories for environmental samples. After presenting briefly the methodology of isotopic analysis at the particle scale, this paper will focused on two recent developments carried out on small geometry SIMS, a Cameca IMS 7F : the detection of fluorine as a fingerprint of the uranium conversion and enrichment activities and the determination of the age of nuclear material.

## 2. Description of the uranium isotopic measurement by SIMS at the particle scale

### 2.1. Sample preparation

The two main objectives of sample preparation for particle analysis are first, not to alter the particulate matter collected on swipe sample and secondly, to preserve it from other environment dust coming for instance from the sample preparation laboratory. To prevent from any contamination, sample preparation is generally performed inside a disposable glove bag under a laminar flow box. Particles are extracted from the swipe using the vacuum impactor technique [7]. This method consists of impacting particles on a carbon planchet beforehand covered with an organic compound, polyisobutylene in nonane, acting as a sticky agent.

### 2.2. SIMS analytical protocol

The determination of the isotopic composition of a uranium particle is generally a two-step protocol. The first step consists in detecting, locating and estimating the  $^{235}\text{U}$  abundance in every particle containing uranium at the surface of the carbon planchet. This search for U particles has been greatly improved by the development of the Automatic Particle Measurement, APM, software by CAMECA which consists in a two-dimensional image scan over a large surface [8].  $^{235}\text{U}^+$  and  $^{238}\text{U}^+$  ion images are acquired by field of  $500\ \mu\text{m} \times 500\ \mu\text{m}$  and data treatment enables to get the particle boundaries, their coordinates and the ratio of  $^{235}\text{U}^+ / ^{238}\text{U}^+$  signals. Therefore, we have access to the isotopic distribution of all the particles collected in the carbon planchet. Particles of interest can be selected according to the  $^{235}\text{U}$  abundance and a precise determination of their isotopic composition is obtained by microbeam analysis which consists of focusing the primary beam onto individual particle and recording the ion intensities of  $^{234}\text{U}^+$ ,  $^{235}\text{U}^+$ ,  $^{236}\text{U}^+$  and  $^{238}\text{U}^+$ . The analytical settings for the two analyses are given in table 1.

Operating conditions	APM	Microbeam
Primary ion current (O2+)	150 nA	250 pA
Raster area	500 $\mu\text{m} \times 500\ \mu\text{m}$	No raster
Dynamic transfer	100%	0%
Mass resolution	450	450
Analyzed masses, in bracket: acquisition time	233 (6s), 234 (6s), $^{235}\text{U}$ (15s), $^{238}\text{U}$ (15s)	$^{234}\text{U}$ (4s), $^{235}\text{U}$ (2s), $^{236}\text{U}$ (4s), $^{238}\text{U}$ (1s), $^{238}\text{UH}$ (1s)
Presputtering time	6 s	0 s

Table 1: SIMS settings for U particle measurement (APM) and U isotopic measurement (microbeam)

## 3. Application of SIMS particle analysis to the detection of fluorine

Fluorine is used in the uranium fuel cycle to convert uranium firstly into uranium tetrafluoride ( $\text{UF}_4$ ) and then into uranium hexafluoride ( $\text{UF}_6$ ) for enrichment purposes.  $\text{UF}_6$  is a very reactive gas that reacts with atmospheric moisture to form uranium oxyfluoride ( $\text{UO}_2\text{F}_2$ ) [9,10]. Given the large amounts of  $\text{UF}_4$

and  $UF_6$  used at conversion and enrichment facilities, very small releases to the atmosphere are common and result in the deposition of particulate  $UF_4$  and/or  $UO_2F_2$  material. So, the detection of a significant amount of fluorine in such uranium particles is a proof that uranium has been converted at one point before the sampling. Based on the same analytical approach, the previous methodology has been modified to enable the simultaneously detection of fluorine and uranium isotopic composition measurement in individual particle.

### 3.1. Materials

Certified Reference Materials and real-life samples collected in a nuclear facility were used to develop the methodology. These materials correspond to different uranium chemical composition representative of some steps of the nuclear fuel cycle. Regarding CRM materials,  $UF_4$  particles from the CRM 17-b material (New Brunswick Laboratory, DOE, USA) and Uranium Ore Concentrate particles from CRMs CETAMA (CEA, France) were used. The nuclear facility that was sampled was an uranium conversion plant that produces  $UF_4$  from UOC. Particles were collected on cotton cloths inside and outside the buildings, but not directly on the bulk nuclear material itself. CP 1 and CP 2 correspond to two different sample locations outside the buildings.  $CP_{Purif.}$  and  $CP_{Fluor.}$  samples were taken inside the buildings, respectively in the purification and fluorination workshops.

For each material, particles were deposited on a cotton cloth (TX 303, Texwipe, NC, U.S.A.) by means of a plastic tip. The particles were then transferred onto a carbon planchet using the vacuum impactor technique.

### 3.2. SIMS analytical protocol

As for the SIMS protocol for the measurement of the uranium isotopic composition, the first step of this new methodology is the automatic search of uranium particles with the APM software. The parameters correspond to those described in table 1 but with the adding of  $^{238}UF$  measurement.

The detection of fluorine is based on the  $^{238}UF$  measurement rather than the F measurement because a preliminary study on  $UF_4$  particles showed that fluorine is better detected at the m/z ratio corresponding to the  $^{238}UF^+$  ions. Once the data acquisition is completed, particles of interest can be selected based on the  $^{235}U$  abundance and/or on the amount of fluorine. Microbeam measurements were then performed on selected individual particles using the same microbeam conditions than those described in Table 1 but once again with the adding of  $^{238}UF$  measurement. The work presented here is based only on the comparison of the relative amount of fluorine between reference materials and real samples. Therefore, the concentration of fluorine in the different particles was not calculated.

### 3.3. Results

Particles coming from the CRM UOC and  $UF_4$  samples and the conversion plant samples were measured according to the methodology described previously. After detection and location of uranium particles with the APM software, fluorine and isotopic measurements were carried out in microbeam mode. Uranium isotopic compositions were all in agreement with the natural uranium composition, with an average atomic isotopic ratio  $^{235}U/^{238}U$  of  $(7.27 \pm 0.21) \cdot 10^{-3}$  (2s). Relative amounts of fluorine for about 10 particles of each sample and their average amounts are compared in figure 1. Fluorine was detected in all the particles. That could be explained by the fact that hydrofluoric acid is used during SIMS manufacturing and that fluorine is released under vacuum from the different parts of the instrument. Nevertheless UOC and  $UF_4$  can be easily identified according to their relative amount of fluorine: fluorine amount in  $UF_4$  particles is two decades higher than in UOC particles. Significant amounts of fluorine were also detected in some particles from the conversion plant. The highest and lowest amounts of fluorine in these CP samples were logically found in the fluorination and purification workshops respectively. However the average amount of fluorine measured in the  $CP_{Purif.}$  sample was higher than the one measured in pure UOC samples. This can be attributed to the closeness between the purification and the fluorination workshops which allows exchange of  $UF_4$  and UOC particles between the two workshops. Concerning the CP1 and CP2 samples, which contain particles collected outside the buildings, larger variations of the amounts of fluorine were observed which is in agreement with the different types of particles present in the facility.

These results confirm that the measurement of the relative amount of fluorine allows discrimination between particles coming from pure UOC material and converted uranium whereas isotopic measurements cannot.

This database can now be used to compare the relative amount of fluorine in unknown real-life samples and to help identifying anthropic uranium from natural uranium.

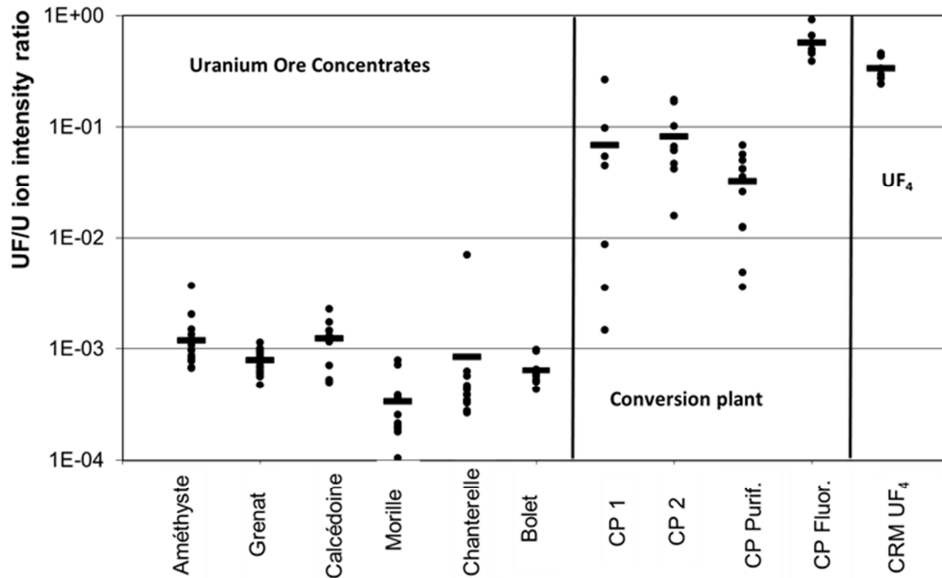


**Figure 1:** Relative amounts of fluorine in uranium particles coming from CRM UOC, conversion plant and CRM UF<sub>4</sub>. Individual measurements are represented by the black dots. The average amount of each sample is represented by the horizontal lines.

#### 4. Application of SIMS particle analysis to the detection of fluorine

In the nuclear field, the “age” refers to the latest purification date. During this step, all the elements are separated from uranium, its daughters included. Two chronometers are of major interest to measure the age of uranium: <sup>230</sup>Th/<sup>234</sup>U and <sup>231</sup>Pa/<sup>235</sup>U. The statement that the measured age corresponds to the purification date can be established under the assumptions of the completeness of the purification of the uranium from its daughter at time zero and the absence of fractionation since production. Because of these assumptions, the “ages” measured by the use of such chronometers are called “model ages”. The model age of uranium particle at time t was calculated using the Bateman equation:

$$t = \frac{1}{\lambda_{234U} - \lambda_{230Th}} \ln\left(1 - R \frac{\lambda_{230Th} - \lambda_{234U}}{\lambda_{234U}}\right) \quad R = \frac{{}^{230}\text{Th}_t}{{}^{234}\text{U}_t}$$

where  $\lambda_{230Th}$  and  $\lambda_{234U}$  are the decay constants of <sup>230</sup>Th and <sup>234</sup>U. The initial amount of <sup>230</sup>Th is assumed to be zero, and the amount of <sup>234</sup>U is assumed to be constant during the elapsed time. More precisely, the decay of <sup>234</sup>U induces a variation of 0.01% in the total number of <sup>234</sup>U atoms over a period of 50 years, which has no effect on the age determination.

The purpose of this work is to develop a direct analysis that simultaneously gives access to the age of uranium particles (by means of <sup>230</sup>Th–<sup>234</sup>U chronometer) and to the isotopic composition.

##### 4.1. Materials

Uranium CRMs (New Brunswick Laboratory, DOE, USA), whose purification dates are known [11], were used to develop the methodology. In order to measure the 230Th+ signal on an individual particle, only enriched CRM were used in this study: U100, U850, U900, and U970. For each CRM, particles were deposited on a cotton cloth (TX 303, Texwipe, NC, U.S.A.) by means of a plastic tip. The particles were then transferred onto a carbon planchet using the vacuum impactor technique. Once the particles were deposited on the carbon disk, the disk was placed in an oven at 400 °C for 30 min in order to eliminate any organic residue that can interfere during SIMS analysis.

The list of the samples used in this paper and their characteristics (isotopic composition and date of purification) are reported in Table 2. The amount of  $^{230}\text{Th}$  per particle was estimated from the equivalent spherical diameter measured with Scanning Electron Microscope XL-30 (FEI, U.S.A.) on 100 particles coming from the reference material U850. Assuming a  $\text{U}_3\text{O}_8$  density ( $8.3 \text{ g}\cdot\text{cm}^{-3}$ ) with a porosity of 30%, the equivalent spherical diameters range from 0.8 to 2.8  $\mu\text{m}$ .

Because size distributions of the other reference materials were comparable, similar equivalent spherical diameters were used to estimate the amount of  $^{230}\text{Th}$  in individual U100, U900, and U970 particles.

CRM	%at $^{234}\text{U}$ ( $\times 10^{-2}$ )	%at $^{235}\text{U}$	Reference date	Estimated $^{230}\text{Th}$ amount per particle (ag)
U100	$6.76 \pm 0.02$	$10.190 \pm 0.010$	8-Jan-1959	0.2–10
U850	$64.37 \pm 0.14$	$85.137 \pm 0.0017$	31-Dec-1957	1.6–69
U900	$77.77 \pm 0.15$	$90.196 \pm 0.011$	24-Jan-1958	2.0–85
U970	$166.53 \pm 0.17$	$97.663 \pm 0.003$	March 1965	3.5–154

<sup>a</sup>Only  $^{234}\text{U}$  and  $^{235}\text{U}$  abundances are reported in this table. Reference date corresponds to the date when purification of the material was completed.

**Table 2:** Characteristics of the uranium CRMs used in this study<sup>a</sup>

## 4.2. SIMS analytical protocol

Two different protocols were used to develop and validate the methodology. The first protocol corresponds to the analysis of carbon planchets containing particles coming from only one CRM. Uranium particles are located with a primary beam intensity of 150 nA and a raster of  $500 \times 500 \mu\text{m}$  at mass to charge ratio,  $m/z$ , corresponding to  $^{238}\text{U}^+$ . Once a particle was located, the age measurement was performed using microbeam conditions to record the ion intensities of  $^{230}\text{Th}^+$  and  $^{234}\text{U}^+$ . The second protocol was used to analyse a carbon planchet containing particles coming from three different CRMs. The first step consists of locating the particles and estimating their  $^{235}\text{U}$  abundance using the APM software in order to identify the different particle populations. The second step consists of analysing individual particles to get their precise uranium isotopic composition and their age. For that purpose, two successive analyses in microbeam conditions are required. Isotopic composition is performed with a very low primary intensity and lasts less than 1 min, keeping enough signals to measure the age. The integration times of  $^{235}\text{U}$  and  $^{238}\text{U}$  isotopes were also fitted to the estimated isotopic composition given by APM measurement in order to get higher counting rates.

Age measurement was carried out in the same conditions as the ones previously described for the first protocol. All the SIMS operating parameters are described in table 3.

Operating Conditions	Protocol 1 Age measurement	Protocol 2 APM measurement	Protocol 2 Isotopic measurement
Primary ion current (O <sub>2</sub> <sup>+</sup> )	2 nA – 5 nA	150 nA	250 pA
Raster area	5 $\mu\text{m} \times 5 \mu\text{m}$ or no raster	500 $\mu\text{m} \times 500 \mu\text{m}$	No raster
Dynamic transfer	0%	100%	0%
Mass resolution	450	450	450
Analyzed masses, in	$^{230}\text{Th}$ (2s), $^{234}\text{U}$ (1s)	$^{235}\text{U}$ (5), $^{238}\text{U}$ (5)	For LEU: $^{235}\text{U}$ (2), $^{238}\text{U}$ (1)

<b>bracket: acquisition time</b>	For HEU: $^{235}\text{U}$ (1), $^{238}\text{U}$ (2)		
<b>Presputtering time</b>	0 s	6 s	0 s

**Table 3:** SIMS settings for age dating measurement

### 4.3. Results

#### 4.3.1 Application to single CRM sample

To demonstrate the feasibility of determining the age of individual particles, each CRM was analyzed separately. Three to five analytical sessions were performed on each material. Results are given in Figure 2.

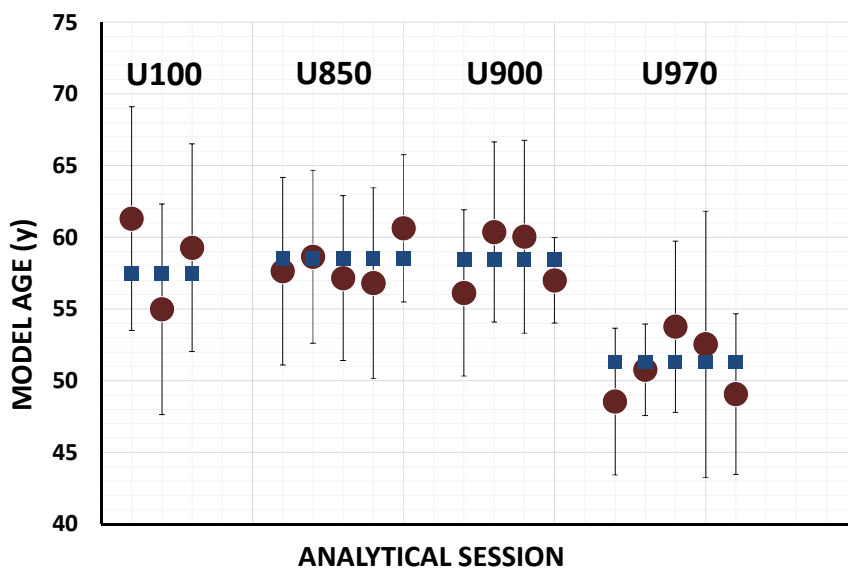


**Figure 2:** Model ages (red circle) of the different CRM particles measured by SIMS. Each point corresponds to an analytical session, in which 4 to 19 particles were analysed. The blue squares represent the reference age. Uncertainties correspond to the standard deviation of each analytical session.

These first results on individual CRM demonstrate the potential of SIMS to determine the age of micrometer-sized particles. Nevertheless, the uncertainties on the model age measured on an individual particle are approximately 10% for HEU CRMs (U850, U900 and U970) and approximately 20% for U100 which are far above the uncertainties achievable by the analysis of ponderable amounts of nuclear materials [12,13].

#### 4.3.2 Application to a mixture of U100 and HEU particles

The methodology was then adapted to be applied to a mixture of U100, U850, and U970 particles loaded on a same carbon planchet in order to demonstrate the possibility of measuring individual ages on a mixture of different isotopic compositions. As described in the paragraph entitled "SIMS analytical protocol", APM was carried out in a first step in order to distinguish and locate uranium particles according their  $^{235}\text{U}$  abundance. The biggest particles of each population were then selected and microbeam analyses were performed. Accuracy on the  $^{235}\text{U}$  abundances is better than 0.5%, even if very short analyses (less than 1 min). Accuracy on the age determination is also better than 4%, which corresponds to about 2 years for the analysed particles. A combination of isotopic measurement and age determination is illustrated in figure 3.

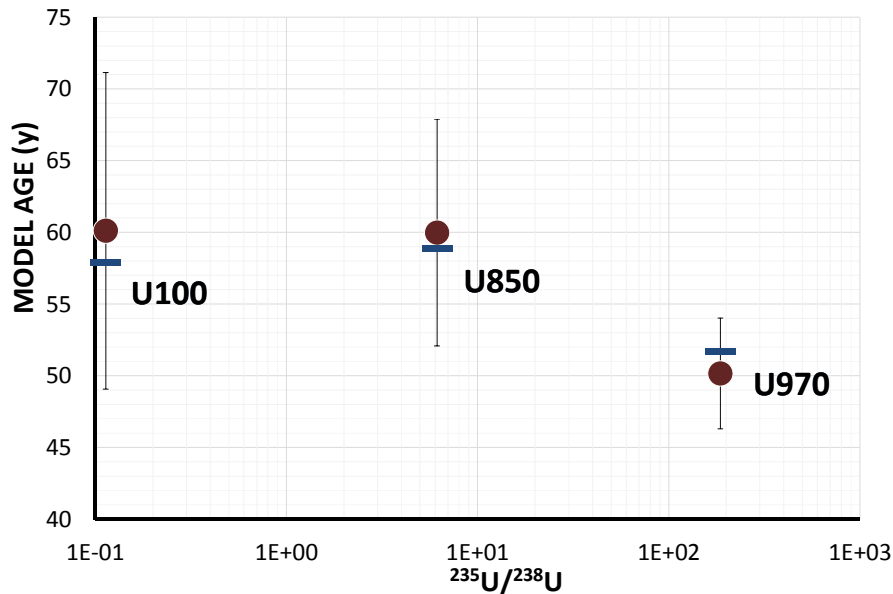


**Figure 1:** Comparison of the model ages and the isotopic composition determined by SIMS at the particle scale (full red circles) and the CRM certified data (blue bars). Uncertainties correspond to one standard deviation.

By comparison, the model age and uranium isotopic ratio that would have been obtained with a bulk methodology have been calculated. Such bulk analysis would have consisted in the dissolution of the entire samples followed by U and Th separation by means of radiochemical treatment. The calculated model age is  $53.1 \pm 1.6$  years, and the calculated uranium isotopic ratio is  $16.458 \pm 0.008$ , which do not correspond to the actual composition of the sample. Consequently, coupling uranium isotopic measurements and age dating at the particle scale is currently the only way to identify the three components of this mixture of materials.

## 5. Conclusion

Thanks to its triple capacity, particle mapping, trace element measurements and isotopic ratio measurements, SIMS can be used well beyond “traditional” nuclear safeguard measurements (U isotope ratio measurements in micrometer-sized particles). SIMS analysis can provide information on the industrial origin of particles and allows for instance the identification of UOC purification, U conversion and U enrichment steps thanks to the simultaneous detection of fluorine and isotopic measurement on individual particle. They can also identify different types of particles that differ in their age and isotopic composition. These measurements enable to trace the history of the nuclear activities of a facility.

## References

- [1] Kuhn E, Fisher D. and Ryjinski M., Environmental sampling for IAEA Safeguards: a five year review. IAEA-SM-367/10/01 2001.
- [2] Pidduck A.J., Houlton M.R., Williams G.M. and Donohue D.L., in Micro-analytical characterization of Uranium particles in support of environmental sampling for safeguards, Institute of Nuclear Materials Management Annual Meeting, Nashville, TN, 2006.
- [3] Tamborini G., Betti M., Forcina V., Hiernaut T., Giovannon B. and Koch L., Spectrochim. Acta, Part A, 1998, 53, 1289–1302.

- [4] Hedberg P.M.L., Peres P., Fernandes F., Albert N. and Vincent C., Journal of Vacuum Science and technology B, Nanotechnology and Microelectronics: materials, Processing, Measurement and Phenomna 36, 03F108 (2018) doi:10.1116/1.5016943
- [5] Lee C. G., Iguchi K., Inagawa J., Suzuki D., Esaka F., M. Magara M., Sakurai S., Watanabe K. and Usuda S., J. Radioanal. Nucl. Chem., 2007, 272, 299–302.
- [6] Baude S. and Chiappini R., IAEA-SM-367-10105, 2002.
- [7] Esaka F., K. Watanabe K., Fukuyama H., Onodera T., Esaka K. T., Magara M., Sakurai S. and Usuda S., J. Nucl. Sci. Technol., 2004, 41(11), 1027–1032.
- [8] Hedberg P. M. L., Peres P., Cliff J. B., Rabemananjara F., Littmann S., Thiele H., Vincent C. and Albert N., J. Anal. At. Spectrom., 2011, 26(2), 406–413.
- [9] Carter J. A. and Hembree D. M., Formation and characterization of UO<sub>2</sub>F<sub>2</sub> particles as a result of UF<sub>6</sub> hydrolysis, Task A.200.3, K/NSP-777, Oak Ridge Gaseous Diffusion Plant, 1998.
- [10] Pickrell P. W., Characterization of the solid, airborne materials created by the interaction of UF<sub>6</sub> with atmospheric moisture in a contained volume, K/PS-144– DE82 015436, Union Carbide Corporation, Nuclear Division, Oak Ridge Gaseous Diffusion plant, 1982
- [11] Croatto, P. U Series Production History; New Brunswick Laboratory: November 2014; p.158
- [12] Lamont, S.P.; Hall, G. J. Radioanal. Nucl. Chem., 2005, 264, 423-427
- [13] Varga, Z.; Suranyi Anal. Chim. Acta, 2007, 599, 16-23

## **Session 5:**

# **Muon and Antineutrino- based methods**

# The AIT-WATCHMAN Project for Remote Monitoring of Nuclear Reactors

Yan-Jie Schnellbach on behalf of the AIT-WATCHMAN Collaboration

University of Liverpool  
Department of Physics  
The Oliver Lodge Laboratory  
Liverpool L69 7ZE, United Kingdom  
E-mail: y.schnellbach@liverpool.ac.uk

## **Abstract:**

*Reactors release antineutrinos in copious amounts linked with the fission process which cannot be shielded. Due to this penetrating property, antineutrino detectors could complement conventional safeguards methods to determine the power and fissile content of reactors under safeguards independent of knowledge of reactor operations, or even exclude the existence of reactors in wide geographical regions. In this presentation, we describe a new initiative known as the Advanced Instrumentation Testbed (AIT). AIT is a joint United States and United Kingdom project to test and demonstrate a range of antineutrino-based monitoring technologies for of nuclear reactors. The first project of AIT is an antineutrino detector located in the North-East England in the Boulby Underground Laboratory with a 1.1 km overburden shielding the detector from cosmic ray interactions. The detector will be located at 25 km standoff distance from the Hartlepool Reactor Complex housing two operational 1.5 GWth reactors. The detector will use 6,000 tons of gadolinium doped water as its antineutrino target and detection medium. The detector walls will be instrumented with several thousand light detectors known as photomultiplier tubes. When an antineutrino from the reactor interacts with the medium, it will produce a tell-tale signature of a prompt flash of light when the antineutrino hits a proton, separated within about 30 microseconds from another flash of light when the neutron released from the original interaction is absorbed on a gadolinium atom. This signal can be easily distinguished from most background signals. The goals of the experiment will be to determine the sensitivity for determining that any reactor is present, and when one, or both of the reactors are shutdown. By measuring signal efficiencies and backgrounds in a controlled but realistic real-world environment, AIT will help explore the prospect of detecting and monitoring smaller reactors at greater standoffs using a scalable water-based technology.*

**Keywords:** remote; monitoring; antineutrino; detector

## **1. Introduction**

Modern nuclear safeguards utilise a wide variety of tools to ensure the goal of non-proliferation of nuclear material. Two key aspects of a comprehensive safeguards regime are validating declared operations and verifying the presence or absence of reactor sites. Antineutrinos have first been recognised as potential signature for reactor monitoring in the 1970s but were challenged by the technical difficulty to do so. However, more recent experiments in the 2000s and 2010s and a greater understanding of the properties of neutrinos/antineutrinos have caused a recent resurgence in interest in antineutrino technology.

This interest in antineutrino monitoring as a safeguards tool is motivated by the fact that antineutrinos are near impossible to block or shield, making their presence an unmistakable marker for a nuclear site. Furthermore, as their emission spectrum and rate are directly related to the burn-up of the fuel, they can also reveal information of the reactor status. Due to the low interaction rate of antineutrinos, such monitoring efforts can be roughly classified into two categories: detectors aimed at validating the declared sites and detectors aimed at determining the absence or presence of an active potentially

unknown reactor. As the former requires a high sample rate, they are usually efforts at small, compact systems to be deployed within near-field (few to tens of meters) of a reactor, such as the SONGS1 experiment requiring access to the reactor site [1]. The latter tends to eschew detailed information about the status and aims to only reveal the presence of a reactor, requiring lower sample rates and larger stand-off distance (hundreds of meters to multiple kilometres) outside of the reactor complex perimeter.

The Advanced Instrumentation Testbed/WATER Cherenkov Monitor for AntiNeutrinos (AIT-WATCHMAN) aims to do the latter by demonstrating nuclear reactor monitoring for non-proliferation purposes over tens of kilometres using a scalable technology.

## 2. Reactor Antineutrinos

As fissile nuclei undergo fission in nuclear reactor, they release energy and leave various fission fragments behind. These fission fragments undergo radioactive decay processes, some of which can release electron antineutrinos. These antineutrinos have very low interaction cross-sections but can be detected in appropriately setup and designed detectors.

### 2.1. Production of Reactor Antineutrinos

During the fission of fissile isotopes, especially uranium and plutonium, various fission fragments are produced, producing antineutrinos while undergoing decay. On average, each fission in a nuclear reactor results in approximately six electron antineutrinos through beta-decay. Hence, an active reactor core emits ca.  $2 \times 10^{21}$  antineutrinos per second per GWth. The energy spectrum of these antineutrinos is dependent on the originating fissile isotope [2]. On average, the antineutrino energy from isotopes in active reactors is ca. 3.5 MeV. Antineutrinos in this energy range have an interaction rate of the order of ca.  $10^{-42} \text{ cm}^2$ , making it very unlikely for them to interact with most matter [3]. As a result, they can leave the reactor itself as well as all surrounding material effectively unhindered. Due to this property, they are a clear and unshieldable signal of any active nuclear reactor, provided they can be detected.

### 2.2. Detection of Reactor Antineutrinos

The main detection mechanism for antineutrinos in the MeV energy range is inverse beta-decay. This process involves the interaction of an electron antineutrino with a proton, resulting in a neutron and positron. Due to the kinematics, the process has a minimum antineutrino energy threshold of 1.8 MeV. While the interaction cross-section is extremely low, the distinct coincidence signal of a neutron and positron provides a power background rejection method.

Water Cherenkov detectors utilise large volumes of water as detection medium. The hydrogen in water acts as target protons for the inverse beta-decay process and the produced positrons can be detected as ring of Cherenkov light inside the volume as they are produced. Due to the optical properties and cost of water, this also allows very large target volumes (ktons to Mtons), which is vital to scale to the large target masses necessary for antineutrinos. The neutrons produced in the inverse beta-decay will thermalize in water for a short period of time (tens of  $\mu\text{s}$ ) and then capture on a nucleus. The gamma-ray cascade produced by the neutron capture will then create Compton electrons in the water, which produce a second Cherenkov light flash. These tell-tale time-delayed coincidence light flashes will originate from a small volume within the water ( $< 1 \text{ m}$  of each other).

Without further dopants, the neutrons will dominantly capture on hydrogen. However, the relatively low neutron capture cross-section of hydrogen (ca. 0.3 b) and energy of the subsequent gamma cascade (2.2 MeV) makes this infeasible for a Cherenkov detector due to the low efficiency and light yield. Hence, in the past, long range observation of reactor antineutrinos was chiefly demonstrated in scintillator-based detectors [4]. However, gadolinium, usually in the form of gadolinium sulphate, can be loaded into the water at a low concentration to increase the neutron efficiency of a Cherenkov detector. Natural gadolinium has a neutron capture cross-section of ca. 49,000 b and releases a ca. 8 MeV gamma-ray cascade upon capture, of which ca. 4-5 MeV are above the Cherenkov threshold and hence visible to the detector. As a result, gadolinium loading at the level of less than a percent allows for a ca. 50% detection efficiency in a water detector, making remote monitoring with a scalable water-based detector feasible.

### 3. The AIT-WATCHMAN Project

The AIT-WATCHMAN project is an initiative to build a water-based, Gd-doped Cherenkov demonstrator detector specifically for detecting nuclear reactors at large distances. This project is driven by a US-UK collaboration. The Boulby Underground Laboratory, 25 km from the Hartlepool power plant, was chosen as site for the AIT-WATCHMAN project in order to provide a stringent test for the capabilities of the technology.

#### 3.1. Hartlepool Reactor Complex

The Hartlepool power plant is an Advanced Gas-cooled Reactor (AGR) commissioned in 1983 and located in northern England and currently operated by EDF Energy. The complex houses two 1575 MWth reactors running in different on/off cycles. As a result, even during shutdowns of one reactor, the second reactor remains active. Hence, this power plant not only allows for a test of AIT-WATCHMAN's ability to merely establish the presence of an active reactor but it also provides an opportunity trial the technology in a more complex reactor cycle representative of real-world monitoring situations where a mix of declared and undeclared reactors might be in geographic proximity of each other.

#### 3.2. Boulby Underground Laboratory

The STFC Boulby Underground Laboratory is located at the Boulby Mine, a working potash, polyhalite and rock-salt mine. The mine, and hence the laboratory site, is located 1,100m underground, making it an ideal site for ultra-low-background experiments due to the attenuation of cosmic rays by a factor of ca.  $10^6$ . Furthermore, the site is ca. 25 km away from the Hartlepool power plant, placing it at a viable distance for a reactor antineutrino monitoring experiment.

The Boulby Underground Laboratory is already host to several underground experiments but due to the size of the AIT-WATCHMAN detector, a new dedicated cavern, 25m tall and 25m in diameter will excavated to house the project.

#### 3.3. AIT-WATCHMAN Detector

The AIT-WATCHMAN detector is a water Cherenkov detector with a planned fiducial volume of ca. 1 kton of water [5]. The current baseline design is a cylindrical tank, 20 m in height and diameter, as shown in figure 1. Within this tank, a steel structure ca. 1-2 m away from the tank walls will support 3600-4400 photomultiplier tubes (PMTs) as photodetection devices for the Cherenkov light flashes, providing 20-25% photocoverage. These PMTs are 10 inch in diameter and are using a low-activity variant to minimise backgrounds. The PMTs allow for imaging the Cherenkov rings, providing localisation of the interaction position for event discrimination.

The majority of PMTs will be pointing inwards into the fiducial region of the detector, which is a virtual volume ca. 1.5m separated from the PMT structure. Veto PMTs will also observe the outer volume, acting as an active veto to reject any cosmic rays that manage to penetrate the surface and reach the detector. Furthermore, this outer water volume also acts as shielding from external radiation

The water is doped with 0.1% gadolinium sulphate salt as neutron capture agent. Previous experiments have demonstrated the feasibility of the gadolinium loading, its interactions with the structure inside the tank and its low impact on the optical quality of the water [6]. For inverse beta-decay events, the average neutron thermalisation and capture time at this gadolinium concentration will be ca. 30  $\mu$ s, which can easily be resolved with PMTs.



**Figure 1:** Illustration of the current baseline design for the AIT-WATCHMAN tank and internal steel frame housing the readout PMTs. The overall tank dimensions are 20 m diameter and height, with the interior frame ca. 1-2 m away from the other tank walls and the virtual fiducial volume inside the PMT structure. For light collection, 3600-4400 PMTs will be mounted on the steel support frame.

### 3.4. Planned Reactor Observation Measurements

At the Boulby site, the total antineutrino flux is a mixture of antineutrinos from the Hartlepool power plant, other reactors as well as geoneutrinos (antineutrinos emitted by radionuclide decay within the Earth itself). Due to its proximity, the Hartlepool power plant dominates the total flux, providing ca. 83.4% of the total flux or causing about 1,000 interactions within a 1 kton water detector per year [7][8]. Including detection efficiencies and background rates based on a detailed GEANT4 simulation of the baseline design, AIT-WATCHMAN is expected to see about 4.8 events per reactor core per week as shown in table 1.

Component	Events/week
Hartlepool Core 1	4.8
Hartlepool Core 2	4.8
World reactors	1.5
Accidentals	0.6
Fast neutrons	0.6
Radionuclides	0.1

**Table 1:** Expected weekly event rate for events classified as inverse beta-decays in the AIT-WATCHMAN detector.

During its data taking period, the AIT-WATCHMAN detector will be used for three measurement campaigns: First, an unblinded analysis with full knowledge of both reactors states at Hartlepool will be conducted to verify predictions and establish the detector’s capabilities to detect the presence of a known reactor. Subsequently, a single reactor analysis will be performed, where knowledge of a single reactor will be combined with the detector measurement to infer the on/off status of the second reactor. Finally, a fully blinded analysis will be run with no knowledge of the status of either reactor.

Due to the two-reactor configuration of the Hartlepool plant, there are two different reactor configurations during this analysis: Both reactors at full power and one reactor on, one reactor off. Due to the similarity of both reactors in power output (and hence antineutrino flux), reactor A on and B off and reactor A off and B on are treated the same. The scenario of both reactors off has historically been rare and is therefore neglected [9]. A statistical analysis has shown that ca. 270 days (under nine months) of experiment time, 95% of all trial experiments will observe a 3-sigma difference between the one- and two-reactor state, as shown in figure 2. At lower standoff distances, an indicative signal (as opposed to a 3-sigma observation) would be obtained much earlier. This also represents one of the most challenging scenarios due to the large standoff distance with reactors operating in closely aligned cycles and a conservative requirement for the observation, as the average trial experiment will observe the 3-sigma difference after ca. 150 days.

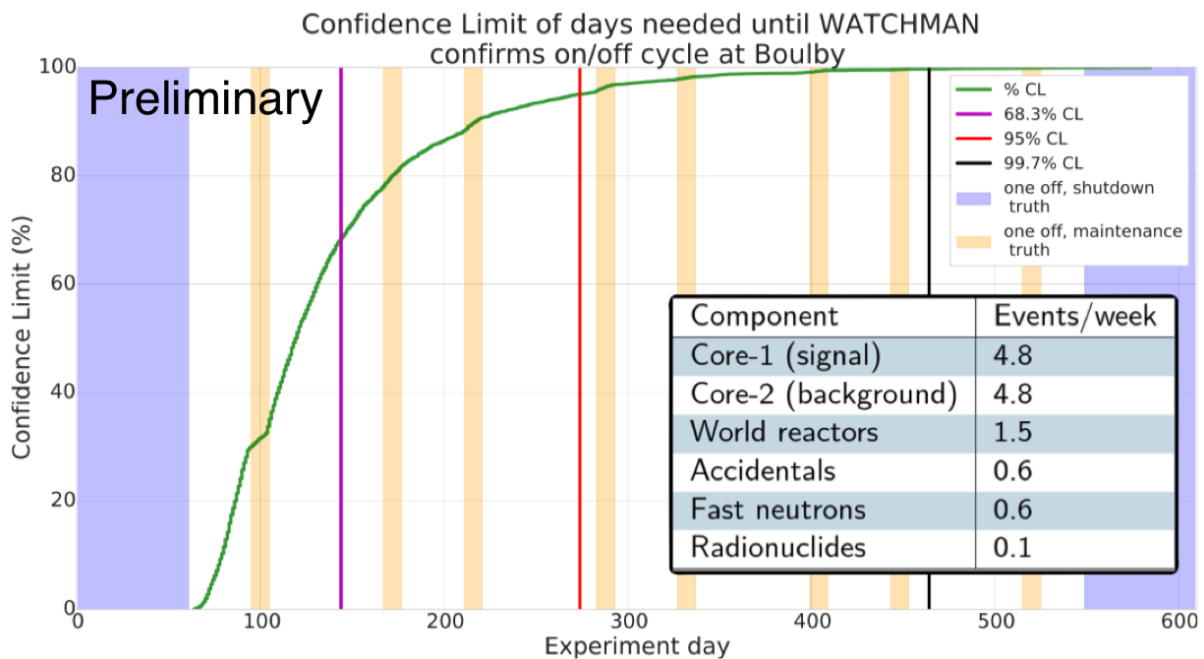


**Figure 2:** Expected confidence limit for the observation of the reactor on/off status of the two Hartlepool reactors at the Boulby site. The 95% confidence limit is indicated as vertical red line at just ca. 270 days of data taking and represents 95% of all trial experiments observing a 3-sigma deviation between one- and two-reactor operation.

#### 4. Outlook and Future Studies

The current timeline expects the AIT-WATCHMAN design and build process to continue take several years and consists of several stages, starting with the cavern design and excavation and finishing with the installation of the detector systems inside the tank. The current draft timeline foresees the WATCHMAN detector to be ready in 2024, followed by several years of full regular data taking. Afterwards, work on the next generation studies and R&D is planned as part of the AIT project.

The site and detector are planned to be used for future studies, specifically for detector R&D. AIT will be a testbed for WbLS (Water-based Liquid Scintillator), LAPPD (Large Area Picosecond Photodetector) sensors with enhanced timing resolution and further R&D projects and studies. These future enhancements will explore the technology capability for non-proliferation purposes, such as the directionality studies, as well as scientific studies.

## 5. Summary

The AIT-WATCHMAN collaboration is currently underway to build a kiloton-scale water Cherenkov detector for remote observation of nuclear reactors at large distances. This US-UK project has secured a site to build and test an antineutrino monitoring demonstrator using a scalable technology for non-proliferation uses. The goal is to not only merely observe the presence of an active power plant but also show the capability to resolve two-reactor nature of the Hartlepool power plant to demonstrate the robustness of the technique in challenging deployment scenarios. Further R&D efforts are also planned to enhance the technology after a successful trial.

## Acknowledgements

The author wishes to thank the US Department of Energy, the National Nuclear Security Association, the UK Science and Technology Funding Council, the Atomic Weapons Establishment and the Boulby Underground Laboratory for supporting the AIT-WATCHMAN collaboration and project.

## Legal matters

I agree that ESARDA may print my name/contact data/photograph/article in the ESARDA Bulletin/Symposium proceedings or any other ESARDA publications and when necessary for any other purposes connected with ESARDA activities.

## References

- [1] Bowden, N.S. et al; *Experimental results from an antineutrino reactor for cooperative monitoring of nuclear reactors*; Nucl. Instrum. Meth. A572; Elsevier; 2006; p. 985-008.
- [2] Mueller, Th. A. et al; *Improved Predictions of Reactor Antineutrino Spectra*; Phys. Rev. C83; American Physical Society; 2011; p. 054615.
- [3] Vogel, P. and Beacom, J.F.; *The angular distribution of the reaction  $\bar{\nu}_e + p \rightarrow e^+ + n$* ; Phys. Rev. D60; American Physical Society; 1999; p. 053003.
- [4] The KamLAND Collaboration; *Constraints on  $\theta_{13}$  from A Three-Flavor Oscillation Analysis of Reactor Antineutrinos at KamLAND*; Phys. Rev. D83; American Physical Society; 2011; p. 052002.
- [5] Askins, M. et al; *The Physics and Nuclear Nonproliferation Goals of WATCHMAN: A WATER Cherenkov Monitor for ANtineutrinos*; ArXiv:1502.01132 [physics.ins-det]; 2015.
- [6] Dazeley, S., Bernstein, A., Bowden, N.S. and Svoboda, R.; *Observation of Neutrons with a Gadolinium Doped Water Cerenkov Detector*; Nucl. Instrum. Meth. A607; Elsevier; 2009; p. 616-619.
- [7] Barna, A. and Dye, S., *Global Antineutrino Modeling: A Web Application*; ArXiv:1510.05633 [physics.ins-det]; 2015.
- [8] Dye, S., *Reactor Antineutrino Signals at Morton and Boulby*; ArXiv:1611.01575 [nucl-ex]; 2016.
- [9] Burns, J., *Remote detection of undeclared nuclear reactors using the WATCHMAN detector*. NuPhys 2017 Proceedings; 2017; p 129-133.

# Liquid Argon - Based Antineutrino Detection Techniques for Nuclear Waste Verification

Mădălina Witte<sup>[1]</sup>

Malte Göttsche<sup>[1,2]</sup>

Achim Stahl<sup>[2]</sup>

[1] AICES - RWTH Aachen University, Schinkelstraße 2, 52062 Aachen

[2] III Physikalisches Institut B, RWTH Aachen University, Otto-Blumenthal-Straße  
52074 Aachen

E-mail: wittel@aices.rwth-aachen.de

## Abstract:

*A significant amount of nuclear fuel has been used both in civilian as well as in military applications of nuclear energy in the past decades. The resulting radioactive waste presents an important verification challenge. Several detection techniques can be employed for verifying declarations of nuclear waste repositories. In contrast to other measurement techniques, antineutrinos, produced by isotopes still present in the nuclear waste that undergo beta decay, e.g. strontium-90, would be capable of propagating through a significant amount of shielding material without being attenuated. Clearly, this poses considerable challenges for the detector design and realisation. The detection technology usually involves measuring scintillation light or Cherenkov radiation. For verification purposes, the directionality of the observed antineutrino events is crucial, for instance, when searching for potentially undeclared storage sites. In this paper, we investigate the prospect of utilising a new neutrino detection technique involving highly granular, imaging liquid argon detectors. This technology is presently developed and validated by the neutrino physics community. It offers the advantage of unprecedented precision in measuring (anti)neutrino energies, incidence directions, and would have a remarkable spatial resolution which is needed to filter out background events. In this work, we perform and discuss a preliminary feasibility study for employing this emergent type of (anti-)neutrino detectors in the context of nuclear waste verification efforts.*

**Keywords:** spent nuclear fuel; safeguards; anti-neutrino applications; liquid argon detectors

## 1. Introduction

The nuclear fuel used to operate any type of fission reactor, for civilian, research and military use, has a finite lifetime. Once it reaches the point where it can no longer sustain a chain reaction inside the reactor core, i.e. it becomes *spent fuel*, it is removed and replaced by fresh fuel. Depending on the reactor type (light-water moderated, CANDU, etc.) and, more importantly, on the reactor operation, between one quarter and one third of the core is typically extracted every 12-18 months and replenished with fresh fuel.

The International Atomic Energy Agency (IAEA) [1] evaluated that the global cumulative amount of spent fuel was approximately 380,500 tonnes heavy metal at the end of 2014 [2]. Furthermore, based on the output of the 438 reactors in operation in 2014, the IAEA estimated that about 10,000 tonnes heavy metal of spent fuel is discharged every year from the nuclear power plants operated by the IAEA member states. This implies that, presently, more than 430,000 tonnes heavy metal of spent fuel are stored around the world. Moreover, due to the growing demand for clean energy, several countries like China, India, Russia are planning to increase their nuclear capacity which would in turn lead to a more rapid increase in the quantity of spent fuel than the IAEA estimate.

Besides the technical and societal-political challenges that must be overcome in order to safely store the large amount of produced spent fuel, the possibility that a fraction of it can be covertly diverted for producing nuclear weapons raises strong concerns and presents a clear necessity for safeguarding.

This paper discusses the need for safeguarding the spent nuclear fuel (SNF) in section 2. The existing monitoring techniques as well as the new technologies currently under scrutiny are overviewed in section 3. In section 4, we examine a specific detector concept: liquid-argon based time projection chambers for detecting anti-neutrinos emitted by the isotopes present in SNF. Lastly, section 5 outlines the feasibility study concerning the use of liquid-argon detectors currently undertaken by our group.

## 2. The Necessity of Safeguarding Spent Nuclear Fuel

The typical spent nuclear fuel composition depends on how the reactor was operated, specifically, on burnup. The table below shows the evaluated composition of SNF extracted from a light-water reactor considering a burnup of 50GWd/t heavy metal [3]:

Material	Relative amount
Uranium (< 1% <sup>235</sup> U, mostly <sup>238</sup> U)	93.4%
Fission products ( <sup>129</sup> I, <sup>90</sup> Sr, <sup>135</sup> Cs, etc.)	5.2%
Plutonium	1.2%
Minor actinides ( <sup>237</sup> Np, <sup>241</sup> Am, <sup>243</sup> Cm, etc.)	0.2%

**Table 1:** Typical isotopic composition of spent nuclear fuel [3]

In the first 100 years after being removed from the reactor, the dominant radioactivity of the SNF stems from the β-decaying fission products, thus being an abundant source of anti-neutrinos. While many isotopes have rather short half-lives (in the order of several hours or a few days), a few like <sup>90</sup>Sr (T<sub>1/2</sub> = 28.78a) and <sup>137</sup>Cs (T<sub>1/2</sub> = 30.17a) still contribute, even decades later. This is particularly relevant when considering long term spent fuel storage solutions.

In addition to its high radioactivity, the presence of plutonium, a key ingredient in the fabrication of nuclear weapons, in the spent fuel reinforces the necessity of safeguarding it. The Institute for Science and International Security [4] estimated that, at the end of 2014, the amount of irradiated (i.e. present in spent fuel) and unirradiated (directly usable for nuclear weapons) plutonium was approximately 2,400 tonnes [5]. A breakdown of the civil plutonium stocks per country at the end of 2014 is given in Fig.1.

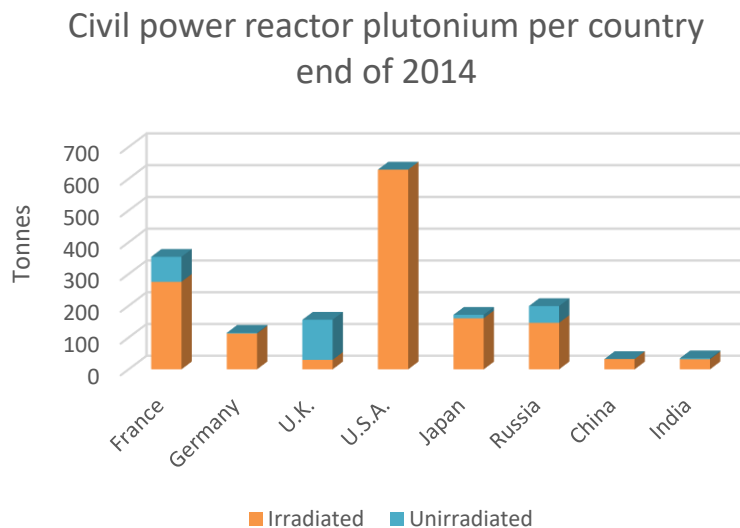


**Figure 1:** The amounts of irradiated and unirradiated plutonium held by country at the end of 2014. [5]

The IAEA current significant quantity definition for plutonium, i.e. the minimum amount of plutonium required for the construction of a nuclear weapon, is 8kg [6]. This implies that the quantity of irradiated and unirradiated plutonium at the end of 2014 would have been sufficient to produce 300,000 more

nuclear weapons. Furthermore, the Institute for Science and International Security evaluated that in the time period between 2004 and 2014, the plutonium stock has increased by a rate of approximately 50 tonnes per year.

The unirradiated plutonium is more susceptible for proliferation, since it can be readily used for nuclear weapons production. However, as can be seen in Fig. 1, a significantly larger amount of plutonium is found in spent fuel from where it can also be extracted through reprocessing techniques like e.g. PUREX, a process that separates the components based on their solubility in two different solutions. On a much smaller scale, plutonium can also be separated in hot cells, i.e. heavily shielded chambers with a controlled atmosphere where remotely manipulated devices can be used to work on radioactive materials.

Presently, civilian reprocessing facilities are operated in France, the United Kingdom, Japan, Russia and India. Approximately 2000 tonnes heavy metal of the total amount of produced spent fuel are reprocessed yearly [3]. The obtained uranium and plutonium are typically meant to be used for refuelling reactors. Nevertheless, safeguards are necessary to ensure that they are not diverted for weapons production.

### 3. Spent Nuclear Fuel Monitoring

Due to the considerable amount of decay heat and the high radiotoxicity, the spent fuel, once removed from the reactor, is immediately stored on-site, in water pools, for a cooling down period ranging from a few months to several decades. After the cooling down time, the SNF can be moved to wet or dry (air-cooled) storage facilities located either on the reactor site or in dedicated centralised repositories. From there, it can be either reprocessed or deposited in long-term geological storage.

The IAEA is presently monitoring the spent fuel during all the management stages in NPT non-nuclear-weapons states and, together with Euratom, in France and the United Kingdom, including their civilian SNF reprocessing programmes. In addition to on-site inspections, several technologies that provide continuous remote surveillance are deployed. This is crucial for providing the necessary continuity of knowledge, ensuring that no amount of fissile material obtained from SNF is diverted for weapons production. A brief overview of the technologies presently employed for this purpose is given in the following subsection [7] [8].

#### 3.1 Current Monitoring Technologies

- **Camera surveillance system:** the cameras are placed in sealed containers (“tamper-indicating”) and are powered by long lasting batteries. The authenticity of the recorded data is ensured by three different levels of cryptographic security systems. The cameras are installed in storage areas and in the vicinity of spent fuel water pools and take images at time intervals between one second and ten minutes. Specialised software is then used to pre-scan the recorded images. Finally, inspectors evaluate the data and verify that it was consistent with the normal operation of the monitored facility.
- **Non-destructive assay systems:** consist of radiation detectors to measure gamma and neutron radiation and other sensors that monitor the temperature, etc. The data collected by these sensors are usually corroborated with the images taken by the surveillance cameras. In addition, a mobile unit neutron detector can be mounted onto the spent fuel casks to ensure that material is not removed from the cask during transportation.
- **Seals:** (i) single use metal cap seals, numbered and with unique markings on their inner surface, (ii) COBRA seals, containing a multicore optic fibre cable, (iii) electronic optical sealing system which can provide remote information and can be linked with the video surveillance system, (iv) laser mapping for containment verification.

### 3.2 Continuity of Knowledge

As the amount of spent fuel in storage accumulates, the probability that one of the monitoring techniques mentioned above may fail also increases with time. Should such a failure occur, especially in the case of cask seals, the contents of the affected casks can no longer be accounted for. While measuring the radiation that escapes from a cask with a damaged seal can demonstrate that its content is radioactive, it cannot provide enough information to determine if any amount of spent fuel is missing. Neutron or photon radiography techniques are also not feasible in this case due to the heavy shielding of the cask.

In order to verify the content of the cask and restore the continuity of knowledge, a tomographic technique based on cosmic muons was proposed and is currently under consideration [9]. The muons are produced when highly energetic astrophysical nuclei interact in the upper atmosphere and follow a broad energy distribution with the mean of approximately 4 GeV. Their average rate is of about  $10^4$  muons per minute and  $m^2$  [9]. Muons can penetrate through significant amounts of material and provide important information about the cask's internal structure. Two tracking detectors, each consisting of several layers of drift-tubes, are placed on opposite sides of the cask. The tomographic information is obtained by measuring the muon attenuation [10], scattering [11] and associated particle production [12]. Thus, measurements of cosmic muons can be used as a stand-alone technique for verifying the contents of dry-storage casks.

A complementary approach, first proposed by P. Huber et al. [13], envisages measuring the anti-neutrino emissions coming directly from the spent fuel itself for long term monitoring and for ensuring continuity of knowledge. This application of anti-neutrino measurements, carried out in particular with liquid argon detectors, represents the main focus of this paper.

### 3.2 Anti-neutrinos as Potential Source of Information

As mentioned in section 2, the main source of radioactivity in the spent fuel comes from beta-decaying isotopes. The emitted anti-neutrinos can constitute a valuable source of information about the amount and content of the spent fuel in storage. Due to their weakly interacting nature, with cross-sections lower than  $10^{-38}$   $cm^2$ , they inevitably escape even large amounts of shielding. Clearly, this also implies that their detection raises considerable challenges which will be addressed later. In addition, since they are neutral particles, their travel directions are not modified by magnetic fields or by traversing matter. Thus, they can also provide direct information concerning the location of the SNF repository.

### 3.3. Characteristics of Anti-neutrinos from Spent Fuel

To evaluate the feasibility of using anti-neutrinos for measuring spent fuel, the characteristics of the emitted anti-neutrinos, i.e. the expected flux and energy range must be first considered.

This preliminary study relies on the anti-neutrino spectra calculations performed by P. Huber et al. [13]. For this purpose, a simulation of a pressurised-water Westinghouse reactor was implemented by the authors of [13] in the simulation code SCALE [14]. A fuel assembly configuration of  $16 \times 16$  elements and an initial enrichment of 4% were assumed. The simulated reactor operation considered a burnup of 45GWd/t heavy metal [15].

The output of the simulation was the isotopic composition of the spent fuel at the time of discharge. This was considered the baseline. Making use of the ENSDF [16] decay data library, the beta-decay electron spectrum for each of the SNF isotopes was calculated at different points in time, e.g. 1 year, 10 years, etc, after being extracted from the reactor. The corresponding anti-neutrino spectra were then individually obtained by applying the conversion method, described for instance in [17].

The cumulative anti-neutrino spectra for 10, 30 and 50 years, respectively, after the spent fuel was discharged are illustrated in Fig. 2. As mentioned previously, after 10 years in storage, the main contributions to the anti-neutrino spectrum come from  $^{90}Sr$  and  $^{137}Cs$ . The discontinuities in the three spectra shown in Fig. 2 illustrate the fact that some isotopes decay in two stages: the first one characterised by a very small Q and, implicitly, a long lifetime, while the second is exactly the opposite [13]; here, Q represents the total energy released in the decay.

It is important to note the low energy of the anti-neutrinos coming from spent fuel: they are comparable to the solar neutrino spectra, as described in [18]. This constitutes additional challenges for the anti-neutrino detection.

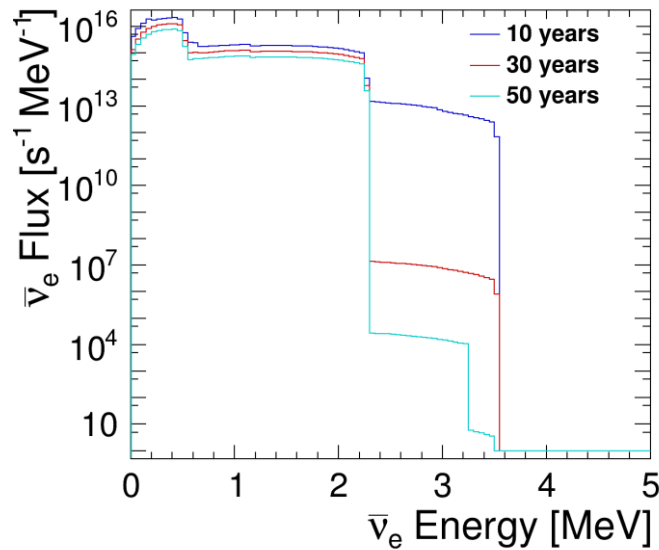


**Figure 2:** Energy spectra of anti-neutrinos emitted in the beta decays of isotopes present in the spent nuclear fuel. The figure was produced based on the calculations performed by P. Huber et al., [13]

### 3.4. Motivation for New Anti-Neutrino Detection Technologies in the Safeguards Context

The use of anti-neutrino measurements for monitoring purposes has already been considered in the case of nuclear reactors: for determining reactor shut-down periods or estimating the plutonium content in the core.

For instance, the WATCHMAN project [19] envisages an anti-neutrino detector containing 1810 tonnes of Gadolinium-doped water as sensitive material and an additional 1730 tonnes of the same material acting as a veto. The detector, in effect a cylindrical tank with a diameter and height of 15.8 metres, will be located in the Boulby mine in the United Kingdom and will measure anti-neutrinos coming from the Hartlepool two-reactor complex situated 25 km away. A similar project, called CHANDLER [20], proposes a smaller detector comprising up to 20 layers of 6 cm cubes of wavelength shifting plastic scintillator and thin sheets of lithium-6 ( ${}^6\text{Li}$ ) loaded zinc sulfide ( $\text{ZnS}$ ) scintillator.

In both WATCHMAN and CHANDLER detectors, the anti-neutrinos interact with the sensitive material by means of the so-called inverse beta decay (IBD) reaction:  $\bar{\nu}_e + p \rightarrow e^+ + n$  (where the proton represents a hydrogen nucleus in water or plastic scintillator). The Cherenkov and scintillation light, respectively, produced as a result of an anti-neutrino interaction is read out by photomultiplier tubes in both detectors.

Since anti-neutrinos interact only weakly, the interaction target, i.e. the detector, must provide a large mass and a high density, such that the interaction rate is significant. The potential use water-Cherenkov detectors for spent fuel verification purposes may be limited especially by their size, e.g. 3.5 kT in the case of the WATCHMAN project.

An additional limitation stems from the energetic threshold of the inverse beta decay reaction itself, i.e.  $E_\nu > 1.8$  MeV. As can be seen from Fig. 2, this would essentially remove more than 80% of the anti-neutrinos emitted in beta-decays from spent fuel, thus significantly reducing the interaction probability. Consequently, a sensitive material which would enable anti-neutrino reactions without an intrinsic energetic threshold would be desirable.

Recently, as the interest in the field of fundamental neutrino research is gradually encompassing the energy range of solar and supernova anti-neutrinos, new detection methods are proposed and/or prototyped. In view of the spent fuel safeguarding requirements, anti-neutrino detectors based on liquid-

argon time-projection chambers (LARTPC) seem to be particularly promising. Such detectors have already been built and tested in experiments like, e.g. ArgoNeuT [21] and MicroBoone [22] and are considered for large-scale neutrino fundamental research experiments like DUNE [23].

## 4. Prospects for Safeguarding Spent Fuel with Liquid-Argon Detectors

The idea of using liquid-argon time projection chambers for neutrino detection was first proposed by Carlo Rubbia in 1977 [24]. It is only in the last decade that LARTPCs prototypes have been realised and tested. The working principles and advantages of this type of detectors are discussed in the following.

### 4.1. Fundamentals of Liquid-Argon Time Projection Chambers

A LARTPC consists of a large volume of liquid argon encompassed by a high-voltage cathode on one side and an anode on the opposite surface. In addition, several read-out wire planes are also located on the anode side. To be liquid, the argon must be cooled to a temperature of 87K (-186.15° C). The uniform electric field realised between the cathode and the anode planes typically has a strength of 500V/cm.

When an (anti-)neutrino interacts via charged or neutral current exchange with an argon atom, i.e. either with the orbital electrons or the nucleus itself, the emergent charged particles ionise and excite further argon atoms along their trajectory. The emitted free electrons drift in the liquid argon, under the force of the electric field, until they reach the read-out wires, in which they generate small currents. The wires are placed at very close distance to each-other, e.g. 3-5mm, and constitute a very dense net. To obtain multi-dimensional information about the charged particles' tracks, several wire planes can be used, placed under different angles with respect to each other.

In addition, the excited argon atoms also emit scintillation light in the ultraviolet range ( $\lambda=128\text{nm}$ ) which can be measured with photosensors (PMTs). The light signal can provide highly useful timing information about the initial point of the anti-neutrino interaction and, implicitly, a way of determining its position along the drift trajectory. This is very useful in reconstructing a three-dimensional image of the charged particle's track.

### 4.2. Advantages of Liquid-Argon Anti-neutrino Detectors

The first benefit of using liquid-argon-based time projection chambers stems directly from their mode of operation: unlike water or scintillator detectors, they are *imaging* detectors - providing a three-dimensional reconstruction of the tracks left by the charged particles emerging from an anti-neutrino interaction. This is crucial for ensuring a good background rejection: in a safeguards context, the detectors will be deployed at the surface, i.e. without too much shielding from cosmic and cosmogenic background sources of neutrinos. The imaging properties of the LARTPCs ensure a very accurate energy reconstruction, based on the track length, and provide a means to infer the directionality of the incoming anti-neutrinos on an event-by-event basis. The SNF anti-neutrinos could be distinguished from the background using these two criteria.

The second advantage is the fact that argon ( $^{40}\text{Ar}$ ) is in fact denser than both water and oil-based scintillator material. Having 18 protons (and electrons) and 22 neutrons, the number of targets for anti-neutrino interactions is higher in argon than in water, for instance, which has only 10 protons/electrons and 8 neutrons.

Furthermore, anti-neutrino interactions in argon produce two types of signal: the free electrons that drift and are collected on the read-out wires and the light emitted during the de-excitation of the argon atoms. In contrast, water or scintillator-based detectors provide only light as detection signal. In fact, liquid argon is an excellent scintillator, providing approximately 5000 photons/mm per minimum ionising particle.

Lastly, since argon constitutes approximately 1% of Earth's atmosphere, especially the  $^{40}\text{Ar}$  isotope with an abundance of 99.6%, it is usually cheap to produce (and to liquify) and it is commercially available.

## 4.2. Relevant Interactions of Anti-Neutrinos in Liquid-Argon

In the standard water-Cherenkov or organic-scintillator-based detectors, (anti-)neutrinos mostly interact by means of the inverse beta decay process:  $\bar{\nu}_e + p \rightarrow e^+ + n$ . However, since there are no free protons available in liquid argon, this reaction cannot take place. Furthermore, as mentioned in section 3.4, its kinematic threshold of 1.8 MeV would severely limit the interaction rate of anti-neutrinos from spent fuel. The analogous reaction in liquid argon is the charged current absorption:  $\bar{\nu}_e + {}^{40}\text{Ar} \rightarrow e^+ + {}^{40}\text{Cl}^*$ . However, its energy threshold in the case of anti-neutrinos is even higher:  $E_\nu > 7.5$  MeV, which makes it unfeasible for SNF safeguarding (cf. Fig. 2).

Nevertheless, there are several other anti-neutrino interactions that may be helpful. The cross-sections of all the (anti-)neutrino interactions in liquid argon as well as other materials, for comparison, are summarised in Fig. 3.

- **Neutral current excitation:**  $\bar{\nu}_e + {}^{40}\text{Ar} \rightarrow \bar{\nu}_e + {}^{40}\text{Ar}^*$   
In this reaction, the excited argon atom would emit photons that could be measured by the photomultipliers.
- **Elastic scattering:**  $\bar{\nu}_e + e^- \rightarrow \bar{\nu}_e + e^-$   
The anti-neutrino scatters off electrons of the argon atoms. This reaction is very important for directionality and, implicitly, background rejection: the outgoing electron is scattered in the direction of the incoming anti-neutrino. However, the cross section of this interaction (blue line in Fig. 3) is rather low. In principle, it has no kinematic threshold, but there are limits to how small the energy of the emergent electron can be, i.e. it should be capable of leaving a measurable track in the detector. Based on a simple  $dE/dx$  calculation, we estimated that a 1 MeV scattered electron would leave a track with a length of approximately 1.4cm in a LArTPC. While this clearly posits a challenge for the read-out technology, these tracks are certainly not invisible in the detector. We are currently also investigating the feasibility of other potential read-out technologies.
- **Coherent elastic neutrino-nucleus scattering:**  
This interaction occurs via weak neutral current and essentially refers to anti-neutrinos being scattered off protons or entire nuclei. The cross-section of this reaction in liquid argon is presently being measure by experiments such as e.g. COHERENT [25] Despite the rather high cross-section (orange line in Fig. 3), the recoil energy is very low and it remains to be seen whether this reaction is detectable at all.

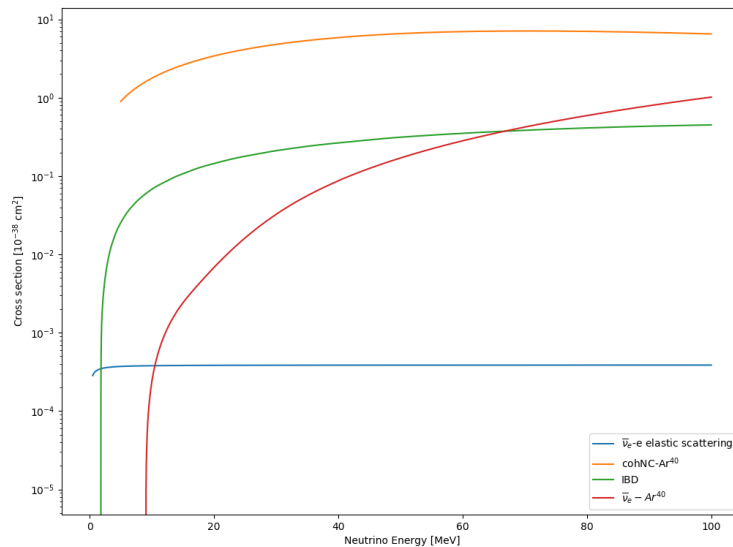


**Figure 3:** Cross-sections of anti-neutrino interactions in various materials. Figure based on SNOwGLoBES [26] cross section calculations.

### 4.3. Expected Event Rate

As a preliminary feasibility study, we have estimated the expected spent fuel anti-neutrino event rate in a liquid-argon time projection chamber and compared it with the rate expected in a water-Cherenkov detector of the same size. For this purpose, we assumed that both detectors have the standard volume of a shipping container, i.e. 80 m<sup>3</sup> [27], and that this entire volume is active and fully instrumented.

The event rate was calculated according to the known formula:  $N_\nu(E_\nu) = \Phi_\nu(E_\nu) \cdot T \cdot \sigma(E_\nu)$ , where  $\Phi_\nu$  is the energy dependent anti-neutrino flux,  $T$  is the number of targets in the detector active volume and  $\sigma$  is one of the relevant anti-neutrino differential cross-sections from Fig. 3.

For the LArTPC, we considered only the anti-neutrino-electron elastic scattering interaction (blue line in Fig. 3). Consequently, the number of *electron* targets present in the volume of liquid argon was computed with the formula:  $T = (N_A \cdot \rho \cdot V) / M_W$ , where  $N_A$  is Avogadro's number,  $\rho$  is the density of liquid argon,  $V$  is the detector active volume and  $M_W$  represents the molecular weight of argon. The anti-neutrino-electron elastic scattering differential cross-section was calculated by the authors of the SNOwGLoBES software package [26], based on [28].

In contrast, the inverse beta-decay reaction (green line in Fig. 3) was considered in the case of the water-Cherenkov detector and the number of *proton* targets was calculated in this case, similarly, for the same volume of ultra-pure water. The IBD differential cross-section was computed as mentioned previously, based on [29].

The anti-neutrino flux was determined based on the spent fuel anti-neutrino emission calculation carried out by P. Huber et al. [13] at time  $t = 10$  years after discharge from the reactor core and assuming one tonne of spent fuel. A distance of 50 m between the detector and the SNF repository was taken into account in the  $\bar{\nu}_e$  flux calculation.

The estimated anti-neutrino event rates, both for liquid argon (black) and water-Cherenkov (red) detectors are shown in Fig. 4. While both detection technologies have very low event rates it can be seen that the rate in the water-Cherenkov detector can be up to 3 orders of magnitude larger. However, as mentioned previously in this section, the IBD reaction has the disadvantage of an energy threshold at 1.8 MeV; hence the shift in the starting point of the IBD (red) curve from Fig. 4.

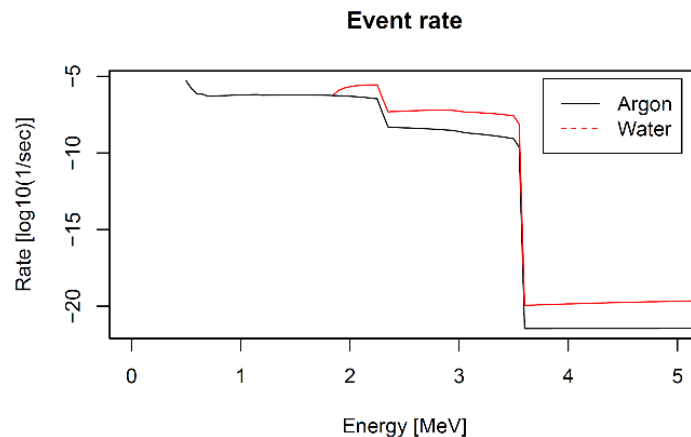


**Figure 4:** The estimated event rate in a LArTPC (black) and a water-Cherenkov (red) detector, respectively, with a volume of 80 m<sup>3</sup>. This estimation assumes a 100% detector efficiency and only 1 tonne of SNF.

When comparing the event rate, integrated over the energy range between 0.5 and 3.2 MeV, the liquid argon and water-Cherenkov performance is very similar, with the former even slightly higher. This clearly indicates the limiting effect of the IBD energy threshold.

It must be noted that the shown anti-neutrino event rates represent an optimistic estimation, since this preliminary calculation assumes a 100% detector and background rejection efficiency.

## 5. Conclusions and Outlook

As the quantity of spent nuclear fuel increases worldwide, the risk of clandestine reprocessing activities with the specific purpose of diverting plutonium for nuclear weapons production informs the necessity of safeguarding known SNF repositories. Alongside cosmic muons that can traverse the shielding and content of the dry-storage casks, the only other messenger particles that could escape would be the anti-neutrinos emitted even decades later through the beta decays of isotopes like  $^{90}\text{Sr}$  and  $^{137}\text{Cs}$  still present in the spent fuel.

In this paper, we proposed the use of liquid-argon based time projection chambers for spent fuel monitoring. This technology is presently developed and validated by the neutrino physics community, thus aligning the nuclear verification efforts with the forefront of fundamental science. It presents several advantages in comparison to traditional detectors: (i) excellent track imaging capabilities – used for efficient background subtraction, (ii) a higher number of targets per unit volume which could somewhat compensate the lower reaction cross-sections, (iii) the emittance of two types of signal which enables three-dimensional track reconstruction and (iv) the relatively low production costs.

We performed a very preliminary calculation of the expected event rate in LArTPCs and compared it with the one achievable with a water-Cherenkov detector. Despite the significantly larger cross-section of the IBD reaction, the latter have the disadvantage of a relatively high energy threshold.

However, this estimate assumes perfect detector efficiency and background rejection. For a realistic feasibility study, the LArTPC performance should be studied in a full simulation that also takes the cosmic, cosmogenic and reactor background into account. This simulation together with a detailed treatment of the background form the subject of our future studies.

## 6. Acknowledgements

This work is funded by the Volkswagen Foundation through the “Freigeist” fellowship programme.

## 7. References

- [1] IAEA - International Atomic Energy Agency, <https://www.iaea.org/>.
- [2] International Atomic Energy Agency, *Nuclear Technology Review*, 2015. [Online]. Available: <https://www.iaea.org/sites/default/files/ntr2015.pdf>.
- [3] International Panel on Fissile Materials, *Managing Spent Fuel from Nuclear Power Reactors*, 2011. [Online]. Available: <http://fissilematerials.org/library/rr10.pdf>.
- [4] Institute for Science and International Security, [www.isis-online.org/](http://www.isis-online.org/).
- [5] D. Albright, S. Kelleher-Vergantini, D. Schnur, *Plutonium and Highly Enriched Uranium Inventories*, Institute for Science and International Security, 2015.
- [6] International Atomic Energy Agency, *The Present Status of IAEA Safeguards on Nuclear Fuel Cycle Facilities*; IAEA BULLETIN- VOL.22, NO.3/4, [Online]. Available: [https://www.iaea.org/sites/default/files/publications/magazines/bulletin/bull22-3/223\\_403400240.pdf](https://www.iaea.org/sites/default/files/publications/magazines/bulletin/bull22-3/223_403400240.pdf).
- [7] International Atomic Energy Agency, <https://www.iaea.org/topics/safeguards-and-verification>.
- [8] International Atomic Energy Agency, <https://www.iaea.org/newscenter/news/surveying-safeguarded-material-24/7>.
- [9] J.M. Durham et al., *Verification of Spent Nuclear Fuel in Sealed Dry Storage Casks via Measurements of Cosmic-Ray Muon Scattering*, *Phys. Rev. App.*, vol. 9, p. 044013, 2018.
- [10] J. Marteau et al., *DIAPHANE: muon tomography applied to volcanoes, civil engineering, archaeology*, *Journal of Instrumentation*, vol. 12, p. C02008, 2017.
- [11] K. N. Borozdin et al., *Surveillance: Radiographic imaging with cosmic ray muons*, *Nature*, vol. 422, p. 277, 2003.
- [12] E. Guardincerri et al., *Detecting special nuclear material using muon-induced neutron emission*, *Nucl. Instrum. Methods Phys. Res.*, vol. A, n. 789, p. 109, 2015.

- [13] V. Brdar, P. Huber, J. Kopp, *Antineutrino Monitoring of Spent Nuclear Fuel*, Phys. Rev. Applied, vol. 8, DOI: 10.1103/PhysRevApplied.8.054050, 2017.
- [14] SCALE, Oak Ridge National Laboratory, <https://www.ornl.gov/scale>.
- [15] P. Huber, *private communication*.
- [16] Evaluated Nuclear Structure Data File» [Online]. Available: <https://nucleus.iaea.org/Pages/evaluated-nuclear-structure-data-file.aspx>.
- [17] A. C. Hayes and P. Vogel, *Reactor Neutrino Spectra*, 2016. [Online]. Available: <https://arxiv.org/abs/1605.02047v1>.
- [18] K. Nakamura - The Particle Data Group, *Solar Neutrinos*, 2002. [Online]. Available: [http://pdg.lbl.gov/2002/solarnu\\_s005313.pdf](http://pdg.lbl.gov/2002/solarnu_s005313.pdf).
- [19] M. Askins et al., *The Physics and Nuclear Nonproliferation Goals of WATCHMAN: A WATER Cherenkov Monitor for ANtineutrinos*, 2015, arXiv:1502.01132v1.
- [20] The CHANDLER Detector Project , <http://cnp.phys.vt.edu/chandler/>.
- [21] C. Anderson et al., *The ArgoNeuT Detector in the NuMI Low-Energy beam line at Fermilab*, 2012. [Online]. Available: <https://arxiv.org/abs/1205.6747>.
- [22] R. Acciarri et al.- The MicroBooNE Collaboration, *Design and Construction of the MicroBooNE Detector*, 2017. [Online]. Available: <https://arxiv.org/abs/1612.05824>.
- [23] The DUNE Collaboration, <https://www.fnal.gov/pub/science/lbnf-dune/index.html>
- [24] C. Rubbia, *The liquid-argon time projection chamber: a new concept for neutrino detectors*, 1977. [Online]. Available: <https://cds.cern.ch/record/117852?ln=en>.
- [25] The COHERENT Collaboration, <https://sites.duke.edu/coherent/>.
- [26] SNOwGLoBES: SuperNova Observatories with GLoBES, <http://webhome.phy.duke.edu/~schol/snowglobes/>.
- [27] International Organization for Standardization, «ISO 668:2013 - Series 1 freight containers - Classification, dimensions and ratings,» 2013. [Online]. Available: <https://www.iso.org/standard/59673.html>.
- [28] Z. P. William J Marciano, *Neutrino–electron scattering theory*, Journal Phys. G, vol. 29, DOI:10.1088/0954-3899/29/11/013, 2003.
- [29] F. V. Alessandro Strumia, *Precise quasielastic neutrino/nucleon cross section*, Phys. Lett. B, vol. 564, DOI:10.1016/S0370-2693(03)00616-6, 2003.

## Modelling of safeguards verification of spent fuel dry storage casks using muon trackers

D. Ancius<sup>5</sup>, K. Aymanns<sup>4</sup>, P. Calvini<sup>1</sup>, \*P. Checchia<sup>2</sup>, F. Gonella<sup>2</sup>, A. Jussofie<sup>6</sup>, F. Montecassiano<sup>2</sup>, M. Murtezi<sup>5</sup>, P. Schwalbach<sup>5</sup>, K. Schoop<sup>5</sup>, S. Vanini<sup>2,3</sup>, G. Zumerle<sup>2</sup>.

<sup>1</sup>Department of Physics, University of Genova, Via Dodecaneso 33, 16146 Genova, Italy.

<sup>2</sup>Istituto Nazionale di Fisica Nucleare (INFN), Sezione di Padova, Via Marzolo, 8, 35131 Padova, Italy.

<sup>3</sup>Dipartimento di Fisica e Astronomia, Università di Padova, Via Marzolo, 8, 35131 Padova, Italy.

<sup>4</sup>Forschungszentrum Jülich GmbH, IEK-6, 52425 Jülich, Germany.

<sup>5</sup>European Commission, DG ENER, Euratom Safeguards, 1, rue Henri M. Schnadt, 2530, Luxembourg.

<sup>6</sup>BGZ Gesellschaft für Zwischenlagerung mbH, Frohnhauser Str. 67, 45127, Essen, Germany.

\*E-mail: paolo.checchia@pd.infn.it

### Abstract:

*The growing number of dry spent fuel casks in intermediate storage sites in EU increases the effort of safeguards inspectorates. The needs for efficient tools for non-destructive routine verifications or re-verifications in case of a loss of continuity of knowledge grow continuously. Ideally, future instruments should have at least a detection limit of one Significant Quantity of nuclear material and thus be able to detect 1 missing PWR or 4 missing BWR spent fuel assemblies. Making use of available cosmic muons shows a promising way towards a tool that helps inspectors to optimize inspection approaches.*

*Muon trackers based on drift tubes have been used in several particle physics experiments, like CMS and ATLAS at CERN. Recently, a small muon-tracking module consisting of an array of 8 x 8 drift tubes has been successfully tested at proximity of a CASTOR<sup>®</sup> V/19 cask in Germany. The tests have convincingly proved that the background created by gamma and neutron radiation from spent fuel stored in the cask represented only about 1% of the useful signal from muon detection. These experimental results justify further investigation related to the use of the muon trackers for spent fuel safeguards.*

*Cosmic muons have been simulated according to the measured energy and the angular spectrum. The geometry has been modelled with Geant4, taking into account two muon trackers measuring the incident cosmic muons that entered the CASTOR<sup>®</sup> V/21 cask and then left it after having crossed its body. Analysis of muons' absorption and their deflection angles allows imaging of the internal structure of the cask and of the enclosed spent fuel. In the first test, the modelled trackers cover only 1/3 of the CASTOR<sup>®</sup> V/21 cask surface. Modelling results that show the proposed prototype detector and prove the feasibility are presented in this paper. Future detectors that may be used for nuclear safeguards would be larger, in order to provide a more complete image of the cask contents in a reasonable time. Therefore, different geometric configurations, up to a full coverage detector, are also simulated and the minimum measurement time to confirm the absence of missing material is estimated. Conditions for future field tests with a fully or partially loaded CASTOR<sup>®</sup> cask are discussed.*

**Keywords:** Safeguards; muon detection; spent fuel; CASTOR<sup>®</sup> V-cask.

## 1. Introduction

Current handling practice of spent nuclear fuel includes its storage in transport and storage casks (dual purpose casks, hereafter referred to as DPC) located in spent fuel storage facilities (SFSF). Spent nuclear fuel contains plutonium and uranium. The measure to evaluate the consequences of diversion of nuclear material is a Significant Quantity (SQ), which is a sufficient quantity of nuclear material to produce an explosive device. One SQ equals to 8 kg of plutonium or 25 kg of highly (>20%) enriched uranium. One DPC usually contains from 20 to 50 SQs and makes an important target material for EURATOM and IAEA safeguards. There were more than 1500 DPCs in all EU member states at the beginning of 2019.

The current safeguards is based on traditional containment and surveillance (C/S) methods, which assure the continuity of knowledge (CoK) of the nuclear material between the physical inventory verifications (PIV). However, given the large and continuously growing number of DPC some cases of loss of CoK cannot be excluded over the long storage times. Moreover, the safeguards experts worldwide are considering several types of nuclear material diversion from DPC scenarios. Identification of such diversion or confirmation that the nuclear material has not been diverted would require reliable non-destructive assay verification tools. Today safeguards inspectorates do not have enough performant technical solutions which may measure diversion of one SQ from DPC.

## 2. The experimental environment

Typical DPCs are CASTOR® V casks. There are different types of CASTOR® V casks with typical height of about 5 m, an external diameter of 2.4 m and a mass of more than 120 tons when fully loaded.

For non-destructive verification of those casks, two techniques, based on different physical processes, could be considered simultaneously: the transmission of cosmic muons, which is related to the density of the investigated volume and the muon scattering which allows to estimate the product of the density and the average atomic number of the elements contained in this volume. As a consequence, to obtain information about the material distribution inside the DPC thanks to these phenomena, one should place muon detectors around the cask. Detectors should measure, with good precision, position and direction of particles that enter the cask as well as those of muons that exit from lateral surface. Despite of the significant radioactivity emanating from spent fuel stored in a DPC, it has been proven that muon tracks can be successfully reconstructed [ 3]. In more details, INFN has built a prototype of a drift tube detector based on eight layers of eight two metre-long drift tubes. The detector has been successfully tested in proximity of a CASTOR® V/19 cask loaded with spent fuel (Fig.1) demonstrating the capability of the system to reconstruct muon tracks under those conditions.



**Figure 1:** the detector near the CASTOR®.

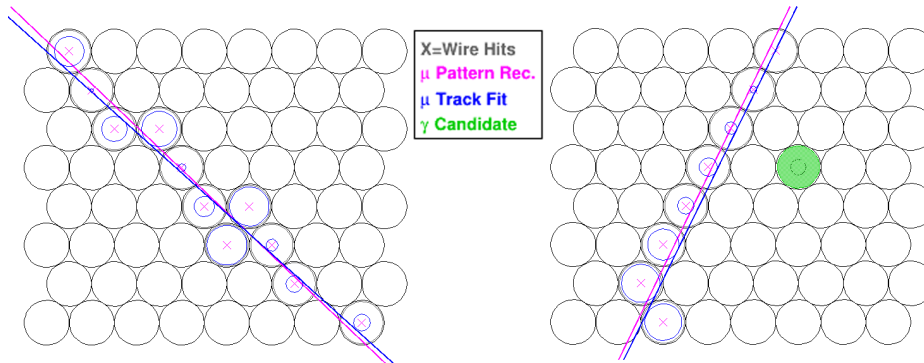


**Figure 2:** Display of two reconstructed muon tracks, recorded with the detector positioned near the CASTOR<sup>®</sup> as in Fig. 1. Black circles represent to the drift tubes, pink crosses correspond to the position of the wires with a signal used to reconstruct the muon path, the blue circles correspond to the measured drift time translated into radial distance from the wire. The green area represents a tube with a signal candidate to be due to emitted radiation.

The field test has been performed in the interim storage facility of the EnKK nuclear power station at Neckarwestheim (Germany). The dose measured at a distance of 22 cm from the CASTOR<sup>®</sup> V/19 cask (approximately the position of the 1<sup>st</sup> detector layer) was 14  $\mu\text{Sv/h}$  ( $\gamma$ ) and 29  $\mu\text{Sv/h}$  (neutron). Two examples of reconstructed tracks recorded with the detector positioned near the cask are shown in Fig. 2. In both cases a clear pattern of hits in tubes in different layers is visible. Additional signals, compatible in time with the muon passage and distinguishable from the muon pattern are also represented in green. The number of additional signals, in the time window ( $\sim 1.2 \mu\text{s}$ ) of a muon track, attributed to CASTOR<sup>®</sup> radiation depends on the number of channels and on their length. For the INFN prototype, containing 64 cells, a value of  $n_{\gamma/\mu}^{64} = 0.4 \pm 0.2$  has been measured, where the error is dominated by systematic effects. A different representation of this result is given in terms of the probability,  $p_{\gamma/\mu}^{\text{ch}}$ , for a 2m long channel to have a signal produced by radioactivity in the time window used to collect all the hits of a muon track. It has been obtained  $p_{\gamma/\mu}^{\text{ch}} = (6 \pm 3) \cdot 10^{-3}$ . This value can be extrapolated to different detector dimensions and different emitted doses. As an example, operating a detector with 5 m long tubes in proximity of a DPC with 3 times more activity we would have  $p_{\gamma/\mu}^{\text{ch}} < 10\%$  even considering the uncertainty. This value is sufficiently low to exclude problems with other DPC.

### 3. The detector

The detector proposed for the DPC inspection is based on drift tubes. The elementary cell is a 50 mm diameter Al tube, with a length up to 6 metres and a coaxial CuBe wire of 100  $\mu\text{m}$  diameter. Commercial tubes with 50 mm external diameter and 1,5 mm thickness can be used. The internal volume is filled with an Ar-based gas mixture. The wire is connected to a  $\sim 3000 \text{ V}$  voltage supply, a ground electrical contact is ensured to the external tube surface and hence a radial electric field is present in the tube. The electrons, produced in the gas ionization due to crossing charged particles, drift toward the anodic wire. The high electric field present near the wire amplifies the number of electrons, producing a measurable signal and then the drift time can be recorded. More details on the cell design can be found in [2].

As discussed above, a detector to reconstruct the content of a DPC should surround the cask. Given the DPC geometry, a good solution to obtain a full DPC coverage is a detector of hexagonal shape as illustrated in Fig.3. Using two modules only, as depicted in red in Fig.3, an effective reconstruction test can be performed before completing the full detector.

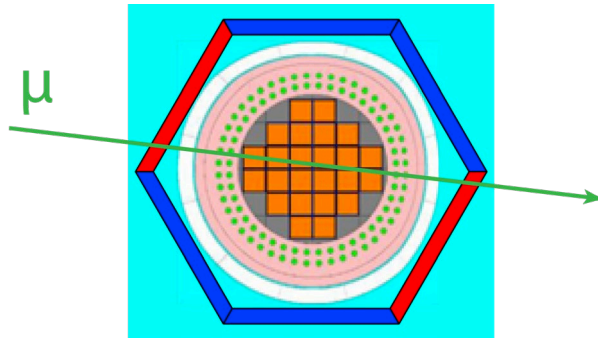


**Figure 3:** Schematic view of a full size detector with hexagonal shape surrounding a DPC (blue segments). Red segments represent a middle size prototype covering 1/3 of the DPC surface.

A detector configuration which would ensure a good performance at a moderate cost, would be a detector based on 6 layers of 5 metres long tubes with the geometry shown in Fig.4. In order to minimise the path ambiguities due to drift time circular symmetry, the 3<sup>rd</sup> and the 4<sup>th</sup> layers are not staggered by half tube. A properly designed support structure design will allow to move the detector to ensure, with longer data recording time, a reasonable reconstruction.

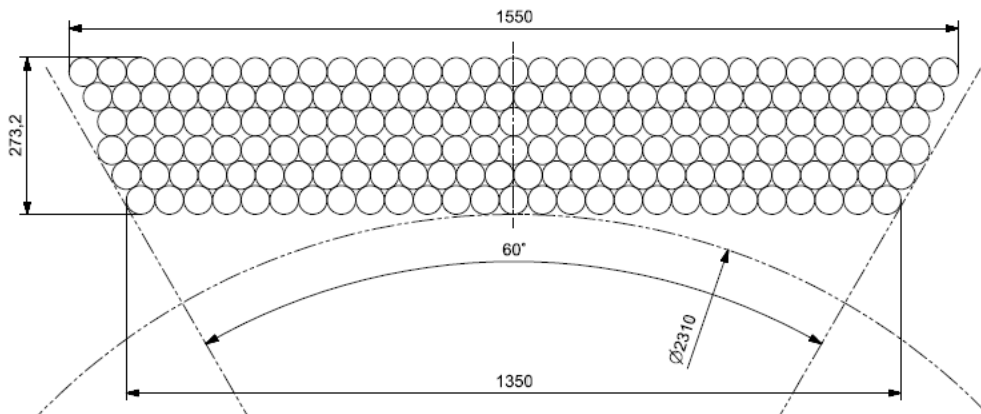


**Figure 4:** Detailed view of a detector segment assembled with six layers of drift tubes. The 3<sup>rd</sup> and 4<sup>th</sup> layers are not staggered in order to minimize path ambiguities due to the circular symmetry of drift time measurements.

A dedicated system based on double read-out ensures a low precision (~20 cm) measurement of the coordinate along wires which is sufficiently accurate given the geometry of this application.

#### 4. Simulation

Cosmic muons are generated according to experimental measurements of their energy spectrum and angular distribution. An accurate description of CASTOR® V/21 is modelled in GEANT4 framework [3]. GEANT4 includes all the physical phenomena occurring to a particle crossing a variety of materials. In particular, it foresees the particle scattering and its absorption when its energy is not sufficient to cross the whole amount of material present in its path. Full loaded casks as well as casks with missing fuel assemblies are considered. Generated cosmic muons are then traced, within the GEANT4 framework, inside the casks.

In order to study the acceptance effects of a limited coverage prototype as shown in Fig. 3, only muons crossing one detector with a direction pointing to the opposite one are considered. However, to ensure a reconstruction of the whole volume, it is possible to rotate the detectors and to collect data as depicted

in Fig. 5. A dataset containing simulated muons corresponding to the three positions of Fig. 5 has been generated.

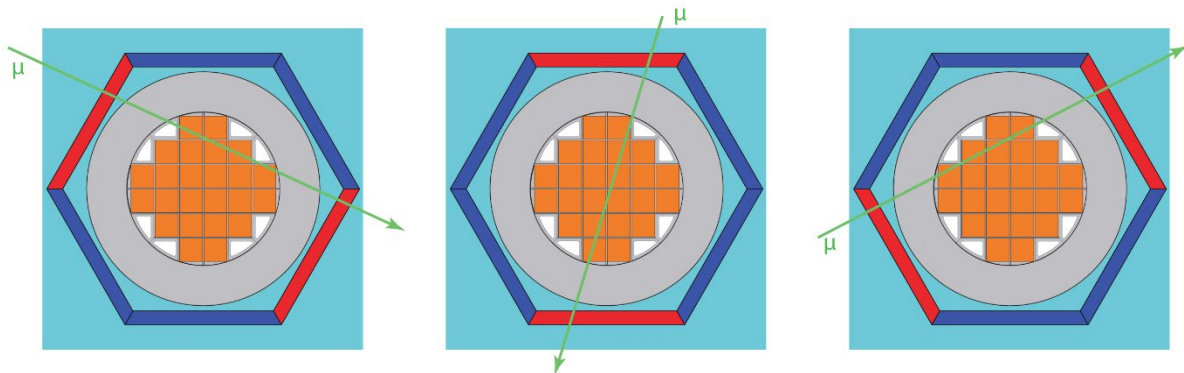


**Figure 5:** Schematic view of three data taking positions, for a middle size prototype covering 1/3 of the DPC surface.

In addition, to study effects induced by the detector response, the muon signal on the detector channels is also simulated by assigning an uncertainty corresponding to the experimental error measured in such a type of detectors. In detail, a 300 μm error is considered in the horizontal plane, while an uncertainty of 20 cm is given to the measurement of the vertical coordinate. The muon track is then reconstructed by a linear fit to all the measured points. A dedicated study of the effects induced by wrong track reconstruction due to the drift time circular symmetry has also been included.

## 5. Simulation results

The results obtained with simulated data corresponding to a full coverage detector demonstrate the capability of this technology to recognise the absence of fuel assemblies from a CASTOR® V/21 as shown in Fig. 6. The image on the right was obtained with a transmission algorithm [4], with a dataset corresponding to 12 hours of recording time. It shows in a colour scale the measured quantity, called stopping power (SP), which is the energy lost by the muon per unit length of crossed material. It is roughly proportional to the material density.

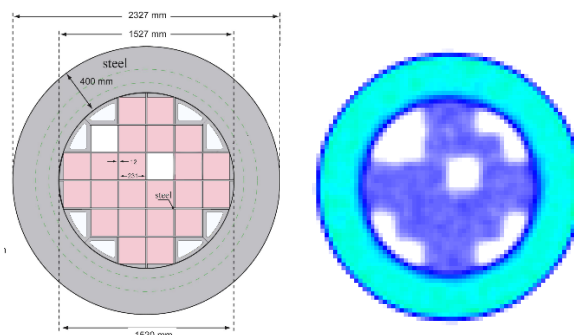


**Figure 6:** Layout of a CASTOR® V/21 with two missing assemblies (left) and the reconstructed image obtained with a full coverage detector and 12 hours of data taking (right).

With a prototype detector covering only 1/3 of the DPC surface, similar results on fuel assembly information can be obtained provided data are recorded with detectors placed in several positions, as shown in Fig.5.

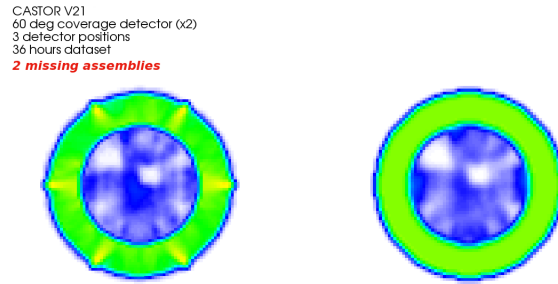


**Figure 7:** Reconstructed image of a CASTOR® V/21 with two missing assemblies obtained with a 1/3 coverage detector and 12 hours of data taking in three positions as indicated in Fig. 5 (left). The image obtained after fixing the SP of the cask structure to its known value (right).

The image of the same CASTOR® cask of Fig. 6 reconstructed on the basis of data collected with a detector covering 1/3 of the DPC surface in three positions is shown in Fig. 7. The image is obtained with three sets of data each corresponding to 12 hours of recording time. The left image in fig. 7 shows artefacts due to limited acceptance at the detector borders. They can be removed, as can be seen the right image, by fixing the SP value in the volume corresponding to the cask structure. The average stopping power for each volume containing a fuel assembly is shown in Fig. 8. Clearly, the positions with missing assemblies correspond to negligible values of stopping power. The results shown in Fig. 7 and 8 are obtained on the basis of simulated tracks, without considering measurement errors induced by the proposed detectors.

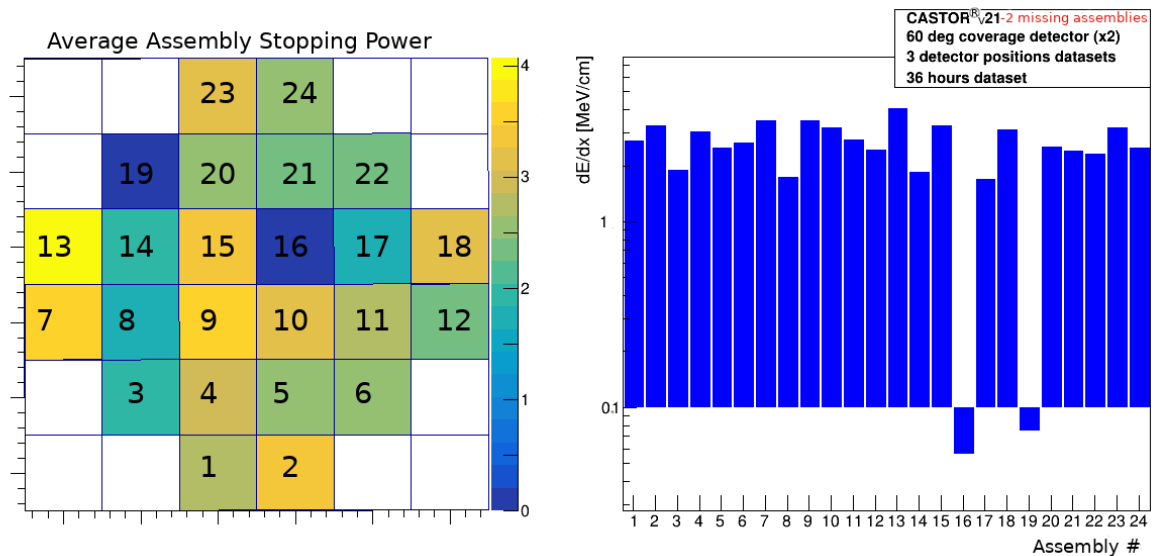


**Figure 8:** Average stopping power for the volumes supposed to contain a fuel assembly in a CASTOR® V/21 with two missing assemblies obtained with a 1/3 coverage detector and 12 hours of data taking in three positions as indicated in Fig. 5. Map with a colour scale (left); histogram with a logarithmic scale (right).

## 6. Conclusions

Recent field tests performed in 2018 by INFN and EURATOM with a small INFN prototype muon drift tube detector has shown excellent performance close to a fully loaded CASTOR® V/19 cask. GEANT4 simulations have been performed on similar CASTOR® V/21 cask to investigate whether the muon trackers could be used for safeguards purposes to identify the missing fuel assemblies. Two investigated scenarios, one with a full CASTOR® V/21 surface coverage trackers and another with 1/3 coverage trackers have proved that in both cases the missing assemblies can be identified within 12 hours of

measurement time. The calculations prove that the muon tomography is a perfectly adequate technique for the inspection of DPC.

## 7. Acknowledgements

This work has been supported by EURATOM and the special project INFN\_E (from INFN).

## 8. References

- [1] Checchia P. et al. *Muography of spent fuel containers for safeguards purposes* IAEA Symposium on International Safeguards CN267-048 (2018)
- [2] Marton, E. et al, *Muons scanner to detect radioactive sources hidden in scrap metal containers* Mu-Steel Final report DOI:10.2777/75975
- [3] Agostinelli S. et. al., *GEANT4 – a simulation toolkit*, Nucl. Instrum. Met. A 506 (2003) 250  
[https://doi.org/10.1016/S0168-9002\(03\)01368-8](https://doi.org/10.1016/S0168-9002(03)01368-8)
- [4] Vanini, S. et al. *Muography of different structures using muon scattering and absorption algorithms* Phil. Trans. R. Soc. A377: 20180051 <https://doi.org/10.1098/rsta.2018.0051>

# **Session 6:**

# **Spent Fuel II**

# Use of machine learning models for the detection of fuel pin replacement in spent fuel assemblies

**Riccardo Rossa, Alessandro Borella**

SCK•CEN Belgian Nuclear Research Centre  
Boeretang 200 – 2400 Mol, Belgium  
E-mail: [rossa@sckcen.be](mailto:rossa@sckcen.be)

## **Abstract:**

*The nuclear material contained in the spent fuel assemblies represents the majority of the material verified during the safeguards inspections, and the replacement of spent fuel pins from an assembly is one of the possible scenarios to divert nuclear material.*

*Due to the high number of fuel pins contained in a fuel assembly (e.g. 264 pins in a PWR 17x17 geometry), a practically infinite number of diversion scenarios can be considered by a potential proliferator. In this framework, Monte Carlo simulations were used to model some of the possible diversion scenarios and to develop a database of detector responses corresponding to different non-destructive assay (NDA) techniques. In addition, the database contains the detector responses obtained with complete fuel assemblies with different initial enrichment, burnup, and cooling time.*

*Given the large size of the database and the multiple detector responses resulting from the NDA techniques, the use of machine learning is proposed for the data analysis. In this work we focus on the classification problem with the aim of classifying the diversion scenarios based on the percentage of replaced pins. Several machine learning models were developed for this problem using decision trees, discriminant analysis, support vector machine, and nearest neighbors algorithms. The accuracy of the models was calculated as the number of correct classifications in the whole dataset.*

*The results from the study show that the selection of the detector type used as input in the machine learning model has a strong impact on the accuracy of the developed model. In general the use of gamma-ray detectors leads to higher accuracies compared to the use of neutron detector responses. In addition, several machine learning models achieved a classification accuracy of more than 90%.*

**Keywords:** Machine learning, fuel diversion, Monte Carlo, spent fuel, non-destructive assays

## **1. Introduction**

As defined in the INFCIRC/153 [1] the technical objective of safeguards is the timely detection of diversion of significant quantities of nuclear material. The nuclear material contained in the spent fuel assemblies represents the majority of the material verified during the safeguards inspections [2], and the replacement of spent fuel pins from an assembly is one of the possible scenarios to divert nuclear material.

The capabilities to detect missing or replaced spent fuel pins, the so-called partial defect testing, were assessed in the past for the Fork detector [3]. In addition, several non-destructive assay (NDA) techniques are proposed to improve the current capabilities for partial defect testing [4], [5]. Among others NDA techniques, the Self-Indication Neutron Resonance Densitometry (SINRD) and the Partial Defect Tester (PDET) have been investigated in the past years at SCK•CEN [6].

Given the large number of diversion scenarios that can be developed and the multiple detector responses resulting from the two NDA techniques, the use of machine learning [7] is proposed for the data analysis as alternative to a previous approach chosen in recent work [8]. Due also to the continuous increase in the computer power, machine learning is extensively used in many fields where large amount of data is available [9], [10]. Within SCK•CEN, research on machine learning applied to the safeguards field focused so far on the use of artificial neural networks (ANN) for the determination of initial enrichment, burnup, and cooling time of spent fuel assemblies [11].

In this contribution the two NDA techniques chosen for the study are described in Section 2, whereas the overview of the Monte Carlo simulations is presented in Section 3, and the description of the machine learning models is included in Section 4. The results from the data analysis are discussed in Section 5, followed by the conclusion and outlook for future work in Section 6.

## 2. Description of the NDA techniques

### 2.1. Models geometry

The NDA techniques chosen for this study are the Self-Interrogation Neutron Resonance Densitometry (SINRD) and the Partial Defect Tester (PDET).

The SINRD technique is a passive NDA technique that was originally developed by LANL based on the passive neutron emission from spent fuel due to spontaneous fissions and ( $\alpha$ ,n) reactions [12]. The principle of the SINRD technique is to measure the attenuation of the neutron flux in the 0.3 eV energy region to obtain a direct estimation of the  $^{239}\text{Pu}$  content in the spent fuel. The technique has been studied for the measurement of spent fuel underwater at LANL [13], [14], [15], whereas a measurement approach in air has been investigated at SCK•CEN [16], [6]. The SINRD detector setup adopted in this study is shown on the left side of Figure 1. The PWR 17x17 fuel assembly geometry was considered in all simulations. The fuel assembly is kept in air and surrounded by a thick slab of polyethylene to ensure neutron moderation. A set of detectors are placed in the fuel assembly guide tubes (red and yellow positions in Figure 1) and in the air gap between the fuel and the polyethylene (green positions).

The Partial Defect Tester (PDET) is a NDA technique that measures the passive neutron and gamma emission from the fuel assembly [17], [18], [19]. The PDET was originally proposed by LLNL with the aim of detecting partial defects, and a PDET prototype has been built and tested in a measurement campaign at the Swedish Interim Storage Facility CLAB in January 2015 [20]. The approach for the PDET detector chosen in this study employs the same detector setup of the SINRD technique, with the difference that the fuel assembly is stored in fresh water. The PDET detector setup is shown on the right side of Figure 1.

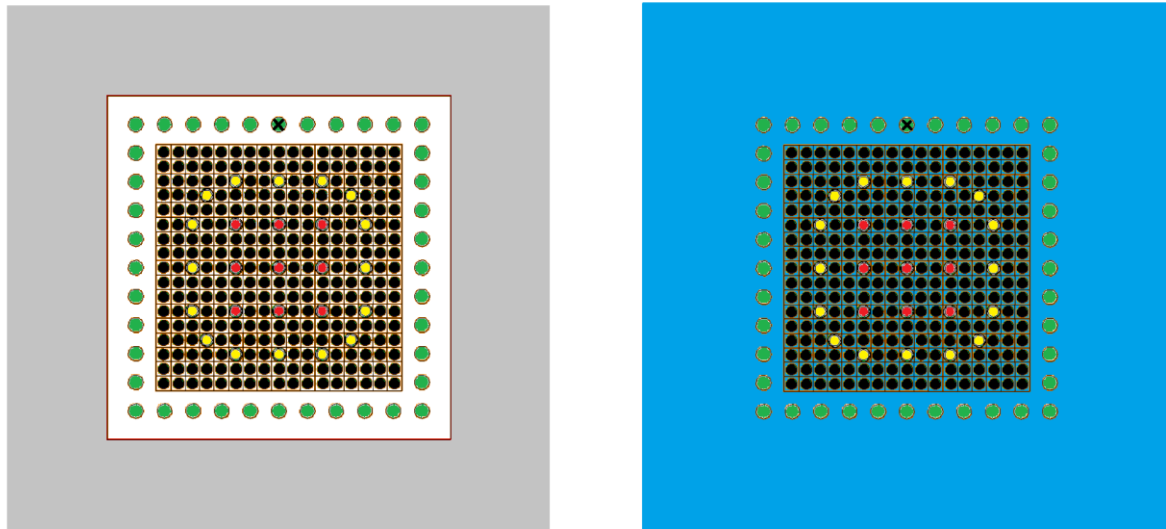


**Figure 1:** Monte Carlo models of the detector setups chosen in this study. The PWR 17x17 fuel assembly is represented with the fuel pins shown in black. The positions of the detectors are depicted in red, yellow, and green. The detector responses are normalized to the value obtained for the detector position marked with a cross. The picture on the left shows the setup for SINRD, with the polyethylene slab in grey surrounding the fuel assembly, and the picture on the right shows the setup for PDET with water depicted in blue.

### 2.2. Detector responses

The detector responses were calculated from the results of the Monte Carlo simulations and following the approach proposed in [6]. As shown in Figure 1, for both SINRD and PDET the detector positions and the detector types are identical. The calculated detector responses include:

- Thermal neutrons (TH): bare  $^{235}\text{U}$  fission chamber;
- Fast neutrons (FAST): bare  $^{238}\text{U}$  fission chamber;

- Resonance region neutrons (RES): difference between the neutron counts with a  $^{239}\text{Pu}$  fission chamber covered by Gd foil and a  $^{239}\text{Pu}$  fission chamber covered by Cd foil;
- Gamma-rays (P): ionization chamber.

### 3. Overview of the Monte Carlo simulations

#### 3.1. Complete fuel assemblies

The same set of Monte Carlo simulations was performed both for SINRD and PDET. From each simulation the detector responses were normalized to the value obtained for the detector marked with a cross in Figure 1. The average value was then calculated for the nine central guide tube positions, the sixteen peripheral guide tube positions, and the forty detector positions outside the fuel assembly.

A first set of simulations was performed with complete fuel assemblies, i.e. assemblies with all the fuel pins with equal material composition and source strength, considering different values of:

- Initial enrichment: 2.0, 2.5, 3.0, 3.5, 4.0, 4.5, 5.0%;
- Burnup: 5, 10, 15, 20, 30, 40, 60  $\text{GWd}/t_{\text{HM}}$ ;
- Cooling time: 1, 5, 10, 50 years.

A total of 196 simulations resulted from all combinations of these parameters. The aim of these simulations is to assess the influence of the fuel irradiation history on the calculated detector responses. The fuel composition and source strength were taken from the SCK•CEN reference spent fuel library [21].

#### 3.2. Diversion scenarios

A second set of simulations considered twelve diversion scenarios, where some of the spent fuel pins were replaced by dummies made of stainless steel. The remaining spent fuel pins had equal material composition and source strength as in the case for complete fuel assemblies, whereas no source term was included in the dummy pins. The scenario with pin replacement is expected to be more difficult to detect compared to the case of diversion without replacement.

The diversion scenarios are shown in Figure 2 and they cover cases with replacement between 50% and 15% of the total number of fuel pins. The fuel pins are depicted in grey, the dummy pins in white, and the guide tube positions in yellow. Most of the replacement occurs on the outer region of the fuel assembly, but also a chess-board pattern (Diversion 1) and diversion from the inner section of the fuel assembly (Diversion 5) are included.

All simulations concerning the diversion scenarios considered fuel with a cooling time of 5 years, but the influence of the irradiation history was taken into account simulating fuel with different values of:

- Initial enrichment: 2.0, 3.5, 5.0%;
- Burnup: 10, 30, 60  $\text{GWd}/t_{\text{HM}}$ .

A total of 108 simulations were carried out in this set of simulations.

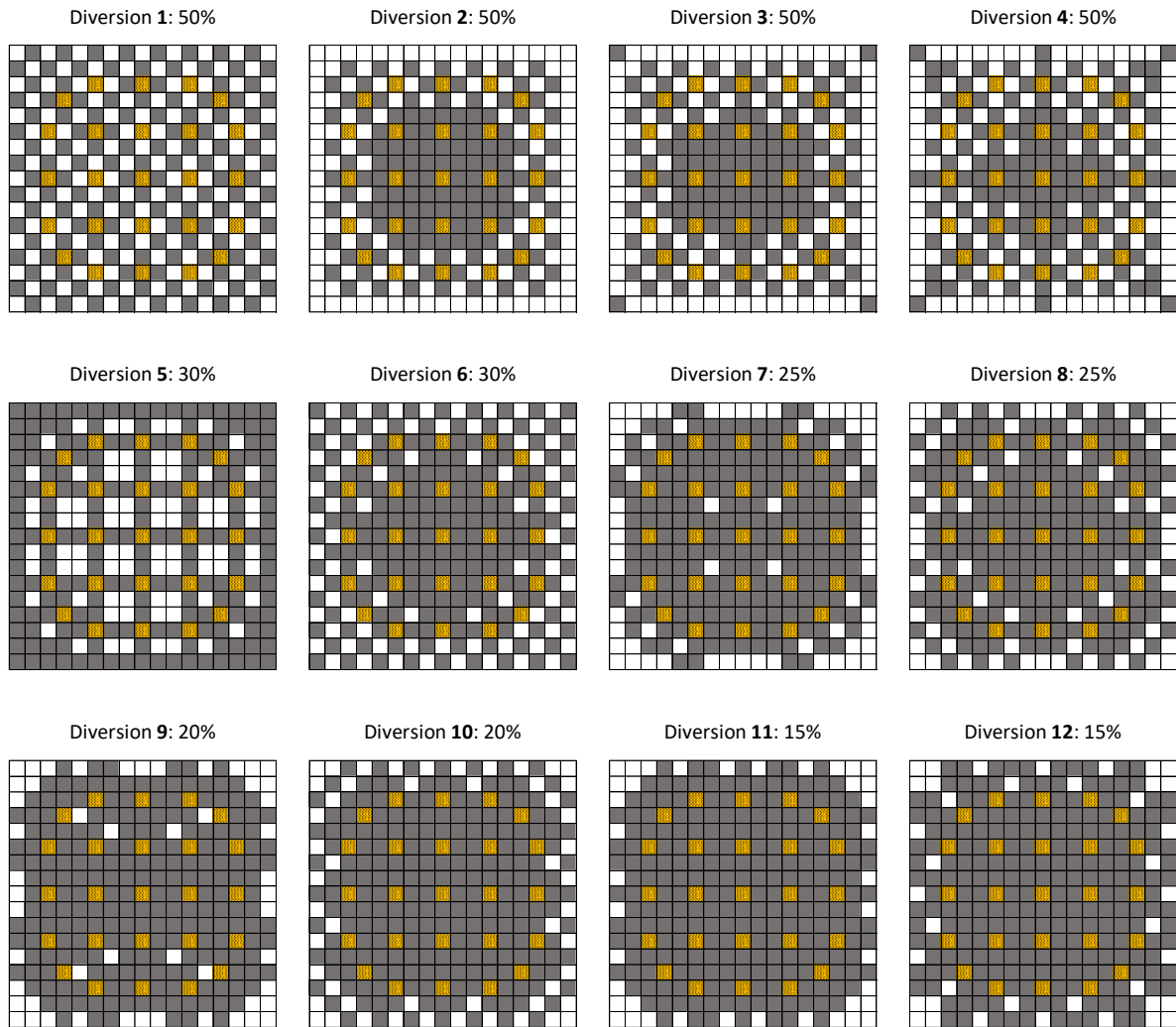


**Figure 2:** Overview of the diversions scenarios considered in this study. The fuel pins are marked in grey, the dummy pins in white, and the guide tube positions in yellow. The percentage of dummy pins is mentioned for each scenario.

## 4. Machine learning models used for the data analysis

### 4.1. Introduction to machine learning

Machine learning is used nowadays for a broad range of applications such as speech recognition, financial fraud detection, and cancer prognosis. [22], [23], [24], [25], [26]

The machine learning models can be divided into two broad categories of supervised and unsupervised learning [27]. In the case of supervised learning the observations in the dataset have associated output values, whereas in the case of unsupervised learning the input data does not have corresponding output values.

A machine learning model for supervised learning is first developed during the training phase on a set of known input and output data. Once the model is trained, it is used to predict (prediction phase) new input data for which the output data is unknown. The generic workflow for supervised learning is shown in Figure 3. The machine learning model developed by supervised learning uses regression or classification techniques depending on the type of output data. Regression techniques are used to predict output data that can assume continuous values (e.g. changes in temperature or pressure, fluctuations in housing prices), whereas classification techniques are used to classify input data into categories that can assume only a limited set of values (e.g. type of fruit, benign/malign tumor). [9]

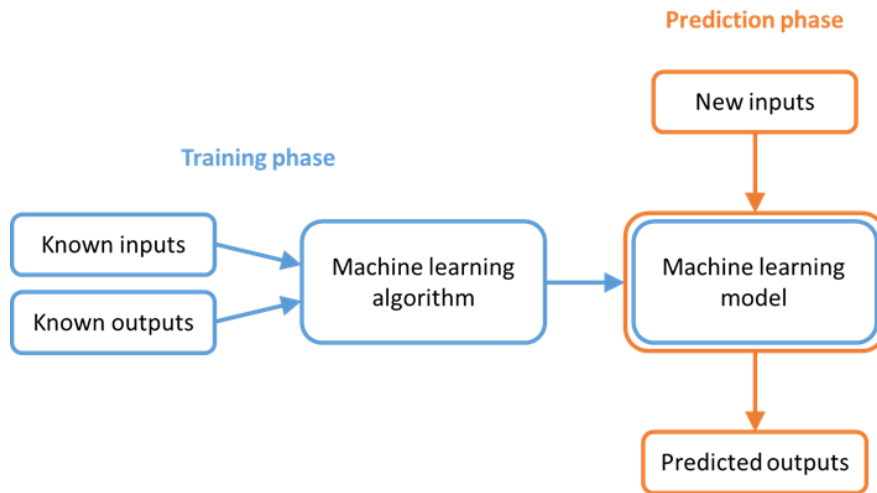


**Figure 3:** Generic workflow in case of supervised learning. The development of the machine learning model from known inputs and outputs is indicated as training phase, whereas the prediction of outputs from new inputs is referred to as prediction phase.

Independently from the machine learning algorithm chosen, the data needed to develop a machine learning model is generally organized in a database. According to the machine learning terminology the records in the database are called observations and the input variables are called features or predictors. In case of supervised learning the output variables are called responses. Specific to classification techniques, the responses can assume only a finite set of values (either in numerical or text format) called classes.

The detector responses calculated with the Monte Carlo simulations described in Section 3 were organized in a database where the normalized average detector responses were the features and the percentage of replaced pins represented the response. Six classes were defined for the response, representing 50, 30, 25, 20, 15, and 0% of replaced pins. Therefore, each observation in the database consisted in 12 features and 1 response. An extract of the database for the SINRD technique is shown in Table 1; the same database structure was used for the data of the PDET detector. Since each observation in the training database contained the corresponding response class, the detection of fuel pins diversion was treated as a supervised machine learning problem to be solved with classification techniques.

The accuracy of the models was calculated as the number of correct classifications in the whole dataset, and this metric was used to compare the different machine learning models developed.

**Table 1:** Extract of the training database for the SINRD technique.

Features												Resp.
Central det. positions				Peripheral det. positions				External det. positions				
TH	FA	RES	P	TH	FA	RES	P	TH	FA	RES	P	
0.35	1.85	0.40	2.09	0.52	1.64	0.56	1.91	1.10	0.86	1.04	0.85	0
0.34	1.85	0.35	2.09	0.51	1.64	0.51	1.91	1.10	0.86	1.05	0.85	0
0.34	1.86	0.32	2.09	0.51	1.64	0.48	1.91	1.10	0.86	1.06	0.85	0
0.34	1.86	0.30	2.09	0.51	1.64	0.47	1.91	1.10	0.86	1.06	0.85	0
0.33	1.87	0.28	2.08	0.51	1.65	0.45	1.91	1.10	0.86	1.06	0.85	0

## 4.2. Parameters chosen for the machine learning models

The machine learning models for this study were developed using the Classification Learner App that is part of the MATLAB Statistics and Machine Learning Toolbox [28].

The toolbox offers the choice of several machine learning algorithms that can be used for supervised and unsupervised learning problems. The Classification Learner App has a graphical user interface

(GUI) that allows the user to select in the first window the training database, the variables to be used as features, and those to be used as responses.

The selection of the validation scheme used to assess the accuracy of the developed model is the next step in the GUI. The default MATLAB 5-fold cross-validation approach was chosen, where the training database is divided into five equal-sized subsections. As noted in [28], the validation scheme is used only for the estimation of the model accuracy; the final model is always trained using the complete training database.

The next section in the GUI is the selection of the model type and model parameters, and the training of the model. Four main families of machine learning models were used for the data analysis: decision trees, discriminant analysis, support vector machines, and nearest neighbours classifiers. The principles of the models are described extensively in literature [28], [22], [9], [29], [30], [31]. The parameters used for each developed model are listed in Tables 2-5.

**Table 2:** Parameters chosen for the decision trees models.

Model name	Maximum number of splits	Split criterion	Surrogate decision splits
Simple tree	5	Gini's diversity index	Off
Medium tree	10	Gini's diversity index	Off
Complex tree	30	Gini's diversity index	Off

**Table 3:** Parameters chosen for the discriminant analysis models.

Model name	Function used to separate classes	Covariance matrix
Linear discriminant	Linear	Diagonal
Quadratic discriminant	Quadratic	Diagonal

**Table 4:** Parameters chosen for the support vector machine models. In the first three models the kernel scale mode was set to Auto, so the option Manual kernel scale was not used.

Model name	Kernel function	Box constraint level	Kernel scale mode	Manual kernel scale	Multiclass method	Standardize data
Linear SVM	Linear	1	Auto	-----	1-vs-1	Yes
Quadratic SVM	Quadratic	1	Auto	-----	1-vs-1	Yes
Cubic SVM	Cubic	1	Auto	-----	1-vs-1	Yes
Coarse Gaussian SVM	Gaussian	1	Manual	4	1-vs-1	Yes
Medium Gaussian SVM	Gaussian	1	Manual	1	1-vs-1	Yes
Fine Gaussian SVM	Gaussian	1	Manual	0.25	1-vs-1	Yes

**Table 5:** Parameters chosen for the nearest neighbors models.

Model name	Number of neighbors	Distance metric	Distance weight	Standardize data
Coarse kNN	100	Euclidean	Equal	Yes
Medium kNN	10	Euclidean	Equal	Yes
Fine kNN	1	Euclidean	Equal	Yes

Cosine kNN	10	Cosine	Equal	Yes
Cubic kNN	10	Minkowski (cubic)	Equal	Yes
Weighted kNN	10	Euclidean	Squared inverse	Yes

## 5. Results

### 5.1. Self-Indication Neutron Resonance Densitometry

The classifier models described in Section 4.2 were applied to the detector responses for the SINRD technique. The accuracies of all models developed using as features the detector responses from the external detector positions are shown in Table 6, whereas the results obtained using all input features are shown in Table 7. These results were selected because they represent the lowest and highest accuracies among the models developed.

The rows of Tables 6-7 indicate the names of the machine learning models, whereas the columns indicate the normalized detector responses used for the analysis. As described in Section 2.2 the detector responses refer to neutron detectors sensitive to the thermal (TH), resonance (RES), or fast (FA) energy regions, and to the total gamma-ray emission (P). One or more detector responses were considered in the analysis and are included in the table. In Table 6 only one feature per detector response was used, namely the average detector response from the detectors in the external positions. In Table 7 three separate features were used for each detector response, corresponding to the average values from the detectors in the central, peripheral, and external positions, respectively. The values included in the table are the accuracy of each model, which is defined as the percentage of observations with correct classification.

The results of Table 6 indicate that the selection of the features used as input variable in the model is important to obtain a reliable classification, and in general the use of the gamma-ray detector response leads to higher accuracy of the model compared to other detector types. This result is in line with previous research [8]. However, the addition of multiple features does not strongly improve the accuracy of the model in most of the cases.

Once the features used in the model are chosen, similar accuracies were obtained for most of the machine learning models applied in this study. However, "Linear discriminant", "Coarse kNN", and "Cosine kNN" models showed several cases where the accuracy was lower than 75%. Complete correct classifications were reached for the "Complex tree", "Fine Gaussian SVM", "Fine kNN", and "Weighted kNN" models when the gamma-ray detector response (P) was used as feature alone or in combination with the fast neutron detector response (FA).

The accuracies calculated for the machine learning models using the detector responses from all positions (i.e. central, peripheral, and external) are included in Table 7. Most of the conclusions drawn from the results in Table 6 are also applicable for Table 7, but in general the use of the detector responses from all available positions lead to an increase in the model accuracy. The largest accuracies are obtained using the responses of detectors sensitive to fast neutrons or gamma-rays. Accuracies lower than 75% were obtained for all cases using "Fine Gaussian SVM" and "Coarse kNN" models except when the feature used was only the fast neutron detector response (FA) or the gamma-ray detector response (P). Complete correct classifications were reached for several models, usually when the gamma-ray detector response (P) was used as feature either alone or in combination with other features.

### 5.2. Partial defect tester

Machine learning models based on the parameters described in Section 4.2 were also developed from the detector responses of the PDET detector. The accuracy for each model was computed and compared to the accuracy of the corresponding model developed for the SINRD technique. Tables 8-9 show the accuracy calculated for the PDET detector using the detector responses from the external positions or from all positions, respectively.

The results in the tables show that in most of the cases the accuracy calculated for the two techniques is within  $\pm 5\%$ . Therefore, the comments reported for the SINRD technique in Section 5.1 are also valid for the PDET detector. Focusing on the cases where the difference in accuracy is larger than 5%, the accuracy for the PDET detector is generally higher than the corresponding value obtained for the

SINRD technique. This is observed in Table 8 when the responses of detectors sensitive to thermal neutrons (TH) or resonance region neutrons (RES) are used as features alone or in combination. On the contrary, a decrease between 5 and 10% was observed for several models when the responses of detectors sensitive to resonance region neutrons (RES) or fast neutrons (FA) are both used as features. Complete correct classifications were achieved using the "Fine Gaussian SVM" model with the (FA,P) features, the "Fine kNN" model using the (FA,P), (TH,FA,P), and (RES,FA,P) features, and the "Weighted kNN" model using the (FA,P) feature.

It is worth to note that for the PDET detector no detector response alone is able to reach a complete classification using the detector positions located outside the fuel assembly. This is in contrast to the results obtained for the SINRD technique, where the gamma-ray detector response reached a complete classification with several machine learning models. The results obtained with SINRD are remarkable in the sense that they indicate that a passive gamma measurement in air has the potential for a complete classification. In addition, if neutron detectors such as fission chambers are not needed, it would significantly simplify the design of a measurement device for spent fuel assay.

However, a safeguards verification underwater, like the one based on the PDET approach, is probably more realistic than a measurement in air, like the one based on the SINRD approach.

Hence future work will be targeted at improving the accuracy of the current models to reach a complete classification also for the PDET detector.

Considering the accuracies calculated using all detector positions in Table 9, the largest difference between SINRD and PDET were obtained using as input features the responses of detectors sensitive to thermal neutrons (TH) or resonance neutrons (RES) either alone or in combinations. An increase of efficiency calculated for the PDET detector between 5 and 10% was obtained for decision tree and discriminant analysis models, whereas a decrease between -5% and -10% was obtained for "Linear SVM", "Quadratic SVM", and "Cubic SVM" models. Several models reached a complete correct classification using the features of the PDET detector, especially when the gamma-ray detector response (P) was used alone or in combinations with other detector responses.

**Table 6:** Accuracy (%) of the machine learning models using the detector responses from the external detector positions. Results for the SINRD technique. The cases with complete correct classification are highlighted in bold.

Detector response 1	Detector positions considered: external (1 feature per detector response)															
	TH	RES	FA	P	TH	TH	TH	RES	RES	FA	TH	TH	TH	RES	TH	RES
Detector response 2					RES	FA	P	FA	P	P	RES	RES	FA	FA	FA	RES
Detector response 3											FA	P	P	P	P	FA
Detector response 4																P
Simple tree	67.8	70.1	83.9	84.9	72.0	82.9	85.9	82.2	84.5	86.2	84.5	83.6	87.2	88.8	87.2	
Medium tree	68.8	68.4	86.2	94.4	69.4	84.5	94.7	85.9	92.1	99.0	87.2	93.1	97.4	96.4	94.7	
Complex tree	63.8	62.5	85.9	<b>100</b>	66.8	84.9	97.7	87.2	94.1	99.3	85.9	93.8	98.4	96.1	96.4	
Linear discriminant	68.1	69.4	70.4	73.4	71.1	79.9	74.3	83.2	78.9	76.6	79.6	79.6	80.3	81.6	81.3	
Quadratic discriminant	67.8	69.7	79.9	85.2	70.4	84.9	85.2	87.8	90.5	85.2	85.2	88.2	85.9	87.5	85.9	
Linear SVM	67.4	70.1	76.0	80.6	69.7	83.9	79.9	85.2	87.2	86.5	84.9	84.9	88.5	89.8	90.1	
Quadratic SVM	69.7	70.1	81.3	89.5	69.7	86.2	89.1	88.8	94.1	94.7	90.1	92.4	96.4	95.4	96.7	
Cubic SVM	39.8	53.9	79.9	96.4	72.0	86.8	94.4	90.5	94.1	96.7	86.8	91.4	97.7	96.4	96.4	
Coarse Gaussian SVM	64.5	70.1	78.3	79.3	70.1	83.9	78.0	86.2	83.9	83.9	86.2	84.5	86.5	90.1	90.1	
Medium Gaussian SVM	68.4	70.4	80.9	90.8	70.4	85.5	87.5	89.8	95.1	99.3	89.8	93.4	97.4	96.7	96.7	
Fine Gaussian SVM	67.4	68.8	88.8	<b>100</b>	70.1	85.2	89.8	81.6	94.4	<b>100</b>	69.7	71.4	84.9	81.3	68.8	
Coarse kNN	64.5	64.5	70.4	64.5	64.5	65.5	64.5	67.4	64.5	67.4	64.5	64.5	67.1	67.4	67.4	
Medium kNN	67.4	68.8	87.5	98.7	70.1	83.2	81.3	89.1	92.4	98.4	84.9	86.2	87.8	96.4	89.5	
Fine kNN	56.9	54.9	84.9	<b>100</b>	62.5	88.5	90.5	88.8	94.7	<b>100</b>	86.2	91.4	97.4	98.0	96.1	
Cosine kNN	64.5	64.5	75.7	69.4	72.0	80.9	74.0	81.3	82.2	89.8	82.6	81.6	82.9	88.5	85.2	
Cubic kNN	66.8	69.7	86.8	98.0	72.0	81.3	81.6	89.5	88.5	97.0	84.9	85.5	85.9	94.1	90.1	
Weighted kNN	60.2	59.9	87.2	<b>100</b>	68.8	84.2	92.8	88.8	95.4	<b>100</b>	86.5	92.1	97.0	97.7	94.1	

**Table 7:** Accuracy (%) of the machine learning models using the detector responses from all detector positions. Results for the SINRD technique. The cases with complete correct classification are highlighted in bold.

Detector response 1	Detector positions considered: central, peripheral, external (3 features per detector response)														
	TH	RES	FA	P	TH	TH	TH	RES	RES	FA	TH	TH	TH	RES	TH
Detector response 2					RES	FA	P	FA	P	P	RES	RES	FA	FA	RES
Detector response 3											FA	P	P	P	FA
Detector response 4															P
Simple tree	70.7	70.7	92.4	92.8	72.0	92.4	92.8	92.4	93.1	93.1	92.4	93.1	92.1	92.4	91.4
Medium tree	70.4	71.4	98.0	<b>100</b>	72.7	97.4	<b>100</b>	97.7	<b>100</b>	99.7	96.4	<b>100</b>	99.3	99.3	99.0
Complex tree	71.7	68.4	98.0	<b>100</b>	71.1	97.4	<b>100</b>	98.0	<b>100</b>	99.7	97.7	<b>100</b>	99.0	99.3	99.3
Linear discriminant	71.1	68.8	90.1	88.8	63.5	87.2	86.2	85.5	85.9	88.5	82.6	84.2	90.5	87.5	88.2
Quadratic discriminant	71.7	66.8	92.4	94.4	66.1	93.1	95.1	93.1	95.1	94.4	91.8	95.1	94.4	95.4	95.4
Linear SVM	89.8	78.6	94.1	94.1	87.5	94.1	93.8	94.1	93.1	96.1	94.7	96.4	94.1	95.4	94.4
Quadratic SVM	92.8	80.6	97.7	98.7	93.1	99.7	99.7	98.7	97.7	98.4	99.0	99.0	98.4	99.3	99.7
Cubic SVM	91.8	82.6	99.3	<b>100</b>	92.1	<b>100</b>	<b>100</b>	98.7	99.7	<b>100</b>	98.7	98.4	<b>100</b>	99.7	98.7
Coarse Gaussian SVM	74.7	73.4	92.8	94.4	77.6	94.7	94.1	93.1	94.7	96.1	95.1	95.7	97.0	97.7	97.4
Medium Gaussian SVM	83.6	75.0	99.7	<b>100</b>	80.9	98.7	99.0	95.4	97.7	<b>100</b>	87.8	86.8	98.0	95.7	86.2
Fine Gaussian SVM	79.3	70.1	98.0	<b>100</b>	64.5	68.1	77.3	64.5	70.4	98.7	64.5	64.5	67.4	64.5	64.5
Coarse kNN	64.5	64.5	73.4	67.4	64.5	72.0	67.4	70.7	66.8	73.0	69.7	66.8	71.7	71.7	70.1
Medium kNN	76.0	73.4	98.7	<b>100</b>	75.3	86.2	87.5	90.1	91.1	99.7	85.2	87.8	90.8	93.4	91.4
Fine kNN	83.6	81.3	99.7	<b>100</b>	80.3	98.7	99.7	97.4	97.7	<b>100</b>	94.7	95.4	<b>100</b>	99.0	97.4
Cosine kNN	81.3	73.0	96.1	99.3	78.6	85.2	86.8	87.2	85.2	97.7	85.5	83.2	85.5	88.2	86.2
Cubic kNN	79.6	73.4	99.3	<b>100</b>	75.3	85.5	87.5	88.5	89.8	98.7	84.5	85.9	89.5	92.4	87.5
Weighted kNN	82.2	80.3	99.7	<b>100</b>	79.6	98.4	97.7	95.7	96.1	<b>100</b>	92.1	91.1	99.0	99.0	96.4

**Table 8:** Accuracy (%) of the machine learning models using the detector responses from the external detector positions. Results for the PDET detector. The cases with complete correct classification are highlighted in bold.

Detector response 1 Detector response 2 Detector response 3 Detector response 4	Detector positions considered: external (1 feature per detector response)														
	TH	RES	FA	P	TH	TH	TH	RES	RES	FA	TH	TH	TH	RES	TH
					RES	FA	P	FA	P	P	RES	RES	FA	FA	RES
											FA	P	P	P	FA
															P
Simple tree	76.0	74.7	82.2	87.2	78.0	82.9	86.2	83.6	87.2	88.5	84.2	85.9	88.2	89.1	88.8
Medium tree	77.6	75.7	85.2	96.1	79.9	88.8	95.7	84.9	97.7	97.4	88.2	95.1	96.4	95.4	94.7
Complex tree	77.6	74.0	86.2	98.7	78.6	88.5	96.4	84.9	96.4	97.0	88.5	95.1	96.1	93.1	96.7
Linear discriminant	71.4	71.1	69.4	74.0	71.7	72.0	79.6	73.4	77.3	79.3	73.0	80.3	80.9	78.6	80.9
Quadratic discriminant	78.3	76.6	78.3	85.5	77.0	81.3	87.8	80.6	85.2	86.8	83.9	88.8	89.8	87.2	91.4
Linear SVM	75.0	73.7	76.6	82.6	74.7	78.0	87.5	76.6	83.9	85.5	77.6	87.5	90.1	84.2	91.4
Quadratic SVM	77.0	75.7	78.6	88.2	77.3	88.8	92.4	85.9	90.1	98.0	86.8	92.8	95.7	95.4	95.7
Cubic SVM	72.0	69.4	78.3	91.8	76.0	89.1	95.1	85.2	93.1	99.0	88.8	94.7	98.4	97.7	97.7
Coarse Gaussian SVM	77.3	74.3	76.6	80.3	77.3	79.3	88.5	77.3	84.2	82.9	79.6	88.8	89.8	88.5	91.8
Medium Gaussian SVM	77.6	76.0	81.6	85.9	78.3	87.2	93.8	83.6	90.1	96.7	87.5	92.4	99.0	97.7	99.3
Fine Gaussian SVM	78.9	77.6	87.2	97.0	76.3	87.5	95.7	82.9	92.8	<b>100</b>	78.9	79.6	96.7	93.1	76.6
Coarse kNN	71.4	68.8	70.4	64.5	69.7	70.4	67.4	70.4	67.4	68.4	70.4	67.4	68.1	67.8	68.8
Medium kNN	77.3	73.4	83.6	98.4	78.6	87.2	93.1	82.6	89.1	99.7	85.5	88.5	97.7	91.1	93.1
Fine kNN	74.7	75.0	84.5	97.0	79.3	89.5	97.7	84.2	95.4	<b>100</b>	88.8	93.1	<b>100</b>	<b>100</b>	99.3
Cosine kNN	75.0	64.5	73.7	72.0	72.0	76.6	88.5	76.3	82.6	86.5	78.6	83.6	90.5	87.2	89.8
Cubic kNN	79.9	73.7	83.6	98.7	78.6	89.1	89.5	81.3	87.5	96.7	83.6	89.1	96.4	92.4	93.1
Weighted kNN	74.0	75.3	83.2	97.4	78.6	90.8	97.0	82.9	94.1	<b>100</b>	87.8	93.1	99.3	97.7	97.7

**Table 9:** Accuracy (%) of the machine learning models using the detector responses from all detector positions. Results for the PDET detector. The cases with complete correct classification are highlighted in bold.

Detector response	Detector positions considered: central, peripheral, external (3 features per detector response)														
	TH	RES	FA	P	TH	TH	TH	RES	RES	FA	TH	TH	TH	RES	TH
Detector response 1															
Detector response 2					RES	FA	P	FA	P	P	RES	RES	FA	FA	RES
Detector response 3											FA	P	P	P	FA
Detector response 4															P
Simple tree	78.6	82.2	93.4	94.1	84.5	93.4	94.1	87.8	88.5	94.1	88.8	88.8	93.8	88.8	89.8
Medium tree	81.6	81.9	98.4	<b>100</b>	83.9	98.7	<b>100</b>	96.7	97.0	99.7	96.7	96.7	99.7	96.4	95.7
Complex tree	81.6	83.2	99.0	<b>100</b>	85.5	99.0	<b>100</b>	95.7	97.0	99.7	97.0	95.7	99.3	97.0	96.1
Linear discriminant	75.7	75.0	90.5	86.8	73.0	86.5	86.8	85.5	87.2	91.1	81.3	81.6	89.1	88.5	86.2
Quadratic discriminant	83.6	80.3	93.4	94.7	80.6	93.8	95.4	95.4	96.1	94.7	92.8	95.1	95.7	96.1	95.7
Linear SVM	80.6	81.9	94.1	93.4	82.9	92.8	93.8	95.4	96.7	95.7	95.4	94.4	93.4	95.4	94.4
Quadratic SVM	84.9	84.9	99.0	98.4	87.5	99.7	99.3	99.0	99.7	98.4	99.0	99.7	99.0	99.7	99.7
Cubic SVM	84.2	85.9	<b>100</b>	<b>100</b>	84.9	<b>100</b>	99.3	99.3	<b>100</b>	<b>100</b>	99.3	99.3	<b>100</b>	99.7	<b>100</b>
Coarse Gaussian SVM	81.3	83.6	93.4	94.1	83.6	93.8	95.1	95.7	98.4	96.4	94.7	97.4	97.4	99.0	98.0
Medium Gaussian SVM	84.9	82.6	<b>100</b>	<b>100</b>	84.2	98.7	98.4	97.4	96.7	<b>100</b>	89.5	93.1	99.0	97.0	89.1
Fine Gaussian SVM	76.3	69.1	99.7	<b>100</b>	65.1	68.1	69.7	65.5	65.8	98.7	64.5	65.1	64.5	65.1	64.5
Coarse KNN	65.1	68.8	73.4	67.4	66.4	72.0	68.1	73.4	71.4	73.4	73.0	69.1	73.0	73.4	73.4
Medium KNN	78.9	81.3	99.3	<b>100</b>	82.2	88.2	90.5	94.1	95.7	<b>100</b>	90.8	92.8	94.4	99.0	95.4
Fine KNN	81.9	80.9	<b>100</b>	<b>100</b>	82.9	<b>100</b>	<b>100</b>	98.0	99.7	<b>100</b>	95.1	97.7	<b>100</b>	<b>100</b>	99.7
Cosine KNN	76.0	77.3	93.8	98.7	81.3	85.5	86.8	90.5	92.1	98.7	88.2	89.8	90.1	95.1	91.1
Cubic KNN	77.3	80.3	97.7	<b>100</b>	82.2	85.5	89.5	91.1	94.7	<b>100</b>	88.5	90.5	92.4	94.7	93.1
Weighted KNN	82.9	80.6	<b>100</b>	<b>100</b>	82.9	98.4	98.0	98.0	98.7	<b>100</b>	95.1	96.4	99.7	<b>100</b>	99.0

## 6. Conclusion

The detector responses of a set of detector types were modelled to assess the capability of SINRD and PDET to detect the diversion of fuel pins from a fuel assembly. Several machine learning models were applied for the data analysis for both NDA techniques.

The different models were evaluated in terms of accuracy, which was defined as the percentage of cases with correct classifications compared to the total dataset. The two NDA techniques were also compared using this metric.

The results for both NDA techniques showed that the detector response used for the data analysis plays an important role in the accuracy of the model, and in general the gamma-ray detector response obtained the highest accuracy compared to the neutron detector responses. However, the addition of multiple detector responses did not improve significantly the accuracy of the models.

Comparing the two NDA techniques, similar results in terms of accuracy were obtained for the majority of the models, with only some cases where the accuracy calculated for the PDET detector was more than 5% higher compared to the value obtained for the SINRD technique.

Several models reached for both NDA techniques a complete correct classification over the dataset used in this study, especially when the gamma-ray detector response was used alone or in combination with other features.

Future work will refine the models developed in this study by investigating different model parameters with the aim of increasing the accuracy of the current models. In addition the training database will be further expanded by generating several additional diversion scenarios and including other detector responses to be used as input features.

## 7. Legal matters

I agree that ESARDA may print my name/contact data/photograph/article in the ESARDA Bulletin/Symposium proceedings or any other ESARDA publications and when necessary for any other purposes connected with ESARDA activities.

This manuscript has been submitted to the ESARDA Bulletin and it is under review for publication in the ESARDA Bulletin Issue 58.

## 8. References

[1] International Atomic Energy Agency (IAEA). "*The structure and content of agreements between the Agency and States required in connection with the treaty on the nonproliferation of nuclear weapons*". INFCIRC/153 (corrected), 1972.

[2] International Atomic Energy Agency (IAEA). "*IAEA annual report for 2013*". IAEAGC(58)/3, 2014.

[3] van der Meer K., et al. "*An assessment of the FORK detector as a partial defect tester*". Proceedings of the 27th ESARDA Symposium on Safeguards and Nuclear Material Management, London, 10-12 May, 2005.

[4] Grape S., et al. "*Recent modelling studies for analysing the partial-defect detection capability of the Digital Cherenkov Viewing Device*". Proceedings of the 2013 ESARDA annual meeting, 2013.

[5] White T., et al. "*Application of Passive Gamma Emission Tomography (PGET) to the inspection of spent nuclear fuel*". Proceedings of the 2018 INMM annual meeting, 2018.

[6] Rossa R. "*Advanced non-destructive methods for criticality safety and safeguards of used nuclear fuel*". Ph.D. dissertation at Université libre de Bruxelles, 2016.

[7] Smola A., et al. "*Introduction to Machine Learning*". Cambridge University Press. ISBN 0 521 82583 0, 2008.

[8] Rossa R. "*Comparison of the SINRD and PDET detectors for the detection of fuel pins diversion in PWR fuel assemblies*". Proceedings of the 59th INMM Annual Meeting, 2018.

- [9] Kotsiantis S. B. "Supervised Machine Learning: A Review of Classification Techniques". *Informatica* 31, 2007, Pages 249-268.
- [10] Soofi A. A., et al. "Classification techniques in machine learning: applications and issues". *Journal of basic & applied sciences*, 2017, 13, Pages 459-465.
- [11] Borella A., et al. "Signatures from the spent fuel: simulations and interpretation of the data with neural network analysis". *ESARDA Bulletin*, No. 55, December 2017, Pages 29-38.
- [12] Menlove H. O., et al. "A resonance self-indication technique for isotopic assay of fissile material". *Nuclear applications*, volume 6, 1969, Pages 401-408.
- [13] LaFleur A. M. "Development of self-interrogation neutron resonance densitometry (SINRD) to measure the fissile content in nuclear fuel". Ph.D. dissertation at Texas A&M University, 2011.
- [14] LaFleur A. M., et al. "Development of self interrogation neutron resonance densitometry to improve detection of partial defects in PWR spent fuel assemblies". *Nuclear Technology*, 181, 2013, Pages 354-370.
- [15] LaFleur A. M., et al. "Analysis of experimental measurements of PWR fresh and spent fuel assemblies using self-interrogation neutron resonance densitometry". *Nuclear Instruments and Methods Section A*, 781, 2015, Pages 86-95.
- [16] Rossa R., et al. "Investigation of the self-interrogation neutron resonance densitometry applied to spent fuel using Monte Carlo simulations". *Annals of Nuclear Energy* 75, 2015, Pages 176-183.
- [17] Sitaraman S., et al. "Characterization of a safeguards verification methodology to detect pin diversion from pressurized water reactor (PWR) spent fuel assemblies using Monte Carlo techniques". *Proceedings of the 48th INMM annual meeting*, 2007.
- [18] Ham Y. S., et al. "Development of a safeguards verification method and instrument to detect pin diversion from pressurized water reactor (PWR) spent fuel assemblies phase I study". Lawrence Livermore National Laboratory technical report LLNL-TR-409660, 2009.
- [19] Ham Y. S., et al. "A new versatile safeguards tool for verification of PWR spent fuel". *Proceedings of the 53rd INMM annual meeting*, 2012.
- [20] Ham Y. S., et al. "Partial defect verification of spent fuel assemblies by PDET: principle and field testing in interim spent fuel storage facility (CLAB) in Sweden". *Proceedings of the 2015 ANIMMA conference*, 2015.
- [21] Rossa R., et al. "Development of a reference spent fuel library of 17x17 PWR fuel assemblies". *ESARDA Bulletin* n. 50, 2013, Pages 48-60.
- [22] Mitchell T. M. "Machine Learning". McGraw-Hill editor, 1997.
- [23] Bishop C. M. "Pattern recognition and machine learning". Springer, 2006, ISBN-13: 978-0387-31073-2.
- [24] Oudeyer P-Y. "The production and recognition of emotions in speech: features and algorithms". *International Journal of Human-Computer Studies*, Volume 59, Issues 1–2, 2003, Pages 157-183.
- [25] Ngai E. W. T., et al. "The application of data mining techniques in financial fraud detection: A classification framework and an academic review of literature". *Decision Support Systems*, Volume 50, Issue 3, 2011, Pages 559-569.
- [26] Kourou K., et al. "Machine learning applications in cancer prognosis and prediction". *Computational and Structural Biotechnology Journal*, Volume 13, 2015, Pages 8-17.

- [27] Murphy K. P. "*Machine learning: a probabilistic perspective*". Massachusetts Institute of Technology, 2012, ISBN 978-0-262-01802-9.
- [28] MathWorks, Inc. "*Statistics and Machine Learning Toolbox™ - User's Guide*", 2018.
- [29] Li T., et al. "*Using discriminant analysis for multi-class classification: an experimental investigation*". Knowledge and Information Systems 10 (4), 2006, Pages 453-472.
- [30] Kecman V. "*Support Vector Machines – An Introduction*". Studies in Fuzziness and Soft Computing, Springer, 2005.
- [31] Iggane M., et al. "*Self-training using a k-Nearest Neighbor as a base classifier reinforced by Support Vector Machines*". International Journal of Computer Applications (0975 – 8887) Volume 56–No. 6, 2012.

# Investigating the gamma and neutron radiation around quivers for verification purposes

Zs. Elter, V. Mishra, S. Grape, E. Branger, P. Jansson, L. Caldeira Balkeståhl

Uppsala University, Division of Applied Nuclear Physics

## Abstract:

*Before encapsulation of spent nuclear fuel in a geological repository, the fuels need to be verified for safeguards purposes. This requirement applies to all spent fuel assemblies, including those with properties or designs that are especially challenging to verify. One such example are quivers, a new type of containers used to hold damaged spent fuel rods. After placing damaged rods inside the quivers, they are sealed with a thick lid and the water is removed. The lid is thick enough to significantly reduce the amount of the gamma radiation penetrating through it, which can make safeguards verification from the top using gamma techniques difficult.*

*In this paper we make a first feasibility study related to safeguards verification of quivers, aimed at investigating the gamma and neutron radiation field around a quiver using a simplified quiver geometry. The nuclide inventory of the rods placed in the quiver is calculated with Serpent and Origen-Arp, and the radiation transport is modeled with Serpent. The objective is to assess the capability of existing non-destructive assay instruments, measuring the gamma and/or neutron radiation from the object, to verify the content for nuclear safeguards purposes. The results show that the thick quiver lid attenuates the gamma radiation, thereby making gamma-radiation based verification from above the quiver difficult. Verification using neutron instruments above the quiver, or gamma and/or neutron instruments on the side may be possible. These results are in agreement with measurements of a BWR quiver using a DCVD, performed by the authors.*

**Keywords:** quiver; safeguards verification; gamma radiation; neutron radiation; spent fuel; PWR; modeling

## 1. Introduction

Spent light water reactor (LWR) fuel in Sweden is currently stored at the nuclear power plants (NPPs) for up to a few years, before being shipped to a central interim storage for spent nuclear fuel (Clab). In some cases, fuel rods in the fuel assemblies are found to be damaged or leaking. Since the central storage for spent nuclear fuel is not able to dismantle fuel assemblies, handling of damaged fuel rods needs to be taken care of at the NPPs. Recently, Westinghouse has presented a new storage solution for failed fuel rods called quivers [quiver]. A quiver is a container for failed rods, with outer dimensions that allows it to be handled as any other LWR fuel assembly. The quiver is made of stainless steel and can store 4-28 boiling water reactor (BWR) fuel rods, or 30-60 pressurized water reactor (PWR) fuel rods in different positions in a Helium environment. A gas- and water-tight lid prevents gases from being released into the surrounding environment. Quivers are still relatively rare, only around a dozen of them

are currently used at the various NPP:s in Sweden. However, they are expected to increase in numbers as operators prepare for a more long-term storage alternative for damaged fuel rods.

Before encapsulating spent nuclear fuel and placing it in a geological storage, the fuel needs to be verified for safeguards purposes. There are several instruments and measurement techniques developed and under development for the safeguards verification of spent nuclear fuel. The majority of these instruments rely on the detection of gamma and/or neutron radiation emitted from the fuel object. Quivers may however be challenging to verify since its design attenuates, and therefore reduces, the radiation to be measured. This was recently discovered during a measurement campaign at the Ringhals NPP in Sweden, where the IAEA performed an SFAT (Spent Fuel Attribute Tester [1]) measurement of a quiver object. The SFAT measures gamma radiation from a fuel object in the water above the object.

The objective of this work is to make a feasibility study concerning the ability to verify the nuclear material inside a quiver filled with PWR fuel rods. We present a methodology for modelling the quiver objects with an assumed content and estimate the gamma and neutron radiation fields around it. We also provide a qualitative discussion, using experience from Digital Cherenkov Viewing Device (DCVD) measurements on a BWR quiver. Since the detailed design of the quiver was not known to the authors, a simplified model of the design was constructed using openly available information from Westinghouse [2, 3].

## 2. Quiver model

The quiver design presented here is based on publicly available information [2], and estimations by the authors. The internal arrangement of a quiver and the number of tubes depends on the operators' needs and may be different from quiver to quiver. However, the outer dimensions are standardized to PWR and BWR fuel assembly sizes, to allow storage and handling as for regular assemblies. In this paper, we tried to estimate a realistic design for PWR quivers.

In our model, the quiver contains 45 steel tubes, which may be filled with fuel pins. Each tube has an outer diameter of 14 mm, and a wall thickness of 0.2 mm. These tubes are arranged in a circular cluster array of 4 rings. The number of pins in each ring, the central radii and the angle of rotation of each ring is summarized in Table 1. A radial cross section of the quiver is shown in the left side of Fig. 1.

#Ring	Central radius (cm)	Number of pins	Rotation (degrees)
1	0	1	0.0
2	2.2	8	45.0
3	4.4	16	22.5
4	6.6	20	18.0

**Table 1:** Parameters of the circular cluster array of the modeled quiver.

The fuel pins are considered to be 400 cm long (although in some of the simulations only the upper part of the fuel rods was considered), out of which the lower 393 cm is surrounded by water, 2 cm is passing through a grid spacer, and 5 centimeters are sticking out into a cavity, in order to make the rods retrievable. In practice, partial length fuel rods may be inserted into quivers, however then, first a space

holder rod is inserted into the tube to guarantee that the top of the fuel rods reach the cavity. This cavity is sealed by a long term steel storage lid, which has an axial height of 8.5 cm in our model. Once the long term storage lid is placed, the water is evacuated and the cavity will be filled with helium. Regarding safeguards verification measurements of the quiver content, performed above the quiver, this lid plays an important role. Thus the conclusions drawn in this paper are sensitive to the thickness of the lid. The side length of the lid is 21.42 cm, same as that of a common PWR fuel assembly. The cavity, and the lid structure is shown in an axial cut in the right side of Fig. 1.

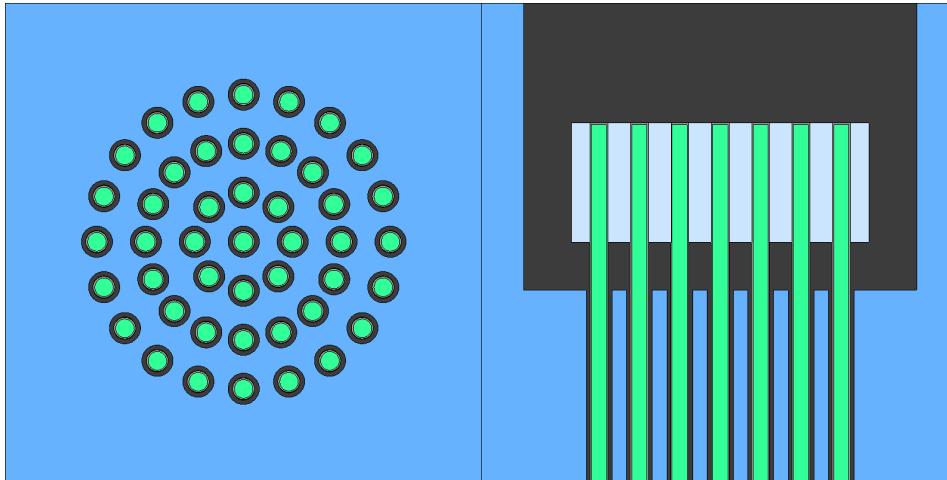


**Figure 1:** X-Y cross section of the modelled fuel rod pattern in the quiver (left). On the right, the X-Z cross section of the modelled quiver and the top lid is shown. The colour map indicates blue= water, light blue=helium, black= steel, green=fuel rod.

We have made several simplifying assumptions in our quiver model. We haven't placed any grid spacer along the quiver axially, since that is anyhow expected to have a negligible effect in our studies. Similarly, we have not included the four corner beams for the quiver, which may have an impact on measurements performed from the side of the quiver, such as FORK measurements, but not on measurements from above. The quiver lid has several seals in order to evacuate the water and to fill the tubes with helium. The geometry of these seals could not be estimate based on the publicly available information, and were thus omitted from the model. One could expect that the shielding is slightly weaker around these seals, which may have an impact on SFAT measurements.

The fuel pins placed in the quiver tubes had standard PWR 17x17 pin sizes summarized in Table 2. Note that the pitch size does not play a role in the quiver model, but it is used in the burnup calculations described in the next section. The quiver is supposed to hold fuel pins of various operational history. For this simplified study, we have decided to use only one pin type, as shown in Fig. 1, although the computational methodology was tested with more pin types as well. All pins have the same dimensions, initial enrichment, burnup and cooling time as specified in section 3.1.

Pellet radius (cm)	Clad in/out radius (cm)	Pitch (cm)
0.41	0.42/0.48	1.26

**Table 2:** Properties of modeled PWR pins.

### 3. Computational methodology

In this feasibility study, two different methodologies were used in order to benchmark the results. One was based purely on the use of the software code Serpent for all steps: the nuclide inventory of the source pins was computed with a Serpent pin-cell burnup calculation, then the gamma and neutron radiation were calculated in a subsequent Serpent simulation. The second methodology was based on the use of Origen-Arp for the depletion calculation, and the use of Serpent for the gamma and neutron transport steps. The gamma and neutron flux results were extracted and analyzed with the help of the SerpentTools suite [4].

Serpent is a Monte Carlo reactor physics code that also includes photon and neutron transport capabilities [5]. In this work the 2.1.28 version of Serpent was used. Given that the quiver geometry was implemented in Serpent, it was natural to consider this code also for the depletion and particle transportation parts. However, Serpent is a relatively new code, and is not as well-validated and verified as the Origen-Arp software, a standardized method for isotope depletion analysis for spent nuclear fuel. Hence, it was decided to use both programs in the study for the depletion calculations.

In both methodologies, the input geometry was the same for both the gamma and neutron transport calculations as described in Sec. 2. Furthermore, the modelled irradiation histories were similar to what one would expect for regular fuel assemblies (although, slightly different in the two methodologies, which is to be resolved later). However, in the case of failed rods that are removed from an assembly and later placed in a quiver, the irradiation history may well be different from that of a regular assembly, which should be taken into account in the future.

#### 3.1. Burnup calculations

##### 3.1.1 Calculations using Serpent

The fuel was considered as a single PWR fuel rod, as described in Table 2, with reflective boundary conditions. The fuel temperature was set to 1500 K, the zirconium cladding temperature to 900 K and the light water moderator temperature to 600 K. The initial enrichment was 3.5 %. The power density was set corresponding to the fuel being burned at a constant rate of 10 MWd/kgU each year up to 50 MWd/kgU. A 30-day revision time was included after each 365-day long irradiation period in the reactor. The nuclide inventory was evaluated after multiple cooling times (CT= 1, 5, 10, 20 and 40 years). The material composition was printed both with the "rfw" option into a binary restart file (for the subsequent radioactive decay source calculation, see Sec. 3.2.1), and into bumat files (for the subsequent neutron transport calculations, see Sec. 3.3.1). The neutron cross-sections were taken from JEFF 3.1, and the decay data was used from ENDF-B-VI-8.

##### 3.1.2 Calculations using Origen-Arp

The gamma and neutron emission spectra from the fuel rods were calculated using Origen-Arp [6]. In Origen-Arp, the depletion of a complete PWR assembly was modelled, using burnups of 10-50 MWd/kgU in steps of 10 MWd/kgU, and multiple cooling times (CT=1, 5, 10, 20 and 40 years). The fuel depletion was modelled as three consecutive irradiation cycles for a discharge burnup of up to 30 MWd/kgU, and four irradiation cycles for the discharge burnups of 40 and 50 MWd/kgU. Each irradiation cycle lasted 333 days and was followed by 32 days of outage. From the Origen-Arp output, the gamma and neutron emission spectra were used as source terms in subsequent Serpent particle transport calculations.

With respect to cross-section libraries used in the Origen-Arp calculations, gamma and X-ray data were regenerated from the Evaluated Nuclear Structure Data File (ENSDF). Additional data for 52 nuclides

without ENSDF data were adopted from ENDF/B-VI data. Decay data comes from NDF/B-VII.0. For neutron emission spectra, the SOURCES code package was used, and the neutron cross-sections come from JEFF-3.0/A.

## 3.2 Gamma flux calculations

In order to obtain the resulting gamma flux from the quiver, the gamma radiation from the fuel rods to the surrounding environment was simulated with Serpent based on the source term from the two different methodologies.

### 3.2.1 Calculations using Serpent

Serpent allows for the definition of radioactive decay sources, in which the source term (emission spectrum and source rate) is created automatically based on a previous burnup calculation. The use of this method greatly simplifies the modelling efforts, nevertheless during the work we have encountered some drawbacks. The main issue emerged from the fact that the method tends to work well only if the material composition is read from a binary restart file. Nevertheless, at the moment only one binary file can be read in an input file. Thus, in case pins with different material compositions are present in the quiver, one needs to run separate input files and sum up the detector scores. Also, currently the method is limited to discrete photon emitting reactions.

### 3.2.2 Calculations using Origen-Arp

As an alternative, the depletion code Origen-Arp was used instead of Serpent. The gamma emission spectrum was obtained in a 47-bin format from the Origen-Arp output, and after renormalization to the mass of the emitting spent fuel material, a gamma source term was created for the Serpent gamma transport calculation. In this methodology, the pin material was considered to be fresh fuel in the gamma transport step, which may result in 1-2% overestimation of the mass attenuation coefficients of the fuel as shown in [7].

## 3.3. Neutron flux calculations

In order to obtain the resulting neutron flux from the quiver, the neutron radiation from the fuel rods to the surrounding environment was simulated with Serpent based on the source term from the two different methodologies.

### 3.3.1 Calculations using Serpent

The spent fuel composition was taken from the Serpent output files (bumat), which provide Serpent-compatible material definitions. Using this option to describe the spent fuel composition allows to handle geometries with various pin compositions in a single run. The source rate of neutrons was based on the total spontaneous fission rate printed in the depletion output. Nevertheless, Serpent does not give any information on the neutron emission spectrum, thus as an approximation, the Watt-spectrum of U-235 was used to describe the emission spectrum.

### 3.3.2 Calculations using Origen-Arp

The total neutron emission spectrum was obtained in a 27-bin format from the Origen-Arp output, and after renormalization (with the mass of the emitting spent fuel material), a neutron source term was created for the Serpent neutron transport calculation. In this methodology, the pin material was considered to be fresh fuel in the neutron transport step, which may result in an underestimation of neutron absorption.

### 3.4. Cherenkov light transport calculations

The results of the gamma transport simulations include a calculation of the gamma spectrum just above the quiver lid. Using the methodology described in [8], where the number of produced Cherenkov photons is estimated from a gamma spectrum, the amount of Cherenkov light produced in the water above the lid was simulated. From this, the intensity of the detectable Cherenkov light directed towards to assumed DCVD position is estimated. In order to assess whether or not the estimated Cherenkov light intensity is detectable using a DCVD, the Cherenkov light intensity from the quiver was compared to that of a corresponding fuel assembly, ie. a 17x17 PWR fuel assembly with fuel rods having identical burnup and cooling time as the rods in the quiver. This approach of course means that the total intensity of the quiver will be lower, since the fuel assembly consists of 264 fuel rods and the quiver only of 45. However, the approach is justified by the fact that it is likely that inspecting authorities will try to verify the quivers using the same methodology and instruments that have been developed for fuel assemblies, and the question is whether or not that will result in a detectable signal.

## 4. Comparison of methodologies

In order to compare the two methodologies, the resulting gamma and the neutron spectra were evaluated in a 2 cm high water volume above the lid for a quiver containing rods with an inventory related to BU=50 MWd/kgU and CT=1 y. The left side Fig 2. shows that there is a good agreement both in shape and amplitude between the two gamma spectra computed using the two methodologies up to 3 MeV. The pure Serpent methodology estimates a slightly higher gamma flux for energies lower than 1 MeV, which may be a result of the accurate material composition model in that case. Above 3 MeV, the flux from the Serpent calculations reduces rapidly to zero, whereas Origen-Arp calculates a low flux of high-energy gamma rays. The neutron spectra, presented in the right side of Fig. 2, show less agreement in absolute values, however the shapes of the spectra are similar up to 0.1 MeV. Above 0.1 MeV, the Watt-spectrum does not seem to be appropriate to describe the total emission spectrum.

Based on these results, it can be concluded that the two methodologies need to be further improved, by either providing the pure Serpent method with more realistic neutron emission spectra, or by updating the combined Origen-Arp and Serpent methodology with more realistic material compositions. The emission spectra from Origen-Arp seem to be more reliable for high energies for both the gamma and neutron radiation.

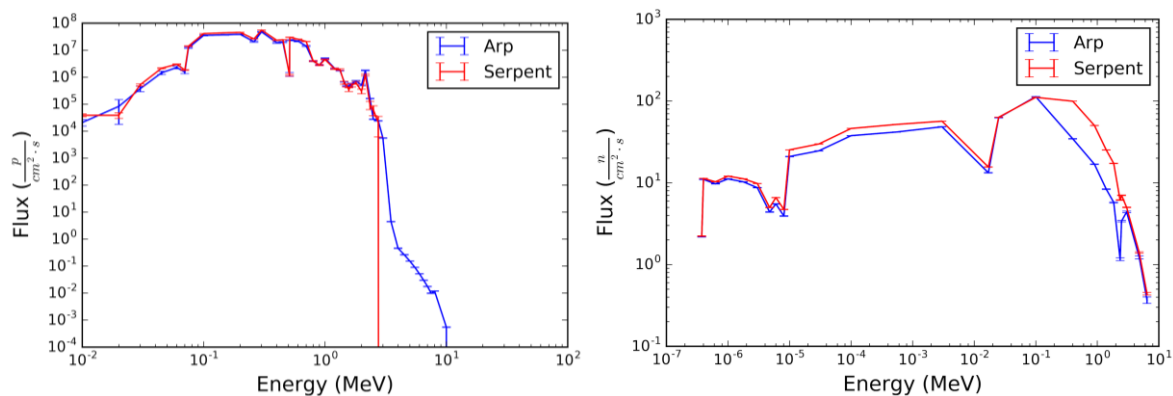


**Figure 2:** Left: gamma spectrum above the quiver lid for fuel with a CT of 1 year. Right: neutron spectrum above the quiver lid for fuel with CT=1 year.

## 5. Results on the radiation fluxes

The gamma and neutron radiation around and above the quiver was visualized with the use of mesh tallies. The size of a voxel was set to  $0.43 \times 0.43 \times 0.5 \text{ cm}^3$ . For the gamma radiation, the flux within the 600-800 keV bin was scored, since it covers the 662 keV peak from Cs-137 which is most frequently used by gamma-ray sensitive safeguards instruments. For the neutron radiation, the flux between 0-14 MeV was scored. We have chosen only to show the results of fuel rods with IE=3.5%, BU=50 MWd/kgU and CT=1 year, since that corresponds to the highest radiation fluxes.

Figs. 3 and 4 show the gamma and neutron radiation around the upper part of the quiver filled with 45 rods, respectively. In the figures, the axial length of the rod is shown between -200 and 200 cm. At an axial height of 193-195 cm a steel spacer grid is present, the helium-filled cavity is located at 195-200 cm, and the quiver lid is located at 200-208.5 cm. Above 208.5 cm there is only water. The source particles were sampled only from the upper 50 cm of the rods for variance reduction, since it was found that particles emitted from lower regions do not contribute to the flux around the lid. This was established by performing gamma transport simulation with Serpent by modeling the source placed at increasing distances from the detector region. The fuel region emitting the source particles was moved away by replacing the top region of the fuel rods with fresh fuel instead of irradiated fuel. It was observed that the flux recorded at the top of the lid from this arrangement declined rapidly and eventually vanished as the region emitting the photons was moved to distances greater than 20 cm from the quiver lid.

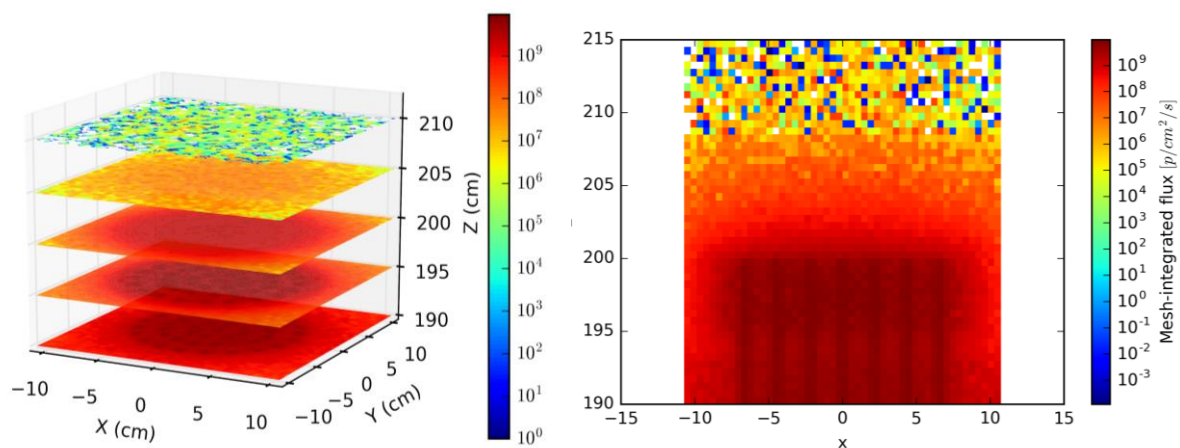


**Figure 3:** Left: Radial cut of mesh-integrated gamma flux at different heights. Right: Axial cut of mesh-integrated gamma flux at the center of the assembly. The gamma-ray energy is 600-800 keV.

Fig. 3 shows that the gamma flux is one order of magnitude lower in the water between the rods as compared to inside the fuel rods due to self-attenuation, and that the total flux drops three orders of magnitude within the lid, which is expected. Above the lid, the mesh tally results are rather noisy due to poor statistics: only a few source particles manage to escape the quiver, thus in several voxels no particle left any score. The results indicate that performing a verification with an SFAT device, which would measure the flux 50-100 cm further away from the lid, will become difficult even for short cooled rods. However, measuring the gamma radiation close to the lid or from the side may be feasible.

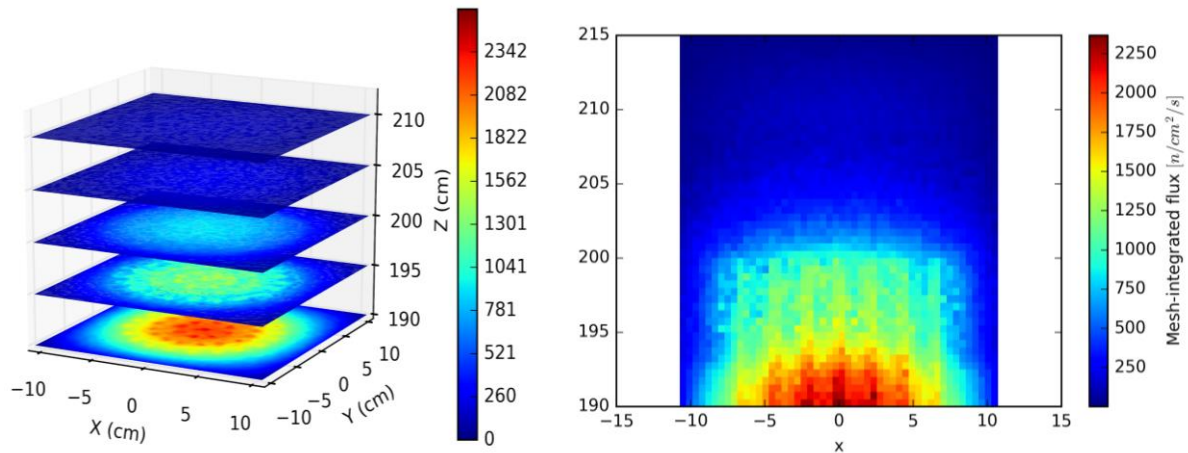


**Figure 4:** Left: Radial cut of mesh integrated neutron flux at different heights. Right: Axial cut of mesh integrated neutron flux at the center of the assembly. The neutron energy is between 0 and 14 MeV.

The neutron flux is shown in Fig. 4. The flux between the rods is again lower than inside the rods, but the reduction is not as large as for the gamma-rays. However, the flux drops one order of magnitude inside the helium-filled cavity. Since the neutron flux is low and approaching zero at the top of the quiver, passive measurements should preferably be done from the side of the fuel assembly.

The gamma and neutron flux as a function of energy were calculated in a 2 cm high water volume for several cooling times, and can be seen in Fig. 5. The base of this volume had the same size as the radial area of the lid. Thus, the spectra represent the observable spectra just above the quiver. The gamma spectra are shown using the default 47-bin structure from Origen-Arp, and the neutron spectra using the default 28-bin structure.

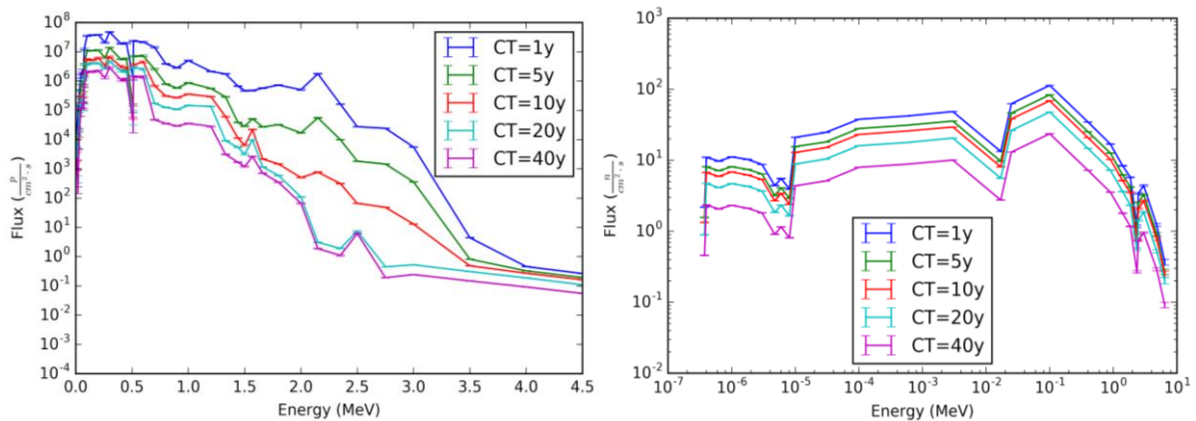


**Figure 5:** Left: gamma spectra from Origen-Arp above the quiver lid for various CTs. Right: neutron spectra above the quiver lid for various CTs.

The results are in agreement with expectations that the longer the cooling time is, the lower the total flux becomes. The source rate for a 40 year cooled fuel drops with 95% compared to a 1 year cooled fuel. We also expect low-lived fission products to decay, leaving the Cs-137 peak at 662 keV to dominate the spectrum. In Fig. 5 (left) we indeed see the reduction of the total flux, although it is difficult to see the dominance of the 662 keV peak. However, if we analyze the simulated gamma spectrum

above the quiver lid and compare it to the corresponding spectrum of a PWR 17x17 fuel assembly, we see that the Cs-137 gamma signal above the quiver is about 2-3 orders of magnitude lower due to the presence of the quiver lid. For a quiver containing low-burnup and long-cooled rods, this signal may actually be too weak to be detected using an SFAT system (which according to [1] is able to verify the 662 keV peak of Cs-137 for CTs > 14 years and BUs in the order of a few MWd/kgU), though further simulations are required to quantify the detected signal for a detector placed on top of the quiver.

With respect to verification using neutron detection techniques, the question is what neutron count rates that are needed for the given instrument (this is of course related to the type and number of detectors considered, and detection times). The right side of Fig. 5 shows that the source rate of the total neutron emission rate decreases by 80% for a 40 years old cooled fuel compared to a 1-year old fuel. However, the shape of the neutron spectra does not change over time. This implies that the same neutron detection can be used both for short and long cooled fuel, since the reaction rates in the detector will be comparable.

With respect to total Cherenkov light intensity, the results show that the estimated detectable Cherenkov light intensity just above the quiver lid is around three orders of magnitude lower than from a corresponding fuel assembly, when the quiver and assembly contains rods of the same burnup and cooling time. This result holds for all assemblies and quivers with a cooling time longer than about 10 years. For a quiver loaded with fuel rods with having more than 10 years cooling time, the expected intensity is estimated to be too low to be accurately measured using the DCVD with the regular measurement methodology.

## 6. Validation of results using fuel measurements

Although the authors are aware that the implemented PWR quiver model is crude and allows only for a feasibility study at this stage, we are able to provide some qualitative validation of the results using DCVD-measurements performed by the authors on a BWR quiver at the Forsmark NPP in late 2018. Although the BWR and PWR quivers differ in terms of size and dimensions, this is what we are able to compare our simulations with at this stage. Due to time constraints, the DCVD settings could not be optimized for the low intensity of the quiver, but for settings applicable to short-cooled assemblies, no discernable Cherenkov light intensity could be seen from the quiver. Furthermore, the lid of the quiver was found to be highly reflective. This significantly increases the amount of ambient light detected in a measurement and complicates the measurement situation by introducing a significant background component. It was therefore immediately found that the regular DCVD measurement methodology where the DCVD is centered above the fuel object to be measured, cannot be applied to verification of quivers. Possibly other measurement methodologies may work, such as measuring the Cherenkov light produced at the side of the quiver rather than on top of it could work. Further investigations are required to assess if such a methodology is feasible, considering both the Cherenkov light intensity and the specific measurement setup.

## 7. Conclusion and outlook

Quivers are container objects for damaged LWR fuel rods. They are made of steel and have a thick lid, which efficiently reduces the amount of gamma radiation that is able to escape. In nuclear safeguards verification of fuel objects, it is an advantage if the fuel object does not need to be moved or handled by the operator in connection to the measurements. In this work we have made a simplified model of a

quiver filled with PWR fuel rods in order to estimate the gamma and neutron flux around, and especially above the quiver.

The results show that it will be difficult to verify the content of quivers using gamma radiation measured at the top of the quiver, due to the steel lid which efficiently attenuates the radiation. This is also the reason why it will be difficult to use the DCVD, which measures Cherenkov light in the water caused by mainly gamma-emitting fission products. The results also show that the neutron radiation is not as heavily affected by the quiver and the flux above the quiver is approximately as large as on its side. Among existing safeguards verification instruments, possibly verification using instruments positioned at the side of the quiver, such as the Irradiated fuel attribute tester (IRAT) or the FORK, may be a better alternative to using instruments that verify the fuel from the above. Verification of the quiver using such instruments will likely be able to reveal the presence of nuclear material (gross verification), but it will be a challenge to verify the content beyond that unless a more accurate verification technique such as i.e. the Passive Gamma Emission Tomography (PGET) instrument. We emphasize that the fact that verification of the quiver seems difficult already for fuel with cooling times of a few years, indicate that verification of fuel with cooling times up to decades will require considerable efforts.

With respect to the modelling methodology, we will in the future work update the material composition for the mixed methodology as well, and create serpent-compatible material definitions from the Origen-Arp output files. Nevertheless, in the following the results of the mixed methodology will be presented. We also hope to be able to get more accurate information on the actual quiver design, such as the thickness and composition of the lid which affects the gamma radiation that can be measured from above. We are also investigating the possibility to access both the proper fuel content of the measured quiver object at Ringhals NPP, and experimental measurement data that was collected by IAEA using the SFAT. Inserting this information into our models, it would be possibly to validate both the model and the results.

## 8. Acknowledgement

We would like to acknowledge the Swedish Radiation Safety Authority for supporting this work under contract SSM2017-5979 and for fruitful discussions. We would also like to thank Westinghouse in Västerås, Sweden, for their interest in this work and for discussing quivers with us. Finally, we want to acknowledge Ringhals NPP for discussing SFAT measurements and quiver contents with us and Forsmark NPP for letting us do DCVD measurements on a quiver.

## 9. References

- [1] Hlavathy Z. et al., *Spent fuel attribute tester realization and application*, In the Proceedings of the IAEA-Hotlab technical meeting in Smolenice, Slovakia, 23–27 MAY 2011.
- [2] Westinghouse Electric Company; *Quiver system for Storing Failed Fuel rods*, video uploaded to <https://www.youtube.com/watch?v=SNtszjtYKzc>, 2017, accessed: 2019. March
- [3] Westinghouse Electric Company; *Westinghouse quiver*, leaflet uploaded to <http://westinghousenuclear.com/Portals/0/operating%20plant%20services/fuel/Fuel%20Outage%20and%20Field%20Services/WestinghouseQuiver-12823.pdf> 2017, accessed: 2019. March

[4] Johnson A., Kotlyar D., Ridley G., Terlizzi S. and Romano P.; *serpent-tools: A collection of parsing tools and data containers to make interacting with SERPENT outputs easy, intuitive, and flawless*, <https://doi.org/10.5281/zenodo.1301036>, 2018

[5] Leppänen J. et al.; *The Serpent Monte Carlo code: Status, development and applications in 2013*, Annals of Nuclear Energy, vol. 82, 2015, pp. 142-150

[6] Bowman S., Leal L., Hermann O. and Parks C.; *ORIGEN-ARP, a fast and easy to use source term generation tool*, Journal of Nuclear Science and Technology, vol. 37, 2000, pp. 575-579

[7] Atak et al. H.; *The degradation of gamma-ray mass attenuation of UO<sub>2</sub> and MOX fuels with nuclear burnup*, To be submitted, 2019

[8] Branger E., Grape S., Jansson P., Jacobsson Svård S.; *Comparison of prediction models for Cherenkov light emissions from nuclear fuel assemblies*, Journal of Instrumentation, 2017

# Validating the Reported Irradiation History of Spent Fuel Assemblies using High-Resolution Gamma Spectrometry and the ORIGEN 2.2 Burnup Code

**Péter Kirchknopf<sup>1</sup>, István Almási<sup>1</sup>, András Kocsonya<sup>2</sup>, Cong Tam Nguyen<sup>1</sup>,  
László Lakosi<sup>1</sup>, Zoltán Hlavathy<sup>1</sup>, Péter Völgyesi<sup>1</sup>**

<sup>1</sup>Hungarian Academy of Sciences, Centre for Energy Research, Nuclear Security Department, 29-33 Konkoly-Thege Miklós út, H-1121 Budapest, Hungary

<sup>2</sup>International Atomic Energy Agency, Wagramer Straße 5, A-1400 Vienna, Austria  
E-mail: peter.kirchknopf@energia.mta.hu, istvan.almasi@energia.mta.hu

## **Abstract:**

*In the last 10 years, the Nuclear Security Department (MTA EK) has been conducting gamma-spectroscopy measurements on the spent fuel assemblies of Paks NPP, Hungary. The primary goal was to check the declared value of burnup by Cs-measurements. The aim of this work is to expand the scope of these measurements: (i) we examine the usability of <sup>106</sup>Ru and <sup>154</sup>Eu for checking the declared value of burnup and (ii) developing a method to independently verify the irradiation history of spent nuclear fuel reported by the NPP operator. We also investigate a method based on the measured activity ratio of <sup>106</sup>Ru and <sup>154</sup>Eu to independently determine the cooling time of spent fuel assemblies.*

*In principle, these aims could be achieved by measuring the activities of gamma-ray emitting fission products using a high-purity germanium (HPGe) detector. The majority of these nuclides have unique production routes, i.e. direct production from fission, decays and neutron captures, and distinct half-lives. This means that a specific fission product activity-map corresponds to each different irradiation scenario. Those nuclides which can be detected under our measurement circumstances cover a half-life interval of 1–30 years. The activity of <sup>137</sup>Cs is proportional to the total burnup of the fuel, while the other activities change in different ways for different irradiation profiles.*

*We use the ORIGEN 2.2 code to calculate the activities of the aforementioned nuclides for various irradiation scenarios. This obtained information could be used to quickly validate the total burnup of the assemblies. The present method would be useful to validate the operator's statement on the balance of nuclear materials in the fuel assemblies.*

**Keywords:** non-destructive assay; spent fuel verification; fission products; irradiation history

## **1. Introduction**

One of the main safeguards objectives of spent fuel measurements is to determine the burnup of the fuel, from which the remaining and produced nuclear material content can be assessed. In some cases, the <sup>134</sup>Cs/<sup>137</sup>Cs fission product activity ratio yields a good approximation of the burnup [1,2]. The use of this ratio is recommended for assemblies having short cooling times, but it can also work if the cooling time is not more than 14 years [3]. The <sup>134</sup>Cs/<sup>137</sup>Cs ratio is most commonly measured by using high-resolution gamma spectrometry (HRGS), which is a non-destructive assay requires less than an hour measurement time to give satisfactory results. However, this method has a disadvantage: the <sup>134</sup>Cs/<sup>137</sup>Cs ratio is dependent on the irradiation history of the fuel. Cesium-137 has a relatively long half-life of 30 years, so its activity is practically history-independent. On the other hand, the activity of <sup>134</sup>Cs, due to its 2-year long half-life, can change considerably depending on the time structure of irradiation (e.g. fuel outages between cycles). Another concern is the varying

assembly power (or neutron flux) during the last cycle because in this case the  $^{134}\text{Cs}$  activity can also change significantly while the impact on  $^{137}\text{Cs}$  is relatively small [3]. These effects result in that, in a general case, the  $^{134}\text{Cs}/^{137}\text{Cs}$  ratio does not correspond uniquely to the burnup. In the scope of this work, the irradiation history is only considered as burnup history, so the effect of varying time intervals is not investigated.

Similar to  $^{134}\text{Cs}$  and  $^{137}\text{Cs}$ , the nuclides  $^{106}\text{Ru}(\rightarrow^{106}\text{Rh})$  ( $T_{1/2} = 1$  y) and  $^{154}\text{Eu}$  ( $T_{1/2} = 8.6$  y) are also gamma-ray emitting fission products. Our measurement experiences at Paks NPP show that both of the latter isotopes can be detected in many spent fuel assemblies. By utilizing not only the  $^{134}\text{Cs}/^{137}\text{Cs}$  activity ratio, but also the  $^{106}\text{Ru}/^{137}\text{Cs}$  and  $^{154}\text{Eu}/^{137}\text{Cs}$  ratios, we may be able to obtain additional information related to the burnup and the irradiation history. The distinct half-lives of 1, 2 and 8.6 years promise this technique to be useful for detecting short, medium and long term differences during the time of operation.

In this paper we examine the measured data of VVER-440 type spent fuel assemblies to see how the  $^{106}\text{Ru}/^{137}\text{Cs}$  and  $^{154}\text{Eu}/^{137}\text{Cs}$  activity ratios change depending on the irradiation history. Our aim is to develop a method that gives us information on the fuel history without using the operator's declaration. This could be achieved with the use of high-resolution gamma spectrometry (HRGS) and theoretical calculations for a supposed history. For the calculations, we use the ORIGEN 2.2 burnup code, developed by ORNL [4].

## 2. Theory

The time dependence of the amount of a specific fission product in a reactor fuel assembly is governed by various nuclear processes. The production of an isotope can occur as a result of the following reactions:

- Fission of a fissile nuclide (i.e.  $^{235}\text{U}$ ,  $^{239}\text{Pu}$  etc.)
- Neutron induced reactions, most commonly radiative capture by another nucleus
- Radioactive decay of another nucleus

Similar to the above processes, the consumption of an isotope can happen in two ways:

- Neutron absorption by the nucleus in question
- Radioactive decay of the nucleus in question

The total change in time of the nuclide number of isotope  $i$  at a given spatial coordinate (point in the reactor) can be expressed with the following equation:

$$\frac{dN_i}{dt} = \sum_{j=1}^n Y_{ij} N_j(t) \int_0^{E_{\max}} \sigma_j^f(E) \phi(E) dE + \sum_{k=1}^n C_{ik} N_k(t) \int_0^{E_{\max}} \sigma_k^c(E) \phi(E) dE + \sum_{m=1}^n D_{im} N_m(t) \lambda_m - N_i(t) \int_0^{E_{\max}} \sigma_i^a(E) \phi(E) dE - N_i(t) \lambda_i \quad (1)$$

Here,  $Y_{ij}$  is the fission yield of isotope  $i$  from the fission of isotope  $j$ ,  $C_{ik}$  is the fraction of isotope  $k$  that transforms into isotope  $i$  with neutron capture and  $D_{im}$  is the fraction of isotope  $m$  that decays into isotope  $i$ .  $N$  is the nuclide number,  $\sigma^f$ ,  $\sigma^c$  and  $\sigma^a$  are the microscopic fission, neutron capture and absorption cross-sections, respectively,  $\phi$  is the neutron energy flux,  $\lambda$  is the decay constant and  $E_{\max}$  is the maximum energy of neutrons in the reactor (commonly used value is 10 MeV). To obtain the amount of nuclides for  $i = 1, \dots, n$ , one has to solve a system of first-order ordinary differential equations (ODEs) composed of  $n$  equations similar to (1). To solve such a system, the knowledge of the initial fuel composition and the neutron energy flux (at the given point) is required. However, the integrals over the energy can be replaced with the product of energy-averaged, one-group cross-sections and fluxes. Thus, (Eq. 1) can be simplified to:

$$\frac{dN_i}{dt} = \sum_{j=1}^n Y_{ij} N_j(t) \langle \sigma_j^f \rangle \langle \phi \rangle + \sum_{k=1}^n C_{ik} N_k(t) \langle \sigma_k^c \rangle \langle \phi \rangle + \sum_{m=1}^n D_{im} N_m(t) \lambda_m - N_i(t) \langle \sigma_i^a \rangle \langle \phi \rangle - N_i(t) \lambda_i \quad (2)$$

In (2),  $\langle \sigma^f \rangle$ ,  $\langle \sigma^c \rangle$ ,  $\langle \sigma^a \rangle$  and  $\langle \phi \rangle$  are one-group averages of the cross-sections and the neutron flux, respectively. The advantage of calculating this way is that only the one-group cross-sections need to be stored and only the one-group fluxes need to be put in or calculated. The latter can be easily done if the thermal power output of the assembly is known. In this case, the cross-section data used must be computed for the fuel composition and geometry for the specific reactor type in question.

The figure below (Fig. 1) shows the production and consumption processes for the nuclides investigated in this work, originating from the thermal neutron induced fission of  $^{235}\text{U}$ .

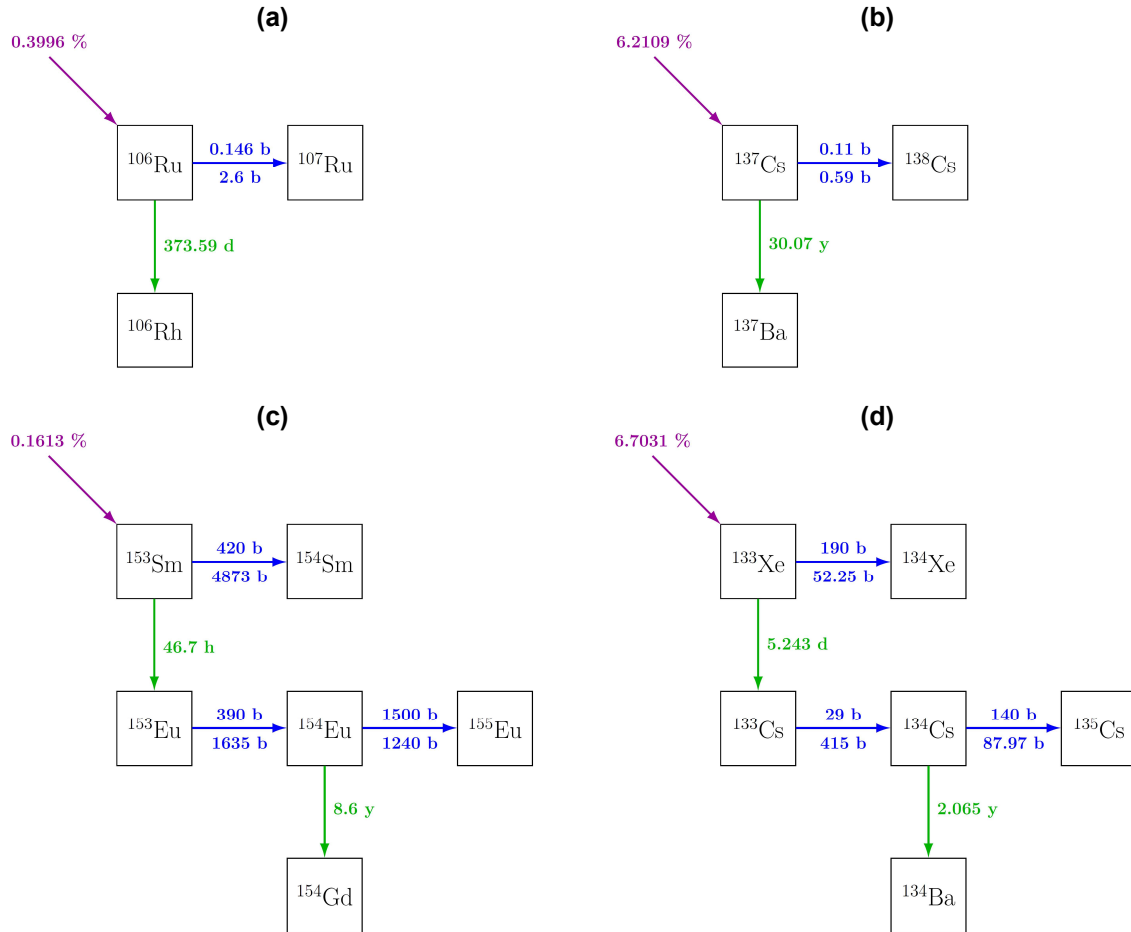


**Fig. 1:** The simplified production routes of (a)  $^{106}\text{Ru}$ , (b)  $^{137}\text{Cs}$ , (c)  $^{154}\text{Eu}$  and (d)  $^{134}\text{Cs}$ . The purple arrows represent the production from fission and show the cumulative fission yield from the thermal neutron induced fission of  $^{235}\text{U}$ . The blue arrows represent neutron capture, the numbers above and below the arrow are the thermal capture cross-sections and resonance integrals, respectively. The green arrows represent radioactive decay with the half-lives shown on their right-hand side. The numerical values are taken from [5], except for the neutron capture of  $^{153}\text{Sm}$ , where the ENDF/B-VII database was used [6].

In reality, the schemes shown on Fig. 1 are more complex, but many nuclides can be practically neglected because they either have short half-lives or small capture cross-sections. The production of  $^{106}\text{Ru}$  and  $^{137}\text{Cs}$  is similar to each other and is proportional to the neutron flux. However, the yield of  $^{106}\text{Ru}$  from the thermal fission of  $^{239}\text{Pu}$  is 4.3085% [5], which is more than 10-times the value from the fission of  $^{235}\text{U}$ . The consequence is that the amount of  $^{106}\text{Ru}$  is superlinear in time, while the amount of  $^{137}\text{Cs}$  is linear. Similarity is also apparent between  $^{134}\text{Cs}$  and  $^{154}\text{Eu}$ . Their production is proportional to the square of the neutron flux, as their formation requires two neutron induced reactions to happen. Cesium-134 decays faster than  $^{154}\text{Eu}$ , so for long time (4-5 years) operation the amount of  $^{134}\text{Cs}$  as a function of the burnup will not be entirely quadratic, while the same will still hold for  $^{154}\text{Eu}$ . These aforementioned differences of the amount or activity of the nuclides as a function of time and burnup give the foundation of the irradiation history determination method presented in this work.

### 3. Experimental

The details about the spent fuel measurements with HPGe detectors at Paks NPP can be found in previous publications [1,2,7]. In this paper, only a brief summary and information about the measurements that took place in 2018 are presented.

The assemblies were measured while they were hung up on the refuelling machine in a service pit that was filled with water. The wall of the pit and the concrete structure around it has a built-in low background collimator tube. The dimensions of the rectangle based conic tube are: 1255 mm length, 3 mm height, 170 mm width at the opening window and 10 mm width at the ending window. The usual distance of the assembly from the collimator opening is between 40-60 cm. Depending on the exact distance and the assembly history, the dead time of the detector is mostly between 10-20%. The detector used for the 2018 measurements was an Ortec GEM 10P4-70 model that has a 70 cm<sup>3</sup> large coaxial type Ge crystal. When measuring live times of around 5 hours per assembly, the most significant peaks of <sup>106</sup>Ru-<sup>106</sup>Rh, <sup>134</sup>Cs, <sup>137</sup>Cs, and <sup>154</sup>Eu could be detected.

Three groups of assemblies with similar operational parameters were selected for measurements, each group containing three assemblies. The assemblies in a group were used in the same cycles and were in equivalent positions in the reactor (i.e. in different sectors but in the same position inside the sectors). Table 1 contains information on the operating history of the measured assemblies.

Assembly group	Initial enrich. (%)	Cooling time (years)	Cycle length (days)				Burnup (GWd/tUi)				
			Cycle 1	Cycle 2	Cycle 3	Cycle 4	Cycle 1	Cycle 2	Cycle 3	Cycle 4	Total
1	4.2	5.3	327.4	308.0	335.9	326.6	9.89	13.18	12.92	10.48	46.47
2	4.2	2.1	326.6	323.0	359.0	367.3	13.87	13.28	12.84	10.99	50.98
3	3.8	5.3	327.4	308.0	335.9	326.6	8.75	7.63	12.95	5.97	35.30

**Table 1:** The operating history information of the three assembly groups provided for the measurements by the NPP operator. The cooling time is the time elapsed from the end of operation until the time of the measurement.

The collected gamma spectra were analysed with GammaVision [8]. After determining the count-rates for the peaks, an intrinsic efficiency calibration method [9] was used to calculate relative activities for four nuclides studied in this work. An example of the relative efficiency function can be seen on Fig. 2.

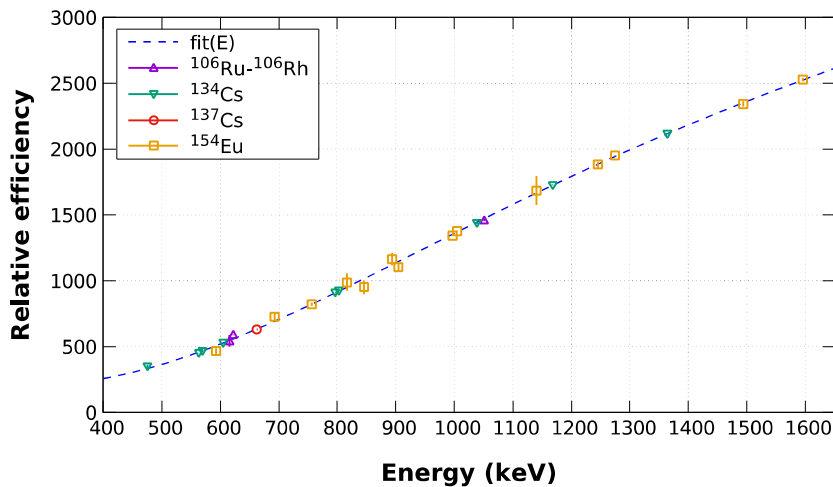


**Fig. 2:** The relative efficiency function calculated from the peaks of <sup>106</sup>Ru-<sup>106</sup>Rh, <sup>134</sup>Cs, <sup>137</sup>Cs and <sup>154</sup>Eu. The peaks of <sup>134</sup>Cs were used as base, the other nuclides' peaks were multiplied with a scaling factor to match with <sup>134</sup>Cs. The fitted function 'fit(E)' is a general 4<sup>th</sup> order polynomial. The increasing characteristic of the efficiency curve is due to the absorption of water between the assembly and the collimator.

As there is no activity calibration for the spent fuel measurements, only the values relative to the activity of  $^{137}\text{Cs}$  were determined. Thus, the result of each measurement can be given with three quantities:  $R_{Ru106}$ ,  $R_{Cs134}$  and  $R_{Eu154}$ , where is  $R_{ig}$  the relative activity of nuclide  $i$  calculated from the gamma peak  $g$  defined by (Eq. 3).

$$R_{ig} = A_{ig}/A_{Cs-137} \quad (3)$$

These activity ratios were calculated for most detected gamma peaks of  $^{106}\text{Ru}$ ,  $^{134}\text{Cs}$  and  $^{154}\text{Eu}$ . The ratio corresponding to a nuclide and its uncertainty was calculated as a weighted mean using the following formulas:

$$\bar{R}_i = \frac{\sum_{g=1}^{n_i} R_{ig}}{\sum_{g=1}^{n_i} \frac{1}{\sigma_{ig}}} \quad (4)$$

$$\Delta \bar{R}_i = \sqrt{\frac{1}{n_i}} \quad (5)$$

In (Eq. 4) and (Eq. 5)  $\sigma_{ig}$  is the standard deviation of  $R_{ig}$  and  $n_i$  is the number of gamma peaks used in the calculations for the nuclide  $i$ .

The results obtained by using the formulas (Eq. 4) and (Eq. 5) are included in Table 2 and are shown on Fig. 3.

Assembly group	Assembly number	Measurement live time (s)	$A_{Ru-106}/A_{Cs-137}$		$A_{Cs-134}/A_{Cs-137}$		$A_{Eu-154}/A_{Cs-137}$	
			mean	std. dev.	mean	std. dev.	mean	std. dev.
1	11	11015	4.64	1.67%	1.979	0.21%	0.0689	0.60%
	12	16156	4.70	1.38%	1.988	0.17%	0.0698	0.46%
	13	16586	4.71	1.32%	1.994	0.15%	0.0692	0.45%
2	21	18183	4.39	0.59%	1.983	0.20%	0.0714	0.69%
	22	15408	4.44	0.59%	1.990	0.21%	0.0712	0.67%
	23	17346	4.42	0.59%	1.986	0.20%	0.0708	0.71%
3	31	18890	4.25	1.53%	1.647	0.19%	0.0631	0.55%
	32	18897	4.26	1.49%	1.641	0.20%	0.0620	0.50%
	33	19190	4.24	1.48%	1.643	0.18%	0.0622	0.49%

**Table 2:** Lives times and the calculated activity ratios of the spent fuel measurements.

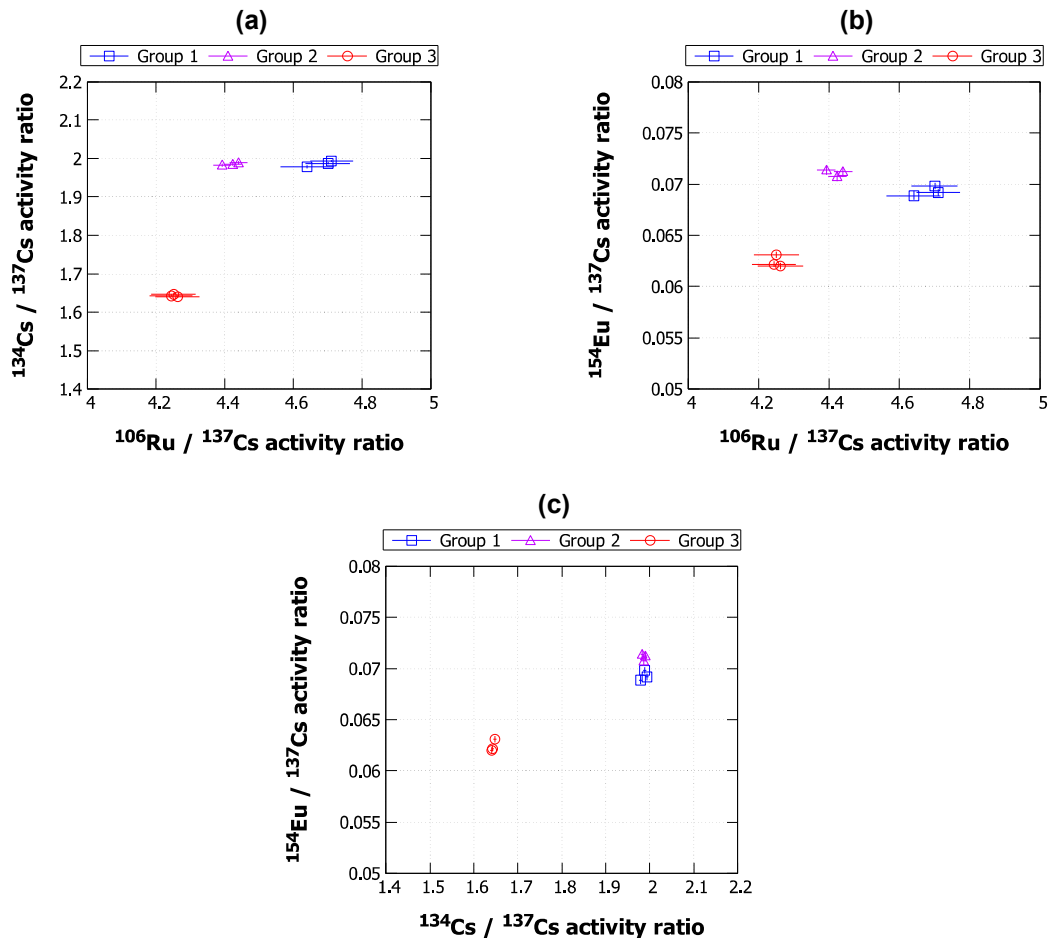


**Fig. 3:** The  $^{106}\text{Ru}$ ,  $^{134}\text{Cs}$  and  $^{154}\text{Eu}$  ratios of assembly groups 1, 2 and 3 measured by HRGS, plotted as 2D graphs. Part (a) shows the  $^{134}\text{Cs}/^{137}\text{Cs}$  ratio as a function of the  $^{106}\text{Ru}/^{137}\text{Cs}$  ratio, (b) is the  $^{154}\text{Eu}/^{137}\text{Cs}$  ratio vs the  $^{106}\text{Ru}/^{137}\text{Cs}$  ratio and (c) is the  $^{154}\text{Eu}/^{137}\text{Cs}$  ratio vs the  $^{134}\text{Cs}/^{137}\text{Cs}$  ratio.

On Fig. 3a and 3c, no difference can be seen between the  $^{134}\text{Cs}/^{137}\text{Cs}$  ratios of group 1 and 2. This means that the  $^{134}\text{Cs}/^{137}\text{Cs}$  ratio does not “remember” the first cycle, from where the burnup difference originates. However, on Fig. 3b and 3c, the  $^{154}\text{Eu}/^{137}\text{Cs}$  ratio of group 2 is higher than that of group 1, so the  $^{154}\text{Eu}/^{137}\text{Cs}$  ratio retains the burnup information on a bigger timescale. The  $^{106}\text{Ru}/^{137}\text{Cs}$  ratio is affected by the operational history of the last cycle, but also by the total burnup via the  $^{137}\text{Cs}$  activity. This could be a possible reason for the  $^{106}\text{Ru}/^{137}\text{Cs}$  ratio of group 2 being smaller than the ratio of group 1, despite them having similar burnup in the last cycle. Group 3 has lower total burnup than group 1 and 2, but it also has lower burnup in the last cycle, so the  $^{106}\text{Ru}/^{137}\text{Cs}$  ratio is smaller.

#### 4. Calculations with ORIGEN 2.2

The computer code ORIGEN 2.2 is capable of calculating the depletion of nuclear fuel and the radioactive decay of its isotopic components. To achieve this, ORIGEN 2.2 solves a large system of ODEs with elements similar to (2). This is carried out by using the matrix exponential technique [10] and also by calculating asymptotic solutions and using the Gauss-Seidel iteration for short-lived nuclides [11]. The one-group neutron flux is either an input parameter or is calculated from the specified power level. An ORIGEN 2.2 input file contains the initial isotopic composition of the fuel, the IDs of the cross-section and decay data libraries used and the irradiation and decay information of the specific problem. This information contains the time intervals of irradiation and decay, and either the neutron flux or the thermal power during the irradiation period.

Calculations were performed for a Westinghouse design 17x17 PWR fuel element with 4.2 wt % initial enrichment. In these calculations, the PWRUE “extended-burnup” cross-section library [12], developed

for the ORIGEN2 code, was utilized. In general, two types of cases were considered: (i) constant total burnup with different burnup-per-cycle structures and (ii) the "H4" structure but with varying values of the high and low burnups. These scenarios are listed in Table 3. Each cycle length is 330 days, with 30 days out-of-operation time between them. The calculated  $^{106}\text{Ru}/^{137}\text{Cs}$ ,  $^{134}\text{Cs}/^{137}\text{Cs}$  and  $^{154}\text{Eu}/^{137}\text{Cs}$  ratios are presented in Table 4 and plotted on Fig. 4 as 2D projections.

Case ID	Burnup (GWd/tUi)					Case ID	Burnup (GWd/tUi)				
	Cycle 1	Cycle 2	Cycle 3	Cycle 4	Total		Cycle 1	Cycle 2	Cycle 3	Cycle 4	Total
H1	14	12	12	12	50	H4C1	12.3	12.3	12.3	13.1	50
H2	12	14	12	12	50	H4C2	12.2	12.2	12.2	13.4	50
H3	12	12	14	12	50	H4C3	12.1	12.1	12.1	13.7	50
H4	12	12	12	14	50	H4C4	11.9	11.9	11.9	14.3	50
L1	11	13	13	13	50	H4C5	11.8	11.8	11.8	14.6	50
L2	13	11	13	13	50	H4C6	11.7	11.7	11.7	14.9	50
L3	13	13	11	13	50						
L4	13	13	13	11	50						
AV	12.5	12.5	12.5	12.5	50						

**Table 3:** The burnup levels per cycle of the examined irradiation history scenarios for the ORIGEN calculations.

Case ID	$A_{\text{Ru-106}}/A_{\text{Cs-137}}$	$A_{\text{Cs-134}}/A_{\text{Cs-137}}$	$A_{\text{Eu-154}}/A_{\text{Cs-137}}$	Case ID	$A_{\text{Ru-106}}/A_{\text{Cs-137}}$	$A_{\text{Cs-134}}/A_{\text{Cs-137}}$	$A_{\text{Eu-154}}/A_{\text{Cs-137}}$
H1	4.7726	1.9096	0.11325	H4C1	4.9312	1.9516	0.11350
H2	4.7822	1.9140	0.11325	H4C2	4.9732	1.9605	0.11357
H3	4.8414	1.9312	0.11319	H4C3	4.9790	1.9694	0.11369
H4	4.9981	1.9777	0.11376	H4C4	5.0389	1.9866	0.11389
L1	4.9643	1.9573	0.11357	H4C5	5.0790	1.9949	0.11395
L2	4.9344	1.9529	0.11350	H4C6	5.1191	2.0032	0.11408
L3	4.9006	1.9357	0.11357				
L4	4.6541	1.8873	0.11280				
AV	4.8726	1.9336	0.11331				

**Table 4:** The values of the activity ratios calculated with ORIGEN 2.2 for each of the examined irradiation history cases.

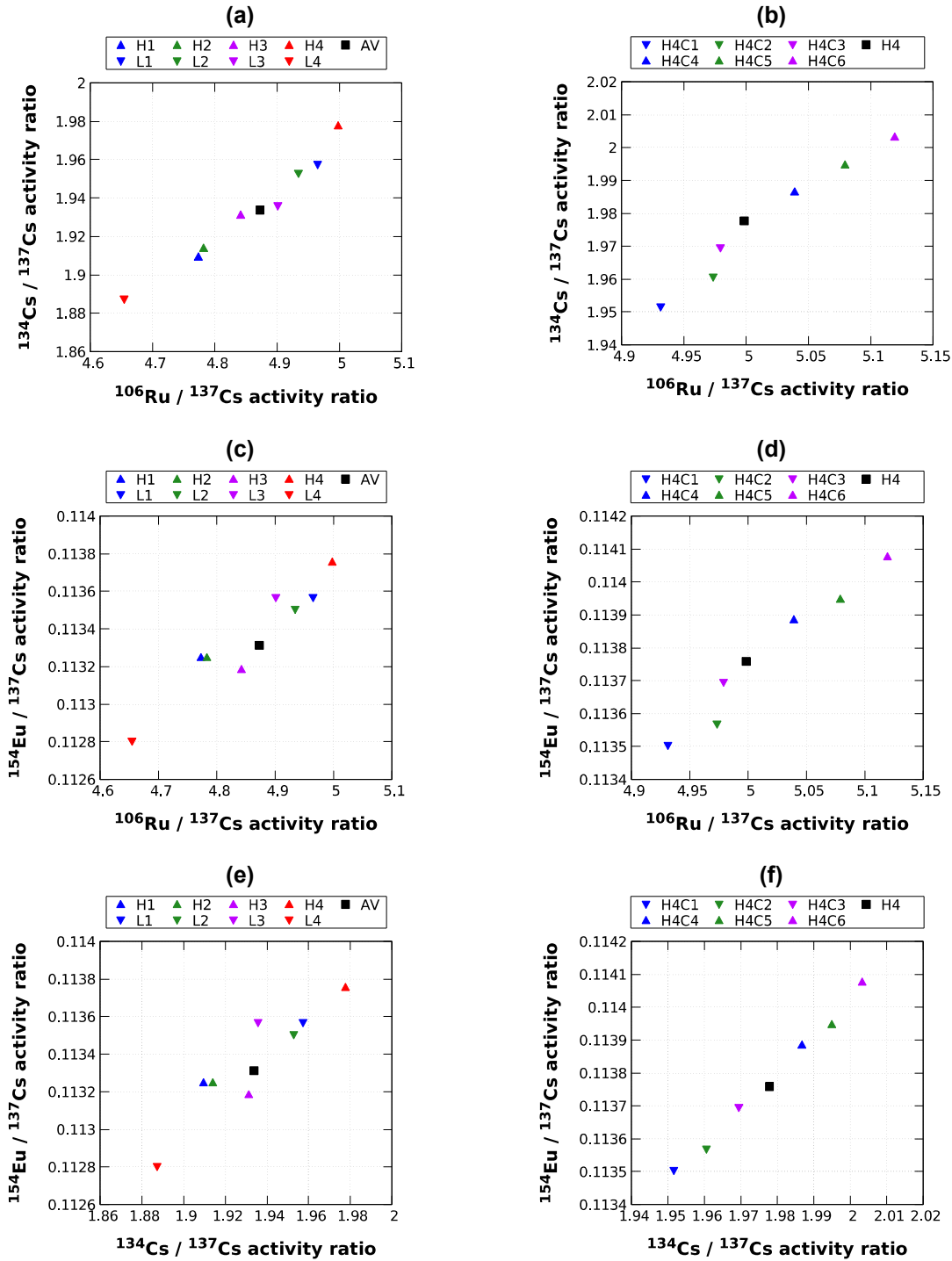


**Fig. 4:** The 2D graphs of the activity ratios calculated with ORIGEN 2.2 for cases H1–H4, L1–L4 and AV on (a), (c) and (e) and for cases H4C1–H4C6 and H4 on (b), (d) and (f).

The difference between cases H1 and H2 is very small on Fig. 4a, 4c and 4e. The same thing can be said for cases L1 and L2. This means that by using these three ratios one cannot say whether an increase/decrease in burnup occurred in the first or the second cycle. H3, L3 and AV are also close to each other, except in the  $^{154}\text{Eu}/^{137}\text{Cs}$  ratio, but the absolute difference is still small. The cases H4 and L4 are distinct from the rest. The ratios also change for a given history structure (H4) if the values of the high and low burnups are different. This is seen on Fig. 4b, 4d and 4f. The impact of this change is that it becomes hard to distinguish histories from each other if the values of the high and low burnups are unknown. Another problem is that, in the examined scenarios, the  $^{154}\text{Eu}/^{137}\text{Cs}$  ratio changes only about 1% between the minimum and the maximum value. So in essence, the  $^{154}\text{Eu}/^{137}\text{Cs}$  ratio needs

to be measured with more than 1% accuracy for history determination purposes. However, an upside is that the  $^{154}\text{Eu}/^{137}\text{Cs}$  ratio can more precisely estimate the total burnup for assemblies of different histories than the  $^{134}\text{Cs}/^{137}\text{Cs}$  ratio, which varies about 5% in the examined scenarios. This is because the longer half-life of  $^{154}\text{Eu}$ , which means that it will conserve more information from the whole operational period.

The cooling time can be determined with the use of the  $^{106}\text{Ru}/^{154}\text{Eu}$  activity ratio. As time elapses, this ratio, denoted with  $R$ , decreases exponentially:

$$R = R_0 \exp[-(\lambda_{\text{Ru-106}} - \lambda_{\text{Eu-154}})t_c] \quad (6)$$

In (Eq. 6),  $R_0$  is the value of the ratio at the end of operation,  $\lambda$  is the decay constant and  $t_c$  is the cooling time. Rearranged for  $t_c$ , (Eq. 6) takes the form of (Eq. 7):

$$t_c = a + b \ln(R) \quad (7)$$

$$a = \ln(R_0) / (\lambda_{\text{Ru-106}} - \lambda_{\text{Eu-154}}) \quad (8)$$

$$b = -1 / (\lambda_{\text{Ru-106}} - \lambda_{\text{Eu-154}}) \quad (9)$$

The value of parameter  $b$  is exactly -1.67507 y, as it only depends on the decay constants. In contrast, parameter  $a$  depends on  $R_0$  as well. Using the result of case AV for the mean of  $R_0$  and its difference from the biggest value (case H4C6) as the uncertainty, the value of  $a$  can be determined as  $6.300 \text{ y} \pm 0.073 \text{ y}$ , so it has about 1% relative uncertainty. It must be noted, that the uncertainty might increase if many more burnup history scenarios are taken into account. Also, the value of  $a$  has to be calculated for each different fuel assembly type.

Direct comparison of the investigated scenarios calculated with ORIGEN 2.2 and the spent fuel measurement results described in Section 3 cannot be made. The reason for this is because the measured assemblies were used in a VVER-440 type reactor and the calculations were carried out for a Westinghouse PWR. The difference between the reactor-core geometries and used materials means that the neutron-energy flux is different and this affects the activity ratios. Nevertheless, the results obtained from the calculations help in understanding the behaviour of the activity ratios for varying assembly histories.

## 5. Burnup validation method

Based on the findings of this work, the following method is recommended to be used for the burnup history validation of spent fuel by HRGS measurements:

1. HRGS measurement of the selected spent fuel assembly, evaluation of the  $^{134}\text{Cs}/^{137}\text{Cs}$  and  $^{154}\text{Eu}/^{137}\text{Cs}$  activity ratios at the end-of-operation time using (Eq. 7).
2. Calculating the  $^{154}\text{Eu}/^{137}\text{Cs}$  ratio with an appropriate burnup code (e.g. ORIGEN2), while supposing a uniform burnup scenario. The total burnup should be adjusted until the measured and calculated ratios agree.
3. Calculating the  $^{134}\text{Cs}/^{137}\text{Cs}$  ratio using the determined total burnup for various burnup per cycle scenarios.
4. Accepting the examined scenario as the burnup history when both the  $^{154}\text{Eu}/^{137}\text{Cs}$  and  $^{134}\text{Cs}/^{137}\text{Cs}$  ratios agree with the measured values.

This method could be supplemented by testing for the  $^{106}\text{Ru}/^{137}\text{Cs}$  ratio as well, mainly to improve the estimated burnup of the last cycle. The knowledge of the operational times is required, but approximating with the usual in- and out-of-operation times for a given reactor should not disturb the results much. The accuracy of this method depends much on the accuracy of the reactor model used in the burnup code. However, the method is relatively fast, as it only requires about 5 hours of measurement time and the calculations can be done very quickly, provided that the necessary data libraries were obtained beforehand.

## 6. Conclusions

It is evident, both from the measurements and the burnup code calculations with ORIGEN 2.2, that the  $^{134}\text{Cs}/^{137}\text{Cs}$  activity ratio, which is commonly used to estimate the burnup, cannot yield a precise burnup value if the burnup history of the fuel is unknown. Instead, the  $^{154}\text{Eu}/^{137}\text{Cs}$  ratio should be used, because its dependence on the burnup history is relatively small. The variation of the  $^{154}\text{Eu}/^{137}\text{Cs}$  ratio could only be a concern if the last cycle's burnup is significantly different from the rest. It should be noted that, since the activity of  $^{154}\text{Eu}$  is an order of magnitude smaller than  $^{134}\text{Cs}$ , the HRGS measurements require longer times (3 hours at least) to achieve the desired precision, which is usually below 1% standard deviation.

The usage of the  $^{106}\text{Ru}/^{154}\text{Eu}$  activity ratio to independently measure the cooling time of an assembly has been investigated. Using ORIGEN 2.2 calculations, it was found that this ratio changes little for fuel assemblies of different burnup history. Based on these investigations, this technique seems promising to independently measure the cooling time with HRGS.

We proposed a method based on the  $^{154}\text{Eu}/^{137}\text{Cs}$  and  $^{134}\text{Cs}/^{137}\text{Cs}$  ratios to more accurately determine the total burnup of a spent fuel assembly. In addition to this, it also gives an estimation of the burnup history. This method yields burnup information independent from the operator's statement. The only required knowledge outside of the measurement is the initial enrichment and the in- and out-of-operation times. The former information is on the assembly itself (VVER-440 assembly) and the latter ones can be approximated well enough.

Further work is needed to test out both the proposed cooling time and burnup determination methods.

## 7. Acknowledgements

The authors would like to acknowledge the sponsorship of Paks NPP and its personnel for assisting at the measurements and for supplying the required burnup data. This project was partly supported by the Hungarian Atomic Energy Authority.

## 8. References

- [1] Almási I, Nguyen CT, Hlavathy Z, Zsigrai J, Lakosi L, Nagy P; *Burnup monitoring of VVER-440 spent fuel assemblies*, ESARDA Bulletin, ed. H. Tagziria, JRC Ispra, No. 50; Dec. 2013; p 41-47.
- [2] Nguyen CT, Almási I, Hlavathy Z, Zsigrai J, Lakosi L, Nagy P, Parkó T, Pós I, *Monitoring burn-up of spent fuel assemblies by gamma spectrometry*, IEEE Transactions on Nuclear Science 60/2 (2013) 1107-1110.
- [3] Lebrun A, Bignan G; *Non Destructive Assay of Nuclear LEU Spent Fuel for Burnup Credit Application*, Nuclear Technology, Vol. 135:3; 2001; p 216-229.
- [4] Croff AG; *A User's Manual for the ORIGEN2 Computer Code*, ORNL/TM-7175; Oak Ridge, TN; 1980.
- [5] Ihara H, Matumoto Z, Tasaka K, Akiyama M, Yoshida T, Nakasima R; *JNDC FP Decay and Yield Data, JAERI-M 9715*; Japanese Nuclear Data Committee, Tokai Research Establishment, JAERI; 1981.
- [6] IAEA, Nuclear Data Services; ENDF/B-VII; <https://www-nds.iaea.org/exfor/endl.htm> (2019.04.23.)
- [7] Lakosi L, Sáfár J, Józsa I; *Spent fuel measurements at NPP Paks*, ESARDA Bulletin, ed. L. Stanchi, JRC Ispra, No. 13; Oct. 1987; p 31-32.
- [8] GammaVision – Gamma Analysis for Windows; Advanced Measurement Technology, Inc.; 2003

[9] Le TA, Nguyen CT, Bui VL, Lakosi L; *Relative efficiency calibration for determining isotopic composition and age of HEU items by passive non-destructive gamma spectrometry*, Applied Radiation and Isotopes 142 (2018) 220-228.

[10] Ball SJ, Adams RK; "MATEXP," *A General Purpose Digital Computer Program for Solving Ordinary Differential Equations by the Matrix Exponential Method*, ORNL/TM-1933; Oak Ridge, TN; 1967.

[11] Croff AG; *ORIGEN2: A Versatile Computer Code for Calculating the Nuclide Compositions and Characteristics of Nuclear Materials*; Nuclear Technology, Vol. 62; September 1983; p 335-352.

[12] Ludwig SB, Renier JP; *Standard- and Extended-Burnup PWR and BWR Reactor Models for the ORIGEN2 Computer Code*, ORNL/TM-11018; Oak Ridge, TN; 1989.

# **Session 7:**

# **Destructive Analysis**

# Optimising the use of reference materials for destructive analysis in nuclear safeguards

Ana María SÁNCHEZ HERNÁNDEZ, Claudia ANDOR, Razvan BUDA,  
Lorelei COMMIN, Francesco D'AMATI, Joan HORTA DOMENECH,  
Sylvain MOREL, Adrian NICHOLL, Christophe NOURRY, Gert SUURKUUSK,  
Martin VARGAS ZUÑIGA, Denis WOJNOWSKI, Evelyn ZULEGER

JRC Directorate G - Nuclear Safety and Security  
JRC G.II.6 Nuclear Safeguards and Forensics  
Hermann-von-Helmholtz-Platz 1, 76344 Eggenstein-Leopoldshafen, Germany  
E-mail: ana-maria.sanchez-hernandez@ec.europa.eu

## **Abstract:**

*The European Commission is responsible for the control of all civil fissile nuclear material in the European Union and one of the Joint Research Centre (JRC) activities is supporting EURATOM safeguards with analytical measurements. The JRC-Karlsruhe Analytical Service (AS) is an ISO/IEC 17025 accredited laboratory which supports the European and International Safeguards authorities and the JRC for sample characterisation mainly related to nuclear research.*

*The AS deals with a large sample variety particularly concerning uranium and plutonium content and isotopic composition determination by Isotope Dilution - Thermal Ionisation Mass Spectrometry (ID-TIMS) and TIMS analyses. To cover the large diversity and amount of samples, a system has been optimised to reduce resource consumption and assure measurement accuracy in compliance with quality standards and the International Target Values (ITVs)-2010.*

*Usually samples need to be diluted to concentration and matrix suitable for Mass Spectrometry (MS) measurements. ID-TIMS is used for content determination. Samples are mixed with a known amount of solution - called spike - containing the investigated element in a well characterised isotopic concentration. Furthermore, for mixed uranium/plutonium samples the two elements need to be chromatographically separated.*

*For quality assurance all samples are treated for spiking, chemical separation and MS measurements together with quality control samples (standards) in the same way. The AS prepares a representative set of standards and spikes with defined MS concentration to cover uranium, plutonium and mixed uranium and plutonium samples. All the samples are prepared such as to have matrix and concentration similar to the reference solutions. In order to reduce the use of valuable Certified Reference Materials (CRMs), the AS uses in-house reference solutions characterised against CRMs. This paper presents the stringent protocol used for production and characterisation of in-house reference solutions in order to keep analysis uncertainties below the ITVs-2010.*

**Keywords:** Safeguards; Destructive Analyses (DA); Laboratory Reference Materials (LRMs); Spike; ITVs-2010

## **1. Introduction**

The European Commission is responsible for the control of all civil fissile nuclear material in the European Union (EURATOM Treaty Chapter VII). One of the main activities of the Directorate General Joint Research Centre (DG JRC) is to give support to EURATOM safeguards by providing high quality analytical measurements. Three main laboratories have been established in the European Commission, the Analytical Service (AS) of JRC-Karlsruhe where samples from different nuclear

facilities are sent for verification and the two EURATOM on-site laboratories located at the reprocessing plants in Sellafield (UK) and La Hague (France) operated by JRC-Karlsruhe on behalf of DG ENERGY. The three laboratories are run by the unit JRC.G.II.6 Nuclear Safeguards and Forensics and share resources in terms of personnel, analytical methods, knowledge, experience and expertise.

The AS is an ISO/IEC 17025 accredited laboratory which supports the European and International Safeguards authorities. Besides, the AS gives support to the JRC for sample characterisation for nuclear research, waste removal and transport of nuclear material to other facilities.

The AS has received an average of ten requests per month in the last years, with more than 400 samples to be characterised every year. More than the half of the samples are coming from Safeguards authorities and the rest from different units of Directorate G based in Karlsruhe and Geel. Figure 1 shows the proportion of samples per customer in 2018. This can be considered a representative feature for the last years.

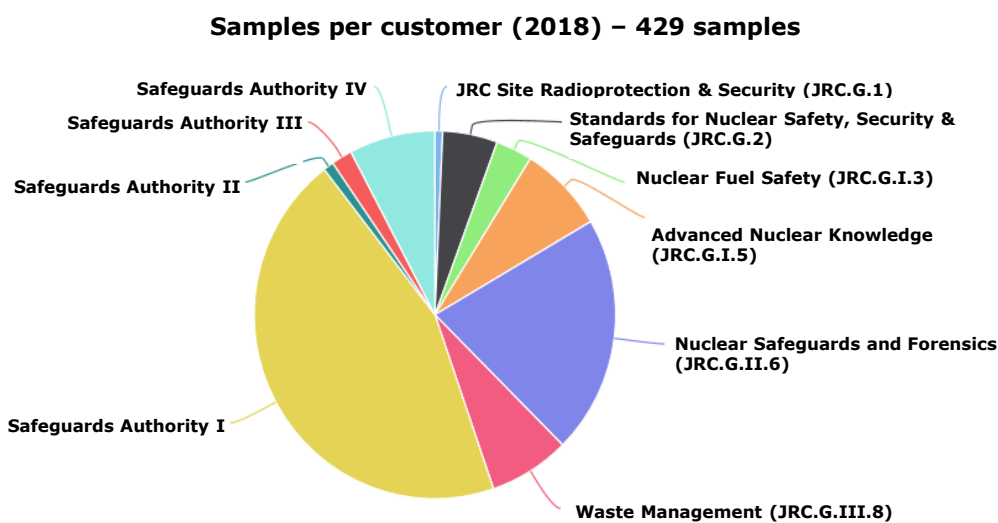


**Figure 1.** Proportion of samples per organisation

The analyses offered by the AS are the determination of uranium, plutonium and boron isotopic composition and the assay of main elements such as uranium, plutonium, americium, or of impurities for more than 70 elements, including light elements carbon, nitrogen and oxygen, in various matrices. Included are uranium particle analyses for isotopic composition determination. The AS also performs evaluation of activity for several radioisotopes including fission products.

The AS offers a big variety of non-destructive radiometric and destructive analyses. The methods used to provide Nuclear Safeguards related measurements are compliant with the International Atomic Energy Agency IAEA/ESARDA International Target Values (ITVs)-2010 [1].

The best fit-for-purpose technique is selected based on the request of the customer and on the characteristics of the samples. Figure 2 presents an overview of the amount of analyses per technique performed in 2018:

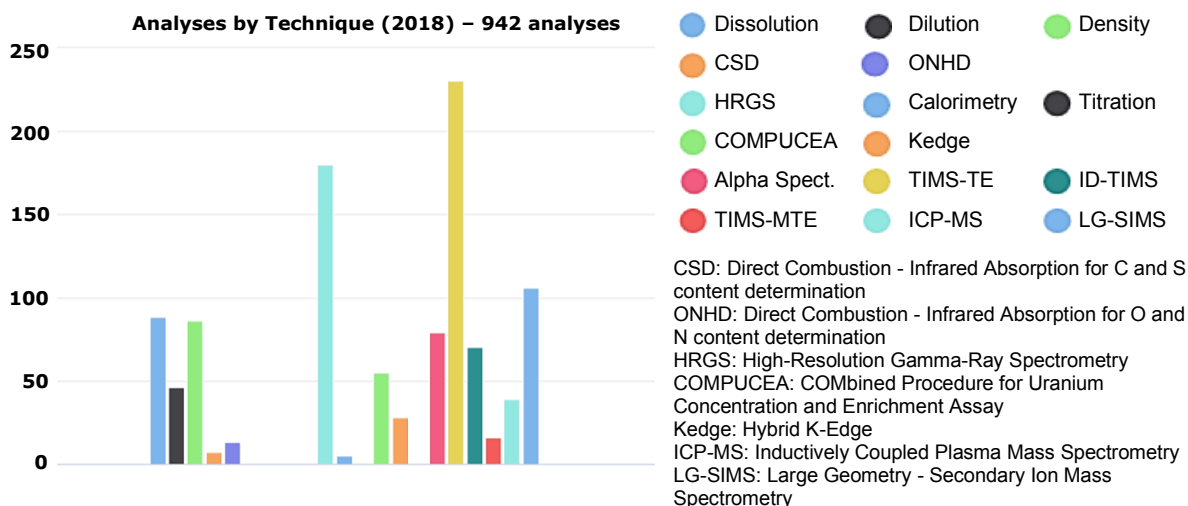


**Figure 2.** Analyses by technique in the AS in 2018

Many of the requested analyses concern the determination of the uranium and plutonium content and/or of their isotopic composition by Thermal Ionisation Mass Spectrometry (TIMS). The methods offered by AS for these analyses are listed below together with their most important characteristics:

- Total Evaporation (TE): Uranium, plutonium and boron isotopic determination – fast, precise and accurate for the major isotope ratios.
- Modified Total Evaporation (MTE): Uranium isotope measurements - high accuracy and precision for determining the minor isotope ratios.
- Isotope Dilution - Thermal Ionisation Mass Spectrometry (ID-TIMS) – used to determine the uranium and plutonium contents. A known amount of spike (material with known concentration and isotopic composition) is added to the sample. The mixture is then measured by TE-TIMS to calculate the concentration in the sample.

TE and ID-TIMS are combined with Alpha Spectrometry to determine the ratio  $n(^{238}\text{Pu})/n(^{239}\text{Pu})$ .

To guarantee accuracy and to establish traceability of the results to the International System of Units (SI), Certified Reference Materials (CRMs) are used as one layer of Quality Control (QC). Besides, the use of CRMs for quality assurance is a requirement for the ISO/IEC 17025 accredited laboratories. These materials are not always available in a suitable form. Consequently, the alternative is the in-house produced Reference Materials (RMs). An overview of the use of (C)RMs in the AS and EURATOM laboratories is presented in reference [2].

The use of CRMs, in particular for plutonium with low commercial availability, is optimised and substituted by in-house prepared RMs as much as feasible. Besides, JRC-Karlsruhe owns a vast range of uranium and plutonium bearing materials in different forms and with various isotopic compositions. The AS has large experience purifying, blending and characterising nuclear materials in order to get uranium and/or plutonium with a target concentration, isotopic composition and form [3], [4]. Making use of the existing material is part of the strategy for optimising the consumption of nuclear material and particularly valuable CRMs.

Another layer of QC of the analytical methods is the participation to Inter Laboratory Comparisons (ILC) exercises such as the Commissariat à l'Énergie Atomique et aux Énergies Alternatives/Commission d'Établissement des Méthodes d'Analyse (CEA/CETAMA) – Evaluation de la Qualité des Résultats d'Analyse dans l'Industrie Nucléaire (EQRAIN), IAEA - Nuclear Material Round Robin and the New Brunswick Laboratories (NBL) - Standard Material Evaluation (SME).

To deal with the large diversity and amount of samples for destructive analysis, the AS has optimised a system to process samples and to prepare in-house reference solutions, called laboratory reference materials (LRMs). This approach allows the reduction of resource consumption while assuring the accuracy of the measurements and compliance with ISO/IEC 17025 quality standards and ITVs-2010.

This paper focuses on the use of RMs by the AS for Mass Spectrometry (MS) measurements and in particular the stringent protocol used for production and characterisation of LRMs which allow keeping analysis uncertainties below the ITVs-2010.

## 2. Sample preparation process for MS and quality control

Samples from different requests and customers can be grouped in batches (called hereafter runs) and prepared/measured in duplicate. The different types of runs depend on the elements to be analysed and the type of determination. The process for the preparation of routine samples for MS is shown in Figure 3:

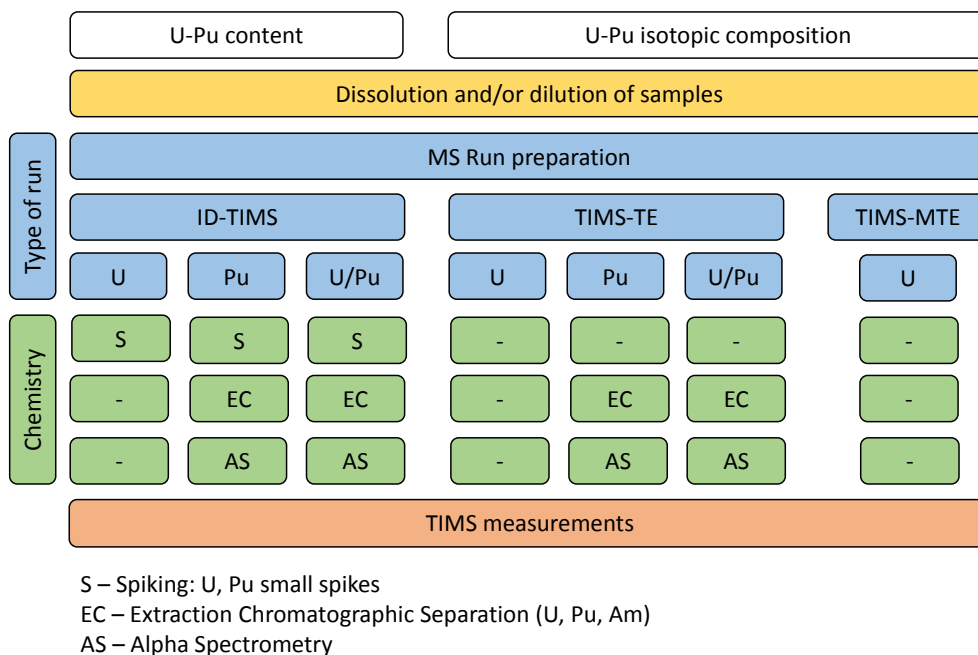


Figure 3. Types of runs and sample preparation for MS

To cover the QC needs of the different type of runs the AS prepares a representative set of standards with concentration and matrix suitable for mass spectrometry. Two different spikes used for uranium and plutonium elemental assay with comparable characteristics are produced (see section 3).

For quality assurance all samples are treated for spiking, chemical separation, Alpha Spectrometry and MS measurements together with QC samples (standards) in the same way.

All the relevant data from the different steps for the preparation of the sample are uploaded in the Laboratory Information Management System (LIMS) of the AS [5]. The results are calculated by the system and the QC is done in the following layers:

- QC Instrument by checking the machine performance and calibration
- QC MS measurements:
  - QC process - verification QC sample
  - QC individual samples - duplicates

Only if the measurement results are accepted according to all the QC criteria, LIMS allows the analyst to create the results assigning the appropriate uncertainty. Finally, the MS task officer or another authorised analyst double check the results and release them in LIMS for the preparation of the final report by the Data Managers.

By grouping the samples in batches, the AS reduces the total amount of spike solutions and RMs used for QC. Furthermore, the chemicals and reagents used during the chromatographic separation procedure is optimised; particularly the use of UTEVA resin for element purification - only a small amount is needed for the typical quantities of uranium and plutonium [6]. Besides, using element concentrations directly usable for MS measurements, the sample (after radiochemistry if needed) can be loaded on the filament without evaporation to dryness and reconstitution. Another main advantage is that the radiochemistry and alpha spectrometry measurements can be performed in a glove box with low level of radioactivity reducing the exposition of the operator.

### 3. Use of reference materials for destructive analyses in the Analytical Service

CRMs are used in the AS for method validation, instrument calibration and QC but also for the production of RMs and LRMs.

The AS uses CRMs provided by the European Commission, JRC.G.2, Standards for Nuclear Safety, Security and Safeguards unit, by CEA/CETAMA and by NBL.

RMs with reference values assigned by the AS have been used regularly by the AS during the last years and measured with different instruments. For those that have been characterised decade ago, the reference values can be re-evaluated with better statistical treatment of the data to be more consistent with the more precise modern techniques. Reference [7] presents a re-evaluation of reference values of plutonium isotopic composition of the RM SM4.

The different types of uranium and/or plutonium LRMs produced by the AS for MS measurements are listed below:

- LRMs used as QC standards:
  - QC instrument
  - QC process
- LRMs used as Spikes:
  - Small spikes for routine samples and ILC exercises.
  - Calibrants for the Large-Sized Dried (LSD) spikes verification procedure [8], [9]

The LRMs target concentration and matrix for alpha spectrometry and MS measurements are summarized in Table 1. The typical amount of nuclear material used in one year for QC standards and spike material for routine samples is about 2 mg of plutonium and 15 mg of uranium:

QC STANDARDS and SPIKES for TIMS-TE, ID-TIMS	
Concentration U ( $\mu\text{g/g}$ )	75-125
Concentration Pu ( $\mu\text{g/g}$ )	7-13
Matrix U	4 M $\text{HNO}_3$
Matrix Pu	8 M $\text{HNO}_3$
Matrix U/Pu	8 M $\text{HNO}_3$
QC STANDARDS for TIMS-MTE	
Concentration U ( $\mu\text{g/g}$ )	3000-6000
Matrix U	1-4 M $\text{HNO}_3$

**Table 1:** Concentration and media for QC and spike solutions.

All LRMs certified for uranium and/or plutonium concentration, depend on guaranteed stability and long-term integrity of the solution to avoid changes in the concentration. The AS developed its own system to store the solutions in ampoules sealed by Laser (see section 4).

In the last years the verification/characterisation procedure has been optimised and implemented in the LIMS. The procedure and statistical treatment depend on the intended use of the reference solution i.e. as QC sample or as spike, see sections 3.1 and 3.2.

### 3.1. LRMs used as QC standards

QC standards are produced by diluting or mixing the appropriate CRMs or RMs. All newly prepared QC LMRs are verified for isotopic composition and/or concentration as per need. This is done by analysing different aliquots or ampoules of the respective solutions using the analytical method for which they are intended. All data processing and calculation of reference values, QC charts depictions and the assigning of the uncertainties to the LMRs are performed by the LIMS. The quality of this verification is crucial as the accuracy and precision of the results provided by the AS depend directly on the uncertainties of the QC reference solutions.

The reference values of the QC LRMs are verified using at least five different ampoules/aliquots representative of the whole batch. This is the minimum number of individual points established to set up preliminary QC charts. The solution aliquots are analysed following the same process as the one for the routine samples. Once the results are validated in compliance with the QC system, the measured values are used for the evaluation of homogeneity and stability of the batch (see section 3.2.1), and for determining the preliminary control charts and uncertainty in LIMS. Before a new standard batch is taken into use, it is utilised in parallel with the remaining running standard; at least three QC runs are performed with double standards - one from the new batch and the one from the one to be replaced - to verify the accuracy of the data entered in LIMS for the new standard.

The QC charts are updated and maintained in LIMS with a maximum of 25 points for the calculation of control limits and uncertainties. The uncertainty assigned to the reference values of the QC standard is calculated considering three components:

- Random component determined from the measured values.
- Deviation contribution which considers the bias of the measurements from the reference values.
- Uncertainty of the reference values from the certificate or verification.

### 3.2. LRMs used as spikes

The different types of ID-TIMS spikes used in the AS are listed below:

- Small spikes – routine samples and ILC exercises:
  - U content assay:  $^{233}\text{U}$  spike
  - Pu content assay:  $^{242}\text{Pu}$  spike
- LSD spikes verification:
  - U content assay: EC-NMR-110  $^{238}\text{U}$  spike
  - Pu content assay: SM4  $^{240}\text{Pu}$  spike

The plutonium assay reference solutions for LSD spikes verification prepared from RM SM4 are characterised against the CRM MP2 (CETAMA).

For uranium and plutonium assay of routine samples, the AS spikes with sufficiently different isotopic compositions of spike and sample and adjusting the sample to spike ratio. The AS makes use of spikes with elevated relative mass fraction (>97%) of  $^{233}\text{U}$  and  $^{242}\text{Pu}$  since the concentration of the sample being measured is suitable for handling in a low level radiochemical laboratory. The  $^{233}\text{U}$  and  $^{242}\text{Pu}$  spikes are produced in-house from material available in the AS and characterised against CRMs.

The  $^{233}\text{U}$  spike is prepared by purifying, if necessary, a uranium nitrate mother solution. If thorium or plutonium is expected a purification step on TEVA resin is included. The  $^{242}\text{Pu}$  spike mother solution is purified using UTEVA resin to remove any uranium and americium in the sample. Once the solutions are purified they are diluted to the target concentration. Alpha spectrometry is used to estimate the content of  $^{233}\text{U}$  or  $^{242}\text{Pu}$ . Section 4 describes the steps taken for ensuring the stability of the material batches by sealing them in glass ampoules.

The spikes used for uranium determination are verified against three different CRMs: EC-NMR-110, EC-NMR-101 (provided by the European Commission, JRC-Geel) and the NBL CRM 125-A. Small spikes for plutonium assay are characterised against three calibrants prepared from different dilutions of the CRM MP2 provided by CETAMA.

For the characterisation of new batches, solution aliquots are analysed following the same process as for the routine samples. The spike characterisation module was implemented in LIMS in 2014 [10]. Once the results are accepted according to the QC system, LIMS starts using the data for the evaluation of the reference values for concentration and isotopic composition. Furthermore, the analysts perform outliers test, and homogeneity and stability studies. Paragraph 3.2.1 presents an example of the characterisation of a  $^{233}\text{U}$  spike produced in the AS, the small spike U-24.

After characterisation, the reference values are verified by using the new spike in parallel with the analogue spike still in use for at least three runs to confirm the accuracy of the assigned values.

In order to rule out any possible cross contaminations of the uranium and plutonium spikes with plutonium and uranium respectively, the final solution is analysed by Inductively Coupled Plasma Mass Spectrometry (ICP-MS).

### 3.2.1. U-24 small spike characterisation

The U-24 mother solution was distributed in three bottles fitted with a large bore dispenser tubing to pour the solution into the marked ampoules. The filling sequence was in numerical order - 125 ampoules were sealed with different volumes of solution. The stability of the ampoules is checked gravimetrically as described in section 4. Four ampoules were rejected resulting in the success rate 96.8% for the sealing.

The three calibrants from different dilutions of CRMs mentioned in section 3.2 were used for the characterisation. Two ampoules from every bottle were randomly chosen. The protocol for the concentration characterisation is shown in Figure 4. The uranium content determination was based on the results of two ID-TIMS runs and the isotopic composition was determined from two TIMS runs. For the ID-TIMS runs one of the calibrants was used as QC sample. It was spiked with the small spike U-23 which was still in-use at that time.

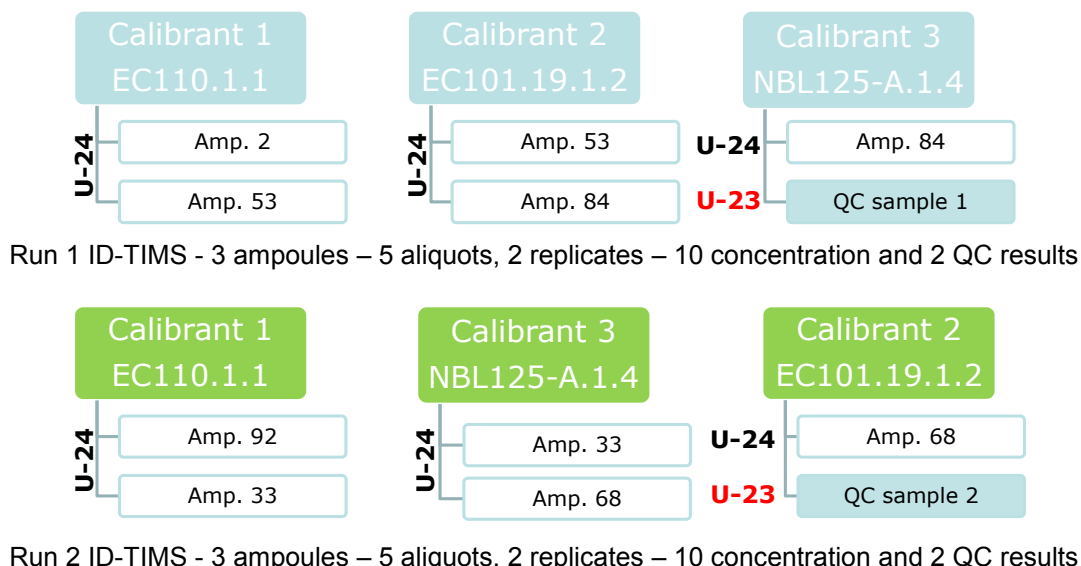


**Figure 4.** Small spike characterisation protocol

The results of the different runs have been treated in compliance with the AS QC system. Afterwards, they have been used for the determination of the reference values of the spike. The Grubbs test was applied to check for outliers among the 20 concentration values; no outliers were found in the data set.



Figure 7 presents the 20 concentration results sorted by calibrants. In this case, the ANOVA test shows that the means of two or more groups are significantly different from each other. To see which populations are different a t-Test (Two-Sample Assuming Equal Variances) has been applied to the different sets of data. The data coming from calibrant 1 and calibrant 3 are significantly different.

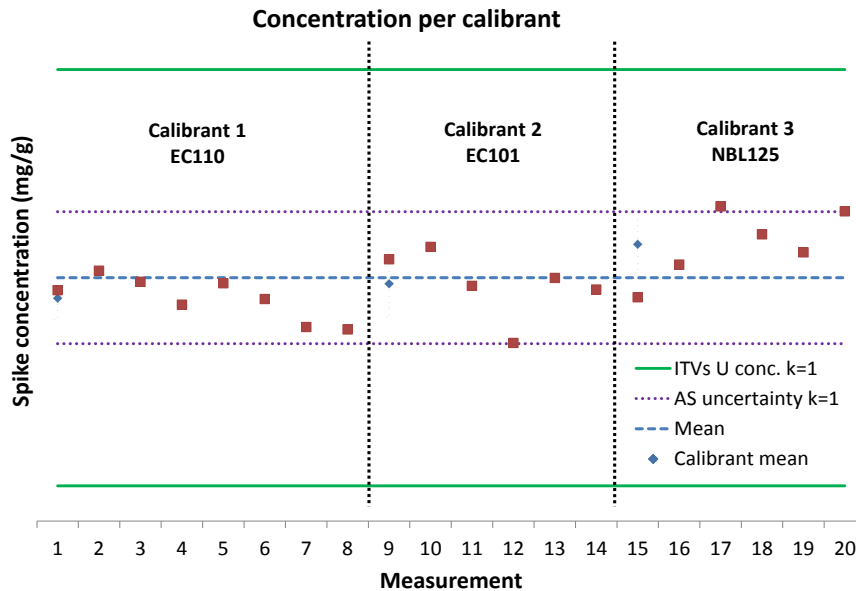


Figure 7. Concentration results per calibrant

However, because the difference between the groups does not impact the measurement uncertainty, the spike U-24 can be considered fit for purpose. The reference values assigned by the LIMS system [10] have been accepted. Nevertheless, in order to improve further the quality of the small spikes, the source of this statistical discrepancy is under investigation.

The performance of the AS small spikes is checked as well by participating in ILC exercises. Two plutonium spikes were evaluated during the EQRAIN Pu14 ILC results, see Figure 8. The concentration determined with the second spike, Pu-31 was closer to the reference value. This effect was observed in the three sub-samples analysed for the determination of the final result. However, since the Pu-31 spike was still under verification only the results of the Pu-30 spike were reported for evaluation:

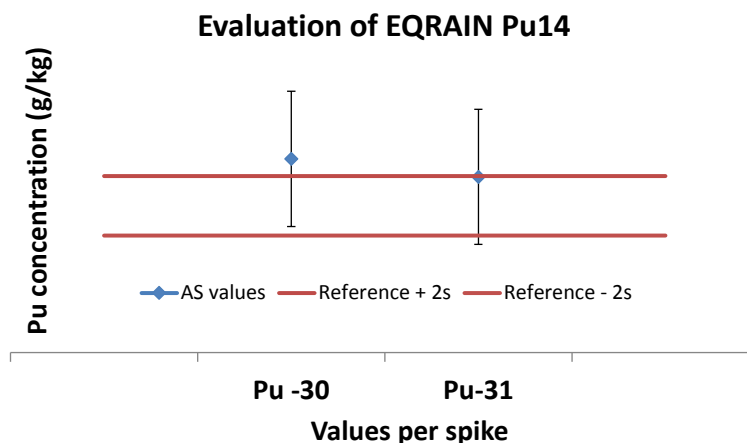


Figure 8. Comparison of results using Pu-30 and Pu-31 spikes.

#### 4. Storage of LRMs in ampoules sealed by Laser

As mentioned in section 2, the stability and long-term integrity of the ID-TIMS QC samples and small spikes is guaranteed by keeping the solutions in Laser sealed ampoules. The AS system is based on the Laser sealing system used in CEA, Marcoule (France). A glove box is dedicated to this activity; the Laser is located outside and connected to the glove box. The ampoules are welded inside the box. The process of sealing one batch of ampoules (100-130 units) is done in 3-4 hours to avoid significant evaporation of the ID-TIMS solutions.

To ensure that the ampoules are properly sealed and that there is no leakage or evaporation of solution, a stability check based on weight control is done on the whole batch of ampoules. The ampoules are weighed the day after welding and again at least three weeks after the sealing date. All ampoules that show a loss of mass higher than the established limit (0.01%) are removed from the batch. The stability check is repeated before usage of every single ampoule.

The sealing system has contributed to the improvement of the stability of the ID-TIMS QC solutions and spikes in the AS [2]. However, during the first years of usage of the technique, the efficiency of the sealing system (in terms of number of ampoules produced per batch and amount of ampoules tightly sealed) was not totally satisfactory. The success rate of tightly sealed ampoules was not constant and below 75 %.

In the last years, efforts have been made to improve the performance of the technique by adjusting and optimising the instrument settings. A QC check on the ampoules before sealing has also been introduced: the quality of the empty ampoules is verified by checking that the dimensions relevant for the welding process are within tolerance limits. The success rate of tightly sealed ampoules increased from 50-75 % in the first years of usage to above 90% during the last four years.

Furthermore, in order to optimise the use of these LRMs and to increase the number of ampoules produced per batch, the volume of solution dispensed in the ampoules has been adjusted according to the intended use of the ampoule. In the case of the QC samples only one aliquot (consisting of 2 duplicates) is needed per run. Accordingly, 1.5-2 mL of solution are dispensed into small ampoules. In the case of small spikes, one ampoule is used per run. Thus, several types of ampoules are used with volumes of solution between 3 and 7 mL to be used in sample runs from 2 to 6 samples.

Producing LRMs requires large amount of resources, time and effort - from the solution preparation and ampoules sealing, to the characterisation with several analyses and evaluation. Using a large number of ampoules provides better statistics for the characterisation and as a result, better accuracy of reference values and uncertainty assigned.

#### 5. Summary

The AS of the JRC-Karlsruhe has been successfully operated for almost four decades. Since 2006 it is an ISO17025 accredited laboratory. Based on the experience acquired over the years the different processes have been optimised and further developed. The AS has a mature quality system oriented towards continuous development of new features for the different methods.

The techniques with higher operation rates have easily reached a high level of reliability. Mass spectrometry, is one of the most applied techniques in the AS. Much progress has been done in the last years, particularly in the improvement of the preparation of LRMs and the data process which has been implemented in the LIMS. The features with higher impact on the optimisation of the use of (C)RMs are listed below:

- Choice of appropriate nuclear material as starting material for RMs and LRMs preparation.
- Use of RMs and LRMs
  - Preparation of LRMs batches with higher quality in terms of reliability and accuracy:
    - Better characterisation (contamination detection, bias and failures prevention)
    - Larger amount of ampoules (longer-lasting sets)

- Handling sample aliquots with reduced concentration for MS preparation process
- Grouping samples in batches for MS measurements
- Optimising the use of spike ampoules (one ampoule per run with customised volume)

Furthermore, producing better quality LRMs allows reducing resources, time and effort. Moreover, a better statistical treatment helps to improve the accuracy and precision of the delivered results.

Future challenges are the implementation of some of the developments above to other techniques, for instance the preparation and characterisation process of LRMs for methods like ICP-MS or Davies-Gray titration and data processing in LIMS.

## 6. Acknowledgements

The authors would like to acknowledge Karin Casteleyn and the former colleagues Ramón Carlos Márquez, Lily Duinslaeger, Lorenza Emblico and Sebastien Mialle for their contribution to the continuous development and improvement of the Analytical Service of the JRC.G.II.6 Nuclear Safeguards and Forensics Unit.

## 7. Legal matters

### 7.1. Privacy regulations and protection of personal data

In order to comply with the European Directive 95/46/EC as approved by the European Parliament and the Council of Ministers on the 24th October 1995 relating to the protection of individuals with respect to the processing of data of personal nature and on the free circulation of such data, it is necessary that you provide us with written consent. Feel free to use the example below as a template:

"I agree that ESARDA may print my name/contact data/photograph/article in the ESARDA Bulletin/Symposium proceedings or any other ESARDA publications and when necessary for any other purposes connected with ESARDA activities."

### 7.2. Copyright

The author agrees that submission of an article automatically authorises ESARDA to publish the work/article in whole or in part in all ESARDA publications – the bulletin, meeting proceedings, and on the website.

The author declares that their work/article is original and not a violation or infringement of any existing copyright.

## 8. References

[1] IAEA; *International Target Values 2010 for Measurement Uncertainties in Safeguarding Nuclear Materials*; IAEA-STR-368, 2010.

[2] Zuleger, E., Casteleyn, K., Duinslaeger, L., Buda, R., Vargas Zuñiga, M., Carlos Marquez, R., Rasmussen, G., Emblico, L., Sánchez Hernández, A.M., Nicholl, A., Luetzenkirchen, K., Schwalbach, P.; *Use of Reference Materials for Destructive Analysis at the Institute for Transuranium Elements (ITU) and the Euratom On-Site Laboratories at Sellafield and La Hague*; INMM Annual Meeting, 2015.

[3] Sánchez Hernández, A.M., Toth, K., Aregbe, Y., Banik, N., Bauwens, J., Buda, R., Bujak, R., Carlos Marquez, R., Casteleyn, K., Duinslaeger, L., Hennessy, C., Jakopic, R., Kehoe, F., Van Belle, P., Zuleger, E.; *Alternative nuclear certified reference materials for safeguards and industry*; Proceedings 39<sup>th</sup> Annual Meeting, Düsseldorf, 2017.

[4] Aregbe, Y., Banik, N., Bauwens, J., Buda, R., Bujak, R., Carlos Marquez, R., Casteleyn, K., Duinslaeger, L., Hennessy, C., Jakopic, R., Kehoe, F., Sánchez Hernández, A.M., Toth, K., Zuleger,

E.; *INS-CRM: Innovative nuclear certified reference materials for EURATOM safeguards and industry*. JRC114518, 2019.

[5] Sánchez Hernández, A.M., Wojnowski, D., Zuleger, E., Pravdova, J.; *User Manual LIMS: Description of the laboratory information management system in Analytical Service: M0024/S5/R1*; JRC99469; Karlsruhe, 2016.

[6] Morgenstern, A., Apostolidis, C., Carlos-Marquez, R., Mayer, K., Molinet, R.; *Single-column extraction chromatographic separation of U, Pu, Np and Am*; *Radiochimica*, vol. 90, p. 81, 2002.

[7] Mialle, S., Casteleyn, K., Sánchez Hernández, A.M., Morel, S., Zuleger, E.; *Internal Re-evaluation of the SM4 Isotopic Composition*; JRC101050, Karlsruhe, 2016.

[8] Van Belle, P., Zuleger, E.; *Procedure for the verification of large scale U/Pu dried spikes*; Technical Note JRC-ITU-TPW-2009/22; 2009.

[9] Jakopič, R., Aregbe, Y., Richter, S., Zuleger, E., Mialle, S., Balsley, S. D., Repinc, U., Hiess, J.; *Verification Measurements of the IRMM-1027 and the IAEA Large-Sized Dried (LSD) Spikes*; *J Radioanal Nucl Chem.* 311:1781-1791, 2017

[10] Sánchez Hernández, A.M., Wojnowski, D., Buda, R., Zuleger, E.; *Validation of the LIMS module: Spike characterisation*; JRC91897, Karlsruhe, 2014.

# **EQRAIN U and EQRAIN Pu interlaboratory comparisons from 1997 to 2016 - Comparison to ITVs-2010**

**Crozet Marielle<sup>1</sup>, Roudil Danièle<sup>1</sup>, Rigaux Corinne<sup>1</sup>, Bertorello Caroline<sup>1</sup>, Picart Sébastien<sup>1</sup>, Maillard Christophe<sup>2</sup>**

1 CEA, DEN, MAR/DMRC/CETAMA, F-30207 Bagnols-sur-Cèze Cedex, France

2 CEA, DEN, MAR/DMRC/SE2A/L2AT, F-30207 Bagnols-sur-Cèze Cedex, France

E-mail address of the corresponding author: marielle.crozet@cea.fr

## **Abstract:**

*Since 1987, the CEA's Committee for the Establishment of Analysis Methods (CETAMA) has regularly implemented interlaboratory comparisons, entitled Evaluation of the Quality Results of Analysis in the Nuclear Industry (EQRAIN). Notably, the EQRAIN U and EQRAIN Pu interlaboratory comparisons assess proficiency in measuring a mass content of uranium or plutonium in reference solutions.*

*This presentation deals with the results of measurement uncertainty assessments from EQRAIN U and EQRAIN Pu comparisons over 20 years of exercises (1997-2016). The mathematical approach developed allows to estimate the impact of short-term systematic and random errors to the overall uncertainty of each analytical method used in the interlaboratory comparison program. This statistical analysis shows a good consistency between measurement uncertainty values from EQRAINs and the measurement uncertainty target values established by the International Atomic Energy Agency (IAEA) for nuclear material balances (ITVs-2010).*

**Keywords:** EQRAIN, uranium, plutonium, proficiency test, interlaboratory comparisons, ITVs-2010, Measurement uncertainty assessment

## **1. Introduction**

The management of nuclear materials is based on accurate knowledge of the quantities and grades of nuclear material present in nuclear facilities and involved in material transfers between facilities. This knowledge is obtained by direct analysis as well as by Destructive sample Analysis (DA). DA has the advantage of providing more accurate measurements. In the nuclear industry and especially in fuel cycle activities, uranium (U) and plutonium (Pu) mass content determination accuracy is crucial for ensuring the safety of nuclear facilities, and for preparing accurate material flow balances [1]. For this purpose, Certified Reference Materials (CRM) are used for the development or validation of analytical methods, for the calibration of analysis methods, and for the preparation of secondary Reference Materials (RM). One of the principal missions of the Committee for the Establishment of Analysis Methods (CETAMA) is to provide (C)RM to meet the analytical needs of laboratories in the French nuclear sector. Concurrently, the CETAMA has implemented the "quality assessment of analysis results in the nuclear industry" program EQRAIN (Évaluation de la Qualité des Résultats d'Analyse dans les Installations Nucléaires) since 1987. In particular, the program organized U or Pu mass content analysis proficiency tests (EQRAIN U and EQRAIN Pu, respectively) in alternate years. These exercises are done in compliance with ISO 17043 [2] through French and international nuclear domain networks, to meet the needs of both industrial and institutional analysis laboratories. The U or Pu reference solution samples for EQRAIN U ILC or EQRAIN Pu ILC, are produced by the CETAMA metrology laboratory (LAMMAN) - located in the Atalante facility at CEA Marcoule - in compliance with the ISO 17034 standard [3] and ISO Guide 35 [4]. EQRAIN U and EQRAIN Pu ILC results are processed in compliance with the ISO 13528 [5] standard.

Given the interest shown in such programs, these ILCs have been repeated regularly and provide the participating laboratories with an opportunity to evaluate their proficiency to measure either U or Pu

mass content in a nitric acid reference solution. These ILCs results over 20 years could be analysed to evaluate method uncertainty.

## 2. CETAMA: EQRAIN U and EQRAIN Pu

### 2.1. Samples

The reference solutions produced by LAMMAN are defined in this paragraph.

The EQRAIN U reference solutions are made by dissolution from the CRM uranium oxide  $U_3O_8$  "AGARIC" [6] certified in impurity amount content, or "OTU-1" [7] certified in U amount content. EQRAIN U reference solutions are uranyl nitrate in nitric acid (2 – 5 M) solution, with the reference value of the U amount content expressed in grams per kilogram of solution (Figure 1). The relative expanded uncertainty ( $k = 2$ , taking into account characterization, homogeneity, and stability components according to [5]) associated with the reference value in EQRAIN U reference solutions is less than or equal to 0.1%. In this article, only EQRAIN U ILCs with U amount content reference values  $x_{ref}$  close to 200 g/kg are taken into account i.e. 7 ILCs, named EQRAIN U08 to EQRAIN U14.

The EQRAIN Pu reference solutions are made by dissolution from the "MP2" [8], plutonium metal CRM, certified in mass, Pu amount content, and Pu isotopic composition. EQRAIN Pu reference solutions are plutonium nitrate in nitric acid (2 – 5 M) solution, and the reference value of the Pu amount content in these solutions is expressed in grams per kilogram of solution (Figure 1). The relative expanded uncertainty ( $k = 2$ , in compliance with [5]) associated with the reference value in EQRAIN Pu reference solutions is less than or equal to 0.12%. In this article, EQRAIN Pu ILCs results with Pu amount content reference values  $x_{ref}$  from 2 to 5 g/kg solution are taken into account i.e. 7 ILCs, named EQRAIN Pu07 to EQRAIN Pu13.

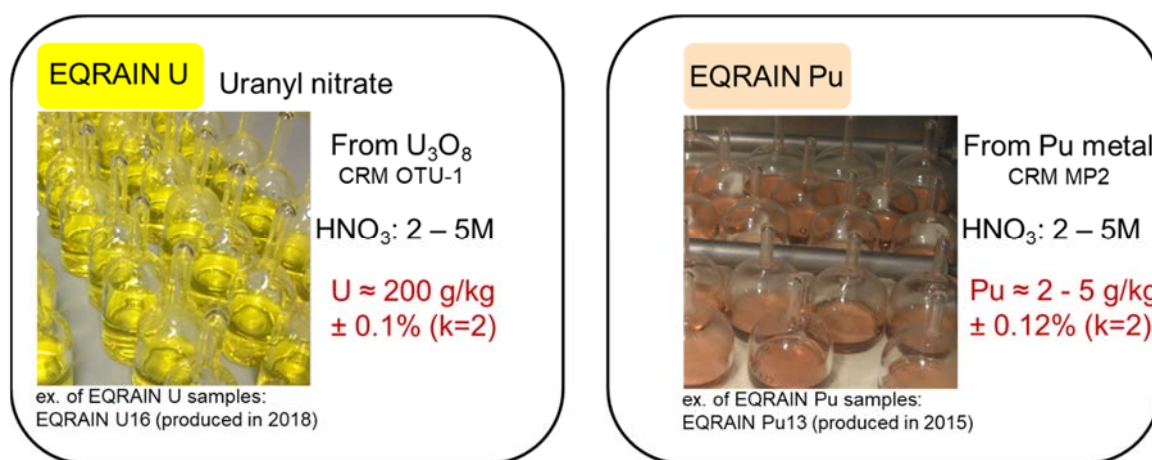


Figure 1: EQRAIN U and EQRAIN Pu ILCs samples

### 2.1. Interlaboratory comparisons

EQRAIN ILCs (noted EQRAINs hereafter) are proficiency tests in which the participating laboratories are free to choose their own analytical method. For each EQRAIN  $j$ , each laboratory has to report its result(s)  $x_{ij}$  (i.e. amount content of U or Pu in grams per kilogram), with its associated expanded uncertainty as estimated by the laboratory and the corresponding coverage factor  $k$ . Laboratories' results are analyzed in compliance with the ISO 13528 [5] standard by the CETAMA and collated in the EQRAIN ILC technical report which is transmitted to each participant.

In this technical report, individual laboratory performance is expressed among others in terms of deviation from the reference value  $d_{ij}$  (Figure 2).

$$d_{ij} = \frac{x_{ij} - x_{ref j}}{x_{ref j}}$$

where  $x_{ij}$  is the measurement result of laboratory the EQRAIN j and  $x_{ref j}$  is the reference value of the EQRAIN j.

The reference value is provided by the metrology laboratory of CETAMA which produces the EQRAIN solution RM. It is calculated from the certified U or Pu amount content of a solid RM that has been dissolved, all quantities used in the dissolution process have been accurately weighed.

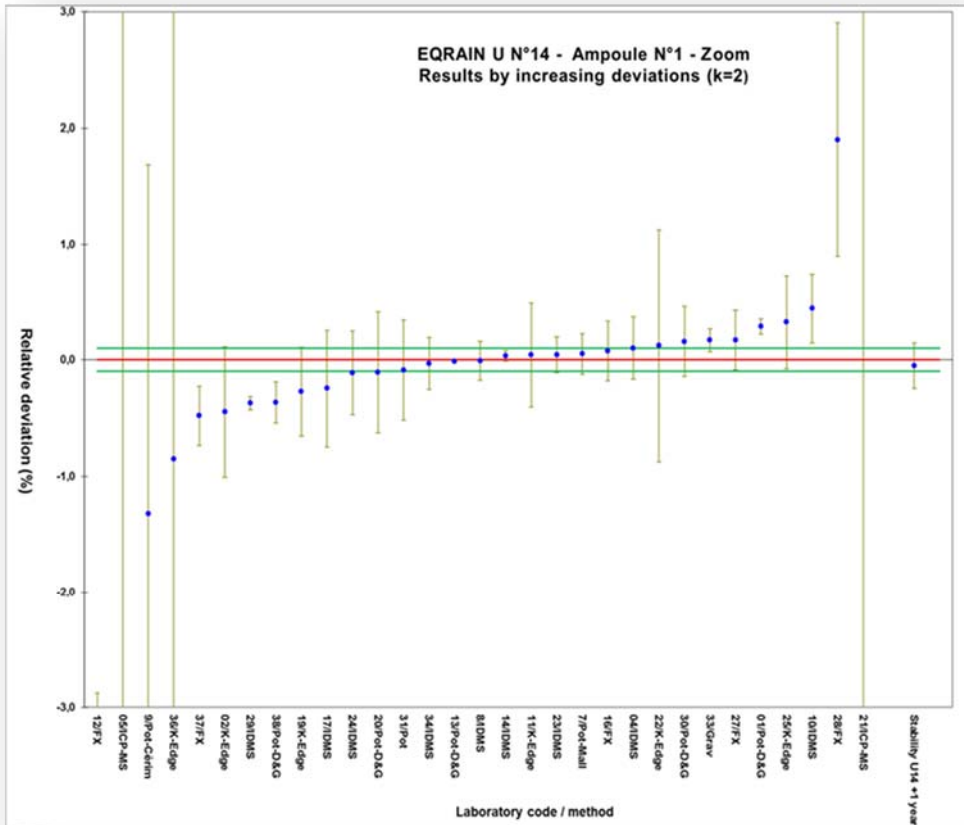


Figure 2: Example of a graph presented in technical report (corresponding to EQRAIN U14)

Thus for each EQRAIN j of the corresponding p EQRAINS (U or Pu) from 1997 to 2016 ( $j = 1$  to  $p$ ), the CETAMA receives  $n_i$  laboratory results ( $i = 1$  to  $n$ ).

In this paper, it is assumed that all  $x_{ij}$  are mutually independent (potential correlations due, for example, to the use of the same spike are neglected) and independent from  $x_{ref j}$ .

### 3. Analysis of ILCs results from 1997 to 2016

#### 3.1. Analytical methods

The number of participating laboratories in EQRAIN U is on average 25, with a stable international participation of 10 laboratories, meaning 25 to 35 results per EQRAIN U ILC (each laboratory can apply several methods and therefore report several results). The analytical methods<sup>1</sup> routinely used [9] are

<sup>1</sup> Abbreviations for the analytical methods are those used in ITVs-2010 document [6], except for Mallinckrodt method (MALL).

illustrated in Figure 3. During the years, the use of Isotope Dilution Mass Spectrometry (IDMS) [10, 11], X-Ray Fluorescence (XRF), and Hybrid K Edge (HKED) increased whereas the use of titrimetric (TITR [12]) methods decreased (TITR is MALL [13] and Davies and Gray (D&G) [14 - 22]).

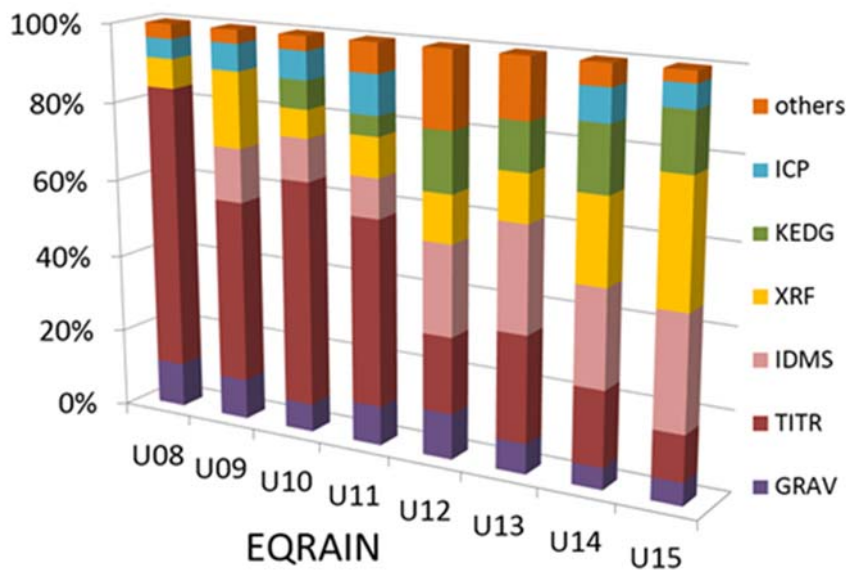


**Figure 3:** Evolution of U analytical methods used in EQRAINs U

The number of participating laboratories in EQRAIN Pu is on average 12, with an international participation of about 6 laboratories, meaning 20 to 25 results per EQRAIN Pu ILC, since a laboratory can report several results. The analytical methods routinely used are illustrated in Figure 4, with an increasing use of IDMS.

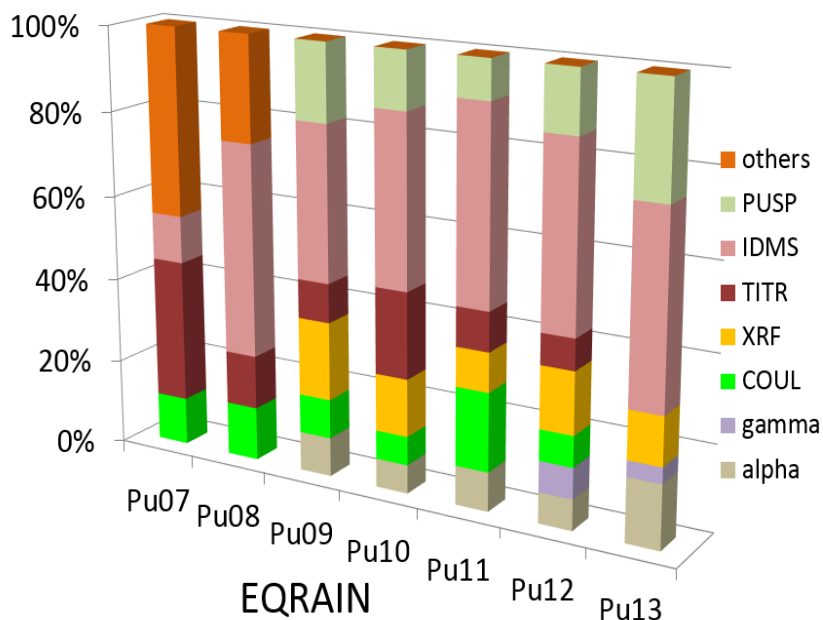


**Figure 4:** Evolution of Pu analytical methods used in EQRAINs Pu

NB: As the EQRAIN Pu solutions are made by dissolving MP2, the isotopy used by the laboratories is that certified from the MP2 certificate.

### 3.2. Mathematical model

The deviation  $d_{ij}$  can be expressed as:

$$d_{ij} = \bar{d} + b_j + e_{ij}$$

where  $\bar{d}$  is the mean difference calculated on the  $p$  EQRAINS,  $b_j$  is the short-term systematic error of  $d_{ij}$  due to the EQRAIN  $j$ , and  $e_{ij}$  is the random error of  $d_{ij}$ .  $b_j$  is the creation of a random variable  $B$ , normal, with a null expectation and with a variance  $\sigma(d)_s^2$  i.e.  $B \sim N(0, \sigma(d)_s^2)$ .  $\sigma(d)_s^2$  is a variance of short-term systematic error due to the factor EQRAIN  $j$ , estimated from a between-EQRAINS variance obtained from an analysis of variances (ANOVA with the study of EQRAIN factor) of the  $d_{ij}$ . The estimation of  $\sigma(d)_s^2$  by ANOVA is  $u(d)_s^2$ .  $e_{ij}$  is the creation of a random variable  $\varepsilon$ , normal, with a null expectation and with a variance  $\sigma(d)_r^2$ , i.e.  $\varepsilon \sim N(0, \sigma(d)_r^2)$ . This variance is a within-EQRAIN variance for which the estimation by ANOVA carried out on the  $d_{ij}$  is  $u(d)_r^2$  [23, 24].

The variance estimation  $u(d)^2$  from ANOVA on  $d_{ij}$  is:

$$u(d)^2 = u(d)_s^2 + u(d)_r^2$$

Variance of  $d$  can also be estimated by applying the variance propagation law [25], generalized to any independent method measurement result  $x$ ; so  $u(d)^2$  can be written:

$$u(d)^2 = \frac{1}{x_{ref}^2} u(x)^2 + \frac{x^2}{x_{ref}^4} u(x_{ref})^2$$

where  $u(x)$  is the standard uncertainty associated with result  $x$  obtained using the analysis method, in other words the method (standard) uncertainty, and  $u(x_{ref})$  is the standard uncertainty on the reference value.

As  $x \sim x_{ref}$ , (only  $d$  values corresponding to laboratory results with an absolute value of  $z$  and zeta scores less than 3 are considered), it can be simplified into:

$$u(d)^2 = \frac{1}{x_{ref}^2} (u(x)^2 + u(x_{ref})^2)$$

By further separating the components related to short-term systematic and random errors, the method relative standard uncertainty related to the short-term systematic error  $u_{rel}(x)_s$  and the method relative standard uncertainty related to the random error  $u_{rel}(x)_r$  can be written as:

$$u_{rel}(x)_s = \frac{\sqrt{x_{ref}^2 u(d)_s^2 - u(x_{ref})^2}}{x_{ref}} \text{ as } x \sim x_{ref} \qquad u_{rel}(x)_r = \frac{\sqrt{x_{ref}^2 u(d)_r^2 - u(x_{ref})^2}}{x_{ref}} \text{ as } x \sim x_{ref}$$

In a conservative approach to evaluating the method uncertainty, it was chosen to disregard the subtraction of the  $u(x_{ref})$  (in an EQRAIN, the reference value is a gravimetric value traceable to the SI Units and with small uncertainties with respect to the reported uncertainties of the participants), thus leading to:

$$u_{rel}(x)_s = u(d)_s \qquad u_{rel}(x)_r = u(d)_r$$

$$u_{rel}(x) = \sqrt{u_{rel}(x)_s^2 + u_{rel}(x)_r^2} = \sqrt{u(d)_s^2 + u(d)_r^2}$$

$u_{rel}(x)$ , method relative standard uncertainty, and its components  $u_{rel}(x)_s$  and  $u_{rel}(x)_r$  can be estimated by an ANOVA applied to the relative difference  $d_{ij}$  between laboratory results and the reference value, as calculated from EQRAIN results  $x_{ij}$  during the EQRAINS from 1997 to 2016. In this ANOVA of  $d_{ij}$ ,  $u(d)_s^2$  corresponds to the EQRAIN factor variance, and  $u(d)_r^2$  characterizes the within-EQRAIN variance. This mathematical model is illustrated in Figure 5.

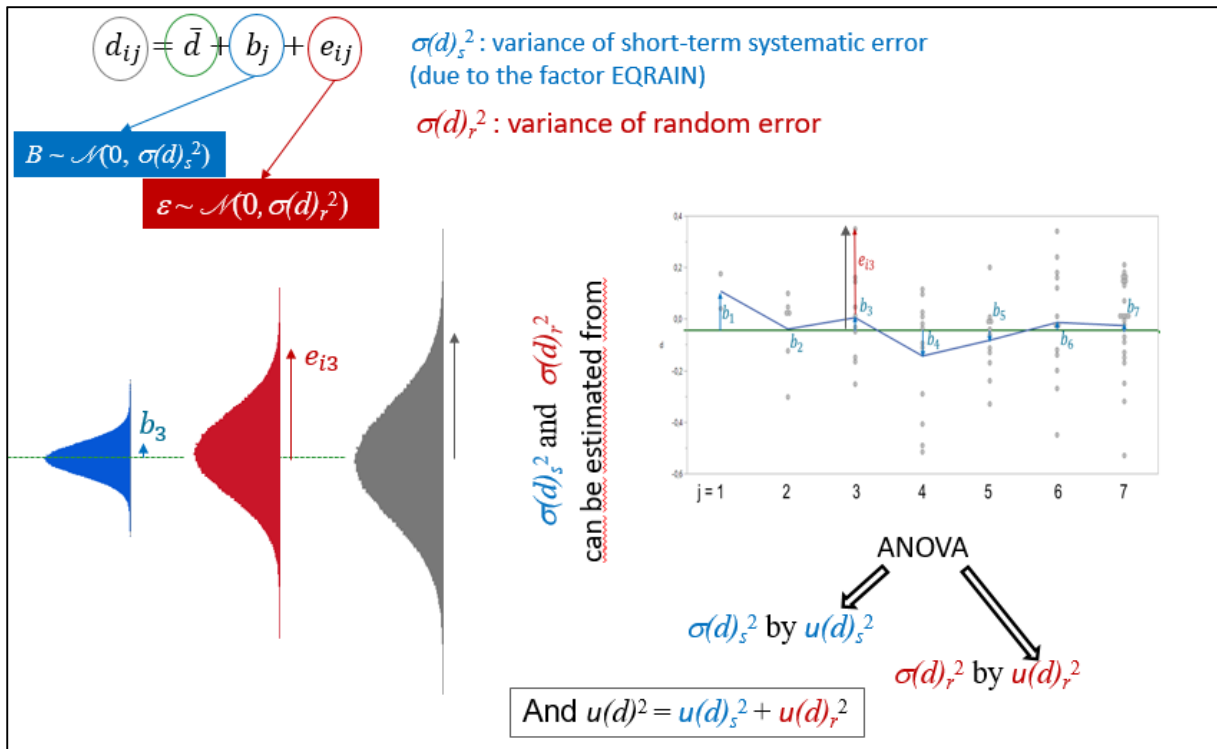


Figure 5: Illustration of the used mathematical model

This uncertainty,  $u_{rel}(x)$ , is the estimated standard uncertainty associated with one U or Pu amount content measurement result obtained by the analytical method in question on pure reference solutions containing respectively hundreds of grams of U per kilogram of solution or a few grams of Pu per kilogram of solution.

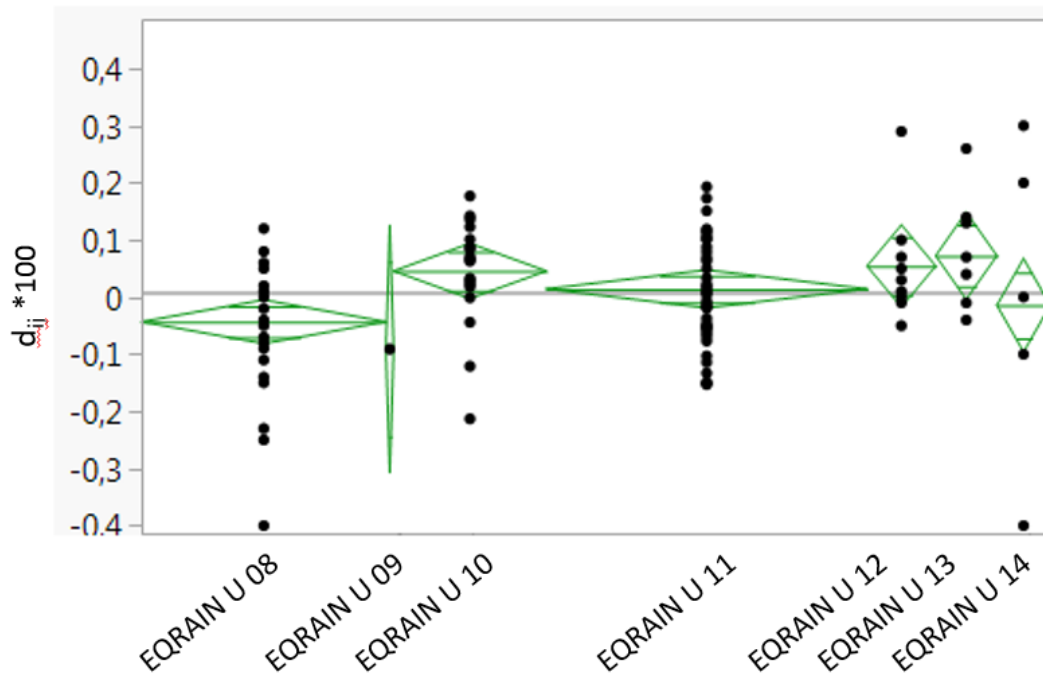
### 3.3. Measurement method uncertainty

For U and Pu, data  $d_{ij}$  from EQRAINS have been divided according to the analytical method. The analytical methods studied are gravimetry (GRAV), MALL, D&G, IDMS, XRF, and HKED for U amount content measurements, and coulometry (COUL), TITR, IDMS, Spectrophotometry (PUSP), and XRF for Pu amount content measurements. For each analytical method for EQRAINS U as well as for EQRAINS Pu, an ANOVA was performed on  $d_{ij}$  leading to the variance due to the EQRAIN factor  $u(d)_s^2$  and to the within-EQRAIN variance  $u(d)_r^2$ . From these two estimated variances,  $u_{rel}(x)_s$ ,  $u_{rel}(x)_r$  and  $u_{rel}(x)$  values were calculated for each analytical method. This approach is illustrated by the statistical processing of the D&G method for EQRAINS U and of IDMS for EQRAINS Pu. These two methods are chosen as they are still the most commonly used within nuclear fuel cycle facilities (more data processing results for the other methods can be found in [26]).

Analyses of variance were performed using the software JMP® 13.0.0 (Statistical Discovery) from SAS Institute Inc [27].

The D&G titration method developed at New Brunswick Laboratory (NBL) has been used since 1970s for U content measurements in the nuclear fuel cycle. This method was applied during the 7 EQRAINS U studied, from EQRAIN U08 in 1997 to EQRAIN U14 in 2015. The ANOVA processed on the  $d_{ij}$  obtained with D&G is illustrated in Figure 6 and in Table 1.

**D&G**



Diamond: middle horizontal line: mean of  $d_{ij} * 100$  for EQRAIN  $U_j$ , upper and lower horizontal lines: coverage interval (95%) of  $d_{ij} * 100$

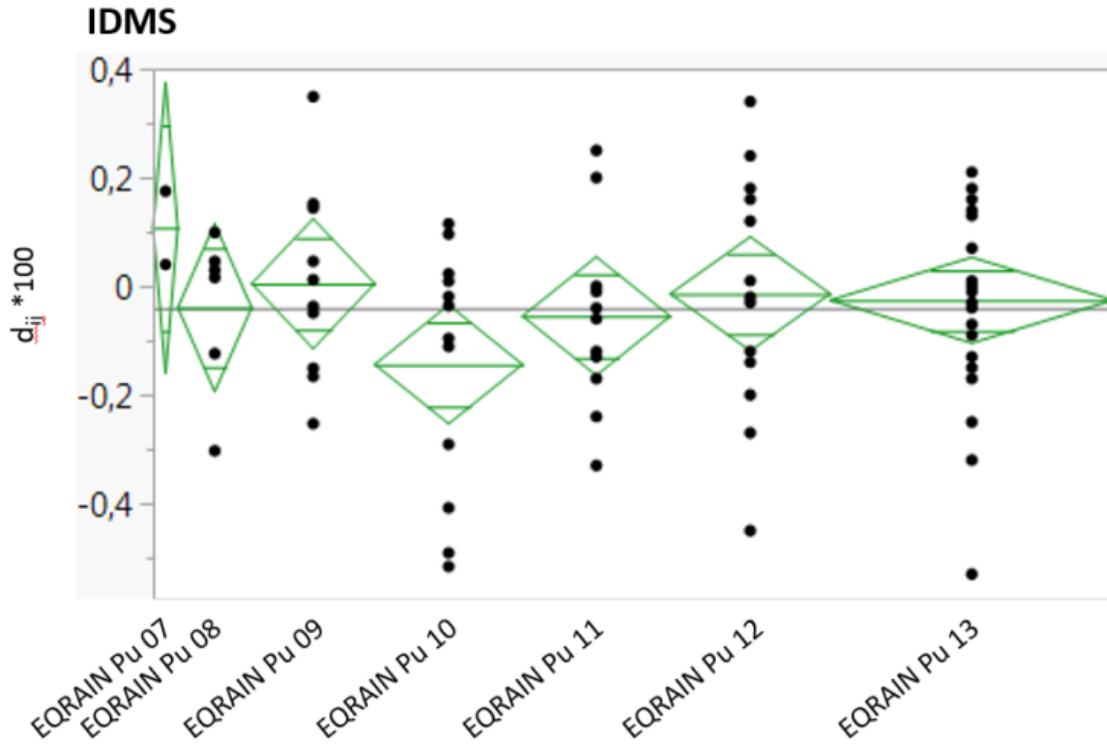
**Figure 6:** D&G: Oneway ANOVA of ( $d_{ij} * 100$ ), from EQRAIN U08 to EQRAIN U14

Source of variation	Sum of squares	Degree of freedom	Mean square
Between-EQRAIN	0.180	6	0.0300
Within-EQRAIN	1.331	112	0.0119
Total	1.511	119	

**Table 1:** D&G: Numerical results of the ANOVA of ( $d_{ij} * 100$ ) from EQRAINs U

From this ANOVA on EQRAINs U, the estimated relative standard uncertainty of a measurement result obtained by D&G,  $U_{rel}(x)_{D\&G}$  is equal to 0.11%, with its components corresponding respectively to short-term systematic and random errors, i.e.  $U_{rel}(x)_s$  equal to 0.04% and  $U_{rel}(x)_r$  equal to 0.12%.

The IDMS method was used to assess the amount content of Pu in solutions of the 7 EQRAINs Pu from EQRAIN Pu07 to EQRAIN Pu13. The ANOVA processed on the  $d_{ij}$  is illustrated in Figure 7 and in Table 2.



Diamond: middle horizontal line: mean of  $d_{ij} * 100$  for EQRAIN  $Pu_j$ , upper and lower horizontal lines: coverage interval (95%) of  $d_{ij} * 100$

Figure 7: IDMS: Oneway ANOVA of ( $d_{ij} * 100$ ), from EQRAIN Pu07 to EQRAIN Pu13

Source of variation	Sum of squares	Degree of freedom	Mean square
Between-EQRAIN	0.2090	6	0.0348
Within-EQRAIN	2.558	71	0.0360
Total	2.767	77	

Table 2: IDMS: Numerical results of the ANOVA of ( $d_{ij} * 100$ ) from EQRAINs Pu

From this ANOVA on EQRAINs Pu, the estimated relative standard uncertainty of a measurement result  $x$  obtained by IDMS,  $U_{rel}(x)_{IDMS}$  is equal to 0.19%, with a negligible component related to short-term systematic error  $U_{rel}(x)_{s, IDMS}$  and a component related to random error  $U_{rel}(x)_{r, IDMS}$  equal to 0.19%.

#### 4. Comparison to ITVs-2010

Table 3 and Table 4 summarize the measurement method uncertainties estimated from EQRAINs U and EQRAINs Pu by one factor ANOVA on  $d_{ij}$ , and also give the corresponding ITVs-2010 and their components related to short-term systematic and random errors for comparison.

	Number of $d_{ij}$	$u_{rel}(x)_s$	$u_{rel}(x)_r$	$u_{rel}(x)$	$u(s)$	$u(r)$	ITV
<b>GRAV</b>	45	<b>0.01</b>	<b>0.16</b>	<b>0.16</b>	<b>0.05</b>	<b>0.05</b>	<b>0.07</b>
<b>TITRI (MALL)</b>	33	<b>0.05</b>	<b>0.06</b>	<b>0.08</b>	<b>0.1</b>	<b>0.1</b>	<b>0.14</b>
<b>TITRI (D&amp;G)</b>	119	<b>0.04</b>	<b>0.11</b>	<b>0.12</b>	<b>0.1</b>	<b>0.1</b>	<b>0.14</b>
<b>IDMS</b>	74	<b>0.03</b>	<b>0.12</b>	<b>0.13</b>	<b>0.1</b>	<b>0.15</b>	<b>0.18</b>
<b>XRF *</b>	42	<b>0.11</b>	<b>0.27</b>	<b>0.29</b>	<b>2</b>	<b>2</b>	<b>2.8</b>
<b>HKED **</b>	40	<b>0.05</b>	<b>0.19</b>	<b>0.20</b>	<b>0.2</b>	<b>0.2</b>	<b>0.28</b>

\* ITVs-2010: 1 to 50 g/L U

\*\* ITVs-2010: typically 150 to 250 g/L U with a U/Pu ratio of 80 to 150 and measurement time of 3x1000 s

**Table 3:** Measurement method uncertainties from EQRAINS U and corresponding ITVs-2010 (%)

	EQRAIN Pu			ITVs-2010			
	Number of $d_{ij}$	$u_{rel}(x)_s$	$u_{rel}(x)_r$	$u_{rel}(x)$	$u(s)$	$u(r)$	ITV
<b>COUL</b>	17	<b>0.07</b>	<b>0.06</b>	<b>0.09</b>	<b>0.1</b>	<b>0.1</b>	<b>0.14</b>
<b>TITR</b>	8	<b>0.21</b>	<b>0.11</b>	<b>0.24</b>	<b>0.15</b>	<b>0.15</b>	<b>0.21</b>
<b>IDMS</b>	78	<b>0</b>	<b>0.19</b>	<b>0.19</b>	<b>0.2</b>	<b>0.2</b>	<b>0.28</b>
<b>PUSP *</b>	22	<b>0</b>	<b>1.5</b>	<b>1.5</b>	<b>2</b>	<b>2</b>	<b>2.8</b>
<b>XRF **</b>	13	<b>0.53</b>	<b>0.48</b>	<b>0.72</b>	<b>2</b>	<b>2</b>	<b>2.8</b>

\* ITVs-2010: process solutions

\*\* ITVs-2010: Pu concentration from 1 to 50 g/L

**Table 4:** Measurement method uncertainties from EQRAINS Pu and corresponding ITVs-2010 (%)

#### EQRAINS U:

MALL, D&G, IDMS and HKED method uncertainties from EQRAINS U are slightly lower than, and in accordance with, the ITVs-2010 and their components related to short-term systematic and random errors.

For GRAV, the difference between ITV (i.e. 0.07%) and the corresponding value  $u_{rel}(x)$  from EQRAIN U (i.e. 0.16%) is due to the component related to random error, which is three times higher for EQRAIN U (0.16% versus 0.05%). This difference is not consistent with the fact that EQRAIN uses solution samples, whilst ITVs are mainly established for powders and other solids. However, it should be noted that these uncertainty values are relative values and it would be useful to compare the mass ranges involved in each case. This could be a subject for further discussion with the IAEA.

XRF uncertainties from EQRAINS U are much lower than the corresponding ITV components (related to short-term systematic error: 0.11%; related to random errors: 0.27%; combined: 0.29% versus 2%; 2% and 2.8% respectively). This could be explained by the fact that the U amount content in EQRAINS U solutions is close to 200 g/kg, i.e. a U concentration of about 290 g/L, whereas the ITVs-2010 are given for process solutions with lower concentration of U (1 to 50 g/L).

#### EQRAINS Pu:

For COUL, TITR, IDMS, and PUSP, uncertainties from EQRAINS Pu are slightly lower or in accordance with the ITVs, except for the component related to short-term systematic error in TITR which is somewhat larger than the component related to short-term systematic error of ITVs-2010 (0.21% versus 0.15%). This could be explained by the low degrees of freedom (only 8  $d_{ij}$  available) for the estimation of variances in ANOVA processing.

XRF uncertainties from EQRAINS Pu are much lower than the corresponding ITVs (but larger than the values obtained from EQRAINS for U). The Pu amount content in EQRAIN Pu solutions is close to 2 - 5 g/kg, i.e. in the same range as ITVs-2010 concentrations (1 to 50 g/L). There is no explanation for this difference at the moment but it should be noted that for this technique, the degrees of freedom in the ANOVA process are low (only 13  $d_{ij}$  available). This means that the uncertainty associated with estimations from EQRAINS Pu is high. As such, the values obtained from EQRAIN should be used with caution.

In general, the estimated values  $u_{rel}(x)$ ,  $u_{rel}(x)_s$  and  $u_{rel}(x)_r$  from EQRAINS are in good agreement with the corresponding ITV,  $u(s)$  and  $u(r)$  respectively published in 2010 ([6]). Most of the time the EQRAINS values were lower or slightly lower than the corresponding ITV. This could be expected due to the fact that samples in EQRAINS are pure reference solutions. These values confirm the ITVs and their components. The component related to random errors concerning gravimetry for U concentration measurement could be studied further in collaboration with the IAEA.

## 5. Conclusion

For most of the analytical methods studied, the estimated method uncertainties from EQRAINS are lower than their corresponding ITVs-2010 and therefore confirm their current validity. As ITVs-2010 are international target values for the measurement uncertainties when applying analytical techniques to industrial nuclear and fissile material (process solutions), the method uncertainty estimated from EQRAINS, i.e.  $u_{rel}(x)$  (and their components  $u_{rel}(x)_s$  and  $u_{rel}(x)_r$ ) could be used as international target values for the uncertainties of analytical techniques applied to pure U (around 200 grams per kilogram) or Pu (around a few grams per kilogram) reference solutions, i.e. the lowest achievable method uncertainties for process solutions. This information may be useful for the next revision of the ITVs. Furthermore, the representativeness of the reference solutions compared to real process solutions could be increased with mixed uranium plutonium reference solutions and/or the controlled addition of impurities, although not yet made available by CETAMA.

## 6. Acknowledgements

The authors wish to thank all members of Working Group "Uranium" (CETAMA WG2) and Working Group "Plutonium" (CETAMA WG3) from 1997 up to now, without whom this paper would not exist, and particularly the WG chairs: Michel Sourrouille (chair of WG2 from 1997 to 2004), Charles Kiper (chair of WG2 from 2004 to 2012), Manuel Organista (chair of WG2 from 2012 to 2018), Serge Amoravain (chair of WG3 from 1994 to 1999), Hervé Chollet (chair of WG3 from 1999 to 2008), Carole Viallesoubranne (chair of WG3 from 2008 to 2009), Jean-Marc Adnet (chair of WG3 from 2009 to 2013), and Alexandre Ruas (chair of WG3 from 2013 to 2015). We are also grateful to the LAMMAN staff and ORANO for financial support.

## References

- [1] International Atomic Energy Agency, IAEA Safeguards Glossary, 2001 edition, para. 6.35, International Nuclear Verification Series No.3, Vienna
- [2] ISO 17043:2010, Conformity assessment – general requirements for proficiency testing, International Organization for Standardization, Geneva, Switzerland
- [3] ISO 17034:2016, General requirements for the competence of reference materials producers, International Organization for Standardization, Geneva, Switzerland
- [4] ISO Guide 35, 2006 Reference materials – General and statistical principles for certification, International Organization for Standardization, Geneva, Switzerland
- [5] ISO 13528:2015, ISO/TC69/SC6, Statistical methods for use in proficiency testing by interlaboratory comparison, International Organization for Standardization, Geneva, Switzerland
- [6] Certificat de matériau de référence "AGARIC", Lot 2001/1, Version 3 2017, available on request to the CETAMA
- [7] Certificat de matériau de référence "OTU-1", Lot 1993/1, Version 3 2017, available on request to [cetama@cea.fr](mailto:cetama@cea.fr)
- [6] International Atomic Energy Agency, Department of Safeguards, STR-368 (November 2010) International Target Values 2010 for Measurement Uncertainties in Safeguarding Nuclear Materials, Vienna, IAEA

- [7] Srinivasan B, Mathew KJ, Croatto P, Narayanan U, Neuhoff N (2007) New Brunswick Laboratory Safeguards Measurement Evaluation (SME) Program: Operational Features, *Int. Journal of Nuclear Knowledge Management* Vol 1
- [8] Certificat du matériau de référence plutonium métal « MP2 », Lot 1987/1, Version 09-2016, available on request to [cetama@cea.fr](mailto:cetama@cea.fr)
- [8] Regular European Interlaboratory Measurement Evaluation Program, REIMEP, <https://ec.europa.eu/jrc/en/interlaboratory-comparisons/REIMEP>
- [9] Wagner JF, Vian A (1999), *Techniques de l'Ingénieur*, P3720 V2
- [10] Handbook of Stable Isotope Analytical Techniques (2004), Volume I Pages 820-834 Chapter 37 - Introduction to Isotope Dilution Mass Spectrometry (IDMS), Michale Berglund, <https://doi.org/10.1016/B978-044451114-0/50039-9>
- [11] Bedson P (2007) Guidelines for Achieving High Accuracy in Isotope Dilution Mass Spectrometry (IDMS), Royal Society of Chemistry, Analytical Methods Committee, Sub-Committee on High Accuracy Analysis by Mass Spectrometry, Coordinating Editors Sargent M, Harte R, Harrington C.
- [12] ISO 7097-2: 2004, Nuclear fuel technology – Determination of uranium in solutions, uranium hexafluoride and solids – part 2: Iron(II) reduction/cerium(IV) oxidation titrimetric method, International Organization for Standardization, Geneva, Switzerland
- [13] <https://inis.iaea.org/collection/NCLCollectionStore/Public/08/339/8339826.pdf> ; <http://www.iaea.org/inis/collection/NCLCollectionStore/Public/08/345/8345998.pdf>
- [14] Davies W, Gray W (1964) *Talanta* 11:1203
- [15] Eberle AR, Lerner MW, Goldbeck CG, Rodden CJ (1970) U.S. Atomic Energy Commission, New Brunswick, NJ, NBL-252
- [16] Aigner H, Hollenthoner S, Keroe E, Kuhn E, Delle Site A, Zoigner A (1983) Fifth annual symposium on Safeguards and Nuclear Materials Management, Versailles, France
- [17] Harrar JE, Boyle WG, Breshears JD, Pomernacki CL, Brand HR, Kray AM, Sherry RJ, Pastrone JA (1976) Proc. Inst. of Nuclear Materials Management Meeting, Seattle
- [18] Reeder SD, Delmastro JR (1978) NBS Publication – 528
- [19] Zook AC, Collins LL, Moran BW 980 NBL-293, New Brunswick Laboratory, USDOE
- [20] Goldbeck CG, Lerner MW (1972) *Anal Chem* 44:594
- [21] Goldbeck CG, Lerner MW, Peoples GE (1973) Annual Progress Report for the Period July 1972 to June 1973, U.S. Atomic Energy Commission, New Brunswick Laboratory, NJ, NBL-267
- [22] Mathew KJ, Bürger S, Vogt S, Mason P, Morales-Arteaga ME, Narayanan I (2009) *J Radioanal Nucl Chem* 282:939–944
- [23] ISO 3534-1:2006, Statistics \_ Vocabulary and symbols \_ Part 1: General statistical terms and terms used in probability
- [24] JCGM 200:2012, International vocabulary of metrology – Basic and general concepts and associated terms (VIM), 3rd edition, 2008 version with minor corrections
- [25] JCGM 100:2008, Evaluation of measurement data — Guide to the expression of uncertainty in measurement, GUM 1995 with minor corrections
- [26] Crozet M *et al.*, *J Radioanal Nucl Chem* (2019) 319:1013-1021
- [27] JMP® 13.0.0 (Statistical Discovery), SAS Institute Inc, <http://www.jmp.com/software/>

## International certification process of the ABACC-Cristallini method for UF<sub>6</sub> sampling – current status

Aníbal Bonino<sup>1</sup>, Fábio Dias<sup>1</sup>, Luis Machado da Silva<sup>1</sup>, Marcos Moreira<sup>1</sup>, Max Facchinetti<sup>1</sup>, Sonia Fernandez Moreno<sup>1</sup>, Olívio Pereira de Oliveira Jr.<sup>2</sup>, Eduardo Gautier<sup>3</sup>, Adolfo Esteban<sup>3</sup>, David Amaraggi<sup>4</sup>

<sup>1</sup> Brazilian-Argentine Agency for Accounting and Control of Nuclear Materials (ABACC), Av. Rio Branco 123, Gr 515, 20040-005, Rio de Janeiro, Brazil.

<sup>2</sup> Laboratório de Caracterização de Urânio - Centro Tecnológico da Marinha em São Paulo (CTMSP), Av. Prof. Lineu Prestes 2468, 05508-000, Cidade Universitária, São Paulo, SP, Brazil.

<sup>3</sup> Laboratorios de Control Químico y Físico y de Espectrometría de Masas - Comisión Nacional de Energía Atómica (CNEA). Centro Atómico Constituyentes, Av. Gral. Paz 1499, (B1650KNA) San Martín – Pcia. de Buenos Aires – Argentina.

<sup>4</sup> Safeguards Analytical Services, Nuclear Material Laboratory, International Atomic Energy Agency (IAEA), Seibersdorf laboratories, Vienna A-2444, Seibersdorf, Austria.

### **Abstract:**

Based on the conceptual development and empirical validation of the Argentine chemist Dr. Osvaldo Cristallini, Brazilian and Argentinean researches developed, with the support of ABACC, a new UF<sub>6</sub> sampling method suitable for uranium isotopic determination. This new method, known as the ABACC-Cristallini method, has been successfully tested by ABACC in Argentine and Brazilian laboratories and in pilot plants. The method was renamed as “Standard Practice for Sampling Gaseous Uranium Hexafluoride using Alumina Pellets” and has been submitted to the ASTM International. It is now in its final process of approval.

This paper describes the steps of this process and presents preliminary results associated with the application of the method. This sampling practice offers significant advantages over the conventional sampling practice because it allows handling non-reactive, non-volatile, solid UO<sub>2</sub>F<sub>2</sub> sample instead of highly reactive and volatile UF<sub>6</sub>. The sample amount is minimum and can be transported with lower radioactivity level and reduced radiological risks. Additionally, there is no risk of airborne uranium particle and HF release.

Uranium isotopic ratios measured with mass spectrometry techniques in UF<sub>6</sub>, sampled by both the conventional and the ABACC-Cristallini methods provided results which are in good agreement within the stated uncertainties.

The acceptance of the ABACC-Cristallini method by facility operators is key to the success of this project. Therefore, it is relevant to confirm, by field testing, the practicalities and advantages of the method, which includes the conformance with facility safety procedures, work instructions and training programs.

**Keywords:** nuclear material safeguards, uranium hexafluoride sampling, uranium isotope composition.

## 1. Introduction

The ABACC-Cristallini Method for sampling UF<sub>6</sub> by adsorption and hydrolysis in alumina pellets inside a Fluoroethene P-10 tube has been developed by the Brazilian-Argentine Agency for Accounting and Control of Nuclear Materials (ABACC) [1] [2]. This method has advantages compared to the currently used sampling method, for which UF<sub>6</sub> is cryogenically transferred into

a stainless-steel vessel for transportation, with hydrolysis and isotopic analysis being performed after shipping to the analytical laboratory.

Facility operators and safeguards inspectors routinely take UF<sub>6</sub> samples from processing lines or storage cylinders to determine the uranium isotopic composition, most important its major ratio (<sup>235</sup>U/<sup>238</sup>U). The conventional sampling method collects gaseous samples containing 5-10g of UF<sub>6</sub> and requires the use of liquid nitrogen.

UF<sub>6</sub> samples must be safely transported to external laboratories for analysis. Transport includes, among others, public roads and international air shipment. Due to the hazards of UF<sub>6</sub>, air transport has become difficult with many transport operators and regulators refusing to carry the material.

The proposed method results in sample vessels suitable for transport, because contain no UF<sub>6</sub>, but just a significantly smaller amount of uranium, in the form of UO<sub>2</sub>F<sub>2</sub>, sufficient to prepare the solution for the determination of the isotope composition. Once the sampling process is complete, the vessel can be transported and handled in a less restrictive manner due to the lessened hazard of handling non-volatile, non-acid UO<sub>2</sub>F<sub>2</sub> versus UF<sub>6</sub>.

Another advantage of the method using P-10 made of PCTFE, a change in colour of the alumina pellets, from white to yellowish, will be visible as UO<sub>2</sub>F<sub>2</sub> is formed. The degree of colour change is a rough indicator of the sufficient amount of uranium adsorbed as presented in Figure 1.

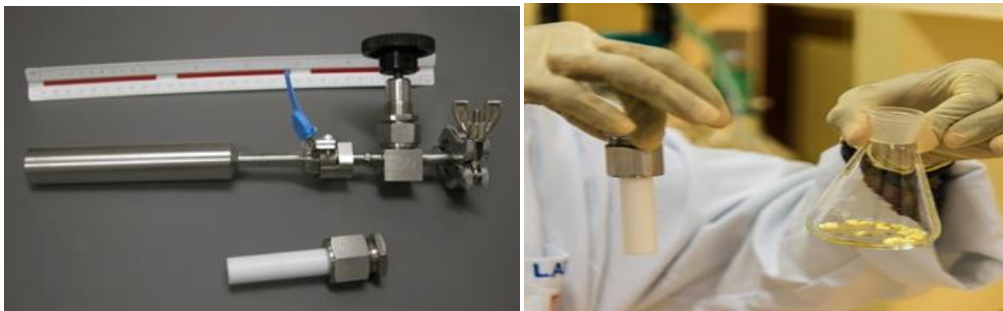


Figure 1: Sample vessels and alumina pellets

## 2. Qualification for safeguards application

ABACC proposed a rigorous validation program to establish the reliability of the method for nuclear safeguards applications and <sup>235</sup>U enrichment determination. The primary evaluation objective of the validation exercise was to determine if the ABACC-Cristallini and direct hydrolysis sampling methods give uranium isotopic measurements in agreement with each other. This program has been successfully carried out under a framework of international collaboration.

This included using four UF<sub>6</sub> Certified Reference Materials (CRM) showed at the table 1, as a source of uranium hexafluoride, and sampling each of the four CRMs by using two different sampling methods: adsorption on alumina (ABACC-Cristallini method) and the standard direct hydrolysis method. Additionally, the two sampling methods measurement results were compared with the certified values for the CRMs to ensure sample integrity.

CRM	$n(^{235}\text{U})/n(^{238}\text{U})$	U	% rel U	ITV-2010
IRMM-020	0.00209570	0.00000060	0.029	0.70%
IRMM-022	0.0072562	0.0000012	0.017	0.28%
IRMM-023	0.0338810	0.0000060	0.018	0.14%
IRMM-029	0.044052	0.000014	0.032	0.14%

Table 1: IRMM UF<sub>6</sub> n(235U)/n(238U) certified values with their expanded uncertainties

The worldwide joint validation program was started in 2016. The samples were distributed to following participating laboratories:

- CNEA (Laboratorios de Control Químico y Físico y de Espectrometría de Masas, Argentina)
- IAEA (Safeguards Analytical Services, Nuclear Material Laboratory, Austria)
- JRC-Geel (Directorate G - Nuclear Safeguards and Forensics, European Commission, Belgium)
- CTMSP (Laboratório de Caracterização de Urânio, Brazil)
- LANIE-CEA/Saclay (Laboratoire de Development Analytique Nucleaire, Isotopique et Elementaire, France)
- JRC- Karlsruhe (Directorate G - Nuclear Safeguards and Forensics, Analytical Service, European Commission, Germany)
- ORNL (Nuclear Analytical Chemistry and Isotopics Laboratory, USA) and NBL (New Brunswick Laboratory, USA)

These samples were measured by these laboratories using their mass spectrometric methods for uranium isotopic composition, particularly  $^{235}\text{U}/^{238}\text{U}$ . The conclusion of the validation program for the purpose of nuclear material accountancy (e.g. safeguards), the ABACC-Cristallini  $\text{UF}_6$  sampling method provides comparable results to a direct hydrolysis method for uranium isotopic determinations [3].

The Cristallini method was proposed to ASTM International in 2017 with the collaboration of NBL under the framework of the technical cooperation between ABACC and DoE and with the support of specialists of Brazil and Argentina.

### 3. The process at ASTM International

ABACC is proposing a new procedure to be verified independently by ASTM experts and to be approved by consensus as an official ASTM standard.

The related procedure “Standard Practice for Sampling Gaseous Uranium Hexafluoride using Alumina Pellets”, commonly referred as “ABACC-Cristallini Method”, describes a technique for sampling gaseous uranium hexafluoride ( $\text{UF}_6$ ) with subsequent recovery of the uranium in the sample for use in the determination of its isotopic composition, in particular, its major amount ratio ( $^{235}\text{U}/^{238}\text{U}$ ).

The practice involves the use of a small sample vessel filled with aluminum oxide ( $\text{Al}_2\text{O}_3$ ) pellets which serve as a substrate upon which  $\text{UF}_6$  gas hydrolyzes predominantly to uranyl fluoride ( $\text{UO}_2\text{F}_2$ ). After pumping the remaining volatile compounds, the vessel contains no  $\text{UF}_6$  and may be handled and shipped under appropriate conditions just for  $\text{UO}_2\text{F}_2$ .

Uranium is then leached from the alumina pellets to yield an aqueous solution suitable for the determination of uranium isotopic composition, which can be performed by several mass spectrometric techniques.

Figure 2 illustrates a set-up for sampling gas from a process line or a  $\text{UF}_6$  cylinder using a typical manifold system and a P-10 tube containing alumina pellets.

The “Standard Practice for Sampling Gaseous Uranium Hexafluoride using Alumina Pellets” is under analysis by the Committee on Standards Review and if approved the procedure may be published by ASTM International by July 2019.

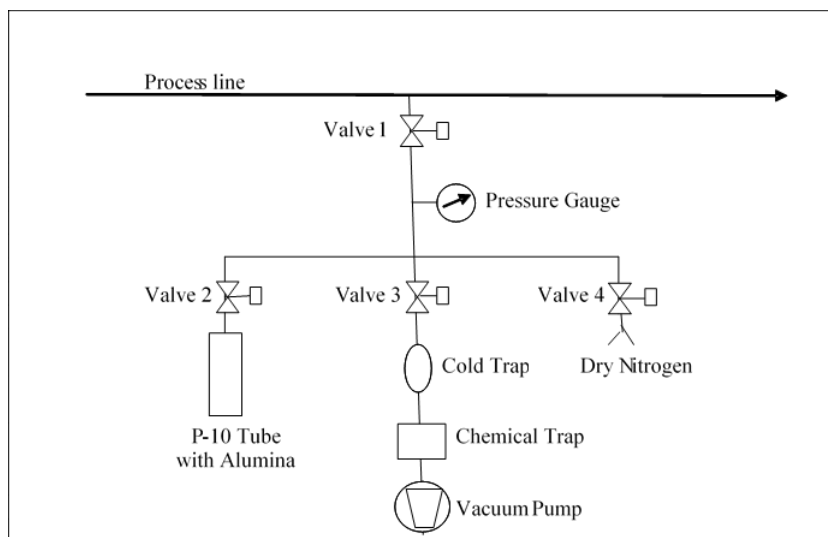


Figure 2: Scheme of equipment setup for UF<sub>6</sub> sampling using alumina pellets

#### 4. UF<sub>6</sub> Sampling Procedure

The principle of the method was first demonstrated at the “Comisión Nacional de Energía Atómica (CNEA)” laboratories in Buenos Aires, Argentina. UF<sub>6</sub> sample bottles with isotope composition in the range of 0.31 and 4.05 <sup>235</sup>U % in mass were used to evaluate the influence of UF<sub>6</sub> pressure and sampling time on the amount of uranium absorbed by alumina pellets loaded in P-10 fluorothene tubes. An amount of 1 g of alumina and a sampling time between 10-30 minutes were considered sufficient to collect the amount of U needed for isotope ratio measurements by thermal ionization mass spectrometry (TIMS) [1] [2]. A procedure to recover the U adsorbed was also developed.

Although the first results obtained at the bench were encouraging, concerns were raised whether the method could effectively work in an isotope enrichment facility, mainly due to different gas flowrate and pressures ranges verified in a typical facility.

The proposed standard practice is applicable to sampling gaseous uranium hexafluoride (UF<sub>6</sub>) from processing facilities, isotope enrichment cascades or storage cylinders, using the sorbent properties of aluminum oxide (Al<sub>2</sub>O<sub>3</sub>).

The sampling procedure consider that a tared sample vessel is filled with a weighed quantity of alumina pellets, attached to a sampling manifold, and exposed to gaseous UF<sub>6</sub> for a timed period, typically 10-30 minutes depending on the gas pressure in the installation and the desired uranium amount in the sample. UF<sub>6</sub> readily hydrolyzes in contact with alumina pellets generating predominantly uranyl fluoride (UO<sub>2</sub>F<sub>2</sub>).

After the required amount of UF<sub>6</sub> has been hydrolyzed by the alumina pellets, the vessel and the manifold are evacuated to remove remaining volatile gas. The valve that connects the installation to the manifold is closed and the vessel and the manifold are pressurized to atmospheric pressure with dry nitrogen (N<sub>2</sub>). The vessel can now be safely removed from the manifold and sealed. The amount of uranium contained in the vessel can be determined by reweighing the vessel.

Using a P-10 vessel loaded with 1 g of alumina pellets, and sampling from a UF<sub>6</sub> cylinder or processing lines under typical conditions will easily allow the adsorption of 100-300 mg of uranium, depending on the gas pressure, temperature and time of exposure. The maximum adsorption capacity for uranium is approximately 600 mg.

The alumina pellets are then removed from the vessel and leached firstly with distilled water and secondly with nitric acid. The alumina fines produced must be carefully removed from the uranium solution. Finally, the solution can be prepared for the determination of uranium isotopic composition.

## 5. Analytical measurements

The P-10 tubes containing alumina and uranium fluoride ( $\text{UO}_2\text{F}_2$ ) were submitted to alpha and beta particles counting. The average activity obtained in this sampling exercise was 313 cpm, a value 10-100 smaller than the values usually obtained for  $\text{UF}_6$  samples collected using the conventional method.

First P-10 tubes were reweighted; then safely disassembled under a fume hood. Alumina pellets were transferred to an Erlenmeyer flask and leached initially with distilled water and finally with nitric acid. The alumina fines were carefully removed from the solution so that it could be prepared for the further measurements. The U contained in the solution was separated by the use of an ion exchange resin. The U recovery was in the range of 80-85%.

The amount of U collected in the  $\text{UF}_6$  sampling exercise for the three streams (F, P and T) was in average equal to 187 mg. It is important to say there were differences in flowrate and pressure between these three streams. Despite, this value is much higher than the 200 ng needed to perform the U isotope ratio measurements by total evaporation method (TE) applied to TIMS.

This method samples a much smaller amount of  $\text{UF}_6$  than the traditional method, in the order of a few milligrams instead of grams. This small amount of  $\text{UF}_6$  combined with the procedure of pumping and flushing the P-10 bottles with dry nitrogen to the atmospheric pressure, that assures that no volatile gas or  $\text{UF}_6$  are present in the P-10 tube, will facilitate the characterization of the sample to be transported under the IATA regulations [4].

The number of pellets in each P-10 tube was also counted, resulting in 32 pellets in approximately 1 g of  $\text{Al}_2\text{O}_3$ . This means each pellet absorbed about 6 mg U. This is an important value because the objective is to recover U from just few pellets, or at least the most yellowish ones, instead of the whole set of pellets within the tube. The goal of this initiative is to reduce the sample waste.

The isotope measurements were easily carried out using the total evaporation method with a thermal ionization mass spectrometer. CRM materials from NBL-DOE-USA were used to correct mass discrimination.  $(n^{235}\text{U})/(n^{238}\text{U})$  isotope ratio typical expanded uncertainties were in the range of 0.02 - 0.05%.

## 6. Conclusions

The procedure "Standard Practice for Sampling Gaseous Uranium Hexafluoride using Alumina Pellets" is under analysis by the Committee on Standards Review. It is expected that the procedure may be published by ASTM by July 2019.

The procedure for sampling gaseous  $\text{UF}_6$  in P10- tubes using alumina pellets was easily executed. The procedure is safe, simple and straightforward, with no impact on the safety and in the process operation of the facility. It was repeated in slightly different gas flowrate and pressure conditions, proving to be also flexible and robust, requirements to be successfully implemented worldwide in facilities operating at unpredictable process conditions.

The ABACC-Cristallini sampling practice offers significant advantages over the conventional sampling practice because it allows handling non-reactive, non-volatile, solid  $\text{UO}_2\text{F}_2$  sample instead of highly reactive and volatile  $\text{UF}_6$ . The sample amount is minimum and can be transported with lower radioactivity level and reduced radiological risks. Additionally, there is no risk of airborne uranium particle and HF release.

U adsorbed in alumina pellets could be readily recovered by repeated washings with good yields. The suggested sampling time provided U amounts much higher than the amount needed for isotope ratio measurements by thermal ionization mass spectrometry.

The U amount recovered was enough even if repetitions of isotope ratio measurement were needed. There was no need to know details the process parameters of the isotope enrichment facility, which preserved its data confidentiality.

## 7. Recommendations

Extensive testing and validation exercises of the ABACC-Cristallini UF<sub>6</sub> sampling method have been carried out since Dr. Osvaldo Cristallini envisaged the absorption of UF<sub>6</sub> gas in alumina pellets to analyze UF<sub>6</sub> uranium isotopic determination in nuclear material samples for safeguards purposes more a decade ago.

ABACC in cooperation with prestigious high-level recognized organizations and laboratories demonstrated that ABACC-Cristallini UF<sub>6</sub> sampling method is equally effective and safe for the operation of the nuclear installations as the traditional UF<sub>6</sub> gaseous method and has significant advantages than the traditional method. Therefore, ABACC has a great expectation that stakeholders could use this method in lieu of the traditional one.

ABACC encourages the use of ABACC-Cristallini UF<sub>6</sub> sampling method to relevant stakeholders, like the enrichment facilities operators and safeguards organizations since this new method for sampling gaseous UF<sub>6</sub> using alumina pellets is much more efficient in reducing the quantity of sampled nuclear material, minimizes waste production at the facility and laboratories, it has advantages from the radiation protection viewpoint and solves the issue of the transport of UF<sub>6</sub> samples.

The advantages of this method are such that we encourage relevant parties to consider facing safety authorities' and operators' requirements to obtain pertinent authorizations to try and use the ABACC-Cristallini method.

ABACC with the cooperation of NBL has been proposing this method to be considered by ASTM as a standard practice. The ASTM procedure "Standard Practice for Sampling Gaseous Uranium Hexafluoride using Alumina Pellets" is under ASTM's review and the approval process and it should be finalized with the ASTM publication of this standard by July 2019.

## 8. References

- [1] A. Esteban, O. Cristallini, J. Perrotta, "UF<sub>6</sub> Sampling Method Using Alumina", 29<sup>th</sup> ESARDA Annual Meeting, France (2007).
- [2] E. Galdoz, A. Esteban, O. Cristallini, J. Perrotta, "UF<sub>6</sub> Sampling Method Using Alumina", 49<sup>th</sup> INMM Annual Meeting, USA (2008).
- [3] A. Esteban, E. Gautier, L. Machado da Silva, S. Fernández Moreno, G. Renha, A. Bonino, F. Dias, O. Pereira de Oliveira Jr., D. Amaraggi, P. Mason, M. Soriano, P. Croatto, E. Zuleger, J. Giaquinto, C. Hexel, T. Vercouter, E. Paredes-Paredes, H. Isnard and S. Richter, "Qualification for Safeguards Purposes of UF<sub>6</sub> Sampling using Alumina – Results of the Evaluation Campaign of ABACC-Cristallini Method", 58<sup>th</sup> INMM Annual Meeting, USA (2017).
- [4] *Dangerous Goods Regulation (DGR)*, International Air Transport Association (IATA) (2019).

# **Session 8:**

# **Geological Disposal**

## Aspects on declared accountancy data for the Final Spent Fuel Disposal in Sweden

S. Lindgren<sup>1</sup>, G. af Ekenstam<sup>1</sup>, L. Hildingsson<sup>1</sup>, R. Fagerholm<sup>1</sup>, A. Sjöland<sup>2</sup>, J-O, Stål<sup>2</sup>

<sup>1</sup>Section for nuclear non-proliferation, Swedish Radiation Safety Authority  
Solna strandväg 96, Stockholm, Sweden

<sup>2</sup>Swedish Nuclear Fuel and Waste Management Company  
Evenemangsgatan 13, 169 79 Solna, Sweden

E-mail: Sara.Lindgren@ssm.se

### **Abstract:**

Sweden is in the final stages of planning and licensing an encapsulation plant and a geological repository that together will handle and dispose of all spent fuel from the nuclear programme. This process will include approximately 50,000 spent fuel assemblies which are planned to be stored in about 6000 copper canisters 500 m below ground. This paper outlines some important principal questions in relation to the declared accountancy data.

The Operator will recalculate and by measurement verify the isotopic composition for all spent fuel assemblies. The purpose is to have the best possible knowledge of important parameters of each individual assembly. This data is a key information for a safe and optimal use of the copper canisters and repository capacity. As a consequence of the re-evaluation, updated and most likely different safeguards accountancy data will need to be reported. All relevant data for the fuel, such as its operating history, initial enrichment, burn-up etc. will be used for the best possible determination of desired parameters together with the measurements of gammas and neutrons. Calorimetric measurement of the heat will be done on part of the fuel inventory as a way to anchor and verify the determinations.

The nuclear State Authority is responsible for supervising the safety, security and safeguards in the country. These three areas are partly interconnected. National control measures for these areas consist of traditional authority supervision by legislation, documentation and paper trail of Operator's data. From the national perspective, it is of the highest importance to ensure that all deposited spent fuel is correctly declared and safely disposed. In case of anomaly and potential future dispute over past nuclear activities the completeness of the documentation of relevant operational data is essential.

**Keywords:** safeguards, final repository, encapsulation plant, spent fuel characterization

### **1. Introduction**

As the planning for the final geological repository proceeds the issue of how to characterize the spent fuel before encapsulation is getting more attention. For safety reasons, it is essential to have the best estimates of important parameters such as the decay heat and criticality. Furthermore, it is important to define the different roles of the Operator, State Authority and the international organizations, respectively, and how the Operator's data is related to safeguards declarations.

According to the Swedish Act on Nuclear Activities the nuclear power plants are responsible to establish a system to manage and dispose of all radioactive waste from the Swedish nuclear programme. This is handled by the Swedish Nuclear Fuel and Waste Management Company (SKB). The proposed system, KBS-3, includes the transport from the nuclear power plants, the interim storage facility (Clab), the encapsulation facility for spent nuclear fuel (Clink), the transport vessel Sigrid, the canister transport cask (KTB) and the geological repository for spent nuclear fuel (SFK).

SKB has applied for permission to build the encapsulation plant co-located with the existing interim storage facility Clab as an extension above ground. The combined facility will be named 'Clink'. The fuel will be encapsulated in copper canisters and temporarily stored at the facility in transport casks before shipped to the geological repository site at Forsmark. It is envisaged that an average of 150 canisters will be disposed per year. During routine operation, this means loading one canister per workday. The encapsulation plant and the geological repository are planned to be in operation for about 45 years. After this period of operations the surface buildings will be removed and the repository closed and sealed. A schematic view of the geological repository is shown in Figure 1.

Data records of the spent fuel are supplied by the Operators of the nuclear power plants. The data is based on for example the computational codes for calculating the reactor power. The data includes initial enrichment (IE), irradiation history, cooling time (CT), burn-up (BU) and amount of fissile material. For safety reasons the spent fuel will be characterized and verified and this can be done at the latest at the encapsulation plant. Important parameters for safety are for example the thermal residual power and burn-up. The characterization of the spent nuclear fuel is expected to generate updated safeguards relevant data.

This paper discusses the planned fuel characterization by the Operator (SKB), the different roles and responsibilities of the Operator and the State Authority (SSM) and also points to some issues that need to be further discussed.

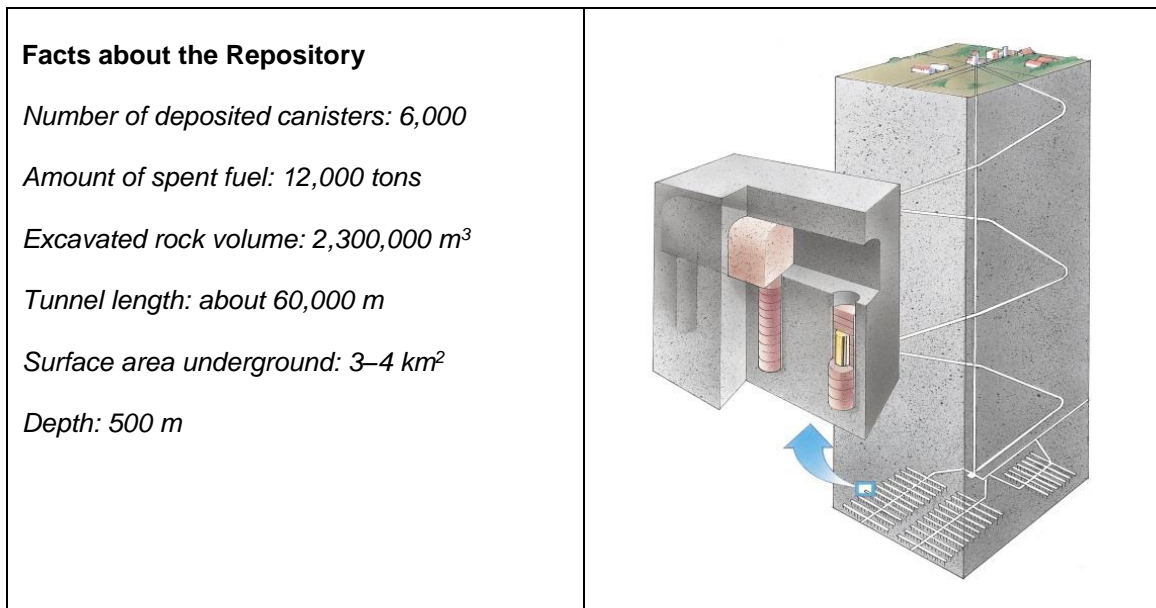


**Figure 1:** Schematic picture of the future final repository.

## 2. Verification methods

The basic underlying principle is that it is the Operator that has full responsibility to manage the nuclear installations in a safe manner and to obey relevant national and international requirements, including requirements on safeguards.

## 2.1 Operator's fuel characterization and measurements

SKB as Operator has to determine, to the best possible extent, the key characteristic parameters of each individual spent fuel assembly in order to design and operate a safe and economically optimized disposal system of the spent fuel. These parameters include the following:

- Decay heat – to fulfil temperature requirement on canister and bentonite
- Criticality – multiplicity
- Radiation doses – both gamma and neutrons
- Nuclide inventory
- Safeguard – identify correct fuel, missing pins
- Contents of fuel – amount of fissile material

The parameters are planned to be determined by a gamma and neutron measurement system in conjunction with the encapsulation process, combined with modelling codes using the known history and properties of the fuel assemblies.

The concept of uncertainty plays an important role in the strategy. For a safe and cost efficient disposal of the spent fuel SKB estimate the demands of accuracy and uncertainty for the final verification of the different parameter to be:

- Decay heat: very high accuracy, order of few percent uncertainty
- Criticality: very high accuracy < 10 %
- Radiation doses: high accuracy, order of 10 %
- Nuclide inventory: for most nuclides fairly low accuracy need; <100 % (for some nuclides higher accuracy needed)
- Contents of fuel – amount of fissile material - Burn-up (BU), Initial enrichment (IE), Cooling time (CT) – intermediate accuracy

## 2.2 Fuel characterization activities

Various activities have been initiated by SKB aiming at obtaining sufficient measurement methods, codes, fuel data and knowledge and understanding of the nuclear fuel for operational and safeguards purposes and in the end for long term safety. In addition to this there must be sufficient competent available human resources.

In a collaboration between SKB, Euratom and the US Department of Energy (DoE) a set of 25 BWR assemblies and 25 PWR assemblies (the so called SKB-50) stored at the interim storage facility Clab has been selected for testing with a variety of measurement techniques. It includes calorimetric measurements, measurements of gamma rays and neutrons. In addition, computational codes are being developed to re-calculate fuel parameters from known irradiation history.

SKB has one of the few (if not the only) calorimeter that can measure whole fuel assemblies, see e.g. [2]. The measurements have a very high accuracy and is therefore important for an optimization of the safety parameters. The method has the potential to be accurate, in the order of 2 %. However, this requires long measurement times for each assembly, several days for the highest accuracy, which is not possible with the planned throughput in the encapsulation plant with up to 12 assemblies per day. So indirect determination methods must be developed to a reasonable accuracy. However, calorimetric measurement of the heat will be done on part of the fuel inventory as a way to anchor and verify the determinations. In Fig. 2 an example is shown of a number of calorimetric decay power measurements of fuels in the SKB-50 with the so called gradient method, where the temperature gradient is determined, which is one of the possible ways to do calorimetric determinations of decay heat. The decay power is corrected for gammas that escape the calorimeter, with gamma detectors employed to determine the amount of gammas escaping.

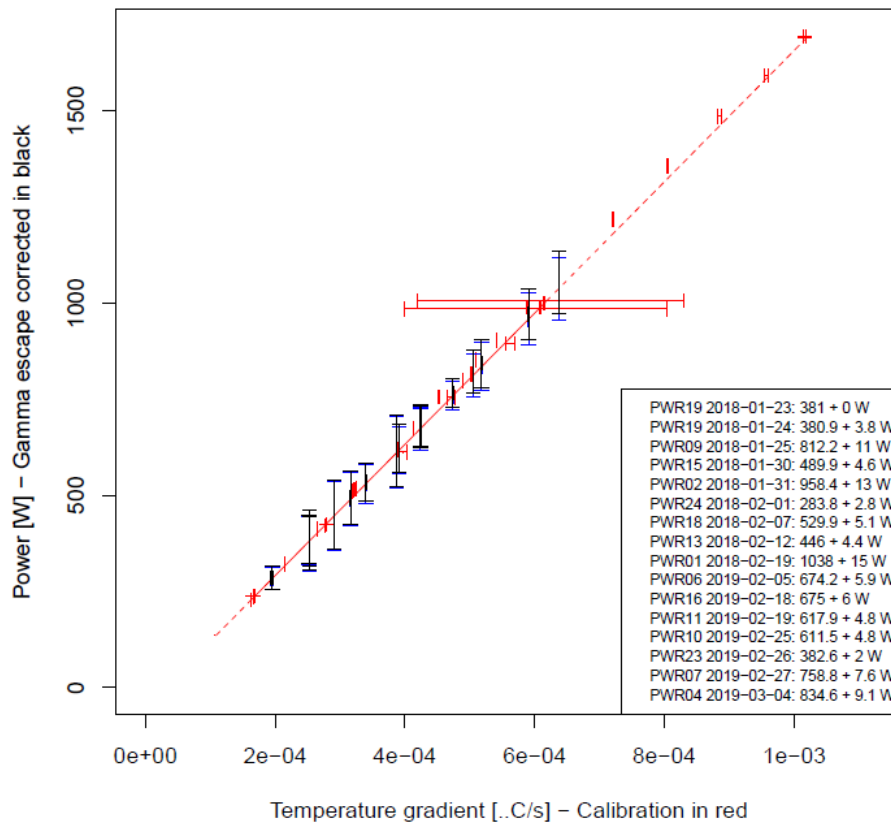


**Figure 2:** Results from calorimetric measurements corrected with escaped gammas of a number of fuel assemblies in the so called SKB-50. On the x-axis the temperature gradient of the measurement. The fuel assemblies have anonymous names with arbitrary numbering. The calibration (in red) is done with an electric heater.

Gamma and neutron measurements include measuring a spent fuel assembly with for instance a high resolution germanium detector and detecting neutrons in for example a differential die-away detector. Various alternatives are being investigated and developed. One challenge is to understand the detector response when the geometry and physical content of the assemblies differ. Data mining tools could be applied to determine the optimal mathematical structure to match the complexity of spent fuel NDA signals and to enable a range of quantities to be estimated (heat, IE, BU, CT, Pu mass, partial defects). References 3 - 7 contain examples of work done. Cherenkov radiation techniques have been extensively developed by among others SSM and it is expected to be a useful addition to the measurement system. Weighing of the fuel assemblies is planned to be performed systematically.

Data records on the fuel assemblies are to be found at fuel suppliers, the nuclear power plants, and SKB. In some cases information could be found at the State Authority SSM and at test laboratories. Also the international authorities IAEA and Euratom have information. A problem associated with the data is that before 1980 most of the data records exist only in paper archives and not in electronic form [8]. It will be a considerable undertaking for SKB to collect and validate all information of the spent fuel.

SKB intends to measure and characterize all spent fuel before encapsulation. To fully do this characterization, SKB will develop a method that most likely will be based on a combination of fuel data, computational models and measurements. SKB, together with the Competent Authority need to define what data has to be preserved and available for the final repository (and partly for other parts of the back-end system).

### 3. Roles of the State Authority and the Operator

The Swedish Radiation Safety Authority (SSM) is the Competent State Authority for all nuclear related activities in the country. SSM should have a comprehensive view of the safety, security and safeguards in all stages of the operation of the domestic nuclear facilities and locations. This includes all steps in handling the spent nuclear fuel in the disposal process, including the long-term behavior of the geological repository after closure.

SSM have reviewed SKB's application for an encapsulation plant and a geological repository. An assessment has been made of the Operators expected capability to fulfill national and international requirements on safety, security and safeguards. SSM has its own internal competence, but for certain issues external expertise has been used to get a more in-depth and independent view.

The role of SSM, after an eventually approved application by the Swedish government, will be to supervise all aspects of the construction and operation of the encapsulation plant and the geological repository. There will be a step-wise process where SSM will evaluate the safety, security and safeguards of the system before SKB can proceed to the next step. SKB needs the permission from SSM to start construction, trial operation, routine operation and final closure of the facilities. During this process SSM will review for example Safety Analysis Reports (SAR), audit special themes relevant for safety, security or safeguards, and do site visits.

It is the responsibility of SKB to assure that the declared parameters of the spent fuel are correct. SSM will ensure that measurements conducted by SKB cover the important parameters and fulfill requirements on accuracy, but SSM do not plan to perform measurements by itself. SKB has also to show in a transparent way the method for estimating the fuel parameters from measurements, fuel data and model calculations mentioned above. When evaluating the activities of SKB, SSM may also use external experts. These experts are planned to be from research groups that SSM supports at Swedish universities.

It is the responsibility of SKB to have a system that tracks all movements and locations of the spent fuel and their disposal canisters. This tracking system will be reviewed by SSM to ensure that it fulfill requirements on safety, security and safeguards. But SSM will not monitor the movements of the disposal canisters at the encapsulation plant, during transport or during receipt and placement underground in the geological repository.

Data records on the spent fuel originate from the nuclear power plants. This information is sent to SKB when the fuel is shipped to the interim storage facility Clab. In addition, SSM has safeguards data on all spent fuel, for example, irradiation dates, burn-up, if any rod exchange has occurred and content of fissile material. It is the responsibility of the Operators to have sufficient and correct data. SKB's data may be compared with the SSM safeguards database. In the case of discrepancy between those registers the potential impact on safety, security or safeguards has to be evaluated.

### 4. Safeguards Considerations

Several of the parameters that are planned to be determined by SKB are safeguards related. The operation of a final disposal system requires these parameters to be determined in the best possible and optimal way. The main reason is the direct operational optimization of the system but also the long term risk. For example that it must not be reassessed in the future so that the safety and dependability of the disposal is put into question.

For practical, financial and logistic reasons the use of a joint measurement system should be proposed. For an independent conclusion of a verification by the IAEA and Euratom the measurement system must be authenticated. Or in other words, a system in which the inspecting authorities (IAEA and Euratom) could confirm the Operators updated declared data by using part of or the entire SKB's verification equipment. For such a system all relevant data for the fuel, such as its operating history, initial enrichment, burn-up etc, will be used for the best possible determination of the parameters with the measurements of gammas and neutrons.

Another issue with verification of declared data is that several of the parameters have been calculated by a certain version of a code at a certain time. For example, a fuel assembly declared in 1980 would most likely get different values than the same fuel assembly, with exactly the same operational history, declared in 2019 just because of a new version of the used code is employed.

A further issue that has to be considered is the mistakes in the records and data bases. We find these in the Swedish records. These errors are non-systematic. In the proposed system they would be found due to the multi-parameter approach which would raise flags for abnormalities. The multi-approach determination still gives reliable value for these, although possibly with a slightly larger uncertainty.

The investigations of the spent fuel will most likely result in values different from the current declared safeguards accountancy data. There is a need to adjust the safeguards data to reflect the Operator's measurement results, for example by using the Euratom code New Measurement (NM). It is of utmost importance that data stored at the Operator, State authority and international authorities are consistent to avoid misunderstandings in the future. Even if the re-evaluation of the spent fuel parameters results in new safeguards data, it is important to ascertain that the fuel disposed is as declared according to the best estimate. As the spent fuel cannot be re-verified after it has been disposed, safeguards will rely on robust C/S systems. In addition, Complementary Access (CA) and other tools in the Safeguards agreements, including the Additional Protocol can be used. With this feature of no possibility to re-verify, we propose that the international inspectorates consider a new inventory change code, for example TG - Transfer to a geological repository.

Lastly, the question can always be elaborated if a final disposal requires other or additional data for future safeguards that is currently not part of the safeguard system and also which information must be recorded and stored for future generations.

## 5. Summary

SKB as the Operator has the full responsibility to manage the encapsulation plant and the geological repository in a safe manner. SSM as the Competent State Authority should have a comprehensive view of the safety, security and safeguards in all stages of the operation.

SKB will measure and characterize all spent fuel before encapsulation. The state Authority SSM will ensure the quality of these measurements.

SKB need to have a system that tracks all movements and locations of the spent fuel and their disposal canisters. SSM will not directly on site monitor the individual movements but ensure the correctness and quality in a supervisory role.

It should be continued to be investigated if it is possible to develop one joint measurement system to be used by both the Operator and the IAEA/Euratom which will provide required safeguards data including the insurance that no rods have been removed and the continuity-of-knowledge for each fuel assembly.

It is proposed that at the time of disposal the to-date best possible characterization of the fuel assemblies is done, using the history and properties of the fuels, and state-of-art codes and measurements. This determination should then represents the future safeguards accountancy records which are expected to differ from the current figures. This can be implemented by using the Euratom code New Measurement (NM). For the transfer to a geological repository where there is no possibility to re-verify the spent fuel, we propose a new inventory change code.

## 6. References

[1] IAEA, *Model Integrated Safeguards Approach for a Spent Fuel Encapsulation Plant*, SG-PR-1305, ver. 1, 2010-10-06

[2] Fredrik Sturek, Lennart Agrenius. *Measurements of decay heat in spent nuclear fuel at the Swedish interim storage facility, Clab*, SKB report R-05-62

- [3] S. Vaccaro, S.J. Tobin, A. Favalli, B. Grogan, P. Jansson, H. Liljenfeldt, V. Mozin, J. Hu, P. Schwalbach, A. Sjöland, H. Trelle, and D. Vo. *PWR and BWR spent fuel assembly gamma spectra measurements*. Nuclear Instruments and Methods in Physics Research Section A: Accelerators, Spectrometers, Detectors and Associated Equipment, 2016, Volume 833, p. 208-225
- [4] Peter Jansson, Stephen Tobin, Henrik Liljenfeldt, Michael Fugate, Andrea Favalli, and Anders Sjöland. *Axial and azimuthal gamma scanning of nuclear fuel - implications for spent fuel characterization*. Journal of Nuclear Materials Management, ISSN 0893-6188, Volume 45, nr 1, s. 34-47
- [5] Martin Bengtsson and Peter Jansson. *Methodology for evaluation of gamma spectroscopy measurements at Clab*, 2016, SKB Doc 1540466, version 1.0
- [6] Peter Jansson. *Comparison of a simple gamma-ray spectroscopy peak area evaluation method to the 2002 IAEA intercomparison test spectra*. Submitted to Nuclear Instruments and Methods in Physics Research Section A: Accelerators, Spectrometers, Detectors and Associated Equipment, 2017
- [7] SKB, *Analysis of gamma-ray spectroscopy measurements of 25 PWR nuclear fuel assemblies performed at Clab during September and November 2016*, SKB Doc 1683508, version 1.0
- [8] Henrik Lindahl, *A study of Availability of Fuel Data for Sweden's Spent Nuclear Fuel*. SSM Technical Note 2014:50, 2014

# Identification of copper canisters for spent nuclear fuel: the ultrasonic method

C. Clementi<sup>1,2</sup>, L. Capineri<sup>2</sup>, F. Littmann<sup>1</sup>

<sup>1</sup> Nuclear Security Unit, Joint Research Centre, European Commission, Ispra (VA), Italy

<sup>2</sup> Dept. Information Engineering, University of Florence, Florence, Italy  
E-mail: [chiara.clementi@ec.europa.eu](mailto:chiara.clementi@ec.europa.eu), [francois.littmann@ec.europa.eu](mailto:francois.littmann@ec.europa.eu), [lorenzo.capineri@unifi.it](mailto:lorenzo.capineri@unifi.it)

## Abstract:

*The long-term storage of spent nuclear fuel in geological repositories has introduced the need to develop new safeguards procedures, measures and technologies. For the proposed Swedish disposal process, the Continuity of Knowledge (CoK) of fuel during transport from Oskarshamn and deposition of the same copper canisters at Forsmark is a challenging topic. Several Containment and Surveillance (C/S) measures could be used for this purpose; among them, the identification and authentication of copper canisters could be useful to trace canisters during transport. Ultrasonic techniques are used by authors to acquire unique fingerprints from each container. The ultrasonic amplitude response of a series of chamfers machined in the inner part of the copper lid can be used as a unique signature readable from outside the canister. In addition, canisters can be authenticated by investigating the welding area between the lid and the canister itself. The robustness of this approach is guaranteed by the angular matching between the identification and authentication fingerprints to produce a third unique fingerprint, more reliable than the other two. Several experimental tests are performed to validate the approach and optimize the design of a device for the acquisition of ultrasonic fingerprints. A potential implementation of this device within the Swedish disposal process is also studied. The acquisition of ultrasonic references could be carried out after canisters' final machining at the encapsulation plant and the process could be completely automated. The reduced cost of realization and its ease of use are the main advantages of the method. However, the machining of chamfers on copper lids requires the introduction of further steps in the manufacturing process of containers.*

**Keywords:** ultrasound, identification, authentication, copper canisters.

## 1. Introduction

The final disposal of spent nuclear fuel in geological repositories introduces the need to revise safeguards approaches for a safe and secure handling of the fuel [1]. In 2011 the Swedish Nuclear Fuel and Waste Management Co. (SKB) submitted an application for the construction of a long-term geological repository in Forsmark (Sweden). The SKB method for final disposal is based on a multi-barrier system: copper canisters with iron inserts are used to host fuel assemblies; the bentonite clay is then used to cover canisters once deposited in tunnels and the bedrock isolates canisters from human-beings and the environment for thousands of years. The spent nuclear fuel coming from nuclear power plants will be stored for a period in pools at the Central Interim Storage Facility (Clab) in Oskarshamn. Then fuel assemblies will be dried and inserted in copper canisters with iron inserts at the encapsulation plant (that will be built next to the Clab). Canisters are big cylinders, about 5 m high and 1 m in diameter with a lid and a tube welded together by Friction Stir Welding (FSW). After the encapsulation of the fuel, copper canisters will be placed in transport casks and temporarily stored before being shipped to the final repository in Forsmark (Figure 1). At this facility, canisters will be reloaded to a deposition machine in the underground central area and then the canisters will be deposited in tunnels, later backfilled and sealed with a concrete plug. A total amount of 6,000 canisters will be deposited underground with an average of one canister per day, over roughly 40

years [2]. The International Atomic Energy Agency (IAEA) model integrated safeguards approach for geological repositories foresee that Containment and Surveillance (C/S) measures should be applied to guarantee Continuity of Knowledge (CoK) of spent nuclear fuel during storage and transport of copper canisters [3].



**Figure 1.** The spent fuel transfers in the Swedish system for final disposal of spent nuclear fuel.

Since in Sweden the encapsulation plant and the geological repository are not located on the same site, safeguards approaches defined by the IAEA should be adapted to ensure CoK throughout the handling chain of the copper canisters. Surveillance systems could be used inside facilities to monitor the flow of spent nuclear fuel, while seals applied on transport casks could guarantee the identity of canisters during the transport from the encapsulation plant to the geological repository. However, in case of failure of one of the two measures, the identification of copper canisters by a unique tag could be adopted to recover CoK. Tagging devices should give a unique identifier to each canister (identification fingerprint) and return evidence of falsification attempts (authentication fingerprint). External engraving of canisters should be avoided because it could trigger a corrosion process. Moreover, according to geometrical features, the minimum copper thickness to assure the stability of canisters' structure is 50 mm. The majority of conventional tagging devices used to identify uniquely nuclear items are analysed in [4] to see to what extent they could be adopted in the case of copper canisters. As a result, even if the identification of canisters could be realized with different methods, such as Reflective Particle Tags (RPT), ultrasonic methods or Tungsten-based Identifiers, the verification of authenticity is complex since it should be accomplished by techniques which analyse intrinsic properties of a canister. The ultrasonic method seems to be the only one able to identify and authenticate copper canisters. A description of this method for copper canisters identification and authentication is reported in the paper, discussing advantages and disadvantages for a potential implementation in the Swedish system for final disposal.

## 2. The ultrasonic method

Ultrasound constitutes pressure-waves which can propagate across a specimen and are reflected whenever a discontinuity is encountered, i.e. a boundary between means of different acoustic impedances. At the interface between air and copper, for example, since the acoustic impedance mismatch is large, a couplant, such as water, is necessary to allow the transmission of the ultrasonic beam in copper. Canisters for spent nuclear fuel are made of copper to provide safety during handling and emplacement of the fuel in the repository and also to ensure isolation from the biosphere for thousands of years. Ultrasonic non-destructive testing is used to check the integrity of copper canisters and also the quality of the weld between lid and tube after the encapsulation of the fuel. However, the investigation of canisters by ultrasound could also be adopted for the acquisition of a unique identifier from each container. Ultrasonic techniques for reading bolt seals with artificial cavities applied on nuclear casks deposited in underwater and dry storages have been used in the nuclear field for twenty years. In the case of copper canisters for spent nuclear fuel, the ultrasonic method for the identification and authentication of each container is based on the acquisition of two fingerprints by ultrasound.

The identification signature is created by machining a series of chamfers in the inner surface of the canister's lid where the copper thickness is greater than 50 mm. Chamfers are arranged around the lid circumference creating a unique code for each canister, readable by rotating a transducer as placed in

Figure 2. The ultrasonic probe is kept inclined, in order to maintain the probe perpendicular to chamfer surfaces to obtain reflections according to Snell's law. Whenever a chamfer is detected, an echo is received by the probe and values of amplitude and time of flight are collected. By a 360° rotation of the probe around the lid circumference, a unique code, strictly related to chamfers' position, can be acquired. In particular, the ultrasonic amplitude response of the chamfers represents an identification fingerprint for each copper canister. Acquiring this signature can be accomplished by immersion testing with water and the probe could be rotated automatically with a motor remotely controlled.

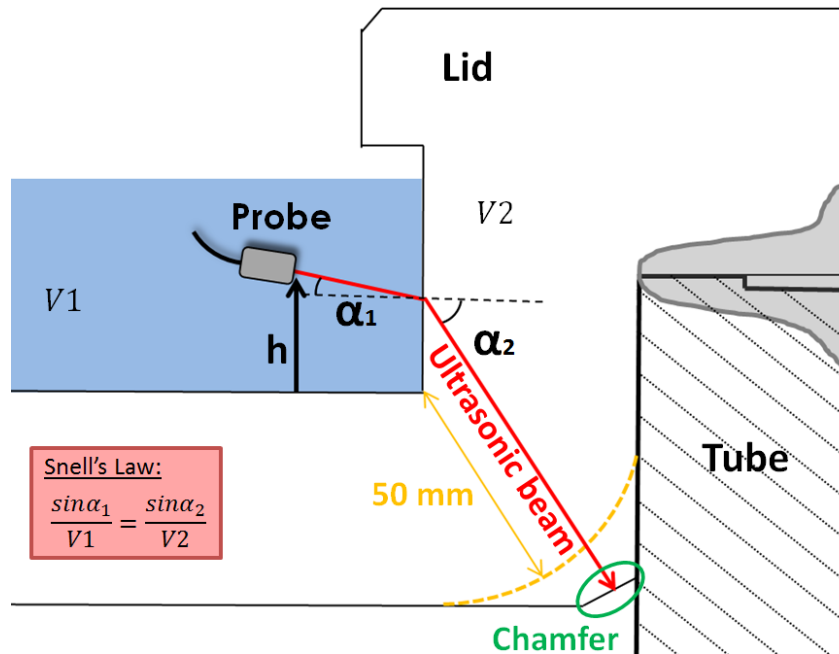


**Figure 2.** Ultrasonic investigation of chamfer (circled in green) machined in the inner part of the copper canisters' lid. V1 and V2 are the velocities of sound in water and copper respectively while  $\alpha_1$  and  $\alpha_2$  are the angles of incidence and transmission of the ultrasonic beam (red arrow).

The geometry of chamfers should be defined, on the one hand, to maximize the signal-to-noise ratio of the ultrasonic investigation and, on the other, to not affect the copper canisters' geometry too much. For this purpose, simulations and experimental tests on a laboratory mock-up have been carried out. As reported in [5] the acquisition of chamfers' amplitude response was carried out on a 1/4 scaled version of the copper lid with chamfers arranged around the circumference. The immersion test with an inclined probe, rotating 360° around the mock-up, confirmed the possibility of acquisition of an ultrasonic amplitude echo, whose variation is correlated to chamfers position.

Afterwards, results of simulations with CIVA software [6], revealed that the best compromise to meet all the requirements is a 10 mm wide chamfer with an inclination of 55°. This solution involves removing only 4.3 g of copper out of the full-sized 708 kg lid. Moreover, this chamfer length will ensure a good signal-to-noise ratio in the ultrasonic inspection also when varying the probe inclination, and in case of temperature variations in the water used for the immersion test. Temperature changes, in fact, affect the velocity of sound in medium and, as a result, the ultrasonic investigation itself. While in copper these variations are negligible, in water the velocity of sound fluctuates from 1403 m/s at 0°C up to a maximum of 1555 m/s at 74°C with a percent variation of about 11% [7]. According to the Swedish design criteria, the maximum temperature of the canisters' outer surface is around 100°C. The CIVA simulations show that 10 mm wide chamfers can be clearly distinguished from the rest of the lid even in varying temperatures as shown in Figure 3. The echo amplitude of the chamfer 10 mm wide (green curve) is higher than without chamfers (blue curve). Therefore, in a range of temperatures between 5°C and 100°C, a chamfer 10 mm wide can be detected with a good margin: as shown in Figure 3 the amplitude acceptance threshold at 0.04 (red line) is 10 times bigger than the maximum amplitude without chamfers. In case of inspection with water temperatures below 7°C, chamfers can be discriminated as well, but the signal-to-noise ratio is lower than in the case of inspections with higher water temperature.

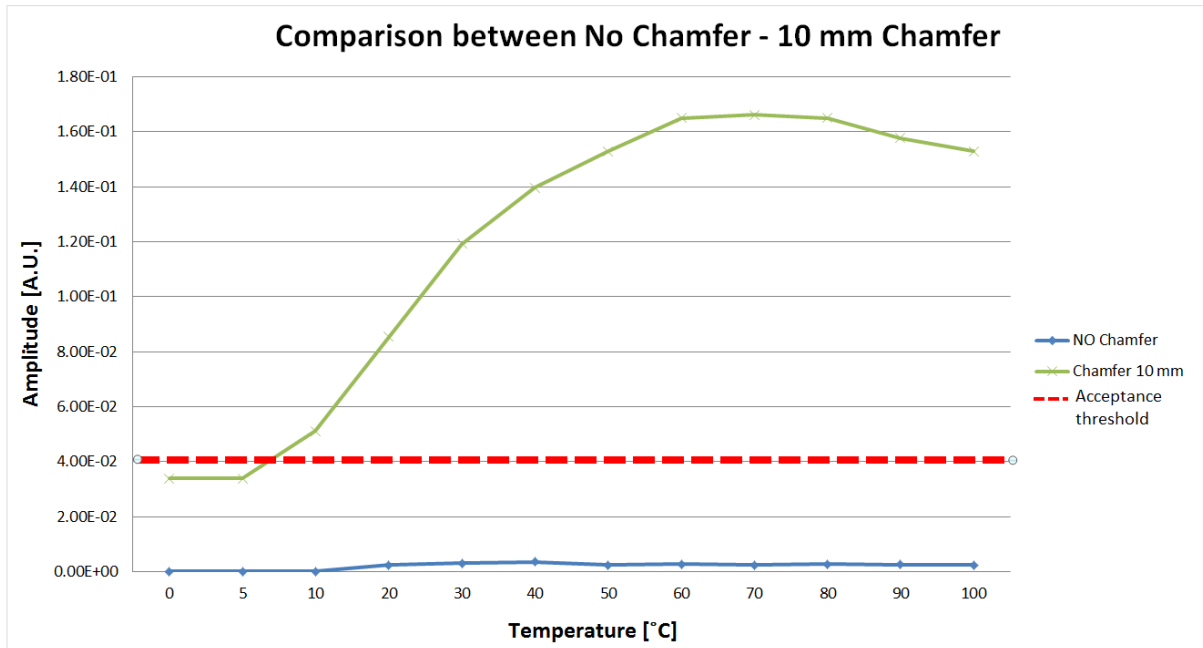


**Figure 3.** Simulation of the ultrasonic amplitude response acquired by the investigation of lid with (green curve) and without (blue curve) a chamfer 10 mm wide, considering a temperature variation from 0°C to 100°C. The red curve represents the acceptance threshold above which a chamfer 10 mm wide is well discriminated from the case with no chamfer.

The angular extension of chamfers is another important parameter which can impact on canister's geometry. The unique reflection realized by chamfers arranged around the lid circumference should be optimized in order to reduce the amount of copper to be removed. As a consequence, the early idea of a binary code with at least 13 chamfers and a reference for the identification of about 6,000 containers has been replaced with another coding. The new solution (Figure 4) splits the lid circumference into four imaginary sections 27° wide representing thousands, hundreds, tens and units. Each division is in turn divided into nine slots, which may or may not host a chamfer inclined 55°, 10 mm wide and with an angular extension of 3°. In this way, depending on which slot of each section is occupied by the chamfer, it is possible to give a unique ID number to a canister with only four chamfers plus the reference.

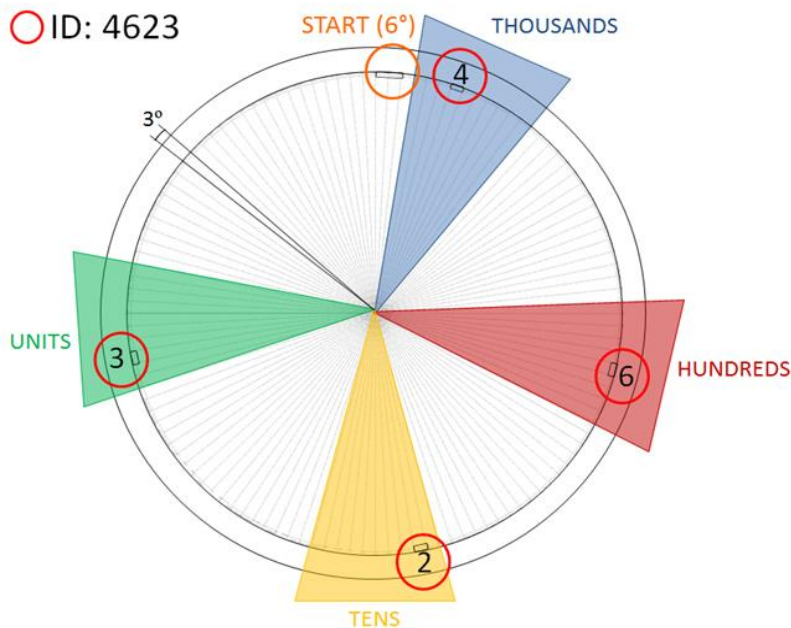


**Figure 4.** Proposed coding for chamfers to uniquely identify a copper canister (ID 4623).

To conclude, the identification of canisters could be realized by chamfers machined on the lids inner surface, readable from outside by an ultrasonic probe. Nevertheless, the code created by chamfers could be duplicated and then another solution should be implemented to verify attempts of falsification. For this purpose, taking advantage of the ultrasonic transducer already implemented in the identification concept, a method to verify the canister's authenticity is developed.

In contrast to the identification fingerprint, the authentication signature is an intrinsic property of each copper canister. After the fuel assemblies have been encapsulated, the copper lid is welded onto the tube by Friction Stir Welding (FSW). A rotating tool penetrates between the two surfaces, heats the material and creates a joint [8]. According to the geometry design, two faces of the lid lean against the tube: at the end of the welding process, only one of them is welded to the tube and the other represents a gap between the lid and the tube. This discontinuity can be detected by an ultrasonic transducer as placed in Figure 5.

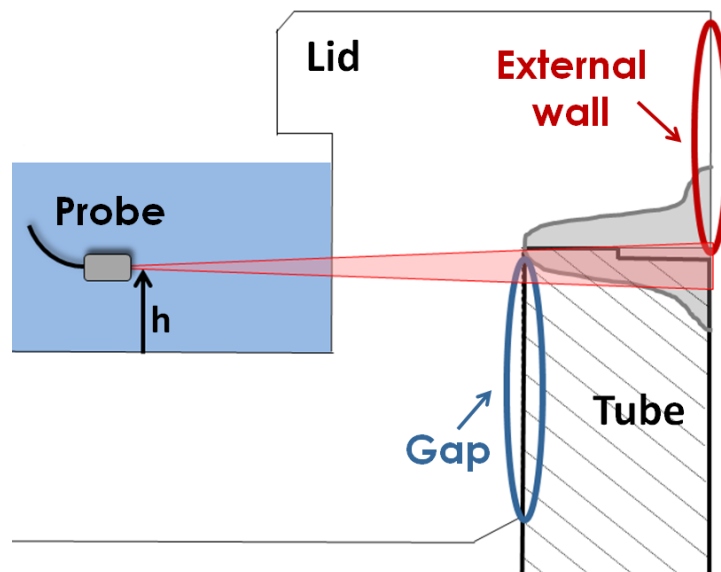


**Figure 5.** Ultrasonic investigation of the welding area between lid and tube of a copper canister. The probe is kept at a fixed height "h".

The ultrasonic amplitude response changes according to the variations of the gap height all around the lid circumference. Preliminary studies on copper flanges, i.e. slices of a copper lid already welded onto the tube, demonstrates the feasibility of the method: ultrasonic echoes from the internal gap and external wall surfaces have been acquired with a good signal-to-noise ratio using a 10 MHz immersion transducer [9]. Afterwards, experimental tests are carried out on full scale welded lids at the SKB's Canister Laboratory in Oskarshamn (Sweden). For this purpose, an ad hoc acquisition system prototype was designed. The reader, i.e. the device used to read authentication fingerprints, is made up by three steel arms, a motor devoted to the probe movement and a rotating bar to keep the transducer perpendicular to surfaces to be investigated. Signals are transmitted and received by an electronic module which is connected to another board for the control of the motor and power supply. Results of investigations are then processed and displayed on a computer [10]. The set-up of measurements for the investigation of welded copper lid is shown in Figure 6. Several measurements have been carried out, changing the position of the reader above the lid and the probe height in order to verify the repeatability of measurements and inspect a wide area of the welded region. Two time windows are used to acquire the maximum amplitude echo between the internal gap and the external wall.

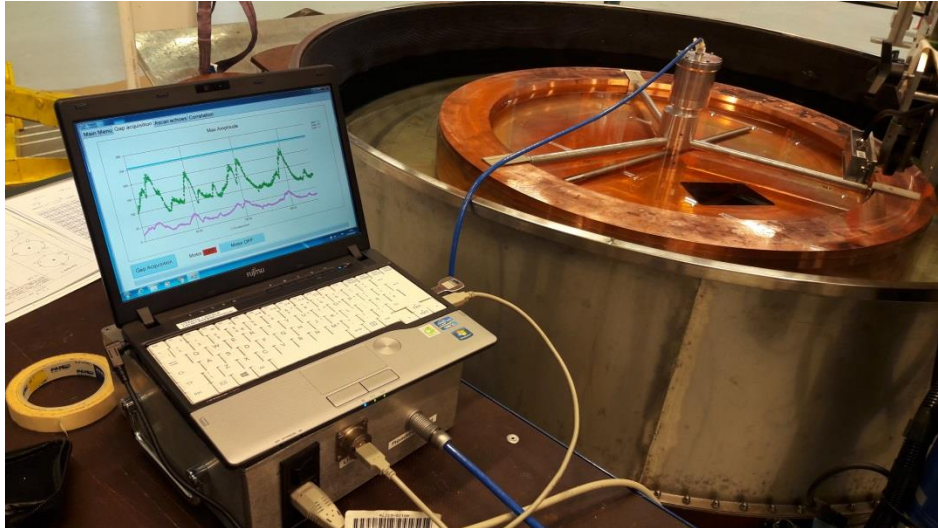


**Figure 6.** Set-up of measurements on copper samples: the reader for the scanning of the welding area is centred on the lid and signals are transmitted/received to/from the ultrasonic transducer by a control box connected to a computer for the processing and display of acquisitions.

After a complete rotation of the probe, the ultrasonic amplitude responses are collected and analysed. In Figure 7 is a display of the ultrasonic amplitude response of the internal gap (in blue) and the external wall (in red) on rotation angle of the probe. The two curves are quite fluctuating and present interesting peculiarities which can be unique to each container. However, the uniqueness of the welding area should be verified undertaking a statistical analysis of a consistent number of samples.

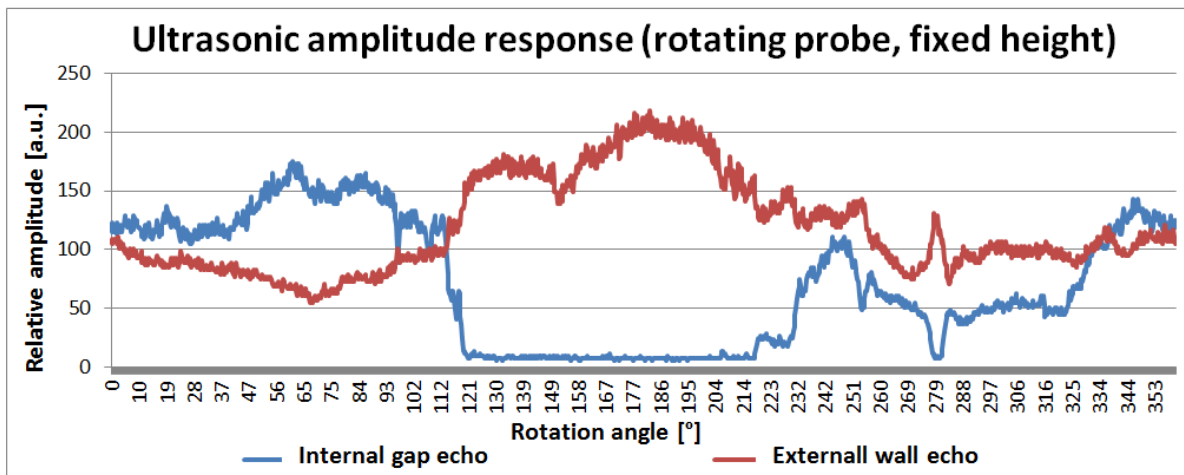


**Figure 7.** Ultrasonic amplitude response acquired rotating the transducer around the copper sample circumference with fixed height  $h$ . The red line is the amplitude response of the external wall while the blue line is the amplitude response of the internal gap.

The ultrasonic method is based on the acquisition of ultrasonic-amplitude responses of chamfers (identification) and welded regions (authentication). While the first can discriminate each canister from another, the second helps to verify the authenticity of each canister. However, duplication of both fingerprints could make it difficult to ascertain the authenticity of a given canister. Therefore, we introduce a third fingerprint to our method to increase the reliability. The new fingerprint is simply realized connecting the intersection points between identification and authentication fingerprints. In this way, as shown in Figure 8, if the angular matching between the two fingerprints (blue line for the identification and yellow line for the authentication) is not the same as in the reference, it is possible to detect anomalies and demonstrate potential counterfeit canisters. A patent has been filed for both the identification and authentication approaches [11].

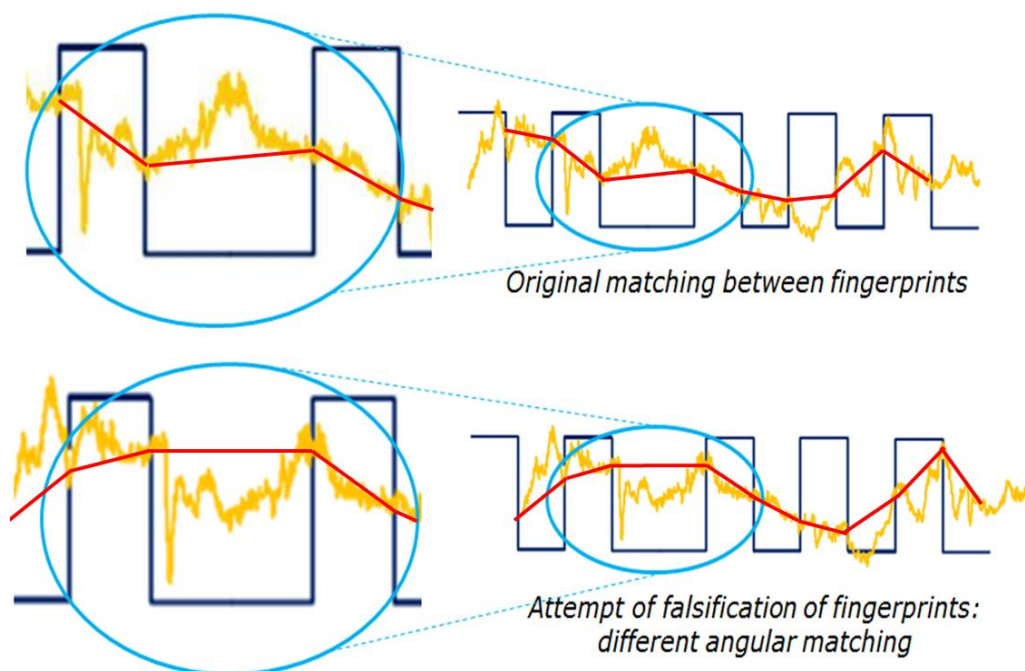


**Figure 8.** Comparison between a real fingerprint and a copy: the differences in angular matching between the identification (blue curve) and authentication (yellow curve) fingerprints can be detected analysing the trend of the third fingerprint (in red).

### 3. Potential implementation in the Swedish system

The adoption of the ultrasonic system could be extremely important in the case of failures of the other two main C/S measures: the monitoring devices and seals applied on transport casks. The encapsulation plant and the geological repository could be considered as black boxes where additional C/S measures are not necessary. However, during transport of copper canisters between the two sites, the use of dual C/S measures is recommended. Therefore, the implementation of an additional system to identify and uniquely authenticate each canister could be considered as a useful way to recover CoK in case of losses and not as a routine measure. The introduction of a unique identifier should also be combined with other techniques to verify the integrity of the canister and the fuel inside. This section describes how the ultrasonic method could be included within the Swedish system for final disposal.

The identification and authentication fingerprints, to be used as references, could be acquired at the encapsulation plant, stored in a database and then verified with other measured fingerprints, only in case of necessity. In general, performing verification measurements to assess the fuel and the canisters' integrity at the geological repository is not desirable, but since this should not be a periodic procedure, it could be useful to recover CoK using ultrasonic methods in case of the failure of other C/S measures. Ultrasonic fingerprints could be acquired at the encapsulation plant and a reference could be stored for each container. At the geological repository, these fingerprints could be verified in case of necessity and acquired responses could then be compared with references. At the encapsulation plant, after the encapsulation of the fuel, canisters are welded and ultrasonic and radiographic tests are then performed on each container to verify the quality of the weld. At this stage, reference fingerprints could be acquired. In particular, an ad hoc system could be developed to acquire automatically a reference signature from each canister. Ultrasonic measurements could be performed in the same room as the radiographic inspection of welds. A section view of the possible ultrasonic reader placed above a canister is shown in Figure 9. The device can be seen as an optimized version of prototypes already developed for laboratory tests. This new system includes a cylindrical box which hosts a tank for water, plus a motor and a rotating bar which supports two transducers (highlighted in yellow in Figure 9). One transducer is kept perpendicular to the welding area to acquire the authentication fingerprint and the other transducer is inclined according to Snell's

law to receive echoes and furthermore to generate the identification code produced by the chamfers. The speed of the motor can be adjusted to optimize the acquisition of signals and different inspections can be performed changing the transducer height for the collection of a larger amount of data.

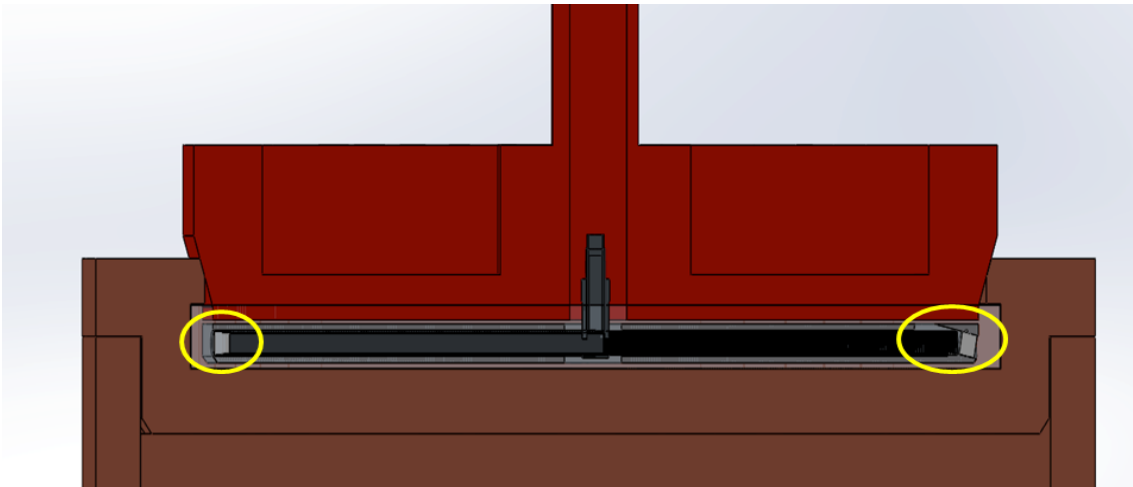


**Figure 9.** Section view of a CAD design of the ultrasonic reader device placed above a canister. Two probes (highlighted in yellow) rotate around the lid circumference to acquire the identification and the authentication fingerprints.

All ultrasonic measurements could be accomplished without the involvement of an operator: the reader system could be put in place by a crane or robotic arm and automatically centred on the lid (Figure 10). Once in place, water can be poured on the external concave of the lid and the ultrasonic immersion testing could be launched. After a complete rotation of both probes, the two curves are registered, stored in a memory card and sent wirelessly to a control station. The processing of signals for the definition of the third fingerprint can be done at the post-processing of data. At the end of the inspection, water will be pumped away from the lid.

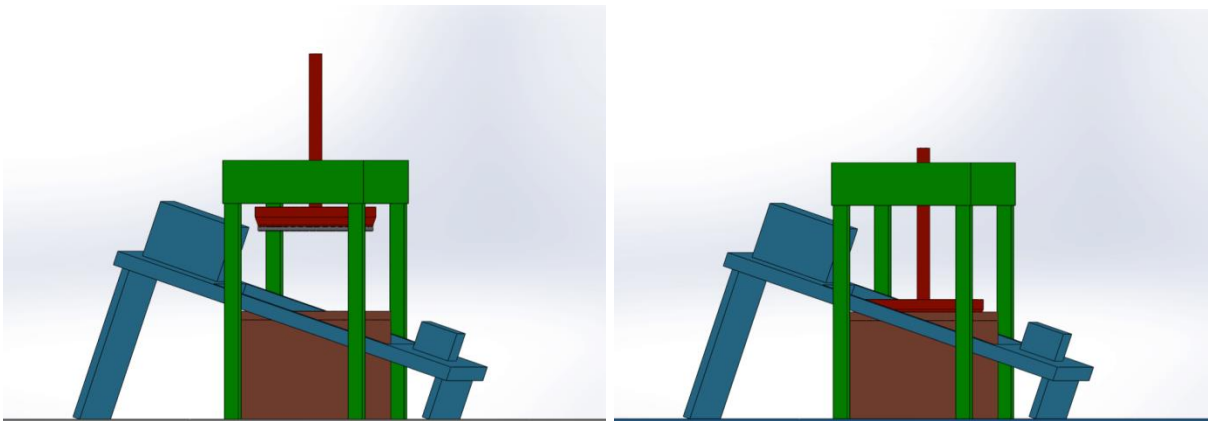


**Figure 10.** The ultrasonic acquisition of identification and authentication fingerprints could be performed in correspondence of the radiographic station for weld verification (in blue). On the left, the ultrasonic reader (in red) is lifted above the copper canister. On the right, a crane (in green) arranges the device on the canister.

All the electronics useful for the control of the motor and the transmission/reception of signals could be developed in an embedded version to fit inside a cabinet which could be placed in the same room as the measurements set-up (far from radiation emitted by the spent fuel inside the canister). All the reading processes could be monitored by surveillance devices and a complete rotation of transducers could be completed in a few minutes. Differently from other identification methods, the ultrasonic method is easy to implement and use, since it works automatically without the need of operators. In addition the cost of signatures' manufacturing is practically included in the canisters production costs. However, the realization of unique configurations of chamfers around copper lids involves the introduction of an additional step within the manufacturing process of canisters.

In the case of verification of fingerprints at the geological repository, a portable version of the same reader could be developed to make an easy verification whenever it is required.

A State might require that canisters be retrieved from a repository as a safety measure [12], as is the case for Sweden. Safeguards approaches have not been pre-determined for any retrieval scenarios. However, having a unique reference for each container could be useful to keep the CoK in case of retrieval, based on the hypothesis that the identification and authentication fingerprints would not be altered at that time, and there is knowledge available to use the ultrasonic methods for the identification of the canisters.

## 4. Conclusions

The final disposal of spent nuclear fuel introduces new challenges in the field of nuclear safeguards. The transport of copper canisters with spent nuclear fuel from the encapsulation plant to the final repository, as planned in Sweden, requires the implementation of supplementary C/S measures, in addition to dual surveillance and sealing systems, to be used in case of CoK losses. The ultrasonic method for the identification and authentication of copper canister is a potential way to help the recovering of CoK if necessary. However, canister identification should be combined with other techniques to verify the fuel integrity in order to recover the CoK. This method is based on the ultrasonic acquisition of two fingerprints. The ultrasonic amplitude response of a series of chamfers machined around the lid's inner surface could be used to generate an identification fingerprint. In addition, the ultrasonic amplitude response of the welding area between the copper lid and the canister can be used as an intrinsic fingerprint which authenticates each container since the ultrasonic amplitude response is only related to material properties and the welding process. Experimental tests were performed to validate both concepts and our results confirmed expectations. We recommend that future tests be performed on a full-scale copper lid with chamfers already welded to a canister tube in order to validate the third fingerprint described in Section 3. In fact, the angular matching between the identification and authentication signals could realize a third unique signature, increasing the robustness and reliability of the whole method. The design of an ultrasonic reader has been presented and its use has been optimized to avoid the involvement of an operator during the acquisition of fingerprints. The proposed version could be adopted within the encapsulation plant but a second version could be developed for the geological repository, by adapting of the one designed for the encapsulation plant.

## 5. Acknowledgements

This research has been accomplished by the Seals and Identification Lab (SILab) of the Joint Research Centre of the European Commission in Ispra in collaboration with the Department of Information engineering of the University of Florence. We would like to thank our colleagues from SKB for the copper samples provided to us for tests and all the expertise shared with us.

## 6 Legal matters

### 6.1. Privacy regulations and protection of personal data

The authors agree to allow ESARDA to print our names/ contact data/photographs/article in the ESARDA Bulletin/ Symposium proceedings, or any other ESARDA publications and, when necessary, for any other purposes connected with ESARDA activities.

### 6.2. Copyright

The authors agree that submission of an article automatically authorises ESARDA to publish the work/article in whole or in part in all ESARDA publications – the bulletin, meeting proceedings, and on the website.

The authors declare that their work/article is original and not a violation or infringement of any existing copyright.

## 7. References

- [1] af Ekenstam G.; Hildingsson L.; Fagerholm R.; Andersson C.; *Elements of a Swedish Safeguards Policy for a Spent Fuel Disposal System*; ESARDA Bulletin 54; June 2018; pp.36-41.
- [2] Hildingsson L.; Andersson C.; Fagerholm R.; *Safeguards Aspects Regarding a Geological Repository in Sweden*; IAEA Safeguards Symposium, Paper CN-220-166; Swedish Radiation Safety Authority: Stockholm; Sweden; 2014.
- [3] International Atomic Energy Agency: IAEA; *Model Integrated Safeguards Approach for a Spent Fuel Encapsulation Plant*; SG-PR-1305; ver. 1; 10 June 2010.
- [4] Clementi C.; Littmann F.; Capineri L.; *Comparison of Tagging Technologies for Safeguards of Copper Canisters for Nuclear Spent Fuel*; Sensors 2018 18(4) 929; March 2018. Available online (accessed on Sept 28 2018): <https://doi.org/10.3390/s18040929>.
- [5] Clementi C.; Littmann F.; Capineri L.; Andersson C.; Ronneteg U.; *Ultrasonic Identification Methods of Copper Canisters for Final Geological Repository*; ESARDA Bull. N.54; 2017, pp. 75–81.
- [6] Ultrasonic Testing with Civa- Extende. Available online (accessed on April 15 2019): <http://www.extende.com/ultrasonic-testing-with-civa>.
- [7] Engineering ToolBox, *Speed of Sound in Water*, 2004. Available online (accessed on Nov 10, 2017): [https://www.engineeringtoolbox.com/sound-speed-water-d\\_598.html](https://www.engineeringtoolbox.com/sound-speed-water-d_598.html).
- [8] Stepinski T.; Engholm M.; Olofsson T.; *Inspection of copper canisters for spent nuclear fuel by means of ultrasound Copper characterization, FSW monitoring with acoustic emission and ultrasonic imagin*; Uppsala University; Signals and Systems Department of Technical Sciences; Sweden; August 2009.
- [9] Clementi C.; Capineri L.; Littmann F.; *Innovative Method to Authenticate Copper Canisters Used for Spent Nuclear Fuel Based on the Ultrasonic Investigation of the Friction Stir Weld*; IEEE Access 2017; Vol. 5; doi:10.1109/ACCESS.2017.2694878.
- [10] Clementi C.; Littmann F.; Capineri L.; *Ultrasonic Investigation of the Welding Area of Copper Canisters for Spent Nuclear Fuel*; ESARDA Bull. N.56; 2018; pp. 19-27.
- [11] Littmann F.; *Ultrasonic identification and authentication of containers for hazardous materials*; EP 16166465; April 21; 2016.
- [12] Mongello R.; Finch R. J.; Baldwin G.; *Safeguards Approaches for Geological Repositories: Status and Gap Analysis*. Available online (accessed on Feb 02 2019): [https://www.researchgate.net/publication/280655578\\_Safeguards\\_Approaches\\_for\\_Geological\\_Repositories\\_Status\\_and\\_Gap\\_Analysis](https://www.researchgate.net/publication/280655578_Safeguards_Approaches_for_Geological_Repositories_Status_and_Gap_Analysis).

## National Safeguards Concept for Encapsulation Plant and Geological Repository

Tapani Honkamaa  
Marko Hämäläinen  
Elina Martikka  
Mikael Moring  
Olli Okko  
Topi Tupasela  
STUK-  
Radiation and Nuclear Safety Authority  
Po-BOX 14  
00881 Helsinki FINLAND  
Tapani.Honkamaa@stuk.fi

### **Abstract:**

*To make geological disposal of spent nuclear fuel project successful from safeguards point of view, we need to answer two basic questions 1) Are the declarations of the fuel correct and complete? 2) Can we and future generations be and stay assured at any point of time that all verified fuel is disposed and securely kept in the repository as declared?*

*STUK has created a national safeguards concept for the Finnish encapsulation plant and geological repository. The concept describes at a general level the principles and practices of the safeguards measures from the intermediate storage to the closure of the geological repository.*

*Recommendations of the IAEA Group of Experts ASTOR (Application of Safeguards TO Repositories) are followed in the national concept. All fuel items will be verified prior to encapsulation and disposal. The verification technology proposed is a combined system of PGET and PNAR/FORK verification tools. Shared access to the measurement data between all inspectorates shall be secured, since all of them will draw their individual conclusions.*

*On order to draw conclusions about continuity-of-knowledge and detection of undeclared activities, STUK will exploit on the conclusions of EC and the IAEA. In addition, STUK will make use of its own continuous 3S inspection efforts, observations of other authorities in Finland and the results of the ongoing environmental monitoring programme.*

*At the moment no one can provide fully satisfying answers to how post-closure safeguards activities will be arranged. There are concerns that these activities may cause undesired burden on future generations with never ending surveillance of the site. However, there is still time to resolve these concerns. Present understanding is that safeguards may continue with the existing institutions and arrangements as long as the safeguards agreements are in force.*

**Keywords:** Geological Disposal of Spent Nuclear Fuel, Safeguards concept

## 1. Introduction

The geological disposal program of spent nuclear fuel creates unique and unrepresented challenges for international and national nuclear safeguards. These can be divided in two separate areas:

- After disposal the fuel is beyond any traditional verification possibilities
- Final repository has safeguards relevance after emplacement and closure.

STUK, Radiation and Nuclear Safety Authority in Finland has prepared national concept for spent fuel disposal to recover these challenges.

The first challenge is addressed by performing verifications and maintaining Continuity of Knowledge (CoK) throughout the process. If all fuel to be disposed is verified with the best available methodology, the inspectorates will generate comprehensive information about the fuel going underground. After verification the continuity of knowledge shall be maintained until emplacement and closure of the canister into the disposal position. As a result a dataset is generated, which provides future generations accurate information about the disposed fuel and they can satisfy themselves about the content of the repository without the possibility to re-verify the disposed fuel ever again.

The second challenge is the cooperation with waste management that relies on a repository concept without long-term institutional arrangements. It is obvious that site characterization, construction, operational documents and verification activities will provide the CoK needed for safeguards during the operational phase of the repository. The assurance about the intact bedrock will provide society with safety and security provisions. However, the debate about termination of safeguards and post-closure activities could create open-ended questions that may cause undesired burden on future generations. At the moment satisfactory answers to these issues are not available. Present IAEA policy is that safeguards may continue with the existing institutions and arrangements as long as the safeguards agreements are in force [2]. However, this debate is not acute at this point of time. There is about 100 years time to resolve this issue, develop new technical tools and create new concepts. By selecting the disposal option Finnish society has chosen the way which would, if successfully implemented, resolve the safety issue forever. Leaving the fuel in the intermediate storages waiting for possible reprocessing, transmutation or some other future technology would, in theory, solve the philosophical, long term safeguards issue, but much more concrete safety and security concerns would remain for future generations.

## Development of National Concept

The development of national concept was the main output of national GOSSER (Geological Disposal Safeguards and Security R&D) project. Project has concentrated in development of verification technologies and investigation how the continuity of the verified fuel can be maintained after verification until emplacement of the fuel into the repository and beyond.

GOSSER project first phase lasted from 2015-2019 and the second phase of the project has started in early 2019. The national concept was finalised also in the early 2019. The concept is not a public document itself yet, but it will be communicated to stakeholders and international collaborators need to know basis. This paper describes basic elements of the concept.

The concept provides answers two basic questions,

1. Are the declarations of the fuel correct and complete?
2. Can we and future generations be and stay assured at any point of time that all verified fuel is disposed and securely kept in the repository?"

The answers are discussed in the next two chapters. Correctness and completeness are resolved with comprehensive verification. Providing assurances is discussed in chapter 4.

## Verification prior disposal

Starting point of the concept is that all spent fuel will be verified with the best available technology. Creating as much as possible verification information prior disposal is minimizes the risk of future generation facing the situation of failing to make necessary conclusions about the disposed fuel.

In practice, recommendations of ASTOR (Application of Safeguards TO geological Repositories) group of experts final report [1] will be followed. The technology proposed by ASTOR report can be assumed to be available in 2025 when disposal is expected to start. The recommended system is comprised of Passive Gamma Emission Tomographer (PGET), Passive Neutron Albedo Reactivity (PNAR) verifier. This verification system will be made available at the intermediate storage. In addition method to verify the weight of the assembly in dry environment in the encapsulation plant is needed.

PGET will contribute pin level detection and provide gamma spectrometric measurement for verifying the presence of  $^{137}\text{Cs}$  and  $^{154}\text{Eu}$ . PNAR will verify gross gamma, neutrons and multiplication. Signatures of  $^{137}\text{Cs}$  and  $^{154}\text{Eu}$  intensities, gross gamma intensity, total neutron intensity, multiplication, and pin level fission product distribution can be predicted using the SCALE/MCNP code used by the European Commission.

Weighing is a relatively accurate method and can also reveal pin removals or substitutions with lower density materials. Verified results will be compared to predicted data and if no discrepancy is found and no unreported, replaced, or removed pins are detected, the verification can be considered as conclusive. Falsifying all this information for a would-be proliferator is very difficult.

When the disposal starts the PNAR and PGET verification will take place in the Olkiluoto spent fuel storage. The weight of the assemblies will be recorded at the encapsulation facility. At this point it should be noted that PNAR is still in the development phase and its performance and operation needs to be confirmed by test measurements. If the development of PNAR fails, the well proven FORK verifier will be the alternative method.

The verification is done against reports provided by the operator. PGET and PNAR are methods, which require sophisticated analyses and interpretation of the results require access to more detail information than is usually provided in regular reports. STUK has right as a national regulator request all fuel data required for the analyses.

The verification process shall be highly automated. Automatic analysis provides traffic light signal (Green-Yellow-Red) supporting the decision. In detail analysis can be done for every assembly.

## Maintaining continuity of knowledge

The encapsulation process will be carried out under international surveillance. The critical moment is the welding of the canister containing the spent fuel after which it is foreseen that no questions concerning the content of the canisters is raised. The international inspectorates have indicated that they need to have a few days time to confirm the successful surveillance before the canister is transferred to the underground storage and further to the repository.

STUK as the national regulatory authority shall require and control that the individual canisters are actually emplaced in a safe and secure manner at their specified emplacement locations. The documentation needed for this regulatory control will be provided by the operator and will be verified by STUK with inspection activities on and off site. Also the backfilling of the tunnels will be documented and controlled. National design information verification is conducted to confirm that the underground premises are constructed and backfilled according to the safety and security requirements, and thus excluding all activities in the vicinity of the emplaced canisters. In addition, geoscientific monitoring is addressed to confirm that the host rock is intact.

## **Safeguards measures for emplaced fuel in operational and post-operational phase**

The creation of credible assurance about the absence of undeclared activities in the vicinity of the repository by the international inspectorates can be raised as an open question. Nationally, this issue will be dealt with as follows:

- 1) STUK follows the daily work plans and the continuous monitoring of the site. These are reviewed by weekly inspections and monthly meetings;
- 2) STUK has contacts with other authorities in Finland that can report about any unreported safeguards-relevant activities, e.g. concerning land-use; and
- 3) STUK also receives and reviews environmental monitoring data around Olkiluoto repository. Some part of this data can reveal unreported activities. This data, for example, from seismic monitoring, hydrogeology and groundwater chemistry monitoring programs, will be reviewed in STUK also from point of view that someone is deliberately intruding the repository.

Nationally, the information described above is enough for making sufficiently credible conclusions about the absence of undeclared activities underground. For possible intrusion the concept provides true deterrence of detection.

### **Long term safeguards data management**

During the disposal process Posiva also receives the fuel data from the NPP operators. It is a national requirement that NPP operators shall maintain the data for five years after the shipment. Posiva shall keep the information until the end of its operations. Eventually this information shall be transferred to the state, but this may happen more than 100 years from now.

Safeguards systems produce a large amount of data. The highest data volumes can be expected to be produced by surveillance cameras and laser scanning systems. Most of this data can be disregarded some time after positive conclusions have been drawn. As a minimum, the annual conclusions based on the data obtained from cameras, seals and other C/S systems shall also be preserved for further generations. All NDA verification data shall be maintained as a representation of the disposed fuel. The size of this data is, however, modest and will not constitute an issue as to data volume.

The inventory of nuclear materials will be presented in standard means of monthly Inventory change reports and annual material balance area reports and physical inventory lists. The storage maps will be updated and preserved by the operator during the operational phase of the disposal facility. The European commission may prepare more precise Safeguards Provisions, but this basic principle for annual inspections and conclusions can be expected to continue. At STUK, the information management for the records will be similar as that with other facilities aiming for permanent preservation of information.

The geoscientific site characterization and site monitoring using multidisciplinary methods collects a high number of different types of data and observations. Currently, this data is collected according to safety requirements and thus are not documented specifically for safeguards. In the annual conclusion, this data and observations can be referred and assessed for a safeguards conclusion about the intact host rock. Typically, the annual monitoring reports are published during the following year after safeguards conclusion are drawn. Therefore, the STUK Safeguards Section will follow the monthly follow-up meetings for safety assessment.

The seismic network was built on the site to detect micro earthquakes, but the network is applied also to record and document all the blasts observed in the vicinity of the repository to confirm that they are related to known earthworks. The monthly reports have been submitted to STUK from the beginning of the excavations. Currently the seismic data is not stored, but the detected and analyzed events are reported by the operator of the seismic system. The need to archive systematically geoscientific or earth observation data for safeguards purposes need to be reassessed with the international inspectorates before the operational phase of the repository begins.

## **Cooperation with the IAEA and EC.**

The concept relies on good cooperation with the EC and the IAEA. STUK is ready to provide its findings, as necessary, to other inspectorates and will make use of the safeguards conclusions by them. The cooperation is organized through EPGR group which was established in 2012 and consists of the IAEA, EC and authorities and operators from Finland and Sweden.

## **Conclusions**

The principle of the concept is that all spent fuel items shall be verified before encapsulation and disposal with a method capable of single pin verification. This eliminates effectively the possibility that future generations, who has no access to the fuel, will have unresolved questions regarding to the fuel characteristics. Another principle is that the verified information shall be effectively maintained until the emplacement of the canister into the deposition hole. After emplacement the national concept relies on the every-day oversight activities of STUK, societal verification between authorities and the people. Review of a selected set of environmental observations is also part of the concept.

The concept is planned to avoid duplication of the work and investment between STUK, the EC, and the IAEA. As a consequence, the inspection burden to the operator and risks to the disposal process can be kept acceptable without endangering the concept's ability to provide credible safeguards conclusions.

## **8. References**

- [1] STR-384, TECHNOLOGIES POTENTIALLY USEFUL FOR SAFEGUARDING GEOLOGICAL REPOSITORIES, ASTOR Group Report 2011-2016, Vienna, August 2017
- [2] IAEA POLICY PAPER 15: SAFEGUARDS FOR FINAL DISPOSAL OF SPENT FUEL IN GEOLOGICAL REPOSITORIES, Date of Entry into Force: 1997-06-19

## Potential SG equipment infrastructure for the Geological Repository in Finland

**K. Khrustalev (IAEA), M.Lahti (POSIVA OY), E. Martikka (STUK), T. Honkamaa (STUK), M. Moring (STUK), M.Murtezi (EC), W.-S. Park (IAEA), I.Tsvetkov (IAEA), K. Baird (IAEA)**

### **Abstract:**

*Responding to the need for establishing an effective safeguards approach for the future Geological Repository (GR) in Finland, and implementing its measures and techniques identified in line with safeguards-by-design concept, the European Commission (EC), the International Atomic Energy Agency (IAEA) and Finnish Radiation and Nuclear Safety Authority (STUK) are jointly working on the Equipment Infrastructure Requirements Specification for the GR.*

*The identification of possible safeguards measures is carried out in such a way as to allow each of the international safeguards inspectorates (EC and IAEA), as well as the national authority (STUK) to effectively fulfil its mandate and to draw independent conclusions, while at the same time having the least possible impact on the spent nuclear fuel geological disposal process.*

*The infrastructure requirements for a GR are derived from a need that all nuclear material transported into and out of the GR must be accounted for and characterized; and the opportunities for monitoring of nuclear material movements later below the surface will be limited. The safeguards approach shall provide for future re-verification of nuclear material in the event of its retrieval from the GR, while the control and maintenance of the safeguard equipment installed on the GR boundary should be simple and economical in view of the long period of the GR operation (planned for at least 100 years).*

*Consideration is being given to containment and surveillance measures complemented by radiation monitoring applied to all penetrations leading to and out of the GR disposal area. In addition, a system for continuous monitoring of potential undeclared spent fuel reprocessing and other activities is under consideration. Kr-85 monitoring on the GR ventilation system (located in the Ventilation Building), and seismic array data analysis are proposed as possible components of such system.*

### **Introduction**

Storage of spent nuclear fuel is an ever-growing issue around the world. The spent nuclear fuel is stored either in dry storage concrete casks above ground or in spent fuel storage ponds (sometimes located in shallow underground tunnels like CLAB at Oskarshamn, Sweden). However, for long-term storage another solution is required. Finland is the first country to have licensed and begun the construction of a final deposition for spent nuclear fuel assemblies underground in a deep geological repository. This concept, which has originated in the 80s, was proposed as one of the most long-term safe, effective and nuclear proliferation-resistant ways of disposal of used nuclear fuel. Geological repositories are utilizing natural as well as engineered barriers to prevent the radioactivity release into the environment and to protect future generations from exposure.

An Advisory Group Meeting (AGM-660) hosted by the IAEA in 1988 recommended that the IAEA should not terminate safeguards on spent fuel before or after emplacement in a geological repository. Since then, various expert groups from the IAEA Member States (SAGOR, ASTOR) worked on the development of the safeguard approach and technical measures to verify spent nuclear fuel and safeguard it while it is being disposed underground [ASTOR 2017; Murtezi et al.,

2018]. The below described potential safeguards measures were shaped in close cooperation between the IAEA, Euratom, STUK and Posiva. Involvement of the Safeguards Inspectorates, the National Regulator and the Operator assured thorough understanding of the operational aspects on the planned geological disposal system and its design features. The identified safeguards measures and the safeguards infrastructure needed for its implementation evolved over the last decade leading to the here presented mature concept that is shared by all the parties involved and is being gradually incorporated into the facility design. However, despite our best efforts in the application of the Safeguards-by-Design approach, it should be noted that it is not realistic to expect to cover all possibilities in advance for a first-of-a-kind facility which shall be operational for more than 100 years. We have to keep an open mind and to allow flexibility and inventiveness for all parties involved in

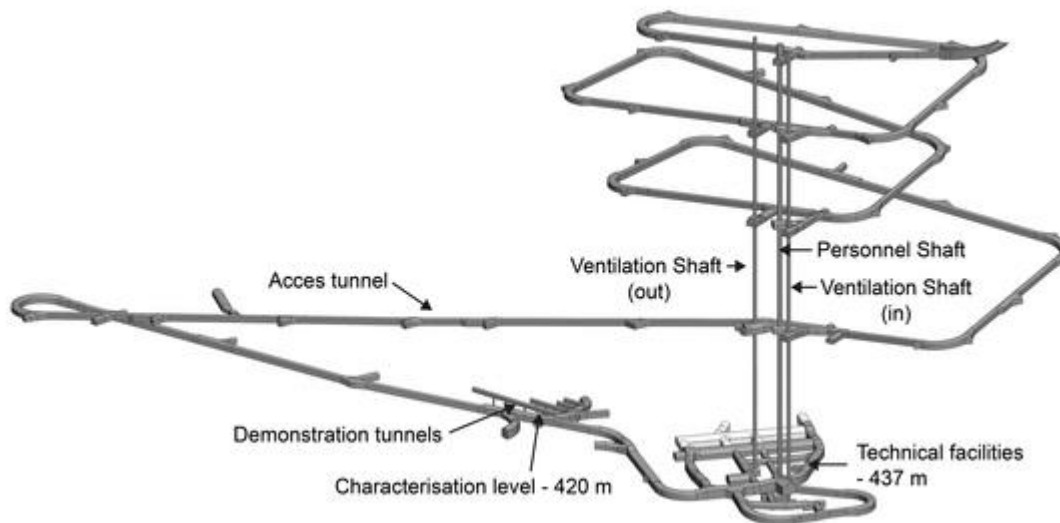
this work. Working step by step, improving when better knowledge available and having good communication and cooperation with all parties, the best result will be achieved.

## Finnish Geological Repository at Olkiluoto

The Finnish Geological Repository at Olkiluoto is comprised of two facilities – the Encapsulation Plant, where the spent nuclear fuel will be prepared and packaged into copper and cast iron canisters, and the Geological Repository – a system of shafts and tunnels at 450 meters depth below the surface, where the canisters will be deposited in the prepared emplacement holes.

The disposal canisters will be transported from the EP to the underground repository with a dedicated lift through a canister shaft. Other access points to the underground repository are the vehicle access tunnel and the Ventilation and Hoist Building shafts (personnel shaft and the inlet/exhaust air shafts).

The declared throughput of the Encapsulation Plant (EP) is 1 canister per week. Canisters are lowered from the EP into the GR underground canister temporary storage. The disposal of canisters from the temporary storage into the deposition holes will be done in campaigns of about 30 canisters per campaign, depending on the design capacity of a particular emplacement tunnel.



Source: Posiva webpage

## Potential safeguards measures

The potential safeguards measures have been identified with the aim to have the least possible impact on the spent nuclear fuel geological disposal process, while allowing each safeguards authority: national Finnish STUK and international - European Atomic Energy Community and International Atomic Energy Agency, to effectively fulfil their mandate and draw independent conclusions. The technical measures have been specified widely enough to cover the expected scope of the final safeguards approach, allowing for a degree of flexibility for possible future changes in the safeguards strategy. In accordance with the Safeguards-by-Design principle the joint work on safeguarding the repository has started well in advance already at the design stage, and continues in close cooperation between the facility operator – Posiva Oy and the national and international safeguards inspectorates.

The international safeguards measures are proposed following the "black box" approach for the geological repository (GR). This approach means that all the nuclear material transported into and out of the underground repository must be accounted for and characterised, and C/S measures will be applied around the boundaries of the "black box", but there will be no monitoring of nuclear material movements below the surface – within the

“black box”. This approach shall permit future re-verification of nuclear material outside of the GR in the event of retrieval, while simplifying the control and maintenance of the safeguard equipment installed on the boundary and making it more economical in view of the long period of the GR operation (planned for 100 years). This containment-like black-box option is in agreement with the rationale of the GR concept and its wider context of safeguards, safety and security (the so-called 3S approach).

To assure this approach it is important to define black-box margins. The proposed solution is limiting the black box to the disposal level and treating the overlaying rock masses as a confinement (with almost 450 meters thickness). This solution enables:

- tighter control on a smaller black box confirming transfers of the disposal canisters to the repository level, and
- earlier warning in case of undeclared or unexpected activities and occurrences.

To accommodate the needs for the nuclear material accounting in GR, while at the same time to facilitate the ease of the equipment maintenance, we propose to create the logical boundary between the Encapsulation Plant (EP) and the GR at the entrance door of the elevator shaft in the EP building. Thus, material (welded canisters with spent fuel assemblies) entering the elevator shaft to be lowered into the underground level will be considered as received and item counted at the GR.

Following the current safeguards model, portal radiation monitoring complemented by containment and surveillance will be applied to all penetrations leading to the disposal area.

In addition, non-invasive perimeter monitoring methods for detection of potential undeclared activities underground are being studied. The prospective technologies comprise Kr-85 stack monitoring on the GR ventilation system, with exhaust stacks located in the Ventilation Building for regular areas and Encapsulation Plant – for controlled areas, and a joint-use seismic array operated by Posiva Oy.

Periodical reviews of the technical characteristics of the GR (including underground) will be conducted (Design Information Verification activities).

Due to the distributed nature of the access points to the GR the safeguards equipment and local cabinets will be distributed accordingly and will have to send data to the IAEA HQ either through independent VPN links, or through a dedicated IAEA-protected local area network with a centralized VPN link.

The sites for the equipment installation are:

1. Encapsulation Plant (EP) building (Canister lift shaft and controlled area exhaust stack)
2. Access tunnel entrance
3. Ventilation and Hoist buildings (Personnel lift and GR ventilation system)

The black box definition is a function of the GR life. It will change when the underground access tunnels leading to the deposition tunnels will be backfilled. Following the evolution of safeguards needs and approaches, as well as technological developments in safeguards methods, additional black box monitoring methods can be introduced in the future, which may require changes to the safeguards-related infrastructure during the consecutive stages of the GR operation.

Remote monitoring (SG data transmission over a VPN to the international SG inspectorates) will play a major role in the safeguarding of the GR as it allows to provide almost real-time SG data review with minimal interference to the facility operations and reducing the need of inspector presence. Modern review tools such as IRAP allow to build correlated events merging together data from a variety of sources (radiation monitors, seals, laser curtains, surveillance cameras) and thus providing the inspectors with software tools which facilitate the efficient and timely verification of the activities at the site by comparing them with the information provided in computer-processed operator declarations.

## **Proposed SG measures for GR entrance points.**

There are three main entry points to the underground repository: A canister shaft, where the disposal canisters are lowered into the GR from EP (this shaft also serves as an exhaust air path for the canister buffer storage underground, which comprises a controlled area); a vehicle tunnel entrance, where the trucks and other heavy machinery enters the GR. This tunnel will see a flurry of the activity as heavy trucks will be transporting out the rock excavated underground, and bring in the bentonite for the emplacement holes and backfilling. And finally, there is a personnel shaft which will transport workers in and out of the GR working areas.

The personnel shaft and the intake and exhaust ventilation shafts are located in the Ventilation and Hoist buildings, but by design they are blocked by the air blowers and are not equipped with any machinery suitable of raising any materials from underground. These features will be verified during the periodic Design Information Verification activities.

Thus, at the three major penetrations to the GR standard safeguard means such as portal radiation monitors (neutron and gamma, possibly with spectroscopic capabilities) and surveillance cameras will be installed. In addition, truck balances might be considered at the tunnel entrance to spot-check the expected load weight of the trucks transporting the crushed rocks out of the underground repository.

Infrared cameras capable of detecting rest heat emitted by radioactive decays may also be considered.

The portal monitor at the entrance to the tunnel may observe rather large spikes of gamma radiation due to the natural radioactivity contained in the excavated rock (U, Th natural decay chains) and bentonite (K-40) transports. Therefore it is important to design the portal monitors in such a way as to minimize the rate of false positives alarms.

## SG measures for verification of the declared use

In order to detect potential undeclared activities various methods can be used [Okko 2006; Pentti 2017]. During the Design Information Verification inspectors will access the tunnel system of the GR and conduct a periodic 3D laser scanning of the tunnels in order to establish that no undeclared penetrations have been created in the tunnel walls. Furthermore, the ground penetrating radar (GPR) can be used to check the walls for any hidden spaces. The penetration depth of the GPR in hard crystalline rock can reach up to 10-15 meters [Carchon et al., 2006; Saksa 2005]

### Kr-85 intake and exhaust monitoring

Kr-85 has been long established as a key indicator of fuel reprocessing. Setting up spent nuclear fuel reprocessing capabilities deep underground may sound as a far cry, but it has been done previously for various reasons and such an undertaking is definitely feasible.

Keeping it clandestine will be no small feat, but history showed us that even very large scale projects can be kept hidden from the world. Hiding them in plain sight in an already operational facility which deals with large quantities of nuclear material can be one of the options. Even if a state has no plans for diversion or misuse at the current time, it may be reasonable, taking into account the long term operation of the facility and safeguards-by-design approach, to install Kr-85 monitors in the beginning of the facility operations period in order to establish a baseline of expected emissions.

As a noble gas Kr-85 will be one of the first effluents to escape and enter the ventilation system. A monitoring systems with sensitivity to low concentrations of Kr-85 can also be used as an indicator of leaking fuel pins or canisters which could have been accidentally damaged or tampered with.

The half-life of Kr-85 is about 11 years, and the current background concentration of Kr-85 in atmosphere in the Northern hemisphere is about 1 Bq/m<sup>3</sup> [Ahlsvede et al., 2013]. This background is caused by a number of sources – previous nuclear tests, nuclear fuel reprocessing activities (e.g. Le Hague in France), medical isotope production (e.g. from the dissolution of the irradiated U-235 targets used for production of Mo-99 generators, as at IRE, Belgium), as well as normal emissions of nuclear power plants. In addition, the proximity of the Onkalo site to the Olkiluoto power plant and the possibility of small releases of Kr-85 from the Encapsulation plant make it necessary to monitor not only the exhaust of the GR ventilation system, but also the intake – in order to establish the baseline “normal” Kr-85 concentration in the GR ventilation system.

The source term for Kr-85 for one ton of heavy metal in spent fuel (roughly equivalent to HM content of one disposal canister) is on the order of 10<sup>12-15</sup> Bq [Kalinowski 1997].

Kr-85 can be partially scrubbed after a release from sheared and dissolved spent fuel. However, various studies conducted on Kr-85 scrubbing over the course of last 50 years never showed that a 100% scrubbing can be achieved [Schoetter, 2009]. Even if a scrubbing system is extremely efficient and can reduce the concentration of the Kr-85 in the ventilation air million-fold, that still leaves a large amount of activity to be detected.

Existing Kr-85 monitoring systems are mostly installed in the stacks of nuclear facilities for regulatory purposes and, since the emission limits on Kr-85 are rather high as it constitutes very low health risk, such monitors are hardly suitable to detect Kr-85 concentrations which are close to the background level.

Atmospheric backgrounds of Kr-85 are studied in a handful of laboratories around the world, the most prominent of them being Bundesamt für Strahlenschutz, Freiburg, Germany [Schlosser et al., 2017] and UniBern environmental laboratory, Switzerland [Loosli et al., 2005]. BFS collects samples cryogenically from around the world at various sampling points over extended periods of time (weeks). The whole air samples are then shipped to the laboratory in Freiburg where they undergo purification using preparative chromatography and then measured using low-level detector systems based on proportional counters. While achieving superbly low minimum detectable activities (Uni Bern underground lab is using Kr-85 for dating ground water, which has very low concentrations of krypton), these lab systems are not suitable for an unattended continuous use.

Different methods are possible for sampling and measuring krypton: cryogenic separation, preparative gas chromatography with pressure and/or temperature swing traps.

Large scale krypton production is happening during the traditional air liquefaction process, in which krypton/xenon mix is produced as a heavy fraction after nitrogen, oxygen and argon are removed using selective evaporation. However, due to the continuous nature of the liquefaction process where part of the cold air is recycled to cool the incoming air a spike in the Kr-85 concentration can be diluted and missed or weakened. Also, cryogenic systems require extra safety precautions and may not be welcome at nuclear installations.

Preparative (large scale vs. analytical which deals with minute amounts of samples) gas chromatography is a common way to separate and enrich various gaseous media. Utilizing the recent progress in manufacturing synthetic zeolites with required properties, more and more industrial gas separations are relying on the chromatographic processes.

Existing systems based on chromatographic separation for noble gases monitoring in air are the Noble Gas (Xenon) monitoring systems of the International Monitoring System of CTBTO [Auer et al., 2004]. The xenon monitoring systems operate continuously in unattended mode even in the most remote regions of the world, with very limited consumables (carrier gases like helium or nitrogen which are required for the gas chromatographic process), and efforts were made in the early 2000s to develop a prototype Kr-85 monitoring systems based on one of the designs (SPARK – SPALAX). The detection capabilities requirement for the IMS Xenon systems are 1 mBq/m<sup>3</sup> (Xe-133), which is 1000 times lower than the natural background of Kr-85, which sets an approximate lower limit for the required detection capabilities of a detection system for a GR ventilation system. Furthermore, the spectroscopy of xenon isotopes is quite complex and subject to interference from radon progeny. Radon has similar molecular size as xenon and is therefore hard to separate from it in the gas chromatographic process. Krypton, on the other hand, is 100 times more abundant in the atmosphere compared to xenon, which makes it a much easier extractable gas. Krypton molecules behave differently and recent studies [Soelberg et al. 2013] shown that silver zeolite adsorbers can be successfully used for krypton separation from ventilation air.

The almost pure beta decay mode of Kr-85 can simplify the analysis of the data, and using an anti-coincidence veto detector system using, for example, a combination of a plastic scintillator gas cell surrounded by a NaI(Cs) crystal scintillator [Khrustalev et al., 2016] can reduce the requirements for the shielding and reduce the size of the monitoring system as a whole.

IAEA, in close cooperation with European Atomic Energy Community, STUK and Posiva Oy is currently working on the development of concept of operation and technical requirements for a Kr-85 monitoring systems designed specifically for monitoring geological repositories

## Microseismic activity monitoring

Posiva Oy is employing a range of geophysical techniques for ensuring the safety of GR operation [Haapalehto et al., 2018]. One of those monitoring tools is a seismic network comprising 17 stations in and around the GR site. The operator is monitoring the site for eventual man-made (induced) seismicity, which may cause a problem in the operations. But the same data can be used to monitor activities underground, such as construction of new shafts, or moving heavy machinery. Using modern digital signal processing methods even signals well below the noise threshold can be identified and located with high precision (less than 10 meters resolution underneath 450 m of hard rock). Such capabilities have not been developed with safeguards purposes in mind, but applications exist already where carefully designed local seismic monitoring networks installed on the surface are used for monitoring commercial mining and drilling activities. One example is fracking where local surface based seismic monitoring networks are used as a state of health diagnostic system allowing the drilling rig operator to locate precisely the position of the drilling head and detect explosions of small (<100g TNT) casing perforation charges which are used to create holes in the concrete casing of the borehole and let the gas or oil from the fracked rocks to flow in and up to the surface. Other use of such network is monitoring for induced seismic events which may cause safety concerns for local populations or the drilling operations.

Another example is the use of Seismic Aftershock Monitoring System (SAMS) for the purposes of discovering aftershocks and cavity collapse after a clandestine nuclear tests as used in the On-Site Inspection verification by the Comprehensive Nuclear Test-ban Treaty Organization (CTBTO) [Gestermann et al., 2013]. SAMS is using a network of surface based detectors which can be deployed in a very short time and provide information on the locations of very weak local events. These technologies developed in the recent years way past the

simple ground motion detection to providing the capabilities to literally hear a rock fall deep underground. Taking those developments and adapting them for safeguards can help ensure the GR black box containment is not breached. IAEA is currently working on a feasibility study for the microseismic data evaluation for safeguards purposes and its data authentication.

## **Conclusion**

The operational phase of the first geological repository for spent nuclear fuel is coming close. A lot of work has been put into thinking about safeguarding such repositories, and many technologies listed as potential candidates. It is high time now to develop detailed requirements for the specific case of the Finnish GR which is well under progress. It is a big step from being a candidate technology to reaching a technological readiness level sufficient for actual safeguards use, and all counterparts to this project are now working towards a realistic safeguard approach. We believe that using the combination of safeguards measures described in this paper we can assure the international community of the continued peaceful use of nuclear material for years to come even when these materials are deposited deep underground.

## References

1. M. Auer, A. Axelson, X. Blanchard, T.W. Bowyer, G. Brachet, I. Bulowski, Y. Dubasov, K. Elmgren, J.P. Fontaine, W. Harms, J.C. Hayes, T.R. Heimbigner, J.I. McIntyre, M.E. Panisko, Y. Popov, A. Ringbom, H. Sartorius, S. Schmid, J. Schulze, C. Schlosser, T. Taffary, W. Weiss, B. Wernsperger. Intercomparison experiment of systems for the measurement of xenon radionuclides in the atmosphere. *Appl. Radiat. Isot.*, 60 (2004), pp. 863-877
2. O. Okko, J. Rautjärvi. EVALUATION OF MONITORING METHODS AVAILABLE FOR SAFEGUARDS USE AT OLKILUOTO GEOLOGICAL REPOSITORY Report on Task FIN C 1572 of the Finnish Support Programme to IAEA Safeguards, 2006, STUK YTO-TR 216, retrieved on May 5, 2019 <http://www.julkari.fi/handle/10024/123299>
3. E. Pentti, E. Heikkinen. Usability of Olkiluoto Monitoring Programme for implementing nuclear safeguards. STUK-TR 28 / DECEMBER 2017, retrieved on May 5 at <https://www.julkari.fi/bitstream/handle/10024/135668/stuk-tr28.pdf?sequence=1>
4. ASTOR (Application of Safeguards TO Geological Repositories) Group of Experts Final report 2017, retrieved on May 5, 2019 from <https://nucleus.iaea.org/Pages/ASTOR.aspx>
5. N. Gestermann, B. Sick, M. Häge, T. Blake, P. Labak, M. Joswig, The Seismic Aftershock Monitoring System (SAMS) for OSI-Experiences from IFE14, *Geophysical Research Abstracts*, Vol. 18, EGU2016-12350-2, 2016, EGU General Assembly 2016
6. C. Schlosser, A. Bollhöfer, S. Schmid, R. Kraiss, J. Bieringer, M. Konrad, Analysis of radionuclides and Krypton-85 at the BfS noble gas laboratory, *Applied Radiation and Isotopes*, Volume 126, 2017, Pages 16-19, ISSN 0969-8043, <https://doi.org/10.1016/j.apradiso.2016.12.043>.
7. Ahlswede, J., Hebel, S., Ross, J. O., Schoetter, R. & Kalinowski, M. B. Update and improvement of the global krypton-85 emission inventory. *J. Environ. Radioact.* 115, 34–42 (2013).
8. K. Khrestalev, J.S.E. Wieslander, M. Auer, A. Gheddou, Calibration of low-level beta-gamma coincidence detector systems for xenon isotope detection, *Applied Radiation and Isotopes*, Volume 109, 2016, Pages 418-424, ISSN 0969-8043, <https://doi.org/10.1016/j.apradiso.2015.11.032>.
9. Loosli, H. H. & Purtschert, R. *Isotopes in the Water Cycle: Past, Present and Future of a Developing Science*, edited by Aggarwal, P., Gat, J. R., & Froehlich, K. (IAEA, Vienna, 2005) pp. 91–95.
10. Kalinowski, M. B., 1997. Measurements and Modelling of Atmospheric Krypton-85 as Indicator for Plutonium Separation. In: *Proc. International Workshop on the Status of Measurement Techniques for the Identification of Nuclear Signatures*, IRMM, Geel 25–27 February 1997.
11. Schoetter, R. Krypton-85 Retention Technologies, in: O. Ross, J. Ahlswede, R. Annewandter, R. Schoetter, P. Stanoszek, M. Kalinowski. First year project report GER1643 (task C.38) Simulation of atmospheric noble gas concentrations to assess sampling procedures for the detection of clandestine reprocessing, JOPAG/01.09-PRG-373, 2009
12. Nick R. Soelberg, Troy G. Garn, Mitchell R. Greenhalgh, et al., "Radioactive Iodine and Krypton Control for Nuclear Fuel Reprocessing Facilities," *Science and Technology of Nuclear Installations*, vol. 2013, Article ID 702496, 12 pages, 2013. <https://doi.org/10.1155/2013/702496>.
13. Haapalehto, S., Malm, M., Kaisko, O., Lahtinen, S., Saaranen, V., Results of Monitoring at Olkiluoto in 2017, *Rock Mechanics*, Working report 2018-47, retrieved on May 5, 2019 from [http://www.posiva.fi/en/databank/workreports/results\\_of\\_monitoring\\_at\\_olkiluoto\\_in\\_2017\\_rock\\_mechanics.1874.xhtml](http://www.posiva.fi/en/databank/workreports/results_of_monitoring_at_olkiluoto_in_2017_rock_mechanics.1874.xhtml)
14. Carchon, Roland, Stefan Jung, Tesfaye Ayalew, Alain Lebrun, Manfred Zendel, Claude Antoine, Xavier Dérobert, Jean-Louis Chazelas, and Michel Larroque. "Ground Penetrating Radar (GPR) for Nuclear Safeguards Design Information Verification." In 11th International Conference on Ground Penetrating Radar. 2006.
15. Saksap, Heikkinen E; Lehtimäki T. Geophysical radar method for safeguards application at Olkiluoto spent fuel disposal site in Finland (STUK-YTO-TR:213), 2005, retrieved on May 5, 2019 at <http://www.julkari.fi/handle/10024/124585>
16. Murtezi M. et al., Getting Ready for Final Disposal of Spent Fuel in Finland—Lessons Learned down the path of the Safeguards-by-Design Cooperation, 2018 IAEA Safeguards Symposium, Vienna

# Verification of Spent Fuel Inside Dry Storage Casks Using Fast Neutrons

Young Ham, Shivakumar Sitaraman, Phil Kerr

Lawrence Livermore National Laboratory  
Livermore, CA 94550  
[Ham4@llnl.gov](mailto:Ham4@llnl.gov)

## **Abstract:**

*Verification of spent nuclear fuel assemblies within dry storage casks has been a major technical challenge for the safeguards regime for decades. Multiple significant quantities and individual accountable items can be present in a single cask, and the substantial amount of irradiated nuclear materials in the world inventory is currently stored in dry storage casks. Conventionally, spent fuel accountancy in dry storage relies on containment and surveillance approaches, and there are no reliable technical means to re-verify the casks content once a breach in the continuity-of-knowledge occurs or an intrusion is suspected. Application of non-destructive assay methods is significantly limited by close packing of assemblies in storage configuration and extensive shielding that prevent reliable evaluation of gamma-ray and neutron signatures on the periphery of the cask. Although multiple solutions have been investigated in the past, none of them worked properly. This problem remains as the priority for the IAEA Spent Fuel Verification and Monitoring Programs and national regulatory authorities.*

*The Lawrence Livermore National Laboratory research team has developed a new approach to dry storage inventory verification. A modeling and experimental study investigates a spatially-dependent fast- and epi-thermal neutron flux distribution measured at the top surface of the dry storage cask. The neutron intensity pattern is collected over a grid within a specified energy range, resulting in a set of images that characterize the assembly loading configuration. If a gross defect is present (due to an assembly diversion) the neutron map image is expected to demonstrate a strong deviation from the expected distribution. The project is evaluating a number of candidate fast neutron detectors and conducting a parametric design study for a prototype instrument. It is expected that this verification methodology can be adapted to a variety of spent fuel cask configurations: from typical concrete enclosures for above-ground interim storage, to metal capsules designated for deep geological disposal.*

*This paper will describe the details and assumptions behind the proposed dry cask verification approach and discuss its capabilities and limitations. Performance of the candidate neutron detection systems and potential design implementations will be discussed. Calculated responses for various spent fuel assembly dry storage configurations and experimental results from laboratory tests will be presented.*

**Keywords:** spent nuclear fuel; dry cask storage; fast neutron spectroscopy; stilbene

## **1. Introduction**

Spent fuel in dry storage is vulnerable to diversion, and there are currently no technical means to re-verify the contents of dry storage casks, once seals attached to the dry storage casks are damaged or inadvertently removed on a closed cask. The difficulty arises as no useful gamma rays or neutrons from the inner spent fuel can penetrate to the outer side surface where measurements can be

performed. Multiple studies in the past based on measuring thermal neutrons or gammas have failed to satisfy IAEA requirements [1] [2][3]. Active interrogation methods using conventional external gamma or neutron sources also are impossible to sufficiently detect diversion because they cannot reach the innermost spent fuel assembly. This problem of re-verification of the integrity of spent fuel inside dry storage has been one of the most technically challenging problems for many decades facing the IAEA as well as other international safeguards communities such as EURATOM or ABACC, and it remains the top priority for the IAEA Spent Fuel Verification and Monitoring Project, one of the top priority R&D needs in the IAEA R&D Plan (T.1.R6), and one of the immediate objectives under Development and Implementation Support Programme for Nuclear Verification 2018-2019 [4] [5].

Lawrence Livermore National Laboratory has embarked upon developing a novel methodology for verification of spent fuel inside dry storage casks through detailed modeling. The verification concept to be developed is based upon collecting and analyzing fast/epi-thermal neutrons coming from the top surface of the dry storage casks. When a set of data is collected with an energy selective/sensitive neutron detector on a grid pattern at the top surface of the dry storage cask, the data can produce a neutron image with epi-thermal neutrons or fast neutrons depending upon what type of neutron is used for data acquisition. In the case of diversion of one or more spent fuel assemblies, the neutron image is expected to show deviation from the typical neutron image. Simulated scenarios using MCNP have demonstrated this behavior.

Having collected the neutron signals from the multiple locations above the subject Dry Storage Cask, one does not rely upon a method of using past measurement results, known as the “fingerprinting” method, because the measured profile can show the diversion in a very clear visual manner.

The first part of this report describes the development of a neutron transport model of a realistic dry storage cask Castor V/21 for performing Monte Carlo simulations. The second part describes laboratory experiments that support the verification concept performed using a Cf252 source and a stilbene fast neutron detector with Castor V/21 measurement geometry.

## 2. Monte Carlo Modeling

We have performed MCNP [6] simulations for a limited set of scenarios. Spent fuel sources were estimated for PWR17x17 fuel from an operating reactor. Castor V/21 was selected for our modeling study partially for the reason that Castor type casks are widely used throughout the world, and much of its design information was available in the open documents. More than 1,300 Castor type casks have already been loaded and stored in sites all over the world.

### 2.1 Spent fuel source term evaluation for Monte Carlo Techniques

Source terms for PWR spent fuel assemblies (SFA) were generated with data obtained from discharged fuel from an actual nuclear power plant. Detailed data on the plant operating conditions were obtained in order to obtain realistic source spectra and isotopics.

Pin by pin burnup estimates were available for a few SFAs. Using this information and the average assembly burnup, pin by pin relative burnup levels were calculated. The average pin power can also be calculated using the assembly average power derived from the data from the power plant. Based on these two parameters, the average power generated by each pin was determined. The total irradiation time was obtained by combining the pin power, the absolute pin burnup and the mass of heavy metal in each pin.

Using these data, ORIGEN-ARP runs were made for each specific burnup using the fuel composition based on the initial enrichment of the SFA [7]. Using the pin power consistent with a burnup level, the initial fuel was burned to that level in discrete time steps over the total number of days of the fuel cycle. A run was made to attain each desired burnup level and decayed to obtain spectra in BUGLE 47 group structure for neutrons and 20 group structure for gammas at various cooling times. The neutron source terms included contributions from both spontaneous fission and ( $\alpha$ , n) events. Neutrons produced by subcritical multiplication are accounted for during the radiation transport process. The isotopics (actinides as well as fission products) consistent with the specific burnup were

also obtained for various cooling times. All ORIGEN runs were based on the mass contained in one fuel rod.

SFAs with uniform burnup and real assemblies with non-uniform burnups can be composed using this set of data. In the case of this specific 17x17 SFA, several sets of data were obtained. Given below are two sample sets of data: at 35 GWd/t at 20 years cooling time and 56 GWd/t at 17 years cooling time.

For a spent fuel assembly that is at least 2 years old since its discharge, the neutron source is dominated by spontaneous fission from Cm244 which has a half life of 18.1 years, and to a lesser extent from Pu240 with half life of 6561 years. Although the ( $\alpha$ , n) component is one to two orders of magnitude less than the spontaneous fission component, the ( $\alpha$ , n) component was still included in the LLNL analyses in the estimation of neutron source. Ignoring the neutron source signal from Cm242 with half-life of only 0.5 years is perfectly acceptable as most of this isotope has decayed away by the time the spent fuel assemblies are transferred into dry storage casks. In the unlikely event that spent fuel less than 2 years old is placed into the dry storage cask, the neutron source from Cm242 cannot be ignored. Thus, the overall spectrum resembles that from a fission source. A set of data of neutron data per fuel rod for 56 GWd/t and 35 GWd/t are provided below in Figure 1.

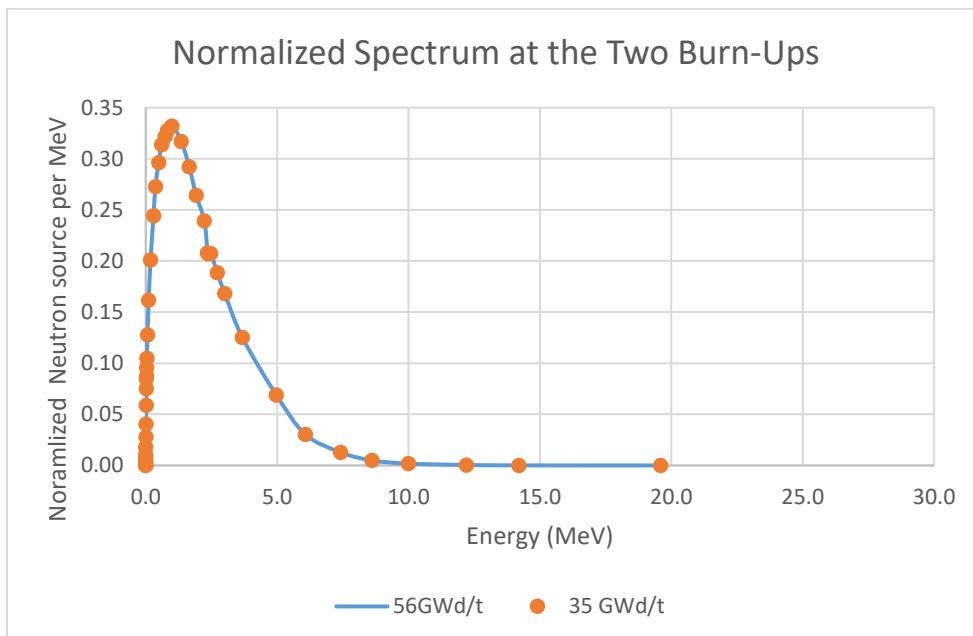


Figure 1: The normalized neutron source spectrum used for the MCNP modelling study for both 35 and 56 GWd/t.

## 2.2 MCNP Modeling with Dry Storage Cask (CASTOR V/21)

The CASTOR V/21 cask was selected for its wide use, and availability here in US for experimental validation of the proposed verification method. The cask is licensed to contain irradiated 14 x 14, 15 x

15 and 17 x 17 PWR fuel assemblies with Zircaloy fuel rod cladding. Total assemblies allowed per cask is less than or equal to 21 [5]. A picture of V21 is shown in Figure 2.

Table 1 shows information and parameters of Castor V/21 used for MCNP modeling. MCNP input information used in the modeling was presented in the form of cross-sectional images of a Castor V/21 DSC that holds 21 17x17 PWR spent fuel assemblies and 21 detectors in Figure 3. One can observe the 290 mm thick primary lid and 90 mm thick secondary lid. Those two lids are dominant shielding material for neutrons coming out of the spent fuel assemblies. In order to optimize computer runtime, 21 detectors with 9.76 cm thick polyethylene (from now on poly in this paper) were placed near the top surface of the DSC. The thickness of the poly was restricted by the need to prevent an overlap with adjacent detectors in the MCNP model. In actuality this restriction will not apply if only one detector system will be used, allowing the poly thickness to be different. Multiple detectors used simultaneously will obviously have limits on the poly thickness. Every detector was placed directly above the center of the PWR spent fuel assembly. Figure 4 shows a close up view of the axial cross-sectional image in which one can observe fuel rods with plenum region as well as the top nozzles, and the poly (blue region) wrapped detectors (wide black region inside the poly and centered on each SFA).



Figure 2: Figure 2 Picture of Castor V/21 which can accommodate PWR 15x15, 16x16 and 17x17.

Parameter Description	Dimension
Overall length of cask	4.866 m (192.4 in)
cross-sectional diameter of the cask body	2.4 m (94.5 in)
Side wall thickness	37.9 cm (14.9 in)
Length of cask cavity	4.154 m (163.5 in)
Diameter of cask cavity	1.527 m (60.1 in)
PWR spent fuel used	Burnup: 50.76 MWd/kg Cooling time: 17 years
Primary lid thickness	29 cm (11.4 in) stainless steel
Secondary lid thickness	9 cm (3.5 in) stainless steel
Detector cylinder	1 inch radius and 10 cm high
Detector shielding	9.76 cm thick poly
Number of histories in MCNP	9x10 <sup>8</sup>
Variance reductions applied	Source biasing Geometry splitting
Energy bins used for tally	.4 eV, .5 MeV, 1 MeV, 2 MeV, 5 MeV, 10 MeV, 20 MeV

Table 1: Information and parameters of Castor V21 used for MCNP

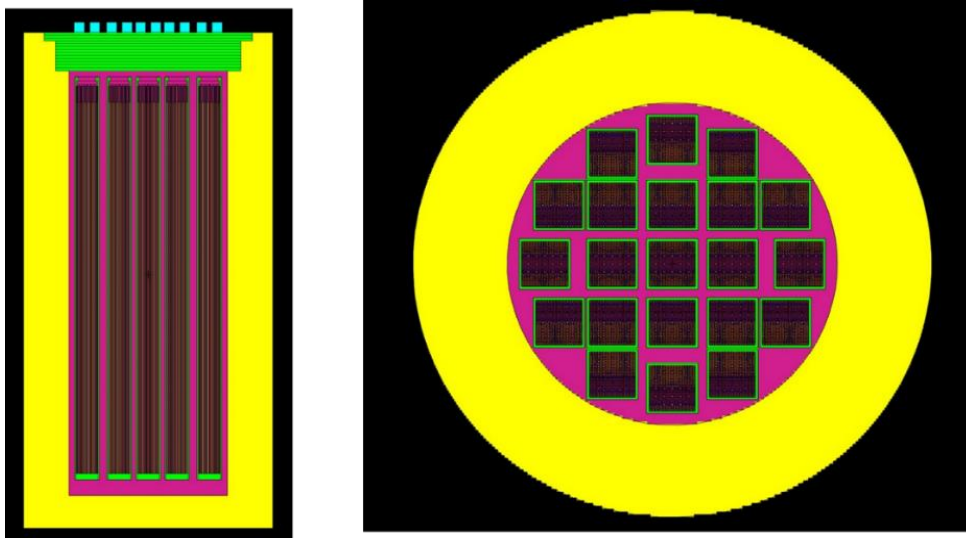


Figure 3: Cut away views of fully loaded CASTOR with 21 17x17 PWR spent fuel assemblies

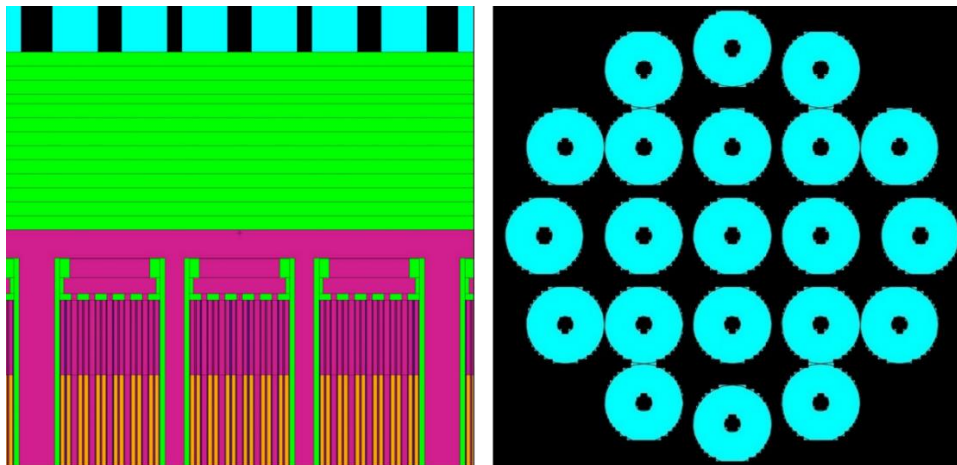


Figure 4: Close up cross-sectional view of MCNP set up. The neutron detectors with poly around them are positioned on the top surface of the CASTOR 21. Every detector is located directly above the center of the PWR spent fuel assembly.

With MCNP input parameters described above, two cases were used in order to investigate the proposed concept of using different neutron energy ranges to detect the diversion of a spent fuel assembly. One case was run with the dry storage cask filled with all 21 spent fuel assemblies. Every spent fuel assembly had a burn-up of 56 GWd/t and 17 years of cooling time. Another case was run with the same condition but with the center assembly replaced with a dummy stainless-steel assembly. This means that the detector 2001 (see Figure 5) would be directly above the diverted spent fuel assembly.

### 2.3 MCNP Results and Discussions

The MCNP results were tabulated using the format shown in Figure 5 below. The left image indicates the five detectors used to generate the flux profile. The numbers in the right image indicate the number used to designate each detector (tally region) where the flux was calculated. Figure 6 shows the MCNP results in a 2D surface plot. The left plot of Figure 6 is obtained for the case of non-diversion whereas the right plot is for the case of diversion where the center assembly was replaced with a dummy stainless steel assembly. Note that how the center part of the surface plot deviated from the non-diversion case.

Table 2 presents the tally results at the 5 detectors in the center vertical line of the basket (see Figure 5) as a function of neutron energy with all 21 spent fuel assemblies whereas Table 3 presents the results when the center assembly (corresponding to detector 2001) is replaced with a dummy stainless-steel assembly. Figure 7 shows the vertical tally profiles, i.e., detector tally through 2003-2002-2001-2004-2005, as the energy tally bin increases. One can observe a cosine-like shape for the case of no diversion. (The last plot in Figure 7, which corresponds to the tally for the neutron energy 10-20 MeV, did not show a cosine-like shape as the statistical uncertainty for that value was too high. You can find this information in Table 4.) Note how the vertical tally profile obtained with a diversion (orange line) deviates further from the profile with no diversion (blue line) as neutron energy increases. In particular, the profiles with the neutron energies above 1 MeV can visually demonstrate the case of a diversion. This profile method can be a powerful tool as the methodology detects a diversion and it does not require earlier measurement for comparison as in the fingerprinting method.

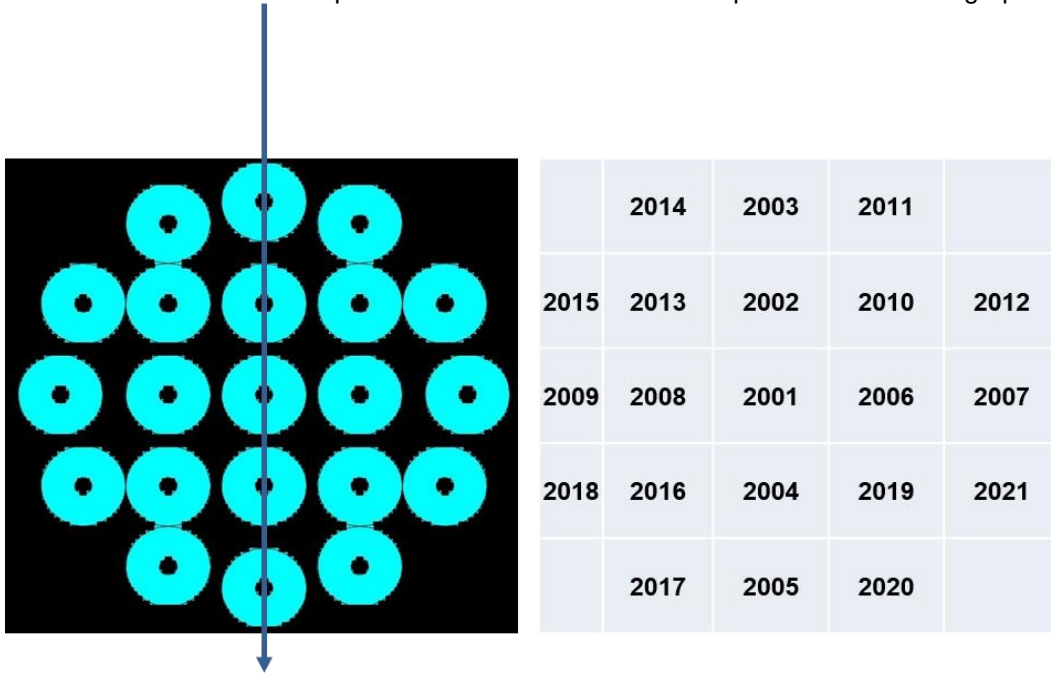


Figure 5: The left figure indicate how data were read and shown as a graph later for easy analysis and results presentation. The numbers in the right figure indicate neutron tally (detector) number which is essentially relative neutron flux.

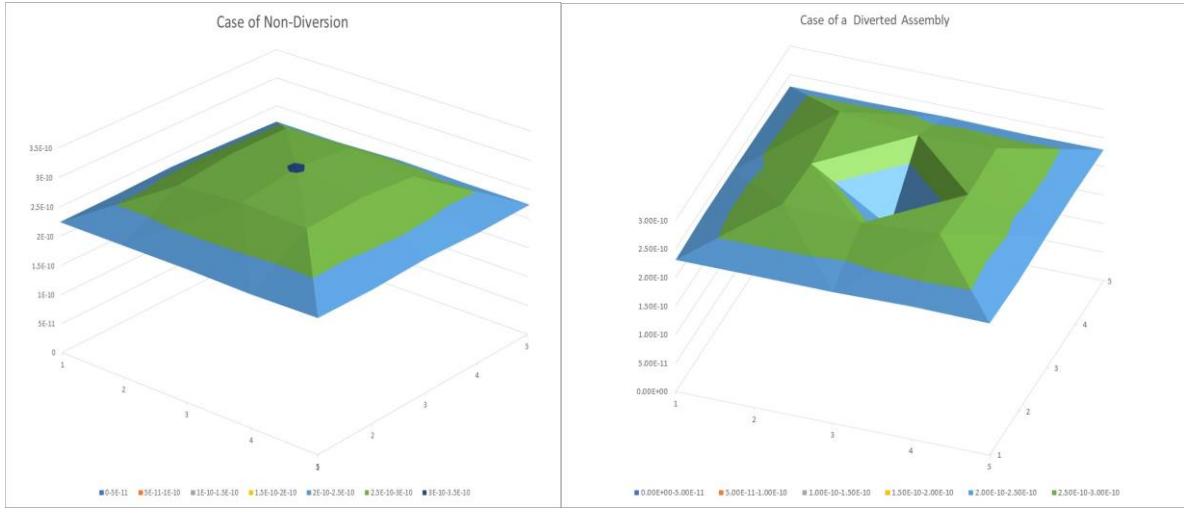


Figure 6: The left figure is obtained for the case of non-diversion. The right figure is for the case where the center assembly was replaced with a dummy stainless steel assembly. Note the deviation in the center in the right figure. This method does not depend on any past measurements. The verification can be easily done by a visual method.

	Tally (Detector) Number for full assemblies				
Neutron Energy	2003	2002	2001	2004	2005
0 - 0.4 eV	4.18E-07	5.74E-07	6.06E-07	5.74E-07	4.18E-07
0.4 eV - 0.5 MeV	3.82E-07	5.25E-07	5.53E-07	5.24E-07	3.82E-07
0.5-1 MeV	1.40E-08	1.89E-08	1.88E-08	1.89E-08	1.38E-08
1-2 MeV	1.97E-09	2.56E-09	2.21E-09	2.52E-09	1.96E-09
2-5 MeV	2.30E-10	2.75E-10	1.92E-10	2.76E-10	2.31E-10
5-10 MeV	3.09E-11	3.55E-11	2.36E-11	3.82E-11	3.12E-11
10-20 MeV	1.52E-12	2.28E-12	1.28E-12	2.29E-12	1.92E-12
Total	8.16E-07	1.12E-06	1.18E-06	1.12E-06	8.16E-07

Table 2: Tally at vertical center 5 detectors as a function of neutron energy with full intact assemblies.

	Tally (Detector) Number with a dummy assembly (2001)				
Neutron Energy	2003	2002	2001	2004	2005
0 - 0.4 eV	4.16E-07	5.84E-07	6.29E-07	5.83E-07	4.16E-07
0.4 eV - 0.5 MeV	3.80E-07	5.34E-07	5.75E-07	5.33E-07	3.80E-07
0.5-1 MeV	1.38E-08	1.96E-08	2.10E-08	1.95E-08	1.37E-08
1-2 MeV	1.92E-09	2.65E-09	2.76E-09	2.64E-09	1.92E-09
2-5 MeV	2.24E-10	2.88E-10	3.02E-10	2.92E-10	2.26E-10
5-10 MeV	3.05E-11	3.85E-11	3.95E-11	3.83E-11	3.07E-11
10-20 MeV	1.74E-12	2.00E-12	2.14E-12	2.34E-12	1.93E-12
Total	8.12E-07	1.14E-06	1.23E-06	1.14E-06	8.11E-07

Table 3: Tally at vertical center 5 detectors as a function of neutron energy with the center assembly replaced with a dummy stainless-steel assembly.

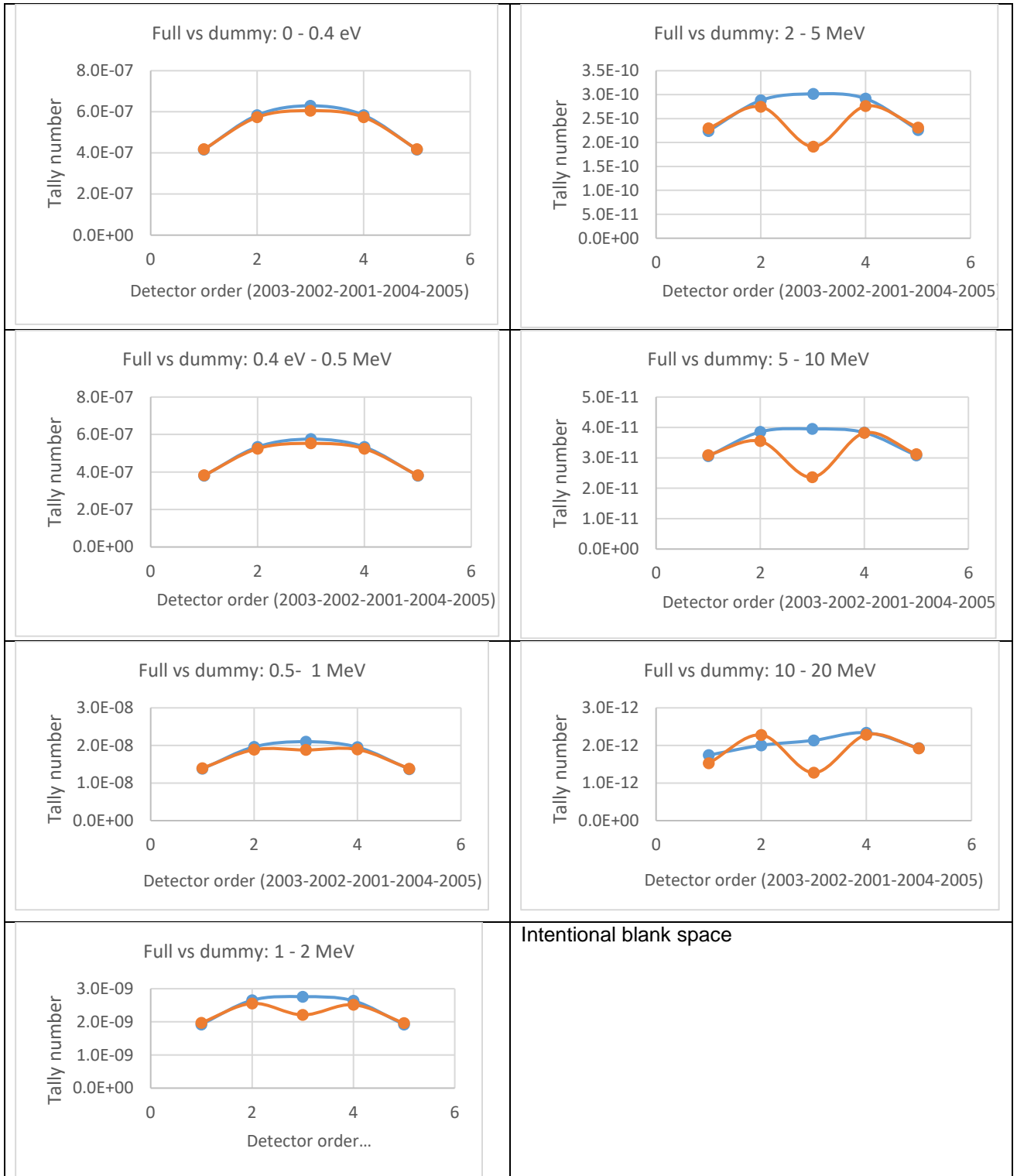


Figure 7: Vertical tally profiles, i.e., detector tally through 2003-2002-2001-2004-2005, as the energy tally bin increases.

Table 4 shows the neutron tally at the detector 2001 for the case of non-diversion as well as the case with the diversion of an assembly at the center. While the neutron detector tally decreases exponentially with increasing energy, the difference in the flux between the non-diverted and diverted case increases with increasing energy. The amount of deviation,  $\varepsilon$ , is defined as

$$\varepsilon = (\text{neutron tally with no diversion} - \text{neutron tally with diversion of an assembly that is subject to verification}) / \text{neutron tally with no diversion}$$

The deviation is a useful quantitative indicator of the diversion of an assembly. The amount of deviation was plotted in terms of neutron energy in Figure 8. For example, if one uses a neutron detector that measures neutron energy in the 2-5 MeV, the relative difference would be 36.4%

Cell	2001 (Full)		2001 (Diverted)		Deviation ( $\epsilon$ )
Neutron Energy (MeV)	Tally	Error	Tally	Error	
0 - 0.4 eV	6.29E-07	0.07%	6.06E-07	0.07%	<b>3.66%</b>
0.4 eV - 0.5	5.75E-07	0.07%	5.53E-07	0.08%	<b>3.83%</b>
0.5-1	2.10E-08	0.24%	1.88E-08	0.25%	<b>10.5%</b>
1-2	2.76E-09	0.55%	2.21E-09	0.76%	<b>19.9%</b>
2-5	3.02E-10	0.89%	1.92E-10	1.21%	<b>36.4%</b>
5-10	3.95E-11	2.12%	2.36E-11	3.13%	<b>40.3%</b>
10-20	2.14E-12	8.55%	1.28E-12	14.24%	<b>40.2%</b>
Total	1.23E-06	0.07%	1.18E-06	0.07%	<b>3.90%</b>

Table 4: neutron intensity, the tally at detector 2001, for the case of non-diversion and the case with the diversion of an assembly at the center. Relative difference can be interpreted as deviation.

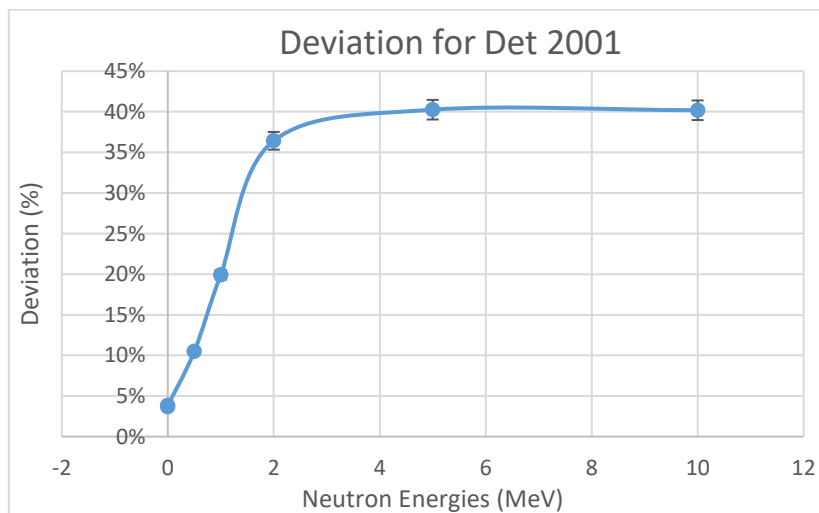


Figure 8: Deviation for detector 2001 in terms of neutron energy. Note how the deviation increases rapidly as neutron energy increases. Here deviation shows the degree of deviation from the case of non-diversion.

It is important to note that the tally used in the MCNP simulation did not account for detector efficiency as the choice of the ideal fast neutron detector to be implemented in the verification tool has not been determined yet.

### 3. Experiments

An experiment was set up in the laboratory to validate the verification concept as a precursor before doing actual validation measurements at a dry storage cask site. The measurement geometry was arranged to mimic the data acquisition for the dry storage measurement environment (see Figure 9.) For the experiments, we selected a stilbene detector, one of the several fast neutron detectors to be studied, to obtain fast neutron signals due to its high efficiency, commercial availability of large sizes, and good characterization of gamma discrimination by use of pulse shape discrimination (PSD). As stilbene is known to be very responsive to gamma rays, PSD application to the measured data is critically important to assess neutron signals. The PSD method is based on the difference in the decay time of fluorescence emitted within an organic scintillator as a result of a reaction between the

ionizing particle and the scintillator. The fluorescence decay time for heavy particles, such as protons, or neutrons is much longer than that of electrons.

The data acquisition system consists of a Fast Comtec MPA-3 four channel multiparameter system, and a Mesytec MPD-4 pulse shape discriminator unit. The MPD-4 unit examines the time structure of the electrical pulse from the PMT to discriminate between neutrons and gamma rays that interact with the stilbene scintillator.

As shown in Figure 9, a 4-inch diameter, 2-inch deep stilbene was used to collect one set of data when the Cf252 was placed directly below the detector in the center of the collimator space (position 1), and another set of data when the Cf252 placed at the off-collimator position (position 2). The detector was placed at 8.5 cm above the top surface of the steel inside the cavity of a poly collimator. Each set of data was collected over a measurement time of 1 day. The distance between the two Cf252 source positions was set to be at 27.75 cm representing actual pitch of two adjacent SFAs on the center line of two SFAs as stored in the Castor cask.

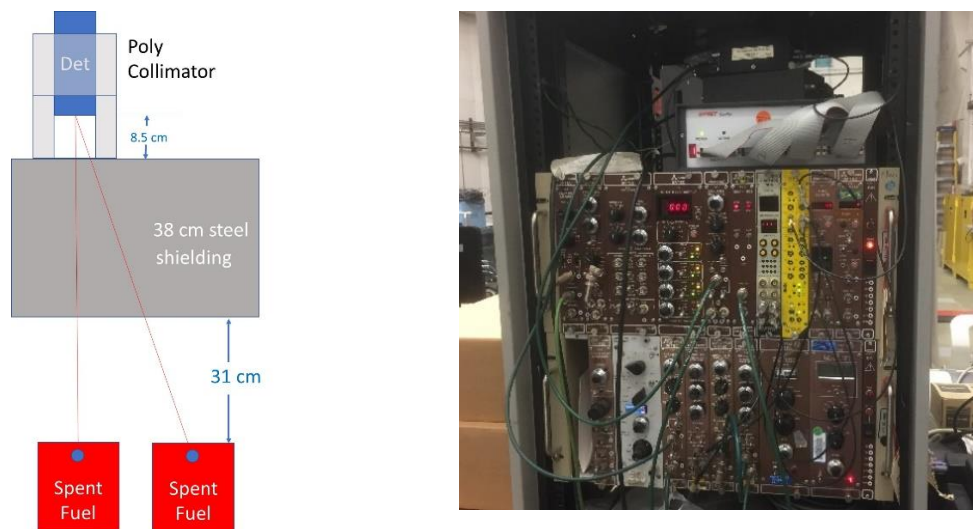


Figure 9: Experimental set up and data acquisition electronics. The picture on the right shows the Fast Comtec MPA-3 four channel multiparameter system on the top, and a Mesytec MPD-4 pulse shape discriminator unit in the NIM bins.

#### 4. Results and Data Analysis

PSD plots obtained with the stilbene scintillator using PSD electronics for the case of a Cf252 source placed directly below the detector and the source at the off-collimator position are shown in Figure 10. The neutron signals were attenuated by 38 cm of steel which is the thickness of the Castor V/21 lids. The upper neutron band signals were well separated from the lower gamma band signals.

Note that in the PSD plots in Figure 10, the neutron signal bands contain energy information, but they do not represent the direct neutron energy information. Thus, the PSD plots cannot be treated as neutron energy spectra requiring unfolding of the PSD plots. As the process of unfolding spectra requires substantial efforts and is perhaps cumbersome to apply for verification, we explore a method for the PSD plots be directly applicable for verification. As our verification methodology requires information on the energy of neutrons that come into the detector, particularly, the energy threshold of 1 MeV or 2 MeV in the measured spectra produced by poly-energetic neutron source, i.e. spent fuel, an effective neutron calibration method is needed. One approach that we adopted is making use of a D-D neutron generator knowing that it produces near monoenergetic neutrons approximately at 2.4 MeV.

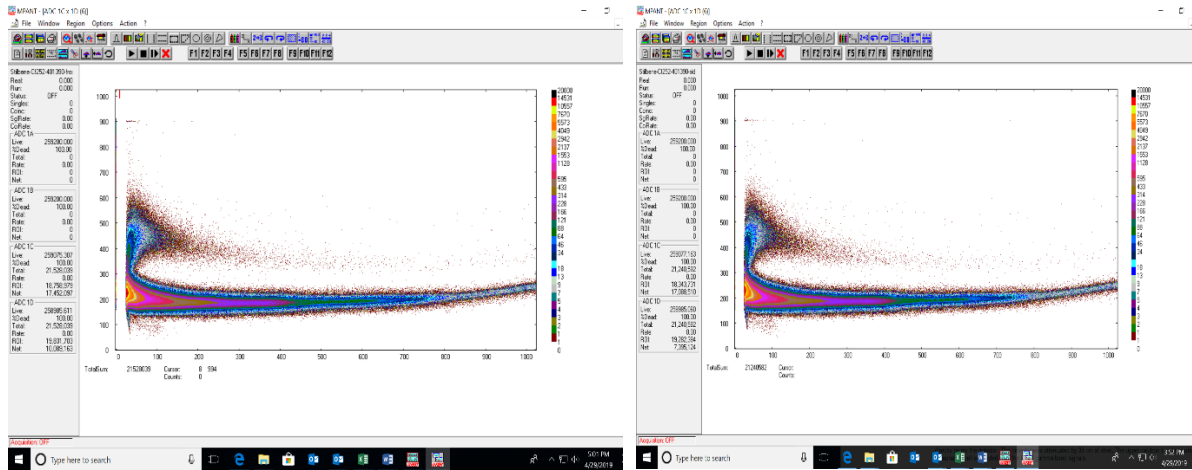


Figure 10: PSD plots obtained with the stilbene scintillator using PSD electronics for the case of Cf source placed directly below the detector and the source off the collimator position. The radiations were attenuated by 38 cm of steel. The upper neutron band signals were well separated from the lower gamma band signals.

The left plot in Figure 11 shows the PSD plot produced by stilbene with the use of a D-D 2.4 MeV neutron generator. Observe a distinctive end of neutron band that ends in near channel 170, a feature that can be useful to separate neutron signals below 2.4 MeV for the data obtained with poly-energetic neutron source such as Cf252 or spent fuel. Using this piece of information, the region of interest (ROI) was selected to capture neutrons above 2.4 MeV from the PSD plots obtained at two source positions (see the right plot in Figure 11.)

D

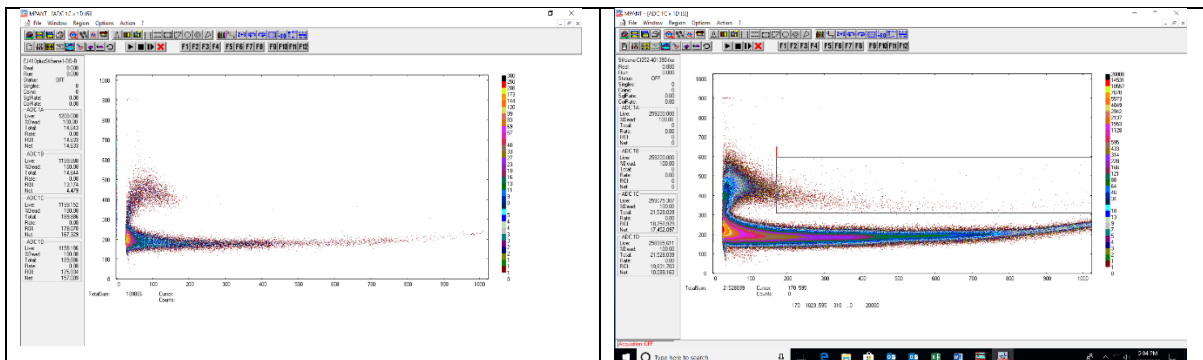


Figure 11: PSD plot in the left obtained with the stilbene scintillator using PSD electronics and DD 2.4 MeV neutrons. Note that there is a distinctive end of neutron band, showing a feature that can be useful to separate neutron signals. The information is used to select a rectangular ROI that predominantly has neutrons with energy greater than approximately 2.4 MeV. An example of ROI selection is shown in the right plot.

**The neutron counts in the ROIs were found to be 8051 +/- 1.2% and 5753 +/- 1.3% with background subtraction respectively for source position 1 (on collimator axis) and position 2 (off collimator axis).** This corresponds to the difference in neutron signals by 27.7%. The amount of deviation is difficult to estimate with this value alone in the V/21 arrangement, but the deviation would be close to 20%. The experimental result will significantly be improved by selecting a smaller diameter stilbene, a thicker collimator and the optimal position of the detector. Further experiments are in progress.

The results obtained in these experiments showed that verification of spent fuel inside dry storage casks is possible by use of stilbene and a simple 2.4 MeV energy threshold method. The results are also consistent with MCNP modeling results, although a direct comparison of the experimental results with the MCNP modeling results was not possible due to different geometry and inability of using spent fuel in the experiments in the lab environment. Besides the stilbene, several different types of

fast neutron detectors are also being explored as a potential fast neutron detector to be a part of the verification system for verification of spent fuel in dry storage casks.

## 5. Conclusions

A novel methodology was proposed to address the long unsolved technical problem of verification of spent fuel inside dry storage casks. The verification concept uses an energy selective neutron detector measuring neutron signals on a grid pattern at the top surface of the dry storage cask. In the case of diversion of one or more spent fuel assemblies, the neutron image is expected to show deviation from the typical neutron image. The verification method is intuitive, easy to interpret, and does not rely upon any past measurement results. Simulated scenarios using MCNP have demonstrated this capability. A simplified laboratory experimental results using Cf252 and a stilbene scintillator showed that the proposed methodology is indeed very promising.

## 6. Acknowledgements

This work was sponsored by the U.S. Department of Energy, National Nuclear Security Administration, Office of Nonproliferation and Arms Control, International Nuclear Safeguards program, and performed under the auspices of the US Department of Energy by Lawrence Livermore National Laboratory under Contract DE-AC52-07NA27344.

## 7. References

1. Ziock K .et. al.; *The Feasibility of Cask "Fingerprinting" as a Spent-Fuel, Dry-Storage Cask Safeguards Technique*; UCRL-TR-215943; 2005
2. Jayson C. et. al.; *Summary Report: INL CDCIS Cask Scanner Testing at Doel, Belgium*; 2013
3. Santi P. et. al.; *Initial Measurement of BN-350 Spent Fuel in Dry Storage Casks using the Dual Slab Verification Detector*; LA-UR-10-03849; 51<sup>st</sup> INMM Annual Meeting Baltimore MD; 2010
4. STR-385, *Research and Development Plan*, IAEA; 2018
5. STR-386, *Development and Implementation Support Programme for Nuclear Verification 2018-2019*
6. Werner C.J. (editor); *MCNP Users Manual - Code Version 6.2*; Los Alamos National Laboratory, report LA-UR-17-29981; 2017.
7. Reardon, B. T. et. al.; *Scale Code System, Version 6.2.3, ORNL/TM-2005/39*; Oakridge National Laboratory; 2018.

# **Session 9:**

# **Nuclear Security**

# **Detection**

# Development of active non-destructive analysis technologies for nuclear nonproliferation and security of JAEA

Mitsuo Koizumi

Japan Atomic Energy Agency (JAEA)  
Shirakata Shirane 2-4, Toukaimura, Naka, Ibaraki 319-1195, Japan  
E-mail: koizumi.mitsuo@jaea.go.jp

## Abstract:

*The Japan atomic energy agency (JAEA) is developing active non-destructive assay (NDA) technologies for nuclear nonproliferation and security under the support of the subsidiary of for "promotion of strengthening nuclear security or the like" of the Japanese government MEXT. One of the programs is "development of active neutron NDA techniques", in which four techniques are developed: i.e., Differential Die Away Analysis (DDA), Delayed Gamma-ray Analysis (DGA), Neutron Resonance Transmission Analysis (NRTA), and Prompt Gamma-ray Analysis (PGA). These techniques are used to complement each other. They would be useful for nuclear material accountancy, applicable to both low- and high-level radioactive nuclear materials (NMs), and for nuclear security purposes such as detection of NM and explosive materials. Another program is "development of nuclear resonance fluorescence (NRF) technique" for measurement/detection of NM. This technique utilizes quasi monochromatic gamma-rays produced by laser Compton scattering (LCS) to irradiate a suspicious sample and observe NRF gamma-rays from that. Demonstration experiment of NM hidden in a shield is being prepared.*

**Keywords:** active interrogation; non-destructive assay; neutron interrogation; Nuclear Resonance Fluorescence (NRF)

## 1. Introduction

Along with the global increase of use of nuclear materials (NMs), the requirements are growing for the development of effective characterization methods used for nuclear material accountancy. Non-destructive Assay (NDA) methods are an efficient and quick way for detection and quantification of NMs. They are commonly used in accountancy and safeguards together with more accurate destructive analysis (DA) methods. However, commonly used passive NDA techniques are not applicable to measure a high-level radioactive NM sample because of the interference of the radiation background from a sample. Department of safeguards are encouraged by IAEA [1,2].

Active NDA techniques utilize interrogation particles (such as photons and neutrons) to induce nuclear reactions to produce a radiation signature from a sample. Measurement and analysis of the induced differences in radiations and incident particles are used to extract information of nuclear and matrix materials in the sample. These methods are potentially applicable to analysis of high-level radioactive NM samples and to detection of NMs hidden in a shield.

The Japan atomic energy agency (JAEA) is developing active non-destructive assay (NDA) technologies for nuclear nonproliferation and security under the support of the subsidiary for "promotion of strengthening nuclear security or the like" of the Japanese government MEXT. One of the programs currently running is "development of active neutron NDA techniques", in which four techniques are developed: i.e., Differential Die Away Analysis (DDA), Delayed Gamma-ray Analysis (DGA), Neutron Resonance Transmission Analysis (NRTA), and Prompt Gamma-ray Analysis (PGA). These techniques are briefly given in table 1 and could be used to complement each other. It would be applicable to nuclear material accountancy for both low- and high-level radioactive NM sample, and to nuclear security purposes for detection of NM and explosive materials.

Another program is “development of nuclear resonance fluorescence (NRF) technique” for detection of NM hidden in a shield. This technique utilizes quasi monochromatic gamma-ray beams produced by laser Compton scattering (LCS). The energy of LCS gamma-rays is tuned to a nuclear resonance energy of a nuclide to be found. NRF gamma-rays induced by LCS gamma-rays are observed by gamma-ray detectors.

This paper will present the project activities of “Development of active neutron NDA techniques” and “Demonstration of NRF NDA technique for NM detection”.

Active Neutron Technique	Description	Quantification
DDA	Pulsed neutron interrogation method that measures a time-dependent neutron die-away curve depending on the neutron emission of induced fission reactions.	$^{239}\text{Pu}$ -effective mass
PGA	Measurement of prompt gamma rays induced by (n, gamma) and the other reactions. Characteristic gamma rays are used to identify nuclides within the sample.	Existence, and qualification/quantification of specific nuclide
NRTA	Neutron time-of-flight (TOF) measurement, in which nuclide characteristic dips are observed in an energy-dependent transmission spectrum at the nuclear reaction resonance energy.	Quantity of each of U/Pu nuclides
DGA	Measurement of gamma rays in decay of fission products resulting from neutron induced fission reactions	Ratio of $^{235}\text{U}/^{239}\text{Pu}/^{241}\text{Pu}$

**Table 1:** four neutron interrogation techniques

## 2. Development of active neutron NDA techniques

Development of active neutron NDA techniques started as a program of “Development of neutron resonance densitometry (NRD)” between 2012 to 2015 Japanese Fiscal year (JFY). NRD was proposed as an analysing method of particle like debris of melted fuel, which has a complicated components, shape and high radioactivity. This method is a combination of NRTA for NM quantification in a debris sample within few % accuracy, and PGA or neutron resonance capture analysis (NRCA) for qualification/identification of matrix elements of the sample [3-7].

After this program, “Development of active neutron NDA techniques” was started. Figure 1 roughly shows the time line of the program. Basic technological development of four active interrogation methods, DDA, DGA, PGA, and NRTA, was conducted. In the phase I program, from 2015 to 2017 JFY. Measurement of low-level radioactive materials were the goal of the basic technological development [8,9].

DDA is a neutron interrogation technique used to measure total amount of effective  $^{239}\text{Pu}$  mass in a sample [10]. A DDA system consists of a sample cavity surrounded by reflector walls, a pulsed neutron source (a DT neutron generator, for example), neutron detectors that measure the time-dependent neutron die-away curve, and an outermost radiation shielding. The quantity of fissile material in a sample can be determined from the observed neutron die-away curve that changes due to the neutron emission from neutron-induced fission reactions.

A JAEA-DDA system is based on the Fast Neutron Direct Interrogation (FNDI) technique [11-13], which utilizes fast and epi-thermal neutrons. A sample cavity made of neutron reflector walls such as stainless steel (SUS) are used instead of a conventional graphite reflector. This increases fast neutron flux and reduces neutron absorption at the surface of a sample. The fast neutrons are thermalized in sample matrix materials and high-density polyethylene (HDPE) surrounding the sample. This increases induced fission reactions inside the sample. The detection efficiency of fast neutrons of fission reactions inside the sample is, oppositely, lower than that from near the surface of the sample. The both effects compensate to flatten the position sensitivity of the system. That is an advantage of the

FENDI technique. This reduces the uncertainty of the system owing to the distribution of NMs within a large sample volume.

PGA utilizes the neutron-capture reactions resulting in prompt gamma-ray emissions that are specific to the reacting nuclide [12]. Existence and qualification/quantification of the nuclides are analysed from the observed prompt gamma rays. Addressing nuclear safeguards, this technique can be applied to analyse nuclides that influence the other measurements (i.e., neutron toxins, absorbers, and the other composing materials). In the NRD technique, PGA/NRCA identify/quantify boron and the other matrix elements in a melted fuel debris sample; that information would be used to the analysis of quantification of NM in a sample measured by NRTA. The other application of PGA relevant to nuclear security is detection of explosive material and toxic chemicals in a suspicious object found somewhere.

An integrated DDA and PGA system, named Active-N Mark-II, has been constructed at the NUCEF (Nuclear Fuel Cycle Safety Engineering Research Facility) facility of JAEA [13]. A high intensity DT neutron source is installed to the system. A Pu sample of 0.002-1 g in a small volume (vial bottle size) was successfully detected by the DDA part. Detection of nitrogen (contained in high explosives) and other elements potentially contained in chemical warfare agents (As, P, Cl, and S) were detected by the PGA part. In this development, it was found that strong prompt gamma-ray background came from cavity materials and reduced the sensitivity of the PGA measurements. Further development is in progress for reducing the background to improve detection efficiency by changing the structure materials, and passive and active detector shielding.

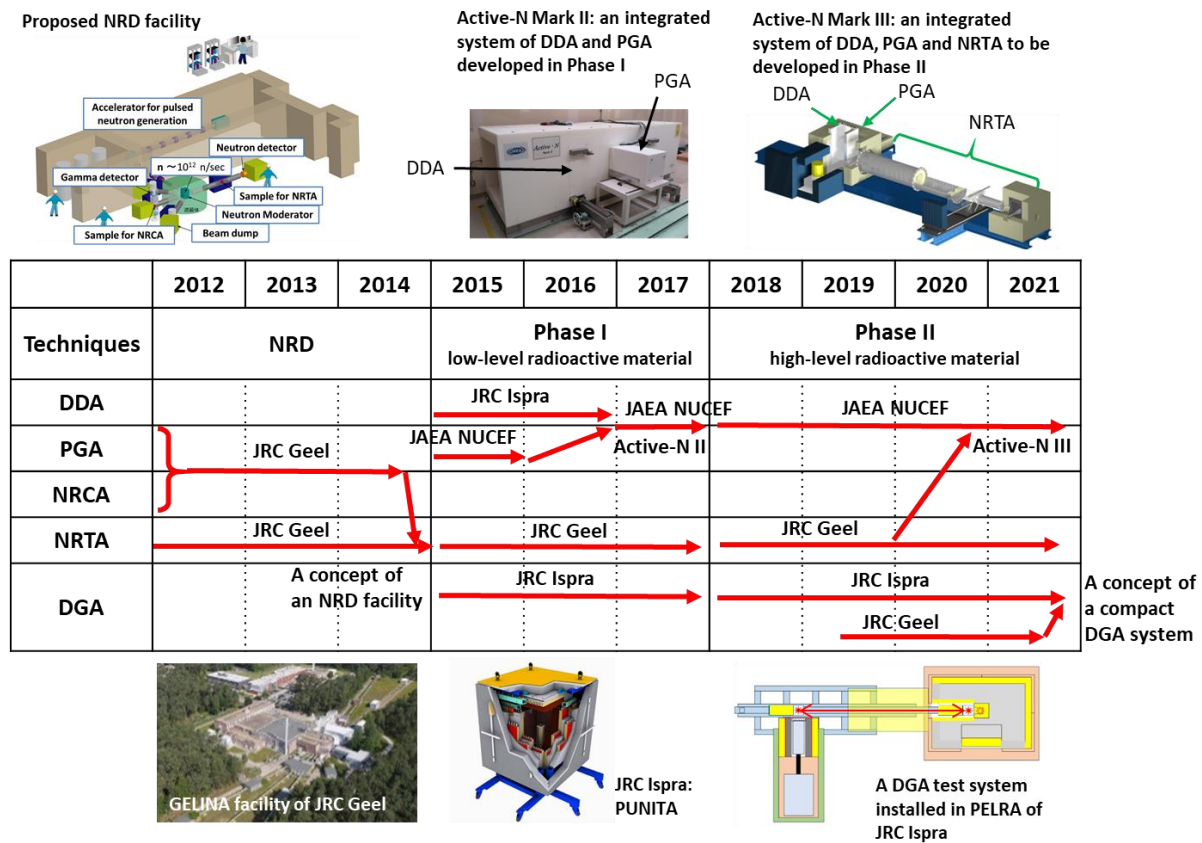
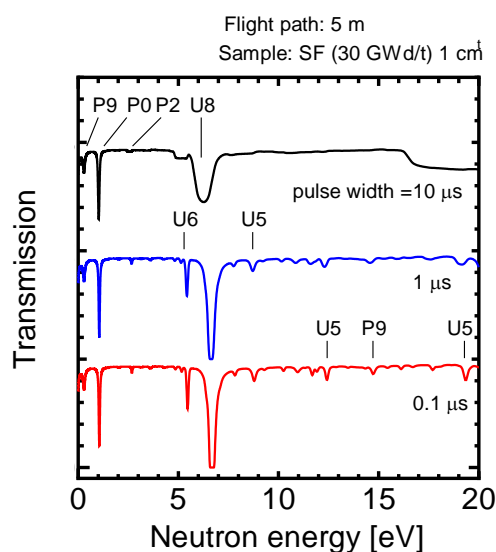


Fig. 1: Time line of development of active neutron NDA techniques conducted under the collaboration between the JAEA and the JRC.

NRTA is a pulsed neutron interrogation NDA technique for quantitative analysis of each nuclide [14]. Neutrons having a broad energy distribution fly from a moderator placed near a neutron generator to a distant neutron detector. A sample is placed in the flight path. Time of flight (TOF) of a neutron is used to evaluate the velocity (or kinetic energy). Then, an energy dependent neutron transmission spectrum is achieved. Because neutrons are resonantly absorbed or scattered in a sample according to the nuclide-specific neutron reaction, dips appear in a neutron transmission spectrum, from which an areal

density of each nuclide is deduced. This technique can be applicable for quantification of NM, MA and the other nuclides as demonstrated in refs. [15-17].

The energy resolution of an NRTA spectrum at high energy region increases with decreasing neutron pulse width and increasing flight path length. For practical applications, a compact NRTA system with a short flight path are desirable. Figure 3 shows simulated energy-dependent transmission spectra of neutrons passing through a 1-cm-thick sample in which compositions of a spent fuel of a 30 GWd/t spent fuel is used [17,18]. The flight path length is fixed to be 5 m, and neutron pulse width is varied. It can be seen that the width of dips at high neutron energy becomes narrow with decreasing pulse width. By using a DT neutron source (pulse width of 10  $\mu$ s), areal densities of  $^{238}\text{U}$  and  $^{239,240,242}\text{Pu}$  can be deduced from the TOF spectrum [17]. An integrated NDA system Active N Mark-II will be upgraded by installing a NRTA system. The system for DDA, PGA, and NRTA, named Active-N Mark-III, can perform three different kind of analysing methods by using one DT neutron source.



**Fig. 2:** Simulated energy-dependent transmission spectra of neutrons passing through a 1-cm-thick sample in which compositions of a spent fuel of 30 GWd/t spent fuel is used [17,18]. The flight path length is fixed to be 5 m. Neutron pulse width is varied: 10  $\mu$ s (black), 1  $\mu$ s (blue), and 0.1  $\mu$ s (red). The vertical positions of the plots are moved for the sake of clarity. The notation of P9, P0, P2, U5, U6, and U8 are relevant to nuclides of  $^{239,240,242}\text{Pu}$ , and  $^{235,236,238}\text{U}$ , respectively.

In order to improve the analysing power of a compact NRTA system, a short-pulsed neutron source is required. One of such neutron sources that provide pulsed neutron with less than 0.1  $\mu$ s is an electron accelerator driven neutron source. A laser driven neutron source (LDNS) could be the one in future. By utilizing a high intensity short pulsed laser beam to produce dense plasma and to accelerate ion beam, an LDNS generates neutrons through nuclear reaction between the accelerated particle and a target material. The neutron production area is small and the pulse width is narrow. Because a laser system can be placed outside a laboratory where NM are analysed and laser beams can be transferred by mirrors, installation and maintenance of an LDNS probably easy. In order realize such LDNS, required developments are on size, power and repetition rate of a laser system, efficient neutron production target system, and neutron moderator system. A feasibility study LDNS for NRTA measurement is implemented in a four-year program starting from 2018 JFY.

DGA utilizes neutrons to induce fission reactions. Resulting radioactive fission products (FPs) emit gamma rays following their radioactive decay chains. The decay gamma rays are measured after stopping neutron irradiation. A measurement-after-irradiation sequence is repeated to achieve enough statistics of the gamma rays of interest. Because the fission yield (FY) distribution of each fissile nuclide differ, the strengths of delayed gamma rays are characterised by each of the fissile nuclide. The relative peak intensities of an observed gamma-ray spectrum are, therefore, used to analyse the ratios of fissile nuclide in a sample. Strong gamma-ray background from radioactivity of  $^{137}\text{Cs}$  and other relatively long-lived FPs is expected in a measurement of high-level radioactive sample. However, those background

gamma rays do not interfere high energy delayed gamma-ray peaks above 3 MeV from relatively short-lived FPs [19,20].

DGA experiments were carried out with an apparatus, PUNITA (Pulsed Neutron Interrogation Test Assembly) [21,22], of EC-JRC Ispra, which consists of a large graphite inner box and a HDPE outer box. The inside of the box is a sample cavity of 50 cm in width (W), 50 cm in length (L), and 80 cm in height (H). A standard pulsed 14-MeV DT neutron generator ( $2 \times 10^8$  n/s neutron emission) is placed in it. Around the generator, tungsten rings with a thickness of 4.5 cm is used for neutron multiplication by (n, 2n) reaction and slowing down the neutrons [23]. Further neutron moderator (carbon bricks and HDPE cavity surrounding the sample) were additionally installed in the sample cavity to increase thermalized neutrons. This induces more fission reaction and increases gamma-ray peak yields. Furthermore, the following contributions are reduced: (1) fission reaction of  $^{238}\text{U}$ , the cross-section of which becomes higher with a neutron energy above 1 MeV, and (2) different fission reaction channel induced by high energy neutrons.

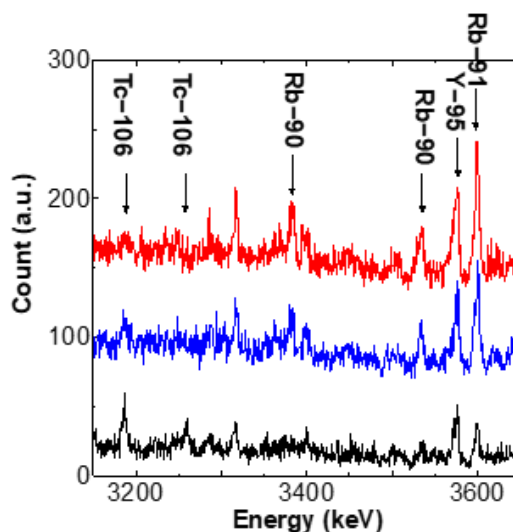


**Fig 3:** High energy delayed gamma-ray spectra measured with PUNITA (Pulsed Neutron Interrogation Test Assembly) of EC-JRC Ispra. The samples used are combinations of 170-g U ( $^{235}\text{U}$  concentration is varied from 0.0 to 4.46 wt% ) and  $^{239}\text{Pu}$  (the weight is varied from 10 mg to 9.5 g). The total fissile masses were approximately 10 g. The difference of each spectrum is due to the mass ratio of  $^{235}\text{U} : ^{239}\text{Pu} = 1:0$  (red), 1:1 (blue ), and 0:1 (black), respectively. The measurements were repeated 50 times of 50-sec neutron-irradiation and 50-sec gamma-ray-measurement sequence.

An experiment was carried out with samples that are combinations of 170-g U ( $^{235}\text{U}$  concentration is varied from 0.0 to 4.46 wt% ) and  $^{239}\text{Pu}$  (the weight is varied from 10 mg to 9.5 g). The total fissile masses were controlled to be approximately 10 g. The measurements were repeated 50 times of 50-sec neutron-irradiation and 50-sec gamma-ray-measurement sequence. The time for sample transportation between the position for irradiation and measurement was less than 1 s. Figure 3 shows gamma-ray spectra observed by using different fissile nuclide ratios: i.e.,  $^{235}\text{U} : ^{239}\text{Pu} = 1:0$  (blue), 1:1 (black), and 0:1 (red), respectively. This confirm a potential for analysing concentration of fissile nuclides.

In the phase II program of DGA development, design of a compact NDA system is in progress. A Cf neutron source and a DD neutron generator are considered because the initial neutron energy are less than that of a DT neutron source, this enables to make the size of moderator, reflector and radiation shielding smaller. A test experiments are in progress at a Performance Test Laboratory (PERLA) of EC-JRC Ispra.

The four techniques can be applied for complementary analysis of a NM sample. Table 2 shows examples of nuclear safeguards applications. PGA technique is used for elemental analysis of sample matrix materials, which may help precise analysis of the other techniques. In addition, a combination of DDA and PGA techniques would be useful for nuclear security application for detecting nuclear, chemical and explosive material in a suspicious object.

Combination	Measured quantities	Deduced nuclides masses
DDA + DGA	fissile mass + ratios of fissile nuclides	U: 235; Pu: 239, 241
HKE + DDA + DGA	masses of elements + fissile mass + ratios of fissile nuclides	U: 235, 238; Pu: 239, 241; sum of the other Pu isotopes
NRTA (10- $\mu$ s)	masses of nuclides	U: 238; Pu: 239, 240, 242
NETA (10- $\mu$ s) + DGA	masses of nuclides + ratio of fissile nuclides	U: 235, 238, Pu: 239, 240, 241, 242

HKE: hybrid k-edge densitometry [24]. Masses of each element are achieved.

**Table 2:** Examples of combinations of NDA techniques.

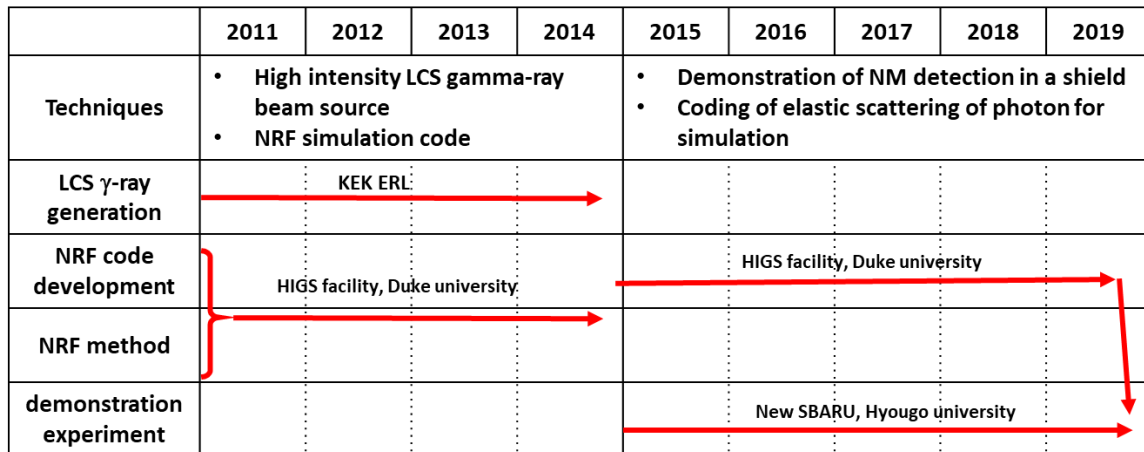
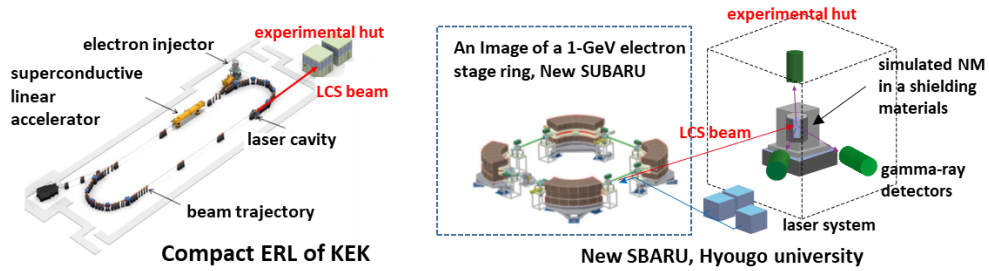


**Fig. 4:** Time line of development of NRF nuclear material detection and measurement technique.

### 3. Development of nuclear resonance fluorescence

Utilization of high-intensity quasi-monochromatic gamma-ray beam for NM detection and measurement was proposed [25-27]. Because nuclear resonance with a photon is characterized by the nuclear structure of a nuclide, the objective nuclide can be measured independently from the sample shape and chemical state of the material. In addition, the penetration ability of gamma-ray beams enables one to detect or assay specific nuclides even inside a shield. This technique should be useful for identifying as well as quantifying NMs and others.

One of the key technologies of NRF is generation of high-intensity quasi-monochromatic gamma-ray beams with photon energy of few MeV. An energy-recovery LINAC (ERL) based laser Compton scattering (LCS) source employing a laser enhancement cavity demonstrated a capability of high-flux and narrow-bandwidth photon beam generation [26]. Figure 4 shows the time line of the development of NRF techniques.

Simulation study is essential for designing an NRF detection/measurement system. Spent fuel assembly measurement in a water pool was investigated [25,27]. It was found that elastic scattering of incident gamma-ray with atoms becomes a competing background of NRF signal when a quantity of objective material is not enough. However, a simulation code such as MCNP and EGS5 only deals with the primary contributor Rayleigh scattering. Simulation tool kit GEANT4 also does not covers all the

important photon scattering processes. They could not reproduce such a high energy photon scattering. Development of a GEANT4 subroutine to reproduce elastic photon scattering was therefore implemented [28]. Experiments are in progress to take photon scattering data to compare with simulation output by using High Intensity Gamma-Ray Source (HIGS), which is a Free-Electron Laser (FEL) based Compton backscattering gamma-ray source, in Duke University of US.

In 2019 JFY, a demonstration experiment of NRF technique for NM detection hidden in a shield will be performed. Figure 5 shows a schematic drawing of the experimental setup, which imitates a NM sample hidden in a shield. The preparation is in progress at the new SUBARU, a 1.5 GeV electron storage ring of the Univ. of Hyogo, under a collaboration of the national institutes for Quantum and Radiological Science and Technology (QST), the Univ. of Hyogo.

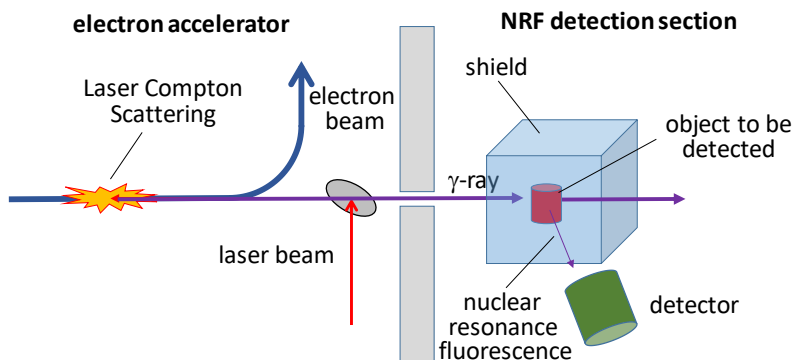


**Fig. 5:** A schematic drawing of an NRF NM detection experiment. Laser photons are injected to make a collision with an accelerated electron and achieves energy by Compton scattering. Energetic gamma-ray coming out through a collimator is quasi-monochromatic. NRF Gamma-rays from the object material is measured by a detector system.

## 4. Summary

The Japan Atomic Energy Agency (JAEA) is conducting R&D projects on technologies of NM detection and measurement for nuclear security and non-proliferation. The activity is based on the Japan's commitment of the 2010 Nuclear Security Summit. In this paper, some of the current projects and activity on active interrogation technique development are shortly overviewed.

## Acknowledgements

This technological development was supported by the Japanese government (MEXT: Ministry of Education, Culture, Sports, Science and Technology), subsidiary for "promotion of strengthening nuclear security and the like". The technological developments are conducted by the Nuclear Science and Engineering Centre (NSEC) of JAEA for DDA, PGA, and NRTA, and by the Integrated Support Centre for Nuclear Nonproliferation and Nuclear Security (ISCN) for LDNS and DGA. Those development of active neutron NDA techniques are carried out under a collaboration between EC-JRC Geel and Ispra, and JAEA. The technological development of NRF was implemented under a collaboration between QST, Hyogo-University, and ISCN of JAEA.

## References

- [1] "Research and development plan – Enhancing capabilities for nuclear verification", Department of Safeguards, IAEA, SRT-385
- [2] "Long-term R&D Plan, 2012-2023", Department of Safeguards, IAEA, SRT-375.
- [3] Harada, H., Kitatani, F., Koizumi, M., Takamine, J., Kureta, M., Tsutiya, H., Imura, H., Seya, M., Becker, B., Kopecky, S., Schillebeeckx, P., Nuclear Data Sheets, 118 (2014) 502-504.
- [4] Kitatani, F., Harada, H., Takamine, J., Kureta, M., Seya, M., J. Nucl. Sci. Technol., 51 (2014) 1107-1113.

- [5] Becker, B., Kopecky, S., Harada, H., Schillebeeckx, P., *Eur. Phys. J. Plus* 129, (2014) 58 (1-9).
- [6] Harada, H., Kimura, A., Kitatani, F., Koizumi, M., Tsuchiya, H., Becker, B., Kopecky, S., and Schillebeeckx, P., *J. of Nucl. Sci. and Tech.* 52 (2015) 837–843.
- [7] Koizumi, M., Tsuchiya, H., Kitatani, F., Harada, H., Heyse, J., Kopecky, S., Mondelaers, W., Paradela, C., Schillebeeckx, P., *Nucl. Instr. and Meth. in Phys. Res. A* 837 (2016) 153-160.
- [8] Toh, Y., Ohzu, A., Tsuchiya, H., Furutaka, K., Kitatani, F., Komeda, M., Maeda, M., Kureta, M., Koizumi, M., Seya, M., Heyse, J., Paradela, C., Mondelaers, W., Schillebeeckx, P., Bogucarska, T., Crochemore, J.-M., Varasano, G., Abbas, K., Pedersen, B., “Development of Active Neutron NDA Techniques for Nuclear Non-proliferation and Nuclear Security”, *Proceedings of 39th ESARDA Symposium on Safeguards and Nuclear Non-Proliferation, Meliá Düsseldorf, Düsseldorf, Germany, (2017) 684-693.*
- [9] Toh, Y., Ohzu, A., Tsuchiya, H., Furutaka, K., Kitatani, F., Komeda, M., Maeda, M., Koizumi, Heyse, J., Paradela, C., Mondelaers, W., Schillebeeckx, P., Bogucarska, T., Crochemore, J.-M., Varasano, G., Abbas K., and Pedersen, B., “Development of Active Neutron NDA System for Nuclear Materials”, *Proceedings of INMM 59th annual meeting (2018).*
- [10] Kunz, W. E., Atencio, J. D., Caldwell, J. T., “A 1-nCi/g Sensitivity transuranic waste assay system using pulsed neutron interrogation”, LA-UR-80-1794, Los Alamos Scientific Laboratory (1980).
- [11] Ohzu, A., Maeda, M., Komeda, M., Tobita, H., Kureta, M., Koizumi, M., and Seya, M., “Design Study on Differential Die-away Technique in an Integrated Active Neutron NDA System for Non-nuclear Proliferation”, 2016 IEEE Nuclear Science Symposium, Medical Imaging Conference and Room-Temperature Semiconductor Detector Workshop (NSS/MIC/RTSD), Strasbourg, (2016) 1-4.
- [12] Haruyama, M., Takase, M., Tobita, H., *J. Nucl. Sci. Technol.* 45, 432-440 (2008).
- [13] Ohzu, A., Komeda, M., Kureta, M., Zaima, N., Nakatsuka, Y., Nakashima, S., *Transactions of the Atomic Energy Society of Japan*, 15 (2015) 115-127 (in Japanese).
- [12] Rossbach, M., *Anal. Chem.* 63 (1991) 2156–2162.
- [13] “Design study on differential die-away technique in an integrated active neutron NDA system for non-nuclear proliferation”, Ohzu, A., Maeda, M., Komeda, M., Tobita, H., Kureta, M., Koizumi, M., and Seya, M., the proceedings of Nuclear Science Symposium in IEEE conference 2016.
- [14] Postma, H., and Schillebeeckx, P., “Neutron Resonance Capture and Transmission Analysis”, *Encyclopedia of Analytical Chemistry (John Wiley & Sons Ltd)* (2009) 1-22.
- [15] Schillebeeckx, P., Becker, B., Harada, H., Kopecky, S., “Neutron Resonance Spectroscopy for the Characterisation of Materials and Object”, *JRC Science and Policy Reports EUR 26848 EN* (2014).
- [16] Paradela, C., Alaerts, G., Heyse, J., Kopecky, S., Salamon, L., Schillebeeckx, P., Wynants, R., Harada, H., Kitatani, F., Koizumi, M., Kureta, M., Tsuchiya, H., “Neutron Resonance Analysis System Requirements”, *JRC Technical Reports EUR 28239 EN* (2016).
- [17] Tsuchiya, H., Kitatani, F., Maeda, M., Toh Y., and Kureta M., *Plasma and Fusion Research* 13 (2018) 2406004.
- [18] Uetsuka, H., Nagase, F., *JAERI-Rep. 95-084* (1995) [in Japanese].
- [19] Campbell, L.W., Smith, L.E., and Misner, A.C., *IEEE Transactions on Nucl. Sci.* 58, 231 (2011).
- [20] Ludewigt, B., Mozin, V., Campbell, L., Favalli, A., Hunt, A., Reedy, E., Seipel, H., “Delayed Gamma Ray Spectroscopy for Non-Destructive Assay of Nuclear Materials”, *LLNL-TR-677606*, (2015).
- [21] Favalli, A., Mehner, H.-C., Crochemore, J.-M., Pedersen, B., *IEEE Transactions on Nucl. Sci.* 56, 1292 (2009).
- [22] Rennhofer, H., Crochemore, J.-M., Roesgen, E., Pedersen, B., *Nucl. Instr. Meth. in Phys. Res. A* 652, 140 (2011).
- [23] Koizumi, M., Rossi, F., Rodriguez, D.C., Takamine, J., Seya, M., Bogucarska, T., Crochemore, J.-M., Varasano, G., Abbas, K., Pederson, B., Kureta, M., Heyse, J., Paradela, C., Mondelaers, W., Schillebeeckx P., *EPJ Web of Conferences* 146, 09018 (2017).
- [24] Gavron, A., Hsue, S.-T., “KED/KCRF Hybrid Densitometer”, *Application Note LALP-96-49* (1996).
- [25] Hayakawa, T., Kikuzawa, N., Hajima, R., Shizuma, T., Nishimori, N., Fujiwara, M., and Seya, M., *Nucl. Instrum. and Meth. Phys. Res., A* 621, 695-700 (2010).
- [26] Hajima, R., Hayakawa, T., Shizuma, T., Angell, C.T., Nagai, R., Nishimori, N., Sawamura, M., Matsuba, S., Kosuge, A., Mori M., and Seya M., *Eur. Phys. J. Special Topics*, 223, 1229–1236 (2014).
- [27] Shizuma, T., Hayakawa, T., Angell, C.T., Hajima, R., Minato, F., Suyama, K., Seya, M., Johnson, M.S., McNabb, D.P., *Nuclear Instruments and Methods in Physics Research A* 737 (2014) 170–175.
- [28] Omer, M., Hajima, R., *Nuclear Instruments and Methods in Physics Research B* 405 (2017) 43–49.

# Investigation of an alternative RPM concept design for special nuclear material detection

**Débora M. Trombetta<sup>1</sup>, Kåre Axell<sup>1,2</sup>, and Bo Cederwall<sup>1</sup>**

<sup>1</sup>Department of Physics, KTH Royal Institute of Technology

<sup>2</sup>Swedish Radiation Safety Authority

## Abstract

*The IAEA Incident Trafficking Database (ITDB) 2018 Fact Sheet reported a total of 166 confirmed interceptions of nuclear or radioactive materials in 34 member states, indicating that unauthorized activities and events involving nuclear and other radioactive materials, including incidents of trafficking and malicious use, continue to occur. Confirmed incidents included highly enriched uranium, plutonium, and plutonium beryllium neutron sources. Radiation Portal Monitors (RPMs) at state borders, ports and other areas of concern (such as nuclear facilities and tunnels) to screen objects and persons passing through them are a key component in the efforts to detect and prevent trafficking of nuclear and radiological materials. Recent experiments with organic scintillator-based detection systems, replacing the historically common <sup>3</sup>He proportional tubes, has demonstrated an added benefit of using the same detection medium for neutron counting and radionuclide identification via gamma-ray measurements. In addition, the fast timing of such detector systems enables coincidence counting on the time scale of tens of nanoseconds, significantly reducing the effects of accidental, false triggers. Following the promising use of organic scintillation detectors as a neutron detector substitute for <sup>3</sup>He-based systems, this paper presents an alternative conceptual design for an organic liquid scintillator-based RPM that makes use of prompt fast-neutron and gamma-ray emission to detect SNM with enhanced performance. Aiding the design, Monte Carlo simulations were performed with version 6.2 of the code MCNP and with the use of the PTRAC option in order to calculate fast coincidence counting rates.*

**Keywords:** liquid organic scintillator detector; MCNP; RPM; nuclear security; SNM.

## 1. Introduction

The detection of special nuclear materials (SNM) is one of the main challenges of nuclear security. The IAEA Incident Trafficking Database (ITDB) 2018 Fact Sheet reported a total of 166 confirmed interceptions of nuclear or radioactive materials in 34 member states, indicating that unauthorized activities and events involving nuclear and other radioactive material, including incidents of trafficking and malicious use, continue to occur. Since 1993, there were 278 incidents that involved confirmed or likely acts of trafficking or malicious use. Confirmed incidents included highly enriched uranium, plutonium, and plutonium beryllium neutron sources [1].

Radiation Portal Monitors (RPMs) are used to screen objects and persons passing through them in order to detect and prevent illicit trafficking of nuclear and radiological materials. These systems should basically compare the measured neutron and gamma-ray counting rates with a predefined count level and set an alarm if these rates are above this defined level – related to background radiation.

A technology that has gained attention in recent years is the use of organic scintillators to not only detect, but quantify special nuclear material [2-5], which due to their fast timing and pulse shape discrimination capabilities enable efficient detection and identification of gamma rays and neutrons for such purposes [6-7]. Recent experiments using organic scintillator-based RPMs, replacing the historically common <sup>3</sup>He proportional tubes, has demonstrated an added benefit of using the same detection medium for neutron counting and radionuclide identification via gamma-ray measurements [8]. The use of this type of detectors may result in a higher sensitivity for detecting SNM, since nuclear fission is associated with the emission of neutrons and "cascades" of gamma rays depopulating excited states in the fission products. Most of these gamma rays are "prompt", i.e. emanate from short-lived nuclear states, and their multiplicity can extend significantly beyond an

average of 5-10 [9-11]. The use of particle coincidences has been extensively used in the quantitative analysis of samples with respect to their content of SNM, in particular for multiplying sources. Background radiation from cosmic rays, naturally occurring radioactive materials (NORM) and the low signal-to-noise ratios in shielded environments can affect the identification of nuclear materials, especially in small quantities. Nuisance alarms triggered by NORM gamma-rays still have high frequency in commonly shipped cargo such as ceramic, fertilizer, and granite tile. For pedestrian RPMs gamma rays emanating from radioactive nuclides remaining in the body after nuclear medical diagnostic procedures like SPECT and PET also contribute to false alarms and may additionally mask the presence of SNM. The use of fast coincidence detection provides additional information that can add significant improvements for reducing false alarm rates in such cases and aid in the detection of SNM.

This paper presents an alternative conceptual design for an organic liquid scintillator-based RPM that makes use of the novel method of prompt fast-neutron and gamma-ray coincidence detection to identify the presence of SNM with enhanced sensitivity [12] focused on security screening applications.

## 2. Method

The ability of theory to accurately reproduce the particle and photon emission from fission and its implementation in state-of-the-art Monte Carlo codes [13] was used in this work to perform an initial investigation on the proposed methodology. Monte Carlo simulations have proven to be a powerful tool for the development of such nuclear security devices, for an overview see e.g. [14] and references there in.

The code MCNP (Monte Carlo N-particle), version 6 was used to perform the computational simulations. Version 6 of MCNP is a merge between MCNP5 and MCNPX, including fission multiplicity options and a new model applied for correlated prompt secondary particle production [15]. The spontaneous decay option that was implemented in MCNPX (2008) was extended in version 6 to include spontaneous fission neutrons (PAR=SN), and the codes CGMF and FREYA which includes gamma ray multiplicity information for fission events [16].

In order to implement fast gamma-neutron coincidence detection as an additional feature, the proposed design consists of a double-sided RPM, with one detection assembly in each pillar separated by 1m. The detection assemblies are composed by four fast neutron detectors each, see Fig.1.

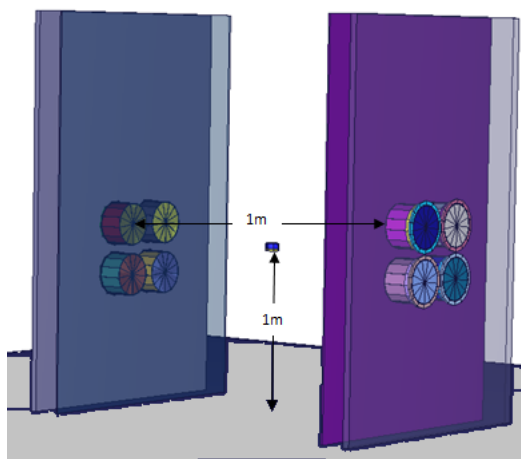


**Fig.1:** Visualization of the RPM computational model from MCNP code.

EJ-309 organic liquid scintillator detectors [17] with 12.7cm diameter and 12.7cm length were modelled according to the manufacture's manual and their modelling validated in a previous work [18]. The detection system is based on pulse shape discrimination that allows the separation between the neutron- and photon-induced signals in the scintillators. In the computational environment, this system was modeled considering that every elastic scattering suffered by neutrons and photons inside the active volume of scintillator material,

taking into account the pre-defined defined energy and time threshold, causes a detector count. The PTRAC card was used to follow the particles, track the scattering events, and the time between correlated emitted fast neutrons from fission events and their deposited energy as predicted by the simulations was accessed. A MATLAB™ [19] post processing code was created to filter the events and perform the calculations of correlation time and energy deposition. The script identifies scattering events for neutrons/photons generated in the same fission event that occurred in different detectors within a given coincidence time window. Here, a coincidence time window of 200ns was used and the energy range cuts applied was from 0.6MeV to 6.6 MeV for neutrons and above 0.05 MeV for photons.

An initial computational calculation test of the setup was done for a Cf-252 source modelled according the ANSI N42.35-2016 [20] standard, with  $2 \times 10^4$  neutrons/s, encapsulated by 1cm of steel and 0.5 of lead in the bare condition and by a 4cm thick high-density polyethylene (HDPE) spherical container, in the moderated condition. To validate the source modelling the calculated rate of single neutrons per detector area was compared with experimental and MCNP-PoliMi results presented in Ref. [21].

Simulations were also performed for a small PuO<sub>2</sub> sample in the setup - not part of the ANSI standard - for which the isotopic mass composition was: 0.064g of <sup>238</sup>Pu, 4.140g of <sup>239</sup>Pu, 1.679g of <sup>240</sup>Pu, 0.099g of <sup>241</sup>Pu and 0.091g of <sup>16</sup>O [22]. The response of the EJ-309 detectors to this sample was also modelled and validated in a previous study [18].

For both sources, spontaneous fission of the specific nucleus was sampled uniformly in the source and the multiplicities for gamma-rays and neutrons were sampled using the FREYA code and multiplicity distributions, respectively. The sources were modelled with isotropic emission and 10<sup>6</sup> histories normalized to the neutron emission rate of each source.

The detection system was placed at the centre of a 100m<sup>2</sup> measurement room with a ceiling height of 4m modelled with concrete [23], density 2.250 g/cm<sup>3</sup>.

### 3. Results

In Ref. [21] Pozzi *et al.* present measured and simulated neutron fluxes for a bare and moderated Cf-252 source with  $3.59 \cdot 10^6 \text{ s}^{-1}$  neutron emission rate placed at a distance of 2m of from a cylindrical EJ-309 liquid scintillator detector with a front surface area of 127cm<sup>2</sup>. A neutron flux of  $18.0 \text{ s}^{-1} \text{ cm}^{-2}$  was measured and a corresponding detected flux of  $24.5 \text{ s}^{-1} \text{ cm}^{-2}$  was predicted by MCNP-PoliMi simulations for the bare source. The simulations performed in this work using the MCNP6.2 produced  $17.0 \pm 1.0 \text{ s}^{-1} \text{ cm}^{-2}$  for the same conditions. In the moderated setup Ref. [21] reports a measured flux of  $13.0 \text{ s}^{-1} \text{ cm}^{-2}$  while a detected flux of  $17.0 \text{ s}^{-1} \text{ cm}^{-2}$  was predicted by the MCNP-PoliMi simulations. The simulations performed in this work produced a detected flux of  $11.5 \pm 1.0 \text{ s}^{-1} \text{ cm}^{-2}$ . Hence, our simulations slightly under-predict the experimental results although the agreement with the experimental data is somewhat better than for the MCNP-PoliMi results reported in Ref. [21]. This could be due to differences between the coincidence time window or energy thresholds applied in the simulations and measurements, respectively and we consider the both the MCNP-PoliMi simulations and the MCNP6.2 simulations performed in this work to well reproduce the experimental data presented in Ref. [21].

The results from the Monte Carlo simulations of the conceptual RPM design studied in this work are given below. Single-neutron and coincidence rates for fast neutrons and gamma-rays are presented for the PuO<sub>2</sub> and Cf-252 source in Table 1 and Table 2, respectively.

	single neutrons/s	neutron-neutron/s	gamma-neutron/s
Bare source	44.2	0.09	2.47

Shielded by 4cm of HDPE	27.7	0.02	1.37
-------------------------------	------	------	------

**Table 1: Calculated** single-neutron and coincidence rates for the PuO<sub>2</sub> sample using MCNP 6.2.

	single neutrons/s	neutron- neutron/s	gamma- neutron/s
Bare source	378.0	2.6	21.6
Shielded by 4cm of HDPE	264.5	1.7	15.1

**Table 2: Calculated** single-neutron and coincidence rates for the Cf-252 source using MCNP 6.2.

The standard ANSI N42.35 defines for RPM tests a background rate of 5-10 $\mu$ R/h for gamma radiation and 200 neutrons s<sup>-1</sup>m<sup>-2</sup> which produces around 1000 gammas/s and 1 neutron/s per detector in the proposed system. Neutron background radiation from cosmic rays could be a concern because, it can be high enough to be comparable with or even more intense than radiation emission from highly enriched uranium (HEU) [24]. Miloshevsky *et al.* [26] studied the correlation of cosmic-ray-induced neutrons and gamma rays at sea level and reported singles fluxes of 0.0175 cm<sup>-2</sup>s<sup>-1</sup> and 0.0024 cm<sup>-2</sup>s<sup>-1</sup> for gamma rays and neutrons, respectively, at 40°N latitude. Moreover, the multiplicities and time correlations between neutrons and gamma rays originating from cosmic rays should also be considered. Cosmic-ray induced coincidence rates were reported in Ref. [26] to be up to five orders of magnitude lower than the singles rates. For example, neutron-neutron coincidences were reported at a rate of 0.12 s<sup>-1</sup> in an interval of 50 $\mu$ s within an area of 100m<sup>2</sup> with average time correlations of ~50-70 $\mu$ s. This already small cosmic-ray-induced background coincidence rate reduces dramatically on the coincidence time scales applied for fast-neutron and gamma detection with organic scintillators of up to 200 ns and they can be safely neglected. Therefore, even with low signal-to-noise ratios in shielded environments can coincidence detection using fast organic scintillators can be used as a way to enhance the identification of nuclear materials, especially in small quantities.

In organic scintillator detectors employed in PSD mode the contribution from particle misidentification to the detected neutron background rate also needs to be taken into account. It is proportional to the average single gamma rate in the scintillator with a factor typically around a few per mille [25] depending on the PSD cuts applied. Here, the gamma to neutron misidentification probability is considered to be 2 per mille, leading to an additional background rate of approximately 2 neutrons/s per detector. Each detector will then count approximately 3 neutrons per second as “background”. The background rates and accidental coincidence count rates were calculated in order to estimate the threshold to activate a positive alarm in the system for different trigger conditions, see Table 3. Considering that the detection threshold is estimated by the sum of background (B) in a given interval time and the product of the standard deviation sigma ( $\sigma$ ) and a multiplier factor (N), i.e. (B + N x  $\sigma$ ) - for an interrogation time of 3 s the sigma multiplier factor was calculated for the different rates and presented in Tables 4 and 5.

	Background Rate (s <sup>-1</sup> )
Single neutrons	24
Single gammas	8000
Neutron-neutron	5x10 <sup>-5</sup>
Gamma-neutron	0.034

**Table 3: Total** (including PSD misidentification) single-particle and coincidence background rates.

Bare source	Multiplier factor (N)		
	single neutrons	neutron-neutron	gamma-neutron
<b>PuO<sub>2</sub></b>	7.1	22.1	22.9
<b>Cf-252</b>	125	639	202

**Table 4:** Calculated sigma multiplier factors for single-neutron and coincidence counts for the PuO<sub>2</sub> sample and Cf-252 source using MCNP 6.2 for an interrogation time of 3s in bare conditions.

Shielded by 4cm of HDPE	Multiplier factor (N)		
	single neutrons	neutron-neutron	gamma-neutron
<b>PuO<sub>2</sub></b>	1.3	4.9	12.5
<b>Cf-252</b>	84.9	416	142

**Table 5:** Calculated sigma multiplier factors for single-neutron and coincidence counts for the PuO<sub>2</sub> sample and Cf-252 source using MCNP 6.2 for an interrogation time of 3s and 4cm of HDPE shielding surrounding the sample/source.

A commonly used positive alarm threshold is five sigma above the mean background rate. As can be seen from Table 4 the performance of the 8-detector RPM system modeled here by far exceeds this standard alarm trigger threshold for both the PuO<sub>2</sub> sample and Cf-252 source as well as the requirements of the ANSI N42.35 standards. Note, however, that due to the low neutron emission rate from the PuO<sub>2</sub> sample it is only detectable in neutron singles and gamma-neutron coincidence mode with an interrogation time of 3 s.

In the shielded conditions the detected single-neutron rate from the PuO<sub>2</sub> sample reduces to 1.3  $\sigma$  above the estimated background rate while the gamma-neutron rate is still 12.5  $\sigma$  above background.

Hence, detection of the PuO<sub>2</sub> sample would be possible via gamma-neutron coincidences only and essentially without background when the sample is moderated with 4cm of HDPE.

## 4. Conclusions

As already demonstrated in the literature [21], a detection system using organic scintillators presents a high potential for substituting He-3 counters in the detection of small amounts of SNM.

This paper investigates an alternative conceptual design for an organic liquid scintillator-based RPM that makes use of gamma-neutron coincidences as a means to improve detection by increasing the sensitivity of the system. Aiding the design, Monte Carlo simulations were performed with version 6.2 of the code MCNP, and coincidences between neutrons and gamma-neutrons were calculated for a standard Cf-252 source and for a PuO<sub>2</sub> sample.

Neutron-neutron coincidence detection is the commonly preferred technique in safeguards applications as they are also subject to low natural background rates, even though the spread in the correlation time for neutrons pairs is larger than for photons, due to the time-of-flight dependence on the neutron energy. However, the rates of neutron-neutron coincidences are often very low, requiring large interrogation times, which is not realistic in the majority of RPM applications. The novel method of gamma-neutron coincidence detection in this context provides reasonable rates that could be used as signature for SNM due to the high gamma-ray multiplicity and the unique time correlations between the photons and neutrons emitted in fission, reducing the number of secondary inspections performed. For the 8-module double-sided RPM investigated in this work the gamma-fast neutron coincidence rates were found to be at least 10 times higher than neutron-

neutron coincidences in the bare source condition. For a mixed PuO<sub>2</sub> sample of less than 2 g <sup>240</sup>Pu<sub>eff</sub> mass we found a true signal of more than 7 times (neutron singles) and more than 22 times (fast gamma-neutron coincidences) the calculated sigma above background for a 3s measurement time in bare conditions. When a shielding of 4 cm HDPE was applied the neutron singles counts reduced to 1.3 sigma above background while the detected fast gamma-neutron coincidence counts were more than 12 sigma above background. In such conditions gamma-neutron coincidence counting would therefore be the only tolerable detection mode. We conclude that gamma – fast neutron coincidence detection is a highly promising solution for detection of small quantities of SNM with RPMs based on fast organic scintillation detectors. It is a detection mode that is relatively insensitive to moderate amounts of shielding that could easily be applied without detection in normal RPM conditions as well as to masking by legitimate radioactive gamma-ray sources such as from medical examinations.

## References

1. IAEA INCIDENT AND TRAFFICKING DATABASE (ITDB) *Incidents of nuclear and other radioactive material out of regulatory control 2018 Fact Sheet*, <https://www.iaea.org/sites/default/files/18/12/itdb-factsheet-2018.pdf>
2. Robinson, S.M., Runkle, R.C., Newby, R.J., *A comparison of performance between organic scintillation and moderated 3He-base detectors for fission neutron detection*, Nuclear Instruments and Methods in Physics Research A 784, 2011.
3. Dolan, J.L., Flaska, M., Poitrasson-Riviere, A., Enqvist, A., Peerani, P., Chichester, D.L., Pozzi, S.A., *Plutonium measurements with a fast-neutron multiplicity counter for nuclear safeguards applications*, Nuclear Instruments and Methods in Physics Research A 763, 2014.
4. Paff, M.G., Monterial, M., Marleau, P., Kiff, S., Nowack, A., Clarke, S.D., Pozzi, S.A., *Gamma/neutron time-correlation for special nuclear material detection – Active stimulation on highly enriched uranium*, Annals of Nuclear Energy 72, 2014.
5. Paff, M.G., Ruch, M.L., Riviere, A.P., Sagadevan, A., Clarke, S.D., Pozzi, S.A., *Organic liquid scintillation detection for on-the-fly neutron/gamma alarming and radionuclide identification in a pedestrian radiation portal monitor*, Nuclear Instruments and Methods in Physics Research A 789, 2015.
6. Kaplan, A.C., Flaska, M., Enqvist, A., Dolan, J.L., Pozzi, S.A., *EJ-309 pulse shape discrimination performance with a high gamma-ray-to-neutron ration and low threshold*, Nuclear Instruments and Methods Physic Research Sect. A 729, 2013, p. 463-468.
7. Enqvist, A., Lawrence, C.C., Wieger, B.M., Pozzi, S.A., Massey, T.N., *Neutron light output and resolution functions in EJ-309 liquid scintillation detectors*, Nuclear Instruments and Methods Physic Research Sect. A 715, 2013, p. 79-86.
8. Marc Gerrit Paff, Marc L. Ruch, Alexis Poitrasson-Riviere, Athena Sagadevan, Shaun D. Clarke and Sara Pozzi, *Organic liquid scintillation detectors for on-the-fly neutron/gamma alarming and radionuclide identification in a pedestrian radiation portal monitor*, Nuclear Instruments and Methods in Physics Research A 789, 2015.
9. Lemaire, S., Talou, P., Kawano, T., Chadwick, M.B., Madland, D.G. *Phys. Rev. C* 72, 014602 2005.
10. Hamilton, J.H., Ramayya, A.V., Zhu, S.J., Ter-Akopian, G.M., Oganessian, Yu.Ts., Cole, J.D., Rasmussen, J.O., Stoyer, M.A., *Prog. Part. Nucl. Phys.* 35, 635, 1995.
11. Bleuel, D.L. et al, Nuclear Instruments and Methods in Physics Research A624 691, 2010.
12. Trombetta, D.M.; Klintefjord, M.; Axell, K.; Cederwall, B., *Fast neutron and  $\gamma$ -ray coincidence detection for nuclear security and safeguards applications*, Nuclear Instrumentations and methods in physics research, A. 927, 2019, p.119-124.
13. Talou, P., Vogt, R., Randrup, J., Rising, M.E., Pozzi, S.A., Verbeke, J., Andrews, M.T., Clarke, S.D., Jaffke, P., Jandel, M., Kawano, T., Marcath, M.J., Meierbachtol, K., Nakae, L., Rusev, G., Sood, A., Stetcu I., and Walker, C., *Correlated prompt fission data in transport simuations*. The European Physical Journal A. 54:9, 2018.
14. Krystal Alfonso, Mashal Elsaid, Michael King, Dan Strellis and Tsahi Gozani, *MCNP simulation benchmarks for a portable inspection system for narcotics, explosives, and nuclear material detection*, IEEE Transition on nuclear science, vol.60, no.2, 2013.
15. *MCNP® USER'S MANUAL Code Version 6.2* Los Alamos National Laboratory report LA-UR-17-29981 (October 2017).

16. Rising, M.E., et al., *Using the MCNP6.2 correlated fission multiplicity models*, CGMF and FREYA, Transactions of the American Nuclear Society, Vol.116, 2017.
17. Eljen Technology, Neutron/gamma PSD liquid Scintillator EJ-301, EJ-309, (n.d.) <<http://www.eljentechnology.com/products/liquid-scintillators/ej-301-ej-309>> (accessed 20 April 2019).
18. Trombetta, D. M.; Axell, K.; Cederwall, B., *MCNP6 simulation validation of fast neutron coincidence detection system for nuclear security and safeguards applications*, ESARDA Symposium 2018, paper 15, 2018, p.49-57.
19. MATLAB R2017a, *The MathWorks, Inc.*, Natick, Massachusetts, United States.
20. ANSI N42.35-2016
21. Pozzi, S.A. Clarke, S.D., Paff, M., Fulvio, A. Di, Kouzes, R.T., *Comparative neutron detection efficiency in He-3 proportional counters and liquid scintillators*, Nuclear Inst. And Methods in Physics Research, A 929, 2019, p. 107-112.
22. *Certificate of analysis*, CBNM nuclear reference material 271, Tech. Rep. Commission of the Europe Communities, JRC, Central Bureau for Nuclear Measurements, 1989.
23. *Compendium of Material Composition Data for Radiation Transport Modelling*, PIET-43741-TM-963 PNNL-15870 Rev. 1, 2011.
24. Ferrari, F., Peerani, P., Radiat. Meas. 45 1034, 2010.
25. J. Cederkäll et al. Nucl. Inst. Meth. Phys Res. A 385, 1997.
26. Miloshecsky, G., Hassanen, A., Time correlation of cosmic-ray-induced neutrons and gammas rays at sea level, Nuclear Inst. And Methd. In Phys. Research A.737, 2014, p.33-41.

# Testing of a Radiation Portal Monitor on the Detection Thresholds

**Arturs Rozite**

European Commission, Joint Research Centre  
Nuclear Safety and Security Directorate, Nuclear Security Unit  
Via E. Fermi 2749, 21027 Ispra (VA), Italy  
E-mail: arturs.rozite@ec.europa.eu

## **Abstract**

*In the present article, a methodology of testing of the Radiation Portal Monitors (RPM) is suggested. The methodology initially was applied to the testing of the RPM based on a single NaI detector; however, the considerations have been extended to the RPM composed from multiple identical NaI detectors. The goal of the testing was in the measurement of the detection thresholds for different radionuclides and in the mapping of the detection thresholds depending on the RPM configuration and parameters of the detection zone. The detection thresholds were determined based on the static and dynamic sensitivity measurements and accounting for default alarm comparison algorithms. The results are presented in the form of the detection threshold maps. Depending on the task of the installation, such maps help decide an optimal RPM configuration.*

**Keywords:** Radiation Portal Monitor, detection thresholds, NaI detector, nuclear security

## **1. Introduction**

The concept of the Radiation Portal Monitor (RPM) has been introduced in 1980<sup>th</sup> in Los Alamos [1]. It is a passive radiation detection system used to detect presence or absence of radioactive source in its detection zone. The RPM usually contains gamma and neutron detectors.

Modern RPMs are intelligent system that provide an operator not only with the user-level information such as type and intensity of the radiation alarm or radiation profile of the occupancy but also with the description of the operational algorithms. Moreover, the modern systems allow operator adjust all-important settings such as alarm thresholds and extract all measured data.

In the RPM, an alarm decision is made comparing radiation signal measured during occupancy to the background signal measured when the detection zone of the RPM is unoccupied.

In case of gamma-ray detectors, the RPM usually triggers an alarm when the current signal is higher than the background signal for a certain number of standard deviations. For the neutron detectors, the alarm-triggering algorithm may be different as the neutron background is very low.

The parameter that describes performance of any RPM is a detection threshold. The detection threshold is a minimum amount of radioactive material that RPM is able to detect.

The detection threshold depends on such RPM characteristics as:

- RPM configuration (type and number of the detectors, their sensitive volume, their shielding);
- Operational algorithms of the RPM (alarm comparison algorithms).

The detection thresholds for different radionuclides are specified along with the set of measurement conditions. Changes of any of these conditions affect the values of the detection thresholds. These conditions are:

- Physical parameters of the detection zone (widths and height);
- Velocity of source;
- False alarm rate;
- Radiation background level;
- Probability of detection.

A simple method of RPM testing on the detection thresholds represents the following procedure [2, 3]: a source of known activity is transferred through the least sensitive point of the detection zone with a certain speed. If the RPM triggers sufficient number of alarms out of fixed sufficiently large number of occupancies, the test is passed and the detection threshold is confirmed.

For a dual-pillar RPM with symmetrical arrangement of the detectors, the least sensitive point is at the middle between the pillars and usually at the top of the detection zone. To verify this a vertical static sensitivity profile is measured. Such test method may also include usage of a grid for static sensitivity measurements for the determination of the least sensitive point of the detection zone [4].

This, rather straight method of testing is often applied, however it doesn't provide one with the precise values of the detection thresholds, it only gives information that the detection threshold is better than a certain value defined by the actual activity of the source being used for dynamic measurements.

The IAEA [5] introduces a parameter called sigma multiplier in order to assay performance of gamma-ray detectors of an RPM. This parameter is linked to the operational algorithm of the RPM.

Is it possible to measure precise values of the detection thresholds?

Is it possible to calculate the values of the detection thresholds for variable physical parameters of the detection zone?

Is it possible to make the map of the detection thresholds depending on the position of the source in the detection zone?

This article provides answers to these questions.

## 2. RPM and its operational algorithms

The developed methodology of testing was applied to the gamma-ray channel of a spectrometric RPM. For the modelling of different RPM configurations (different number of gamma-ray detectors and their arrangement) a mobile and transportable radiation monitor, model SPIR-Ident Mobile [6] produced by Mirion Technologies was used. The monitor is based on a single large volume NaI(Tl) detector having rectangular shape and a sensitive volume of 2 liters (10 x 5 x 40 cm). The detector is placed in the hard-sided transport case that can be installed vertically or horizontally.

A default alarm comparison algorithm is based on the comparison of the net signal value measured during occupancy to the square root from background value. Alarm comparisons are made every second for a rolling spectrum. The rolling spectrum represents a sum of two 1 second spectra. By default, the alarm comparisons are made in the following four regions of interests (ROI):

- a) ROI 1 – from 30 to 300 keV – low-energy window
- b) ROI 2 – from 300 to 800 keV – middle-energy window
- c) ROI 3 – from 800 to 3000 keV – high-energy window
- d) ROI 4 – from 30 to 3000 keV – total energy window

Detection alarm is triggered when the sum of counts in a single alarm comparison time interval in one of four regions of interests is higher than

$$B + N \times \sigma \quad (1), \text{ where}$$

**B** is a sum of background counts in a given ROI for a given alarm comparison interval;

**$\sigma$**  is a standard deviation of background counts;

**N** is a sigma multiplier that defines an alarm threshold and a false alarm rate.

For the Gaussian distribution of background counts a  $5 \times \sigma$  value of a detection threshold corresponds to the false alarm rate (FAR) of 1:3 489 000 seconds in case if one alarm comparison per second is made and to the FAR of 1:872 000 seconds when four alarm comparisons per second are made (the default algorithm). The default value of the sigma multiplier is user adjustable. Actual (not theoretical) FAR was checked during instrument testing.

Single NaI detector could operate as an RPM or several NaI detectors can be connected together to form an RPM with improved detection thresholds for a given physical parameters of the detection zone. The goal of the work was in the creation of 3D maps of detection thresholds for various radionuclides

and for different number of NaI detectors, their arrangement and parameters of the detection zone. Depending on the task of the analysis, these maps could help to decide an optimal configuration of the RPM.

### 3. Methodology of testing

The developed methodology of testing is based on a large number of static sensitivity measurements made using a 2D grid and followed by a set of dynamic sensitivity measurements transferring the source through a single representative point of the detection zone.

The testing went through the following steps:

1. Measurement of spectra of radiation background;
2. Distance and geometry dependent measurements of static sensitivities using a rectangular grid;
3. Calculation of the net static sensitivities;
4. Dynamic testing at 1 m distance to the reference point using dynamic test bench;
5. Determination of dynamic correction coefficient;
6. Calculation of values of sigma multipliers (geometry dependent) per unit of source activity;
7. Calculation of the detection thresholds for the different radionuclides depending on the RPM configurations and as a function of radiation background, false alarm rate, detection probability, velocity of source, parameters of the detection zone and counting algorithms;
8. Creation of the detection threshold maps.

### 4. Measurements

#### 4.1. Measurement conditions

The NaI detector is placed in a hard-sided transport case that represents a rectangular parallelepiped with dimensions of 25 x 25 x 84 cm. The detector can be positioned vertically or horizontally (Figure 1). For vertical orientation in space, the distance from the floor to the geometrical centre of the detector is 29 cm. For the horizontal orientation of the device, the distance from floor to the geometrical centre of the detector is 12.5 cm.

For simplicity of further mapping, the following approximation is made: the detector in its case represents a rectangular parallelepiped with a height of 75 cm. Distance from the floor to geometrical centre of NaI detector is 25 cm when case with a detector is installed vertically on the floor.

Measured background dose-rate at the facility is 0.14  $\mu\text{Sv/h}$ . Average dose-rate of has been recorded using survey meter with a pressurized ionization chamber, model Fluke 451P.

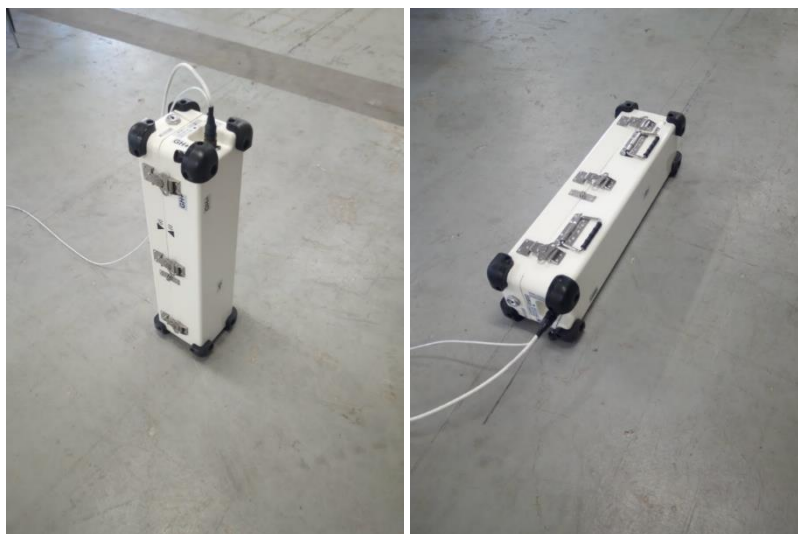


Figure 1 – NaI detector in the housing

## 4.2. False alarm rate testing

The FAR tests were made at three alarm thresholds (values of sigma multiplier). The obtained results are shown in Table 1. Actual FAR is higher than the theoretical one.

Table 1 – FAR tests at the JRC Ispra

Measurement time	Alarm threshold	False alarms	False alarm rate
1 day	4 sigma	39	1:37 minutes
5 days	5 sigma	7	1:17 hours
7 days	6 sigma	0	-

## 4.2. Measurement of radiation background

Radiation background signal was measured for 500 seconds. The values of background in all ROIs per are shown in Table 2. The values are normalized for default alarm comparison interval of 2 seconds.

Table 2 – Background in the ROIs

Region of interest	Background, counts per 2 seconds	Sigma
ROI 1 30 - 300 keV	3228	56.8
ROI 2 300 - 800 keV	1108	33.3
ROI 3 800 - 3000 keV	598	24.5
ROI 4 30 - 3000 keV	4934	70.2

## 4.3. Static sensitivity measurements

For the static sensitivity measurements, the NaI detector in its case was placed on the concrete floor and positioned horizontally along Y-axis of a 2D grid (Figure 3). The dimensions of one cell of the grid are 25 cm x 25 cm.

Static sensitivity measurements were made using a  $^{60}\text{Co}$  source having activity of 205 kBq. The source was sequentially positioned in the nodes of the 2D grid. The source was on a Styrofoam support having 12.5 cm height. The red spot in Figure 2 corresponds to the (100; 0; 12.5) coordinate (X; Y; Z) of the source expressed in cm. Duration of each measurement was 100 seconds. In total 64 measurements were made. The results have been normalized to the measurement time of 2 seconds (default alarm comparison interval).

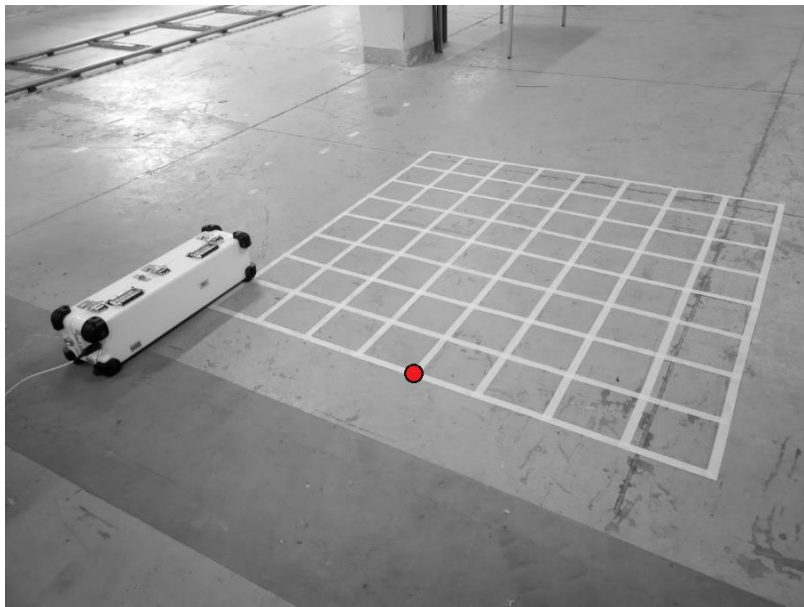


Figure 2 – Coordinates grid. Each cell of the grid has 25 cm widths and 25 cm depth. For the static sensitivity measurements the sources have been positioned in the nodes of the grid.

The results of static sensitivity measurements represent 8x8 coordinate matrix (Table 3). For the vertically oriented detector Y coordinate designates the height of the detection zone and X coordinate the widths of the detection zone. The position of the source indicated by the red spot corresponds to the position **d1** of the grid.

Table 3 – coordinate matrix (8x8)

			X- coordinate, cm							
			25	50	75	100	125	150	175	200
			a	b	c	d	e	f	g	h
Y coordinate, cm	0	1				X				
	25	2								
	50	3								
	75	4								
	100	5								
	125	6								
	150	7								
	175	8								

The results of gross static sensitivity measurement at point **d1** are shown in Table 4.

Table 4 – Gross static sensitivity at point d1 in the ROIs

Region of interest	Gross static sensitivity, counts per 2 seconds
ROI 1 30 - 300 keV	3786
ROI 2 300 - 800 keV	1684
ROI 3 800 - 3000 keV	1384
ROI 4 30 - 3000 keV	6854

A comparison of the radiation background spectrum (in blue) with the <sup>60</sup>Co source spectra at two different positions on the grid are shown in Figure 3.

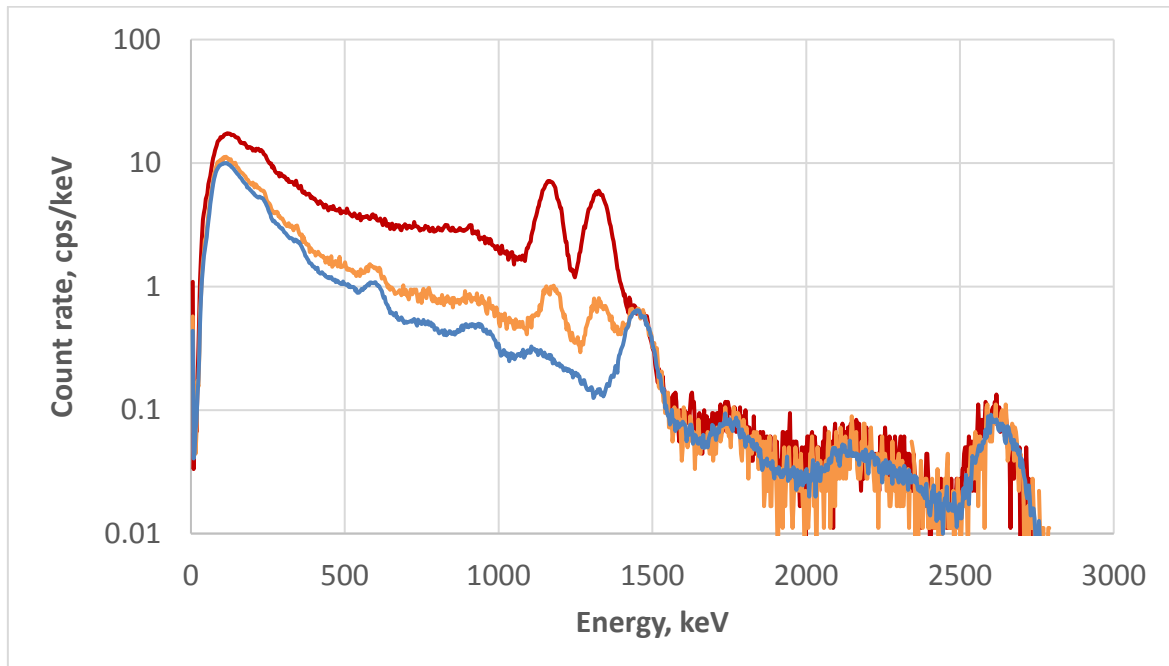


Figure 3 – Comparison of the background and <sup>60</sup>Co source spectra collected during static sensitivity measurements.

### 4.3. Net static sensitivity

Values of net static sensitivity have been obtained subtracting background values from the results of gross static sensitivity measurements. The results of net static sensitivity calculated for the point **d1** are shown in Table 5.

Table 5 – Net static sensitivity at point d1 in the ROIs

Region of interest	Net static sensitivity, counts per 2 seconds	Sigma multiplier	
<b>ROI 1</b>	30 - 300 keV	558	9.8
<b>ROI 2</b>	300 - 800 keV	576	17.3
<b>ROI 3</b>	800 - 3000 keV	786	32.1
<b>ROI 4</b>	30 - 3000 keV	1920	27.3

In the last column the values of sigma multipliers (SM) are indicated. SM describes how many times measured net signal (NS) is higher (SM > 1) or lower (SM < 1) in terms of standard deviations than the background value. SM is defined according to the following formula:

$$SM = \frac{NS}{\sqrt{B}} \quad (2)$$

The highest value of sigma multiplier is obtained in ROI 3, so the best detection threshold is obtained for the alarm comparisons made in this ROI.

The matrix of relative net static sensitivities is shown in Table 6. All values are normalized to the value obtained at the reference **d1** point. The matrix is based on the net static sensitivity measurements in the ROI 3. This matrix can be used for the determination of the relative static sensitivities for any radionuclide. There are measurable effects of Compton scattering for the low energy ROIs at low source-to-detector distances of 25 and 50 cm due to the proximity of concrete floor, so the matrix of relative sensitivities based on the measured data in ROI 3 is the most correct.

Table 6 – matrix of the net static sensitivities (relative values)

			X- coordinate, cm							
			25	50	75	100	125	150	175	200
			a	b	c	d	e	f	g	h
Y coordinate, cm	0	1	7.49	3.05	1.61	<b>1.00</b>	0.66	0.47	0.34	0.27
	25	2	5.15	2.53	1.45	0.90	0.62	0.45	0.33	0.26
	50	3	2.29	1.67	1.13	0.77	0.55	0.41	0.32	0.25
	75	4	0.99	0.97	0.76	0.59	0.46	0.36	0.28	0.24
	100	5	0.47	0.60	0.54	0.46	0.38	0.32	0.25	0.22
	125	6	0.24	0.36	0.35	0.33	0.30	0.25	0.22	0.18
	150	7	0.15	0.24	0.26	0.26	0.22	0.22	0.19	0.17
	175	8	0.10	0.15	0.18	0.19	0.18	0.16	0.15	0.13

### 4.4. Values of sigma multiplier for static measurements

The values of sigma multipliers were calculated per unit of source activity and are presented in Table 7.

Table 7 – ROI 3, matrix of sigma multipliers per one kBq of <sup>60</sup>Co

			X- coordinate, cm							
			25	50	75	100	125	150	175	200
			a	b	c	d	e	f	g	h
Y coordinate, cm	0	1	1.174	0.478	0.252	0.157	0.103	0.074	0.053	0.042
	25	2	0.807	0.397	0.227	0.141	0.097	0.071	0.052	0.041
	50	3	0.359	0.262	0.177	0.121	0.086	0.064	0.050	0.039
	75	4	0.155	0.152	0.119	0.093	0.072	0.056	0.044	0.038
	100	5	0.074	0.094	0.085	0.072	0.060	0.050	0.039	0.034
	125	6	0.038	0.056	0.055	0.052	0.047	0.039	0.034	0.028
	150	7	0.024	0.038	0.041	0.041	0.034	0.034	0.030	0.027
	175	8	0.016	0.024	0.028	0.030	0.028	0.025	0.024	0.020

#### 4.5. Dynamic sensitivity measurements

The <sup>60</sup>Co source was placed in a source holder of a track, so to be at 1 m distance to the detector and in front of the detector reference point, when the track is passing the detector (Figure 4).

Dynamic sensitivity measurement were made. The source has been transferred with velocity of 1.2 m/s. Maximum amplitudes of alarms have been recorded for 30 sequential trials. The average values and corresponding measurement error have been calculated for the ROIs (Table 8). The results of dynamic sensitivity measurements have been compared with the results of static sensitivity measurements in position **d1**. Average dynamic correction coefficients equal to **2.8** has been found.



Figure 4 – Measurements of dynamic sensitivity using the JRC track

Table 8 – Average dynamic correction coefficient for source velocity 1.2 m/s has been found

	Dynamic measurements, average maximum net signal per alarm comparison interval (of 2 seconds)	Dynamic measurements error (StD), %	Static measurements, average net signal, counts per 2 seconds	Static to dynamic sensitivity ratio
ROI 1	224.9	18.1	558	2.5
ROI 2	185.6	11.1	576	3.1
ROI 3	277	11.4	786	2.8
ROI 4	687.5	6.3	1920	2.8

#### 4.6. Correction of the results of static sensitivity measurements

Based on the dynamic trials all results of the matrix of net static sensitivity measurements have been divided by 2.8.

#### 4.7. Dynamic detection thresholds

For determination of the dynamic detection thresholds the values of source activity per 1×SM have been multiplied by N. Value of  $N \times \sigma$  defines false alarm rate. Table 9 provides dynamic detection thresholds for  $5 \times \sigma$  alarm threshold settings.

Table 9 –  $^{60}\text{Co}$  detection thresholds at  $5 \times \sigma$ 

			X- coordinate, cm							
			25	50	75	100	125	150	175	200
			a	b	c	d	e	f	g	h
Y coordinate, cm	0	1	11.9	29.3	55.5	89.3	135.3	190.0	262.6	330.7
	25	2	17.3	35.3	61.6	99.2	144.0	198.4	270.6	343.4
	50	3	39.0	53.5	79.0	116.0	162.3	217.8	279.0	357.2
	75	4	90.2	92.1	117.5	151.3	194.1	248.0	318.9	372.0
	100	5	190.0	148.8	165.4	194.1	235.0	279.0	357.2	405.9
	125	6	372.0	248.0	255.1	270.6	297.6	357.2	405.9	496.1
	150	7	595.3	372.0	343.4	343.4	405.9	405.9	470.0	525.2
	175	8	892.9	595.3	496.1	470.0	496.1	558.1	595.3	686.9

Detection thresholds are specified for an RPM based on single vertically arranged NaI detector:

- for the alarm threshold of 5 sigma
- with 0.5 probability of detection
- for the velocity of source of 1.2 m/s
- at radiation background of 0.14  $\mu\text{Sv/h}$

Detector sensitive volume is 2 liters. Distance from the midpoint of the detector to the floor is 25 cm.

### 5. Mapping of the detection thresholds for $^{60}\text{Co}$

Maps of detection thresholds are created for  $^{60}\text{Co}$  and for different RPM configurations (number and arrangement of identical detector) and physical parameters of the detection zone (Figures 5 – 8). The detection thresholds are specified for the alarm comparisons in the ROI 3 and along with the conditions mentioned in the paragraph 4.7. The height of the detection zone is 200 cm because the distance from the detector midpoint to the floor is 25 cm and therefore for the vertically installed detector the response at the height of the floor and at 50 cm to the floor is the same.

Figure 5 represent values of the detection thresholds for  $^{60}\text{Co}$  for a single vertically positioned NaI detector. Distance from the midpoint of the detector to the floor is 25 cm.

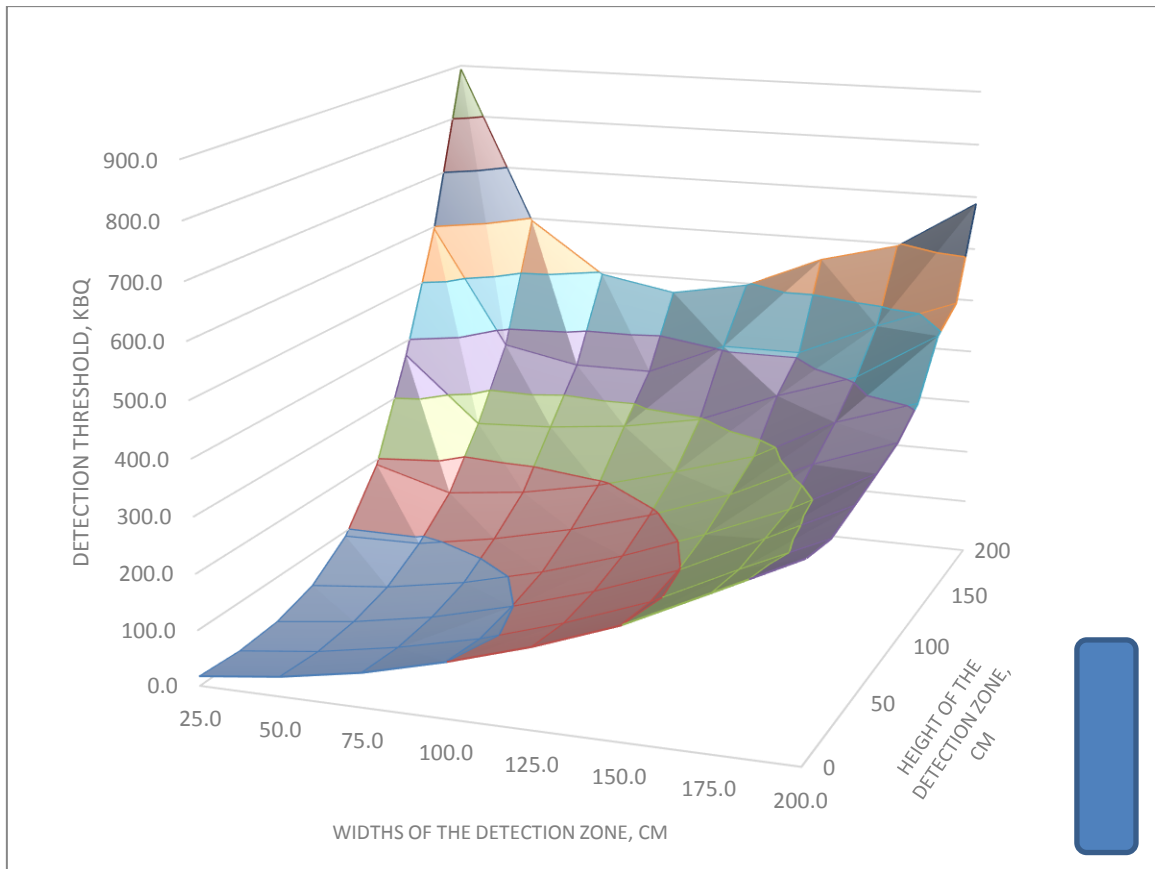


Figure 5 –  $^{60}\text{Co}$  detection thresholds (one detector, one pillar)

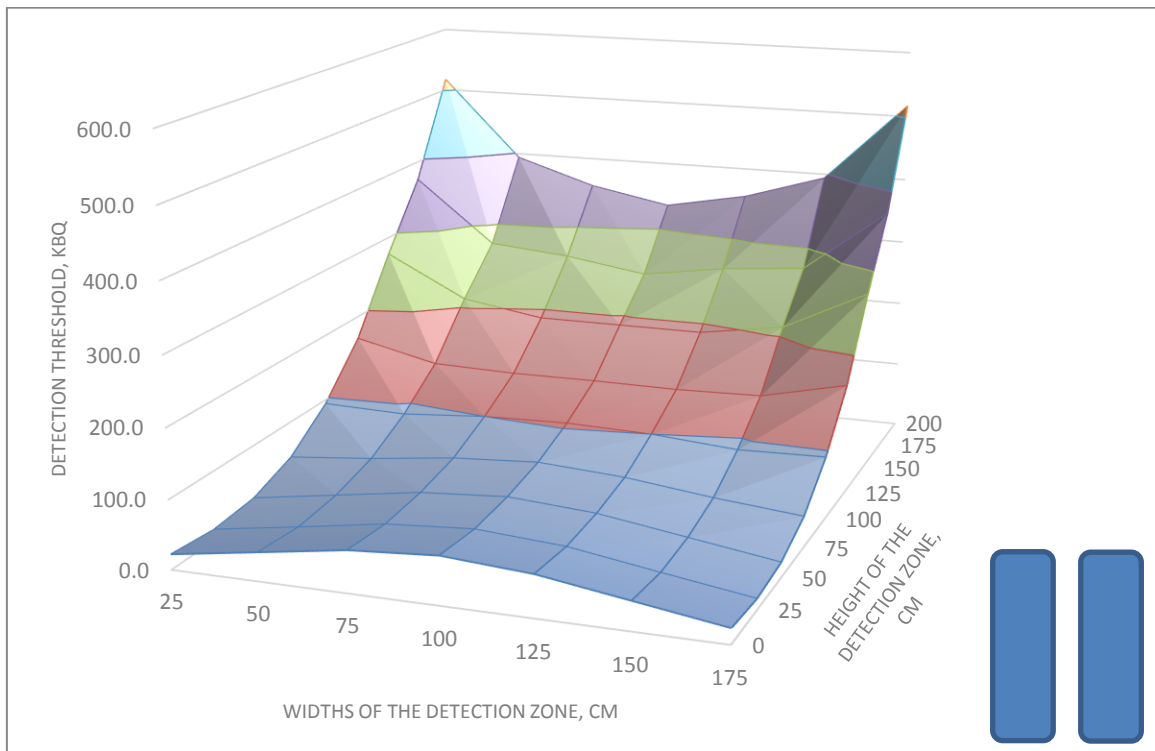


Figure 6 –  $^{60}\text{Co}$  detection thresholds (two detectors, two pillars, distance between pillars 2 m)

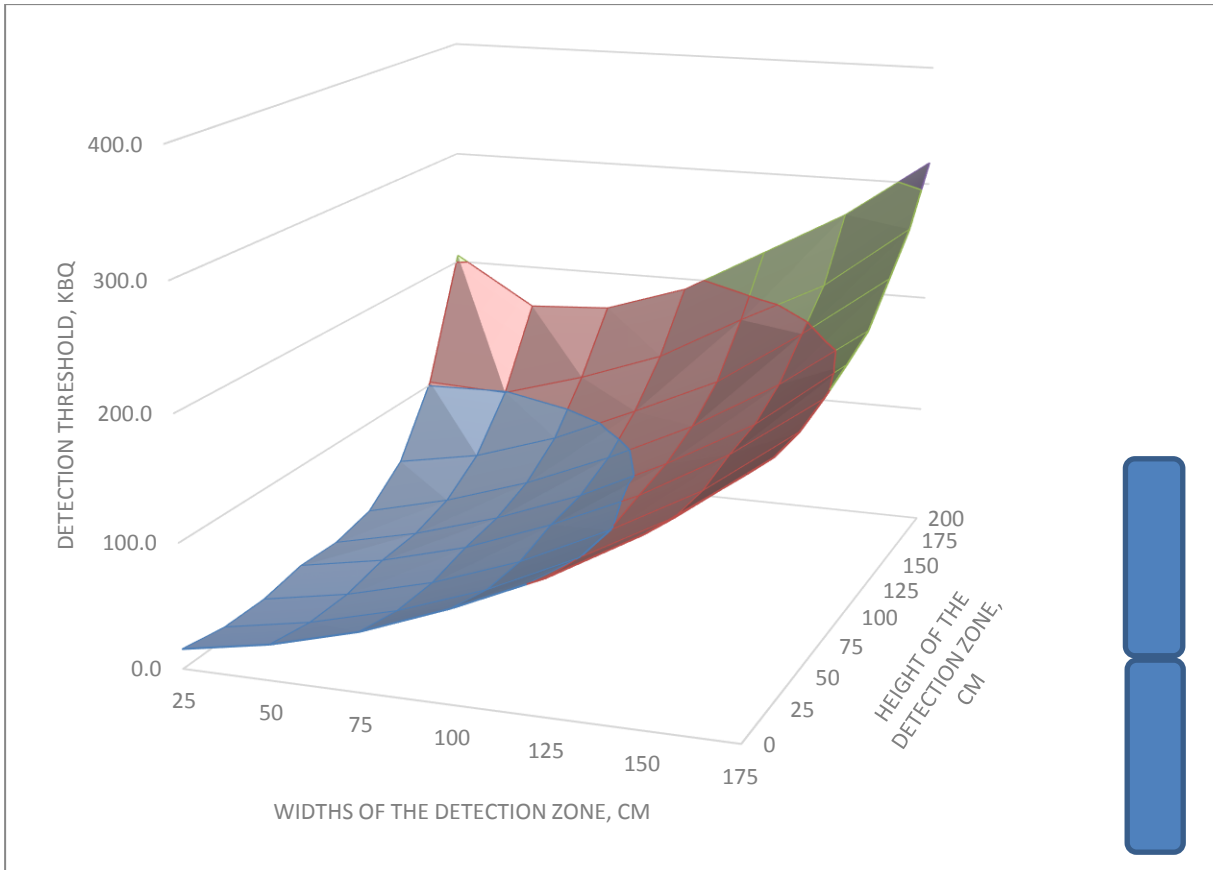


Figure 7 –  $^{60}\text{Co}$  detection thresholds (two detectors, one pillar)

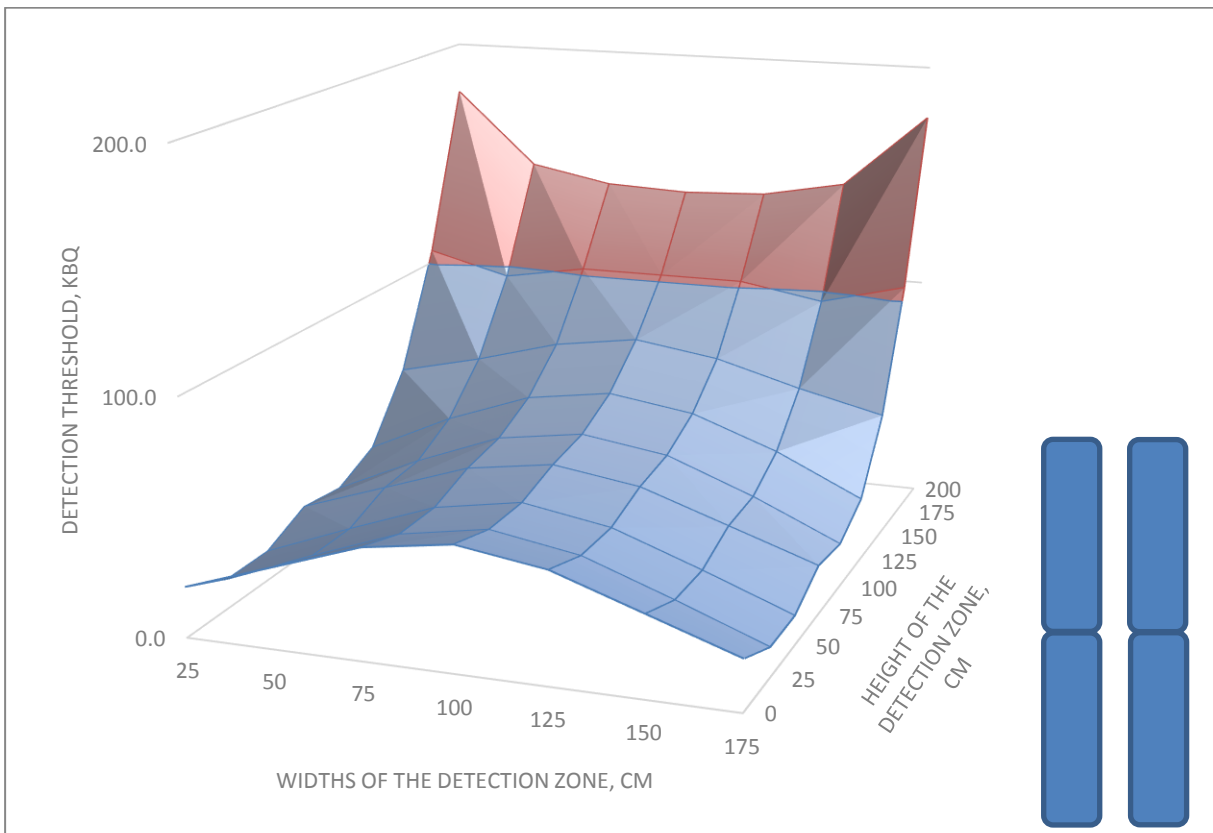


Figure 8 –  $^{60}\text{Co}$  detection thresholds (four detectors, two pillars, distance between pillars 2 m)

Figure 6 represents the detection thresholds for the dual-pillar RPM based on two identical NaI detectors installed vertically on the floor at 2 m distance to each other. Distances from the midpoints of the detectors to the floor are 25 cm. The map was constructed based on the matrix of net static sensitivities shown in Table 10.

Table 10 – 8x8 matrix of net static sensitivities for dual-pillar RPM based on 2 identical NaI detectors

			X- coordinate, cm						
			25	50	75	100	125	150	175
			a	b	c	d	e	f	g
Y coordinate, cm	0	1	<b>a1+g1</b>	<b>b1+f1</b>	<b>c1+e1</b>	<b>2x d1</b>	<b>c1+e1</b>	<b>b1+f1</b>	<b>a1+g1</b>
	25	2	a2+g2	b2+f2	c2+e2	2x d2	c2+e2	b2+f2	a2+g2
	50	3	a3+g3	b3+f3	c3+e3	2x d3	c3+e3	b3+f3	a3+g3
	75	4	a4+g4	b4+f4	c4+e4	2x d4	c4+e4	b4+f4	a4+g4
	100	5	a5+g5	b5+f5	c5+e5	2x d5	c5+e5	b5+f5	a5+g5
	125	6	a6+g6	b6+f6	c6+e6	2x d6	c6+e6	b6+f6	a6+g6
	150	7	a7+g7	b7+f7	c7+e7	2x d7	c7+e7	b7+f7	a7+g7
	175	8	a8+g8	b8+f8	c8+e8	2x d8	c8+e8	b8+f8	a8+g8

Figure 7 represents the detection thresholds for the single-pillar RPM based on two identical NaI detectors installed vertically on the floor and on the top of each other. Distance from the midpoint of the bottom detector to the floor is 25 cm. Distance between the midpoints of two detectors is 75 cm. The map was constructed based on the matrix of net static sensitivities shown in Table 11.

Table 11 - 8x8 matrix of net static sensitivities for single-pillar RPM based on 2 identical NaI detectors

			X-coordinate, cm							
			25	50	75	100	125	150	175	200
			a	b	c	d	e	f	g	h
Y coordinate, cm	0	1	a1+a4	b1+b4	c1+c4	<b>d1+d4</b>	e1+e4	f1+f4	g1+g4	h1+h4
	25	2	a2+a3	b2+b3	c2+c3	<b>d2+d3</b>	e2+e3	f2+f3	g2+g3	h2+h3
	50	3	a3+a2	b3+b2	c3+c2	<b>d3+d2</b>	e3+e2	f3+f2	g3+g2	h3+h2
	75	4	a4+a1	b4+b1	c4+c1	<b>d4+d1</b>	e4+e1	f4+f1	g4+g1	h4+h1
	100	5	a5+a2	b5+b2	c5+c2	<b>d5+d2</b>	e5+e2	f5+f2	g5+g2	h5+h2
	125	6	a6+a3	b6+b3	c6+c3	<b>d6+d3</b>	e6+e3	f6+f3	g6+g3	h6+h3
	150	7	a7+a4	b7+b4	c7+c4	<b>d7+d4</b>	e7+e4	f7+f4	g7+g4	h7+h4
	175	8	a8+a5	b8+b5	c8+c5	<b>d8+d5</b>	e8+e5	f8+f5	g8+g5	h8+h5

### 6. Detection thresholds for other radionuclides

For the calculation and mapping of the detection thresholds for any other radionuclide, it is sufficient to measure a spectrum of this radionuclide for the source positioned in the position **d1** (or any other position of the grid), and

- calculate values of net static sensitivities for position d1 in the ROIs
- calculate values of sigma multipliers in the ROIs and define most sensitive ROI
- apply matrix of relative net static sensitivities obtained using <sup>60</sup>Co source
- apply dynamic correction coefficient by dividing values of net static sensitivities by 2.8.
- fill the matrix of sigma multipliers per unit of source activity
- calculate detection thresholds for N×sigma
- construct map of the detection thresholds

## 7. Conclusion

The methodology of testing of RPMs on the detection thresholds is suggested. The methodology is described on the example of testing of an RPM based on 1, 2, 3 and 4 identical NaI detectors.

The methodology includes a set of static sensitivity measurements using a rectangular grid that models the detection zone, followed by a set of dynamic trials at the reference geometry (source-to-detector distance). The methodology allows define precisely the detection thresholds and construct maps of the dynamic detection thresholds for the different configuration of the RPM and for the arbitrary parameters of the detection zone.

## 8. References

- [1] Chambers, W.H.; Atwater, H.F.; Fehlau, P.E.; Hastings, R.D.; Henry, C.N.; Kunz, W.E.; Sampson, T.E.; Whittlesey, T.H.; Worth, G.M. *Portal Monitor for Diversion Safeguards*. Los Alamos National Laboratory, LA-5681, 1974.
- [2] *Illicit Trafficking Radiation Detection Assessment Program (ITRAP+10). Test campaign summary report*. January 26, 2016.
- [3] *American National Standard for Evaluation and Performance of Radiation Detection Portal Monitors for Use in Homeland Security*. IEEE/ANSI N42.35-2016.
- [4] ГОССТАНДАРТ РОССИИ. МОНИТОРЫ РАДИАЦИОННЫЕ ЯДЕРНЫХ МАТЕРИАЛОВ. Общие технические условия. ГОСТ Р 51635-2000.
- [5] IAEA. *Nuclear Security Series No. 1. Technical and Functional Specifications for Border Monitoring Equipment. Reference Manual*. 2016.
- [6] Mirion Technologies. *SPIR-Ident Mobile. User's Manual*. 2018.

## Capacity building in EU Member States for the testing and assessment of detection equipment in nuclear security within ITRAP+10 Phase II

**F. Raiola<sup>1</sup>, A. Rozite<sup>1</sup>, M. Goncalves<sup>2</sup> and H. Tagziria<sup>1a</sup>**

<sup>1</sup>European Commission, Joint Research Centre, Nuclear Safety and Security Directorate G, Nuclear Security Unit G.II.7, Ispra (Italy); <sup>2</sup>EU EC Directorate A, Brussels (Belgium)

**T. Köble, M. Risse, H. Friedrich, M. C. Bornhöft, J. Glabian**

Fraunhofer-Institut für Naturwissenschaftlich-Technische Trendanalysen INT Appelsgarten 2, 53879 Euskirchen, Germany

**C. Deyglun, P. Funk, N. Pepin and AL. Weber**

Institut de Radioprotection et de Sureté Nucléaire, 31 avenue de la Division Leclerc, 92260 Fontenay-aux-Roses, France

**Cs. Csöme, G. Dosa, A. Kovacs, Gy. Nagy, Cs. Toth and P. Völgyesi**  
Hungarian Academy of Sciences, Centre for Energy Research, Nuclear Security Department, Konkoly-Thege Miklós út. 29-33, Budapest, H-1121, Hungary

**T. Schroettner, F. Strebl and R. Mudri**

Seibersdorf Labor GmbH 2444 Seibersdorf, Austria

**M. Belin<sup>3</sup>, C. Boucq<sup>4</sup>, M. Convers<sup>4</sup> and S. Vayre<sup>4</sup>**

<sup>3</sup>CEA, DAM, VALDUC, <sup>4</sup>CEA, DAM, DIF, F-91297 Arpajon, France

---

### Abstract

*Phase II of the Illicit Trafficking Radiation Detection Assessment Program (ITRAP+10) for nuclear security primarily aimed to build testing and performance assessment capacity within EU member states (MS), which can be the basis towards certification of radiation detection equipment in a medium to long term. In addition, commercially available mobile and transportable detection systems which were not previously assessed in Phase I were tested and the extensive data acquired. This contributed to further improving international standardization and detection capabilities through innovation and a fair competition. Capacity building was achieved through the provision by the JRC to a consortium of EU laboratories of testing procedures and training as well as the organization of a round robin exercise. In essence a set of representative detection instruments (PRD, RID and SRPM) were provided by the JRC and circulated amongst the laboratories. The equipment had been thoroughly tested at the ITRAP facility of the JRC-Ispra which allowed an inter-comparison where appropriate between the partner laboratories on one hand and JRC-measurements as the reference on the other. The EU consortium was partially funded by the EU (under H2020) to develop and construct testing facilities similar to that of the JRC be it on a smaller scale and each one with its advantages and some understandable limitations. These facilities will be described and results of the measurements and inter-comparison will be given where appropriate.*

**Keywords:** ITRAP, Nuclear Security, Radiation Detection, Illicit Trafficking, Capacity building

<sup>a</sup> Contact and technical responsible: [hamid.tagziria@ec.europa.eu](mailto:hamid.tagziria@ec.europa.eu)

## 1. Introduction

In line with European Commission's (EC) CBRN 2010-2015 action plan [1], the Joint Research Centre carried out from 2011 to 2014 a far reaching ITRAP+10 programme funded by DG-Home with the aim to assess the performance of the most families of commercially available nuclear and radioactive material (NRM) detection instruments and test them against international standards. Extensive data was collected the results of which were subsequently communicated to standards committees (for new or improved standards) and to participating commercial companies thus helping them to improve the performance of their detection equipment.

In 2015 ITRAP+10 Phase II was launched by the European Commission with the scope to:

1. Test at the ITRAP facility of the JRC in Ispra and in real external environmental conditions the remaining families of detection systems which are either novel (e.g.  $^3\text{He}$  alternatives) or those which were not previously tested in Phase I such as the mobile and transportable.
2. Make good strides and contribution towards improving international standards and generally move towards certification of nuclear detection equipment for nuclear security.
3. Consequently contribute to innovation, a fair completion and improvement of detection technologies.
4. Build the capacity of a selected consortium of EU laboratories (partially funded by the EC's DG-Home) to test and (ultimately) certify nuclear security detection equipment through the provision by the JRC of testing procedures and the organization of a round robin exercise based on a set of representative instruments (PRD, RID and SRPM) which had been thoroughly tested in Ispra. Noteworthy that the particular brand were selected for no specific reason or motivation except for their availability in numbers to the consortium. It is not the aim in this exercise to evaluate the performance of this equipment, which was done within Phase I of ITRAP+10.

This Phase II of ITRAP+10 is also well in line with the 2017-2020 CBRN action plan [2].

Phase I of ITRAP+10 has been previously presented and described [3-5] together with points 1 to 3 of Phase II above. This paper thus aims to describe the all-important point 4, the capacity building in EU MS for the testing and assessment of detection equipment in nuclear security within ITRAP+10 Phase II. The facilities developed, the testing campaigns carried out by each laboratory including at the ITRAP+10 facility of the JRC in Ispra (Italy).

Testing within the round robin exercise was carried out from 2017 to end of 2018, coordinated by France Expertise and implemented by the JRC and the following consortium of EU laboratories:

1. IRSN (France)
2. CEA (France)
3. MTA EK (Hungary)
4. Fraunhofer INT (Germany)
5. Seibersdorf Labor (Austria)

## 2. The Round Robin Exercise

The transfer of know-how to EU Member States' laboratories was ensured through a round robin exercise (**Figure 1**) whereby:

- 1) A limited but representative set of instruments were circulated namely (**Figure 2**):
  - a. Personal Radiation Detectors (PRD) – IEC 62401
  - b. Radioisotope Identifiers (RID) – IEC 62327
  - c. Spectrometric Radiation Portal Monitor (SRPM) – IEC 62484

These particular representatives were selected for no specific reason or motivation except for their availability to the consortium.

- 2) Test procedures have been developed and validated at the JRC and provided to a consortium of participating EU laboratories
- 3) Testing of instruments were carried out at the JRC in Ispra
- 4) Training and demonstrations were offered to the participating laboratories at the JRC-Ispra ITRAP facility

- 5) Testing of the equipment was made by the consortium of EU laboratories using the same procedures
- 6) Results were compared with those of reference measurements by the JRC in Ispra and if meaningful between different laboratories (including the JRC)

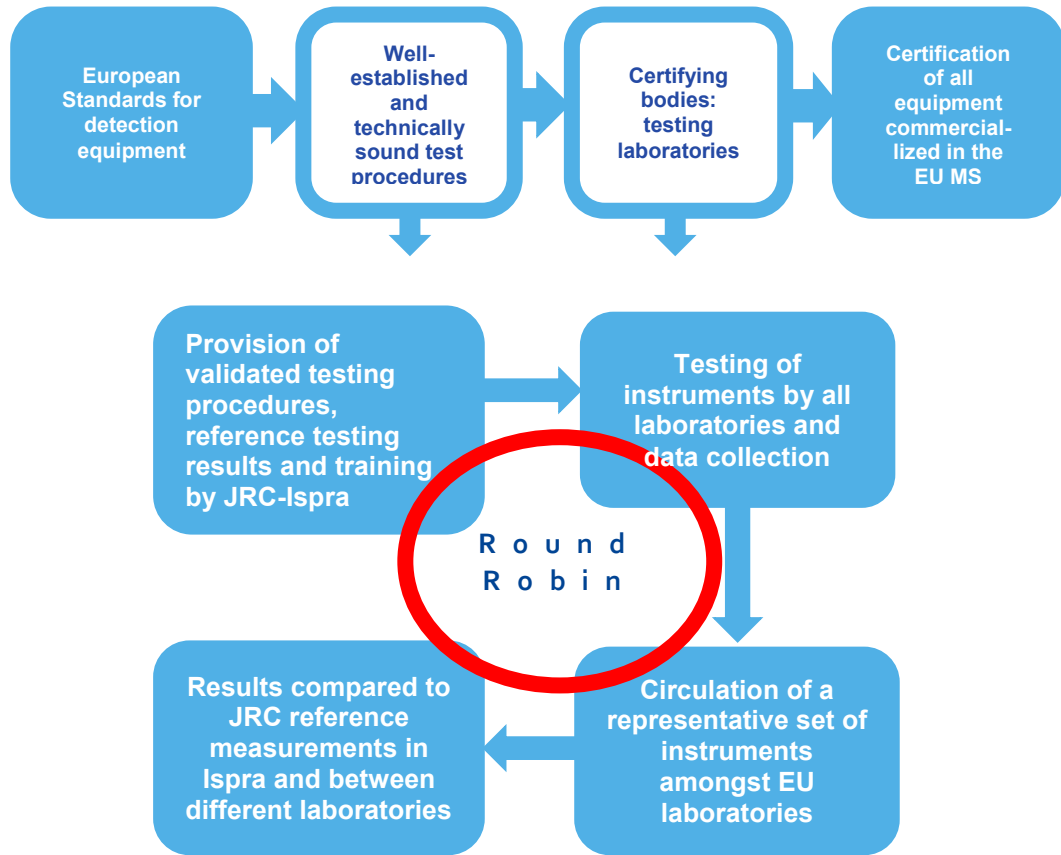


**Figure 1:** Schematic representation of the round robin exercise.



**Figure 2:** Three categories of instruments taking part in the round robin exercise.

### 3. Test bed facilities at the JRC in Ispra

#### 3.1. Dynamic tests with sources

These are carried out using the test bed facility shown in **Figure 3** which has the following characteristics:

- 27 m long conveyor/rail;
- Speed varying from 0.02 to 3.0 m/s;
- 10 to 300 cm vertical elevation of source;
- With/without moderator;
- Various shielding arrangement;
- 2 source mounting options: automatic and manual for testing with heavily moderated or shielded sources;
- Data Collection System (DCS) described below.



**Figure 3:** Dynamic test bed facility at the JRC in Ispra.

#### 3.2. Static testing on purpose built irradiators

Two purposely built irradiators (shown in **Figures 4 and 5**) are installed with the following specifications:

- 2 separate irradiators for neutron and gamma sources
- Full control of exposure time and duration
- Complete record of instrument's response
- Extensive data collection and management using a client-server based Data Collection System



Figure 4: Panoramic view of the static test facility.



Figure 5: Neutron and gamma irradiators at the static test bed facility at the JRC in Ispra.

### 3.3. The Data Collection System

A client-server based Data Collection System (DCS) shown in **Figure 6** was developed by DNDO and implemented at the JRC Ispra for the acquisition and management of data within ITRAP+10. Eight different databases have been created to accurately record any single piece of information that could help to analyze the results. This allowed a quality assured collection and management of vast amount of data (pictures, spectra etc.) during these extensive testing campaigns.

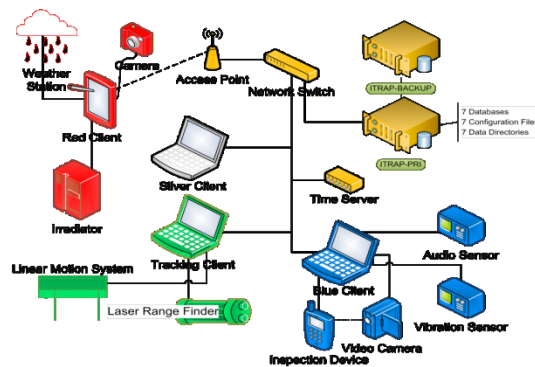


Figure 6: Schematic of the Data Collection System at the JRC's ITRAP facility in Ispra.

### 3.4. Nuclear material and radioactive sources available

A full set of a variety of gamma-ray and neutron sources as required by standards, SNM, NORM and medical isotopes on request.

## 4. The MTA EK test facility

The Detector Testing Laboratory of the MTA EK is located in a semi-basement building-section at the campus of the Centre for Energy Research, Budapest. The Testing Laboratory consists of two irradiation rooms, both equipped for different types of testing applications.

### 4.1. Dynamic test room

Specific parts of the ITRAP+10 Phase II measurements required the target materials to move with defined speeds in front of the radiation detector, simulating the passage of people or vehicles. These tests were done in the dynamic test room (**Figure 7**).

The dynamic test room is equipped with a rail based source moving mechanism, with 11 m track length, and scalable speed and source-height settings, ranging from 0.01 to 2.5 m/s and from 0 to 2.5 m, respectively. All the dynamic parameters, like the speed, height and repetition time are pre-programmable by a remote computer. Furthermore, a light beam curtain and a dosimetry monitoring system ensure the safe working conditions.

During the ITRAP tests, an additional modular framework had to be constructed to carry the heavier shielding materials, which hindered the capability of the moving mechanism to easily change the source-heights. For the safe mounting and easy movement of the SRPM, a special holder was made.

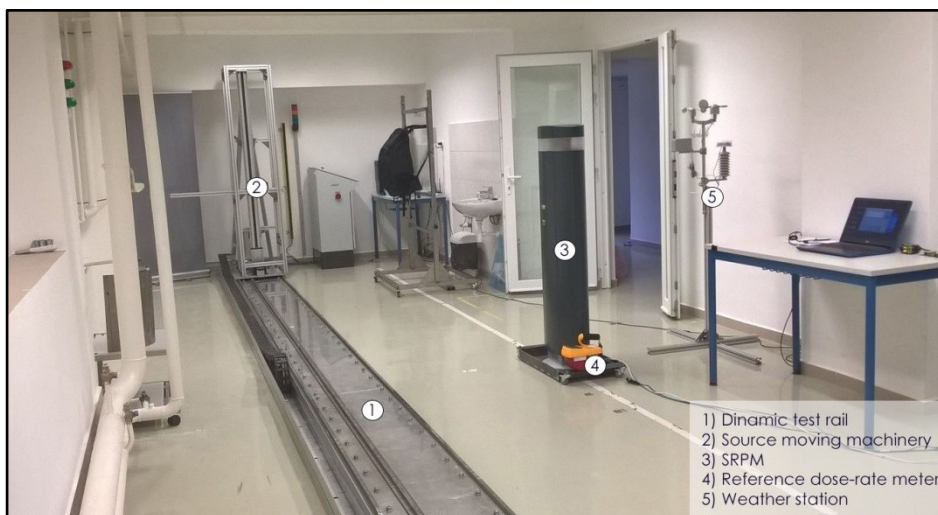


**Figure 7:** Dynamic test bed facility at MTA EK with the SRPM detector under test.

### 4.2. Static test room

The other part of the ITRAP+10 tests was carried out at the static test room, where the accuracy and response time of the handheld radiation detector and the radioisotope identifier were tested (**Figure 8**).

The static test room consists of two irradiators, one for gamma and one for neutron radiation. Each irradiator is equipped with a lead shielding and a neutron moderator container, and a radiation source torpedo to rapidly increase the radiation field. The irradiators are controlled by a remote computer, where the irradiation parameters, like the irradiation interval, cooling time and repetition rate can be pre-programmed.

During the ITRAP tests, a special optical character recognition based technology had to be used for data recording, because none of the tested handheld devices had a built-in data transfer option to a computer.



**Figure 8:** Static test bed facility at MTA EK with the PRD detector under test.

### 4.3. The Data Collection System

The software used for controlling the dynamic and static systems is a self-developed, LabView based, modular and expandable control software. This software provides a manual or pre-programmed automated control and supervision over both of the systems, with a wide range of operational parameters. Additionally, a weather station is mounted in the test laboratory in order to monitor the environmental conditions, like pressure, temperature and humidity. This station has a portable design, separate indoor display and wireless communication with the control software.

### 4.4. Nuclear material and radioactive sources available

MTA EK possesses different radiation sources and a wide scale licence for use of various radioactive and nuclear materials within its campus, making available the usage of a broad range of industrial and medical radiation sources, and different kind of NORM and nuclear materials (e.g. DU, LEU, HEU,  $^{239}\text{Pu}$ ) for the testing purposes. The operation of a 10 MW research reactor and a private enterprise producing radioisotopes together with experienced trading companies at the MTA EK campus assure the availability of various radiation sources, satisfying even special requests for test sources. Beside this technical background, a longstanding expert knowledge and experience in nuclear measurement techniques provides help to perform the different tests based on the relevant international standards.

## 5. The IRSN test facility

### 5.1. Dynamic tests with sources

These are carried out using the test bed facility shown in **Figure 9** and **Figure 10** which has the following characteristics:

- Compact and transportable design
- 10 m long conveyor/rail
- Speed varying from 0.02 to 2 m/s
- 10 to 200 cm vertical elevation of source with manual mounting
- Possibility to install different kind of shield and/or moderator
- Full control of the speed, timing and number of crossings with on-board computer
- Checking of the timing based on webcams, infra-red sensors and nano-computer Raspberry-Pi
- Complete record of instrument's response based on commercially available webcam and alarm detectors
- External environmental conditions record (temperature, atmospheric pressure and humidity sensors) based on nano-computer Raspberry-Pi



Figure 9: Dynamic test bed facility at the IRSN.

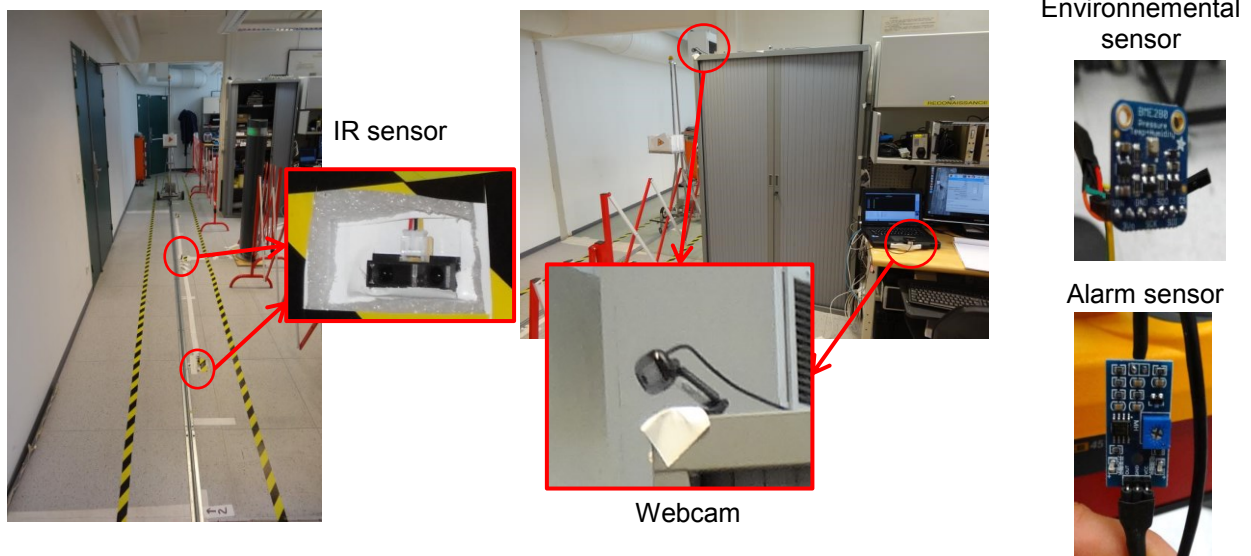
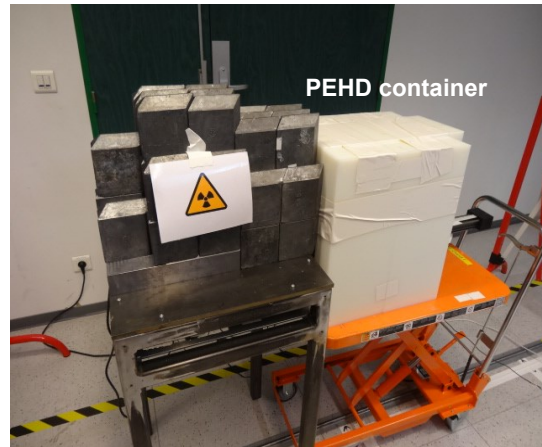
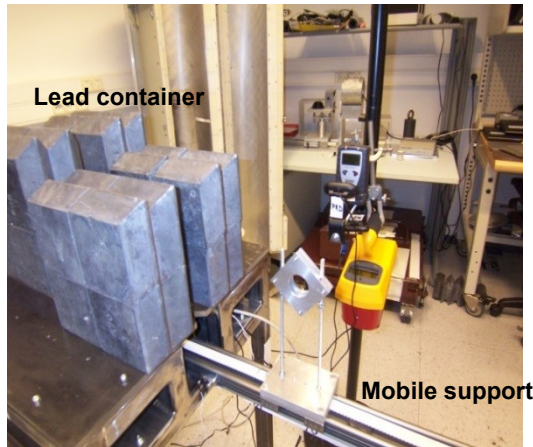


Figure 10: Acquisition devices (temperature, atmospheric pressure and humidity sensors, webcams, alarm sensor and infra-red sensors along the rail) mastered by nano-computer Raspberry-P (IRSN).

## 5.2. Static testing on purpose built irradiators

One purposely built irradiator (shown in **Figure 11** and 12) is installed with the following specifications:

- 1 irradiator for neutron and gamma sources
- removable and adaptable shields (lead blocks to hide gamma sources or HDPE and borated wrap to hide neutron source)
- Full control of exposure time and duration based on nano-computer Raspberry-Pi
- Complete record of instrument's response based on commercially available webcam and alarm detectors
- External environmental conditions record (temperature, atmospheric pressure and humidity sensors) based on nano-computer Raspberry-Pi



**Figure 11:** Static platform for gamma source (lead blocks) with bare source and source surrounded by 4 cm of HDPE (IRSN).

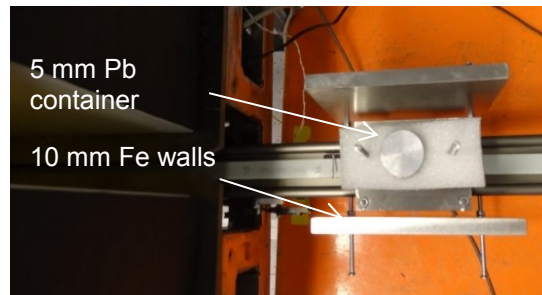


**Figure 12:** Static platform for neutron source (PEHD and borated wrap).

### 5.3. Nuclear material and radioactive sources available

A full set of a variety of gamma-ray and neutron sources as required by standards, SNM, NORM and industrial isotopes on request. The **Table 1** below presents:

1. The recommendations of the IEC 62484 norm (Radiation protection instrumentation – Spectroscopy-based portal monitors used for the detection and identification of illicit trafficking of radioactive materials).
2. The recommendations of the JRC technical reports (Illicit Trafficking Radiation Detection Assessment Program, ITRAP+10 Phase II, Round Robin, Spectroscopic Radiation Portal Monitor, Test Methods).
3. IRSN's sources activities and the distance source-detector calculated to have the same photon flux than the recommendations.
4. The distance SNM-detector was 100 cm.

**Table 1:** List of the radioactive sources used at IRSN.

Source	IEC 62484		IRSN		
	Activity [kBq]	Distance source-detector [cm]	Activity [kBq]	Distance source-detector [cm]	Distance source - surface of the monitor [cm]
<sup>241</sup> Am	1.7E3	100	1.74E3	100	88
<sup>137</sup> Cs	580	100	8.9E3 + 2 cm Pb	135	123
<sup>60</sup> Co	250	100	407	127	115
<sup>133</sup> Ba	320	100	621.2	139	127
<sup>232</sup> Th	500	100	420.8	91	79
<sup>252</sup> Cf	20,000 n/s	100	20,000 n/s	100	88
HEU	221 g U-235	100	77 g U-235	100	88
Nat. U	A few kilos	100	177 g Unat.	100	88
WGPu	15 g + 1 cm Fe	100	2.987 g	100	88

## 6. The Seibersdorf test facility

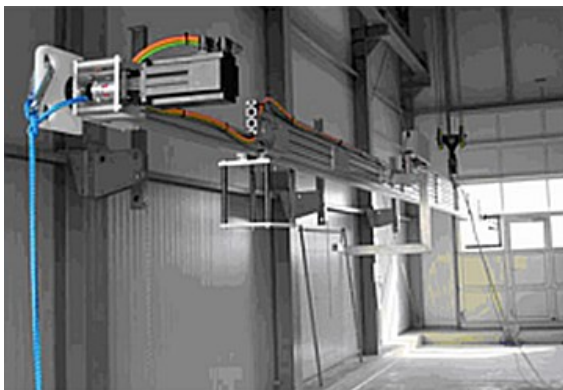
### 6.1. Dynamic tests facility

For dynamic tests a flexible test hangar (Figure 13) with a computer-controlled source transportation system is available with following characteristics:

- 13 m long conveyor/rail
- source speed varying from 0.01 to 5 m/s
- 1 to 500 cm vertical elevation of source
- sources can be mounted with/without moderator
- sources are mounted manually to the moveable “wagon”
- various shielding arrangements (up to 5 kg is possible)
- LabView PC software for source transportation allows definition of multiple passages with precise speed, length of way, pre-set stops and time breaks between passages.

As test sources a variety of radioactive materials are available:

- On site production of pharmaceutical radionuclides (<sup>18</sup>F, <sup>131</sup>I, <sup>99m</sup>Tc)
- Set of calibration sources (app. 500 kBq activity)
- Drum filled with <sup>40</sup>K (fertilizer); High activity <sup>226</sup>Ra sources
- <sup>252</sup>Cf neutron source (app. 20.000 n/s)
- No permission to handle SNM like HEU, Pu isotopes



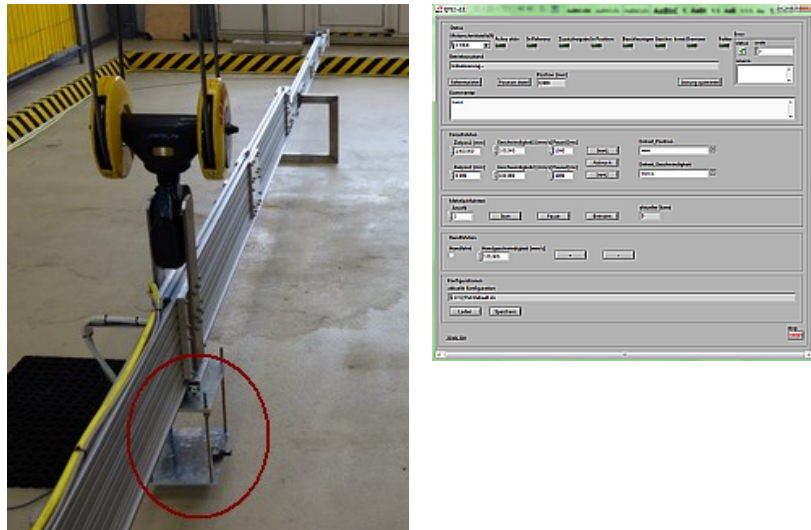


Figure 13: Dynamic test bed facility at the Seibersdorf Labor GmbH (Austria).

### 6.2. Static irradiation test facility:

The dosimetry reference irradiation facility at Seibersdorf is equipped with strong  $^{137}\text{Cs}$  and  $^{60}\text{Co}$  sources as well as strong X-ray tubes with a variety of filters to produce different radiation qualities.

This testing facility for static tests (Figure 14) has two measurement rooms with following characteristics:

- Different radiation qualities can be produced ( $^{137}\text{Cs}$  and  $^{60}\text{Co}$  sources; one > 30 TBq  $^{60}\text{Co}$  tele-therapy source), 320 kV x-ray tube with a variety of filters;
- Dose rates from ambient background values up to 100 Sv (in 30 cm distance) can be realized;
- Pneumatic source movement device to expose radioactive radiation sources;
- Ionization chamber for precise dose-rate monitoring (Austrian primary normal for metrology);
- Monitoring of environmental conditions (air pressure, temperature, humidity) and video surveillance;
- Automatic data logging system to integrate all measurement parameters (lab-view software).



Figure 14: Static test bed facility at the Dosimetry Laboratory of Seibersdorf Labor GmbH (Austria).

## 7. The Fraunhofer INT test facility

The Fraunhofer INT systems for the dynamic and static tests have both a modular design and are transportable. Therefore measurements can be performed at any place, even for already deployed non-movable equipment.

### 7.1. Test facility for dynamic tests

At Fraunhofer INT the dynamic tests are carried out by using a rail guided trolley system which is shown in **Figure 15** and which has the following characteristics:

- A rail system guides a trolley which carries the sources;
- The track length is variable up to 40 m (modular design);
- The trolley is automated and the velocity (0.02 m/s to 2.2 m/s) and acceleration can be chosen;
- Trolley design includes electric stepper motor, control computer, communication systems, and a system for height adjustment of sources;
- Vertical positioning of sources possible up to 230 cm;
- Load capacity of approx. 12 kg for moderator or shielding material as addition to the sources;
- Specially designed fast interchangeable source holders for different source geometries;
- Video observation system for data collection, measurement surveillance, and measurement documentation (see chapter 7.3);
- Reproducibility is achieved by: adjustment with scales, positioning aid for the detectors and sources, and source holder for all types of sources on the same level;
- Equipment for high accuracy: laser distance meter, cross hair laser for height level adjustment.

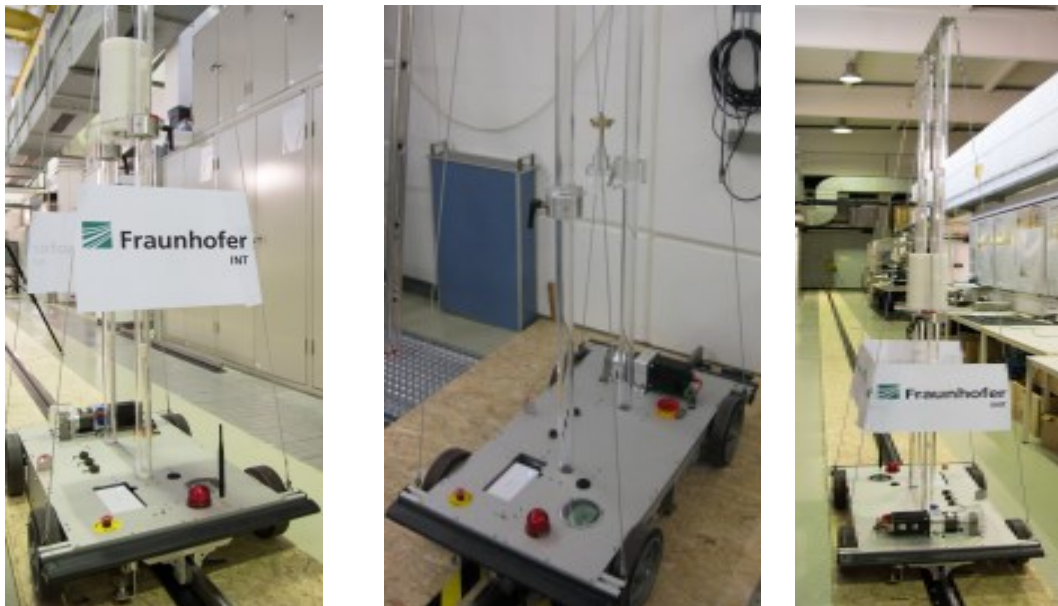


**Figure 15:** Test facility for dynamic tests at Fraunhofer INT.

### 7.2. Test facility for static tests

At Fraunhofer INT the static tests are carried out by using a gamma and neutron irradiation system which is shown in **Figure 16** and which has the following characteristics:

- The system consists of up to three guide rails with roller carriages to perform tests with three detectors at the same time;
- The system design includes roller carriages, guide rails, compressed air system, a timer, cameras for data collection, safety features, and shielding material;
- A lift up mechanism based on compressed air is used for the sources. It enables to have lifting up times (out of the shielding) of about 0.35 s or even faster;
- Source shielding between measurements: for gamma sources lead is used while a structure of borated polyethylene, lead, and high density polyethylene is used for neutron sources;
- Video observation system for data collection, measurement surveillance, and measurement documentation (see chapter 7.3 below);
- Height adjustment of the detector and source by using a cross line laser with the roller carriage lift up mechanism and the special made source holder for the different sources.



**Figure 16:** Test facility for dynamic tests at Fraunhofer INT.

### 7.3. Video observation system

For the surveillance of the static and dynamic measurements, for data collection and for documentation in both cases a video observation system consisting of several free mountable cameras is used. The display and storage of the camera signals is realized by the software Blue Iris (from Perspective Software).

In case of the static tests a timer is used to assure the traceability of the chronology of the time behavior of the tested devices and to document the time correlation of the measured values. This timer is always placed next to the display of the tested detector to be visible in the same video file. It is automatically started by the lift up mechanism when the source is placed in front of the detector. The video of the detector display and the timer is recorded as well as the video of the camera observing the source. In case of the dynamic tests the camera surveillance system is used to observe the detector itself, to track the movement of the trolley, to record the detector display and the computer screen if available.

Naturally, all available data produced by the tested detection systems themselves is also transferred and stored for further analysis. To prevent possible loss of the recorded data an automated back-up system is also used.

### 7.4. Source availability

To perform the static and dynamic tests Fraunhofer INT possess a variety of different gamma and neutron sources:  $^{137}\text{Cs}$ ,  $^{60}\text{Co}$ ,  $^{133}\text{Ba}$ ,  $^{152}\text{Eu}$ , DU,  $^{241}\text{Am}$  for gamma tests and  $^{252}\text{Cf}$ , Am/Be, and Am/Li for neutron tests. If necessary the availability of further sources can be arranged.

## 8. The CEA test facility

The CEA test facility used in the round robin is the Nuclear and Radiological Platform located in CEA-DAM-DIF. It is a facility designed to carry out nuclear metrology measurements with both dynamic and static tests in a controlled environment. Various types of radioactive sources are available for testing, as well as a  $^{60}\text{Co}/^{137}\text{Cs}$  irradiator delivering a collimated photon flux for higher gamma field experiments.

### 8.1. Static testing

A static bench for precise positioning of detectors or radioactive sources is available in the facility (see **Figure 17**). It has a length of 6 m and its 48 x 50 cm table-top maximum weight capacity is 50 kg. It is controlled by an embedded control panel as well as an external wired control panel for remote operating. This bench can be operated on 3 axis with a usable length of 5450 mm, 200 mm and 500 mm, respectively on the x, y and z axis. The static bench is mostly positioned on the collimated photon's flux axis of the irradiator (see **Figure 17** Right) but can be rotated by a 90° angle (see **Figure 17** Left).

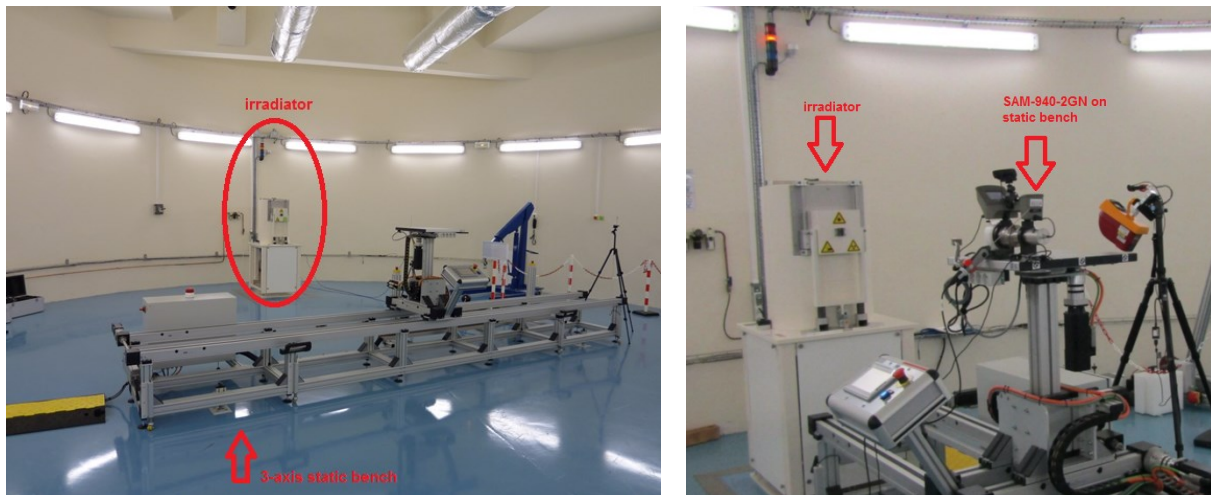


**Figure 17:** (On the left) the  $^{60}\text{Co}/^{137}\text{Cs}$  irradiator and static bench at the CEA facility. (On the right) irradiator and static bench used for high gamma field “Accuracy for photons” test.

### 8.2. Dynamic testing

Dynamic testing is performed with a dedicated dynamic bench from the facility (see **Figure 18**) composed of two components.

The first component is an 8 m long x-axis motorized bench allowing for automated x-axis movement, as well as a z-axis manual positioning of a XX x XX cm table-top with a maximum weight capacity of 23 kg. This x-axis bench can be operated with a maximum velocity of 2.2 m/s (with an acceleration of 3.1 m/s<sup>2</sup>) on the full range of the bench.

The second component is a z-axis automated plate that can be used for fast shielding of radioactive sources, up to a maximum of 23 kg. This automated z-axis component has a range of 1.48 m with a maximum velocity of 1.2 m/s (with an acceleration of 3.0 m/s<sup>2</sup>).

Both components are remote controlled, either with a computer or a dedicated control panel. Computer control allows for programming of various sequences for automated long-run experiments.

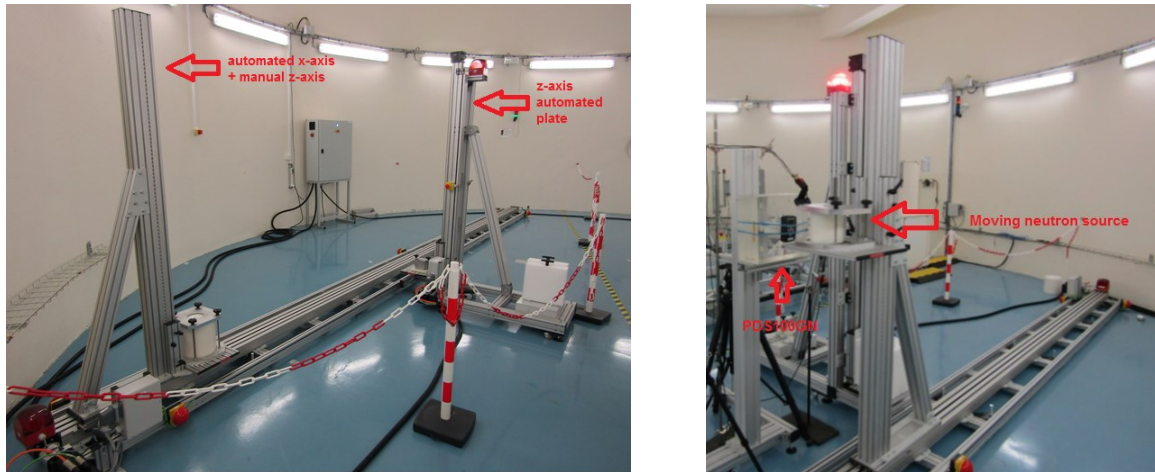


**Figure 18:** (On the left) X-axis and z-axis dynamic bench at the CEA facility. (On the right) Dynamic bench used for the “Dynamic sensitivity to neutron radiation” test.

### 8.3. Data recording

All the primary data coming from the tested devices are recorded using the devices’ own recording capabilities. When devices are not able to record their own data, manual recording from operators performing the test are implemented. Every test performed is also video recorded thanks to multiple camera angles allowing for general facility recording and devices’ screens recording.

As required by metrology standards, room temperature, pressure, humidity and radiological background are controlled and recorded for the duration of the tests.

### 8.4. Radioactive sources

A wide range of industrial gamma-ray sources are available in the facility, along with a few NORM and SMN and neutron sources. Medical sources are not available inside the facility.

## 9. Results

### 9.1. MTA-EK results

Most of the ITRAP+10 tests could be performed at the MTA EK Detector Testing Laboratory, though some modifications had to be made on the testing facility itself, or the test methods, in order to meet the test requirements to a satisfactory level.

The main challenges included the availability of the high activity nuclear sources required for the shielded tests, and the large physical size or difficult handling of the available sources and shielding materials. These problems could only be solved by decreasing the source-detector distance, or by modifying the mounting structure of the source-moving mechanisms, which required additional calculations and decreased the automation capabilities of the test facility.

Another challenge was the data access and the control of the tested detectors. None of the handheld devices had the possibility to automatically start measurement cycles, and the measurement data was not accessible via a cabled or wireless computer connection. This problem had to be solved by manual control of the devices, even during the high repetition rate tests. The measurement data was recorded by a camera, mounted above the detectors, and optical character recognition software, but the precise adjustment of this technique was a technical difficulty and required additional and constant supervision by the colleagues performing the tests.

The above modifications and the required fluence calculations (based on HPGe spectrometry) together with the dose-rate measurements significantly extended the test campaign, especially in the case of the medical isotopes.

Based on our experiences, the accessibility of the required  $^{252}\text{Cf}$  neutron sources poses the biggest challenge. The sources used during the ITRAP+10 Phase II tests were relatively old (manufactured a couple of decades before), and the neutron spectra significantly differed from that of a newly produced source. The exact determination of the neutron yield originating from the  $^{252}\text{Cf}$  isotope compared to the daughter elements proved to be quite difficult even with the combined usage of gamma-spectrometry and neutron-counting techniques. The determination of the acceptable test results was even more difficult since there was no performance data available for the detection of older  $^{252}\text{Cf}$  sources, compared to the new ones. The high prices and the relatively short half-life make the procurement of the new  $^{252}\text{Cf}$  sources problematic and likely not cost-effective.

## 9.2. The IRSN results

### 1. PRD results:

Many scenarios were tested with the static and dynamic platforms, and the following sources:

- Neutron source:  $^{252}\text{Cf}$  (unmoderated and moderated)
- Gamma sources:  $^{241}\text{Am}$ ,  $^{137}\text{Cs}$ ,  $^{60}\text{Co}$

All radiological tests described in the test procedure were performed, except the accuracy tests for photons from  $^{241}\text{Am}$  and  $^{60}\text{Co}$  at a high dose rate of 50  $\mu\text{Sv/h}$  due to sources activities. In addition, it was observed that if the equivalent dose rate is too high (close to 100  $\mu\text{Sv/h}$ ), the PRD device went to "DANGER" mode and gamma and neutron alarms cannot be discriminated.

### 2. RID results:

Many scenarios were tested with the static and dynamic platforms and the following sources:

- Neutron source:  $^{252}\text{Cf}$  (unmoderated and moderated)
- Gamma sources:  $^{241}\text{Am}$ ,  $^{137}\text{Cs}$ ,  $^{60}\text{Co}$ ,  $^{133}\text{Ba}$
- Special Nuclear materials: HEU, Pu

All radiological tests described in the test procedure were performed, except the accuracy tests for photons from  $^{241}\text{Am}$  and  $^{60}\text{Co}$  at a high dose rate of 50 and 100  $\mu\text{Sv/h}$ , some of the mixed and masking scenarios ( $^{137}\text{Cs}+\text{HEU}$ ,  $^{57}\text{Co}+\text{HEU}$ , SNM+medical and SNM+NORM) and interfering beta radiation test mainly due to sources activity but also unavailability of medical and pure beta emitter isotopes. The main difficulties encountered during accuracy and identification tests for photons were probably due to a bad calibration during the auto-calibration process, leading to an overestimation of the measured dose rate and false-identification. A manual calibration of the instrument corrected most of the issues. Regarding overload characteristics, the maximum exposure rate was not reported in the user manual, but the instrument was able to identify  $^{137}\text{Cs}$  at a dose rate of 200  $\mu\text{Sv/h}$  and notify a dangerous radioactivity level.

### 3. SRPM results:

Many scenarios were tested with the static and dynamic platforms and the following sources:

- Neutron source:  $^{252}\text{Cf}$  (unmoderated and moderated)
- Gamma sources:  $^{241}\text{Am}$ ,  $^{137}\text{Cs}$ ,  $^{60}\text{Co}$ , Th, natural U
- Special Nuclear materials: HEU, Pu

All radiological tests described in the test procedure were performed, except the identification tests involving medical isotopes.

The neutron testing presented some issues. The main lesson learned is the impact of the room dimensions. The room where the tests were performed was too small so that scattered neutrons increased the neutron background. Hence, during the test the detection limit became too high to detect the  $^{252}\text{Cf}$ - source. One solution consists in designing a PEHD shield to hide the neutron source between each repetitive measurement and maintain a stable background.

### 9.3. The Seibersdorf results

Only tests with the SPRM system have been performed during the ITRAP+10 round robin exercise. Tests applying SNM sources were not carried, as the permit for handling such materials has been expired before the start of the project.

Following tests have been performed according to ITRAP+10 procedures, based on IEC standards:

- Vertical profile test ( $^{137}\text{Cs}$ ,  $^{241}\text{Am}$ ,  $^{60}\text{Co}$ ,  $^{252}\text{Cf}$  unmoderated, HDPE moderated, shielded in 1 cm steel plus 0.5 cm lead)
- False alarm test
- Background effects ( $^{226}\text{Ra}$ ,  $^{137}\text{Cs}$ ,  $^{252}\text{Cf}$ )
- Response to Gamma radiation / Single radionuclide identification ( $^{137}\text{Cs}$ ,  $^{57}\text{Co}$ ,  $^{60}\text{Co}$ ,  $^{133}\text{Ba}$ ,  $^{22}\text{Na}$ ,  $^{226}\text{Ra}$ ,  $^{241}\text{Am}$ ,  $^{152}\text{Eu}$ )
- Response to neutron radiation (moderated by HDPE, unmoderated)
- Overload test (with  $^{137}\text{Cs}$  with dose rate of 100  $\mu\text{Sv/h}$  and 10 mSv/h)
- Neutron indication in the presence of photon radiation (at background dose rate 100  $\mu\text{Sv/h}$ )
- Identification shielded radionuclides ( $^{131}\text{I}$ ,  $^{18}\text{F}$  in 8 cm HDPE)
- Over range characteristics for identification ( $^{60}\text{Co}$  and  $^{137}\text{Cs}$  of different activity with a  $^{226}\text{Ra}$  background of 1  $\mu\text{Sv/h}$ )

The tested SPRM instrument was very sensitive, therefore, most of the tests could be performed with the available sources, although some of them had lower activities as demanded by the testing standards. Moreover, for the background effect test, with the given test method it was impossible to raise the radiation background without triggering an alarm, i.e. the intended effect wasn't a challenge for the SPRM.

For testing neutron capability it turned out that the available  $^{252}\text{Cf}$  source and also the testing arrangement was not optimal:

- Due to its age the source already contained a lot of decay products leading to considerable emission of gamma radiation, which produced interfering gamma detection events.
- Because of backscattering of neutrons from the floor lead to higher count rates in the lower measurement positions, therefore the detector sensitivity in vertical profile test turned out to be lowest in the highest measurement positions.

The round-robin exercise was an excellent opportunity to optimize the work-flow for performing detector tests under commercial framework conditions in our laboratory. There has been considerable effort for set-up of the testing facility and making available all necessary components and experienced staff required for the performance of detector tests according to IEC standards, especially the effort for documentation and report writing turned out to be very time consuming. At the moment there is no business model for testing facilities carrying out detector tests as a routine task, as such testing is not required by the market or by companies. Therefore, under given market conditions, keeping up the infrastructure and availability of qualified personnel without envisaged future incomes seems very difficult for a commercial company like Seibersdorf Labor GmbH.

### 9.4. The Fraunhofer results

In the set of tests for SRPM device we encounter a major memory problem which led to the fact that no data could be stored any longer, respectively was visible and analyzable in the SPIRIdent software

(SpirPortal Replay). After contacting the manufacturer we received a SQL script with which it was possible to empty the database (e.g. delete the old images data) and perform measurements with longer measurement times without any further problems. Due to the absence of HEU, WGPu, medical isotopes and pure Beta sources the following measurements couldn't be conducted in the Fraunhofer INT laboratory: identification of mixed radionuclides, masking and interfering beta radiation.

For the RID we could not get the following information out of the manual or from the device: reference points for the gamma and the neutron measurements are not marked.

In the **Tables 2 - 4** below the time spent on each measurement performed for the SRPM, RID and the PRD is shown.

**Table 2:** Summary of the Fraunhofer INT testing of the SRPM device.

Test	Time effort [h]	
	Measurement + preparation time	Performed test
General test requirements	3.5	✓
Vertical profile <sup>1</sup>	2.4	✓
False alarm <sup>1</sup>	1.4	✓
Background effects	2.00 <sup>2</sup>	✓
Over range characteristics for ambient dose equivalent rate indication	0.55	✓
Response to gamma	16.5	✓
Response to neutrons	7.6	✓
Neutron indication in the presence of photons	3.8	✓
Single Radionuclide Identification	0 <sup>3</sup>	✓
Identification of shielded radionuclide	-	✗
Simultaneous identification & masking	-	✗
Over-range characteristics for identification	0.75	✓
<b>Total</b>	<b>63.0<sup>4</sup></b>	<b>ten: ✓ two: ✗</b>

<sup>1</sup>Due to the enormous problems with the data storage the real times for these tests have been much larger. Given here are the times which would have been needed without storage problems.

<sup>2</sup>Two people are needed. This is the time for one person for the measurement.

<sup>3</sup>Measurement was done under Response to gamma

<sup>4</sup>This total include also unattended measurements (i.e. False alarm)

**Table 3:** Summary of the Fraunhofer INT testing of the RID device

Test ID	Time effort [h]: Measurement + preparation time	Performed test
Accuracy test for photons	17	✓
Over range characteristics for ambient dose equivalent rate indication	2.5	✓
Time-to-alarm; photons	3	✓
Time-to-alarm; Neutrons	2	✓
Neutron indication in the presence of photons	1	✓
False identification rate	2	✓
Single Radionuclide Identification	25	✓
Identification of mixed radionuclides	-	✗
Masking	-	✗
Interfering beta radiation	-	✗
Overload characteristics for identification	6	✓
Spectra:	4	✓
<b>Total</b>	<b>62.5</b>	<b>eight: ✓ three: ✗</b>

**Table 4:** Summary of the Fraunhofer INT testing of the PRD device.

Test ID	Time effort [h]: Measurement + preparation time	Performed test
<b>General Test Requirements</b>		
Test configuration	partly 3 persons had to perform the tests altogether the time needed was 2.5	✓
Acceptance Test		✓
Display		✓
Audible and vibration alarm – gamma		✓
Reference point marking		✓
Instrument size		✓
Clips and lanyards		✓
User interface		✓
Documentation		✓

Battery Requirements	100 <sup>1</sup>	✓
<b>Radiological Tests static</b>		
False identification rate	23 <sup>1</sup>	✓
Time-to-alarm; Photons	4.3	✓
Time-to-alarm; Neutrons	2.75	--
Accuracy test for photons	10.8	✓
Over range characteristics for ambient dose equivalent rate indication	0.9	✓
Gamma response of neutron detector and neutron response in the presence of Gamma	4	--
<b>Radiological Tests - dynamic</b>		
Dynamic sensitivity to gamma and neutron radiations	2.3	✓
<b>Total</b>	<b>152</b>	✓

<sup>1</sup>Times including the measurement where no person is needed to observe the measurement.

## 9.5. The CEA results

The following tables represent a non-exhaustive summary of the various tests and manpower dedicated to testing the PRD (see **Table 5**), the RID (see **Table 6**) and the SRPM (see **Table 7**). The manpower and time effort numbers only answer for the actual testing of the instrument. They do not include documentation's preparation, results' validation or report writing, which can add up from 7 to 18 days depending on the instrument.

Every instrument showed different rate of success. The PRD mostly failed tests regarding response time and detection of neutrons but was successful on photons accuracy measurements and false identification testing. The RID failed most tests involving neutrons, single and masked radionuclide identification but was successful for basic gamma-ray alarms (time response test) and identification of mixed radionuclides. The SRPM also mostly failed all tests concerning neutrons but was successful in the field of single and masked radionuclides identification.

The main difficulties revealed by the tests were the unavailability of radioactive sources required by the standards' requirements, especially for SNM sources. Some tests were also only partially performed due to unavailability of SNM and medical sources. Aside from this topic, some standards' requirements could be clarified in order to help the testing process. For example during accuracy for photons testing, to accommodate for the low activity sources having to be used at closer distances, the notion of "homogeneous radiation field" should be clearly established. Also, a possibility of including further investigating the instrument's response in the standards would be beneficial. In order to obtain more information in cases where the instruments fail, such as neutron indication in the presence of photons or neutrons time-to-alarm, it would be worth investigating at which neutron rates or times the instruments pass the tests. Finally, the overall workflow at CEA could be optimized to improve time spent during experimental set-ups.

**Table 5:** Summary of the CEA's testing on the PRD device.

PRD Testing	Manpower and time effort	Performed test	
General PRD requirements	3p x 2h	✓	
False identification rate	6h	✓	
Accuracy tests for photons	2p x 12h	✓	
Over-range characteristics for ambient dose equivalent	2p x 3h	✓	
Time-to-alarm (photons)	2p x 4h	✓	
Time-to-alarm (neutrons)	2p x 4h	✓	
Dynamic sensitivity to gamma and neutron radiations	2p x 5h	✓	
Gamma response of a neutron detector and neutron response in the presence of gamma-rays	2p x 4h	✓	
<b>Total</b>	<b>~ 5 days with 2p</b>	✓	<b>8</b>
		x	<b>0</b>

**Table 6:** Summary of the CEA's testing on the RID device.

RID Testing	Manpower and time effort	Performed test	
Accuracy for photons	2p x 16h	✓	
Over-range characteristics for ambient dose equivalent	2p x 3h	✓	
Time-to-alarm (photons)	2p x 3h	✓	
Time-to-alarm (neutrons)	2p x 4h	✓	
Neutron indication in the presence of photons	2p x 3h	✓	
False identification rate	2p x 3h	✓	
Single radionuclide identification	2p x 28h	✓	
Mixed radionuclides identification	2p x 5h	✓	
Masking	2p x 6h	✓	
Interfering beta radiation	-	x	
Overload characteristics for identification	2p x 3h	✓	
<b>Total</b>	<b>~ 10 days with 2p</b>	✓	<b>10</b>
		x	<b>1</b>

**Table 7:** Summary of the CEA's testing on the SRPM device.

SRPM Testing	Manpower and time effort	Performed test	
Vertical profile	2p x 2.5d	✓	
False alarm and false identification rates	0.5d	✓	
Background effects	2p x 5h	✓	
Over-range characteristics for ambient dose equivalent	2p x 4h	✓	
Response to gamma-rays	2p x 10h	✓	
Response to neutrons	2p x 3h	✓	
Neutron indication in the presence of photons	2p x 1.5h	✓	
Single radionuclide identification	2p x 7h	✓	
Shielded radionuclides identification	2p x 4.5h	✓	
Simultaneous identification and masking	2p x 5.5h	✓	
Overload characteristics for identification	2p x 2h	✓	
<b>Total</b>	<b>~ 8 days with 2p</b>	✓ x	<b>11</b> <b>0</b>

## 10. Inter-comparison of results

### 10.1. Introduction and scope

The JRC team received for the three families of detector (SRPM, RID, and PRD) a total of 13 reports with the following distribution:

1. Commissariat à l'Energie Atomique et aux Energies Alternatives (CEA): 1x PRD report, 1x RID report, 1 SRPM report
2. Fraunhofer Institute for Technological Trend Analysis (Fraunhofer): 1x PRD report, 1x RID report, 1 SRPM report
3. Center for Energy Research (MTA EK): 1x PRD report, 1x RID report, 1x SRPM report
4. Institut de Radioprotection et de Sûreté Nucléaire (IRSN): 1x PRD report, 1x RID report, 1 SRPM report
5. Seibersdorf Labor GmbH (SL): 1x SRPM report

The data and comments from the different laboratories has been taken in account with the reference values from the test data of the same three families of detector and an inter-comparison has been performed. It is important to highlight the importance of evaluate the capacity building in testing and evaluating RN detection equipment for all the laboratories. The round robin exercise has shown the performance of the different laboratories to assess the radiological performance of the mentioned three families of RN detection systems against standards. The JRC has provided, equally to all 5 laboratories before the round robin exercise, three documents (i.e. "PRD test method", "RID test method" and "SRPM test method") that describe the procedure that shall be followed by them in order to perform the radiological tests against the IEC standards.

In this section the cross comparison results will be shown in a form of table for each of the three families of detector (PRD, RID, and SRPM) as deduced from the laboratory reports. A simple color coding structure will have the following meaning on the mentioned tables:

	Test successful completed
	Test partially completed
	Test not performed

In particular the terminology “test successful completed” it means that the laboratory was able to perform the test following the relative test method provided by the JRC and the data were put in comparison with the JRC results. The terminology “test partially completed” means that the laboratory was not able to perform fully the test and it provided a partial result/s to JRC team with possible comments on their incurred difficulties. The terminology “test not performed” shall indicate a test that the laboratory was not able to perform for practical reason (e.g. unavailability of a radioactive source, absence of enough shielding material and so on) or for unforeseen difficulty during the round robin exercise (storage or user documentation issues). Remember the indication of “test successful completed” is not an indication of the pass of a test from the evaluated instrument because no performance instrumentation will be reported in this document.

### 10.2. PRD measurements

**Table 8** is reporting all the data collected from the five involved laboratories. It is foreseen that not all required tests described in the current standard can be done by a single laboratory and the below table will evidence it but at the same time it showed the feasibility of having a set of laboratory that can perform all tests required for a valid certificate for the user.

**Table 8:** Reported data of the **PRD** from the five participant laboratories.

	Fraunhofer INT	SL <sup>1</sup>	MTA EK	CEA	IRSN
<b>False alarm</b>					
<b>Time-to-alarm: photons</b>					
<b>Time-to-alarm: neutrons</b>	2				
<b>Accuracy test for photons</b>			3		
<b>Over range characteristics for ambient dose equivalent rate Indication</b>					
<b>Gamma response of a neutron detector and Neutron response in the presence of Gamma</b>	2				
<b>Dynamic sensitivity to gamma and neutron radiations</b>					

### 10.3. RID measurements

**Table 9** is reporting all the data collected from the five involved laboratories. It is foreseen that not all required tests described in the current standard can be done by a single laboratory and the below table will evidence it but at the same time it showed the feasibility of having a set of laboratory that can perform all tests required for a valid certificate for the user.

<sup>1</sup> The Austrian Seibersdorf Labor GmbH

<sup>2</sup> Not enough information available at the current moment.

<sup>3</sup> The test was not complete as a whole because of the unavailability of some radioactive sources.

**Table 9:** Reported data of the **RID** from the five participant laboratories.

	Fraunhofer INT	Seibersdorf	MTA EK	CEA	IRSN
False identification rate					
Accuracy tests for photons			4		5
Over range characteristics for ambient dose equivalent rate Indication					
Time-to-alarm: photons					
Time-to-alarm: neutrons					
Neutron indication in the presence of photons			6		
Single Radionuclide Identification				7	8
Identification of mixed radionuclides	9			6	10
Simultaneous identification & masking	7			9	11
Interfering beta radiation	12		13	14	15
Overload characteristics for identification					16

#### 10.4. SRPM measurements

**Table 10** is reporting all the data collected from the five involved laboratories. It is foreseen that not all required tests described in the current standard can be done by a single laboratory and the below table will evidence it but at the same time it showed the feasibility of having a set of laboratory that can perform all tests required for a valid certificate for the user.

<sup>4</sup> Not a complete list of sources available.

<sup>5</sup> Not completed for <sup>241</sup>Am and <sup>60</sup>Co sources due to low activity availability.

<sup>6</sup> Due to the results from the "Time-to-alarm: photons" this test was skipped.

<sup>7</sup> No medical or Pu sources available.

<sup>8</sup> Absence of medical radioisotopes.

<sup>9</sup> Due to the absence of HEU and WGPu sources.

<sup>10</sup> Not enough activity for the <sup>137</sup>Cs and <sup>60</sup>Co to perform this test.

<sup>11</sup> Absence of medical radioisotopes and NORM radioisotopes.

<sup>12</sup> Due to the absence of needed beta emitter (<sup>32</sup>P, <sup>90</sup>Sr/<sup>90</sup>Y).

<sup>13</sup> Not available beta emitter source.

<sup>14</sup> A <sup>90</sup>Sr/<sup>90</sup>Y 4MBq source was ordered but not delivered in time for the tests.

<sup>15</sup> Beta emitter source not available.

<sup>16</sup> Not high activity radioactive sources available.

**Table 10:** Reported data of the **SRPM** from the five participant laboratories.

	Fraunhofer INT	Seibersdorf	MTA EK	CEA	IRSN
<b>Vertical profile</b>	<sup>17</sup>				
<b>False alarm</b>					
<b>Background effects</b>					
<b>Response to gamma-rays</b>					
<b>Response to neutrons</b>					
<b>Over-range characteristics</b>					
<b>Neutron indication in the presence of photons</b>					
<b>Single Radionuclide Identification</b>	<sup>18</sup>	<sup>19</sup>		<sup>20</sup>	<sup>21</sup>
<b>Identification of shielded radionuclide</b>	<sup>21</sup>			<sup>21</sup>	
<b>Simultaneous identification &amp; masking</b>	<sup>21</sup>	<sup>22</sup>		<sup>21</sup>	<sup>21</sup>
<b>Over-range characteristics for identification</b>					

### 10.5. Summary of results

All laboratories were able to perform both dynamic and static tests using different concepts of operation in term of dynamic of the trolley system (dynamic tests) and acquisition system for the different type of data (i.e. environmental parameters, dose rate, image acquisition, and data acquisition/storage). It was noted by most laboratories that one of the main difficulties was the availability of the radioactive sources in term of type of isotopes as well as range of activity. Thus some laboratories were able to perform a specific set of measurements not others and vice versa.

The following spider plot (see **Figure 19**) highlighted the strength and weakness that different laboratories experienced during the round robin exercise as evaluated by each laboratory.

The long testing experience of the JRC over many years covering more than 100 RN instruments in the 8 families range for nuclear security allowed the provision of adequate testing procedures and a sound assessment, planning and preparations for the tests against the standards. Time required by the measurements and data analysis is of course costly and demanding in term of human resources. The availability of radioactive sources required by the standards in terms of type and activity is essential for the completion of all the required (by standards) tests. Although not extensively mentioned, it is also necessary to have a full understanding of the instruments characteristics in term of mode/s of use, configuration settings, installation instructions and not least its scope of use in the real environment. A full and active interaction in term of communication with the instrument owner is

<sup>17</sup> Not performed with <sup>241</sup>Am and <sup>60</sup>Co.

<sup>18</sup> Not a full extends of the radioactive isotopes were available (i.e. medical and nuclear).

<sup>19</sup> Tests applying SNM sources were not carried out due to regulatory restrictions in handling such materials.

<sup>20</sup> No medical radioactive sources available or <sup>239</sup>Pu.

<sup>21</sup> No medical radioactive source available.

<sup>22</sup> Tests applying SNM sources were not carried out due to regulatory restrictions in handling such materials.

also fundamental to cover all the unknown characteristics that are not mentioned in the operation manual.

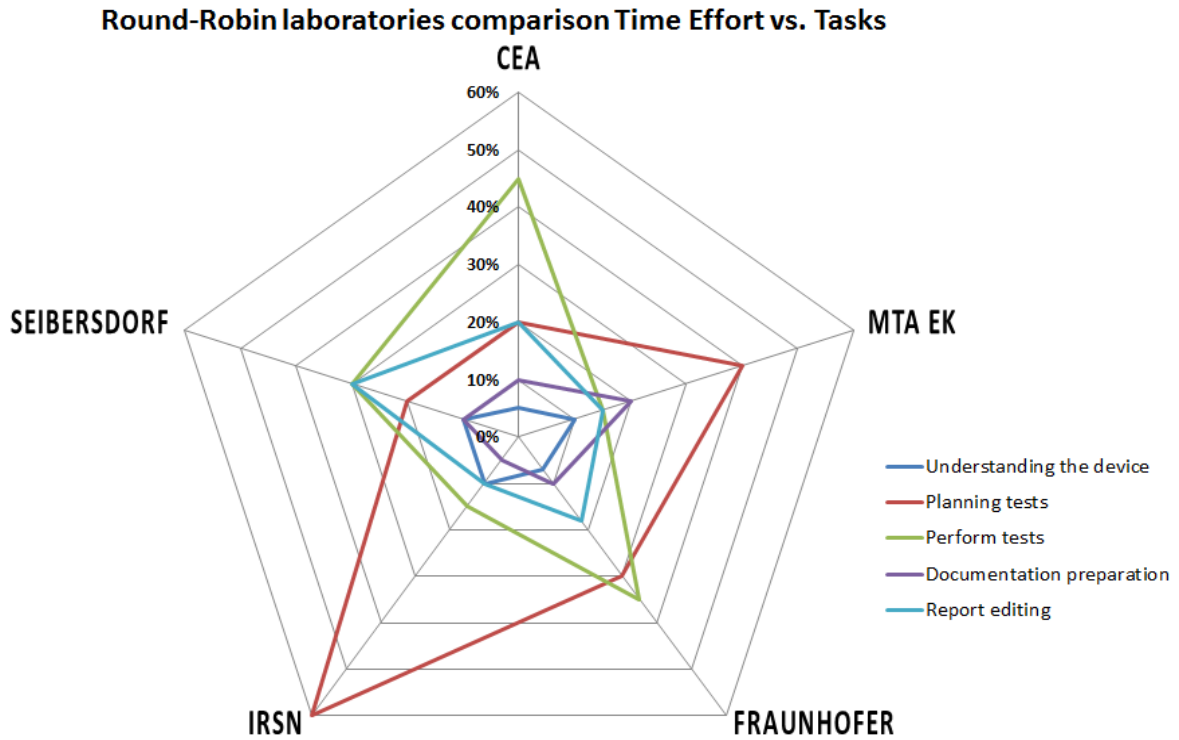


**Figure 19:** Spider diagram of the time spent in each specific task by the five involved laboratories in the round robin exercise.

## 11. Conclusion

Within ITRAP+10 Phase II, good progress was made to build capacity in EU members states for testing and performance evaluation of nuclear security detection equipment used to combat the illicit trafficking of nuclear and other radioactive materials and out of regulatory control. Capacity building was achieved through the provision by JRC to a consortium of EU laboratories of testing procedures and the organization of a round robin exercise based on a set of representative instruments (PRD, RID and SRPM). The detection equipment had been thoroughly tested at JRC-Ispra and inter-compared where appropriate between the participating laboratories on one hand and with JRC-measurements as the reference on the other.

Each of the EU laboratories (partly funded by the EU) was thus able to develop and construct testing facilities similar to the ITRAP facility in Ispra be it on a smaller scale and each one with its characteristics, advantages and some understandable limitations initially at least. Collaboration between different testing laboratories to complement each other's capabilities in order to provide a full service may thus be essential and recommended in the short term at least.

These EU facilities are now ready to be used by EU companies, research laboratories and operators for testing and R&D regarding detection equipment in nuclear security thus setting up an important milestone towards further standardization and certification which consequently will enhance nuclear security, innovation and competition.

## 12. References

- [1] Council of the EU, document 15505/1/09 REV 1, adopted in Dec 2009 by the council with the aim of strengthening CBRN security throughout the EU
- [2] CBRN action plan to enhance preparedness against chemical, biological, radiological and nuclear security risks COM (2017) 610 final of 18.10.2017 (Communication to the EU parliament, the council, the EU economic and social committee and the committee of the regions)
- [3] ITRAP +10 test campaign summary report, 25 Jan 2016, EUR publication no. 27958 <https://ec.europa.eu/jrc> Available from EU Bookshop (<http://bookshop.europa.eu>)
- [4] The ITRAP+10 summary report is also made available by the U.S. Department of Homeland Security – Domestic Nuclear Detection Office with the following identifiers:  
Guidance: DHS SCG DNDO-001.1, 12/12 Document Number: 200-ITRAP-124860V1.0
- [5] S. Abousahl, C. Carrapico, G. Eklund, V. Forcina, M. Goncalves, M. Marin-Ferrer, A. Ossola, J. Paepen, P. Peerani, F. Raiola, R. Rossa, F. Rosas, A. Rozite, A. Tomanin and H. Tagziria, 'The Illicit Trafficking Radiation Assessment Program (ITRAP+10) for Detection Equipment in Nuclear Security' 39th ESARDA symposium Dusseldorf May 2017, <https://esarda.jrc.ec.europa.eu/>

## Acknowledgements

The funding of the EC's DG-Home as well as the coordination by Expertise France are acknowledged

# **Session 10:**

# **Sealing / Dry Storage**

## Spent fuel cask reverification Brief technology survey for an integrated multi-method toolkit

Stefano Vaccaro<sup>1</sup>, Hamid Tagziria<sup>2</sup>, Darius Ancius<sup>1</sup>, Alice Tomanin<sup>1</sup>, Peter Schwalbach<sup>1</sup>, Katharina Aymanns<sup>3</sup>

<sup>1</sup>European Commission, Directorate General Energy, Directorate Euratom Safeguards, Luxembourg

<sup>2</sup>European Commission, Directorate General Joint Research Centre, Ispra, Italy

<sup>3</sup>Forschungszentrum Jülich GmbH, IEK-6, 52425 Jülich, Germany.

### Abstract:

*The back end of the nuclear fuel cycle requires more and more attention by the Safeguards Community in the next decades. With more than 50 out of the 129 reactors currently in operation in the EU planned to be shut down by 2025, a large amount of nuclear-material-bearing spent fuel will require interim storage for between 40 and 100 years mostly in dedicated facilities hosting casks. Moreover, once their design capacity has been reached, these interim storages will move from a dynamic phase, where the material inventory is constantly increasing by the continuous influx of material, to a static one, with a constant inventory of nuclear material, practically inaccessible for verification purposes.*

*In such a context, the Continuity of Knowledge (CoK) regarding previously verified fuel is a key element of the safeguards strategy and consequently the risk of its loss becomes the biggest liability in the absence of adequate cask (re)verification methods. Current methods, such as neutron fingerprinting by dual slab detector, do not always supply conclusive evidence for the absence of material diversion. As a result, the risk of CoK loss can currently only be mitigated by redundant multilayer containment and surveillance (C/S), whose robustness comes with a high cost in terms of resources, inspectors' radiation dose burden and safety. New (re-)verification tools are thus of high importance.*

*The current paper assesses methods and technologies with the goal to define the user requirements they respond to (e.g detection of a missing assembly), current technology readiness levels, deployment cost etc. These methods include state-of-the-art NDA methods, used in nuclear safeguards generally and spent fuel verification in particular, as well as other potential technologies that either may be under development or applied elsewhere, such as muon, gamma and neutron imaging, active interrogation etc. The final objective is to stimulate the scientific community to propose and develop an integrated multi-method toolkit for cask reverification, that could become a fundamental building block for a new, more effective and efficient inspection approach to interim dry spent fuel storages.*

**Keywords:** Spent Fuel; Dry Storage; Verification; NDA

### 1. Introduction

European Union Member States need to apply the highest standards of nuclear safety, security, waste management and non-proliferation. Recently, the back-end of the nuclear fuel cycle, defined as the phase after the productive life of the fuel, where the fuel needs to be either recycled or stored safely and securely, receives increased attention, due to the growing number of spent fuel assemblies being stored in dry spent fuel storage facilities (SFSF) facilities. This has resulted in a situation where the currently used techniques for safeguarding these facilities are causing a disproportionately high work load for both DG ENER and IAEA inspectorates. Further, the large number of spent fuel containers is causing a considerable radiation dose intake for the inspectors applying these techniques as well as for the facility operators accompanying these inspectors.

The current paper focuses on promising ideas and developments regarding potential reverification techniques that, applied in the future in European SFSF, may complement the safeguards approaches in case of a loss of *Continuity of Knowledge* (CoK).

## 2. Problem statement

Safeguards inspectorates worldwide are considering several type of spent fuel diversion scenarios from a dry spent fuel cask.

Confirmation a nuclear material diversion after a loss of Continuity of Knowledge (CoK) or its detection by routine measurements would require reliable and performant verification tools, aiming at re-establishing the assurance on the integrity of the container and its content [1]. Today safeguards inspectorates do not have performant and independent technical solutions for that. A loss of CoK entails a heavy effort on the inspectorates and operators.

The best available technique, so far, has been neutron fingerprinting, whose limits in terms of diversion detection capability have been discussed in the past [2]. Moreover, the growing number of loaded spent fuel cask in centralised and on-site stores increases the need for verification tools to be available for safeguards inspectors.

## 3. Solutions under consideration

Conventional and well-proven non-destructive safeguards verification techniques are based on low energy emitted or interrogating particles. Spent fuel cask have strong shielding for high radiation protection and only high-energy particles could penetrate spent fuel cask shielding and thus be used for interrogation. The practical choice of verification methods, to be deployed within a horizon of about 5 years, can be narrowed to cosmic muons and fast spontaneous fission neutrons present in spent fuel. Direct verification of Pu and U isotopes would be the inspectors' strict requirement, if technically feasible. However, the radiation emanating from spent fuel is predominantly coming from fission products (e.g. gammas, Cs) and transuranium elements (e.g. neutrons, Cm). Only a very small fraction of the radiation comes from Pu and U. Thus, the signals are indirect verifications of nuclear material.

In view of application of high-energy neutrons and looking at longer time perspective, the compact laser-driven neutron sources could be another novel technology that may allow direct verification of nuclear material in spent fuel casks. This technology was proposed by Technical University of Darmstadt and its feasibility demonstrated in Los Alamos National Laboratory.

### 3.1 Imaging with cosmic muons (muography)

#### 3.1.1 Physical principles

Muons are charged leptons, with physical properties similar to those of the electrons, but with a free rest mass 207 times heavier and a rest lifetime of 2.2 microseconds, before decaying in an electron and two neutrinos (muon-neutrino, electron-anti-neutrino). Cosmic muons are born in upper layers of the terrestrial atmosphere because of primary cosmic radiation. These relativistic particles reach earth's surface with a flux of about 10,000 muons/m<sup>2</sup> min and average energy of 3 GeV. Being charged particles, muons mostly loose energy by ionization of atoms on their path (Coulomb interaction). Because ionization dissipates energy in relatively small amounts, muons of some GeV energy are still capable to penetrate meters of steel and hundreds of meters of rock, allowing their use for imaging of massive and heavily shielded objects [4]. The simplest muon imaging technique is the radiographic picture, which shows the distribution of the densities inside the sampled volume.

However, since the basic mechanism of cosmic muons' interaction with the matter is Coulomb scattering, higher Z-material, like U and Pu, would create higher scattering angles. The cosmic muon imaging is based on measurements of muons' transmission and of their multiple scattering angles.

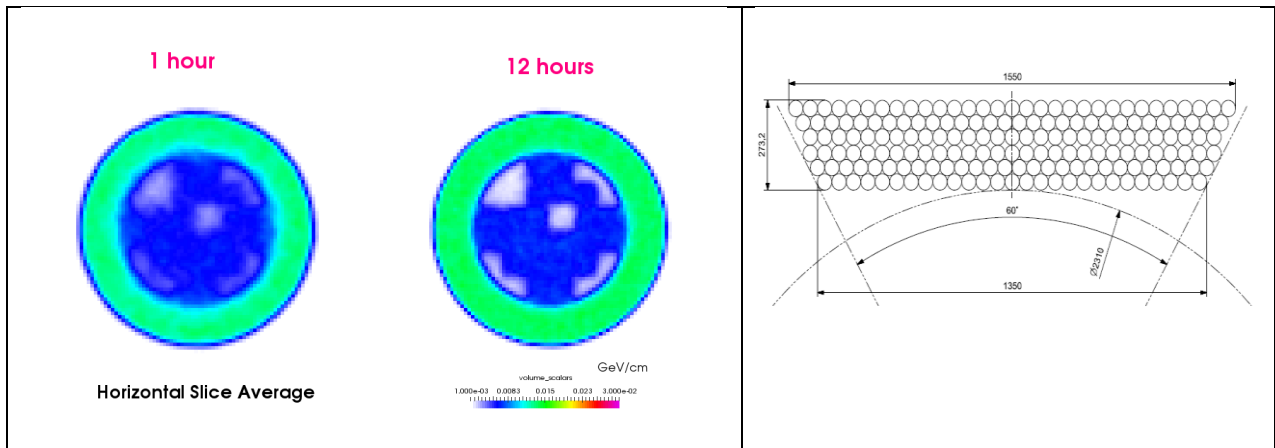


Figure 3: *Left*: Geant4 simulation of a full coverage 360° muon detector on CASTOR-24. Two missing fuel assemblies: one in the centre and one in upper left corner and their simulated measurement times taking into account the natural muon flux. *Right*: INFN proposed 1/3 full coverage prototype muon detector (two such slab trackers will be used for field tests).

### 3.1.2 Maturity of the technology

Muon measurements are one of the most developed areas of experimental high-energy particle physics. The recent development of the Compact Muon Solenoid (CMS) at CERN and of other high-energy particle detectors offer multiple solutions to measure muon energy and its momentum. Whereas evaluation of muon's momentum is the most important task in colliders and accelerators, Los Alamos National Laboratory scientists proved that its measurement for imaging purposes is not necessary [5]. This significantly simplifies muon detectors for imaging purpose, by eliminating the use of magnets and absorbers.

During the last 15 years, muography (combination of muon radiography and scattering angle measurements) has seen an impressive development from purely scientific to industrial application, spanning from volcano monitoring to national security and nuclear waste characterisation [6]. In 2018, a first industrial nuclear waste tomographer using scintillation fibres technology has been deployed at the Sellafield site, UK [7][8].

The same year, DG ENER and Padova INFN (Italian Institute for Nuclear Physics) have effectively tested a small-scale drift-tubes-based muon tracker prototype at a dry store in Neckarwestheim, Germany. The test proved that the cosmic muons can be successfully measured in proximity of a fully loaded spent fuel cask. The background gamma and neutron radiation resulting from the spent fuel cask represented only ~1% of the useful signal [9]. Monte Carlo calculations by Geant4 [10], suggest that it is feasible to obtain a tomographic image allowing to determine if an assembly is missing inside a cask, by using a 1/3 full-scale prototype tomographer based on drift tubes. Therefore, the basic technology can be considered mature for in field tests.

## 3.2 Imaging with fast spontaneous fission neutrons from spent fuel

### 3.2.1 Physical principles

Spent nuclear reactor fuel is a strong neutron emitter due to spontaneous fission of transuranium elements (mainly Cm). The neutron flux can be characterised by a spontaneous fission spectrum, since the other neutron emitting processes, like  $(\alpha;n)$  reactions, usually contribute by one or two orders of magnitudes less to the emitted flux. Although the spectrum maximum lies between 2 and 3 MeV there is a non-negligible tail towards higher energies up to 10 MeV and beyond. Conventionally, the neutrons of several hundred keV and above are defined as fast neutrons. Since the probability of interaction of the neutrons with matter is usually inversely proportional to their velocity, fast neutrons have high penetrability and can escape the heavy shielding with straight trajectories, thus giving important information on their origin, once suitably measured. In fact, the detectors of fast neutrons can also be considered as a camera giving an image of the spontaneous fission source distribution

behind the shielding. Thus, one interesting question is: could a measurement of the fast neutron flux on the top of a spent fuel cask provide a map of the fuel assemblies inside it?

### 3.2.2 Maturity of the technology

Detection of thermal and cold neutrons is a known and well-established area of measurements and of object tomography. A number of neutron detectors coupled with cameras are available on the market. Fast neutron detectors are rather custom built and usually operated in physics experiments, like in neutron beam detection. The detectors use light elements, such as H, He or C, which convert a scattered incident neutron's energy to light. A number of plastic, liquid scintillators or diamond detectors are available on the market. The technology still needs to be demonstrated in field. Several detectors maybe needed for field tests with spent fuel casks.

Setting up the fast neutron detectors for an actual physics experiment is a complex process and the final result depends on the correct assessment of the boundary conditions. Since, the use of fast neutron detectors for spent fuel cask is a novelty, which has not yet been tested, research experiments will be useful to develop the optimal system. In this view, special circumstances, such as the thick shielding, the presence of a background of intense gamma radiation and of thermal neutrons have to be taken into account to ensure the actual applicability of the system. Optimal fast neutron detection conditions involving efficient gamma-neutron signal separation, shape of collimator and/or of low energy cut off filters as well as corrections due to burn up should be modelled before the start of the field test.

Important development and research of fast neutron detectors for safeguards purposes has been made by IAEA, Michigan University and by Lawrence Livermore, Los Alamos, Oak Ridge, Brookhaven National Laboratories [12][13][14]. Co-operation of safeguards inspectorates with such organizations is a natural way forward for the development of fast neutron detectors for spent fuel cask safeguards. The detection through the lid of the container is very promising because it may allow distinguishing the signal from individual elements in the cask, which may not be the case from the side. Some interesting investigation and review of plausible detection solutions for spent fuel cask verification has been done by Lawrence Livermore National Laboratory. Monte Carlo calculations suggest that the fast neutron flux as measured on the top of spent fuel cask is by 20 to 40 % lower on the upright position of a missing assembly [12].

The new fast neutron measurement technology is quickly developing today due to new era accelerators and associated electronics. Some study and modelling of the most promising solution for spent fuel cask should be performed before in field tests.

### 3.3 Complementarity of the two described methods: towards a multi-method toolkit for cask reverification

Both, muon and neutron, technologies are mature for field tests with a loaded cask which can be performed in 1 – 1.5 years' time.

- Muon detectors have good possibilities to detect missing assemblies in a spent fuel cask and are not dependent on the burn up of spent fuel, whereas the fast neutron detectors may not be applicable in case of low burn up. However, fast neutron detectors, in principle, have in theory excellent capability to distinguish a dummy assembly from a real one, whereas a muon detector's detection sensitivity is limited.
- The physical processes behind muography and fast neutron detection are very different, as the two techniques focus on different physical observables. The two methods are therefore complementary and offer to safeguards inspectors the possibility to apply the technology combination, which fits best the actual safeguards inspection scenario.

The complementarity of the two technologies described makes them the most mature candidates to be integrated in a multi-method toolkit for cask reverification.

**Summary of key features of the two already existing technologies for spent fuel verification in spent fuel casks.**

	<b>Muon Tomograph</b>	<b>Fast Neutron imaging</b>
<b>Maturity for field test (Technology Readiness Level, TRL, according to [15])</b>	Mature (TRL = 6, “technology demonstrated in relevant environment”)	Fairly mature, developing (TRL = 5, “technology validated in relevant environment”)
<b>Time needed to set up prototype for field tests</b>	1 year	1 – 1.5 years
<b>Estimated cost of prototype</b>	>100,000 euros	Several ten thousands of euros estimated (several detectors + electronics + mechanical structure, initial simulation)
<b>Potential to identify a missing assembly in a spent fuel cask</b>	Very high according to Monte Carlo simulations	Very probable. Preliminary Monte Carlo simulation promising.
<b>Potential to identify a dummy assembly in a spent fuel cask</b>	Very challenging. Depends on dummy material. Monte Carlo simulation for stainless steel dummies is ongoing	Very probable.
<b>Dependence on burn up and delay after discharge from reactor</b>	Does not depend on burn up and after reactor storage time.	The higher the burnup and the shorter the delay after reactor storage, the better. Low burn up fuel could be challenging to detect.
<b>Effort to operate during inspection</b>	Requires potentially cumbersome manipulation due to large dimensions of detector. Access from all cask sides needed. The spent fuel cask needs to be moved to maintenance area for verification.	Medium-easy to use. Access to the top of spent fuel cask is needed. Presumably no need to move spent fuel cask from its store position.
<b>Potential use of technology in other types of installation</b>	Yes:  Encapsulation Plant – hot cell, confirmation of emptiness of discharged transport cask. Deep geological repository – confirmation of completeness of copper canisters after transport from interim store.	Yes:  Encapsulation Plant – hot cell, confirmation of emptiness of discharged transport cask. Encapsulation Plant – hot cell, monitoring of transport casks’ unloading process.

### 3.4 Potential of High-energy Neutron Sources to image the structure of a spent fuel cask

#### 3.4.1 Physical principles

The uniqueness of neutrons to probe materials relies in their high penetrability due to their neutral charge. However, without reactors or accelerators it is difficult to create the high energy and intensity neutron sources, which could be used to probe spent fuel cask. One of the possible solutions under investigation (another could be using small cavity linear accelerators, beyond the scope of this paper [16]) to this issue has been observed experimentally with the recent developments of the high-energy short pulse lasers (HESP), which show the technical feasibility of compact and mobile laser systems to image structured objects. Such systems are able to generate intense and directed ion beams, which can be used to produce short and intense neutron pulses. Darmstadt Technical University and Los Alamos National Laboratory proved that an intense, laser-generated, 170 MeV deuteron beam on a Be converter creates a forward directed neutron beam pulse with peak energies at 70 MeV and maximum energies of 150 MeV[17][18]. Such high-energy neutrons can penetrate dense and thick material. A preliminary Geant4 [10] simulation of a V/19 CASTOR shows that the high-energy neutrons would penetrate the spent fuel cask walls and create a significant number of the high-energy secondary neutrons. These secondary neutrons can be used for probing the internal structure of a spent fuel cask, could be measured by an array of external detectors and might allow assessing the amount of fissile material in the probed volume.

However there are still many unknown about the constraints to the actual depolyability of such a system and its cost, so it makes premature to add it to the comparison in table 1.

#### 3.4.2 Maturity of the technology

HESP neutron sources is a new developing technology (Technology Readiness Level = 3, i.e. "experimental proof of concept" according to [15]). It opens many possibilities for small-scale laboratories and universities worldwide, which have no reactors or accelerators giving them access to a strong neutron source. This technology will likely create a great interest for material sciences, fusion technology and the mobile and compact systems may become more accessible and cheap. Safeguards of spent fuel may benefit from this development. Important features of HESP neutron source are very short and high intensity, directed neutrons. As Figure 4 shows this flux would generate a number of secondary neutrons, which are one order of magnitude higher than the primary neutrons (which itself represent a very bright source - up to  $1 \times 10^{10}$  neutrons/sr during one shot in Darmstadt & LANL experiment). DG ENER is following this development. Especially interesting would be the detection of the secondary neutron flux created by the HESP and its possible use for imaging of a spent fuel cask. Other interesting phenomena, that may be used for safeguards purposes, are the induced fissions on U and Pu isotopes, multiple scattering of secondary neutrons, the use of fast neutron detectors to track the neutrons leaked from a cask. Therefore, DG ENER will continue to follow up the development and availability of compact and mobile HESP neutron sources.

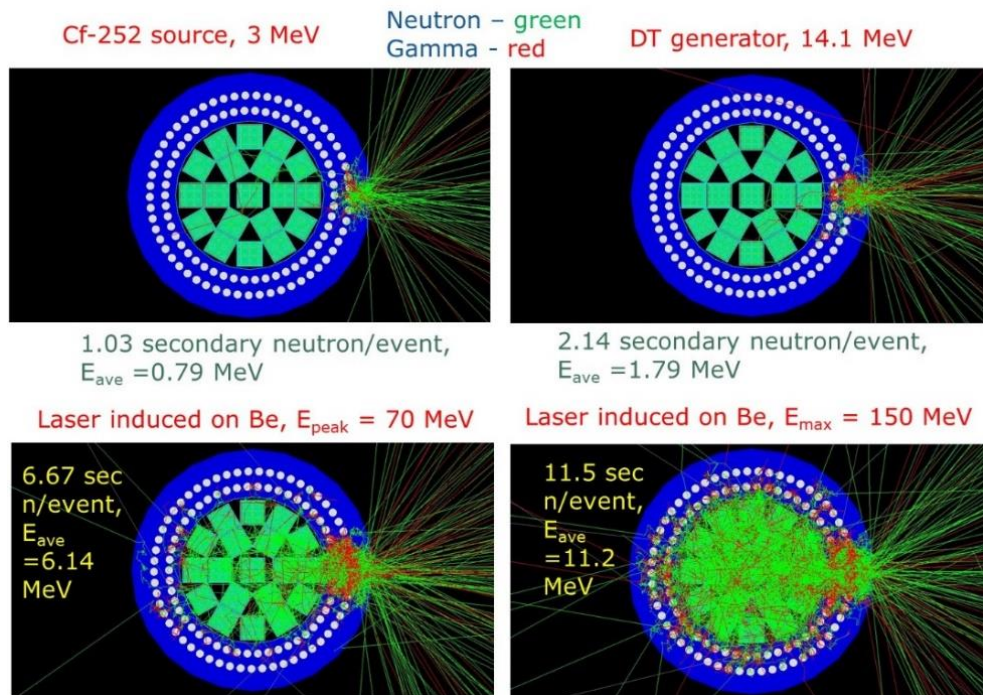


Figure 4: Geant4 simulation of CASTOR V/19 spent fuel cask and of an incident perpendicular neutron source from the right side. In all cases, the 100 neutrons at a given energies are simulated. Comparison of conventional (Cf-252, DT generator) and HESP induced neutron sources.

## 4. Conclusions

Reverification of spent fuel casks is one of the bigger challenges that safeguards inspectorates are currently facing. In fact, in the next 5-10 years, the quantity of fuel stored in interim dry storages is foreseen to grow steadily due to the aging and phase out of nuclear power plants, which started operations between the 1980s and the 1990.

In this context, the availability of a tool (or, more probably, a system of complementary tools) for spent fuel cask reverification would: firstly, drastically reduce the risk resulting from the loss of CoK; secondly, allow the safeguards inspectorates to revise their inspection approaches; and thirdly, to optimise the resources needed to ensure the absence of diversion of nuclear material at dry spent fuel storages.

In terms of their technological readiness level, cost and contribution to a reverification method two technologies, muon tomography and fast neutron, are ready to be proposed, in terms of maturity, as suitable for safeguards use in the near future and can easily be integrated in a multi-method toolkit. Based on the scientific observations available, laser-driven neutron active imaging technology could further improve the effectiveness of safeguards verifications, if it reaches a technology readiness level appropriate for industrial application.

However, in order to deploy these next generation technologies for safeguards use, the additional developments and adjustments need to be carried-out in cooperation between safeguards inspectorates and research institutions. The current paper, does not aim to provide conclusive indications, but rather to be a survey stimulating this discussion and cooperation.

## References

- [1] Katharina Aymanns, Astrid Jussofie, Peter Schwalbach, Konrad Schoop, Juha Pekkarinen, Lukasz Matloch, Darius Ancius, Mentor Murtezi, Arnold Rezniczek, Marcel Hahn, Thomas Krieger, Irmgard Niemeyer, *Aspects of Safeguarding On-Site Dry Storage Facilities*, Current conference proceedings, 2019.
- [2] Peerani P., Galletta M., *Re-Establishment of the Continuity of Knowledge in the Safeguards of Interim Storages using NDA Techniques*, Nuclear Engineering and Design vol. 237 no. 1 p. 94-99, 2007.
- [3] P. Checchia, *Review of possible applications of cosmic muon tomography*, Journal of Instrumentation, vol. 11, 2016.
- [4] Alvarez, L.W. et al. *Search for hidden chambers in the pyramids using cosmic rays*, Science 167, 832., 1970.
- [5] Borodzin, K.R. et al., *Surveillance: Radiographic imaging with cosmic-ray muons*, Nature 422 (2003) 277.
- [6] G. Jonkmanns, V. N. P. Anghel, C. Jewett and M. Thompson, *Nuclear waste imaging and spent fuel verification by muon tomography*, Annals of Nuclear Energy, vol. 53, 2013.
- [7] D.F. Mahon, A. Clarkson, D.J. Hamilton, M. Hoek, D.G. Ireland, J.R. Johnstone, R. Kaiser, T. Keri, S. Lumsden, B. McKinnon, M. Murray, S. Nutbeam-Tuffs, C. Shearer, C. Staines, G. Yang, C. Zimmerman, *A prototype scintillating-fibre tracker for the cosmic-ray muon tomography of legacy nuclear waste containers*, Nuclear Instruments and Methods in Physics Research Section A: Accelerators, Spectrometers, Detectors and Associated Equipment, Volume 732, 2013,
- [8] Mahon David, Clarkson Anthony, Gardner Simon, Ireland David, Jebali Ramsey, Kaiser Ralf, Ryan Matthew, Shearer Craig and Yang Guangliang, *First-of-a-kind muography for nuclear waste characterization*, 377, Philosophical Transactions of the Royal Society A: Mathematical, Physical and Engineering Sciences, 2018.
- [9] P. Checchia, D. Ancius, F. Gonella, G. Zumerle, K. Aymanns, N. Erdmann, P. Schwalbach and S. Vanini, *Muography of spent fuel containers for Safeguards*, in IAEA Symposium on International Safeguards: Building Future Safeguards Capabilities - Proceedings, Vienna, 2018.
- [10] Agostinelli S. et al., *GEANT4 – a simulation toolkit*, Nucl. Instrum. Met. A 506 (2003) 250 [https://doi.org/10.1016/S0168-9002\(03\)01368-8](https://doi.org/10.1016/S0168-9002(03)01368-8)
- [11] Darius Ancius, Katharina Aymanns, Paolo Checchia, Franco Gonella, Astrid Jussofie, Fabio Montecassiano, Mentor Murtezi, Peter Schwalbach, Konrad Schoop, Stefano Vaccaro, Sara Vanini and Gianni Zumerle, *Modelling of safeguards verification of spent fuel dry storage containers using muon trackers*, Current Conference Proceedings, 2019.
- [12] Y. Ham, *Verification of Spent Fuel Inside Dry Storage Casks by Fast/Epi-thermal Neutron Mapping*, Lawrence Livermore National Laboratory technical report, LLNL-TR-763971.
- [13] P. Vanier, *Radiation Templates of Spent Fuel in Casks*, Brookhaven National Laboratory Report, BNL-203645-2018-FORE (2018).
- [14] Mateusz Monterial, Peter Marleau, Sara Pozzi, *Characterizing subcritical assemblies with time of flight fixed by energy estimation distributions*, Nuclear Instruments and Methods in Physics Research Section A: Accelerators, Spectrometers, Detectors and Associated Equipment, Volume 888, Pages 240-249, ISSN 0168-9002, <https://doi.org/10.1016/j.nima.2018.01.080> (2018).
- [15] EUROPEAN COMMISSION, Technology readiness levels (TRL), HORIZON 2020 – WORK PROGRAMME 2018-2020 General Annexes, Extract from Part 19 - Commission Decision C(2017)7124, 2017.
- [16] d'Errico, F., Felici, G., Chierici, A. et al. *Detection of special nuclear material with a transportable active interrogation system* Eur. Phys. J. Plus (2018) 133: 451. <https://doi.org/10.1140/epjp/i2018-12292-6>
- [17] M. Roth, *Neutron Generation by Laser-Driven Proton Sources*, in 39th ESARDA Symposium- Proceedings, Düsseldorf, 2017.
- [18] Roth, M. et al., *Bright Laser-Driven Neutron Source Based on the Relativistic Transparency of Solids*. Physical Review Letters, 110(4), 1-5. (2013)

## Aspects of Safeguarding On-Site Dry Storage Facilities

**Katharina Aymanns<sup>1</sup>, Astrid Jussofie<sup>2</sup>, Peter Schwalbach<sup>3</sup>, Konrad Schoop<sup>3</sup>, Juha Pekkarinen<sup>3</sup>, Lukasz Matloch<sup>3</sup>, Darius Ancius<sup>3</sup>, Mentor Murtezi<sup>3</sup>, Arnold Rezniczek<sup>4</sup>, Marcel Hahn<sup>5</sup>, Thomas Krieger<sup>1</sup>, Irmgard Niemeyer<sup>1</sup>**

**<sup>1</sup> Forschungszentrum Jülich GmbH  
IEK-6: Nuclear Waste Management and Reactor Safety,  
Jülich, Germany**

**<sup>2</sup> BGZ Gesellschaft für Zwischenlagerung mbH,  
Essen, Germany**

**<sup>3</sup> European Commission, DG ENER, Euratom Safeguards,  
Luxembourg, Luxembourg**

**<sup>4</sup> UBA Unternehmensberatung GmbH  
Herzogenrath, Germany**

**<sup>5</sup> PreussenElektra GmbH,  
Emmerthal, Germany**

### **Abstract:**

*This paper describes current aspects related to German on-site spent fuel dry storage facilities (SFSFs) with regard to Germany's energy transition. The last nuclear reactor will be disconnected from the power grid in 2022. It is foreseen that about five years later the defueling of the reactors will be completed and all spent fuel loaded into dry storage casks and transferred to the SFSFs. Once the fuel is moved to storage and the loading pit in the reactor is decommissioned there is no possibility to open the spent fuel casks for re-verification of the inventory on the site. Until a disposal facility becomes available, in total more than 1.000 spent fuel casks (from light water reactors) will remain in 12 German on-site SFSFs and the three central SFSFs in Ahaus, Gorleben and Lubmin for several decades without further receipt or shipments.*

*Maintaining continuity of knowledge (CoK) of the inventory of nuclear material in spent fuel casks is a key safeguards requirement. In order to meet this requirement, the current practice is to implement a dual containment and surveillance (C/S) system using two independent sealing systems supplemented with camera surveillance. Gaining access to the top of the casks for seal verification is a time consuming procedure due to the dense packaging of the spent fuel casks. A longer stay in this high radiation environment leads to a high dose rate for inspectors and accompanying operators. Given this situation, there is an urgent need to explore alternative C/S methods and develop substantially improved re-verification capabilities for use by the inspectorates.*

*The paper will discuss technical solutions and concepts under consideration.*

**Keywords:** dry storage facilities, spent fuel, C/S systems, re-verification

## 1. Introduction

After the nuclear accident in Fukushima Daiichi the German federal government decided in June 2011 to exit nuclear power production with the commitment to complete the phase-out by end of 2022. As a consequence 10 of 17 nuclear power reactors (NPPs) have been shut down until now. The ongoing defueling of the reactors has caused a temporary sharp increase in the number of spent fuel casks loadings and transfers to dry on-site spent fuel storage facilities (SFSFs). This has led to a significant increase of inspections needed to verify nuclear material in spent fuel assemblies as well as loading of spent fuel casks and their transfer to the on-site SFSFs. Presumably by the end of the year 2027 all spent fuel assemblies will have been packed in transport and storage casks and transferred to SFSFs. Once the transfer is completed the on-site SFSFs will have a quasi-static inventory of more than 1,000 casks as no receipts or shipments are expected after the transfer will have been completed. The casks filled with spent fuel will remain in the SFSFs for several decades until the casks will be transported to final disposal. The specific conditions of a SFSF in static operation entail the need for technical solutions to ease safeguards inspections of loaded spent fuel casks and to minimize the radiation exposure of the inspectors and facility staff. Furthermore no sufficiently precise method is currently available for re-verification of nuclear material in spent fuel casks in SFSFs. This will become urgent once the reactors have been decommissioned and the possibility to open loaded spent fuel casks in the loading pool of a reactor would not further exist. Therefore, the investigation and development of potentially suitable technologies for re-verification is required.

## 2. Safeguarding German on-site storage facilities in quasi static operation

With the amendment of the Atomic Energy Act in April 2002, the energy supply companies were obliged to store irradiated fuel assemblies resulting from operation at the nuclear power plants in storage facilities on-site. Decentralized storage facilities in operation ensure that further transports in the Federal Republic of Germany, e.g. from nuclear power plants to central storage facilities, are not necessary. In the years 1998 to 2000, the NPP operators applied for the license to store spent fuel assemblies on-site. Twelve SFSFs were newly constructed and commissioned between 2002 and 2007. According to the storage licenses the spent fuel assemblies have to be stored in dual purpose casks for transport and storage such as CASTOR® V-casks (see figure 1). In addition, three central dry interim storages in Ahaus, Gorleben and Lubmin, and the local dry storage facility in Jülich are operated in Germany [1], making a total of 16 SFSF in Germany. The licensed storage period of all German storage facilities is limited to 40 years beginning with the emplacement of the first spent fuel containing cask in the storage building [1].



Figure 1: Design of CASTOR Type V19 and V/52 (copyright: GNS)

The SFSFs are licensed for an accurately defined quantity of heavy metal (in tons) and for an accurately defined number of storing positions for casks. The licensed mass of heavy metal (HM) in

the on-site SFSFs varies between 450 Mg and 2,250 Mg, which leads to storage capacities between 80 and 192 CASTOR® V-casks [2], [3].

The on-site SFSFs were built according to three different design-types the STEAG, WTI and tunnel design. The layouts of the three different SFSFs-designs are shown in the figure below.

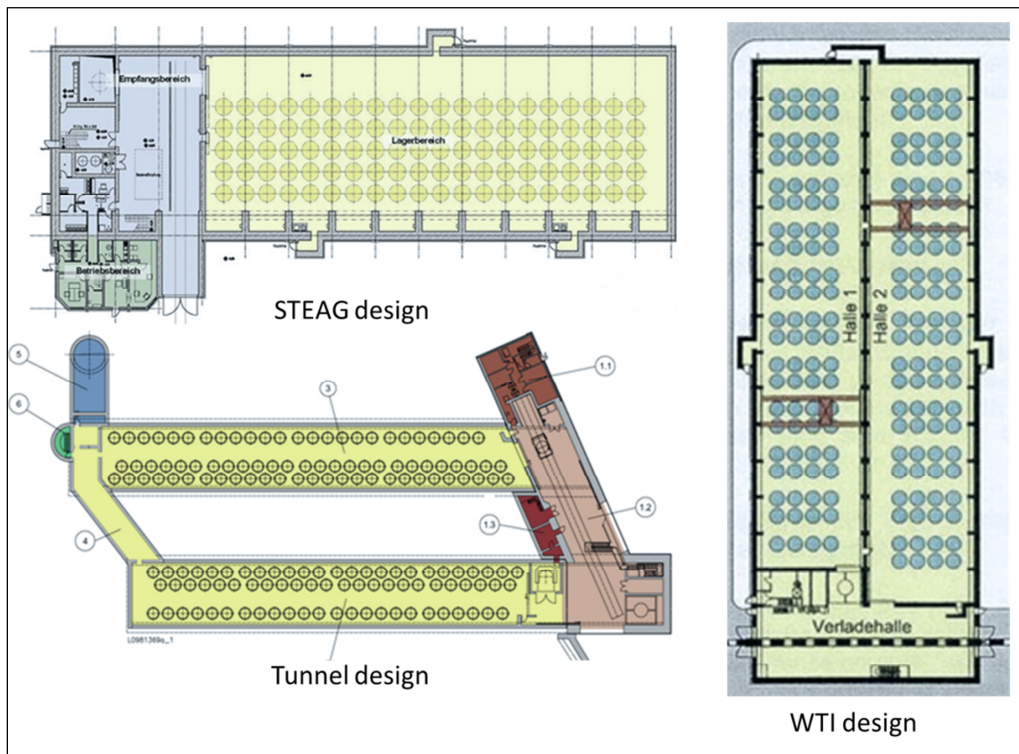


Figure 2: Designs of dry on-site storage facilities in Germany (courtesy: BGE)

The STEAG facilities consist of one storage hall, where the spent fuel casks are stored densely (about 55 cm space between the casks in a row). Facilities of this type were built on-site of six NPPs in the northern part of Germany. The storage facilities constructed according to the WTI design have two halls, where the spent fuel casks are stored group-wise (a group consists of eight casks with a distance of about 50 cm between the casks in a row). This design type was realized at five NPPs in the southern part of Germany. The tunnel design was only realized once at the NPP Neckarwestheim due to spatial reasons on-site. Here, two tunnel tubes are used as storage areas, where the casks are stored in a single and a double row, with a distance between each cask of approximately 44 cm [1], [2].

It can be seen from the layouts of the three SFSFs (shown in figure 2), that the casks are packed densely in the storage area. Due to this arrangement; spent fuel casks cannot be moved between other casks. A lifting of a six meter high CASTOR® cask over other casks of this type is technically not possible due to the limited lifting height of the crane, which is 9 m from the ground [2].

With regard to safeguards requirements continuity of knowledge (CoK) has to be maintained during long term storage of spent fuel. Therefore casks loaded with spent fuel should be under dual containment and surveillance (C/S). In order to meet this requirement, two independent sealing systems are attached to the protection plate of each spent fuel cask by the inspectorates - supplemented by surveillance through video cameras in the storage hall. In addition, group sealing is commonly applied for cask immobilization. The final seal configuration applied to dual purpose casks in German SFSFs consists of two individual seals per cask, a Cobra seal and, as a second seal, a further Cobra seal or a copper-brass seal as a backup attached at the top of the casks. In addition group seals are attached as a backup for surveillance. At the time being mostly Cobra seals are used in the SFSFs for group-sealing, in some cases the Electronic Optical Sealing System (EOSS) is alternatively in use.

Almost all SFSFs are equipped with remote data transmission (RDT) systems for surveillance. Here safeguards data collected by unattended monitoring and measurement systems is transmitted off-site via communication networks to inspectorate's headquarters for review and evaluation.

In several German SFSFs connection boxes for electronic group seals were installed during the construction phase to allow remote verification of electronic seals. Those boxes are mounted on the wall for every group of 8 or 10 spent fuel casks. They provide electrical power and a data cable to the Euratom equipment rack, available in every SFSF. The connection box is connected to the RDT-system of the SFSF and thus allows inspectorates to monitor seal status from headquarters. .

## 2.1. Considerations of a new C/S approach for German SFSFs

The verification and replacement of copper-brass seals attached on the top of the casks is challenging in those facilities, where the CASTOR® V-casks are stored so closely together that the distance between the casks does not allow to introduce lifting equipment to reach the top of the spent fuel casks from ground level (see figure 3). Accessing the top of the casks is only possible by using a crane or a special movable scaffolding. As a consequence gaining access to the top of the casks is a time consuming procedure in a relative high radiation environment. The total dose rate (gamma and neutrons) in the immediate vicinity of the CASTOR® V-casks is of concern. The maximum permitted dose value averaged over the shell surface of the spent fuel casks differs for the individual German SFSFs: the allowed values range between 0.35 mSv/h and 0.50 mSv/h in case of the CASTOR® V-cask (96 design). The continuously increasing number of spent fuel casks in the SFSFs will lead to an increase of the radiation level inside the respective storage hall. The principle guideline for radiation protection 'As Low As Reasonably Achievable' (ALARA) [4] calls for a reduction in the duration of stay as achievable in such an environment. Furthermore, work safety rules do not allow unsecured movements between casks and thus enforce time-consuming positioning of persons for each cask separately to carry out seal verification or replacements on the top of the casks [5].



Figure 3: CASTOR® V casks stored in SFSF at NPP Grohnde (courtesy: BGZ)

Given this situation, there is an urgent need to optimize the current approach and to find improved C/S solutions tailored to the application for a long-term interim storage in a quasi-statically operated on-site SFSF. To address this challenge, a working group has been established to review and discuss suitable alternative C/S technologies for safeguarding German SFSFs. It should be noted that the secured containment is currently defined as a spent fuel cask. The inclusion of the perimeter of the entire SFSF hall or building as a relevant component of the containment for static SFSFs is currently under consideration. A move from the current dual C/S to a monitoring of the storage-boundaries would significantly improve the efficiency and reduce the need for on-site inspections. Additionally the extended use of RDT capable systems for seals and other monitoring systems would be very beneficial allowing remote near real-time monitoring of the SFSF and potentially reduce frequency of inspections.

Based on these reflections Euratom conducted a preliminary site analysis of the SFSFs and identified the following devices suitable for a field trial in a German SFSF [5]:

**Laser curtain for containment and tracking (LCCT):**

The LCCT is a virtual fence, which provides a containment measure by detecting movement through a defined boundary. This system operates with real-time sensors that continuously acquire time-of-flight distance information to monitor the area of interest. The LCCT can be combined with surveillance and remote data transmission. This system is currently under approval by the IAEA for safeguards use and has been routinely applied by Euratom for more than 20 years [6], [7].

**Ultrasonic Optical Sealing Bolt (UOSB):** The UOSB consists of a special tamper-indicating uniquely identifiable bolt, combined with an electronic or a Cobra seal. An UOSB replaces one of the bolts securing the protective cover of a spent fuel cask. A detailed description of the seal can be found in [8]. The combination of the two sealing systems enables the verification of the secondary seal (electronic or Cobra seal) from ground level. The UOSB itself is verified by reading out the ultrasonic fingerprint. The initial installation and the re-verification of the UOSB require access to the top of the cask, and have to be performed by inspectors. However, periodic exchange is normally not required and the lifetime of the seal is expected to be many tens of years, likely exceeding the lifetime of the German SFSFs. This device has been approved for safeguards use by the IAEA and Euratom.

To verify the applicability of these technologies to safeguarding the SFSFs, the working group decided to facilitate a field trial in a facility in Germany. The inspectorates will define beforehand the essential technical requirements needed for the installation of the instruments as well as the optimal on-site conditions in the facility, such as facility layout, quasi-static operation or dynamic storage etc. Once those requirements are clearly defined, a suitable field test facility will be chosen to carry out the trials.

**2.2. Potential technologies for spent fuel cask re-verification**

In the event of “loss of CoK” the only option to open a spent fuel cask for re-verification purposes would be the cask loading position in the wet storage in the reactor building, or a hot cell within the storage facility. The wet storage is no longer available when the reactor building is under decommissioning and no storage facility is equipped with a hot cell. Consequently no on-site installation will be available to open spent fuel casks once all German nuclear power plants will be decommissioned. At the moment no sufficiently accurate method is available to re-verify the spent fuel assemblies stored in a shielded and closed CASTOR<sup>®</sup> V-cask. The state of the art is described in [9]. Recent research results indicate that muon tomography could be a suitable technique for re-verification of a shielded spent fuel cask [10]-[15]. Muons are a part of the natural cosmic radiation and are able to penetrate dense materials. Consequently, images of the inner components of shielded spent fuel casks can be obtained by measuring deflection angles of muons passing through the cask. Thus, muon tomography could potentially be used to verify presence or absence of spent fuel assemblies in casks.

In 2018 a first pre-field test has been carried out at a German nuclear power plant, initiated by Euratom and in cooperation with the National Institute of Nuclear Physics (INFN, Italy), Energie Baden-Württemberg AG (EnBW) and the German Member State Support Programme (GER MSSP). The aim of this field test was to demonstrate, that muons can be tracked in a high radiation environment. Therefore a prototype-detector developed by the National Institute of Nuclear Physics (INFN) in Italy measured the muon flow through a CASTOR<sup>®</sup> V-cask [12]. The field test showed that it is possible to reconstruct successfully muon tracks in an environment with a significant background radiation. A follow up field test to further investigate the suitability of muon tomography for re-verification purposes is planned for 2020 in a German SFSF. Based on the results of the first test, the prototype detector will be technically optimized and further developed. The new detector shall be capable to image a complete inner structure of a CASTOR<sup>®</sup> V cask including all fuel assemblies. It is planned to examine the generated images of a spent fuel cask for their suitability for re-verification measures. The results of this field test will contribute fundamentally to the evaluation of muon tomography for the re-verification of spent fuel casks.

The innovative re-verification methods above could be available relatively soon but are still somewhat limited as they do not measure directly what is of interest for safeguards, plutonium and uranium. The neutron radiation from spent fuel is dominated by emission from Cm, the gamma radiation stems from fission products (mainly 137 Cs).

At the horizon there appears a new technology, which may have the potential to measure the nuclear material directly. Laser induced neutron sources [16], [17] can provide a high neutron flux density with neutrons in the energy range of 100 MeV. Such neutrons can penetrate into the cask and induce fission. The related signatures could in principle be used to verify the nuclear material content directly. This very promising technology will be further investigated.

Criticality questions will be addressed during the detailed modeling, but are not expected to be an issue due to the boundary conditions in the cask and the relatively small number of additional thermal neutrons generated.

### 2.3. Selection probabilities and random Physical Inventory Verification

In some States such as Germany, randomly scheduled inspections (RSIs) of SFSFs are performed. For the RSI planning, the probability that any particular SFSF in the State is selected at least once per year for an RSI is considered, and the number of RSIs to achieve the required selection probability is determined.

Based on this requirement three topics arise immediately: First, how are the SFSFs selected for the RSIs and when are the RSIs performed (time aspect)?

Second, how many RSIs have to be performed to achieve the required selection probability? In this context the number of RSIs can be understood as a fixed or an expected number. For example: If the number of RSIs is set to three (fixed), then exactly three RSIs are performed. In the case of an expected number of three, none, one, two, or more RSIs could be carried out.

Third, the fixed or expected number of RSIs that assure the required selection probability  $p$  is not equal to  $p \times 100\%$  of the number of SFSFs in the State.

Regarding future inspection regimes for static long term SFSFs, instead of regular physical inventory verification (PIV) only random PIVs could be considered. One possible inspection scheme assumes that at least one PIV has to be scheduled within (say) 5 consecutive years. What is the probability of performing a PIV in any year?

All these topics are addressed and discussed in detail in [18] and [19].

## 3. Summary and Outlook

The verification and replacement of copper-brass seals attached on the top of spent fuel casks is challenging in those German SFSFs, where the CASTOR<sup>®</sup> V-casks are stored so closely together that the distance between the casks does not allow introducing lifting equipment to reach the top of the spent fuel casks from ground level. As a consequence gaining access to the top of the casks is a time consuming procedure in a relative high radiation environment. Given this situation, there is an urgent need to optimize the current approach and to find improved C/S technologies as well as suitable technologies for re-verification purposes tailored to the application for a long-term interim storage in a quasi-statically operated on-site SFSF. To address this challenge the working group dedicated to safeguarding German SFSFs decided to carry out field trials to investigate further the mentioned C/S technologies and the muon tomography system described above. Therefore suitable field test storage facilities will be chosen based on defined criteria. New technologies such as active neutron interrogation, which could potentially be used for re-verification purposes of spent fuel casks, will also be further investigated.

In addition selection probabilities of randomly scheduled inspections (RSIs) in SFSFs as well as random Physical Inventory Verification (PIV) for SFSFs in quasi static operation are considered in this paper.

## **4. Acknowledgments**

This paper was prepared as an account of work sponsored by the Government of the Federal Republic of Germany within the Joint Programme on the Technical Development and Further Improvement of IAEA Safeguards between the Federal Republic of Germany and the IAEA.

## **5. Legal matters**

### **5.1. Privacy regulations and protection of personal data**

I agree that ESARDA may print my name/contact data/photograph/article in the ESARDA Bulletin/Symposium proceedings or any other ESARDA publications and when necessary for any other purposes connected with ESARDA activities.

### **5.2. Copyright**

The authors agree that submission of an article automatically authorises ESARDA to publish the work/article in whole or in part in all ESARDA publications – the bulletin, meeting proceedings, and on the website.

Once the article has been accepted for publication the copyright is reserved, but part of the publication may be reproduced, stored in a retrieval system, or transmitted in any form or by any means, mechanical, photocopy, recording, or otherwise, provided that the source is properly acknowledged.

The authors declare that their work/article is original and not a violation or infringement of any existing copyright.

### **5.3 Disclaimer**

Neither the authors of this paper, nor the organization or industrial company they are affiliated with, nor the Federal Government assume any liability whatsoever for any use of this paper or parts of it. Furthermore, the content of this paper does not reflect any policy of the Federal Government.

## 6. References

- [1] B. f. k. Entsorgungssicherheit, "Zwischenlager für hochradioaktive Abfälle: Sicherheit bis zur Endlagerung," Berlin, 2018.
- [2] K. Aymanns, A. Rezniczek, A. Jussofie and I. Niemeyer, "Sealing Systems in German Spent Fuel Storage Facilities," *Esarda Bulletin*, vol. 55, 2017.
- [3] A. Jussofie, R. Graf and W. Filbert, "Germany's accelerated exit from nuclear energy: challenges and perspectives with regard to Safeguards," in *IAEA-CN-220/Symposium on International Safeguards: Linking Strategy, Implementation and People*, Vienna, 2010.
- [4] StrlSchV, „Verordnung über den Schutz vor Schäden durch ionisierende Strahlen,“ 2001.
- [5] K. Aymanns, D. Weinberg, A. Jussofie, P. Schwalbach, K. Schoop, J. Pekkarinen, D. Ancius and L. Matloch, "Cooperation between Germany the European Commission and the IAEA in safeguarding spent fuel intermediate storage facilities," in *Symposium on International Safeguards: Building Future Safeguards Capabilities*, Vienna, 2018.
- [6] P. Schwalbach et al., "Euratom Safeguards: Improving Safeguards by Cooperation in R&D and Implementation," in *IAEA Symposium on International Safeguards: Linking Strategy, Implementation and People -Proceedings*, Vienna, 2014.
- [7] P. Richir, A. Homer, A. Polkey, D. Ancius, K. Benn, L. Persson, L. Dechamp, L. Pierssens, N. Edmonds, P. Peerani, P. Dransart, P. Buchet, S. Synetos and Z. Dzbikowicz, "Design and Implementation of Equipment for Enhanced Safeguards of a Plutonium Storage in a Reprocessing Plant," in *IAEA Symposium on International Safeguards: Linking Strategy, Implementation and People -Proceedings*, Vienna, 2014.
- [8] F. Littmann, M. Sironi, P. Schwalbach, L. Matloch, B. Wishard and V. Kravtchenko, "New Ultrasonic Optical Sealing Bolts for Dry Storage Containers," in *37th ESARDA Symposium- Proceedings*, Manchester, 2015.
- [9] P. Peerani and M. Galletta, "Re-establishment of the continuity of knowledge in the safeguards of interim storages using NDA techniques," *Nuclear Engineering and Design*, vol. 237, pp. 94-99, 2007.
- [10] S. Chatzidakis, C. K. Choi and L. H. Tsoukalas, "Analysis of Spent Nuclear Fuel Imaging Using Multiple Coulomb Scattering of Cosmic Muons," *IEEE Transactions on Nuclear Science*, vol. 63, 2016.
- [11] J. M. Durham, D. Poulson, J. Bacon, D. L. Chichester, E. Guardincerri, C. L. Morris, K. Plaud-Ramos, W. Schwendiman, T. J. D. and P. Winston, "Verification of spent nuclear fuel in sealed dry storage casks via measurements of cosmic ray muon scattering," *Phys. Rev. Applied*, vol. 9, 2018.
- [12] J. M. Durham, D. Poulson, E. Guardincerri, J. D. Bacon, C. Morris, K. Plaud-Ramos, D. Morley and A. Hecht, "Cosmic ray muon imaging of spent fuel in dry storage casks," *Journal of Nuclear Materials Management*, vol. 44, no. 3, 2016.
- [13] P. Checchia, "Review of possible applications of cosmic muon tomography," *Journal of Instrumentation*, vol. 11, 2016.
- [14] P. Checchia, D. Ancius, F. Gonella, G. Zumerle, K. Aymanns, N. Erdmann, P. Schwalbach and S. Vanini, "Muography of spent fuel containers for Safeguards," in *IAEA Symposium on International Safeguards: Building Future Safeguards Capabilities - Proceedings*, Vienna, 2018.
- [15] G. Jonkmanns, V. N. P. Anghel, C. Jewett and M. Thompson, "Nuclear waste imaging and spent fuel verification by muon tomography," *Annals of Nuclear Energy*, vol. 53, 2013.
- [16] M. Roth et al., "Neutron Generation by Laser-Driven Proton Sources," in *39th ESARDA Symposium-Proceedings*, Düsseldorf, 2017.
- [17] M. Roth et al., "Bright laser-driven neutron source based on the relativistic transparency of solids," *Physical Review Letters*, pp. 044802-1 - 044802-5, 25 January 2013.
- [18] T. Krieger, R. Avenhaus and T. L. Burr, "Modellers meet practitioners: On 20% SFSF selection probability and random physical inventory verifications," in *Proceedings of the ESARDA Symposium (41st Annual Meeting)*, Stresa, Italy, May 14-16, 2019.
- [19] T. Krieger, R. Avenhaus and T. L. Burr, "Modellers meet practitioners: On 20% SFSF selection probability and random physical inventory verifications -- Derivations and extensions," *ESARDA Bulletin*, 2019 (in preparation).

# Laser Scanning for Safeguarding Spent Fuel Storage Facilities

Erik Wolfart, Gunnar Boström, Vítor Sequeira

EC Directorate General Joint Research Centre, Directorate G - Nuclear Safety and Security, Ispra, Italy

## **Abstract:**

*The interim storage facilities that are coming into operation following the nuclear phase-out in Germany require substantial resources from the safeguards authorities. Other countries will follow with similar facilities in the near future. Once the fuel transfer from the reactors has been completed, the facilities will be quasi-static. This will pose new challenges to the inspectorates requiring new safeguards concepts and technologies. Two laser scanning applications might be used for addressing those challenges: i) continuous surveillance using 2D laser curtains and ii) change detection using static 3D laser scanners:*

*Laser curtains are installed in the facilities for continuous surveillance. The acquired data is analyzed in real-time and triggers an alarm if specific activities are detected in the area of interest. Laser curtains support an automated, event-based verification process with minimum need for inspector presence and data review.*

*Change detection is based on 3D models that the inspector acquires during on-site visits using portable, high-precision 3D laser scanners. By comparing 3D models acquired at two inspections, the inspector can verify the absence of undeclared container movements between the inspections.*

*The paper describes the two technologies and proposes a complete monitoring system using them as core components.*

**Keywords:** surveillance & containment; laser scanning; spent fuel storage facilities

## **1. Introduction**

Safeguarding spent fuel storage facilities (SFSF) is becoming an increasingly important task for the international safeguards authorities. For example, Germany will phase out its nuclear reactors by 2022 and is expected to transfer all spent fuel to interim storages by 2027. Once the fuel transfer is completed, the German storage facilities will have a total inventory of more than 1000 casks and will remain quasi-static for several decades, i.e. no cask shipments are expected and only limited movement within the facility will be necessary for maintenance purposes [1].

The safeguards authorities need to maintain continuity of knowledge on the spent fuel over the entire life time of the SFSF. The present IAEA procedures require a dual C/S system, because the nuclear material is enclosed in the cask and re-verification would be very challenging [2]. In practice, the casks in the German SFSFs are currently sealed with two passive seals (COBRA and/or metal seal), which need to be regularly verified and replaced. Since the casks are spatially very close and the radiation level is high, this obligation has a significant impact for both, operators and inspectors [3].

The IAEA and Euratom are currently discussing alternative technologies for maintaining the continuity of knowledge in spent fuel storage facilities, which could ease the burden of the current safeguards concept. This paper describes two laser scanning technologies that are considered as core components of a future monitoring system:

- *Laser Curtain for Containment and Tracking (LCCT)*. LCCT is an active, continuous surveillance system based on real-time laser scanners, which allows an automatic, event-based monitoring of the storage facility without the need of inspector reviews. It is proposed as the primary layer of a future safeguards concept and provides complete monitoring during normal operation.
- *3D Laser Verification System (3DLVS)*. 3D laser scanning can be applied to create a highly accurate 3D model of the storage casks in the facility, which is used to verify the absence of undeclared changes between on-site visits. 3DLVS can be considered a passive sealing system, which is used as a first-layer backup of the primary LCCT system. Additionally, 3DLVS can be used for DIV/BTC verification of the SFSF buildings.

The purpose of the document is to provide a basis for discussing a concept for safeguarding spent fuel storage facilities using laser scanning. As example, the document assumes a STEAG-concept storage facility, which is operated at six German sites [4]. The system can be adapted for other facility designs as required.

Sections two and three provide an overview of LCCT and 3DLVS and illustrate how they can be applied for safeguarding a spent fuel storage facility. Section four puts the two technologies in the context of possible safeguards scenarios and illustrates how they can be combined with other technologies to form a complete monitoring system. Section five provides conclusion and an outlook to future activities.

## 2. Laser Curtain for Containment and Tracking (LCCT)

The LCCT is a fixed installation based on multiple real-time laser scanners that continuously acquire depth information to monitor an area of interest. The sensors use the time-of-flight (ToF) principle to acquire the distance to an object by emitting a laser pulse and measuring the time for the signal to be returned. The sensors use a scanning mechanism that rotates around one axis to generate a line scan within a single plane. Figure 1 illustrates the data that would be acquired in a SFSF by a system using two laser scanners. The accuracy of a single 3D measurement is typically around 1cm.



**Figure 1:** *Left:* Image of spent fuel casks at the SFSF Unterweser, Germany (*source:* bgz.de). *Right:* Schematic top-down view of LCCT based on two laser scanners. The blue lines depict the data that would be acquired by the scanner on the left (LS2). The red lines correspond to the scanner on the bottom (LS1).

On a local server running at the SFSF, all laser data is fused into a single 3D data set and analysed in real-time to monitor and track the movements of the spent fuel casks. Since the analysis works on geometric measurements in 3D space, event detection can be restricted to a pre-defined area of interest. Furthermore, the measurements are based on an active laser light and therefore the analysis is much more robust than event detection based on optical video surveillance (which is influenced by ambient light conditions).

If LCCT detects a safeguards-relevant event (e.g. movement of a spent fuel cask), the event information is sent via remote data transmission to the inspectors headquarter. Using a data review tool such as iRAP [5], the inspector correlates the LCCT events with complementary sensor data (e.g.

surveillance imagery and radiation measurements) and verifies that the activities are in compliance with the operator declarations. Since the facility is quasi-static, safeguards-relevant events will be rare and regular data review is not required.

The technology has already been proven during operational use for safeguards applications at the reprocessing plant in La Hague, where Euratom has been using it since 2015 for monitoring activities over a spent fuel pond. The IAEA is currently testing its use at Atucha, Argentina.

The following use cases provide examples how different scanners could be installed according to the monitoring objectives. In order to provide redundancy, at least two scanners are proposed for each use case. In the final system, only a subset of the scanners might be used if the full functionality is not required. Figure 2 shows the proposed scanner locations for the case of a STEAG-type facility.

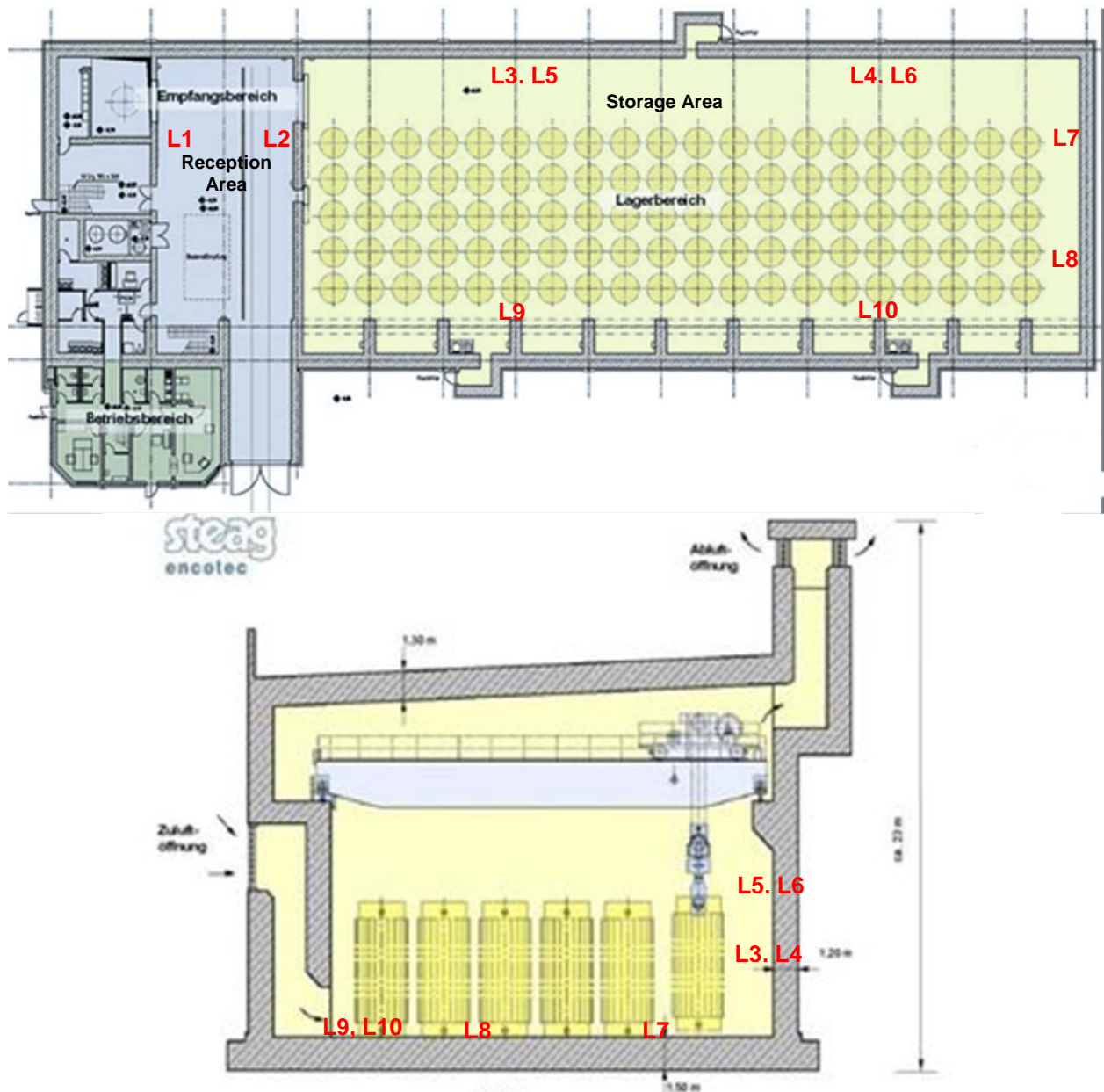


Figure 2: Layout of a STEAG-concept storage facility (source: bgz.de). L1 to L10 indicate the positions of the laser scanners as proposed below. L1 to L6 are wall mounted; L7 to L10 are mounted on the floor or on the wall.

**Use Case 1: Track cask movement in the reception area.** The objective is to track cask movement in the reception area. The laser scanners L1 and L2 are installed on the wall at 3m meters height monitoring a horizontal plane.

**Use Case 2: Track cask movement in the storage area.** The objective is to track cask movement in the storage area. The laser scanners L3 and L4 are installed on the wall at 3m meters height monitoring a horizontal plane.

**Use Case 3: Track crane movement above the cask level.** The objective is to track movement of the crane and detect when the crane is lifting a cask. The laser scanners L5 and L6 are installed on the wall at approximately 7 meters height monitoring a horizontal plane.

Use Case 1 to 3 allow tracking the cask over the entire movement, i.e. continuity of knowledge regarding the cask IDs and respective storage positions will be maintained.

**Use Case 4 and 5: Perimeter monitoring of outer walls.** The objective is to detect the removal of casks through the two outer walls (the other two walls are already monitored by use case 1 to 3). The laser scanners L7 to L10 can be installed on the floor or on the wall monitoring vertical planes parallel to the outer walls to detect passage of any object.

### 3. 3D Laser Verification (3DLVS)

3D laser scanners have been used in nuclear safeguards for several years in order to create as-built 3D models of nuclear facilities [6,7,8]. The models are used for documenting the facility; for Design Information Verification (i.e. to verify that the facility layout corresponds to the design information provided by the operator); and for monitoring changes over time. The systems are based on high-accuracy, high-resolution 3D laser scanners mounted on a tripod during data acquisition. In order to completely cover a given area of interest, several scans are acquired and then registered into a single coordinate frame in an offline post-processing phase. The resulting 3D model is used to verify the correctness and completeness of the design drawings provided by the operator and is stored as a reference for subsequent visits. On return, the inspector re-scans the area of interest to verify that no undeclared modifications to the facility have occurred. (see Figure 3)



Figure 3: *Left:* 3D Laser scanner mounted on a tripod. *Middle:* snapshot of a 3D model of a (non-nuclear) facility; *Right:* change map generated by comparing the 3D model acquired before and after modifying the scene. Blue pixels correspond to unchanged objects; red pixels correspond to objects that moved closer to the scan position or were inserted to the scene; green pixels correspond to objects that were moved away from the sensor or removed from the scene.

In the context of SFSFs, 3D Laser Verification can be applied as follows: the inspectors scan the spent fuel storage casks with high-accuracy 3D laser scanners during subsequent on-site inspections. The change analysis of the scan data verifies that the casks have not been moved and therefore continuity-of-knowledge has been maintained between the acquisitions. 3DLVS can be considered a 'passive sealing' system in the sense that the 'sealing' is based on the position of the casks, i.e. a

power outage between the inspections would not compromise the continuity of knowledge. The approach is illustrated in Figure 4 and described in more detail hereafter:

- The 'outer' ring of casks (blue circles in Figure 4) is the seal; the integrity of the seal is based on the cask position. Since the inner casks (red circles in Figure 4) cannot be lifted above the outer casks (due to a limitation of the crane and facility height), the continuity of knowledge is maintained when the integrity of the seal (i.e. position of the outer casks) is verified. The sealing system is passive because the integrity is based only on the cask position.
- The laser scanner can be considered the *seal reader*: it is used to take a reference of the positions of the outer casks and to verify the seal integrity (i.e. absence of movement for the outer casks).
- The seal is closed when the 3D reference model of the outer casks has been acquired: the laser scanner is mounted on a tripod which is placed at different locations in the storage hall. The stars in Figure 4 represent the scanning positions for creating the reference model.
- The seal is opened by moving one of the outer casks, e.g. when it needs to be moved to the maintenance area.
- The seal can be re-closed by scanning the position of the outer cask after the movement (e.g. after a cask returns from maintenance). The reference model will be updated accordingly. The scanning could be carried out by the operator if data authenticity can be ensured.
- The seal is verified by taking a complete verification model, i.e. acquiring scans from all positions indicated in Figure 4, and verifying the absence of changes for all outer casks.

Optionally, it would be possible to acquire 3D data from a level above the storage casks, e.g. by mounting the scanner on the crane, to simultaneously verify the position of all storage casks and carry out the DIV/BTC verification of the storage building.

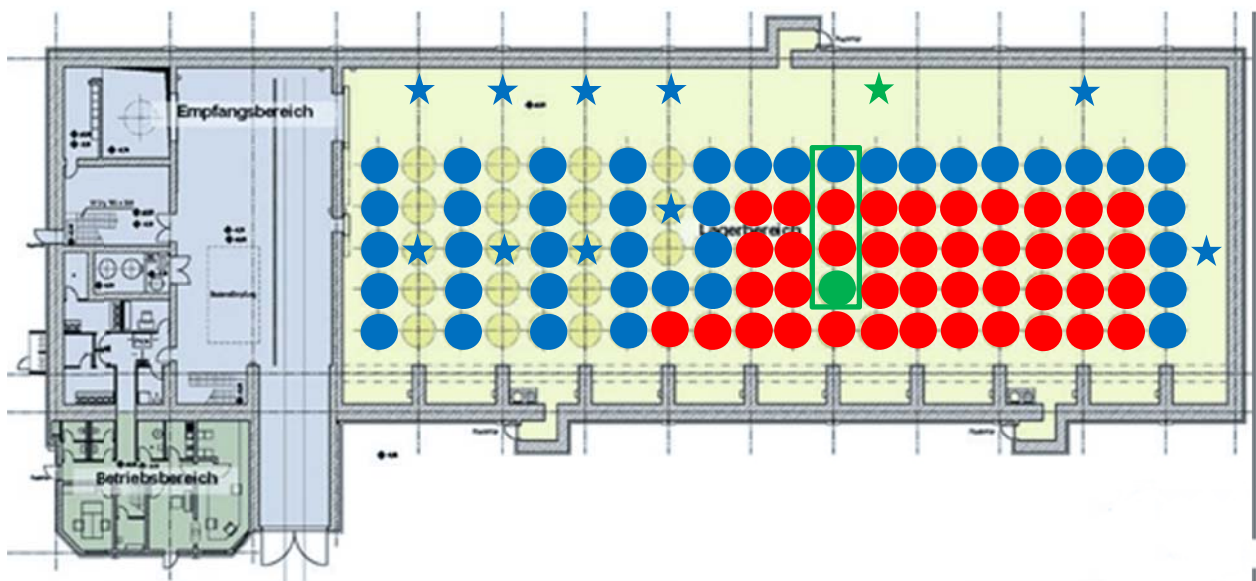


Figure 4: A partially-filled storage facility. Stars depict scan positions (blue: for initial reference and verification; green: needs to be re-scanned after green casks returns from maintenance) and circles cask positions (blue: outer casks visible in the scans; red: inner casks not visible by the scans; green: to be moved to maintenance cell). All casks in the green rectangle need to be moved when the green cask goes to maintenance.

#### 4. Application Scenarios

This section briefly describes different scenarios for spent fuel storage facilities and illustrates how the proposed laser scanning technologies are applied for safeguards purposes. It is assumed that the

LCCT system is installed and connected via remote data transmission to the inspector headquarters and that the inspectors have already acquired a complete 3D reference model with 3DLVS.

- *Static Storage.* LCCT continuously monitors the storage hall and automatically verifies the absence of undeclared movements of the storage casks. The inspector is automatically notified if LCCT detects an unexpected event. If necessary, s/he can make a follow-up analysis using the data from the surveillance camera and radiation monitor using an integrated analysis tools, such as iRAP.
- *Cask maintenance.* When the operator moves a cask to the maintenance cell, LCCT detects the movement and tracks all casks (several casks may need to be moved to temporary storage) along the movement. When a cask enters the maintenance cell, LCCT temporarily loses visibility and notifies the inspector accordingly. The inspector can then cover this period with video surveillance review. Once all casks are returned to their positions, the operator makes a 3D laser scan to update the 3D reference model (i.e. to close the 3DLVS seal).
- *Arrival of new cask.* LCCT detects the new cask in the arrival hall and tracks it through the process until the storage position. Once the task has arrived at its position, the operator makes a 3D laser scan to update the 3D reference model (i.e. to close the 3DLVS seal).
- *LCCT failure during static storage.* LCCT monitors its state-of-health and will notify the inspector in the unlikely case of a system failure. 3DLVS will act as first-layer backup and guarantee the continuity of knowledge during LCCT downtime. Once LCCT is restored, the inspector needs to carry out an on-site inspection to verify the 3D reference model (i.e. the integrity of 3DLVS seal). The operator is not allowed to move any cask between the LCCT failure and the verification of the 3D reference model.
- *LCCT and 3DLVS failure:* In the following cases, 3DLVS could fail as first-layer backup: if LCCT fails during cask maintenance (i.e. the 3DLVS seal was open); if the operator moves a cask after LCCT failure (i.e. the 3DLVS seal is broken); in case of technical failure (e.g. corrupted 3D reference data). In any of those cases, continuity of knowledge needs to be restored through one of the complimentary sensors (surveillance camera or radiation monitor).

## 5. Conclusions and Outlook

The number of interim spent fuel storage facilities (SFSF) will increase significantly over the next years. The facilities will be quasi-static once the fuel transfer is completed, but will remain under nuclear safeguards for several decades. The current approach for maintaining continuity of knowledge is based on two independent sealing systems for each spent fuel cask. The requirement for periodic validation and/or replacement of the seals and the relatively high radiation levels in the proximity of the casks constitute a significant issue to the inspectors and facility operators. Therefore, Euratom and IAEA have started discussing alternative technologies that can significantly reduce the inspection effort for safeguarding quasi-static SFSFs.

Laser scanning can be a core technology of an unattended monitoring system that requires less inspector presence: Laser curtains (LCCT) allow to continuously monitor the spent fuel casks and automatically notify the inspectors through remote data transmission in case any safeguards-relevant events are detected. Change detection using static laser scanners (3DLVS) is a complementary technology that can be used to maintain the continuity of knowledge in case that continuous LCCT surveillance fails, e.g. due to an extended power outage.

Updating the current approach will require extensive analysis and testing of the proposed technologies. A field test will be carried out in one of the German SFSFs in order to support this analysis and collect valuable information for decision process.

## References

- [1] K Aymanns, D. Weinberg, A. Jussofie, P. Schwalbach, K. Schoop, J. Pekkarinen, D. Ancius, L. Matloch, I. Niemeyer, T. Krieger, A. Rezniczek, "Cooperation between Germany, the European

*Commission and the IAEA in safeguarding spent fuel intermediate storage facilities*,  
Symposium on International Safeguards, Vienna, 2018

- [2] IAEA, IAEA Safeguards Glossary, 2001 Edition, IAEA International Nuclear Verification Series No. 3, Vienna (2002).
- [3] K Aymanns, A Rezniczek, A. Jussofie. I. Niemeyer, "Sealing Systems in German Spent Fuel Storage Facilities", Esarda Bulletin 55,(2017) 39-43.
- [4] <https://www.bfe.bund.de/EN/nwm/interim-storage/decentralised/design/design.html>
- [5] A. Smejkal, A. Angelo, J. Regula, J.Longo, R. Linnebach, S. Bertl, "IRAP: a New System for Integrated Analysis and Visualization of Multi-Source Safeguards Data: Challenges and Techniques", Symposium on International Safeguards, Vienna, 2018
- [6] E. Agboraw, S. Johnson, C. Creusot, S. Poirier, H. Saukkonen, B. Chesnay and V. Sequeira, "IAEA experience using the 3-Dimensional Laser Range Finder," in IAEA Safeguards Symposium: Addressing Verification Challenges, Vienna, 2006.
- [7] J. Oddou, "The Application of 3D Laser Scanning Techniques for the Efficient Safeguarding of Fairly Static Storage Facilities for Natural, Depleted and Reprocessed Uranium", Proceedings of the 51st Annual Meeting of the Institute for Nuclear Materials Management (INMM), 2010.
- [8] P. Chare, Y. Lahogue, P. Schwalbach, A. Smejkal and B. Patel, "Safeguards By Design – As applied to the Sellafield Product and Residue Store (SPRS)" ESARDA Bulletin (46), pp. 72-78, 2011.

# Mechanical Design of the Operator Applied & Removed Sealing Bolt

Littmann François EC JRC Ispra  
Gutierrez San Simon Jorge Politecnico di Milano

## Abstract:

*With the phasing out of nuclear plants, a lot of nuclear spent fuel will have to be stored in dry storage casks, in Europe and throughout the world. Inspectors from Safeguards agencies won't be able to be physically present for the sealing operations needed for all those casks. Firstly because of the huge costs in manpower, travel and radiation dose but also because the operators are filling those casks at random intervals depending on the process speed.*

*The need for a sealing device able to be installed by the operator without the presence of inspector is then of utmost importance and urgency.*

*The solution proposed by the JRC is based on the following:*

- *A remotely operated Tamper-resistant Remotely Controlled Locker (TRCL) containing several compartments, each with a door and an internal communication connection to a central computer system.*
- *Several Operator Applied & Removed Seals (OARS), each connected to an Active Optical Loop Seal (AOLS) and including an optical leash passing through the bolt connected to the TRCL.*
- *A surveillance camera managed remotely by inspectors from headquarters or triggered by the central computer of the TRCL, fixed and sealed on a wall near the TRCL and within its field of view.*

*The sealing system could be applied by the operator and removed by the inspector, or applied & removed by the operator. The paper will describe the overall concept but mainly the mechanical design of the OARS.*

**Keywords:** seal; operator; cask; active; C/S

## 1. Introduction

The number of spent fuel dry storage casks is rapidly growing throughout the world. From a Safeguards point of view, the operations of closing the casks must be carried out, or supervised, by inspectors from international agencies, such as the International Atomic Energy Agency (IAEA) or Euratom (European Atomic Energy Community), so as to ensure that the nuclear material is not diverted from its original use.

Number of inspector/days of mission duties and associated radiation doses should grow accordingly, but it is not financially sustainable. Even if there are some solutions already on service, none of them completely release inspectors from sealing operations: current IAEA practices may permit operators to apply or remove seals, but not both; an inspector must only be involved in one of the operations

The paper will describe the concept of operator applied sealing systems: a temporary active seal, known as Operator Applied and Removed Sealing bolt (OARS). The solution proposed by the JRC is where a seal can be both placed and removed (if needed) by operators, without the need of the physical presence of inspectors, as they include some features ensuring their correct installation and allowing for remote verification.

## 2. State of the Art: Operator Applied Seals

IAEA has already approved some activities in which operators are allowed to insert or remove Safeguards seals without an inspector, saving time and resources. Such activities have been approved in coordination with State agencies, operators and regional inspectorates. For example in Germany, operators are allowed to apply Safeguards seals on the lid of CASTOR® casks. The identity

of the seals and the application procedure is recorded by video surveillance. Once the casks arrive to the interim storage facilities, inspectors verify the accuracy of the sealing systems.

Responding to EURATOM & IAEA's need of seals to be implemented by operators to reduce inspectorates' efforts, the Seals & Identification Laboratory (SILab) of the Joint Research Centre in Ispra (Italy) has over the last two years been working on a seal that meet these requirements. The conceptual design is set out in the patent WO 2017/140575 (for the sealing bolt itself) and another one pending, which relates to the overall operator sealing concept.

### 3. The concept: Operator Applied & Removed Sealing System

The solution proposed by the JRC is based on the following items (figure 1):

- A Tamper-resistant Remotely Controlled Locker (TRCL) containing several compartments, each with a door and internal electronics that can store event data with secure network capabilities for remote data transmission. It is considered as a Tamper Indicating Enclosure, fixed and sealed in the ground or wall in a determined position.
- Several OARS, each including a dedicated Active Optical Loop Seal (AOLS) able to detect a torque threshold during installation and to monitor various installation parameters. Optionally, each OARS may include an optical fiber leash connected inside the TRCL.
- A surveillance camera triggered by the electronics of the TRCL, ensures that the TRCL and the spent fuel cask in its field of view at all times.
- An Ultrasonic Thread Integrity Verifier (UTIV), stored in one of the TRCL compartments, connected to it by an optical leash limit the operational radius. This equipment verifies the integrity of the M36 thread before installation of each sealing bolt.

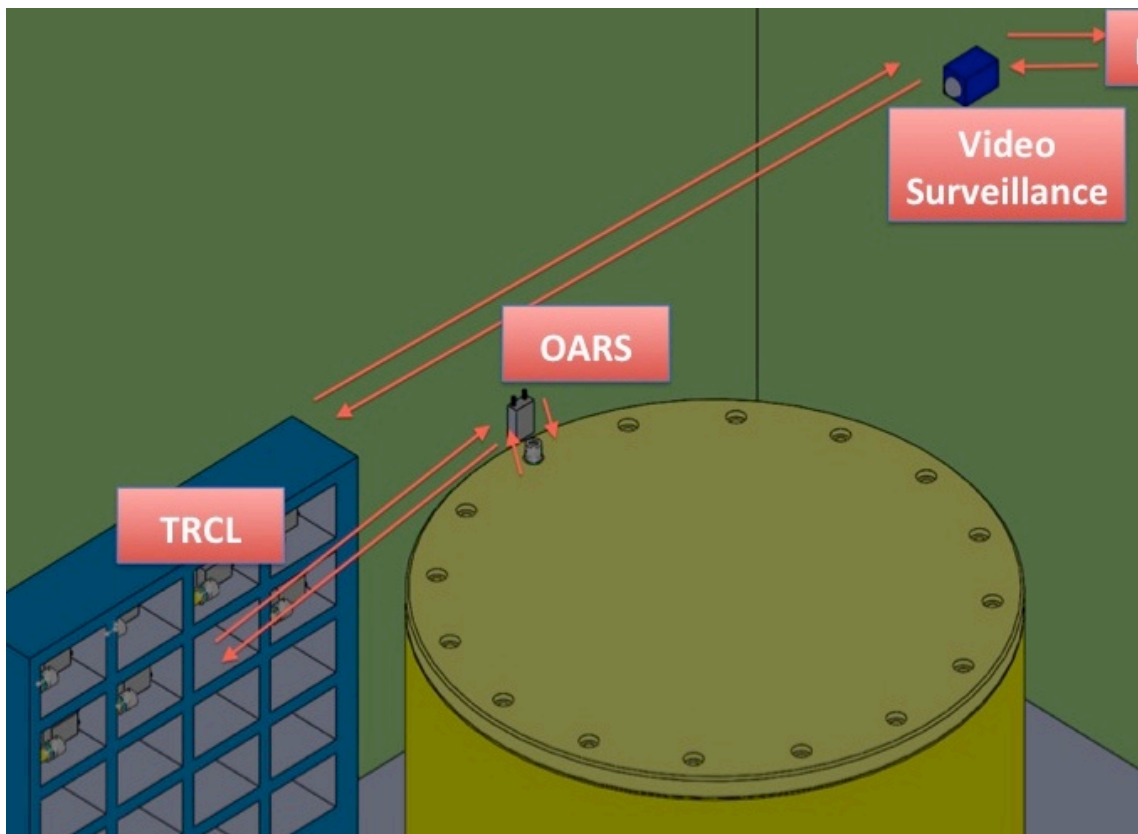


Figure 1: View of the various items needed for the Operator Applied & Removed Sealing concept

During installation the seal remains connected to the locker via the optical leash. In this way, through the video-surveillance camera and the data collected by the locker, inspectors can be sure that the correct seal, and not a dummy one, is installed.

When the operator has applied the seal and green light is given by the monitoring system, he is allowed to disconnect the leash from the TRCL. The cask is now considered sealed and can be moved from where it was and transported to another location, for example a dry storage facility or a encapsulation plant.

If the seal has to be removed later, the procedure is repeated by the operator in reverse order. Another TRCL should be previously installed by inspectors in the unsealing zone. When the operator has to remove the seal, he firstly connects the leash to the TRCL, and reads the AOLS to verify that the correct seal is removed. After removal, the operator puts the seal back in the locker, ending the procedure.

How it works in more detail:

- The TRCL is initially filled by an inspector with OARS. Each OARS is put into a separate compartment with a door that can be unlocked remotely by inspectors or by a central computer.
- Each OARS is connected to its compartment by a short optical fiber leash, to limit the radius of operations around the TRCL impeding the sealing of a fake cask. This fiber is connected directly to the TRCL central control system, able to detect any cutting of the fiber.
- The cask to be sealed is moved by the operator close to the TRCL and in the field of view of the surveillance camera. The operator can access the compartment where the UTIV is located with a time limited code and use it on a selected thread on the cask lid where the first OARS will be later installed. Once the integrity of the thread is verified, the operator can put back the UTIV in its compartment and close the door. The operator then opens a compartment with another authorization code and retrieves one OARS, (connected to its optical leash, of a few meters long) and tightens it on the empty threaded hole, previously verified by the UTIV, at the required torque. The OARS monitoring system will detect and register in its internal memory when the seal is correctly installed at the specified torque. A light and/or sound indication can be produced to indicate correct operation. Once the procedure is completed, data from the OALS monitoring system is sent to the TRCL and the optical leash can be cut off or disconnected. The AOLS and all optical fibers are put back in the open compartment, which is then closed. TRCL compartments opening and closing status together with AOLS data related to the correct installation of the OARS bolt are stored in the TRCL central computer.
- The above procedure has to be repeated to install a second OARS cask lid (if two are necessary to avoid opening the lid by rotation around one only).
- The cask is now considered sealed. Information collected by the TRCL electronics can be sent to the inspectors headquarters or stored locally for later verification. Inspectors have assurance that the right cask was correctly sealed and thus a physical verification is no longer needed.

## 4. Mechanical Design of the Operator Applied & Removed Seal

This chapter is dedicated to the mechanical design of the Operator Applied and Removed Sealing Bolt (OARS) and presents its working principle and general aspects considered during its design. As a preamble, it describes the Active Optical Loop Seal, which will be used as a monitoring device.

### 4.1 Active Optical Loop Seal

Developed by JRC, the Active Optical Loop Seal (AOLS) (Figure 2) is the first active seal (electronic seal) with an open hardware and software architecture. The seal is able to monitor the amplitude of a light pulse going through a plastic optical fiber and detect opening and closing of the loop. The seal is

also equipped with mechanical and electronic anti-tampering devices, and data from its monitoring activity can be collected securely through a digitally signed data transmission.



**Figure 2:** Active Optical Loop Seal (AOLS)

The AOLS design aims at combining the simplicity of passive seals with the core advantages of electronic seals, namely the continuous monitoring of the fiber and the possibility to interact with the seal through the reader, simplifying the inspector's work and providing more complete information.

The fact that the seal was designed entirely at the JRC (hardware and software) provides a good platform to develop new applications, modifying the light pulse detection algorithm or eventually adding other sensors.

#### 4.2 Main features of the patented design

The innovative element with respect to previous sealing bolts developed at SIlab is the presence of a conductor, preferably a Plastic Optical Fibre that is in different conditions before installing (unbolted condition) and after bolting (bolted condition) the seal [1]:

- unbolted condition: the fiber is compressed, limiting the signal transmission through it (Figure 3)
- bolted condition: the fiber is released, allowing full signal transmission (Figure 4)

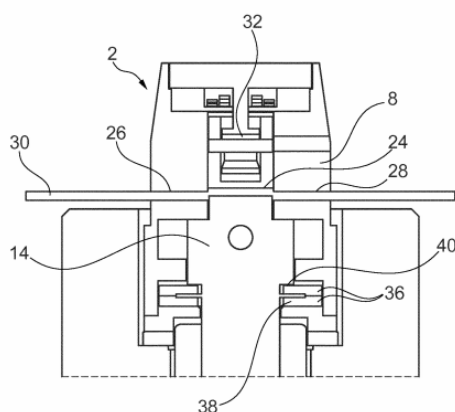


**Figure 3:** Unbolted condition, with conductor (30) compressed

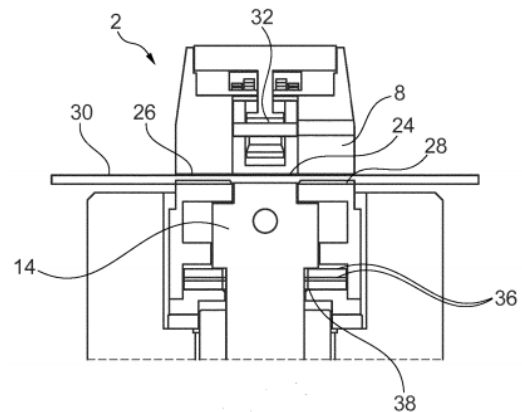


**Figure 4:** Bolted condition, with conductor (30) released

### 4.3 Operator Applied & Removed Seal Working Principle

OARS is an active seal; it comprises a mechanical part connected to an electronic reader (referred in the patent WO 2017/140575 as monitoring and detection unit), preferably an AOLS.

The operating principle to determine whether the seal is installed or not, or if it has been tampered with, is the different light output through the plastic optical fibre housed inside the seal.

The maximum light output should take place when the seal is correctly installed; therefore, the incorrect installation and tampering-once-installed attempts are easily detected: light output won't be the maximum expected.

When the seal is not installed, the state is from hereon referred to as unbolted condition, the light transmitted is just a fraction of the maximum available light output. This is due to a mechanical obstacle the light beam faces along its path inside the seal (Figure 5). The loss of part of the light beam due to the said obstacle leads to lower values of light output through the conductors.

When the seal is installed, the state from hereon is referred to as bolted condition, the mechanical obstacle changes its position due to the compression of disc springs inside the seal, freeing the Plastic Optical Fiber (POF) cross section from any solid material obstruction (Figure 6). This leads to the maximum available light output through the seal.

After the removal of the seal, the springs return to their original deflection and the obstacle obstructs the light beam again. Also, if the POF is cut the light output will decrease drastically and will be detected by the AOLS.

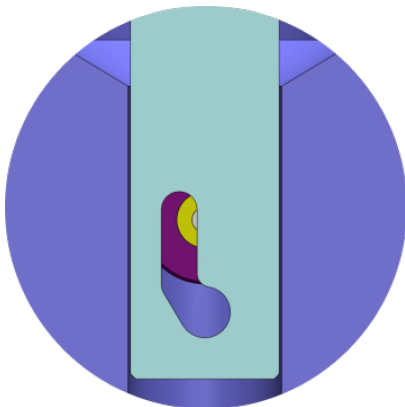


**Figure 5:** Section view of OARS in unbolted condition

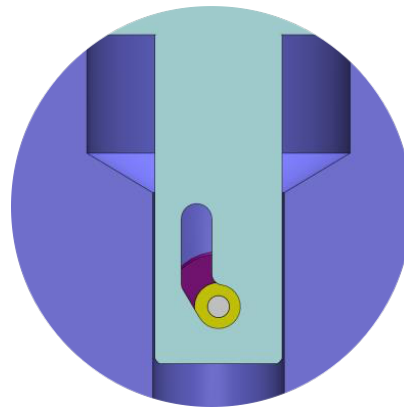


**Figure 6:** Section view of OARS in bolted condition

According to the working principle described previously, the difference can be observed with respect to the patented functioning:

(a) Patented design: one POF cable; light output variation accomplished by compressing the POF cable.

(b) Current design: two POF cables; light output variation accomplished by placing a mechanical obstacle in the gap between cables' ends.

This change is due to the tests performed at SILab. In these tests, POF showed plastic behaviour for the compression required to provoke desired light power attenuation in the unbolted condition. Therefore, when the conductor was being released (bolted condition), it was keeping the deformed shape and the light output wasn't the maximum available. This could be interpreted by a monitoring unit as tampering of the seal. As a conclusion, the light output losses cannot be provoked by compressing the conductor, as initially pretended.

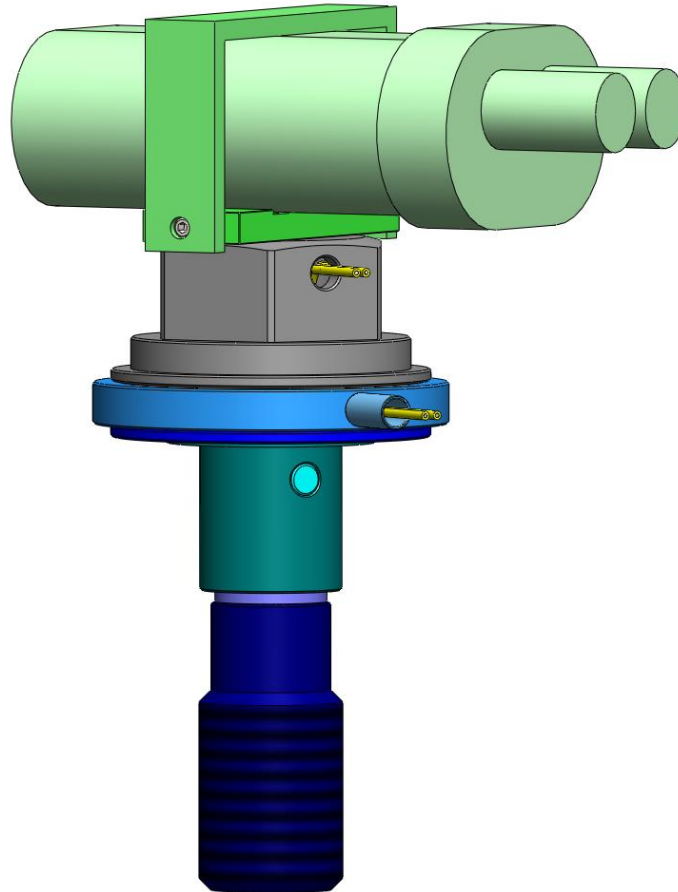


**Figure 7:** 3D view (CAD model) of OARS

## 5. Manufacturing

All components were 3D printed and/or manufactured at the mechanical workshop of SILab in Ispra (Figure 8).



Figure 8: 3D printers and various machines used for prototyping

### 5.1 Resin Prototypes

Prototypes manufactured by stereo-lithography (SLA) 3D printings have been essential in OARS design process, mainly for testing the different design proposals to assess the correct light transmission.

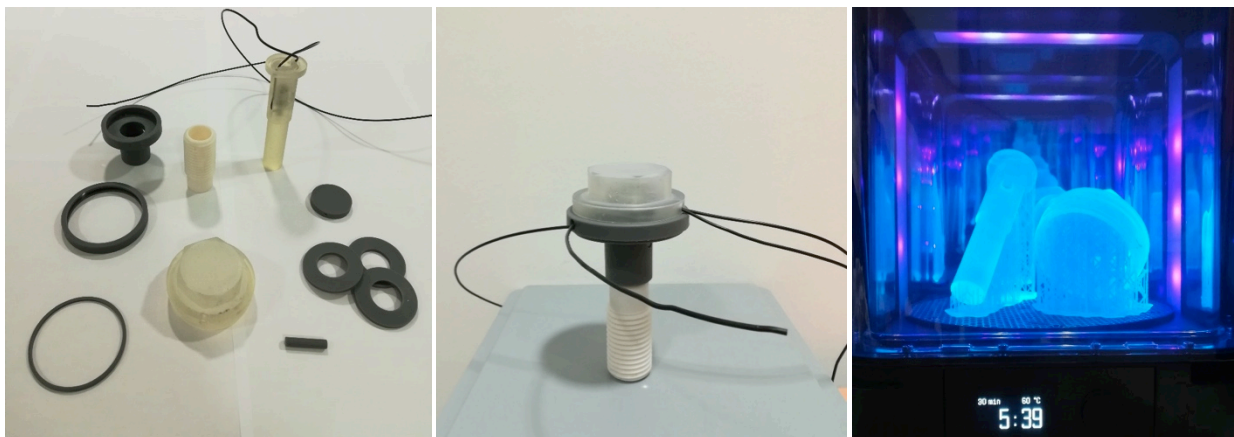


Figure 9: 3D printed components (left), once assembled (middle) and when cured (UV + heat) after printing (right)

## 5.2 Steel Prototypes

Several partial prototypes were built with the aim of selecting the correct springs in order to give enough torque and the right displacement. Others were dedicated to light transmission, which forced us to leave out the preliminary concept of compressing the fiber to the adoption of the new concept of blocking the light instead. After this intensive testing phase, the final mechanical design was validated first on SLA models and then manufactured in stainless steel.



**Figure 10:** OARS components corresponding to second functional prototype before their assembly

In particular, the assembly of the various components including the upfront installation of the fiber, and later the welding were studied carefully. It proves to be efficient and the prototype worked as foreseen. In particular the torque and mainly the two phases of power light transmission were assessed and successfully tested.



**Figure 11:** OARS final steel prototype with AOLS connected on top and optical leach (bottom right)

## 6. References

- [1] F. Littmann and M. Sironi, Patent “Sealing bolt and method of installing a sealing bolt” WO 2017/140575

# **Session 11:**

# **NDA Neutrons**

## Nuclear and Atomic Data Needs for Safeguards

**Chris A. Pickett<sup>1, 2</sup>, Christopher Ramos<sup>2</sup>, Fredrik Tovesson<sup>2</sup>, Karen Ventura<sup>2, 3</sup>**

<sup>1</sup> Oak Ridge National Laboratory

<sup>2</sup> National Nuclear Security Administration

<sup>3</sup>Pacific Northwest National Laboratory

[pickettca@ornl.gov](mailto:pickettca@ornl.gov)

[Christopher.ramos@nnsa.doe.gov](mailto:Christopher.ramos@nnsa.doe.gov)

[Fredrik.Tovesson@nnsa.doe.gov](mailto:Fredrik.Tovesson@nnsa.doe.gov)

[Karen.ventura@nnsa.doe.gov](mailto:Karen.ventura@nnsa.doe.gov)

### Abstract

The International and Domestic Nuclear Safeguards programs are foundationally based on obtaining accurate and precise nuclear material measurements with quantifiable uncertainties. These programs employ several types of both non-destructive assay (NDA) and destructive analysis (DA) methods to measure material quantity, chemistry, and physical properties. Each measurement method has the goal of meeting the International Atomic Energy Agency (IAEA) established international target values (ITVs); which are based on the utilized measurement methods. Common NDA methods used for domestic and international Safeguards are; passive gamma spectroscopy, passive and active neutron correlation counting, nuclear calorimetry, and X-ray fluorescence techniques. The most common DA methods are mass spectrometry and Davis-Gray titration. All of the commonly used NDA and DA methods have dependence on atomic and nuclear data. These data typically exist in measurement codes (embedded software) that are either supplied by a commercial entity or government laboratory. However, it is not always clear what nuclear and atomic data sources are being utilized by these commercial and lab developed codes. Without this information or adequate calibration standards, accurate quantification of NDA and DA measurement uncertainties cannot be properly determined. In this paper, we highlight on-going efforts by the Defense Nuclear Nonproliferation Research and Development (DNN R&D) program that focus on determining nuclear and atomic data most pertinent for global Safeguards and other Nonproliferation missions. We also provide status on recent efforts to improve the quality of nuclear and atomic data used for NDA and DA measurements of special nuclear materials (SNMs).

**Keywords:** International Target Values, Safeguards, Nuclear Data, Atomic Data, NDA, DA

### 1. Introduction

Destructive and non-destructive measurement methods used to characterize and quantify special nuclear material (SNM) are foundational to all Domestic and International Safeguards programs. Additionally, they are utilized by many global nuclear safety and security programs. The primary safeguards objective for these measurements methods is to determine the completeness and correctness of a facility or state declared SNM inventory. The underlying codes (software) associated with these measurement methods are reliant on the quality of nuclear and atomic data being utilized to determine elemental and isotopic quantities. In many cases (for nuclear data being used today), the original source of the data and its associated uncertainties are unknown. Without this information, safeguards measurement methods are limited in their ability to accurately quantify measurement uncertainty; or in other words in their ability to effectively verify the completeness and correctness of a safeguards declaration.

Safeguards practices require excellence in the performance of **nuclear material accountability** (NMA) and **containment/surveillance** (C/S), domestically referred to as material control. Material accountability deals with measurements that determine the material type and the material amounts. Containment and Surveillance deals with **protecting the integrity of measured values** and works to maintain chain of custody of the SNM as it is processed, stored, and transported. Built on a foundation of effective NMA

and C/S, these measures provide confidence and Continuity of Knowledge (CoK) that supports overall safeguards conclusions (see Figure1). Our ability to obtain quality measurements and maintain the integrity of these measured values is necessary for drawing meaningful safeguards conclusions!

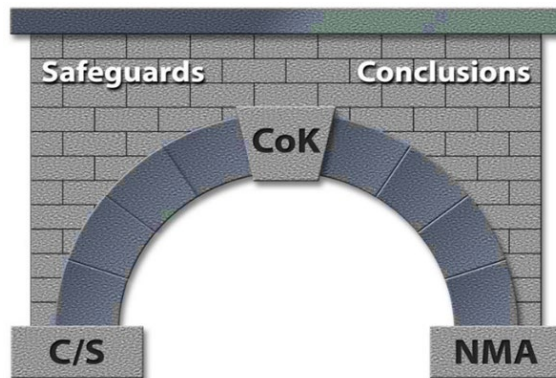


**Figure 1:** CoK is the Keystone for Drawing Safeguards Conclusions that relies on Effective Nuclear Material Measurements and Containment & surveillance

## 2. Deriving the Material Balance equation

Safeguards monitoring is summarized as a need to understand a particular process and identify key measurement points. Every process contains an input and an output (see Figure 2). In Safeguards, we must characterize both, taking into account that in some cases the understanding of the process to get from the input to the output is necessary. Consequently, the material balance equation becomes fundamental for determining and verifying nuclear material inventories.

A process in safeguards is anything that has inputs and outputs. We define Material Balance Areas or MBAs as distinct geographical areas where inventories can be performed (meaning where inputs and outputs can be measured and tracked). MBAs are typically actual physical processes, sub-processes, storage areas, shipments, etc. MBAs can be as large as an entire facility or as small as a source storage cabinet.



**Figure 2:** Simple Nuclear Material Process Model

Figure 2 illustrates a simple process. The material enters, leaves, and/or may remain in a process. If all nuclear material that enters the process leaves the process, then:

$$\text{Inputs} = \text{Outputs (ideal case)}$$

When some material remains in the process from previous processing, then the inventory at a specific point in time will be:

$$\text{Inputs} = \text{Outputs} + \text{Ending Inventory (EI)} \quad (\text{EI is the material left in the process})$$

Thus, for the very first inventory period (beginning inventory  $n = 0$ ):

$$0 = \text{Inputs} - \text{Outputs} - EI$$

For a second inventory at a point in time, the ending inventory of the first period becomes the beginning inventory (BI) of the second period, i.e.  $BI_2 = EI_1$ :

$$0 = \text{Beginning Inventory}_2 + \text{Inputs}_2 - \text{Outputs}_2 - \text{Ending Inventory}_2$$

$$0 = BI_2 + I_2 - O_2 - EI_2$$

Which leads to:

$$0 = BI_n + I_n - O_n - EI_n$$

or

$$0 = EI_{n-1} + I_n - O_n - EI_n$$

Where  $n$  is the  $n^{\text{th}}$  inventory period.

However, in nearly all nuclear material processes, each term is subject to an unknown uncertainty. Therefore, we define the Inventory Difference (ID) or Material Unaccounted for (MUF) as:

$$ID = MUF = BI + I - O - EI \quad (\text{Material Balance Equation})$$

**Note:** Sometimes Inputs (I) and Outputs (O) are referred to as Additions (A) and Removals (R)

Unfortunately, most material balances at nuclear processing facilities are non-trivial. In these facilities, materials can change physical form and/or chemical composition as they are processed. These processes also result in process losses that cannot be recovered for measurement (see Figure 3).

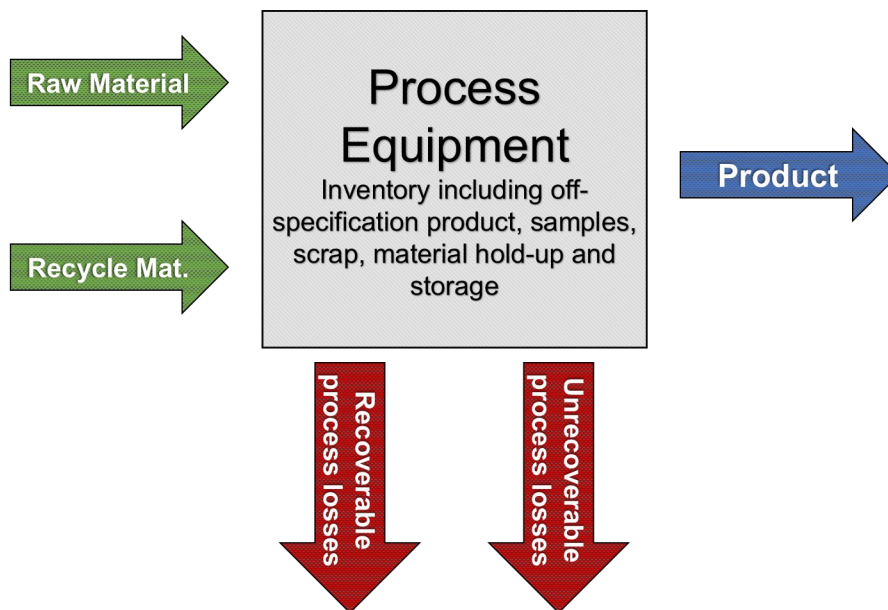


**Figure 3:** Representative Nuclear Material Process Model

Our ability to effectively determine IDs or MUFs is fundamental for obtaining meaningful safeguards conclusions. Examples of event that contribute to MUFs are:

- Errors in the inventory
- Errors in the inventory process
- Process upset
- Human errors

- Measurement uncertainty
- Incorrect adjustments
- Unmeasured losses
- Theft/Diversion.

Even when all sources of contribution to MUF are minimized, there still are factors that must be considered when drawing safeguards conclusions. These include:

- **Prior knowledge:** (What is the quality of past information? What do we know and what we not know?)
- **Technical capabilities:** (How good are the initial tools and methods versus the current tools and methods?)
- **Time** (When was the information acquired? Could the material have changed since it was last measured?)
- **Ability to monitor** (When and where can measurements be taken?)

Since there are many contributors to MUFs it is very important that we ensure that our measurement uncertainties can be sufficiently quantified. When MUFs start to equal significant quantities of nuclear material, the effectiveness of Safeguard measures for detecting material theft or diversion will be questioned. Some of the previously mentioned factors can be mitigated with an effective measurement control program, documentation of calibration methods, standards, and use of meta-data (i.e., operational records, etc.), and maintaining effective C/S.

Next, we will discuss the DA and NDA measurement methods used for safeguards and the underlying nuclear and atomic data that it relies on to accurately determine elemental and isotopic quantities of SNM.

### 3. Destructive Analysis Methods Used for Safeguards

Destructive analyses are methods that require obtaining a physical sample of the item for analyses. The obtained sample is typically “destroyed” as part of these analyses. The advantages of DA methods are high precision and accuracy. They are useful for the characterization of standards and allow for total analysis (providing information on other actinides of interest). On the other hand, the disadvantages of these techniques are the removal of material from the process, they are labour intensive, time consuming, subject to sampling errors, and they typically generate chemical, radiological and mixed wastes.

In 2010, the International Atomic Energy Agency (IAEA) STR-368 established International Target Values (ITVs) for DA methodologies used for Uranium and Plutonium [1]. The ITVs estimate the capability that could reasonably and realistically be expected from industrial-type laboratories on a routine basis.

Example of common DA techniques include:

- **Gravimetric Analysis:** Where uranium tetrafluoride ( $UF_4$ ) is converted to uranium oxide ( $U_3O_8$ ) using pyrohydrolysis in a furnace at 850 °C
- **Davies-Gray Uranium Titration:** Chemical titration where Uranium (U) is reduced to  $U^{IV}$  then titrated to  $U^{VI}$
- **Coulometric Determination of Plutonium; Electrochemical “titration”** where Plutonium (Pu) is oxidized from  $Pu^{III}$  to  $Pu^{IV}$
- **Mass Spectrometry:** Thermal ionization mass spectrometry (TIMS) and isotope dilution mass spectrometry (IDMS) (These measurements are not absolute. The measurements are relative to an external (standard bracketing) or internal (isotope dilution) standard)
- **X-ray Fluorescence:** Can be used to quantify U in materials; may be considered an NDA method as well depending on how the sample is prepared.

It is important to mention that the uncertainties for most of the DA methods are limited to the instrumental measurement uncertainty and availability of appropriate reference materials. In addition, DA methods

depend on nuclear and atomic data, such as, atomic masses, half-lives, etc. One of the major safeguards needs in the area of destructive analysis is the ability to age date nuclear materials.

### 3.1 Nuclear Data Needs for Destructive Analyses

Atomic masses are used in a variety of techniques such as mass spectrometry calculations. The uncertainty of these values is so small that it is usually neglected. Most of the time these well-known values are treated as constants. However, there are ongoing discussions whether to continue to disregard these uncertainties.

Half-lives are very important when accounting for material. The short Half-lives of  $^{241}\text{Am}$ ,  $^{238}\text{Pu}$  and  $^{241}\text{Pu}$  have uncertainties significant enough to have non-trivial effects on accountancy. A near-term goal for the safeguards community is to have consistent values of half-lives among national laboratories. In addition, a literature review of the current state of use of such values could help us better understand the extent of the problem. It is also important to mention that  $^{241}\text{Pu}$  has a string effect on measurements because it is used as a reference material. Some of the primary or most specific needs for improved nuclear data for destructive analyses methods involve:

- **Consensus/improved half-lives for  $^{229}\text{Th}$ ,  $^{230}\text{Th}$ .** Improvements in these half-lives would benefit age dating of Uranium materials
- For Pu determinations, IDMS and TIMS isotopic methods can benefit from **consensus/improved half-lives for  $^{238}\text{Pu}$ ,  $^{241}\text{Pu}$ ,  $^{241}\text{Am}$**
- Age dating of Pu materials are dependent on how well we know the **half-lives of  $^{241}\text{Pu}$  and  $^{241}\text{Am}$**

Some other important points to take into consideration when improving nuclear data to support DA methods are:

- Improve data for  $^{241}\text{Am}$ ,  $^{234}\text{U}$  and  $^{230}\text{Th}$ . Special attention should be given to  $^{229}\text{Th}$ , since discussion about the value of its half-life still exists and it is currently being used as an IDMS tracer for age dating of uranium materials.
- The half-life of  $^{241}\text{Pu}$  has direct impact in accountancy when propagating a measurement through time.
- A study on burn-up effects on fission product is needed. The yield of these products can be used for quantifying the number of fissions in a sample

## 4. Nuclear and Atomic Data Needs for Nondestructive Data Analysis (NDA) Measurements and Metrology in Nuclear Safeguards

International Nuclear Safeguards and Nuclear Material Accounting and Control (NMAC) rely on accurate and quantifiable physical inventory measurements. For instance, the commercial nuclear fuel cycle requires the verification of material in a variety of forms under a diverse set of measurement conditions. To perform these measurements the nuclear safeguards inspectorates employ a wide suite of non-destructive assay techniques and instruments. NDA methods based on passive gamma spectroscopy, passive and active neutron correlation counting, nuclear calorimetry, and x-ray fluorescence techniques are the most widely established, but a number of techniques are under development to meet emerging difficult to measure items and material flows.

A common feature for all NDA techniques is their dependence from implementation to analysis and interpretation on atomic and nuclear data. A physical model supported by data may be used to justify technique selection. Scientific design and optimization of measurement systems using forward prediction models rest on the quality of physical data. Basic data is often needed to support the characterization and calibration of instruments. During NDA analyses, correction factors and interference corrections typically require basic data as does the inversion of the measurement data collected into quantitative assay results and the interpretation of the nuclear material source term. Historically, nuclear safeguards measurement applications have relied on atomic and nuclear data that was evaluated for purposes other than safeguards. The uncertainties in this nuclear and atomic data are often the limiting factors in the overall uncertainties achievable with an NDA technique. For accurate

uncertainty quantification (UQ), it is also important to evaluate co-variance data, but unfortunately this is rarely done.

Minimizing systematic uncertainties due to nuclear and atomic data would improve the accuracies that are achieved by the NDA instruments. Efforts in this area, will drive the revision of ITVs [see e.g. STR-368 (2010), ESARDA Bulletin 48 (2012)], resulting in better measurements. The ITVs reflect the current state of practice, given the knowledge of the uncertainties. We are obligated to develop and utilize the best metrological practices.

The following sections provide details on the current status of different types of nuclear data that is utilized by common NDA measurement methods [2].

#### 4.1 Status of Existing Nuclear Data Uncertainties: Fission yields

- Fission Yields: Accurate estimation of neutron absorbing fission products is vital.
  - Build-up of neutron absorbing fission products reduces the net neutron population inside and escaping from the source and, therefore, the count rate measured by an NDA instrument.
  - ORIGEN estimations of fission products such as  $^{133}\text{Cs}$ ,  $^{143}\text{Nd}$ ,  $^{149}\text{Sm}$ ,  $^{154}\text{Eu}$  are within a few % of experimental values.
  - Absorption cross sections of some of the fission products ( $^{155}\text{Gd}$ ) have relatively large uncertainties (~5.3%).
  - Calculated/Experimental ratios for  $^{109}\text{Ag}$ ,  $^{106}\text{Rh}$ , and  $^{125}\text{Sb}$ : 170%, 67%, and 100%, respectively.
  - Inconsistencies have been observed with respect to quoted uncertainties on legacy nuclear fission yield data on noble gas fission products; (e.g.  $^{85}\text{Kr}$ )
  - $^{244}\text{Cm}$  is the dominant source of spontaneous fission neutrons as well as delayed neutrons from spent fuel: the nuclear data uncertainties are relatively high (8%).

#### 4.2 Status of Nuclear Data Uncertainties – Actinide Reaction Cross-sections

- High-fidelity covariance matrices for evaluated ENDF/B-VII files are available for three major actinides,  $^{235}\text{U}$ ,  $^{238}\text{U}$  and  $^{239}\text{Pu}$  [3]
- Covariance matrix evaluations for all major reaction cross sections are available- total, capture, fission, elastic, total inelastic, and (n,xn). [3]
  - Need: Angular distribution, uncertainties for discrete inelastic reaction cross sections
- Fission cross sections: Important for source term definition and interpretation of the response of active and passive neutron NDA system measurements for safeguards (e.g. Active Well Coincidence Counter, Neutron Coincidence Collar).
- Neutron-induced fission cross section of  $^{235}\text{U}$  was evaluated by the IAEA Standards Group [4],
  - ENDF/B-VII.0 evaluation incorporates their findings without modification, **including the associated covariance matrix for this reaction**
  - UQ for the neutron-induced fission cross-section of  $^{235}\text{U}$  is of major importance as most other actinide fission cross-section uncertainties are driven by it.
- Evaluation by the IAEA Standards Group is the result of major efforts from experts in the domain.

### 5. The Type of Measurements Needed for ( $\alpha$ , n) Reaction Data for Safeguards Science

Neutron emissions include spontaneous fission, induced fission, and ( $\alpha$ , n) reactions. Nuclear data related to neutron emission are vital in accurate definition of the source term and the detector response.  $\text{UF}_6$  is the most abundant material in the fuel cycle, and one way that the material production is verified is by neutron counting highlighting the importance of the ( $\alpha$ , n) reactions. A 10% uncertainty in ( $\alpha$ ,n) cross sections measurements can represent several significant quantities (SQs) of uncertainty in the MUF at the quantities of material handled in industrial facilities.

## 5.1 Sealed sources

Sealed neutron source measurements are convenient, since sources can be transferred to other centres for independent measurement, as part of inter-comparison exercises, or to use and calibrate different kinds of instruments. Once source measurements are taken they can be used for several years (working life in excess of 20 years, although the radiolysis of high activity sources and helium gas build up must be considered). They are readily accessible for laboratory experiments as routine quality control items. These source measurements can be set up to validate new spectroscopy and yield measurement methods that might be developed. They can be certified for absolute neutron emission using the  $\text{MnSO}_4$ -bath technique and provide an important link to national standards. Sources of various types can be used to validate the energy dependence of detectors to realistic  $(\alpha, n)$  spectra. By developing an  $(\alpha, n)$  yield and spectrum measurement program, sealed sources can play an essential role as well as providing important benchmark/integral/normalization data in their own right.

## 5.2 Accelerator measurements

Thick target ( $\alpha$ -particles stop in the material) integrated-over-angle (TT IOA) yield measurements in steady state using flat a well characterized energy  $4\pi$  are needed for the elements mentioned. A variety of target materials should be measured to check consistency and scaling rules. Using the same instrumentation is recommended to avoid bias. Target degradation under bombardment should be included as part of the experimental evaluation

## 6. Nuclear Data Needs for NDA Methods for Safeguards Applications

Accurate knowledge of gamma ray energies, half-life, and gamma ray yields are extremely important for identifying and quantifying radionuclides of interest for non-proliferation applications. NDA instruments based on gamma spectrometry, and analysis software depend on gamma ray related nuclear data and their associated uncertainties. Nuclear data related to gamma ray emission are used in libraries for nuclide identification in gamma ray analysis, and activity or mass determination.

Branching ratios of gamma-rays emitted by uranium, plutonium, and other actinide isotopes are needed with greater accuracies so that the uncertainties in the isotopic analyses can be driven down. Similarly, atomic data such as mass attenuation coefficients of actinide elements and X-ray yield data have large uncertainties. These limit the accuracy of U and Pu elemental concentration results that are of importance to nuclear safeguards.

A Workshop for Applied Nuclear Data Activities (WANDA) was held at the Elliot School of International Affairs at George Washington University in January 2019 [5]. The purpose of WANDA was to bring subject matter experts from the national laboratories, universities and industry together with government program managers and their advisors to develop collaborative plans of action (e.g., roadmaps) to address outstanding issues in nuclear data that affect applications in nuclear non-proliferation. During a brainstorming session focussed on NDA measurements used in Safeguards, the following comprehensive list of nuclear data needs were obtained:

- Knowledge of nuclear and atomic data can become the limiting factors in design and calibration of NDA systems and physics-based modelling of responses from NDA systems used in safeguards applications.
- The neutron yields from  $(\alpha, n)$  reaction on low Z nuclides (for example the  $F(\alpha, n)$  reaction, important in the safeguards of the enrichment of uranium) are not well known. [6]
- Uncertainty quantification, taking into account co-variances, is needed for cross-section (fission and other reactions) data in the evaluated nuclear data libraries.
- Relative abundances of delayed neutron groups available in the literature have large uncertainties.
- Branching ratios of gamma-rays emitted by uranium, plutonium, and other actinide isotopes are needed with greater accuracies so that the uncertainties in the isotopic analyses can be improved.
- Atomic data such as interaction cross sections and X-ray yield data have large uncertainties, which limit the accuracy of U and Pu elemental concentration results that are of importance to nuclear safeguards.

- It is a high priority to have improved ( $\alpha, n$ ) cross sections on low-Z material (e.g. Fluorine, Oxygen, Nitrogen) for uranium enrichment measurements.
  - Improved stopping power measurements are needed for alphas in these materials for alpha energies of  $\sim 10$  MeV down to threshold of relevant ( $\alpha, n$ ) reactions.
- $^{13}\text{C}$  ( $\alpha, n$ ) is important for calibration neutron detectors used in safeguards.
  - This information is also relevant to molten salt reactor studies such as low-Z isotopes found in F, Li, Be in other salts.
- A study on burn-up effects of fission products is needed. The yield of these products can be used for quantifying the number of fissions in a sample.
- Intensity of gamma-ray emissions and branching ratios in the decay of  $^{234\text{m}}\text{Pa}$  can have immediate impact on safeguards applications.
- Delayed gamma-ray spectra and models thereof are affected strongly by fission yields. These calculations of fission yields are important for assaying nuclear materials.
  - For fissile materials and a variety of energy-group/energy-differential irradiations.  $^{235}\text{U}$ ,  $^{238}\text{U}$ ,  $^{239}\text{Pu}$ ,  $^{241}\text{Pu}$
  - For fast neutron spectra more fissionable isotopes become relevant
  - Carefully selected energy groups can be useful to different applications because they can be selected/applied in an intuitive fashion.
- There are a number of active projects to measure fast neutron fission. [7] However, low-energy neutron irradiations would likely require additional efforts.
- High-energy gamma intensities for fission products.
- A list of high priority fission products is needed, especially those with short half-lives ( $< 10$  min) and high energy gamma emission lines over 2.5 MeV
- Eventually it would be ideal to obtain fission yields for minor actinides as these are also found in spent fuel.
- There are about 156 fission products. Not all of them contribute to the fission spectra. We are looking for high energy gammas. ( $^{142}\text{La}$ , Cm that is in spent fuel has a high cross section that causes some interference,  $^{237}\text{Np}$ ,  $^{233}\text{Pu}$ )
- New high-precision measurements of  $^{252}\text{Cf}$  (nu-bar), including the quantification of the delayed neutron component are needed. Moments and distributions are desired.
- Evaluations of distributions need to be updated for applications like MCNP [8].
- Improved measurements of low energy X- and gamma-ray line intensities of U and Pu.) and their daughters

A summary comment made by several workshop attendees indicated that just like there are benchmarks for criticality safety, benchmarks are needed for safeguards measurements; however there first should be an effort to define a safeguards benchmark. If appropriate safeguards benchmarks can be established, then we can truly perform measurements of excellence!

## 7. Concluding Remarks

The entire global safeguards community needs to achieve a better understanding of the underlying nuclear and atomic data used by safeguards measurement systems. It is very important that the source(s) of nuclear and atomic data utilized by these measurement methods can be referenced and the uncertainties with this data are well understood. This will improve our ability to quantify measurement uncertainty and move the global safeguards community toward measurements of improved quality.

## 8. Acknowledgements

The material in this report is based upon work supported by the U.S. Department of Energy (DOE) National Nuclear Security Administration (NNSA) Office of Defense Nuclear Nonproliferation R&D. The authors would like to acknowledge the many important contributions of Stephen Croft and Brian Ticknor from Oak Ridge National Laboratory, and Andrea Favalli from Los Alamos National Laboratory. Without their contributions, much of the information represented in this paper would have taken much more time to compile.

## 9 Legal matters

### 9.1. Privacy regulations and protection of personal data

"I agree that ESARDA may print my name/contact data/photograph/article in the ESARDA Bulletin/Symposium proceedings or any other ESARDA publications and when necessary for any other purposes connected with ESARDA activities."

### 9.2. Disclaimer

This paper was prepared as an account of work sponsored by an agency of the United States Government. Neither the United States Government nor any agency thereof, nor any of their employees, makes any warranty, express or limited, or assumes any legal liability or responsibility for the accuracy, completeness, or usefulness of any information, apparatus, product, or process disclosed, or represents that its use would not infringe privately owned rights. Reference herein to any specific commercial product, process, or service by trade name, trademark, manufacturer, or otherwise does not necessarily constitute or imply its endorsement, recommendation, or favoring by the United States Government or any agency thereof. The views and opinions of authors expressed herein do not necessarily state or reflect those of the United States Government or any agency thereof.

## 10. References

1. STR – 368, International Target Values 2010 for Measurement Uncertainties in Safeguarding Nuclear Materials, international Atomic Energy Agency, Vienna, Austria, November 2010.
2. Venkataraman, R.; Worrall, L. G.; McElroy Jr., R. D.; Favalli, A.; and Croft, S.; *Nuclear & Atomic Data Needs for NDA Measurements in Nuclear Safeguards*, in proceedings of Annual Meeting of the Institute of Nuclear Material and Management, Baltimore, USA, 2018.
3. P. Talou et al., Nuclear Data Sheets 112 (2011) 3054–3074
4. A.D. Carlson et al., Nuclear Data Sheets, 110, 3215 (2009)
5. Bernstein, L.; Romano, C.; Brown, D.A.; Casperson, R.; Descalle, M.; Devlin, M.; Pickett, C.; Rearden, B.; and Vermeulen, C.; *Final Report for the Workshop for Applied Nuclear Data Activities*, George Washington University, Washington, DC, January 22-24, 2019, LLNL-PROC-769849.
6. Croft, S.; Favalli, A.; Fugate, G. A.; Gould, I.; McElroy Jr., R. D.; Simone, A.; Swinhoe, M. T.; Venkataraman, R.; *The specific ( $\alpha, n$ ) production rate in  $^{234}\text{U}$  in UF<sub>6</sub>*, *Nuclear Instruments and Methods A*, (online:Nov.2018), in press. <https://doi.org/10.1016/j.nima.2018.11.067>
7. Croft, S.; Favalli, A.; McElroy Jr., R. D.; *A review of the prompt neutron nu-bar value for  $^{252}\text{Cf}$  spontaneous fission*, *Nuclear Instruments and Methods A*, (online:Jan.2019), in press, <https://doi.org/10.1016/j.nima.2018.11.064>
8. Croft, S.; Nicholson, A.; Henzlova, D.; Favalli, A.; *Representing the uncertainty structure of the factorial moments of  $^{252}\text{Cf}$  and  $^{238, 240, 242}\text{Pu}$* , Advances in Nuclear Nonproliferation Technology & Policy Conference, ANS. Santa Fe, NM, US, September 25-30, 2016.

## New developments in neutron counting chains for safeguards

Giovanni Varasano, Mahel Abousahl, Tatjana Bogucarska, Bent Pedersen

European Commission, Joint Research Centre,  
Nuclear Safety & Security Directorate, Nuclear Safeguards & Security Department  
Nuclear Security Unit  
Via E. Fermi 2749, Ispra 21027 (VA), Italy  
E-mail: giovanni.varasano@ec.europa.eu

### Abstract:

*Standard neutron counting systems in nuclear safeguards typically use a thermal neutron absorber material in gas proportional counters embedded in a neutron moderator a block, and surrounding the central sample cavity. Multiple detector tubes are normally connected to one electronics chain composed of a pre-amplifier, amplifier, a single channel analyser, and a digital signal mixer summing signals from multiple chains to producing a single pulse train representing the neutron detection events. This has typically been the design compromise considering factors such as dead-time of detection system, electronics reliability, complexity, and cost.*

*In this paper we describe the ongoing developments at JRC for modernizing the entire electronics chain including all individual components mentioned above as well as the digital signal analyser. A key element of this work concerns an in-house designed digitizer board capable of processing pre-amplifier outputs to identify neutron detection events. The board has multiple analogue inputs, a multi-channel ADC, pulse processing in FPGA hardware, and output of timestamps of neutron detection events. The benefits from this work is expected to be a reduced pulse processing time in the electronics, better pulse pair resolution, elimination of the physical signal analyser, and better systems diagnostics.*

*The new electronics developments are being assembled and tested in the JRC reference passive neutron counter, and will be ready for demonstration in the coming year. The reference counter is a cylindrical well-counter incorporating 126  $^3\text{He}$  neutron detector tubes.*

**Keywords:** NDA; neutron counter; digitizer; list-mode; safeguards

## 1. Introduction

Several non-destructive techniques (NDA) and devices for safeguards using passive or active neutron measurement methods have been developed and tested at the JRC over decades.

Traditionally a neutron measurement chain consists of analogue and digital components: a detector with high voltage bias supply, a preamplifier, an amplifier/shaper circuit, and finally a digital discriminator. Modern neutron detection systems apply many  $^3\text{He}$  or  $\text{BF}_3$  gas proportional counters in order to increase the neutron detection probability and also to reduce the paralyzing, or updating, dead-time effects.

A necessary requirement for systems of multiple detection chains is that the resulting digital signal lines must be summed to produce one signal pulse train for the analysis, without suffering loss of real signals and without causing false spurious signals. An analogue electronics chain performs rather well when only few parallel measurement chains are used i.e. when several detectors grouped together within a moderator block, are connected to a single measurement chain.

High efficiency neutron well-counters often use tens of such measurement chains. Particular care must be observed when manufacturing such devices in order to eliminate internally or externally generated electromagnetic noise. Such precautions can include using proper filters on the high voltage rail, using multi-layer printed circuit boards (PCBs), separating analogue and digital ground planes, avoiding to create inductive paths which may amplify ground bounces, etc.

Such passive neutron counting systems currently operated at JRC includes e.g. the Drum Monitor, the Boron Based Neutron Coincidence counter (BBNCC), and neutron slab counters, applying 28, 6 and 1 analogue chains, respectively. These systems output TTL pulse signals, representing neutron detection events, to be counted by means of standard signal analysers such as multi-channel scalers (MCS) or shift registers (SH/R) commonly used in multiplicity analysis. The analysers are routinely used with standardised measurement software for example for nuclear inspectors.

Most often Transistor-to-Transistor Logic (TTL) signal outputs are used to maintain compatibility with existing analysers. An important part of the analogue electronics is the discriminator which filters out signals not originating from neutron detections but from other effects for example gamma-ray background, and false bursts caused by electromagnetic noise. The discriminator level is set carefully not avoid eliminating real neutron signals, and not to trigger multiple output signals from a single analogue pulse. Correctly setting the discriminator can in part eliminate gamma background and spikes of noise caused for example by TTL ground bounces whose noise contribution to the analogue signal can increase significantly when multiple parallel measurement chains are in use. Each analogue pulse crossing the discrimination level triggers the output of a logical pulse for further processing.

Modern technologies offer alternative approaches to the solution of problems encountered in a standard analogue chain. For example implementing measurement components using field programmable gate arrays (FPGA), and using low-voltage differential signal standards (M-LVDS) to propagate signals within the neutron counter [1]. In case a TTL output signal is needed to maintain compatibility with external instrumentation, a digital pulse can easily be produced as output.

The text below describes such techniques and components, we have implemented so far, together with other efforts currently under development in order to process neutron detection events using more modern digital techniques.

We use a Moving Window Deconvolution (MWD) algorithm [2] to process a signal in an entirely digital fashion using appropriate digital filters implemented in FPGA state-of-the-art technology. Another effort concerns implementing a novel low-noise charge pre-amplifier to be implemented eventually with every single  $^3\text{He}$  tube thus avoiding connecting several tubes to a single pre-amplifier. This will reduce the updating dead-time of the combined system. An analogue pulse shaper will no longer be used, but will be substituted by a digital filter featuring a comparable or possibly shorter shaping time. A final advantage of the digital pulse processing chain is expected simply by all data being transmitted via high-speed optical USB3.0 link. Avoiding the usage of multiple 50-Ohm coaxial cables will simplify the implementation of the overall system as expected for example in a planned high-efficiency counter using 126  $^3\text{He}$  tubes. Multiplicity analysis and/or multichannel scalers are easily integrated inside the FPGA fabric.

Applying a pre-amplifier on each detector tube makes the individual tubes independent rather than integrated in the shared detection system. This fact greatly facilitates the sharing of  $^3\text{He}$  proportional counters between neutron well-counters thus avoiding the purchase of many  $^3\text{He}$  tubes with a single usage in mind.

## 1.1 Digital techniques

The main advantages, proposed in this paper, for changing to digital processing techniques in neutron NDA instrumentation for safeguards, are:

- 1) Elimination of noise spikes returning to the pre-amplifier input and generated by TTL digital output signals from another electronics chain. Low-voltage differential signal lines (M-LVDS Standard) can be an alternative to single ended TTL logic.
- 2) Reduction of the dead-time, and possibly improved detection of pile-up pulses.
- 3) Recording of both timestamp and energy information of a radiation detection event. The added energy information can help discriminate high-energy events e.g. caused by cosmic radiation or unwanted ionizations.
- 4) If compatibility with existing instrumentation needs to be maintained, a TTL output pulse can be generated at the same time the timestamp is computed.

## 1.2 Time digitizers for neutron counting applications in safeguards

Neutron coincidence counting is the reference NDA technique used in nuclear safeguards to measure the mass of nuclear material in samples. Most neutron counting systems are based on the original shift register technology. The analogue signal from the  $^3\text{He}$  tubes is processed by a charge amplifier/discriminator producing a train of TTL digital pulses that are fed into an electronics unit which records frequency distributions of neutron detections in short time intervals. In recent years many research laboratories instead produce the frequency distributions based on software based analysis of timestamps of detection events. For this purpose so-called list-mode acquisition devices produce the list of timestamps. Often seen are standard laptops or desktop computers (PCs) utilising external acquisition boards based on FPGA technology providing a time stamp for every incoming digital signal. The acquisition can be performed at high data rates utilising the ubiquitous Universal Serial Buses (USB2.0 or USB3.0) for transfers to the host PC with typical data throughput in the order of 40MB/s and 300MB/s, respectively.

The timestamps of a given measurement are often saved to storage devices. This has the advantage that measurement data can be re-analysed with different parameter values such as gate pre-delay and gate width. Other useful diagnostics information such as die-away time, dead-time, performance of individual electronics chains, and eventually electronics noise can be filtered from the original data stream. The diagnostics information can be extracted from this stored data, or even in real-time under certain circumstances.

At JRC two models of the Time Digitizers for Safeguards (models TDS8 and TDS32) were developed with the timestamp features described above. The TDS8 and TDS32 are shown in Figure 1. The devices record the arrival time of digital pulses with a 20 ns resolution, and feature 8 or 32 input channels, respectively. Also the channel number is recorded for each event. Data are transferred to host PC over USB2.0 or USB3.0 data links. Data throughputs are 38 MB/s and 300 MB/s, respectively. The devices are housed in a small extruded aluminium enclosure and in a standard 19-inch rack 1U enclosure, respectively. Other features include powering over USB (TDS8), and front panel Light Emitting Diodes (LED) for each input line allowing the user to observe the incoming pulses on individual channels (TDS32). A signal output on the rear panel is the sum of all input channels, and can be routed for example to a standard Shift Register analyser for comparison and/or test purposes. In both devices the recorded events are written into a dual port memory block in the FPGA. Dual port memories guarantee independence between the processes of writing and reading data simultaneously. Decoupling the data producer and data consumer allows a simpler but very efficient hardware/firmware design,



**Figure 1.** The models TDS8 and TDS32 list-mode devices developed at JRC. One with 8 front panel inputs, the other with 32.

A state machine, evolving through several states: (IDLE, WRITE\_START\_RECORD, WAIT FOR PULSE, WRITE\_PULSE\_EVENT, WRITE\_ROLLOVER\_EVENT AND WRITE\_STOP\_RECORD) transfers into dual port memory the time of arrival of TTL or LVTTLL signal on individual input channels. The TDS8 uses a timestamp of 32 bits so a roll-over event happens every 85.59 s, while the TDS32 uses timestamps of 29 bits, giving roll-over events every  $(2^{29}-1 \times 20\text{ns})$  equals 10.37 s. The generation of a roll-over event allows to measure arrival times in absolute time.

A Wishbone system on chip (SOC) bus [3] makes data available to the host PC using a buffered USB transmission.



5-bit Gray code counters have been implemented so that 16 slots (4 bits) are available on each individual line. Bursts of noise, such as the ones detected by the post-processing analysis of the pulse train (Tables 1,2), are eliminated by including a simple inhibit filter into the mixer FPGA fabric. This real-time filtering action should be performed only at low count rates or background measurements.

### 1.3 Signal Digitizer for Safeguards

At JRC we are currently in the process of developing an analogue signal digitizer to substitute the standard signal amplifier used in neutron counting instrumentation for safeguards. The signal digitizer will have eight analogue signal input lines intended for pre-amplifier signals from gas proportional counters. The main benefits of this prototype compared to the standard analogue front-end electronics are expected to be:

- reduced updating dead-time on each signal line
- improved discrimination of pile-up events

The digitizer will process the analogue charge pre-amplifier output with the characteristic long exponential decay by means of a Moving Window Deconvolution (MWD) and "feature extraction algorithm" (FEA). The algorithms are currently being tested in our laboratory. The hardware is expected to be operational by end of 2019.

A larger version featuring up to 128 channels to be housed inside a detector head is the final goal. In this way a single optical USB cable from the detector eliminates the complex wirings of multiple coaxial cables normally interfacing a neutron detector head to a signal analyser.

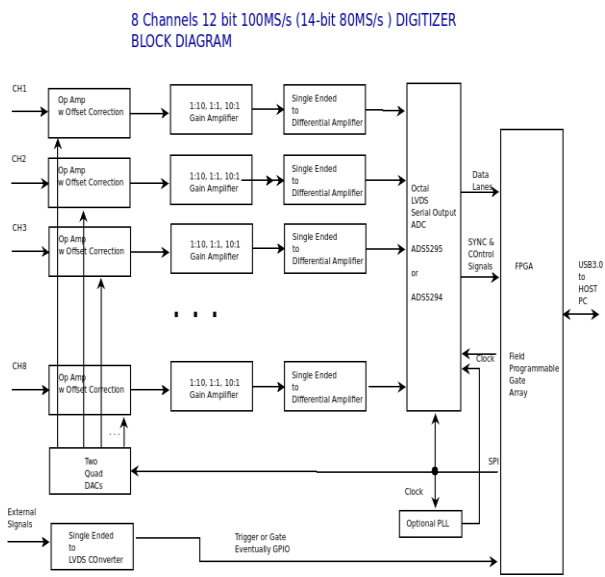
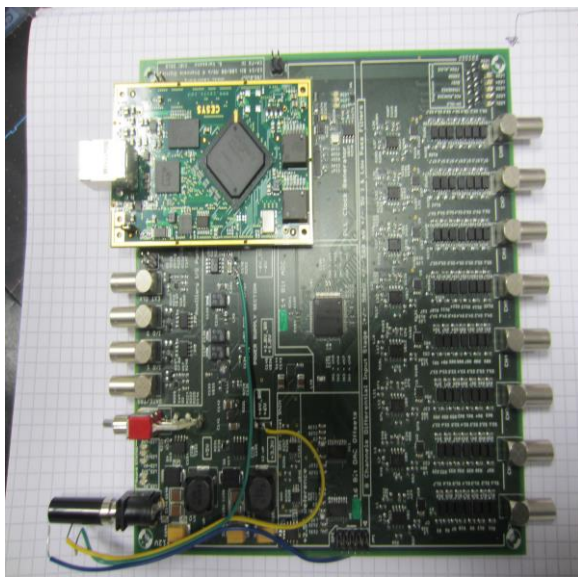


**Figure 2.** The prototype signal digitizer board and corresponding block diagramme.

The hardware is enclosed in an extruded aluminium box (170 mm x 163mm x 51.5 mm) of the following characteristics:

- Sampling rate up to 100MS/s ( ADS5295) and 80MS/s ( ADS5294) depending on chipset.
- Resolution 12-bit (ADS5295 ) or 14 bit (ADS5294).
- 8 channels, DC coupled, fixed input impedance: moderately high impedance (kΩ) or 50Ω.
- Trigger options: internal (software or driven by channel(s) criteria), or external (TTL logic levels).
- Gate: external TTL signal.
- Clock options: internal or external.
- Digitally controlled gain – In principle settable independently for each channel (the current version uses the same gain for all channels to simplify the board design on a 4 layers PCB).
- Input sensitivity covers the range from +/- 50mV (100mVpp) , +/-500mV (1Vpp) , +/- 5V (10Vpp) for ADC full scale.

- 50 (40) MHz analogue bandwidth, anti-aliasing LC filter included. Coefficients for low-pass filters can also be uploaded to the ADC registers.

## 2. Digital filter using Moving Window Deconvolution and feature extraction algorithm

The MWD algorithm, see Georgiev, Gast and Lieder [2], consists in a technique to determine a value proportional to the step amplitude of an exponential decaying signal (the output of a charge pre-amplifier) by looking at the sequence of values of the signal at successive time intervals. The values evidently contain an indication of the step value A assumed at t=0. In the continuous time domain, an exponential signal is defined as:

$$y(t) = \begin{cases} Ae^{-\frac{t}{\tau}} & t \geq 0 \\ 0 & t < 0 \end{cases} \quad (1)$$

To determine the step amplitude (A), we define a function  $f(t) = A$ . A term  $y(t)$  is added and subtracted:

$$f(t) = y(t) + A - y(t) \quad (2)$$

Then inserting the definition of the exponentially decaying function, the equation reads:

$$f(t) = y(t) + A \left(1 - e^{-\frac{t}{\tau}}\right) \quad (3)$$

By applying the fundamental theorem of integral calculus and using a variable substitution  $u = \frac{t}{\tau}$ ,

$$\text{because } \tau \int_0^t e^{-u} du = -\tau e^{-u} \Big|_0^t = \tau \left(1 - e^{-\left(\frac{t}{\tau}\right)}\right) \quad (4)$$

we get:

$$f(t) = y(t) + \frac{1}{\tau} \int_0^t y(u) du \quad (5)$$

The sum can be extended to  $-\infty$  because the signal is a null function for  $t < 0$ .

In the time domain this corresponds to a step function, i.e. the response of an ideal integrator.

To avoid saturation of a real pre-amplifier a continuous discharge is applied by a resistor in parallel to the integrating capacitor, so that the exponential response of the real filter is de-convoluted to a step function. In the discrete time domain the integral becomes a sum, also extensible to  $-\infty$ :

$$A(n) = x(n) + \frac{\Delta}{\tau} \sum_{k=0}^{n-1} x(k) \quad \text{where } \Delta = \frac{1}{\text{samplingrate}} \quad (6)$$

which can also be expressed as a recursion:

$$A(n) = x(n) - \left(1 - \left(\frac{1}{\tau}\right)\right) x(n-1) + A(n-1) \quad (7)$$

Equation 5 is differentiated (in discrete time) because we are interested only in the amplitude step of the signal from the radiation detector, we get:

$$MWD(n) = A(n) - A(n-M) = x(n) - x(n-M) + \frac{\Delta}{\tau} \sum_{k=n-M}^{n-1} x(k) \quad (8)$$

The MWD can be seen as a composition of two elementary blocks: Delay and Subtract (DS), and Moving Average (MA). The DS block takes the amplitude difference at two sampling points which are M sampling intervals apart  $y[n] = (x[n] - x[n-M])$ . M is the MWD differentiation filter length. The value of M can be taken as an integer power-of-two in order to easily implement a fast binary division.

## 2.1. Algorithm Implementation

The block diagram of the algorithm as implemented in Very High Speed Integrated Circuits Hardware Description Language (VHDL) code is presented in Figure 3.

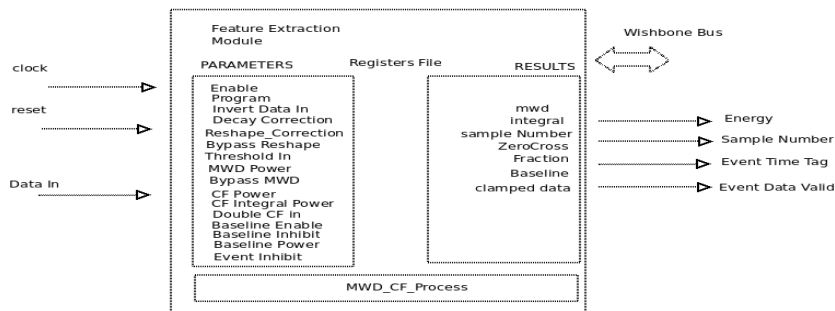


Figure 3. Block diagramme in VHDL.

The top level block of the MWD filter dialogues with the external word using a Wishbone bus interface [3]. Several registers are available to the user in order to store parameters and constant values for controlling the algorithm. The module outputs are:

- a timestamp indicating when the step value A is recognized,
- the corresponding energy (step height),
- an indication about the validity of the data recorded

The main registers to control the behaviour of the algorithm are:

- Decay and Reshape correction
- MWD Power (of 2) to give a length (M)
- Cross Fraction Power (division by  $\frac{1}{4}$  or  $\frac{1}{2}$ ) and Cross Fraction Integral Power (of 2) length of pipeline
- Baseline Power (of 2) so pipeline length
- Baseline inhibit and enable bits
- Event detect inhibit or enable
- Threshold input

A detail of the top-level diagram is given in Figure 4.

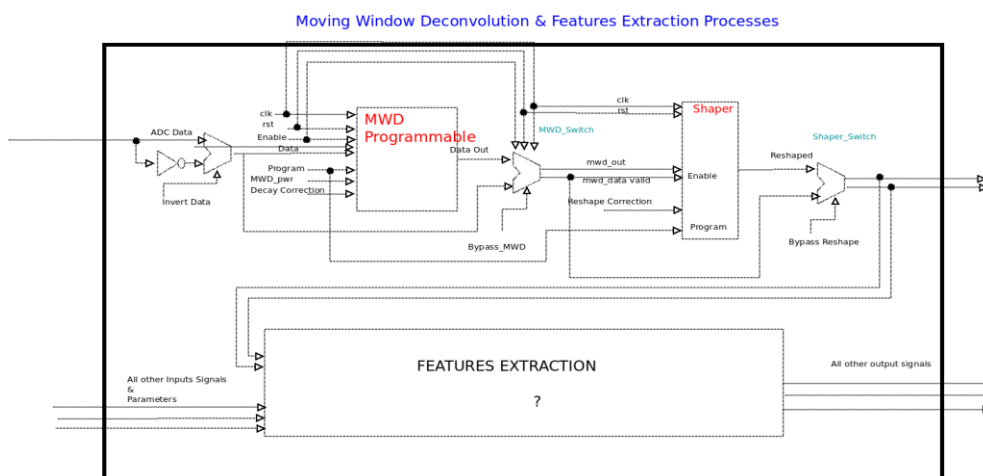


Figure 4. MWD and Shaper Block diagramme.

The ADC input data, or an inverted value representation, becomes the input of the programmable MWD module which can optionally be bypassed. The data can become an input for a shaper module which may also be bypassed. Following the MWD and shaper blocks a further more complex Features

Extraction block follows in Figure 5. Implementing a MWD, consisting of a DS and an MA block, is an easy task. The Features Extraction module however is not easily implemented. The latter module has been edited and adapted from a remarkable open source code [4], [5], [6] and [7].

The MWD logic consists of the Moving Sum and the Difference blocks. Fixed point arithmetic operations can be easily performed. However, the normalization constant  $\frac{A}{T}$ , expressed in units of the ADC sampling period  $T = 10$  ns, is a real number ( $<1$ ). A typical value is  $1/14000$  for the Cremat CR110 preamplifier decay constant of  $140 \mu\text{s}$ . In order to make the FPGA implementation of the MWD filter algorithm possible, the normalization constant is multiplied by an arbitrarily large power-of-two value, and after the multiplication operation the result is divided by the same factor.

### 2.1.1. Moving Sum or Moving Average (MA)

The MA entity is a basic building block for the MWD and in general also for FEA. The block is composed by an accumulator register, an adder/subtractor, and a delay line. The accumulator contains the sum of the delay line elements. Each value coming out of the delay line is subtracted from the accumulator. After an initial delay, an averaged value is output at each clock-tick (10ns). It is straightforward to divide (shift right operation) by  $N$  if the delay line length ( $N$ ) is a power of two.

### 2.1.2 The Features Extraction Algorithm (FEA)

A clamped data signal is obtained from the signal coming out from the previous MWD block and from the signal baseline information, which must be taken into account and subtracted from the input data. Of course the baseline computation must be disabled during the energy pulse duration interval otherwise a false value for the baseline would be obtained. In order to compute the energy and timestamp information of the step value  $A$ , a trigger signal must be determined at the same time.

The Features Extraction module (Figure 5) contains several blocks which compute different information more or less simultaneously by use of delayed pipelines, just to get information at a later time after other events have been already detected. In this way the algorithms can be executed in parallel and global information can be figured out after a delay when a final trigger signal is generated. The algorithm can be run continuously and is trigger-less because the trigger is extracted from incoming data.

A constant-fraction discrimination (CFD) module is used as a preferred choice with respect to the simpler leading-edge discriminator. The CFD entity is implemented by subtracting a delayed copy of the clamped signal, which has been scaled (values are divided by 2 or 4 for the sake of simplicity and implementation). The obtained CDF signal has a zero-crossing timing independent from the shape and rise time of the clamped signal. After detection of the zero-crossing a trigger is sent to the event detection module.

An event is detected when an area of the pulse is above the set threshold. The area is computed by means of a trapezoidal filter: another MA module which computes averaged values of the flat top portion of the pulse (can be seen in Figure 8). In order to detect the highest pulse level, which is contaminated by noise, a pulse detector is implemented by collecting a limited history of input signals. A timestamp is generated by means of a free running counter, and read upon arrival of the trigger signal. A linear interpolation is then used to determine a less arbitrary and more precise timestamp value. The zero-crossing indication is obtained by a simple algorithm which looks at a sequence of consecutive "one negative and two positive" values. The time information is between two samples. A linear interpolation of 4, 8 or more interpolated points can give an even better approximated value.

Parametric values are setup by the user by means of several registers (see Figure 3) in order to fine-tune the behaviour and performance of the algorithm.

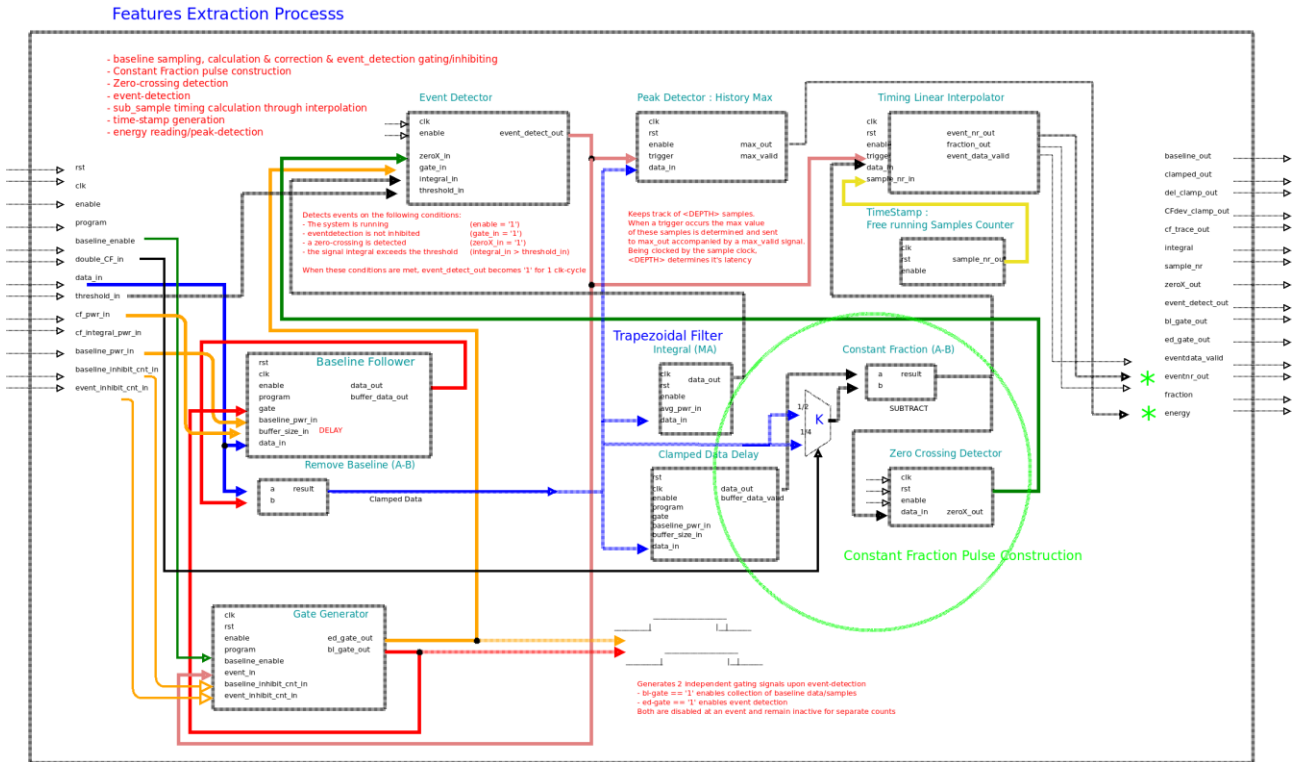


Figure 5. Feature Extraction module.

### 2.1.3 Simulations

The following figures, Figure 6-8, are the results of simulations performed using an open source hardware description language simulator. The analogue signals are a representation of digital values which, if represented only as numerical values, would have been less expressive of the dynamics of the signals.

The results of the MWD and FEA are shown below.

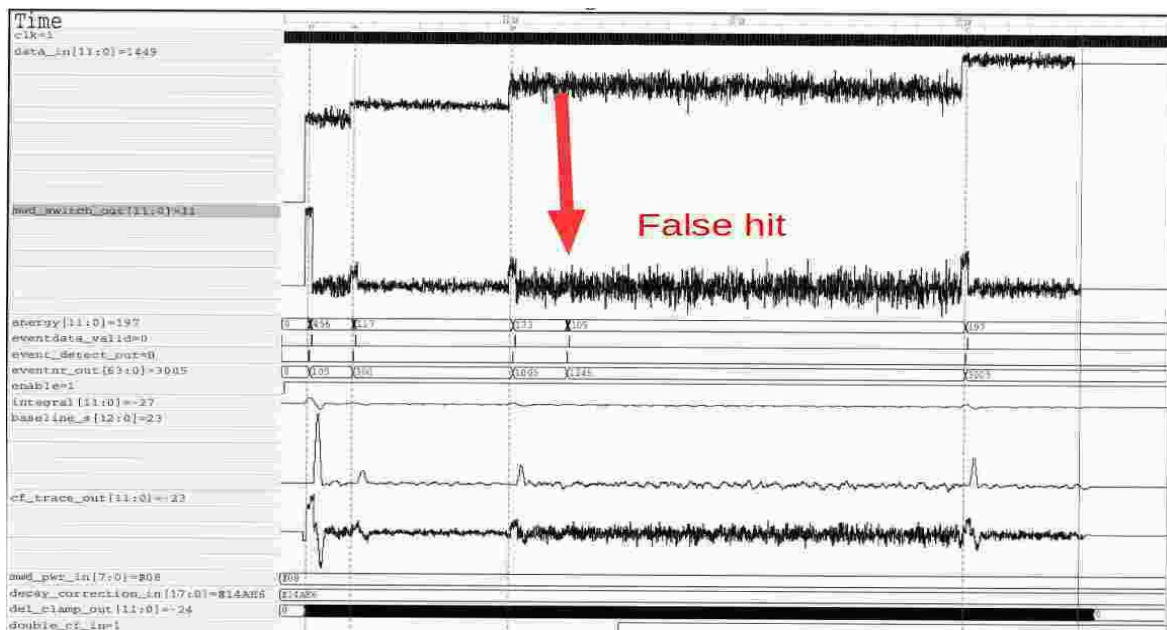


Figure 6. Simulation Result no 1

Figure 6 shows an input signal, which is a superposition of the exponential decaying waveform having a 140 us decay time (simulated pre-amplifier pulse). After the 3<sup>rd</sup> step the noise level has been increased purposely in order to generate a false detection of a time stamp and a corresponding energy value.

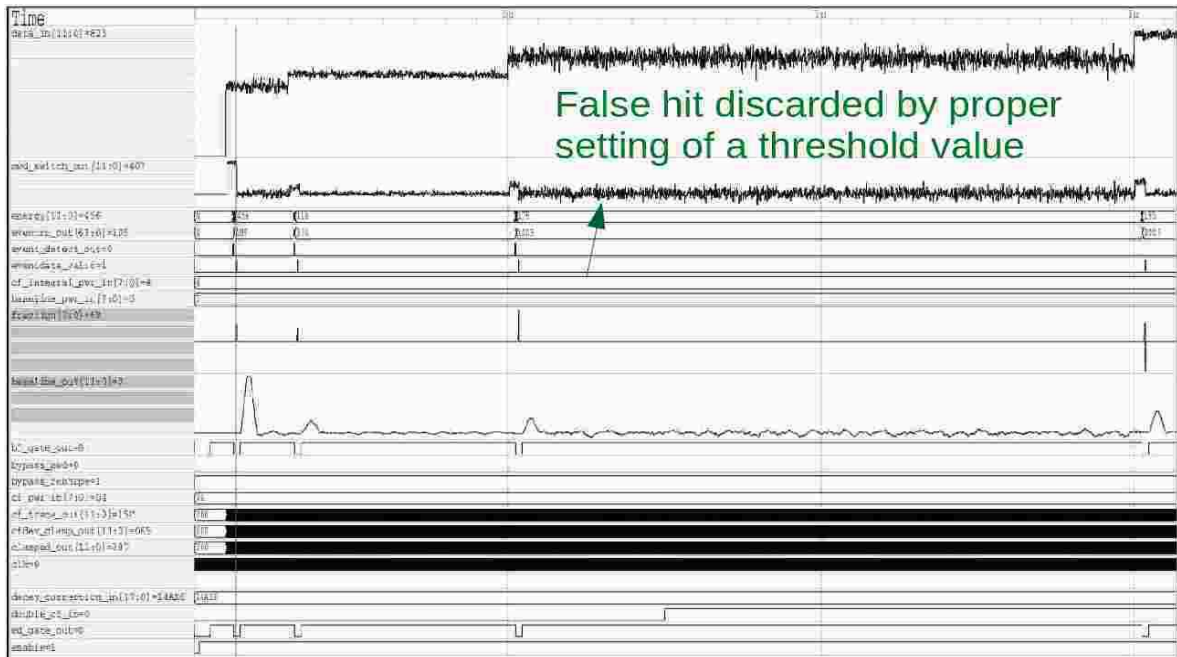


Figure 7. Simulation Result no 2

After having changed the threshold parameter (Figure 7), the false pulse in Figure 6 has been discarded. This fact means that tuning the digital algorithm can be as simple and effective as an analogue threshold discrimination circuit.

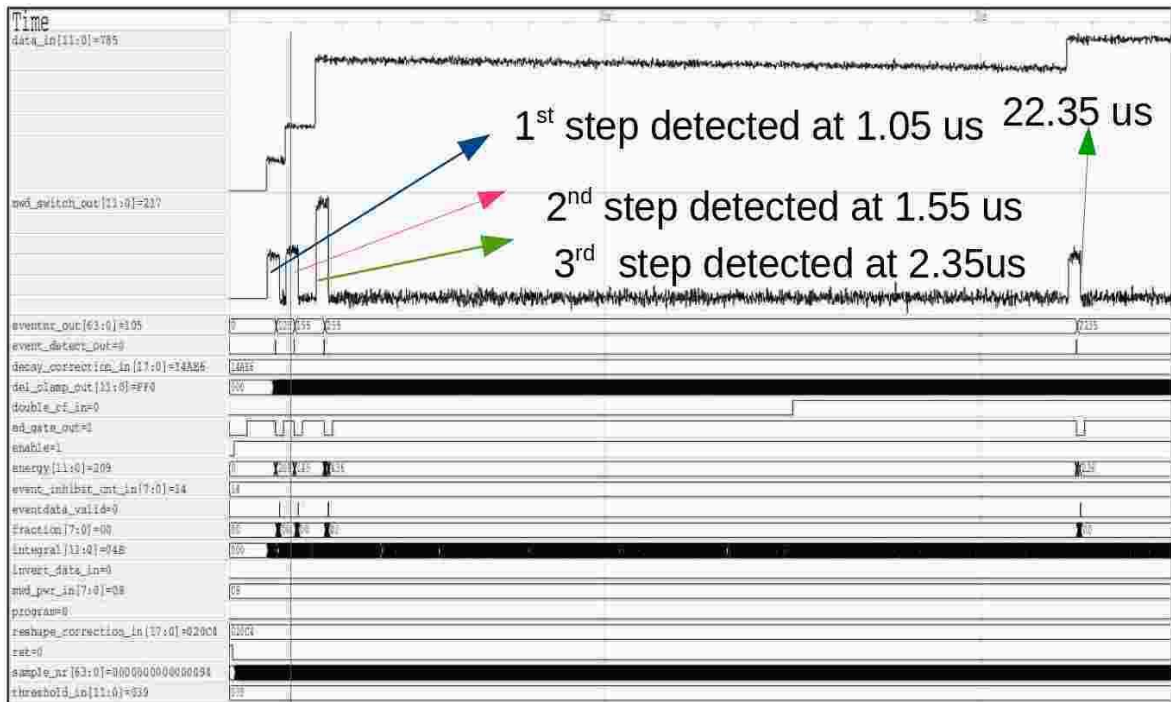


Figure 8. Simulation Result no 3

In Figure 8 a series of nearby pile-up events have been simulated. Pulses were correctly discriminated by the MWD FEA; timestamp and energy information have been generated.

### 3. Conclusion

At JRC we are working to improve the electronics chain in neutron counting systems for safeguards. This concerns all the steps from the charge collection pre-amplifier connected to neutron sensitive gas proportional counters to the measured frequency distributions of neutron detection events, as used typically in well-counters for neutron multiplicity counting.

We have presented elements of noise suppression methods used in the development of new pre-amplifiers/amplifier circuits. Also the new list-mode devices developed at JRC to substitute the standard Shift Register analysers were presented and the data elaboration and diagnostics possible in these devices was discussed. The main focus however was the ongoing development of digitizer circuit we propose for replacing the traditional signal amplifier and digital signal formation following a neutron detection event. The advantages of the digital approach are expected to be first of all better dead-time performance and pile-up rejection, but also much improved system diagnostics and lower cost. Tests are ongoing on a prototype digitizer board with eight input lines. The promising simulations show the feasibility of implementation, what is basically a digital filter, with potential for substitution of the widely used analogue methods for the neutron pulse processing in safeguards.

An added advantage from the digital approach derives from the entire signal processing being completely parallelized, starting from the single  $^3\text{He}$  detector tube until the final step of data analysis. This offers the possibility that individual  $^3\text{He}$  detectors can be moved between detector heads without affecting the electronics design - provided the neutron detection heads are purposely designed for easy removal of the tubes. A better utilisation of the  $^3\text{He}$  tubes in this fashion could alleviate the present shortage of  $^3\text{He}$ .

### 4. References

- 1) National Semiconductor, "LVDS Owner's Manual", 4th Edition; 2008.
- 2) A.Georgiev,W.Gast, R.M.Lieder,AN analog-to-digital conversion based on a moving window deconvolution, IEEE Transactions on Nuclear Science, Volume: 41 , Issue4 , Aug 1994 )
- 3) Wishbone B4 , Wishbone System-on-Chip (SoC) Interconnection Architecture for portable IP cores, [cdn.opencores.org](http://cdn.opencores.org)
- 4) P. Lemmes, M.Kavatsyuk, " General purpose pulse-processing algorithm" <[http://opencores.org/project.pulse\\_processing\\_algorithm](http://opencores.org/project.pulse_processing_algorithm)>.
- 5) E. Guliyev, M. Kavatsyuk, P.J.J. Lemmens, G. Tambave, H. Loehner, "VHDL Implementation of Feature-Extraction Algorithm for the PANDA Electromagnetic Calorimeter" , Nuclear Inst. and Methods in Physics Research, A 664(2012) 22-28
- 6) E. Guliyev, Verification of a novel calorimeter concept for studies of charmonium states, University of Groningen(2011).
- 7) M.Kavatsyuk,E.Guliyev,P.J.Lemmens,H.Lohner,G.Tambave, Digital signal processing in the PANDA Electromagnetic Calorimeter for the Panda collaboration, KVI, University of Groningen, Groningen, The Netherlands

# High rate approximation for extendable dead time corrections in elaborate settings

Chen Dubi<sup>1,2</sup>, Rami Atar<sup>3</sup>

<sup>1</sup>Physics Department, NRCN,, Beer Sheva, Israel

<sup>2</sup>Department of mathematics, Ben-Gurion University of the Negev, Beer-Sheva  
84105, Israel

<sup>3</sup>Viterbi Faculty of Electrical Engineering, Technion, Haifa 32000, Israel  
E-mail: chendb331@gmail.com

## Abstract:

*Measuring occurrence times of random events, aimed to determine the statistical properties of the governing stochastic process, is a basic topic in science and engineering, and has been the subject of numerous mathematical modelling approaches. Often, true statistical properties deviate from measured properties due to the so called {it dead time} phenomenon, where for a certain time period following detection, the detection system is not operational. Understanding the dead time effect is especially important in radiation measurements, often characterized by high count rates and a non reducible detector dead time (originating in the physics of particle detection). The effect of dead time can be interpreted as a suitable rarefied sequence of the original time sequence.*

*In a very recent study, a central limit approximation was introduced for high rate counters with extendable (Type II) dead time in a very general setting- allowing a general distribution for both the inter arrival waiting time and the duration- but providing that the inter arrival waiting times are independent and identically distributed.*

*The outline of the present study is to demonstrate new implementations of the above mentioned approximation, and to demonstrate its applicability in analysing the dead effect in elaborated settings*

**Keywords:** Dead time; Renewal process; Type II counters

## 1. Introduction

Counting and measuring occurrence times of random events in order to estimate statistical properties of underlying stochastic processes is a basic topic in science and engineering, and has been the subject of numerous mathematical modeling approaches. One of the most prominent problems in high rate measurement is the {it dead time} phenomenon, where the sensing device takes a certain time to recover after each detection, during which the counter is not functional.

The effect of dead time on the detection signal can be interpreted as the process of rarefying the sequence of occurrence times, by removing events within the dead time period following a previous event. One distinguishes two types of dead time models [1]. In a *non extendable* dead time (or *type I counter*), only counts that are within a dead time period following an actual detection are lost.

Thus, for an event to inflict a dead time, it must appear in the rarefied sequence. In an *extendable* dead time (or *type II counter*), counts within a dead time period following an original event (detected or not) are lost. Thus, all events in the original sequence inflict a dead time.

The practical significance of the dead time phenomenon has been widely recognized. It is observed in all types of measurement systems provided that the count rate is sufficiently high. Since high detection rates are very often in radiation measurements, there is a wide treatment of the subject in radiation literature [2,3,4] (to state a few), but questions of identifying and compensating for the dead time have also been studied in control theory [5], signal processing [5], medical imaging [7], mass spectrometry [8] and more. A very recent literature review is provided in [9].

In a fairly trivial (and intuitive) manner, the effect of the dead time on the count distribution is determined by two basic quantities: the waiting time between consecutive events (which is often referred to as the *inter-arrival* time, and the duration of the dead time following a detection. Notice that both quantities are, by nature, random variables. A special case of interest is when both the waiting times and the dead times (each one by itself) form a set of Independent Identically Distributed (IID) sequence of random variables. In such case, the counting process is known as a *renewal process* [10], and is uniquely determined by two distributions: the waiting time distribution, which we will denote by  $f_{\theta}(t)$ , and the dead time distribution, which we denote by  $f_{\tau}(t)$ .

In general, computing the count distribution from the inter arrival distribution  $f_{\theta}(t)$  (even without any dead time) might be very hard to do, and (to the best of our knowledge) there is no simple and closed formula to connect between the two. However, if the measurement time is sufficiently larger than the average waiting time, we may use the so called *diffusion scale* approximations, which simply connect between the first two moments waiting time distribution and the count distribution. Hereon, we denote by  $\mu = \int_0^{\infty} t f_{\theta}(t) dt$  the average waiting time, and by  $\sigma^2 = \int_0^{\infty} (t - \mu)^2 f_{\theta}(t) dt$  the variance of the waiting time (in the presence of dead time  $\tau$ , a subscript will be added).

The first approximation, known as the *elementary renewal theorem*, states that the average count in an interval of duration  $t \gg \mu$ , which we denote by  $m(t)$ , is given by:

$$(1) \quad m(t) \approx \frac{t}{\mu};$$

The approximation in (1) is vary intuitive: it simply states that for large measurement times, the average number of detections is simple the measurement time divided by the average waiting time between consecutive counts.

An even stronger version is the *central limit theorem* for renewal process, stating the following (Th. 14.6 of [10]). Let ‘ $\Rightarrow$ ’ denote convergence in distribution, and  $\mathcal{N}(0,1)$  denote the standard normal distribution.

**Theorem 1.** Let  $R(t)$  be a renewal process corresponding to waiting times  $\{\theta_i\}_{i=1}^{\infty}$ . Denote  $\mu = E[\theta_1]$  and  $\sigma^2 = Var[\theta_1] < \infty$ . Then, as  $t \rightarrow \infty$ ,

$$\frac{R(t) - \frac{t}{\mu}}{\sigma \sqrt{t/\mu^3}} \Rightarrow \mathcal{N}(0,1).$$

Which leads to the approximation:

$$(2) \quad R(t) \approx \mathcal{N}\left(\frac{1}{\mu}t, \frac{\sigma^2}{\mu^3}t\right)$$

Formulas (1,2) not only give an explicit description of the count distribution (under the assumption that the count rate is sufficiently high), by rise an important fact: to quantify the effect of a dead time on the count distribution, it is suffice to quantify the effect of the dead time of the first two moments of the inter-arrival dead time.

In a recent study introduced by the authors [11], it has been proving that for an original waiting time distribution by  $f_{\theta}(t)$ , and a dead time distribution  $f_{\tau}(t)$ , the first two moments of the waiting time (with the dead time) are given by:

$$(3) \quad \mu_{\tau} = \frac{\mu}{1-S}, \quad \sigma_{\tau}^2 = \frac{\sigma^2 + \mu^2}{1-S} + \frac{\int_0^{\infty} \left[ \int_0^t x F_{\theta}(x) dx \right]^2 f_{\tau}(t) dt}{(1-S)^2} - \frac{\int_0^{\infty} \left[ \int_t^{\infty} x f_{\theta}(x) dx \right]^2 F_{\tau}(t) dt}{(1-S)^2}$$

Where  $S$  is the average probability of two consecutive events to occur within the dead time interval:

$$(4) \quad S = \int_0^{\infty} \int_0^t f_{\theta}(x) dx f_{\tau}(t) dt$$

In particular, the average count rate is reduced by multiplication with the factor  $1 - S$ .

If the dead time is fixed, then  $f_{\tau}(t)$  is a delta function, and (3,4) obtain a simpler form:

$$(5) \quad \mu_{\tau_0} = \frac{\mu}{1 - P_{\tau_0}}$$

$$(6) \quad \sigma_{\tau_0} = \frac{\sigma^2 + \mu^2}{1 - P_{\tau_0}} + \left[ \frac{\int_0^{\tau_0} x f_{\theta}(x) dx}{1 - P_{\tau_0}} \right]^2 - \left[ \frac{\int_{\tau_0}^{\infty} x f_{\theta}(x) dx}{1 - P_{\tau_0}} \right]^2$$

The outline of the proposed study is to introduce the reader with some simple implementations of the above formulas, and to demonstrate their applicability in radiation measurements. In what follows, we focus on two aspects: in the next section, we consider the effect of a non-constant dead time on the average count rate, and in section 3 we study the problem of serially connected components. In section 4 we conclude

## 2. Constant Vs. Random dead time

The dead time in a radiation detector often has, by nature, a random duration [3]. However, it is often assumed that the dead time is constant, for two main reasons: first, the nature of the dead time distribution is not known, and second, it is often too hard to analyse. However, using the approximations introduced in the previous section, the effect of dead time on the average count can be quantified by computing  $S$ .

If we assume that the dead time is fixed, the natural choice for the duration of the dead time is the average duration, which we will denote by  $\langle \tau \rangle$ . Then,  $S$  simply become the probability of two consecutive events within a waiting time  $\langle \tau \rangle$ , given by  $P = \int_0^{\langle \tau \rangle} f_{\theta}(t) dt$ , and the average count distribution is corrected by the simple factor  $1 - P$

In the present section, we assume that the original waiting time has a simple exponential distribution with parameter  $\lambda$  (corresponding to simple radioactive decay), and consider two dead time distributions: exponential and normal. Throughout this section we use the notations  $n$  for the real (theoretical) count-rate (without the dead time) and  $m$  for the actual count rate

### 2.1. Exponentially distributed dead time

We now consider the case where  $f_{\theta}(t) = \lambda e^{-\lambda t}$  and  $f_{\tau}(t) = \frac{1}{\langle \tau \rangle} e^{-\frac{1}{\langle \tau \rangle} t}$ . If we assume a fixed dead time value of  $\langle \tau \rangle$ , then  $P = \int_0^{\langle \tau \rangle} f_{\theta}(t) dt = \int_0^{\langle \tau \rangle} \lambda e^{-\lambda t} dt = 1 - e^{-\lambda \langle \tau \rangle}$ , and we obtain the well-known correction the average count rate  $m = n e^{-\lambda \langle \tau \rangle}$ . However, looking at equation (4), taking the average dead time will deviate from the true value, and for the true correction we must average over  $1 - e^{-\lambda \tau}$ . Through direct calculations, we obtain that:

$$S = \int_0^{\infty} (1 - e^{-\lambda \tau}) \frac{1}{\langle \tau \rangle} e^{-\frac{1}{\langle \tau \rangle} \tau} d\tau = 1 - \frac{1}{1 + \lambda \langle \tau \rangle}$$

Which leads to the correction  $m = \frac{n}{1 + \lambda \langle \tau \rangle}$  - which is exactly the correction for a non-extendable dead time! This a surprizing result: an exponentially distributed dead in an extendable model will create the same average count loss as a fixed dead time (with the exact same average) in a non extendable setting.

## 2.2. Normally distributed dead time

As we often do in engineering, if the dead time distribution is not known, a normal distribution is considered. We thus consider the case  $f_\theta(t) = \lambda e^{-\lambda t}$  and  $f_\tau(t) = \frac{1}{\sqrt{2\pi}\sigma_1} e^{-\frac{(t-\tau)^2}{2\sigma_1^2}}$ . Again, the correction term  $S$  can be computed directly:

$$S = \frac{1}{\sqrt{2\pi}\sigma_1} \int_{-\infty}^{\infty} e^{-\frac{(t-\tau)^2}{2\sigma_1^2}} \int_0^t \lambda e^{-\lambda x} dx dt = 1 - e^{-\lambda\tau} e^{\frac{(\lambda\sigma_1)^2}{2}}$$

And the correction is given by  $m = ne^{-\lambda\tau} e^{\frac{(\lambda\sigma_1)^2}{2}}$ . As we can see, assuming a normal distribution will *reduce* the effect of the dead time. One may argue that there is something wrong with the above expression, since if  $\sigma_1$  is sufficiently large, then  $m > n$ . While this is theoretically true, this is always a risk we are taking when using normal distribution to “emulate” a positive random variable, and the using a normal distribution for the dead time makes sense only if  $\sigma_1$  is sufficiently small.

## 3. serially connected components

In most counting models, the model consists of two elements: the source and the detector (counter). However, in real life, the detector itself is often constructed as a serial connection of two (or more) elements [9]. In radiation measurements, for instance, the detector module is often constructed from the physical detector, which is a tube containing materials that create a noticeable reaction with the detected particles, serially connected to a signal amplifier, or a computer sampling card. This is not a unique attribute of radiation measurements, and often counters consist of two serially connected elements: a physical component ( $A$ ) which detects the events, and a second component ( $B$ ), which digitally records them. In the terminology used so far, if both components ( $A$ ) and ( $B$ ) have a dead time period (and to some extent they always do), then the rarefied (output) signal from component ( $A$ ) becomes the non-rarefied input signal for component ( $B$ ).

To demonstrate the applicability of our results, we will consider the following two settings: in both we assume that the original inter-arrival time is exponentially distributed with an average waiting time of  $1/\lambda$ . In the first setting we assume that component ( $A$ ) has a fixed non extendable (Type I) dead time  $\tau_0$  and component ( $B$ ) has a fixed extendable (Type II) dead time  $\tau_1$ . In the second we will look at a slightly more elaborate setting, where the duration of the dead time of component ( $B$ ) has an exponential distribution, with a mean value  $\tau_1$ .

### 3.1. Example I: Both components suffer from fixed dead time

In the first example, since the original waiting time between consecutive events has an exponential distribution, the waiting time between the recuperation of the detector ( $A$ ) and the following detection is once again exponential with the exact same parameters. Therefore, the inter-arrival time in the rarefied series created by detector ( $A$ )- which serves as the unrarefied series for component ( $B$ ) - is of the form  $x + \tau_0$ , where  $x$  is a random variable exponentially distributed with mean value  $1/\lambda$ . The PDF of inter arrival time is given by  $f_\theta(x) = U_0(x - \tau_0)\lambda e^{-\lambda(x-\tau_0)}$  (where  $U_0(x) = 0$  if  $x < 0$  and  $U_0(x) = 1$  if  $x \geq 0$ ), and:

$$\begin{aligned} \mu &= E[x] + \tau_0 = \frac{1}{\lambda} + \tau_0 \\ \sigma^2 &= \frac{1}{\lambda^2} \end{aligned}$$

Again, since we assume that the dead time of component ( $B$ ) is fixed, we may apply formulas (5) and (6). We now divide into two cases:  $\tau_1 \leq \tau_0$  and  $\tau_1 > \tau_0$ . For the first, the dead time of the second component ( $B$ ) is irrelevant, since the minimal waiting time in the signal entering the component is  $\tau_0$ . For  $\tau_1 > \tau_0$  we compute directly:

$$P_{\tau_1} = 1 - e^{-\lambda(\tau_1-\tau_0)}, \quad \int_0^{\tau_1} \theta f_\theta(\theta) d\theta = \lambda \int_{\tau_0}^{\tau_1} \theta e^{-\lambda(\theta-\tau_0)} d\theta = \left(\frac{1}{\lambda} + \tau_0\right) - \left(\frac{1}{\lambda} + \tau_1\right) e^{-\lambda(\tau_1-\tau_0)}$$

$$\int_{\tau_1}^{\infty} \theta f_{\theta}(\theta) d\theta = \left(\frac{1}{\lambda} + \tau_1\right) e^{-\lambda(\tau_1 - \tau_0)}$$

and we have:

$$\begin{aligned} \mu &= e^{\lambda(\tau_1 - \tau_0)} \left(\frac{1}{\lambda} + \tau_0\right); \\ \sigma^2 &= e^{\lambda(\tau_1 - \tau_0)} \left(\frac{1}{\lambda^2} + \left(\frac{1}{\lambda} + \tau_0\right)^2\right) + \\ &\quad \left(\frac{\left(\frac{1}{\lambda} + \tau_0\right) - \left(\frac{1}{\lambda} + \tau_1\right) e^{-\lambda(\tau_1 - \tau_0)}}{1 - e^{-\lambda(\tau_1 - \tau_0)}}\right)^2 - \left(\frac{\left(\frac{1}{\lambda} + \tau_1\right) e^{-\lambda(\tau_1 - \tau_0)}}{1 - e^{-\lambda(\tau_1 - \tau_0)}}\right)^2 \end{aligned}$$

### 3.2 Example II: component (A) suffer from fixed dead time, and component (B) has an exponentially distributed dead time

In the second example, we use the set of equations (3) and (4), with:

$$\begin{aligned} f_{\theta}(x) &= U_0(t - \tau_0) \lambda e^{-\lambda(t - \tau_0)}; \\ f_{\tau}(x) &= \frac{1}{\tau_1} e^{-\frac{x}{\tau_1}} \end{aligned}$$

Through direct computation

$$S = \int_0^{\infty} \left(\int_0^t f_{\theta}(x) dx\right) f_{\tau}(t) dt = e^{-\frac{\tau_0}{\tau_1}} \left(1 - \frac{1}{1 + \lambda\tau_1}\right)$$

and thus

$$\mu(\tau_0, \tau_1) = \frac{\frac{1}{\lambda} + \tau_0}{1 - e^{-\frac{\tau_0}{\tau_1}} \left(1 - \frac{1}{1 + \lambda\tau_1}\right)}$$

For the variance, computations are more complicated. First, we have that  $\sigma^2 + \mu^2 = \frac{1}{\lambda^2} + \left(\frac{1}{\lambda} + \tau_0\right)^2$ . For the integral terms in (3) we have:

$$\begin{aligned} \int_0^{\infty} \left[\int_0^t x f_{\theta}(x) dx\right]^2 f_{\tau}(t) dt &= \int_{\tau_0}^{\infty} \left[\int_{\tau_0}^t x \lambda e^{-\lambda(x - \tau_0)} dx\right]^2 \frac{1}{\tau_1} e^{-\frac{t}{\tau_1}} dt \\ \int_0^{\infty} \left[\int_t^{\infty} x f_{\theta}(x) dx\right]^2 f_{\tau}(t) dt &= \int_0^{\tau_0} \left[\int_{\tau_0}^{\infty} x \lambda e^{-\lambda(x - \tau_0)} dx\right]^2 \frac{1}{\tau_1} e^{-\frac{t}{\tau_1}} dt + \\ &\quad \int_{\tau_0}^{\infty} \left[\int_t^{\infty} x \lambda e^{-\lambda(x - \tau_0)} dx\right]^2 \frac{1}{\tau_1} e^{-\frac{t}{\tau_1}} dt \end{aligned}$$

The last integrations can be executed fully (although the results would be fairly lengthy), and once substituted in (3) and (4) would then give explicit formulas for  $\sigma^2$ , from which the parameters of the diffusion scale approximation can be computed.

## 4. Concluding Remarks

In the study, we have introduced implementation of the formulas developed in [11] for the dead time effect on the count distribution, to some elaborated settings associated with radiation measurement. In particular, we have been able to introduce new formulas for a random dead time with exponential and normal distribution, and formulas for a detection system with serially connected components. Future work should include experimental validation of the formulas, and extending the results to a non-paralyzing setting

## 5. References

- [1] Takacs, L ; *On a probability problem arising in the theory of counters*, Mathematical Proceedings of the Cambridge Philosophical Society; Vol. 52; p 488-498
- [2] G. F. Knoll: *Radiation Detection and Measurement*. John Wiley and Sons, Inc., 2000.
- [3] L. Pal, I. Pázsit: *On some problems in the counting statistics of nuclear particles investigation of the dead time problems*. Nuclear Instruments and Methods, Vol. 693, pp.26-50, 2012.
- [4] J. W. Muller: *Dead time problems*. Nuclear instruments and methods, Vol. 112, pp. 47-57, 1973.
- [5] J. E. Normey-Rico, E. F. Camacho: *Dead-time compensators: A survey Control Engineering Practice*, Vol. 16, pp. 407-428, 2008.
- [6] S. Jeong, M. Park: *The Analysis and Compensation of Dead-Time Effects in PWM Inverters* IEEE Transactions on Industrial Electronics, Vol. 38, pp. 108-114, 1991.
- [7] T.J Spinks, T. Jones, M.C Gilardi, J.D. Heather: *Physical performance of the latest generation of commercial positron scanner* IEEE Trans Nucl Sci, Vol. 35, pp.721-725, 1988.
- [8] S. M. Nelms, C. R. Quetel, T. Prohaska, J. Vogl, P D. Taylor: *Evaluation of detector dead time calculation models for ICP-MS* J. Anal. At. Spectrom. Vol. 16, pp.333-338, 2001.
- [9] S. Usman, A. Patil: *Radiation detector dead time and pile up: A review of the status of science* Nuclear Engineering and Technology, Vol. 50, pp.1006-1016, 2018
- [10] P. Billingsley: *Convergence of Probability Measures*, John Wiley & Sons, 2013.

## Sample shape effect on nuclear material quantification with neutron resonance transmission analysis

**H. Tsuchiya<sup>1</sup>, F. Ma<sup>1</sup>, F. Kitatani<sup>1</sup>, C. Paradella<sup>2</sup>, J. Heyse<sup>2</sup>, S. Kopecky<sup>2</sup>, P. Schillebeeckx<sup>2</sup>**

1. JAEA

2. EC-JRC Geel

E-mail: [tsuchiya.harufumi@jaea.go.jp](mailto:tsuchiya.harufumi@jaea.go.jp)

### **Abstract:**

*Experiments of Neutron resonance transmission analysis (NRTA) were performed at GELINA with a Cu cuboid in order to investigate how a hole fraction and a sample irregularity affects accuracy of NRTA measurement. For this aim, the Cu cuboid was arranged with rotated by 0 degrees, 30 degrees or 45 degrees relative to an incident direction of neutron beams. By considering the hole fraction, the experimental transmission spectrum for the 0 degrees were analysed to derived an areal density, which is found to be consistent with a declared areal density within 1% accuracy. In addition, we found that the areal density for the other rotation angles can be well evaluated with an analytical model considering both the hole fraction and the sample irregularity. This work shows a careful consideration of a sample shape can improve the accuracy of the NRTA measurement.*

**Keywords:** neutron resonance transmission analysis; sample irregularity; hole fraction

### **1. Introduction**

From the viewpoint of nuclear safeguards and security, it is expected that special nuclear materials (SNM) of uranium and plutonium in the debris should be accurately quantified after its removal. One plausible technique for the measurement is Neutron Resonance Transmission Analysis (NRTA). A detailed description of its application for various materials as well as the principle of NRTA is given in Refs. [1]. With respect to its application for nuclear fuels, Bowman et al. [2] and Behrens et al. [3] applied NRTA to quantify SNM in fresh and spent fuel pellets and determined the abundance of <sup>239,240,242</sup>Pu and <sup>235,236,238</sup>U in the pellets with an accuracy better than 4%. Furthermore, a feasibility study with Monte Carlo simulations was carried out to investigate how NRTA can quantify the amount of SNMs in a spent fuel assembly [4]. However, unlike such fresh and spent fuel pins, a method to assess SNMs in debris caused by a severe accident like the Fukushima case has not been established yet.

NRTA is based on the transmission experiments in which homogeneous samples with a constant thickness are generally used, and hence it has been mainly applied to such a homogeneous sample so far. It is easily expected that debris in a severe accident has inhomogeneous characteristics, which may strongly affect accuracy of the NRTA measurements. One of the inhomogeneities is thought to be density variations in powder samples, and it has been already investigated by Becker et al. [5]. Another is a shape-shape irregularity. To consider the irregularity such as a variable shape and a hole fraction, Harada et al. [6] have proposed analytical models to treat those effects. However, experimental validations of the proposed models have not been done yet. In this work, we report how the proposed models are applied to a real NRTA experiment with a Cu cuboid sample which simulates the sample irregularity.

### **2. NRTA**

To examine characteristics of a sample, NRTA utilizes an intense pulsed white neutron source as a diagnostic beam. We measure, as a function of neutron energy, the fraction of neutron beams that is

transmitted through the sample. The neutron energy is obtained by the time-of-flight (TOF) technique. TOF is the time difference between a start signal (*c.f.*, from an accelerator) and a stop signal (*c.f.*, from a detector). The transmitted spectrum has characteristic dips resulting from resonance structures in neutron-induced reaction cross sections of nuclides in the sample.

In an actual measurement, the observed quantity is the fraction of the neutron beam that traverses the sample without any interactions. For a parallel neutron beam that is perpendicular to a sample material, the transmission  $T$  is ideally represented by

$$T = e^{-\sum_k n_k \bar{\sigma}_{tot,k}}, \quad (1)$$

where  $\bar{\sigma}_{tot,k}$  is Doppler broadening total cross section and  $n_k$  is the number of atoms per unit area of nuclide  $k$ , which is also shown as an areal density.

Experimentally, the transmission  $T_{exp}$  is computed from the ratio of counts of a sample-in measurement  $C_{in}$  and a sample-out measurement  $C_{out}$ , after subtraction of background contributions  $B_{in}$  and  $B_{out}$ , respectively,

$$T_{exp} = N_T \frac{C_{in} - B_{in}}{C_{out} - B_{out}}, \quad (2)$$

where  $N_T$  is a normalization factor that is the ratio of the total intensities of the incident neutron beam during the sample-out and sample-in cycles. The background,  $B_{in}$  and  $B_{out}$ , is determined by an analytical expression applying the black resonance technique [1].

Eq. (2) indicates that the experimental transmission is independent of both the detection efficiency and neutron flux incident to the sample. Therefore, we can consider that NRTA provides an absolute measurement that does not require additional calibration experiments.

Generally, the transmission expressed by Eq. (1) is applicable under the condition that a sample size is larger than a neutron beam diameter. When the sample size is smaller than the beam diameter, we have to modify the formula with considering a hole fraction,  $f_h$ . The  $f_h$  is the fraction of neutron beams that reach a detector without passing through a sample. According to Harada et al., [6], a transmission spectrum considering  $f_h$  can be denoted by

$$T = f_h + (1 - f_h) e^{-\sum_k n_k \bar{\sigma}_{tot,k}}. \quad (3)$$

Moreover, they have proposed general analytical models to treat irregular shapes (Eq. (8) or (9) in Ref. [6]) and we modified it to treat the experimental data in this work as

$$T = f_h + (1 - f_h) \left[ \frac{b}{\sum_k n_k \bar{\sigma}_{tot,k}} (1 - e^{-\sum_k n_k \bar{\sigma}_{tot,k}}) + (1 - b) e^{-\sum_k n_k \bar{\sigma}_{tot,k}} \right]. \quad (4)$$

This formula considers not only the  $f_h$ , but also a sample rotation,  $b$ , corresponding to a sample irregularity. Later we use them to derive areal density for a simulated irregular-shaped sample.

### 3. Experiments

The experiments in this work were performed at the TOF-facility GELINA of the EC-JRC Geel. GELINA has a linear electron accelerator. The linear electron accelerator was operated at 800 Hz with an average current of 30  $\mu$ A, providing electron pulses with an average energy of 100 MeV and a pulse width of 2 ns. To produce a white neutron beam, the pulsed electron beam impinges on a mercury-cooled rotating uranium target. Then, bremsstrahlung radiation is generated and produce neutrons via ( $\gamma, n$ ) and ( $\gamma, f$ ) reactions. To obtain a neutron spectrum ranging from thermal energy to a few MeV, the produced neutrons are moderated by two 4-cm thick beryllium containers filled with water that are placed beneath and above the target. The total neutron intensity is monitored by  $BF_3$  proportional counters located in the concrete ceiling of the target hall.

The measurements were carried out at a 50 m measurement station. For the sake of examining sample shape effects, we prepared a Cu cuboid with the weight, width, and thickness of  $85.434 \pm 0.001$  g,  $9.94 \pm 0.02$  mm, and  $10.05 \pm 0.02$  mm, respectively. These values give an areal density of the Cu cuboid as  $(8.508 \pm 0.017) \times 10^{-2}$  atom/b.

To shield a neutron detector from the  $\gamma$ -ray flash and fast neutrons, a shadow bar made out of Cu and Pb was placed close to the uranium target. The moderated neutrons were collimated into the flight path through evacuated aluminium pipes of 50 cm diameter with annular collimators, consisting of

borated wax, copper and lead. A combination of Li-carbonate plus resin, Pb and Cu-collimators was used to reduce the neutron beam to a diameter of around 35 mm at the sample position. Close to the sample position a  $^{10}\text{B}$  overlap filter was placed to absorb slow neutrons from a previous burst. The impact of the  $\gamma$ -ray flash was reduced by a 5-mm Pb filter.

The neutrons passing through the sample were detected by a 6.35-mm thick and 101.6-mm diameter Li-glass scintillator (NE905) enriched to 95% in  $^6\text{Li}$ . The Li-glass scintillator is connected to a boron-free quartz windowed photomultiplier. The detector was placed at around 48 m from the neutron target. The PMT anode signal was fed into a constant fraction discriminator to make a fast logic signal that defines the neutron detection time. In all measurements, we placed fixed Na, Bi and Co black resonance filters close to a Cu sample.

For the purpose of investigating the sample shape effects on the NRTA measurement, we performed three experiments with the Cu cuboid under different angles relative to incoming neutron beams. Figure 1 shows individual schematic conditions. In each measurement, the neutron beam diameter was always larger than the sample width. This means all neutrons did not pass through the sample, and some of them directly arrived at the neutron detector.

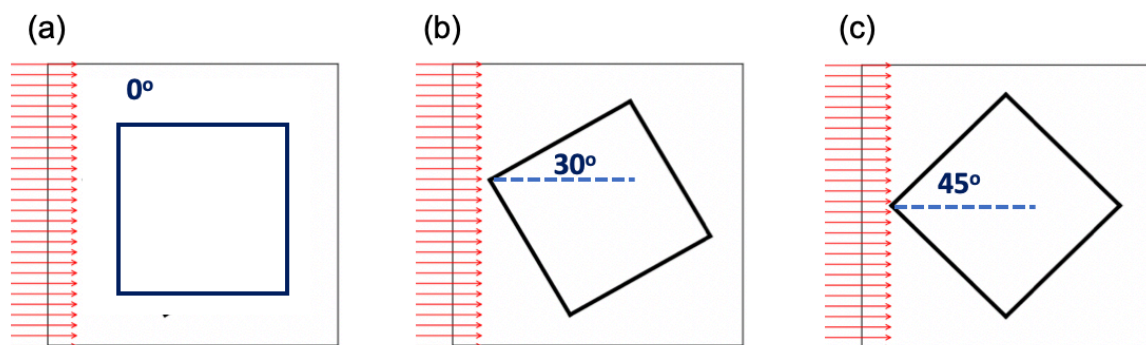


Figure 1: Arrangements of the Cu cuboid sample with respect to neutron beams. Panels (a), (b), and (c) correspond to a rotation angle of 0 degrees., 30 degrees, and 45 degrees, respectively. Red arrows in each panel represent direction of incoming neutrons.

### 3. Results

Figure 2 shows the transmission spectra under the condition (a), (b), and (c) of Fig. 1. Transmission spectra change according to rotation angles. These changes are ascribed to variations of track length of neutron beams in the cuboid sample, according to incident positions of neutron beams.

Analysing the experimental data for 0 degrees with Eq. (3), we evaluated an areal density for 0 degrees as  $(8.542 \pm 0.025) \times 10^{-2}$  atom/b, which gives its ratio to the declared one as  $1.004 \pm 0.004$ . Without considering the hole fraction, the ratio was to  $0.200 \pm 0.021$ , being inconsistent with the declared areal density.

To quantitatively analyse the transmission spectra for the rotated sample, Eq. (4) was applied to the experimental data. As shown in Table 2, the fitting result with Eq. (4) well agrees with the experimental data. Obviously, Eq. (4) is found to give more consistent results compared with Eq. (3). Table 2 indicates that the derived areal density based on Eq. (4) provides the accuracy of 2.1% and 0.2%, for 30 degrees and 45 degrees, respectively. It is found that the Eq. (4) much more improved the accuracy of the areal

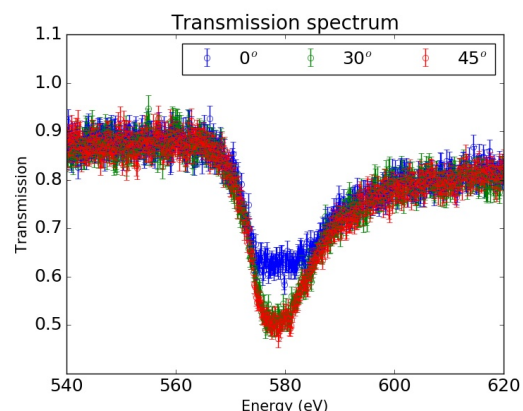


Figure 2: Transmission spectra measured for the cuboid sample under the conditions (a), (b), and (c) of Fig. 1.

density in comparison with the Eq. (3). Given these results, we may conclude that a sample shape must be properly considered to analyze a NRTA measurement with an irregular shape sample.

	30 deg.	45 deg.
Eq. (3)	0.915±0.014	0.958±0.013
Eq. (4)	1.021±0.012	0.998±0.008

Table 2: Ratios of experimental areal density to the declared one.

#### 4. Summary

We experimentally investigated how a sample shape affects the NRTA measurement. For this aim, the experiments with a Cu cuboid sample were carried out at a neutron TOF facility of GELINA. To study a hole fraction, the cuboid sample was used with its size smaller than the neutron beam diameter. In order to simulate a sample irregularity, the sample was arranged with rotated by 0 degrees, 30 degrees, and 45 degrees relative to an incident direction of the neutron beams. To treat the hole fraction and the sample irregularity, analytical models have been proposed by Harada et al., [6]. In this work, we studied how well the proposed models reproduce the experimental data. It was found that considering the hole-fraction effect, the derived areal density for 0 degrees was well consistent with the declared one. We then analyzed the experimental data for 30 degrees and 45 degrees with considering both the hole fraction and the sample irregularity. Consequently, by using the model considering the above two effects, the derived areal densities were found to be consistent with the declared ones, with ~2% or better accuracy.

#### 5. Acknowledgements

This work was partly done under the agreement between JAEA and EURATOM in the field of nuclear materials safeguards research and development. This research was implemented under the subsidiary for nuclear security promotion of MEXT.

#### 6. References

- [1] Schillebeeckx P., Borella A., Emiliani F., Gorini G., Kockelmann W., Kopecky S., Lampoudis C., Moxon M., Perelli Cippo E., Postma H., Rhodes N.J., Schooneveld E.M., Van Beveren C.; *Neutron resonance spectroscopy for the characterization of materials and objects*; JINST 7, C03009; 2012.
- [2] Bowman C.D., Schrack R.A., Behrens J.W., Johnson R.G.; *Neutron resonance transmission analysis of reactor spent fuel assemblies*, Neut. Radiography 503-511; 1983.
- [3] Behrens J.W., Johnson R.G., Schrack R.A.; *Neutron resonance transmission analysis of reactor fuel samples*, Nuclear technology 67, 162-168; 1984.
- [4] Strebentz J.W., Chichester D.L.; *Neutron resonance transmission analysis (NRTA): A non-destructive assay technique for the next generation safeguards initiative's plutonium assay Challenge*; INL/EXT-10-20620; 2010.
- [5] Becker B., Harada H., Kauwenberghs K., Kitatani F., Koizumi M., Kopecky S., Moens A., Schillebeeckx P., Sibbens G., Tsuchiya H.; *Particle Size Inhomogeneity Effect on Neutron Resonance Densitometry*; ESARDA BULLETIN, No. 50, 2-8; 2013.
- [6] Harada H., Kimura A., Kitatani F., Koizumi M., Tsuchiya H., Becker B., Kopecky S., Schillebeeckx P.; *Generalized analysis method for neutron resonance transmission analysis*; J. Nucl. Sci. and Tech.52, 837-843; 2015.

# Inter-Comparison Exercise for the Safeguards Verification of PWR Fresh Fuel Assemblies using Fast and Thermal Neutron Coincidence Collars

A. Tomanin<sup>1</sup>, L. Bourva<sup>2</sup>, J. Beaumont<sup>2</sup>, P. De Baere<sup>1</sup>, A. Terrasi<sup>1</sup>, V. De pooter<sup>1</sup>, M. Arias Arenas<sup>1</sup>

<sup>1</sup> European Commission, Directorate General Energy, Directorate Euratom Safeguards, Luxembourg

<sup>2</sup> International Atomic Energy Agency, Vienna, Austria

## Abstract:

*The verification of Light Water Reactor (LWR) fresh fuel relies on independently establishing the linear mass of  $^{235}\text{U}$  ( $\text{g}\cdot\text{cm}^{-1}$ ) present in the assembly. To perform this task using Non-Destructive Assay (NDA) methods, series of thermal neutron detectors (Uranium Neutron Coincidence Collar or UNCL) have been developed since the early 1980s. Independence of the verification has been progressively eroded by the introduction of correction factors based on unverifiable concentrations of burnable poison in fresh fuel. The EURATOM and Los Alamos National Laboratory (LANL) have developed a high efficiency neutron collar that operates in fast mode (EURATOM Fast Collar for PWR fuel or EFCP), where the thermal detector's sensitivity to burnable poison is reduced by removing thermal neutrons from the interrogation of the assembly. The EFCP is routinely used for Safeguards verification. The International Atomic Energy Agency (IAEA) is currently introducing a new liquid scintillator-based fast neutron coincidence collar (FNCL) which detects fast fission neutrons from the assembly without any requirement for moderation, aiming to significantly reduce the verification measurement times and eliminate the dependency on declared burnable poison concentrations. Following field testing in Brazil and South Korea and in order to further qualify the performances of the new measurement system, an inter-comparison exercise between the FNCL and the EFCP was organised with the support of the FRAMATOME fuel fabrication plant in Romans-sur-Isère, France.*

*After benchmarking the numerical calibration of the FNCL measuring 17x17 PWR assemblies, covering a very wide range of  $^{235}\text{U}$  enrichments, a set of 10 fresh fuel assemblies was measured with both collars. Based on available inventories at the time of the exercise, the selected set included fuel assemblies with fuel pins loaded with 3.2 wt.%  $^{235}\text{U}$ , half of which had 12 fuel pins substituted with burnable neutron poison pins containing 8 wt.%  $\text{Gd}_2\text{O}_3$ .*

*The present publication describes in detail the modality of the measurement inter-comparison and the performance results obtained with both the FNCL and EFCP collars. In particular, information about the counting precision, measurement times, FNCL calibration, and the sensitivity of the measurements to the presence of  $\text{Gd}_2\text{O}_3$  in the fuel are provided.*

**Keywords:** NDA, FNCL, EFCP, Gadolinium, Safeguards Verification

## 1. Introduction

Neutron coincidence counting is a Non-Destructive Assay (NDA) measurement technique which is widely used in nuclear Safeguards to verify independently from the operator's declaration the amount of fissile material. The technique relies on the detection of time-correlated neutrons emitted during fission events. It can therefore be used as a passive measurement technique, to detect burst of neutrons emitted from spontaneous fission event in  $^{238}\text{Pu}$ ,  $^{240}\text{Pu}$  and  $^{242}\text{Pu}$  isotopes. It can also be used with the active interrogation of a sample, where neutrons from an external source (typically an  $^{241}\text{AmLi}$  ( $\alpha, n$ ) neutron source) are used to induce fission events in fissile uranium isotopes ( $^{233}\text{U}$ ,  $^{235}\text{U}$ ). Using a reproducible measurement geometry for which a calibration curve has been established and validated, the detection rate of time-correlated - or coincident - neutrons can be directly related to the mass of fissile isotope(s) present in the measured sample.

Neutron detection in traditional neutron coincidence counters is based on  $^3\text{He}$  gas proportional counters. These detectors have both high efficiency, due to the high thermal neutron cross section of

the  ${}^3\text{He}(n,p){}^3\text{H}$  reaction they rely upon for neutron detection, and low sensitivity to gamma-rays. Typical counters are made of such  ${}^3\text{He}$  gas proportional tubes embedded in a good neutron moderator, like High Density Poly-Ethylene (HDPE). Generic designs include well or cavity counters as well as collars. The formers completely enclose the sample, and are used for measuring limited size items, while the latter, open at the bottom and at the top, and with a removable side panel, are mainly used for measuring the fissile uranium content (per unit length) of power reactor fresh fuel assemblies, and are the main focus of this publication.

The development of Uranium Neutron Coincidence Collars (UNCL) started at the Los Alamos National Laboratory (LANL) in the 1980s [Menlove81]. Since, the nuclear industry has progressively introduced new commercial fuel designs with higher nominal  ${}^{235}\text{U}$  linear mass loadings, but compensated by burnable neutron poison rods. Burnable poisons are strong thermal neutron absorbers aiming to keep the reactivity of the fuel to a low controllable level despite higher initial enrichments. Nowadays, the most commonly used burnable poison material is gadolinium. The presence of thermal neutron poisons in the fuel assemblies have made the UNCL measurement challenging because of their impact on the rate of detected coincidence events. Starting from the 1990s, correction coefficients have been developed and applied to the verification measurement to account for such effect on the basis of the operator's declaration of the burnable poison content [Menlove90]. The independence of the verification from the operator declaration was at that point no longer assured.

Initial UNCL designs were operated using a "thermal" neutron interrogation mode, where the  ${}^{241}\text{AmLi}$  interrogation neutrons are thermalised in the UNCL panels so as to maximize the induced fission rate in the Fresh Fuel Assembly (FFA). In this design both thermal interrogation neutrons and thermalised fission neutrons are highly affected by the gadolinium. In order to reduce the gadolinium impact on the measured coincidence rates, an alternative "Fast" neutron interrogation mode was proposed. Collars operated in "fast" interrogation mode have a thin cadmium layer covering the inner sides of the measurement cavity. Given cadmium's high neutron absorption cross section for neutrons with energy below 0.5 eV, thermal neutrons moderated in the collar's HDPE structure are prevented from penetrating the FFA measurement cavity. The resulting energy distribution of the interrogating neutron flux in the FFA is therefore less perturbed by the gadolinium captures. Nevertheless, gadolinium correction factors based on operator's declarations are still applied to the measurements in "fast" interrogation mode, although these being in the range of few percent compared to the tens of percent needed to compensate for poison absorption in "thermal" interrogation mode [Menlove90]. Another consequence of the energy hardening of the neutron interrogation flux is the significant decrease in the induced fission rate in the FFA. As a result measurement times in "Fast" interrogation mode are significantly longer. To give an example, the measurement time needed to achieve a 2% statistical uncertainty on the coincidence counts increases from few minutes to around 2 hours for the UNCL respectively in "thermal" and "fast" interrogation modes. This is also compelled by the fact that, for thermal neutron detector based measurement systems, a direct increase in the activity of the  ${}^{241}\text{AmLi}$  source does not provide any significant improvement in the measurement precision. This is due to the fact that the random coincidence noise originating from the  ${}^{241}\text{AmLi}$  source itself is in direct competition with the induced fission coincident signal measured in the shift register electronics. Instead, neutron collars with increasingly higher efficiencies to fission neutrons from the FFA and lesser sensitivity to  ${}^{241}\text{AmLi}$  neutrons have been developed in an attempt to further compensate for the smaller "Fast" interrogation coincidence count rates and improve measurement performances. These developments include the UNCL-II from the 1990s [Menlove90], the IAEA's fast-UNCL [Tagziria2012] and most recently the EURATOM Fast Collar developed by LANL in collaboration with the European Commission's Safeguards Directorate in its design for PWR [Swinhoe2015] and BWR, respectively called EFCP and EFCB. The EFCP is currently routinely used for Safeguards verification by EC inspectors at the FRAMATOME fuel fabrication plant located in Romans sur Isère, France, whereas the EFCB has been developed and is currently undergoing a test phase.

The Fast Neutron Collar (FNCL) developed by the IAEA in recent years [Plenteda2016] is about to be introduced as an authorised Safeguards verification tool. Contrary to the UNCL designs, which as mentioned before rely on thermal neutron detectors, the FNCL was developed around non-hazardous EJ-309 liquid-scintillation detectors which directly detect fast neutrons [EljenTechnology2019]. Neutron detection is performed through recoil protons generated by neutron scattering events with hydrogen atoms. Photons are also detected through Compton scattering with electrons. Consequently, Pulse Shape Discrimination (PSD) on the signal waveforms collected by fast electronic digitiser needs to be performed to segregate incident neutrons from gamma-ray signals.

The system only operates in "Fast" interrogation mode to reduce sensitivity to gadolinium. Since fast neutrons are measured without moderation, the detection time interval of coincident neutron occurs over time scales of the order of 10's of nanoseconds, and the random coincidence noise originating from the  $^{241}\text{AmLi}$  source is quasi inexistent for the typical  $^{241}\text{AmLi}$  sources used in active neutron counters. Additionally, functioning as a neutron spectrometer, energy thresholds are applied to prevent the detection of neutrons below about 0.5 MeV, which minimises the response of the FNCL to  $^{241}\text{AmLi}$  source neutrons and further de-sensitises the system to the influence of gadolinium (lower energy fission neutrons have a higher chance of being captured by gadolinium when scattering in the fuel). This also opens the possibility to use such a system with stronger interrogation sources and hence reduce even further the required measurement times.

The two most recently developed neutron coincidence collars for Safeguards application, respectively the EC's EFCP and the IAEA's FNCL described above, open the possibility to perform all verification measurements in "fast mode" during time-constrained inspections, and to reduce or even ignore the dependence of the raw measurement on operator's declaration for the neutron poison content of FFAs. To assess and compare the relative capabilities of the two instruments, the EC and the IAEA have organised an inter-comparison exercise with both detectors in a realistic verification scenario. The tests took place in November 2018 at the FRAMATOME fuel fabrication plant of Romans sur Isère, France. The following section will describe the features of the two instruments and the conditions of the test. Later, the results will be discussed with a comparison of the two system's performances.

## 2. Inter-comparison Exercise

The Inter-comparison exercise took place between the 12<sup>th</sup> and 14<sup>th</sup> November 2018 and was carried out by measuring a wide range of PWR 17 x 17 fresh fuel assemblies at the FRAMATOME fuel fabrication plant located in Romans sur Isere in France.

### 2.1 EURATOM Fast Collar (EFCP)

#### 2.1.1 EFCP Design

The Euratom Fast Collar for PWR fuel elements (EFCP) was designed by LANL in 2013 in cooperation with the Euratom Safeguards Directorate of the European Commission [Evans2013]. The target requirements driving the instrument's design were: 1) an assay time of 15 minutes or less for a "fast mode" measurement of a fuel element with 4.5 w%  $^{235}\text{U}$  enrichment and containing poison rods, and 2) a 2% relative uncertainty in the coincident count rates, hereafter referred as doubles count rates or D. Both of these requirements had to be met with a standard AmLi interrogation source strength of  $5.7 \cdot 10^4$  neutrons/s. The EFCP design has been optimised against the target requirements by means of Monte Carlo simulation. The detector contains 33  $^3\text{He}$  tubes with 10 atm. gas pressure, providing high detection efficiency to thermal neutrons. Illustration of the EFCP design is shown in Figure 1.

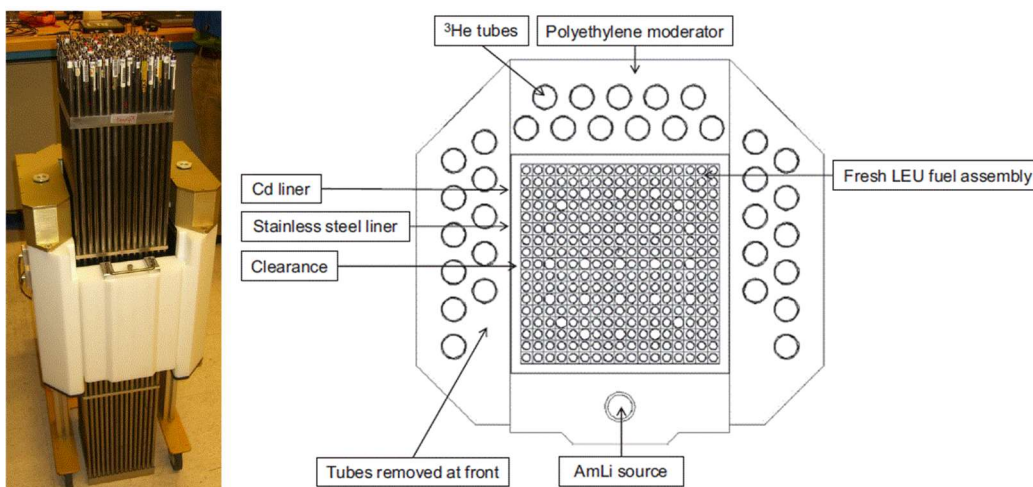


Figure 1. Photograph on the left hand side of the EFCP with a mock fuel assembly [Swinhoe2014] and on the right hand side a top view of the MCNPX model of the EFCP [Evans2013].

The tubes are arranged in two rows within the polyethylene moderator, and the configuration of the rows is optimised to minimise the counts of uncorrelated neutrons from the AmLi interrogation source (i.e. the noise). A fixed cadmium liner surrounds the fuel cavity, therefore the EFCP operates only in "fast mode".

### 2.1.2 EFCP Calibration

The instrument was calibrated with a mock-up fuel assembly of variable enrichment at LANL [Swinhoe2014] and with actual assemblies at the FRAMATOME Fuel Fabrication Plant in Lingen, Germany [Swinhoe2015]. The calibration curve is normalised to the strength of the  $^{241}\text{AmLi}$  source MCR-95, which was used as a reference source for the initial calibration at LANL. This is a common convention for  $^3\text{He}$  based collars which dates back to the original calibration procedure developed for the UNCL in the 80s. In its current application the EFCP operates with the  $^{241}\text{AmLi}$  source C941, which has a certified strength of  $9 \cdot 10^4 \pm 10\%$  neutrons/s.

### 2.1.3 EFCP Normalisation Factors

The  $k_0$  source yield correction factor, which is used to normalise the measured counts to those expected with the MCR-95 reference source, is based on the ratio of the two source's strengths corrected by the decay since the calibration date and it was 0.482 at the time of the inter-comparison exercise. The correction parameters for poison content were evaluated by Monte Carlo simulation and then validated in the field. A fuel configuration containing 32 poison rods with 12% weight concentration of gadolinium was chosen as the upper limit for the establishment of the correction factor and it reflects the most advanced poisoned fuel design currently available. For such an assembly, the maximum correction factor applied to the EFCP counts is 12.9% [Evans2013].

The EFCP normalisation was validated once per day by measurement of the neutron singles rate emitted by  $^{241}\text{AmLi}$  source C941. The source orientation was kept constant throughout all the measurements to eliminate uncertainties due to source anisotropy.

## 2.2 Fast Neutron Collar (FNCL)

### 2.2.1 FNCL Design

The FNCL design, shown in Figure 2, is based upon 12 EJ-309 fast neutron liquid scintillators configured in three detector panels (four each). This forms three sides of the measurement cavity. The fourth side is a source panel specific to the type of FFA being measured (PWR, BWR or VVER-1000). Each source panel holds two  $^{241}\text{AmLi}$  sources for active interrogation. Each detector is coupled to a photomultiplier tube and operated between 1500 and 2000 V.

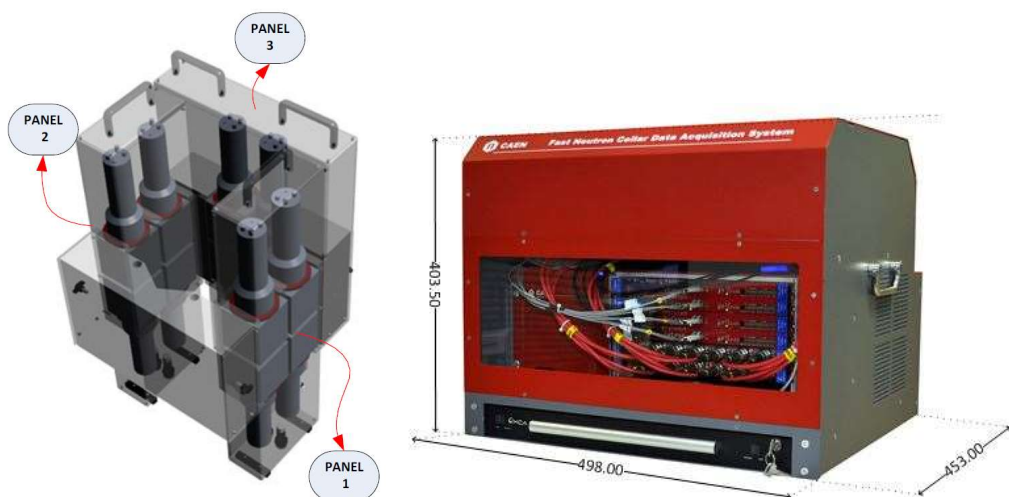


Figure 2. Illustration on the left hand side of the FNCL detector/source panels defining the FNCL measurement cavity, and on the right hand side, a photograph of the FNCL All-in-One DAQ.

The 12 detector channels are fed into a compact all-in-one Data Acquisition System (DAQ) where the collected signals are digitised using 500 MHz 14-bit digitizers and all resulting signal wave forms, sampled over 256 ns, are recorded with respective time stamp and detector address. The FNCL is

therefore a full list-mode system with additional waveform data. During operation data is analysed on-the-fly and includes steps for detector cross talk rejection, pulse energy threshold rejection, pulse shape discrimination, and gamma pile-up rejection. The resulting neutron pulse train is then analysed digitally by conventional shift register analysis to derive singles and doubles neutron count rates. All FNCL detection data can be re-analysed in an off-line mode with flexibility to adjust all analysis parameters. Since fast neutrons are measured without moderation time the FNCL operates with a coincidence gate of 60 ns, one thousand times smaller than conventional  $^3\text{He}$  detection systems. This virtually eliminates accidental coincidence neutrons and resultantly improves measurement statistics. The FNCL is further described in [Beaumont2017].

### 2.2.2 FNCL Normalisations

Prior to FFA measurements, the FNCL energy calibration and neutron efficiency normalisation measurements (including background measurements) were performed at the start of each day. The energy calibration was also repeated in the afternoon on the second day, following an unscheduled power cut.

The FNCL functions as a neutron spectrometer and therefore requires an energy calibration. This was accomplished measuring a  $^{137}\text{Cs}$  source (UC-785 – nominal activity 3.91 MBq) placed at the centre of the FNCL cavity. This energy calibration is performed by determining the position of the  $^{137}\text{Cs}$  Compton edge for each detector. The  $^{137}\text{Cs}$  energy spectrum was collected for 60 seconds which provided ample statistics. The use of a relatively strong  $^{137}\text{Cs}$  source also alleviated any issues due to the background radiation from approximately 100 unshielded fuel assemblies stored in the relative vicinity of the FNCL.

Neutron efficiency normalisation was performed by measuring two  $^{241}\text{AmLi}$  sources referenced as C941 and C940, both of them having a certified neutron strength of  $9 \cdot 10^4 \pm 10\%$  neutrons/s. Normalisation counts were performed every day, including a 10 minutes background measurement, and a 10 minutes  $^{241}\text{AmLi}$  sources measurement (reduced to two 5 min measurements on the third day). Both sources orientation were kept constant throughout all the measurements.

Figure 3 shows data for the neutron efficiency normalisation of the FNCL during the exercise. The calculated doubles efficiencies were within the acceptance limit of 5% and therefore no correction was applied to the FNCL.

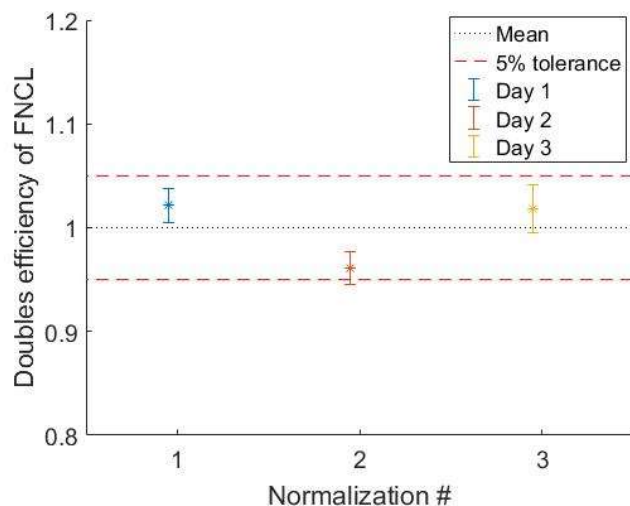


Figure 3. Normalisation values calculated using neutron singles and the net doubles matrix during the measurement campaign (statistical uncertainties shown at  $3\sigma$ ).

### 2.2.3 Empirical Calibration Data

Prior to positioning an FFA in the FNCL, all radioisotope sources were stored away from the FNCL and the FNCL source panel was removed. The FFA was brought by the operator using an overhead crane from the storage rack into the measurement cavity. The source panel was replaced and secured. A mechanical fuel spacer at the back and foam spacers at the sides were used to ensure that the FFA was properly aligned within the FNCL measurement cavity. Passive (no  $^{241}\text{AmLi}$ ) and

active (with  $^{241}\text{AmLi}$ ) measurements were then performed sequentially. Measurement pre-set times of 180 s for the passive assays and 420 s for the active assays were used for the FFA calibration measurements.

Nine fuel assemblies covering an enrichment range between 1.4% and 4.2% in  $^{235}\text{U}$  were measured with the FNCL to provide empirical benchmarking for the  $^{235}\text{U}$  linear concentration calibration. All assemblies to the exception of the 2.3% assembly have no gadolinium poison rods in their design.

Processing of the collected data was performed in real time for the majority of assemblies, and produced verification results within less than 2 minutes from the end of the data collection. Coincidence doubles rates were derived with relative uncertainties between 0.8 and 1.4% (at  $1\sigma$ ) depending on enrichment and gadolinium content. Figure 4 presents a plot of the obtained doubles rates as a function of FFA uranium loading alongside the Monte Carlo based calibration curve for the measured FFA.

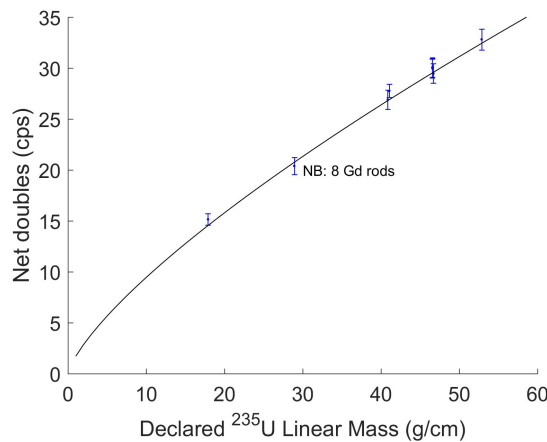


Figure 4. Plot of the net doubles rates measured with the FNCL for a set of FFA covering a wide range of  $^{235}\text{U}$  loading. Statistical uncertainties shown at  $3\sigma$ .

### 2.2.4 FNCL Monte Carlo Calibration

Extensive details on the modelling approach taken to simulate the FNCL response has been published elsewhere [Beaumont2018]. Monte Carlo simulation results derived using the MCNP Polimi [Pozzi2003] package are used with a post processing algorithm to fully simulate the wave form digitisation process and subsequent filtering and pulse rejection steps performed by the FNCL DAQ software. Once normalised to the  $^{241}\text{AmLi}$  interrogation neutron source output, this simulation approach allows to provide reliable Doubles count rates. Figure 5 shows good agreement obtained when comparing empirical Doubles rates with simulated Doubles count rates.

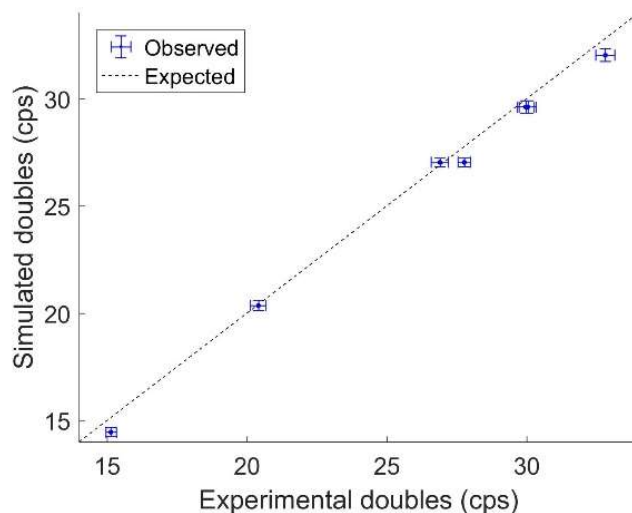


Figure 5. Comparative plot between empirical FNCL Doubles count rates and Doubles count rates obtained from normalised Monte Carlo simulations. Statistical uncertainties shown at  $1\sigma$ .



Figure 6. The EFCP (left) and the FNCL (right) in their measurement configuration for the inter-comparison.

### 2.3 Test configuration

The two instruments were placed in front of each other at around 3 meters distance in the fresh fuel storage hall of the facility as shown in Figure 6. The FFAs were stored above ground and located about 10 metres from the instruments.

The selection of the fuel assemblies for the inter-comparison was based on available inventories at the time of the exercise. It consisted of 10 fuel assemblies with fuel pins loaded with 3.2 wt.%  $^{235}\text{U}$ , half of which had 12 fuel pins substituted with burnable neutron poison pins containing 8 wt.%  $\text{Gd}_2\text{O}_3$ . The details of the fuel assemblies selected for the measurement are reported in Table 1.

Assembly ID	Enrichment	Linear $^{235}\text{U}$ mass (g/cm)	Gd rods	$\text{Gd}_2\text{O}_3$ weight (%)
Exp_1	3.2	41.08	0	-
Exp_2	3.2	41.05	0	-
Exp_3	3.2	40.89	0	-
Exp_4	3.2	40.89	0	-
Exp_5	3.2	40.81	0	-
Exp_Gd_1	3.2	39.67	12	7.48
Exp_Gd_2	3.2	39.70	12	7.48
Exp_Gd_3	3.2	39.79	12	7.45
Exp_Gd_4	3.2	39.63	12	7.48
Exp_Gd_5	3.2	39.70	12	7.48

Table 1. Operator's declared characteristics of the assemblies measured in the inter-comparison exercise.

Each of the selected assemblies was measured by both collars in sequence. The measurements were divided in two parts: a passive short measurement of the fuel without the interrogation source(s) assessed the background doubles from the spontaneous fissions in the  $^{238}\text{U}$  isotopes; an active longer measurement with the interrogation source(s) measures the doubles from both the spontaneous and the induced fissions respectively in  $^{238}\text{U}$  and  $^{235}\text{U}$ . The net doubles rate is given by subtraction of the passive from the active doubles rate. The total measurement time per assembly for the EFCP was set to 20 minutes (5 minutes passive and 15 minutes active measurement), whereas for the FNCL the total measurement time was 15 minutes (4.3 minutes passive and 10.6 minutes active measurement).

### 3. Results

Table 2 gives a summary of the results of the two instruments. Table 3 reports in more details including the Doubles count rates and the assayed  $^{235}\text{U}$  masses. Figure 7 shows extracts of the calibration curves of the EFCP and FNCL and the respective Doubles rate: the net uncorrected and corrected Doubles rates measured by the EFCP for Gd and non-Gd assemblies respectively (bottom graph) and the net uncorrected FNCL Doubles rates (top). The displayed  $\pm 1 \sigma$  confidence limits of the calibration curve were derived by considering systematic uncertainties associated with the fitted calibration curve coefficients.

By virtue of the higher interrogation rate and the lower sensitivity to uncorrelated noise from the  $^{241}\text{AmLi}$  sources, the FNCL's average relative random uncertainty on the net doubles rate is 0.96% (at  $1 \sigma$ ), significantly smaller than the EFCP's value of 1.85% (at  $1 \sigma$ ), in their respective measurement times. The uncertainty on the doubles count rates are the random uncertainty component contributing to the total uncertainty of the assayed  $^{235}\text{U}$  masses.

The net doubles rates measured by the EFCP for the fuel assemblies containing poison rods are corrected by the poison content declared by the operator. Uncorrected doubles rate are also reported in table 3 and figure 7 for comparison. For the specific case of 12 poison rods at 8 wt.%  $\text{Gd}_2\text{O}_3$  content, the calculated correction is 3.7%. The net double rates measured by the FNCL are not corrected for the poison content, thus restoring the independence of the Safeguard verification approach for FFAs. Derived from the FNCL data in table 3, the mean net doubles rates of the Gd group exhibit a relative drop of  $2.8 \% \pm 1.0 \%$  (at  $1 \sigma$ ) with respect to the Doubles rate estimated by the calibration curve at the mean  $^{235}\text{U}$  mass loading. This is the average gadolinium effect on the FNCL doubles rate for this fuel design, and for the enrichment and poison loading considered in this exercise. Simulations using the benchmarked FNCL MCNP model described in section 2.2.4 were performed for the assemblies described in [Evans2013] to provide for a direct comparison of the bias caused by 32 Gd rods at 12% wt. gadolinium oxide. For the FNCL the bias was  $-8.4 \pm 0.3 \%$  to the doubles rate compared with  $-12.9\%$  calculated for the EFCP. The value for 24 Gd rods at 10% wt. gadolinium oxide (the expected upper limit) was also calculated to give a  $-4.5 \pm 0.3 \%$  bias to the doubles rate.

The average relative uncertainty of the EFCP's assayed  $^{235}\text{U}$  mass is around 2.3% (at  $1 \sigma$ ). For the FNCL it was around 1.3%. The Operator-Inspector Differences (OID) were calculated for each measurement as the ratio of the difference between the declared (Operator) mass and the measured (Inspector) mass over the declared (Operator) mass. These are commonly compared to the relative uncertainty of the assayed  $^{235}\text{U}$  mass at the  $1 \sigma$  confidence level in order to evaluate whether any mass discrepancies can be attributed to the reasonable statistical dispersion of the measurement values. For the EFCP measurements, the OIDs lie in the range of  $-2.9\%$  to  $2.8\%$ . As a matter of comparison, the OIDs if the count rates were uncorrected for the poison content would lie in the range  $-2.5\%$  to  $6.4\%$ . For the FNCL measurements, the OIDs are in the range of  $-3.6\%$  to  $4.9\%$  without any gadolinium correction.

	Measurement time (min)	Gd correction	Doubles Rel. Uncert.	Assayed $^{235}\text{U}$ mass Rel. Uncert.	OIDs	
					Non-corrected	Gd-Corrected
<b>EFCP</b>	20	3.70%	1.85%	$\sim 2.3\%$	$-2.5 \div 6.4 \%$	$-2.9 \div 2.8 \%$
<b>FNCL</b>	15	None	0.96%	$\sim 1.3\%$	$-3.6 \div 4.9\%$	N.A.

Table 2. Results summary for the inter-comparison exercise. Relative uncertainties are expressed at  $1 \sigma$ .

A useful reference to understand the magnitude of the OIDs in Safeguards measurements is offered by the International Target Values (ITVs). The ITVs represent uncertainty evaluations to be considered in judging the reliability of measurement techniques applied to Safeguards verification. They are compiled for each measurement technique by a team of experts and they are periodically revised. The most recent version of the ITV was published in 2010 [ITV2010] and it is about to be revised with a dedicated discussion session planned at the 2019 ESARDA symposium. For reference, the ITV associated with the verification of the  $^{235}\text{U}$  mass by uranium collar measurement of low enriched fuel assembly is reported as 4.5%. This value applies to fuel without and with gadolinium content not exceeding the calibration range. In the presence of higher gadolinium content, the systematic uncertainty component can increase up to 10%, and the total relative target uncertainty increases to 10.8%.

FFA ID	Declared linear <sup>235</sup> U mass [g·cm <sup>-1</sup> ]	EFCP							FNCL					
		Corrected Net Doubles [DPS]	Doubles Rel. Uncert. [%]	Assayed linear <sup>235</sup> U mass [g·cm <sup>-1</sup> ]	<sup>235</sup> U Rel. Uncert. [%]	OID [%]	Uncorrected Net Doubles [DPS]	OID without Gd correction [%]	Uncorrected Net Doubles [DPS]	Doubles Rel. Uncert. [%]	Assayed linear <sup>235</sup> U mass [g·cm <sup>-1</sup> ]	<sup>235</sup> U Rel. Uncert. [%]	OID [%]	
EXP_1	41.08	29.41	1.78	41.95	2.26	-2.1	/			26.57	0.96	40.38	1.30	1.7
EXP_2	41.05	28.75	1.81	40.81	2.30	0.6				27.51	0.93	42.32	1.25	-3.1
EXP_3	40.89	28.75	1.83	40.53	2.32	0.9				26.32	0.94	39.87	1.27	2.5
EXP_4	40.89	29.38	1.77	41.90	2.27	-2.5				27.26	0.94	41.80	1.26	-2.2
EXP_5	40.81	28.69	1.82	40.69	2.31	0.3				27.5	0.95	42.30	1.28	-3.6
EXP_Gd_1	39.67	28.19	1.89	39.84	2.40	-0.4	27.20	3.9	25.44	0.97	38.08	1.31	4.0	
EXP_Gd_2	39.70	28.77	1.84	40.85	2.34	-2.9	27.76	1.5	25.95	0.95	39.11	1.28	1.5	
EXP_Gd_3	39.79	27.55	1.92	38.74	2.42	2.7	26.62	5.8	26.47	0.93	40.17	1.26	-1.0	
EXP_Gd_4	39.63	28.16	1.88	39.78	2.38	-0.4	27.17	3.3	25.24	1.00	37.67	1.35	4.9	
EXP_Gd_5	39.70	27.46	1.94	38.59	2.44	2.8	26.49	6.4	25.39	0.99	37.98	1.34	4.3	

Table 3. Summary table of the Doubles count rates obtained with the EFCP and FNCL for the 10 measured FFA. Relative uncertainties are expressed at 1σ. The net Doubles count rates and the OIDs of the EFCP for the gadolinium containing FFAs are reported with and without correction to perform a direct comparison with the uncorrected results of the FNCL.

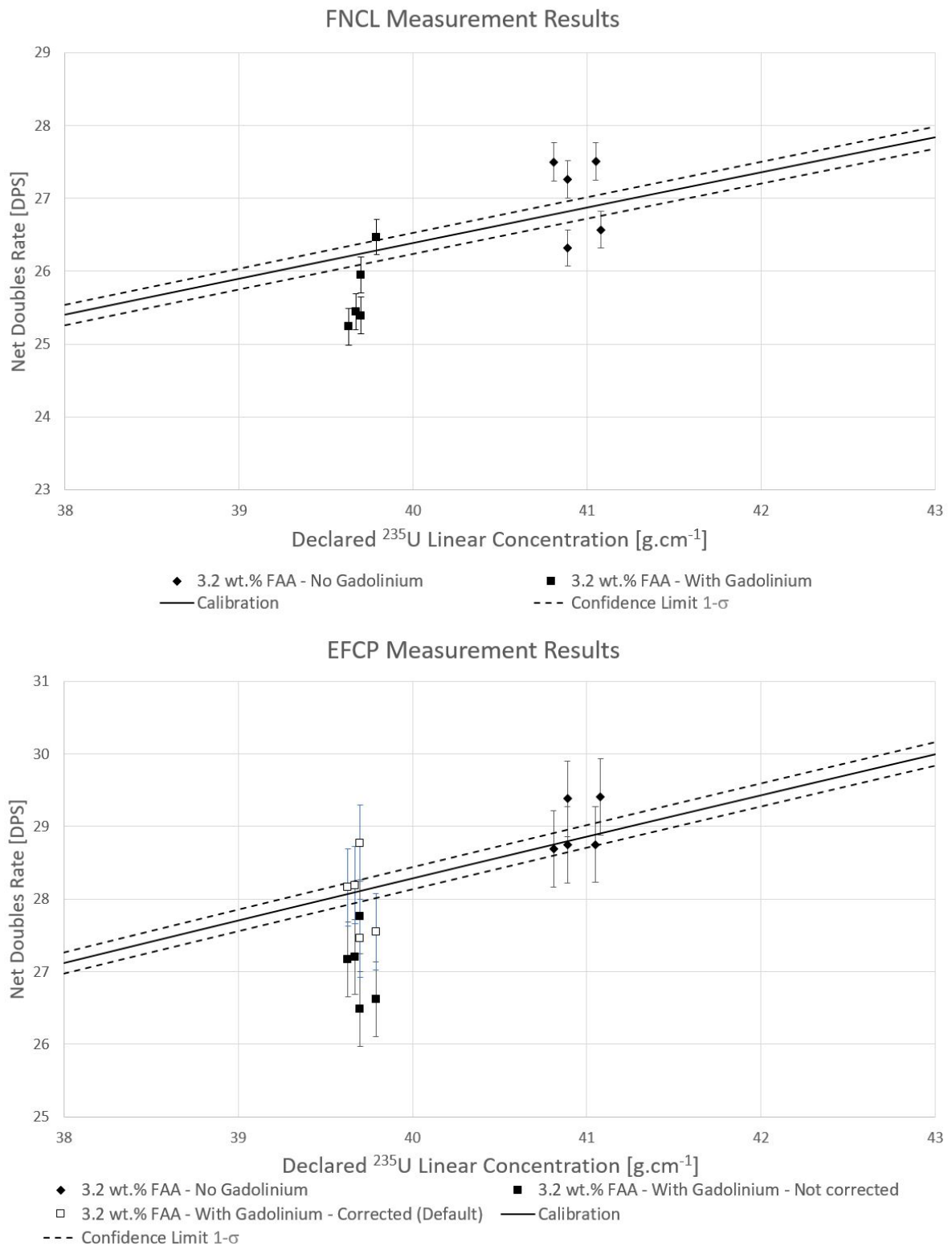


Figure 7. Plots of the FNCL (top) and EFCP (bottom) calibration curves and the net uncorrected/corrected doubles rates obtained for FFA with and without gadolinium rods. Uncertainties are shown at  $1\sigma$ .

## 4. Conclusions

The EC's EFCP and the IAEA's FNCL were compared in a realistic verification scenario at the FRAMATOME Fuel fabrication plant of Romans sur Isère in November 2018. The inter-comparison exercise focused on the measurement of 10 fuel assemblies with 3.2 wt.%  $^{235}\text{U}$ , half of which had 12 fuel pins substituted with burnable neutron poison pins containing 8 wt.%  $\text{Gd}_2\text{O}_3$ .

Both measurement systems performed satisfactorily in providing fissile material estimates for all measured FFA. The FNCL, by detecting directly fast neutrons from fission, is far less sensitive to the randomly correlated  $^{241}\text{AmLi}$  interrogation background than the thermal neutron detectors of the EFCP. This allows the FNCL to operate with two  $^{241}\text{AmLi}$  interrogation sources (or more) instead of one and to achieve lower statistical uncertainties in less time since the neutron accidentals can be neglected. Additionally, for the FFAs containing burnable neutron poison, the EFCP results were corrected by a factor of 3.7% derived from the declared poison content. This approach ties the verification measurements to the operator declarations, but in turn provides results with high accuracy (within  $1.3 \sigma$ ) after correction. The FNCL results showed that even with no corrections for the gadolinium assemblies the quantified  $^{235}\text{U}$  masses were consistently within the ITVs, therefore removing the need to introduce an unverifiable parameter from the assay. Hence, it can be concluded that the FNCL delivers more robust results for Safeguards verification of FFAs.

## 5. Acknowledgement

The authors would like to thank the FRAMATOME fuel fabrication plant of Romans sur Isère, France, for having hosted the tests and in particular Mr. P. Marion, Mrs. P. de Lavarène and Mr. P. Turbiault for having facilitated the organisation and the measurement campaign.

## 6. References

- [Beaumont2017] J. Beaumont, T. H. Lee, M. Mayorov, C. Tintori, F. Rogo, B. Angelucci, M. Corbo, A fast-neutron coincidence collar using liquid scintillators for fresh fuel verification, *J Radioanal Nucl Chem* (2017) 314: 803.
- [Beaumont2018] J. Beaumont, M. Milovidov, M. Mayorov, A Semi-empirical Approach to Validating Results from a Fast-neutron Coincidence Collar, *Conference Proceedings, ESARDA NM-NDA-IMNS18, May 16-17 2018, Luxembourg.*
- [EljenTechnology2019] Eljen Technology, Neutron/Gamma PSD EJ-301, EJ-309, <https://eljentechnology.com/products/liquid-scintillators/ej-301-ej-309>
- [Evans2013] L.G. Evans, M.T. Swinhoe, H.O. Menlove, P. Schwalbach, P. De Baere, M.C. Browne, A new fast neutron collar for safeguards inspection measurements of fresh low enriched uranium fuel assemblies containing burnable poison rods, *Nuclear Instruments and Methods in Physics Research A* 729 (2013) 740-746
- [ITV2010] K. Zhao, M. Penkin, C. Norman, S. Balsley, K. Mayer, P. Peerani, C. Pietri, S. Tapodi, Y. Tsutaki, M. Boella, G. Rehna Jr., E. Kuhn, *International Target Values 2010 for Measurement Uncertainties in Safeguarding Nuclear Materials*, ESARDA Bulletin, No. 48, December 2012.
- [Menlove81] H.O. Menlove, Description and performance characteristics for the neutron Coincidence Collar for the verification of reactor fuel assemblies, LA-8939-MS, 1981
- [Menlove90] H.O. Menlove, J.E. Stewart, S.Z. Qiao, T.R. Wenz, G.P.D. Verrecchia, Neutron collar calibration and evaluation for assay of LWR fuel assemblies containing burnable neutron absorbers, LA-11965-MS, 1990
- [Plenteda2016] R. Plenteda, K. Baird, A. Tomanin, A. Lavietes, J. Adamczyk, P. Peerani, N. Mascarenhas, M.J. Joyce, M. Aspinall, F. Cave, *Development of a Prototype Fast Neutron Active Coincidence Collar for Safeguards*, *Journal of Nuclear Materials Management*, Vol. XL IV, No.2, pp. 45-51 (2016).
- [Pozzi2003] Sara A Pozzi, Enrico Padovani, Marzio Marseguerra, MCNP-PoliMi: a Monte-Carlo code for correlation measurements, *Nuclear Instruments and Methods in Physics Research Section A: Accelerators, Spectrometers, Detectors and Associated Equipment*, Volume 513, Issue 3, 2003.
- [Swinhoe2014] M.T. Swinhoe, C.D. Rael, H.O. Menlove, P. De Baere, *Euratom Fast Collar (EFC) Calibration Report*, LA-UR-14-23275, 2014
- [Swinhoe2015] M.T. Swinhoe, P. De Baere, In-field Calibration of a Fast Neutron Collar for the Measurement of Fresh PWR Fuel Assemblies, LA-UR-15-22843, 2015
- [Tagziria2012] H. Tagziria, J. Bagi, P. Peerani, A. Belian, *Calibration, characterisation and Monte Carlo modelling of a fast-UNCL*, *Nuclear Instruments and Methods in Physics Research A* 687 (2012) 82–91

# **Session 12:**

# **Statistics**

## **Statistical design of experiments: a powerful tool in your nonproliferation toolbox**

### **Robert Brigantic**

Pacific Northwest National Laboratory  
902 Battelle Blvd.  
Richland, WA 99352  
e-mail: robert.brigantic@pnnl.gov

### **Andrea Trevino-Gavito**

Northwestern University  
2145 Sheridan Road, room C210.  
Evanston, IL 60208  
e-mail: andrea.tg@u.northwestern.edu

### **Nick Betzsold**

Pacific Northwest National Laboratory  
902 Battelle Blvd.  
Richland, WA 99352  
e-mail: nicholas.betzsold@pnnl.gov

### **Casey Perkins**

Pacific Northwest National Laboratory  
902 Battelle Blvd.  
Richland, WA 99352  
e-mail: casey.perkins@pnnl.gov

### **Gregg Mckinney**

Los Alamos National Laboratory  
MS E521  
Los Alamos, NM 87545  
e-mail: gwm@lanl.gov

### **Abstract:**

*Regardless of the domain, statistical design of experiments (DOE) is a powerful methodology that can be used to identify the most influential factors in a simulation, experiment, or operational process; explore interactions between factors; understand and manage variation; and help to improve the overall efficiency of a system--all based on running only a limited number of experiments. In this paper we present how DOE was used to efficiently explore the representative output space from the Nuclear Inspection Node Event SIMulator (NINESIM) across its full space of input parameters. NINESIM integrates state-of-the-art capabilities in user interfaces, statistical discrete-event processing, human intervention modeling, background and clutter algorithms, and radiation transport modeling using open-source software. We focus on the DOE approach and setup that was used to test and evaluate the model. This includes, delineating input factors of interest and corresponding levels, selecting appropriate design and performance metrics, running the NINESIM model across the design space, and analyzing output results to identify the most significant factors and interactions in terms of their impact on output performance metrics. Lastly, we present the results of the DOE analysis, which includes a review of the*

*most influential factors in the NINESIM model and important interactions between factors that might otherwise be unaccounted for and could result in erroneous or less than optimal decision outcomes.*

**Keywords:** design of experiments; nonproliferation; statistics; NINESIM; modelling and simulation

## 1. Introduction

Regardless of the domain, statistical design of experiments (DOE) is a powerful methodology that can be used to identify the most influential factors in a simulation, experiment, or operational process; explore interactions between factors; understand and manage variation; and help to improve the overall efficiency of a system--all based on running only a limited number of experiments. In this paper we present how DOE was used to efficiently explore the representative output space from the Nuclear Inspection Node Event SIMulator (NINESIM) across its full space of input parameters.

After introducing NINESIM, we will focus on the DOE approach and setup that was used to test and evaluate the model. This includes, delineating input factors of interest and corresponding levels, selecting appropriate design and performance metrics, running the NINESIM model across the design space, and analyzing output results to identify the most significant factors and interactions in terms of their impact on output performance metrics. Lastly, we present the results of the DOE analysis, which includes a review of the most influential factors in the NINESIM model and important interactions between factors that might otherwise be unaccounted for and could result in erroneous or less than optimal decision outcomes.

The remainder of this paper is organized as follows. First we provide a short introduction to statistical design of experiments (DOE) methodology. This is followed by an overview of the Nuclear Inspection Node Event SIMulator (NINESIM) model. Next, we present the DOE approach and setup that was used to test and evaluate NINESIM and then present results from the DOE analysis. Finally, we present findings from this work.

## 2. Introduction to DOE methodology

Statistical design of experiments is a structured approach to help analyze a system or process that makes use of designed experiments to help determine 1) which inputs have the most a significant impact on the system or process response (output) and 2) appropriate target levels for inputs to achieve a desired system or process response [1]. Additional benefits of using a DOE approach include [2-4]:

- Applying a more rigorous/informative approach than traditional methods, such as changing one-factor at a time
- DOE helps to establish important interrelationships among numerous system variables that might otherwise not be accounted for, such as:
  - Important variables that need to be controlled
  - Unimportant variables that may not need to be controlled
  - Interactions between variables
  - DOE can also help to eliminate confounding between variables
- Enables more informed decisions/better solutions in less time and with less cost
- DOE is applicable to any domain

### 2.1. Key characteristics of DOE

Key characteristics of DOE include specification of the following:

- *Factors* – system or process inputs to the experiment; these case be can controllable or uncontrollable
- *Levels* – input settings for each factor
- *Response* – the system or process output from the experiment that is based on the input factor settings

In summary, the goal of DOE is to run a set of experiments in which the levels of the factors are systematically varied to ascertain their impact on the system or process response.

## 2.2. Basic steps

The basic steps to implement a DOE approach include:

- 1) Choose factors ( $k$  of them) and determine a valid range for each
- 2) Determine the measured response variable(s)
- 3) Select a statistical test design; there are many to choose from but a typical standard test design is a  $2^k$  factorial design [5]
- 4) Run the experiments and collect outputs
- 5) Analyze data and develop statistical models
- 6) Interpret results
- 7) Make recommendations

Of course the above steps could be repeated or updated (e.g., add or remove factors, vary factor levels, include additional design points, etc.) based on results and information learned from the DOE approach.

## 2.3. $2^k$ factorial design

A  $2^k$  factorial design is a common starting point for conducting an DOE analysis. Key features of a  $2^k$  design include:

- $k$  factors, each with 2 levels -- high (+) and low (–)
- For a single replication of each “design point,” this yields  $2^k$  total experiments or treatments
- A full-factorial design uses all possible  $2^k$  treatments

An advantage of using a  $2^k$  design is that it allows for conducting a simple statistical analysis and estimate of the main effects (i.e., how does the response change with a change in the level of a factor?) and interactions (i.e., how does the response change with a change in two factors at the same time) as well as statistical significance of such affects. Figure 1 shows a  $2^k$  factorial design for  $k = 3$  factors (A, B, and C) and a typical table of standard factor level settings for each of the  $2^3 = 8$  total design points or trials.

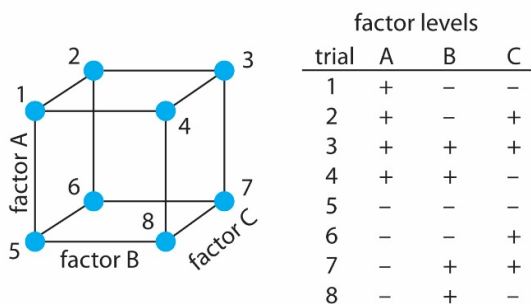


Figure 1:  $2^3$  full factorial design

## 3. Nuclear Inspection Node Event SIMulator (NINESIM) overview

The Nuclear Inspection Node Event SIMulator was developed for the U.S. Department of Homeland Security’s Countering Weapons of Mass Destruction (CWMD) Office to provide an adaptable, high-fidelity, and faster-than-real-time modeling and simulation capability of special nuclear material (SNM) radiation detection at ports-of-entry (POE). NINESIM integrates state-of-the-art capabilities in user interfaces, statistical discrete-event processing, human intervention modeling, background and clutter algorithms, and radiation transport modeling using open-source software. Furthermore, this tool could be extended to support other objectives, to include an assessment of potential concepts of operations

(CONOPS) in support nonproliferation activities. Figure 2 provides an overview of the modules which comprise NINESIM and its key features. The various modules provide a means for users to fully specify the configuration of a POE (i.e., number of lanes, detector types, etc.) and various assumptions about the radiological material (i.e., type, mass, shielding) being scanned, background, and CONOPS. All of permutations associated with these settings would yield more than 1 million design points. For a single configuration, NINESIM will typically output a receiver operating characteristic (ROC) curve. From this, a single output can be used for the DOE response, namely the true positive (TP) rate.

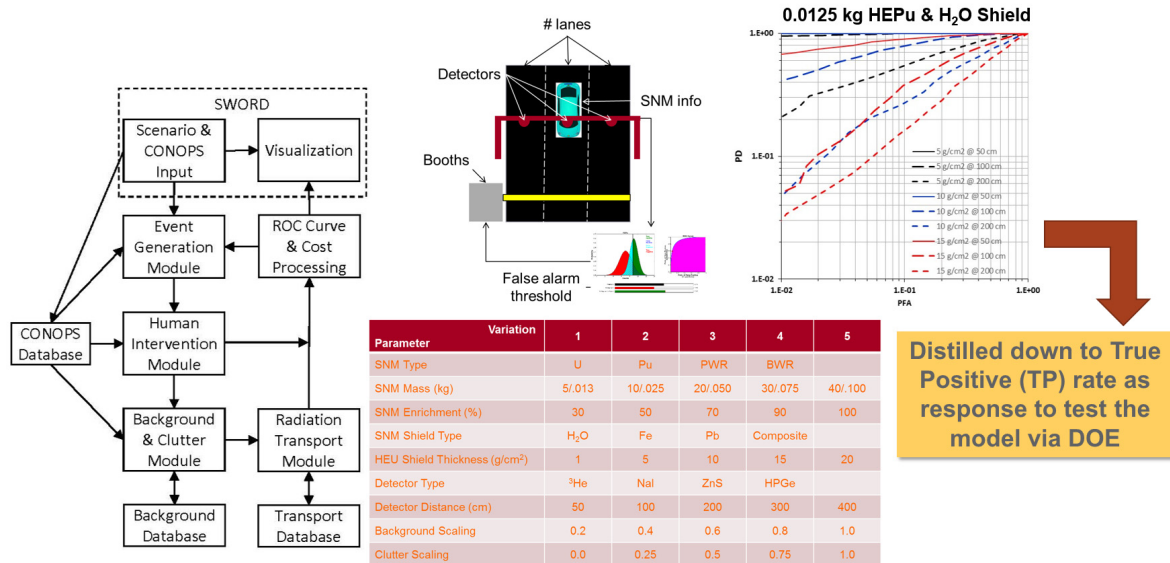


Figure 2: Overview of NINESIM modules and key features

#### 4. DOE approach and setup for test and evaluation

Having introduced DOE methodology and NINESIM, we next outline our approach and setup to test the model. In summary this involves, the following steps:

- Delineate NINESIM input factors of interest and corresponding levels
- Determine an appropriate response metric
  - As mentioned, we used overall true positive (TP) rate as output from NINESIM for each design point
  - At each design point, the mean TP rate was computed based on total number of true positives from 48 arriving conveyances
- Select an appropriate DOE design and response metric
  - We used a standard  $2^k$  full-factorial design with  $k = 6$  for total of  $2^6 = 64$  design points
  - We ran this setup for each source (5 of them), detector type (3 of them) and shielding type (3 of them) = 45 permutations
  - Over total of  $64 \times 45 = 2,880$  experimental design points
  - The overall input setup is shown in Table 1 (Note: HIM is short for the Human Intervention Module which characterizes human proficiency in the screening process)
- Run NINESIM model across design space
- Analyze output results to identify most significant factors and interactions in terms of their impact on the TP rate

	SNM		Shield		HIM	Detector	Velocity at Detectors (mph)	Distance to Detector (cm)	PFA
	Type	Mass	Type	Thickness (g/cm <sup>2</sup> )					
No. Levels	5	2	3	2	2	3	2	2	2
LEVELS	U	10 kg 20 kg	H2O Fe Pb	10 20	High Low	He3 Nal ZnS	5 10	Short Far	0.05 0.1
	Pu	0.025 kg 0.05 kg							
	K-40	100 kg 200 kg							
	Tc-99	0.001 mCi 0.01 mCi							
	Co-60	0.01 mCi 0.1 mCi							

Table 1: Summary of the full DOE settings for NINESIM

### 5. DOE results

Next we summarize the results for the DOE evaluation of NINESIM.

#### 5.1. Main effects

Main effects refers to a change in the response produced by a change in the level of a factor averaged over the other factors. In a main effects plot, a line which is parallel to the x-axis would indicate no main effect. If the line is not horizontal, we can say that there is a main effect and that the slope of the line represents its magnitude. Figures 3-5 shows main effects plots for the source U, Pb, and K-40 respectively. Rows in each figure represent different detector types (He3, Nal, and ZnS) and columns represent different shielding types (Fe, H2O, and Pb).

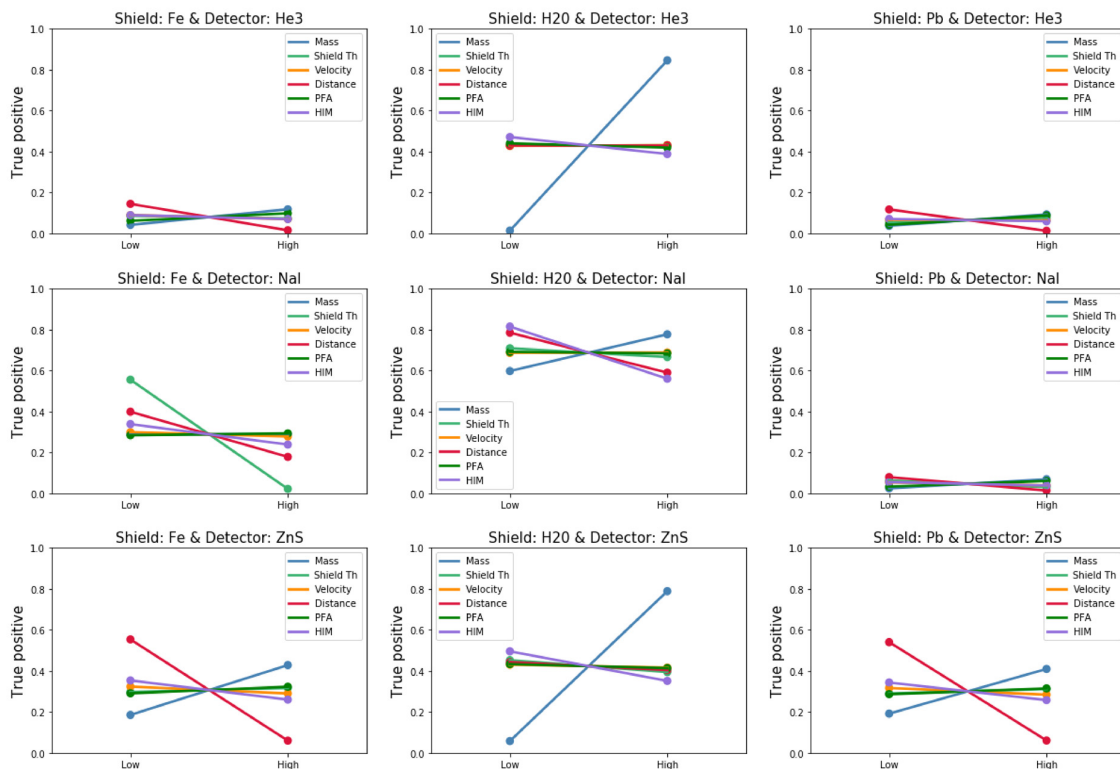


Figure 3: Main effects plots for U

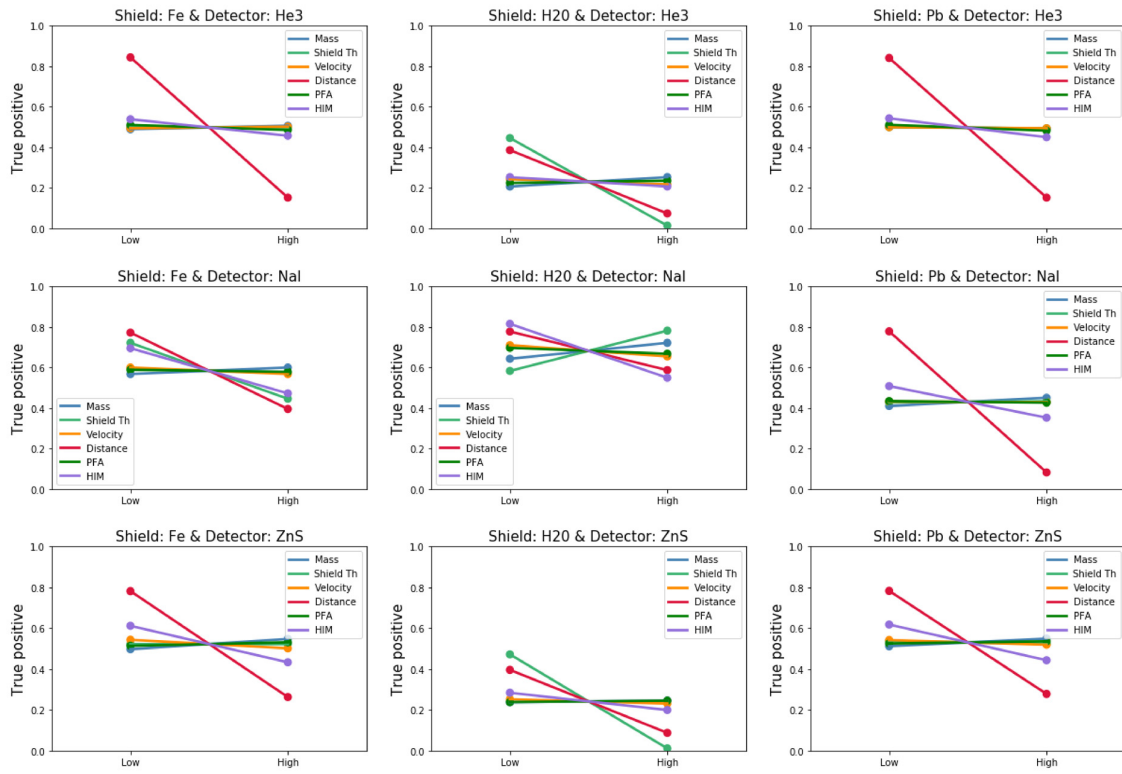


Figure 4: Main effects plots for Pu

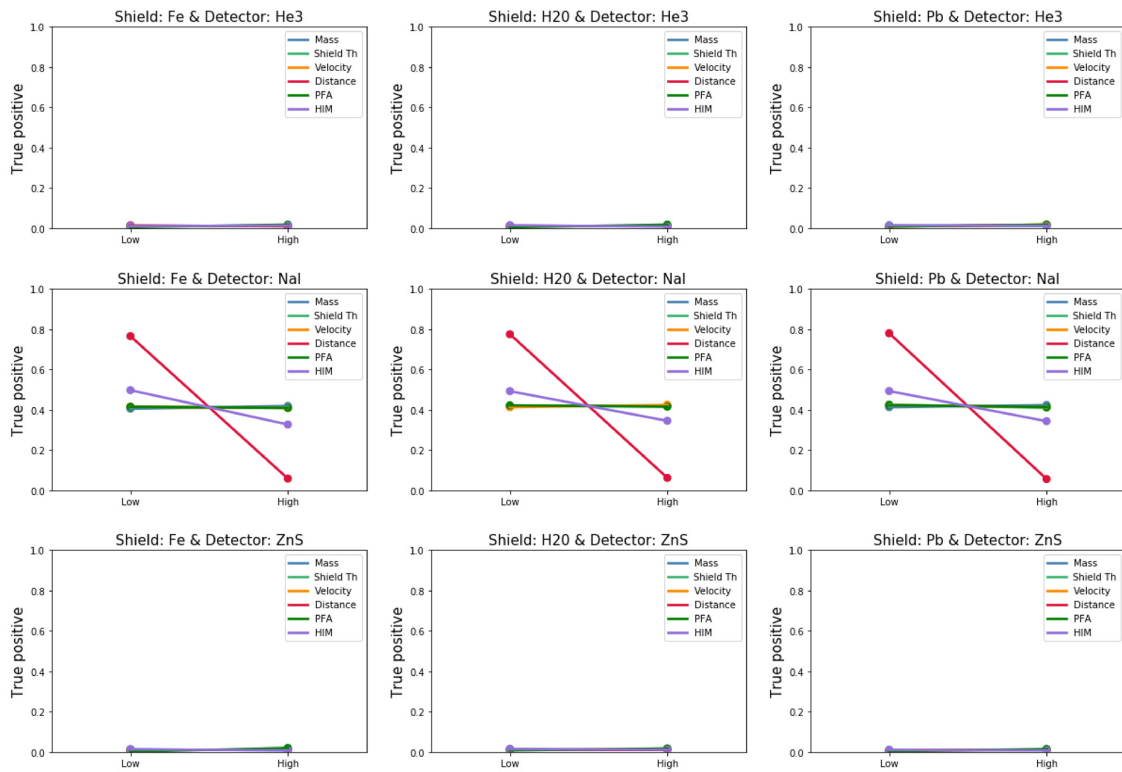


Figure 5: Main effects plots for K-40

We also provide a summary of significant main effects for U and Pb as shown in Tables 2 and 3 respectively. Here we define significant based on effects having a statistical significance (p-value < 0.05) and practical significance (regression coefficient >0.05).

Uranium				
Shielding	Detector Type	Significant Main Effects	p-value	Regression Coefficient
Fe	He3	Distance	5.74E-12	-0.064697
		Distance	1.06E-07	-0.110205
	Nal	Shield Thickness	4.45E-21	-0.266813
		Mass	4.02E-12	0.121354
H2O	ZnS	Distance	6.52E-25	-0.246549
		Mass	2.45E-57	0.416227
	He3	Mass	2.00E-06	0.089779
		Distance	2.61E-07	-0.097689
Nal	HIM	2.90E-10	-0.127507	
	Mass	1.65E-37	0.365202	
Pb	ZnS	HIM	7.86E-08	-0.072135
		Distance	1.34E-10	-0.052279
	He3	Mass	1.97E-10	0.108968
		Distance	5.63E-24	-0.239665

Table 2: Significant main effects for U

Plutonium				
Shielding	Detector Type	Significant Main Effects	p-value	Regression Coefficient
Fe	He3	Distance	1.49E-46	-0.34611
		Distance	6.05E-12	-0.188574
	Nal	Shield Thickness	4.24E-08	-0.138021
		HIM	4.00E-06	-0.111523
	ZnS	Distance	3.84E-34	-0.25931
		HIM	5.06E-13	-0.089388
H2O	He3	Distance	4.34E-09	-0.156478
		Shield Thickness	1.87E-13	-0.216309
	Nal	Distance	4.92E-08	-0.095264
		Shield Thickness	1.70E-08	0.099495
	ZnS	HIM	3.56E-12	-0.133089
		Distance	4.41E-09	-0.154118
Pb	ZnS	Shield Thickness	1.13E-14	-0.230257
		Distance	3.13E-49	-0.344564
	He3	Distance	2.07E-38	-0.34834
		HIM	1.14E-09	-0.078125
	Nal	Distance	2.72E-31	-0.252262
		HIM	2.67E-11	-0.087419

Table 3: Significant main effects for Pb

## 5.2. Interaction effects

Interaction effects refers to the difference in the response between the levels of one factor not being the same at all levels of the other factors. In interaction plots, we plot the response of a given factor for the levels of another factor. If the plotted lines for a factor are parallel to each other, this would indicate no presence of interaction between factors, whereas two lines that are not parallel would indicate an interaction between them. Figures 6-7 shows interactions plots for the source U and Pb respectively. Rows in each figure represent different detector types (He3, Nal, and ZnS) and columns represent different shielding types (Fe, H2O, and Pb).

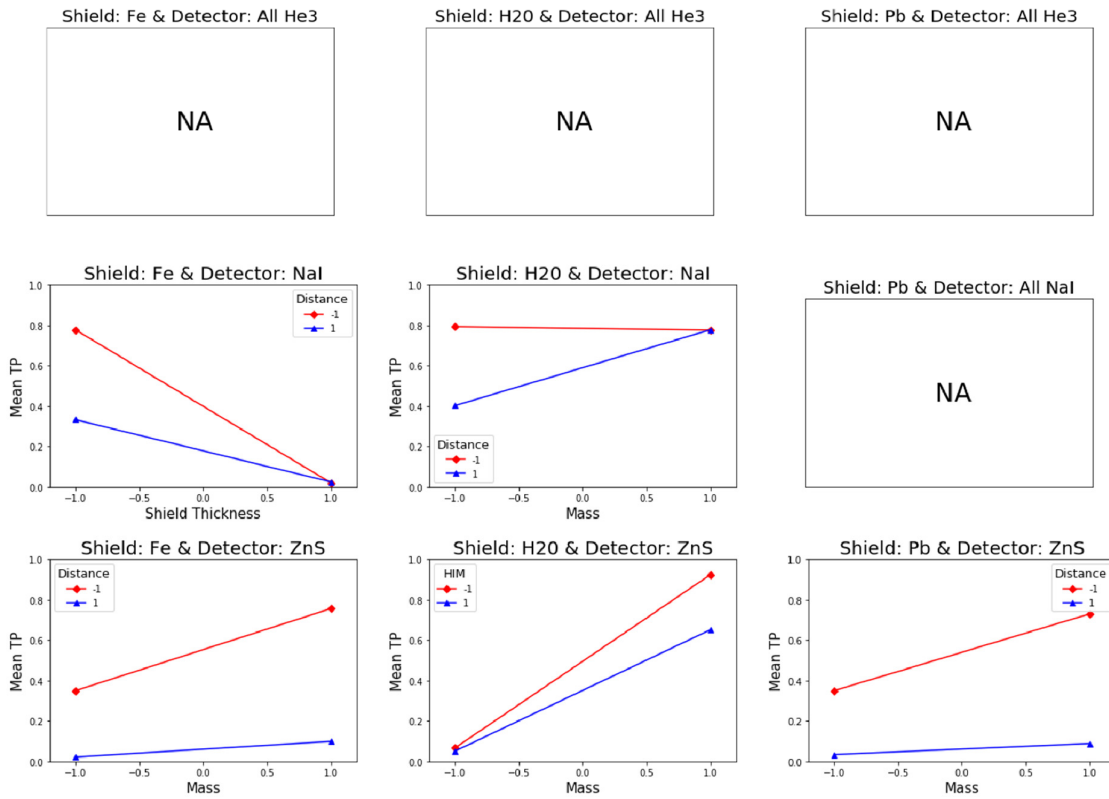


Figure 6: Interaction plots for U

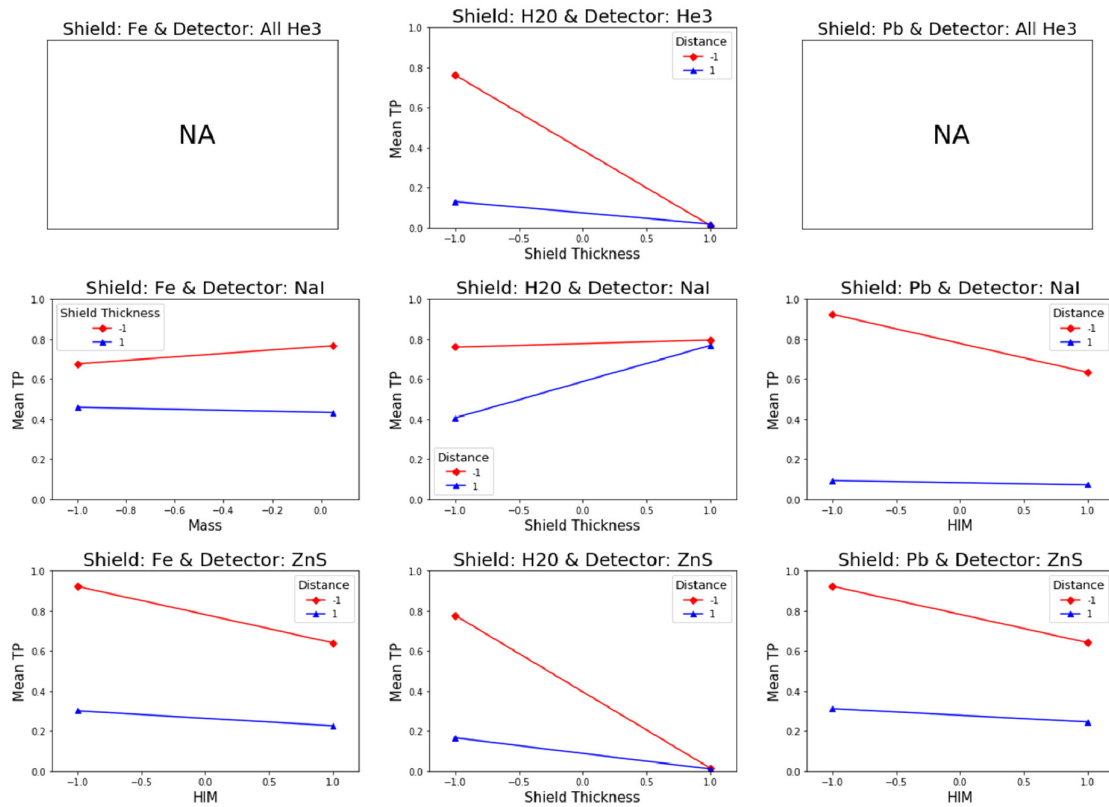


Figure 7: Interaction plots for Pb

As before, we also provide a summary of significant interaction effects for U and Pb as shown in Tables 4 and 5 respectively. Again, we define significant based on effects having a statistical significance (p-value < 0.05) and practical significance (regression coefficient >0.05).

Uranium				
Shielding	Detector Type	Significant Interactions	p-value	Regression Coefficient
Fe	Nal	Shield Thickness-Distance	1.55E-19	0.112484
	ZnS	Mass-Distance	1.09E-18	-0.082357
H2O	Nal	Mass-Distance	2.40E-16	0.09834
	ZnS	Mass-HIM	3.06E-12	-0.064355
Pb	ZnS	Mass-Distance	3.20E-16	-0.081462

**Table 4:** Significant main effects for U

Plutonium				
Shielding	Detector Type	Significant Interactions	p-value	Regression Coefficient
Fe	Nal	Mass-Shield Thickness	1.66E-03	-0.05506
		Shield Thickness-Distance	1.40E-19	-0.138444
	ZnS	HIM-Distance	5.14E-13	0.051725
H2O	He3	Shield Thickness-Distance	1.68E-27	0.159961
		Mass-Distance	4.54E-03	0.053788
	Nal	Shield Thickness-Distance	6.00E-11	0.08195
		Shield Thickness-Distance	3.37E-24	0.152295
Pb	Nal	HIM-Distance	2.91E-15	0.066992
	ZnS	HIM-Distance	2.59E-12	0.053825

**Table 5:** Significant main effects for U

## 6. Findings

Next, we provide a summary of findings based on the results of the DOE evaluation of NINESIM. First, the results show that NINESIM is behaving as expected across the levels of different input factors. In regard to main effects, the results show the following:

- Distance to from the source to the detectors is consistently an influential factor among all sources
- SNM mass stands out by having a large impact for U
- For the tested levels, velocity does not show a significant influence
- TP results can vary dramatically as detector types change for different SNM sources
  - K-40 shows poor TP results for He-3 and ZnS detectors compared to Nal detector
  - Because latter two detectors are geared at detecting neutrons which are absent from K-40 whereas Nal is geared at gamma detection
  - All of the above results conform to expectations

In regard to interactions, the results show the following:

- Mass is the most influential factor for U, as all but one of its most significant interactions per shielding and detector type involve mass
- Distance, shield thickness, and HIM are consistently influential for Pu when interacting among them

In summary, we have shown that statistical design of experiments is an effective and efficient approach to assess a wide variety of input settings that affect overall system performance for the test and evaluation of NINESIM. DOE also allows us to explore how results change when factors are simultaneously varied and it enables us to also assess the interactions between factors. DOE can be a powerful tool in your nonproliferation toolbox too!

## 5. Acknowledgements

This work has been supported by the U.S. Department of Homeland Security's Countering Weapons of Mass Destruction (CWMD) Office under contract/IAA HSHQDN-16-X-00060. This support does not constitute an express or implied endorsement on the part of the Government.

## 8. References

- [1] MoreSteam, *Design of Experiments (DOE)*, <https://www.moresteam.com/toolbox/design-of-experiments.cfm>, accessed 15 Feb 19.
- [2] Treglia, M., *Understanding Design of Experiments*, <https://www.qualitydigest.com/inside/quality-insider-article/understanding-design-experiments.html>, accessed 15 Feb 19.
- [3] Montgomery, D.; *Design and Analysis of Experiments*, 9th. ed.; New York: John Wiley and Sons; 2017.
- [4] DOES; *Statistical Design of Experiments (DOE)*; <http://www.doesinc.com/knowledge.htm#miracle>, accessed 15 Feb 19.
- [5] Antony, J.; *Design of Experiments for Engineers and Scientists*, 2nd Edition; Amsterdam: Elsevier; 2014; p 63-85; <https://doi.org/10.1016/B978-0-08-099417-8.00001-8>.

# Modellers meet practitioners: On 20% SFSF selection probability and random physical inventory verifications

**Thomas Krieger**

Forschungszentrum Jülich GmbH, Jülich, Germany  
E-mail: t.krieger@fz-juelich.de

**Rudolf Avenhaus**

Universität der Bundeswehr München, Neubiberg, Germany  
E-mail: rudolf.avenhaus@unibw.de

**Tom L. Burr**

Los Alamos National Laboratory, Los Alamos, USA  
E-mail: tburr@lanl.gov

## **Abstract:**

*Due to Germany's phase out of nuclear energy production, discussion on current and future inspection regimes for long term spent fuel storage facilities (SFSFs) with static inventory has revived recently. In current practice, in some States, randomly scheduled inspections (RSIs) of SFSFs are performed such that in each year any particular SFSF of the State is selected for RSIs with a required selection probability of (say) 20%. Three questions arise from such a requirement: First, how are the SFSFs selected for the RSIs and when are the RSIs performed? Second, how many – a fixed or expected number of RSIs – have to be performed to achieve the required selection probability? Third, if a fixed or expected number of RSIs assure the 20% selection probability, is this number equal to 20% of the number of SFSFs in the State? Regarding future inspection regimes for static long term SFSFs, instead of a regular physical inventory verification (PIV) only random PIVs are being considered. Here the question is to calculate the probability that a PIV is performed in any year, under the requirement that at least one PIV has to be scheduled within (say) 5 years?*

*This paper addresses all these questions, and instead of a typical conference paper the format is a fictitious meeting between modellers and practitioners, e.g. statisticians and inspectors. This way both parties' ideas and concepts and the ways of thinking are made explicit, and the surprises that can happen on both sides in the course of those meetings are illustrated.*

**Keywords:** Spent fuel storage facilities, Selection probability, Random PIVs, Safeguards approach

## **1 Introduction**

Due to Germany's phase out of nuclear energy production, discussion on current and future inspection regimes for long term spent fuel storage facilities (SFSFs) with static inventory has revived recently. In current practice, in some States, randomly scheduled inspections (RSIs) of SFSFs are performed such that in each year any particular SFSF of the State is selected for RSIs with a required selection probability (SP) of (say) 20%.

In section 2, an inspection scheme is developed under three assumptions, namely:

- i) the order of the SFSFs selected for verification is important,
- ii) the number of RSIs is a fixed integer, and
- iii) timing of the RSIs is not taken into account.

In ii) the fixed integer must not be understood as an expected value even though practitioners might prefer that. We justify our model by arguing that on one hand, planning is easier with fixed numbers of annual RSIs, and that on the other, if one wishes so, an expected number of e.g. five RSIs per year can be realized by 9, 3, 7 and 1 RSI(s) in four years.

For this model, the number of RSIs is determined to achieve a required SP. In this context two recurring statements are discussed: The number of RSIs needed to achieve a required SP of (say)  $p$  is usually not equal to  $p \times 100\%$  (rounded up) of the number of SFSFs in the State. Second, suppose the number of inspected SFSFs is  $p \times 100\%$  of the number of SFSFs in the State (rounded up). Does this imply that the achieved SP is at least  $p$ ?

In section 3 the probabilistic model developed in section 2 is extended and limited repetitions are taken into account, which means that a SFSF can be selected for verification at most (say) three times. Limited repetitions are needed to exclude cases in which all RSIs are performed in one SFSF.

In section 4 an inspection scheme for random PIVs is analysed, where in a certain number of consecutive years at least one PIV has to be performed. This scheme is simulated and the limiting distribution for performing a PIV is determined. Also the approximate year in which the steady state is reached is assessed using simulation.

Sections 2 to 4 can be seen as a transcription of meetings between practitioner(s) (P) and modellers (M). Therefore, the wording fits in with a meeting atmosphere.

The derivations of the results in this paper as well as extensions can be found in [1].

## 2 First meeting: Problem formulation and probabilistic modelling

P: Hello and good morning. Thanks for making this meeting possible. Today we want to discuss probabilistic aspects of planning verifications in long term spent fuel storage facilities (SFSFs).

First let me describe the situation: We consider a State with a number of SFSFs in which a number of inspections is performed per year. The number of inspections is chosen such that any particular facility in the State is selected for verification with 20% selection probability (SP) per year.

M: Interesting! Do you know where the “20% SP requirement” comes from, or stating it differently: Is there a systems analysis view point behind that?

P: Unfortunately, not. I have never seen any justification behind that. I know that you guys could come up with models that can be used to determine the required SP such that the State is deterred from behaving illegally, but for the moment let us just assume that the “20% SP requirement” is agreed upon.

M: That’s okay for the moment. When you talk about “20% SP requirement” does this mean that you allow for random physical inventory verifications (random PIVs) in SFSFs?

P: Oh no, not yet, at least. This idea is appealing especially for static long term SFSFs but let us postpone this topic to a later meeting. For now, we assume that in each SFSF one PIV is performed.

M: So, the PIV’s are scheduled at fixed time points. What kind of inspections are we talking about?

P: Typically, in SFSFs two types of inspections are distinguished: “Regularly scheduled inspections and design information verification”, for example PIVs, and “Randomly scheduled inspections” (RSIs). The purpose of RSIs is to detect and deter undeclared activities, which may take place at a SFSF.

M: Well, if there is a 20% probability that any particular facility is selected at least once per year for an RSI, and if this selection is done independently of the selection of other SFSFs, then the probability that no RSI is performed at all, is given by  $0.8^n$ , which simplifies to  $\approx 0.07$  in case of (say)  $n = 12$  SFSFs in the State.

P: Oh, no! Sorry, I forgot to mention that at least one RSI must be performed per year in all SFSFs in the State.

M: Well, that’s indeed an important information that corrupts the independence assumption! That means just “rolling a dice” for each SFSF independently will not meet this requirement because none of the facilities might be inspected. So .... How do we model this situation appropriately?

Let us develop it together. The simplest case is that exactly  $k = 1$  RSI is performed in the State. Then the inspector chooses the SFSF randomly from the set  $\{1, \dots, 12\}$ , and each elementary event, i.e. to choose SFSF no.  $i = 1, \dots, 12$  for inspection, has the probability  $1/12 < 0.2$ .

P: Well, that is obvious. The result implies that one RSI in the State will not achieve the “20% SP requirement”. Can we try two RSIs?

M: Sure! In that case the inspector chooses the SFSF(s) to be inspected from the set

$$\{(1,1), (1,2), \dots, (1, n), (2,1), \dots, (2, n), (3,1), \dots, (n, n)\}$$

where for example (1,1) means that both RSIs are performed in SFSF no. 1, and (1,2) means that the first RSI is performed in SFSF no. 1 and the second RSI in SFSF no. 2. This set is sometimes referred to as the sample space of the random experiment because it contains all possible outcomes of the random trial.

P: That means you assume that the order the SFSFs are selected for inspection is important. So you do not explicitly talk about the time or day of inspection, but only about the order the SFSFs are inspected.

M: Right! This is a modelling assumption that can be questioned. But for now we keep it.

P: I think that is fine for now. So, what is in this case the probability that any particular SFSF in the State is selected for verification?

M: Well first we have to define the probability of the elementary events  $(i, j)$ , i.e. what is the probability that the pair  $(i, j)$  of SFSF(s) is/are inspected? Because the SFSFs are assumed to be equal, it is natural to use the equal distribution, thus any elementary event has the probability  $1/n^2$ . Which elementary events are in favour for the selection of (say) SFSF no. 1? Well that’s easy. They are given by  $(1,1), (1,2), \dots, (1, n), (2,1), (3,1) \dots, (n, 1)$ . Thus, the probability to inspect SFSF no.  $i = 1, \dots, n$  at least once per year is

$$\frac{2n - 1}{n^2} = 1 - \frac{(n - 1)^2}{n^2}.$$

P: Can you give an example?

M: The above result implies that if less than 10 SFSFs are in a State, then the “20% SP requirement” is fulfilled, because we have (rounded to the second digit):

$n$	2	3	4	5	6	7	8	9	10
$\frac{2n-1}{n^2}$	0.75	0.56	0.44	0.36	0.31	0.27	0.23	0.21	0.19

P: This is a useful result because we have quite a few States with 9 or fewer SFSFs. So, in case of more than 9 SFSFs in a State we certainly achieve less than 20% SP with two RSIs. What we need is a formula which gives the selection probability as a function of the number  $n$  of SFSFs and the number  $k$  of RSIs.

M: Agreed. In the general case of  $k$  RSIs, the selection probability, i.e. the probability of selecting any particular SFSF at least once per year, is given by

$$\mathbb{P}(\text{at least one RSI in SFSF no. } i) = 1 - \mathbb{P}(\text{no RSI in SFSF no. } i) = 1 - \frac{(n-1)^k}{n^k}, \quad (1)$$

which is the same for all SFSFs – as expected, because the SFSFs are assumed to have the same characteristics.

P: That's nice. Now I realize how  $n$  and  $k$  are related to each other. What I like about Eq. (1) is that it can be used in two ways: 1) For evaluating current approaches regarding the question of the achieved selection probability, and 2) For determining the number of RSIs for any given selection probability  $p$ , and not just for  $p = 0.2$ !!

M: That's right! Regarding your remark 1): Using Eq. (1) for the assessment of existing approaches you have to assure that current inspection planning is done according to the model. Otherwise you compare apples and oranges and your conclusions are incorrect.

P: I agree. So, I need to go back to our software description and check whether the model developed here coincides with the one implemented in the software.

M: Right. Regarding your comment 2): For a fixed number  $n$  of SFSFs in a State and a given required selection probability  $p$ , the number of RSIs has to be (at least)

$$k \geq \frac{\ln(1-p)}{\ln(1-1/n)} \quad (2)$$

to achieve  $100 \times p\%$ . For a State with  $n = 12$  SFSFs and  $p = .2$  we get  $k \geq 3$ .

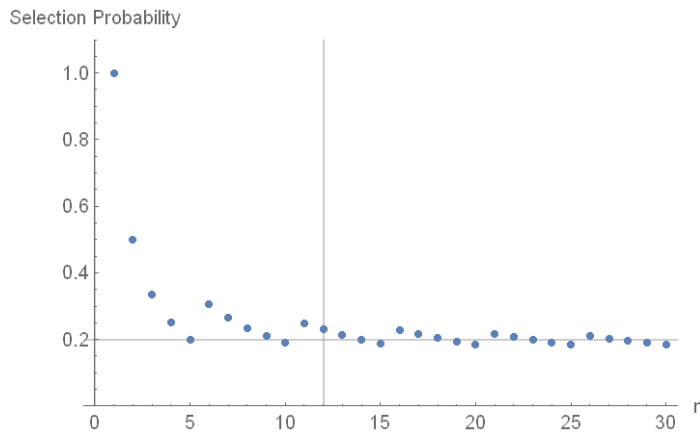
P: Let us discuss a little bit Eqs. (1) and (2). Because the number  $n$  of SFSFs is given – and if we stay with the 20% SP, then Eq. (2) gives us the number  $k$  of RSIs. Is this number the same as 20% of the number of SFSFs in the State (rounded up)?

M: (Sceptical frown) What? Do you ask the question if the number of RSI is 20% of the number of SFSFs, i.e.  $k = [0.2 n]$ ,<sup>1</sup> then the selection probability is (at least) 20%?

P: Yes, this is the question. In [2] on page 13 this relation is used.

M: Well, this is not always true! Using Eq. (1), we get for  $k = [0.2 n]$  the following figure for a State with up to 30 SFSFs.

<sup>1</sup>  $[a]$ : the ceiling is the smallest integer not less than  $a$ , e.g.,  $[2.3] = 3$  and  $[5] = 5$ .



You see that for some  $n$  the selection probability is smaller than the required 20% SP. In the example case of  $n = 12$  SFSFs, however, the 20% SP can be assured with  $k = \lceil 0.2 \times 12 \rceil = 3$  RSIs.

P: I am surprised! Thus the two statements “the number  $k$  of RSIs to achieve a 20% SP” and “ $k = \lceil 0.2 n \rceil$  guarantees a 20% SP” do not mean the same.

M: Yes, they are not equivalent!! We recommend deleting the “ $k = \lceil 0.2 n \rceil$  guarantees a 20% SP” statement. By the way, there is another formulation which is sometimes used in this context: “If 20% of the SFSFs are inspected then a 20% SP is achieved”.

P: I can’t see the difference between both statements.

M: Well, in the “ $k = \lceil 0.2 n \rceil$ ” statement the number of RSIs is addressed, while in the second statement the number of inspected SFSFs is referred to: at least  $\lceil 0.2 n \rceil$  different SFSFs are inspected.

P: I see. Both statements sound so similar and only after digesting and thinking about them you realize the difference between them. Is it difficult to determine the probability for at least one RSI in any arbitrary facility?

M: This is quite challenging. Why? Because you must exclude all elements from the sample space that do not contain at least  $\lceil 0.2 n \rceil$  different SFSFs. For example:  $(1, \dots, 1), \dots, (n, \dots, n)$  must be excluded and many more. Your last question is too difficult to be answered on the fly.<sup>2</sup>

P: Okay. Thanks for the joint development effort. I think we should stop here, digest the model developed today and discuss any arising questions in the next meeting.

Note: If the order of the SFSFs to be inspected does not matter, then the selection probability is given by

$$\mathbb{P}(\text{at least one RSI in SFSF no. } i) = 1 - \frac{\binom{n-1+k-1}{k}}{\binom{n+k-1}{k}} = \frac{k}{n+k-1},$$

see [1] for further details.

<sup>2</sup> A related topic is addressed in section 3.

### 3 Second meeting: Extension of the probabilistic model

P: Hi folks, thanks for being back to discuss the RSI approaches. Let me summarize the model we discussed in the last meeting:

We consider a State with  $n$  SFSFs in which  $k$  RSIs are performed. The number  $k$  is understood as a fixed integer, and not as an average value, e.g., four RSIs are performed per year. The case that the expected number of RSI per year is considered is deferred to another meeting. Furthermore, the order in which the SFSF are selected for verification is important, but timing aspects are neglected here.

M: Exactly, these are the model assumptions.

P: According to our model, all RSIs might have to be performed in the same SFSF, right?

M: Yes, this probability is

$$\mathbb{P}(\text{all } k \text{ RSIs are performed in the same SFSF}) = \frac{n}{n^k} = \frac{1}{n^{k-1}},$$

which yields  $1/144 \approx 0.00694$  in case of  $n = 12$  SFSFs and  $k = 3$  RSIs, and which is small but positive!

P: Yes, this probability is small and, by the way, we would never perform all three RSIs in one SFSF.

M: (Angry) But these are boundary conditions you have to tell us beforehand! So ... a quick but dirty solution is to run the computer program again if e.g.  $(1, \dots, 1)$  is selected by the computer.

P: I think we can live with that.

M: You might, but from a modelling point of view this is not convincing at all. First we allow that, e.g.,  $(1, \dots, 1)$  is an element of the sample space knowing beforehand that if this element is chosen, then it will be rejected. These possibilities should be excluded from the very beginning.

P: I see your point. What would be the difference in the models, and how does the selection probability change?

M: Let  $c$  be the number of maximal repetitions of an SFSF to be inspected. For example: If  $c = 3$  then any of the  $n$  SFSFs can only be inspected up to three times per year. Clearly we have to have  $cn \geq k$  because otherwise we cannot schedule  $k$  RSIs.

Unfortunately, the formula of the selection probability gets more complicated, and analytical results only exists for some cases of  $c$ :

$$\begin{aligned} & \mathbb{P}(\text{at least one RSI in SFSF no. } i) \\ &= \begin{cases} 1 - \frac{(n-1)^k}{n^k} & \text{for } c = k \\ 1 - \frac{(n-1)^k - (n-1)}{n^k - n} & \text{for } c = k - 1 \\ 1 - \frac{(n-1)^k - (n-1) - k(n-1)(n-2)}{n^k - n - k n (n-1)} & \text{for } c = k - 2 \\ 1 - \frac{\binom{n-1}{k} k!}{\binom{n}{k} k!} = \frac{k}{n} & \text{for } c = 1. \end{cases} \quad (3) \end{aligned}$$

For  $k \geq 5$ , and the cases  $c = 2, \dots, k - 3$  a computer program needs to be used to determine the number of elements in the sample space, and the interesting probabilities.

P: Well, that is getting complicated fast. Why is that?

M: Let us consider the case  $c = k - 2$ , i.e. at most  $(k - 2)$  repetitions are possible. Then you have to exclude from the original sample space the  $n$  tuples  $(1, \dots, 1), \dots, (n, \dots, n)$  and the  $k n (n - 1)$  tuples  $(i, \dots, i, j), (i, \dots, j, i) \dots, (j, i \dots, i)$  with  $i \neq j$ , where  $i$  appears  $k - 1$  times. You have to count all these elements and then you get the expression for  $c = k - 2$ .

P: I see. What does it mean for the example State with  $n = 12$  SFSFs and  $k = 3$  RSIs?

M: We have seen that  $k = 3$  RSIs are enough to achieve a 20% SP. If a priori any particular SFSF can only be inspected up to two times, i.e.  $c = 2$ , then Eq. (3) implies  $3/13 \approx 0.2308$  which is higher than the respective probability  $397/1728 \approx 0.2297$  for  $c = 3$ , as expected.

P: Got it. I suggest that we do not put too much effort in the case with limited repetitions because we can live with the fact to run the program again if an unfortunate combination, such as all RSIs have to be performed in the same SFSF, is chosen by the computer.

In the next meeting I want to consider random PIVs. Thanks and see you then!

Note: In [1] a Mathematica® program to calculate the probabilities in Eq. (3) for all values  $c = 2, \dots, k - 3$  is presented. Also, the model in which the order of the SFSFs to be inspected does not matter is analysed in the case of limited repetitions. Furthermore, in [1] an approach is developed in which the number of RSIs is regarded as an expected number and timing aspects are included.

#### 4 Third meeting: Random PIVs

P: Good afternoon. After having talked about RSI planning in the last meetings, today we want to approach the topic of random PIVs, an idea that is in the air for the last few years.

M: That sounds interesting! Especially from the material balance evaluation point of view in which PIV data are really essential.

P: You are right. Today, however, we do not want to discuss the data evaluation topic but a specific PIV inspection scheme: Suppose a PIV has to be carried out at least every five years. What is the probability to have a PIV in arbitrary year?

M: To get it right: Do you mean to have at least one PIV in five consecutive years?

P: Yes, that is the design. And we want to know the probability that a PIV is performed in any particular year.

M: Let's try to formalize this inspection scheme. For year 1,2,3 and 4, let  $p$  be the probability that a PIV is performed that year. What happens in year 5? If at least one PIV is performed during years 1, ..., 4, then the probability that a PIV is performed in year 5 is  $p$  again. If there is no PIV during years 1, ..., 4, then there must be a PIV in year 5.

P: I agree. What is the probability of a PIV in year 5?

M: It is given by

$$p(1 - (1 - p)^4) + 1(1 - p)^4 = 1 - 4p + 10p^2 - 10p^3 + 5p^4 - p^5, \quad (4)$$

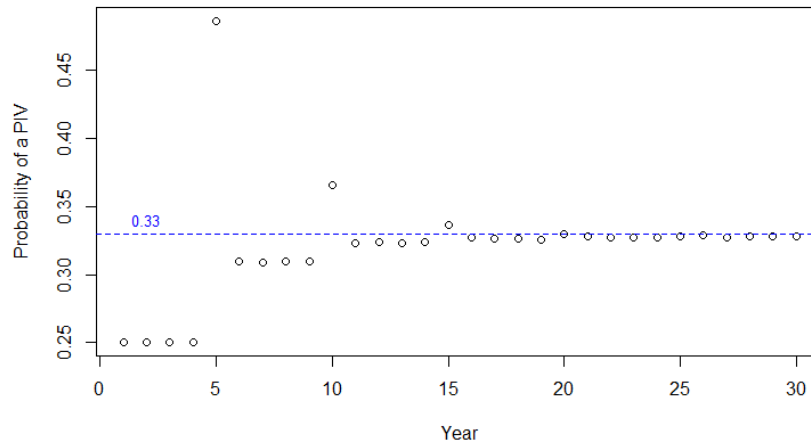
because a PIV is performed with probability  $p$  in year 5 if there is at least one in years 1, ..., 4 which happens with probability  $1 - (1 - p)^4$ , and a PIV is performed with probability 1 in year 5 if there is none in years 1, ..., 4 which happens with probability  $(1 - p)^4$ .

P: The probability in Eq. (4) is obviously much more complicated compared to the probability  $p$  for the years 1, ..., 4.

M: Yes, this is due to the inspection regime: at least one PIV in five consecutive years.

P: I guess that the equations for years 6,7, .... gets even more complicated.

M: Yes, indeed. We model this PIV scheme as Markov chain, and then you can determine the probabilities using the so-called Chapman–Kolmogorov equation. Here, instead of deriving the probabilities for years 6,7, ..., we perform  $10^6$  simulation of this PIV scheme for  $p = .25$  and get the figure:



P: Wow, that is interesting. The probabilities to have a PIV seem to be the same for all years between the multiples of five years. And there is a limit of 0.33 reached for say 20 and more years.

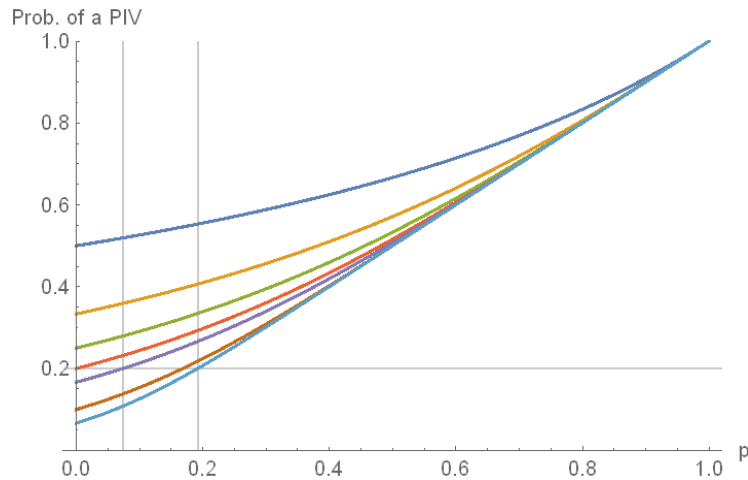
M: That's right. The probabilities seem to be the same for all years between the multiples of  $\ell$  years. However, it is difficult to give a simple explicit expression of the probabilities before the steady state is reached. In the limit or in the long run as you might also call it, however, this is not difficult at all! It can be shown that the steady state probability is

$$\frac{p}{1 - (1 - p)^\ell}, \quad (5)$$

if  $\ell$  is the number of consecutive years in which at least one PIV must be performed.

P: This expression is simple as compared to the probability in Eq. (4) to perform a PIV in year five. Does it mean that the system settles after some years at the probability given by Eq. (5)?

M: Right you are. Eq. (5) gives the probability that a PIV is performed in any year in the long run. Here is a visualization:



It shows Eq. (5) for  $\ell = 2, \dots, 6, 10, 15$  from top to bottom. For  $p = 0$  we have  $1/\ell$  as expected, because the PIVs are only performed in years  $\ell, 2\ell, 3\ell, \dots$

P: And as you have indicated with the horizontal line: The 20% probability can be reached using different  $\ell$  values. So, I might have at least one PIV in six consecutive years and  $p$  is approximately 0.07, or I achieve the same probability of 20% with at least one PIV in 15 consecutive years with a  $p$  of about 0.19.

M: Exactly! You can play with the parameters  $\ell, p$  and the required probability.

P: Yes, this is helpful. Though, one thing is still unclear to me. You said that this limit is reached when the system is somehow settled. But when is it settled?

M: This is an important question, and we are going to answer it by simulation. Let  $n$  be the minimum time step at which the absolute difference between the probability to perform a PIV in year  $n$  and the steady state probability given by Eq. (5) is smaller or equal to  $\varepsilon$ , where we choose arbitrarily  $\varepsilon = .04$ . The table shows estimated values of  $n$  using an R simulation:

```
> tempmat
      [,1] [,2] [,3] [,4] [,5] [,6] [,7] [,8]
[1,]  52  57  56  55  57  57  55  61
[2,]  25  25  26  25  29  25  28  21
[3,]  16  17  16  13  15  17  19  11
[4,]  13  13  11  13   8   9  10  11
[5,]  10   9  11   7   8   9  10   1
[6,]   7   5   6   7   8   1   1   1
[7,]   7   5   6   7   1   1   1   1
[8,]   4   5   6   1   1   1   1   1
[9,]   4   5   1   1   1   1   1   1
[10,]  4   1   1   1   1   1   1   1
> |
```

The first row represents the  $\ell$ -values from 3, ..., 10, and the first column the probabilities  $p$  from 0.05 to 0.5 in steps of 0.05. The entries in the matrix give the estimated minimum time steps to reach the steady state probability in  $10^5$  simulations. We see for example that in case of  $\ell = 3$  and  $p = 0.05$  about 52 years have to be waited until the steady state is reached.

P: How do we relate the values in this table to the steady state probability?

M: If, e.g., we require that a PIV is performed every year with 20% probability, then Eq. (5) yields different  $p$ -values for different  $\ell$ -values, and the above table can be used to give boundaries on the expected minimum number of time steps until the steady state probability is reached:

$\ell$	5	6	7	8	9	10
$p$	0.0	0.07	0.11	0.14	0.16	0.17
Estimated year	$\geq 56$	25, ..., 55	15, ..., 29	17, ..., 25	10, ..., 19	11

P: Now I see the relation, and I am surprised that it takes so long in some cases. I think that for some combinations of  $\ell$  and  $p$  values we will have to rely on the exact probabilities. Just working with the limiting distribution will not be sufficient.

M: Yes, this may well be the case. The exact probabilities can be derived with computer programs, if you decide you will rely on them.

P: Wrapping up we can say that for the specific random PIV scheme discussed today the steady state probability that a PIV is performed in any year can be determined.

Regarding State-Level considerations, however, I am now curious how this scheme can be generalized to more than one facility.

M: That's indeed an interesting topic. Unfortunately, we have to postpone its discussion until our next meeting. Please keep in mind that the work on these topics cannot be done overnight and is often associated with substantial development effort!

P: Yes, we keep that in mind and will come back to you in due time.

Note: Using a Theorem by Doeblin, see [3] or [4], it can be shown that the absolute difference between the probability of a PIV and the steady state probability given by Eq. (5) is smaller or equal to  $\varepsilon$  for all  $n \geq n_0$  where

$$n_0 := \frac{\ln(\varepsilon/2)}{\ln(1-p)}.$$

For the Markov chain considered here, the steady state probability is usually reached earlier than in year  $n_0$ : The Theorem by Doeblin only gives upper limits. Details can be found in [1].

## 5 References

- [1] T. Krieger, R. Avenhaus and T. L. Burr, "Modellers meet practitioners: On 20% SFSF selection probability and random physical inventory verifications: Derivations and Extensions," *ESARDA Bulletin*, 2019 (in preparation).
- [2] IAEA/EURATOM, "Partnership Approach under Integrated Safeguards for Spent Fuel Storage Facilities (SFSFs)," 2008.
- [3] W. Doeblin, "Exposé de la Théorie des chaînes simples constantes de Markoff à un nombre fini d'États," *Revue Math. de l'Union Interbalkanique*, vol. 2, p. 77–105, 1938.
- [4] D. W. Stroock, *An Introduction to Markov Processes*, 2nd ed., Berlin Heidelberg: Springer, 2014.

## Improve a weighing scale with operator concerns

Vincent Bruel<sup>1</sup>, Stéphane Puydarrieux<sup>2</sup>, Bernard Thauvel<sup>3</sup>, Marcel Mokili<sup>4</sup>

1 Orano Chemistry & Enrichment, 2 Orano Recycling, 3 Consultant engineer in metrology, 4 SUBATECH – IMT Atlantique, CNRS/IN2P3, Université de Nantes

E-mail: [vincent.bruel@orano.group](mailto:vincent.bruel@orano.group)

### **Abstract:**

*In principle, in a nuclear plant context, the precision of accounting scales shall be equal to or lower to International Target Values. A pragmatic approach should observe that ITVS and the impacts on a material balance test may differ, for example, depending on the intensity of use of each instrument.*

*Improving the precision of an instrument should be profitable to both operator and inspector:*

- *For inspector: to reduce the Material Unaccounted For in order to reduce the risk of misuses.*
- *For operator: to reduce non-quality costs due to handling errors.*

*On the other hand, making a weighing scale more precise while the system is already active in the plant may be a complex task, while the cost of the project may be very expensive.*

*This article reminds mainly that the material balance is actually a statistical hypotheses test. We suggest therefore an approach in order to help the operator to build the best strategy to improve the power of the material balance test with an economic viewpoint, especially for weighing systems.*

*A summary of the approach could be:*

- *Select the instruments that most impact the uncertainty of the material balance.*
- *Determine the significant parameters that most impact the material balance.*
- *Avoid basic mistakes while using a weighing system.*
- *Define the best project according to costs and precision objectives.*

*This is a very pragmatic method, based on a real return of experience and statistical analysis. This approach has been shared with the CETAMA<sup>1</sup> working group in Statistics, in order to write a methodological guide applied on statistical tools for the material balance.*

**Keywords:** material balance, ITV, MUF, weighing, operational research

# 1 Introduction

The material balance is actually a statistical test which evaluates 2 decisions in function of 2 hypotheses.

Statistical hypothesis test		True situation	
		Accounting is correct	Accounting is false
Decision	Accounting is accepted	Right decision $1 - \alpha$ is the confidence level	Wrong decision $\beta$ is the probability to falsely accept
	Accounting is refused	Wrong decision $\alpha$ is the probability to falsely refuse	Right decision $1 - \beta$ is the power of the test

Table 1 : the material balance is a statistical hypothesis test

$1 - \beta$  is indeed the most important criteria of the statistical hypothesis test: it measures the capacity of the test to detect something wrong with the nuclear accounting of the process, like accounting errors or misuses.  $1 - \beta$  depends on  $\alpha$  which is fixed by the regulator, the mass value to detect which is a variable value, and  $\sigma$  which is the uncertainty (the noise) of the Material Unaccounted For estimator. Therefore, increasing the power of this test means to reduce the  $\sigma$  value. This article suggests several common sense ideas in order to improve the power of the test.

## 2 Method to improve the power of the material balance test

### 2.1 Select the few largest contributors on the material balance

As an MUF estimator is the sum of all measurement errors, we should improve the accuracy of all instruments involved in the material balance test. As improving all instruments could cost too much, a better strategy is to select only the instruments that significantly impact the MUF estimator.

The Pareto principle is often respected for the material balance: the majority of the errors are explained by only 3 or 4 instruments involved in the material balance. Therefore, improving the power means selecting the major contributors and then improving them.

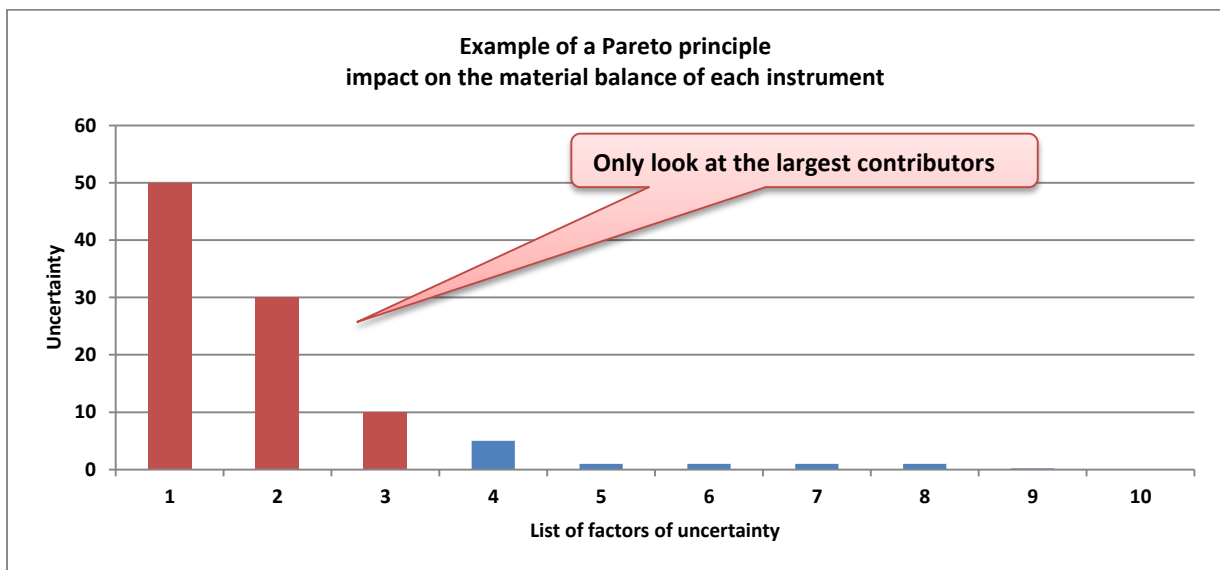


Figure 1 : impacts of instrument on sigma follow a Pareto distribution

## 2.2 Error parameters that most affect the material balance

The global error of all instruments  $\sigma$  is composed of numerous different sources of uncertainty  $\sigma_i$  that we should summarize before proceeding to the error propagation calculations. 4 error parameters are important to consider:

- The value of the standard-uncertainty.
- The duration of the material balance period (1 month, 1 year, several years).
- The intensity of use of the instrument: number of articles measured in a period of time.
- The duration of the fixed error: random or systematic error in time unit.

For this last level, an explanation is necessary. In first approach, the error is so composed of:

- Random error: sum calculation of several random errors is quadratic :  $\sqrt{\sum_i \sigma_i^2}$
- Systematic error: sum calculation of several systematic errors is algebraic:  $\sqrt{(\sum_i \sigma_i)^2}$

In further analysis, the duration is also important as it modifies the rules of propagation calculations. Systematic error could be:

- short-term, like “few months”,
- medium term, like “few years”,
- long-term, like “several years”.

The longer the duration, the larger the impact is on the material balance. It is common sense: more articles are calculated with algebraic way instead of quadratic way. This explains why long-term systematic errors represent the majority of the  $\sigma$  value of the MUF estimator.

Just consider this example: 1000 articles measured during a material balance period of 10 years, value of systematic error = 1. For each one: a different duration of the systematic term:

Duration of the systematic term	Number of terms	Number of articles by term	Impact: propagation error
No duration : random	1000	1	$1 \times \sqrt{1000} = 31.6$
1 month	120	8	$8 \times \sqrt{120} = 91.3$
1 year	10	100	$100 \times \sqrt{10} = 316.2$
2 years	5	200	$200 \times \sqrt{5} = 447.2$
10 years	1	1 000	$1000 \times 1 = 1000$

Table 2 : impact analysis of the duration of the systematic term

Same values are showed in this graph:

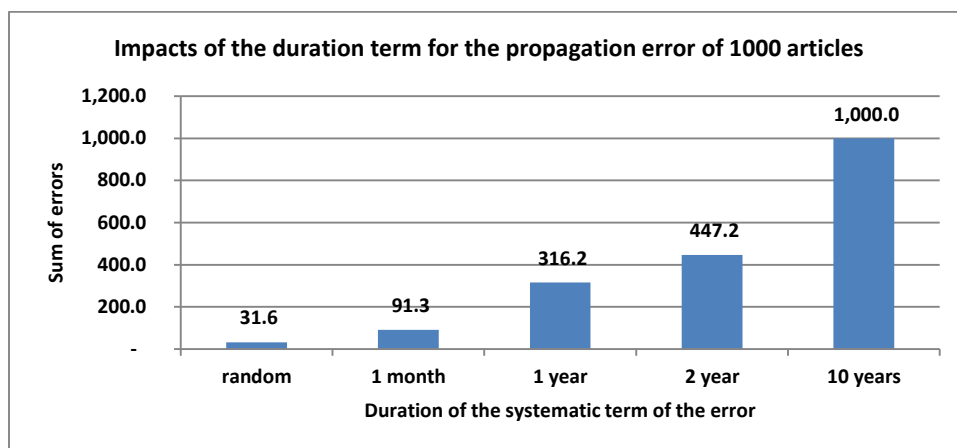


Figure 2 : example of an impact analysis of the duration of the systematic term

## 2.3 Evaluate the impact of only one instrument

### 2.3.1 Evaluation of main factors of an instrument

This excellent diagram from Ishikawa named “causes and consequence” shows how several causes can explain a consequence. The diagram groups together 5 items in a general law.

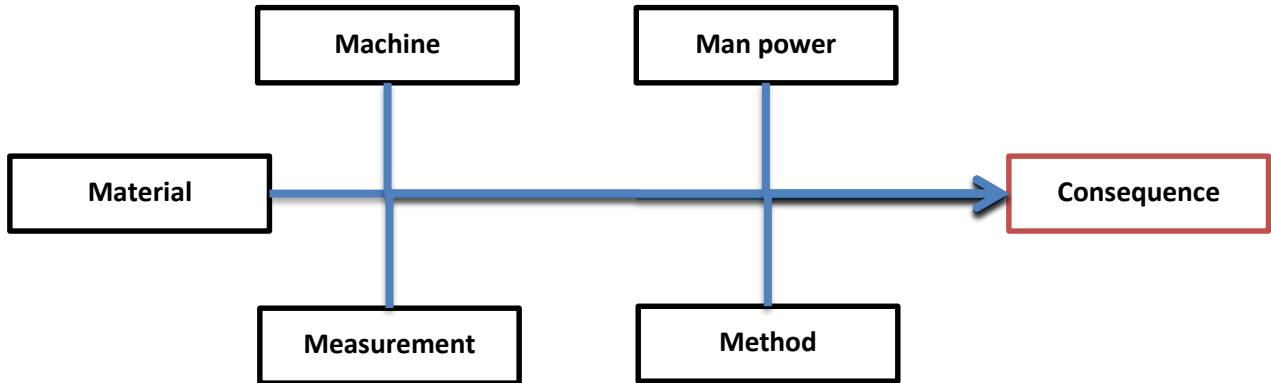


Figure 3 : Ishikawa diagram<sup>2</sup>

For the specific case of “uncertainties of the instrument”, this next diagram, which explains the rule “specific main causes  $\Rightarrow$  impact on uncertainty of the measurement chain”, is more appropriate, actually easier to use, for reasons which will be explained afterwards:

- 3 main basic factors which are always present, and are nearly equal :
  - o Calibration: the capability of the calibrator to calibrate (at the exact time of calibration)
  - o Deviation: the capability to maintain the calibration accuracy (process control)
  - o instrument: the capability of the instrument (weighing technologies)
- 2 main factors which could occur but level depends specifically on the case:
  - o Use: occurs once in a while due to a failure to comply with the procedure, (“human and organisational factor”)
  - o Methodology: sum of methodological biases (measurement standards, technical limits, error of conception, laboratory methodology)

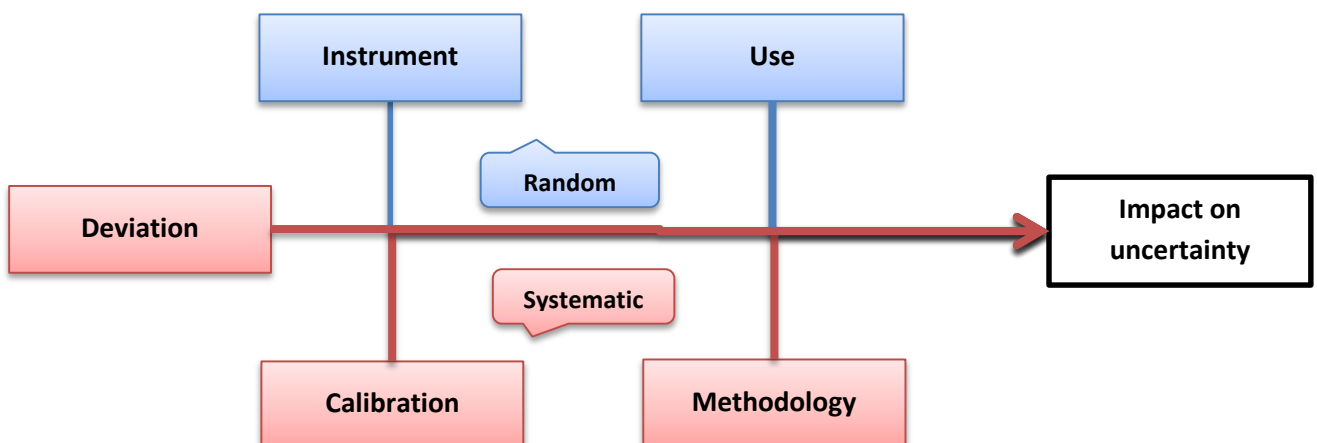


Figure 4 : “causes and consequence” diagram adapted to uncertainty calculation

These 5 main causes are clustered specifically for these 2 raisons: “Source of information” and “duration of the systematic error”, which are nearly identical for each factor.

### 2.3.2 Source of information

- ❖ **Methodology:** sum of bias due to technical limits defined by the measurement methodology

“Methodology” factor clusters all systematic biases, fixed for a very long time and always with the same sign. A basic error is measurement standards, like calibration weights. The source of information is essentially the measurement methodology and technological limits, less frequently error of conception of the measurement system or bias due to a technical difference between calibration and use.

- ❖ **Calibration:** the capability of the calibrator to calibrate the instrument

Source of information is the calibration report that the calibrator must provide, according to the regulations. This value is no less than the capability of the instrument, so if the calibration job is carried out right, this value is almost equal to the capability of the instrument.

- ❖ **Deviation:** the capability of the operator to maintain the post-calibration accuracy

Source of information is the quality control charts and thus the maximum deviation accepted by the operator after the calibration. If the work is carried out right, this value is almost equal to the capability of the instrument.

- ❖ **Instrument:** the capability of the instrument:

Source of information is the technical information report given by the supplier of the instrument. Reader must note that the capability is evaluated by the supplier with very advantageous conditions of use, as laboratory conditions.

- ❖ **Use:** the capability of user to respect the compliance

Source of information is the compliance monitoring and observations during use.

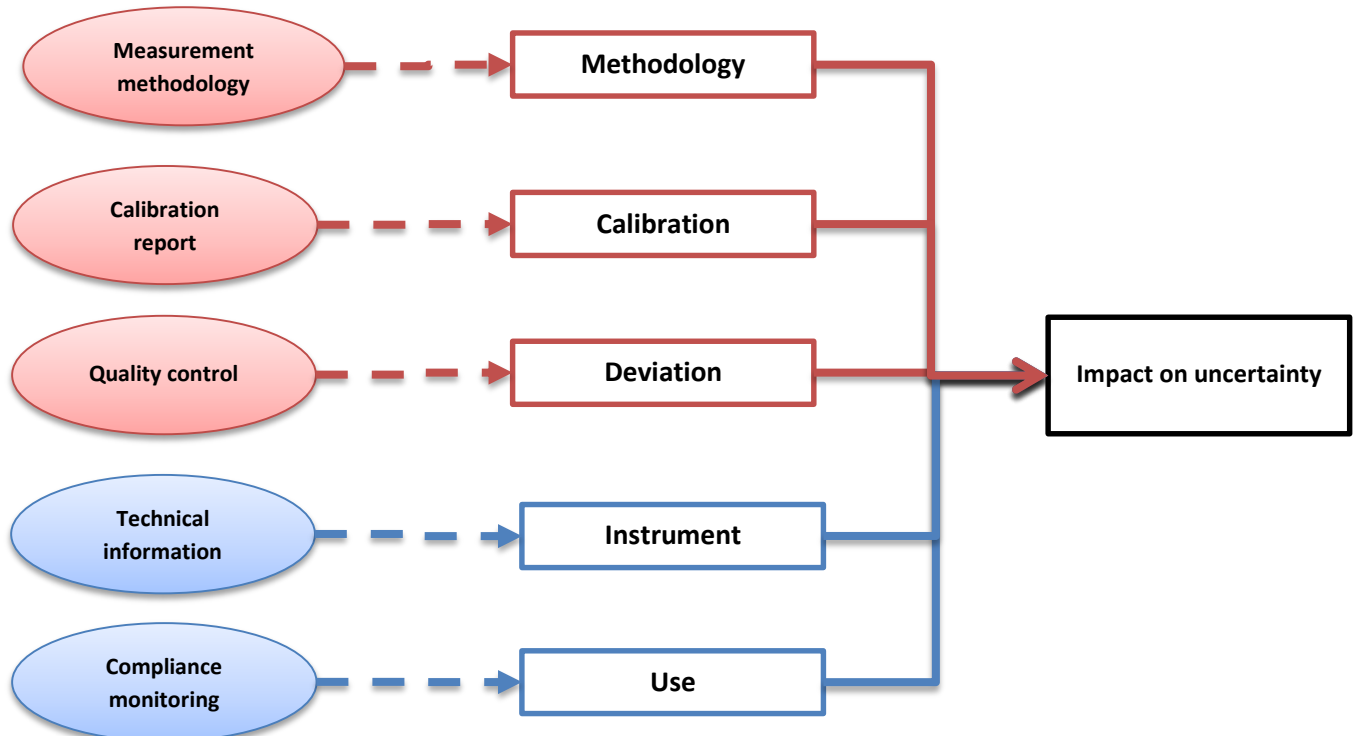


Figure 5 : each main factor has the same source of information

### 2.3.3 Duration of the systematic error

These 5 main causes have different terms for each systematic error: no-term, short-term, medium-term, long-term... actually, it depends of the case, but the general law is often this one:

- **Methodology:** long-term

The duration lasts as long as the methodology is used, and could last up to the life of the plant.

- **Calibration:** medium term between 2 calibration operations.

The duration of this error depends on the time between 2 calibrations: if and only if the calibrator modifies the calibration coefficients of the instrument.

- **Deviation:** short-term systematic error, as a trend due to biases moving within the tolerance accepted by the operator.

The main trend is due to the outside temperature (12 months) or intensity of use that could lead to material fatigue.

- **Instrument:** random error due to the capability of the instrument
- **Use:** the error occurs only once in a while

In order to represent the main factors with the duration context, let us look at this graph that shows that the 5 main factors could impact the observed value of the instrument in different ways.

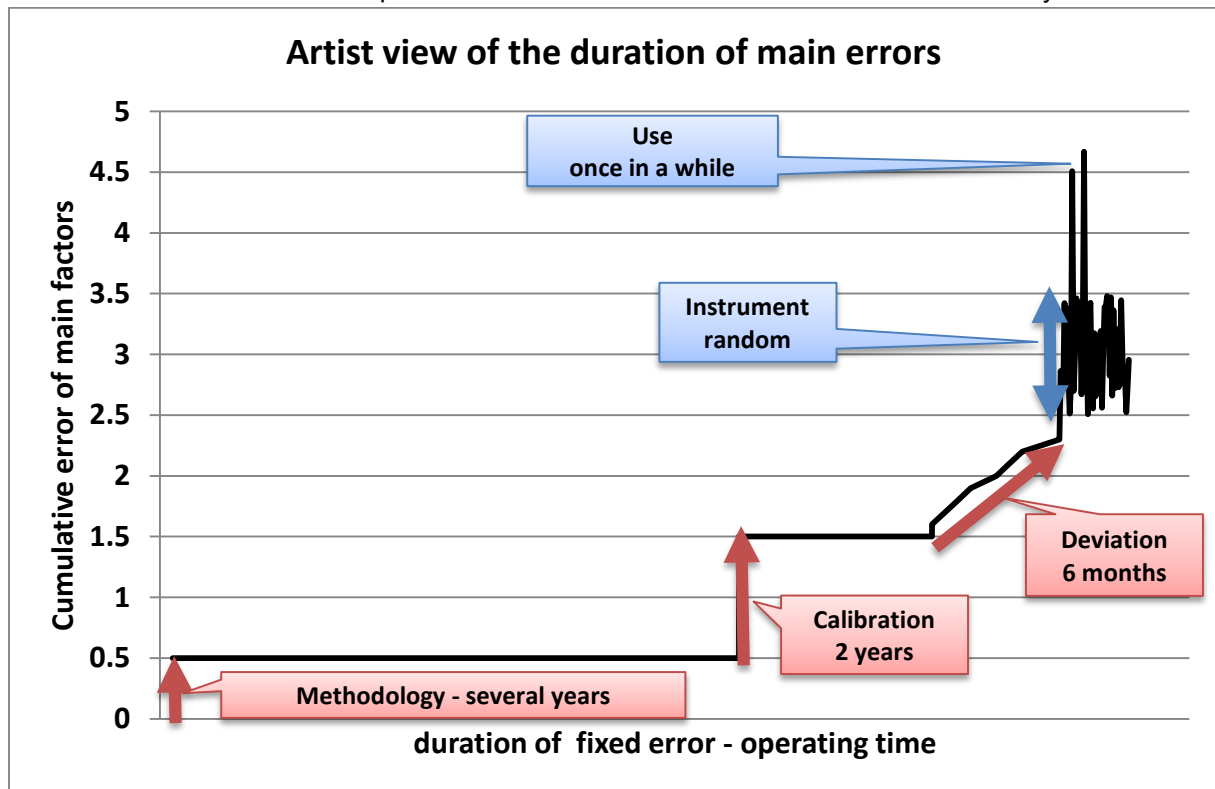


Figure 6 : each main factor has a different duration of its error

**2.3.4 Summary of the duration and the composition of the error of the instrument**

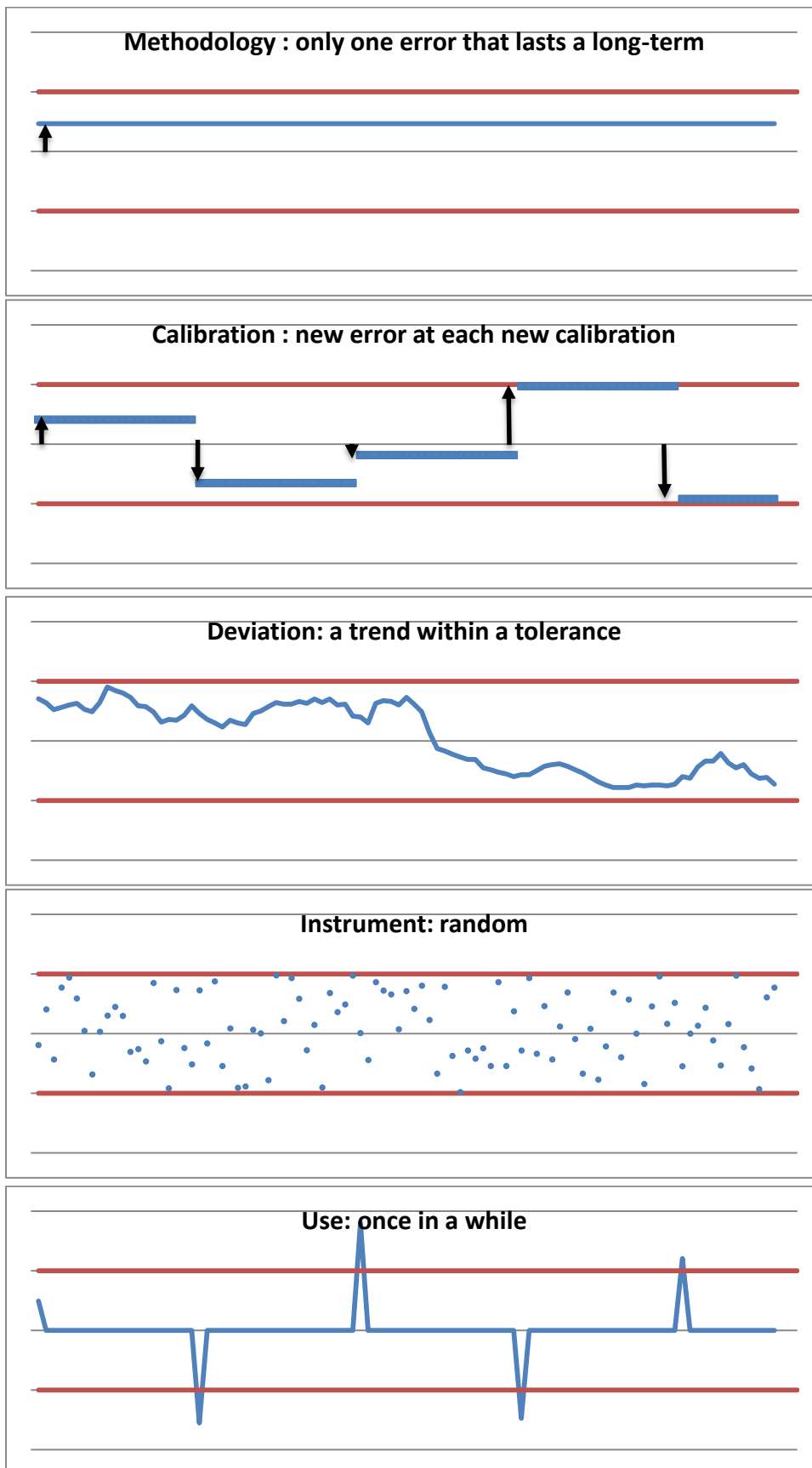


Figure 7 : the error of the instrument is a composition of 5 different main factors of error

## 2.4 Representative example from a weighing system

### 2.4.1 Example of evaluation of the 5 main factors for a weighing system

Look at this example given from a representative scale in a nuclear plant. Assume that “Instrument”, “Deviation” and “Calibration” factors are normalized to 1, “Use” factor is often larger but less frequently and “Methodology” factor is often lower but continuously.

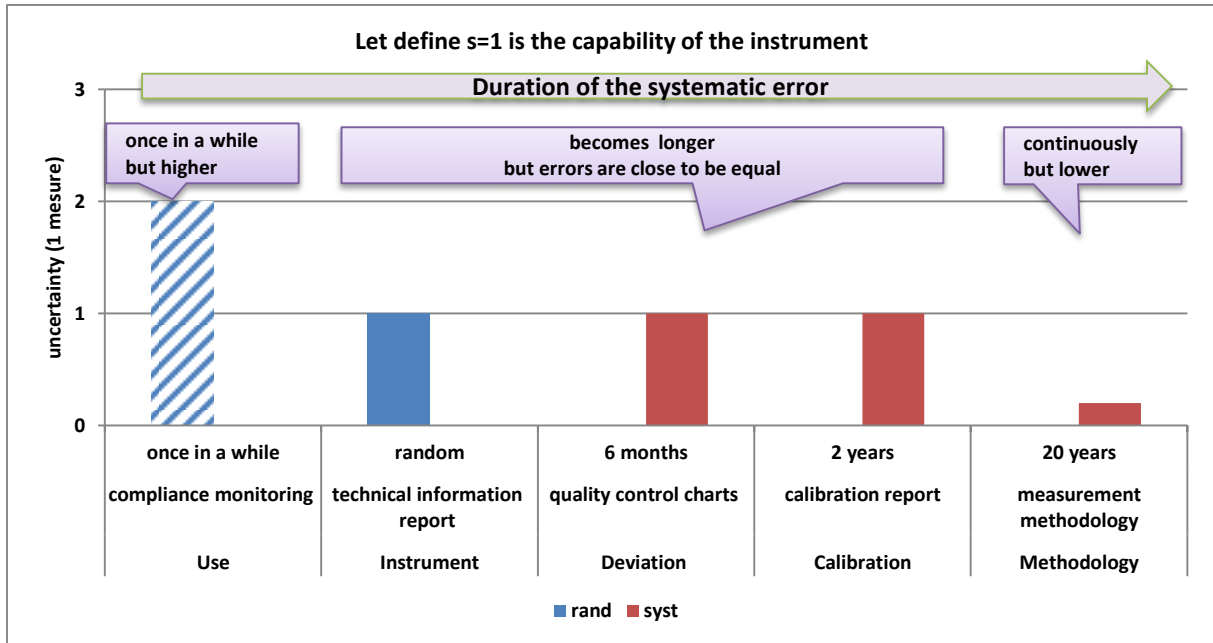


Figure 8 : representative example of frequency and level analysis for the 5 main factors for a weighing instrument

The reader will notice that the impact distribution is different between one measurement of an instrument and the cumulative error of 1000 measurements: the material balance.

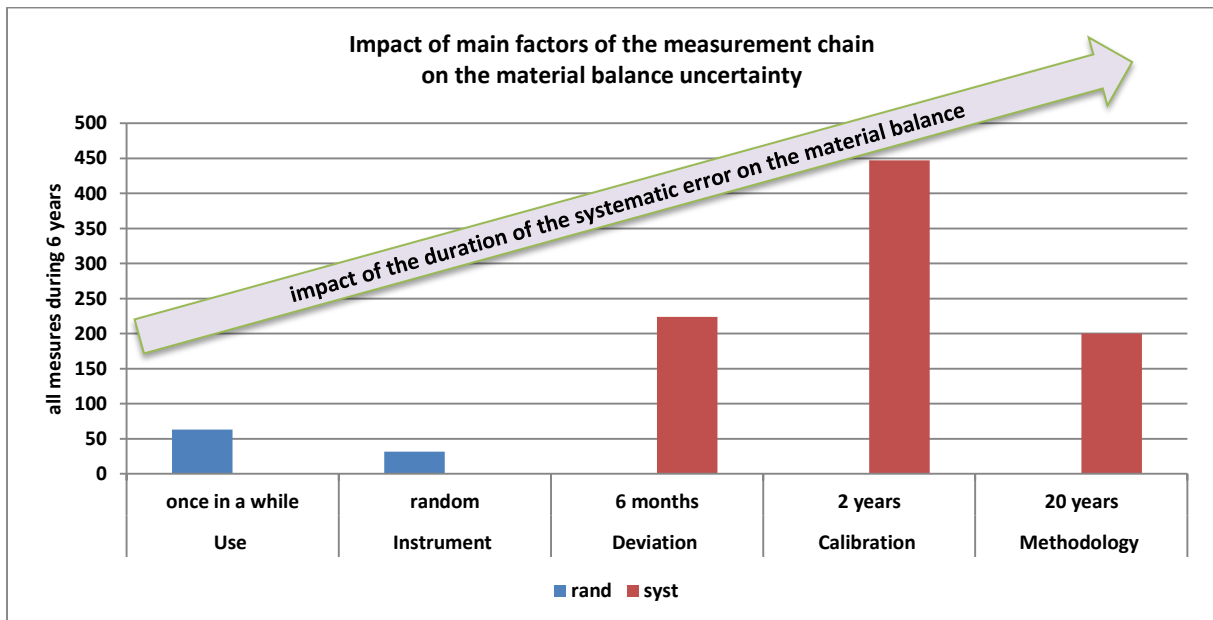


Figure 9 : Same example but with the impact on material balance due to the 5 main factors

### 2.4.2 Same example but visualisation with radar graphics

This visualisation shows that uncertainty of only one measure and the impact on uncertainty of the material balance test are different. This demonstrates that several parameters are necessary to analyse the impact on mass balance.

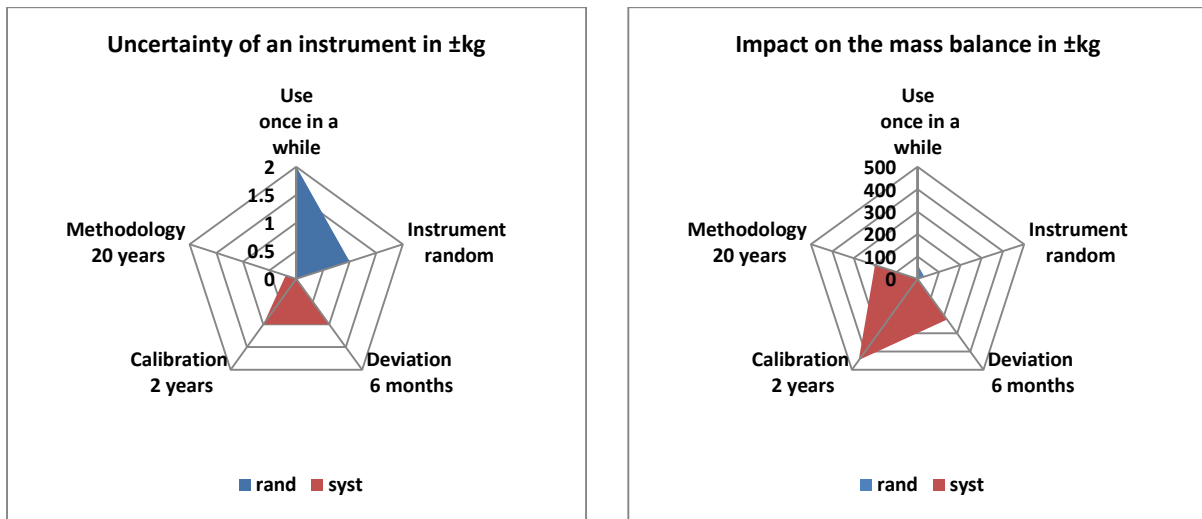


Figure 10 : comparison between uncertainties of one measure and several measures for an instrument

## 2.5 Conclusion

The evaluation of the impact on the material balance of an instrument is due to:

- The value of the standard-uncertainty of the instrument.
- The number of articles measured by the instrument.
- The type of error: random or systematic and then the duration of the systematic error.

In order to carry out properly the uncertainty calculations, 5 main factors which represent each step of the error of a measure are introduced.

- Precision of the instrument
  - o due to the capability of the **Instrument**
  - o due to the **Use** of the instrument
- Accuracy of the **Methodology**
- Accuracy of the instrument :
  - o error of **Calibration** (at the exact time of the calibration)
  - o **Deviation** of the accuracy after the calibration

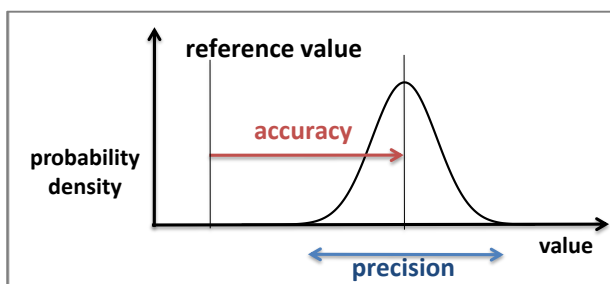


Figure 11 : This figure reminds the difference between accuracy and precision.

This table summarizes the 5 main factors or error:

Actor	Main factor	What	From	Duration	Source of information	Impact on material balance
All	Methodology	accuracy of the Methodology	methodological bias	systematic long-term	measurement methodology	***
Calibrator	Calibration	accuracy of the instrument	error of calibration	systematic medium-term	calibration report	***
Operator	Deviation	accuracy of the instrument	deviation of accuracy post-calibration	systematic short-term	quality control charts	***
Supplier	Instrument	precision of the instrument	capability of the instrument	random	technical information report	*
User	Use	precision of the measure	due to the use	random once in a while	compliance monitoring	*

Table 3 : organisation of the 5 main factors of error

### 2.5.1 First consequence with the application of the main factors

The uncertainty given with “laboratory conditions”, *id est* the instrument capability, is smaller than the uncertainty in use of the measurement system.

3 times is possible between the “instrument” factors and the sum of the uncertainty of the 5 factors.

### 2.5.2 Second consequence with the application of the main factors

In order to improve a material balance test, the operator should take a closer look at these 3 main factors, with priority:

- First : Methodology factor

This factor must absolutely be reduced to almost 0. The impact could be very high on the material balance if something wrong occurs. Unfortunately, this factor is not easy to detect, and sometimes technical limits prevents improvement.

- Second : Calibration factor

The aim is to reduce the Calibration factor up to the supplier capability. The operator should understand that is the best and easiest moment to reduce the impact on the material balance test.

- Third: Deviation factor

The aim is to reduce the Deviation factor up to the instrument capability. “Statistical Process Control” like quality control charts could help.

### 3 Avoid basic mistakes while using a weighing system

This part explains with common-sense ideas, how to improve the accuracy without any investment. Weighing system is chosen because it is the most frequently used instrument, and also it is an amazing measurement system if we consider the ratio “ease of use” and “numerous factors of errors”.

#### 3.1 Methodology: the Archimedes buoyancy

##### 3.1.1 Definitions according to the OIML

The OIML<sup>3</sup> definition of this physical bias is: “Air buoyancy is equal to the weight of the displaced air”.

The OIML<sup>4</sup> adds: “The mass of an object is obtained by weighing in air. Because the weighing instrument indicates a value that is proportional to the gravitational force on the object reduced by the buoyancy of air, the instrument’s indication in general has to be corrected for the buoyancy effect. The value of this correction depends on the density of the object and the density of the air.”

**Mass:** the physical quantity  $m$ , which can be ascribed to any material object and which gives a measure of its quantity of matter. The unit of mass is the kilogram.

**Weight:** Material measure of mass, regulated in regard to its physical and metrological characteristics: shape, dimensions...

The **Conventional mass**  $m_c$  of a body is equal to the mass of a standard that balances this body under conventionally chosen conditions”. The conventionally chosen conditions are:

- $\rho_0 = 8000 \text{ kg/m}^3$ : Conventional density of weight standards made of stainless steel
- $a_0 = 1.2 \text{ kg/m}^3$ : Conventional density of air at  $t_0 = 20^\circ\text{C}$ .

##### 3.1.2 Estimate the real mass

This bias cannot be detected by any other weighing measurement system, as all these systems are affected by the same physical bias.

- $a$ : density of air in use
- $L = L(\text{package}) - L(0)$ : the observed weight of the load of a body by weighing in air
- $m$ ;  $V$ ;  $\rho = \frac{m}{V}$ : Mass; volume, density of the body

Starting from the balance equation of the weighing<sup>4</sup>:

$$m \left(1 - \frac{a}{\rho}\right) = L \left(1 - \frac{a}{\rho_0}\right)$$

Also write the real mass:

$$m = L + aL \left(\frac{1}{\rho} - \frac{1}{\rho_0}\right)$$

The author defines:  $V_0 = \frac{L}{\rho_0}$ : the fictitious volume of standards that would balance the body. The atmospheric bias should be simplified with:

$$C_a \cong a(V - V_0)$$

Conclusion: the correction of a weighing measurement in air consists of 2 biases:

- A first buoyancy force is fixed at the time of the calibration with the volume of the mass standards.
- In use, a second buoyancy force is defined with the volume of the body.

### 3.1.3 Estimate the conventional mass

The conventional mass is given by:

$$m_c = L + (a - a_0)L \left( \frac{1}{\rho} - \frac{1}{\rho_0} \right)$$

### 3.1.4 Impact on the material balance

The legal metrology (and thus the conventional mass) is always used by operators for trade. If all measurement systems are scale, all bias are subtracted, but if the conventional mass is compared with another systems of measurement, like volume and concentration, we should look at the impact.

The declared mass has to be real and not conventional in order to be compared without bias with another system of measurement on the material balance.

Thus a simple weight of a package costs an error of:

$$a_0(V - V_0)$$

Let us see this general case: estimate the nett mass of a package:  $m_c^{nett} = m_c^{Full} - m_c^{empty}$ .

$$m^{nett} = m_c^{Full} + a_0(V^{full} - V_0^{full}) - m_c^{empty} - a_0V^{empty} - V_0^{empty}$$

As the volume of the package is subtracted, but not the volume of the fictitious standards:

$$m^{nett} = m_c^{Full} + -m_c^{empty} + a_0(V_0^{empty} - V_0^{full})$$

### 3.1.5 Summary and solution to manage the atmospheric bias on the material balance

This bias has a little impact on the material balance if all input/output packages are measured by weighing. On the opposite, this bias could impact the mass balance if a weighing measurement system is compared with not-weighing measurement system.

For the nuclear context: as the nuclear material is carried with airtight package, buoyancy effect is only due to the volume of fictitious standards, because the volume of the package is subtracted.

As operators have to respect commercial regulations, the conventional mass is required (Legal metrology).

In order to take into account these constraints, the solution is to:

- Calculate the real mass.
- Estimate the impact on the material balance: real – conventional estimations.
- Decide if a correction is necessary.

### 3.2 Methodology: try to subtract the systematic part of an instrument

#### 3.2.1 Classic way to use an industrial scale

Assume a process where scale1 measures inputs and scale2 measures outputs.



Figure 12 : representation of the classic way to use industrial scales

Assuming that the 2 scales measure 1000 input and 1000 output items: random error is = 1; systematic error is = 1. An easy computation shows that both systematic errors of the 2 scales explain the majority of the errors: the total impact on the material balance is close to  $\sqrt{2} \times 1000$ .

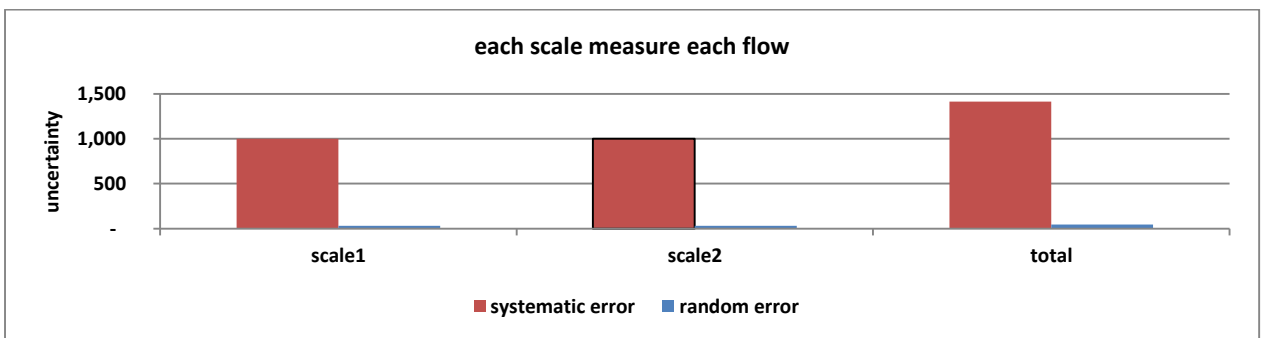


Figure 13 : with the classic use, 2 systematic errors add up

#### 3.2.2 Best way to use an input/output industrial scale

The best way is to use only one scale (or both scales) in order to weight equally input/output flows.

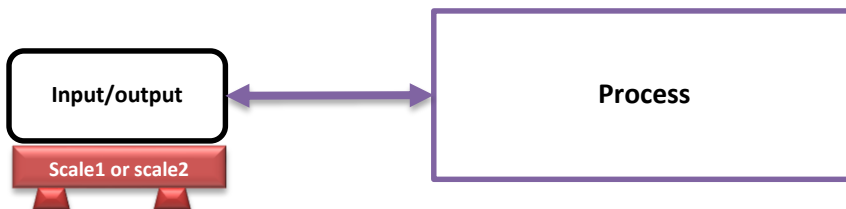


Figure 14 : best way to use the accounting scale for input/output flows

Amazing: with any technical modification, this method subtracts the systematic error and it is possible to significantly reduce the impact on the material balance.

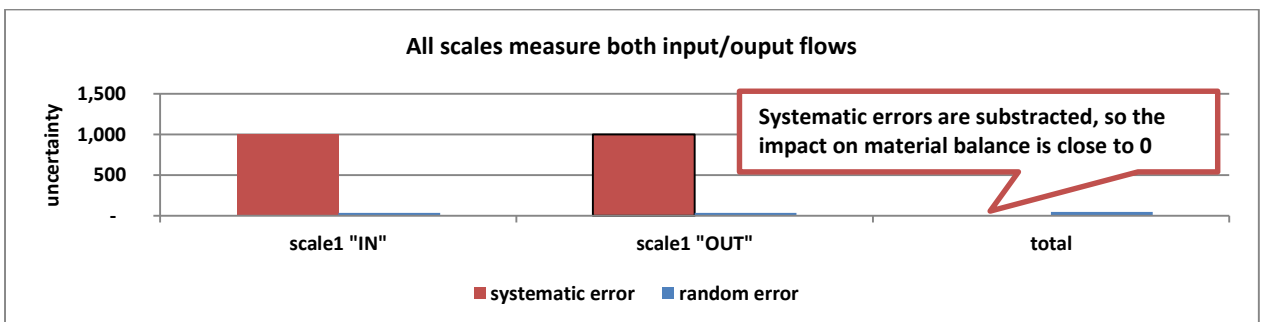


Figure 15 : best way: either only one or both scales measure the both input/output flows

### 3.3 Methodology: make sure to vacuum the empty package

The operator should make sure to vacuum the empty cylinder in order to avoid air bias:

- It is obvious for cylinders or for nuclear materials that could react with water (in this cases a high vacuum is done for those process reasons).
- But much less for barrels whose resistance is not designed for a high vacuum.

#### 3.3.1 Impact of no-vacuum empty package

Consider a full input package, which then comes out empty.

For the output, the operator does not proceed to vacuum the package:

- as there is not air-filled for the full package,
  - and if there is air-filled for the empty package,
- an air-filled bias is created for the net mass and so on the material balance.



Figure 16 : Air-filled inside the package plays a role on the material balance

For example, a package with an enclosed volume of 1 m<sup>3</sup>, calculations are:

- As 1 m<sup>3</sup> of air weights almost 1.2 kg,
- 1000 barrels of 1 m<sup>3</sup>, "full air-filled", cost a bias of 1200 kg on the material balance.

#### 3.3.2 Solutions

3 ways with such a situation:

- Best way is always to high vacuum the package:



Figure 17 : the best way is to vacuum the package

- If it is not technically possible:
  - o Check if it is not significant compared to the uncertainty of the scale.
  - o If it is significant, the final option is to take this bias into account as a correction in the nuclear accounting.

### 3.4 Calibration: Ask the calibrator to reset the instrument

As defined, the calibrator factor is one of the main impact factors. And this leads to try to reduce the tolerance from the calibrator factor to a minimum.

The calibrator has to respect the tolerance as defined by the regulator, and not seek to regularly adjust the instrument to 0, because the time needed to reset is longer.

Additionally, the calibrator has no apparent reason to change the procedure especially for nuclear sites in comparison to other industries. However, this is the best opportunity to improve the instrument: the weight standards and the calibrator are there at that point and no more than once a year.

Allow the weighing machine to be newly calibrated, and assume a tolerance of 1 kg as defined by the regulator:

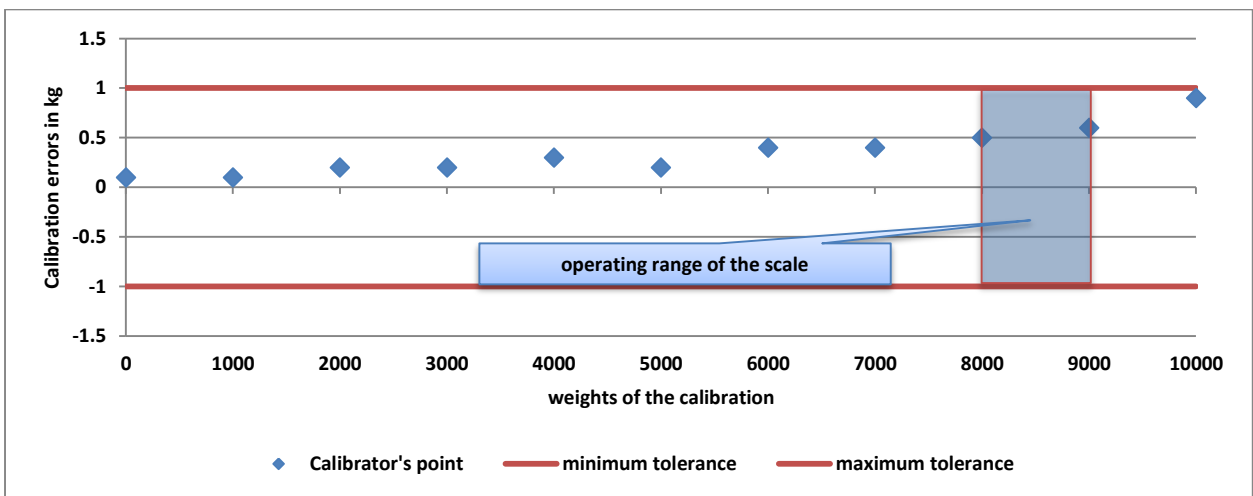


Figure 18 : This calibration is acceptable by the regulation but costs an impact on the material balance

The operator accepts the result of this calibration, because all points are within the tolerance. But this case costs a systematic error of 0.5 kg for at least 2 years, located on the main operating range, and so will have a large impact on the material balance test.

Interest-based negotiations are necessary between operator and calibrator in order to explain the needs and constraints of each side. The calibrator should make a special effort to calibrate in the nuclear industry. It is possible and necessary for the operator. Good calibration is shown below:

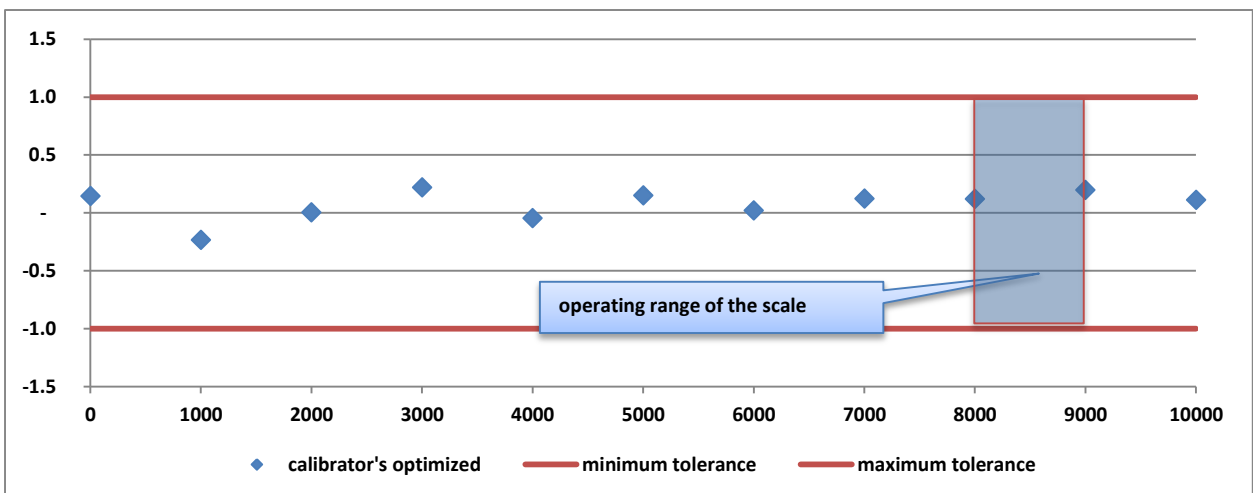


Figure 19 : impose additional conditions as regards with the material balance requirements

### 3.5 Deviation: reduce the impact of the temperature

Numerous environmental factors could affect the error of a weighing machine, such as the temperature (recorded at the place where are located the weighing sensors), which is in fact correlated with the outside temperature.

A sensitivity coefficient for the temperature exists, provided by the supplier for the majority of weighing technologies and is expressed in this unit: "bias in kg / weighed load in kg / °C.

For example, assume a sensitivity coefficient  $c = 0.002\%$  for your industrial scale, 15000 kg of load and a range of temperature of  $\pm 5^\circ\text{C}$ .

The impact is calculated as:  $0.002\% \times 15000 \text{ kg} \times \pm 5^\circ\text{C} = \pm 1.5 \text{ kg}$ .

#### - Classic situation

Even if the temperature is regulated by the air-conditioner: outside temperature plays a role on the temperature and this could affect the accuracy of the scale. The operator asks usually to calibrate in function of operational requirements, like a decrease in activity of the workshop. Unfortunately, a decrease of activity is often during winter or summer, which is in extreme temperature conditions. This fact moves the temperature bias towards a "methodology" systematic bias: and produces such a high impact on the material balance.

#### - Best choices for the calibration time

The best moment to calibrate the instrument is to choose the periods when the temperature is close to the average of the year. This will reduce the temperature bias.

If air-conditioning system is in use, we should regulate it at a single set point temperature, equal to the average of the ambient temperature of the year. This will reduce the temperature deviation.

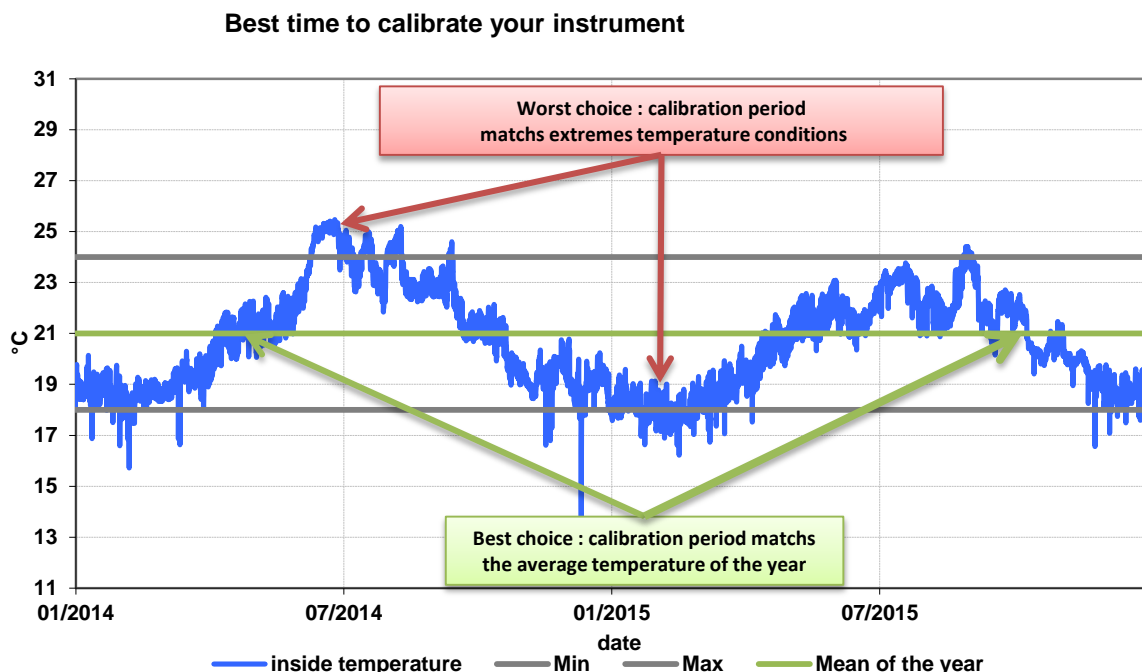


Figure 20 : best periods to calibrate the instrument

### 3.6 Others parameters for industrial scale

This describes several recurring errors for an industrial scale. It is not comprehensive...there is plenty of factors of error with a weighing machine.

#### 3.6.1 Vertical or horizontal impacts, vibration

This could cause:

- A damage of the structure of the scale
- A swaying during the weighing that could impact the accuracy

#### 3.6.2 Diagonal line of load

The diagonal line of load is a mechanic phenomenon that occurs if the scale is a "4 sensors technology". Like a chair with 4 feet, a diagonal line of load unbalances the load of each sensor.



Figure 21 : diagonal line of load in case of 4 sensors

#### 3.6.3 Overload of the sensors

In case of off-centre phenomena, a sensor could receive an overload:

- This could damage the sensor
- The overload exceeds the range of the calibration of the sensor (it is not calibrated at this load), uncertainty is then uncontrolled.

#### 3.6.4 Height of the centre of gravity

The centre of gravity of the package should be located close to the scale.

#### 3.6.5 Operational duration of the weighing

The duration of weighing causes a material fatigue of the sensors named "creep behaviour" that could impact a permanent inaccuracy.

#### 3.6.6 Magnetism

The balance must be protected from magnetism problems. Above all for a laboratory balance, as it is very sensitive instrument.

#### 3.6.7 Levelling

A weighing device must always be level (the air bubble must stay in the mark centre). The bubble position must be corrected, if needed,. In this example, the balance measures only the P component, perpendicular to the pan.

## 4 Improve an instrument with an economic approach

The proposed approach, based on a representative example from an industrial application, provides the key general ideas for project progress in regards with operational efficiency.

### 4.1 Evaluation of costs of the project

An industrial scale is subject to various sources of uncertainty which negatively affect the workload of the operator. These overloads are expressed as non-quality costs. A project to improve the material balance test is planned, and so costs of improvement are evaluated. The operator would like to improve the accuracy by optimizing the economic perspective.

#### 4.1.1 Non-quality costs

Non-quality costs are the economic losses resulting from nonconformities:

- Work overload for the operator (time taken to search for the error and its justification, operational remeasurement, administrative recovery of erroneous measurements).
- Penalties or additional constraints imposed on the operator by the supervisory authorities

These costs can be significant for an operator managing many items that may be non-compliant. For this example, the operator estimated the non-quality costs based on the uncertainty of an instrument:

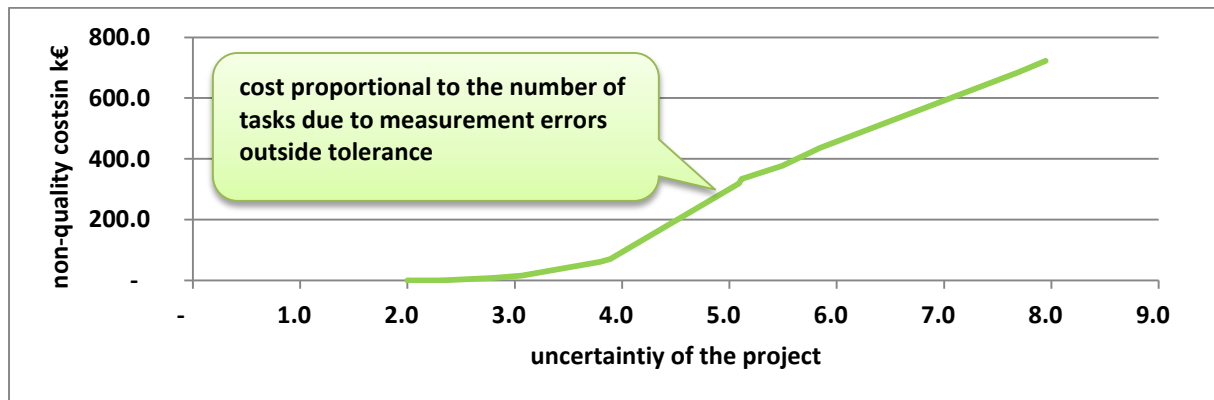


Figure 22 : Evaluation of non-quality costs by the project in function of the uncertainty of the instrument

#### 4.1.2 Gain and costs of the improvement project

The project suggests a list of solutions for each source of errors. For each solution, estimation is made of the uncertainty gain introduced by the operation as well as the evaluation of the operation cost.

Solution	Win in $\pm$ kg	Cost in k€
1	5.0	50.0
2	3.0	4.0
3	2.0	7.5
4	2.0	8.7
5	0.5	1.0
6	3.3	55.8
7	0.9	5.0
8	2.0	15.0
9	2.2	125.4
10	1.2	71.5
11	1.5	152.5
12	0.7	46.8
13	0.5	165.0
14	0.7	71.8
15	0.5	74.0
16	0.5	50.0
<b>Total</b>	<b>8.26</b>	<b>903.9</b>

Table 4 : List of solution and the Gain / Cost evaluations (assume that the technical project suggests this list)

### 4.2 Evaluation of the win of the solutions

For each error source, there are one or more solutions that improve the accuracy of the material balance. Each of these solutions:

- requires a cost  $C_k = I_k + E_k t$  composed of:
  - o an investment cost  $I_k$ ,
  - o an additional annual  $E_k$  cost of operation where  $t$  is the operating time.
- provides a win to a source of error evaluated at  $\pm u_M(k)$ 
  - o therefore allows a gain in precision  $\sqrt{u_M^2 - u_M(k)^2}$

### 4.3 Select solutions using the gain / effort matrix

The graph below uses the data from the previous table, and each blue point shows a solution according to the technical gain compared to the implementation cost.

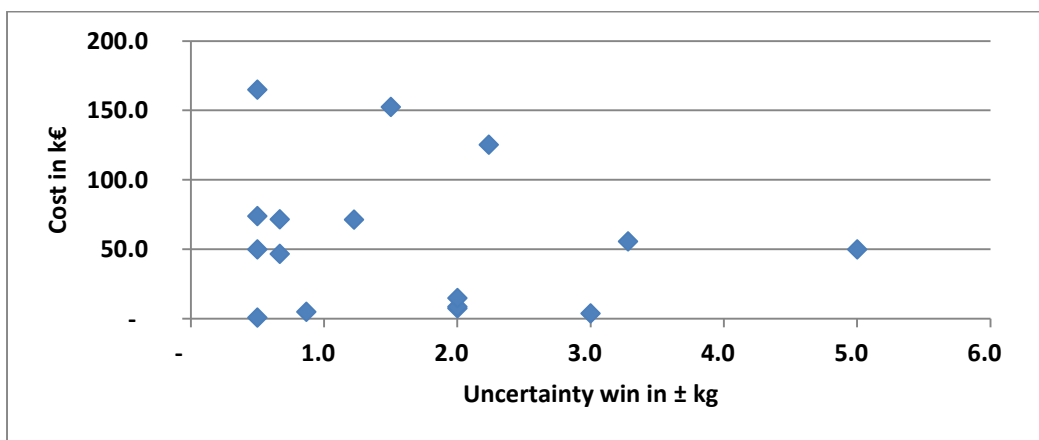


Figure 23 : List of all solutions suggested by the technical project

The cost-benefit analysis method from operational performance proposes to select the best solutions. This matrix is given by the preceding table which groups the solutions into 4 qualitative items.

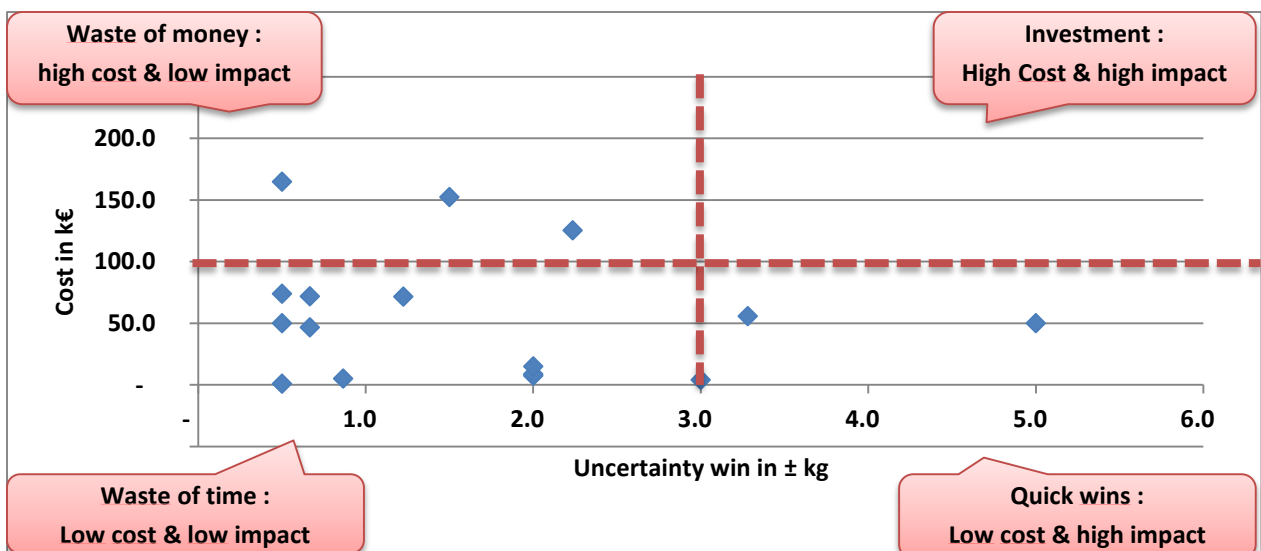


Figure 24 : classic “cost-benefit” analysis

For this example, we could choose the 3 “Quick Win” solutions and leave the others. Unfortunately, if that is insufficient, the project would have difficulty figuring out the way forward.

#### 4.4 Application of Operational Research

Operational research can be defined as the set of mathematical methods and techniques directed towards discovering the best operational choice in order to achieve the desired result or the best possible result.

Indeed, this approach produces a large number of solutions and then becomes a question of selecting these according to a technical-economic criterion. However, in this case, it is particularly interesting to think differently, Operational Research offers a more suitable method to determine the best way to pilot the project.

Imagine that the project targets improvement actions one by one from the best solution to the worst: this is called “**looking for the optimal path**” between:

- The “do nothing” scenario: 0 actions decided and thus zero cost
- The “do the maximum” scenario: maximum action and maximum cost

What is the best economic approach?

##### 4.4.1 Cost / Gain prioritisation of solutions

The improvement made by the solution in terms of precision must be expressed by the variance: the square of the uncertainty, which is the right parameter for these prioritisations, given that the variance has an additivity property. The underlying prioritisation criterion is the Cost / Win<sup>2</sup> ratio:

$$r(k) = \frac{C_k}{\pm u_M^2(k)}$$

$r(k)$  is the linear coefficient of the line passing through the point (0 ; 0) and the point ( $u_M^2(k)$  ;  $C_k$ ). First operation is to begin with the one with the lower ratio, and idem for the following operations.

On the following graph the best actions are prioritised by polar sectors.

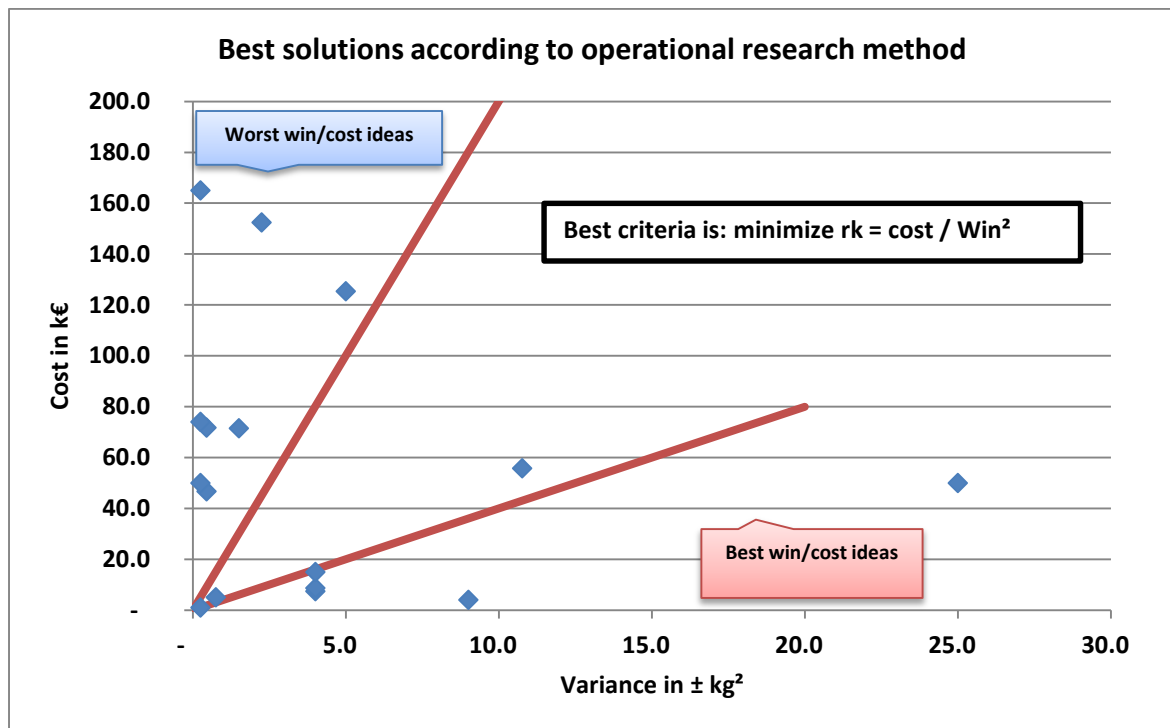


Figure 25 : operational research view to select and prioritize solutions

#### 4.4.2 Comparison with all possible paths

A path is the cumulative and ranked operations carried out by the project from the initial point (nothing is done) towards the final point (all the operations are done).

One way to demonstrate that the criterion  $r(k)$  provides the optimal path for the project is to look for all possible paths. In the following graph, the red path is the best path because for every €, the gain of precision obtained is greatest.

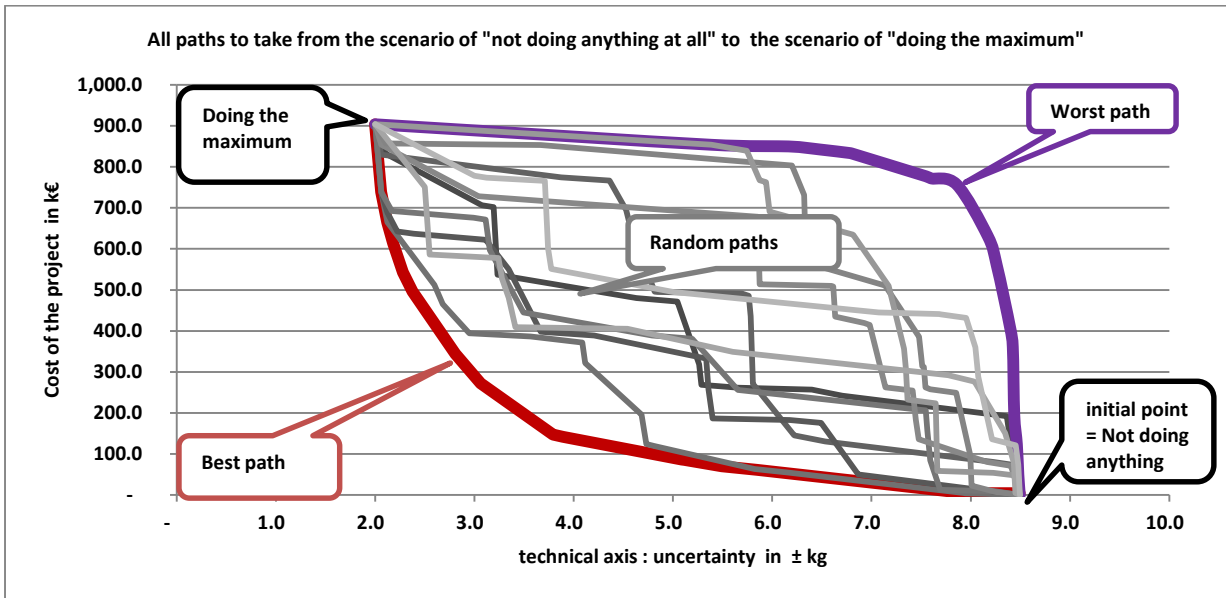


Figure 26 : all possible paths from initial point to final point. This figure shows that the red one is the appropriate order

#### 4.5 Choice of the best project in function of an allocated budget

This determines the best project, if a cost limit equals to 550 k€, is defined:

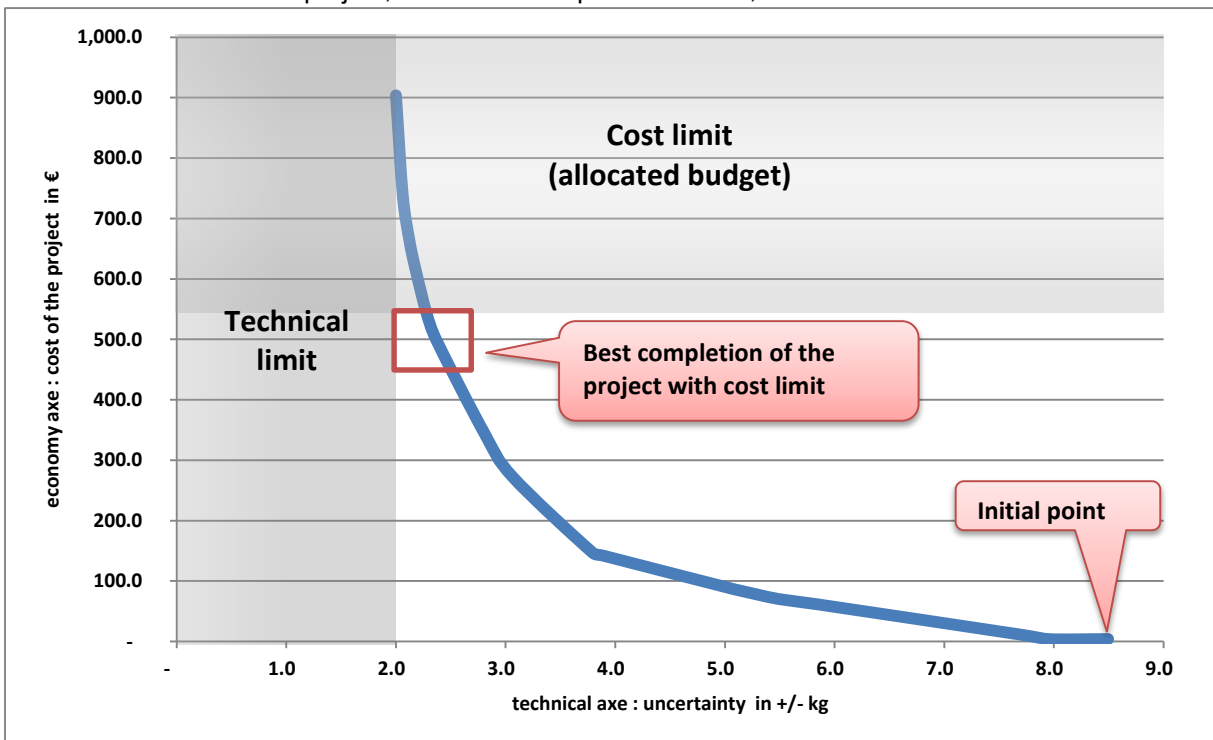


Figure 27 : Determine the best project if a cost limit is defined Technical versus cost of the project

#### 4.6 Overall economic optimisation

The final step is to define the best project with economic performance.

First, this graph reminds the both costs: non-quality and improvement project, in function of accuracy gain achieved thanks to the project.

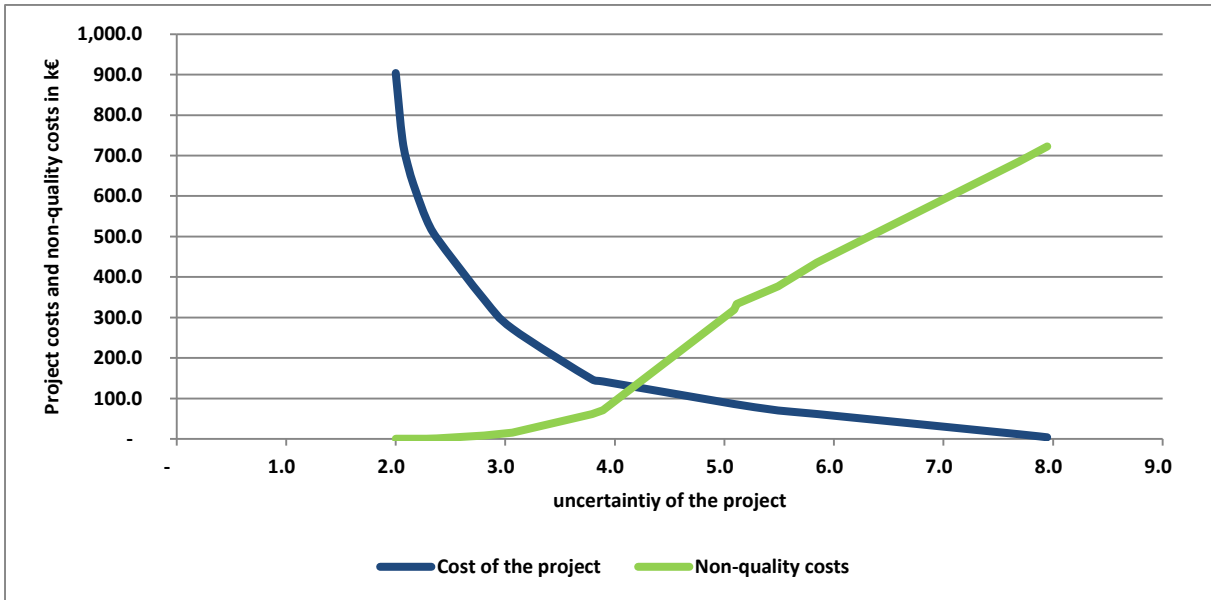


Figure 28 : non-quality costs and project costs together

Let us define: “overall costs” are “cost of non-quality + cost of improvement”.

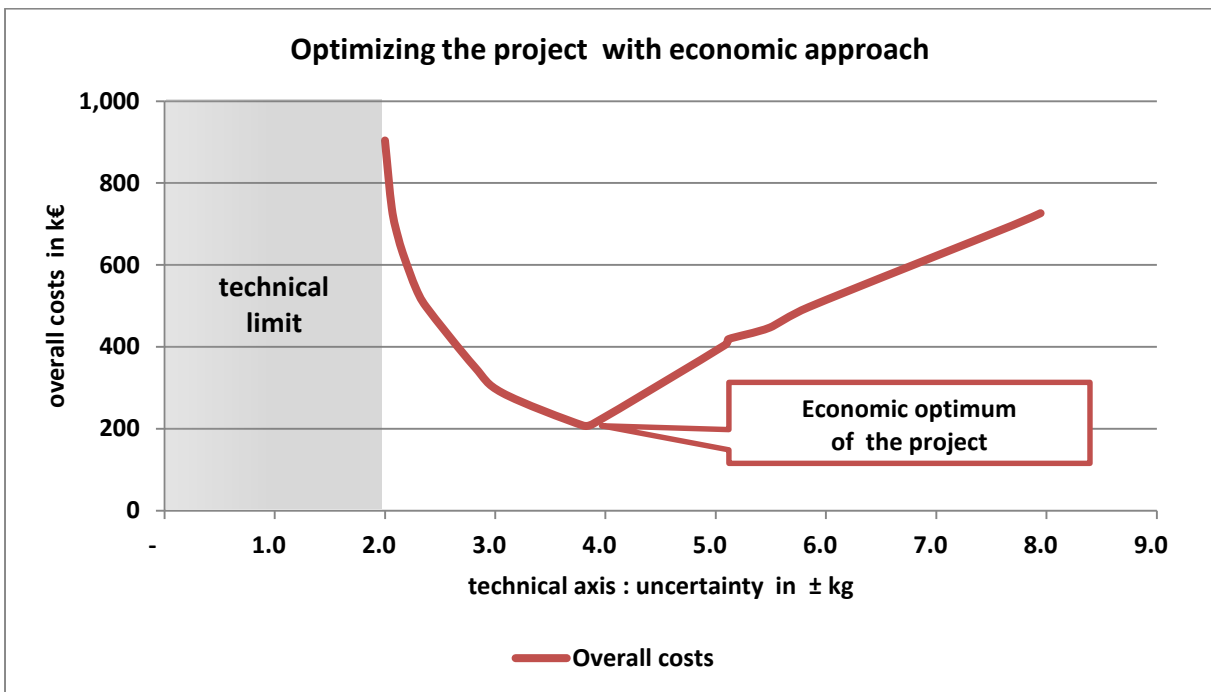


Figure 29 : The best project minimizes the overall costs

#### Conclusion:

- ⇒ The decision-maker will ask the project leader for a target of  $\pm 4$  kg.

## 5 References

[1] *Commission d'ETablissement des Méthodes d'Analyse – Statistical working group. CETAMA is a French committee responsible for improving the quality of measurement and analysis results. <https://cetama.partenaires.cea.fr/>*

[2] *Ishikawa, Kaoru (1968). Guide to Quality Control. Tokyo: JUSE.*

*“The International Organization of Legal Metrology (OIML) is a worldwide, intergovernmental organization whose primary aim is to harmonize the regulations and metrological controls applied by the national metrological services, or related organizations, of its Member States.”*

[3] *International Organization of Legal Metrology – OIML R111-1: International recommendations – Metrological and technical requirements.*

[4] *International Organization of Legal Metrology – OIML D28: Conventional value of the result of weighing in air*

# Unaccounted for uncertainties in radioaerosol assays as used in plume reconstruction or treaty verification

Robert B. Hayes

North Carolina State University, Nuclear Engineering Department, 2500 Stinson Dr.  
Raleigh, NC 27695-7909 USA  
E-mail: rbhayes@ncsu.edu

## **Abstract:**

*The typical approach used in air sampling is to ascribe the radiological concentration of interest in an air sample to the ratio of filter activity to volume pulled. This attribution is reasonable provided the sample is representative, however, the uncertainties ascribed to this concentration are generally considered Poisson errors from the counting scheme used. This work will show how the actual dispersion can be one or two orders of magnitude larger in some cases even when the radioaerosol has constant specific activity due to the lognormal size distribution of the particulate sampled. Applications in plume monitoring and the actual release from the February 2014 event at the Waste Isolation Pilot Plant in New Mexico USA will be considered and presented.*

**Keywords:** air monitoring; uncertainty; dispersion; sampling

## **1. Introduction**

Air sampling is one of the key aspects to the comprehensive test ban treaty (CTBT) monitoring regime. Samples of interest include radioaerosols (eg radioiodines and transuranics) along with noble gases (eg. Xe isotopes). This work addresses only the aerosol physics of this sampling but as such, it also has applicability to operational health physics and radiological emergency response. The application to the February 2014 transuranic waste drum deflagration at the Waste Isolation Pilot Plant (WIPP) in southeast New Mexico USA will be evaluated as a case in point on the effect described here.[1] The effects of aerosol physics on the sample collection will demonstrate how typical air sampling interpretations for common assays will underestimate true dispersion by as much as an order of magnitude in most cases, possibly even 2 orders.

### **1.1. Aerosol sampling and assay**

The process for taking an air sample has largely been unchanged for the past 70 years. This method involves pulling a known volume of air through a filter and then assaying that filter. The sampled air is then ascribed a concentration value equal to the ratio of the filter assay activity to the volume of air pulled.

Typically, the volume of air is known quite precisely and the assay is constrained to Poisson statistics relegating the dominant uncertainty in the airborne concentration estimate to that of the Poisson counting in the assay.

### **1.2. Representative sampling**

In order to obtain a quality sample, the collection of all particulate must be representative of the total population present in the space of interest. This is typically only considered to be an issue when the sampling is taking place in a duct or exhaust system. When sampling an effluent, the linear face velocity through the filter has to be equal to that of the general volume surrounding it to prevent over or under sampling of the particulate. This can be challenging when the linear flow rates of the effluent vary or are turbulent.

Undersampling is expected to occur when the linear face velocity through the filter is lower than the bulk volume around the sampling head. This will cause some of the smaller particulate to follow the flow path avoiding the filter even though it would have initially traversed it were the sampling head not present.

Oversampling is expected when the linear face velocity through the filter is higher than the bulk volume around the sampling head. This would cause particulate which otherwise would not have passed along the intake face of the filter to divert from its ambient path into the filter due to the higher sampling flow rate.

One way to overcome this challenge for dynamic flow conditions is to use a shrouded probe as shown in Figure 1. The shroud forces air through the outer channel to take a more linear path surrounding the filter's sample head and therefore can prevent any under- or oversampling.

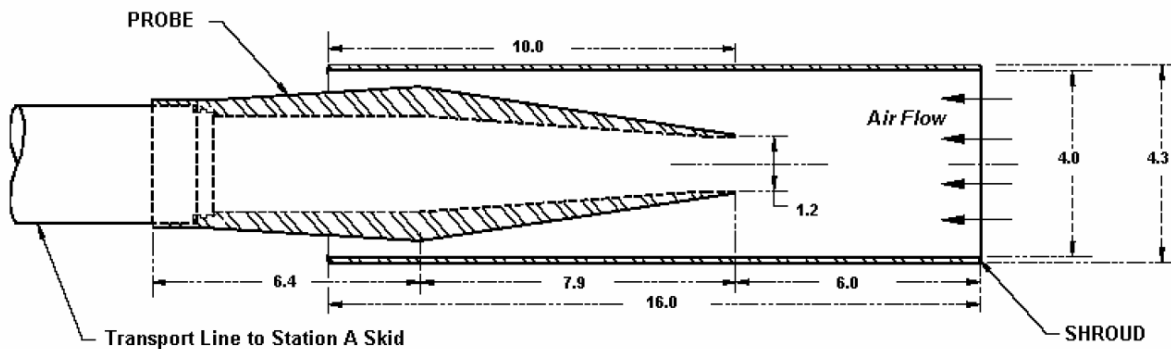


Figure 1: Shrouded probe schematic show from a cross sectional view. [2]

### 1.3. Aerosol physics

Aerosols evolve in an effectively fractal manner. They are not generally spherical but rather dendritic and are composed primarily of organic matter, micron-sized silicates and ocean mist near the coast. [3] Their evolution will depend on relative humidity, particle density and types.

Typical binding forces are those of Van der Waals when gross kinetic impact of any kind occurs. Aerosol particulate growth is not spherical but erratic resulting in dynamic properties such as changing density, heat capacity and obviously aerodynamic radii. Reviews of the intricacies of these dynamic dependencies can be found elsewhere. [4, 5]

#### 1.3.1. Radioaerosol physics

Radioaerosols in particular can be extremely erratic in their evolution when they decay through charged particle emission. When a gaseous radionuclide (such as radon or its progeny) decays through charged particle emission, the resulting heavy metal gas has a charge that will induce a polarization in all nearby aerosols. The resultant dipoles in the vicinity of a point charge will result in an attractive potential to pull the radionuclide into a bound state with one or more ambient aerosols.

This additional Coulomb-based potential in radioaerosol physics only further exacerbates the evolutionary growth properties in any given species. The radical electric potential shift which can occur when spontaneous charge generation is placed on the aerosol or gas (from charged particle emission in radioactive decay) allows for rapid growth and is unique to the radioactive decay process.

A radioactive aerosol can begin as an inert isolated gaseous species such as radon, radon progeny or radioiodines. With radioiodines, these can combine with atmospheric water or other materials to become an aerosol. Radon progeny can remain as a gas through its decay series or combine with ambient aerosols to become part of the bound fraction of the progeny (conversely, that part which does not combine with any aerosols is simply the unbound fraction). These fractions are expected to depend on relative abundances of the radionuclide and ambient aerosols along with temperature, relative humidity etc.

### 1.3.2. Sampling physics

The action of sampling a gas or aerosol for assay requires either measurement in some in-situ fashion (generally resulting in dismal sensitivity with low concentrations) or concentrating it in some medium for characterization. With an aerosol, this is done by pulling air through a filter such that the filter concentrates the particulate within its volume. Gaseous species are typically collected by pulling air through zeolite or activated charcoal to later be boiled off in a vacuum and then concentrated for assay.

With the air filter, there are 4 main mechanisms for fixing the analyte in the medium. These are inertial impaction (similar to a projectile into mud), interception (particles too massive to fit through the pores), diffusion (Van der-Waals adhesion) and electrostatic attraction (requiring a net charge, although not seen in Figure 2, see section 1.3.1).

As a result of the variety of physics taking place when sampling an aerosol, the particle size collection efficiency is dependent on a number of factors (including flow rate, filter characteristics etc.). As a generalization, the particle size efficiency shown in Figure 2 [5] can be used as a reasonable approximation to typical behaviours. Here, dominant sampling mechanism regimes are shown as a function of aerosol size.

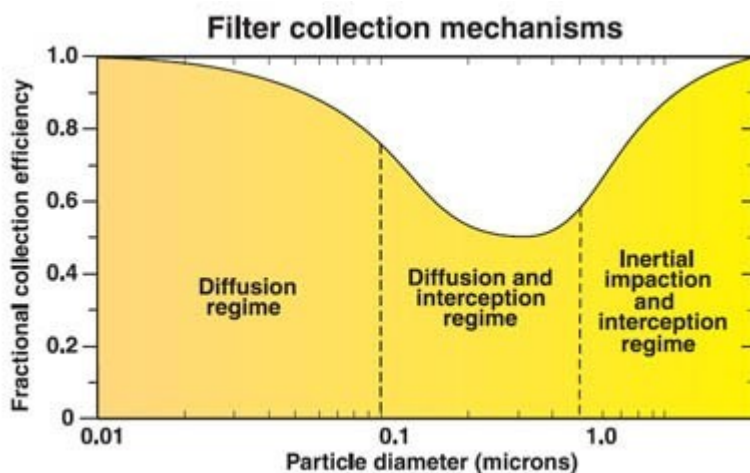


**Figure 2:** Filter collection mechanisms labelling dominant sampling efficiencies grouped by particle size. Note the abscissa is given in logarithmic scale. [3]

It is significant to note that in the respirable range (when particulate is able to make it all the way down into the lung alveoli and be retained for a dose intake) is exactly where the filter efficiency is both lowest and has the largest changes (0.1 to 5  $\mu\text{m}$ ). This uncertainty in filter efficiency for the respirable range is contributes to the reason why dose cannot legally be ascribed to individuals based only on air monitoring data [6] compared to the far more reliable and standard bioassay in determining actual radionuclide intake. This is one important contribution to dispersion in aerosol monitoring which is independent of the final filter assay but there are others.

## 2. Plume monitoring

With the advent of any nuclear detonation, leakage of the gaseous constituents from the event will then pour into the environment creating a plume. The simplest propagation model for plume evolution is probably Gaussian diffusion with advective transport. This means that as the material follows airflow, it will diffuse in all directions driven by simple Fickian mechanics. Atmospheric stratification along with ground boundaries complicate the transport along with any convective or turbulent flows.

To the extent that the plume propagation can be accurately predicted, multiple sample points would then enable characterization of the same. Two or three points are likely inadequate to fully characterize any plume unless the source term itself was already well known in time and space. Backtracking a potential

plume around the globe can quickly become intractable without source term knowledge or real time monitoring of the plume itself. [6]

## 2.1. Footprint characterization

If a known release had occurred, sampling teams would generally prefer to stay on the penumbra of the fallout footprint caused by the plume passage and deposition. This prevents the sampling teams from being required to don personal protective equipment (PPE) and so prevent skin contamination. Further, vehicle contamination would also occur if sampling missions were not constrained to the outskirts of the fallout. Any vehicle and personnel radioactivity accumulation would create the need for decontamination and so full hotline support to eventually doff the PPE and reuse of the vehicle. These activities would necessitate additional manpower and resources for decontamination rather than sampling, assessment and control.

### 2.1.2. Low concentration sample drivers

Due to these inhibitions from sampling in contaminated areas, only those areas that have barely detectable levels of the radionuclides of interest may be measured so that PPE is not required. Higher levels of the plume footprint are then characterized from the air using large arrays of NaI logs for gamma detection [7]. This means that air and soil samples taken from ground teams are invariably acquired from those regions of low or very low contamination.

The same result is generally realized for routine air samples, even those taken from an effluent stack. This is because facility release limits are generally sufficiently low that the maximum possible public or environmental dose consequence is a small fraction of normal background dose. In order to comply with facility limits, effluent content of any controlled radionuclides have to be low. In many cases, the dominant TRU release content is from resuspended fallout created by atmospheric weapons testing in the past century [8]. The purpose for most air samples is to prove that no release did occur so again, overwhelmingly, air samples for controlled radionuclides have low to very low anthropogenic radionuclide content.

## 2.2. WIPP event

On February 14 of 2014, a deflagration took place in a TRU drum sent to the WIPP for permanent disposal by the Los Alamos National Laboratory. The facility itself is a deep salt mine and the radiation monitoring system detected the breach shifting the airflow to a suite of HEPA filters preventing a large environmental release. The system had a small leak due to industrial bypass filters designed for mining operations to divert the airflow which were not rated for nuclear operations (they were designed and built in the 1980's prior to modern nuclear standards for geological repository ventilation systems). The event took place while the regulatory compliant radiation monitoring system was functioning including on and offsite air sampling stations.

The resultant plume along with offsite sampling station labelled as pink flags is shown in Figure 3. Here, the effluent stack was measured via representative sampling and so the plume was predicted using the NARAC modelling code allowing comparison with offsite sampling stations. [9]

### 2.2.1. Source of the WIPP release

The release itself was comprised of a nitric salt with many curies of  $^{241}\text{Am}$  contained therein. The cause of the deflagration was eventually traced back to the use of organic kitty litter with the nitric salt based on a miscommunication of the words, "inorganic" with "an organic". Detailed descriptions of the sequence of events culminating in the release can be found elsewhere. [10]

### 2.2.2. Air monitoring results

A graph of the predicted versus measured air concentration values from the WIPP event is provided in Figure 4 [1, 6]. Here it is clear that at high airborne concentrations, excellent linear correlation is realized resulting in an almost unity correspondence. At lower concentrations however, a drastically larger relative deviation is clearly seen in Figure 4.

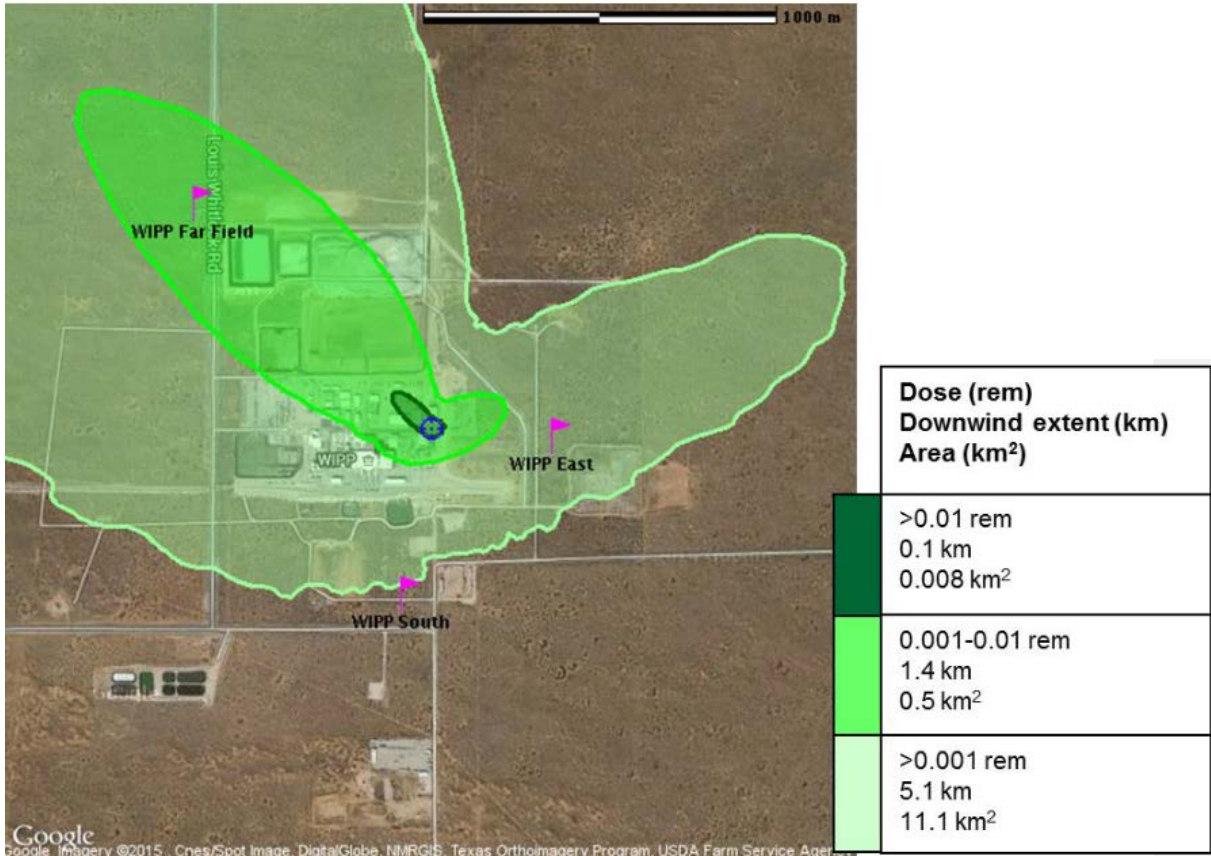


**Figure 3:** Dose contours determined from the WIPP release based on effluent assays which could then be correlated with field air sampling results. Inner locations for air sampling are represented by maroon flags labelled WIPP Far Field, WIPP East and WIPP South.

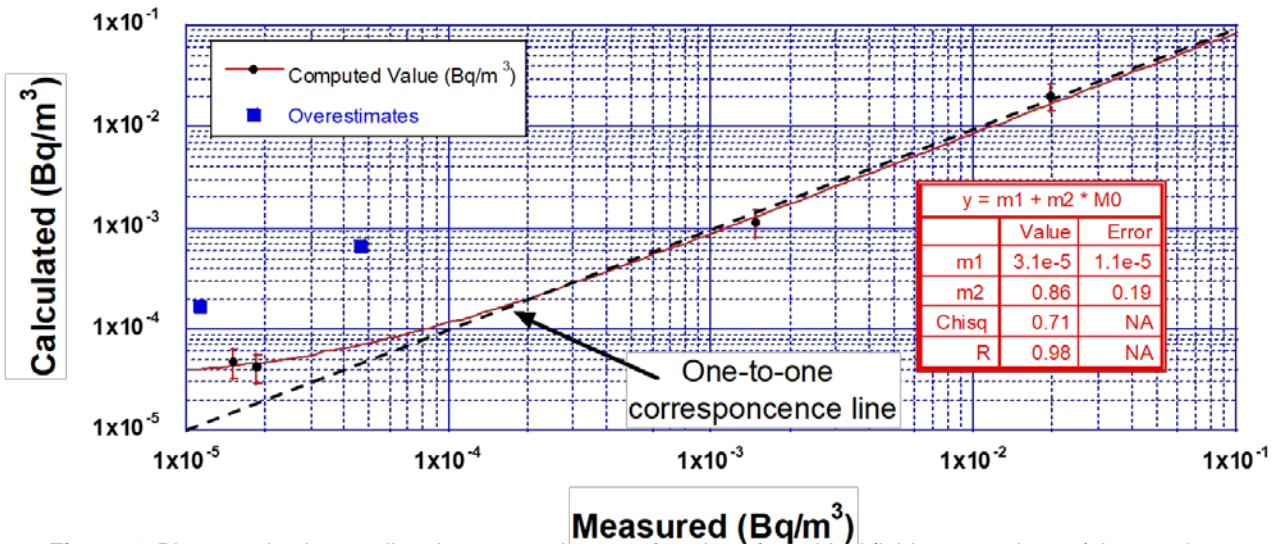


**Figure 4:** Plume projection predicted concentration as a function of empirical field assay values of the passing plume based on regulatory compliance air sampling infrastructure.

The linear correlation shown in Figure 4 does not include the pair of noted overestimates. The agreement seen at high concentrations largely forces the high correlation. The scatter at low concentrations is noted to vary by an order of magnitude relative to the expected value with apparent presence of positive bias in overpredicting. Overpredictions will be shown later to be an expected event from small probability, large particle size radioaerosols being sampled.

### 3. Aerosol statistics

The shape parameter for an aerosol is based on its settling velocity in ambient air when compared to a spherical droplet of water. The equivalent water droplet with the same settling velocity as the aerosol then fixes the mass median aerodynamic diameter (MMAD). Similarly, the activity median aerodynamic diameter (AMAD) is used for defining respirable particle sizes which when inhaled can be incorporated into bodily fluids through the lung membrane of the alveoli.

An equivalence between the MMAD and AMAD can be found only when a radioaerosol has a constant specific activity. If the entire particle has uniform radioactivity present, then the activity will be directly proportional to the mass and so the reference diameter which gravitationally falls at the same rate as the standard droplets normalize them to have the same size distribution values of mode, median and mean as shown in Figure 5.

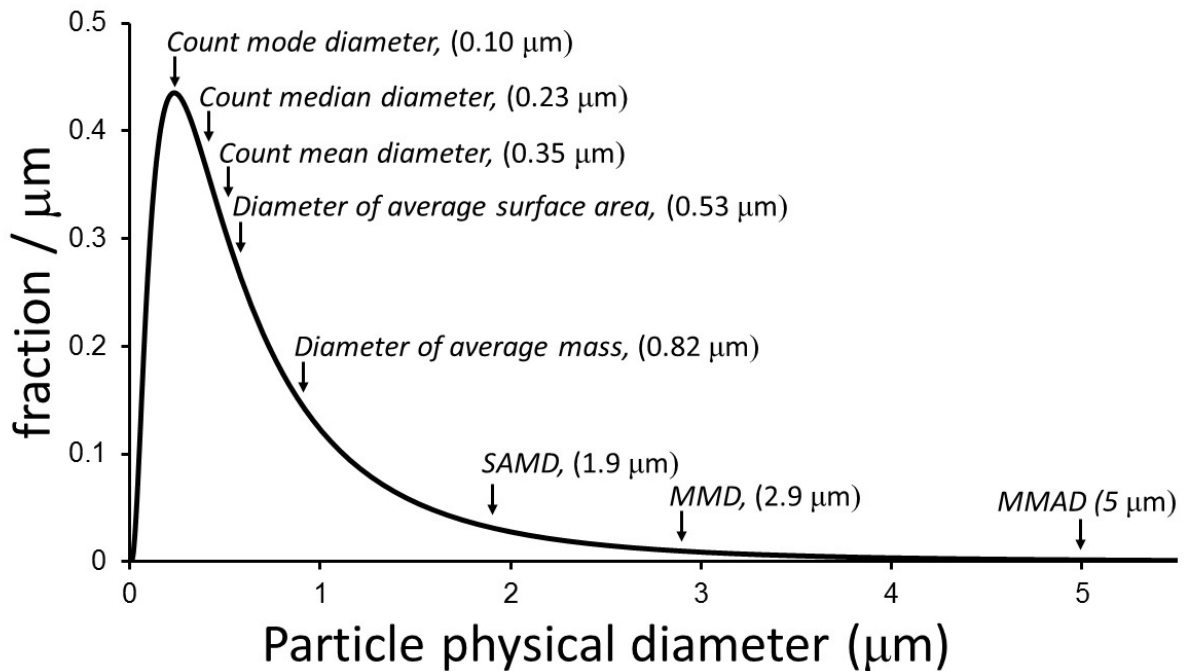


**Figure 5:** Probability distribution of 5 µm AMAD particles as a function of their particle physical diameter [M] (Hoover 2016). Marked in the figure are many properties of potential significance in evaluating statistical properties of a distribution from an aerosol with an AMAD of 5 µm.

#### 3.1. Lognormal

The functional relationship describing the shape distribution of aerosols (Fig. 5) is given by Equation 1. Here, the argument of the exponential is a logarithmic abscissa and so a typical shape for a 5 µm MMAD aerosol is shown in Figure 5. Here, the skew is evident in that the parameter describing the shape equivalent of a standard aerosol (MMAD or equivalently the AMAD) is far up into the tail and very different than the mode or median.

$$f(x; \mu, \sigma^2) = \frac{1}{\sqrt{2\pi\sigma x}} e^{-[\ln(x)-\mu]^2/(2\sigma^2)} \tag{Eqn. 1}$$

The basic probability density function is approximated here by Equation 1 where more detailed physical interpretations can be obtained elsewhere [12]. An example of such a distribution is shown in Figure 5 where a frequency distribution of various diameter related metrics are provided. Here, the mode (0.1 µm) is recognized to be less than half the median (0.23 µm) which is more than an order of magnitude below the effective mean or the mass median aerodynamic diameter (MMAD at 5 µm). It is the MMAD

(effectively equivalent to the activity median aerodynamic diameter or AMAD) which is standardized based on settling velocities compared to a monodisperse material such as water. This is important given the dependency on the effective shape distributions driven by conforming to Equation 1 relative to the total respirable fraction present. This can become much more complicated with multimodal distributions although these are assumed simple superpositions of multiple lognormals.

### 3.1.1. Health consequences

The drastic skew in particle size distributions of an aerosol (Fig. 5) can significantly effect the inhalation intake from incorporation into bodily fluids through transfer across the tissue interface of the lung alveoli. The respirable range is generally in the 0.1 to 5  $\mu\text{m}$  range where most planar disc air sample filters have the largest variation in collection efficiency as seen in Figure 2.

If the shape distribution peaks (has a mode) in the respirable range where sampling efficiency demonstrates the largest variability (Figure 2), evolution in the peak location will only exacerbate the resultant health effect dispersion. This contributes to overall error but the true uncertainty has to also account for sampling statistics driven by the distributions following the form of Equation 1.

### 3.1.2. Sampling statistics

By definition, a small number of aerosols sampled from the diameter distribution shown in Figure 5 will likely come from the mode. On average, half of these should be above the median which itself is just over double the mode. The dispersion in diameters sampled for a small sample number would then be expected to look like a Gaussian, centered between the mode and median in this sense.

The population however has members with sufficiently large diameters which cause the aerodynamic average to be more than an order of magnitude larger than either of the erroneous Gaussian approximations to the mode or median. Based on the frequency distribution seen in Figure 5, the probability of sampling one of these large diameter particles is vanishingly small. If the activity of each aerosol particle is uniform throughout its volume, then the true sampling dispersion can become egregious at best.

### 3.1.3. Shape parameter dependencies

The shape of the distribution seen in Figure 5 is strongly dependent on the geometrical standard deviation of the lognormal. A family of curves for the lognormal having different shape parameters are shown in Figure 6 where each curve shown has the same integrated area (note both base axes are not linear in the traditional sense as  $\log(x)$  is plotted as an axis).

Here the family of curves is normalized to have the same integral to highlight the large variation possible from a lognormal distribution, specifically when they all have equivalent probability interpretations. This results in each curve having a different mode, median and mean. The curves are graphed together along the sigma scale for display only and not intended to describe the

### 3.1.4. Monte Carlo modelling

A normal random variable of mean  $\bar{x}$  and variance  $\sigma^2$  is represented by  $N(\bar{x}, \sigma^2)$ . A normal random variable with zero mean and unity variance is represented by the symbol  $N(0, 1)$ . This was used to create a lognormal distribution in the form of  $e^{N(0,1)}$  such that it would have a mode of  $e^{-1}=0.37 \mu\text{m}$ , a median of  $e^0=1 \mu\text{m}$ , and a mean of  $e^{1/2}=1.65 \mu\text{m}$ . With this mean radius, the average diameter then becomes 3.3  $\mu\text{m}$  which places it in the range of the most penetrating size for biological intake and so makes for a simplified mathematical example for consideration.

A random sampling from the  $e^{N(0,1)}$  distribution was done using a generated normal random variable in Microsoft Excel to allow for simulating these effects. Doing this 1e6 times resulted in the overall distribution shown in Figure 7 where the insets show the distribution's appearance when displayed with differing logarithmic axes. The upper center inset has a logarithmic abscissa resulting in an apparent normal distribution. The upper right inset has a logarithmic ordinate axis showing the effect of the unique tail approximated by the Monte Carlo calculation.

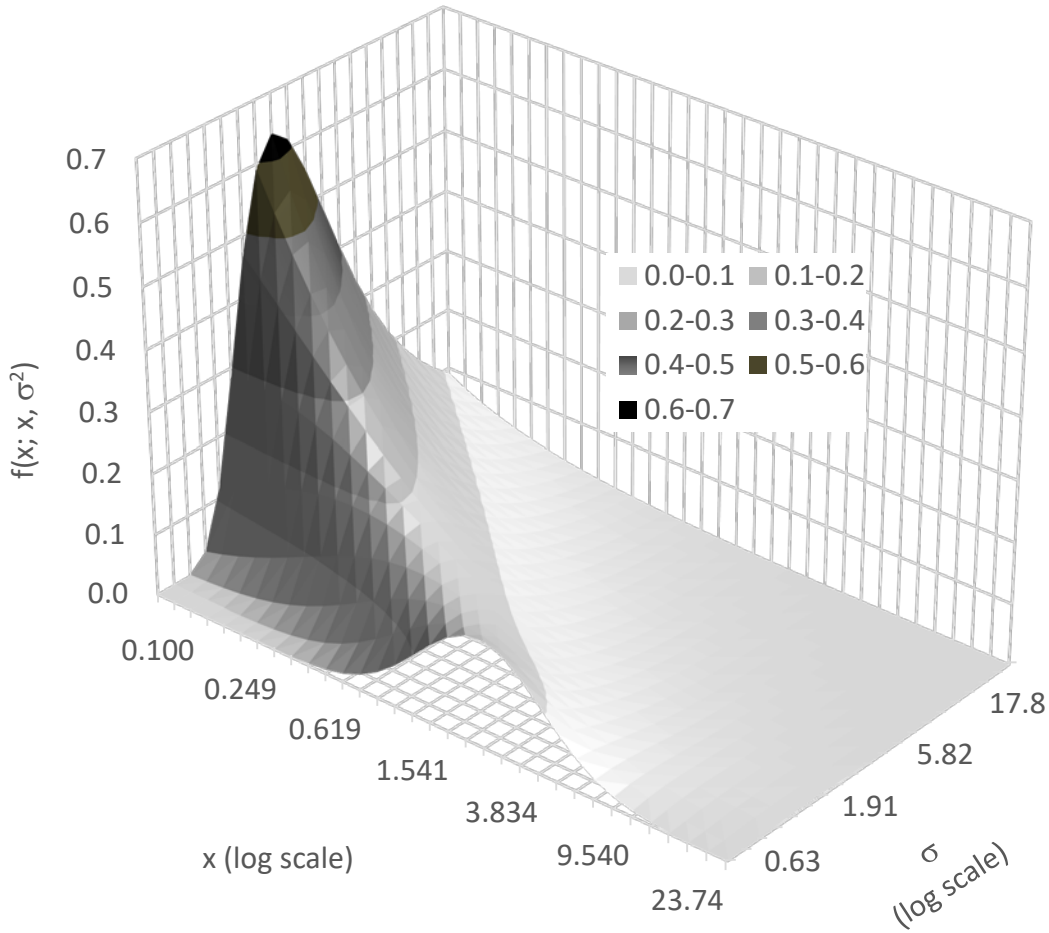


**Figure 6:** Family of lognormal distributions having a mean  $\mu=1.5 \mu\text{m}$  based on a progressive increase in shape parameters as listed in the legend. Note the shape parameter is the  $\sigma$  value in Equation 1.

Taking a random sample from a lognormal population distribution will then result in a dispersion strongly dependent on sample number. As the sample number becomes large, the true lognormal distribution will by definition be observed. Smaller sets will appear normal demonstrating skew with increasing size. Estimating this effect by simple Monte Carlo sampling from the population probability density function can provide a good estimate on these effects.

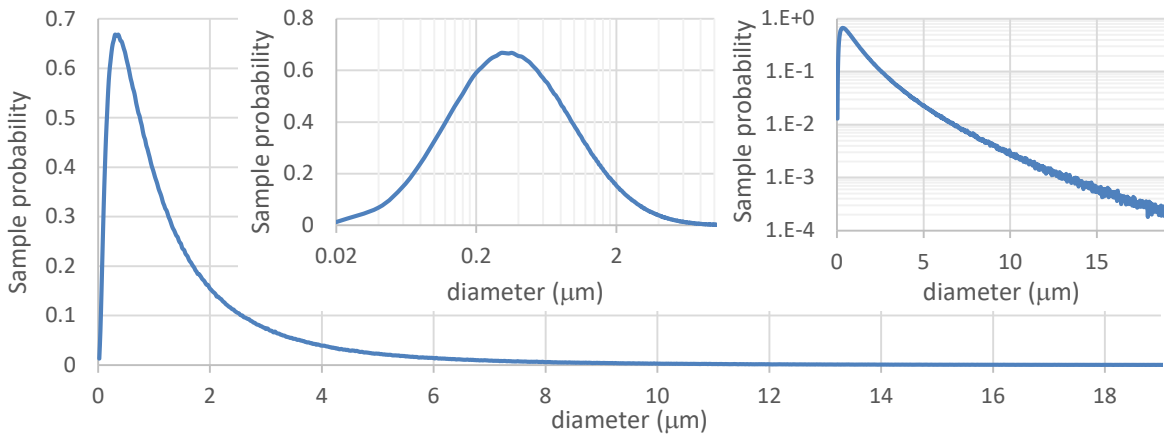


**Figure 7:** Monte Carlo calculated standard lognormal probability distribution from  $1e6$  values generated from  $\exp(N(0,1))$ . This distribution has a mode at  $0.34 \mu\text{m}$ , a median at  $1.0 \mu\text{m}$  and a mean at  $1.65 \mu\text{m}$ .

### 3.1.4.1. Normal variance as a function of sample size

Due to the choice of a simplified distribution parameter set, the normal standard deviation as a function of sample size is  $\sigma(n)$  then given by the expectation function  $\sigma(n) = \sqrt{E(\bar{x} - x)^2}$  such that  $\sigma(n) = 2/\sqrt{n}$  for the particle radii distribution. This means that at the upper 95%CL, the limit becomes  $3.29/\sqrt{n}$  which relative to the defined mean (e.g. AMAD) value of  $\bar{x}=1.65$  shows that there must be at least 4 randomly sampled aerosol particulates to have a normal standard deviation of 2. This may not seem terrible at first glance but note that the activity of a transuranic or similar radioaerosol will not scale with the radii but rather the radii cubed. With low particle numbers, this activity value becomes large, effectively an order of magnitude.

A very relevant question then becomes the effect of those instances when a low probability aerosol of a large diameter is sampled from the distribution given that very large radii are possible from this very simple distribution (Figure 7,  $e^{N(0,1)}$ ). Here, the activity (or mass) scales with the effective radius cubed. A single 2.2  $\mu\text{m}$  radius particle will have 10 times the activity of a single 1  $\mu\text{m}$  radii particle. Likewise, a 1  $\mu\text{m}$  radius particle will have 1000 times the activity of a 0.1  $\mu\text{m}$  particle. More egregious cases could be considered (e.g. multimodal distributions etc.) but the salient point is that this is truly an independent dispersion source in the overall assay results.

## 4. Discussion

Applications of this work in treaty verification and plume monitoring demonstrate how plume density or activity measurements will have large dispersion from penumbra samples where particulate density is low or very low. Unless the aerosol itself is not homogenous in composition, this will only effect integrated activity or centerline projection estimates. The key facet in aerosol physics identifies that the dispersion mechanisms do not change the average as a whole but only the variance of that mean if more common statistics (normal or Poisson) are assumed. Correspondingly, a small sample number from low concentration air will be expected to have very high dispersion as seen empirically from historical air monitoring assays when the sampled particulate number is small [12].

The key finding here considers that the Poisson dispersion in air filter assays may actually prove to be an insignificant contribution to the overall uncertainty in the characterization effort of any airborne contamination events. The extent to which this dispersion plays a role will be dependent on a product of the sample volume and actual airborne contamination concentration as this will scale the number of particles acquired on the filter media. Assays of high activity samples will not be subject to this additional dispersion effect to the same extent as low activity samples and so can be considered accordingly.

The functional dependence of particle size distributions was demonstrated using a mathematically simplified distribution scaled to have relevance to radiological risk scenarios for aerosol assay. More egregious cases could be constructed as done elsewhere [6] although clearly, less egregious cases could also be constructed and considered realistic for potential real world applications in operational health physics scenarios. The moderate approach utilized here was offered as an insightful perspective into the effects from particle size distributions in final assay results and their interpretations.

## 5. Conclusions

This work has shown that the true dispersion in most radioaerosol samples can potentially be orders of magnitude larger than the uncertainty ascribed only from Poisson counting errors in the sample assay. Interpretations which require quantitative estimates of the radiological concentration then are subject to additional uncertainty terms which have not historically been considered when characterizing radiological air sample assay results.

## 6. Acknowledgements

Special thanks are extended to S. Joseph Cope for critical reviews and comments on this work.

This material is based upon work supported by the Department of Energy National Nuclear Security Administration under Award Number DE-NA0002576. This work partially paid for by the Nuclear Regulatory Commission grant NRC-HQ-84-14-G-0059. Additional support of this work was through a joint faculty appointment between North Carolina State University and Oak Ridge National Laboratory in coordination with the Office of Defence Nuclear Nonproliferation R&D of the National Nuclear Security Administration sponsored Consortium for Nonproliferation Enabling Capabilities.

## 7. References

- [1] Hayes RB; (2016) Consequence assessment of the WIPP radiological release from February 2014. *Health Phys.* **110**(4), 342-360.
- [2] Frank-Supka L, Harward DJ, Casey SC; *Overview of the WIPP Effluent Monitoring Program, Compliance with Title 40 CFR Part 191, Subpart A, Environmental Standards for Management and Storage* US Department of Energy, Carlsbad New Mexico, May 2005. Last accessed 4/19/2019 [https://wipp.energy.gov/library/Overview\\_WIPPEffluentMonitoring.pdf](https://wipp.energy.gov/library/Overview_WIPPEffluentMonitoring.pdf)
- [3] Maiello ML, Hoover MD Editors; *Radioactive Air Sampling Methods*, CRC Press, Boca Raton, FL, 2011.
- [4] Kleinstreuer C, Feng Y. Computational Analysis of Non-Spherical Particle Transport and Deposition in Shear Flow With Application to Lung Aerosol Dynamics—A Review. *ASME. J Biomech Eng.* 2013;**135**(2):021008-021008-19. doi:10.1115/1.4023236
- [5] Vehkamäki H, Riipinen I, Stockholms universitet, Naturvetenskapliga fakulteten, Institutionen för tillämpad miljövetenskap (ITM). Thermodynamics and kinetics of atmospheric aerosol particle formation and growth. *Chemical Society reviews.* 2012;**41**:516-5173.
- [6] Hayes RB. (2017) Reconstruction of a radiological release using aerosol sampling *Health Phys.* **112**(4), 326-337.
- [7] 34) Hendricks T, Hayes R. Enhancement of aerial gamma surveillance utilizing complementary characteristics of NaI and HPGe detection. *1st Joint Emergency Preparedness and Response/Robotic and Remote Systems Topical Meeting*. Salt Lake City, UT, February 11-16, 2006. ISBN: 978-0-89448-692-0 CD-ROM.
- [8] Hayes RB, Akbarzadeh M. (2014) Using isotopic ratios for discrimination of environmental anthropogenic radioactivity. *Health Phys.* **107**, 277-291.
- [9] Hayes R. B. (2016) Consequence assessment of the WIPP radiological release from February 2014. *Health Phys.* **110**(4), 342-360.
- [10] Accident Investigation Board. *Radiological Release Event at the Waste Isolation Pilot Plant, February 14, 2014*. US Department of Energy, Carlsbad, New Mexico. April 2015. Accessed 4/20/19 [https://www.wipp.energy.gov/Special/AIB\\_WIPP%20Rad\\_Event%20Report\\_Phase%20II.pdf](https://www.wipp.energy.gov/Special/AIB_WIPP%20Rad_Event%20Report_Phase%20II.pdf)
- [11] Crow EL, Kunio Shimizu K, Editors; *Lognormal distributions : theory and applications* Taylor and Francis, London, 2017
- [12] Alvarez JL, Bennett WS, Davidson TL; Design of an Airborne Plutonium Survey Program for Personnel Protection. *Health Physics.* **66**(6):634-642, June 1994.

# **Session 13:**

# **Containment &**

# **Surveillance**

## JRC Embedded Universal Seal Reader

**Gunnar Boström, David Puig, Claudio Bergonzi, Aurora Fassi, Vitor Sequeira**

European Commission, Joint Research Centre  
Directorate for Nuclear Safety and Security, Ispra, Italy

E-mail: [gunnar.bostrom@ec.europa.eu](mailto:gunnar.bostrom@ec.europa.eu)

### **Abstract:**

*Active and passive seals are important tools for Nuclear Safeguards Inspectors. They are widely used to immobilize equipment and preventing casks, flasks, doors and other objects from being opened in-between inspections without being detected. The amount of seals at hand are increasing. Consequently, the inspector needs to carry in-field and to be trained on more devices for seal verification.*

*This paper presents a recent development by Joint Research Centre in Ispra, Italy: the Embedded Universal Seal Reader, which is an all-in-one reading device for both active and passive seals leading to a more efficient and effective safeguards use. The seal reader is built and designed to be a versatile tool carrying a high-resolution camera with dedicated illumination to be able to handle all aspects of Cobra seals from installation and verification. It is also capable of reading the status-logs from active seals such as EOSS and AOLS using serial communication. The device is further equipped with USB-connectors to enable in-field generating digital signatures on images and data to guarantee the authenticity of data. The inspector can use the device without stylus or similar, thanks to the dedicated human-interface and embedded touch-screen.*

*The article will present the device in detail, its capacities and design. For the passive Cobra seal, the article presents the new innovative automated image-analysis procedure that highlights relevant changes between reference and new images and proposes a result for the Inspector to endorse. The tool automatically generates a report with relevant information and confirmation by the inspector. For active seals, like AOLS and EOSS, the article presents the device's log-reading functionality and the major improvements related to traditional active seal interaction.*

**Keywords:** Seal reading device; Active and passive seals; Surveillance and verification; Nuclear Safeguards.

## **1. Introduction**

Passive and active seals are corner-stones of the Nuclear Safeguards Inspector toolbox [1]. Whenever an object must be immobilized or a door verified closed, either a seal or a safeguard camera are used. Nuclear surveillance cameras are highly robust and can be used to verify objects over time. However, their results come with a certain manual intense activity, namely the video-review [2]. Passive and active seals are tamper-indicating devices which can be used to detect if a particular object has been moved or changed, in order to prevent unauthorized access within secured containments [3]. The general needs for these types of seals are large. These devices are put in place by an Inspector or Operator and remain on site until next time a verification is requested. The passive seal can verify that the wire connected to the seal has not been opened at the seal-end and, thereby, that the object under control has not been altered or removed. In contrary to the passive seal, which can only show that an object change has occurred since last installation or validation date, the active seal can tell when an opening or tampering activity happened. Tens of thousands of passive and active seals are applied annually by Nuclear Inspectors, motivating the need for a very efficient and effective seal handling, including pre-installation work, installation and post-verification activities.

There are several approved passive and active seals used currently by the Safeguards Inspector community. Passive seals are primarily Cobra and metal-cap seals, while active seals are mostly EOSS and future AOLS. The Cobra seal [4] uses a multi-strand optical fibre cable, forming a loop with both fibre-ends enclosed in the central end-cap of the seal head. During the closure of the seal, the head cuts both fibre-ends and blocks the light-passage for a random number of fibres in the cable. A picture of the fibre-end unique pattern can be acquired with a digital camera and dedicated illumination. This fibre-end image, together with specific reflective particles embedded in the head, makes it possible for an Inspector to verify the integrity of the optical fibre cable. The EOSS (Electronic Optical Sealing System) [5] consists of a fibre-optic loop connected to a monitoring device, which continuously/randomly sends laser pulses through the loop and measures the transmitted pulse. Every opening and closing of the seal wire, resulting in missing pulse response, is recorded and stored in the internal activity log of the device. All communication with the EOSS seal is encrypted. The unit-specific crypto keys are stored in a separate USB Crypto-token, which handles the encryption/decryption of the transferred messages. The AOLS (Active Optical Loop Seal) has the same working principle as the EOSS but with a few differences. It uses a plastic multi-mode fibre, which is more flexible and less sensitive than the silica-based single-mode fibre in the EOSS. This means that the attenuation in the AOLS fibre is significantly higher, leading to shorter fibre-length, but this does not impose any practical limitation in most cases. Considering the AOLS seal, the log file information is transmitted in clear text but carries an additional digital signature that guarantees the authenticity of the data, without the need of any Crypto-token.

Currently, the different seal technologies require different tools to be used for reading and verification purposes. The active EOSS and AOLS need a laptop computer with a RS-422 connection to retrieve and analyse the log files stored in the seal, while the Cobra needs a camera-based device for the acquisition of reference and verification fibre-ends images. In order to stream-line the inspector operations and limit the number of equipments which must be carried on site, there is certainly the need for an all-in-one tool performing the different in-field activities related to both passive and active seals. For this reason, the JRC has designed the Embedded Universal Seal Reader (EUSR), which is a portable device that handles all aspects of the daily in-field activity of Nuclear Safeguards Inspectors, related to the reading and validation of active seals and to the installation and verification of passive seals. Moreover, the EUSR adds a number of advantages and improved processing functionalities compared to other available systems applied for the acquisition and verification of Cobra seals. In current Cobra readers [6], the serial number of the seal must be manually typed by the user and the reference/verification comparison is performed by manually switching between the two seal images. In order to speed up and facilitate Nuclear Inspectors in Cobra verification processes, the EUSR provides useful tools for the automatic recognition of the head serial number and for the assisted comparison between reference and verification seal images. Finally, it allows authenticating the Cobra seal by analysing the intrinsic reflective particles, which are present on the seal body.

## 2. Hardware design

Figure 1 shows a picture of the developed compact hand-held EUSR system. The mechanical design of the EUSR device is depicted in Figure 2, highlighting the main components. The EUSR system is mainly based on commercially available Off-the-Shelf items. The only tailored components are represented by the connection electronic board and the mechanical housing. The housing (Figure 1a) is designed in SolidWorks and is produced in a 3D printer either with the ABS-M30i plastic or with Nylon material. No mounting screws are present on the outer shell. The EUSR can be held in a single hand due to the compact design, resulting in a length of 18 cm, a width of 12 cm and a height of 7 cm. A stretchable palm-strap is added to secure the device to the hand.



**Figure 1:** (a) Implemented EUSR device, depicting the external housing and the embedded touch-screen. (b) EUSR internal view, showing the central camera surrounded by a squared LEDs array, with the exchangeable seal-holder placed on the right side.

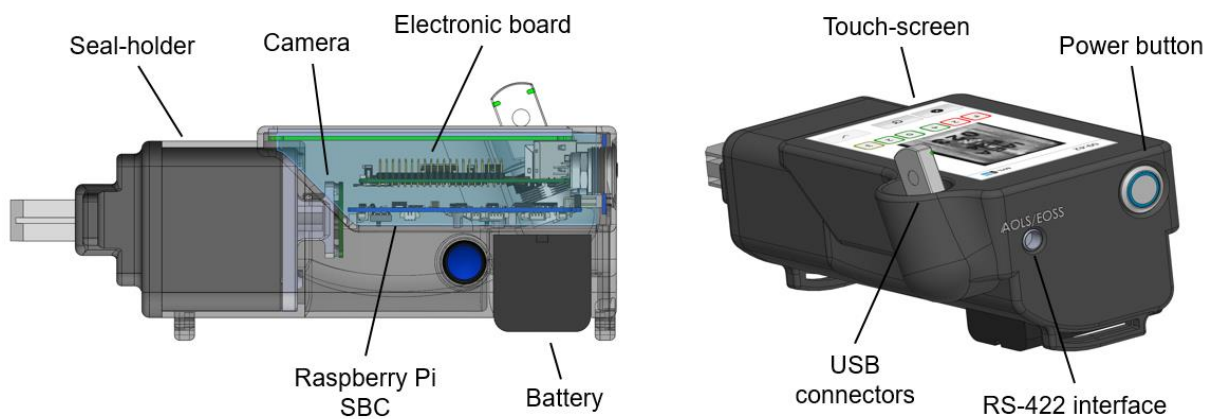


**Figure 2:** Mechanical drawings of the EUSR device, showing the main hardware components.

Concerning the electrical design, the EUSR application runs on a Raspberry Pi single board computer (SBC). An on-board battery provides power to the SBC and other electronic components, resulting in an autonomy of an entire day in case of normal use. A power button circuit is added on the interface board to control the power-on and shutdown of the device. A touch-screen is provided for user operations, showing large buttons on the application interface to allow finger use. The on/off control of the touch-screen back-light is implemented through interface board, in order to save a significant amount of battery. Two external USB connectors are present for a Crypto-device, used to digitally sign the result data, and for data transfer, to allow the import and export of data without the need of a laptop. The EUSR is equipped with a serial RS-422 interface to be able to communicate with EOSS and AOLS active seals and read-out their activity log files. Finally, the EUSR carries a dedicated reading device, including a built-in USB camera with active illumination, to acquire images of Cobra passive seals. As can be seen in Figure 1b, the seal-holder is exchangeable, supporting different back-ends for other seals or objects to be analysed. The optical design is further described in the following section.

## 2.1. Camera and light configuration

The EUSR device is equipped with a high-quality CMOS camera with 5MP resolution, to be able to accurately acquire and compare reference and verification scans of passive seals. Although a monochromatic camera would be needed for the grey-scale Cobra seals, a colour camera is used to account for possible future extension to different sealing objects that can carry a specific colorized pattern on the seal body, such as the Glass seals. Concerning the illumination system, a neutral white illumination is chosen in order to cover the full spectra of visible light. Traditional 2-pin LEDs are used for the EUSR design, with a high energy efficiency and focused angular distribution in order to optimize the light introduction into the fibre-cores and increase the fibre-end illumination to account for long optical cables.

The light configuration is designed to minimize the specular reflections back-projected onto the imaging sensor, which reduce image quality. As depicted in Figure 1b, the EUSR device is provided with a

squared configuration of 28 white LEDs arranged in four arrays around the camera. For the illumination of the flat Cobra head surface, all four LEDs arrays are activated in such a way that the light never reflects back to the sensor and the highest amount of light is introduced in the fibre-cores (Figure 3a). Instead, for the illumination of future cylindrical sealing objects only two lines of illumination can be activated, in order to reduce the glossy response generated by the round structure (Figure 3b).

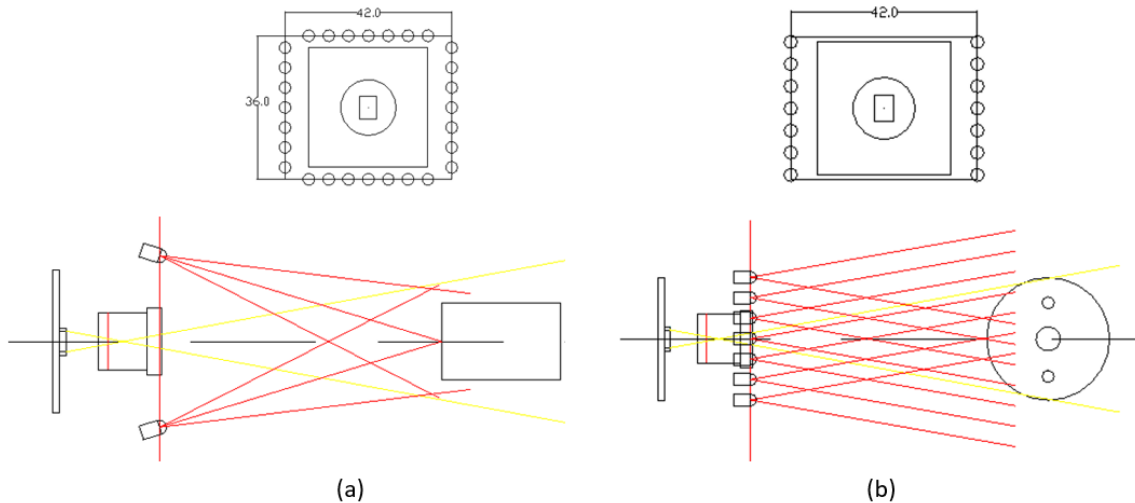


**Figure 3:** Optical design of the EUSR illumination, which can be applicable to both flat seals, by activating all LEDs arrays (a), and to cylindrical sealing objects, by activating only two opposite LEDs lines in order to avoid specular reflections of the round surface (b).

### 3. Software application

The EUSR hosts a number of “Seal-applications”, which can be loaded as dynamic modules depending on the requirement of a specific EUSR device. Each Seal-application can expose one or more actions, which are represented as selectable buttons on the main interface of the application (shown in Figure 4). The application uses a “Facility” concept and all actions performed by a Seal-application, such as image acquisition or data transfer, manage files in the Facility-folder stored on the disk. The EUSR also hosts a number of internal services available to all loaded Seal-applications, which are mainly camera support, Optical Character Recognition (OCR) engine, PDF-report generator and data import/export resource.

The camera resource can provide both a single image or a live stream of images, with a given gain and exposure time specified by the requesting Seal-application. In case of single image, the High Dynamic Range (HDR) algorithm [7] can be applied to obtain the best possible balanced image. As depicted in Figure 5, multiple images with different exposure times are merged to compensate the loss of details in the over-exposed or under-exposed parts of each single image, thus increasing the image contrast both in bright and dark regions. This makes the system robust to varying ambient lighting and active light-conditions. As another internal resource, the EUSR can provide the automatic identification of the alphanumeric serial number present on the seal head by using OCR techniques [8]. Results obtained from each Seal-application can be included in a PDF report, which is tailored according to the information of the template supported by each Seal-application or Facility. Finally, data can be exported or imported from a connected removable USB memory, with the possibility for each Seal-application to specify the files that should be copied. In the following sections, the main Seal-applications will be described in detail.

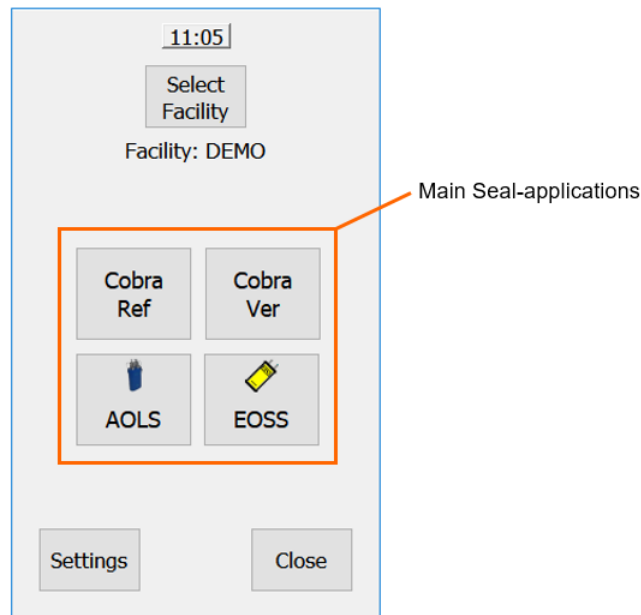


**Figure 4:** Main graphical user interface of the EUSR device, highlighting the main Seal-applications for the acquisition of reference and verification Cobra seal images and for the communication with AOLS and EOSS seals.

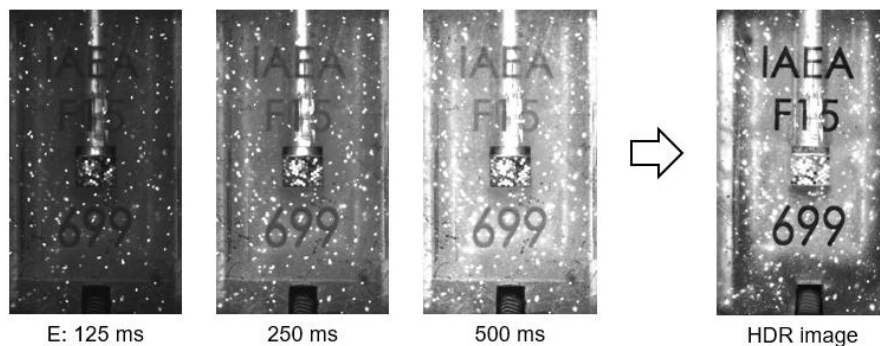


**Figure 5:** Example of Cobra seal image acquired with the EUSR device, obtained by merging three different exposure times (E) with the HDR algorithm.

### 3.1. Cobra Seal-application

Figure 6 shows all the different head revisions of Cobra seals that can be handled by the EUSR application, accounting for different character position/orientation and font variations. As shown in Figure 4, the Cobra Seal-application exposes two main functionalities to the user, namely the acquisition of reference images and the acquisition/evaluation of verification images. The processing of Cobra seal scans is summarized in the flow-chart depicted in Figure 7. Due to possible mechanical variations in the assembly of the EUSR optical components and in the insertion of the Cobra head in the seal-holder, the head position within the acquired full image (Figure 8a) can change between different devices and acquisitions. Therefore, as a first image processing step, the Region of Interest (ROI) of the Cobra head (Figure 8b) is extracted from the surrounding black background by applying thresholding techniques. The correct placement of the Cobra head in the seal-holder is also checked. The software automatically recognize which head revision is under evaluation and consequently adapt the ROIs for the extraction of the characters and fibre-end images (Figure 8b). OCR techniques [8] are applied to the characters ROIs for the automatic identification of the Cobra head serial number (Figure 8c). A level of confidence is assigned to each recognized character and the user can manually edit wrong items using an alphanumeric keyboard. Low confidence values can be, for example, due to the overlap of the bright control pin, which makes the character interpretation difficult (as depicted in Figure 8b).

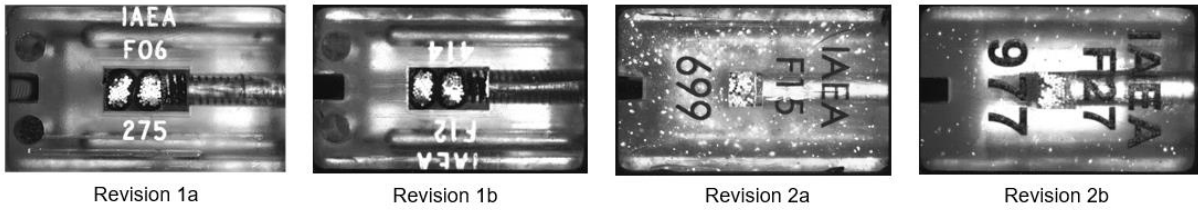


Figure 6: Samples of Cobra head revisions that can be handled by the EUSR system.

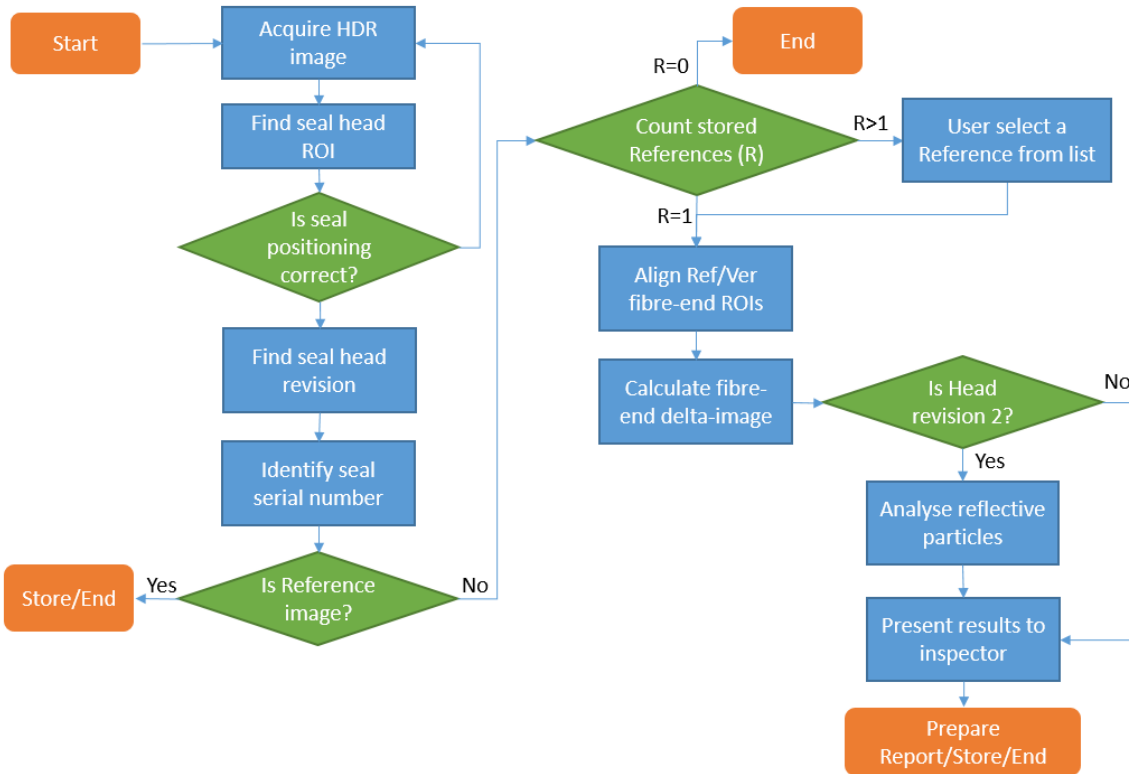


Figure 7: Flow-chart showing all Cobra image processing steps.

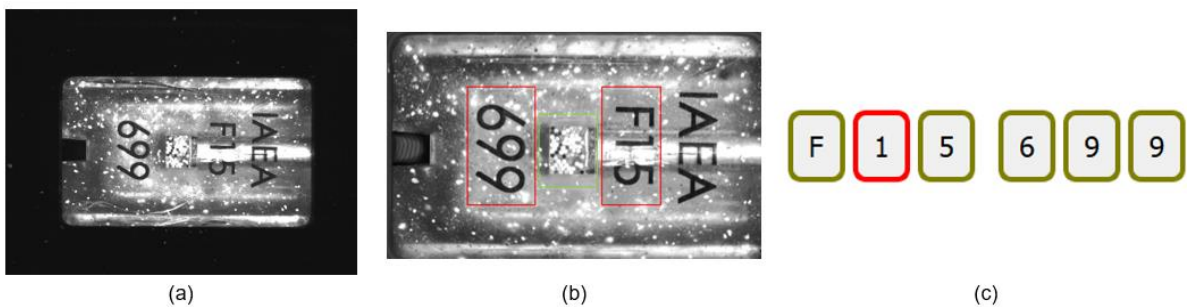
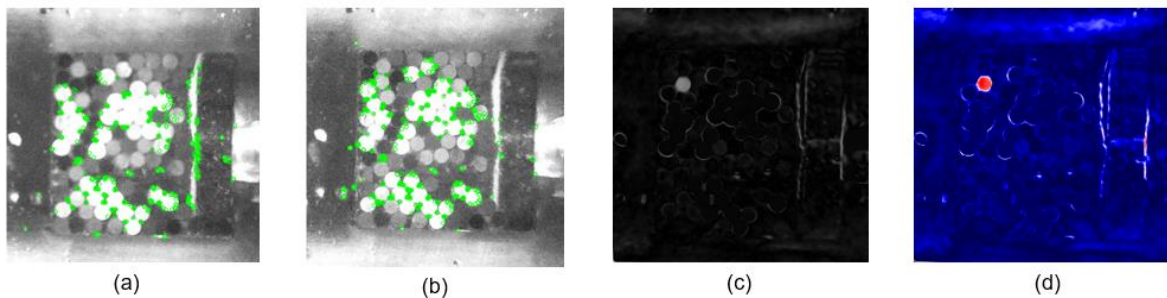


Figure 8: (a) Full image of a Cobra seal acquired by the EUSR camera. (b) Seal head ROI extracted from the full image, highlighting the fibre-end region in green and the characters regions in red. (c) Results of the OCR analysis applied to the characters ROIs, as shown on the EUSR interface. The box around each character denotes the level of confidence in the character recognition, i.e. high confidence for green boxes, medium confidence for dark green boxes and low confidence for red boxes.

In case of a reference scan, after the validation of the serial number, the image is stored in the Facility folder, adding EXIV meta-data fields in the image file. The stored EXIV tags allow retrieving for each image the Cobra head serial number, the image type (reference or verification) and the date/time it was acquired. In case of a verification scan, instead, an assisted comparison is performed with a reference image stored in the database and carrying the corresponding serial number. The EUSR application also works with reference images acquired with current available Cobra seal readers [6]. To account for imperfections in the imaging systems and optical differences between individual EUSR devices and

current available systems, the reference and verification fibre-end ROIs are aligned through image registration. The optimum transform is obtained by matching corresponding features identified on both reference (Figure 9a) and verification (Figure 9b) ROIs [9]. The aligned reference and verification fibre-ends ROIs are then equalized and grey-scale corrected using an intensity compensation algorithm [10]. A delta image is finally obtained by subtracting the two aligned ROIs. In order to assist the Nuclear Inspector in evaluating the differences between reference and verification images, the user interface shows the grey-scale (Figure 9c) or pseudo-colour (Figure 9d) delta image and allows switching between the two aligned ROIs. In case of intrinsic reflective particles present on the seal body (as seen for revision 2 in Figure 6), the positions of these particles are analysed to check the authenticity of the Cobra head. The seal head ROI, excluding fibre-end and character regions, is extracted from both reference and verification images. Intensity compensation and feature matching are applied to these ROIs [9,10]. After alignment, the extracted features corresponding to the reflective particles are depicted on the reference and verification images for visual inspection, warning the user in case of poor correlation.



**Figure 9:** Fibre-end ROIs extracted from the reference (a) and verification (b) Cobra seal images, depicting in green the corresponding features used for image alignment. The subtraction of the aligned ROIs generates a delta image, which is shown on the EUSR interface both in grey-scale (c) and in pseudo-colour (d).

### 3.1. AOLS and EOSS Seal-application

Both for AOLS and EOSS active seals, a single seal or several daisy-chained seals (up to 16 interconnected units) can be connected to the EUSR device via the RS-422 interface. The Seal-application is able to query which seals are available and download each individual activity log files. Using the hosted import/export resource, the log information can be copied to a USB memory for further transfer to the headquarters. In case of the AOLS seals, the EUSR application can show the content of the activity log files, since they are transmitted in clear text. The attached signature for data authentication is transferred by the EUSR application along with the files. In case of the EOSS seals, the EUSR device is also able to connect to the EOSS Crypto-token. If this token carries the digital private keys for the encrypted data format, the EUSR application can decrypt the transferred information and show its content.

## 4. Discussion

This document presents the detailed design, improvements and advantages of the developed EUSR device, which provides a single tool to handle the most common types of Nuclear Safeguards seals, namely the Cobra passive seal and the EOSS/AOLS active seals. Compared to the current approach requiring the use of different tools for each sealing activity, the EUSR system adds a number of benefits for Safeguards organizations. It requires a single training course and manual for the Inspectors and it simplifies the equipment logistics, since only one type of battery needs to be charged and one device needs to be maintained by technicians.

The EUSR built-in functionalities were designed as generic as possible for extended future use. The system architecture is modular and versatile, meaning that a new application can be easily added to the EUSR. The exchangeable seal holder, as well as the RS-422 interface and camera resources, allows for possible future adaptations to new seals or objects to be pictured or analysed. Another advantage of the EUSR is the user friendliness, since the device can be held in a single hand and the user interface shown on the touch-screen is easy-to-use and optimized for finger use, without the need of a stylus.

The device is designed to be used also in outdoor environments accounting for dust and different weather conditions. As generic resources, it provides the automated reporting of the obtained results and the digital signing and authentication of the transferred data.

The EUSR device offers improved functionalities for Cobra seal analysis compared to current available reading systems [6]. The high quality camera and the applied HDR algorithm allow acquiring seal images with better quality, increasing the contrast and reducing blurring and distortion artefacts. This enables the analysis of the reflective particles on the Cobra head for a further seal authentication, which is prevented in current reading systems by the low image quality. The dedicated illumination designed for the EUSR optimizes the light introduction in the fibre-cores, allowing the analysis of longer optical cables (up to 30 meters). The device adds the automatic recognition of the Cobra head serial number and performs a much stronger evaluation and comparison between reference and verification Cobra scans, providing a delta image that can assist the Inspectors in taking decision. Finally, the backwards compatibility is guaranteed, since the EUSR application allows the comparison with reference images acquired with current Cobra reading systems. At the same time, the EUSR provides reference images converted in a proper format to be used in current systems for analysis.

As a future development, by acquiring a sufficient amount of information and experience data, the EUSR application can potentially provide to the Inspector a final proposal on the comparison between reference and verification Cobra images to be authenticated. In case of strong image correlation, the Inspector would not be obliged to manually compare the two scans. Future extensions of the EUSR hardware are also planned. A new version dedicated only to Nuclear Safeguards Operators is foreseen, with further optimized mechanical design and a docking station for automated data transfer. An optimized version to read only the active seals is also planned. In this version, the camera and illumination will be removed, thus reducing the overall mechanical size. This type of device is expected to play a key role in the active seal handling in future safeguards installations, since it can be used in-field by an Operator to issue readings of the active seals.

## 5. References

- [1] Waddoups IG; *Advances in containment and surveillance (C/S) which enhance the interaction between safeguards authorities and the operators*; SAND-83-0826C; United States; 1983.
- [2] Rocchi S, Hadfi G, John M, et al; *Evaluation of a Surveillance Review Software based on Automatic Image Summaries*; IAEA-CN-220; International Atomic Energy Agency (IAEA); 2015.
- [3] U. N. R. Commission; *Tamper-indicating seals for the protection and control of special nuclear material*; Revision 1 to Regulatory Guide 5.15; U.S. NRC; 1997.
- [4] Vodrazka P, Cermak L; *Cobra sealing system*; Nuclear Materials Management; 1991; p 852-856.
- [5] Jussofie A, Van Bevern K, Hahn M, Trautwein W; *Germany's Accelerated Exit from Nuclear Energy: Challenges and Perspectives with Regard to Safeguards*; IAEA-CN-220; International Atomic Energy Agency (IAEA); 2015.
- [6] iCobra Quick-Start Guide, v. 1.1; Aquila; 2012.
- [7] Mertens T, Kautz J, Van Reeth F; *Exposure fusion*. Proceedings of 2007 IEEE Computer Graphics and Applications; 2007; p 382-390.
- [8] Patel C, Patel A, Patel D; *Optical Character Recognition by Open source OCR Tool Tesseract: A Case Study*; International Journal of Computer Applications 55 (10); 2012; p 50-56.
- [9] Rublee E, Rabaud V, Konolige K, Bradski GR; *ORB: An efficient alternative to SIFT or SURF*; ICCV; 2011; p 2564-2571.
- [10] Xu W, Mulligan J; *Performance evaluation of color correction approaches for automatic multi-view image and video stitching*; Proceedings of 2010 IEEE Computer Vision and Pattern Recognition; 2010; p 263-270.

# Use of commercial components for a future Surveillance Camera

G. Boström, F. Ghiringhelli, V. Sequeira

European Commission, Directorate Joint Research Centre, Nuclear Security Unit,  
Ispra, Italy,

E-mail: [gunnar.bostrom@ec.europa.eu](mailto:gunnar.bostrom@ec.europa.eu)

## **Abstract:**

*The commercial market is filled with cameras of various kinds and with informatics components such as ready-made single board computers and robust operating systems. In the area of software development, many tools are available and very often free to use even in a commercial system. In the nuclear safeguard community, there has not been a tradition to use much of these resources. Often, dedicated development projects with closed solutions from a single supplier or a consortium have been applied.*

*In the application area of nuclear safeguards, specific requirements apply such as mean time between failures (MTBF), long-term battery operation, tamper-indication and equally important the ability to operate in areas with ionizing radiation. Will this pose problems or prevent a system from being built using commercially available components?*

*This article presents a study that aimed at identifying commercial systems or commercial components and open source initiatives suitable for a future nuclear surveillance camera. It summarizes the main requirements of the camera and analyses the consequences from the commercial component perspective. We list the most suitable components taking into account both second-source and long-term availability. Based on the findings, a future prospective technical project is sketched for which a future nuclear surveillance camera could be drafted.*

**Keywords:** surveillance; camera; embedded systems.

## **1. Introduction**

The development of a nuclear safeguards camera must be carefully planned in advance because the overall development cycle, from the analysis phase to the moment of commissioning, requires a considerable amount of time. For example, the nuclear safeguards camera currently in use, the 'Next Generation Surveillance System' (NGSS), required about eight years from initial design to be deployed in the field. And this includes not only for the technical work (i.e. requirements, design, development, and testing) but also for the authorization process, which is also quite long.

Furthermore, the development of such a camera is never finalized as the system needs to be continuously maintained to cope with design limitations, change requests and to extend functionalities. Specifically, the level of cyber-security embedded in the surveillance camera requires a developer to always be ready to patch or update the camera when new cyber-attack techniques are discovered.

The existing NGSS camera will continue to serve the nuclear safeguards organizations around the world for many years to come. Still, considering the lead time for any safeguards instrument development, the design of the successor of the NGSS camera should not be delayed. The NGSS is a well-designed and robust camera that meets the high requirements of a nuclear safeguards camera. However, it also suffers from some design limitations such as single volatile memory store. The SD-card memory itself faces increased single event upset sensitivity because the manufacturers optimize their storage capacity, e.g. decreasing size of intrinsic memory cells.

It is not easy to identify a new camera. Commercial systems may be available, but it is unlikely that a replacement camera can be found that fulfils the requirements. Additionally, other factors such as the risk of depending on a single supplier, costs, and long-term stability for supplies must be taken into account. Objectives like MTBF and service needs have a central role in the search for a successor to NGSS. For example, if a camera has needs more service in the field, the overall economy will change dramatically.

Section 3 and 4 of this article summarize a study requested by DG-ENER/Luxembourg that aimed at exploring whether a new camera platform can be considered using Commercial-Off-The-Shelf (COTS) components or systems. The study investigated whether existing complete camera systems can fully support the requirements or whether they can be extended to fulfil these requirements. In case one would find a suitable system, would it be possible to guarantee a stable supply of systems for 10 years from the initial release? Would there be issues with intellectual property rights preventing the possibility to create a future critical security patch? Would even the supplier exist?

In addition, the study also analysed the possibility to build a camera system using existing off-the-shelf components. In this way, the development could re-use knowledge from the commercial market and potentially lead to a faster and more cost effective development. Also this approach comes with some concerns: would the component manufacturers exist in 10-20 years? Are there existing second-source components?

To further motivate and support this study, one can conclude that cameras have been introduced into a broad selection of today's technical appliances over the last years. The camera technology is cheap and the industry is overwhelmed with small to medium sized companies selling systems or components suitable for building fully functional surveillance camera systems.

Based on the study results, the JRC started the development of a test-bed and prototype that can support the design and development of a future safeguards surveillance camera. Section 4 describes the ongoing developments and section 5 provides some conclusions.

## 2. Requirements and implications

In order to set the boundary conditions for a study of existing cameras or existing commercial sub-components, a list of the critical high-level system requirements is needed. Table 1 lists the requirements as defined by the European Commission, Directorate ENER.E.1 [1], divided in sub-groups.

Most of requirements are met by many commercially available surveillance cameras, but some requirements are very specific. For example, if we focus our attention on power consumption and battery backup aspects, we see that the ideal camera-system must be able to: (a) acquire 5 frames per second (in burst mode), (b) evaluate at least 1 frame per second with (c) 10 individual motion detection zones, and (d) perform mpeg-encoding. In worst case, (e) this is has to be done on a battery for several days. The statements (a)-(d) indicate that a CPU/DSP with proper capacity must be used while the power-related statement (e) suggests that the system should use low-power components in order to save as much energy as possible. This directly indicates that very few, if any, commercial off-the-shelf system can match these requirements.

Most requirements such as those related to image-processing, triggering, cryptographic operations and mechanics are easier to satisfy as they do not impose any restrictions on the evaluation of the commercial components for a new surveillance system. However, three of the requirements reported in Table 1 are particularly difficult to satisfy for existing commercial cameras:

Group	Identifier	Requirement
General req.	GEN1	Flexible configuration (use as much standard devices and COTS)
Environmental requirements	ENV1	Must pass environmental tests: thermal, vibration, shock, electromagnetic interference, and electrostatic discharge
	ENV2	Radiation tolerant by covering Single Event Upset (SEU)
Reliability	REL1	Unattended and reliable operations for long period in harsh environment (MTBF $\geq$ 20 years)
Camera optical sensor	OPT1	Progressive scan optical sensor
	OPT2	Resolution $\geq$ 2M pixel
	OPT3	Sensitivity 50 IRE (fully opened diaphragm)
Camera housing	HOUSE1	Tamper indicating enclosure
	HOUSE2	CCTV input (RGB or B/W) for video signal branching
	HOUSE3	Dimensions (WxLxH) $\leq$ 180x290x140 mm
Image compression and resolution	IMG1	Compression algorithms: JPEG, MPEG2, MPEG4, or H.264
	IMG2	Image quality from 4CIF (704x576) to HD1080p (1920x1080)
Data authentication	AUTH1	AES with asymmetric keys, PKI, or port based
	AUTH2	Information to authenticate (e.g. image, timestamp, metadata)
Network	NET1	Secured network communication via TLS
	NET2	Multicast to provide images to at least 2 servers
	NET3	SNMP support to get SOH from the camera
Data buffering	BUF1	Store images for $\geq$ 7 days in case of power loss
	BUF2	Store images for $\geq$ 20 days to compensate server connection loss
Data encryption	ENC1	Encrypt data stored in local buffers (SD card)
Setup	SETUP1	Remote setup and readout of images, ideally via Web interface
	SETUP2	Secured network communication via TLS
	SETUP3	Password protected access
Power	PWR1	Two independent power sources (power redundancy)
	PWR2	Power back-up $\geq$ 7 days
	PWR3	Low voltage $<$ 60Vdc or 230 Vac with optional power supply unit
Image triggering	TRG1	Trigger by Time Lapse (programmable PTI in the range 1s to 30min)
	TRG2	Trigger by Motion Detection
	TRG3	Trigger by External Source

**Table 1:** List of requirements for the safeguard camera.

**ENV2:** The requirement defines that the camera should cope with a Single Event Upset (SEU) or more generally, be able to work in an environment with ionizing radiation and high-energy particles. The two primary ways radiation can affect electronics are: Total Ionizing Dose (TID), a long term destructive effect, and Single Event Effect (SEE), normally random non-destructive event. The TID effect is difficult to handle and for cases with very high radiation levels, specific hardened camera-systems are used.

In case of SEE, any nuclear surveillance camera must be able to address these problems. The effect can be a bit-flip in memory or program registers (i.e. SEU) [2]. In order to maintain a system with a high MTBF, watchdogs and an embedded capacity to power-cycle the device are crucial. One could consider using hardened Single Board Computers or components found in satellite electronics. In general, these are very expensive and difficult to be found as COTS. A watchdog together with a built in memory sanity checker (i.e. Data Scrubber, [3]) could potentially solve the issue for events related to running RAM.

**REL1:** A Mean Time Between Failure (MTBF) of 20 years or more is desired. However this level of MTBF is difficult to guarantee for any system, unless one would have a production based on individual components environmentally tested as it is done for satellite-electronics. Nevertheless, several measures at all design steps can increase the operational life. These would include (as also indicated in requirements above) redundant critical components such as power supplies and external memory plus an external independent health-monitor/watchdog with power-cycling capacity.

**PWR2:** The power autonomy is another concern. This requirement stipulates an autonomy on embedded battery for more than 7 days. As indicated in the introductory example, the system

functionality needs to be balanced with respect to processing speed and hibernate capacity. What processing power is needed to keep the core functionality running while remaining as efficient as possible? What basic services must be shut down on battery operation? For example, by definition the tamper indicating service must always be active. The same applies to the maintenance of private cryptographic keys. Some commercial surveillance cameras are equipped with back-up batteries which however guarantee limited autonomy. Such cameras are not meant and designed to perform on battery for days. Instead, they are designed to guarantee operation in the event of short power outages, i.e. a few hours.

### 3. Solutions

The industry today is overwhelmed with camera systems and components. They can be found in any small device, from toys and smart-phones to sophisticated systems for tracking of human faces in open spaces and airports. In recent years, the arrival of low-cost electronics, CPUs and optical CMOS sensors has enabled very small organizations and companies to develop complete camera systems in-house.

Many of these systems are the result of assembling basic commercial components that represent the cornerstones of a camera. This is possible thanks to the wide availability of these components on the market today. Single Board Computers (SBC) with built-in drivers for the most popular CMOS sensors can be deployed in a short time.

With the availability of many COTS components, open source libraries and operating systems, it is not too difficult to develop a surveillance camera with customized system functionality. However, the ease of making a commercial product can also have a negative impact: the competition between camera vendors is obvious and the long-term stable supply of a specific camera may be impacted on the commercial success of the chosen company. Thus, selecting the right camera system to adapt is crucial.

Finally, as we discussed in Chapter 2, the long-term availability of the new safeguards camera and its spare parts must be guaranteed, which suggests that second-sources and equivalent replacements need to be identified from the initial stages.

We have identified three different strategies to build a complete camera system. They are shown in table 2 and further elaborated in the following sections.

Strategy	Description
Adapted COTS system	Reconfigure, extend and adapt an existing camera as needed
Use of COTS components	Build the camera by assembling commercial components and modules
Dedicated development	Build the camera from scratch by designing dedicated HW and SW

**Table 2:** Three strategies to build a complete camera system.

#### 3.1. Adapted COTS system

The current needs for professional camera systems come mainly from two sectors: the ever-increasing surveillance sector and the process automation sector. Camera systems of both sectors consist of ready-made cameras with limited but existing extension capabilities.

##### 3.1.1. Surveillance sector camera systems

In general, surveillance cameras are cost-optimized products with all the logics and processing power embedded in energy-optimized ASIC's. For fine-tuning, they offer numerous configuration options such as motion detection, network interaction, optical/lens aspects, image-masks and storage features. An example of surveillance camera from Bosch is shown in figure 1a.

Compared to others, this is the most economical solution that also has the advantage of drastically reducing development time. The disadvantage of these systems is that they offer no extension capability since the vast majority of customers would accept existing configurable options. This makes them not suitable for building a safeguards surveillance camera.

### 3.1.2. Automation sector camera systems

The automation sector has a long history in using video camera systems typically for process and quality monitoring. These cameras are complete video systems that use image processing algorithms to identify anomalies, count objects in view, guide robot-arms or other relevant tasks. An example of such cameras is the Tattile S200 shown in figure 1b.

They offer on-board extension capacity. Unfortunately, they lack important features such as embedded encryption and authentication. Tamper indication is also missing but, in some cases, can be implemented by mounting the camera in a designed enclosure and using a programmable digital input for the tamper sensor.



(a)



(b)

**Figure 1:** (a) Bosch DINION IP 5000 MP surveillance camera: CMOS 1/3" sensor, 2592x1944 resolution, 12 fps. (b) Tattile S200 automation sector camera: Dual Core ARM Cortex-A9 800 MHz, CMOS CMV4000 sensor, 2048x2048 resolution, 180 fps.

## 3.2. Use of COTS components

An alternative solution of using commercially available complete systems is to design the camera by assembling low-level COTS components. This approach has several advantages including a proprietary design, reduced development time and costs, the possibility of pre-building interfaces for future sensors, etc.

In addition, this solution offers maximum flexibility both in hardware and software. For example, the design can be "second-source-aware" in order to minimize the impact in terms of time and cost of replacing any component. Moreover, having control over the entire software development, it is possible to integrate any custom artificial vision algorithm. This would potentially allow to process the video in real time and save the results in the camera so that they are immediately available at the time of review.

There is a large amount of COTS components which can serve the purpose when designing a dedicated nuclear surveillance camera. This category includes both complete cameras that could form the basis for further extensions and adaptations and low-level COTS components such as board cameras and Single Board Computers (SBC).

### 3.2.1. Off-the-shelf cameras

Assembled in a proprietary housing, these cameras provide a digital interface for triggering and image streaming. Usually they do not have internal memory for saving images locally. They must also be connected to a host (embedded) computer to form a complete vision system. Figure 2a shows an example of such cameras from Imaging Source.

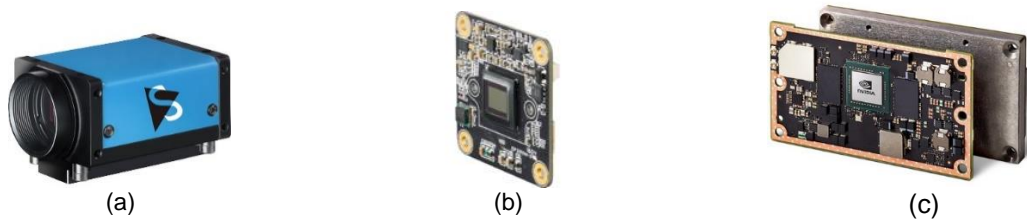


**Figure 2:** (a) Imaging Source DFK 38UX267 off-the-shelf camera. (b) Imaging Source DFM 27UP006-ML board camera and (c) the NVIDIA Jetson TX2 supercomputer.

### 3.2.2. Board cameras and Single Board Computers

Board cameras lack housing and higher level electrical interface for triggering and power supply. They can be connected to many SBC platforms of various capacity available on the market. For example, a board camera such as DFM 27UP006-ML from Imaging Source (figure 2b) can be easily interfaced with popular low-cost SBCs like Raspberry Pi or the more powerful NVIDIA Jetson TX2 (figure 2c).

### 3.3. Dedicated development

The last option is to design a camera system from scratch. The development would involve the design of a dedicated Printed Circuit Board (PCB) as well as a dedicated programmable logics to extract images from CMOS sensors and to run the low-level sequencers.

At first, this may seem like a long process, but with the wide range of examples and reference projects for electronics along with open source software, it could be a very reasonable way forward. A sample reference design from Elphel [4] giving an idea of how to build a modular camera system is shown in figure 3. In this example, a camera board is interfaced with a computer board that in turn is connected to an extension board that provides additional interfaces. This reference design is not meant to be used “as is” but it can serve as a template to assist the design.

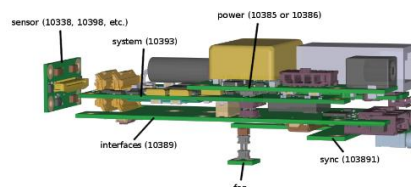


**Figure 3:** Sample reference design for a modular camera system from Elphel.

## 4. Summary and next steps

Based on the findings, as briefly summarized in chapter 3, we conclude that the different approaches have advantages and disadvantages. The possibility to identify a ready-made system, as in the adapted COTS system strategy that supports our requirements, can be ruled out for several reasons. First, the requirements cannot be met by any identified system. Large scale adaptations and extensions would cost development resources and by the end one would depend on a commercial company for decades to come. This is neither recommended nor cost-efficient. The second strategy mentioned, ‘use of COTS components’, is interesting since there is a large amount of available standardized components available which could serve as the foundation for a safeguards device. Surely, this strategy would require some amount of dedicated design to support the commercial components but having the base for camera and board computer would give the development a head start. The third strategy identified, ‘Dedicated development’ is always the fall-back scenario. Selecting and using dedicated components, a skilled electronics designer would in a reasonable amount of time design the base for a new safeguards system.

In conclusion, we consider the second strategy the best way forward and have therefore started an extended analysis and test-development project in order to better evaluate the possibility to use such components as the basis for a future generation surveillance camera.

The development process for a new complex safeguards device such as a surveillance camera with all the requirements is long and winding. Taking into account that one also wants to make use of existing commercial modules one should potentially not start the design work without some initial test-cases. Some explorative developments are needed to exclude certain designs and components and validate others. In order to rapidly get some hands-on experience of a system design using varying level of commercial components, we will perform an explorative study including two steps of increasing system completeness which are described in the following sub-sections. We hope and believe that these steps will lead to a shorter and more efficient future development project whoever is undertaking this task.

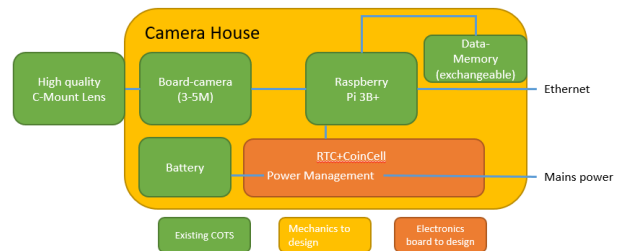
#### 4.1. First development stage, “test-bed”

The first step, denoted “test-bed” will be based on existing components from the Embedded Universal Seal reader (EUSR) [5]. The aim is to build a test-bed within a short amount of time to evaluate the basic concepts of using commercial components and to implement a first design of supporting firmware which is able to support many of the basic requirements for a nuclear surveillance camera. The development tool-chain, low-level hardware access and camera are inherited from the EUSR design in order to get a flying start. Mechanically, the camera will be built using a rapid prototyped shell together with a supported aluminium frame where tolerances and stronger structures are needed. Internally, the system would carry a backup battery for a limited time off mains supply. The design will enable the use of high quality C-mount camera-lenses.

In order to be able to test the cryptographic functionalities, an attached crypto-device will provide the private key and the full support for encryption, data-authentication and secure encrypted inter-process communication will be present. This solution will not be used in a final design but it is added in order for the test-bed system to validate the higher-level cryptographic capacities.

A short summary of the components are listed in figure 4a and a descriptive schematic of the simple test-bed architecture in figure 4b.

Components	Brand/type
SBC	Raspberry PI 3+
Camera	Imaging Source 5MP
Crypto-device	Card-contact HSM
Backup-Battery	Tracer LiFePo <sub>4</sub>
Electronics board	Dedicated design



(a)

(b)

**Figure 4:** Indicative ‘test-bed’ design: (a) major components and (b) brief system design.

Since the hardware was not designed to support low-power modes such as system hibernate, reduced clock-frequency or low-amp sequencer, we cannot expect this system to meet the battery autonomy requirement. The same applies for the environmental requirements and complete tamper-detecting casing that will not be considered in this phase. However, many of requirements are expected to be met: for example, the system will provide full support for capacities such as image-quality, video-compression, storage-design and configurable requirements.

As previously mentioned, ENV2 requirement of table 1 regarding the operation in environment with iodizing radiation is a special test-case and during this phase there will be a dedicated hardware set-up to analyse the effects of SEU. Together with a dedicated firmware we hope to detect SEU during exposure and be able to take proper actions.

#### 4.2. Second development stage, “functional prototype”

The second step, denoted “functional prototype”, will be a more dedicated development activity, based on the experience of the test-bed step and with a more realistic set of hardware components that hopefully will meet all the requirements. By choosing more sophisticated and complete system

components such as layered boards with embedded microcontrollers, we can achieve a functionality that guarantees better performance on battery operation.

At this time, it is not possible to define exactly which components and features should be included, but this system prototype would certainly support long-term power-battery usage, which means that the system must have the ability to hibernate between scheduled activities. The active device always running would be a very power-optimized micro-controller handling sequencing, crypto-activities and tamper-detecting capacities.

Most probably, the more demanding processor part will be based on the versatile SMARC board [6] SBC using layers of CPU's together with a commercial or open Real-Time Operating System (RTOS). As mentioned before, a board camera and a commercial battery-pack are foreseen.

It would also be interesting to evaluate the concept of a modular design [7], which would enable current and future sensors to intrinsically inherit the cryptographic capacity and RDT tools, obligatory in a nuclear surveillance camera. This would potentially be implemented using a cascading bus concept from PC104 [8], dedicated to the new modern inter-process communication for ARM processors. In such a concept depicted in figure 5, each PC104-formatted board would host a single SMARC SBC.

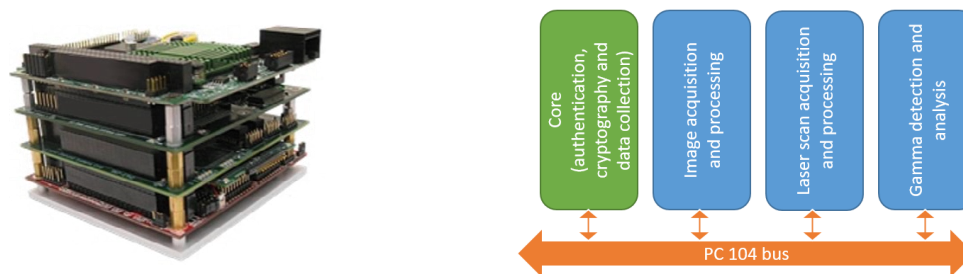


Figure 5: Sample image of a cascading PC104 designed pack.

## 5. Conclusions

In this article, we have reported on a technical study that evaluated the use of commercially available components to be part of a future nuclear safeguards camera development. We have discussed the high level requirements for such a device and put them in the context of commercially graded equipment. We have analysed different strategies of how to develop a future nuclear safeguards camera and we have concluded that a limited amount of the requirements which are specific to the nuclear safeguards sector makes it very difficult to find a commercially available camera that can either be purchased directly or extended. We have also concluded that there is a rich list of standardized components that would allow the cost-efficient development of a customized nuclear safeguards surveillance camera. To support the idea, we started an explorative development project in two steps which will further test the concept. The first stage, denoted 'test-bed' will test the concept of COTS equipment with existing components that have already been used for the universal seal reader. A following step 2 denoted 'functional prototype' will be targeting all requirements and carry more suitable components for a future nuclear surveillance camera.

## 6. Acknowledgements

The authors would like to thank Juha Pekkarinen and Konrad Schoop from DG-ENERGY in Luxembourg for supporting us with a requirement specification, comments and good cooperation during this study.

## 7. References

[1] Directorate E Euratom Safeguards, E.1 Quality assurance and technology, 'Requirements for Safeguards Cameras and Systems'.

[2] Fan Wang et. al., "Single Event Upset: An Embedded Tutorial", in 21st International Conference on VLSI Design 2008, doi:10.1109/VLSI.2008.28

[3] Data scrubber, [https://en.wikipedia.org/wiki/Data\\_scrubbing](https://en.wikipedia.org/wiki/Data_scrubbing)

[4] Elphel reference design, [https://www3.elphel.com/353\\_components](https://www3.elphel.com/353_components)

[5] Boström et. al. "JRC Embedded Universal Seal Reader", in proceedings of ESARDA Symposium 2019

[6] SMARC Standard, [www.sget.org/standards/smarc.html](http://www.sget.org/standards/smarc.html)

[7] Boström, Sequeira and Wolfart, "Containment and Surveillance Systems—reflections on future technology", in proceedings of ESARDA Symposium 2017, doi:10.2760/631364

[8] PC/104 standard, <https://pc104.org/hardware-specifications/pcie104/>

# Tamper-Indicating Enclosures with Visually Obvious Tamper Response

**Heidi A. Smartt, Annabelle I. Benin, Cody Corbin, Joyce Custer, Patrick L. Feng, Matthew Humphries, Amanda Jones, Nicholas R. Myllenbeck**

Sandia National Laboratories  
Albuquerque, New Mexico, USA  
P.O. Box 5800 MS1371 Albuquerque, NM, USA 87185  
E-mail: hasmart@sandia.gov

## **Abstract:**

*Sandia National Laboratories is developing a way to visualize molecular changes that indicate penetration of a tamper-indicating enclosure (TIE). Such “bleeding” materials (analogous to visually obvious, colorful bruised skin that doesn’t heal) allows inspectors to use simple visual observation to readily recognize that penetration into a material used as a TIE has been attempted, without providing adversaries the ability to repair damage. Such a material can enhance the current capability for TIEs, used to support treaty verification regimes. Current approaches rely on time-consuming and subjective visual assessment by an inspector, external equipment, such as eddy current or camera devices, or active approaches that may be limited due to application environment. The complexity of securing whole volumes includes: (1) enclosures that are non-standard in size/shape; (2) enclosures that may be inspectorate- or facility-owned; (3) tamper attempts that are detectable but difficult or timely for an inspector to locate; (4) the requirement for solutions that are robust regarding reliability and environment (including facility handling); and (5) the need for solutions that prevent adversaries from repairing penetrations. The approach is based on a transition metal ion solution within a microsphere changing color irreversibly when the microsphere is ruptured. Investigators examine 3D printing of the microspheres as well as the spray coating formulation. The anticipated benefits of this work are passive, flexible, scalable, cost-effective TIEs with obvious and robust responses to tamper attempts. This results in more efficient and effective monitoring, as inspectors will require little or no additional equipment and will be able to detect tamper without extensive time-consuming visual examination. Applications can include custom TIEs (cabinets or equipment enclosures), spray-coating onto facility-owned items, spray-coating of walls or structures, spray-coatings of circuit boards, and 3D-printed seal bodies. The paper describes research to-date on the sensor compounds and microspheres.*

**Keywords:** tamper-indicating enclosures; international nuclear safeguards

## **1. Introduction**

Tamper-indicating enclosures (TIEs)<sup>a</sup> are used in treaty verification regimes to detect access to an item of interest. Items of interest can include, but are not limited to, (1) inspectorate-owned equipment enclosures in which detecting access is desired to ensure trust in information stored or processed within the enclosure and (2) facility-owned enclosures containing nuclear materials that have been measured by inspectors and require maintaining continuity of knowledge in the absence of the inspector. Current deployed TIEs typically fall within three categories. The first are materials that an inspector will primarily visually inspect for signs of unauthorized access, such as the ubiquitous anodized aluminium enclosures that the IAEA deploys with the RMSA fiber loop seal, the NGSS surveillance system, legacy surveillance systems, and other monitoring equipment. The second category are active electronic methods/materials that continuously monitor the volume for signs of unauthorized access, such as the conductive foil within

<sup>a</sup> Note that TIEs are essentially volumetric seals. As such, they must have an integrity and identity element. The integrity element (tamper-indicating) is the thrust of this work. The identity element will be addressed separately.

the EOSS fiber loop seal and the fiber mesh embedded in the enclosure of the NGSS. The third category are externally deployed indicators of penetration or access to materials, such as eddy current or imaging devices. Note that both the second and third category also require visual inspection. The limitations to these three categories are the subjective and time-consuming process of visually inspecting surfaces, the inability to deploy an active approach in some situations because of batteries or because of environmental conditions or facility requirements, and the limited materials able to be analysed by eddy current and potential inability to bring external equipment into a facility. Further, some approaches rely more on post-mortem analysis rather than in-situ verification.

The existing toolkit for TIEs is limited regarding the complex issues involved, and many technologies are old which may leave them more vulnerable. Simple visual approaches capable of high detection sensitivity have not received adequate research and development, although applications already exist that could benefit from such a capability. Sandia National Laboratories (SNL) recognizes these limitations and is developing “bleeding” materials (analog of visually obvious bruised skin that doesn’t heal) that provide inspectors the ability to readily recognize using simple visual observation that penetration into the material has been attempted without providing adversaries the ability to repair damage. Such material can significantly enhance the current capability for TIEs, used to support treaty verification regimes.

SNL’s approach is research and development of cargo-loaded microspheres embedded in 3D-printed structures or spray-coated onto existing surfaces, that when penetrated or tampered, cause an irreversible color change that is visually obvious<sup>1</sup>. Work comprises the following general tasks: (1) sensor and microsphere development and optimization (i.e., intensity of response, surface area of response, and microsphere composition, size, wall thickness, rupture point), (2) integration of transition metal-loaded microspheres into 3D-printed, spray-coated, or moulded geometries, and (3) testing and evaluation of prototypes, including environmental and industrial considerations. The anticipated benefits of this work are passive, flexible, scalable, cost-effective TIEs with obvious and robust responses to tamper attempts. These responses result in more efficient and effective monitoring as inspectors will require little or no additional equipment and will be able to detect tampering without extensive time-consuming visual examination. Applications can include custom TIEs (cabinets or equipment enclosures), spray-coating onto facility-owned items, spray-coating of walls or structures, spray-coatings of circuit boards, and 3D-printed seal bodies.

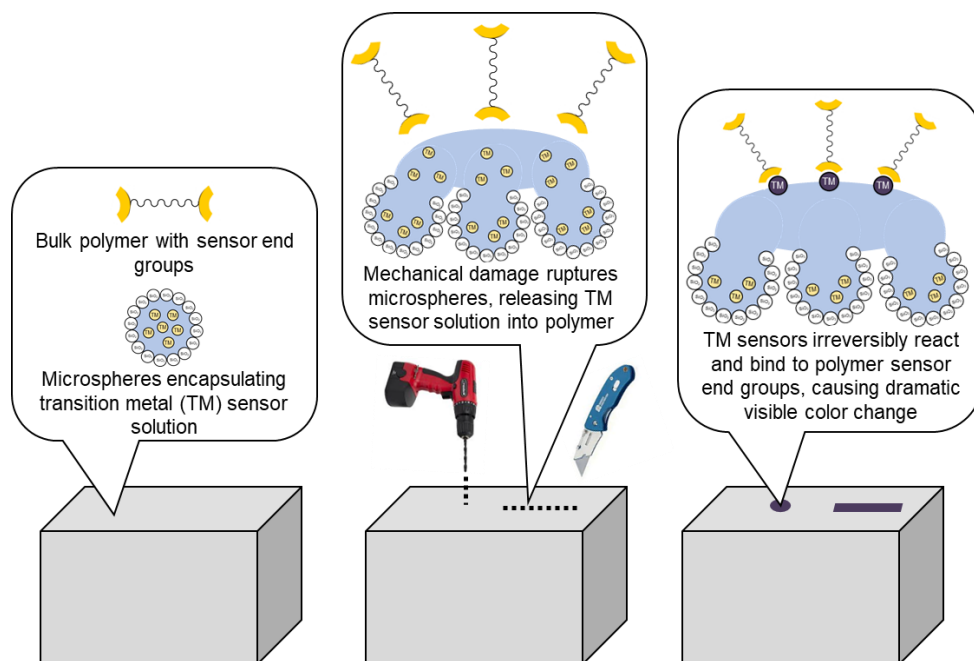


**Figure 1:** General schematic of R&D concept. A two-phase material consisting of a sensing polymer and transition-metal encapsulated microspheres are 3D-printed or spray-coated on to a unique geometry. Upon tampering, the microspheres rupture and the two sensor components interact to form an irreversible visible color change.

## 2. R&D of sensor compounds

Transition metal complexes consist of a transition metal center derived from a metal salt (e.g.  $\text{FeCl}_3$ ) and an organic molecule. The combination of these components can lead to dramatic and highly visible color changes which may be utilized for sensing application spaces. The initial approach for the goal of this project was to perform a scoping study with various 3d transition metals with one organic sensor (2,6-bis(10-methyl-benzimidazolyl)-4-hydroxypyridine, (HOBip)) to establish a qualitative evaluation of color change.<sup>2,3</sup> Figure 2 presents these results along with the chemical structure of the sensor that was utilized.

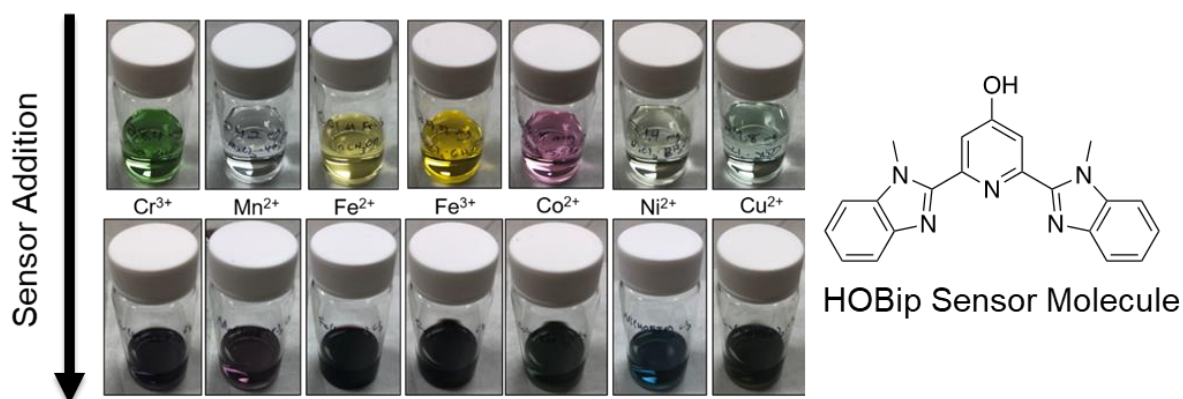


**Figure 2:** Qualitative scoping study results on 3d transition metal color changes with addition of organic sensor in methanol. All metal solutions get significantly darker, and many have a dramatic color change.

Once the plausibility of the mechanism was confirmed, our second goal was to make a series of transition metal complexes with a commercially available sensor. The compound 5,6-epoxy-5,6-dihydro-[1,10]-phenanthroline (Ephen) was chosen as the sensor because it is cheap, colorless, and can be easily polymerized using various methods. The series of transition metal complexes were prepared via combining dilute solutions of the metal salts ( $\text{CrCl}_3$ ,  $\text{Mn}(\text{OAc})_3$ ,  $\text{FeCl}_2$ ,  $\text{FeCl}_3$ ,  $\text{CoCl}_2$ ,  $\text{CuCl}_2$ ,  $\text{NiCl}_2$ , and  $\text{ZnCl}_2$ ) with a dilute solution of Ephen in a 1:1 molar ratio. This ratio was chosen because it represents the minimum binding of the sensor to the metal salt. Two common solvents were investigated, methanol and dimethyl sulfoxide (DMSO). These solvents were chosen as these are expected to have good penetration into epoxy-based polymeric materials while also allowing efficient solubility of the metal salts.

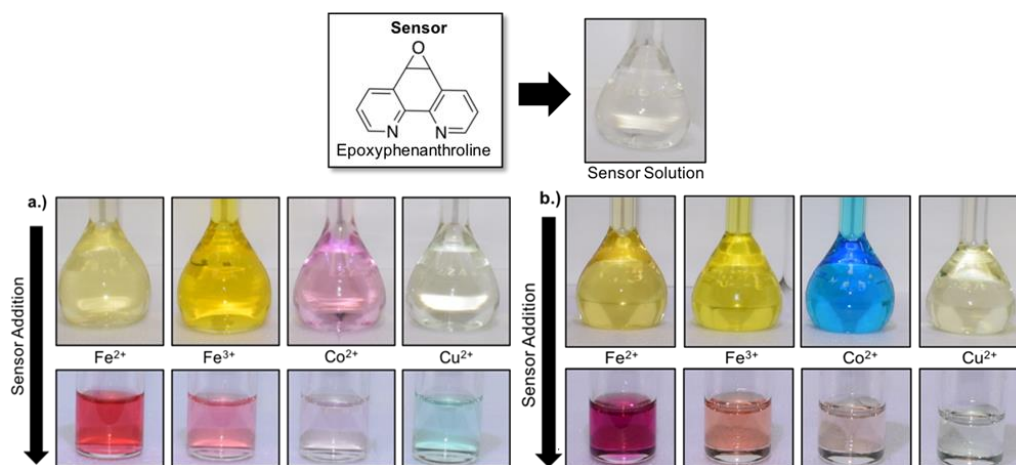


**Figure 3:** Colorless sensor solution in both methanol and DMSO (top); (a) addition of sensor solution to various metal salt solutions in a 1:1 molar ratio in methanol; (b) addition of sensor solution to various metal salt solutions in a 1:1 molar ratio in DMSO.

Figure 3 shows the results of mixing  $\text{FeCl}_2$ ,  $\text{FeCl}_3$ ,  $\text{CoCl}_2$ , and  $\text{CuCl}_2$  with the sensor, Ephen. The other metal salts,  $\text{CrCl}_3$ ,  $\text{Mn}(\text{OAc})_3$ ,  $\text{NiCl}_2$ , and  $\text{ZnCl}_2$ , did not yield an easily visible color change in either solvent. All solutions from Figure 3 have concentrations of 10 mM except the  $\text{Fe}^{3+}$  ( $\text{FeCl}_3$ ), which had to be diluted to 2 mM. The transition metal complexes formed when mixing the Ephen sensor with the  $\text{Fe}^{2+}$ ,  $\text{Fe}^{3+}$ , and  $\text{Co}^{2+}$  solutions, all of which produced dramatic and visibly obvious color changes.

A more quantitative look at the color changes is shown in Figure 4. The solutions above were analyzed by UV-Visible absorbance spectroscopy and the results were plotted as a function of wavelength. The two most intense transitions occur with the  $\text{Fe}^{2+}$  and  $\text{Co}^{2+}$  ions. In the case of  $\text{Fe}^{2+}$  where the solution initially absorbs around 375 nm (visibly yellow), addition of the sensor dramatically shifts the absorbance to around 510 nm (visibly red). The  $\text{Co}^{2+}$  DMSO solution on the other hand begins as an intense, broad peak between 550 nm and 750 nm (visibly blue) and addition of the sensor produces a broad, weak absorbance around 500 nm. The other solutions do not produce such intense transitions.

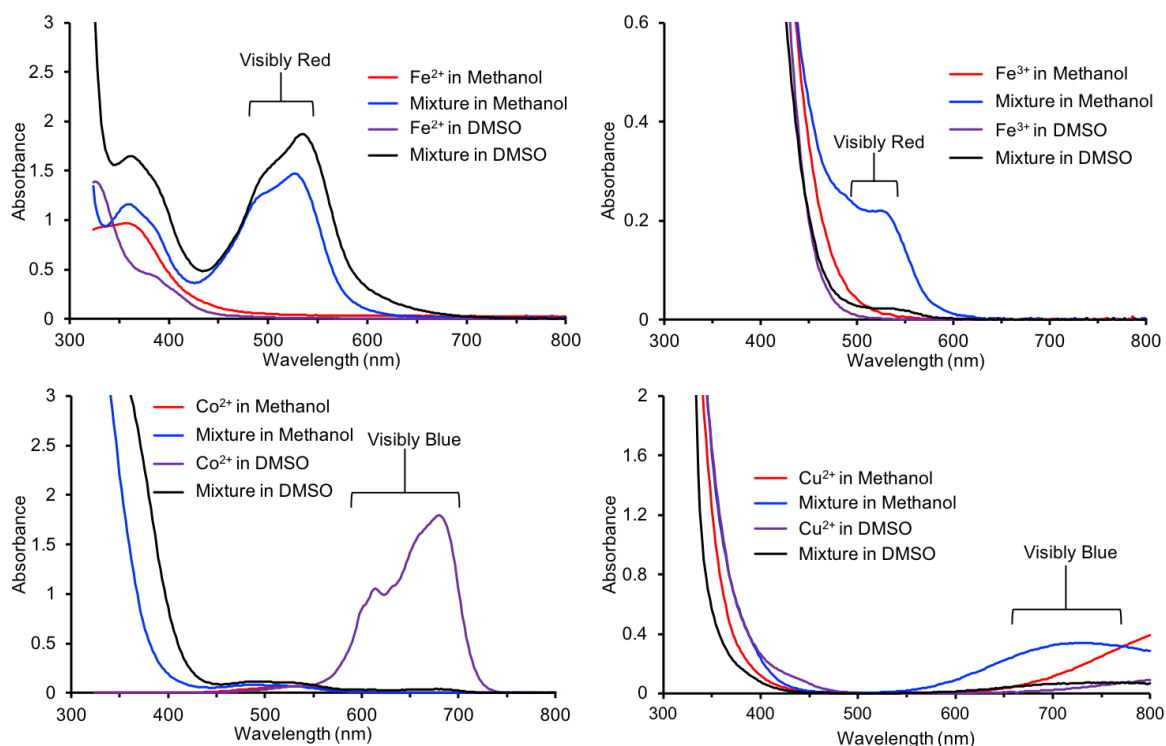


**Figure 4:** UV-Visible absorbance spectroscopy of  $\text{Fe}^{2+}$  (top left),  $\text{Fe}^{3+}$  (top right),  $\text{Co}^{2+}$  (bottom left), and  $\text{Cu}^{2+}$  (bottom right) before and after addition of the sensor. The visible colors of the most intense peaks are labeled.

The most visibly obvious color changes occurred in the solutions of  $\text{Fe}^{2+}$  and  $\text{Fe}^{3+}$  in both methanol and DMSO. The  $\text{Co}^{2+}$  transition was also visibly obvious but only occurred in DMSO. The next goal is to physically incorporate these sensor molecules into a polymer backbone (Figure 5) and to investigate the stability of these complexes over time in air, over heat, and in the presence of corrosive materials. Radiation testing will also be a major characterization required for the safeguards application space, and the R&D in progress has been designed to utilize robust materials. More specifically, thermoset (cross-linked) materials are being prepared instead of thermoplastic materials, which can melt/degrade much quickly over time. The molecular structure of the thermoset materials will also aid in mitigating radiation damage.

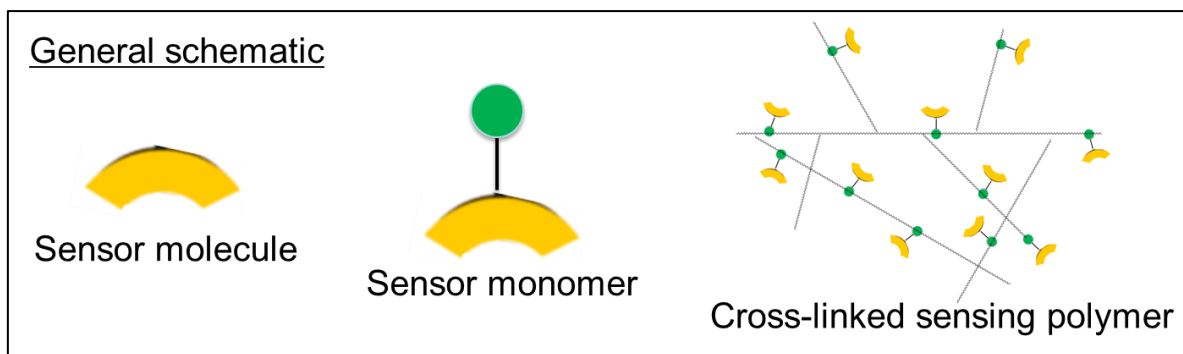


**Figure 5:** General schematic of incorporation of organic sensor into polymeric material. Both UV-curable and heat-curable materials will be prepared and evaluated.

### 3. Development of microspheres

A variety of wet chemistry microsphere synthetic methods have been developed in the literature in which capsule formation is carried out in liquid medium, starting from a solution, a liquid-in-liquid emulsion, or a solid-in-liquid suspension.<sup>4</sup> Template materials are often employed to direct the size and shape of the products during synthesis. One templating strategy involves the use of “soft” templates that are sensitive to synthesis parameters such as temperature, pH, solvent polarity, etc. and have been demonstrated to form hollow nano- and microstructures composed of SiO<sub>2</sub>, carbons, polymers, metals, metal oxides, etc.

Our efforts focus on the use of emulsion templates. Emulsions are defined as two immiscible liquids (usually hydrophobic and hydrophilic pairs) where small droplets of one liquid are finely distributed within another continuous liquid phase. Emulsions can be oil-in-water (o/w) or water-in-oil (w/o), and surfactant compounds are often required to assemble at the interface of the two liquids to decrease the interfacial tension and increase thermodynamic stability. Precursor species for the microsphere shell self-assemble (often with the aid of co-surfactants) at the interface of the droplets and the continuous phase and the shell can subsequently be formed through, for example, polymerization. This method can produce spheres in the nano- to micron- size regime. Cargo species of interest can be incorporated in one step into the microspheres through solubilization within the emulsion droplets.<sup>4,7</sup>

The requirements for the microsphere wall material are primarily structural in nature, serving to mechanically contain the cargo compound. The structural properties of the microsphere must be commensurate with the strains expected for the particular application, i.e. they must be sufficiently robust to withstand ‘normal’ environmental conditions yet able to rupture under tampering conditions. These properties are associated with the intrinsic tensile properties of the wall material itself, as well as the wall thickness and microsphere radius. Based on these criteria, three types of candidate materials were down-selected for investigation and optimization: polymeric, siliceous, and polymer-silica core-shell composites.

Three different polymeric materials were studied: Urea-Formamide (UF), Melamine-Urea-Formamide (MUF), and Poly(methyl methacrylate) (PMMA).<sup>5</sup> The first two materials are copolymers prepared by o/w emulsion polymerization procedures, whereas the third entry comprises a homopolymer microsphere prepared via an evaporation/phase-separation procedure. Microspheres ranging in diameter from 10 – 250 μm were synthesized and filled with the different mobile phase materials such as mineral oil and hexadecane.

Of the three materials studies, UF microspheres performed the best due to several properties: robust synthetic method that afforded the capsules in high yield, a relatively narrow size distribution, uniform particle surface properties, synthetically adjustable sizes across a wide range, and compatibility with all of the tested mobile phase materials. The above combination of desirable attributes was not exhibited by either the MUF copolymer or PMMA microspheres, in spite of other advantages such as higher thermal stability and lower diffusivity in the case of MUF.

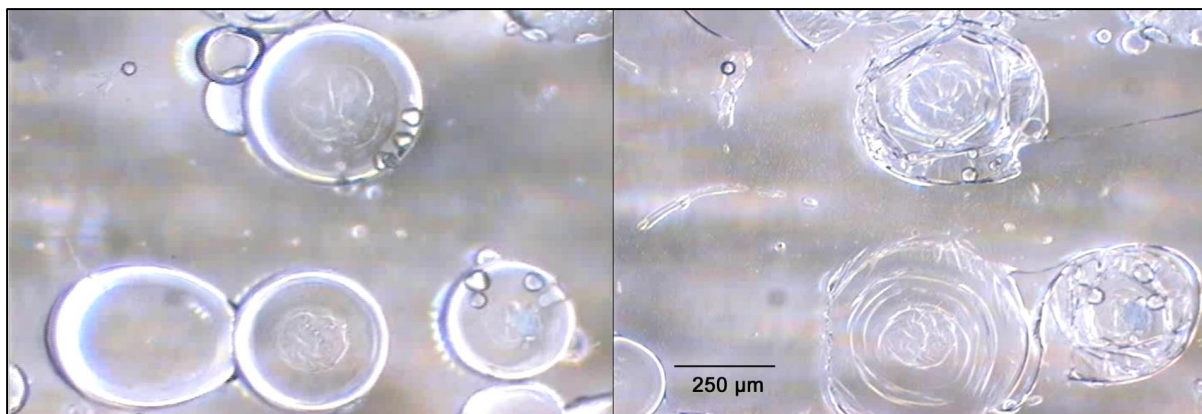


**Figure 6:** Video microscope screen capture images depicting intact (left) and ruptured (right) mineral oil-filled UF microspheres. The mechanical stimulus was exerted by a micro-manipulator tip pressing on the top plate of a microscope cover slip.

The development of a variety of microspheres with different structural properties would provide a flexible selection of materials to coincide with the mechanical characteristics/detection sensitivity of the corresponding tamper-indicating device design. Siliceous systems were subsequently studied to impart increased mechanical strength into the microsphere walls.

Silica microcapsules were prepared by the acid-catalyzed hydrolysis of tetraethyl orthosilicate (TEOS) in a w/o emulsion.<sup>6</sup> Stirring speed and method during the reaction had a large effect on the microsphere size and purity, as shown in Figure 7 below. Overhead stirring at 1000 rpm with a propeller impeller provided the best shear conditions to produce clean silica microspheres with a roughly trimodal size distribution of 0.5 - 1, 2 - 5, and 10 μm. Cu<sup>2+</sup> and Fe<sup>3+</sup> transition metal ions were successfully encapsulated as cargo in the aqueous mobile phase.

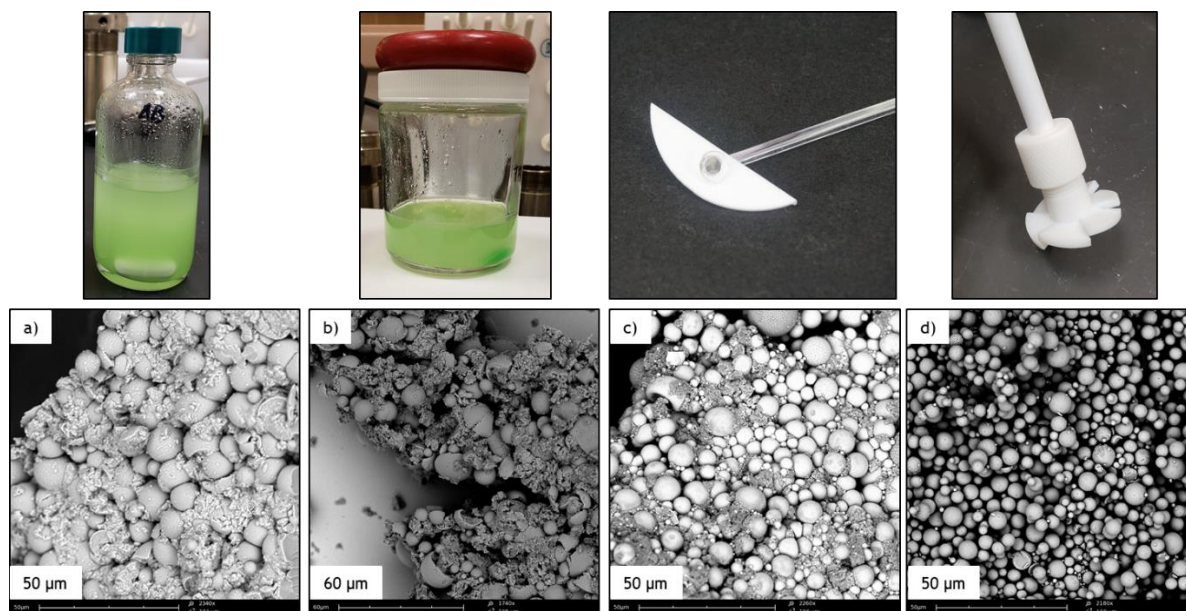


**Figure 7:** Scanning Electron Micrographs (SEMs) of silica microsphere products a) with magnetic stirring in a narrow glass bottle b) magnetic stirring in a wide glass jar c) overhead stirring in a glass round bottomed flask with a paddle impeller and d) overhead stirring in a plastic bottle with a propeller impeller.

Crushing and grinding of these dried microspheres between two glass slides showed very little to no breakage, pointing towards the high mechanical strength of the silica microspheres compared to polymeric. It is well known, however, that silica microspheres contain micro- and mesoporosity,<sup>6</sup> which

is undesirable for long term containment of cargo molecules. Our next efforts will focus on combining the low permeability of the polymers with the mechanical strength of the silica to form a core-shell polymer-silica composite microsphere material.

#### 4. Summary and Next Steps

SNL continues to develop a material that results in an obvious, visual response (irreversible color change) upon tamper. The material will be 3D-printed for customizable inspection equipment, or spray-coated for application to facility-owned equipment. The material adds to the TIE toolbox, which is currently limited in options. R&D will continue on transition metals and microspheres, culminating in the integration of the transition metals and microspheres into 3D-printed and spray-coated prototypes. The prototypes will undergo environmental testing upon fabrication. Future testing for durability and vulnerability will also be conducted.

#### 5. Acknowledgements

The authors would like to acknowledge the U.S. National Nuclear Security Administration (NNSA) Office of Defense Nuclear Nonproliferation R&D Safeguards portfolio for funding and supporting this research.

Sandia National Laboratories is a multi-mission laboratory managed and operated by National Technology and Engineering Solutions of Sandia, LLC, a wholly owned subsidiary of Honeywell International, Inc., for the U.S. Department of Energy's National Nuclear Security Administration under contract DE-NA0003525. SAND2019-2728 R.

#### 6. References

- [1] Smartt, H.A., Corbin W., Feng, P.L., Myllenbeck, N., Patel, S. *Tamper-Indicating Enclosures with Visually Obvious Tamper Response*, Proc. of Symposium on International Nuclear Safeguards, Vienna, Austria, 2018.
- [2] Balkenende, D. W. R.; Coulibaly, S.; Balog, S.; Simon, Y. C.; Fiore, G. L.; Weder, C. *Mechanochemistry with Metallosupramolecular Polymers*, J. Am. Chem. Soc., **136**, 10493-10498, 2014.
- [3] Rowan, S. J.; Beck, J. B. *Metal-ligand induced supramolecular polymerization: A route to responsive materials*. Faraday Discuss., **128**, 43-53, 2005.
- [4] Prieto, G., Tüysüz, H., Duyckaerts, N., Knossalla, J., Wang, G.-H., Schüth, F. *Hollow Nano- and Microstructures as Catalysts*, Chem. Rev., **116**, 14056–14119, 2016.
- [5] Smartt, H. A., Feng, P. L., Romero, J. A., Gastelum, Z. N. *Tamper-Indicating Enclosures Based on "Bleeding" Microcapsules*, SAND2015-8131.
- [6] Wang, J-X, Wang, Z-H, Chen, J-F, Yun, J. *Direct encapsulation of water-soluble drug into silica microcapsules for sustained release applications*, Mater. Res. Bull., **43**, 3374-3381, 2008.
- [7] Zhang, Y., Hsu, B.Y.W., Ren, C., Li, X., Wang, J. *Silica-based nanocapsules: synthesis, structure control and biomedical applications*, Chem. Soc. Rev., **44**, 315-335, 2015.

# Light Field Cameras Offer Surveillance a New Dimension

James R. Garner

Oak Ridge National Laboratory  
1 Bethel Valley Road  
Oak Ridge, TN 37831  
E-mail: GarnerJR@ORNL.gov

## **Abstract:**

*Light field cameras, sometimes called “plenoptic cameras,” are used for a form of computational photography that captures information about the intensity and direction light rays are traveling in a scene. Researchers at Oak Ridge National Laboratory evaluated commercial off-the-shelf light field camera systems from Raytrix and Lytro. This paper describes how light field cameras work, discusses the author’s experience with the systems, proposes potential benefits they may offer for safeguards applications, and identifies limitations that would have to be addressed.*

**Keywords:** surveillance; camera; plenoptic; light field

## **1. Introduction**

Light field or plenoptic cameras combine aspects of plentiful computing, high-resolution digital sensors, and modern optics to produce a camera system that allows a user to “interactively change the focus, point of view and perceived depth of field” after image acquisition [1]. These systems can produce occlusion-free, three-dimensional (3D) images in a single shot using a single lens and sensor.

Plenoptic cameras provide these capabilities by leveraging parallax (i.e., the effect that an object viewed from different perspectives can appear to be in different positions). As shown in Figure 1, the relative position of an object can appear to change when viewed from different viewpoints.

Stereoscopic concepts, which take advantage of parallax to provide the illusion of depth, have been around since 1838 [2]. As shown in Figure 2, when a point in space is projected back through the optical centre of left and right cameras, the point will have an apparent displacement relative to the optical image centre. Modern stereo camera systems triangulate using these relative displacements to infer the depth to an object point.

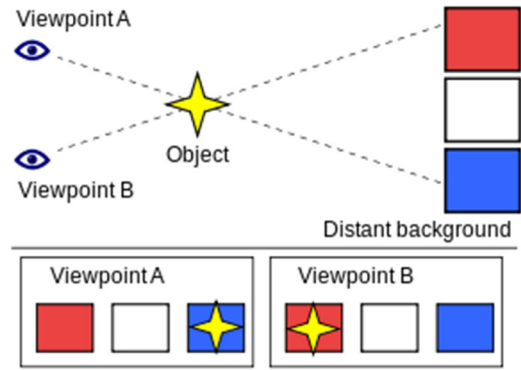


Figure 1. When viewed from Viewpoint A the object appears to be in front of the blue background. When viewed from viewpoint B the object appears to be in front of the red background.

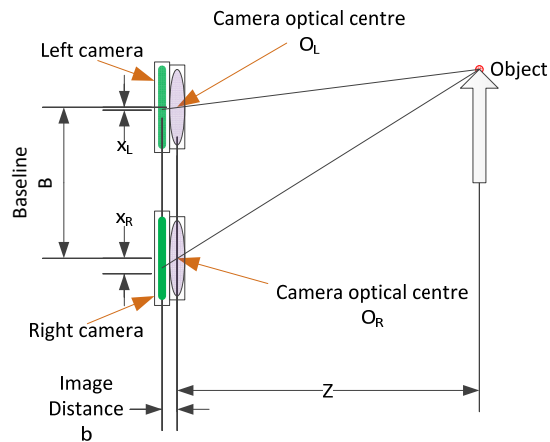


Figure 2. Stereoscopic cameras can be used to infer object depth using triangulation.

Plenoptic cameras can be thought of as an extension of stereo cameras. Instead of two image sensors separated by some baseline, a single image sensor is segmented into many microsensors, each paired with a microlens, as shown in Figure 3.

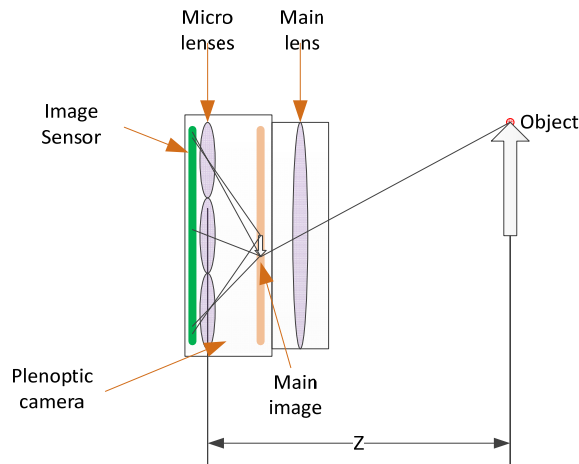


Figure 3. A plenoptic camera adds a microlens array in front of the image sensor, creating many microcameras.

## 2. Raytrix

Raytrix was the first to produce commercial plenoptic cameras, around 2010 [3]. Today Raytrix produces cameras ranging in resolution from 8 to 122 megaray. The cameras use USB3, GigE vision, CXP, or Camera-Link to communicate to a host computer. Most models can be ordered as monochrome, colour, or near-infrared cameras. Raytrix uniquely produces its microlens array with three different focal lengths, which allow Raytrix cameras an extended depth of field [1].

### 2.1. ORNL's Raytrix Experimental Setup

ORNL purchased a Raytrix R42 USB 3.0 camera with a Ricoh 50 mm f/2.4 lens (FL-BC5024-9M). The R42 uses a rolling shutter and a 2/3 in., 7,728 × 5,368 pixel (41.5 megapixel) CMOS sensor made by Toshiba. Each pixel measures 1.1 $\mu$ m.

Raytrix provides two software packages for use with its cameras: RayCam View and RxLive. RayCam View provides a simple interface to acquire 2D images from the camera. RxLive provides a more complex interface to acquire, calculate, and manipulate 3D images. We were surprised to find that 2D images acquired using RayCam View could not be processed by RxLive to calculate 3D information.

The Raytrix RxLive 4.0 software requires a graphics card with at least 4 GB of memory but recommends a graphics card with at least 6 GB of memory for the R42 camera. The Raytrix camera was first used with a Dell Precision 3620 Tower with an Intel i7-7700K @ 4.20 GHz, 32 GB of random-access memory (RAM), and a Nvidia Quadro P4000 graphics card with 8 GB of dedicated graphics processing unit (GPU) memory. Laptop form factor machines with dedicated graphics cards with 4 GB or more of RAM are not common. For a more portable test system, ORNL purchased a Dell Precision 7730 Mobile Workstation with Intel Xeon E-2176M @ 2.7 GHz, 32 GB of RAM, and a Nvidia Quadro P4200 graphics card with 8 GB of dedicated GPU memory.

### 2.2. ORNL's Raytrix Experience

We found working with the Raytrix R42 laborious. We tried to use the camera to capture several different indoor and outdoor scenes. We were able to capture well-lit scenes, but the value of the depth information was disappointing. To demonstrate some of the depth-capturing capabilities, we constructed the test scene that consisted of a standard size keyboard and a load cell cutaway placed on a checkerboard-patterned backdrop (Figure 4). Also shown is the Dell Mobile Workstation used to acquire images from the camera.



*Figure 4. Raytrix experimental setup showing R42 camera on small tripod connected via USB3 to a Dell 7730 Mobile Workstation. The R42 was focused on a keyboard and load cell cutaway.*

The microlens array must be calibrated before useful images can be acquired. Calibration involves several steps:

- (1) focus the scene and adjust the shutter speed to acquire a nominally in-focus, well-lit image;
- (2) attach the white balance filter;
- (3) adjust the aperture until the microlens images just begin to touch one another (as shown in Figure 5); and
- (4) acquire a calibration image and a grey monochrome image.

Refocusing has a second-order effect on the microlens adjustment, so tape was used to fix the aperture and focus of the lens at 500 mm, as shown in Figure 6. Then the distance from the camera to the subject was adjusted until the scene was in focus.

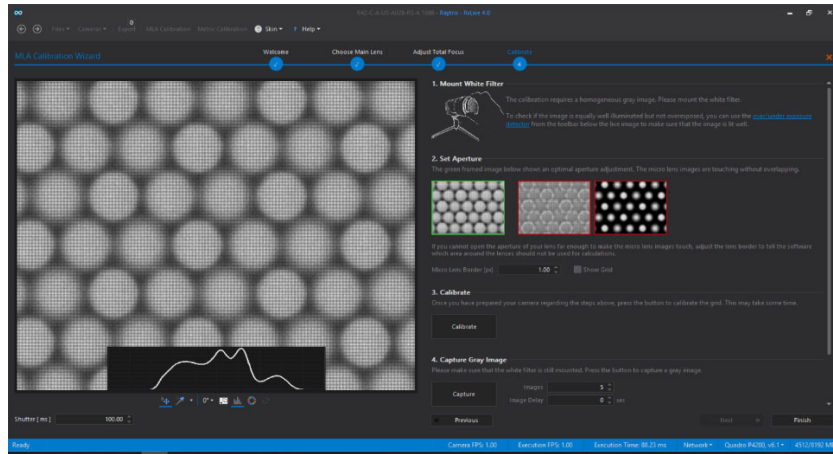


Figure 5. The RxLive software provides a workflow to calibrate the microlens array with example images.



Figure 6. The R42 camera had a Ricoh 50 mm focal length lens. After the microlens array calibration, tape was used to secure the focal distance at 500 mm, and then the camera was moved to various distances away from the subject.

One of the strengths of the Raytrix system is the ability to calculate depth maps from single shots, as shown in Figure 7. Depth maps can be used by RxLive to display a colour-accurate 3D rendering of the scene, as shown in Figure 8. RxLive allows the user to zoom in or out and to rotate the 3D rendering. RxLive can also

use the calculated depth map to refocus each pixel for a “Total Focus” view of the scene, as shown in Figure 9. Figure 9 also shows artefacts in the background that are the result of image reconstruction.

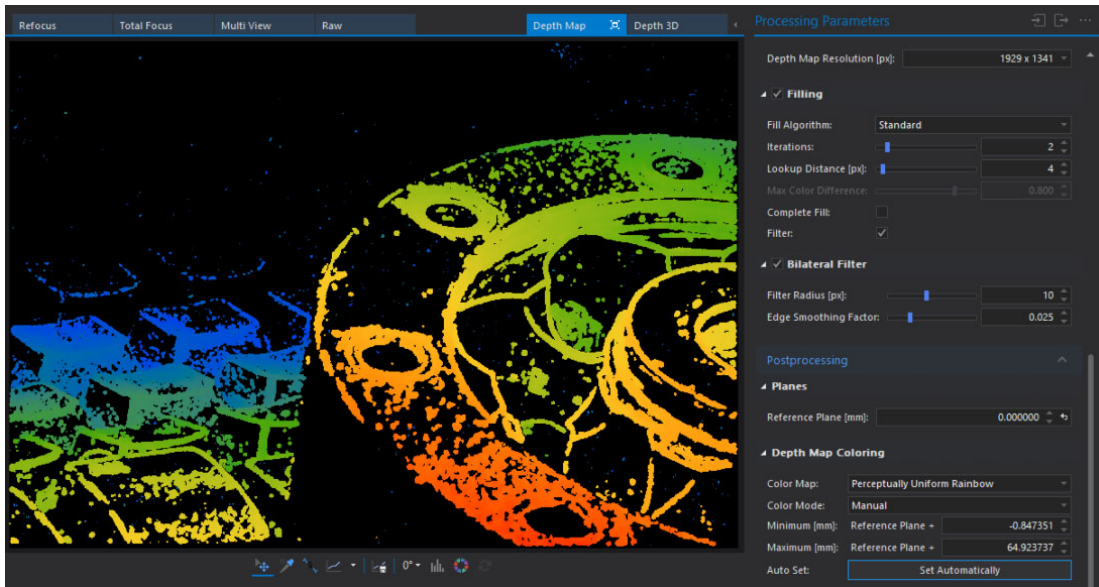


Figure 7. RxLive can display a depth map using warmer colours to represent closer points and cooler colours to represent points that are farther away.

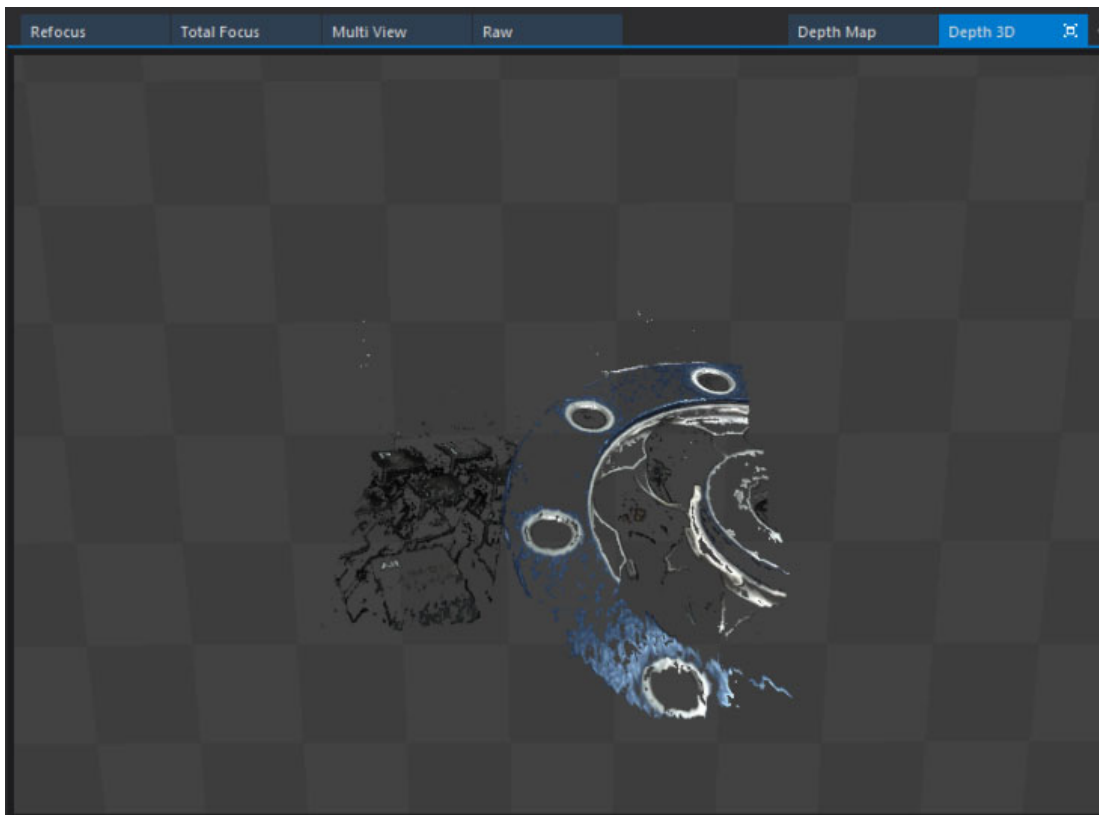


Figure 8. RxLive can display a 3D representation of the part in true colour.

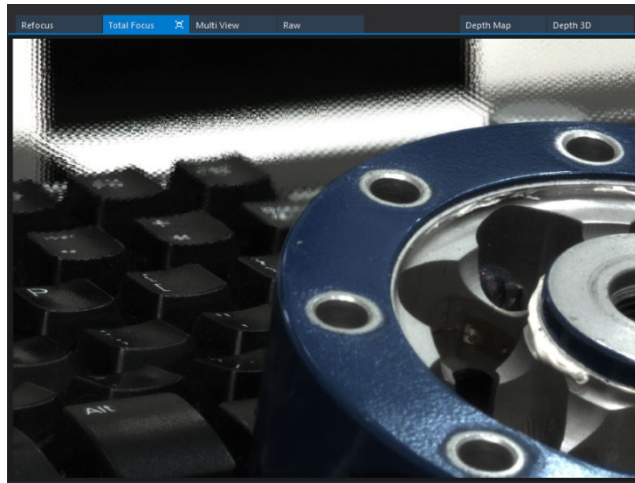


Figure 9. RxLive can display a “TotalFocus” image which focuses each pixel based on the calculated depth map.

As shown in Figure 10, RxLive allows an image to be refocused to different virtual depths.

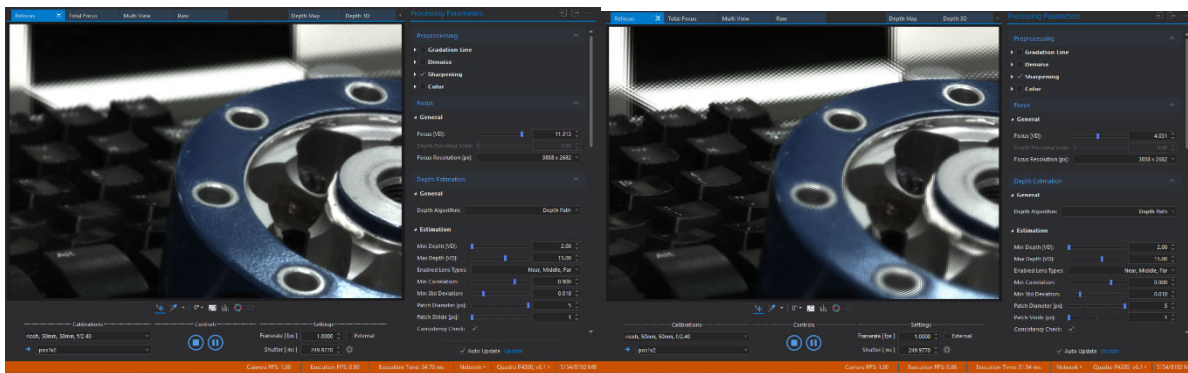


Figure 10. The virtual depth (distance from focal plane parallel to optical axis) can be varied to focus in the near field as shown on the left or the far field as shown on the right.

The R42 was also used to capture several outdoor scenes. The subjects were further from the camera in the outdoor scenes and therefore had a larger depth of field. As a result, the 3D images were not as compelling as the examples shown in Figure 7 through Figure 10. It was also very challenging to use the camera outdoors. Changing lighting conditions and glare on the laptop screen made calibrating the microlens array challenging.

We observed that the R42 used more than 5 GB of the GPU memory, but the Windows 10 Task Manager reported utilization of only a few percent on the GPU and no extraordinary load on the central processing unit (CPU).

### 3. Lytro

Lytro took a different approach to light field photography, and in 2011 and 2012 introduced an 11 megaray camera intended for hobbyists. Capable of producing 1.2 MP 2D image, the original Lytro camera was packaged as a square tube (shown on the left in Figure 11). It featured a 1.52 in. touch screen and an 8× optical zoom. In 2014 Lytro released the Illum (Figure 11, right). The Illum uses a 40 megaray, ½ in. sensor to produce 4 MP 2D images.



Figure 11. The original Lytro Camera. (left) was intended for hobbyists [4]. The Lytro Illum camera (right) has more features for professional use.

### 3.1. ORNL's Lytro Experience

Lytro marketed the Illum to amateur and professional photographers, which was clear from the user experience at ORNL. The Illum camera is comfortable to hold, and the controls are intuitive. The touch screen on the camera itself can be used to review images and to change the focal plane; however, the Windows Lytro Desktop application enables a much richer experience with the Lytro images (see Figures 12–15).

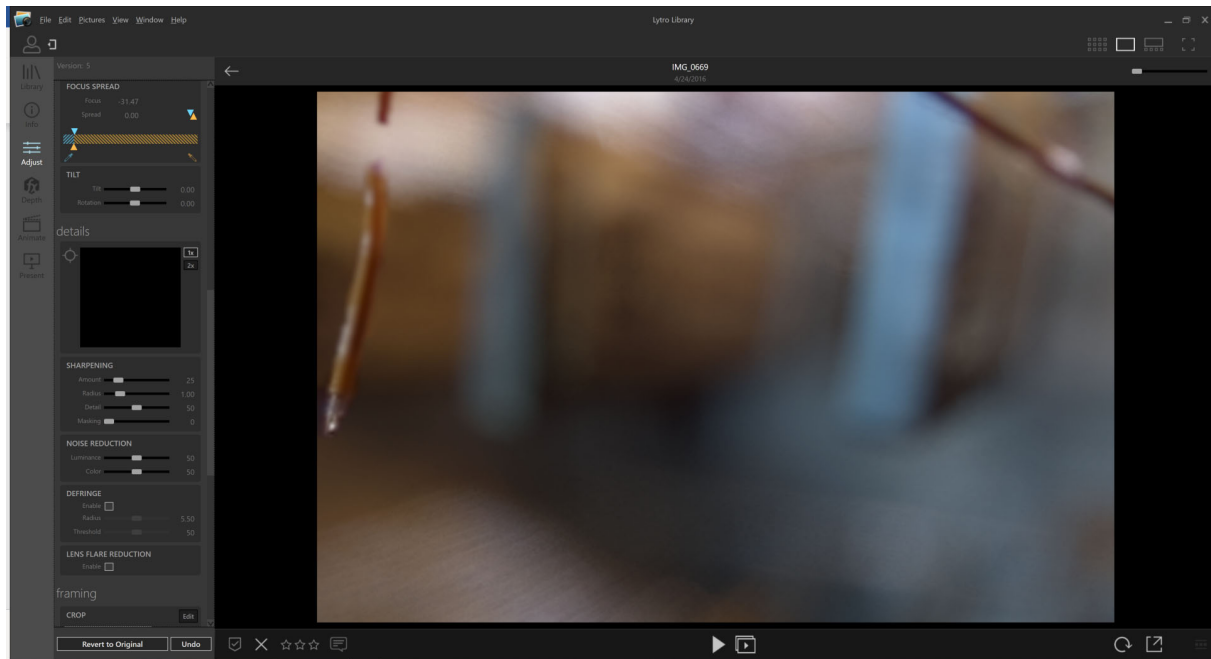


Figure 12. Lytro Illum images can be refocused by clicking on a point in the image. Here a thermocouple is in focus in the near field. This refocused distance can be displayed using the Lytro Library Adjust tab focus spread section.

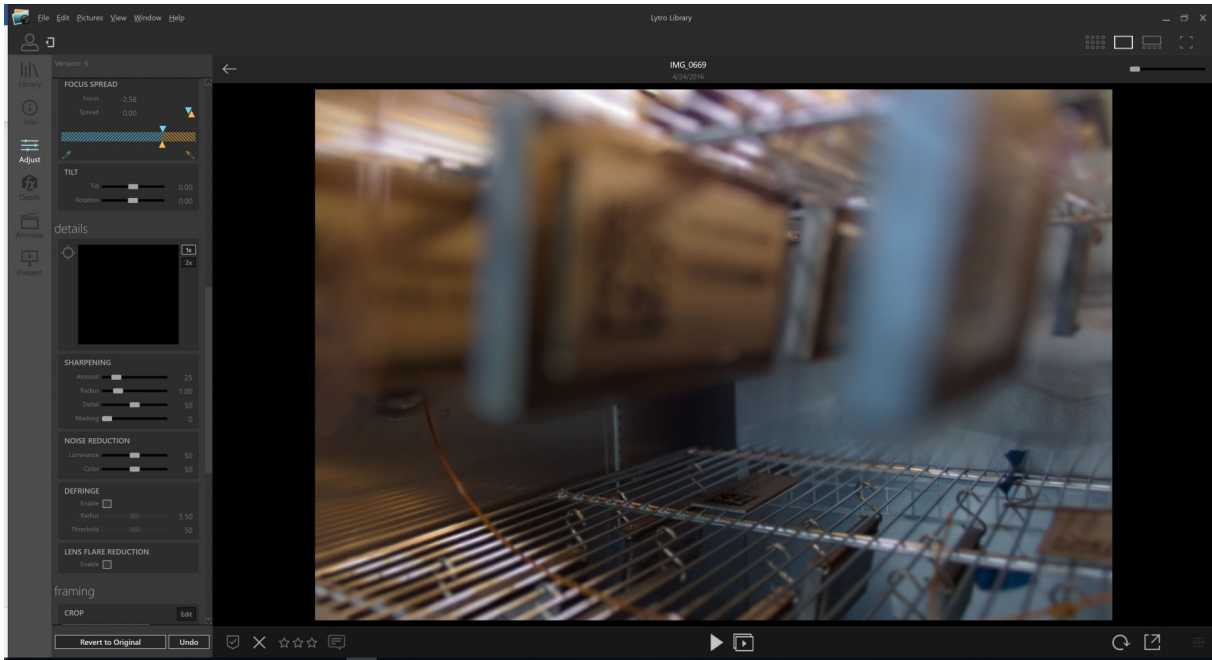


Figure 13. Lytro Illum image focused to a barcode in the background.

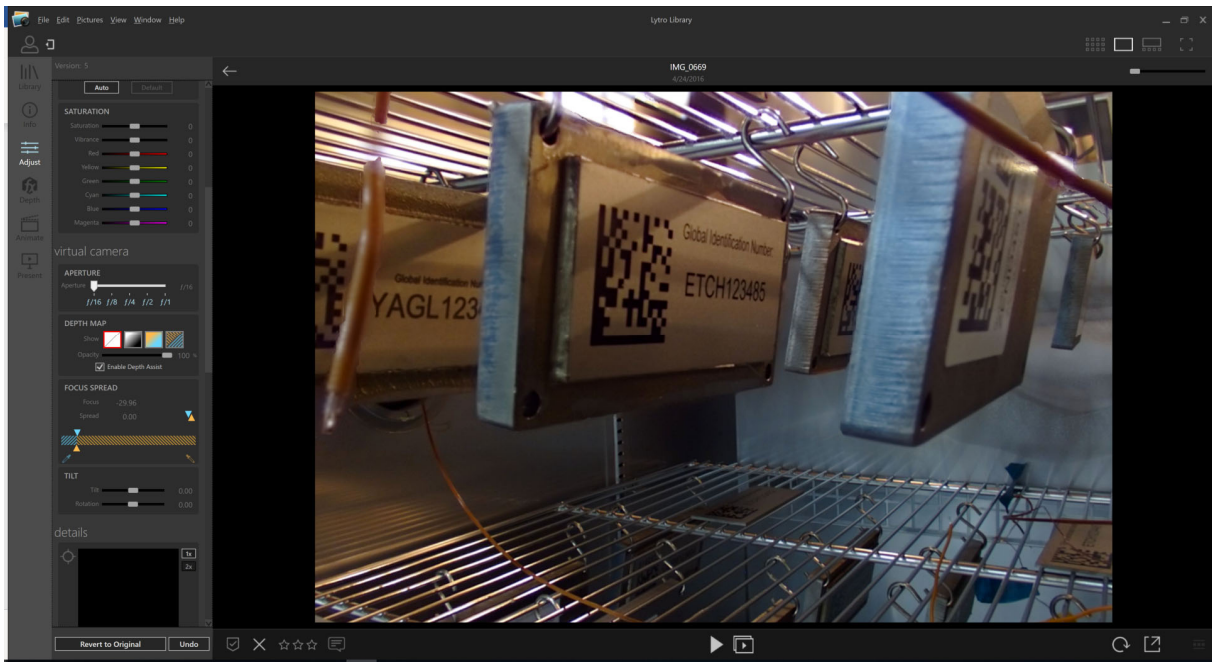


Figure 14. The Lytro Illum captures photographs at  $f/2$  but can synthetically adjust the aperture, which results in a larger depth of field, as shown with this image at  $f/16$ .



Figure 15. Lytro Desktop can display a depth map computed from the image.

The Lytro Illum processes images when they are reviewed on the camera or imported into the Lytro Desktop application. When an image is reviewed on the Lytro Illum, there is a slight delay before the image appears on the interactive touch screen, at which point a user can touch different portions of the screen or rotate one of the lens barrels to refocus the image. We imported images into the Lytro Desktop application from an SD card. Importing images was CPU intensive and fully utilized the Desktop's i7-7700K processor and Mobile Workstation's Intel Xeon E-2176M processor but only utilized about 7% of the GPU in either computer.

## 4. Applicability for Safeguards

Plenoptic cameras could be used as an attended tool similar to traditional digital cameras or as an unattended tool similar to the currently utilized DCM-14 and NGSS cameras.

### 4.1. Notional Attended System

As an attended tool, the Lytro Illum already packages plenoptic camera capabilities in a user-friendly device that could be used by most inspectors. Plenoptic cameras offer depth-map capabilities that traditional digital single-lens reflex or point-and-shoot cameras cannot. These depth maps are particularly effective with subjects that are close to the camera. While higher-precision depth maps can be generated using dedicated 3D laser scanners, such as a Zoller+Froehlich 5016, the Lytro Illum offers ease of use and tripod-free acquisition.

### 4.2. Notional Unattended System

Using plenoptic cameras for unattended applications comes with additional difficulties. International safeguards agencies often use cameras to maintain continuity of knowledge of verified material for days or years between visits. The current generation of international safeguards cameras typically use low-power processors and do not include dedicated graphics cards to facilitate the ability to run from battery.

## 4.2. Limitations

Plenoptic cameras offer depth-map information that traditional cameras cannot offer, but the depth map is limited for distant objects. Figure 16 shows a common use case for IAEA surveillance systems in which the camera is installed in a reactor hall overlooking a reactor vessel. For this use case the object is tens of meters away, likely past the infinite focal distance of the lens. Raytrix suggests that the depth resolution is about 1% of the total depth of field, so for distant objects there would be very little depth information. [5]

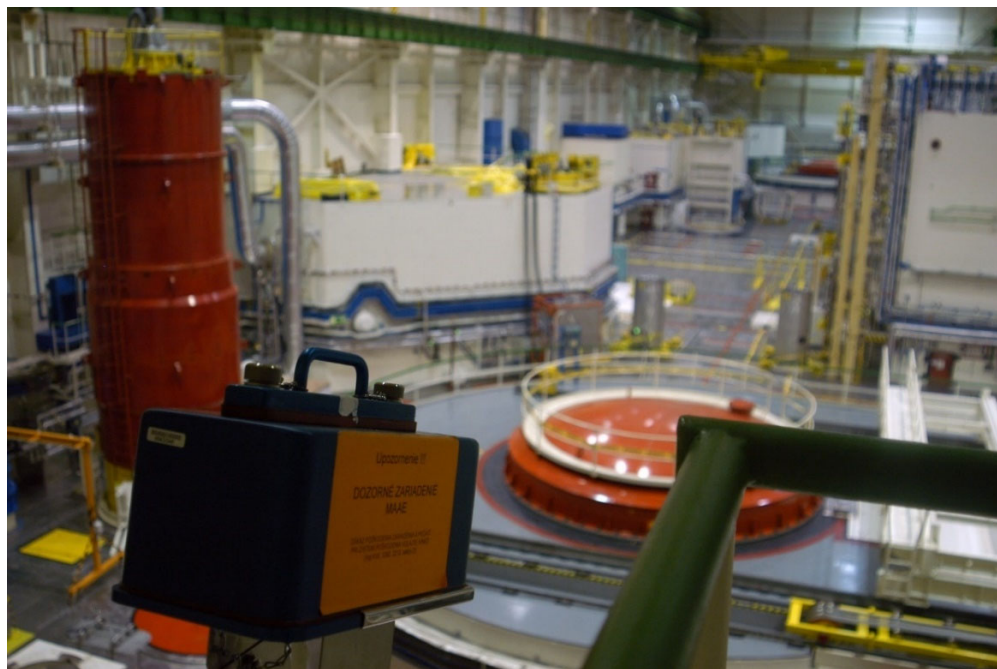


Figure 16. IAEA surveillance camera surveils a reactor vessel at Slovakia's Mochovce nuclear power plant, January 2005. Photo Credit: Dean Calma / IAEA [6]

## 5. Conclusion

Plenoptic cameras offer an interesting approach to capturing 3D images using a single camera; however, there appear to be significant challenges to deploying this technology for safeguards. Many of the benefits plenoptic cameras offer may be better met with other technologies. Different plenoptic sensor configurations may be more suitable (e.g., an array of cameras). For typical safeguards surveillance applications where objects of interest may be tens of meters away, an array of cameras with a wider baseline would provide the same capabilities (e.g., refocusing, 3D) as a compact plenoptic camera, but with richer depth information.

## References

1. Perwaß, C. and L. Wietzke, *Single Lens 3D-Camera with Extended Depth-of-Field*, in *Human Vision and Electronic Imaging*.
2. Hahne, C., *The Standard Plenoptic Camera: Applications of a Geometrical Light Field Model*. 2017.
3. *Raytrix Timeline -- LightField Forum*. 8/2014 4/24/2019]; Available from: <http://lightfield-forum.com/raytrix/raytrix-timeline/>.
4. Coetzee, D., *Lytro light field camera - front.jpg*. 2012.
5. Institute, W.N.T., *UF6 Cylinder Identification*. 2017, WNTI: London, United Kingdom.
6. Calma, D. January 18, 2005.

# **Session 14:**

# **Arms Control Verification**

## Arms Control Verification Technologies

**Eduardo Padilla**

Sandia National Laboratories<sup>1</sup>, Albuquerque, NM, USA

**Jesus Valencia**

Sandia National Laboratories, Albuquerque, NM, USA

### **Abstract:**

*Nuclear arms control treaty verification scenarios present unique challenges which are not always present in safeguards. These challenges include safety related concerns when working on or near warheads, information security when measuring radiation output of weapon systems and unknown material compositions. Conversely, there are many areas in which arms control and safeguards overlap, such as authentication and certification concerns, quantification of trust or confidence and chain of custody.*

*Sandia National Laboratories is engaged in research and development activities aimed at enabling future arms control agreements. As part of this R&D effort, Sandia develops technical solutions in the areas of radiation detection, tamper indicating seals and unique identifying tags. Additionally, we develop tools for authentication and certification of treaty verification hardware, as well as participate in multilateral cooperative exercises aimed at exploring advanced approaches to potential future arms control scenarios. This paper presents an overview of these activities, as well as some ideas for future engagement.*

**Keywords:** Arms Control; Verification; Treaty Monitoring

### **Introduction**

Arms control and safeguards technologies play vital roles in each of the non-proliferation regimes that seek to reduce the spread and development of nuclear material and weapons. Arms control agreements and treaties seek to prevent vertical proliferation within a state that has already developed a nuclear weapon. These agreements aim to control the development, production, stockpiling, proliferation, distribution or the usage of a particular weapon type or its delivery systems. Safeguards are meant to prevent the diversion of dual-use technologies from peaceful uses to military applications. Both safeguards and arms control missions are accomplished using combinations of monitoring, detection, and verification technologies.

While the two technologies have similar goals and uses, there is currently an underutilization of arms control technologies. The amount of treaties and agreements that rely on arms control technologies is very small when compared to the relatively large volume of states and facilities that are currently monitored by safeguards technologies. To increase utilization, and thereby trust, in existing arms control technologies, efforts could be made to co-develop and/or implement arms control technologies into safeguards applications. The following presents an overview of some technologies developed by Sandia National Laboratories for the purposes of arms control verification, with the potential to offer novel capabilities to the safeguards regime.

<sup>1</sup> Sandia National Laboratories is a multimission laboratory managed and operated by National Technology and Engineering Solutions of Sandia, LLC., a wholly owned subsidiary of Honeywell International, Inc., for the U.S. Department of Energy's National Nuclear Security Administration under contract DE-NA-0003525.

## Application of arms control technologies in safeguards

Arms control technologies such as seals and tags are used to prevent access or tampering with previously verified materials. These devices are already widely used throughout the nuclear safeguards regime and serve as an example of the overlap in mission requirements between the arms control and safeguards regimes. However, detection systems such as those that monitor or characterize nuclear material are used differently within the two verification regimes. In arms control inspections, information barriers are typically used in conjunction with detection systems to reduce the amount of information gained by the visiting state in a survey or inspection. However, these systems are designed to allow for verification with levels of confidence significant enough for inspectors to conclude that host states are still beholden to their agreement obligations.

### Current Applications

Currently, there are only two major arms control agreements in place, the Intermediate Range Nuclear Forces Treaty (INF) and the New Strategic Arms Reduction Treaty (New START). The INF Treaty was originally struck between the U.S. and Soviet Union to reduce tensions by eliminating all missiles with a range of 500 to 5,500 kilometers. The treaty was verified through a combination of satellite observations, on-site inspections and monitoring. However, the US is currently on track to withdraw from this treaty on August 2, 2019. New START sought to build off its predecessor the Strategic Arms Reduction Treaty (START) and further reduce offensive arms between the U.S. and the Russian Federation. This treaty has been verified using on-site inspections, data and telemetry exchanges on an agreed number of ICBM and SLBM launches. Unless extended, the New START Treaty will expire in February of 2021.

Thus far, neutron counters have been a primary means of absence verification in bilateral arms control agreements. Figure 1 illustrates a neutron detector developed by Sandia National Laboratories for use in absence verification measurement procedures during New START inspections.



Figure 1 - Radiation Detection Equipment Developed for New START Absence Verification Measurements

In contrast to arms control technologies, safeguards technologies have been widely adopted for use by the International Atomic Energy Agency to ensure that nuclear material is not being diverted from peaceful uses to create nuclear weapons or explosive nuclear devices. As of April 2019, the IAEA implements safeguards in 182 different countries. These agreements between the host state and IAEA utilize a wide array of detection, monitoring and verification techniques. Whereas safeguards technologies are adopted by the IAEA, a foundationally multinational agency, arms control technologies have historically been developed in a closed bilateral negotiation process. The multilateral development approach for safeguards allows for states, as well as the international research community to become more familiar with current technologies and suggest improvements.

### Proposed Applications

In an effort to provide solutions for potentially moving beyond absence verification via neutron counting, Sandia National Laboratories has worked to develop several concepts for warhead confirmation. These concepts can often be grouped into one of several categories of arms control technologies: Template Measurement Systems, Attribute Measurement Systems and the Zero-knowledge Protocol. From the initial concept stage of the development lifecycle, the design methodologies for these technologies consider the inevitable authentication and certification process that would precede adoption into any arms control treaty.

An example template measurement system is the Trusted Radiation Identification System (TRIS) [1]. TRIS utilizes a trusted processor with information barrier to measure a gamma radiation spectrum from an item of interest, compares that against previously acquired spectral templates, and gives a general yes/no/failure indication to an inspector (Figure 2). This method is able to perform highly intrusive gamma spectral analysis without ever revealing sensitive information to an inspector.

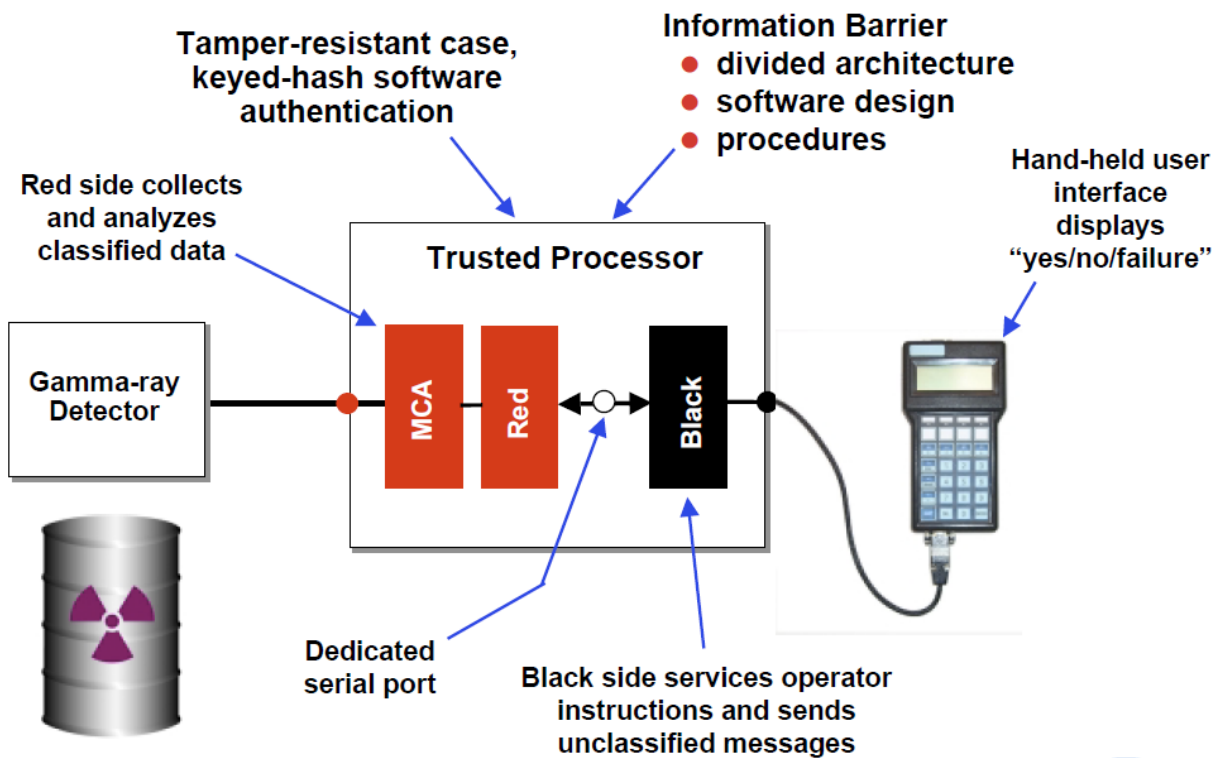


Figure 2 - TRIS System Diagram [2]

The Minimum Mass Estimates for Plutonium Algorithm [3] is an example of what we consider an attribute measurement system. The intent of these systems is not to exactly match an object of interest to an exemplar template, rather to confirm the presence of a material of interest, in this case weapons grade plutonium. This algorithm is capable of demonstrating that an inspected item contains more than a deliberately low amount of plutonium or simple neutron source, without revealing sensitive weapons design information.

The key aspects for this algorithm are to confirm that the amount of plutonium exceeds a declared threshold and the ratio of Pu-240 to Pu-239 is consistent with weapons-grade plutonium, using only high purity germanium measurements. This is achieved via spectral deconvolution, which enables estimations of Pu-240/Pu-239 ratios as well as the amount of scattered source radiation (Figure 3).

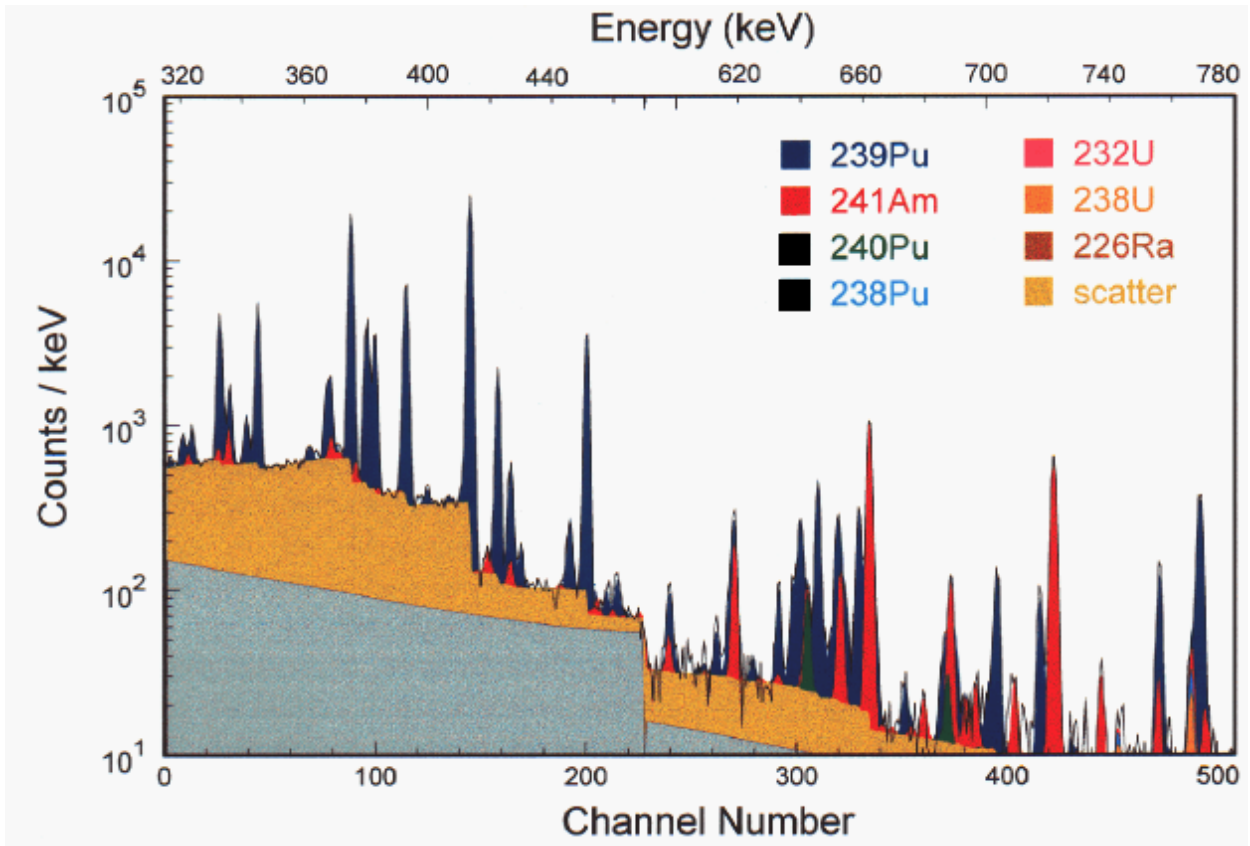


Figure 3 - Plutonium Spectral Deconvolution for Minimum Mass Estimate [3]

A concept which combines aspects of both template and attribute measurement systems is the Unclassified Radioisotope Algorithm [4], which avoids the collection and storage of a potentially sensitive gamma spectrum upfront, processing each incoming pulse in list mode. By constructing simple weight arrays (consisting of -1, 0 or +1 weight values) of desired and undesired pulse heights prior to a measurement, you can then construct scalar values from a set number of pulses counted (Figure 4).

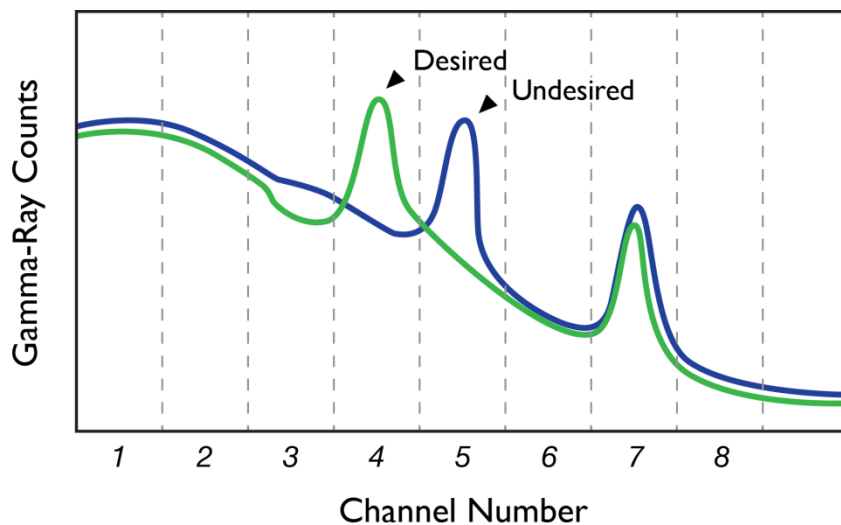


Figure 4 - Desired vs. Undesired Spectra

These scalar weight values at the end of a measurement can then be compared to expected scalar values from both desired sources (e.g. weapons grade plutonium) and potential undesired sources (e.g. reactor grade plutonium). By weighting and de-weighting appropriate regions of the spectra, clear discrimination even in the presence of shielding between desired and undesired sources (Figure 5) can be achieved without ever recording sensitive information such as a gamma radiation spectrum.

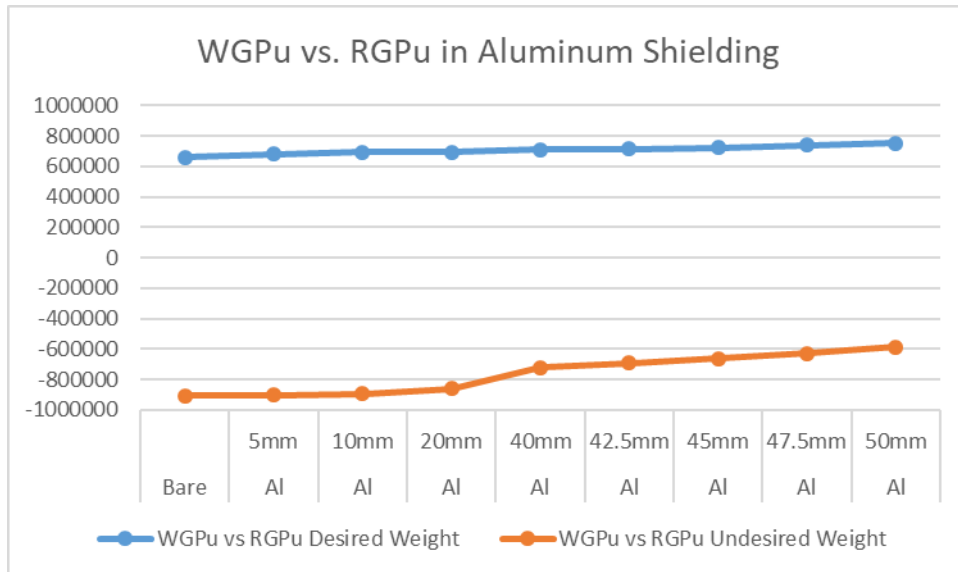


Figure 5 - Unclassified Radioisotope Algorithm Performance Estimate

An alternate approach to warhead verification which does not require a priori knowledge of the treaty item characteristics, or the recording and processing of sensitive data, is the Zero Knowledge Protocol. An example of this is CONFIDANTE using a Fast-neutron Imaging Detector with Anti-image Null-positive Time Encoding (CONFIDANTE). This concept uses time encoded imaging with an anti-image null-pattern coded aperture to compare two radioactive objects declared to be equal (Figure 6).

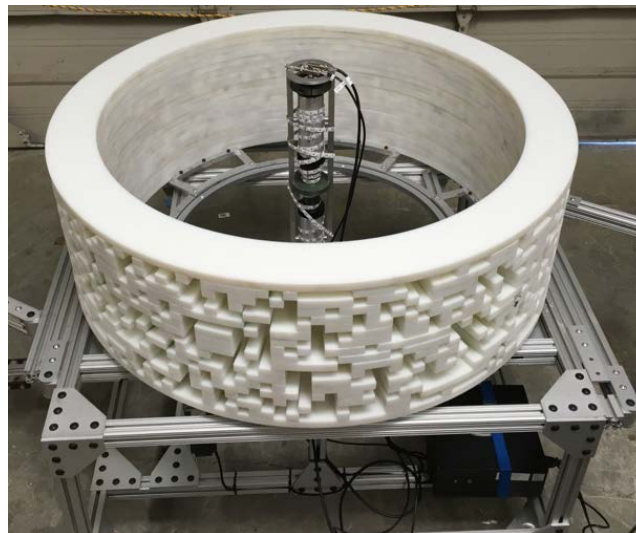


Figure 6 - CONFIDANTE System [5]

The idea with CONFIDANTE is that each open aperture on one side will have a closed aperture exactly opposite, and vice versa. Therefore, if the two items are identical, the net count rate from the single pixel detector located in the center of the cylindrical coded aperture array would be consistent with Poisson noise (Figure 7). This approach enables relatively high resolution imaging, yet avoids the measurement and storage of sensitive information.

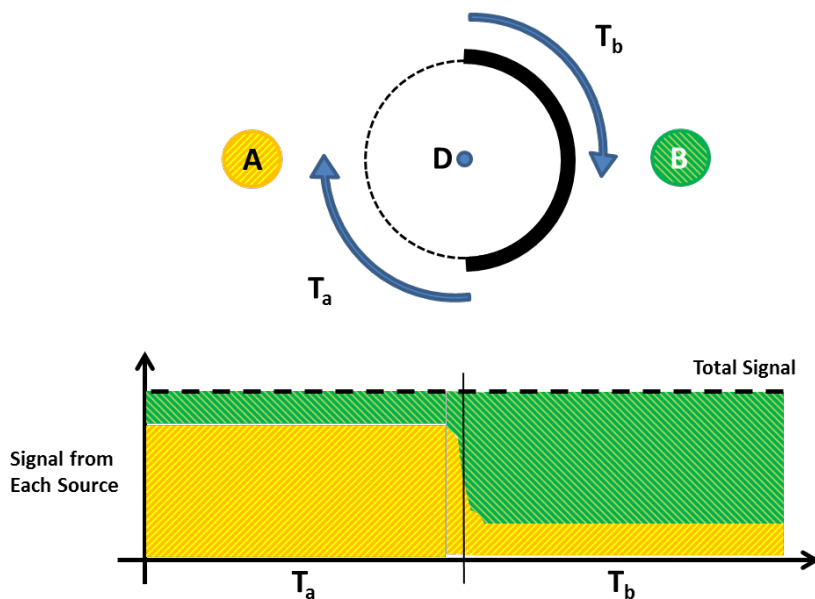


Figure 7 - Null Image Concept [5]

## Challenges with implementation

A potential downside to utilizing arms control technologies in safeguards applications might involve potential competition between the two technologies. Rather than performing a competitive downselect of the two, both technologies can be used in conjunction. A greater level of confidence can be reached regarding compliance if a state passes multiple independent compliance tests. Additionally, having multiple systems capable of measuring similar phenomenologies can offer increased operational flexibility for off-normal situations. However, with increased verification efforts comes increased costs.

To reduce the financial strain placed on the IAEA for implementing safeguards, arms control technologies can potentially be used to reduce the amount of inspection visits. Inspection visits can be reduced by implementing both types of technologies to increase compliance confidence between inspections. By subjecting a country to increased monitoring using both technologies, a lower amount of inspections might be needed to verify compliance. In some scenarios, states may feel this method of verification to be less intrusive since site operations will not be hindered by the on-site inspections. The perceived reduction in intrusiveness also provides a greater feeling of autonomy and privacy to the state. This scenario can be used to ease new safeguards signatories into more intrusive and comprehensive modes of verification and eventual arms control agreements after trust is built. This may be an effective way for arms control talks to resume as current agreements like the INF and New START expire within the next few months and years.

## Conclusion

Despite the appreciable differences in the arms control and safeguards verification regimes, such as information sensitivity, operational constraints and the sheer volume of use cases, the driving requirement for open development (i.e. the ability to authenticate and certify a verification technology for use in a treaty verification scenario) can lead to the development of algorithms and technological solutions which are inherently exportable and easily transferred to international treaty partners. By encouraging technological cross-talk between arms control and safeguards, the resulting increased usage can ultimately lead to increased confidence and trust in the arms control systems. Thus, increased familiarity with well-documented technologies can encourage the adoption of more rigorous verification technologies, resulting in more secure and confidence building treaties.

## References

- [1] Seager K, et al; *Trusted Radiation Identification System*, Sandia National Laboratories, 2000.
- [2] Mitchell D; *1997 and 1999 Pantex Radiation Measurement Campaigns*, Sandia National Laboratories, 2001.
- [3] Mitchell D, Marlow K; *Minimum Mass Estimates for Plutonium Based on the Peak Intensities and Scattered Radiation in HPGe Spectra*, Sandia National Laboratories, 1999.
- [4] Padilla E; *Radioisotope Discrimination Algorithm for Arms Control Inspections*, Sandia National Laboratories, 2018.
- [5] Marleau P, et al; *Proof of concept demonstration of CONFIDANTE (CONFirmation using a Fast-neutron Imaging Detector with Anti-image Null-positive Time Encoding)*, Sandia National Laboratories, 2018.

# The Importance of Understanding the Inverse Problem in an Arms Control Scenario

Jennifer Schofield

AWE Ltd

AWE, Aldermaston

Reading, RG7 4PR

© British Crown Owned Copyright 2019/AWE

E-mail: Jennifer.schofield@awe.co.uk

## **Abstract:**

*The inverse problem is defined as calculating the cause from a given effect. When verifying a treaty, one of the most important aspects is the ability to identify consistency with declarations, for example ensuring the spectra of a measurement (the effect) is consistent with the declared item (the cause). By ensuring we can identify when this information is incorrect, both parties can be held more accountable. When monitoring a treaty limited item declarations may be imprecise, and thus during monitoring, combinations of variables may have the effect of fulfilling the declaration characteristic. In particular, for arms control and treaty verification scenarios, an often-proposed data collection method is radiation measurement, with the emissions being the radioactive components in a treaty limited item. When considering gamma spectra, different combinations of parameters (e.g. mass, time, geometry, distance, shielding, material composition) can provide similar spectra.*

*The issue is how to ensure items presented during measurement are in fact items of interest. Investigating this inverse problem allows all parties in a treaty to understand which declarations are most appropriate for a given treaty.*

*This paper will investigate the inverse model as applied to arms control. It will detail the main methods used to tackle inverse transport problems, such as the adjoint Levenberg-Marquardt method, and Mattingly and Mitchell's differential approach, with their relative strengths. The paper will go on to suggest inverse modelling techniques which could bring multiple solutions to light and allow treaty declarations to be more effective, increasing trust between parties.*

**Keywords:** inverse modelling, arms control, treaty verification

## **1. Introduction**

Inverse problems are ubiquitous in many scientific fields and in a general sense can be described as using effects/results to get back to a cause. This could be, for example, using x-ray detection to reconstruct an image of a patient, or inferring internal properties of the earth from external measurements (i.e. without drilling bore-holes hundreds of metres). Figure 1 shows how the forward problem, going from the object or physical properties and predicting/measuring the observables and the inverse case, are related to each other.

Arms control often takes the form of formal agreements or treaties. Within a treaty, declarations are made regarding the items of interest for that treaty. It is these declarations which are verified to ensure consistency and contribute to the trust between states that the treaty is being carried out as intended.

Depending on the aim of the arms control treaty there are a couple of possible types of declarations and associated verification methods. Absence declarations state that an item or characteristic is not present. Presence declarations state an item's presence and require positive confirmation measurements. The determination that something is in fact a warhead is also called the initialisation problem and is a challenge in verification as the host party may wish to protect sensitive design information [2]. This must be done whilst also giving enough confidence to other parties that the item is as declared. Exactly what

measurements are able to communicate about a given system is therefore important. There is already an existing literature on the difficulty of negotiating agreements as a function of the attributes you wish to measure, as more information is declared the more the treaty is seen as difficult to negotiate [2].

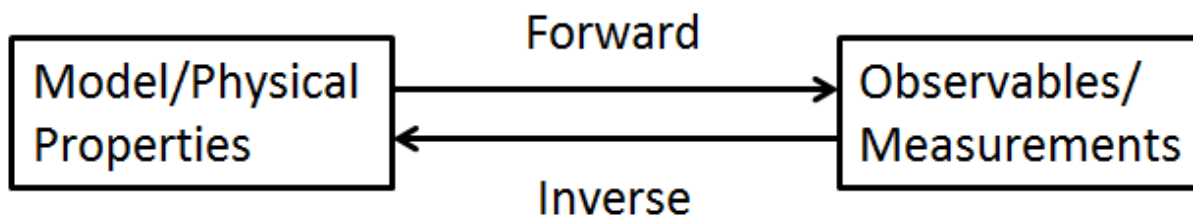


**Figure 1:** The link between a forward and an inverse calculation is simply whether you start with an object, or with the measurements.

In the past, treaties have included declarations in a form that can be verified by confirming the absence of fissile material. Examples of where on-site inspection and measurements have been included to help verify declarations in the treaty are the Intermediate-range Nuclear Forces Treaty, START I (Strategic Arms Reduction Treaty) and New START [1]. All three of these treaties included provisions for the confirmation of the absence of fissile material using neutron radiation measurements. From this it can be seen that absence declarations are easier to negotiate, as they have been included in past treaties, than presence declarations.

In the future, treaties may include a reduction of warhead numbers. Where this is the case, declarations may not only be asserting absence, but may require positive identification of items/aspects of items for dismantlement. In general, for a nuclear warhead we would expect it to emit several types of radiation: neutron and gamma. Both have been suggested as giving attributes of interest for measurements to confirm declarations of item presence [2]. When measuring gamma radiation, a spectrum is generally obtained with peaks found at different energies. This gamma spectrum has a wealth of information intrinsic to it, for example, the type of material emitting radiation (in this case  $U^{235}$  or  $Pu^{239}$ ) or information about the amount of shielding in between the source of the radiation and the detector (the attenuation).

Things that might be included in treaty declarations for the presence of fissile material could include as suggested by Hauck [2]: the type of fissile material (HEU or Pu), the amount above a threshold or the age of the materials involved. For each of these attributes there are already existing equipment to look at/measure these attributes [2]. As already mentioned, depending on the measurement taken, much more information than required could be in the observation than is necessary to satisfy the declaration.

One way of overcoming the competing constraints of host and inspector is the concept of an information barrier, which restricts the information available to the inspecting party. The level of restriction can vary, from as little as a yes/no result to, for example, part of a gamma spectrum. Work has been done by several parties on information barriers and, in the case of the UK Norway Initiative (UKNI), devoted some thought to confidence around designing and building the barrier [3]. This work will focus more on the attributes chosen for measurement and aims to show the importance of choosing treaty declarations carefully in order to allow effective verification with confidence on all sides.

The inverse problem as it pertains to radiation transport will be explored in more depth below, and two particular methods will be described to show some technical aspects of how solving the inverse problem can be done. Where possible in this work mathematical terms have been avoided. For a full technical review of inverse transport in radiation transport see, for example, Bledsoe's "Inverse Methods for Radiation Transport" [4]. The implications for arms control declarations and methods will be discussed.

## 2. Inverse Problems

There are two main methods for tackling inverse problems. These are termed explicit and implicit where explicit models do not involve direct models of the observables. Implicit models take a "first guess" as a

solution, then use a forward model to predict observables. This forward model is iterated and changed according to an optimisation method until the model output matches the unknown spectra closely. The parameters of this forward model are then considered to be the solution for the inverse problem. Common inverse methods for radiation transport use differential or adjoint methods [5, 6]. Increasingly, as computers have become more efficient, the range of tools able to be applied have increased, and global solutions are now being explored.

## 2.1. Differential Methods

Differential methods tend to be simple to understand but can be less efficient than other methods. Mattingly and Mitchell have presented a differential method for radiation transport in the field of non-proliferation and international security [6].

As mentioned, optimisation on forward models is implemented to ensure the outputs match. These optimisations usually use chi-squared,  $\chi^2$ , often described as the “goodness of fit”, shown below.

$$\chi^2 = \sum_{n=1}^N \left( \frac{M_{n,0} - M_n(u)}{\sigma_{n,0}} \right)^2$$

In the equation above  $M_{n,0}$  denotes the measured value which you are using (as an example this might be flux at a particular energy, as Table 1 used in Section 3) and  $M_n(u)$  is that value as calculated using your forward model.  $N$  is the number of measurements and  $u$  is the unknown parameter of interest (e.g. the type of fissile material present). The  $\sigma$  is the uncertainty associated with the measurement.

For differential methods, calculating the required change in the unknown parameter is done by calculating the forward difference between the measurement with a given parameter and the measurement with a slightly different parameter.

$$\delta u = \frac{M(u + \omega) - M(u)}{2\omega}$$

The  $\omega$  should be much smaller than the parameter so for example 0.001 cm if the parameter were the amount of shielding, and this was expected to be on the order of cm. This change in the unknown parameter  $\delta u$  can be added to the original  $u$  to form  $u'$  and the radiation transport system (forward model) run again.

## 2.1. Adjoint Methods

The differential method is probably the simplest to understand. However, a key down-side is how it scales with number of unknown parameters. When there is only one unknown parameter to solve for, for example the ratio of  $\text{Pu}^{239}/\text{Pu}^{240}$  as with the UKNI information barrier, two calculations would be needed per iteration. However, as the number of unknown parameters increases the number of calculations per iteration will also increase as the total number of unknown parameters plus one.

There is another method which has an advantage when it comes to speed. Adjoint methodologies use the forward transport as well as the adjoint transport equation to perform optimisation calculations. The adjoint is sometimes described as the importance of the detector for a particular gamma energy. It effectively applies the radiation transport equation as if the source were placed at the detector. By utilising a method which optimises the problem according to an adjoint method the calculation only has to be performed once for each iteration, regardless of the number of unknown parameters.

Blesoe, Favorite and Aldemir have looked at using the Levenberg-Marquardt method using adjoint equations in order to solve the inverse radiation transport problem [7]. The Levenberg-Marquardt method is a gradient-based optimisation which finds the minimum value of the  $\chi^2$ . The minimisation is done by calculating the first and second derivatives of  $\chi^2$  for the unknown parameters of interest. Using these gradients, a change to the unknown parameter can then be found for the forward model.

$$\sum_{l=1}^p \alpha'_{kl} \delta u = \beta_k$$

The second  $\chi^2$  derivative is wrapped in the  $\alpha'_{kl}$  term which includes a term to determine convergence, the first derivative is in the  $\beta_k$  term. The number of unknown parameters is denoted by  $l$  with the total number,  $p$ . The Levenberg-Marquardt method is very efficient whilst retaining constraints allowing it to move towards a minimum more accurately than differential methods.

### 2.3. Multiple Solutions and Global Searches

When utilising the inverse techniques, as are detailed above, the optimisation is performed on the suggested first guess made by the operator. The ability of the system to look outside of this is often limited. This brings us onto an issue discussed often in the literature, one of non-uniqueness. The argument for this is that, with an almost infinite number of combinations (materials, thicknesses etc.), there is bound to be more than one model which will fulfil the stopping criteria of our method. Now some of these combinations are much less likely than others, but it could be useful in an arms control case to be able to search for these other combinations.

By using a global search for multiple local minima it is hoped a global minimum can be found. In particular, Armstrong and Favorite have looked into this for inverse problems for national security [8]. They have used a technique called multilevel single linkage (MLSL) for the global search. This takes a local search method on a given set of parameters (for this you could use the Levenberg-Marquardt method, although Armstrong and Favorite use a Mesh Adaptive Direct Search algorithm). After this a stochastic global search is performed across the domain of possible parameters, see Figure 2 for a diagram showing the method. For each local search a minima, or “yes” result, may be found – which are all equally correct as solutions to the inverse problem, for a given stopping criteria.

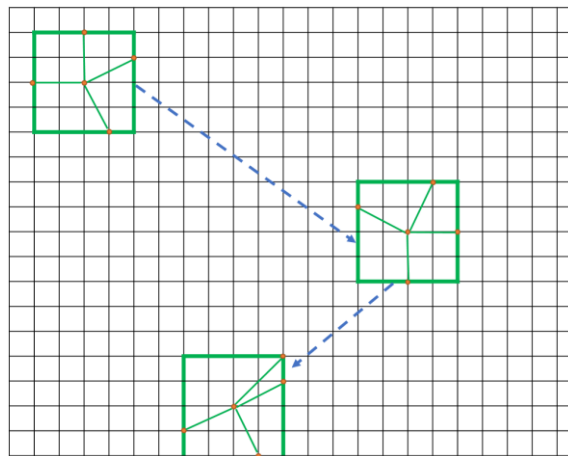


**Figure 2:** Illustration of a global search method, local searches are performed within the green squares and the algorithm moves stochastically around a “mesh”. Figure depicts work from Armstrong and Favorite’s method in [8]. The meshed domain corresponds to different parameter spaces, one green square may find the local minimum for an object constrained by a mass envelope of material and amount of several particular shields; a second green square could depict the local search being found for a different mass envelope, and across different possible isotopic values for fissile material.

### 3. Importance to Arms Control

The importance of understanding inverse problems in arms control derives primarily from the possibility of non-unique solutions (see Section 2.3 above). The challenge affects both the host and the inspecting party in a verification scenario.

As a host the priority is protecting sensitive design information. Making declarations that lead to verification measurements, which could be susceptible to information loss using inverse methods, will

be unwelcome. A suggested solution to this is information barriers. For an inspectorate it is important to be conservative and ensure ambiguous items are unlikely to pass, the information barrier giving a “not proven” result. However, even when provided with a “yes” result, may not give sufficient confidence, despite trust in the equipment. This is due to the possibility of multiple local minima across the global parameter space.

This issue, encountered when using information barriers, can also be described as the unknown number of things that will pass a given declaration. As an example, imagine an information barrier which measures the flux of 1.001 MeV gamma rays and mandates a value above a certain threshold to indicate the presence of fissile material. Two HEU objects can be modelled using MCNP, with the same isotopic composition but different masses, the larger mass being a sphere and the smaller mass a plate. When simulating the flux in a simulated detector the results can be seen in Table 1. Despite being very different amounts of material, they give almost exactly the same response in the detector.

Shape	Volume (cm <sup>3</sup> )	Flux (ph s <sup>-1</sup> cm <sup>-3</sup> )
Sphere	268	9.28
Plate	144	9.39

**Table 1:** Peak flux at 1.001 MeV as calculated by MCNP for a sphere and plate of different volumes.

This means both, when measured with an information barrier, would give a “yes” result. Without knowledge of the inverse problem and without being able to assess global solutions an inspecting party may have unwarranted confidence in a result. Information barriers are also imperfect due to the many causes of false negatives in addition to the possibility of false positives.

Faced with a large domain of parameters (material type, thickness, shielding etc.) where values will all pass a given threshold, a party may negotiate more constraints. From an inspector perspective, this constrains the domain over which “false” negatives will apply. However, extra measurements could mean more measurements of different attributes, leading to possible aggregation of information and more concern on the host-side due to sensitive information release (for the very reason that this would constrain the parameters further).

Inverse analysis is already well established in the context of national and international security, with products such as GADRAS being designed for detector response as well as analysis functions [9]. The use of the inverse in this context is slightly different as sensitive information does not need to be protected, unlike arms control. One area which is of less importance for arms control that comes out of discussing the inverse problem is the time required for different methods. This widens the range of methods which can be applied to solve the inverse problem.

#### 4. Conclusion

It is clear that treaty declarations can be much more complicated than they first appear. Information barriers may appear to solve some issues; however, in reality, they may require so many confinements that they become cumbersome. In the special case of gamma spectra, it should not be considered certain that declarations on these will be included in a treaty, due to the number of constraints required to ensure confidence in a measurement. Declarations that are not towards confirming that something is an item of interest, but rather that distinguishes between categories of items may lead to verification measures which are not as susceptible to the inverse problem. For example, declarations that warheads are in “long term storage” category as opposed to (for example) an “active service” category, may not necessarily lead to verification measures requiring radiation measurements at all; in addition, any radiation measurements required may be subject to a lower level of confidence in the domain space by the inspectors as the initialisation problem can be avoided.

It is immensely difficult to ensure that the measurement presented is in fact from one single object of interest - this is an effect of the fact we are solving an ill-posed, non-unique inverse problem. When declarations are made it is important that aspects such as the inverse problem are considered well in advance. Some even suggest that declarations should be confined to simply the presence of fissile material, rather than specifying anything further [2]. This would actually help confidence of all parties in many respects.

## 5. Acknowledgements

The author would like to acknowledge all those who have reviewed this work.

I agree that ESARDA may print my article in the ESARDA Bulletin/Symposium proceedings.

The authors declare that their work is original and not a violation or infringement of any existing copyright.

## 6. References

[1] The Challenge for Arms Control Verification in the Post-New START World C. R. Wuest, LLNL-TR-564612, July 16, 2012.

[2] Benefits of a “Presence of Fissile Material Attribute for Warhead Confirmation in Treaty Verification”, Danielle K. Hauck, Duncan W. MacArthur, LA-UR-13-25330.

[3] UKNI, “IB Project Context and Concepts”, (2016), <https://ukni.info/>, accessed 01/04/2019.

[4] “Inverse Methods for Radiation Transport”, Keith C. Bledsoe, Dissertation, Ohio State University, 2009.

[5] “Using a derivative-free optimization method for multiple solutions of inverse transport problems”, Jerawan C. Armstrong and Jeffrey A. Favorite, Optimization and Engineering, March 2016, Volume 17, Issue 1, pp 105–125.

[6] “A Framework for The Solution of Inverse Radiation Transport Problems”, John Mattingly and Dean J. Mitchell, IEEE Transactions on Nuclear Science, vol. 57, no. 6, December 2010.

[7] Using the Levenberg-Marquardt Method for Solutions of inverse transport problems in one and two-dimensional geometries, Keith C. Bledsoe, Jeffrey A. Favorite and Tunc Aldemir, 2011, Nuclear Technology, 176:1, 106-126.

[8] Jerawan C. Armstrong, Jeffrey A. Favorite, “using a derivative-free optimization method for multiple solutions of inverse transport problems”, Optimization and engineering, 17 (2016) 105-125.

[9] GADRAS-DRF 18.6 User's Manual, Horne, Steve M. et al., Sandia National Lab. (SNL-NM), Albuquerque, NM (United States), 2016.

# **Session 15:**

# **Process Monitoring**

# Developing a new safeguards sensor control platform and its application in EURATOM safeguards

## IMAP, the Integrated Monitoring and Acquisition Platform, challenges and techniques

Andreas Smejkal<sup>1</sup>  
Ralf Linnebach<sup>1</sup>  
Ludwig Holzleitner<sup>2</sup>

<sup>1</sup> European Commission, Directorate General for Energy, Directorate Euratom Safeguards, Luxembourg

<sup>2</sup> European Commission, Joint Research Centre, Directorate Nuclear Safety and Security, Karlsruhe

### **Abstract:**

*Remote monitoring and unattended data acquisition is a backbone of EURATOM safeguards verifications. Sensor networks are used in many different applications, such as item tracking, containment applications, or automated mass verification of samples. EURATOM started to use unattended systems particularly in the large bulk handling facilities more than 20 years ago. For this purpose the software package RADAR (Remote Acquisition of Data and Review) had been developed, which aimed at standardizing the unattended NDA systems in use. While still being used, RADAR is not always stable and reliable on a Windows 7 architecture or newer environments for which it was not developed. In addition, the data acquisition and transfer processes are not compliant to state-of-the-art data security requirements.*

*This paper presents a new integrated sensing and data acquisition system, designed for instrumentation control, unattended continuous data acquisition, and state of health monitoring, providing at the same time the highest achievable level of reliability and data security. In particular, the new system under development is designed to be consistent with the goals of operation of RAINSTORM (Real-time And INtegrated STream-Oriented Remote Monitoring) and RADAR in terms of data security and modularity. IMAP, the Integrated Monitoring and Acquisition Platform, will be a new smart sensor control platform, facilitating device installation and enabling easy configuration of the system for all safeguards sensors in use. IMAP will support various hardware interfaces and will be as well adaptable to new safeguards devices. The design will also provide for means to configure and update operating and monitoring parameters (such as state of health) for all sensor modules remotely.*

*IMAP will operate as well on sensor networks based on Single Board Computers (SBC). SBCs are gaining greater attention from the safeguards community because they offer great advantages due to their small size, low power consumption and easy integration.*

*This paper aims at providing an overview of challenges and techniques of the IMAP development and prototype testing, based on a cooperation between EURATOM and the JRC Karlsruhe. It describes the state-of-the-art and points to the most probable future challenges and development directions in the next years.*

**Keywords:** remote monitoring, unattended data acquisition, sensor control platform

## **1. Introduction**

For 20 years EURATOM has been using the software platform RADAR [1] as unattended monitoring system deployed for acquiring data at nuclear facilities to verify the facility operator's compliance with

safeguards agreements. While still being used, RADAR is not always stable and reliable on a Windows 7 architecture or newer environments, for which it was not developed. In addition, the data acquisition process and transfer is not compliant with state of the art security requirements.

To address this problem, EURATOM started defining requirements for a new multi sensor control platform providing all necessary tools and functionalities for the installation and configuration of a remote monitoring system which operates completely unattended while ensuring the highest achievable level of data security.

In particular, the new system to be developed should be consistent with the goals of operation of both IAEA's data security protocol "Real-time And INtegrated SStream-Oriented Remote Monitoring" (RAINSTORM) protocol [2] and RADAR. Further, the new architecture should work with existing equipment and be open to new equipment and systems that are intended to be built or purchased.

The system to be developed should reuse existing concepts, processes and components to facilitate a smooth transition from the current legacy system to a new data acquisition platform. Major changes of the currently used IT infrastructure and processes have to be avoided. The system to be developed has to use RAINSTORM for secure transmission and storage of sensor data wherever possible and should follow the modular concepts of RADAR and its Data Acquisition Modules (DAM) as much as possible.

## 2. System description of IMAP

### 2.1 A smooth transition from RADAR to IMAP

RADAR has been in use for nearly 20 years. One of the consequences is that EURATOM's whole data acquisition process and corresponding evaluation and analysis processes are centred on it and its file formats. Replacing such a core tool is a challenging task. As a first consequence, it has been decided that the new IMAP will produce output file formats compatible to RADAR and corresponding evaluation tools like the Integrated Review and Analysis Program IRAP [3] and VisoR [Visualization of RADAR].

In particular, IMAP will produce configuration snapshots of DAMs, the so-called setting files, and sensor specific output files. Additionally, IMAP will be able to read legacy setting files and accept them as input. Thus, replicating current sensor setups does not require creating new configuration files or manual interaction and a "quick-start" into IMAP becomes possible. The new security requirements however demand some new setup and configuration steps.

IMAP will provide a clear and comprehensible web interface to all the functionalities tailored for the specific needs of different user groups. This allows for a flat learning curve for inspectors, technicians and other potential user groups (e.g. 3<sup>rd</sup> party maintenance).

### 2.2 The development method: Actor Model

IMAP development started in late 2018 and is based on a framework known as the actor model [4]. An actor model in computer science is a conceptual model to deal with concurrent computation. It defines some general rules where universal primitives, called actors communicate exclusively via asynchronous messages sent to each other (Figure 1). The most important core-components or "core-actors" of IMAP are the *WatchdogActor*, the *ConfigurationActor*, the *FileInteractionManagerActor*, and the *SecurityActor*. They are "unique" for every instance of IMAP. *DAMActors* for individual measurement devices take care of the actual data acquisition.

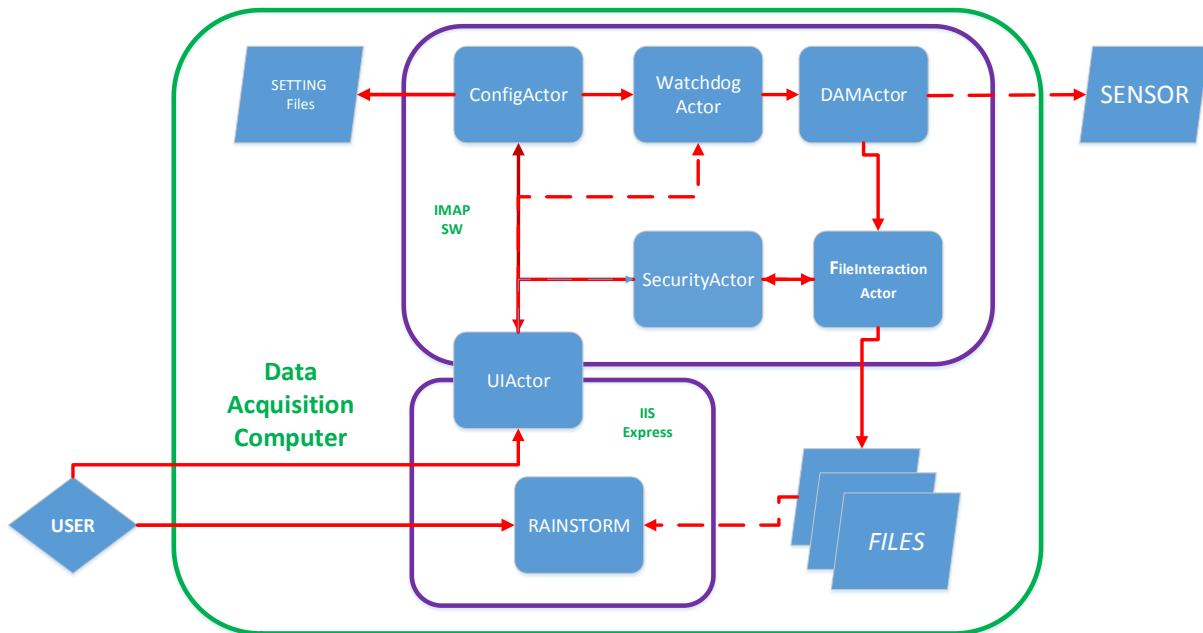


Figure 1: IMAP actor model - simplified overview

### 2.3 The architecture

A main requirement of IMAP is the compatibility to existing safeguards sensors and the ability to provide a maximum flexibility for implementing new sensor electronics. A parallel operation of different sensor types connected to the same computer is a typical use case for an unattended monitoring system. Therefore, it is required that the new system being developed enables simultaneous measurements of numerous analogue and digital channels. The signals can be recorded with a sampling rate up to 1000 samples per second and they can be stored either in a built-in memory card of the acquisition computer or any other connected portable media. Universal Serial Bus (USB), Ethernet and RS232 interfaces allow for a device-computer communication, in particular, setting up acquisition parameters and enables efficient data transfer between device and computer (Figure 2).

As a matter of fact, most safeguards sensors are installed in controlled areas at nuclear facilities and not always easily accessible. Therefore, all devices and measurement electronics can be as well accessed and operated through a computer network and/or remote access via internet lines. They are configured and operated using various web user interfaces.

The software architecture and the design of the system is based on modularity, a concept that has proved to be very successful [5]. The interface to each individual sensor will be represented by a so-called DAM (Data Acquisition Module). However, DAMs might use common libraries in order to avoid duplication of code, e.g. if working with the same hardware. A modular designed system is far more reusable since all (or many) of these modules may be modified and maintained separately. In any case, the modular approach shall allow the modification of existing sensor modules with minimal impact to the overall acquisition framework or the development and integration of new sensor interfaces.

Watchdog processes are used to detect and recover from computer malfunctions. Computer controlled safeguards equipment operates on a 24/7 basis in controlled areas of nuclear facilities. For obvious reasons, it is important that the system is running continuously. As safeguards technicians cannot easily access the equipment or would be unable to react quickly to faults, the computer cannot depend on human intervention, e.g. a reboot, if a device or the computer itself hangs. The system must be self-reliant. Otherwise, such systems could become permanently disabled if they were unable to autonomously recover from faults.

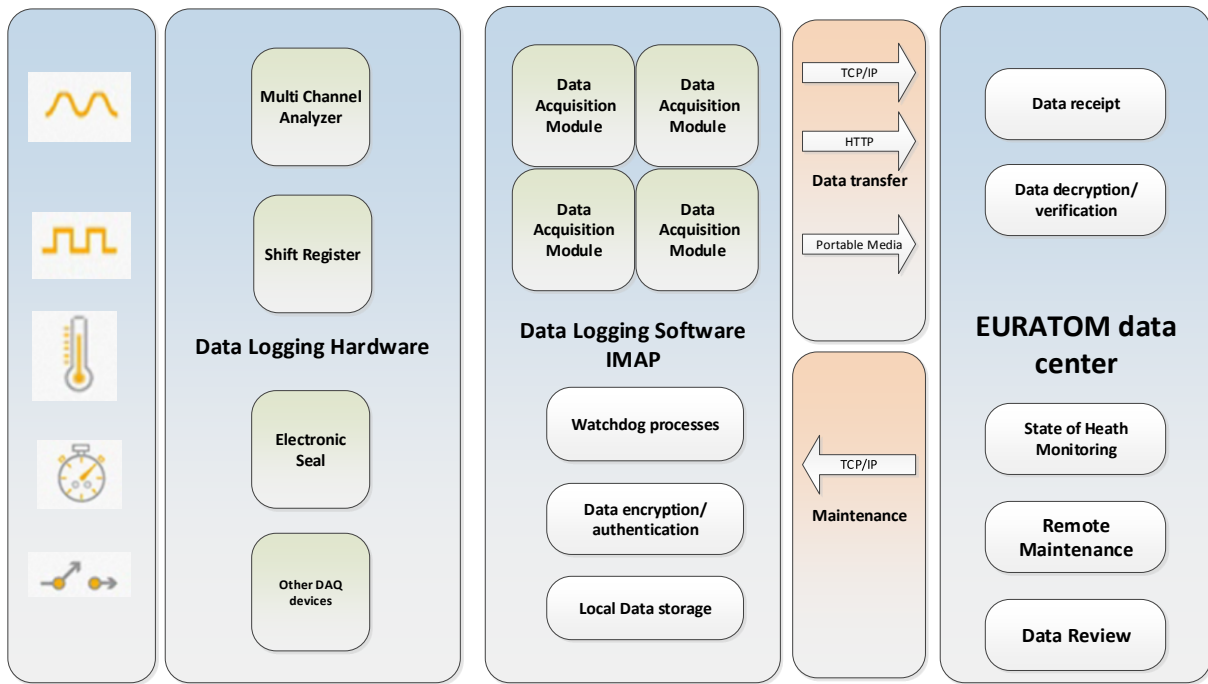


Figure 2: The general architecture of a future IMAP system

## 2.4 Safeguards sensors

EURATOM’s unattended monitoring systems are deployed at many facilities in the European Union, especially in reprocessing plants, fuel fabrication plants, at spent fuel loading campaigns and soon in encapsulation plants and geological repositories [6]. The system architecture of such a system is based on measurement equipment that can be connected to a computer and operated completely unattended. The size of such a system may vary from a single stand-alone unit at spent fuel loading campaigns up to a remote monitoring network with about hundred sensors in a reprocessing plant.

Today EURATOM is using more than 20 different safeguards sensors. The most important measurement devices are sensors to detect and measure gamma and neutron radiation. Other instruments measure e.g. weight, ID or length (Table 1).

Description	Instrument
Gamma Spectroscopy	Multi-channel analysers (MCA-166, MCA-527) [7]
Neutron coincidence counting	Shift registers (JSR12; JRS14, JSR15) [8]
Neutron multiplicity counting	Shift registers (JRS14, JSR15)
Spent fuel verification	Serial Micro Channel SMC 2100 [9]
Containment	Electronic seals, e.g. EOSS [10]
Neutron counting	Counter modules
Identification	ID, barcode reader
Rod length measurement	Multi-Channel Scaling (MCA-166, MCA-527)

Table1: Typical safeguards instruments to be implemented into IMAP

### 3. IMAP User Interface design

Unlike the predecessor system RADAR, the new IMAP may have several types of user interfaces to serve different kinds of users and needs. Those user interfaces will be depending on the user-class and operation mode. Several modes of access to the sensor control platform will be supported by this system. Nevertheless, the entry point will be a *Web User Portal* through which IMAP can be accessed through a local computer and as well remotely in a secure manner from anywhere in the world through the world-wide web. It will not require any extra software than a standard web-browser. It will enable the user to access each individual sensor, submit setup files or modify configuration parameters and download data. There shall be direct instrument control through this interface possible.

- *Inspectors Interface:* This is the interface through which nuclear inspectors will operate the system. There shall be as little direct interaction between this interface and systems parameter of the sensor as possible. The interface shall emphasize the measurement rather than instrument control to reduce the learning curve and enable nuclear inspectors to focus on the measurement results. All functionality provided by this interface shall be within a single integrated application.
- *Sensor Control Panel Interface:* This is the interface through which safeguards technicians will operate the system. The interface enables direct access to each subsystem of the data acquisition system, for setup, diagnostics and monitoring. It shall be a sensor focused interface. Access to the sensor control panel for monitoring purposes shall not adversely affect the performance of functionality of any on-going data acquisition activities under normal circumstances
- *Diagnostic interface:* This interface shall only be available to experienced users and/or developers. It will give access to all critical parameters and allow tracking and analysing issues (bugs) as recorded by the system (Alarm and Log events). Several modes of diagnostic tools will be available (e.g. on-demand when a user wants to investigate issues, background diagnostics to monitor a system for failures or system indicators). This mode provides access to enhanced State of Health (SoH) analysis, diagnostic tools and system parameters not visible in standard operational scenarios. If a system runs in failure mode, the user needs to have quick access to status information of all system components of the program and associated hardware but as well to relevant information related to the host PC and the communication between PC and electronics.
- *User Interface for attended measurement:* Attended measurements will be started by the user for a specific time period only. The duration of the measurement time is either configured in the setup process or triggered by the user via start and stop commands. The user will have direct visual feedback on data acquired.

### 4. IMAP Data security features

Even if EURATOMs data acquisition systems are usually operated in sealed electronic cabinets preventing unauthorized access and data transfer is managed via secure VPN connections to the HQ, additional requirements to achieve a high level of security were defined. A main priority for transfer of safeguards data is to ensure its integrity. IMAP will provide a number of features to apply authentication and encryption to acquired data files.

EURATOM and IAEA began using unattended data acquisition systems and remote monitoring in the late '90s as a means of optimizing inspection efforts. Especially the possibility to use remote data transmission (RDT) has gradually expanded over the last 10 years. EURATOM is currently operating ~60 RDT connections to 14 EU member states. It is expected that this number will continuously grow in the future. To ensure the increasing demands on data security EURATOM decided to be compliant to IAEA's requirements on secure data transmission.

In 2012 the IAEA defined a set of requirements for Real-time And INtegrated SStream-Oriented Remote Monitoring (RAINSTORM) which define the data interface and data security requirements for all new remote-monitoring capable safeguards instruments. Today RAINSTORM is globally deployed by the IAEA for all their remote data acquisition systems. In order to avoid redundant developments and to start working with an approved technology, EURATOM adopted this concept into the new data acquisition system IMAP.

The RAINSTORM concept works in conjunction with a cryptographic token engine, the Universal Instrument Token (UIT) that will provide greater private key protection. The data security requirements are based on public-key infrastructure (PKI). PKI provides a far superior encryption/authentication security than pre-shared keys. The sensor platform requires a TCP/IP over Ethernet implementation and USB access to the cryptographic token. All RAINSTORM components work on top of these requirements and can be easily implemented.

## **5. Challenges – Autonomous operation of a multi-source data acquisition system**

Operational requirements to a nuclear safeguards data acquisition system are challenging. Safeguards data is acquired for the purpose of verifying movements of nuclear material within a facility. In order to maintain the continuity of knowledge this data must be complete and easily available to the inspector and to the review and analysis system. Furthermore, its integrity and authenticity needs be ensured at all times.

The EURATOM technical department operates hundreds of safeguards sensors at nuclear facilities in member states of the European Union. Physical access for technicians to these sensors is limited and very time consuming. As a matter of fact such systems need to operate completely autonomous with a minimum of human intervention necessary.

Because such a data acquisition system is intricately woven into safeguards operations, the highest level of availability is required for the acquisition processes to support 24/7 data availability. Any downtime - planned or unplanned - may directly affect any safeguards conclusion to be made.

The underlying architecture must therefore support features at all levels to maximize the reliability of the systems and minimise data loss in case of unplanned outages such as hardware or software failures, as well as planned outages such as hardware maintenance and application upgrade cycles. The system should also prevent data loss that typically happens due to user or application errors. These new requirements call for a significant effort in pre-operational testing procedures.

### **5.1 Testing facility: The EUSECTRA laboratory**

To verify the correct operation of the IMAP system it has to undergo technical acceptance and long-time performance tests. As the EURATOM HQs in Luxembourg does not provide an adequate environment and infrastructure for such tests, a cooperation with the JRC Karlsruhe was established. The European Nuclear Security Training Centre (EUSECTRA [11]) offers the specific technical infrastructure, the scientific expertise and the availability of a wide range of samples of Plutonium and Uranium with different isotopic composition to verify that the measurements performed by IMAP meet safeguards requirements and deliver correct results.

### **5.2 Test approach: Comparing RADAR and IMAP**

Prototypes of the IMAP software are currently installed on a dedicated PC in the EUSECTRA laboratory. The PC is connected to measurement electronics like MMCA and Shift registers and corresponding neutron monitors and gamma detectors performing long-time tests (Figure 3). Tests will be performed on both Win-7 and Win-10 operating systems in order to ensure compatibility with both systems. A variety of typical safeguards instruments are available at JRC-Karlsruhe for these tests such as MCA527, MCA166, electrically cooled HPGe (High Purity Germanium) detector, HLNCC

(High Level Neutron Coincidence Counter), AWCC (Active Well Coincidence Counter), PSMC (Plutonium Scrap Multiplicity Counter), JSR12 and JSR15R just to mention some.

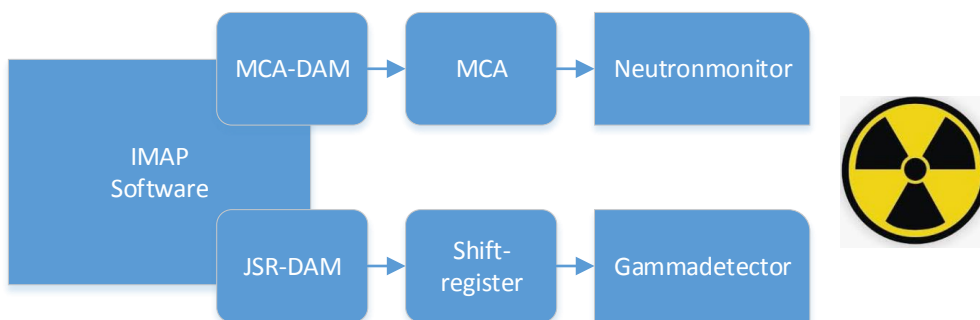


**Figure 3:** EUSECTRA laboratory setup: PC, measurement electronics, monitors, samples

The purpose of these tests is to monitor the behaviour of the measurement infrastructure, the computer’s operating system and the data acquisition system (Table 2). In a later stage sample measurements with IMAP will be repeated with RADAR systems to compare results between both platforms.

Description	RADAR	IMAP
Development environment	Visual basic 5/6, C#	C# .NET, MS Orleans
Operating system	Win NT, Win XP	Win7, 10 and higher
Operating modes	unattended	attended/unattended
Configuration and setup	GeneralConfig in Windows registry	ConfigurationActor
Data security	3 <sup>rd</sup> party tools (e.g. PGP)	PKI infrastructure
Data security modes	On demand	OTFE, scheduled, on demand
Sampling rate/sec	1	1000
Data types	File, OPC	File, OPC
GU Interface	One single configuration interface	User dependent web interface

**Table 2:** A comparison of RADAR and IMAP features

### 5.3 Test evaluations

A main requirement to any autonomous data acquisition system is reliability and stability of all processes during the measurement period. Nevertheless, we have to spend attention to data quality issues as well. Is the measured data consistent with the declaration of the sample? Does the measurement electronics deliver the correct values?

RADAR data is usually analysed by using the review platform IRAP. IRAP is designed to structure and perform an interpretation of massive amounts of data based on the inspectors’ judgement using means of visual representations combined with advanced scientific methods like MGA (Multi Group Analysis) [12], ORIGEN (Oak Ridge Isotope Generation) [13], FRAM (Fixed-Energy, Response Function Analysis with Multiple Efficiency) [14] or INCC (IAEA Neutron Coincidence counting) [15]. All these scientific programs are highly accepted tools in the safeguards community, results delivered by these programs are considered as reliable and accurate.

As IMAP data will be by definition compatible to IRAP data requirements, the effort to analyse new data sets will be minor. The EUSECTRA laboratory provides a declaration on mass and isotopic content of the material for each sample. A verification of the IMAP measurement, comparing the

analysed measurement with the sample by using existing and approved tools is therefore straightforward.

In a second step, we have to exclude any bias from the detector or electronics hardware. Independent replicate measurements with the same sample need to be performed with the RADAR system in order to compare results of both acquisition platforms. Only when it is confirmed by a number of successful laboratory measurements that IMAP processes the acquired information correctly, it can be released for an infield verification test campaign.

#### 5.4 Future applications – low cost data acquisition system

EURATOM operates a huge and growing number of unattended sensors at various nuclear facilities in European member states. An efficient use of financial and human resources requires the optimisation of reliability and maintainability of the data collection process throughout the entire lifecycle.

EURATOM identified the use of *Single board computers* (SBC) as a valuable contribution; they are an ideal platform for a quick and focused design of a specific sensor system (Figure 4). The low-cost and the small size of SBCs enables them to be deployed into situations where a standard PC would not be suitable.

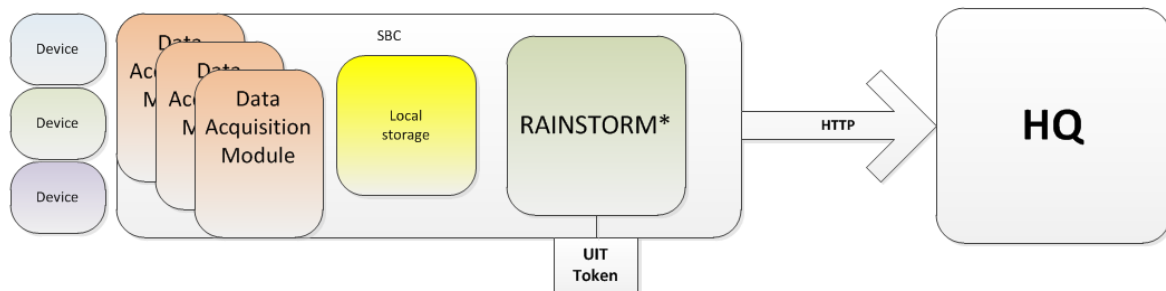


**Figure 4:** Example - possible setup of a low cost secure data acquisition system on a single board computer (SBC) connected to the HQs in Luxembourg

EURATOM has already gained some experience in the field use of SBCs and measurement devices during the execution of the EDAS (Enhanced Data Authentication System) field test [16] at the Springfields site in the UK. Beagle Bone Single Board Computers were used to acquire sensor data from an operators control system during a 6 months trial period. Further laboratory test connecting and operating the system with other safeguards devices like the SMC 2100 (Fork electronics, Figure 5) were successful and promising.

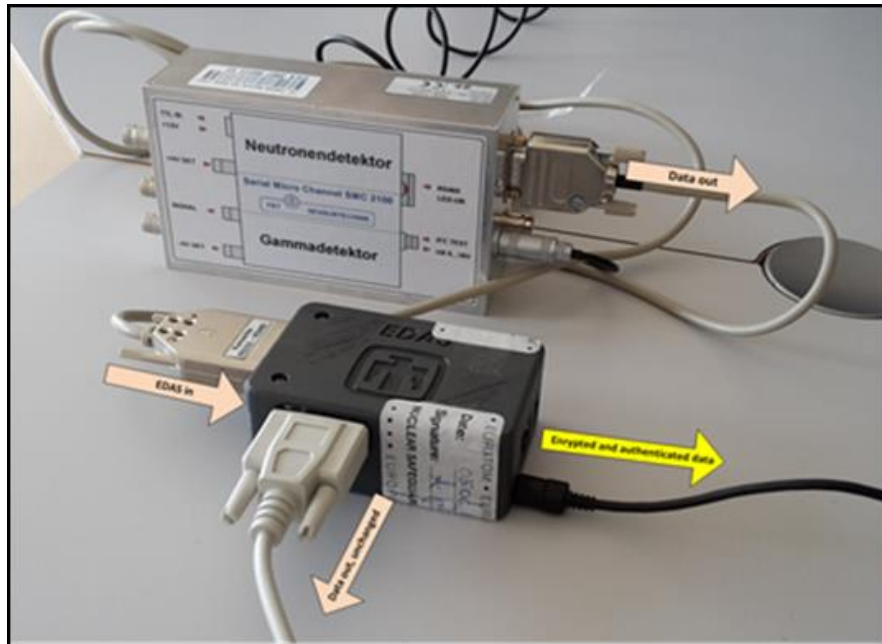


Figure 5: SBC connected to Fork electronics

## 6. Summary

IMAP is a standardized, modular software platform for sensor configuration and autonomous data acquisition. Together with IRAP it forms the backbone of EURATOM's remote monitoring network for unattended data acquisition and automated review. IMAP will operate all current EURATOM sensors in a reliable and secure manner based on a public key infrastructure and will be open to new developments. Technical acceptance and performance tests are subject of a cooperation between EURATOM and the EUSECTRA laboratory of the JRC Karlsruhe.

## 7. References

- [1] Schwalbach, P., Chare, P., Girard, T., Holzleitner, L., Jung, S., Kloeckner, W., Smejkal, A., Swinhoe, M., "RADAR: EURATOM's Standard for Unattended Data Acquisition"; Proceedings IAEA Symposium on International Safeguards, Wien 2001, Austria
- [2] Naumann, I., Morgan, K., Brunhuber, C., Wishard, B., Schwier, A., Thater, F., The IAEA's Universal Instrument Token, Proceedings IAEA Symposium on International Safeguards, Vienna 2014, Austria
- [3] Smejkal, A., Linnebach, R., Longo, J., Nordquist, H., Regula, J., Joint Partnership: a New Software Development Paradigm, Proceedings IAEA Symposium on International Safeguards, Vienna 2014, Austria
- [4] DOKUMENTA, iMAP Software requirements analysis, EURATOM internal report, 2018
- [5] Smejkal, A., Software Requirements Specification for IMAP - integrated Monitoring and Acquisition Platform, A multi sensor control platform IMAP, DG ENERGY – EURATOM Safeguards, Internal Report, 2017
- [6] Park, W.S., Coyne, J., Ingegneri, M., Enkhjin, L., Chew, L.S., Plenteda, R., Sprinkle, J., Yudin, Y., Ciuculescu, C., Baird, K., Koutsoyannopoulos, C., Murtezi, M., Schwalbach, P., Vaccaro, S., Pekkarinen, J., Thomas, M., Zein, A., Hämäläinen, M., Martikka, E., Moring, E., Okko, O., Safeguards by design at the Encapsulation Plant in Finland, IAEA Symposium on International Safeguards, Vienna, 2014
- [7] Mortreau, P.; Berndt, R., Performance test of the multi-channel analyzer MCA-527 for nuclear safeguards applications, Report EUR 26165, 2013
- [8] Mena, N., Villani, M., Evaluation of the LANL hand held multiplicity register and Canberra JSR-15, Nuclear Science Symposium Conference Record, 2007. NSS '07. IEEE Volume: 1
- [9] <http://www.fst-sensortechnik.com/seiten/mca1.html>
- [10] Richter, B., Neumann, G., Lange, S., Goldfarb, M., Tzolov, R., Mackowiak, R., Schoop, K., Design Concept of the Electronic Optical Sealing System EOSS, German Support Programme to the IAEA, report no. 337, Jülich, June 2002; and Proc. 43rd INMM Annual Meeting, Orlando, 2002
- [11] Holzleitner, L., Zsigrai, J., Galy, J., Toma, M., Bagi, J., Peerani, P., Construction of a NDA-Safeguards Training Facility at the ITU Karlsruhe, International Atomic Energy Agency (IAEA), Vienna (Austria); 491 p; 23 Mar 2015; p. 146; 12. Symposium on International Safeguards.
- [12] Gunnink, R., Ruhter, W.D., MGA: A Gamma-Ray Spectrum Analysis Code for Determining Plutonium Isotopic Abundances, Volume I and II, Lawrence Livermore National Laboratory, Livermore, CA., UCRL-LR-103220, 1990
- [13] Gauld, I. C., Bowman, S.M., Murphy, B. D., Schwalbach, P., Applications of ORIGEN to Spent Fuel Safeguards and Non-Proliferation, Proc. of INMM 47th Annual Meeting, July 16–20, 2006, Nashville, Tennessee
- [14] Sampson, T.E., Kelley, T.A., Vo, D.T., Application Guide to Gamma-Ray Isotopic Analysis Using the FRAM Software, Los Alamos National Laboratory, LA-14018, 2003
- [15] Krick, M.S., Harker, W.C., Rinard, W.C., Wenz, T.R., Lewis, W., Pham, P., De Ridder, P., The IAEA neutron coincidence counting (INCC) and the DEMING least-squares fitting programs; Inst. of Nucl. Mater. Mgmt. XXVII (39th Proceedings, Naples, FL (United States), 26-30 Jul 1998
- [16] Thomas, M.A.; Hymel, R.W.; Baldwin, G.; Smejkal, A.; Linnebach, R.; Field trial of the enhanced data authentication system (EDAS), ESARDA Bulletin, Issue n° 54, 2016.

## PRE-NRTA SYSTEMS: OPPORTUNITIES AND CHALLENGES

### **J-B. DARPIN**

Orano  
Courbevoie, France  
Email: jean-baptiste.darphin@orano.group

### **F. BONINO**

Comité Technique Euratom  
Gif-sur-Yvette, France

### **J. ODDOU**

Comité Technique Euratom  
Gif-sur-Yvette, France

#### **Abstract:**

*The principle of verification of the accounting declarations of the ORANO SET GBII enrichment plant is based on a physical control of the uranium masses and isotopic contents, by sampling on the incoming and outgoing containers stored since the last routine inspection. An annual inventory completes this scheme.*

*A computer network collects physical data from the operator. These data are processed by a specific software developed by the European Commission Joint Research Center of Ispra. This software allows the monitoring of the operator's activities in connection with the collection of precise weighing data and determination of U235 concentration from mass spectrometers. The physical data are accessible for the audit of EURATOM Inspectorates and IAEA.*

*To date, the EURATOM information system has been used successfully during the last 4 annual inventories! Moreover, the network makes it possible to contemplate changes in the practices of the current control approach, for instance taking into account the possibilities offered by computer analysis during monthly inspections.*

*At the ORANO reprocessing plant in La Hague, Euratom also implemented an efficient nuclear material control system including measurement, confinement and monitoring devices, as well as a local network system, independent from the operator's system, in order to collect data and send them to the inspectors' office on site. This information system allows the Euratom inspectors to access and process the data while on site. A data transmission system to the Euratom review room in Luxembourg is also being set up.*

*The purpose of the presentation is to take stock of the opportunities that these pre-NRTA systems represent and the challenges that must be overcome, particularly in terms of data protection and cybersecurity.*

## **1. INTRODUCTION**

Pre-NRTA systems are already installed in some existing ORANO facilities and represent actual opportunities for the inspectorates and the operator as their use can result in increased reliability, accuracy, flexibility and effectiveness of safeguards. Those systems allow better verification, less time consuming and more effective inspections.

Without modifications, or with limited ones, it is already possible to take benefit of the wide-ranging information systems installed by Euratom (i.e. the European Commission) in these facilities.

When necessary, update of Safeguards Approaches or simply the way they are applied may allow taking more advantage of the potential of these acquisitions and data processing systems, using the principles of near real time accountancy.

## 2. ACQUISITION NETWORK IN GEORGES BESSE II CENTRIGUGE ENRICHMENT PLANT

### 2.1. Current IAEA and Euratom control in GB II

Like all civil nuclear facilities in France, the Georges Besse II enrichment plant (GB II) is under Euratom control in compliance with the Euratom Treaty and the European Commission regulation n°302-2005. In 2009, the IAEA designated GB II for the application of safeguards under the tripartite safeguards agreement between France, Euratom and the IAEA (INFCIRC/290) with a view to test and develop new safeguards approaches and to enhance safeguards effectiveness while minimizing the impact on the facility operator. Hence, GB II is under Euratom and IAEA safeguards.

The inspectorates' basis for the verification of France's accounting declarations in relation to the ORANO SET GB II enrichment plant is the measurement of the uranium quantities and isotopic contents, by selection of the incoming and outgoing 30B and 48Y containers received from or sent to another facility. The containers are stored in the storage areas between routine monthly inspections.

IAEA and Euratom may also perform LFUA (Low Frequency Unannounced Access) inspections in order to confirm the absence of undeclared production.

An annual physical inventory verification (PIV) completes this control scheme. During this PIV, masses of the containers in the stations are measured and samples are taken from the process and from the cylinders. As for monthly inspections, both IAEA and Euratom inspectors participate.

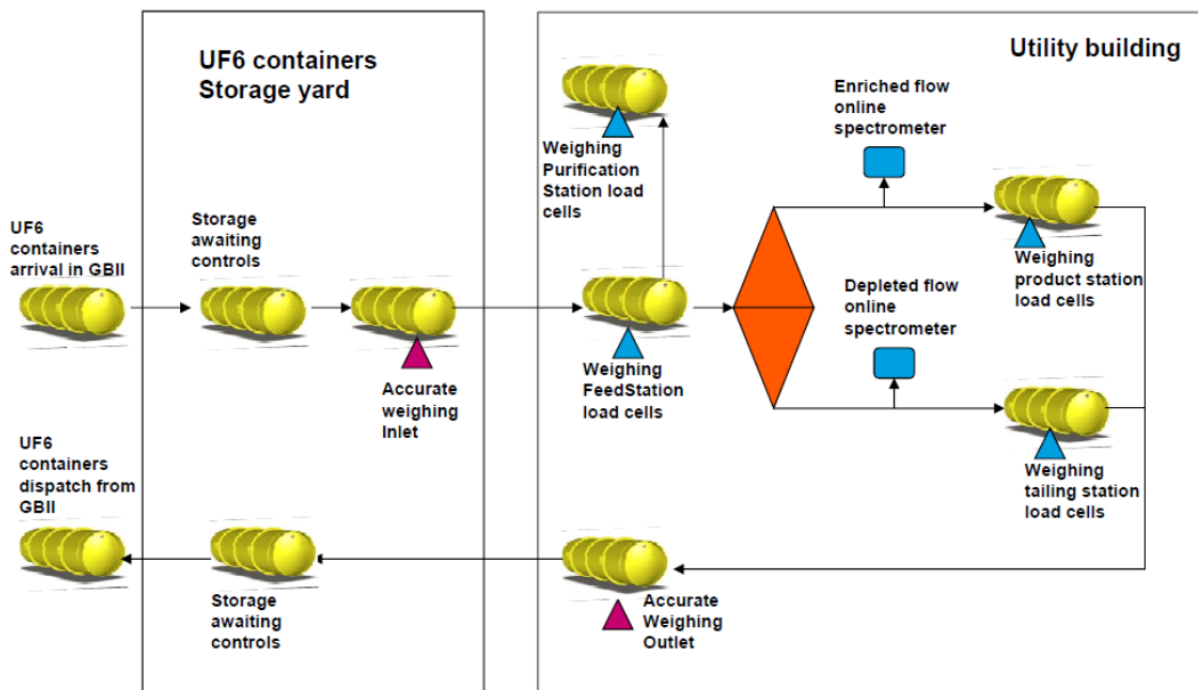


Figure 1

## 2.2. Euratom information system

The aim of the Euratom information system (network) is to bring support to the IAEA and Euratom, for PIV and other safeguards activities, and to reduce the burden on the operator, while respecting non-disclosure requirements of technologically and commercially sensitive information. The Euratom information system is exclusively operated by Euratom, independently from ORANO.

A computer network collects physical tracking data for the operator. In parallel, the Euratom information system collects, practically simultaneously, these data. Inspectors then retrieve, in an on-site dedicated office accessible to them only, the data processed by a specific software developed by the European Commission Joint Research Center of Ispra. This software assists the inspectorates in monitoring the operator's activities through the processing of accurate weighing measurement results. In addition measurements results from mass spectrometers provide data on the U235 enrichment of UF6 from the cascades.

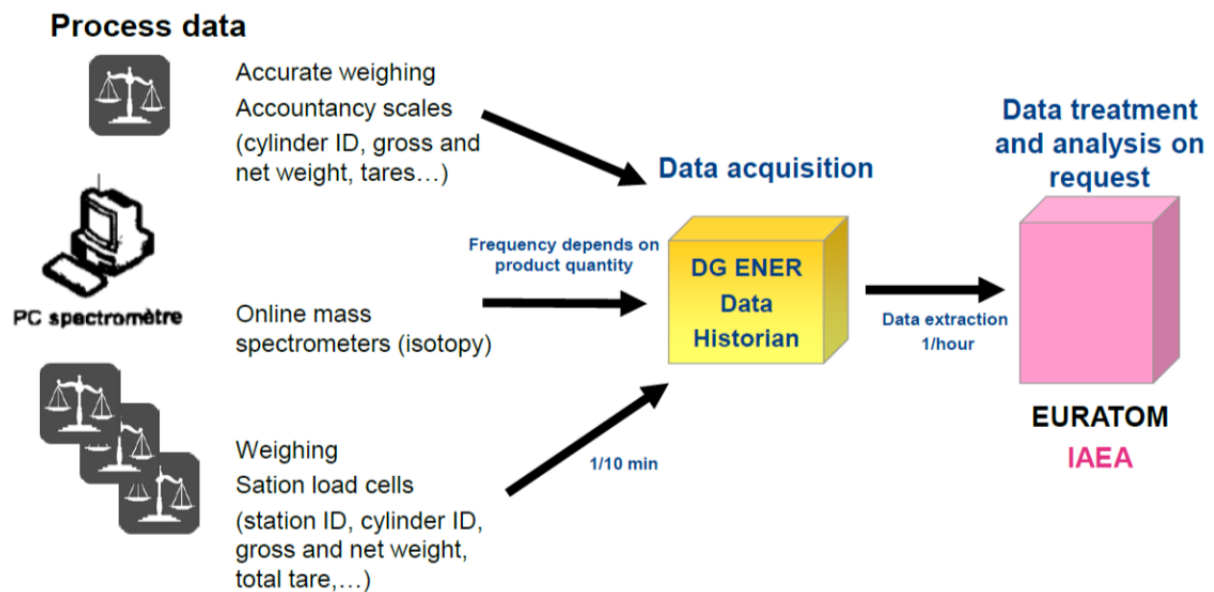


Figure 2

Although the Euratom information system is not used by the inspectorates as an NRTA system, it has all the characteristics necessary for such an application, including the accuracy and the robustness. It could in some way be considered as a pre-NRTA system.

Only data synthesized and elaborated by the software "Inspector Studio" can be transmitted to Euratom and IAEA inspectors. The information remains on site in the inspector's dedicated room with restricted access. French data security policies require this data not be stored more than 5 years. Such data are classified EURA-RESTRICTED (Euratom) or SAFEGUARDS RESTRICTED (IAEA).

## 2.3. Challenges to be overcome

Main challenges were (and remain for some of them):

- Convince the operator of the benefits of the project,
- Assess and reduce the risks, in particular related to cybersecurity, to a level low enough to be considered acceptable,
- Fulfill confidentiality agreements and protect sensitive commercial and technological information,
- Continue to fulfill all existing international and national regulations,
- Get authorization by all relevant French Authorities.

Efforts have to be made at all the stages of the project: to launch it, to get different authorizations, to design it, to implement it and to assure its continuous operation.

A risk assessment was performed in order to minimize and mitigate them.

Main remaining action to get the Euratom information system fully effective is to finalize a Framework agreement for operation of the Euratom network and of its associated software "inspector studio".

The update of the facility attachment has not yet been agreed.

#### **2.4. Main opportunities and benefits already obtained**

Thanks to the Euratom information system, the annual PIV can now be carried out without stopping plant activities for long periods which was previously the case because of the necessity of sealing the feed/withdrawal stations and weighing accurately all the containers (no more plant "switch over"). The burden of such activities would have a negative impact on the production flow. Measured weights in stations during the PIV are authenticated through the monitoring of weight changes collected by the independent Euratom network before and after the PIV. Control of the weighing stations calibration by inspectorates, before the annual PIV, becomes unnecessary.

The verification of the monthly accounting declarations of the containers' masses can be carried out on the basis of precise weighing data, of the monitoring of the weighings in stations, of measurements from mass spectrometers, and of cross-checking between the isotopic contents and declared/calculated masses. The multiple ways of cross-checking data increase the confidence in correctness and completeness of accountancy declarations.

The Euratom information system produces very accurate mass balances for each 500 k SWU module of the plant.

#### **2.5. Additional opportunities and benefits already possible with an update of the safeguards approach**

The network makes it possible to envisage changes in the practices of the current control approach.

All the data transmitted to the inspectorates for the monthly accounting declaration are easily verified thanks to this information system. Moreover, all the physical tracking data used by the operator for its monthly declaration is available in the Euratom network database on site.

Therefore, IAEA and Euratom inspectors could perform a mere computer analysis thanks to this comprehensive system and monthly physical verification would not be necessary anymore. Then partial physical verification of the accounting declaration by sampling (with a few weighing and a few isotopic measurements) may be beneficially replaced by a full and comprehensive verification of mass and assay thanks to the information system.

It would also not be necessary for the operator to keep the incoming and outgoing containers during one month between two routine inspections.

To date, the EURATOM information system is only used during annual PIVs. Taking into account the possibilities offered by computer analysis, its continuous use during monthly inspections should allow greater reliability and greater flexibility for both inspectorates and the operator.

Without any additional modification on site, a monthly verification using Euratom information system would allow an even better effectiveness in the control of the facility. The PIV would be less burdensome, quicker and more reliable. There would be gain for both operator and inspectorates since it would also allow the calculation of a monthly intermediate MUF for each module.

#### **2.6. Additional opportunities and benefits possible after additional modifications**

The European Joint Research Center in ISPRA has suggested an additional modification which would still improve the certification of the measurements and enhance confidence that the plant has been operated as declared.

Two laser scanners forming a double laser curtain (DLC) could be installed at the place where the UF6 cylinders are transferred from the storage yard to the process hall in order to monitor and count the entries and exits of cylinders and to automatically identify their type. In the facility process hall, where the stations are located on both sides, a laser distance sensor could be installed to continuously and accurately monitor the position of the UF6 cylinder conveyor. Combined with the accountancy scale weighing and the station load cell data, the system would also allow making the exact identification of cylinders going from/to the accountancy scales to/from the stations. The monitoring of the position of the UF6 cylinder conveyor in the process hall would also allow controlling that the mass of any cylinder entering or leaving the process hall has been measured by an accountancy scale (reference [2]).

That would still improve the real time monitoring of the material while processed in the GBII facility.

However, these modifications imply use of laser in a nuclear environment, introduction of a new equipment in a nuclear facility and acquisition of new type of data. Therefore it will require additional studies and authorizations from the French authorities for safety, security and safeguards.

### **3. EURATOM INFORMATION SYSTEM IN LA HAGUE REPROCESSING PLANT**

#### **3.1. Euratom verification in La Hague ORANO Plant**

The reprocessing of spent fuel enables the recovery of valuable products such as uranium and plutonium and the volume reduction of highly radioactive waste compared to other solutions.

Given the amount of nuclear material, strict and continuous safeguards activities implemented by international organizations is necessary. IAEA safeguards in La Hague focus on certain areas of the plant, whereas Euratom, in compliance with EC regulation n°302-2005, performs a comprehensive verification of the whole process. The latter requires a large amount of accounting information. This information is subject to verification and confrontation with the reality of measurements and raw data of the operator.

U and Pu contents in process fluids are estimated by precise sampling analyses combined with accurate volume and weight measurements, thus allowing for the verification of the nuclear material inventory with sufficient accuracy.

For verification purposes, Euratom implemented a nuclear material control system in La Hague including measurement, confinement and monitoring devices, as well as a local network system, independent from the operator's network system, in order to collect data from these devices and send them to the inspectors' office located on the La Hague site. These dedicated software systems allow the Euratom inspectors to access and process the data while on site.

Euratom also operates an On Site Laboratory (OSL) to perform physicochemical analysis of samples (U and Pu precise measurements).

#### **3.2. Euratom information system in La Hague**

Two decades ago, advanced nuclear material accountancy techniques, such as Near Real Time Accountancy (NRTA) became the reference for IAEA safeguards in reprocessing plants [1]. The information system in La Hague was initially designed as a full NRTA system and in this respect can be considered as a predecessor of modern NRTA systems. Currently, it is used to perform near real time process monitoring rather than near real time nuclear material accountancy.

Online instrumentation (such as temperature sensors, pressure transducers, etc.), the data acquisition system and the DAI (Data Analysis and Interpretation) software (developed by the European Commission's Joint Research Center in Ispra) are jointly used to accurately determine the volume and density of processed fluids and to ensure the monitoring of their transfer through accountancy tanks all along the process (main flow). These data (volume and density) are stored in the "Historian" database that is processed by the DAI system.

Real time monitoring of tank levels and consistency checking with predefined normal sequences are performed as part of the DAI system's functions. Any inconsistent information or abnormal behaviour will be detected in real time and will result in the activation of a warning or alarm visible in the inspectors' office.

Uranium and plutonium contents are measured in Euratom's OSL, thus allowing for the near real time calculation of the facility's mass balance.

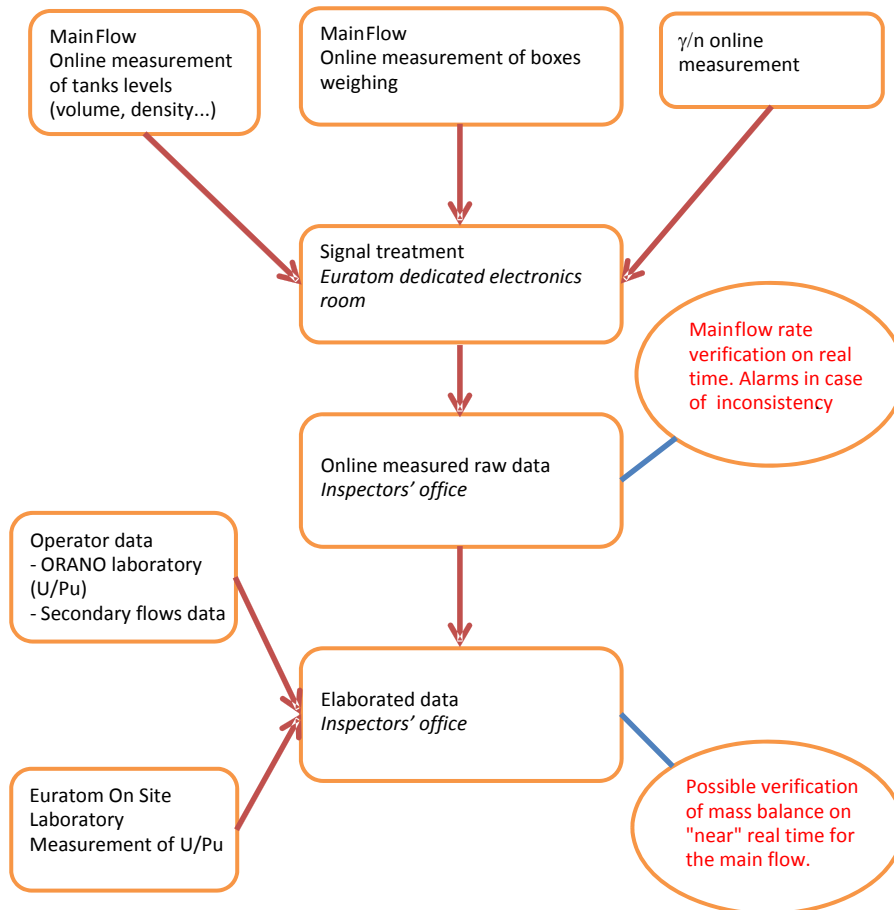


Figure 3

The DAI system can also include other verification data, such as the incremental recording of weight changes as PuO<sub>2</sub> is transferred into cans.

The Euratom information system, in particular the DAI software, has been successfully tested for several years at the La Hague plant.

Euratom network at the La Hague plant is exclusively operated by Euratom, independently from ORANO. However, Euratom has assigned part of the network's maintenance and monitoring to the Projects division of ORANO. In order to provide confidence in the independence of Euratom's activities in relation to the use of its network, all parties signed a framework agreement that clearly defines the different responsibilities of each partner.

In compliance with the current safeguards approach, the Euratom network continuously records data. This data is stored on the Euratom network server and is only accessible to Euratom inspectors when they are on site.

Since Euratom inspectors are in La Hague once per month (for a week), the full benefit of the Euratom information is not drawn, in particular the warning and alarm system. The current plan for

modifying this data analysis approach is described below and should improve the effectiveness of the information system towards the control of the facility.

### 3.3. Euratom Data Transmission project and expected benefits

In order to support and prepare more effectively its inspections, Euratom want to access some data from Luxembourg that are either produced by Euratom measurement devices, processed by Euratom software package, or provided by the operator. To reach this goal, Euratom launched the Remote Data Transmission (RDT) project and entered into discussions with the French authorities and the operator ORANO. This project consists in an upgrade of the existing network and in an addition of a cyphered telecommunication system between Euratom inspectorate offices on site and in Luxembourg.

The local Euratom network is split in two areas:

- A “Real Time” Area that corresponds more or less to the current network (before implementation of the RDT project). It includes all hardware and software allowing for:
  - real time data collection: monitoring, measurement, confinement and surveillance system
  - monitoring, analysis and processing of this data by Euratom inspectors when they are on site.
- A “Delayed Time” Area where “real time” data are placed with a slight time delay, yet allowing for a sufficient reduction in the data’s confidentiality level. Operator declarations and results of laboratory analyses are also sent to this area. This data will be accessible by Euratom inspectors on site and in Luxembourg through the VPN system. As in La Hague, the data can only be accessed in Luxembourg through a separated network, physically isolated from other Euratom networks in a dedicated room. As stated in a specific agreement framework, some data are computed and synthetized in a dedicated review room in La Hague, and sent to the inspectorate offices in Luxembourg.

These two areas are linked by a diode that performs the “push” of “Real Time” Area data to “Delayed Time” Area and introduces the requested delay.

A risk assessment involving French authorities, Euratom and ORANO was performed, leading to the implementation of 59 modifications. In addition to this risk assessment, and to its recommendations and security requirements, French authorities requested a comprehensive security audit in La Hague and in Luxembourg to provide assurances that cyberattacks risks had been correctly assessed and dealt with.

RDT does not imply any changes to the Safeguards Approach. It is currently considered simply as a new mode of transmission of the data.

However, expected benefits are:

- More effective (and efficient) inspections
- Reduction of inspection effort (operator and Euratom). However, this slight gain for the operator shall not be counterbalanced by an increased number of requests/questions from inspectors who may be inclined to clarify data which will be continuously accessible from their headquarters.
- Early detection of malfunctions to avoid re-verifications
- Remote maintenance and adjustments
- Safer data transmission (based on a Sellafield risk analysis)

Eventually this increased inspectorate visibility and confidence may lead to an evolution in the control approach itself and not only in its application.

These RDT systems raise some cybersecurity and confidentiality issues but could effectively complement an NRTA system when inspectorates cannot be continuously present on site.

## **4. CONCLUSION**

These pre-NRTA systems represent great opportunities for the inspectorates and the operator through an increased effectiveness of safeguards. Some immediate benefits are obvious but many parameters should be taken into account, in particular the security and the confidentiality of data.

To allow the deployment of NRTA system deployments among relevant operators, it is important to widen the windows of opportunities allowed by these new systems and to enhance accordingly Safeguards Approaches.

In parallel, some challenges have to be overcome, particularly in terms of data protection and cybersecurity.

## **5. REFERENCES**

[1] LASCAR Forum Report, Large Scale Reprocessing Plant Safeguards, IAEA, STI/PUB/922, Vienna, 1992

[2] Patrice Richir, European commission, JRC Ispra, " Use of Laser Scanners and Laser Distance Sensors to Support Safeguards Activities at Gas Centrifuge Enrichment Plants", SPLG 2017

# **Session 16:**

# **NDA Gamma**

## International testing platform for Uranium & Plutonium gamma-ray isotopic analysis codes: achievements and prospects

P. Funk, AL. Weber

Institut de Radioprotection et de Sûreté Nucléaire (IRSN), France

B. McGinnis<sup>1</sup>, D. Vo<sup>2</sup>, H. Nordquist<sup>2</sup>, J. Dreyer<sup>3</sup>, R. Venkataraman<sup>4</sup>, R. Haddal<sup>5</sup>

<sup>1</sup> Innovative Solutions, LLC, USA

<sup>2</sup> Los Alamos National Laboratory, USA

<sup>3</sup> Lawrence Livermore National Laboratory, USA

<sup>4</sup> Oak Ridge National Laboratory, USA

<sup>5</sup> Sandia National Laboratories, USA

E-mail: anne-laure.weber@irsn.fr

### Abstract:

*A variety of gamma spectrometry systems are routinely used within nuclear fuel cycle facilities by operators and safeguards inspectors to determine the uranium and plutonium isotopic composition needed to support mass verification or to confirm other declared nuclear material attributes. Given concerns expressed by the international community of the need for both code developers and end-users to assess a gamma spectra evaluation codes' applicability, capability, limitations and to ensure their sustainability, members of the International Working Group on Gamma Spectrometry Techniques started to develop a testing platform containing gamma-ray spectra acquired on well-characterized uranium, plutonium and mixed oxide materials. The paper describes the background and utility of this testing platform, which is currently available as an online repository hosted by the European Safeguards Research and Development Association (ESARDA) and details its structure, content, current developments and future evolutions. This project started with the definition of an architecture in three sections: (1) good quality spectra, (2) lower quality spectra acquired under measurement conditions more common in the field, and (3) unusual spectra. Spectra were then collected from the ESARDA Nondestructive Assay (NDA) Working Group (WG) members, the International Atomic Energy Agency (IAEA) and the United States Department of Energy (US-DOE) to populate those sections together with information on sample isotopic composition (reference values) and measurement configuration according to the detector type, electronics settings and nuclear material category (U enrichment, Pu burnup, Pu/U mass ratio). Through bilateral cooperation, IRSN and US-DOE are engaged in the continuing development of high, medium and low-resolution gamma spectra categorization mechanisms and tools according to quality acceptance criteria which have been agreed upon to populate the testing platform sections with the available spectra. Current activities under this collaboration focus on the development of a searchable database structure to facilitate multi-criteria search, the development of metadata display parameters for each spectrum, incorporation of a functionality that supports the download of spectra as return of the query and the definition of mechanisms for spectral contributions.*

**Keywords:** gamma-ray spectra, international database, measurement of plutonium isotopics, measurement of uranium enrichment

### 1. Introduction

A large variety of gamma spectrometry systems are routinely used within nuclear fuel cycle facilities by operators and safeguards inspectors to determine the uranium and plutonium isotopic composition needed to support mass verification or to confirm other declared nuclear material attributes. Given concerns expressed by the international community of the need for both code developers and end-users to assess a gamma spectra evaluation codes' applicability, capability, limitations and to ensure their sustainability, members of the International Working Group on Gamma Spectrometry Techniques (IWG-

GST) that is formally hosted within the ESARDA Non Destructive Assay Working Group, started to develop a testing platform containing gamma-ray spectra acquired on well-characterized uranium, plutonium and mixed oxide materials as a basis to the development of good practice guides and standard test methods [1], [2]. The collection of candidate spectra started in 2010 in Europe, USA and South America. Initial progress was slowed due to a lack of dedicated funding and competing priorities of the various contributors. In order to reactivate collaboration on activities related to the IWG-GST, IRSN and US DOE signed a dedicated action sheet (Action Sheet 6) in 2015 under the *Agreement between the Institut de Radioprotection et de Sûreté Nucléaire for France and the Department of Energy of the United States of America for Cooperation in Research and Development in the Physical Protection of Nuclear Material and Facilities and in Nuclear Material Safeguards Technologies*. The tasks included under Action Sheet 6 focus on developing criteria for selecting good quality spectra, evaluating candidate spectra, adding approved spectra to the database, uploading technical references associated with development and testing of U/Pu isotopics codes on the IWG-GST online repository and developing a searchable database structure. The paper describes the background and utility of this testing platform, which is currently available as an online repository hosted by ESARDA and details its structure, content, achievements under Action Sheet 6 and current developments to evolve towards a multi-criteria searchable database.

## 2. Testing platform structure and utility

The testing platform is devoted to the evaluation of codes used to estimate the isotopic composition of uranium and plutonium for a broad range of hardware configurations, nuclear material types and measurement conditions. This makes it useful for both codes developers and end-users. It also provides powerful training medium to demonstrate code functionality for various types and forms of nuclear materials or measurement situations without physically handling nuclear material. Trainees such as new safeguards practitioners, operators and inspectors, as well as university students can learn and demonstrate their abilities to properly evaluate the uranium or plutonium isotopic composition of a sample from its gamma spectrum with a given analysis code. Such testing platform is useful to qualify a new version of the same code before implementation by comparing the output from the new version to the reference output of the previous version. The spectra may also be used to assess the improvement or at least consistency of the accuracy and precision of both versions when analysing the same set of data.

The architecture of the testing platform, which was defined and agreed to by the IWG-GST members eight years ago [3], contains three sections, which were slightly rearranged according to the spectral contributions received since then.

- Section 1 is dedicated to U, Pu and MOX spectra acquired under normal measurement conditions, qualified as “good quality spectra”. Such a dataset is useful for performance assessment of the accuracy of the codes in their typical ranges of application. Code developers can test newly developed codes or revisions to existing codes to support software quality assurance based on such a dataset. End-users can assess the capabilities of several measurement hardware and software solutions from this dataset and then select the best equipment and analysis code for a given application and/or measurement configuration.

The spectra stored in Section 1 are categorized according to material type (U/Pu/MOX), detector resolution (high resolution / medium resolution / low resolution), detector type (planar / semi-planar / coaxial / portable electrically cooled coaxial or semi-planar / cadmium zinc telluride (CZT) / cadmium telluride (CdTe) / cerium doped lanthanum bromide (LaBr<sub>3</sub>(Ce) / thallium doped sodium iodide (NaI(Tl))), energy range (gain and total number of channels) and isotopic range (depleted uranium (DU) / natural uranium (NU) / low-enriched uranium (LEU) / high-enriched uranium (HEU), plutonium burnup (high / medium / low) and plutonium to uranium ratio for mixed oxide fuel. The current testing platform folder structure detailed for high resolution gamma spectra is shown in figure 1 here after.

- Section 2 is dedicated to U, Pu and MOX spectra that do not meet the criteria to be stored under Section 1. These spectra are typically acquired under measurement conditions that, while not optimal, are common for measurements performed in the field using shorter count times. The dataset provided in this section allows testing of the robustness of the gamma analysis code under harsh or poor measurement conditions that are often encountered by the end-users in the field. It can help the end-user to assess the limitations of a combination of measurement hardware and

software solutions but also can help the developer to improve and validate analysis algorithms to make them more robust to field measurement conditions.

Spectra under this section are further categorised according to measurement anomaly. This currently includes poor counting statistics, poor resolution, count rates that results in excessive deadtime in the electronics or pulse pileup and the presence of strong attenuators between the detector and the sample. Spectra resulting from electronic settings that are not optimal and high background caused by other nuclear material located near the measured item or in a surrounding process would also be of interest for this section.

- Section 3 is dedicated to U, Pu and MOX spectra that are not commonly encountered or are associated with unusual samples. The dataset provided in this section is devoted to the evaluation of the behaviour of the gamma analysis code when expected gamma ray energies are absent in the spectrum or at the extreme ratio of one isotope to another. Once again these spectra can be used to assess the limitations of existing measurement systems but also to develop or revise analysis codes to perform better given the unique type of sample.

Spectra under this section are further categorised according to material type. These materials currently include pure isotopes, nuclear material that is freshly separated and uranium or plutonium contained in inhomogeneous wastes. Spectra resulting from very high burnup plutonium, recycled MOX, aged plutonium with high americium content and nuclear material contaminated with other actinides or fission products would also be of interest for this section.

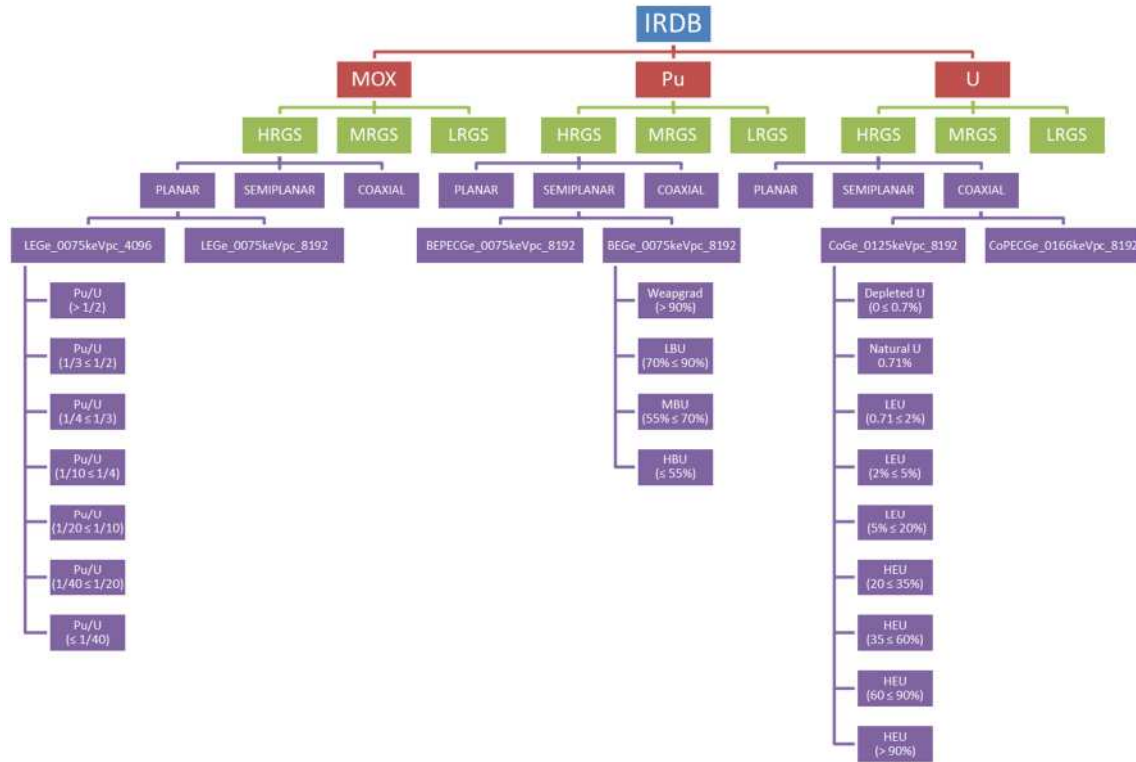


Figure 1: Testing platform folder structure detailed for high resolution gamma spectra

The reference data and measurement configuration associated to each spectrum are currently tabulated in an Excel file which provides, for each spectrum identified by a reference which is also reported in the spectrum file name, the following data:

- uranium isotopic composition and/or plutonium isotopic composition expressed as mass fraction of isotopes 234, 235, 236 and 238 for uranium and 238 to 242 for plutonium and <sup>241</sup>Am, associated uncertainties at 1σ or 2σ (at least characterized by mass spectrometry) and reference date, uranium mass fraction, plutonium mass fraction and U/Pu mass for MOX samples, plutonium isotopic composition updated at the measurement date;
- physicochemical form of uranium and/or plutonium, provider, detector type, analyser type, attenuator material and thickness if any (e.g., Cd filter), matrix in case of U/Pu/MOX in retention, measurement distance, number of channels, energy range, conversion gain, detector resolution

expressed by full width at half the maximum peak height (FWHM) at 185 keV for uranium and 208 keV for plutonium, acquisition date and live time, total number of counts in the spectrum, deadtime and spectrum format;

- Optional supplementary data such as separation date, U/Pu mass and associated optional, certification, detector size and/or model, acquisition electronics, measurement geometry.

### 3. Gamma spectra categorization mechanisms and tools

#### 3.1. Criteria for selecting good quality spectra

The criteria for identifying good quality spectra were developed by a panel of experts with years of experience in developing, testing and using peak ratio based analysis codes [4], [5]. They are defined for different types of semiconductor detectors (germanium, CZT, CdTe) and scintillators (LaBr<sub>3</sub>(Ce) and NaI(Tl)) according to the energy range (low < 307 keV, medium < 600 keV, high up to 1001 keV or 3 MeV) and detailed in [5]. An example is given in table 1 for semi-planar detectors. For high resolution gamma spectrometry, those criteria were drafted considering detector capabilities, gamma spectrometry good practices and typical U and Pu isotopics peak ratio code specifications and/or recommendations. For medium and low resolution gamma spectrometry, good quality spectra criteria were drafted considering their application to confirm or verify the enrichment level for uranium using the enrichment meter method based either on a region of interest approach or response function fitting code in the low energy range, and detector capabilities and gamma spectrometry good practices in the high energy range. Once drafted, the criteria were reviewed by international stakeholders such as ESARDA and Institute of Nuclear Material Management (INMM) members and observers. The IWG-GST co-chairs and experts that have significant experience with gamma analysis codes reviewed international stakeholders' comments and adjusted some of the criteria based on their input.

Energy range	0-600 keV	0-1001 keV	0-1001 keV
Energy calibration slope	0.075 keV/channel	0.075 keV/channel	0.125 keV/channel
Ratio of Full Width Tenth Maximum (FWTM) to Full Width Half Maximum (FWHM)	< 1.95 at a low energy peak > 60 keV (e.g. 129, 186, 208 keV)	< 1.95 at a low energy peak > 60 keV (e.g. 129, 186, 208 keV)	< 1.95 at a low energy peak > 60 keV (e.g. 129, 186, 208 keV)
Analog to Digital Conversion buffer	8192 channels	16384 channels	8192 channels
% Dead Time	<40%	<40%	<40%
Total Counts	>1X10 <sup>6</sup>	>1X10 <sup>6</sup>	>1X10 <sup>6</sup>
Resolution Pu 129 keV	<800 eV	<800 eV	<800 eV
Resolution Pu 662 keV		<1500 eV	<1500 eV
59/[88-104] keV region	0.1 < 59/(88 to 104) < 2.0	0.1 < 59/(88 to 104) < 2.0	0.1 < 59/(88 to 104) < 2.0
Resolution U 186 keV	<1100 eV	<1100 eV	<1100 eV
Resolution U 1001 keV		<2000 eV	<2000 eV
Peak position (channels) 129 keV	1724 +/- 4	1724 +/- 4	1034 +/- 4
Peak position (channels) 662 keV		8832 +/- 8	5300 +/- 8
Peak position (channels) 186 keV	2476 +/- 5	2476 +/- 5	1486 +/- 5
Peak position (channels) 1001 keV		13347 +/- 10	8008 +/- 10

Table 1: Section 1 Criteria for spectra collected using a semi-planar HPGe detector.

### 3.3. Tools for gamma spectra categorization

The spectra collected from the ESARDA and IAEA inter-comparison exercises on high and medium resolution gamma spectrometry techniques for U235 enrichment and/or plutonium isotopic composition measurement, ESARDA members (EC JRC ITU, IRSN) and US National Laboratories (LANL, LLNL) were first categorized according to the characteristics of the measured sample: physicochemical form of the nuclear material, <sup>235</sup>U enrichment in case of uranium, <sup>239</sup>Pu proportion in case of plutonium, Pu/U mass ratio in case of mixed oxide of uranium and plutonium, the type of gamma spectrometry system used to collect the spectrum, and the energy range defined by the amplifier gain and the number of channels of the multi-channel analyzer. They were then converted into a common file format, namely the SPC format. The high resolution gamma spectrometry spectra were automatically analyzed using the AutoISOPLUM [6] in-house software developed by IRSN to extract useful information about the total counts in the spectrum, deadtime, counting rate and counting statistics, FWHM and full width at a tenth of the maximum peak height (FWTM) of gamma lines of interest for quality evaluation purposes. AutoISOPLUM utilizes the region-of-interest (ROI) option of Gammavision [7] to calculate the net peak area of each photopeak, FWHM and FWTM for a spectrum calibrated using a defined energy, and ROI for isolated photopeaks specified by the user. The analysis results were then compared to the criteria previously defined in order to select the spectra to be kept in Section 1. Specific tools were additionally developed to extract information about the filtering of the <sup>241</sup>Am gamma line at 59.54 keV to facilitate easier selection of the plutonium spectra. The criteria and evaluation report will be stored on the European commission's CIRCA-BC ESARDA collaborative platform.

## 4. Testing platform content and Access

### 4.1. Available data

The selection process described above resulted in a set of more than 1700 good quality HPGe spectra (~200 for U, ~100 for Pu and ~ 40 for MOX + additional repetitive measurements), 66 good quality CZT spectra (5 for U and 8 for Pu + additional repetitive measurements) and 65 good quality LaBr3 spectra (5 for U, 8 for Pu + additional repetitive measurements) in the current version of the testing platform. There is a deficit of low resolution gamma spectrometry spectra, but contributors have been identified.

#### 4.1.1. Uranium good quality spectra

The following configurations are available in the high energy range:

- Spectra acquired with coaxial germanium detectors in the range [0-1024] keV (0.125 keV/channel on 8192 channels). In such configuration, at least one spectrum is available in each uranium 235 enrichment subcategory from depleted to high enriched uranium below 90%. Spectra from repetitive measurements acquired on the same sample are also provided for some enrichment subcategories.
- Spectra acquired with portable electrically cooled coaxial germanium detectors in the range [0-3] MeV (0.366 keV/channel on 8192 channels). In such configuration, at least one spectrum is available in each uranium 235 enrichment subcategory from depleted to high enriched uranium. Spectra from repetitive measurements acquired on the same sample are also provided for some enrichment subcategories.
- Spectra acquired with a coaxial Safeguards germanium detector in the range [0-1200] keV (0.075 keV/channel on 16384 channels). In such configuration, at least one spectrum is available in each uranium 235 enrichment subcategory from low enriched to high enriched uranium except the enrichment range 30-35%. Spectra from repetitive measurements acquired on the same sample are also provided for some enrichment subcategories.
- Spectra acquired with a CZT 500 mm<sup>3</sup> hemispherical detector in the range [0-1394] keV (0.34 keV/channel on 4096 channels). In such configuration, at least one spectrum is available in each uranium 235 enrichment subcategory from depleted uranium to low enriched uranium up to 5%. Spectra from repetitive measurements acquired on the same sample are also provided.
- Spectra acquired with a LaBr<sub>3</sub>:Ce 2" x 0.5" detector in the range [0-2800] keV (0.68 keV/channel on 4096 channels). In such configuration, at least one spectrum is available in each uranium 235 enrichment subcategory from depleted uranium to low enriched uranium up to 5%. Spectra from repetitive measurements acquired on the same sample are also provided.

The following configurations are available in the low and medium energy range:

- Spectra acquired with planar germanium detectors in the range [0-307] keV (0.075 keV/channel on 4096 channels). In such configuration, at least one spectrum is available in each uranium 235 enrichment subcategory from depleted to high enriched uranium. Spectra from repetitive measurements acquired on the same sample are also provided for some enrichment subcategories.
- Spectra acquired with planar germanium detectors in the range [0-1229] keV (0.075 keV/channel on 16384 channels). In such configuration, 2 spectra collected on different samples are provided in the U enrichment range [LEU 5-20%] and [HEU 60-90%]. Spectra from repetitive measurements acquired on those 2 samples are also provided.
- Spectra acquired with portable semi-planar germanium detectors in the range [0-614] keV (0.075 keV/channel on 8192 channels). In such configuration, at least one spectrum is available in each uranium 235 enrichment subcategory from depleted to high enriched uranium, except for the categories LEU [0.7-2%] and HEU [20-35%]. Spectra from repetitive measurements acquired on the same sample are also provided for some enrichment subcategories.

#### 4.1.2. Plutonium good quality spectra

The following configurations are available in the high energy range:

- Spectra acquired with coaxial germanium detectors in the range [0-1024] keV (0.125 keV/channel on 8192 channels, "CoGe\_0125keVpc\_8192" block in figure1). In such configuration, at least one spectrum is available in each plutonium burnup subcategory from very low to medium burnup plutonium. Spectra from repetitive measurements acquired on the same sample are also provided for some plutonium burnup subcategories.
- Spectra acquired with coaxial germanium detector in the range [0-614] keV (0.075 keV/channel on 8192 channels, "CoGe\_0075keVpc\_8192" block in figure1). In such configuration, at least one spectrum is available in plutonium medium burnup and very low burnup subcategories. Spectra from repetitive measurements acquired on the same sample are also provided for some burnup subcategories.
- Spectra acquired with coaxial Safeguards germanium detector in the range [0-1200] keV (0.075 keV/channel on 16384 channels, "SGDGe\_0075keVpc\_16384" block in figure1). In such configuration, several spectra collected on different samples are available in plutonium low and medium burnup subcategories. Spectra from repetitive measurements acquired on the same sample are also provided for some burnup subcategories.
- Spectra acquired with portable electrically cooled coaxial germanium detector in the range [0-3] MeV (0.366 keV/channel on 8192 channels, "CoPECGe\_0366keVpc\_8192" block in figure1) on a very low burnup sample.
- Spectra acquired with a CZT 500 mm<sup>3</sup> hemispherical detector in the range [0-1394] keV (0.34 keV/channel on 4096 channels). In such configuration, one spectrum is available in each plutonium burnup subcategory from very low to high burnup. Spectra from repetitive measurements acquired on the same sample are also provided.
- Spectra acquired with a LaBr<sub>3</sub>:Ce 2"x0.5" detector in the range [0-2800] keV (0.68 keV/channel on 4096 channels). In such configuration, one spectrum is available in each plutonium burnup subcategory from very low to high burnup. Spectra from repetitive measurements acquired on the same sample are also provided.

The following configurations are available in the low and medium energy range:

- Spectra acquired with planar detectors in the range [0-307] keV (0.075 keV/channel on 4096 channels). In such configuration, several spectra from different samples are available in the plutonium low burnup subcategory.
- Spectra acquired with planar detectors in the range [0-614] keV (0.075 keV/channel on 8192 channels). In such configuration, at least one spectrum is available in each plutonium burnup subcategory from very low to medium burnup plutonium. Spectra from repetitive measurements acquired on the same sample are also provided for some enrichment subcategories.
- Spectra acquired with semi-planar germanium detectors in the range [0-614] keV (0.075 keV/channel on 8192 channels). In such configuration, several spectra from the same medium burnup plutonium sample are available.

- Spectra acquired with semi-planar germanium detectors in the range [0-1024] keV (0.125 keV/channel on 8192 channels). In such configuration, several spectra from different low and very low burnup plutonium samples are available.
- Spectra acquired with portable semi-planar germanium detectors in the range [0-614] keV (0.075 keV/channel on 8192 channels). In such configuration, spectra from several medium burnup plutonium samples are available. Spectra from repetitive measurements acquired on the same sample are also provided.

#### 4.1.3. MOX good quality spectra

The following configuration is available in the high energy range:

- Spectra acquired with coaxial germanium detectors in the range [0-1024] keV (0.125 keV/channel on 8192 channels). In such configuration, at least one spectrum is available in each MOX Pu/U ratio subcategory from 1/20 to higher than 1/2.

The following configurations are available in the low and medium energy range:

- Spectra acquired with planar detectors in the range [0-307] keV (0.075 keV/channel on 4096 channels). In such configuration, two spectra are available for a sample with  $Pu/U > 1/2$  and  $1/10 < Pu/U < 1/4$ .
- Spectra acquired with planar detectors in the range [0-614] keV (0.075 keV/channel on 8192 channels). In such configuration, at least one spectrum is available in each Pu/U ratio subcategory from 1/40 to higher than 1/2. Spectra from repetitive measurements acquired on the same sample are also provided for some enrichment subcategories.

Such a selection also identified existing gaps in the different material and instrumentation categories such as high burnup plutonium.

Currently, section 2 contains ~700 spectra which were rejected from section 1 selection due to poor counting statistics, poor resolution, or count rates that result in excessive deadtime in the electronics or pulse pileup, and a few additional spectra acquired in presence of strong attenuators between the detector and the sample.

Currently, section 3 still needs to be populated as it only contains a few spectra acquired on fresh uranium, pure  $^{239}Pu$ , pure  $^{240}Pu$  material and some inhomogeneous U and Pu wastes.

## 4.2. Access

The testing platform can currently be accessed upon registration through the European commission's CIRCABC ESARDA collaborative platform. A user's guide was prepared by Oak Ridge National Laboratory (ORNL) and will be made available after the searchable database is finalized.

## 5. Searchable database development for uploading and downloading spectra

Current activities under IRSN and US-DOE collaboration focus on the development of a searchable database structure to facilitate multi-criteria search, the development of metadata display parameters for each spectrum, functionality that supports the download of spectra as return of the query and the definition of mechanisms for spectral contributions.

The software will use standard SQL queries to access the records in a relational database. Calls to this database will be used to filter and download data. The software will allow the user to filter the records based on metadata as defined in sample form presented in figure 2 below, and to combine filter criteria. The software will provide the user the ability to download one or more spectra in SPE format.

Enter your spectra search criteria below, then hit the search button for matching spectra.

Spectra Section  Nuclear Material Type  If MOX, Pu/U Ratio

Composition and Isotopics

Isotope  Enrichment % Range  to

Isotopics:

Pu isotopic composition:  
 Enrichment % Range  
 Pu238  to  %  
 Pu239  to  %  
 Pu240  to  %  
 Pu241  to  %  
 Pu242  to  %  
 Am241  to  %

U isotopic composition:  
 Enrichment % Range  
 U234  to  %  
 U235  to  %  
 U236  to  %  
 U238  to  %

Detector Type

Detector Electronics

Material form

Chemical Composition

Sample mass range  to  g

Attenuators:

Thickness range:  
 1.  to  mm  
 2.  to  mm  
 3.  to  mm

Material:

Container Type

Sample measurement time range  to  seconds

Deadtime range  to  %

Counting statistics range  to  counts

Has Certificate of Analysis

Figure 2: sample form for searching spectra

Regarding spectral contributions, the initial request was to provide spectra in their original format and possibly in ASCII format. The IWG-GST requested that contributors provide instrument and geometrical setup parameters and nuclear material reference values for spectra using an agreed upon template, which is proposed to be replaced by a PDF fillable format in order to make it compatible with a searchable database and to allow the attachment of certificates, detector specification and/or photos of the measurement configuration in addition to the provided spectra [4]. The form developed by Lawrence Livermore National Laboratory (LLNL) is presented in figure 3.

**Spectrum Submission Form**  
 International Working Group on Gamma Spectrometry Techniques For U And Pu Isotopics

Contributor Name \_\_\_\_\_  
 Organization \_\_\_\_\_  
 Contact Information \_\_\_\_\_  
 Address \_\_\_\_\_  
 Email \_\_\_\_\_  
 Attribute contribution to organization?

**3) OPTIONAL SUPPLEMENTARY DATA**  
 Separation date \_\_\_\_\_  
 Certificate Available

	Reference Value	Sigma
U mass (g)	_____	_____
U content	_____	_____
Pu mass (g)	_____	_____
Pu content	_____	_____

**1) SAMPLE COMPOSITION**  
 Click to Attach Spectrum  
 Note: Equivalent measurements of the same sample can be attached to this form.  
 Contains: Uranium  Plutonium

**Uranium**

Isotope	Percent Mass
<sup>234</sup> U	_____
<sup>235</sup> U	_____
<sup>236</sup> U	_____
<sup>238</sup> U	_____
U Mass (g)	_____

**Plutonium**

Isotope	Percent Mass
<sup>238</sup> Pu	_____
<sup>239</sup> Pu	_____
<sup>240</sup> Pu	_____
<sup>241</sup> Pu	_____
<sup>242</sup> Pu	_____
<sup>241</sup> Am	_____
Pu Mass (g)	_____

**2) MEASUREMENT CONFIGURATION**  
 Acquisition Date \_\_\_\_\_  
 Material (check all that apply)  
 Metal  Powder  Solution  
 Oxide  Other \_\_\_\_\_  
 Measurement Geometry  
 Source-Detector Distance (cm) \_\_\_\_\_  
 Attenuators \_\_\_\_\_  
 Cu thickness (cm) \_\_\_\_\_  
 Cd thickness (cm) \_\_\_\_\_  
 Other (material, thickness) \_\_\_\_\_  
 Detector Information  
 HPGE  NaI  LaBr  
 CZT  Other \_\_\_\_\_  
 Model \_\_\_\_\_  
 Detector dimensions (cm) \_\_\_\_\_  
 Readout electronics \_\_\_\_\_  
 Additional Information  
 Click to Attach Detector Specifications  
 Click to Attach Photographs of Measurement Configuration

**4) CERTIFICATE**  
 Click to Attach Source Certificates

**Uranium Certificate**

Reference Date	U Mass (g)	Percent Mass Reference Values	$\sigma$
_____	_____	_____	_____
<sup>234</sup> U	_____	_____	_____
<sup>235</sup> U	_____	_____	_____
<sup>236</sup> U	_____	_____	_____
<sup>238</sup> U	_____	_____	_____
Standard deviation of uncertainties			

**Plutonium Certificate**

Reference Date	Pu Mass (g)	Percent Mass Reference Values	$\sigma$
_____	_____	_____	_____
<sup>238</sup> Pu	_____	_____	_____
<sup>239</sup> Pu	_____	_____	_____
<sup>240</sup> Pu	_____	_____	_____
<sup>241</sup> Pu	_____	_____	_____
<sup>242</sup> Pu	_____	_____	_____
<sup>241</sup> Am	_____	_____	_____
Standard deviation of uncertainties			

**MOX Certificate**

Reference Date	U+Pu Mass (g)	Percent Mass Reference Values	$\sigma$
_____	_____	_____	_____
U (g)	_____	_____	_____
Pu (g)	_____	_____	_____
U/Pu	_____	_____	_____
<sup>234</sup> U	_____	_____	_____
<sup>235</sup> U	_____	_____	_____
<sup>236</sup> U	_____	_____	_____
<sup>238</sup> U	_____	_____	_____
<sup>238</sup> Pu	_____	_____	_____
<sup>239</sup> Pu	_____	_____	_____
<sup>240</sup> Pu	_____	_____	_____
<sup>241</sup> Pu	_____	_____	_____
<sup>242</sup> Pu	_____	_____	_____
<sup>241</sup> Am	_____	_____	_____
Standard deviation of uncertainties			

Figure 3: sample form for searching spectra

Users may submit spectra for consideration using a web submission page, experts should verify newly added spectra to check that they are properly sorted into the appropriate category and only experts may add spectra and their associated metadata to the database at a frequency to be adjusted (once or twice a year for instance).

## 6. Conclusion

Through bilateral cooperation, IRSN and US DOE are engaged in the continuing development of a reference database of U, Pu and MOX spectra accepted by the international safeguards community to test and validate gamma-ray analysis codes for uranium enrichment or uranium and plutonium isotopic composition determination, started under the auspices of the International Working Group on Gamma Spectrometry Techniques (IWG-GST). Mechanisms to select good quality high, medium and low resolution spectra were developed and reviewed by international stakeholders. A software routine called AutoISOPLUM was developed by IRSN to evaluate candidate spectra to be included in the testing

platform section dedicated to good quality spectra for code evaluation in their typical range of application. The testing platform resulting from this evaluation is currently hosted by the European commission's CIRCABC ESARDA collaborative platform and contains more than 1700 spectra, covering a broad range of hardware configurations, nuclear material types and measurement conditions. Specifications have been defined by LANL and LLNL to develop a searchable database structure to facilitate multi-criteria search, the development of metadata display parameters for each spectrum, functionality that supports the download of spectra as return of the query and mechanisms for spectral contributions. A user's guide was prepared by Oak Ridge National Laboratory (ORNL) and will be made available after the searchable database is finalized.

Such database is intended for both code developers and end-users of isotopic analysis codes such as safeguards inspectorates, facility operators or university students. Uranium, plutonium and MOX spectra are categorized into three sections: Section 1 - good quality spectra to be used for code evaluation in their typical range of application, Section 2 - lower quality spectra to be used to test the robustness of the various gamma spectrometry analysis codes against harsh measurement conditions in the field, and Section 3 - unusual spectra to be used for code evaluation outside their typical range of application. Thus code developers can test newly developed codes or revisions to existing codes to support software quality assurance based on such dataset. End-users can assess the capabilities of several measurement hardware and software solutions from this dataset and then select the best equipment and analysis code for a given measurement situation. This dataset also provides training media to demonstrate code functionality for a range of equipment or measurement situations without the need to handle nuclear material.

## 8. References

- [1] WEBER, A.L., FUNK, P., MCGINNIS, B, VO, D., WANG, T.F., BERLIZOV, A, PEERANI, P., ZSIGRAI, J "The need to support and maintain legacy software: ensuring ongoing support for the isotopics codes", IAEA Safeguards symposium, November 2014
- [2] PEERANI, P., MCGINNIS, B, "Working group on gamma spectrometry technique for U/Pu isotopics, terms of reference", ESARDA Bulletin n°38, June 2008
- [2] KOSKELO, M.J., MCGINNIS, B., PEERANI, P. et al, "Sustainability of gamma-ray isotopic evaluation codes", 51th INMM Meeting, July 2010
- [4] MCGINNIS, B., DREYER, J, FUNK, P., HADDAL, R., VO, D., WEBER, A.L., WORRALL, L, VENKATARAMAN, R., INMM Meeting, Baltimore, July 2018
- [5] WEBER, A.L., FUNK, P., MCGINNIS, B, VO, D., DREYER, J., VENKATARAMAN, R, WORRALL, L., HADDAL, R "International database of gamma-ray spectra for uranium and plutonium isotopic analysis", IAEA Safeguards symposium, November 2018
- [6] DUFOUR, J.L. "AUTOISO\_PLUM user's manual", IRSN PDS-DEND/SATE/2011-0680
- [7] <https://www.ortec-online.com/products/application-software/gammavision>

# Application of Delayed Gamma-Ray Spectrometry in Nuclear Safeguards and Non-Proliferation

**K. Abbas<sup>1</sup>, D.C. Rodriguez<sup>2</sup>, J.M. Crochemore<sup>1</sup>, F. Rossi<sup>2</sup>, T. Bogucarska<sup>1</sup>, T. Takahashi<sup>2</sup>, B. Pedersen<sup>1</sup>, M. Seya<sup>2</sup>, S. Nonneman<sup>1</sup> and M. Koizumi<sup>2</sup>**

<sup>1</sup> European Commission, Joint Research Centre, Directorate for Nuclear Safety and Security, Nuclear Security Unit, Via Enrico Fermi 2749, 21027 Ispra (VA), Italy

<sup>2</sup> Integrated Support Center for Nuclear Security and Nuclear Non-proliferation, Japan Atomic Energy Agency, Shirakata Shirane 2-4, Tokai, Naka, Ibaraki, Japan

Kamel.abbas@ec.europa.eu

## Abstract

EC JRC is the science and technology advise provider to the EU policy makers. Its work has a direct impact on the lives of citizens by contributing with its research outcomes to a healthy and safe environment, secure energy supplies, sustainable mobility and consumer health and safety. To do so, EC JRC hosts specialized laboratories and unique research facilities, which are home to thousands of scientists.

New instruments and methods for analysis and characterization of nuclear material are continuously needed to face new challenges of an efficient and an effective nuclear safeguards and non-proliferation. Non-destructive assay (NDA) is among the most important mean for safeguards inspectors verify state system of accounting for and control on nuclear material. In this regard, the Integrated Support Center for Nuclear Security and Nuclear Non-proliferation of the Japan Atomic Energy Agency (ISCN JAEA) and the Nuclear Security Unit of the Joint Research Centre of the European Commission (EC JRC) established a multiannual collaboration on a development of an innovative NDA technique base of delayed gamma ray spectrometry (DGS) for characterization on material containing nuclear material such as spent fuel. This technique aims at filling the gap where existing techniques showed limitations. DGS is based on the detection of relatively short-lived fission products. Fissions in an analyzed sample are induced by an external neutron source and the detection of those FPs is carried out with by high-energy resolution gamma-ray spectrometry although medium energy configuration is envisaged.

After successful experimentation with this technique, carried out with the PUNITA D-T neutron generator, and in view of further fine-tuning of the technique for applicability to nuclear safeguards, new Monte Carlo model-based theoretical simulations are being developed. Intensive experiments were continued with an experimental set-up and with a slightly modified ISCN JAEA DGS system operated in JRC PERLA laboratory (Ispra, Italy). This paper reports the performance of the technique and the results of the last measurement campaigns.

**Keywords:** Nuclear Material Assay Delayed Gamma-ray Spectrometry, DGS, Safeguards

## 1. Introduction

EC JRC is the science and technology advise provider to the EU policy makers. Its work has a direct impact on the lives of citizens by contributing with its research outcomes to a healthy and safe environment, secure energy supplies, sustainable mobility and consumer health and safety. To do so, EC JRC hosts specialized laboratories and unique research facilities, which are home to thousands of scientists.

EC JRC collaborates with over a thousand organizations worldwide whose scientists have access to many JRC facilities through various agreements and arrangements. In this context, the Japan Atomic Energy Agency (JAEA) and EC JRC continue their long standing collaborative work in both R&D and Training in nuclear safeguards and security. This collaboration is structured in different fields and projects (Action Sheets). The Action Sheet -7 (started on 2015) is dedicated to the development of active neutron NDA techniques by further investigating different neutron interrogation techniques such as Differential Dye Away Analysis (DDA), Prompt Gamma-ray Analysis (PGA), Delayed Gamma Spectrometry analysis (DGS) and Neutron Resonance Transmission analysis (NRTA) for the characterization nuclear material. Two JRC sites are involved in this collaboration, which are Ispra (Italy) and Geel (Belgium).

In this regard, the Integrated Support Center for Nuclear Security and Nuclear Non-proliferation of the Japan Atomic Energy Agency (ISCN JAEA) and the Nuclear Security Unit of the Joint Research Centre of the European Commission (EC JRC) established a multiannual collaboration on a development of an innovative NDA technique based on DGS for characterization of material containing nuclear material such as spent fuel.

DGS is based on measurements of gamma-ray spectra of relatively short-lived fission products (FPs) in the analyzed NM sample specially in the high energy gamma range. In fact, low energy gamma-rays peaks of FPs of interest would not be resolved above the high background in that low energy range. Therefore, the utilization of high energy gamma spectrometry is an advantage from the perspective of negligible self-shielding that could occur in case of gamma-ray of low energy traveling in high absorbing material such as NM in spent fuel samples [1, 2]

The aim of this work is not only the development of a new NDA technique and validation of a MC model but also to gather new nuclear data in particular, those at high gamma energy, in the range greater than 3 MeV.

After promising experimentation of this technique, with PUNITA D-T neutron generator to induce fissions and in view of further fine-tuning of the technique for its applicability to nuclear safeguards, new Monte Carlo model-based theoretical simulations were developed. Intensive experiments are currently being performed using an JAEA DGS experimental system installed in JRC PERLA laboratory at Ispra (Italy). This paper presents updated results on the experimentation of DGS in PERLA laboratory using  $^{252}\text{Cf}$  sources including results from the upgraded JAEA DGS system.

## 2. The DGS experimental Set-up

The JAEA DGS experimental set-up is already reported in previous communications. It is being tested in PERLA Laboratory of JRC Ispra [6]. The main objective of this work is to study the applicability of DGS technique in safeguards verification of very active nuclear material such as solutions of dissolved spent nuclear fuel. The established conventional NDA techniques for low activity samples cannot be applied for very active material due to the high gamma background in the energy range 50 keV - 3 MeV. To overcome the issue of high gamma radiation background, DGS was proposed as an alternative NDA technique to utilise the high energy gamma range (above 3 MeV). DGS allows in principle qualitative and quantification characterisation of nuclear material thanks to an external neutron interrogation of the sample.

Presently verifications of contents of some nuclides in spent fuel solution such as  $^{239}\text{Pu}$ ,  $^{241}\text{Pu}$  and  $^{235}\text{U}$ , safeguards inspectors mostly rely on the very time consuming destructive assay methods (DA). DGS aims at replacing some of DA methods therefore would reduce safeguards verification at reprocessing plants.

DGS is based on analysis of selected FPs via high-energy resolution gamma-ray spectrometry analysis [5-9] in the high energy gamma spectrum. In fact DGS aims at analysing fissile material such as  $^{235}\text{U}$ ,  $^{239}\text{Pu}$ , ... through the detection of fission products (FP) induced by an external neutron source.

The external neutron source must be chosen properly to ensure high yields of desired FPs meaning with suitable neutron spectrum and flux considering the fact that fissile nuclides such as  $^{239}\text{Pu}$ ,  $^{241}\text{Pu}$  and  $^{235}\text{U}$ , yields the same FPs but fortunately with different yields.

A development of an effective DGS analysis system requires at least three important considerations, which are the efficient neutron irradiator, the analysis protocol and the acquisition of gamma-ray spectra of the neutron interrogated samples including analysis of those spectra:

### - The neutron irradiator

The neutron irradiator is composed by a neutron source, an irradiation chamber and a shielding system. The neutron source inducing fission in the analysed sample should be chosen properly. Its neutron spectrum and flux should be well known in order to design an efficient irradiation chamber with suitable material and dimensions for neutron moderation, reflexion and buffering including the shielding of the whole apparatus to prevent operators against neutron and gamma radiations. The irradiation chamber should be designed in a such way to ensure high fission yields consequently to lower the minimum detection limits of FP of interest.

In this regard, the modelling is playing an important role in each of the step for the development of a such system.

### **- The analysis protocol**

The meaning of analysis protocol in here is the list of steps to be carried out in a DGS analysis. It starts with a neutron interrogation of the sample in the irradiation chamber, then its transfer for gamma spectrum acquisition and analysis. As mentioned earlier, the gamma energy range of interest for DGS begins at high energy (> 3 MeV). An acquisition of a gamma spectrum with enough statistic in that high energy range may not be reached in a single neutron irradiation - gamma acquisition. This is due mainly to relatively low efficient of high energy resolution available detectors. In order to overcome this issue of acquire a workable a high energy resolution gamma spectrum in high energy range, the spectrum is acquired in a loop of neutron irradiation and gamma acquisition until the necessary statistic of the gamma spectrum is reached for a quantitative determination of the yielded FPs in the analysed sample. When possible, the analysis protocol should start with the preselection of FPs of interest by considering mainly their half-lives, fission yields and theirs high gamma-ray lines to focus on in the analysis. Knowing in advance the FPs of interest would help define of the different times of the analysis meaning the neutron irradiation time, the transfer/decay time, the gamma acquisition time etc considering also that FPs on interest here are relatively short lived.

### **- The delayed gamma spectrum acquisition and analysis**

As mentioned above the gamma-ray spectrum of the neutron irradiated sample should be a acquired with high-energy resolution detector. This allows the identifications of the FPs produced. The detection efficiency of such detectors should be as high as possible. HPGe detectors fulfil these requirements of high energy resolution and efficiency. It important to underline that the gamma background should be as low as possible. In regard, the shielding of the gamma detector including the sample holder and the in The gamma background should be efficient in the high gamma energy.

## **3. The main features of the JAEA DGS system being tested in PERLA laboratory**

All the requirements mentioned in the previous chapter were considered in the development of the JAEA DGS system, which is under testing in JRC Ispra [3, 4, 5]. The system utilizes a  $^{252}\text{Cf}$  sealed source as a neutron source (average energy ~ 2.5 MeV maxi 10 MeV) compared to the D-T generator used in PUNITA (~14.1 MeV). This is the new feature with respect to the research work carried out in this collaboration framework (JAEA-JRC) on DGS in PUNITA facility in Ispra. The moderation of the  $^{252}\text{Cf}$  fission neutrons would require less moderation material with respect to the D-T 14 MeV neutrons. Moreover, in the case of analysis of  $^{235}\text{U}$  in uranium-bearing samples, it's more likely that fissions occur in  $^{235}\text{U}$  than in  $^{238}\text{U}$  with  $^{252}\text{Cf}$  irradiation (neutron energy threshold for fission of  $^{238}\text{U}$  is above 1 MeV). Figure 1. shows a picture of the original JAEA DGS system, which is installed and tested in PERLA laboratory. Preliminary tests were made to investigate the good operation of the system from the view point of software and hardware. The main components of the system are the neutron source transfer feature, the irradiation cavity, the high energy resolution gamma detector including the complex electronic chain for the monitoring of the whole DGS system. The gamma detector is a HPGe planar type of 50% absolute efficiency.

The NM samples used in the testing of the system are uranium of hundreds of grams total U with enrichment varying from depleted to 4.5%. Prior to the testing the JAEA DGS system, some preliminary

experiments were carried as a simple proof of the technique as regards efficient fission yields induced by a  $^{252}\text{Cf}$  sources and the observation of resolved gamma-rays from a neutron irradiated sample.

#### 4. Results and discussions

This paper presents some findings from the experimentation of the JAEA DGS system, which was tested with two  $^{252}\text{Cf}$  sources, first with 10 then with 50 MBq nominal. These capsule source were purchased from Eckert & Ziegler (Germany).

Several analysis protocol were selected for the experimentation of the DGS System. For the neutron irradiation time, 3 to 10 mins time range was experienced. Regarding the gamma spectrum acquisition, the same time range was used. A test on NM sample was accomplished in several loops. As indicated above, a loop includes neutron irradiation, decay time (to let decay the very short lived FPs), gamma acquisition time and again decay time. An over whole time for a gamma spectrum acquisition did not exceed 30 mins.

The tests performed with 10 MBq revealed limited evidence of presence of FPs in the irradiated sample as almost no gamma peaks could be seen above a background continuum. This fact could be due to several reasons such as:

- Little or no fissions were induced in the sample. This could be attributed to a low activity of the  $^{252}\text{Cf}$  source, to a low fission yields or to a design of the irradiation chamber.
- The detection efficiency is low or the gamma background is so high that it masked FP gamma peaks in the high energy range. To overcome this issue, the gamma acquisition chamber must be efficiently shielded.

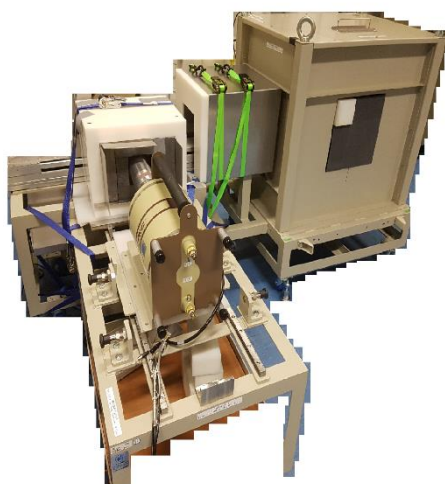


Figure 1: View of the upgraded JAEA DGS system being tested in PERLA. The  $^{252}\text{Cf}$  irradiator is on the right-hand while the gamma-ray acquisition is visible with the HPGe detector.

Tests of the DGS system with 50 MBq was also carried out and it resulted on an increased count rate of the gamma acquisition however without a significant improvement regarding the identification of resolved gamma peaks of FPs in the region of interest. Further MC calculations revealed that the gamma detection geometry and of the positioning of the  $^{252}\text{Cf}$  source in the system could be improved. In the original design, the NM sample for analysis is fixed while the neutron source is shuttled from its home position to the irradiation position. The gamma acquisition starts only when the  $^{252}\text{Cf}$  source is in home position. In this case the NM sample and the HPGe are fixed. After that a modification of the System was undertaken with the emphasis of the improvement of the gamma shielding the HPGe crystal against gamma as well as further shielding of the neutron source to avoid neutron escape that may contribute while in home position with additional cadmium layers. All these requirements, conducted to a modified DGS system where in this case the neutron source is fixed while the sample for analysis is shuttled

between the sample loading position to the neutron irradiation position. The JAEA DGS System is being modified to include further improvements.

In the margin of the modification of the original DGS system, a stand-alone neutron irradiator was built to verify optimum irradiations and a relocatable gamma-ray spectrometry acquisition station was set to anticipate best detection geometry.

The irradiator is based on a  $^{252}\text{Cf}$  capsule surrounded by around 15 cm polyethylene, making so an irradiation chamber of 10 x 10 x 20 high cm<sup>3</sup>. A sample is put at 1 cm thickness of polyethylene from the  $^{252}\text{Cf}$  source capsule in the irradiation chamber.

Figure 2 show a side and top ruff views of the stand-alone irradiator. The portable gamma acquisition station is based of HPGe portable gamma-ray of 50% efficiency.



Figure 2: Side (right) and top (right) view of the stand-alone neutron irradiator used preliminary tests in PERLA Laboratory

As gamma background measurements all around the original DGS system revealed that its gamma-ray acquisition station is sensitive to the relatively high measured gamma background, the built stand-alone irradiator and the gamma station were positioned 10 m away one from the other. This distance between allowed successful acquisitions of gamma spectra with well resolved high energy gamma-ray peaks of FPs. In fact, at such a distance, the gamma station was successfully operated without any shielding of the HPGe Crystal.

Several sample interrogations (neutron irradiation followed by gamma acquisition) were successfully performed using low enriched uranium samples. These tests were performed in many loops by manually putting samples for neutron irradiations and transferring them to the gamma acquisition station to accumulate a satisfactory gamma spectrum where FP gamma-rays peaks are resolved and grown to be quantified.  $^{252}\text{Cf}$  source activity is the range 10 - 70 MBq were used with low enriched uranium samples.

Figure 2 shows a gamma spectrum of a 4.5% enriched uranium sample irradiated with a 10 MBq  $^{252}\text{Cf}$  source in the stand-alone irradiator mentioned above. The gamma spectrum is acquired in the relocatable gamma station in 800 s with the protocol of 4 irradiations and gamma acquisition of 200 s each. The cooling time after each irradiation was 15 s due to the sample transfer time between the stand-alone irradiator and the relocatable gamma station.

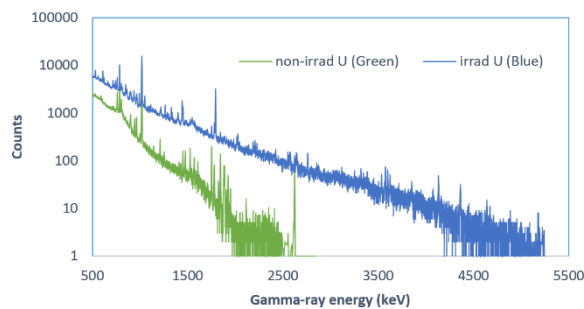


Figure 3: A gamma-ray spectrum of an enriched (4.5%) uranium sample (200 g total U mass) irradiated with 10 MBq  $^{252}\text{Cf}$  source. The gamma-ray spectrum of the non-irradiated U sample is show in green color.

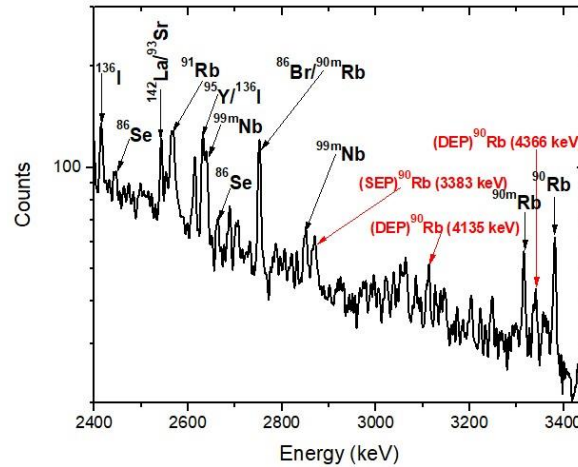


Figure 4: Energy range 2.4-3.4 MeV zoom on the gamma spectrum shown in Figure 2. A single and double escape peaks are pointed out (SEP, DEP).

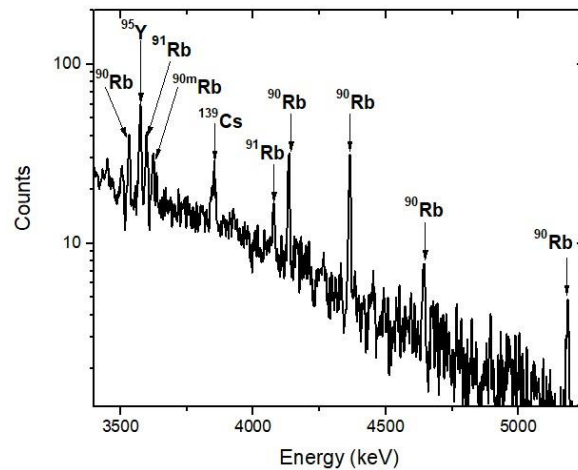


Figure 5: Energy range 3.5-5.4 MeV zoom on the gamma spectrum shown in Figure 2

This gamma spectrum shows a detection with satisfactory confidence of more than 35 FPs (or daughters) that can be used for quantification on NM or identification of signatures for special NM (SNM). Table 1 shows a comprehensive qualitative analysis of the shown gamma spectrum with the list of all detected nuclides, which are identified by their gamma-ray lines taking into account their branching ratios. For each of the detected nuclide, their gamma-ray lines energy and intensity, fission yields (in cases of  $^{235}\text{U}$  and  $^{239}\text{Pu}$ ) with four half-life ranges (Table 1 a/b/c/d) are shown. These nuclide data are retrieved from JEF-3.1 data base with Nucleonica platform [7, 8, 9, 10]. Table 1a, Table 1b, Table 1c and Table 1d show detected FPs (or their daughters) with half-lives in the ranges of below 3 m, 2.7-10 m, 10-19 m and 0.5-3 h respectively. The aim of this classification of detected FPs is the selection of optimum analysis protocol when a focus is desired on particular FPs (see Chap 2). These numerous FPs detected in the high energy gamma-ray spectrum offers a large possibility for non-destructive assay of NM including identification of NM signatures such as in mixtures of  $^{235}\text{U}$ ,  $^{239}\text{Pu}$ , ... The quality of gamma-ray spectrum shown in Figure 1 is similar to those spectra acquired in JRC PUNITA facility, which is equipped with a D-T neutron irradiator [13]. This preliminary work shows a promising results on the testing of the DGS technique with a sealed neutron source as low as 10 MBq  $^{252}\text{Cf}$ . Also these preliminary results allow findings for the ongoing upgrade of the JAEA DGS system being tested in PERLA Laboratory.

**Table 1a. FPs (or daughters) with half-lives below 3 m detected in a 4.5% enriched uranium sample irradiated with 10 MBq  $^{252}\text{Cf}$  source. Their gamma-ray peak energy and intensity, fission yields (in case of  $^{235}\text{U}$  and  $^{239}\text{Pu}$ ) are shown.**

Fission Products	Half-life	Yield $^{235}\text{U}$ (%)	Yield $^{239}\text{Pu}$ (%)	Energy (keV)	Intensity (%)
<b>Se-86</b>	15.3 sec	1.26	0.29	2441.1	43
				2660	21.59
<b>La-144</b>	40.8 sec	5.44	3.59	397.44	94.3
				541.2	39.23
				844.8	22.25
<b>Nb-97m</b>	52.7 sec	5.70	5.00	743.36	100
<b>Br-86</b>	55 sec	1.87	0.67	1534.7	9.28
				1564.92	64
				2751.2	21.06
<b>Rb-91</b>	58.4 sec	5.63	2.17	345.52	8.29
				1970.99	6.7
				2564.19	12.54
				3599.67	10.41
				4078.25	4.078
<b>Sr-94</b>	75.3 sec	6.11	3.71	703.9	2.129
				723.8	2.4
				1427.7	94.2
<b>I-136</b>	83.4 sec	2.93	1.69	1313.02	66.7
				1321.08	24.81
				2289.6	10.41
				2414.6	6.8
				2634.2	6.7
<b>Sb-133</b>	150 sec	2.41	1.30	817.8	18.49
				1096.22	43
<b>Nb-99m</b>	156 sec	2.20	2.12	2641.3	3.693
				2851.5	3.094
<b>Rb-90</b>	158 sec	4.37	1.27	831.69	39.9
				1060.7	9.536
				3383.24	6.7
				3534.24	4.03
				4135.51	6.7
				4365.9	7.98
				4646.45	2.25
5187.44	1.165				

**Table 1b. Table 1a. FPs (or daughters) with half-lives in the range 2.7–10 m detected in a 4.5% enriched uranium sample irradiated with 10 MBq  $^{252}\text{Cf}$  source. Their gamma-ray peak energy and intensity, fission yields (in case of  $^{235}\text{U}$  and  $^{239}\text{Pu}$ ) are shown.**

Fission Products	Half-life	Yield $^{235}\text{U}$ (%)	Yield $^{239}\text{Pu}$ (%)	Energy (keV)	Intensity (%)
<b>Sb-132</b>	2.79 m	1.76	1.32	696.8	86.13
				816.6	10.89

				973.9	99
<b>Ce-145</b>	2.95 m	3.94	3.03	439.71	6.7
				724.33	59
				1148.03	9.14
<b>Se-84</b>	3.1 m	0.99	0.42	408.2	100
				498.5	2.4
<b>Kr-89</b>	3.15 m	4.43	1.42	356.1	4.1
				497.38	6.67
				576.96	5.66
				586.03	16.64
				867.08	5.95
				1472.76	6.9
				1530.04	3.337
				1533.68	5.146
<b>Xe-137</b>	3.82 m	6.15	6.13	455.49	31.2
<b>Sb-132m</b>	4.10 m	0.90	0.83	696.8	100
				973.9	100
<b>Rb-90m</b>	4.30 m	1.36	0.71	831.69	94.09
				1060.7	7.62
				1375.36	16.65
				2752.68	11.48
				3317	14.3
				3620.8	0.574
<b>Br-84m</b>	6.0 m	0.02	0.03	425.3	100
				881.61	98
				1463.84	97
<b>Sr-93</b>	7.42 m	6.36	3.71	590.2	68
				710.3	21.76
				875.73	24.48
				888.13	22.1
				1040.63	3.196
				1122.48	4.012
				1269.47	7.14
				1387.11	3.47
				1699.06	3.332
				2543.84	3.026
<b>Cs-139</b>	9.27 m	6.31	5.72	627.24	1.77
				1283.23	8.3
				3853.87	0.0224

*Table 1c. FPs (or daughters) with half-lives in the range 10-19 m detected in a 4.5% enriched uranium sample irradiated with 10 MBq <sup>252</sup>Cf source. Their gamma-ray peak energy and intensity, fission yields (in case of <sup>235</sup>U and <sup>239</sup>Pu) are shown.*

Fission Products	Half-life	Yield <sup>235</sup> U (%)	Yield <sup>239</sup> Pu (%)	Energy (keV)	Intensity (%)
<b>Y-95</b>	10.3 m	6.47	4.82	954	15.8
				1324	4.91

				1940.3	2.386
				2175.6	6.99
				2632.4	4.756
				3576	6.38
<b>Ba-142</b>	10.6 m	5.80	4.68	895.2	13.86
				1078.7	11.46
				1204.3	14.23
<b>Tc-101</b>	14.2 m	5.17	6.18	306.86	88.7
				545.12	5.96
<b>Xe-138</b>	14.08 m	6.41	5.02	434.56	20.32
				1768.26	16.73
				2004.75	5.355
				2015.82	12.25
				2252.26	2.287
<b>Rb-89</b>	15.4 m	4.69	1.68	345.52	8.29
				657.77	9.97
				947.73	9.22
				1031.94	58
				1248.19	42.57
				2196.02	13.34
				2570.19	9.86
<b>Tc-104</b>	18.3 m	1.88	6.07	358	89
				530.5	15.57
				535.1	14.69
				884.4	10.95
				893.1	10.24
<b>Y-94</b>	18.7 m	6.40	4.30	918.74	56
				1138.88	5.99

*Table 1d. FPs (or daughters) with half-lives in the range 0.5-3 h detected in a 4.5% enriched uranium sample irradiated with 10 MBq  $^{252}\text{Cf}$  source. Their gamma-ray peak energy and intensity, fission yields (in case of  $^{235}\text{U}$  and  $^{239}\text{Pu}$ ) are shown.*

Fission Products	Half-life	Yield $^{235}\text{U}$ (%)	Yield $^{239}\text{Pu}$ (%)	Energy (keV)	Intensity (%)
<b>Cs-138</b>	33.41 m	6.69	5.94	462.79	30.75
				547	10.76
				1009.7	29.83
				1435.7	76.3
				2218	15.18
				2639.59	7.63
<b>Sb-130</b>	39.5 m	1.08	1.45	331.05	78
				793.53	100
				839.49	100
<b>Te-134</b>	41.8 m	6.79	4.40	277.95	21.24
				435.06	18.88
				565.99	18.58
				767.2	29.5
<b>I-134</b>	52.5 m	7.74	6.62	621.79	10.59

				847.025	95.4
				884.09	64.87
<b>Nb-97</b>	72.1 m	6.00	5.29	658.08	98.44
<b>La-142</b>	91.1 m	5.86	4.97	641.28	47.4
				894.9	8.3
				2397.8	13.27
				2542.7	10
<b>Sr-92</b>	2.71 h	6.03	3.00	953.3	3.5
				1383.9	90
<b>Kr-88</b>	2.84 h	3.54	1.25	834.83	12.98
				1529.77	10.93
				2195.8	13.18
				2392.11	34.6

## 5. Conclusion

This paper presented promising experimental results on the DGS as a step further to its development as a new NDA technique for nuclear safeguards verification specially in case of highly active NM such as solution of spent nuclear fuel. Some other tests are ongoing or planned in the perspective of the optimization of the new version of the JAEA DGS System. So far the tests were performed on uranium samples and further tests test with plutonium and also with higher activity of irradiating  $^{252}\text{Cf}$  (up to 0.1 GBq) are planned. Besides the validation of a new NDA technique, this work contributes also to the validation of the theoretical model base on MC but also to the gathering of new nuclear data. In particular, there is a need for new nuclear data and also for new detection instrumentation specially in high gamma-ray energy range.

## 6. References

1. D. C. Rodriguez, J. Takamine, M. Koizumi, and M. Seya, "Utilizing Delayed Gamma Rays for Fissionable Material Measurement in NDA," in 37th Annual Meeting of the European Safeguards Research & Development Association, EUR-27342, May 2015
2. M. Koizumi, F. Rossi, D.C. Rodriguez, J. Takamine, M. Seya, Bogucarska, T., J:M. Crochemore, G. Varasano, K. Abbas, B. Pederson, M. Kureta, J. Heyse, C. Paradela, W. Mondelaers, P. Schillebeeckx, Delayed gamma-ray spectroscopy combined with active neutron interrogation for nuclear security and safeguards EPJ Web of Conferences 146, 09018, 2017
3. D. C. Rodriguez, F. Rossi, J. Takamine, M. Koizumi, M. Seya, J. M. Crochemore, G. Varasano, T. Bogucarska, K. Abbas, and B. Pedersen, "Delayed Gamma-ray Spectroscopy (1): Development and Current Status," in 58th Annual Meeting of the Institute of Nuclear Materials Management, July 2017
4. F. Rossi, M. Koizumi, D. C. Rodriguez, J. Takamine, M. Seya, B. Pedersen, J. M. Crochemore, K. Abbas, T. Bogucarska, and G. Varasano, "Delayed Gamma-ray Spectroscopy (1): Experimental Studies of Fissile Materials Ratios," in 58th Annual Meeting of the Institute of Nuclear, Materials Management, July 2017
5. M. Koizumi, F. Rossi, D.C. Rodriguez, J. Takamine, M. Seya, Bogucarska, T., J:M. Crochemore, G. Varasano, K. Abbas, B. Pederson, M. Kureta, J. Heyse, C. Paradela, W. Mondelaers, P. Schillebeeckx, Delayed gamma-ray spectroscopy combined with active neutron interrogation for nuclear security and safeguards EPJ Web of Conferences 146, 09018, 2017

6. K. Abbas, D.C. Rodriguez, B. Pedersen, F. Rossi, J.M. Crochemore, M. Seya, M. Koizumi, S. Nonneman, T. Bogucarska, T. Takahashi, R&D on NDA techniques for nuclear safeguards and security in JAEA-JRC partnership in Ispra  
Safeguards2018 IAEA symposium, Safeguards: Building Future Safeguards Capabilities  
5–8 November 2018, Vienna, Austria, paper 128.
7. Live Chart of Nuclides, IAEA, Nuclear Data Section,  
<https://www.nds.iaea.org/relnsd/vcharthtml/VChartHTML.html>
8. 8th Table of Radioactive Isotopes, data base with Nucleonica platform
9. Nucleonica GmbH, Nucleonica Nuclear Science Portal ([www.nucleonica.com](http://www.nucleonica.com)), Version 3.0.65, Karlsruhe (2017)
10. JEF-3.1 data base retrieve with Nucleonica platform

# Performance of FRAM isotopic analysis of shielded plutonium with electrically cooled gamma-spectrometers

J. Zsigrai<sup>1</sup>, A. Berlizov<sup>2</sup>, D. van Eerten<sup>1,3</sup>, J. Bagi<sup>1</sup>, A. Muehleisen<sup>1</sup>

<sup>1</sup>European Commission, Joint Research Centre, Directorate G, Karlsruhe, Germany

<sup>2</sup>International Atomic Energy Agency, Vienna, Austria

<sup>3</sup>Durham University, Durham, United Kingdom

## Abstract:

The capability of the FRAM software to accurately determine the isotopic composition of shielded plutonium was tested by the Joint Research Centre in Karlsruhe to support the use of FRAM for the verification of plutonium-bearing items by safeguards inspectors in the field. More than ten thousand spectra of eight certified reference-material items were recorded by a portable electrically cooled gamma spectrometer, "ORTEC microDetective", and analysed using different FRAM parameter sets. The performance of FRAM was evaluated as a function of shielding thickness, measurement time, sample composition and "spectrum quality". The spectrum quality was quantified using a numerical figure of merit that included the uncertainties of the peak areas relevant for the isotopic analysis. Thereby, it combined the effects of shielding, measurement time and sample isotopic composition into a single indicator. It was shown that using FRAM's automatic analysis option improves the isotopic results, especially in the case of lower quality spectra. The results of this work will help safeguards inspectors to optimize the use of electrically cooled gamma-spectrometers and to improve the accuracy of plutonium isotopic composition measurements in the field.

**Keywords:** gamma spectrometry, electrically cooled gamma spectrometer, plutonium isotopic composition, FRAM

## 1. Introduction

The purpose of this work was to study and possibly improve the capability of the FRAM software to determine the isotopic composition of shielded plutonium by portable electrically cooled HPGe detectors. This work, focused on plutonium, is a follow-up of previous work [1] that was focused on uranium. Both tasks were carried out within the European Commission's support programme to the International Atomic Energy Agency (IAEA). For the sake of completeness, some introductory remarks about the task and about FRAM are repeated here.

FRAM is software that calculates uranium and plutonium isotopic composition from the gamma spectra of these materials [2], [3]. It has been developed at Los Alamos National Laboratory (USA) and it has been commercialized by ORTEC and Canberra. The version used in this study was 5.2, which has minor changes compared to version 5.1 [4], which was used in the study on uranium [1].

The so called parameter sets determine what FRAM exactly does. They define the type of material (U, Pu, MOX) and the type of detector. They also contain information about the isotopes and gamma peaks to be analyzed, peak fitting parameters, energy calibration, relative efficiency constraints, etc. FRAM contains a number of default parameter sets built into the software, which cover a large number of typical measurement configurations. However, users can also prepare modified or new parameter sets to suit their specific measurement configuration. In this work we focused on parameter sets for plutonium.

More than 100007000 high-resolution gamma spectra of various certified reference materials were taken by the ORTEC microDetective electrically cooled spectrometer under well-defined measurement conditions with different steel, cadmium and lead screens. These spectra were used to check the performance of FRAM v5.2 for determining the isotopic composition of shielded plutonium. In this paper the results calculated using different parameter sets are compared to each other and the influence of shielding thickness, measurement time and plutonium burn-up is discussed. This way the capabilities and limitations of FRAM became better understood.

## 2. Method and equipment

The ORTEC microDetective electrically cooled spectrometer was used to record the gamma spectra. It has a high-purity coaxial germanium (HPGe) crystal of 50 mm diameter and 30 mm depth (length). The conversion gain of its amplifier was set to 0.125 keV/channel, to match the gain in the default FRAM parameter sets. (Note that for the uranium study [1] an older version of the ORTEC detective was used, having fixed amplifier gain, set in the factory.)

A total of 8 Pu reference items from the "CBNM" [5] and "PIDIE" [6], [7], [8] sets were used in this study. Their isotopic composition is shown in Table 1 and Table 2.

**Table 1.** Isotopic composition of the "CBNM" reference samples in weight % with 2s absolute uncertainty for reference date 20.6.1986.

Reference sample		Isotope					
		<sup>238</sup> Pu	<sup>239</sup> Pu	<sup>240</sup> Pu	<sup>241</sup> Pu	<sup>242</sup> Pu	<sup>241</sup> Am
CBNM Pu93	weight %	0.0117	93.4123	6.3131	0.2235	0.0395	0.1047
	2s	0.00003	0.004	0.0039	0.0004	0.0003	0.0021
CBNM Pu84	weight %	0.0703	84.3377	14.2069	1.0275	0.3576	0.2173
	2s	0.0006	0.0084	0.0085	0.0018	0.001	0.0022
CBNM Pu70	weight %	0.8458	73.3191	18.2945	5.4634	2.0772	1.1705
	2s	0.0018	0.0098	0.0087	0.0034	0.0023	0.0117
CBNM Pu61	weight %	1.1969	62.5255	25.4058	6.6793	4.1925	1.4452
	2s	0.0025	0.0283	0.0241	0.0087	0.0064	0.0144

**Table 2.** Isotopic composition of PIDIE reference samples in weight % (normalized to sum of Pu isotopes) with 2s absolute uncertainty for reference date 1.1.1988.

Reference sample		Isotope					
		<sup>238</sup> Pu	<sup>239</sup> Pu	<sup>240</sup> Pu	<sup>241</sup> Pu	<sup>242</sup> Pu	<sup>241</sup> Am
PIDIE 1	weight %	0.01101	93.7650	5.99025	0.19920	0.0346	0.2304
	2s	0.00033	0.0065	0.0052	0.00255	0.0015	0.0060
PIDIE 3	weight %	0.04716	84.5795	14.1442	0.9953	0.2338	0.6282
	2s	0.00038	0.0094	0.0052	0.0036	0.0075	0.0151
PIDIE 5	weight %	0.1314	75.8862	21.2169	2.0638	0.7017	1.7488
	2s	0.0011	0.0147	0.0115	0.0042	0.0015	0.0387
PIDIE 7	weight %	1.253	61.9848	25.5941	6.4919	4.6763	3.5287
	2s	0.016	0.0420	0.0195	0.0132	0.0081	0.1111

The spectra of each item were recorded using a tungsten collimator and combinations of Fe screens of up to 16 mm thickness, Cd screens up to 2 mm thickness and a Pb screen of 4 mm thickness. The sample to detector distance was 10 cm. The only exception, 20 cm, was the configuration with the CBNM Pu61 source and low shielding (2 mm Cd with no Fe and 1 mm Cd with 4 mm Fe). This means 5 shielding configurations for each sample (Table 3).



Several quantities were calculated for the statistical interpretation of the results.

- Average relative bias (ARB):
  - the systematic component of FRAM's bias, or the expected accuracy of many ( $n$ ) measurements. It can be either positive or negative.
- Relative standard deviation (RSD):
  - the random component of FRAM's bias.
- Combined average relative bias and relative standard deviation (CBD):
  - the overall performance of FRAM, or the expected accuracy of a single measurement.
- Mean absolute value of the relative difference (MARD):
  - Similar to, but different from CBD. It also describes overall performance of FRAM, or the expected accuracy of a single measurement, but using it in error propagation is not straightforward. Here it is only used for comparison with previous work on uranium [1].

All these quantities are calculated for each shielding configuration for each measurement time. They are defined as follows:

$$\text{Average Relative Bias} = \text{ARB} = \frac{\sum_{i=1}^n \frac{x_i - x_{Ref}}{x_{Ref}}}{n},$$

$$\text{Relative Standard Deviation} = \text{RSD} = \frac{1}{x_{Avg}} \sqrt{\frac{\sum_{i=1}^n (x_i - x_{Avg})^2}{n-1}},$$

$$\text{Combined Bias and standard Deviation} = \text{CBD} = \sqrt{\text{ARB}^2 + \text{RSD}^2},$$

$$\text{Mean Absolute value of Relative Difference} = \text{MARD} = \frac{\sum_{i=1}^n \frac{|x_i - x_{Ref}|}{x_{Ref}}}{n}, \quad (1)$$

where  $n$  is the number of spectra analysed (e.g.  $n=192$  for the 5-minute spectra),  $x_i$  is the value calculated by FRAM,  $x_{Ref}$  is the certified reference value and  $x_{Avg}$  is the average of the FRAM results for the given measurement time and shielding configuration.

In this work all isotopic data (declared data and FRAM results) were decay-corrected to 1<sup>st</sup> January 2019 and all quantities were calculated for this reference date.

Two especially important variables used for plotting were the effective iron shielding and the statistical quality indicator of the spectra. The effective iron shielding is the equivalent shielding based on thickness of the shielding screens used and the mean values of the linear attenuation coefficients in the energy range 180-433 keV. It is calculated as:

$$\text{Effective iron shielding} = d_{Fe} + \frac{\bar{\mu}_{Cd}}{\bar{\mu}_{Fe}} d_{Cd} + \frac{\bar{\mu}_{Pb}}{\bar{\mu}_{Fe}} d_{Pb}, \quad (2)$$

where  $dX$ , is the thickness of the Fe, Cd or Pb screens used and  $\bar{\mu}_X$  is the average of 14 equidistant values of the linear attenuation coefficient of these materials in the energy range 180-433 keV. The values for linear attenuation coefficients were taken from the online NIST database [9].

For example, 4 mm of Pb corresponds to 26.8 mm effective iron shielding, while 2 mm of Cd corresponds to 3.6 mm effective iron shielding, according to the above definition.

The indicator of the statistical quality of the spectra ("magic number") is the inverse of the combined relative uncertainty of the "magic peaks":

$$\text{statistical indicator ("magic number")} = \frac{1}{\sqrt{\sum_i \delta_i^2}}, \quad (3)$$

where  $\delta_i$  is the relative uncertainty of the  $i^{\text{th}}$  peak and the sum goes over all magic peaks. The "magic peaks" are those peaks which are used in all parameter sets investigated in this study. In particular, they were the peaks of  $^{239}\text{Pu}$ ,  $^{241}\text{Pu}$  and  $^{241}\text{Am}$  at 413.712, 208.000 and 335.432 keV, respectively.

Figure 2 shows the dependence of the statistical indicator (averaged over all shieldings and samples) on the measurement time, for all investigated parameter sets.

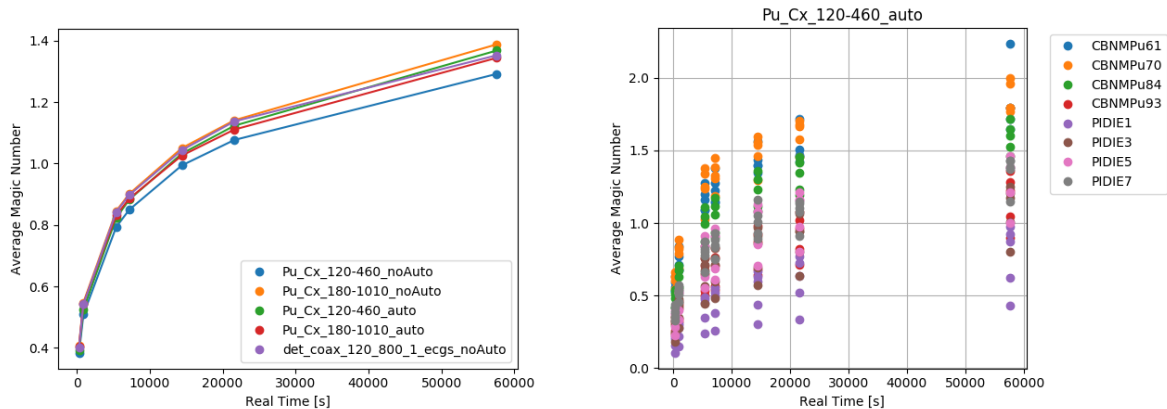


**Figure 2.** Left: statistical quality of the spectra ("magic number") averaged over all shieldings and samples as a function of real measurement time, for all investigated parameter sets. Right: statistical quality of the spectra ("magic number") as a function of real measurement time for all samples calculated using the parameter set Pu\_Cx\_120-460 with auto analysis turned on.

The statistical indicator depends on the measurement time, shielding, sample activity and isotopic composition. It also slightly depends on the parameter set, due to small differences in peak fitting. It increases with measurement time, but for some samples (e.g. PIDIE1) it stays quite low even for long measurement times. As it will be seen later, "good" spectrum quality means that the value of this indicator is around 1 or above 1.

Three different types of plots were prepared from the calculated statistical quantities:

1. "Category plots": The performance indicators (average relative bias, RSD, CBD and MARD) of the isotope ratios relative to  $^{239}\text{Pu}$  and of the  $^{239}\text{Pu}$  isotope fraction were calculated for each configuration, each measurement time, each sample and each parameter set. These values were plotted as a function of various variables for all values of a selected category on a separate graph for each parameter set. For example, the dependence of  $^{239}\text{Pu}$  CBD on spectrum quality for each value of the declared  $^{239}\text{Pu}$  fraction is plotted on a separate graph for a given parameter set (Figure 8). This gives (5 configurations) x (7 different measurement times) x (8 samples) = 280 points on each "category plot".
2. "Average plots": To visualize FRAM's performance in a more compact form, the average of the above quantities was calculated as a function of selected variables and all parameter sets were plotted on the same graph. For example, the  $^{239}\text{Pu}$  average CBD as a function of statistical quality of the spectra (Figure 7) plotted on the same graph for all parameter sets. In this case the number of points on the graph depends on the number of different values that the independent parameter may take.
3. "Grand average plots" (bar charts): To have an even more compact comparison of the parameter sets, the grand averages of all the values of selected quantities calculated by a given parameter set were plotted on a bar chart. An example is the bar chart showing the grand average of the  $^{241}\text{Pu}$  CBD for all parameter sets (Figure 5).

These plots demonstrate the performance of the different FRAM parameter sets for different situations and might be used for improving the parameter sets.

### 3. Results

#### 3.1. General comments on the results

The presentation of the results starts by comparing the parameter sets using the grand average plots for each investigated quantity, and then goes into more detail through the average plots and eventually category plots.

The results for  $^{242}\text{Pu}$  were not investigated in this work, because  $^{242}\text{Pu}$  cannot be directly obtained from the gamma spectrum and empirical correlations have to be used. The discussion of these empirical correlations will be the subject of further work. That is why only isotope ratios to  $^{239}\text{Pu}$  are studied in this work, and not the ratios to total Pu, because the ratios to total Pu are affected by the calculation of  $^{242}\text{Pu}$ . Nevertheless, due to its importance for safeguards, the ratio of  $^{239}\text{Pu}$  to total Pu is also presented in this work.

In certain situations FRAM reports zero for some isotope ratios. Those results are removed from the averages presented in the graphs.

As the MARD used in previous work is no longer used here for the presentation of the results, it is worth to compare it to the CBD, which is used instead of it. The MARD and the CBD are mathematically NOT equivalent, but if all the biases are positive, then for large  $n$  (number of spectra) the values of the MARD and CBD are very close to each other. This is demonstrated in Figure 3, where the CBD for  $^{239}\text{Pu}$  and for the  $^{238}\text{Pu}/^{239}\text{Pu}$  ratio are plotted as a function of MARD.

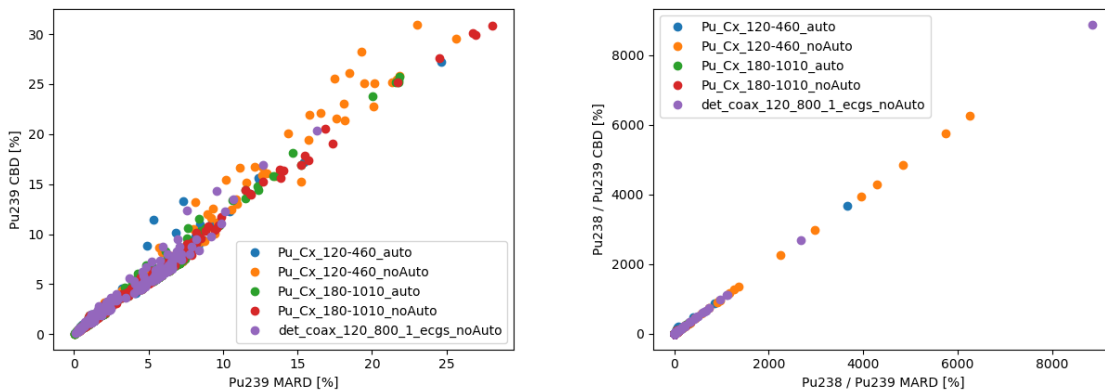


**Figure 3** The CBD as a function of MARD for  $^{239}\text{Pu}$  (left) and for the  $^{238}\text{Pu}/^{239}\text{Pu}$  ratio right, for all investigated parameter sets.

#### 3.2. Grand average plots

For the  $^{239}\text{Pu}$  fraction the lowest grand average relative bias and the lowest grand average CBD are achieved using the parameter set det\_coax\_120\_800\_1\_ecgs (Figure 4). However, for mass ratios of the other isotopes relative to  $^{239}\text{Pu}$  the best results are achieved with the two default parameter sets used in "autoanalysis" mode (Figure 5).

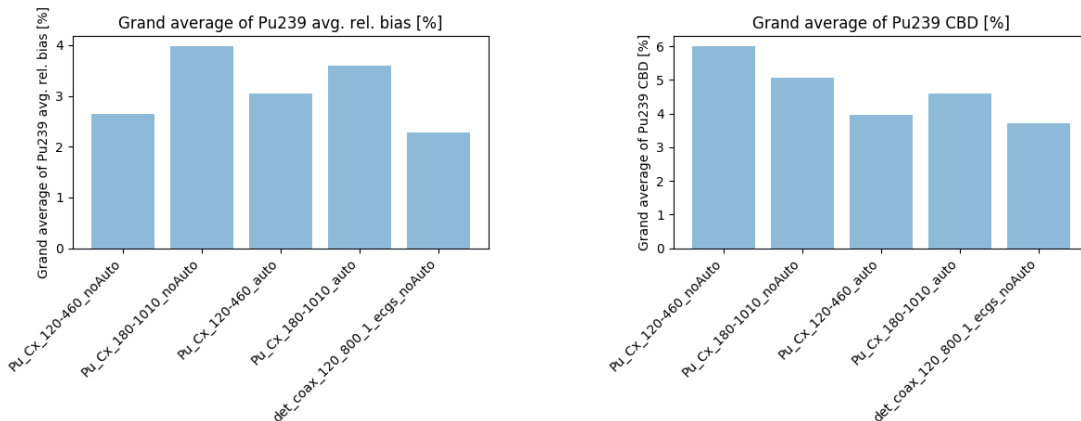


**Figure 4.** The grand average of  $^{239}\text{Pu}/\text{Pu}$  mass fraction relative bias and CBD for all parameter sets

The grand average relative bias and the CBD of the mass ratio relative to <sup>239</sup>Pu are shown for all parameter sets in Figure 5.

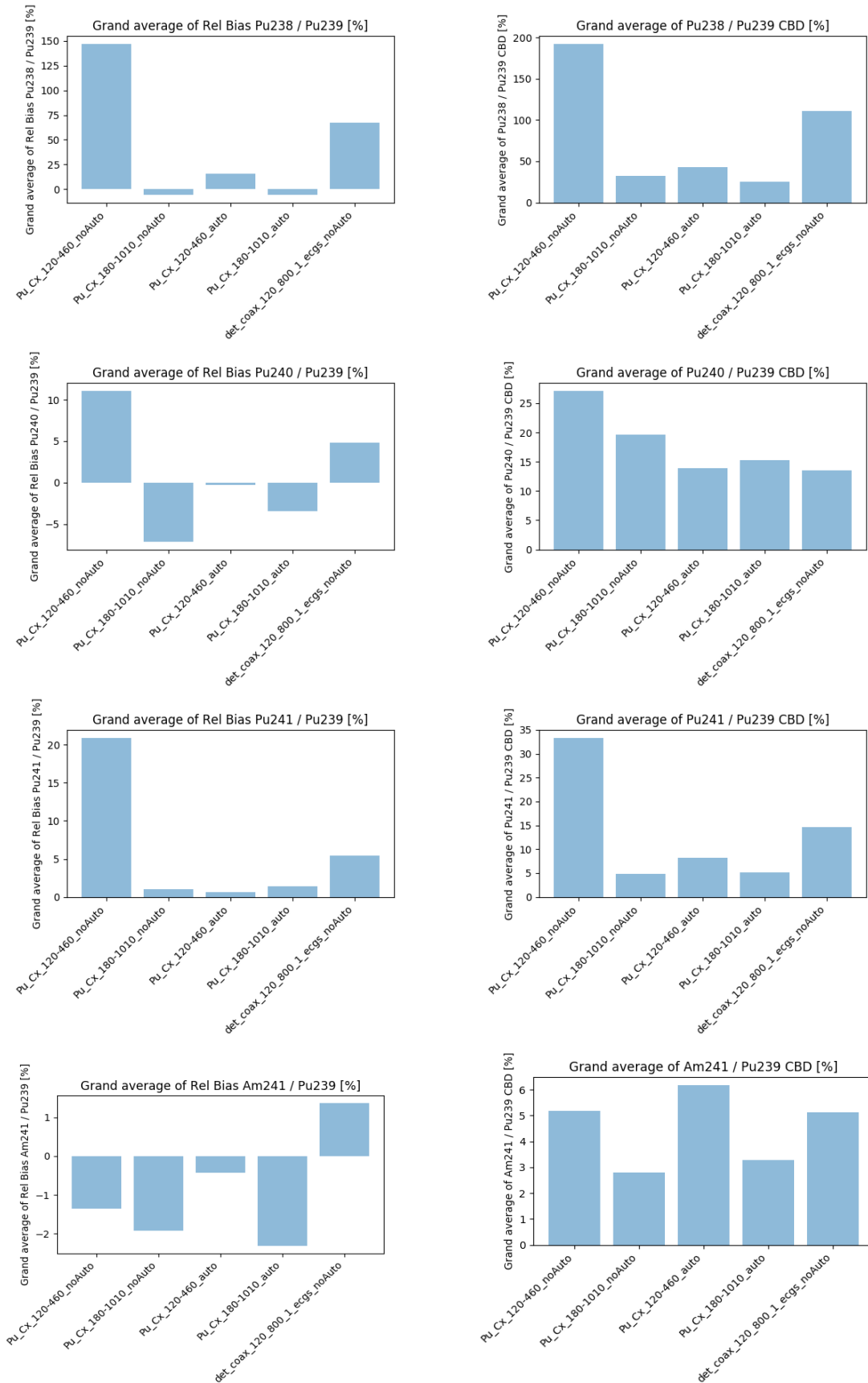


Figure 5. The grand average of the relative bias and CBD of the mass ratios for all parameter sets

### 3.3. The average plots

The "average plots" show the dependence of a selected quantity as a function of a measurement parameter, averaged over all identical values of that parameter in all spectra for which the selected parameter has the same value. For example, one of the points on an average plot can be the average of all spectra for which the effective shielding thickness is 16 mm, for all measurement times, for a given parameter set. The parameters investigated here are the shielding thickness and spectrum statistical quality.

#### 3.3.1. Dependence of FRAM performance on spectrum statistical quality

The dependence of the CBD of the mass ratios on spectrum quality is shown in Figure 6 and the CBD of  $^{239}\text{Pu}/\text{Pu}$  mass fraction is shown in Figure 7 and Figure 8.

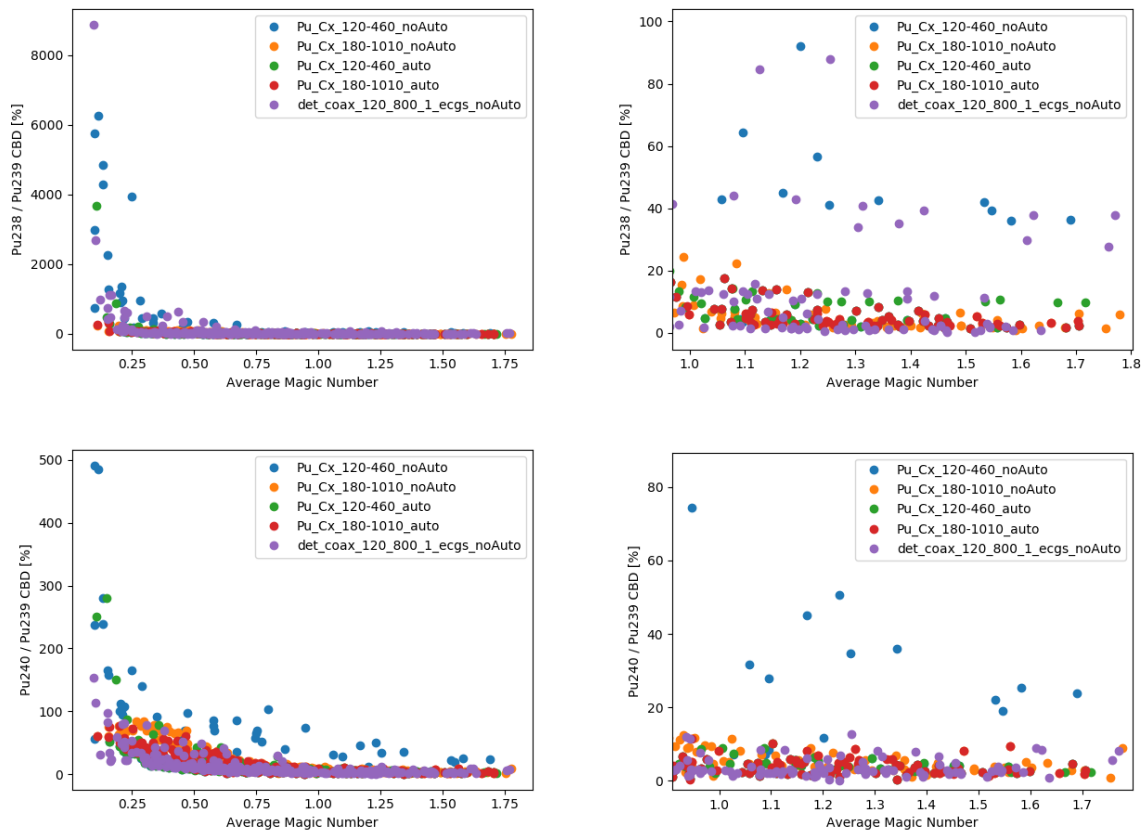


( Figure continued on next page.)

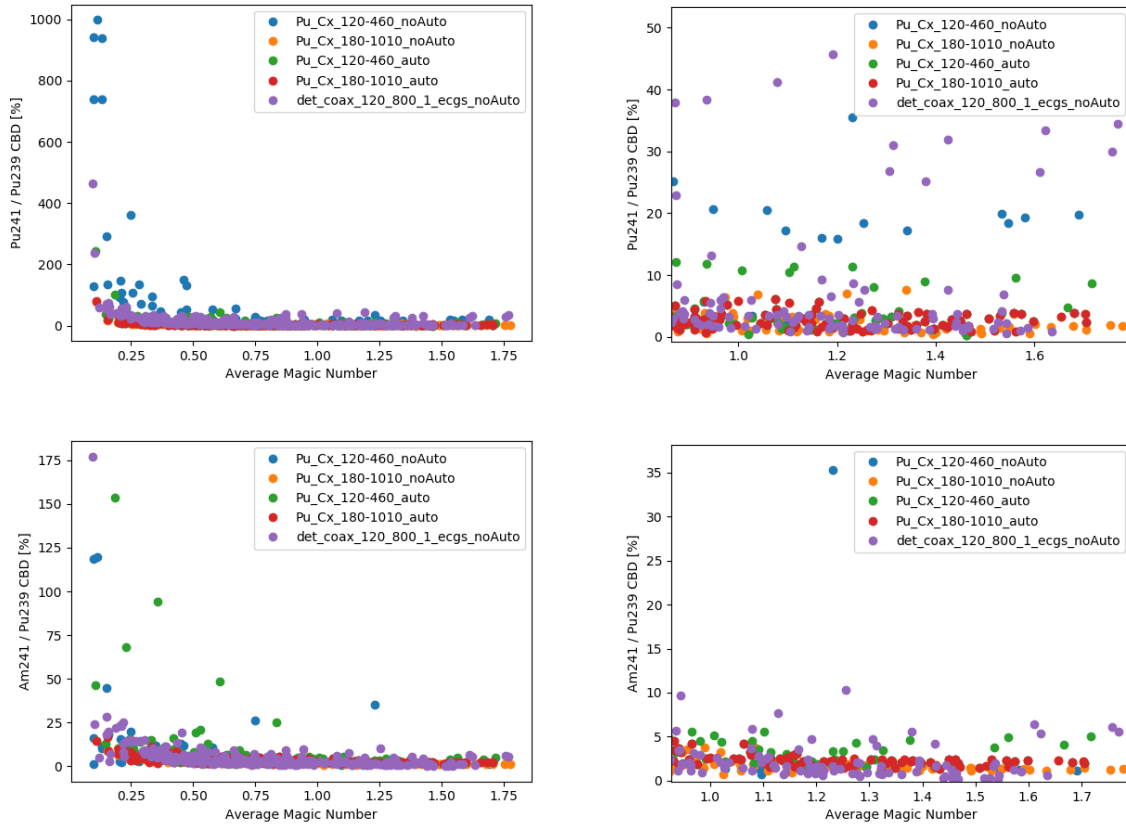


**Figure 6.** Average-plots of the CBD of the mass ratios as a function of statistical quality of the spectra. Left: entire range. Right: zoomed-in to higher spectrum quality

The average plots of the CBD of the mass ratios relative to  $^{239}\text{Pu}$  as a function of statistical quality of the spectra show that all parameter sets give very bad results for low spectrum quality (meaning short measurement time and/or low sample activity and/or thick shielding). If the statistical indicator is above 1, then for most parameter sets the average CBD of  $^{238}\text{Pu}/^{239}\text{Pu}$  becomes lower than 20%, the CBD of  $^{240}\text{Pu}/^{239}\text{Pu}$  lower than 15%, CBD of  $^{241}\text{Pu}/^{239}\text{Pu}$  lower than 10 % and the CBD of  $^{241}\text{Am}/^{239}\text{Pu}$  lower than 5 %.

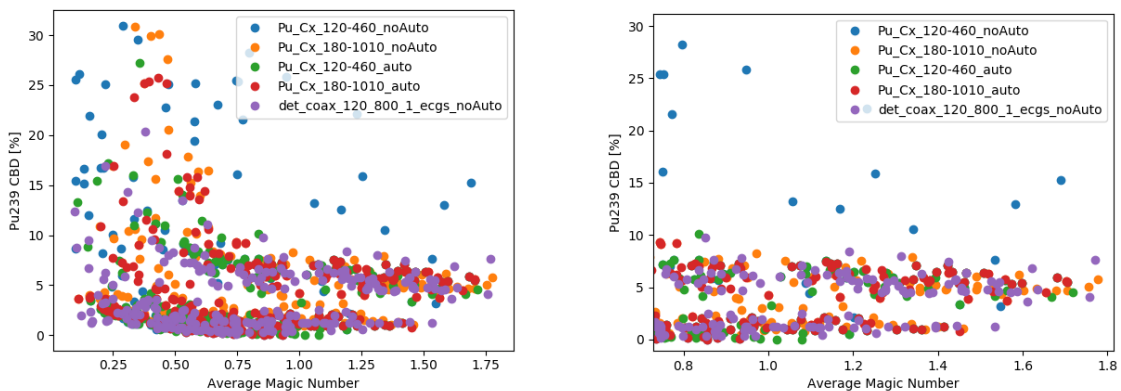


**Figure 7.** Average plot of the CBD of  $^{239}\text{Pu}$  fraction as a function of statistical quality of the spectra: entire range (left) and zoomed-in to higher spectrum quality (right)

The CBD of the  $^{239}\text{Pu}/\text{Pu}$  fraction, for good quality spectra, is lower than 10 % for most parameter sets. However, Figure 7 shows two distinct groups of points: the points denoting higher CBD belong to high-burnup Pu (lower  $^{239}\text{Pu}$  fraction), while the lower CBD belong to low-burnup Pu. This is confirmed by Figure 8, showing the dependence of  $^{239}\text{Pu}$  CBD on spectrum quality for each value of the declared  $^{239}\text{Pu}$  fraction (a "category plot") for the parameter set det\_coax\_120\_800\_1\_ecgs.

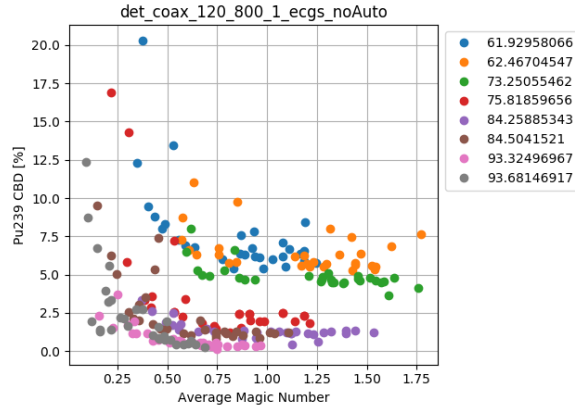


**Figure 8.** Dependence of  $^{239}\text{Pu}$  CBD on spectrum quality for each value of the declared  $^{239}\text{Pu}$  fraction (a "category plot") for the parameter set det\_coax\_120\_800\_1\_ecgs

3.3.2. Dependence of FRAM performance on shielding

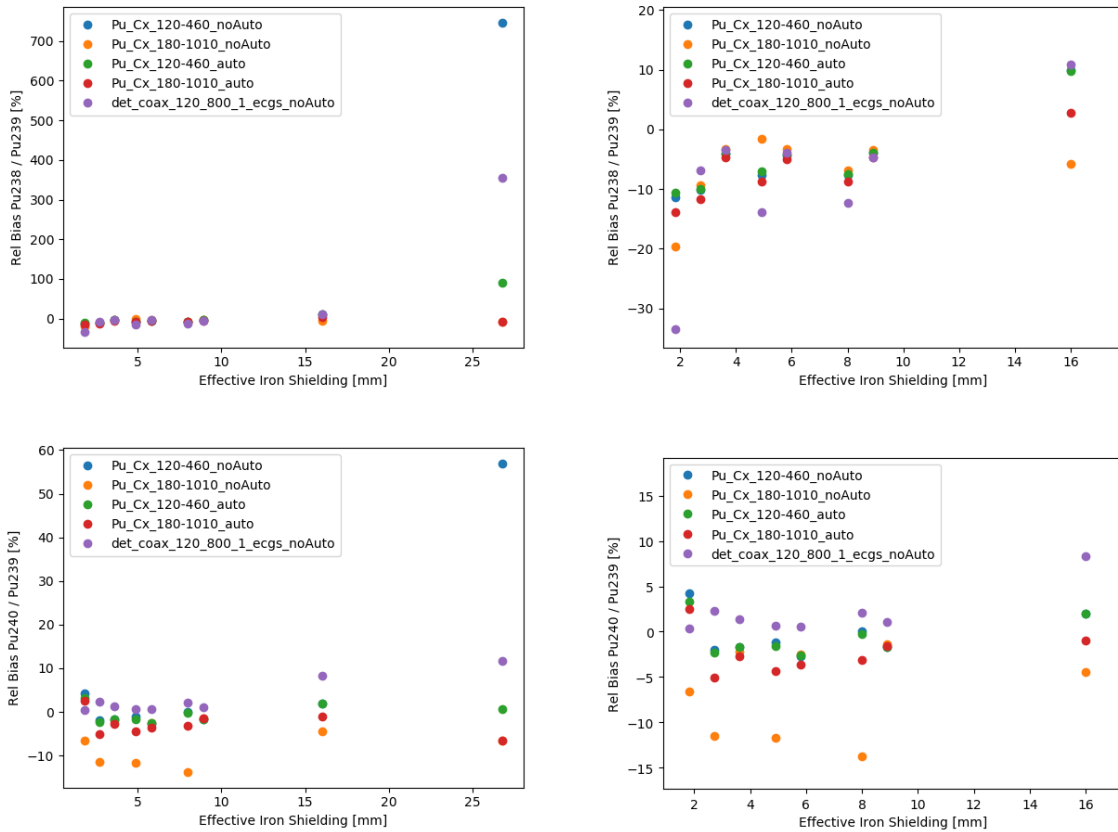


(Figure continued on next page.)

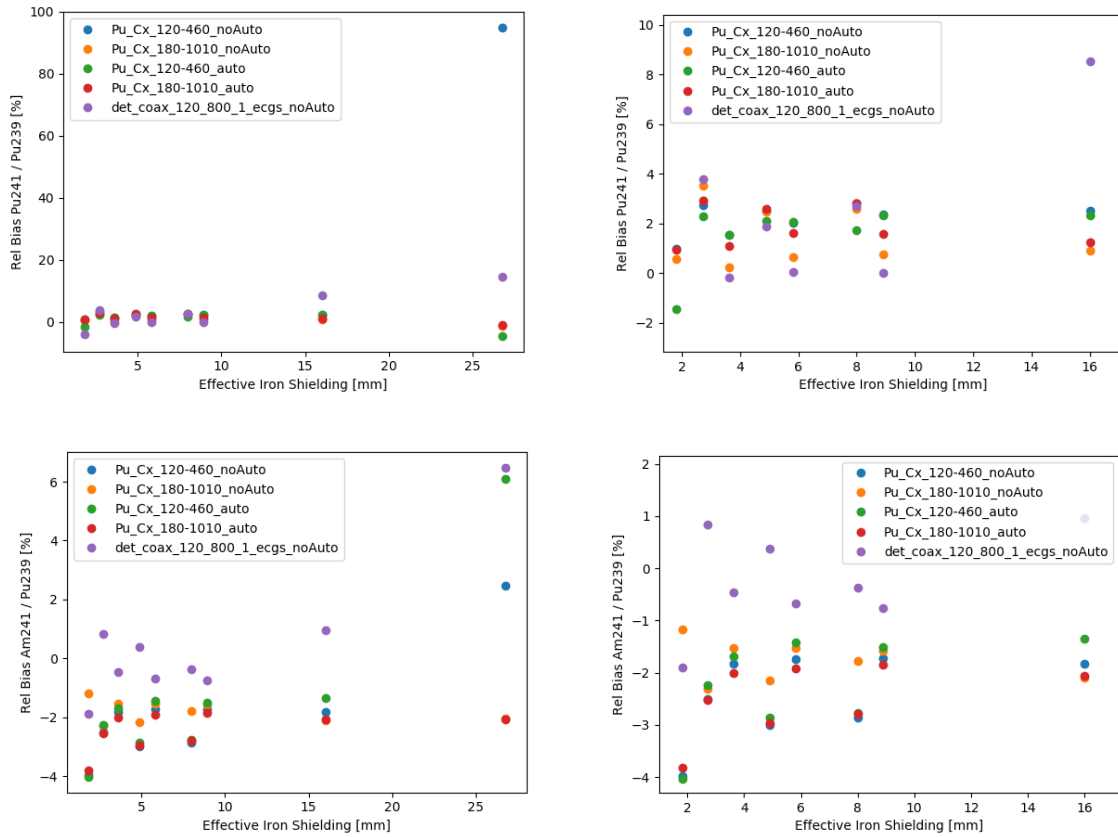


**Figure 9.** The average relative bias of the mass ratios as a function of effective iron shielding thickness: entire range (left) and zoomed-in to lower shielding values (right). Some points overlap, and that is why for some shieldings less than 5 points are visible. For example, Pu\_Cx\_180-1010 and Pu\_Cx\_180-1010\_auto overlap for the highest shielding, because auto analysis always gives the final result using Pu\_Cx\_180-1010 in case of such thick shielding.

Up to 16 mm of effective iron shielding the influence of shielding on the mass ratios is similar for all parameter sets (Figure 9), usually resulting in a negative bias. It is interesting that the best results are obtained between 4-10 mm of effective iron. For effective iron shielding of 27 mm (i.e. a 4 mm sheet of Pb), the mass ratios calculated by those parameter sets that rely on lower energy peaks is biased by a few orders of magnitude.

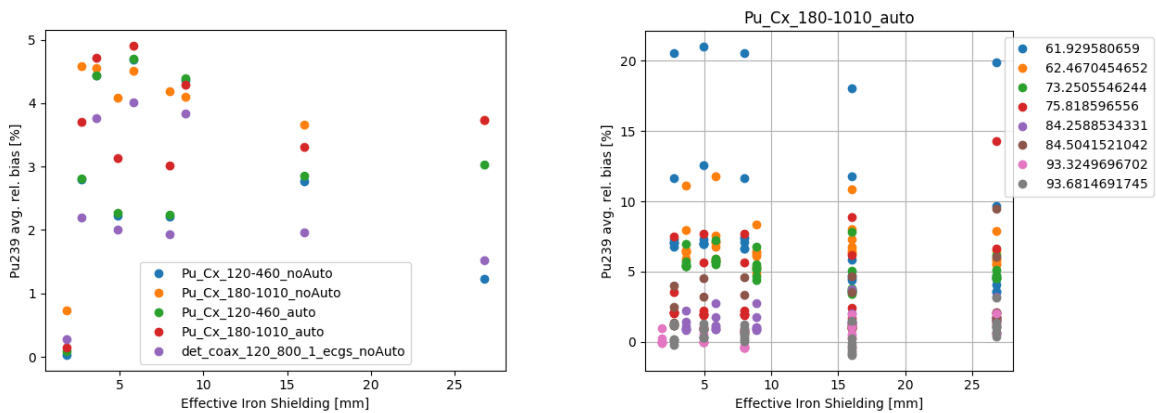


**Figure 10.** Left: Average relative bias of the  $^{239}Pu$  fraction as a function of effective iron shielding thickness for all parameter sets. Right: Average relative bias of the  $^{239}Pu$  fraction as a function of effective iron shielding, calculated using the parameter set Pu\_Cx\_180-1010 with auto analysis turned on, categorized according to the value of the declared  $^{239}Pu$ .

Contrary to the mass ratios, the results for the  $^{239}\text{Pu}$  fraction are the best for the lowest shielding thickness. For all other shielding thicknesses the  $^{239}\text{Pu}$  results are biased between about 2 and 5 % for all parameter sets. In Figure 10 it seems that there are two distinct sets of point for each parameter sets. The explanation for having these two groups is given by the "category plot" on the right of Figure 10 showing the  $^{239}\text{Pu}$  relative bias as a function of effective iron shielding, for all values of the declared  $^{239}\text{Pu}$  for the parameter set Pu\_Cx\_180-1010 with auto analysis turned on. On the right we see that the points with higher burnup (lower  $^{239}\text{Pu}$ ) have higher bias, resulting in the distinct groups on the left.

### 3.4. When FRAM analysis fails

In some situations, especially for low quality spectra and for thick shielding, FRAM is not able to calculate one or more mass ratios and reports a zero for that mass ratio. The spectra for which FRAM gives a zero result were not included in the averages. Figure 11 shows the number of spectra for which a given parameter set failed to calculate a given mass ratio, that is, reported a zero result. Figure 12 shows the average number of zeros as a function of statistical quality.

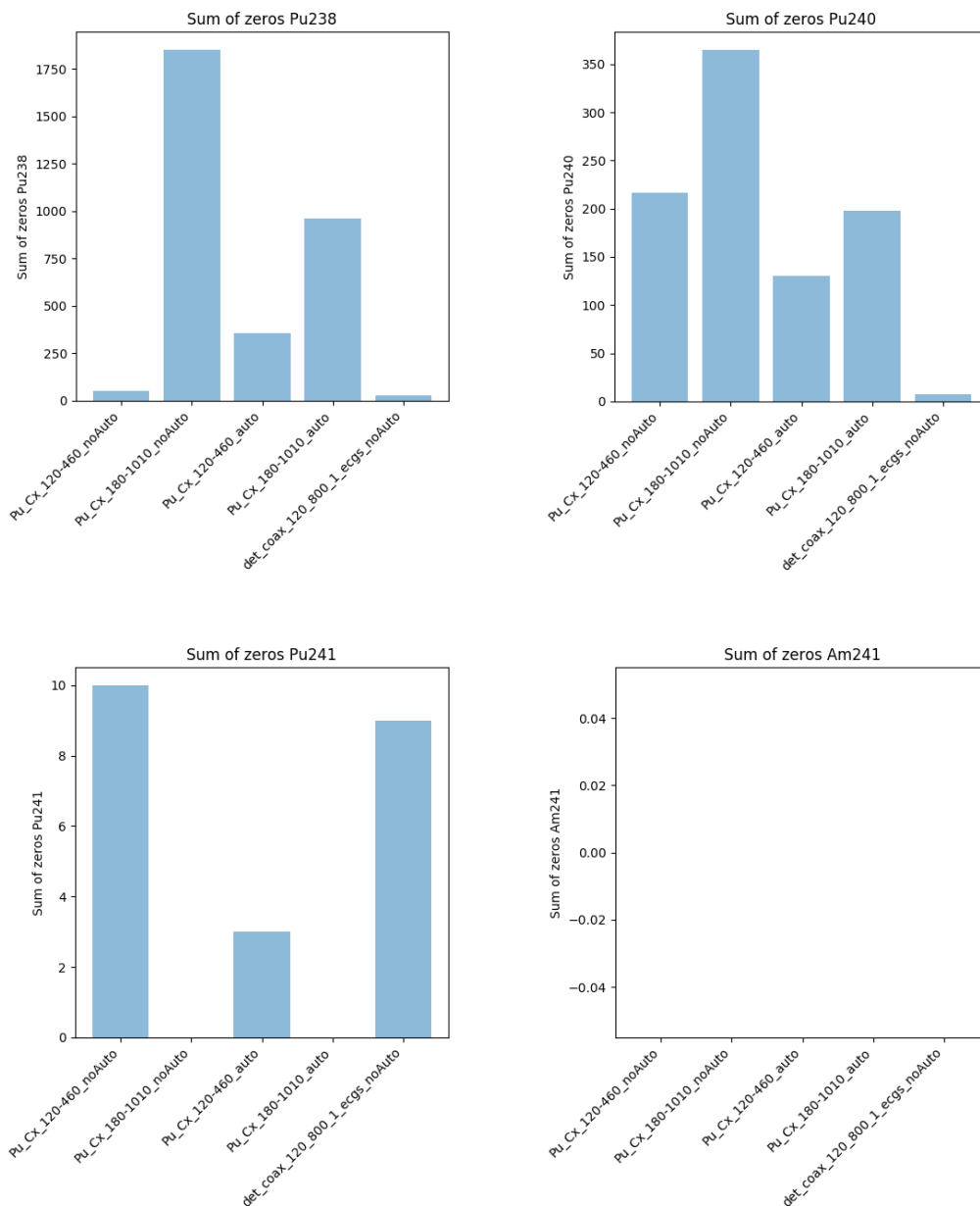


**Figure 11.** The sum of zeros (failures), out of 11240 analysed spectra, for the various mass ratios for different parameter sets. For  $^{241}\text{Am}$  FRAM never fails with zero results.

From Figure 5 to Figure 10 one can see that for good quality spectra the best results for the various mass ratios are reported by the one of the two default parameter sets Pu\_Cx\_120-460 and Pu\_Cx\_180-1010 with auto analysis turned on. However, in case of low spectrum quality the default parameter sets often fail (i.e., report zero mass ratio) and in that case the parameter set det\_coax\_120\_800\_1\_ecgs, which uses simultaneously the high and low energy region, provides the optimum results, as seen on Figure 11 and Figure 12.

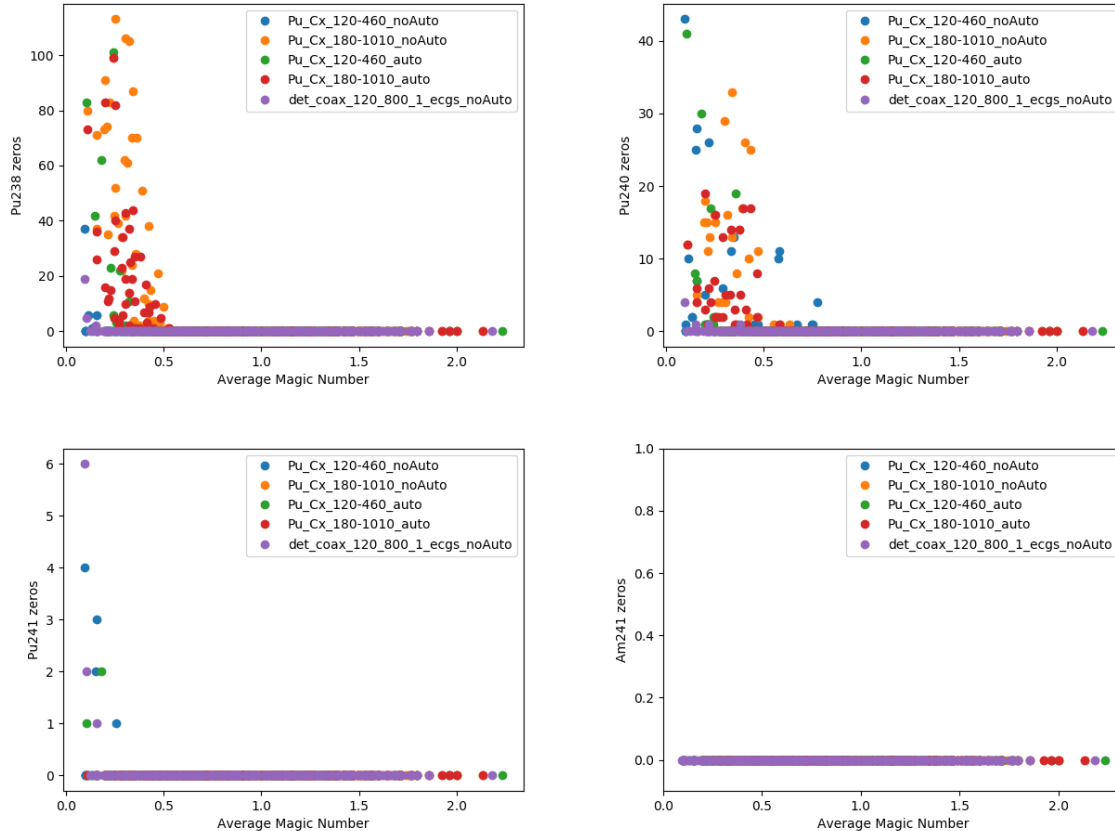


**Figure 12.** The average number of zeros of the various mass ratios as a function of statistical quality of the spectra, for all parameter sets

#### 4. Conclusion

The auto analysis option significantly improves the performance of the default parameter sets Pu\_Cx\_120-460 and Pu\_Cx\_180-1010. This option enables FRAM to distinguish, e.g., shielded and unshielded samples and automatically reanalyse the spectrum using a parameter set that is better suited for the particular setup. For the mass ratios relative to <sup>239</sup>Pu the default parameter sets (with auto analysis on) provide similar results, better than the set det\_coax\_120\_800\_1\_ecgs. However, for the <sup>239</sup>Pu fraction the set det\_coax\_120\_800\_1\_ecgs is superior to both default sets.

FRAM results heavily depend on the statistical quality of the spectra, as expected. An indicator, called the "magic number", was used in this work to measure the statistical quality of the spectra. If this number is below 1, then the bias of the results can go up several orders of magnitude, especially for the <sup>238</sup>Pu/<sup>239</sup>Pu mass ratio. For some of the measured samples the "magic number" does not go above 1, even for long measurement times and thin shielding.

A possible improvement could be to create parameter sets accompanying the set det\_coax\_120\_800\_1\_ecgs, in order to benefit from the possibilities offered by auto analysis.

These conclusions are valid for very old (>20 years), pure Pu samples. The extension of the studies to 1-2 years old MOX samples is planned.

## References

- [1] J. Zsigrai, A. Frigerio, J. Bagi, A. Mühleisen, and A. Berlizov, "Using FRAM to determine enrichment of shielded uranium by portable electrically cooled HPGe detectors," in *Proceedings of the 39th ESARDA Annual Meeting - Symposium, 16-18 May 2017, Düsseldorf, Germany*, 2017, pp. 80–86.
- [2] T. E. Sampson and T. A. Kelley, "PC/FRAM: A code for the non-destructive measurement of the isotopic composition of actinides for safeguards applications, LA-UR-96-3543," 1996.
- [3] T. E. Sampson, T. A. Kelley, and D. T. Vo, "Application Guide to Gamma-Ray Isotopic Analysis Using the FRAM Software, LA-14018," 2003.
- [4] D. T. Vo, "Operation and Performance of FRAM Version 5.1 Proceeding of the 52nd Annual Meeting of The Institute of Nuclear Materials Management, Palm Desert, CA, USA, July 17-21, 2011, LA-UR-11-03016," 2011.
- [5] "CBNM Nuclear Reference Material 271, Certificate of Analysis, Commission of the European Communities, Joint Research Centre, Central Bureau for Nuclear Measurements, Geel," Geel, 1989.
- [6] R.J.S. Harry, "PIDIE, plutonium isotopic determination inter-comparison exercise, ECN-RX--90-044," in *Annual Meeting of the Institute of Nuclear Materials Management*, 1990, no. July, pp. 15–18.
- [7] J. Morel and B. Chauvenet, "Intercomparaison des mesures de composition isotopique du plutonium par spectrometrie X et gamma. Resultats de l'action 'Pidie', rapport final, CEA Centre d'Etudes de Saclay, Gif-sur-Yvette (France). Dept. des Applications et de la Metrologie des Rayonnem."
- [8] J. Morel, B. Chauvenet, and M. Etcheverry, "Final results of the PIDIE intercomparison exercise for the plutonium isotopis determination by gamma spectrometry," in *Proceedings of the 13th ESARDA Symposium, Avignon, France*, 1991, pp. 251–257.
- [9] C. T. Chantler, K. Olsen, R. A. Dragoset, J. Chang, A. R. Kishore, S. A. Kotochigova, and D. S. Zucker, "Detailed Tabulation of Atomic Form Factors, Photoelectric Absorption and Scattering Cross Section, and Mass Attenuation Coefficients for Z = 1-92 from E = 1-10 eV to E = 0.4-1.0 MeV," 2005. [Online]. Available: <https://www.nist.gov/pml/x-ray-form-factor-attenuation-and-scattering-tables>. [Accessed: 01-Aug-2018].

# Optimization and Uncertainty estimation of the Enrichment meter Measurement Technique for UF<sub>6</sub> Cylinder

Jean-Luc DUFOUR, Nicolas PEPIN, Clement DEYGLUN and Anne-Laure WEBER

IRSN

Fontenay-Aux-Roses, France

Email: [jean-luc.dufour@irsn.fr](mailto:jean-luc.dufour@irsn.fr), [nicolas.pepin@irsn.fr](mailto:nicolas.pepin@irsn.fr), [clement.deyglun@irsn.fr](mailto:clement.deyglun@irsn.fr), [anne-laure.weber@irsn.fr](mailto:anne-laure.weber@irsn.fr)

## Abstract:

*IRSN carries out on-site non-destructive assay of nuclear material for domestic safeguards purposes in France. The paper presents the study of uncertainty components and the optimization of the traditional uranium enrichment meter method, applied to UF<sub>6</sub> in 30B and 48Y cylinders. Such calibration based gamma spectrometry technique measures the enrichment by quantifying the count rate in the 185.7 keV peak of uranium 235 in conditions of infinite thickness of the measured material. It is based on high resolution gamma spectrometry measurements coupled with ultrasonic gauge. The calibration is performed with the spectrometer in a collimated geometry using U<sub>3</sub>O<sub>8</sub> laboratory standards, whereas UF<sub>6</sub> assays performed on-site are un-collimated in order to reduce the inspection time. Therefore, corrections need to be done to correct for the differences between laboratory and on-site measurements, and associated uncertainties have to be taken into account. A measurement of the container wall thickness is performed using an ultrasonic gauge in order to correct the gamma-rays attenuation through the container wall. On-site tests and MCNP simulations were also performed to calculate a calibration transfer factor and evaluate the impact of different detector localizations on the count rate acquisition. In addition, these tests showed the impact of the background, mainly due to the higher energy gamma rays of U-238 daughters that Compton scattered within UF<sub>6</sub> and the detector. Finally, the measurement time was estimated, the use range of the technique was defined, and the measured uranium enrichment uncertainty was calculated.*

**Keywords:** enrichment; UF<sub>6</sub>; spectrometry; uncertainty; MCNP

## 1. Introduction

IRSN carries out on site non-destructive assay of nuclear material as part of its mission of technical assistance to the Authority responsible for the protection and control of nuclear material in France. In order to enlarge its measurement control capabilities to uranium hexafluoride (UF<sub>6</sub>) contained in 30B and 48Y cylinders, a study was conducted to develop a dedicated measurement system including software and mechanical support development. For this purpose, the traditional enrichment meter method was adapted to high resolution gamma spectrometry instrumentation and U<sub>3</sub>O<sub>8</sub> standards available within IRSN nuclear material metrology laboratory.

High resolution portable gamma spectrometry measurements are routinely used to verify the U-235 enrichment in large UF<sub>6</sub> cylinders applying the calibration based method known as enrichment meter method in conjunction with an ultrasonic measurement of the container wall thickness, which demonstrated to be a reliable method for inspection purposes [1], [2], [3], [4]. Calibration between the uranium enrichment and the net count rate of the 185.7 keV gamma-ray in a collimated geometry is performed at IRSN using four U<sub>3</sub>O<sub>8</sub> reference materials (U-235 from 0.7 to 89%) and a weighted least-squares linear regression. Due to the small dimensions of the reference materials (104 to 120 g of U<sub>3</sub>O<sub>8</sub> in 48 mm diameter by 26 to 33 mm filling height), the collimation needed during calibration to fulfil the infinite thickness conditions at 185.7 keV. But the collimation can't be applied on UF<sub>6</sub> cylinders on site with reasonable container inspection time [5]. It is then proposed here to measure the net

count rate of the 185.7 keV gamma-ray from the UF<sub>6</sub> container in a non-collimated geometry in order to reduce the container inspection time on-site and correct the differences in gamma-ray attenuation between the container wall of the U<sub>3</sub>O<sub>8</sub> reference material and the container wall of the 30B and/or 48Y cylinder, in measurement geometry and in chemical composition between the reference materials and the item to be measured. This paper presents the methodology and equipment implemented on-site in the framework of a qualification measurement campaign, and the study of uncertainty components. It also discusses some improvements prospects to reduce the measurement uncertainty.

## 2. Measurement principle

The enrichment meter method [6] is based on the proportional relation between U-235 enrichment value and count rate for the 185.7 keV gamma-rays for a calibration reference material and the inspected sample. If the detector views only a fraction of the uranium sample through a collimator, the 185.7 keV gamma rays from only a fraction of the total sample reach the detector because of the strong absorption of uranium. This is the "infinite thickness" criterion (Table 1 lists the mean-free-path and infinite-thickness values). The size of this visible volume is independent from the U-235 enrichment and only depends on the collimated geometry and uranium physicochemical properties.

Uranium Compound	Density	Mean Free Path (cm)	Infinite thickness (cm) *
Metal	18.7	0.04	0.26
UF <sub>6</sub> (solid)	4.7	0.20	1.43
UO <sub>2</sub> (powder)	2.0	0.39	2.75
U <sub>3</sub> O <sub>8</sub> (powder)	7.3	0.11	0.74

\*7 mean free path represent the distance for which the error in assuming infinite-sample size is less than 0.1%

**Table 1:** Mean free paths and infinite thickness for 185.7 keV gamma-rays in uranium compounds [6].

Such method presents limitations:

- Only the near surface depth of the uranium sample is interrogated, which means that the material must be isotopically uniform.
- The available reference materials are small and need a narrow collimator to fulfil the infinite thickness requirements which induce important measurement time. Large measurement times are possible during the calibration within the laboratory, but not consistent with on-site measurements. Thus, a calibration transfer function ( $C_{TFE}$ ) is calculated to measure on-site sample without collimation using calibration performed with collimation on reference materials.
- The calibration is performed with U<sub>3</sub>O<sub>8</sub> but at the end UF<sub>6</sub> is measured. The coefficient  $F/F'$  corrects for the difference of chemical composition.
- If the measured material is embedded within a container, the gamma-rays are attenuated by the container wall. The correction factor  $CF_c = e^{-\mu_c \rho_c T_c}$  corrects for such attenuation ( $\mu_c$ : attenuation coefficient of the container for 185.7 keV gamma-rays,  $\rho_c$ : container material density, and  $T_c$ : container wall thickness).
- The detector efficiency can change between the calibration in the laboratory and the measurement on-site. The correction factor  $CF_\epsilon$  corrects for the variations of efficiency.

Taking into account all these correction factors, U-235 enrichment  $E$  can be expressed as follows:

$$E = (A + B \times [R \times CF_c \times C_{TFE} \times CF_\epsilon]) \times \left(\frac{F}{F'}\right)$$

Where  $A, B$  are constants calculated during the calibration in collimated configuration with U<sub>3</sub>O<sub>8</sub> reference materials. The term in the bracket contains the measured net count rate at 185.7 keV obtained in non-collimated configuration ( $R$ ) and corrections factors. Each component is studied in the following paragraphs.

The measurement system implemented on-site contains a portable high resolution gamma spectrometer Detective type (AMETEK/ORTEC), a computer equipped with both Gammavision software (AMETEK/ORTEC) and in-house Enrichment software to drive the spectrum acquisition and

apply the enrichment meter method, a shielding, a collimator, a spectrometer positioning system and an ultrasonic measurement system. The measurement configuration is shown on Figure 1.

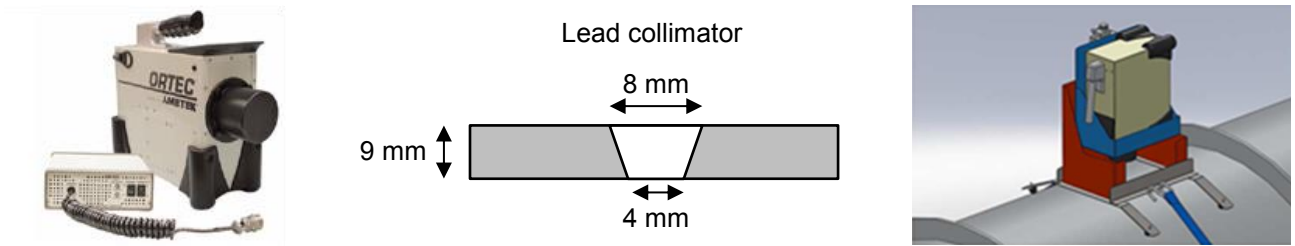


Figure 1: Measurement configuration.

### 3. Container wall impact

The component  $CF_c = e^{-\mu_c \rho_c T_c}$  corrects for the attenuation of gamma-rays by  $UF_6$  container wall.  $\mu_c$  and  $\rho_c$  are known thanks to a bibliographical study and the container wall thickness  $T_c$  can be measured directly using an ultrasonic thickness gauge at the measurement position. The process of container wall attenuation correction is presented in Figure 2.

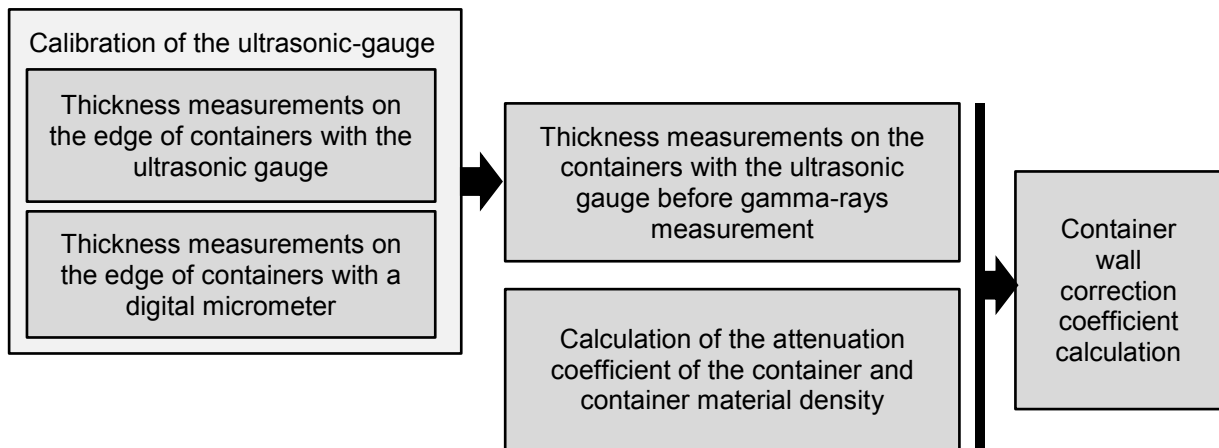
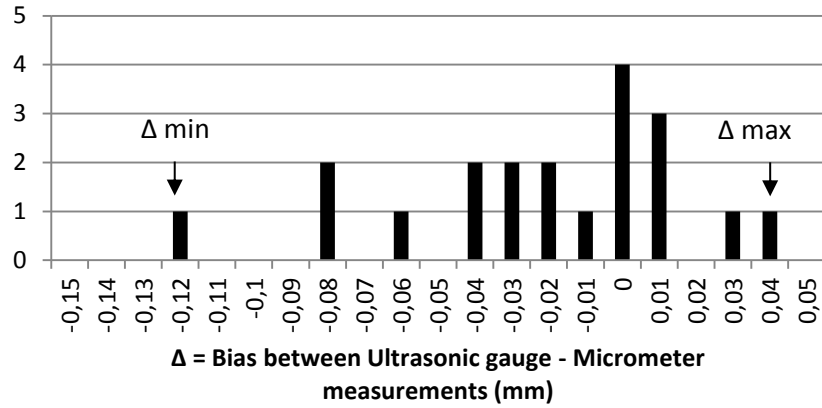


Figure 2. Container wall attenuation correction evaluation process.

#### 3.1. Container wall measurement T

In absence of a known reference standard stainless steel ASTM A516 Grade 65 type block, the ultrasonic gauge calibration was based on thickness measurements on the edge of  $UF_6$  containers with a digital micrometer (0.001 mm resolution and  $\pm 0.002$  mm precision), considered as a reference. Thickness measurements with the ultrasonic gauge were then performed at the same location adjusting the ultrasounds speed according to the thickness value measured with the micrometer. Once speed fixed, the bias and precision of the ultrasonic gauge was evaluated (Figure 3).



**Figure 3:** Distribution of the bias between the ultrasonic gauge and the micrometer during the measurement of the edge of containers.

The best measurements are obtained at a speed of 5925 m/s. The difference between the micrometer and the ultrasonic gauge measurements shows a uniform distribution. The precision and the bias are then calculated as follows:

$$precision = \frac{\Delta_{max} - \Delta_{min}}{2\sqrt{3}} = 0.046 \text{ mm}$$

$$bias = \frac{\sum_{i=1}^n \Delta_i}{n} = -0.043 \text{ mm}$$

The overall uncertainty on the container wall thickness  $u_{Tc}$  also includes components due to resolution, container paint thickness, ultrasound speed variations with temperature and container wall dilatation with temperature. These components are presented in Table 2.

$$u_{Tc} = \sqrt{u_{calib}^2 + u_{resol}^2 + u_{speed}^2 + u_{dilat}^2} = 0.118 \text{ mm}$$

Denomination	Comments	Evaluation
Calibration	Takes into account bias and precision from the calibration, but also additional bias sources such as the curvature of the container ( $u_{curve} = 0.012 \text{ mm}$ ) and coating ( $u_{coating} = 0.031 \text{ mm}$ ).	$u_{calib} = u_{precision} + \frac{ u_{bias} + u_{curve} + u_{coating} }{\sqrt{3}}$ $u_{calib} = 0.096 \text{ mm}$
Resolution	The resolution of the ultrasonic gauge is 0.01 mm. At each measurement there could be an error of $\pm 0.01/2 \text{ mm}$ .	Error is described by a uniform distribution : $u_{resol} = 0.01/2\sqrt{3}$ $u_{resol} = 2.887 \times 10^{-3} \text{ mm}$
Variation of ultrasounds speed with temperature	The ultrasound's speed depends on the matter temperature. If the gauge is calibrated at 20°C but the container wall is warmer, ultrasounds are slower and the wall appears thicker.	In winter, the container wall can be about -10°C and in summer 60°C (range of use defined by the manufacturer of the ultrasonic gauge) $u_{speed} [-10^\circ\text{C};60^\circ\text{C}] = 0.068 \text{ mm}$
Container wall dilatation with temperature	The dilatation of the wall decreases the matrix density and increases the thickness.	$u_{dilat} = 4.191 \times 10^{-3} \text{ mm}$

**Table 2:** Components of the wall thickness measurement overall uncertainty.

### 3.2. Container wall attenuation correction

The typical chemical composition of 30B or 48Y containers (ASTM A516) and maximal fractions are presented in Table 3.

C	Mn	Si	Al	P	S
0.18 (max=0.26)	1.05 (0.85-1.20)	0.32	0.04	0.015 (max = 0.035)	0.008 (max=0.035)

**Table 3:** Typical chemical composition of ASTM A516 Grade 65 and maximum [11].

$\mu_c \rho_c$  for 185.7 keV gamma-rays is calculated using XMuDat software [9] by assuming ASTM A516 Grade 65 and a density of 7.75. The coefficient is calculated for a typical composition and two “extreme” compositions:  $\mu_{min}$  is calculated with the minimal iron concentration and the maximum concentration for the other elements and  $\mu_{max}$  is calculated with only iron.

$$\mu_{typical\ composition} = 1.222\ cm^{-1}$$

$$\mu_{min} = 1.210\ cm^{-1}\ \text{and}\ \mu_{max} = 1.231\ cm^{-1}$$

We assume a uniform distribution of  $\mu$  between  $\mu_{min}$  and  $\mu_{max}$ , thus  $\mu_{wall} = \frac{\mu_{max} + \mu_{min}}{2} = 1.221\ cm$  and  $u_\mu = \frac{\mu_{max} - \mu_{min}}{2\sqrt{3}} = 0.006\ cm^{-1}$ .

### 3.3 Conclusion about the wall impact

The coefficient  $CF_c = e^{-\mu_c \rho_c T_c}$  corrects for the attenuation due to gamma-rays interactions within the wall of the container. The variance of the wall attenuation correction is given by the following expression:

$$u_{CF_c}^2 = \left( \frac{\partial e^{-\mu_c \rho_c T_c}}{\partial \mu_c \rho_c} \right)^2 u_{\mu_c \rho_c}^2 + \left( \frac{\partial e^{-\mu_c \rho_c T_c}}{\partial T_c} \right)^2 u_{T_c}^2$$

$$\left( \frac{u_{CF_c}}{CF_c} \right)^2 = \mu_c \rho_c T_c^2 \left[ \left( \frac{u_{\mu_c \rho_c}}{\mu_c \rho_c} \right)^2 + \left( \frac{u_{T_c}}{T_c} \right)^2 \right]$$

## 4. Impact of the detector location

The distribution of solid  $UF_6$  inside the container is an important, but unknown, measurement parameter. MCNP6 [10] simulations were performed to determine the influence of the detector position and the filling level on the enrichment measurement. On-site tests were also performed to check simulation results.

### 4.1. MCNP6 simulations

MCNP6 was used to model the gamma-rays transport through  $UF_6$  and 30B cylinder. Tally F5 (flux at a point) was used for the gamma-rays spectrum detection and only 185.7 keV gamma-rays were generated. Many hypotheses are assumed for the model:

- H1. Uniform properties of  $UF_6$  (uniform chemical, isotopic composition and uniform density);
- H2. Gamma-rays emitted by the gaseous  $UF_6$  neglected;
- H3. Uniform wall thickness.

The impact of the detector location and the filling level on measurement results is studied by considering different detector locations on 30B container and filling level. Three locations (D1, D2 and D3) and seven filling levels were studied as described on Figure 4.

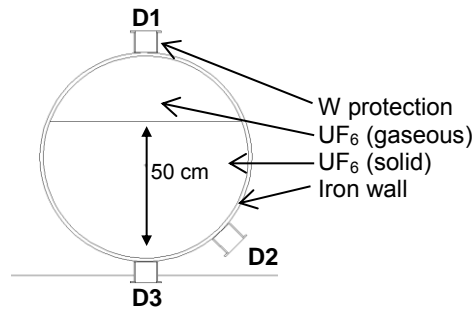


Figure 4: MCNP model of 30B container, detectors and filling level.

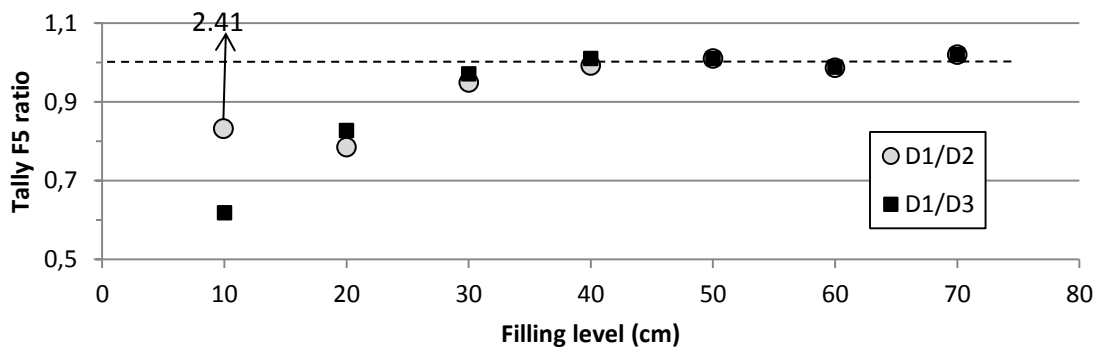


Figure 5: Ratios of tally F5 for different localization (D1, D2 and D3) and filling levels.

As we can see on Figure 5, for filling level higher than 30 cm (approximately 2180 kg) locations D1, D2 and D3 can be interchangeably used.

#### 4.2. On-site measurements

The influence of the detector position on the enrichment measurement is evaluated experimentally for seven detector locations along a 30B container (filled with 2200 kg of UF<sub>6</sub>, at 1.41% enrichment). At each detector position, a thickness measurement is performed with the ultrasonic gauge to correct for the attenuation of the photons in the container wall. Locations and results are provided in Figure 6.

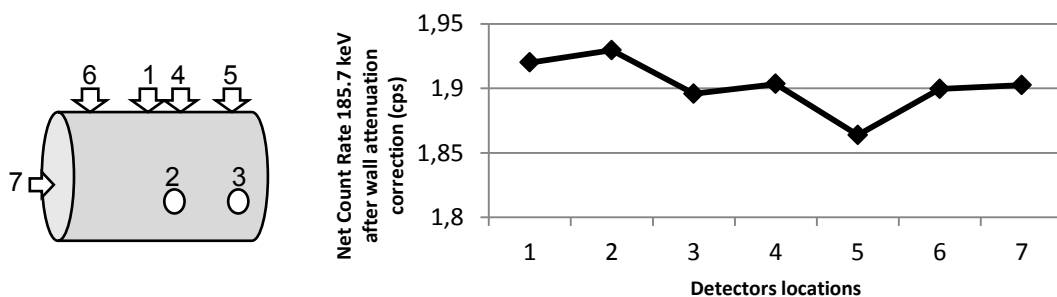


Figure 6: Impact of the detector localization on the 185.7 keV gamma-rays count rate (on-site measurements).

The relative standard deviation of the distribution of the count rate according to the detector position is around 1.1%, which is less than the repeatability uncertainty (1.35%).

#### 4.3. Conclusion about the detector location

Simulation and on-site measurements show that detectors at the top and on the side of the container can be interchangeably used if the 30B container contains at least 2200 kg of UF<sub>6</sub>. A measurement position at the top of the container and centred along the cylinder axis has two advantages:

- It is the most practical location to install the system,
- The acquisition is less impacted by the background generated by surrounding containers.

### 5. Correction due to the differences in chemical composition between reference materials and item to be measured

The coefficient  $\frac{F}{F'}$  corrects the predicted enrichment from the differences in chemical composition between the reference material and the item to be measured (based on the data in Table 4 [6]). In case of UF<sub>6</sub> enrichment measurements based on a calibration performed with U<sub>3</sub>O<sub>8</sub> samples, a correction factor 1.02 needs to be applied to the enrichment value obtained from the calibration.

Nuclear Material of Calibration Standards (Factor F')	Nuclear Material of Items Measured (Factor F)					
	U	UC	UC <sub>2</sub>	UO <sub>2</sub>	U <sub>3</sub> O <sub>8</sub>	UF <sub>6</sub>
U (100% U)	1.00	1.00	1.00	1.01	1.01	1.04
UC (95% U)	1.00	1.00	1.00	1.01	1.01	1.03
UC <sub>2</sub> (91% U)	0.99	1.00	1.00	1.00	1.01	1.03
UO <sub>2</sub> (88% U)	0.99	0.99	1.00	1.00	1.00	1.03
U <sub>3</sub> O <sub>8</sub> (85% U)	0.99	0.99	0.99	1.00	1.00	1.02
UF <sub>6</sub> (68% U)	0.96	0.97	0.97	0.98	0.98	1.00
U nitrate (47% U)	0.92	0.92	0.93	0.93	0.93	0.95

Table 4: Material composition correction factors (F/F') [6].

Table 4 doesn't provide any associated uncertainties  $u_{F/F'}$ . Taking two ratios  $F/F'$  with small difference, e.g.  $F/F'_1=1$  and  $F/F'_2=1.01$ , these two values are random values with mean 1 and 1.01 and associated uncertainties  $u_{F/F'_1}$  and  $u_{F/F'_2}$ . If we use the classic comparison test to compare the two means:

$$\frac{\left|F/F'_1 - F/F'_2\right|}{3\sqrt{u_{F/F'_1}^2 + u_{F/F'_2}^2}} < 1$$

If this test is true, the two means can be considered equals with "false alarm" probability of 0.26% and the difference is due to their associated uncertainties  $u_{F/F'_1}$  and  $u_{F/F'_2}$ .  $\left|F/F'_1 - F/F'_2\right| = 0.01$  and the inequality becomes  $3\sqrt{u_{F/F'_1}^2 + u_{F/F'_2}^2} > 0.01$ . If we assumed the two uncertainties  $u_{F/F'_1}$  and  $u_{F/F'_2}$  are equal, i.e.  $u_{F/F'_1} = u_{F/F'_2} = u_{F/F'}$ , the inequality becomes  $3\sqrt{2u_{F/F'}^2} > 0.01$  and  $u_{F/F'} = \frac{0.01}{3\sqrt{2}} = 0.0024$ .

### 6. Correction due to the non-collimated geometry

Calibration with reference materials is performed in a collimated configuration to fulfil the infinite thickness requirements. By removing the collimator during on-site measurements on UF<sub>6</sub> cylinders, the calibration conditions are modified and then the counting rate measured for an unknown sample needs to be corrected with a calibration transfer function (C<sub>FTE</sub>). C<sub>FTE</sub> is derived from the ratio between the counting rates at 185.7 keV recorded in the two measurement configurations, with and without collimation. MCNP6 simulations were performed to determine the coefficient C<sub>FTE</sub> and compared with on-site measurements.

**6.1. MCNP6 simulations**

MCNP6 was used to model the gamma-rays transport through UF<sub>6</sub>, 30B cylinder and HPGe detector. A precise model of a 12% relative efficiency p-type HPGe coaxial detector was created for photon detection, see Figure 7. Detector resolution and dead layers were determined by different experiments. The model was validated by comparing calculated and experimental full energy peak counting and FWHM for a Eu-152 source.

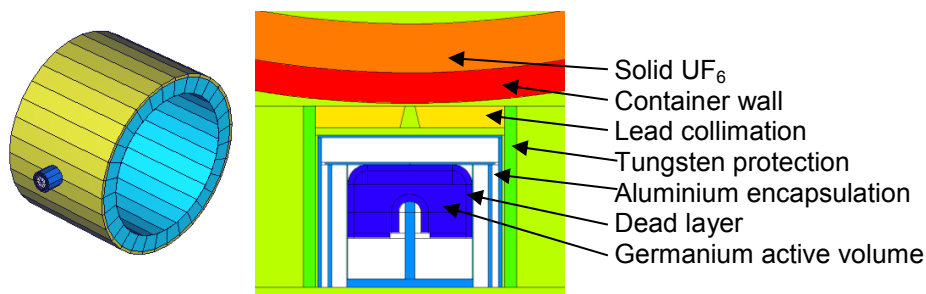


**Figure 7:** Model of the HPGe detector in collimated configuration (lead collimateur is replaced by air in the non-collimated configuration).

The gamma spectra are obtained using tally F8 (pulse height distribution). Collimated and non-collimated simulation results are presented in Figure 8.

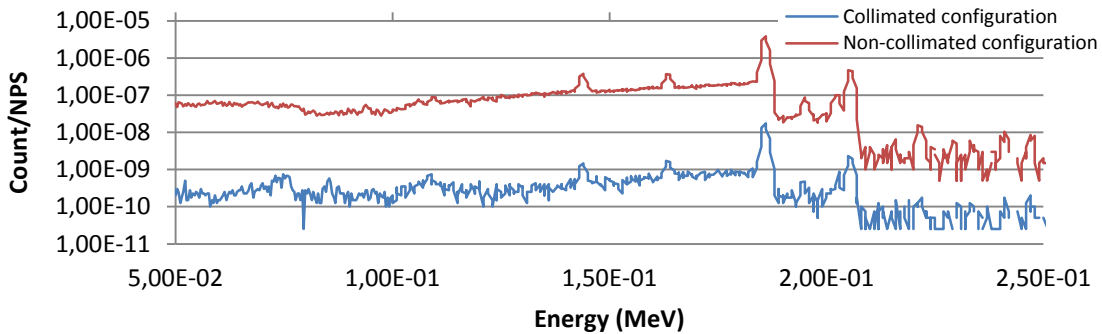


**Figure 8.** MCNP6 spectra of U-235.

C<sub>FTE</sub> is derived from the ratio between the counting rates at 185.7 keV recorded in the two measurement configurations, with and without collimation, and estimated at 0.00456. The associated uncertainty (u<sub>C<sub>FTE</sub></sub>) includes components due to the trueness of the model, statistic and the software deconvolution uncertainties  $u_{C_{FTE}} = \sqrt{u_{model}^2 + u_{stat}^2 + u_{peak}^2} = 9.23\%$ . These components are presented in Table 5.

Designation	Origin	Estimation	Comments
<i>u<sub>model</sub></i>	Adjustment of the MCNP model.	4.65%	Estimated with Eu-152 source between 80 keV and 1408 keV.
<i>u<sub>stat.</sub></i>	Statistical uncertainty of Monte Carlo simulation.	7.65%	Mainly due to the low efficiency of the collimated configuration. Uncertainty

			could be reduced by increasing the calculation time.
$U_{peak}$	Subtraction of the continuum background of the peak area	2.23%	The simulation is free from the background continuum due to U-238.

**Table 5:** Components of  $u_{C_{FTE}}$ .

### 6.2. Experimental $C_{FTE}$

Experimental measurements have been performed on one 30B container to estimate  $C_{FTE}$ . Three 120 seconds measurement time acquisitions are enough to get good counting statistics in non-collimated configuration, but the collimated configuration needs long measurement time (>13h) to have a good statistical uncertainty. The counting rates recorded in the collimated configuration on the side and at the top of the container are different due to the background from the other containers.  $C_{FTE}$  was calculated with the system at the top of the container, where the background contribution of the neighbors' containers is small, and estimated to 0.00476.

NB:

- The difference of counting rate between the two locations was not observed with simulations because only the measured container was modeled.
- To reduce the continuum background impact lead protections around the detector could be added.

$C_{FTE}$  is derived from the ratio between the net counting rates at 185.7 keV recorded in the two measurement configurations, with and without collimation.

$$C_{FTE} = \frac{R_{with\ colli}}{R_{without\ colli}}$$

$$C_{FTE} = \frac{\frac{N_{with\ colli}}{t_{with\ colli}}}{\frac{N_{without\ colli}}{t_{without\ colli}}}$$

Where  $N_{with\ colli}$  is the number of detected 185.7 keV gamma-rays for the collimated configuration and  $t_{with\ colli}$  the measurement time. Thus, the associated uncertainty  $\left(\frac{u_{C_{FTE}}}{C_{FTE}}\right)^2$  is expressed as follows:

$$\left(\frac{u_{C_{FTE}}}{C_{FTE}}\right)^2 = \left(\frac{u_{N_{with\ colli}}}{N_{with\ colli}}\right)^2 + \left(\frac{u_{N_{without\ colli}}}{N_{without\ colli}}\right)^2$$

$$\frac{u_{C_{FTE}}}{C_{FTE}} = 3.40\%$$

NB: the contribution of the measurement time uncertainties  $\left(\frac{u_{t_{with\ colli}}}{t_{with\ colli}}\right)^2$  and  $\left(\frac{u_{t_{without\ colli}}}{t_{without\ colli}}\right)^2$  are neglected.

Despite a long measurement time, the relative uncertainty related to the counting rate with collimation is large (3.4%) due to the poor signal to noise ratio that can be attributed to the Compton continuum of higher energy photons mainly coming from the large amounts of U-238 in the item and the bremsstrahlung emitted by its daughters.

### 6.3. Conclusion about $C_{FTE}$

MCNP6 was used to estimate the calibration transfer function correction but modelling uncertainties and simulation time induce large uncertainties. At the end, the experimental  $C_{FTE}$  has a better uncertainty.  $C_{FTE}$  is needed because on-site measurements and calibration conditions are different.

Calibration could be performed in no-collimated configuration based on large UF<sub>6</sub> reference samples. This could speed up the calibration process and reduce the associated uncertainty.

## 7. Calibration and Inverse Calibration

The reference materials available within the laboratory are four U<sub>3</sub>O<sub>8</sub> powder samples, infinitely thick with respect to the 185.7 keV gamma emission, embedded in a POMC (Acetal Copolymer) container. Their characteristics are summarized in **Erreur ! Source du renvoi introuvable.**

U <sub>3</sub> O <sub>8</sub> Mass (g)	Enrichment (wt %)	Enrichment Unc. (wt %)
120.9	0.714	0.005
114.73	3.038	0.018
106.81	29.187	0.018
104.74	89.303	0.018

**Table 6:** Reference materials <sup>235</sup>U enrichment.

The calibration is performed in a collimated geometry as follows: the reference material is placed on the collimator which is itself positioned against the germanium detector front face, both of them being centred on the coaxial germanium detector axis. The calibration consists in measuring the net counting rate at 185.7 keV for each reference material using the ROI (Region Of Interest) report option of Gammavision software ( $R_i$ ), apply the correction factor  $CF_r$  to correct it from the attenuation of the wall thickness and apply a weighted least-squares linear regression to the couples ( $R_i, E_i$ ),  $E_i$  being the U-235 enrichment value given by the certificate. The measurement time was defined in order to get a counting statistics of around 1% in the 185.7 keV net peak area.

The application of the weighted linear least-squares regression to the couples ( $R_i, E_i$ ), using as weight ( $g_i = \frac{1}{s_i^2}$ ) the inverse of the variance of the counting rate, leads to calibration factors  $a = -0.011496151$  and  $b = 0.806211927$  (calibration  $R = a + b \times E$ ). The coefficients  $a$ ,  $b$  and  $\bar{R}$  are given by the following expressions:

$$b = \frac{\sum g_i \sum g_i E_i R_i CF_r - \sum g_i E_i \sum g_i R_i CF_r}{\sum g_i \sum g_i E_i^2 - (\sum g_i E_i)^2}$$

$$b = CF_r \frac{\sum g_i \sum g_i E_i R_i - \sum g_i E_i \sum g_i R_i}{\sum g_i \sum g_i E_i^2 - (\sum g_i E_i)^2}$$

$$\bar{R} = \frac{\sum g_i R_i CF_r}{\sum g_i} = CF_r \frac{\sum g_i R_i}{\sum g_i}$$

And

$$a = \bar{R} - b\bar{E}$$

NB: The correction factor due to the attenuation from reference material container wall ( $CF_r$ ) is estimated experimentally by performing the ratio  $CF_r = \frac{R_0}{R}$ , where  $R_0$  is the counting rate measured at 184.4 keV with a <sup>166m</sup>Ho source and  $R$  the counting rate measured when an equivalent container wall is installed between the detector and this source.

The enrichment of an “unknown” item can then be predicted using the inverse calibration.

$$R = a + b \times E$$

$$E = A + R \times B$$

Where  $R$  is the measured net counting rate at 185.7 keV obtained in non-collimated configuration,  $E$  the unknown U-235 enrichment,  $A = -\frac{a}{b}$  and  $B = \frac{1}{b}$ .

### 8. Overall uncertainty

The U-235 enrichment is calculated as follows:

$$E = (A + B \times [R \times CF_c \times C_{FTE} \times CF_\epsilon]) \times \left(\frac{F}{F'}\right)$$

Or

$$E = \frac{-a + R \times CF_c \times C_{FTE} \times CF_\epsilon}{b} \times \left(\frac{F}{F'}\right)$$

Where:

- $a, b, A, B$  are constants calculated from the calibration with the reference materials  $U_3O_8$  in collimated configuration (see §7),
- $R$  is the measured net counting rate at 185.7 keV obtained in non-collimated configuration,
- $CF_c$  corrects for the container wall attenuations,
- $C_{FTE}$  corrects for the difference of configuration between measurement in laboratory (collimated configuration) and on-site (non-collimated configuration),
- $CF_\epsilon$  corrects for efficiency variations between measurement in laboratory and on-site,
- $\frac{F}{F'}$  corrects for the difference of chemical composition between the reference material and the measured sample.

The enrichment measurement uncertainty is calculated as follows:

$$u_E = \sqrt{u_{\text{Calibration}}^2 + u_{\frac{F}{F'}}^2 + u_{\text{Trueness}}^2}$$

Where :

- $u_{\text{Calibration}}^2$  depends mainly on the regression model, counting rates uncertainties and corrections applied to these counting rates. Enrichment can be expressed as follows,  $E_{\text{after } \frac{F}{F'} \text{ correction}} = E_{\text{before } \frac{F}{F'} \text{ correction}} \times \frac{F}{F'}$  and thus  $u_{\text{Calibration}}^2 = E_{\text{after } \frac{F}{F'} \text{ correction}}^2 \left( \frac{u_{E_{\text{before } \frac{F}{F'} \text{ correction}}}}{E_{\text{before } \frac{F}{F'} \text{ correction}}} \right)^2$
- $u_{\frac{F}{F'}}^2$  is evaluated based on a difference of 0.01 between the ratios of two matrix material composition correction factors.
- $u_{\text{Trueness}}^2$  is evaluated from the known enrichment items measurements . It is calculated considering a rectangular distribution of the bias, i.e.  $u_{\text{Trueness}} = \frac{|\sum_{i=1}^n (E_{\text{Reference}_i} - E_{\text{Measured}_i})|}{n \cdot \sqrt{3}}$

The inverse calibration is applied to the corrected count rate  $R_{\text{corrected}}$  in order to determine the predicted the enrichment  $\left(E_{\text{before } \frac{F}{F'} \text{ correction}}\right)$ :

$$\overline{R_{\text{corrected}}} = \bar{R} C_{FTE} C_{FC} C_\epsilon \quad u_{\overline{R_{\text{corrected}}}} = \overline{R_{\text{corrected}}} \sqrt{\left(\frac{u_{\bar{R}}}{\bar{R}}\right)^2 + \left(\frac{u_{CF_c}}{CF_c}\right)^2 + \left(\frac{u_{CFTE}}{C_{FTE}}\right)^2 + \left(\frac{u_{C_\epsilon}}{C_\epsilon}\right)^2}$$

$$E_{\text{before } \frac{F}{F'} \text{ correction}} = \left(\frac{R \times C_{PCE} \times C_{FTE} \times C_\epsilon - a}{b}\right)$$

$u_{E_{\text{before } \frac{F}{F'} \text{ correction}}}$  represents the estimation of the predicted enrichment uncertainty (before  $\frac{F}{F'}$  correction) and is calculated from the confidence interval of the predicted enrichment  $IC_{\text{Regression}}$ .

Assuming that the confidence interval variable follows a rectangular probability law, the uncertainty associated to the predicted enrichment is given by  $u_{E_{before \frac{F}{F_1} correction}} = \frac{IC_{Regression}}{2\sqrt{3}}$ .

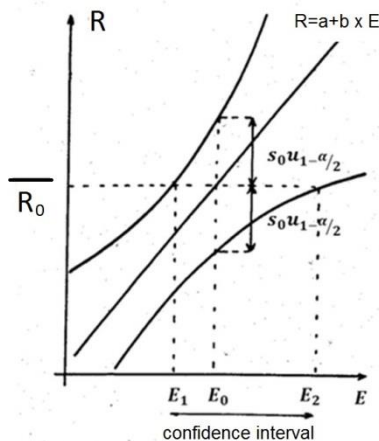


Figure 9. The enrichment confidence interval.

The enrichment confidence interval  $IC_{Regression}$  is limited by  $E_1$  et  $E_2$  (see Figure 9). These boundaries are calculated through the intersection between  $R = \bar{R}_0$  and  $R = a + bE \pm S_0 u_{1-\frac{\alpha}{2}}$ ,  $u_{1-\frac{\alpha}{2}}$  = normal restricted variable = 3 (false alarm risk ~0.26%).

$E_1$  and  $E_2$  are calculated by resolving the two following degree 2 equations :  $\bar{R}_0 = a + bE_0 + S_0 u_{1-\frac{\alpha}{2}}$  and  $\bar{R}_0 = a +$

$$bE_0 - S_0 u_{1-\frac{\alpha}{2}}, \text{ with } S_0 = \sqrt{S_{Rcorrected}^2 + \frac{1}{\sum g_i} + \frac{(E_0 - \bar{E})^2 \sum g_i}{\sum g_i \sum g_i E_i^2 - (\sum g_i E_i)^2}}$$

The confidence interval  $IC_{Regression}$  is then made symmetrical by calculating the boundaries  $E_1 = E_0 - \text{Max}(|E_0 - E_1|, |E_0 - E_2|)$  and  $E_2 = E_0 + \text{Max}(|E_0 - E_1|, |E_0 - E_2|)$

## 9. Conclusions

On-site measurement on UF6 containers and numerical simulations contributed to the validation of the U-235 enrichment calibration based method relying on the small dimensions reference materials available at IRSN. Only small  $U_3O_8$  reference materials are available at IRSN so that collimation is needed to fulfil the infinite thickness conditions during calibration. On the other hand, in order to make on-site verifications compatible with time inspection constraints, the 185.7 keV net counting rate is measured in a non-collimated geometry. Therefore a transfer function between the two different geometries is applied. Such correction was estimated both experimentally and numerically with a good agreement between both of them, but a better uncertainty associated to the experimental evaluation. Longer simulations times and accurate models should improve simulation uncertainty.

The measurement uncertainty, around 5% for low enriched uranium and 10% for depleted uranium, could be improved in the future. Peak-fitting algorithms could be investigated in order to extract net peak area from a high background continuum with a better accuracy. The geometry transfer function coefficient could be useless if the calibration was performed with large uranium reference sample.

## 10. References

- [1] IAEA Safeguards techniques and equipment: 2011 edition, International Nuclear Verification Series n°1 (Rev2).
- [2] International Target Values 2010 for Measurement Uncertainties in Safeguarding Nuclear Materials, STR-368, IAEA, Vienna, November 2010.
- [3] MORTREAU, P., BERNDT, R., "Handbook of gamma spectrometry methods for non-destructive assay of nuclear materials", EUR 19822 EN, Joint Research Centre, Ispra, third revision June 2006.
- [4] MONTGOMERY, J.B., "Enhanced Techniques and improved Results in 235U Enrichment Measurement of Large UF6 Cylinders by Portable Germanium Spectrometer", Journal of Nuclear Materials Management, Winter 2006, Volume XXXIV, N°2.
- [5] DUFOUR, JL., PEPIN N., "Mesure d'enrichissement de l'UF6 en conteneur 30B et 48Y", PDS-DEND/SATE/2013-0748

[6] REILLY, D., ENSSLIN, N., SMITH, H., KREINER, S., "Passive Nondestructive Assay of Nuclear Materials, NUREG/CR-5550, LA-UR-90-732, March 1991.

[7] FEINBERG, M., "Labo-Stat: Guide technique d'accréditation pour l'évaluation des incertitudes de mesure en biologie médicale" SH GTA 14 Rev00".

[8] CETAMA, "Statistique appliquée à l'exploitation des mesures", Ed. MASSON, 1986, 2nd edition.

[9] NOWOTNY, R., "XMuDat : photon attenuation data on PC", version 1.0.1 of August 1998, Institut f. Biomed. Technik und Physik, Univ. Wien, AKH-4L

[10] D. B. PELOWITZ, ed., MCNP6 User's Manual, Version 1.0, Los Alamos National Laboratory report LA-CP-13-00634 (May 2013).

[11] Specification for pressure vessel plates, carbon steel, for moderate- and lower- temperature service, SA-516/SA-516M, 2009b Section II, Part. A

# Poster Session 1: Focus on NDA

# Spectroscopic SiPM based Fast Neutron Detector for Safeguard Applications

**Mohsen Meshkian<sup>1</sup>, Ulisse Gendotti<sup>1</sup>, Giovanna Davatz<sup>1</sup>, Rico Chandra<sup>1</sup>,  
Christoph Philipp<sup>1</sup>, Marco Panniello<sup>1</sup>, Jan Nowakowski<sup>1</sup>**

<sup>1</sup>Arktis Radiation Detectors Ltd., 8045 Zurich, Switzerland  
E-mail: meshkian@arktis-detectors.com

## **Abstract:**

*Traditionally, instruments in the field of nuclear safeguards have relied on He-3 based thermal neutron counters, providing detection capabilities highly desired by such nuclear facilities for many years. Following the He-3 supply crisis in the past decade, novel and innovative He-3-free neutron detectors have been designed and built as replacements, including Commercial Off the Shelf S670 detector series provided by Arktis Radiation Detectors Ltd. These detectors provide advantages such as direct fast neutron detection, precise timing information of the interacting neutron, and rugged SiPM-based light read-out. In addition, the integrated signal processing board performs gamma/neutron discrimination and provides energy deposition information without using digitizers.*

*Recently, such detectors were integrated in an innovative plutonium detection system (PHUMS), for mapping plutonium hotspots, making it lightweight and highly maneuverable compared to conventional systems.*

*The following paper summarizes the performance evaluation of the S670 detectors under various neutron test conditions at the National Metrology Institute of Germany (PTB). The test conditions included a range of low to high neutron energies (144 keV, 565 keV, 1.2 MeV, 2.5 MeV, 5 MeV and 14.8 MeV) to provide an insight on the energy discrimination capabilities of S670 detectors in order to validate their feasibility as nuclear safeguards instruments. The measurements demonstrate crucial energy discrimination capabilities and neutron spectrometry for use in various inspection systems, e.g. safeguards, fuel cask content monitoring, etc.*

**Keywords:** <sup>3</sup>He alternatives; <sup>4</sup>He scintillation; Energy discrimination; Fast Neutron Detection

## **1. Introduction**

Arktis Radiation Detectors Ltd. manufactures <sup>4</sup>He-gas based fast neutron detectors, utilizing the elastic scattering property of the gas, which both serves as the neutron detection and scintillation medium. Selection of <sup>4</sup>He over <sup>3</sup>He as a detection medium is natural as the former stands out as the cheaper alternative, without utilizing a moderator. Previously, it has been demonstrated that the <sup>4</sup>He detector has a wide range of applications, such as measurement of plutonium content in mixed oxide fuel [1], detection of hidden shielded nuclear material [2], and applications in nuclear safeguards and homeland security [3].

The current work focuses on the characterization of <sup>4</sup>He fast neutron detectors by determination of the detector response for neutron energies ranging from 0.144 MeV up to 14.8 MeV. The experimental work was carried out in the low-scatter measurement hall of the PTB accelerator facility (PIAF).

## 2. Helium-4 Detectors

$^4\text{He}$  is an excellent detection medium as it possesses a resonance peak in (n, elastic) cross section around 1 MeV. Succinctly, a helium nucleus gains kinetic energy, from an incident neutron, which in turn excites or ionizes other helium nuclei along its path through the gas, resulting in production of excimers (singlet and triplet excited states). Subsequently, scintillation light is produced as these excimers decay to the ground state. The scintillation mechanism in pressurized  $^4\text{He}$  gas has been thoroughly outlined in [4]. Finally, the light is read out by a series of silicon photomultipliers (SiPM).

The benefits with SiPM based detectors compared to their PMT based counter partners include, insensitivity to magnetic fields, compactness and rugged, cost efficient at large scale production, etc. [5]. The PMT based  $^4\text{He}$  detectors consists of two opposing PMTs at either end of the active volume. The neutron response of such detectors has previously been characterized and reported in [6]. Furthermore, pressurized  $^4\text{He}$  detectors demonstrate performance advantages such as low gamma-ray sensitivity and good pulse shape discrimination capability, making them attractive for applications with high gamma-ray background, such as fission neutron detection from spent fuel assay. Additionally, incident neutron energy retention is possible with  $^4\text{He}$  based detectors due to the lack of moderating materials, which are in contrary crucial for functionality of  $^3\text{He}$  based detectors as these rely on the absorption of thermal neutrons in the gas [7, 8].

The neutron detectors of interest are uniquely designed; having three optically separated segments, each having four pairs of SiPMs that are equilaterally positioned along the SiPM-strip. The design allows for full immersion of the SiPMs inside the pressurized (180 bar)  $^4\text{He}$  gas volume. On-board electronics perform digital pulse shape discrimination to reject gamma-induced events and provide a pulse for every detected neutron. Robustness is achieved by eliminating fragile components such as crystals, photomultiplier tubes and sensitive anode wires.

## 3. Experimental Methods

The neutron irradiations were carried out in the low-scatter measurement hall, 24 x 30 x 14 m<sup>3</sup>, at the PTB accelerator facility (PIAF). The irradiations utilized quasi-monoenergetic neutron fields with mean energies of the direct neutrons of 0.144, 0.565, 1.2, 2.5, 5 and 14.8 MeV. The fields were produced according to the general recommendations of the ISO standard [9-11].

Neutron energy (MeV)	Fluence rate ( $10^5 \text{ cm}^{-2}$ )
0.144	1.40
0.565	2.23
1.2	6.41
2.5	2.41
5	Not known
14.8	6.49

**Table 1:** Neutron energies with corresponding fields, measured at approximately 3 m.

The  $^4\text{He}$  neutron detectors were positioned perpendicularly to the direction of the ion beam for homogenous irradiation of the detector segments, as well as simultaneous irradiation of all the detectors of interest. The detectors were supported and enclosed by foamed material. The distance between the neutron production target and the detectors was around 300 cm. The area between the two horizontally placed detectors intercept the neutron beam, as shown in Figure 1.



**Figure 1:** Setup for the irradiation of the  $^4\text{He}$  detectors. The distance  $d$  is measured from the position of the reactive target layer to the plane containing the vertical axes of the two detectors.

The scintillation pulse height depends on the incident neutron energy and subsequent scattering kinematics given by  $^4\text{He}$  ( $n$ , elastic). Therefore, the amount of energy from the incident neutron to the recoiled  $^4\text{He}$  particle is given by:

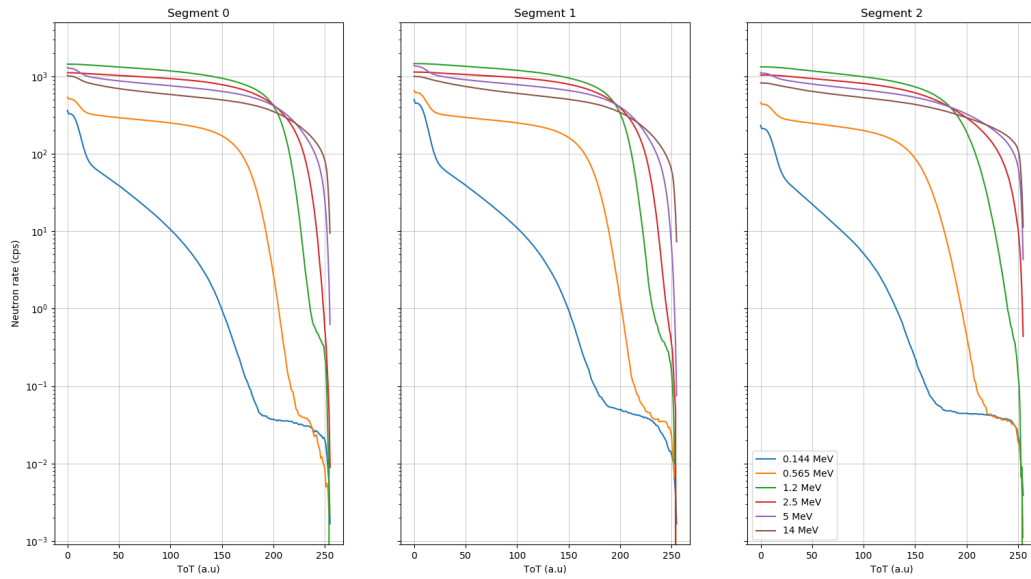
$$E_R = 0.32(1 - \mu)E_i$$

where  $E_i$  is the incident neutron energy and  $\mu$  is the scattering cosine in the center of mass coordinate. The maximum energy transfer equals  $0.64E_i$  when  $\mu = -1$ .

Measurements create a ToT (Time-over-Threshold)-histogram for each segment (see Figure 2). The ToT parameter represents the duration of the detector signal above a predefined pulse height threshold, the so-called *offset*, with values between 400 and 5000. Therefore, the ToT shows a logarithmic relationship with the energy deposited in the scintillator, as larger energy depositions result in longer pulses.

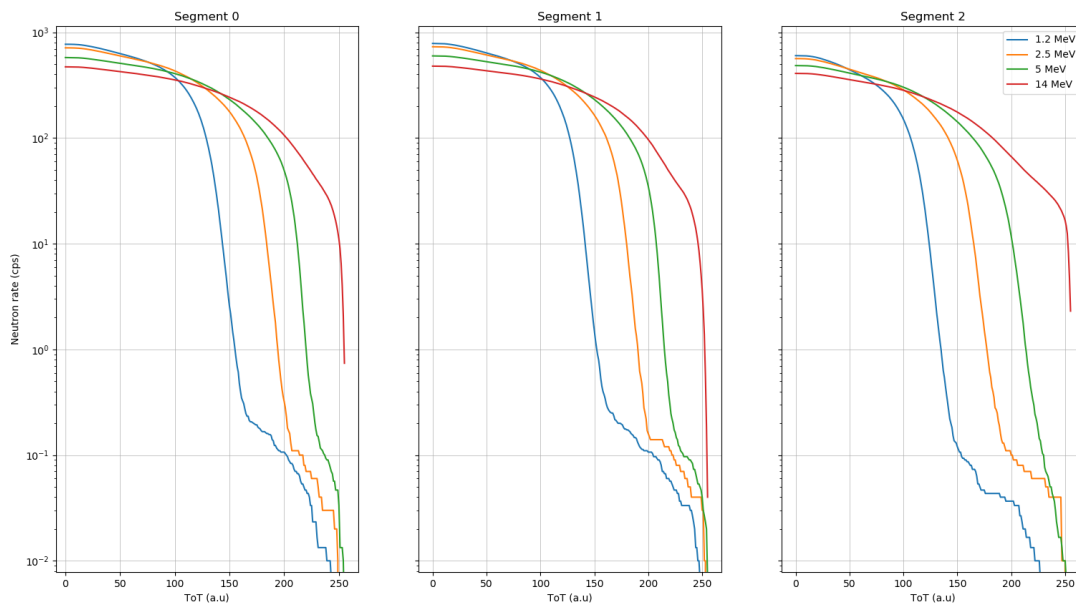
#### 4. Results and Discussion

Figure 2 shows the light collection output for various incident neutron energies, as measured by the  $^4\text{He}$  detector at PTB. The response of the detector is plotted for the incident neutron energies of 0.144, 0.565, 1.2, 2.5, 5, and 14 MeV for offset 600.



**Figure 2:** The response of the neutron detector to different neutron energies at offset 600.

The number of detected neutrons for each incident neutron energy is dependent on the neutron flux from the target, as well as the elastic cross-section of  $^4\text{He}$ . Theoretically, the detector response, for each incident neutron energy, has a sharp cut-off on the upper edge, which corresponds to the maximum energy transfer given by the equation above. The cut-off of the distribution is depicted in Figure 4.



**Figure 3:** The detector response for 1.2, 2.5, 5, and 14.8 MeV neutrons for offset 3000.

Furthermore, utilization of the cut-offs from Figure 3, as well as calculating the maximum energy transfer for the incident neutron energies result in Figure 4, which depicts the relationship between the measured ToT output and deposited energy.

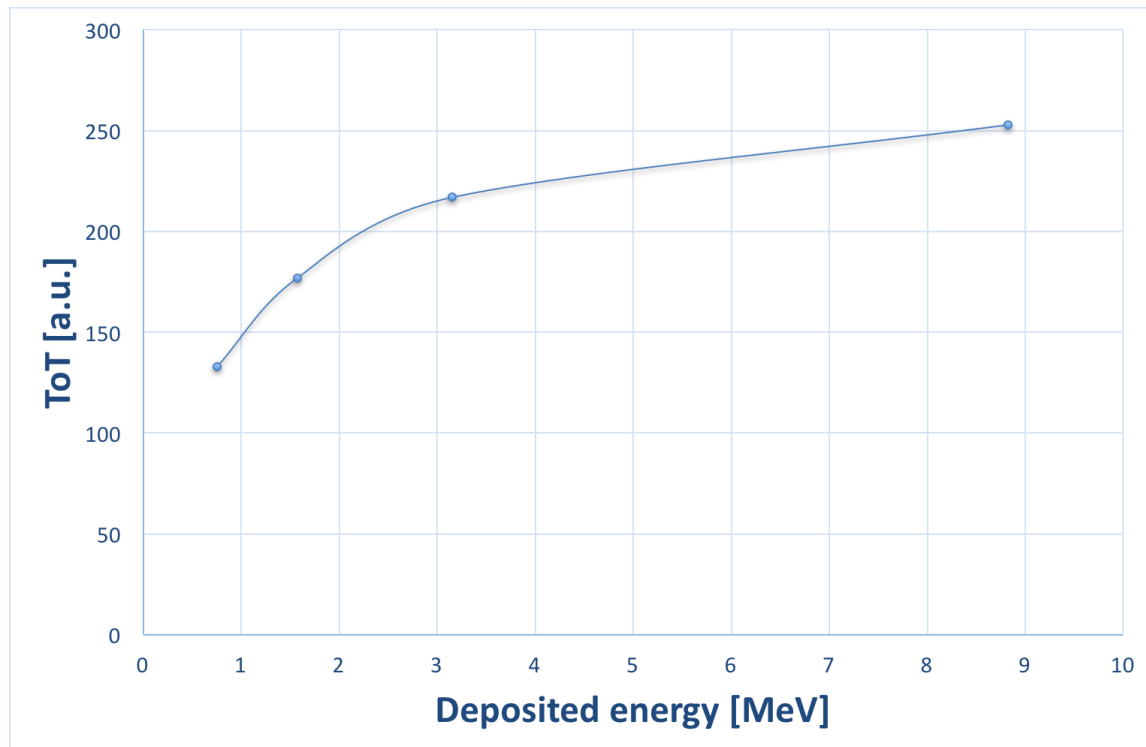


**Figure 4:** The upper edge cut-off of the detector response for the maximum neutron energy transfer to  $^4\text{He}$  nucleus.

## 5. Conclusions

Preservation of incident neutron energy, accurate energy discrimination abilities, and gamma-ray rejection are noteworthy performance advantages of fast neutron  $^4\text{He}$  scintillation detectors, developed by Arktis Radiation Detectors Ltd. This work measured the neutron response of SiPM based  $^4\text{He}$  detectors.

The neutron irradiation facility at PTB was used to conduct this research for various neutron energies, up to 14.8 MeV. The neutron fluence and incident energy were recorded, as well as the detector output for each event. The recorded data was post-analyzed.

In the current work, the detector response for different neutron energies was determined. The results of the current work and the integrated signal processing enable the use of  $^4\text{He}$  detectors in active interrogation application, as the detector is capable of discriminating between the interrogating neutrons and the induced uranium fission neutrons in a strong gamma background. The application of these detectors may also be extended to nuclear safeguards as a means to quantify and characterize fissile materials in nuclear facilities, due to the lack of moderating material around the detector and preservation of incident fast neutron energy. Furthermore, the results of this research will be further analyzed for construction of a future neutron dosimeter based on  $^4\text{He}$  scintillation.

## 8. References

- [1] D. Murer, R. Chandra, G. Davatz, H. Friederich, U. Gendotti, A. Howard, R. Lanza, P. Peerani, A. Tomanin;  *$^4\text{He}$  detectors for Mixed Oxide (MOX) fuel measurements*; IEEE Nuclear Science Symposium Conference Record (2011); p 4858-4864.
- [2] J.M. Lewis, R.P. Kelley, D. Murer, K.A. Jordan; *Fission signal detection using helium-4 gas fast neutron scintillation detectors*; Applied Physics Letters 105 (2014).
- [3] H. Chung, R.P. Kelley, W. Lee, Y.H. Chung, K.A. Jordan; *Spent nuclear fuel cask and storage monitoring with Helium-4 scintillation fast neutron detectors*; Proc. Korean Nucl. Soc. 2014 Fall Meeting, 2014.
- [4] R.P. Kelley, D. Murer, H. Ray, K.A. Jordan; *Analysis of the scintillation mechanism in a pressurized  $^4\text{He}$  fast neutron detector using pulse shape fitting*; AIP Advances 5, 037144 (2015).
- [5] Y. Liang, T. Zhu, A. Enqvist; *Timing Characterization of Helium-4 Fast Neutron Detector with EJ-309 Organic Liquid Scintillator*; EPJ Web of Conferences 170, 07005 (2018).
- [6] R.P. Kelley, L.M. Rolison, J.M. Lewis, D. Murer, T.N. Massey, A. Enqvist, K.A. Jordan; *Neutron response function characterization of  $^4\text{He}$  scintillation detectors*; Nucl. Instr. Meth. A 793 (2015) 101-107.
- [7] T. Zhu et al.; *Improved fission neutron energy discrimination with  $^4\text{He}$  detectors through pulse filtering*; Nucl. Instr. Meth. A 848 (2017) 137-143.
- [8] R.T. Kouzes et al.; *Neutron detection alternatives to  $^3\text{He}$  for national security applications*; Nucl. Instr. Meth. A 623 (2010) 1035-1045.
- [9] International Standard ISO 8529-1; *Reference neutron radiations: Characteristics and methods of production*; 2001.
- [10] International Standard ISO 8529-2; *Calibration fundamentals of radiation protection devices related to the basic quantities characterizing the radiation field*; 2002.
- [11] International Standard ISO 8529-3; *Reference neutron radiations: Calibration of area and personal dosimeters and determination of their response as a function of neutron energy and angle of incidence*; 1998.

# Evaluation of advanced dead time correction algorithms for neutron correlated counting

Daniela Henzlova<sup>1</sup>, Vlad Henzl<sup>1</sup>, L. Holzleitner<sup>2</sup>, M. Lockhart<sup>1</sup>

<sup>1</sup>Los Alamos National Laboratory, Los Alamos, NM 87545, USA

<sup>2</sup>Joint Research Centre, Karlsruhe, Germany

## Abstract:

*Advanced dead time correction algorithms for neutron correlated counting were recently developed at Los Alamos National Laboratory (LANL) and Joint Research Centre (JRC) Karlsruhe. Each of the algorithms provides an independent and standalone method to correct for dead time losses in correlated neutron pulse train with the aim to expand the dead time correction to higher count rates, provide improved dead time correction over traditional empirical approaches, and extend the dead time correction towards higher order correlated rates (Quads and Pents). The advanced dead time correction algorithms provide a novel capability to extract and dead time correct higher order correlated rates (Quads and Pents) that was not readily available before. Such a capability, when connected with appropriate advanced analysis methods, could be used to obtain improved neutron assay results or additional information about assayed item, specifically for items that substantially deviate from the point model assumptions.*

*The LANL algorithms dead time correct measured neutron multiplicity distributions, while the JRC-Karlsruhe method utilizes Rossi-alpha distribution from channel-by-channel list mode record of individual neutron detections. The latter approach, therefore, requires neutron detectors, where the signal from each channel (i.e. amplifier) is available for acquisition. In this paper, an inter-comparison of these algorithms on a broad experimental dataset will be presented.*

**Keywords:** correlated neutron counting; dead time correction; Quads

## 1. Introduction

Currently adopted technique to correct for dead time effects in neutron correlated counting relies on semi-empirical dead time correction expressions, which assume that neutrons are emitted randomly in time. The empirically-determined correction factors in principle compensate for biases present in the dead time model and are limited to count rate ranges for which they were established. Furthermore, the current approach is only developed and implemented up to the third order (i.e. includes Singles, Doubles and Triples) [1,2]. Advanced dead time correction algorithms were developed at LANL and JRC-Karlsruhe to allow for more fundamental dead time treatment without reliance on semi-empirical assumptions and to enable extension to higher order correlated rates beyond Triples. The advanced dead time treatment could provide an improved performance over a broad range of count rates, where some semi-empirical model assumptions may begin to fail.

Current neutron multiplicity analysis techniques utilize the first three correlated rates (Singles through Triples) that are linked to three physical properties of an item (mass, multiplication, contribution of  $(\alpha, n)$  reactions) through point model formalism [1]. For certain measurement scenarios, for example items with significant impurities affecting emitted neutron energies or items with high multiplication, such assumptions can lead to assay bias [3]. In order to reduce the reliance on the point model assumptions, additional information would need to be extracted from the measured multiplicity distributions. Naturally, additional information could be extracted if higher order correlated rates were available (beyond Triples, i.e. Quads and Pents).

Previous attempts to measure and utilize higher order correlated rates have been hampered as techniques to properly correct dead time were not developed. The advanced dead time correction algorithms, evaluated here, provide the first step towards an improved nuclear material assay by enabling extraction of these higher order correlated rates. To fully utilize such extended experimental information, it has to be linked to physical item properties through advanced analysis models beyond point model. Several analysis models were proposed and developed [3,4] and could be used in combination with the advanced dead time correction algorithms in the future.

## 2. Advanced and traditional dead time correction algorithms

Two advanced dead time correction algorithms were developed at LANL to provide improved dead time correction methodology and extension to higher order correlated multiplicity rates. Furthermore, JRC-Karlsruhe developed an independent dead time correction algorithm based on Rossi-alpha distribution, which also provides extension to higher order correlations. Complete documentation on each of these algorithms can be found in [5] for Dytlewski-Croft-Favalli (DCF), [6] for Correlated Neutron Dead Time Model (CNDTM) and [7,8] for JRC-Karlsruhe algorithm. In this section, brief highlights of each of these algorithms will be provided for reference. For completeness, the traditional dead time correction methodology, currently adopted in neutron correlated counting and embedded in INCC software [9], will be briefly reviewed.

### 2.1. Traditional dead time correction

The current INCC implementation applies dead time corrections directly to the measured Singles and Doubles values [9]. The Singles correction is based on the formulation for a paralyzable detector. The Doubles correction is an empirically based variation of the Singles correction. The basis for the dead time corrected Triples value is in a formalism based on work by Dytlewski [10]. The dead time corrected rates in the current INCC implementation are given by:

$$S = S_m e^{(\delta/4)S_m} = S_m e^{\left(\frac{a+bS_m}{4}\right)S_m} \quad (1)$$

$$D = D_m e^{\delta S_m} = D_m e^{(a+bS_m)S_m} \quad (2)$$

$$T = \frac{e^{\delta_{mult} S_m (1+cS_m)} z}{t} \quad (3)$$

Where:

$$z = \sum_{i=2}^{127} \beta_i (N_i - B_i) - \frac{\sum_{i=1}^{127} \alpha_i B_i}{\sum_{i=0}^{127} B_i} \left[ \sum_{i=1}^{127} \alpha_i (N_i - B_i) \right] \quad (4)$$

The  $S_m$ ,  $D_m$  values are the measured quantities,  $S$ ,  $D$ ,  $T$  are the dead time corrected rates,  $t$  is the measurement time. The expression for Triples (3) is a convolution of exponential factor; factor  $(1+cS_m)$ , which is used to make fine adjustments to the dead time correction; and the  $z$  term, which contains an inherent dead time correction based on Dytlewski [10]. The values  $N_i$  and  $B_i$  in (4) are the Real-plus-Accidental and Accidental multiplicity distributions, and  $\alpha_i$ ,  $\beta_i$  are functions of  $\delta_{mult}$  dead time coefficient [9]. The expressions (1-3) require four dead time coefficients. The dead time coefficients  $a$  and  $b$  in factor  $\delta=a+bS_m$  in Singles and Doubles expressions, and two dead time coefficients ( $\delta_{mult}$  and  $c$ ) in the expression for Triples. The coefficients  $a$ ,  $b$ ,  $\delta_{mult}$  and  $c$  are typically extracted from a dedicated calibration, although coefficient  $c$  is usually set to 0.

## 2.2. Correlated Neutron Dead Time Model (CNDTM)

The Correlated Neutron Dead Time Model (CNDTM) is based on work by Hage and Cifarelli [11], among others, to provide an exact dead time model for correlated neutrons. The CNDTM assumes an updating dead time and therefore a paralyzable system, it also assumes that the system die-away contains a single exponential. The derivation of the dead time model is extensive, and is presented in its entirety in [6,12]. The model defines joint probability distribution functions that give the expectation of detection of  $n$  neutron counts after dead time. The distribution functions include contributions from both correlated and uncorrelated neutrons and are used to predict the measured multiplicity moments after dead time effects (and through those the measured count rates), based on the underlying detection rates that would be measured if there were no dead time effects. The formulas for the measured multiplicity moments need to be inverted to extract the true (dead time corrected) detection rates. The corresponding mathematical expressions thus require inversion through numerical integration to obtain the dead time corrected rates.

The CNDTM was developed for the traditional shift-register type analysis in the sense that it combines Real-plus-Accidental and Accidental multiplicity distributions. In addition, it was also developed to extract correlated count rates using separately only Accidental multiplicity distribution (Randomly Triggered Inspection, RTI, approach) or only Real-plus-Accidental multiplicity distribution (Signal Triggered Inspection, STI) [6,12]. These analyses represent two alternative methods to extract multiplicity count rates and thus extend neutron multiplicity counting beyond traditional shift-register type analysis. Initial evaluation of differences and possible advantages of these alternative approaches was performed in [13]. The CNDTM model was developed for any multiplicity order, but fully formulated up to and including Quads. Current CNDTM software implementation only includes Singles through Triples. The model requires a single dead time coefficient parameter, which can be extracted in a dedicated calibration.

## 2.3. Dytlewski-Croft-Favalli (DCF) algorithm

The DCF algorithm was developed as an extension to original Dytlewski [10] formulation, where the dead time correction is applied directly to the measured multiplicity distributions. The DCF builds on this concept and introduces self-consistent treatment of Singles dead time correction as well as extends the methodology up to and including Pents. The DCF formulation for the correlated rates up to Pents offers computational simplicity and is therefore attractive for its straightforward software implementation. The algorithm requires a single dead time coefficient parameter that can be extracted in a dedicated calibration.

The DCF dead time corrected singles,  $S$ , Double,  $D$ , Triples,  $T$ , Quads,  $Q$  and Pents,  $P$  can be expressed as follows:

$$S = C_S \cdot \frac{1}{t} \cdot \sum_{i=0}^{\infty} B_i = \left( \frac{1}{T_g} \cdot \frac{\sum_{i=1}^{\infty} \alpha_i B_i}{\sum_{i=0}^{\infty} B_i} \right) \quad (5)$$

$$D = C_S \cdot \frac{1}{t} \cdot \sum_{i=1}^{\infty} \alpha_i \cdot (N_i - B_i) \quad (6)$$

$$T = C_S \cdot \frac{1}{t} \cdot \sum_{i=2}^{\infty} \beta_i \cdot (N_i - B_i) - S \cdot D \cdot T_g \quad (7)$$

$$Q = C_S \cdot \frac{1}{t} \cdot \sum_{i=3}^{\infty} \gamma_i \cdot (N_i - B_i) - \left( \frac{1}{T_g} \cdot \frac{\sum_{i=2}^{\infty} \beta_i B_i}{\sum_{i=0}^{\infty} B_i} \right) \cdot (D \cdot T_g) - S \cdot (T \cdot T_g) \quad (8)$$

$$P = C_S \cdot \frac{1}{t} \cdot \sum_{i=4}^{\infty} \eta_i \cdot (N_i - B_i) - \left( \frac{1}{T_g} \cdot \frac{\sum_{i=3}^{\infty} \gamma_i B_i}{\sum_{i=0}^{\infty} B_i} \right) \cdot (D \cdot T_g) - \left( \frac{1}{T_g} \cdot \frac{\sum_{i=2}^{\infty} \beta_i B_i}{\sum_{i=0}^{\infty} B_i} \right) \cdot (T \cdot T_g) - S \cdot (Q \cdot T_g) \quad (9)$$

In the equations above,  $N_i$  and  $B_i$  represent Real-plus-accidental and Accidental multiplicity distributions, respectively,  $t$  is the measurement time,  $T_g$  is the coincidence gate width and  $C_S$  is the Singles correction factor:

$$C_S = \frac{\sum_{i=1}^{\infty} \alpha_i \cdot B_i}{\sum_{i=1}^{\infty} i \cdot B_i} \quad (10)$$

The  $\alpha_i$ ,  $\beta_i$ ,  $\gamma_i$  and  $\eta_i$  are functions of dead time coefficient,  $d$ , through parameter  $\Phi = d/T_g$  ([5,14]). The  $C_s$ ,  $\gamma_i$  and  $\eta_i$  expressions represent the DCF extension of the traditional Dytlewski methodology.

Note that the above expressions utilize both, Real-plus-Accidental as well as Accidental histograms, which corresponds to traditional shift-register type analysis. Similarly as in case of CNDTM, the DCF method was also formulated for alternative analysis methods by utilizing solely the information contained in the Accidental histogram (Randomly Triggered Inspection, RTI [5]), which extends neutron multiplicity counting beyond traditional shift-register type analysis. In this approach, the Singles through Pents expressions are rewritten to only depend on  $B_i$  multiplicity distributions.

#### 2.4. JRC-Karlsruhe dead time correction algorithm

The JRC-Karlsruhe algorithm is described in detail in [7,8], an earlier version suitable for lower count-rates only can be found in [15,16]. At the moment it assumes non-updating dead time, but an extension to updating dead time could be possible in the future if the need occurs. The JRC-Karlsruhe algorithm uses information from each amplifier (i.e. channel) within the detector system to establish dead time losses. Therefore, it requires channel-by-channel readout instead of traditional single OR'd output available from standard neutron coincidence/multiplicity counters. It waits for a pulse to occur and the respective channel to be dead. Then it looks to other channels, estimating the lost pulses with the ones occurring on these other channels as reference. However, other channels may be on dead time as well, so the channels and respective lost pulse estimations are interconnected. This could be resolved using a matrix equation, the exact details can be found in [7,8]. In case of JRC-Karlsruhe algorithm, the dead time probability-behaviour is extracted directly from the measured data during each measurement. It is calculated for each channel using an iterative process: It makes use of some basic properties of the Rossi-alpha distribution and the relation of channels to each other in the early parts of this distribution which shall be fulfilled. This is done with actual measurement data, provided the amount of data is large enough to result in good statistics. It has been found that different energies of neutrons have significant influence on this dead time behaviour if several rings of  $^3\text{He}$  tubes are involved. No need for a dedicated dead time coefficient calibration is one of the main advantages of this algorithm.

### 3. Inter-comparison of advanced dead time correction algorithms

To compare performance and merit of the advanced dead time correction algorithms for practical safeguards use, series of measurements were performed to develop common experimental dataset. The measurements were performed in two JRC-Karlsruhe neutron well counters – Active Well Coincidence Counter (AWCC) [17] and Plutonium Scrap Multiplicity Counter (PSMC) [18]. Standard operating parameters (excluding dead time) are summarized in Table 1. Dead time coefficients are reported separately, along with the new dead time coefficients extracted for advanced algorithms, in Table 3.

The measurements were performed using list mode data acquisition [19] to assure sufficient flexibility of data analysis. Furthermore, the counters were equipped with channel-by-channel readout, where signal from each amplifier was recorded separately in list mode. In this way, the level of detail was obtained, which was necessary for the JRC-Karlsruhe algorithm. Detector head of each counter was modified for this purpose by removing derandomizing circuit and connecting the outputs of individual amplifiers directly into list mode.

Detector	Pre Delay ( $\mu$ s)	Gate Width ( $\mu$ s)	High Voltage (V)	Die Away ( $\mu$ s)	Efficiency (%)	Doubles gate fraction fd	Triples gate fraction ft
AWCC	4.5	64	1680	55.43	33.00	0.6314	0.4271
PSMC	4.5	64	1680	49.20	54.42	0.6207	0.3924

**Table 1:** Overview of AWCC and PSMC standard operating parameters.

To obtain a dataset covering a broad count rate range, several  $^{252}\text{Cf}$  and AmLi neutron sources were measured. This dataset was used to evaluate performance of each of the dead time correction algorithms under high count rates, which are difficult to obtain from Pu-bearing materials available in laboratory. Measurement times spanned between 600 s to 1000 s to mimic realistic measurement conditions. Measured sources and detected count rates are summarized in Table 2.

Source material	Activity [Bq]	AWCC count rate	PSMC count rate
$^{252}\text{Cf}$	5.005E+05	21000	30000
$^{252}\text{Cf}+\text{AmLi}$	3.448E+10	37000	52000
	6.896E+10	53000	74000
	11.184E+10	77000	106000
	15.472E+10	100000	137000
	19.760E+10	124000	170000
	24.453E+10	141000	193000
	28.741E+10	164000	225000

**Table 2:** Overview of count rates available for inter-comparison of advanced dead time correction algorithm.

### 3.1. Inter-comparison results

The evaluation metric was based on assessment how each of the advanced DTC algorithms reproduces expected trends (if properly dead time corrected). The evaluation utilized combination of  $^{252}\text{Cf}$  and AmLi sources over a broad count rate range to access regions of high count rate that are more affected by dead time. The measurements used a fixed, medium strength  $^{252}\text{Cf}$  neutron source, which was combined with increasing number of AmLi neutron sources. AmLi neutron sources only emit random (i.e. uncorrelated) neutrons and therefore should not contribute to genuine correlations detected from the  $^{252}\text{Cf}$  source, however, they will increase the overall count rate (Singles) and therefore contribute to dead time. If properly dead time corrected, the correlated count rates should be independent of number of AmLi sources added (i.e. Singles). The correlated count rates included correlated pairs (Doubles, D) up to quadruples (Quads, Q). This provided a basis for assessment of the advanced algorithms not only for their dead time correction performance, but also for their ability to extract correlations beyond Triples. Results for all the algorithms in both counters are summarized in Figures 1 and 2.

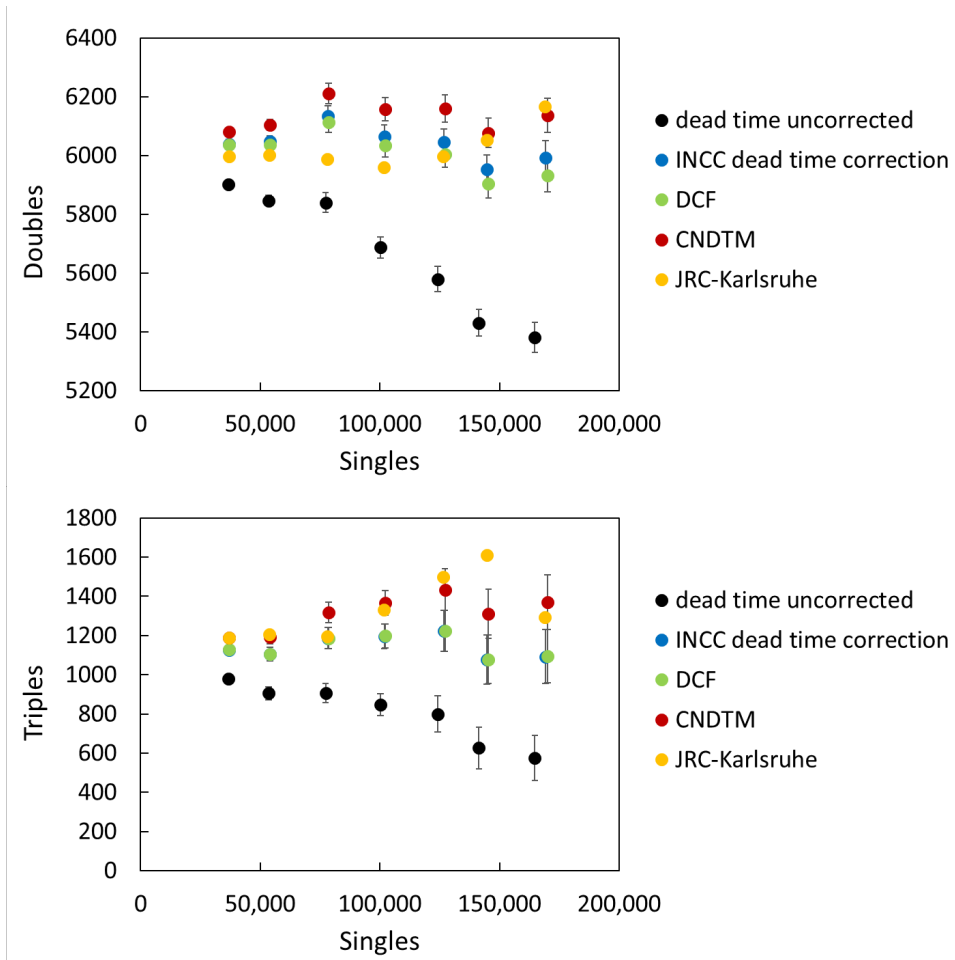


**Figure 1:** AWCC dead time corrected Doubles and Triples rates as a function of increasing count rate (Singles) due to added AmLi sources. Advanced dead time correction algorithms are compared to dead time uncorrected trends and INCC type dead time correction.

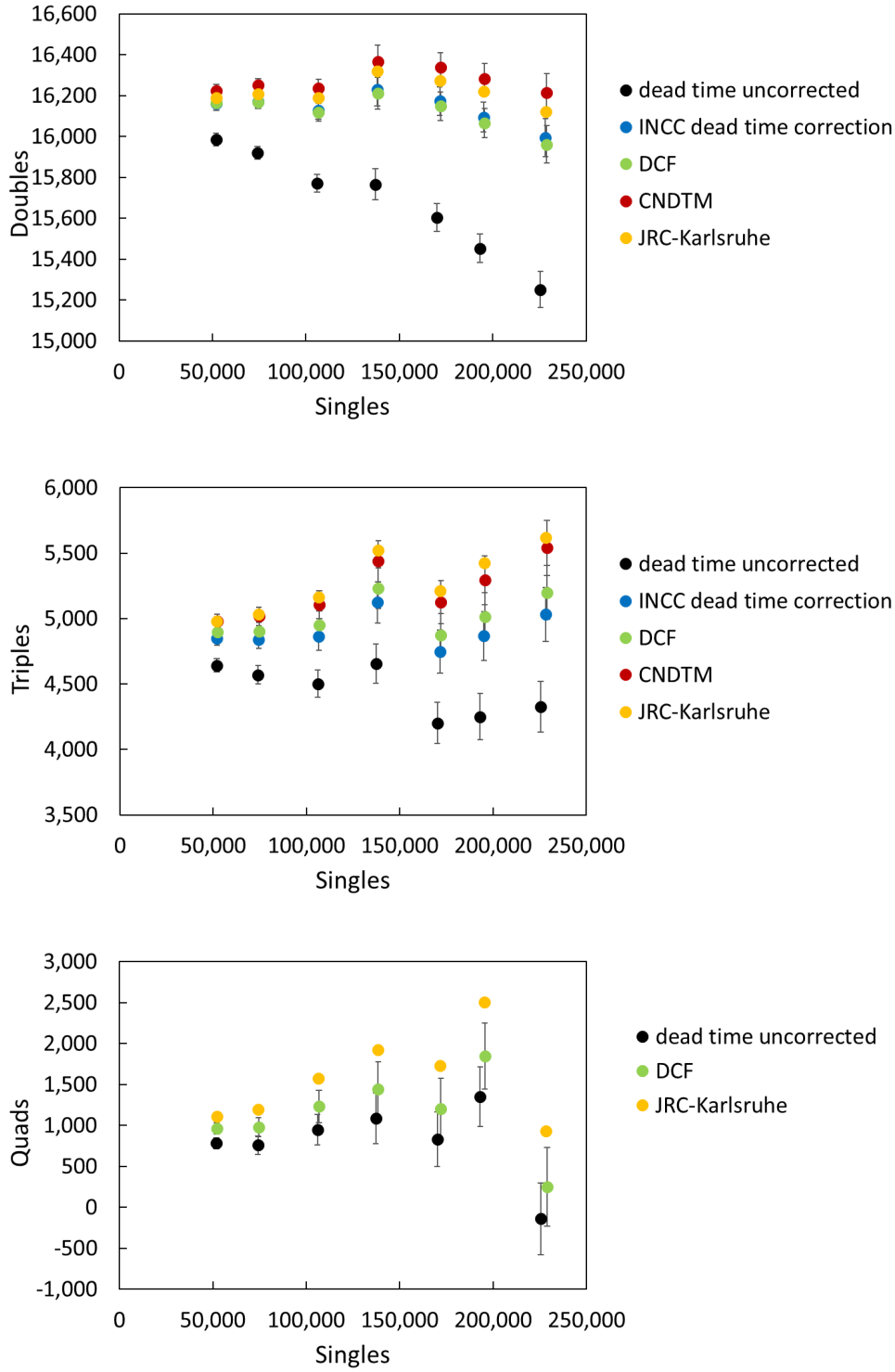


**Figure 2:** PSMC dead time corrected Doubles through Quads rates as a function of increasing count rate (Singles) due to added AmLi sources. Advanced dead time correction algorithms are compared to dead time uncorrected trends and INCC type dead time correction (up to Triples only). Note that CNDTM algorithm is currently only implemented up to Triples.

Figures 1 and 2 provide an overview of performance of individual advanced DTC algorithms over a broad range of count rates. To put the measured count rates into perspective, a 600 g PuO<sub>2</sub> (16% <sup>240</sup>Pu) item produces ~100,000 counts per second in PSMC. The data from AWCC were not used for higher order correlated rates (i.e. beyond Triples) due to the efficiency of this counter of 33% making it more suitable for coincidence rather than multiplicity measurements. As studied in [4], high efficiency (~>50%)

is needed to achieve good statistical precision in higher order correlated measurements. The PSMC with 54% efficiency was therefore selected in the evaluation exercise to enable extraction and assessment of higher order correlated rates.

The dead time corrected correlated count rates in Figures 1 and 2 are compared with dead time uncorrected trends for reference. Further, the traditional INCC type dead time correction results are shown (up to Triples) for comparison. Since the data was acquired in list mode, the traditional INCC type dead time correction was incorporated in the list mode analysis software with standard AWCC and PSMC dead time correction coefficients (see INCC in Table 3). The CNDTM and DCF algorithms only require a single dead time coefficient, which is expected to be different for each algorithm. The value of this coefficient was established in a parametric study by iteratively analysing the full  $^{252}\text{Cf}+\text{AmLi}$  dataset with range of dead time coefficient values until the trend with least dependence of correlated rates on the Singles count rate was established. The corresponding dead time coefficient was selected as an optimum for these analysis methods. As described earlier, the JRC-Karlsruhe algorithm extracts dead time coefficient from each measurement and requires therefore no user input for this parameter. An overview of the dead time coefficients used in the individual algorithms is shown in Table 3.

Detector	CNDTM [ns]	DCF [ns]	INCC			
			A [ $\mu\text{s}$ ]	B [ $\mu\text{s}^2$ ]	C [ns]	$\delta_{\text{mult}}$ [ns]
AWCC	188	188	0.6200	0.2000	0	188.0
PSMC	65	65	0.2110	0	0	54.3

**Table 4:** Overview of dead time coefficients for different dead time correction algorithms.

Based on the results in Figures 1 and 2, it can be seen that the three advanced DTC algorithms show comparable performance in high count rate scenarios. All the algorithms are able to correct the decreasing trend of the correlated rates with increasing Singles rate, observed for uncorrected data. The DCF dead time correction results are very similar to the INCC results. The DCF and JRC-Karlsruhe also demonstrate capability to extract dead time corrected higher order correlated rates as shown in Figure 2 bottom. The results, however, exhibit significant uncertainty, which increases with increasing number of AmLi sources due to the increasing contribution of random correlations (accidentals). This can be expected for such a high order correlations and rather conservative measurement time (1000 s). Note that the measurement times in this comparison were selected to illustrate performance for measurement times typical in practical applications. Increasing measurement time would aid in reducing the uncertainties and may be needed in practical applications to make use of these higher order correlations (Quads). This aspect was discussed in [4], however, it was concluded that uncertainty requirements on higher order correlated rates are yet to be fully established depending on their propagation into final results (through an improved analysis model). Additional evaluation of DCF dead time correction for higher order correlations (Quads and Pents) was performed independently of this research in ref [20] and illustrates DCF capability to extract Quads and Pents for measurements with reduced uncertainty. The measurements in ref [20] were performed without channel-by-channel readout and therefore could not be used to compare with JRC-Karlsruhe method.

### 3. Practical implications and observations

From practical implementation point of view, the advanced dead time correction algorithms offer potential for reduced number of calibration parameters through single dead time coefficient for DCF and CNDTM. The dead time coefficient could be established using similar techniques that are traditionally used to establish INCC dead time coefficients (i.e. two-source method or range of Cf with AmLi sources as used in this evaluation) [1]. Contrary to DCF and CNDTM, the JRC-Karlsruhe provides a practical advantage in that no a-priori knowledge of dead time coefficient is required. The algorithm extracts appropriate dead time coefficient value directly from each measurement. This is one of the key

advantages of the JRC-Karlsruhe algorithm, which would remove any assumptions on dead time coefficient validity over a broad count rate range. In practical applications, dead time coefficient calibration is typically performed only once, during the initial characterization of neutron counting instrument. The same dead time coefficients are then used in all assays with a given instrument and typically do not need to be modified. There are, however, situations, where very broad range of items is measured over extensive count rate range and the dead time coefficients established for different count rates during initial calibration may no longer be valid. The advanced dead time algorithms presented here should largely remove this concern.

List mode data acquisition was used in this evaluation. However, the use of list mode is not requirement for DCF and CNDTM algorithms. In fact, both of these algorithms could be applied to multiplicity distributions available from existing multiplicity shift register hardware. Therefore, no hardware modifications for these algorithms would be required. The JRC-Karlsruhe algorithm relies on the highest level of detail available in neutron counter in order to be more flexible and independent on a-priori knowledge of dead time coefficients. The JRC-Karlsruhe algorithm utilizes signals from each amplifier within the neutron counter to self-calibrate detection efficiencies and establish dead time behaviour and losses. Current neutron coincidence and multiplicity counters typically employ half-a-dozen up to tens of amplifiers to collect signals from  $^3\text{He}$  tubes. All the amplifiers are OR'd or combined in a derandomizing circuit into a single output from the entire instrument. To benefit from JRC-Karlsruhe algorithm flexibility, a modification of junction box in existing neutron counters would be required to enable collection of signals from individual amplifiers (i.e. channel-by-channel acquisition). Such signal collection can only be performed in list mode to support the high number of amplifiers (i.e. channels) and to provide access to all neutron detections required by the JRC-Karlsruhe algorithm. This could be done by replacing the derandomizing circuit with a list mode counter. The data could be transferred using protocols like USB or TCP/IP. This offers the additional advantage of making pulse transfer from the detector insensitive to pick-up of electromagnetic noise or reflections in old coaxial cables.

The CNDTM and DCF algorithms were written in C# in a modular form in order to ease possible transfer and implementation into other software (such as INCC). The JRC-Karlsruhe algorithm was written in FORTRAN-90, which provides a good run-time performance. The very calculation intensive methods made the usage of a high performant language necessary.

## 4. Conclusions

Three advanced dead time correction algorithms with capability to extend neutron multiplicity counting to higher order correlations were evaluated and compared. The performance of the algorithms was compared on a dataset with broad range of count rates from combined  $^{252}\text{Cf}$  and AmLi neutron sources. The comparison focused on capability to correct for dead time effects and extend neutron multiplicity counting towards higher order correlations (beyond Triples). The dead time correction capability of each algorithm was also compared against INCC dead time correction reference.

Overall all the advanced algorithms show capability to correct for dead time observed in the dead time uncorrected trend. The results of the DCF dead time correction are similar to the traditional INCC-based approach for Singles through Triples for the available count rates. The lead contribution of the advanced approaches can be seen in their ability to extract higher order correlations, which was here illustrated for DCF and JRC-Karlsruhe corrections. This aspect provides a path to extend neutron multiplicity counting towards improved nuclear material assay. Quads extraction is currently implemented in INCC, however, lacks dead time correction, which would bias the results in any practical application. To fully utilize the higher order correlated rates, they have to be linked to the assayed item physical properties. Neutron multiplicity analysis is composed of two analysis phases – extraction of dead time corrected correlated rates and analysis model to relate these to item properties. The advanced algorithms evaluated here enable the first analysis phase and the full use of the newly accessible additional experimental information will rely on advanced analysis models (beyond point model) to relate the extended set of measured quantities (S,D,T,Q, (possibly P)) to item characteristics. Several advanced analysis approaches were considered and developed elsewhere [3,4], but have not been extensively evaluated. Future evaluation should focus on combining the advanced algorithms with advanced analysis model(s) to assess benefits of the additional experimental information that now became available in improving nuclear material assay.

The motivation for developments of advanced dead time correction algorithms was to introduce improved methodologies for processing and analysing of correlated neutron data in order to:

- 1/ expand information that can be obtained from multiplicity measurements to improve nuclear material assay
- 2/ improve dead time correction to be applicable to broader range of measurement scenarios (i.e. count rates).

The two above goals are strongly interconnected and the advanced dead time correction algorithms provide tools necessary for extraction of additional information (in form of higher order correlated rates) already available in current neutron multiplicity measurements.

## 5. Acknowledgements

This work was sponsored under “Action Sheet 60 between the United States Department of Energy (DOE) and the European Atomic Energy Community (Euratom) for Cooperation on Joint Comprehensive Evaluation of Advanced Dead time Correction Algorithms for Neutron Multiplicity Counting Developed at LANL and JRC.” The project Action Sheet was developed pursuant to the 2010 Agreement between DOE and Euratom Represented by the European Commission in the Field of Nuclear Material Safeguards and Security Research and Development.

## 6. References

- [1] Ensslin N., Harker W.C., Krick M.S., Langner D.G., Pickrell M.M., Stewart J.E.; *Application guide to neutron multiplicity counting*; Los Alamos National Laboratory Manual LA-13422-M; 1998.
- [2] Reilly D., Ensslin N., Smith H. Jr., and Kreiner S.; *Passive nondestructive assay of nuclear materials*; Los Alamos National Laboratory Technical Report LA-UR-90732; 1991.
- [3] Hauck D.K., Santi P.A., Favalli A., Croft S.; *Variations of Point Model Analysis in Neutron Multiplicity Counting and On-going Theoretical Developments*; INMM 54th Annual Meeting 2013; Palm Desert, California, USA; LA-UR-13-25366.
- [4] Henzlova D., Cutler T., Favalli A., Geist W., Henzl V., Koehler K., Lockhart M., McGahee Ch., Parker R., and Santi P.; *Improving Neutron Measurement Capabilities – Final Report*; Los Alamos National Laboratory Technical Report LA-UR-17-29756; 2017.
- [5] Croft, S. and Favalli A.; *Extension of the Dytlewski-style dead time correction formalism for neutron multiplicity counting to any order*; *Nuclear Instruments and Methods in Physics Research A* 869; 2017; p. 141-152.
- [6] Hauck, D. K., Croft S., Evans L.G., Favalli A., Santi P.A., and Dowell J.; *Study of a theoretical model for the measured gate moments resulting from correlated detection evens and an extending dead time*; *Nuclear Instruments and Methods in Physics Research A* 719; p. 57-69.
- [7] Holzleitner L., Henzlova D. and Swinhoe M.; *Numerical Method for High Count-Rate Dead time Correction in Neutron Multiplicity Counting using Multi-Channel List-Mode Recorders*; 40th ESARDA Annual Meeting, Luxembourg, May 2018.
- [8] Holzleitner L., Henzlova D., Swinhoe M. and Henzl V.; *Estimation of Dead time Loss for high Neutron Count-Rates and associated Multiplicity Correction using Multi-Channel List-Mode Data*; Symposium on International Safeguards, Vienna, Austria, Nov. 2018.
- [9] Harker B., Krick M., Geist W. and Longo J.; *INCC Software Users Manual*; Los Alamos National Laboratory LA-UR-10-6227; March 2009.

- [10] Dytlewski N.; *Dead time corrections for multiplicity counters; Nuclear Instruments and Methods in Physics Research A* 305; p. 492-494.
- [11] Hage W., and Cifarelli D.M.; *Correlation Analysis with Neutron Count Distribution for a Paralyzing Dead time Counter for the Assay of Spontaneous Fissioning Material; Nuclear Science and Engineering* 112; p. 136-158.
- [12] Hauck D.K.; *An Exact Dead Time Model for Correlated Neutron Counting based on the Joint Probability Function*, Los Alamos National Laboratory Technical Report LA-UR-12-24194.
- [13] Henzlova D., Croft S., Menlove H.O., Swinhoe M.T.; *Extraction of correlated count rates using various gate generation techniques: Part II Experiment; Nuclear Instruments and Methods A* 691; p. 159-167; 2012.
- [14] Croft S., Favalli A.; *Higher Order Dead Time Corrections for Neutron Multiplicity Counting*; ESARDA bulletin 47; 2012.
- [15] Holzleitner L., and Swinhoe M.; *Dead time correction for any multiplicity using list mode neutron multiplicity counters: A new approach - Low and medium count-rates; Radiation Measurements* 46; 2011; p. 340-356.
- [16] Holzleitner L. and Swinhoe M.; *Improvements in Dead time Correction Using List-mode Neutron Counters*; 33rd ESARDA Annual Meeting, Symposium on safeguards and nuclear material management, Budapest, Hungary, May 2011.
- [17] Menlove H.O.; *Description and Operation Manual for the Active Well Coincidence Counter*; Los Alamos National Laboratory Report LA-7823-M, 1979.
- [18] Menlove H.O.; *Plutonium Scrap Multiplicity Counter Operation Manual*; Los Alamos National Laboratory LA-12479-M; 1993.
- [19] Henzlova D., Menlove H.O., Swinhoe M.T., Marlow J.B., Martinez I.P., Rael C.D.; *Neutron Data Collection and Analysis Techniques Comparison for Safeguards*; Proceedings of the IAEA Safeguards Symposium: Preparing for Future Verification Challenges, Vienna, Austria, Nov. 1-5, 2010.
- [20] Lockhart M., Henzlova D., Croft S., Cutler T., Favalli A., McGahee Ch., Parker R.; *Experimental evaluation of the extended Dytlewski-style dead time correction formalism for neutron multiplicity counting; Nuclear Instruments and Methods in Physics Research A* 879; p. 69-76; 2018.

## Calibration of a combined PNCC / HRGS non-destructive assay system for measurement of Pu and MOX Packages in order to verify declared inventory

Avril Cormack<sup>1</sup>, Natalie Bain<sup>1</sup>, Paul Mullarkey<sup>1</sup>, Richard Gunn<sup>1</sup>, Antony Towner<sup>2</sup>, John Mason<sup>2</sup>, Kevin Burke<sup>2</sup>, Douglas Paton<sup>1</sup>, Charlie McIntosh<sup>1</sup>

<sup>1</sup>Dounreay Site Restoration Ltd, Dounreay, Thurso, Caithness, Scotland

<sup>2</sup>A.N. Technology Ltd, Unit 6, Thames Park, Wallingford, Oxford, England

E-mail: [avril.cormack@dounreay.com](mailto:avril.cormack@dounreay.com), [natalie.bain@dounreay.com](mailto:natalie.bain@dounreay.com),

### Abstract:

*A historic inventory of plutonium fuel materials packaged in steel cans, including alloys, mixed uranium/plutonium oxides (MOX) and mixed uranium/plutonium carbide required characterisation in order to verify declared content and thus meet safeguards and safety requirements. The non-destructive-assay system used for this work combined high resolution gamma spectrometry (HRGS) with passive neutron coincidence counting (PNCC), in order to measure both the isotopic composition and the <sup>240</sup>Pu-effective mass. From this information, total Pu-mass and power output could also be determined.*

*The main challenge for characterisation was to achieve representative <sup>240</sup>Pu<sub>(effective)</sub> mass calibrations. Certified standards were not available and there was limited information available to support modelling using MCNP. Therefore, it was necessary to calibrate with a selection of the actual fuel cans themselves, using their declared <sup>240</sup>Pu<sub>(eff)</sub> masses as reference. This 'self-verification' method relied heavily on accuracy of the declared inventory. Careful investigation of historical data was required in order to divide the materials into appropriate family groups and choose the most appropriate cans to calibrate for each family.*

*A number of calibrations were performed and these have been used successfully to measure over 1200 cans with power outputs up to 8 Watts. MCNP modelling combined with radiography was used to assist in verification of the calibrations, and explain instances where measured data deviates from declared.*

*This paper describes how the NDA system calibrations were set up and summarises the results. It concludes that 'self-verification' calibrations for <sup>240</sup>Pu<sub>(effective)</sub> mass can work well provided they are fully representative and based on high quality declared data. The combined gamma measurement formed a useful independent check on the accuracy of declared data. MCNP modelling and radiography also proved invaluable tools in the support of this work, both as a means of benchmarking the <sup>240</sup>Pu<sub>(effective)</sub> mass calibrations and as a means of investigating any measurements which fail to agree with declared.*

**Keywords:** non-destructive assay; plutonium; isotopics; <sup>240</sup>Pu-effective calibration; PC-FRAM

## 1. Introduction

The aim of this work was to verify historic declared inventory of plutonium and mixed plutonium / uranium fuel cans in various forms including pellets, powders, carbon coated spheres, ceramic metals (CERMETS), capsules and alloys. A combination of passive neutron coincidence counting (PNCC) and high-resolution gamma spectrometry (HRGS) was chosen as the best available characterisation method, given project timescales and resources.

In terms of project planning, the V-model for system lifecycle from the NDA Good Practice Guide [4] was adopted due to the complexity of the project. The V-model places particular emphasis on commissioning and testing phases, and includes an iteration loop between commissioning and earlier definition phases. Such a loop permitted flexibility to modify calibration plans and make changes to assay system set-up when issues were encountered. This was useful given the uncertainties associated with calibrating since it enabled issues to be dealt with promptly. The project lifecycle is illustrated in Figure 1.

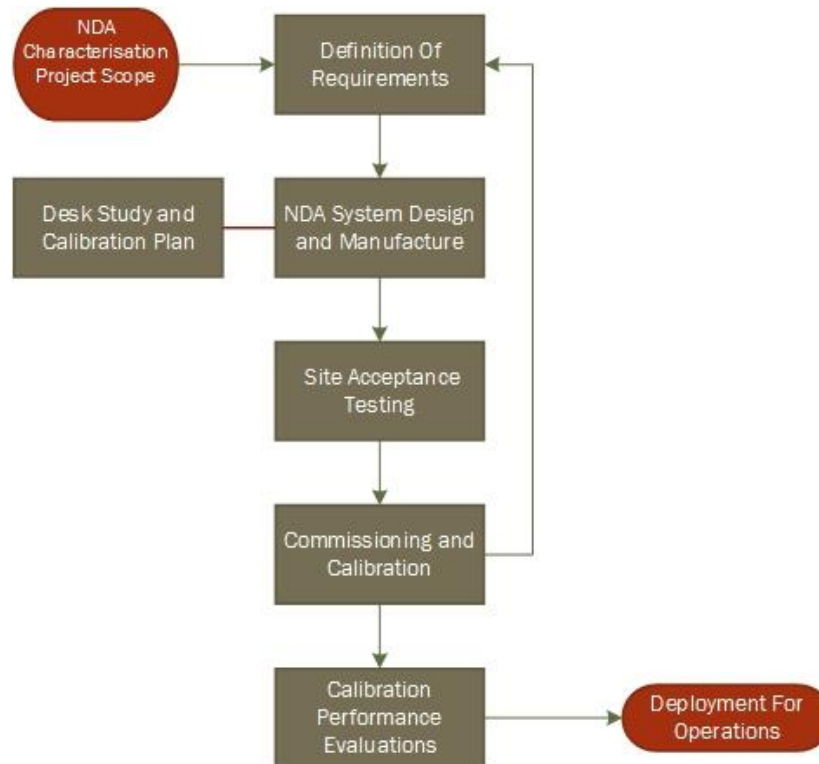


Fig 1: V-Model Of Characterisation Project LifeCycle

Representative, certified standards were not available for this project. The only alternative was to attempt calibrations with a selection of the actual fuel cans to be measured; using their declared  $^{240}\text{Pu}$ -effective masses *in place* of certified reference values. Such a technique has been successfully demonstrated in the past to verify declared inventory for repackaged material [1], but it is recognised that this is not an ideal situation. For any such calibration to work, the declared values must be accurate with good historical provenance.

This project faced a unique challenge in that the material had been in long term storage. It was not possible to open any cans prior to measurement and so there existed a number of 'unknown' quantities with respect to their contents. These 'unknowns' are discussed further in Section 3.1. The inventory was extensive, encompassing materials from a wide range of different origins. Much of the material had declared data based on manufacturing / reprocessing specifications and laboratory analysis which were deemed to be of high quality.

Planning the  $^{240}\text{Pu}_{\text{(eff)}}$  calibrations proved a significant and time-consuming stage of the project due to the diverse range of material types requiring measurement. A comprehensive review of historical inventory enabled the materials to be divided into a number of family groups for calibration and assay based on material form and mass range.

The NDA instrument commissioning phase included system set-up, optimisation, testing, and finally, calibration. The required measurement performance was agreement with declared values to within  $\pm 15\%$ . This level of agreement is greater than the International Target Values [9]. However it should be noted that the target values were not strictly applicable in this case, because the accuracy of the declared (reference) data used for calibration was unknown. Also, for the lower Pu mass cans (in particular, those with high U:Pu ratio), instrument detection limit levels were challenged.

Once commissioning was complete, the calibrations and measurement campaigns commenced in two phases. Phase 1 measured cans with heat outputs up to 3.5W and Phase 2 dealt with higher power cans up to 8W. The timescales were extremely challenging, with the entire lifecycle from initial project definition to the completion of operations, being completed within approximately 18 months.

## 2. Instrumentation Description and Set-Up

The NDA equipment used for this project was manufactured by A.N. Technology Ltd (ANTECH) utilising a design based on a similar instrument which is fully described in [2]. There was a requirement for the instrument to be mobile and fit into areas with space limitations. This led to a design modification where the external shielding around the neutron assay chamber was reduced to just 20cm of polythene and 1mm of cadmium. For the polythene shielding, 20cm is less than ideal, making the instrument vulnerable to background effects as well as providing less radiological protection for operators. However, this has been carefully managed by operational procedures and where required, use of additional portable shielding screens [18].

Fig 2 shows the main unit of the mobile combined system, which comprises of a pair of adjacent assay chambers (gamma and neutron) housed within a single, compact unit. Cans are lowered into each assay chamber in turn for gamma (isotopics) and neutron ( $^{240}\text{Pu}$ -effective mass) measurement. The measurements are software controlled and processed via a separate computer workstation.

All the cans to be measured had been sealed in steel over-packs of fixed dimensions. The assay chambers were designed to fit closely around this over-pack, thus maximising counting efficiency. Surveillance and data signals are routed from the instrument prior to the counting electronics to enable independent monitoring directly by the regulator, EURATOM.



Fig 2: Antech Combined Gamma / PNCC Assay Chamber Unit

### 2.1. $^{240}\text{Pu}_{(\text{effective})}$ Mass Measurement

$^{240}\text{Pu}$  effective mass measurement by passive neutron coincidence counting (PNCC) is a well-established method which is described in detail elsewhere [5,6,20], therefore only the most pertinent points are briefly discussed in this section. In summary, the even-numbered isotopes of Pu have the greatest spontaneous fission yield, and it is these which are critical for passive measurement. The neutrons emitted are time correlated, which enables them to be distinguished from random events such as ( $\alpha, n$ ).

Since the neutrons from individual isotopes cannot be distinguished from one another during measurement, the  $^{240}\text{Pu}$  effective mass is used for PNCC calibration. This is defined as the mass of  $^{240}\text{Pu}$  which would be required to produce the same neutron emission rate as the combined contribution from the even-numbered Pu isotopes [5]. See Equation 1.1.

$$^{240}\text{Pu}(\text{eff}) = 2.52(^{238}\text{Pu}) + ^{240}\text{Pu} + 1.68(^{242}\text{Pu}) \quad \text{Eq 1.1}$$

The neutron assay chamber contains 30 x  $^3\text{He}$  tubes arranged into six banks of five within a thick walled cylindrical high density polyethylene chamber. Each of the six detectors banks are fed through an Amptek A111 high count rate amplifier to a De-Randomising Mixer Buffer Counter (DMBC). The entire slab assembly is lined with a thin sheet of cadmium absorber and 3mm of steel. The DMBC is designed to ensure no losses, even when counting at high count rates and provides two identical output signals. The first signal is fed directly to a TCA (Time Correlation Analyser), and the second to an independent data take-off point for regulatory and safeguards compliance monitoring.

The neutron system settings were initially established during factory acceptance testing, and finalised during on-site commissioning. A background study was carried out to determine the operational detection limit  $L_D$ , which is defined as the minimum amount of material which can be quantified with confidence.  $\sigma_d$  is the standard deviation of the background signal and  $L_C$  is the critical limit [17]

$$L_D = L_C + 1.645\sigma_d \quad \text{Eq 1.2}$$

The detection limit in terms of  $^{240}\text{Pu}(\text{eff})$  mass varied with location of system and calibration, but was for most purposes around **2 - 3.5g**. Some background was observed due to adjacent sources of neutrons in the area and operational activity was shown to affect the background during the course of measurements. This contributed to the detection limits and was initially addressed by restricting access to the area during all NDA measurements. As the project moved into Phase 2 (refer to Section 3.3) however, adjacent background levels increased further and it became necessary to add additional external polyethylene shielding around the neutron assay chamber. The thickness required was calculated by MCNP [18].

Neutron die-away time ( $\tau$ ), was determined by measuring a neutron source at the operational gate-width ( $G_1$ ), then repeating measurement at a second gate-width ( $G_2$ ) which is twice the length of  $G_1$ . The die-away time was then calculated using Eq1.3 where  $R_1$  is the observed real count rate at  $G_1$  and  $R_2$  is the observed real count rate at  $G_2$  [5].

$$\tau = \frac{-G_1}{\ln\left(\frac{R_2}{R_1} - 1\right)} \quad \text{Eq 1.3}$$

Die-away time was measured to be **71.28 $\mu\text{s}$** . The pre-delay was factory set at **4  $\mu\text{s}$**  and a gate-width of **89.6 $\mu\text{s}$**  was used based on Eq 1.4 [5]:

$$G = 1.257\tau \quad \text{Eq 1.4}$$

The neutron counting efficiency was approximately **30%**, (measured using a certified reference  $^{252}\text{Cf}$  neutron source positioned centrally in the chamber). As the cans to be measured were all the same size, geometrical variations in detection efficiency were not a major concern. However, the fill height of the cans was uncertain, and therefore geometrical response profile measurements were performed. The response profiles showed only a very slight increase in efficiency towards the top of the chamber.

Daily performance was monitored using a background and check measurement as per good practice [4]. With repeatability and stability of counting confirmed,  $^{240}\text{Pu}(\text{eff})$  calibration proceeded as per Section 3.

## 2.2. Isotopics Measurement

No calibration as such is required for isotopics measurement because the technique relies on quantifying only the relative peak heights of gamma emitting nuclides from a measured spectrum. As such, the gamma measurement was considered a useful independent check of declared inventory in

addition to forming an integral part of the measurement of each can. In general, lower energy gamma rays are more abundant and give best results for Pu isotopics using FRAM, provided the cans are not shielded. Isotopic homogeneity of cans is essential if accurate results are to be acquired. For a description of the spectral regions used for isotopics analysis, refer to [5].

The gamma system used for this work utilises a single co-axial, electronically cooled Ortec HPGe detector, connected to an Ortec DPEC Jnr 2.0 signal processor. The assay chamber is constructed from thick lead walls, lined in graded copper and tin. Due to dimensional constraints, the detector is mounted underneath the sample chamber and 'views' the can through the floor of the chamber. This design reduced the footprint of the gamma system significantly, almost halving one dimension and reducing detector-sample distance. Such a design maximises efficiency of counting partially filled or lower activity cans from a single detector and eliminates the need for a turntable. However it does mean that only the base of each can is viewed and there is additional requirement for use of filters and collimation when measuring higher activity cans.

The measured spectra are collected using Ortec Maestro emulation software and analysed using FRAM (Fixed Energy Response Function Analysis with Multiple efficiencies). The FRAM code has been developed over a number of years in the Safeguards Science and Technology Group at the Los Alamos National Laboratory and is now well established for isotopics analysis [3].

Gamma detector optimisation is essential to ensure the high quality spectral data required for accurate FRAM analysis. During preliminary commissioning, a  $^{133}\text{Ba}$  certified reference gamma source was used for instrument set-up. This was chosen due to the fact that it has a set of known gamma emission lines which lie within the 120 – 460keV energy range utilised by FRAM.

FRAM Analysis in the 120 – 460keV range utilises a single  $^{240}\text{Pu}$  photo-peak at 160.31keV. The difficulty in measurement of this single low intensity gamma ray is exacerbated by interference from gamma rays at nearby energies and the 59.9keV  $^{241}\text{Am}$  peak which typically dominates the spectrum. These gammas can take up a large proportion of the detector live time.

Refer to Fig3a which is an example of an unfiltered gamma spectrum for a typical can of MOX material taken during early commissioning work. This particular can has a low Pu mass (<50g total Pu) and high U:Pu ratio of 125:1, making it particularly challenging for isotopics measurement due to high levels of self-shielding from the U content. The 59.9keV  $^{241}\text{Am}$  peak region of interest (ROI) is marked and can be clearly seen to dominate the spectrum.

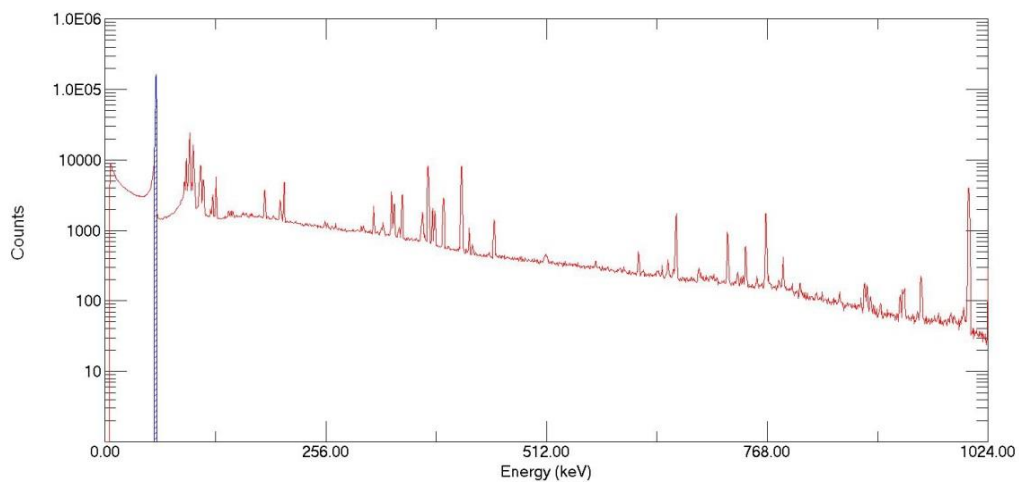


**Fig 3a:** Pu Gamma Spectrum of Low Pu Mass MOX Capsules Can (total Pu = 38.8g, U:Pu 13:1, approx. 12% Pu-240 isotopic content). *Measured with no cadmium filter.*

Cadmium is an effective filter medium which attenuates the 60keV region without having too much effect on the higher energy lines [5]. The widely used 'rule of thumb' recommends balancing the 59.5keV  $^{241}\text{Am}$  peak with the 100keV peak complex. A 2mm thick cadmium filter was initially used in

line with standard recommendations for Pu isotopics measurement [3], but analysis results were consistently poor, both in terms of precision and accuracy because the spectrum appeared over-filtered. Refer to Fig 3b.

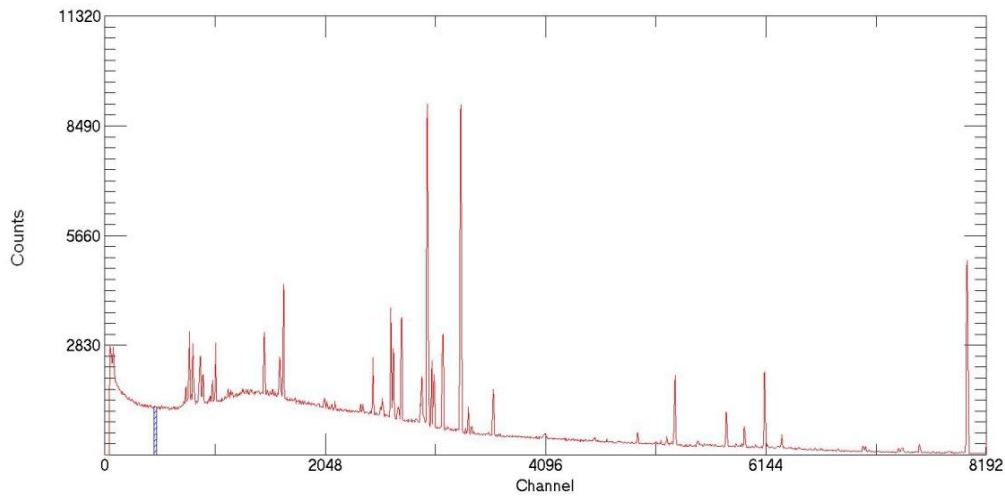


**Fig 3b:** Repeat Measurement of the can in Fig3a using 2mm Cd Filter.

Additional testing was conducted and it was established that 1mm of cadmium gave the best results for this project - refer to Fig 3c.

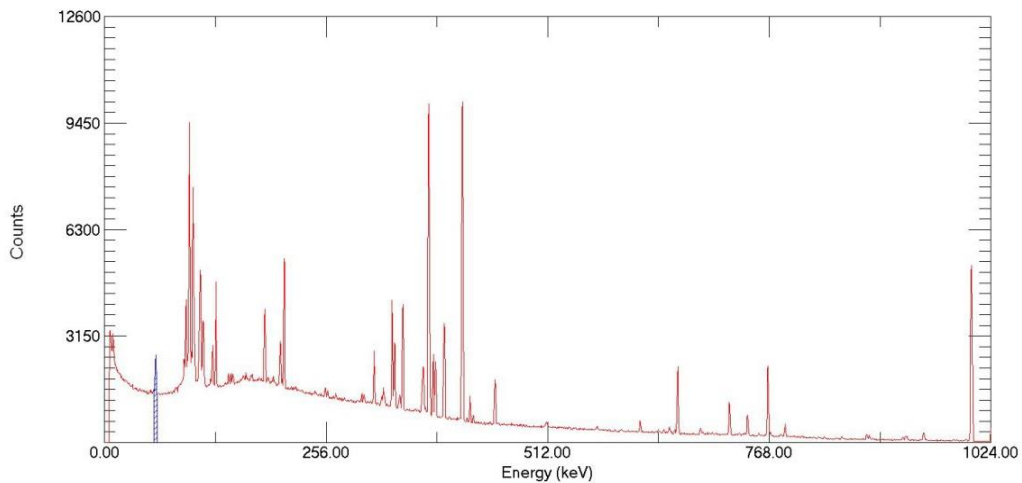


**Fig 3c:** Repeat Measurement of the can in Fig3a using 1mm Cd Filter. This configuration gave the best results for FRAM analysis.

A standard parameter file Mox\_Cx\_120\_460 was used for most materials with a few exceptions. A peak rise time of  $6\mu\text{s}$  was used, with gain setting targeted to achieve  $0.125\text{keV/Ch}$ . The energy calibrated gamma detector typically achieved a resolution (FWHM) of 0.97 for the  $^{133}\text{Ba}$  reference source at 276.4keV with dead-time not exceeding a few percent. For higher mass Pu cans, the 208.1keV peak resolution reduces to around 1.07 at 40% dead-time and 1.16% at 60% dead-time. Whilst spectra were found to be usable with dead-time as high as 50 - 60%, much improved results could be achieved by decreasing the collimator gap width or use of additional filters between detector and sample.

### 2.3. Pu Total Mass and Power Calculation

Pu total mass and power are calculated directly from the measured isotopics and  $^{240}\text{Pu}$  effective mass. The Pu total mass is calculated from the measured  $^{240}\text{Pu}_{\text{eff}}$  mass combined with the measured  $^{238/240/242}\text{Pu}$  isotopic abundances using Eq 1.1. Fig 4 summarises this process

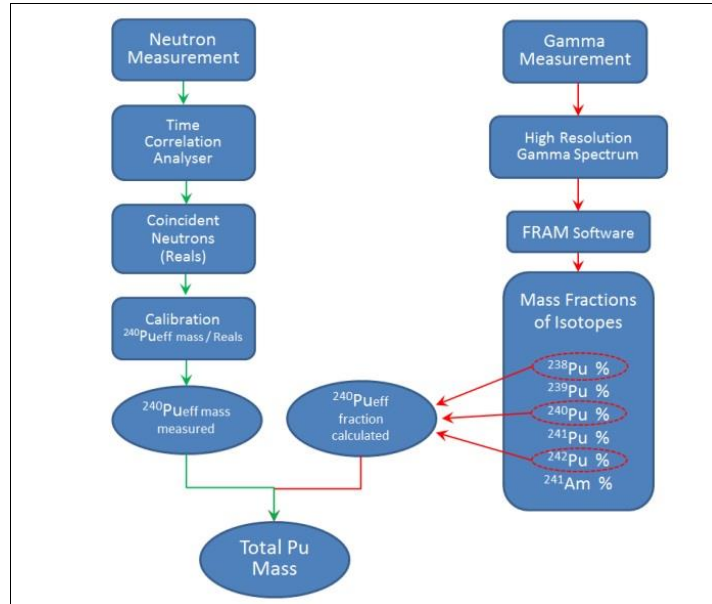


Fig 4: Combined Measurement Process

The power output is subsequently calculated using Equation 1.5, which multiplies the measured Pu/Am isotopic masses by the relevant specific power values in watts per gram [5].

$$P(W) = (0.57x^{238}\text{Pu})+(0.0019x^{239}\text{Pu})+(0.0071x^{240}\text{Pu})+(0.0033x^{241}\text{Pu})+(0.00012x^{242}\text{Pu})+(0.11x^{241}\text{Am})$$

**Eq 1.5**

### 3. Calibration & Results

The aim of calibration was to establish a relationship between declared  $^{240}\text{Pu}$ -effective mass and instrument response for each material group using actual items from the inventory. As discussed previously, the disadvantage of using such a 'self-calibration' strategy is that the accuracy of the declared data is unknown and any variation in can contents may potentially affect the calibration. These factors are likely to dominate a total measurement uncertainty which would have been extremely challenging to quantify in this case. In the absence of any certified reference benchmark, there were also limited options available for verifying the calibrations.

Confidence in the  $^{240}\text{Pu}$ -effective mass calibrations could only be achieved by including a large number of calibration cans which (a) had good provenance on their declared data and (b) originated from a number of different sources. Provided continued correlation was achieved throughout the assay campaign, and the independent isotopics measurement was also consistent with declared data, this added evidence to the conclusion that declared data was accurate. In the absence of reference standards, this large sample number approach was supported when required with use of MCNP modelling as an alternative benchmark of instrument response. Refer to Section 4.

Isotopics measurement formed an essential part of the verification process because it is not calibration dependant. Weight checks, radiography and health physics surveys were also carried out as a means of increased confidence in final measurement results.

### 3.1. Inventory Review & Calibration Planning

The key aim of calibration plans was to review all the inventory information and divide the fuel material into appropriate family groups based on shared characteristics (e.g. chemical composition, physical form, mass range, isotopic grade). From each family group, materials considered suitable for inclusion in the calibration were then selected, ensuring that these had high quality declared data wherever possible. The following inventory information was important to the desk study:-

- Manufacturing / Reprocessing reports / specifications
- Laboratory analysis reports
- Packaging records
- Health physics surveys and previous non-destructive assay results
- Radiographs (*note: limited numbers were available at calibration planning stage*)

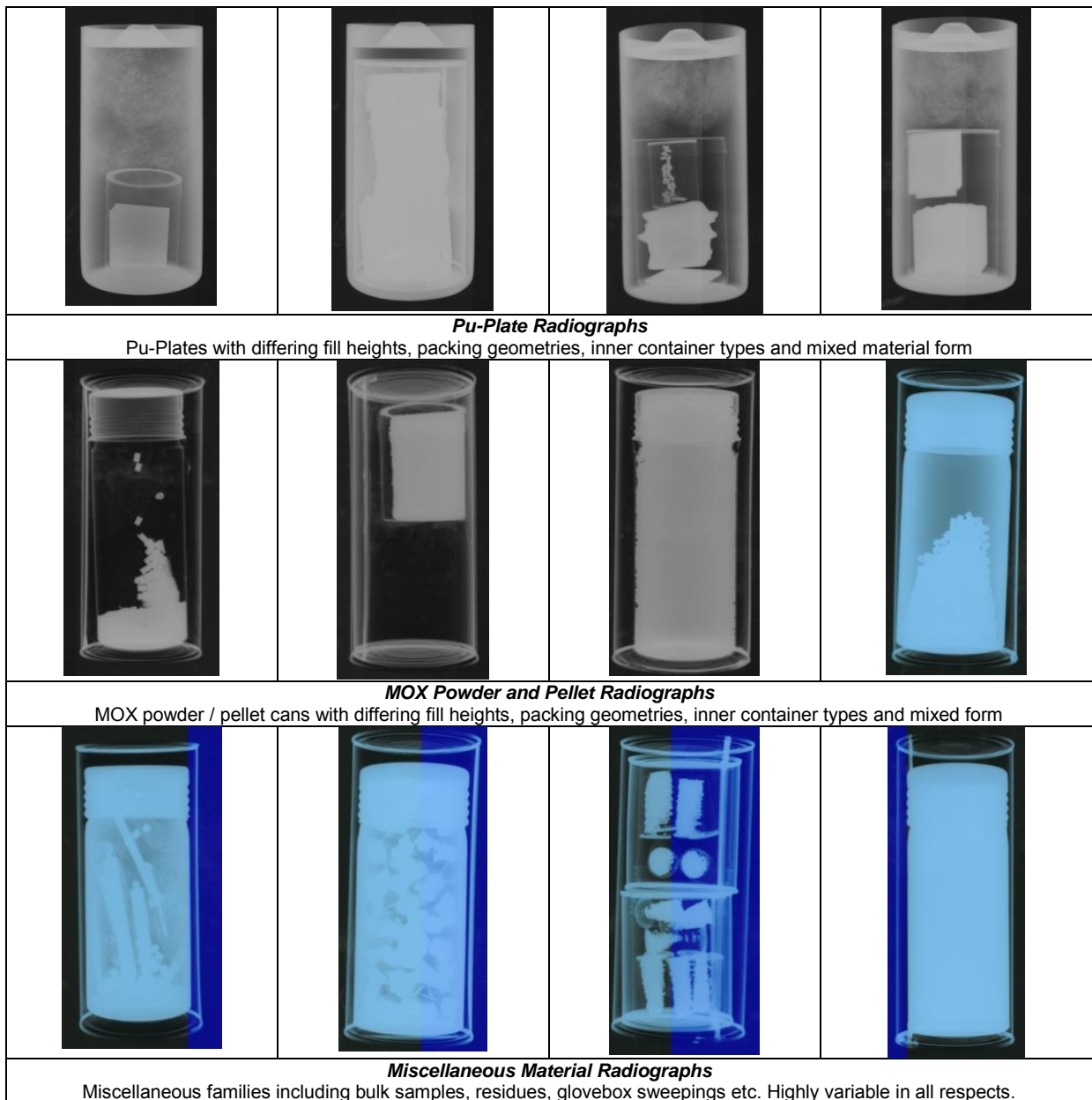


**Fig5:** Historical Radiographs (taken prior to over-packing).

On the whole, most of the inventory had the advantage of good provenance where declared data could be traced to high quality laboratory analysis from original manufacture and / or subsequent

reprocessing. However, the material had been in long term storage and was believed to be highly variable in terms of compositional content and packaging. Furthermore, a number of cans had incomplete inventory. A small portion of the cans had been radiographed in the past and these illustrate some of the issues with potential to affect NDA measurement. Refer to Fig 5.

- i) **Family Grouping Issues** The radiographs indicated that some cans did not fit within a single family group. Mixtures of pellets and powders, or pellets and plates were the most frequently encountered anomaly.
- ii) **Variations in Geometry & Packaging.** Within any given family group there existed an unknown level of geometrical variation in terms of packing and density, fill height and voidage. Packaging also varied with a mixture of steel, aluminium, brass and plastic containers all being used, as well as various types of PVC wrapping. Packaging details were not always clearly defined in inventory records.
- iii) **Variation in Physical / Chemical Form.** Within any given group there were varying characteristics in terms of both chemical and physical form (e.g. *differing alloy compositions, U:Pu ratios, HEU content, presence of moisture, chloride / fluoride, moderator, packaging types*).
- iv) **Mixed isotopics.** Some cans had heterogeneous isotopic content. This was a particular concern, not only because isotopic homogeneity is essential for accurate FRAM analysis, but also because the gamma detector can only 'view' the base of the can.
- v) **High dose rate cans.** Estimated dose rates for some of the higher mass cans could potentially reach mSv/hr levels. Such levels are known to cause issues for both neutron and gamma measurement.

The planned calibration families were split into two phases as illustrated in Fig 6. Phase 1 covers the lower mass materials with power <3.5W. Phase 2 includes all the higher mass materials with power levels up to 8W. The calibrations and results are described in Sections 3.2 – 3.3.

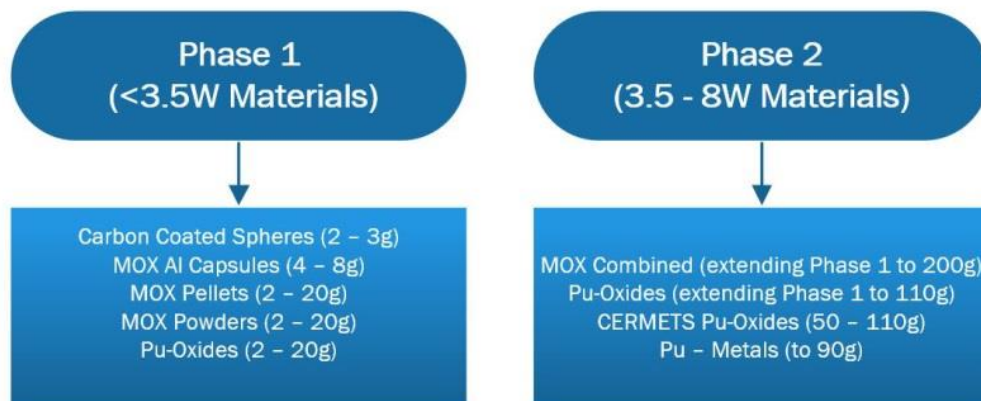


Fig 6: Summarised Calibration Plans with Pu240eff mass ranges.

### 3.2. Phase 1 Calibrations & Results (Low Mass Range MOX Materials)

The Phase 1 group of materials had power outputs <3.5Watt and  $^{240}\text{Pu}_{(\text{eff})}$  masses < 20g. Declared data was comprehensive and considered to be high quality. These were initially segregated into five families for calibration and measurement as follows:-

- Carbon Coated Spheres
- Al Capsules
- MOX Pellets
- MOX Powders
- Pu-Oxide Powders

The carbon coated MOX spheres shared a total Pu mass range of 20 – 30g combined with 700 – 2000g of depleted uranium per can, giving a relatively constant U:Pu ratio of around 80:1. The

material was in the form of MOX spheres / granules with a carbon content of around 1000g per can, and  $^{240}\text{Pu}$  isotopic abundances of 15 – 20%.

The Al-capsules contained MOX pellets with  $^{240}\text{Pu}$  isotopic abundances of around 12%. Each can was similar, with around 4900g of U in depleted form combined with 39g Pu per can, giving a U:Pu ratio of approx.126:1.

The MOX Pellets and Powders family groups covered a wider mass range and more variable declared content. These cans contained uranium in natural, depleted and enriched forms, combined with low Pu mass (not exceeding around 100g total Pu in any can). The  $^{240}\text{Pu}$  isotopic abundance varied from 6% up to around 25%. U:Pu ratios were very variable; typically around 50:1 up to 400:1, but a few were as high as 1000:1 or more. It would have been preferable to further sub-divide this group prior to calibration, but this not possible because there was not enough cans to adequately represent any additional sub-groups.

The Pu-Oxide materials were all in powder form with total Pu mass in the range 3 – 130g and no U content. The  $^{240}\text{Pu}$  isotopic abundance varied from 5 – 15%, although most cans were at the higher end of this range.

The  $^{240}\text{Pu}_{(\text{eff})}$  mass calibration for each of the five Phase 1 families initially consisted of a minimum of six points, where each calibration can was measured three times as a check on repeatability. The average measured reals count-rates were subsequently used as calibration points. Count times were 20 minutes for all neutron measurements (and 50 minutes for gamma).

Although all phase 1 materials were originally measured under individual  $^{240}\text{Pu}_{(\text{eff})}$  mass calibrations, it became increasingly clear as the assay campaigns proceeded, that comparable (if not better) results could have been obtained using a single combined calibration. This is because all five family groups shared similar neutron response relationships. Refer to Fig 7a which combines all five Phase 1 calibrations into one. The main outlier was a higher mass Pu-oxide can which returned a lower than expected count rate. There were no other cans available during Phase 1 with which to compare this outlier and no radiograph. This limited investigation at the time of measurement.

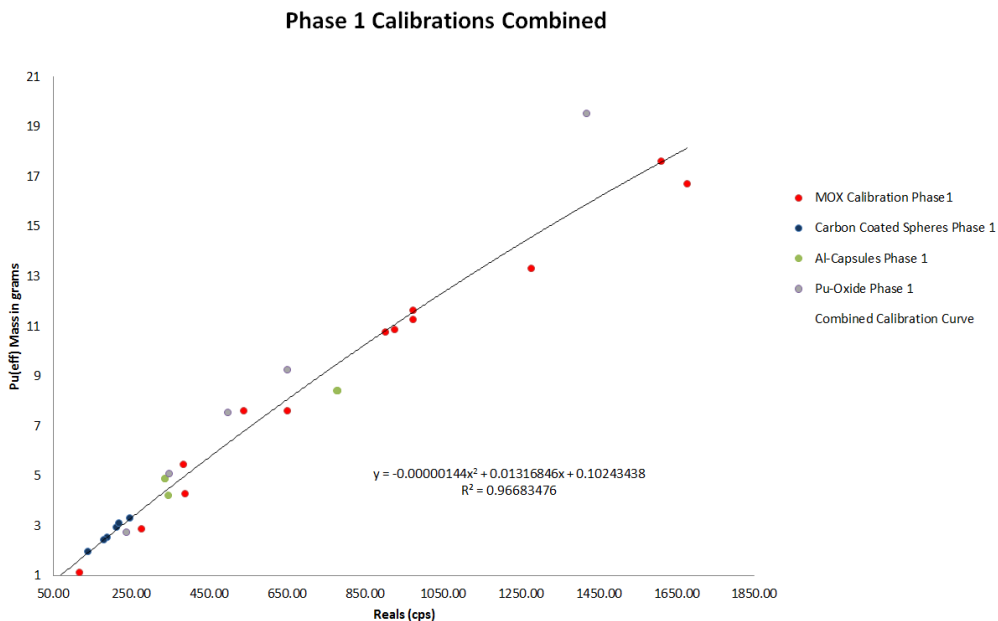


**Fig 7a:** Phase 1 Calibrations

In total, 559 cans were measured as part of Phase 1 and a high percentage of these showed good correlation with the combined calibration. Refer to Fig7b which shows all the neutron measurements plotted against the combined calibrations.

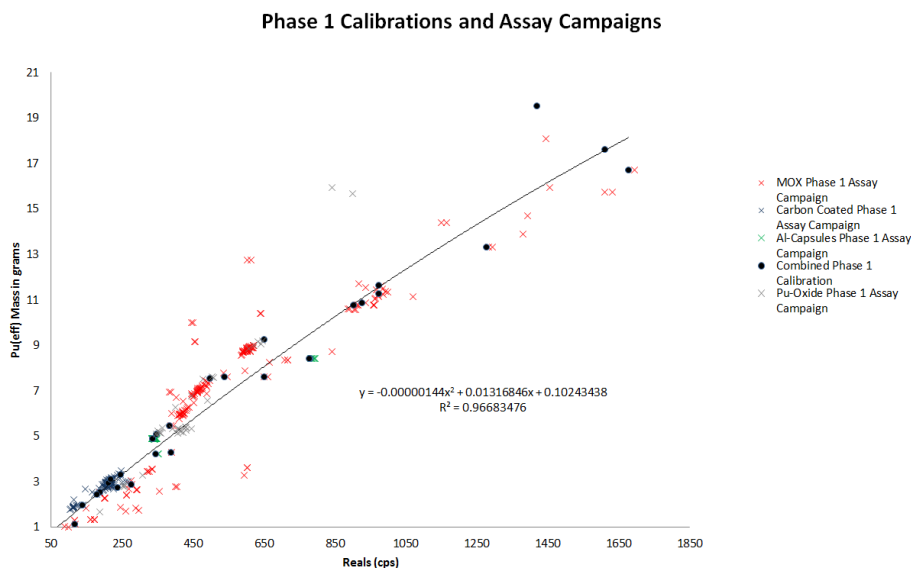


**Fig 7b:** Phase 1 All Cans shown on Combined Calibration

The single calibration worked very well for Al-capsules and carbon coated spheres, with high pass rates of 100% and 86% respectively. Pu-oxides results showed a lower pass rate of 78%, but it should be noted that some of these were below instrument detection limits in terms of  $^{240}\text{Pu}_{(\text{eff})}$  mass. When materials below the detection limit are excluded, the pass rate for Pu-oxides increases to 85%.

The MOX powder / pellet gave mixed results with only 54% of the cans passing, but given the wider declared mass range and content variations within this family group this is not unexpected. Additional calibrations based on material sub-groups in terms of U content may have improved results, but were precluded by timescales and number of cans available. As for Pu-oxides, a large number of the MOX powder / pellet cans measured were below detection limit. If these are excluded, the pass rate for MOX increases to 89%.

The gamma measurements gave very poor isotopics results for Phase 1 material with the exception of the carbon coated spheres and any MOX / Pu-oxides which had  $^{240}\text{Pu}$  isotopic abundances exceeding around 15%. Attempts to improve results by increasing count time and changing filter thickness were unsuccessful. In the case of Pu-oxides, isotopics measurement only failed for those cans which had very low Pu mass (<3g), combined with very low  $^{240}\text{Pu}$  isotopic abundance (<6%). The isotopic content in these cans appeared to be below instrument detection levels, although there was insufficient data to determine a clear isotopics measurement cut-off.

Phase 1 was not supported by MCNP modelling or radiography, but in any case, most of the failed cans had declared masses below instrument detection limits. In these cases, it was agreed that where a measured count rate and declared value was both below detection limit, the NDA result could only be used to confirm that items contained very small amounts of Pu. This was deemed sufficient for verification purposes given the project constraints and instrument measurement limitations.

### 3.3. Phase 2 Calibrations & Results (Intermediate Mass Range MOX & Pu-Oxide Materials)

Phase 2 extended the combined calibration up to 210g  $^{240}\text{Pu}_{(\text{eff})}$  mass. The materials originated from a range of different sources, which were segregated into five families for calibration as follows:

- MOX Powders / Pellets
- Pu - Oxides
- CERMETS
- Metals
- MOX containing HEU

Additional operational restrictions were implemented during Phase 2 which meant that it was no longer possible to carry out repeat measurements on calibration cans at the higher masses. However, radiography of all cans was now included which enabled many of the ‘unknowns’ in can contents to be accounted for. Neutron count times were necessarily reduced to 10 minutes for Phase 2 measurements due to the higher real rates being measured. Gamma measurements were reduced to 15-30 minutes.

The combined MOX powders and pellets calibration was extended in a series of incremental steps, aligned with assay campaigns of increasing  $^{240}\text{Pu}_{(\text{eff})}$  mass.  $^{240}\text{Pu}$  isotopic abundance was mostly within the range 12 – 25%. A total of fifty MOX cans from various origins were used for this calibration extension as a ‘large sample number’ approach – refer to Fig 8a. The uranium present was all in natural or depleted form because there were sufficient cans of MOX containing highly enriched U (HEU) to permit sub-division of these materials into a separate calibration.

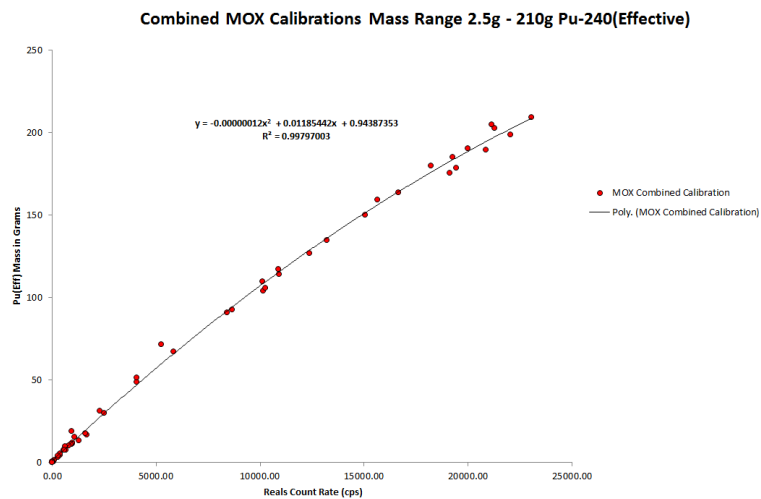


**Fig 8a: Phase 2 MOX  $^{240}\text{Pu}_{(\text{eff})}$  Calibration (incorporating Phase 1 calibration measurements also)**

Over 700 cans have been measured on the Phase 2 MOX calibration, and the results are shown in Fig 8b. Pass rates are very high with almost all cans achieving 15% agreement or better agreement with declared  $^{240}\text{Pu}_{(\text{eff})}$  mass. In the small number of cases where cans failed, valid reasons have generally been found through subsequent investigation and this has led to all the major outliers being removed – refer to Section 3.4.

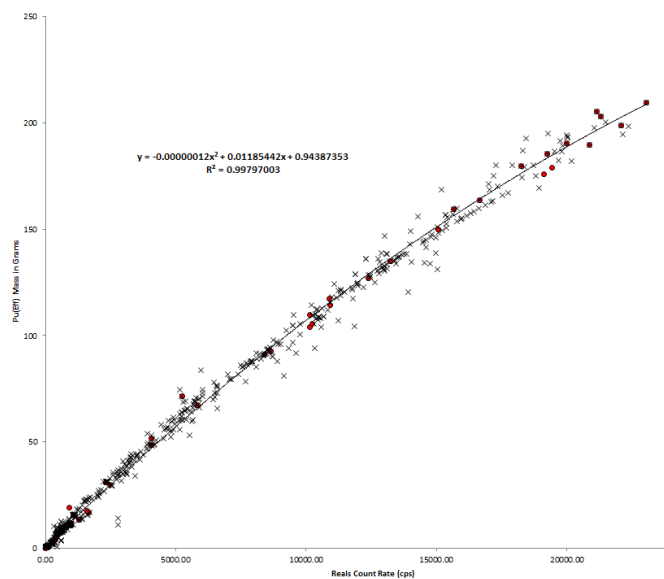


**Fig 8b: MOX Assay Campaign Performance (>700 cans measured to date)**

The Cermet, Pu metal, Pu-oxide and MOX containing HEU calibrations are incomplete, and are therefore only discussed briefly. At the time of writing, the Pu-oxide and CERMET calibrations are comparable with MOX and it appears likely that a combined calibration will continue to apply at higher Pu mass, as was the case for Phase 1 measurements. Refer to Fig 9.

MOX materials containing HEU exhibit a significantly higher real response rate for a given Pu mass and therefore require separate calibration. Three MOX HEU cans with enrichments of around 70%, and  $^{235}\text{U}$  content of around 500 – 900g are plotted on Fig 9 for reference. The observed deviation from the standard MOX calibration for these is attributed to higher levels of self-multiplication due to induced fission of  $^{235}\text{U}$ , and is expected to vary with enrichment and U-235 mass.

Three Pu metal can measurements are also plotted on Fig 9 for reference and show a dramatic increase in real response when compared to the standard MOX calibration. These cans contained around 1kg of Pu metal in a solid billet form. As for the MOX containing HEU, the increased response is attributed to high levels of self-multiplication. MCNP modelling and reference to real enhancement factors [7, 18] indicated that the high measured count rates for Pu metal were consistent with theoretical data. Correction for self-multiplication brought measured results much closer to the other calibration curves.

Work on calibrations for MOX containing HEU and Pu metal is still ongoing and therefore outwith the scope of this paper, but early MCNP modelling work has shown good agreement with the measured results for all family groups. Refer to Section 3.4.

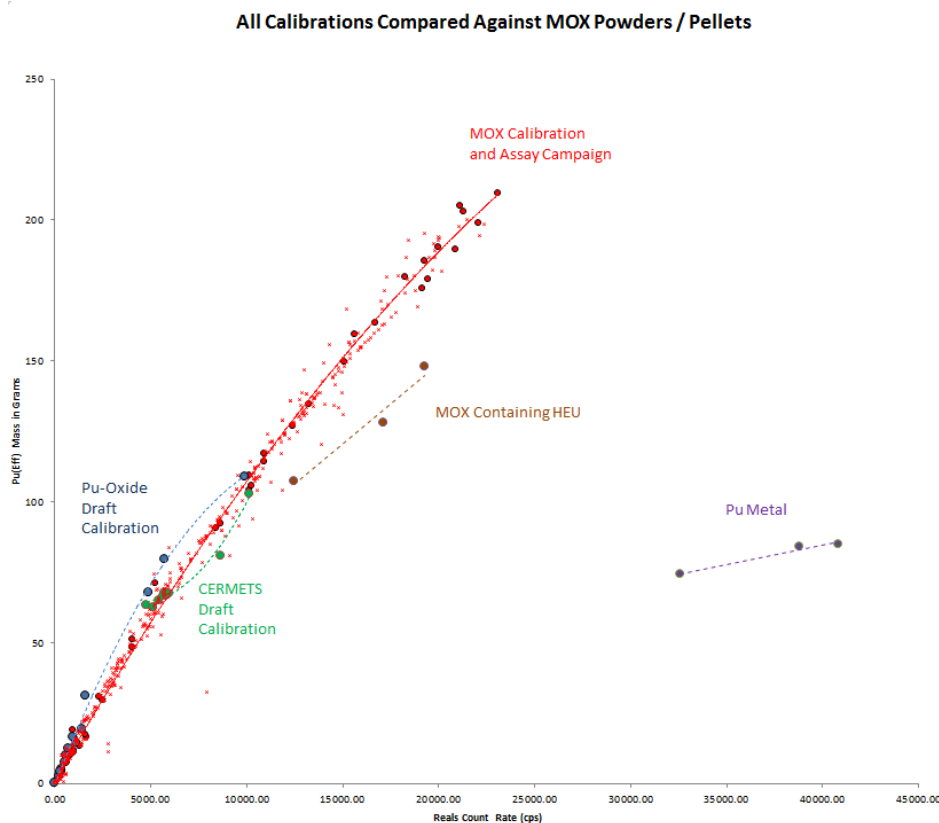


Fig 9: Phase 2 MOX Calibration and Assay Campaign Comparison with Other Phase 2 Materials

The gamma measurement generally showed very good performance for all Phase 2 materials provided that isotopic content was not mixed, achieving 15% or better agreement with declared  $^{240}\text{Pu}$ .

### 3.4. MCNP Support

Where Radiographs and drawings are available for material of known provenance, it is possible to make credible assumptions and use MCNP [04] which can determine the Multiplication "M" and

detection efficiency “ $\epsilon$ ”. This has proved useful in supporting the verification of calibrations, as well as aiding investigation of results where NDA measurements fail to agree with declared data. A radiograph and equivalent simplified MCNP Model of a single can are shown below for comparison in Figure 10. Assumptions have been made by not modelling bulges or screw top lids which are complicated to replicate. However, there is a reasonably accurate like-for-like comparison.

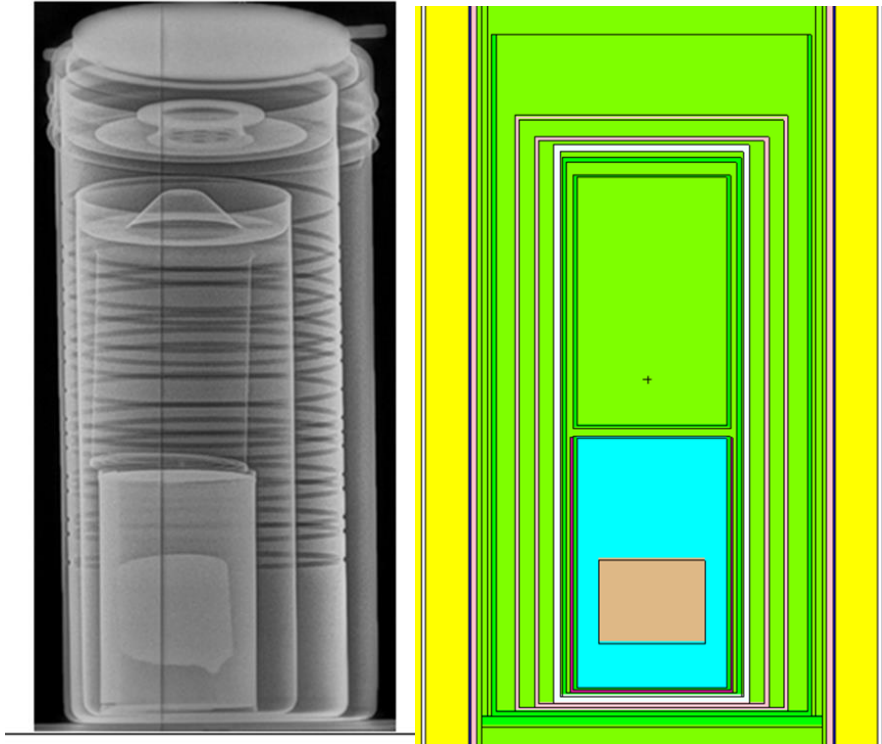


**Figure 10:** Simplified (not-to-scale) assumed MCNP Geometry compared to Can Radiography

Weighing the can prior to assay gives a gross mass. The MCNP output for cells gives masses from the geometry and input density. As further re-assurance that the MCNP model is reasonably accurate, it is possible to compare the measured mass with the MCNP calculated value. In the example above, the outer can difference was calculated to be less than 2.5%. Of course, by an iterative process of adjusting material parameters by small fractions it would be possible to minimise the mass bias further. This is considered to be overcomplicated and unnecessary as the can materials are believed to have a small perturbation effect on the neutron transport.

The analytical point model equations for Reals is useful for providing an independent cross-check on the calibration of the measured Pu mass since it relies on the properties of the material and physical constants. The analytical expressions for the Reals count-rate are given below [6]:

$$R \approx m F \frac{\epsilon^2}{2} f_d M^2 \left[ \nu_{s2} + \frac{(M-1)}{(\nu_{i1}-1)} \nu_{s1} \nu_{i2} (1 + \alpha) \right] \quad \text{Eq 1.6}$$

Where R is the Reals (Doubles) count rate (s), m is the  $^{240}\text{Pu}_{(\text{eff})}$  mass calculated from the gamma PC-FRAM (g), F is the  $^{240}\text{Pu}$  spontaneous fission rate (473 n/s/g),  $\epsilon$  is the instrument detection efficiency (counts per neutron),  $f_d$  is the chamber doubles gate-fraction, M is the leakage Multiplication factor,  $\nu_{i1}$  (3.163),  $\nu_{i2}$  (8.24),  $\nu_{s1}$  (2.156),  $\nu_{s2}$  (3.789) are the 1<sup>st</sup> and 2<sup>nd</sup> reduced moments for induced fission and spontaneous fission respectively and  $\alpha$  is the ( $\alpha$ ,n) to spontaneous fission ratio.

$\epsilon$  may be determined experimentally or by using MCNP. For a given chamber design  $f_d$  is considered to be a constant until such time as the chamber or counting electronics are adjusted and is calculated as follows [5]:

$$f = \exp\left(-\frac{t_p}{\tau}\right) \left[ 1 - \exp\left(-\frac{t_g}{\tau}\right) \right] \quad \text{Eq 1.7}$$

Where,  $t_p$  is the pre-delay time (4  $\mu$ s),  $t_g$  is the gate width setting (89.6  $\mu$ s) and  $\tau$  is the thermal die-away time (73.6  $\mu$ s); and as a sanity check it is a general rule that  $t_g = 1.249 \tau$ .

The leakage Multiplication “M” is calculated directly from the assumed Pu mass (g) and estimated density (g/cc) according to the Croft/Chard et.al. method [15] as follows:

$$M = 1 + \langle a_1 \left( \rho^{\frac{2}{3}} g^{\frac{1}{3}} \right) + a_2 \left( \rho^{\frac{2}{3}} g^{\frac{1}{3}} \right)^2 \rangle \quad \text{Eq 1.8}$$

Where,  $g$  = Mass of Pu (g),  $\rho$  = density of Pu (g/cc),  $a_1 = 4.187 \times 10^{-3}$  and  $a_2 = 39 \times 10^{-6}$  respectively. We accept that “g” is either the declared Pu mass or has been determined by the instrument and “ $\rho$ ” is assumed from knowledge of the sample.

Finally,  $\alpha$ , for PuO<sub>2</sub>, taking into account <sup>241</sup>Am in-growth, can be calculated from the gamma PC-FRAM as follows [5]:

$$\alpha = \frac{13400 \%Pu_{238} + 38.1 \%Pu_{239} + 141 \%Pu_{240} + 1.3 \%Pu_{241} + 2 \%Pu_{242} + 2690 \%Am_{241}}{1020 (2.54 \%Pu_{238} + \%Pu_{240} + 1.69 \%Pu_{240})} \quad \text{Eq 1.9}$$

If all the input assumptions are valid and the values are representative of the material, a theoretical calculation of neutron Reals is possible as all other parameters are known. For Pu Metals and PuO<sub>2</sub>, the analytically derived neutron Reals has matched in most cases to better than 15%, via calibration, the declared Pu mass. This suggests that most input assumptions are approximately valid and also that the calculated neutron reals rate and measured neutron reals rate are representative of the material being assayed.

It is very important to note and understand that this analytical work only supports the declared and measured results. It is not used to determine Pu calibrations or declare Pu masses for accountancy. Where it is useful as an off-line tool is to gain supporting confidence in the validity of declared results.

Lastly, MCNP cannot be used to check every can measurement within the given timescales. As figure 10 above clearly illustrates there are too many variables in can and material type to quickly change all cells and surface cards with the required level of confidence and quality assurance required by following the ESARDA Modelling Good Practice Guide [16].

### 3.5. Radiography and General Assessment

Where measurements fail to meet agreement with declared, these have been investigated on a case by case basis. A level of flexibility requires to be applied to such investigations, but the general protocol is as follows:

- 1) Review the gamma spectra and parameter file used - if deemed necessary, reanalyse on a more appropriate parameter file.
- 2) Check the measured reals response against expected value on relevant calibration to ensure measured value is as expected. If it is not, check that the Totals:Reals ratio is normal for material type. If this ratio is not typical of a given family group it may indicate different material characteristics.
- 3) Study radiographs. These provide a lot of valuable information on can contents.
- 4) Conduct MCNP modelling to verify measured neutron response.
- 5) Revisit historic inventory (packing sheets, analytical reports, manufacturing spec / reprocessing records etc.).
- 6) Checks on physical material weights.

To date, all measured cans which have failed to reach 15% agreement with declared have been explained in a concessionary process by following this investigation protocol. Some examples are discussed below.

#### 3.5.1 Failed Isotopics Analysis

On the occasions where isotopics analysis failed to reach 15% agreement with declared, one (or more) of the following reasons is most likely:

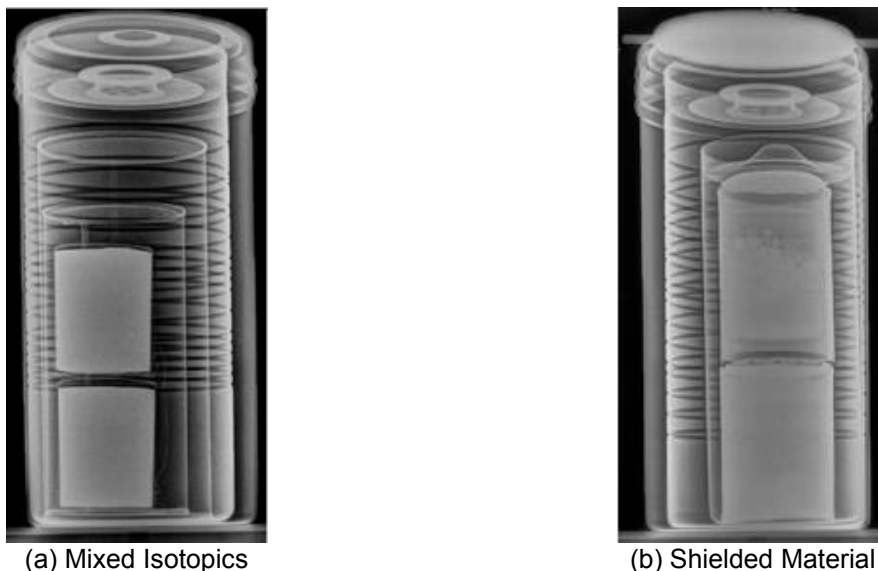
- $^{240}\text{Pu}$  isotopic content below instrument detection limit (due to very low mass and/or isotopic abundance). Very high U:Pu ratio also affected detection due to the high self-shielding properties of U.
- Counting losses due to high dead-time when measuring higher dose rate cans
- Heterogeneous isotopic content or material with mixed isotopics in the same can.
- Use of inappropriate parameter file

In the case of detection limit being the issue, options were limited because the instrument source-detector distance was fixed. Results could sometimes be achieved by increasing count times, but limited success was achieved during Phase 1.

Dead-time issues were improved by reducing collimator gap width. Use of the latest version FRAM software (FRAM-BW v5.2) showed marked improvement in analysis of spectra from higher dose rate cans compared to the earlier version utilised in the NDA system.

In the case of mixed isotopics, little can be done to improve results. However, in cases where the mixed isotopics are due to a can containing two smaller containers of differing declared isotopics, radiography can add some value to the measurement. The gamma detector, which views the can from the base upwards, can only 'see' the lower can. Refer to Fig 11a.

The correct choice of parameter file is important. On one occasion, failed isotopic measurement on an entire batch of cans occurred and a review of the gamma spectra revealed that this was because the low energy peaks had not been detected. The radiographs were studied and clearly confirmed presence of an additional layer of high density material wrapped round the inner cans. See Fig 11b. Subsequent reanalysis of these spectra using the higher energy FRAM parameter file suitable for shielded material (MOX\_Cx\_180-1010), gave much improved agreement with declared.



(a) Mixed Isotopics

(b) Shielded Material

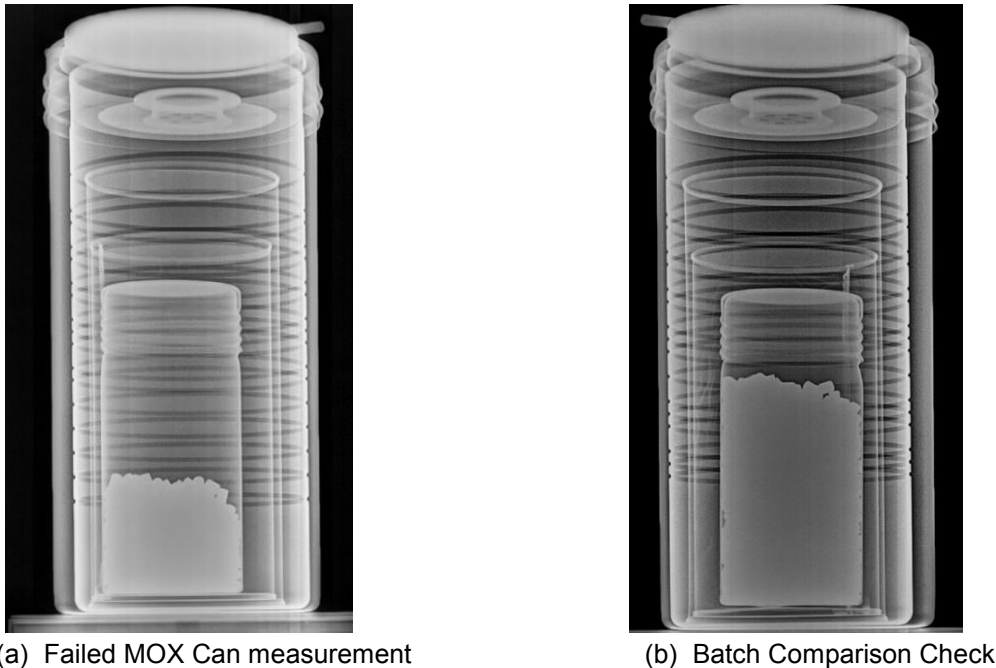
**Figure 11:** Radiograph Examples - Cans Which Failed Isotopics Measurement

### 3.5.2 Failed $^{240}\text{Pu}_{(\text{eff})}$ Mass Measurements

Failure of  $^{240}\text{Pu}_{(\text{eff})}$  measurements to agree with declared were occasionally encountered and the main causes were as follows:

- Incorrect declared inventory
- High Levels Of Self-Multiplication not represented in calibration
- Use of incorrect calibration

Cases of incorrect declared inventory was very rare, but was demonstrated on a few occasions. In such cases radiography combined with measurement against an established calibration was essential in drawing conclusions. An example is shown in Fig 12 where (a) is a failed MOX pellet can which had significantly lower than expected measured reals count and (b) is one of several comparable cans with the same declared content as the failed can. In this particular case, radiography was able to confirm that the failed can was only half full. A physical weight check supported the NDA result and all the evidence taken together enabled confirmation of a historic declared data error.



(a) Failed MOX Can measurement (b) Batch Comparison Check  
**Figure 12:** Radiograph Examples - Cans Which Failed Declared  $^{240}\text{Pu}_{(\text{eff})}$  Mass Measurement

High levels of self-multiplication or  $(\alpha, n)$  contributions which are not represented in the calibration results in higher than expected reals count rates for a given  $^{240}\text{Pu}_{(\text{eff})}$  mass. In the case of additional  $(\alpha, n)$  contributions, a high Totals:Reals ratio proved a very useful diagnostic indicator. The most important  $(\alpha, n)$  contributors are typically oxygen and fluorine [5].

An example of a can failing due to unexpected  $(\alpha, n)$  contribution was encountered during Phase 2. This was a Pu-oxide powder can which showed a very high measured reals rate against the Pu-oxide calibration. Investigation showed that the Totals: Reals ratio for this particular can was almost 50:1 (all the other material from the same batch had a much lower ratio of around 7:1).

There was no evidence of anything unusual in the measured gamma spectrum, and the isotopics analysis gave good agreement with declared. The radiograph confirmed a geometry consistent with the rest of the batch (i.e. two cans of powder stacked inside a larger can). The historical inventory data was examined in detail and it then was established that the top can actually contained Pu-Fluoride rather than Pu-Oxide. This explained both the high ratio and elevated count rates. There was no calibration available for this material so the NDA measurement was unable to verify declared content. However, the results were subsequently modelled by MCNP which confirmed that measured count rates were consistent with theoretical values for the same mass.

If cans are measured on an unsuitable calibration, this will increase fail rates. However, to date this has only applied to cans containing fluoride, HEU or Pu metal - none of which correlate with the combined MOX calibration. Pu metal form has proved straightforward to distinguish from radiographic images and it's low Totals:Reals signature. HEU content is more complex to investigate.

#### 4. Discussion

The lessons learned during Phases 1 and 2 are useful as this project moves on to measurement of higher mass materials with power outputs exceeding 8W (Phase 3). Work so far has demonstrated that this 'self-verifying' strategy can work very effectively for  $^{240}\text{Pu}_{(\text{eff})}$  mass calibration provided the calibrations are fully representative of the material being measured and there is good confidence in the accuracy of declared data.

The work in Phase 1 was limited by very low masses of Pu, particularly when combined with high U masses which contributes to a high level of self-shielding. Instrument detection limits were challenged, both in terms of neutron and gamma measurement and yet high pass rates were achieved. In the case of the gamma measurement, it may have been possible to improve results by moving the gamma detector much closer to the material, but this was not possible due to a system design optimised for very high mass / dose rate cans. The neutron counting detection limit could have been improved by increasing the external shielding to reduce background had space limitations allowed.

Assay results for the Phase 2 materials, where Pu masses were within the system operating limits, achieved very high pass rates. For isotopics measurement, the results are self-standing as they are independent of calibration. However for  $^{240}\text{Pu}_{(\text{eff})}$  mass measurement, calibrations are based on an assumption that declared data was accurate.

When using a 'self-verifying' strategy it is vital to ensure that declared data is accurate. This is best achieved by bench-marking to a certified reference standard. This option was not available. However, the project had the advantage of access to large batches of materials with high quality laboratory analysis data that had been carried out to comparable, traceable standards. Also, the gamma measurement formed a direct, independent check on the isotopic declared information.

Confidence in declared  $^{240}\text{Pu}_{(\text{eff})}$  mass was gained by a 'large sample number approach', whereby calibrations included many cans from different manufacturing and / or reprocessing origins. As more materials from different origins were measured and continued to demonstrate good agreement with the original calibrations, confidence in the results increased and maximised the likelihood of identifying any errors in declared inventory. Further confidence was acquired as the project moved on to Phase 2 by using MCNP modelling and radiography to examine outliers.

The  $^{240}\text{Pu}_{(\text{eff})}$  mass 'self-calibration' method is undoubtedly crude in some respects, but it also has some advantages worthy of consideration. One of the major unknown factors affecting neutron counting response is self-multiplication within the material itself. This effect can be very difficult to quantify and correct for. Correction is usually required in conventional calibrations because they utilise artificially prepared certified reference standards which are fundamentally different in terms of compositional and physical characteristics to the material being measured. Conversely, the method described in this paper uses actual inventory material so the effects of self-multiplication are captured within the calibrations themselves, thus eliminating any requirement to apply complex corrections.

This work has demonstrated that despite considerable variations in material geometry, density and form, it has been possible to create a single calibration which covers a wide range of masses and material types. Partially filled cans, MOX and Pu-oxide in both powder and compacted forms, and varying package type can all be encompassed within a single calibration. Radiography and MCNP modelling proved invaluable support during both calibrations and subsequent assay campaigns.

The measurement data acquired to date is potentially useful for reference and possibly benchmarking during similar assay projects in future.

## 5. Acknowledgements

The authors would like to acknowledge and thank the DSRL Operations staff, the OCEANEERING radiography team and EURATOM safeguards inspectors for their continued support and assistance throughout this project. Special thanks also to Christopher Orr and Patrick Chard for helpful advice on neutron physics theory.

## 6. Legal matters

### 6.1. Privacy regulations and protection of personal data

The authors agree that ESARDA may print our names/contacts and data/photographs/article in the ESARDA Bulletin/Symposium proceedings or any other ESARDA publications and when necessary for any other purposes connected with ESARDA activities.

### 6.2. Copyright

The authors agree that submission of an article automatically authorises ESARDA to publish the work/article in whole or in part in all ESARDA publications – the bulletin, meeting proceedings, and on the website.

Once the article has been accepted for publication the copyright is reserved, but part of the publication may be reproduced, stored in a retrieval system, or transmitted in any form or by any means, mechanical, photocopy, recording, or otherwise, provided that the source is properly acknowledged.

The authors declare that their work/article is original and not a violation or infringement of any existing copyright.

## 7. References

- [1] Wells, G.M., Cookson, J.A., Metcalfe, B.; *NDA Techniques Applied to a Major Transfer of Nuclear Material* (EUR—13686); Commission of the European Communities (CEC); 1991.
- [2] Burke, K.J., Ancius, D., Chaudry, A., Gunn, R.D., Looman, M.R., Maina, J., Mason, J.A., Paton, D., Towner, A.C.N., Wood, G.H.; *Design and Testing of a Combined Neutron and Gamma Assay System for Measuring Fissile Material in Fuel and Waste Items*; ANTECH; WM2015 Conference; 2015.
- [3] Sampson, T.E., Kelley, T.A., Vo, D.T.; *Application Guide to Gamma Ray Isotopic Analysis using the FRAM Software*; Los Alamos National Laboratory; LA-14018; 2003.
- [4] National Physical Laboratory; *Good Practice Guide No. 34 Radiometric Non-Destructive Assay*, ISSN 1368-6550 Issue 2; 2012.
- [5] Reilly, D., Ensslin, N., Smith, Jr., Kreiner, S.; *Passive Non-destructive Assay of Nuclear Materials*; Los Alamos National Laboratory; LA-UR-90-732; 1991.
- [6] L' Annunziata, Michael F.; *Handbook of Radioactivity Analysis*; ISBN 978-0-12-384873-4; Elsevier Academic Press; 3<sup>rd</sup> Edn. USA; 2012
- [7] Croft, S., Chard, P.; *Prompt Self-Multiplication Factors For Squat Cylinders of Weapons Grade Plutonium Metal*; AEA Technology; 1995.
- [8] Henzlova, H., Menlove, H.O., Croft, S., Favalli, A., Santi, P.A.; *The Impact of Gatewidth Setting and Gate Utilization Factors on Plutonium Assay in Passive Correlated Neutron Systems*; Los Alamos; LA-UR-15-21078; 2015.
- [9] IAEA; *International Target Values 2010 for Measurement Uncertainties in Safeguarding Nuclear Materials*; STR-368; 2010.
- [10] Myers, S.C., Porterfield, D.R., Tandon, L.; *Unique Challenges with recent Gamma Spectroscopy Measurements at Los Alamos National Laboratory*; Journal of Radioanalytical Nuclear Chemistry 282:533-537; 2009.
- [11] Vo, D.T.; *Operation and performance of FRAM Version 5.1*; LA-UR-11-03016; 2011.
- [12] Vo, D.T.; *Generalization of the FRAM's Bias*; LA-14253; 2005.
- [13] Vo, D.T.; *FRAM Version 5.1's Bias*; LA-UR-11-02958
- [14] T. Goorley, et al.; *Initial MCNP6 Release Overview*; Nuclear Technology; Dec 2012.
- [15] Croft, S., Stanfield, S., Chard, P.M.J. *Neutron Self Multiplication Effects in PDP Items in the Context of Coincidence Counting*; Paper 10496 Waste Management Conference, Arizona. 2010.
- [16] Chard, P.M.J., Croft, S., Looman, M., Peerani, P., Tagziria, H., Bruggeman, M., Laure-Weber, A.; *A Good Practice Guide for the use of Modelling Codes in Non Destructive Assay of Nuclear Material*; European Commission Joint Research Centre (EC-JRC); ESARDA Bulletin 42; 2009.
- [17] Knoll. G.F.; *Radiation Detection and Measurement*; 3<sup>rd</sup> Edition; John Wiley & Sons, Inc; 1999

- [18] Baldioli, V., Mullarkey, P., Coghill, A., Bain, N., Cormack, A., Gunn, R., Paton, D.; *Using MCNP to Reduce the Background Sensitivity of a Non-Destructive Assay Passive Neutron Coincidence Counting Chamber*; Dounreay Site Restoration Ltd; 2018
- [19] Bourva, L., Croft, S., *Calculation of Neutron Leakage Self-Multiplication Factors For Small Cylindrical Plutonium and Mixed Oxide Samples*; Harwell Instruments Ltd; 1999.
- [20] Mason, J.A., Bondar, W., Hage, B., Pederson, B., Swinhoe, M., Ledebink, E.W.; *The Assay of Pu by Neutron Multiplicity Counting Using Period and Signal Trigger Methods*; Proceedings of INMM93; Scottsdale; Arizona; July 1993

# Research on Uranium Enrichment Determination Using 143-1001keV Region of HPGe Uranium Spectrum

Yuan Tian  
Guorong Liu  
Hao Zhou  
Yonggang Zhao  
Jinghuai LI

China Institute of Atomic Energy  
P.O.Box 275-8, Beijing 102413, China  
E-mail: tianyuan910307@163.com

## **Abstract:**

*Uranium enrichment has been recognized as a significant target of verification in nuclear safeguards. A method for enrichment determination of  $^{235}\text{U}$  by analyzing gamma peaks of  $^{235}\text{U}$ ,  $^{238}\text{U}$  and  $^{228}\text{Th}$  (daughter of  $^{232}\text{U}$ ) to calibrate relative detection efficiency was described. A code to verify the method by analyzing the spectrum was written. A HPGe detector was used to measure two types of uranium samples with enrichment ranging from 1.8%-90.2% repeatedly. For the samples measured, the uranium enrichments are determined with an accuracy of about 3%.*

**Keywords:** uranium, enrichment, efficiency, self-calibration, HPGe

## **1. Introduction**

Leave three line spaces after the keywords and write an introduction title as shown above, leave one line space and begin the main body of the text.

International nuclear safeguards, also known as nuclear safeguards, are activities to verify a country's compliance with its international commitments not to divert its nuclear projects and activities to nuclear weapons. Strengthened and improved nuclear safeguards can also detect the presence of undeclared nuclear material and activities in a state.

The determination of uranium enrichment by gamma spectrum is an important work in the field of nuclear safeguards. The relative detection efficiency self-calibration method has the advantages of no standard source calibration, no special requirements for sample geometry and chemical morphology, and is relatively applicable under heavy shielding. The key technique of this method is how to fit the relative detection efficiency curve covering the whole middle and high energy region. According to the uranium energy spectrum, the characteristic energy peaks of  $^{235}\text{U}$  used to fit the relative detection efficiency curve are 143 keV, 163 keV, 186 keV and 205 keV, and the characteristic energy peaks of  $^{238}\text{U}$  are 258 keV, 743 keV, 766 keV, and 1001 keV. It can be seen that the characteristic energy peaks of  $^{235}\text{U}$  are distributed in the middle energy end of the energy spectrum, while the characteristic energy peaks of  $^{238}\text{U}$  are mainly distributed in the high energy end. Moreover, there is a large gap between the 258 keV and 743 keV characteristic energy peaks of  $^{238}\text{U}$ , so it is very difficult to fit the relative detection efficiency curve accurately. At the same time, the 258 keV characteristic energy peak becomes the key energy peak of fitting the relative detection efficiency curve. This method will mainly solve the technical difficulty, fit out the relative detection efficiency curve covering the whole middle and high energy region and determine the uranium enrichment.

In this paper, the fitting method of relative detection efficiency curve for HPGe uranium spectrum is established, and the corresponding algorithm and program are developed by using Matlab R2013a.

## 2. Method

### 2.1. Calculation of uranium enrichment

Uranium enrichment is defined as the ratio of the mass of the isotope  $^{235}\text{U}$  to the total mass of uranium, usually expressed as a percentage.  $^{235}\text{U}$  enrichment is expressed as follows:

$$nr = \frac{235N_5}{234N_4 + 235N_5 + 236N_6 + 238N_8} \approx \frac{235}{235 + 238 \frac{N_8}{N_5}}$$

The Enr is enrichment of  $^{235}\text{U}$ , and  $N_4$ ,  $N_5$ ,  $N_6$  and  $N_8$  are the atomic numbers of  $^{234}\text{U}$ ,  $^{235}\text{U}$ ,  $^{236}\text{U}$  and  $^{238}\text{U}$  respectively.

Normally, uranium samples contain very low levels of  $^{234}\text{U}$  and  $^{236}\text{U}$ , which were ignored in this work. So the enrichment of  $^{235}\text{U}$  depends only on the ratio of the atomic number of  $^{235}\text{U}$  to  $^{238}\text{U}$ .

### 2.2. Fitting of the relative detection efficiency curve

For each characteristic energy peak of  $^{238}\text{U}$ , the following equations are assumed:

$$\ln(A_8 \cdot \varepsilon) = \ln(\text{Area}_8 / \text{BR}_8) = f(E)$$

$$f(E) = C_1 + C_2/E^2 + C_3 \ln E + C_4 (\ln E)^2 + C_5 (\ln E)^3$$

In the formula,  $A_8$  is the activity of  $^{238}\text{U}$ , Area is the detection efficiency of peak, BR is the branch ratio of peak.

$f(E)$  is a relative detection efficiency curve which is composed of the characteristic energy peaks of  $^{238}\text{U}$ , and another relative detection efficiency curve corresponding to  $^{235}\text{U}$  can also be obtained from the characteristic energy peaks of  $^{235}\text{U}$ . Since there is a fixed difference between the relative detection efficiency curve functions of  $^{235}\text{U}$  and  $^{238}\text{U}$ , and the difference corresponds to the activity ratio  $k$  of the two, the following results are obtained:

$$\ln(A_5 \cdot \varepsilon) = \ln(\text{Area}_5 / \text{BR}_5) = f(e) + k$$

$$k = \frac{A_5}{A_8} = \frac{235}{238} \cdot \frac{T_8}{T_5} \cdot \frac{enr}{1 - enr}$$

Thus, all data points for fitting the curve  $f(E)$  can be obtained: (1) x axis is the energy peak  $e$ , in MeV, (2) Y axis is relative detection efficiency. The relative detection efficiency curves (as shown in figures 4 and 5) can be obtained by fitting the data points  $(E, y)$  into the curve form  $f(E)$ .

In the actual calculation, because the enrichment degree is an unknown quantity, it is necessary to use the exhaustive method to find the value of enrichment degree that minimizes the fitting residuals, that is, the final enrichment degree value. The initial values of the exhaustion can be calculated by using two energy peaks of 205 keV and 258 keV (assuming that the detection efficiencies of the two peaks are equal, the enrichment can be approximately calculated). Starting from the initial enrichment degree, the best enrichment degree can be found by enumerating and comparing.

Fig. 1 shows the relationship between the characteristic peak strength and  $^{235}\text{U}$  enrichment in the energy range of 230-265keV. From Fig. 1, with the increase of  $^{235}\text{U}$  enrichment, the content of  $^{238}\text{U}$  decreases, the 258.3 keV characteristic peak of  $^{238}\text{U}$  becomes weaker, and the characteristic peak of  $^{228}\text{Th}$  becomes stronger. The 258.3 keV characteristic peak of  $^{238}\text{U}$  almost disappears when the enrichment of highly enriched uranium is high (for example, 90.2%), so for the highly enriched uranium sample, the characteristic peaks of  $^{235}\text{U}$  and  $^{238}\text{U}$  can not be used to fit the relative detection efficiency curve correctly. Considering that there is a small amount of  $^{232}\text{U}$  in HEU, the 238.6 keV characteristic energy peak of  $^{228}\text{Th}$  is just at the middle energy region, which plays an important role in fitting the relative detection efficiency curve of HEU.

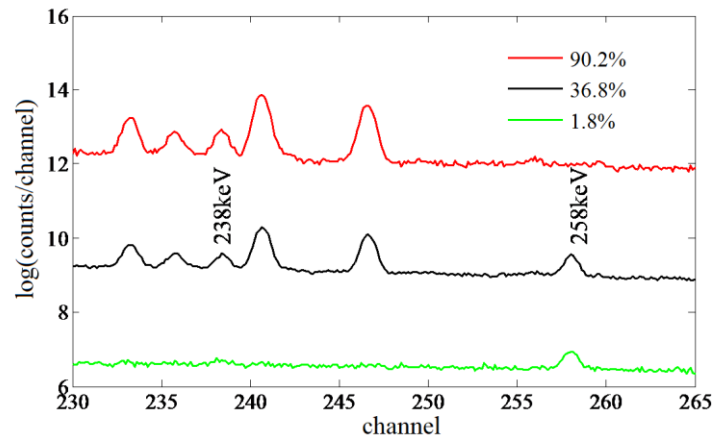


Figure 1: relationship between the intensity of characteristic peak and enrichment of  $^{235}\text{U}$

For highly enriched uranium, the relative detection efficiency curves covering the whole middle and high energy region can be obtained by using the above method through the  $^{235}\text{U}$  and  $^{228}\text{Th}$  characteristic energy peaks (238.6 keV, 583.2 keV, 727.3 keV and 860.5 keV). The enrichment degree of highly enriched uranium can be obtained by fitting the characteristic peaks of  $^{238}\text{U}$  according to the curve of relative detection efficiency.

### 3. Experiment and results

#### 3.1 Experiment

In the experiment,  $\text{U}_3\text{O}_8$  powder,  $\text{UO}_2$  pellets and standard samples with different enrichment degree were measured and analyzed. The uranium enrichment of  $\text{U}_3\text{O}_8$  powder samples was 4.06% and 90.2%, respectively. The uranium enrichment of  $\text{U}_3\text{O}_8$  nuclear fuel pellets was 1.8%, 4.2% and 10%, respectively. The uranium enrichment of standard samples was 14.48% and 18.95%. The nominal values of these samples are all from the results of mass spectrometry, and the relative uncertainty is less than 0.5%.

A GC2018-HPGE detector (relative efficiency 20%, energy resolution about 0.66% at 122 keV) and a Inspector-2000 spectrometer were used to measure and analyse seven samples. During the measurement, the detector was placed in a 1.1 cm thick steel lead shield, with cadmium and copper absorbers placed between the detector and the sample. The parameters such as high pressure and forming time of the spectrometer were kept unchanged. The Spectrometer was set at 8192 channels Channel width set to 0.125 Kev/ch.

#### 3.2 Results and discussion

The fitting effect of the relative efficiency curve of the actual energy spectrum is shown in Fig.2(a) (for the pellet sample with uranium enrichment of 10%) and fig.2(b) (for the powder sample with uranium enrichment of 10%). In the graph, horizontal coordinates represent energy, vertical coordinates represent relative detection efficiency,  $^{235}\text{U}$  data points are calculated data points,  $^{238}\text{U}$  data points and  $^{228}\text{Th}$  data points are fitted data points. As can be seen from the diagram, the data points are uniformly distributed on or on both sides of the fitted relative detection efficiency curve, and the relative detection efficiency curve is relatively smooth, covering the middle and high energy regions. It is shown that the method proposed above can fit the relative detection efficiency curves of LEU and HEU samples well.

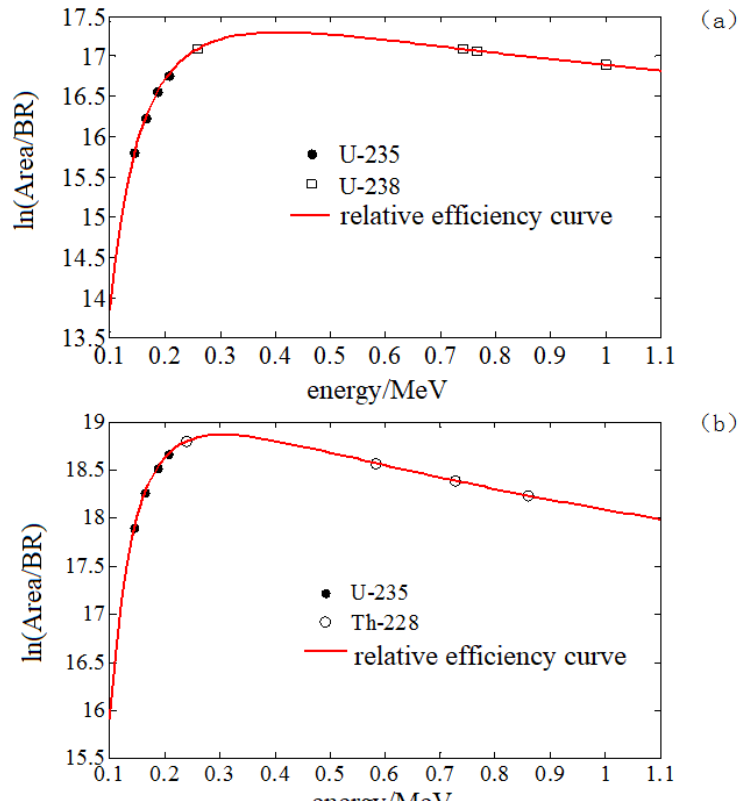


**Figure 2:** examples of a relative efficiency curve of enriched uranium samples

The main results of repeated measurements of spectra for each sample by the spectral UNMIXING program are listed in Table 1. According to the analysis results in Table 1, the relative deviation of the analytical values of core samples and powder samples is not more than 3%.

Samples	Enrichment/%	Determination/%	RD/%
UO <sub>2</sub> Pellet	1.80	1.78±0.04	-1.1
UO <sub>2</sub> Pellet	4.20	4.17±0.09	-0.7
UO <sub>2</sub> Pellet	10.00	10.20±0.22	2.0
U <sub>3</sub> O <sub>8</sub> Powder	4.06	4.18±0.10	3.0
U <sub>3</sub> O <sub>8</sub> Powder	90.2	90.75±0.42	0.6
Standard sanmple	14.84	14.91±0.28	0.4
Standard sanmple	18.95	18.87±0.40	-0.4

**Table 1:** results of different type of samples.

The results show that there is still a big gap between the analytical accuracy of this work and the international level. The reason may be that the characteristic energy peaks of the <sup>238</sup>U sub-body used to analyze uranium enrichment are affected by different degrees of coincidence addition effect, which leads to the decrease of the net peak area and affects the analysis accuracy.

#### 4. Conclusion

A method of fitting the relative detection efficiency curve with the characteristic peaks in the 143-1001 keV region using the uranium spectrum of HPGe is established. A program of the uranium enrichment degree is compiled. The fitting method of relative detection efficiency curve is verified by experiments. The experimental results show that the fitting method established in this paper can fit the relative detection efficiency curve well. For the samples measured, the uranium enrichment can be determined with an accuracy of about 3.0% for LEU samples and 0.6% for HEU ones.

## 5 Legal matters

### 5.1. Privacy regulations and protection of personal data

I agree that ESARDA may print my name/contact data/photograph/article in the ESARDA Bulletin/Symposium proceedings or any other ESARDA publications and when necessary for any other purposes connected with ESARDA activities.

### 5.2. Copyright

We agree that submission of an article automatically authorises ESARDA to publish the work/article in whole or in part in all ESARDA publications – the bulletin, meeting proceedings, and on the website.

Once the article has been accepted for publication the copyright is reserved, but part of the publication may be reproduced, stored in a retrieval system, or transmitted in any form or by any means, mechanical, photocopy, recording, or otherwise, provided that the source is properly acknowledged.

We declare that our work/article is original and not a violation or infringement of any existing copyright.

## 6. References

[1] Sampson T E, Nelson G W, Kelley T A; *FRAM: A versatile code for analyzing the isotopic composition of plutonium from gamma-ray pulse height spectra*; Instrumentation Related to Nuclear Science & Technology, 1989.

[2] Vo D T, Sampson T E; *Uranium Isotopic Analysis with the FRAM Isotopic Analysis Code*; Office of Scientific & Technical Information Technical Reports, 1999.

[3] Sampson T E, Kelley T A, Vo D T; *Application Guide to Gamma-Ray Isotopic Analysis Using the FRAM Software*; 2003.

[4] Sampson T E, Kelley T A; *PC/FRAM: a code for the nondestructive measurement of the isotopic composition of actinides for safeguards applications*; Applied Radiation & Isotopes, 1997, 48(10-12):1543-1548.

## Extended verification of fresh fuel assembly using LaBr<sub>3</sub> scintillation detectors at the Paks Nuclear Power Plant

<sup>1</sup>G. Dósa, <sup>1</sup>I. Almási, <sup>1</sup>Z. Hlavathy, <sup>1</sup>Zs. Kerner, <sup>1</sup>P. Kirchknopf, <sup>1</sup>P. Völgyesi,  
<sup>1,2</sup>A. Kocsonya, <sup>3</sup>D. Mesterházy

<sup>1</sup> Hungarian Academy of Sciences Centre for Energy Research,  
Nuclear Security Department, H-1121 Budapest,  
29-33 Konkoly-Thege Miklós Street, Hungary

<sup>2</sup> International Atomic Energy Agency, 1400 Vienna, Austria

<sup>3</sup> MVM Paks NPP Ltd., H-7031 Paks, Hungary

E-mail: [gergely.dosa@energia.mta.hu](mailto:gergely.dosa@energia.mta.hu), [istvan.almasi@energia.mta.hu](mailto:istvan.almasi@energia.mta.hu)

### Abstract:

*Checking the divergent assemblies in each fresh fuel batch carries the importance of nuclear safety, safeguards and economic optimization. Because of this, enrichment of uniformly and non-uniformly enriched ("profiled") fuel assemblies in the range of 1.6-4.4% were verified by gamma-ray spectrometry at the MVM Paks NPP Ltd. with HPGe and CdZnTe (CZT) detectors. While the HPGe detector was positioned at the side, the CZT was inserted into the central tube of the assemblies. They were thus used for obtaining information not only from the outer but also from the inner fuel rods. Applying these detectors, a procedure was developed to verify the recently arrived shipment of assemblies, and is now in routine use. This procedure is quite time consuming due to the necessary assembly side measurements, which were performed to check the side symmetry of the hexagonal assemblies by changing the sides three or more times. Until now, we were capable to measure around 10-20% of the assemblies within the given time frame, but it can be extended by using additional LaBr<sub>3</sub> scintillation detectors to 100%. We have already tested 3 detectors positioned around the assembly with promising results. Despite the lower resolution, compared to the HPGe, we were able to separate the important 185.7 keV peak using the FitzPeak software, still with acceptable statistics. Balancing between measuring time and statistics, and purchasing additional LaBr<sub>3</sub> detectors, we can measure (almost) each side of the hexagonal fuel assembly at the same time, decreasing the need for rotation. The increased number of detectors also infers the importance of automatization, both in handling and evaluation. This detector setup will potentially contribute to the safety and stability of nuclear energy production and seems a promising technique for the quick enrichment determination.*

**Keywords:** gamma-spectrometry; fuel assembly; fresh fuel; VVER-440; NDA

### 1. Introduction

In the nuclear industry, it is essential to continuously ensure the safe operation (of power plants) by developing and revising inspection methods. Consequently the verification of fresh fuel assemblies has become more and more important, especially for the IAEA and EURATOM. So urged by these authorities, between 2008 and 2012, tentative measurements were carried out by Almási et al. [1] at the VVER-440 type Hungarian Paks Nuclear Power Plant to develop methods suitable for routine use. Based on these measurements, starting from year 2012, the Institute of Isotopes and later the Hungarian Academy of Sciences - Centre for Energy Research - Nuclear Security Department continued to partially check the new fresh fuel shipments up to the present day.

The original goal was to double-check the enrichment of every fresh fuel assembly efficiently and independently from the manufacturer (because the late revelation of deviations may cause significant interruptions due to forced refuelling of the reactor and this comes with high expenses), but could not be done at that time with the available instruments. Our department recently purchased additional scintillation detectors and now eager to finally achieve this goal by extending the foregoing routine measurements and now on the way to verify and optimize this process. But before the detailed

explanation, a basic understanding is needed; the next section summarizes the main points of the routine measurements and the used method.

## 2. Routine measurements until now

For routine measurements, gamma-spectrometry was chosen as a passive (NDA) method. Two types of detectors were used: coaxial HPGe detectors and CdZnTe (CZT) detectors (Table 1). MCNP simulations [1] showed that with gamma-spectrometry the “visibility” is 2-3 fuel rod (pin) rows deep, therefore elaborate detector placement is needed to get enough information from the VVER-440 hexagonal fuel assemblies. Older assemblies are homogeneous in enrichment, while newer assemblies are “profiled” with differently enriched pins and burnable poison ( $Gd_2O_3$ ) (Fig. 1) to achieve higher burnup and longer campaign.

For the HPGe measurements, the fuel assemblies are needed to be brought to the inspector stand. The coaxial HPGe detector is placed on a stand at a distance of 10-30 cm from the assembly’s half-height with a lead plate around the head section to function as a collimator by increasing the signal to noise ratio (Fig. 2, lower-right section). One measurement usually lasts 1400-1500 s real-time (1200-1300 s in live-time) to reach 0.2% uncertainty for the 185.7 keV peak (these uncertainty values limit come from years of convention). To balance between pin visibility coverage and measuring time, it was decided to measure just 3 sides ( $-120^\circ$ ,  $0^\circ$ ,  $+120^\circ$ ). With these adjustments, one fuel assembly needs 1-1.5 h measurement time, therefore 5-8 assemblies can be verified in an 8-hour shift. The HPGe measurement - which includes a lot of assembly crantage (placement and rotation) - is the main bottleneck for the verification, despite its preferred higher resolution.

In the case of the CZT measurements, the fuel assemblies can be measured in the storage rack. These detectors are small enough to fit into the assembly’s central hole (Fig. 3) and 2-3 CZTs can measure in parallel at 10-60 cm depth with 5000-6000 s measuring time to reach 1.15% uncertainty for the 185.7 keV peak (real-time is nearly equal to live-time in this case).

With these measurements, a big portion of the pins in the assembly can be verified; the HPGe can see 2-3 rows on every other side, and the CZT can see in a 2-3 pin radius around the central tube. In case of the “profiled” assemblies, only an average (apparent) enrichment (Table 2) can be measured based on pin visibility. The apparent enrichments were also calculated and verified using MCNP code. The verification of enrichment is being done with the following “enrichment meter” method.

### 2.1. “Enrichment meter” method<sup>[1]</sup>

After discarding the use of the MGAU<sup>[2][3]</sup> code and the intensity ratio of the 185.7 keV peak of  $^{235}U$  to that of the 1001 keV peak of  $^{238}U$  ( $^{234m}Pa$ ) because of their unrequired complexity, a simpler method was chosen in the end. The so called “enrichment meter” method can be described as follows:

1. Spectra of older assemblies with homogeneous composition (1.6, 2.4 or 3.6% enrichment) are taken and used as standards. The background spectrum (with no assembly in the inspector stand) should be taken as well, because it is not insignificant in the fresh fuel storage.
2. Spectra of fresh fuel assemblies are taken one after another. Important note: 3 (side) measurements are needed for the HPGe detector.
3. Count rates of the 185.7 keV peak ( $^{235}U$ ) are plotted and the average enrichments of visible pins (Table 2) are calculated using that of the standards’ with linear interpolation.

Model	Type	Crystal volume [cm <sup>3</sup> ]	FWHM at 122 keV [keV]
Ortec GEM10P4-70	Coaxial HPGe	70	0.615
Ortec GEM15-70-SMP		95	0.651
Ortec SGD-GEM-3615		15	0.513
(2x) Ritec $\mu$ SPEC60	CdZnTe (CZT)	60 [mm <sup>3</sup> ]	10-20

**Table 1:** Used HPGe and CZT detector models. One HPGe detector was used at a time.

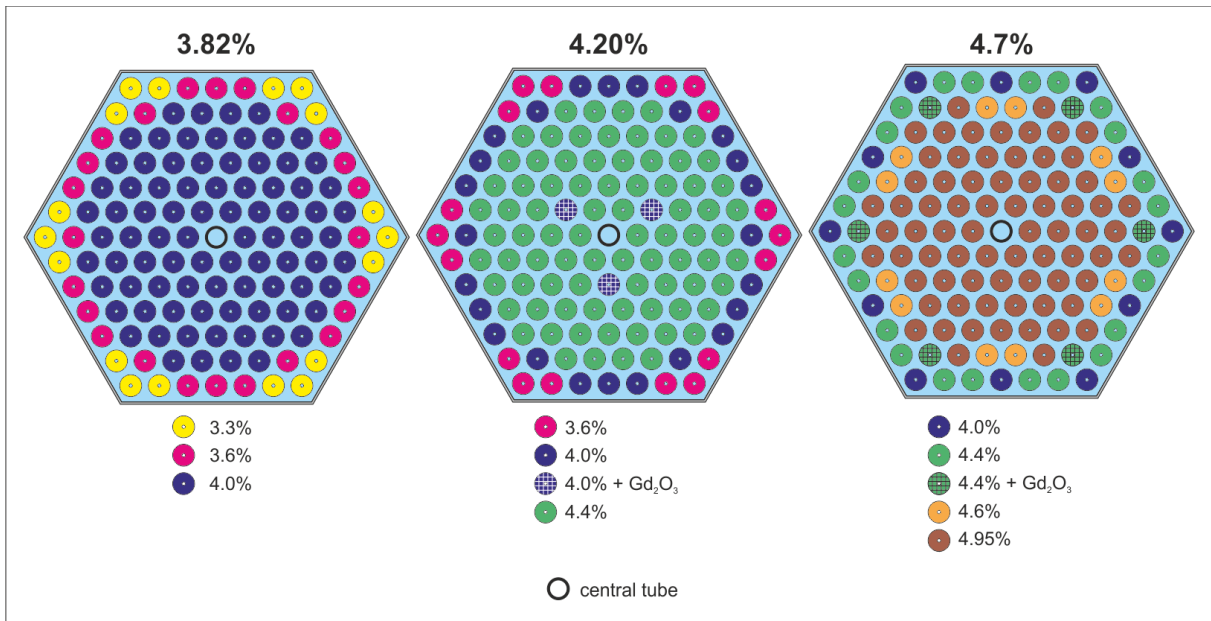


Fig. 1: Schematic diagrams of the “profiled” VVER-440 assemblies

Measuring position	Profiled assembly type		
	”3.82”	”4.20”	”4.7”
side (HPGe, LaBr <sub>3</sub> )	3.55	3.91	4.33
central tube (CZT)	4.00	4.35	4.95

Table 2: Apparent enrichments [%] for “profiled” VVER-440 assemblies from MCNP calculations



Fig. 2: HPGe detector on the detector stand, LaBr<sub>3</sub> detector framework (with detectors) and assembly in measuring position

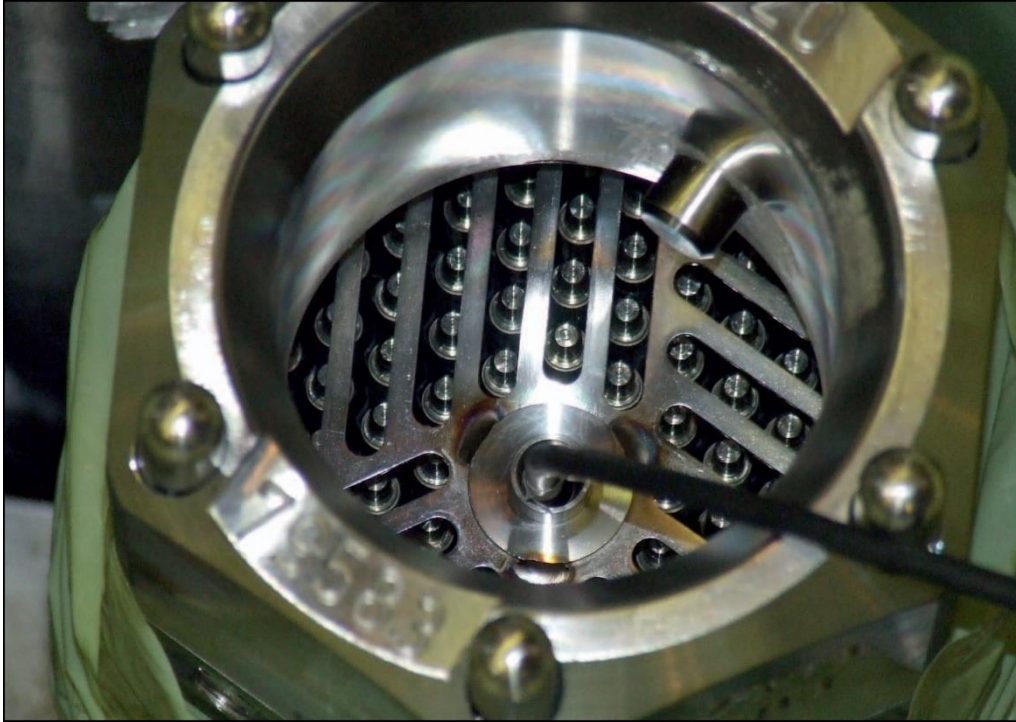


**Fig. 3:** CZT detector in the central hole of the assembly

### 3. Extension and development of the existing measurements

With the above mentioned method and given timeframe, only 10-20% of the arrived fresh fuel assemblies can be verified. It was under consideration in the last few years to invent a new way and/or acquire new equipment to extend this verification coverage. The recently purchased  $\text{LaBr}_3$  scintillation detectors (Table 3) gave a perfect opportunity to test out the possibility of this extension. The reasons why the  $\text{LaBr}_3$  detector type was selected are the following: low dead-time (nearly 0%), high count rate in the 185.7 keV peak, small, compact and cooling is unnecessary. In exchange, the resolution is much lower comparison to the HPGe detectors (Fig. 4), but still better than the NaI detectors'.

After the promising assessment in 2017, a new frame was constructed and placed on the inspector stand in 2018 (Fig. 2, upper-left section). To achieve the mentioned goal in the introduction, we needed to measure more sides in parallel to speed up the verification process and increase the number of verified pins; 3  $\text{LaBr}_3$  detectors were placed with lead-copper collimators at the following angles:  $-60^\circ$ ,  $0^\circ$  (same angle as the HPGe) and  $60^\circ$  (Fig. 5). This way the fresh fuel assembly needs to be rotated just once by  $180^\circ$ , instead of twice by  $120^\circ$ . The measurement time was also cropped to around 1000 s real-time (900 s live-time), hence 2 assemblies can be verified in an hour, that means 16 in an 8-hour shift. This measurement time cutback naturally leads to increased uncertainties, but these are well within acceptable limits: for HPGe 0.3% and for  $\text{LaBr}_3$  0.5-0.6%. This does not interfere with the (already quick enough) CZT measurements. If the main focus was Safeguards instead of Safety, then even less measuring time (around tenth) would be required.

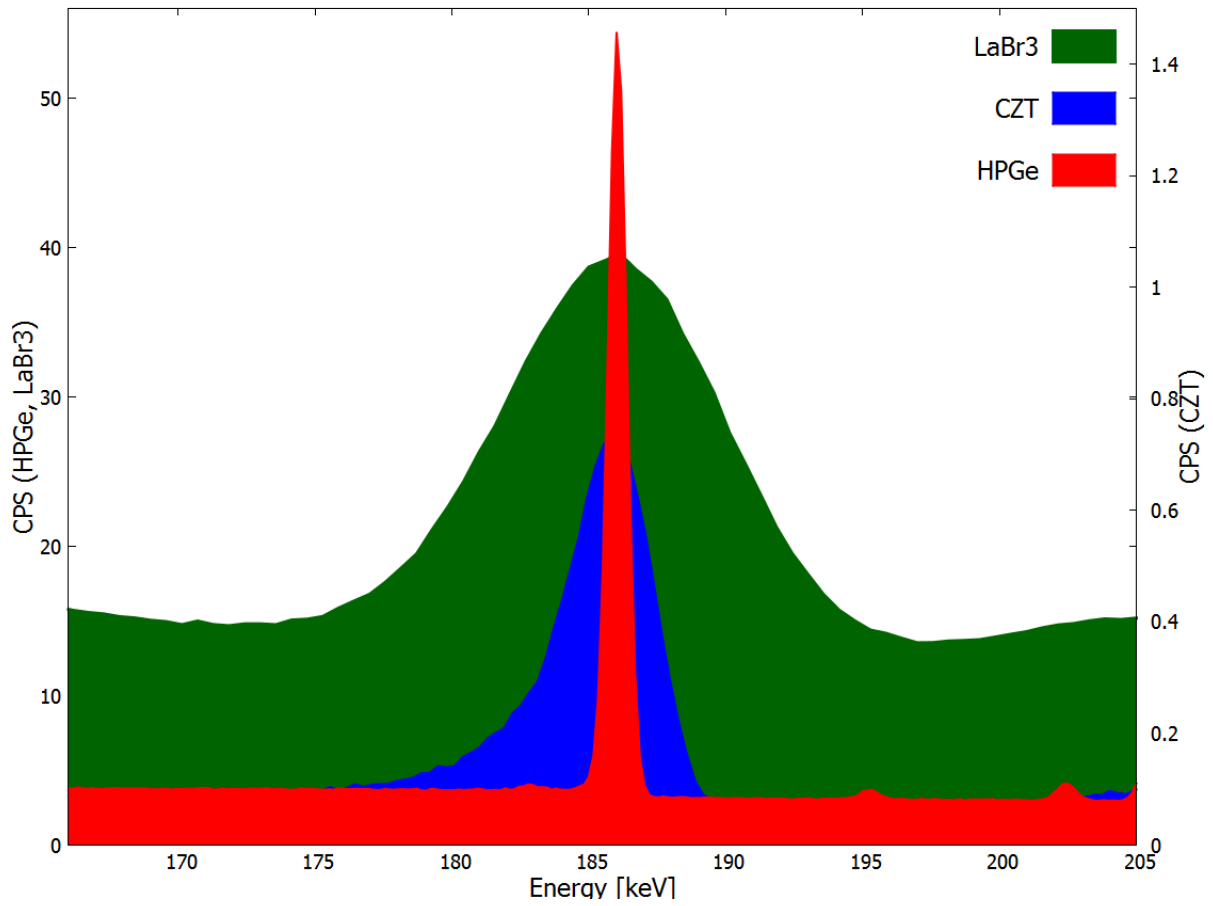


Fig. 4: HPGe, CZT and LaBr<sub>3</sub> detector peak shape comparison at 185.7 keV

Model	Type	Electronics	Resolution at 662 keV [%]
(3x) Saint-Gobain 38S38 (2-4-6115)	scintillation LaBr <sub>3</sub> (Ce)	Ortec digiBASE	2.6

Table 3: Used LaBr<sub>3</sub> detectors

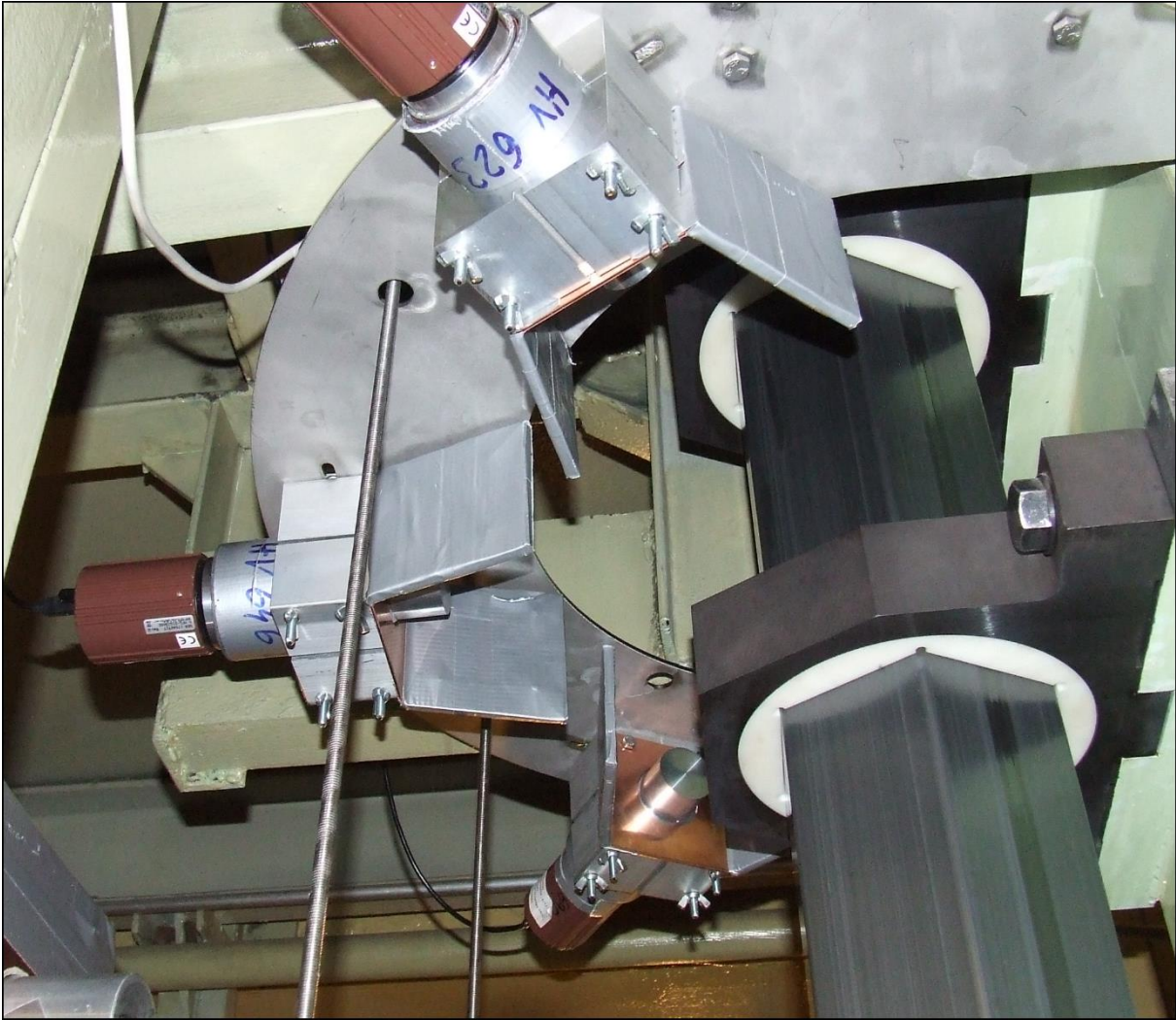


Fig. 5: LaBr<sub>3</sub> detector placement around the assembly

#### 4. First results and observations of the extension test

The first real test to verify the entirety of the fresh fuel shipment was in the first half of 2019. Over 100 fresh fuel assemblies were verified in 10 days with 2 shifts per day and over 1000 spectra were produced. This in addition to the prior tests gave us plenty of experience.

The spectra from HPGe and CZT detectors were analysed with the Ortec *Maestro*<sup>[4]</sup> software so far by precisely selecting the ROI (Region of Interest). This method has limitations, but with the right conditions the evaluation is quick and simple and can be done on site. The LaBr<sub>3</sub> detectors brought in a new kind of challenge in the image of instability. This instability materializes as a constant channel-energy shifting in the spectrum; during a 2-day-long verification, the 185.7 keV peak can shift by 13-18 channels in the 1024 channel MCA. This is not a problem in a HPGe system, but in a scintillation system where the FWHM of the peaks are significantly bigger and the peaks are closer (Fig. 4), the constant redrawing of the ROI is required. This redrawing by hand makes this method less reproducible as a standardized method for the LaBr<sub>3</sub> detectors. To solve this problem, a peak fitting software called *FitzPeaks*<sup>[5]</sup> was tested out with promising results.

With the reduced measurement time and increased number of detectors, the on-site, between-measurement evaluation has become more and more difficult. Pared with the sheer number of fresh fuel assemblies, this monotonous process produced a small number of mistakes that not happened before. Therefore, we are contemplating the need of a new automatized method for the evaluation procedure.

For evaluation, the mentioned “Enrichment meter” method was used for 36 selected “4.20” fresh fuel assemblies (Fig. 6-7). To compare the 185.7 keV peak count rates of different detectors (HPGe, LaBr<sub>3</sub>), one assembly was fully rotated and measured on each (6) side. As can be seen on the mentioned Figs, the average is around 3.91% with both HPGe and LaBr<sub>3</sub> detectors (this corresponds well to the apparent enrichment value of 4.20-side pos. from Table 2), and the (relative) deviations of these values are within  $\pm 1.5\%$  ( $2\sigma$ ) from this average, even including the greater deviation of the LaBr<sub>3</sub> detectors. This means that the selected assemblies did not have detectable discrepancy and passed the criterion. This also means that the new scintillation detectors are a good alternative to the HPGe detectors in our case, but we are not intending to exclude the HPGe measurements in the future.

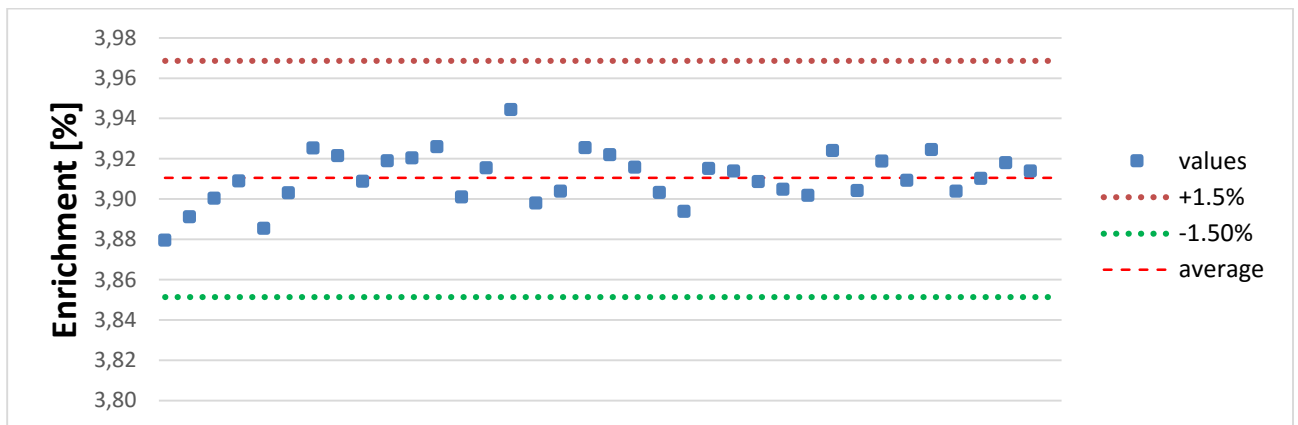


Fig. 6: Evaluated apparent enrichment values from 36 selected “4.20” fresh fuel assemblies with the HPGe detector

## 5. Conclusion

New LaBr<sub>3</sub> detectors were introduced and tested at the MVM Paks NPP Ltd. to extend the fresh fuel verification capabilities. The existing measurements were made simple and reproducible, but only a portion of assemblies could be verified. This will hopefully change in the future based on this big test in 2019; the results and the standard deviations are well within acceptance. Some problems were also identified: the need for a suitable peak fitting software and the need for automatization. After solving these problems, this new extended verification method will be standardized and introduced as a stable way to fully check every arriving fresh fuel shipment.

## 6. Acknowledgements

This work was supported by the MVM Paks NPP Ltd. and the Hungarian Atomic Energy Authority.

## 7. References

- [1] I. Almási, C.T. Nguyen, J. Zsigrai, L. Lakosi, Z. Hlavathy, P. Nagy, N. Buglyó; *Verification of 235U enrichment of fresh VVER-440 fuel assemblies*; ScienceDirect; 2012;
- [2] R. Gunnink et al.; *MGAU: A New Analysis Code for Measuring U-235 Enrichments in Arbitrary Samples*; UCRL-JC-114713, Lawrence Livermore National Laboratory, USA; 1994;
- [3] A.N. Berlizov, R. Gunnink, J. Zsigrai, C.T. Nguyen, V.V. Tryshyn; *Performance testing of the upgraded uranium isotopics multi-group analysis code MGAU*; Nuclear instruments and methods in Physics research A 575 (2007) pp 498-506.
- [4] <https://www.ortec-online.com/products/application-software/maestro-mca> (2019)
- [5] <http://www.jimfitz.co.uk/fitzpeak.htm> (2019)

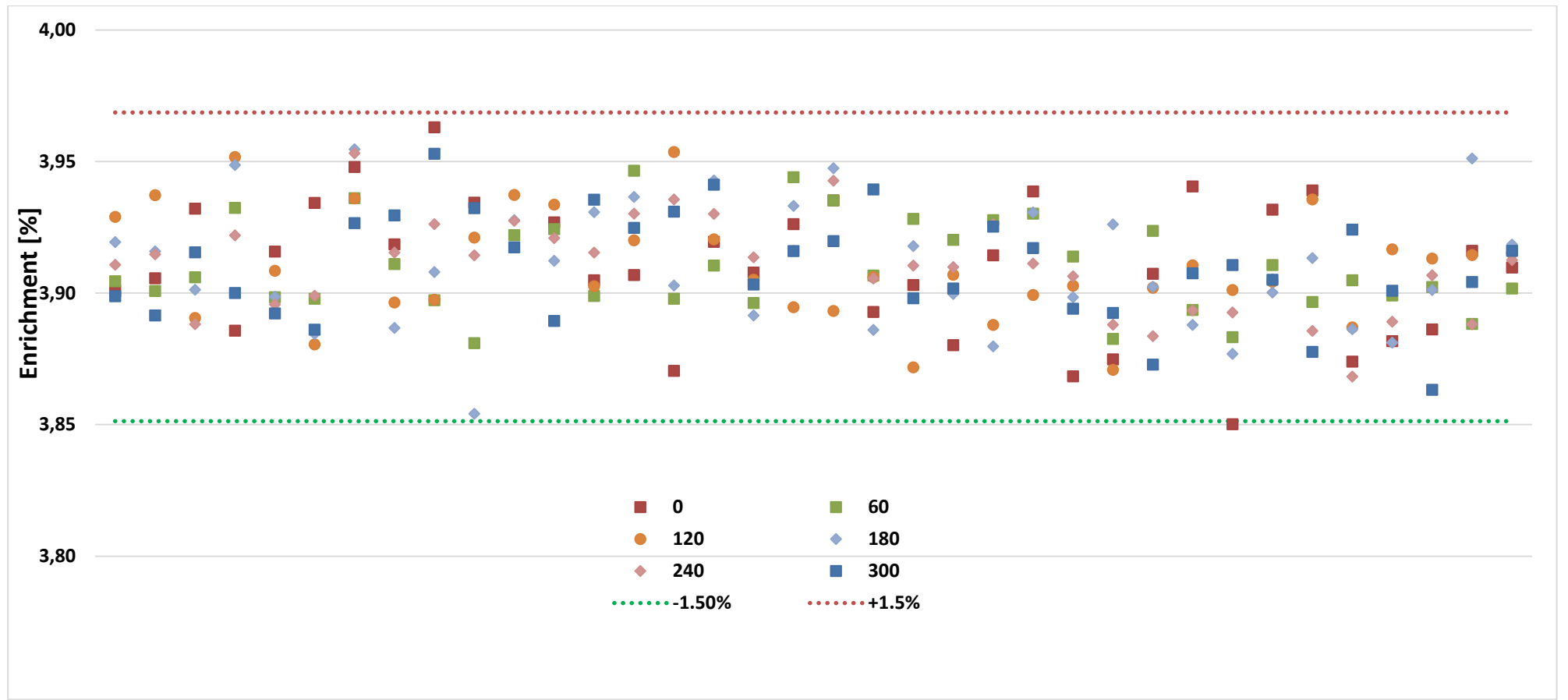


Fig. 7: Evaluated apparent enrichment values from 36 selected "4.20" fresh fuel assemblies with the LaBr<sub>3</sub> detectors

## C-BORD high-level equipment to enhance freight inspection in support to customs

§ G. Sannie<sup>1</sup>, B. Pilorget<sup>2</sup> and H. Tagziria<sup>3</sup>

<sup>1</sup> Commissariat à l'énergie atomique et aux énergies alternatives, Institut List, Saclay France

<sup>2</sup> ARTTIC, 58A rue du Dessous des Berges, 75013 Paris – France

<sup>3</sup> European Commission, Joint Research Centre, Nuclear Security Unit G.II.7, Ispra (Italy)

### **Abstract**

*Thousands of freight containers and trucks pass every day at any small to medium port or border within the EU which potentially makes them an ideal means for the illicit transport and trafficking of radioactive and nuclear materials (including waste and contaminated commodities) as well as for the smuggling of drugs and narcotics, tobacco, weapons, explosives, chemical warfare and humans.*

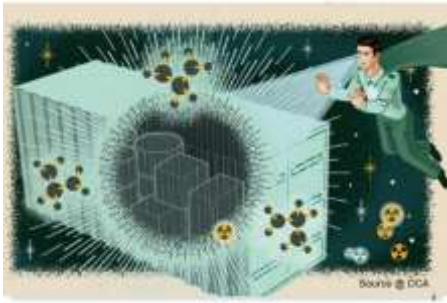
*This creates many challenges for customs and border control authorities who must ensure that adequate inspection means and solutions are in place for an optimum interdiction chain that is safe, practical, and cost-effective and on the other hand remain non-intrusive in order to facilitate trade on one hand and ensure safety and security of the society.*

*To that effect and following the success of earlier EU projects such as SCINTILLA, the Effective Container Inspection at Border Control Point (CBORD) project was launched in June 2005, funded (11.8 M€) within the EU H2020 programme to support a consortium of eighteen partners (industry, universities, research centres, users) and from nine EU member states not only to develop but also integrate five detections and inspection technologies. The technologies selected and pursued namely the next generation cargo X ray, tagged neutron interrogation, evaporation (or sniffer), advanced radiation portal monitors and photo fission were tested in laboratories such as at the JRC-Ispra, CEA (France) and EK (Hungary) followed by extensive field testing (on targeted use cases) prior to closure of the project by a well-attended public workshop which included a demonstration at the Rotterdam harbour in October 2018.*

*This paper aims to report on the project and give some of its main results and conclusions.*

**Keywords:** CBORD, Nuclear Security, Detection of Illicit Trafficking, SNM, explosives, Narcotics, Tobacco

§ on behalf of CBORD partners <http://www.cbord-h2020.eu/>



## 1. Introduction

An efficient non-intrusive inspection (NII) of containerised freight is critical for customs, as freight containers are potential means of smuggling, illegal immigration or even trafficking nuclear material and chemical warfare agents. The objectives of the European project C-BORD was to enable customs to deploy comprehensive and cost-effective solutions for the NII of containers in order to protect the European

Union sea and land borders.

An efficient non-intrusive inspection (NII) of containerised freight is also increasingly critical to trade and society, as the criminal disruption of supply chains can severely harm the economy, as well as endanger public health and safety. The current methods for container NII combine intelligence-supported risk analysis and X-ray technology to combat illicit trafficking. However, this approach is limited due to health and safety regulations, long operator processing time to manually check containers in case of a doubt and a lack of reliability due to insufficient ability to distinguish between innocent items and threats.

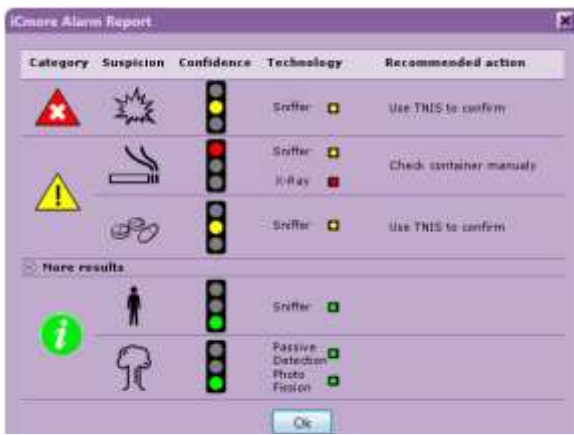
## 2. Combining five NII technologies to ensure reliable inspections

Within the framework of the C-BORD project, a new generation of container inspection system was developed, combining advanced X-ray techniques capable of

### Why inspect freight containers?

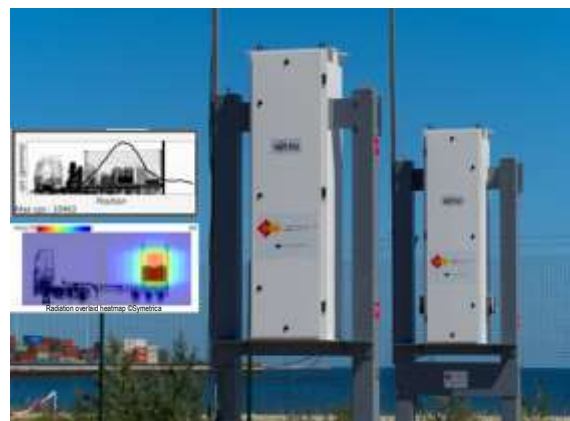
Freight containers can be used for smuggling, illegal immigration, trafficking of drugs and dangerous illicit substances, including nuclear material, chemical warfare agents and radioactively contaminated goods. But no single inspection technology available today can adequately cope with the challenge of reliably detecting all of these threats. This is where C-BORD came in.

locating objects inside a large volume (cargo container) at a high rate, as well as additional techniques more sensitive to specific substances, such as: advanced passive detection technologies, a tagged neutron inspection system, photo-fission technology and artificial sniffing. The data generated by the five technologies were collated in a single graphic user interface for customs decision-making.



Screen captures from DaiSy, an analysis software tool from Smiths Detection. ©Smiths Detection

Passive detection, neutron and gamma detection sub-systems were designed to demonstrate the feasibility of using isotope identification to reduce false positive radiation alarms raised by naturally occurring radioactive materials, such as fertilizer.



Passive neutron-gamma detection system

While previous “artificial sniffing” methods have failed because of the complexity of the problem at hand (notably in terms of sensitivity, due to a wide range of potential targets - the large volume of a

**The C-BORD Toolbox combines complementary innovative NII technologies**

- Next generation cargo X-ray
- Advanced radiation management
- Evaporation-based detection
- Tagged neutron inspection system
- Photo-fission



*Artificial sniffing sampling by introducing canister inside the container*

potentially contaminated cargo adds complexity), a robust and highly sensitive evaporation-based detector was developed to detect volatile chemicals that may be present in a container. The sampling proof of concept for large volume application still needs to be demonstrated.

The “Rapidly Relocatable Tagged Neutron Inspection System” (RRTNIS) was a second-line system to be used on sealed containers. These detectors complement X-ray imaging by enabling molecular-specific detection (providing chemical information instead of the object’s outline), thus improving the discrimination power of the scanning system.



*RRTNIS in operation on field test area*

Within CBORD, the successful detection of targeted drugs and explosive within containers by the RRTNIS was done in real condition, with real targets, explosives and drugs, hidden by customs in containers.

Additionally, the photo-fission technique enabled to detect SNM (Special Nuclear Material – mainly uranium and plutonium isotopes), a crucial issue for homeland security applications. It allows for inspection of the cargo container without opening it, which is a time-consuming and potentially dangerous process. Both these experiences demonstrated the efficiency of the detection capability for these breakthrough techniques and represented a major success for European research and European customs.

The C-BORD project was also an opportunity to improve X-ray techniques, particularly with regard to the accuracy of material discrimination with progress on radiation scattering treatment and correct x-ray image artefacts caused by movement of the x-ray scanner boom.

C-BORD met critical operational requirements and overcame a number of constraints, which altogether enable for:

- Increased throughput of containers per time unit
- Reduced need for costly, time-consuming and dangerous manual container inspections
- Lower false negative and false positive alarm ratios



*Mobile X-ray detection system*

### 3. From the laboratory to customs

If the aim of C-BORD was to develop new and improved NII technologies tailored to the customs' working environment, they were tried and tested in real operational conditions. This is why C-BORD planned field trials jointly with customs partners. The performance of the technologies was tested at three customs sites: Rotterdam, The Netherlands, for testing equipment for a fully automated seaport; Gdańsk, Poland, for implementing a rapidly relocatable checkpoint for ports; and Röszke, Hungary, for deploying mobile equipment for a land border checkpoint.



*Euronews Video during Gdansk tests*

Thanks to the assessment of the enhanced technologies, and how their combined use allows for a reliable detection of radioactive material, explosives, chemicals, drugs and tobacco hidden in cargo containers, C-BORD supported the decision-making of end users, namely customs services, on how to combine and deploy technologies for different needs.

Last but not least, activities were governed by the standard research ethical principles relative to the safety and well-being of researchers, the public, private property and the environment.

All trials were subject to authorisations from the appropriate national civilian health & safety authorities in charge of hazardous materials and active detection methods.



**References:** <http://www.cbord-h2020.eu/>

**Video about the C-BORD project:**  
[www.euronews.com/2018/07/16/how-to-make-customs-controls-more-effective](http://www.euronews.com/2018/07/16/how-to-make-customs-controls-more-effective)




---

#### Tailored and efficient solutions for end users

One of the benefits of the approach is that it proposes tailored solutions for very different customs / border-crossing situations, from mobile devices for a small land border-crossing to fixed installations for an automated system handling large volumes at a major port. Thus, the deployment of C-BORD solutions can address the problem of the weakest link in the control chain.

---

This project has received funding from the European Union's Horizon 2020 research and innovation programme under grant agreement N° 653323. The C-BORD project, with a budget of 11.8M€, was coordinated by CEA, providing its expertise in the CBRNE and detection fields. 18 partners from nine countries were involved in the project.

**Partners of the C-BORD project:**

CEA (coordinator), ARTTIC, BRSU, CAEN, ESIEE, Fraunhofer, MTAEK, NCBJ, OCSS DCA, SYMETRICA, SmithsD, UNIPD, UNIMAN, ICGDy, NTCA, ADM, JRC

# Application of Gamma-Ray Tomography for Waste Characterization

**E. Roesgen<sup>1</sup>, S. Vanzo<sup>1</sup>, F. Raiola<sup>1</sup>, G. Bostrom<sup>1</sup>, P. Hubert<sup>2</sup> and K. Abbas<sup>1</sup>**

<sup>1</sup> European Commission, Joint Research Centre, Directorate for Nuclear Safety and Security, Nuclear Security Unit, Via Enrico Fermi 2749, 21027 Ispra (VA), Italy

<sup>2</sup>European Commission, Joint Research Centre, Nuclear Safety and Security Directorate, Nuclear Decommissioning Unit, Ispra, Italy

eric.roesgen@ec.europa.eu

## Abstract

There is a legal obligation for the Joint Research Centre of the European Commission (EC JRC) to characterize its nuclear waste (NW). In the JRC Ispra site (Italy), part of the waste was generated during six decades of nuclear research activities which will add to waste produced by the decommissioning of the nuclear facilities. This waste includes samples containing small quantities of either irradiated or non-irradiated nuclear material as well as different types of waste produced on site by two research reactors, a charge particle accelerator and some other large research facilities all under decommissioning. A large quantity of waste drums must be radiologically characterized and further processed prior to either their intermediate storage or free release by the Nuclear Decommissioning Unit (NDU) of the JRC which relies on the support of a number other JRC scientific Units for its R&D needs. As part of this support, this paper reports on a refurbishing and testing development of a large facility for waste drum characterization, which was delivered by ANTECH Company (UK). In order to better understand and thus improve the data processing and the characterization of the drums, we have built a lightweight scanner reproducing some features of the ANTECH waste characterization system having all the flexibility necessary first to test different upgraded gamma measurement software/hardware used to assess with high sensitivity, precision and accuracy the activities of selected radionuclide vectors in the analysed drums and secondly to allow a pre-validation of different 3D image reconstruction algorithms using either segmented or tomographic gamma scanning methods of hot spots. The scanner operates autonomously thanks to an in-house development control software. Preliminary results of tests carried out on various geometry configurations and on calibration waste drums are presented and discussed which will be used to implement high standard methods for decommissioning and waste management.

**Keywords:** tomography, gamma imaging, nuclear decommissioning, waste characterisation

## 1- Introduction

The European Commission through its DG Joint Research Centre DG (JRC) has supported for almost sixty years a large number of nuclear research programs. From the eighties onwards, the JRC has reoriented his nuclear research towards decommissioning as others activities were drastically reduced or even completely stopped (research reactors, nuclear laboratories, particles accelerators...). In Ispra, the Nuclear Decommissioning unit of the Nuclear Safety and Security Directorate of the JRC is responsible for decommissioning and waste management activities. The Nuclear Security unit of the Department of Nuclear Security and Safeguards of the same is in charge of a multiannual research program to support JRC nuclear decommissioning and waste management (D&WM) programme. This research program is called ITSP (Innovative Techniques and Standardization of Procedures in nuclear decommissioning and waste management).

In this context, the European Parliament has expressed his support on future EURATOM research program and requested that JRC builds upon its experience with decommissioning of JRC nuclear

facilities and further reinforces its research to support safe decommissioning in Europe. The JRC Director General Vladimir Sucha has reaffirmed his commitment in the following declaration: "In the field of nuclear decommissioning the collaboration with scientific units should increase, taking advantage of the hands-on experience accumulated. The opportunities are huge taking into account the international political context of decommissioning of old nuclear plants."

In JRC Ispra, nuclear research activities over years have generated waste. This so-called historical waste was managed at that time according to the regulations in force. The packaging in ultimate containers was made of segregation, characterisation and storage according rules of regulations of that time. These waste will presently be managed according the present in-force regulations till its final disposal. Furthermore, activities for the preparation for the decommissioning (the so-called POCO (Post-Operational and Clean-Out)) will generate additional waste. The dismantling of large facilities in JRC Ispra such as ESSOR reactor facilities will generate new waste (technological waste). According to the Italian law (Decreto 7 Agosto 2015), prior to any waste disposal, all waste must be characterized. To date in JRC Ispra site, 330 m<sup>3</sup> of technological waste of low activity have already been produced. These waste are mainly conditioned in 220 l drums and it is expected that the future decommissioning activities will generate an additional 20 000 m<sup>3</sup> of waste to be characterized. The present 220 l waste drums are intermediate storage containers that will be packed in final waste containers filled with immobilisation cement (usually six drums for each container). The waste characterisation will rely at least for the large part on the existing Non-Destructive Assay methods (NDA) using gamma-ray spectrometry and neutron coincidence counting and also, when appropriate, imaging techniques such as radiography and tomography. Destructive Assay techniques (DA) are also used to complement NDA measurements, especially for the definition of nuclide vectors and correlation factors for the definition of the homogeneous groups of waste.

This paper reports on a refurbishing and upgrading of a large waste drum characterization system (WCS) manufactured by ANTECH Company (UK). WCS includes two measurement stations; the neutron and gamma stations. The first station performs passive and active neutron interrogations while the second one utilises gamma-ray spectrometry is dedicated to both segmented and tomographic scans (SGS and TGS). This report is focused of the gamma station, the presently ongoing work on the WCS neutron station is not reported here.

In addition to the work of WCS itself, we have built a lightweight scanner reproducing some features of the ANTECH waste characterization system offering more flexibility for testing than WCS. This scanner is used:

- First to test different upgraded gamma measurement software/hardware solution to be implemented in the WCS gamma station from the point of view of sensitivity, precision and accuracy of qualitative and quantitative measurements of the selected radionuclide vectors in the analysed drums.
- Second to allow a pre-validation of different 3D image reconstruction algorithms using for tomographic gamma scans.

Regarding the regulatory requirements for waste characterisation, no specific characterisation method is imposed. Currently waste regulation doesn't require a sophisticated waste characterization instrument such as WCS (with both SGS and TGS). SGS is however considered and used in many nuclear decommissioning and waste management facilities.

## 2. Waste Characterisation System (WCS) Features

WCS is designed to perform high performance characterization of waste drums. The main features of WCS are visualised in Figure 1. As mentioned above, WCS incorporates a neutron station equipped with a D-T neutron generator to perform passive and active neutron interrogations of waste using the Differential Die-Away technique, it's indicated with DDT in the Figure. The second station of WCS indicated with SGS/TGS is the gamma station to perform both segmented and tomographic gamma scanning (SGS or TGS). The gamma and neutron station are the main parts of WCS. Complementary information is provided by many other sub-stations such as:

- Weight measurement: Drum weights are necessary for the analysis of the matrix self-absorption.
- Dose rate measurement: Six Geiger Muller detectors ensure dose measurement of dose rates at different surface positions of a drum including the transport index (dose rate at 1 m).

- Drum buffer conveyor: This conveyor allows loading of twenty drums and can dispense them to each measurement stations in an unattended manner.
- Control room: WCS can be operated manually or in a fully automatic mode. The system is made up of computers running a scada software. In addition, specific software for the two measurement stations runs on two different PCs. All equipment's communicate through a LAN

The JRC Ispra WCS provides a complete solution for waste assay going beyond the present regulation requirements. It's designed to characterise a maximum of 20 drums in a 24 h period without operator supervision.

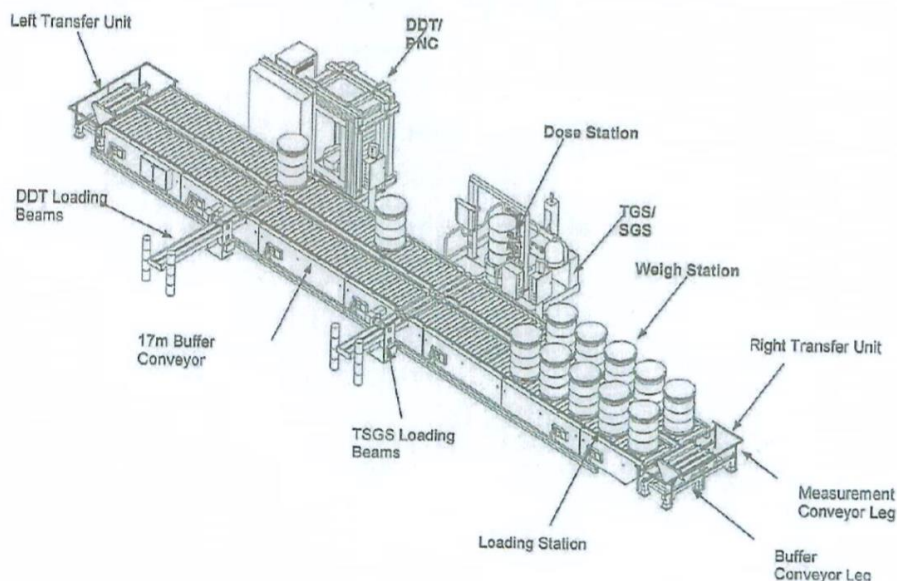


Figure 1: Waste Characterisation System layout.

### 3. The Gamma Station

#### 3.1 Segmented Gamma Scanner

The main objective is to reassess the performance of the system and to find the best parameters to characterize low and intermediate activity 220 l waste drums. The movement of the SGS system is controlled by a PLC that receives its instructions (e.g. number of layers, measurement time...) from a windows PC: In normal conditions of operation, only SGS is used while TGS is used only in particular cases when the results provided by SGS show inconsistencies. One has also to consider the long duration (many hours) of a TGS scan with respect to a SGS one. An SGS scan is generally accomplished in a less than an hour.

A WCS operator has to decide between the scanning and tomographic mode. He then selects and installs the proper tungsten collimator in front of the gamma detector (diamond shape for tomographic scan rectangular shape for segmented gamma scanning) according validated standard procedures.

For the 220 l drum SGS scanning mode, the drum is divided into 16 layers of 5 cm height each (this value can be changed). These layers would be sufficient to cover completely the drum. Each layer is measured twice for a configurable amount of time (100 s by default) while the drum revolves around its axis (neglecting the positioning error) for a 360 degree rotation. At the beginning of the procedure in SGS mode, the system uses a known  $^{152}\text{Eu}$  source that is used to determine the average attenuation coefficient at different energy (those of the  $^{152}\text{Eu}$  peaks) of the measured layer. In the second step the  $^{152}\text{Eu}$  source holder shutter is closed and only the drum internal activity is recorded as an energy spectrum. The internal activity for each drum-layer is corrected for the average attenuation coefficient (the matrix of the drum is considered uniform).

Due to the large aperture angle of the collimator, the total drum activity cannot be calculated as the sum of the 16 individual layers measured. A linear calibration must be performed to give to each layer a different weight.

The main parts of the hardware and software of the SGS (see Figure 2) are described hereafter:

#### a - WCS SGS Hardware

SGS is composed by:

- A rotary table supporting the drums

This rotary table is also equipped with translator

- A pillar with a metallic arm supporting the gamma detector/collimator and a source holder with a  $^{152}\text{Eu}$  source and a shutter;

The gamma detector is a high purity germanium detector from ORTEC company (relative efficiency 50% on  $^{137}\text{Cs}$  and FWHM 0.855 keV for the  $^{57}\text{Co}$  122 keV line). The gamma acquisition electronic chain has been upgraded to DSPEC 50 (ORTEC) connected to the acquisition PC by Ethernet (TCP/IP).

In addition to DSPEC 50, an ORTEC 419 Precision Pulser generates pulses at 1974.5 keV for possible stabilization, energy calibration adjustment and dead time correction.

- A portal with six Geiger Mueller detectors for surface dose rate measurements as mentioned above.



Figure 2: View of the WCS Gamma Station (for both SGS and TGS scanning)

#### b - WCS SGS Software

The rotary table movement, the gamma detector arm and the data acquisition are monitored by a program called Master Scan. This program sends instructions to the PLC in charge of the system motion control and it also controls the Maestro program (by ORTEC) for the gamma acquisition.

Once the acquisition is complete, the analysis is performed by the program Master Analysis then a report is generated giving the activity of each single identified radionuclide. Figure 3 shows an example of a screenshot (Master Analysis software from ANTECH) of an analysis information case of a waste drum containing  $^{137}\text{Cs}$ . The central gamma spectrum is an integrated gamma spectra other the 16 SGS layer while the upper and lower spectra are both those of the transmission source of  $^{152}\text{Eu}$  which are used for the self-attenuation corrections in the different density waste (soil, concrete, plastic, ...). Figure 4 shows the corresponding SGS analysis report.

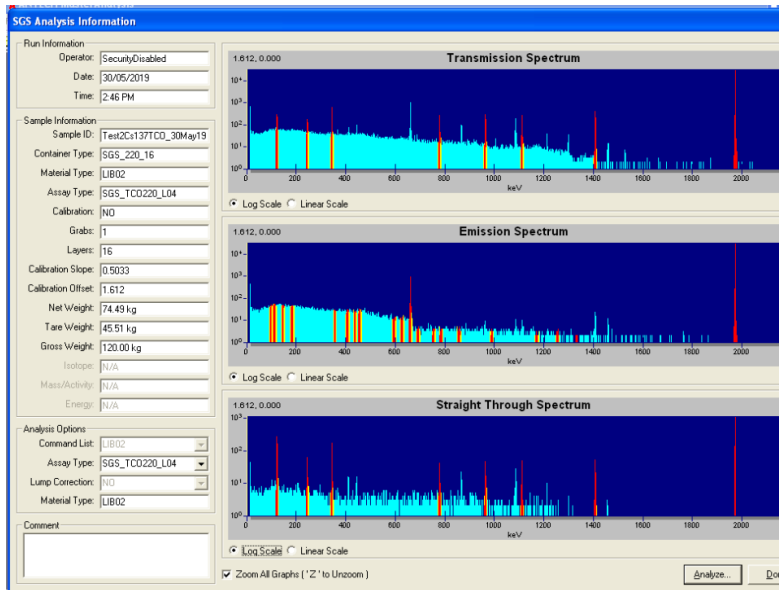


Figure 3: A Master Analysis software (ANTECH) screenshot of an analysis information case of a waste drum containing <sup>137</sup>Cs. In the figure, the gamma-ray spectrum of <sup>137</sup>Cs is the central one while the upper and lower are those of the <sup>152</sup>Eu transmission source.

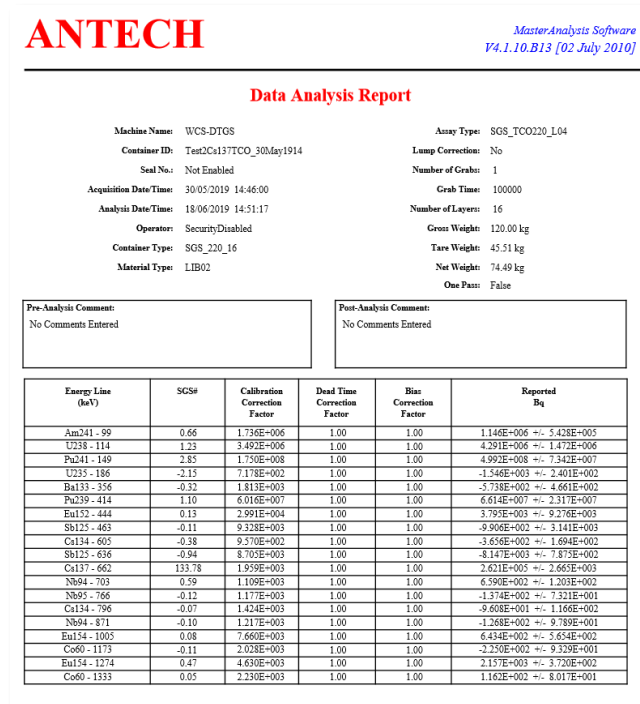


Figure 4: An example of an SGS analysis report (16 layers) on a waste drum containing a source of <sup>137</sup>Cs.

After a long period of verification and testing, repairs, upgrade and improvements have been made to the system for both software and hardware. This has been made necessary because the facility has not been operated for years. The WCS resumption of operation showed no damage and all its mechanical and electromechanical components proved to be robust and reliable however some measurement

station components upgrade were/will be required in particular the upgrade of the operating systems used by the WCS PCs.

Following the system resumption of the operation, a long period was dedicated either for the verification of calibration of different protocols or for the recalibration. This activity was followed by a testing campaign (with SGS) with the first fully dedicated calibration drums with known radioactive sources placed inside and then with real waste drums. The evaluation of the minimum detectable activities for different radionuclide vectors in various waste categories is in progress.

The current status of SGS can be summarised as follows:

- The electromechanical part of is fully operational.
- The Gamma acquisition (software and hardware) components are fully operational.

The measurement parameters are finely tuned and the system performance assessment and the system parameters determination necessary for the evaluation of the system are in progress.

### 3.2 Tomographic Gamma Scanner

As mentioned above WCS combined in a single facility both SGS and TGS. TGS is the second important operational mode of the gamma station of WCS. As in SGS, TGS measures horizontal segmented layers on a waste drum however it's equipped with a translation motion system to allow, while the drum is rotating, horizontal translations of the whole drum/rotary table. A single TGS acquires at least 150 gamma ray spectra related to the different measurement points on the drum. Those spectra include those from the emission and transmission gamma spectra using the  $^{152}\text{Eu}$  source. The purpose is to acquire the drum projection (gamma spectra acquired at different angles and lateral positions) that will be used for the tomographic image reconstruction using image reconstruction calculation codes, which are based on single photon emission computed tomography (SPECT). Presently, TGS is experiencing software issues and the software debugging is currently in progress with the support of ANTECH.

To support additional R&D on gamma emission tomography to what is already possible with the WCS complex TGS mode, a lightweight experimental tomographic device has been built (Figure 5). The results of the R&D gained from the experimental tomographic system should be implemented in the WCS. The experimental tomograph comprises a gamma detector, a gamma radiation collimation assembly, a transmission source holder and a rotary table. The table is designed in such a way that 3D image reconstruction would be possible (3 degree of freedom). This experimental tomography system offers the flexibility to test new scanning configurations, for instance from the gamma signal acquisition such as using other gamma detectors than a high purity germanium. In fact, the system can host CdZnTe (CZT) or scintillation based gamma detectors. The monitoring software was developed to offer also large flexibility for projection acquisition including the utilisation of the existing or in-house development program for tomographic image reconstruction.

The software suite is divided into three parts. The first part is in charge of drums rotation and the detector movement. The second part is in charge of the gamma acquisition. The last one is in charge of the data analysis and image reconstruction.

The control command and the gamma acquisition software have been developed in LabVIEW environment. MATLAB is used for the analysis of data and for the image reconstruction.

Once a satisfactory solution has been found, the MATLAB script is compiled into a Windows executable/assembly which can be integrated in the final WCS system. Our development system has been designed to test different gamma measurement solutions and to decrease the measurement time while preserving a good resolution reconstructed image.

The collimators have a critical part in the performance of our system. We have to find the best compromise between position accuracy and measurement time. Nowadays only lead collimators have been tested. In the future we might use honeycomb tungsten collimators. This will improve the directionality while maximizing the use of the crystal surface.

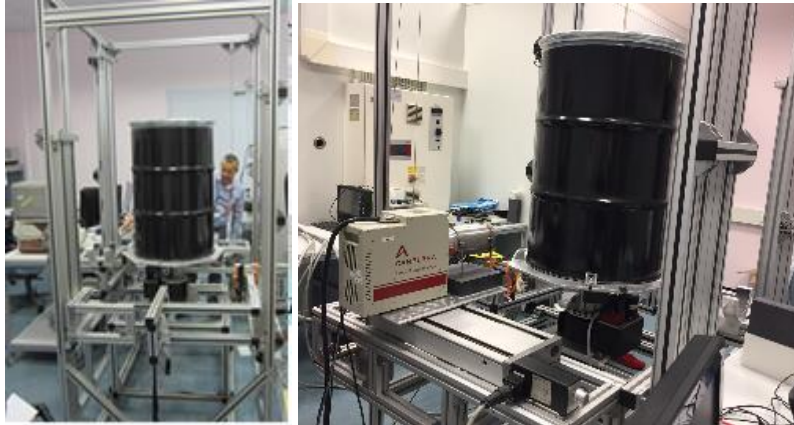


Figure 5: two view perspectives of the experimental tomograph built to support TGS model development in the perspective of their implementations for WCS upgrade.

### 3.2.1. Movement control/command system

The rotary table actuators are connected to a controller (IMC-S8 from ISEL). The controller receives its instructions from a LabVIEW program running either on a Windows 7® PC or on a real time PXI machine (PharLaps). The Real time controller is interfaced to the table controller and connected to a window PC. This control command is synchronized with the gamma acquisition software. Its role is to instruct the controller to perform the sequence of movement necessary for a tomographic scan. Figure 6 shows the rotary table of the experimental tomograph where a set up for three radioactive sources is mounted. Projection of a mixture of  $^{137}\text{Cs}$ ,  $^{60}\text{Co}$ ,  $^{57}\text{Co}$  were acquired in various positions configurations.

Currently we have achieved promising results on 2D tomographic image reconstructions. The whole volum tomographic scan (3D) of a waste drum will be carried by integrating tomographic scans of each horizontal layer of a drum with an attention on the utilisation of adequate collimators.



Figure 6: Rotary table of the experiment tomograph. A set up for radioactive source holders built on the table is visible. The gamma ray detector collimator is also visible on the top-hand of the picture.

Figure 7 shows the graphical interface of the control of the experimental tomographic with on/off-line data processing using LabVIEW/MATLAB and tomographic image reconstruction algorithms.

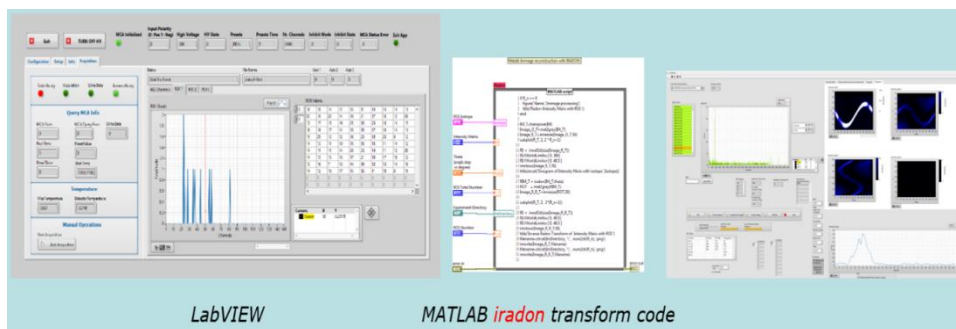


Figure 7: Graphical interface of the control of the experimental tomographic showing on/off-line data processing using LabVIEW/MATLAB and tomographic image reconstruction algorithms.

### 3.2.2. Gamma acquisition system

We have retained three solutions for the gamma acquisition. Two solutions are based on commercial hardware from GBS (mini MCA 527) and from ORTEC (DSPEC 50). The third one is an in-house (in progress) development based on a FPGA board with a 4 channel digitizer from National Instrument.

The gamma acquisition software is written in LabVIEW. This program can either interface with the mini MCA's from GBS or with a DSPEC 50 from ORTEC. It is possible to call from LabVIEW directly the functions contained in the library provided by GBS. ORTEC has developed a driver and a set of functions compatible with LabVIEW. The ORTEC DSPEC 50 solution is similar to the one proposed by ANTECH for WCS but it is not easily scalable and/or as expensive. To reduce the measurement time, the table has been designed to support up to four cryo-cooled HPGe detectors. GBS has developed a new library able to control simultaneously many mini-MCA. This solution will be thoroughly investigated as many mini-MCA are readily available for our 4 cryo-cooled HPGe.

The advance in FPGA (field-programmable gate array) technology has lead us to consider a custom system to process the signals from up to four HPGe detectors using a FPGA board PXIe-7975 interfaced with a 4 channels NI-5761 digitizer (14 bits, 250 MB/s). This development is/will be done in two phases.

The first phase (in progress) consists in connecting one HPGe detector preamplifier to an analog NIM amplifier. The output of the amplifier is sampled by the NI-5761 plugged in the PXIe-7975 which acts as an ADC. The system can be used in a normal PHA mode or in LIST mode.

The detector preamplifier output is connected to a FAN IN/FAN OUT module (Philips scientific 748). Then the signal is sent to a commercial ADC (GBS mini MCA527) and to the NI-5761. The purpose of this extra step is to compare the two systems and validate the FPGA system.

The removal of the analog electronic part (except the High Voltage supply) should be part of the second phase (optional). The four channels available on the NI-5761 would be a perfect fit for our 4 cryo-cooled HPGe detector configuration.

The working principle for any of the mentioned three solutions (DSPEC 50, mini-MCA, and PXI7975+ NI-5761) is always the same. A linear scan is performed in discrete steps (the scan must cover at least the diameter of the drum. The number of step is determined by the collimator aperture.) Afterwards the drum is slightly rotated. This sequence is repeated until the drum has been rotated by at least 180° or preferably 360°. At each step a gamma spectrum is recorded. This spectrum contains the radioisotopes peaks of interest.

At each measurement points the peaks area (subtracted from the background) is inserted in a matrix to create a sinogram for each peak of interest. A sinogram is made for all the predetermined peaks.

Due to the long time necessary to create the sinogram, a new approach is currently being tested.

Instead of incrementing the drum's rotation angle by a fix amount (typically 1° or 3°), the system will rotate the drum in such a way to maximize the angle difference between consecutive measurements.

For example, let say that we want to perform a 180° scan with 3° step. Our first method will consist of rotating by step the detector to 0°, 3°... up to 177°. With the second method, the drum will be rotated according to following sequence 90°, 0°, 177°, 45°, 135°.

After a relatively small amount of projections, a reconstruction attempt can be made. Additional projections will make the reconstruction image sharper.

### 3.2.3. Analysis Software

The reconstruction software has been written in LabVIEW and MATLAB but the critical part of the system is the ASTRA toolbox library [1] (a MATLAB and Python compatible toolbox offering high-performance CPU/GPU primitives for 2D and 3D tomography which implements many reconstruction algorithms).

Similar software has also been written in Python. Decision should be made to decide on a unique development environment after testing both methodologies.

We have performed tests with different point sources. The location source is limited only from the collimator geometry and not by the software. The reconstruction process is made off-line.

A MATLAB script has been written to reconstruct the image. This script calls a ASTRA toolbox library functions. The algorithms implemented in this library are based on algebraic reconstruction method (ART). The algebraic methods have many advantages over analytical ones (less sensitivity to missing/incomplete data...). We have chosen the SIRT (Simultaneous Iterative Reconstructive Technique) which provide better image compared to ART. The ASTRA toolbox can take advantage of the powerful graphics cards available in high-end computer to reconstruct the image (inverse problem). The intensive computation is performed by the GPU (graphic card processor provided the PC is equipped with a compatible NVIDIA graphic card) and not by the PC CPU. This method results in a significant computational time gain. MATLAB and ASTRA toolbox make the utilization of the GPU transparently using CUDA [2].

## 3.3. Mathematical problem with tomographic reconstruction

The problem is to use the detector readings, which have been acquired around the drum. The detector or detectors are placed or positioned in a linear fashion. Then this linear array of detectors are rotated (or the drum is rotated) to acquire readings from many projection angles. The unknown distribution of the material can be represented as an "image" which shows the gamma intensity for the region within each pixel. The problem can be described mathematically as in equation 1.

$$d_{i,r} = \sum_{n=0}^N P(i, r, n) I_n \quad (1)$$

Value  $i$  represent detector number,  $r$  defines the current rotation index,  $N$  is the number of pixels in the final reconstructed image. The function  $P$  defines the projection-fraction seen from the detector of the pixel.  $I_n$  is the number of photons emitted at position  $i, r$  for the  $n$ th voxel crossed by the projection line (defined by  $i$  and the rotation angle  $r$ )

This equation 1 can be written in matrix format as shown in equation 2.

$$D = AI \quad (2)$$

$D$  is an  $m$  sized column vector with all the readings for all the detector positions for all rotations.  $I$  is an  $n$  sized column vector with all the unknown values to search for corresponding to all the pixels in the unknown reconstructed image. The parameter  $A$  is an  $m \times n$  matrix with the projection for each pixel element on each detector.

Reasonable sizes for  $m$  and  $n$  varies and in our case  $m$  may be 6000 (50 projections points and 120 rotations) and  $n$  is typically 16384 (or  $128^2$  the sampling lattice) which defines the image size searched. It follows that the projection matrix will be very large and in the above example it will be a 16384 x 6000 matrix

To solve the equation (2) the usual mathematical methods based on linear algebra such as Single value decomposition, Gaussian elimination or linear regression cannot be applied since the sizes are too large and there are no analytical solutions available. Therefore one can approach the problem with iterative methods where several methods have been proposed [3,4].

The method which gives the best solution for our dataset is the Simultaneous Iterative Reconstruction Technique (SIRT). The SIRT performs a forward and back-projection in each iteration. Iterating over this equation yields a solution. Equation 3 shows the calculation of the unknown vector  $I$  for iteration  $t+1$ .

$$I^{t+1} = I^t + CA^T R(D - AI^t) \quad (3)$$

Here the entities  $C$  and  $R$  are diagonal matrix with the trace representing the inverse of the column and row sum of matrix  $A$  respectively. The term  $A^t$  is the forward projection and the CATR is the weighted back projection. All this is then added to the current searched pixel intensities  $I^t$

In our case, some 20 iterations are needed to achieve the results as shown in Figure 8

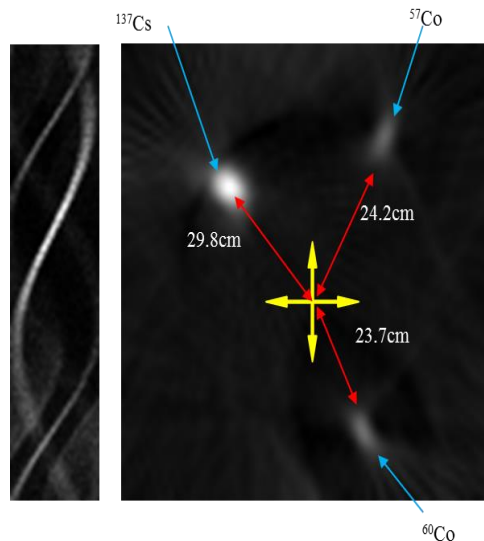


Figure 8: Image reconstruction with the sinograms of three sources (on the Left) and the algebraic reconstruction using Python ASTRA toolbox (on the Right).

The image calibration can be performed by both the MATLAB image processing toolbox or by the NI Vision. The latest one is the preferred option as it can be seamlessly integrated into our program.

Due to the low activity of waste, the statistical fluctuation of our measurement is significant (5 to 10 % but up to 25% in the worst case). These fluctuations generate artefacts as shown in Figure 9. The filtering of these fluctuations is not yet resolved.

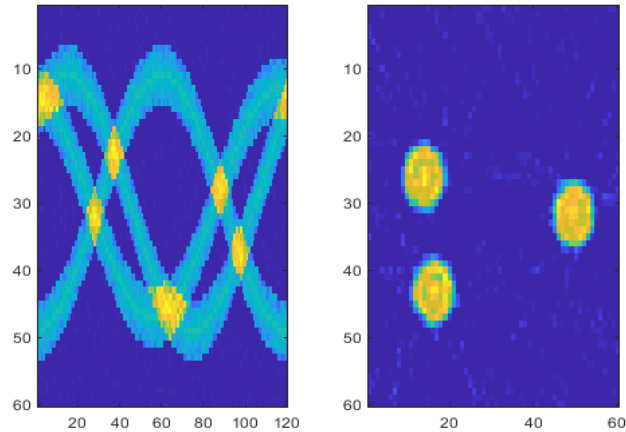


Figure 9: This image shows some artefacts (white spots) generated by the statistical variation of the intensity peak.

Extensive test of the experimental tomograph with a HPGe detector have been performed. Now we have started to use CZT detectors. Thanks to the technological progress, new CZT detectors with large crystal have been developed at an affordable cost. We aim to create a system made of an array of large volume CZT crystals for the gamma acquisition. Such a solution would reduce the measurement time by a factor proportional to the number of detectors (considering size/efficiency of the CZT similar to the one for an HPGe crystal). A preliminary test and its reconstruction image has been performed with a 0.5 cm<sup>3</sup> detector. Figure 10 shows a tomographic image reconstruction obtained a CZT crystal.

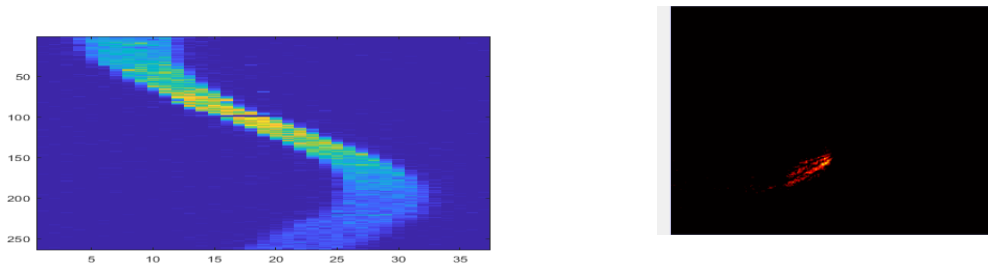


Figure 10: A sinogram (right) and the corresponding tomographic image (left picture) of a <sup>137</sup>Cs point source measured with a CZT cube 527 from GBS (500 mm<sup>3</sup>). Each spectrum has been acquired for 60 sec for a total 37x263 spectra. Some artefacts have been removed.

#### 4. Conclusion

The purpose of this project is to make WCS (Waste Characterisation System) in JRC Ispra fully operational. This paper focused on the work performed on gamma station of WCS that operates in SGS or TGS mode. Presently the SGS mode is fully operational although new calibrations are required and are currently in progress. For emission tomography especially for TGS, an experimental tomographic system has been built and tested successfully with various waste measurement configurations and various tomographic image construction algorithms (inverse Radon, algebraic techniques) implemented in the Astra Toolbox. The experimental tomograph goal is to support new developments of tomographic methods that would be tested before their implementations in WCS. Regarding the TGS mode, some software issues should still be resolved soon. Then both TGS/SGS modes could be used and WCS be fully operational.

There is also a plan to implement new features and technologies in WCS. The main parts for upgrade regard a second pillar to hold the high activity  $^{152}\text{Eu}$  transmission gamma source in a such a way that the gamma radiation background would be reduced significantly for the gamma station. Thus this will result on higher sensitivity on gamma measurements for improved SGS/TGS. This will be accomplished also by adding a variable aperture and efficient gamma tungsten collimator. The hardware and software upgrades are in this plan.

## References

- [1] The ASTRA Toolbox, a MATLAB and Python toolbox of high-performance GPU primitives for 2D and 3D tomography, <http://www.astra-toolbox.com/>] NVIDIA CUDA Compute Unified Device Architecture, Programming Guide Compute Unified Device Architecture (CUDA), [http://developer.download.nvidia.com/compute/cuda/1.0/NVIDIA\\_CUDA\\_Programming\\_Guide\\_1.0.pdf](http://developer.download.nvidia.com/compute/cuda/1.0/NVIDIA_CUDA_Programming_Guide_1.0.pdf)
- [3] Gordon, R; Bender, R; Herman, GT (December 1970). "Algebraic reconstruction techniques (ART) for three-dimensional electron microscopy and x-ray photography". *Journal of Theoretical Biology*. 29 (3): 471–81. doi:10.1016/0022-5193(70)90109-8
- [4] A Simultaneous Iterative Reconstruction Technique (SIRT) for 2D data sets. <https://www.astra-toolbox.com/docs/algs/SIRT.html>
- [5] ] C. I. Epstein, Introduction to the Mathematics of Medical Imaging: Second Edition, SIAM, 1 janv. 2008 - 761 p
- [6] A. V. Oppenheim Ronald W. Schafer, Discrete-Time Signal Processing, Pearson Education (US), 2009

## INS3L – a new NDA laboratory for the European Safeguards R&D Community

Bent Pedersen<sup>1,2</sup>, Tatjana Bogucarska<sup>1,2</sup>, Kamel Abbas<sup>1,2</sup>, Jean-Michel Crochemore<sup>1,2</sup>, Francesco Raiola<sup>1,2</sup>, Eric Roesgen<sup>1,2</sup>, Arturs Rozite<sup>1,2</sup>, Hamid Tagziria<sup>1,2</sup>, Giovanni Varasano<sup>1,2</sup>, Isabella Maschio<sup>1,2</sup>, Stefan Nonneman<sup>1,2</sup>, Willem Janssens<sup>1</sup>

European Commission, Joint Research Centre,

<sup>1</sup>Nuclear Safety & Security Directorate, Nuclear Safeguards & Security Department

<sup>2</sup>Nuclear Security Unit

Via E. Fermi 2749, Ispra 21027 (VA), Italy

E-mail: bent.pedersen@ec.europa.eu

### **Abstract:**

*The Nuclear Security Unit of JRC operates for more than four decades an R&D programme in non-destructive assay (NDA) methods on nuclear materials. The application areas include nuclear safeguards, security and decommissioning. The experimental work is currently carried out in four dedicated laboratories on the ESSOR reactor site in Ispra but also in specific laboratories of the Nuclear Decommissioning Unit on the site. The ongoing decommissioning programme on the JRC Ispra site includes among many other tasks the decommissioning of the ESSOR reactor. In relation to this JRC decided to construct a new infrastructure outside the ESSOR site and to transfer the four laboratories that would otherwise be affected by the decommissioning activities.*

*The new infrastructure, Ispra Nuclear Safeguards, Security and Standardisation Laboratory (INS3L), will allow the continuation of the NDA work programme of the Nuclear Security Unit. INS3L will also be a more versatile NDA infrastructure than the present, and will be able to accommodate a larger range of R&D and training projects in a more agreeable environment. This is part of a deliberate effort to increase the collaborations with our research partners in the EU member states, and to make the infrastructure, the instrumentation and the radioactive source inventory directly available to EU research partners.*

*At present the executive design of INS3L has been completed, the construction site allocated, and the tendering process for the construction contract is in progress. The paper gives an overview of the new infrastructure and intends to provide potential research partners an impression of the range of R&D projects that can be undertaken.*

**Keywords:** NDA; R&D; laboratory; nuclear safeguards; nuclear security; nuclear decommissioning

### **1. Introduction**

Non-destructive assay (NDA) methods and instrumentation are the backbone of radiation measurements in nuclear safeguards, nuclear decommissioning and waste management (ND&WM), and nuclear security implementation. In safeguards and ND&WM, NDA allows scientists, plant operators and safeguards inspectors to make rapid and accurate measurements of sensitive nuclear materials in diverse form and composition as part of the nuclear material declaration/verification or waste categorization. In the security field, NDA allows front line officers to quickly detect and identify radioactive materials transported illicitly.

INS3L (Ispra Nuclear Safeguards, Security & Standardization Laboratory) is the new infrastructure on the JRC Ispra site for hosting all existing and future non-destructive assay (NDA) activities of the Nuclear Security Unit. In 2015 the Director General of JRC approved the realisation of INS3L based on a detailed study taking into account aspects such as future directions in NDA R&D, stakeholder requirements, serviceability of R&D partners and training clients, maintenance and running costs etc.

As such INS3L will incorporate activities currently undertaken in all the experimental facilities of the Nuclear Security Unit concerned with NDA currently located on the ESSOR reactor site (INE), including PERLA, PUNITA, ITRAP and EUSECTRA-Ispra. The relocation of these four laboratories also facilitates the planned decommissioning of INE. Based on the decades of experience with the present laboratories, the INS3L design incorporates an even more versatile and accommodating environment suitable for an even larger range of NDA activities. Generally speaking INS3L will serve the three specific activity areas mentioned below.

### **1.1 Nuclear safeguards support**

JRC provides support to DG ENER (Euratom) and the International Atomic Energy Agency (IAEA) for the implementation of international treaties on safeguards and non-proliferation verifications.

INS3L will provide the framework for continued R&D in NDA methods and instrumentation, development of technical solutions for nuclear inspectors, provide in-field technical support, and training of inspectors. These services are offered both to DG ENER (Euratom) and to IAEA by means of the European Commission Support Programme (EC-SP). The R&D component of the safeguards work in INS3L is greatly complemented through the synergy with the other Nuclear Security Unit safeguards laboratory AS3ML (Advanced Safeguards Measurement, Monitoring and Modelling Laboratory) where state-of-the-art safeguards instrumentation and methodologies are developed for safeguards inspections.

### **1.2 Nuclear security activities**

Nuclear security activities in INS3L includes development of technical tools for implementation of EU policies and instruments for nuclear security on European borders.

The R&D component in the field of nuclear security concerns participation to international R&D projects (recently ITRAP, SCINTILLA, C-BORD) and also research into so-called active NDA methods for detection of nuclear materials in cargo. In the latter case the PUNITA facility of the Nuclear Security Unit implementing active neutron interrogation is an important asset. Other key R&D activities concern standardization, benchmarking, round-robin tests etc. In this work area a good collaboration has been established with the JRC Geel site.

In addition, the infrastructure is used for training of border guards and customs officers in detection and response to illicit trafficking of radioactive and nuclear materials (part of this work takes place in the Outdoor test area indicated in Figure 1). This work is shared and coordinated with the JRC site in Karlsruhe. This work also has strong synergy with a similar Nuclear Security Unit activity on training of border guards and customs officers on export control of dual use items and interception/recognition of these items on EU borders.

### **1.3 Nuclear decommissioning and waste management support**

NDA is an important tool in nuclear decommissioning and waste management (ND&WM) both within JRC and on European scale in form of development of instrumentation and methods for the safe monitoring and characterization of radioactive waste.

In support to ND&WM INS3L expertise and instrumentation is put to work mainly in the area of NDA methods for waste characterization. This work concerns both international R&D projects (e.g. MetroDecom, and MetroDecom-II) and direct support to the Nuclear Decommissioning Unit in their decommissioning activities on the JRC Ispra site. A new activity of this kind is the assay of large historical waste components by means of tomography using atmospheric muons as the interrogating source.

## **2. A European User-Laboratory for NDA methods and Instrumentation**

INS3L has been conceived as a user-laboratory for client DGs of the European Commission, EU member state authorities and national laboratories, international research partners and international organisations.

The layout of the laboratory including support facilities is intended to provide easy access to the external user and their equipment, and to allow different activities take place in parallel in different parts of the laboratory. For this purpose INS3L is designed with a single entry point that gives the user

access to the entire laboratory. Shielding for radiation and noise is applied around specific rooms and sub-areas to avoid interference between ongoing activities.

One important feature of INS3L is the sealed source inventory of unique and well-characterized radioactive and nuclear materials to which access elsewhere in Europe is typically very restricted. The fact that the laboratory operates with radioactive materials exclusively in sealed source form provides a number of advantages for the experimentalist related to easy and simple accessibility. For example novel NDA instrumentation can be brought to INS3L for final testing before field deployment without any risk of contamination, new NDA analysis methods can be tested on well-characterised radioactive or nuclear materials for validation or comparison purposes, and new signal analysers or radiation detectors can be tested or characterised on real materials under controlled conditions. Operating with only sealed sources however does limit the range of NDA applications to the ones concerned with detection of radiation of the penetrating type such as x-rays, gamma-rays, heat, neutrons (and atmospheric muons). Whereas applications based on detection of charged particles from the source such as alpha or beta radiation, or applications requiring radioactive sources in non-solid form, cannot easily be studied due to the permanent source encapsulation. Work on open radioactive sources requires a sealed environment such as a glove-box facility which is not part of the objective of INS3L.

The operational license of INS3L is intentionally limited in scope to NDA activities on sealed radioactive and nuclear materials. This circumstance is key to many aspects of the easy access for experimenters and their equipment, and the range of experimental activities that can be undertaken in the laboratory. The fact that INS3L was designed for this sole purpose makes the infrastructure inexpensive and versatile within the scope. This is indeed difficult to achieve in other laboratories where NDA is a minor part and purpose in a facility with a more extensive scope where safety and security measures are implemented based on the most constraining of the activities.

As is currently the case for the existing NDA laboratories of the Nuclear Security Unit, INS3L will see a variety of research applications and joint projects with external partners taking place simultaneously in the different parts of the laboratory. Some partners will bring instrumentation to INS3L for the purpose of performance testing or validation using the nuclear material source inventory. Some will come to the laboratory to receive specialized training in specific NDA instrumentation and methods, while others will conduct specific research e.g. on innovative detection methods or active neutron interrogation.

INS3L's emphasis on NDA research, and accessibility for external partners, is further reinforced by the INS3L support facilities such as the computer cluster for MCNP calculations in support of the experimental activities, and the electronics laboratory where users can be assisted in modifying detection systems in order to adapt ongoing experiments. Another significant INS3L feature is the catalogue of state-of-the-art NDA instruments as well as the staff's expertise in NDA methods, collected over decades of R&D through the long standing safeguards support programme of JRC.

The layout of INS3L is shown in Figure 1. INS3L can be seen to include three main areas: the main laboratory (right side), the office area (left side), and the outdoor test area (lower part).

## 2.1. The INS3L NDA laboratory

The main laboratory (Figure 1, dotted red line) has a single access point where users and visitors enter via a security portal. Once inside the main laboratory the user can access all the experimental areas shown in Figure 1, except for the Outdoor Test area which is only accessible by special procedure. The size of the laboratory hall is roughly 45 metres length, 20 metres width, and 8 metres height. The laboratory is sub-divided into specific areas to allow activities to proceed undisturbed simultaneously. In general the laboratory is arranged so that activities making use of low radioactivity are located towards the laboratory entrance and the office area, whereas activities using higher radioactivity are concentrated towards the opposite end.



**Figure 1.** Plan of INS3L ground floor showing the access-controlled laboratory (perimeter indicated by red dotted line), and some of the key sub-areas within the laboratory. Some auxiliary rooms located outside the laboratory are shown (left side). Also the outdoor test area is shown.

### 2.1.1. High activity area

A certain area of INS3L is reserved for experiments with strong radiation sources or for example compact particle accelerators. This area (also indicated on Figure 1) of 54 m<sup>2</sup> is surrounded by a one metre thick concrete wall for the purpose of reducing radiation dose rates outside the high activity area to levels well below permissible, and to avoid disturbing detection systems in other parts of the laboratory. As in all parts of INS3L, the high activity area is designed with external users in mind. By means of an overhead crane large detection systems and accelerator systems can be lifted into the area for test campaigns for example in combination with the nuclear material inventory of INS3L. The high activity area is well-equipped for studies of active NDA methods and instrumentation. For example neutron activation studies, or studies of delayed fission signatures, can make use of a built-in transfer system shuffling a sample through the shielding wall between the irradiation station and a low-background measurement station.

Among other instrumentation also the Pulsed Neutron Interrogation Test Assembly (PUNITA) is located in the high activity area and available for users. PUNITA is a versatile research tool for NDA methods in nuclear safeguards and nuclear security.

### 2.1.2 Safeguards training area

An area of INS3L is dedicated to training of safeguards inspectors and is fully equipped with standard safeguards detection and data acquisition systems for hands-on training sessions, primarily on gamma-ray and neutron detection systems. Besides training session this area is used for testing and validation of instrumentation to be used in-field, and safeguards R&D. As such the areas make frequent use of the inventory of reference sealed sources of nuclear materials. As for the former PERLA laboratory this part of INS3L is expected to welcome many external users from EU member states, universities, international partners for projects such as testing and benchmarking of own instrumentation, workshops, training and inter-comparisons.

### 2.1.3 Large test area

This part of INS3L is dedicated to the testing and validation of large integral detection systems. The area has direct access for bulky equipment through the large access door and the Outdoor test area (Figure 1). For example testing of large tomographic systems based on muon detection is likely to take place here.

The area is also home to the dynamic and static test facilities for testing and validating the performance of off-the-shelf radiation detection instrumentation against international standards for the purpose of providing feedback to the manufacturer on the performance of their instruments, to standards committees, as well as to the EU member states. This activity was launched under the Illicit Trafficking Radiation Detection Assessment Programme (ITRAP). By now the infrastructure and testing procedures are offered also to external users for testing and benchmarking their new prototypes, as well as assisting the certification of EU MS laboratories by transfer of expertise.

### 2.1.4 EUSECTRA-Ispra

The European Security Training Centre (EUSECTRA) is coordinated by the sister unit on the JRC Karlsruhe site, and operated on both Ispra and Karlsruhe sites. EUSECTRA provides training to front line officers and their trainers in techniques, instrumentation and procedures to detect, and respond to, events of illicit trafficking of radioactive or nuclear materials. The facility is implemented under the CBRN Action Plan of DG HOME of the European Commission.

In INS3L, the EUSECTRA-Ispra facility is comprised of the dedicated training room and the outdoor test area (Figure 1). The outdoor test area has two sets of permanently installed vehicle radiation portal monitors (RPMs). During training sessions the outdoor portals monitors (RPMs) are monitored and controlled from the bay window of the EUSECTRA-Ispra area. The facility also operates a variety of detection instruments ranging from handheld detectors to pedestrian RPMs, and makes use of the INS3L inventory of sealed nuclear material sources also in the outdoor test area under special procedures. Such training sessions also have strong synergy with a similar Nuclear Security Unit activity on training of border guards and customs officers on export control of dual use items and interception/recognition of these items on EU borders.

## 2.2 Auxiliary rooms and offices

The office area is the only part of the INS3L building which has two floors. The 1<sup>st</sup> floor is dedicated to staff offices and meeting room. The ground floor has the entrance to the building, 1<sup>st</sup> floor access, and auxiliary rooms to support the experimental activities (Figure 1).

The Visitors' Office is the home for external experimentalists outside the access-controlled laboratory. The intention is that data acquisition from experiments can be routed from anywhere inside the laboratory to the office area (including the Visitors' Office). This is to allow the experimenters to retreat from the laboratory while an experiment is ongoing thus reducing the time spent near the radiation sources.

The storage room keeps NDA equipment not currently in use in the laboratory. This room is also the buffer store for equipment belonging to external users before/after a measurement campaign in the INS3L laboratory.

NDA data acquisition systems typically make use of substantial amounts of electronics, cabling and data paths. The electronics laboratory, located outside the access-controlled laboratory, is dedicated to maintenance and repair of acquisition systems, and quick interventions on detector electronics in ongoing campaigns if needed.

To facilitate training lectures in the best possible way one meeting/teaching room is located inside, and one outside, the access-controlled area.

## 3. Project implementation

At the time of the ESARDA Symposium 2019 the project of construction of the INS3L laboratory has already reached a number of key milestones. Most prominently, the executive design phase has been completed, the site allocation for INS3L within the JRC Ispra site is approved, budgetary preparations are completed, and the tender procedure for the construction of INS3L is in the launch phase. Figure 2 is a depiction of the final INS3L design.

The expectation is that a construction contract will be allocated by the end of 2019, followed by the construction phase of little more than one year, completion of the licensing phase and taking into service expected by end of 2021.

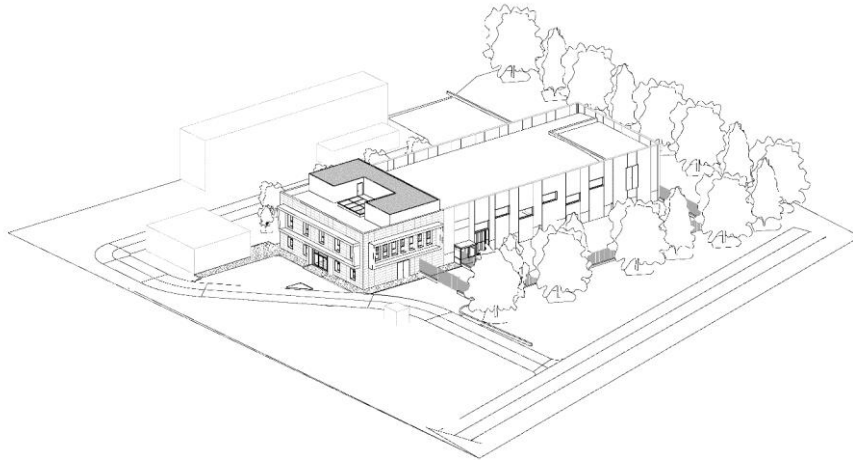


**Figure 2.** INS3L as perceived in the final design drawings. Visible elements are: the two-story office and auxiliary room area, the main laboratory, and the enclosure of the Outdoor test area.

#### **4. Acknowledgements**

The authors represent the NDA users of INS3L and as such have provided the user requirements to the new construction. The authors wish to acknowledge the Nuclear Decommissioning Unit of JRC, and in particular the Operations INE & Infrastructures sector and the Licensing Office, for their leading role in all phases of the INS3L construction project, and their continued support in implementing the user requirements in the best possible manner.

# An SNM detection method based on fission signatures induced by a low-energy neutron source

Bent Pedersen<sup>1</sup>, Aharon Ocherashvili<sup>2</sup>, Giovanni Varasano<sup>1</sup>,  
Tatjana Bogucarska<sup>1</sup>, David Mikhaeli<sup>2</sup>, Guy Heger<sup>2</sup>, Valeriy Mayorov<sup>1</sup>

<sup>1</sup>Joint Research Centre, European Commission  
Directorate Nuclear Safety and Security  
Nuclear Security Unit  
Via E. Fermi 2749, Ispra 21027 (VA), Italy  
E-mail: bent.pedersen@ec.europa.eu

<sup>2</sup>Physics Department, Nuclear Research Center Negev  
P.O. Box 9001, 84190 Beer-Sheva, Israel

## Abstract:

*Liquid scintillation detectors are able to identify fast neutrons by means of the well-known pulse shape discrimination (PSD) analysis method of photomultiplier charge output signals. Detection systems based on this technology have been demonstrated by many groups as a valid alternative to standard neutron detectors, and as a direct detection method for fast neutrons, in passive neutron well-counters for safeguards. We apply this technology combined with a pulsed neutron source as an active system for detection of fissile materials. In the present paper we elaborate on our previous findings based on laboratory experiments towards the application of this active detection system as a potential method for detection of special nuclear materials (SNM) in shielded containers such as air cargo.*

*The use of a pulsed neutron source, a graphite moderator, and prompt fission neutron detection has parallels to the standard differential die-away (DDA) technique used in nuclear safeguards. At less than 100 microseconds after the 14-MeV neutron burst only low-energy and thermal source neutrons persist. The low-energy source neutrons are indistinguishable from gamma rays in the PSD analysis whereas the fast prompt fission neutrons are. This circumstance provides a way of separating the interrogating sources neutrons from the prompt fission neutrons in the detectors. The interrogation by only low-energy neutrons is achieved by time-gating the acquisition system to avoid the period when fast source neutrons interact with the detectors. In contrast to the standard DDA system this means the detectors can be placed in the vicinity of the sample rather than behind the graphite and Cd-liner thus providing a better neutron detection efficiency.*

*We present new performance values achieved in laboratory experiments on HEU uranium samples in terms of detected single and coincident fission neutrons*

**Keywords:** NDA; 14-MeV neutrons; PSD; nuclear security; scintillation detection

## 1. Introduction

Inducing fission by means of an external neutron source is a principle with great potential as an active non-destructive assay (NDA) method for detection of special nuclear materials (SNM). The prompt emissions of neutrons and  $\gamma$ -rays following the fission event are useful signatures for the detection of SNM in shielded containers. Detecting the prompt fission neutrons is particularly useful as they are very penetrating and difficult to deliberately shield from detection, and the simultaneous emission of multiple neutrons provides an additional mechanism to be exploited in the detection method. For this purpose, and for increasing the detection efficiency, it is useful to apply a detection system composed of multiple individual detectors.

Using an external neutron source that can be pulsed so that short bursts of neutrons are emitted periodically can provide further advantages to be exploited in the detection method. By short bursts is understood bursts of neutrons emitted in a time interval much shorter than the combined slowing down time and thermal neutron life-time of the source neutrons. The period between bursts must be long enough that source neutrons from one burst have disappeared before the following burst. In this way the interactions of the epi-thermal source neutrons and the thermal source neutrons can to some extent be separated in time. By proper timing (gating) of the detection period with respect to the neutron emission from the external source, an object can be interrogated by a low energy (epi-thermal or thermal) neutron flux only, providing the possibility to distinguish the fast fission neutrons from the low energy source neutrons in the neutron detection system.

The present report addresses the problems associated with the detection of prompt fission neutrons during the interrogation by the epi-thermal source neutrons. In this time period however the response of the detection system is hard to interpret due to the much larger proportion of gamma detection events. The epi-thermal interrogation however is important from a nuclear security point of view as these source neutrons will to some degree penetrate any thermal neutron shield, such as a Cd liner, purposely placed around an object containing fissile material. An SNM detection instrument seeking to detection neutron induced fission signatures should apply a combined thermal and epi-thermal neutron interrogation regime.

Previously we have reported on measurements in different time periods of the pulse neutron interrogation using the Pulsed Neutron Interrogation Test Assembly (PUNITA) at JRC [1, 2, 3]. Different trigger schemes and time intervals had been used for the purpose of reducing the data rate. The present report is based on new experiments where the detector response during the whole period between neutron pulses could be recorded without data loss. This also allowed recording single neutron detection events as well as two and three-fold neutron detection events in short coincidence intervals. Also a new detector configuration yielding a higher neutron detection probability in the eight scintillation detectors is applied.

## 2. Experimental setup

The PUNITA facility is designed for active neutron interrogation studies of NDA methods for nuclear safeguards and security. Figure 1 shows a cross section of PUNITA and the positioning of the detectors used in this work. The facility is composed of a large graphite liner surrounding a central cavity of volume  $50 \times 50 \times 80 \text{ cm}^3$ . The (D-T) neutron generator producing pulses of 14-MeV neutrons, the sample under investigation and the scintillation detectors used in the present study are all located inside the central cavity. Also indicated in Figure 1 is the so-called source monitor, an array of  $^3\text{He}$  neutron detectors embedded in the polyethylene shield. The source monitor is well shielded from all but the 14-MeV neutrons and can thus be used to normalize detector readings in all experiments to the same total neutron emission from the neutron generator.

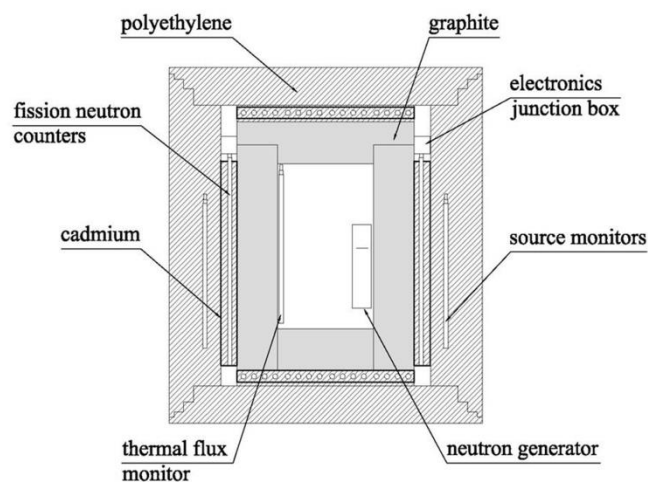


**Figure 1.** Sketch of PUNITA showing the permanently installed fission neutron detectors ( $^3\text{He}$  counters) and the neutron generator mounted inside the sample cavity. An important detector for the present experiments is the so-called source monitor embedded in the polyethylene shielding.

The neutron generator (Model A-211 from Thermo Fisher Scientific Inc.) is pulsed at 100 Hz, yielding a pulse period of 10 milliseconds, which is chosen based on the average thermal neutron life-time in the graphite/cavity configuration. The generator is able to produce short and intense bursts of neutrons with no neutron emission between bursts. This fact, together with the very short duty-cycle of one per mille, allow separation of the neutron interrogation into a fast/epi-thermal period from zero to about 120  $\mu$ s, and a pure thermal period from about 250  $\mu$ s to 9 ms, respectively [1].

We use an array of eight EJ-309 3"x3" liquid scintillation detectors from Eljen Technology ([www.eljentechnology.com](http://www.eljentechnology.com)) for the detection of the prompt radiation from fission events. This type of liquid scintillation detector can distinguish fast neutron interactions from  $\gamma$ -rays by means of pulse shape discrimination (PSD). The performance of scintillation detectors with respect to  $\gamma/n$  discrimination as observed in the PUNITA facility is described in [3]. Due to the very fast response of the scintillation detectors the effect of the neutron generator burst can be followed in detail [2]. In the present work the scintillation detectors were arranged in a new setup for the purpose of increasing the prompt fission neutron detection efficiency, Figure 2.



**Figure 2.** The new setup of the PUNITA cavity including the eight liquid scintillation detectors. The detectors are arranged in closed proximity to the centred sample. In the corner the neutron generator is visible (with the target at the same level as the sample to be irradiated).

Each detector was applied with an individual high voltage allowing to adjust the Compton edge of a given  $\gamma$ -source to same charge response. The detector response was thus calibrated using standard gamma sources including  $^{133}\text{Ba}$  ( $E_{\gamma}=356\text{keV}$ ),  $^{137}\text{Cs}$  ( $E_{\gamma}=662\text{keV}$ ),  $^{54}\text{Mn}$  ( $E_{\gamma}=835\text{keV}$ ), and  $^{22}\text{Na}$  ( $E_{\gamma}=511,1274\text{keV}$ ).

The anode output of the photomultiplier was connected directly to a signal digitizer. For the present experiments two CAEN DT5730B digitizers were used. This model has eight input channels, 14-bit energy resolution, and is capable of 500 MS/s. The model also has built-in proprietary firmware analysing in real time the charge pulse according to the standard PSD charge integration method. The PMT charge pulses were typically 20 - 30 ns duration, and we applied a Long Gate of 120 ns and a Short Gate of 40 ns. The so-called PSD value calculated in firmware equals the ratio of the charge integral of the tail to the charge integral of the whole pulse. As part of the DT5730B firmware analysis of each charge pulse, a time stamp is output together with the PSD value. Unfortunately the internal timer cannot be reset with each synchronisation pulse from the neutron generator. This means that timestamps are not reset with each generator cycle. For this reason we used two digitizers each using four signal inputs, and a 5<sup>th</sup> input channel used for a synchronisation pulse from the generator to obtain the timestamp of relative to the start of the generator cycle. This way all signal timestamps could be related to the start of the generator cycle. Using two digitizers also benefitted the high data throughput over USB 2.0 to the host computer.

## 2.1. Initial experiments

In Figure 3, (a) is a schematic indicating the generator pulsing regime with the periodical pulse of 14-MeV neutrons, and the subsequent formation of the thermal neutron flux caused by the substantial graphite mantle surrounding the central cavity in PUNITA. The graphs (b) - (d) show the signal rate in the liquid scintillation detector at different time intervals following the neutron burst at time zero. The graph (b) shows the response in the 8 ms following the burst of 14-MeV neutrons at time zero. The graphs show 4 distinct intervals of the 10 ms period: 14-MeV neutron emission (0 - 20  $\mu$ s), neutron slowing down (20  $\mu$ s - 300  $\mu$ s), thermal neutron (300  $\mu$ s - 4000  $\mu$ s), and finally the range dominated by activation and signal background (4000  $\mu$ s - 8000  $\mu$ s) in the scintillation detectors. The two distinct single exponential decays visible in (b) and (d) are attributed to the slowing down time and thermal life time, respectively, of neutrons in the graphite/cavity assembly.

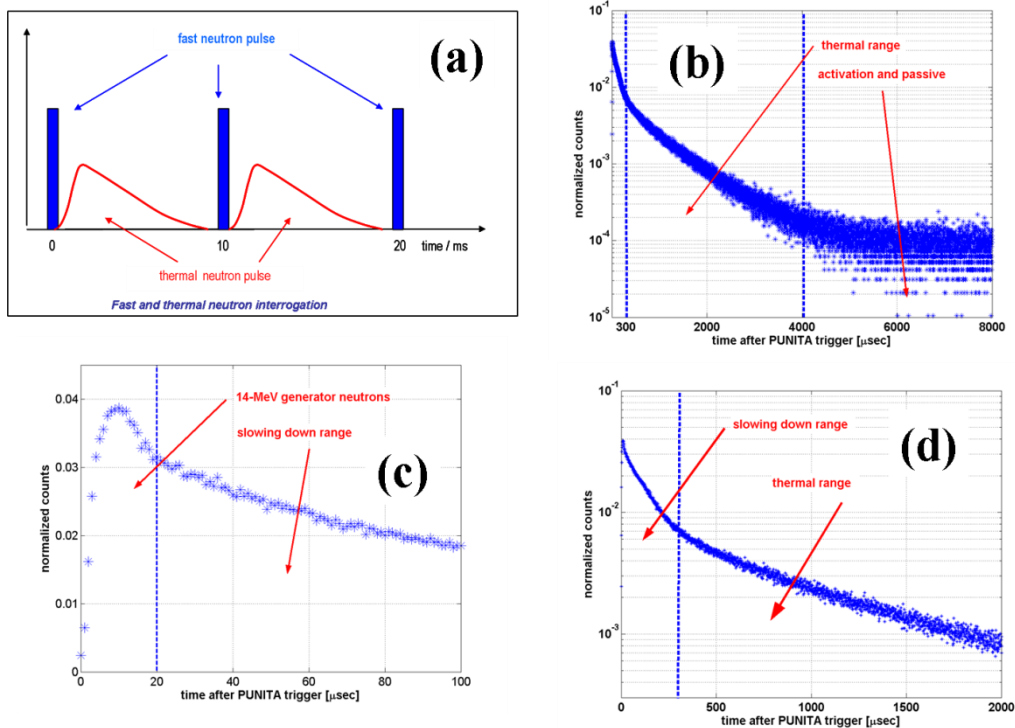


**Figure 3.** Schematic of pulsing regime of the neutron generator (a), and signal rate observed in the scintillation detector as function of time after the burst of neutrons from the generator (b - d). The three graphs are different time scales of the total time spectrum (b). Time zero corresponds to beginning of the 14-MeV neutron pulse.

The PSD analysis of the charge pulse in the liquid scintillation detectors due to the proton recoil reaction allows identification of fast neutrons with energy threshold of approximately 0.6 MeV. In Figure 3 the only source of such neutrons is the 14-MeV generator, and only for the duration that these neutrons have energy above the threshold. After this time only low-energy neutrons (indistinguishable from  $\gamma$ -rays) and  $\gamma$ -rays interact with the detectors.

In Figure 3 time zero corresponds to the trigger output signal from the generator which occurs (conveniently) 27  $\mu$ s before the 14-MeV pulse initiates. The 14-MeV pulse concludes at about 36  $\mu$ s after the trigger pulse. Previous experience shows that up to approximately 30  $\mu$ s after the trigger pulse, the detector readings are meaningless probably due to the current pulse in the transformers of the ion source and the acceleration unit of the neutron generator disturbing the PMTs of the scintillation detectors. For this reason we gate the data acquisition to start at 50  $\mu$ s after the trigger pulse corresponding to approximately 14  $\mu$ s after the end of the 14-MeV pulse. The acquisition gate remains open until 9 ms after the trigger pulse.

## 2.1. Initial experiments

In the new experimental setup of Figure 2, the first experiments included both passive and active measurements aimed at verifying the performance and signal throughput of the online PSD analysis in

the two CAEN DT5730B digitizers, and the optimisation of the signal range to be used when performing the active neutron interrogation. The purpose of these tests was to optimise the selection of useful data in the vast amount of data produced in these experiments. This was done for example by selecting the range of Large Gate integral values where the fission neutron events occur. Figures 4 to 8 show a short summary of these tests.

Figure 4 shows the Long Gate integral for all data from a single detector, in this case detector #4. All detectors however respond in the same way. The normalization of counts as noted in the following graphs refers using the same number of source neutrons (from the 14-MeV generator) in each experiment (run). Although the same measurement time was applied in all runs, the number of source neutrons varies due to the dynamics of the D-T generator (e.g. ion source gas pressure). All runs were normalized to the same source monitor reading (proportional to the neutron emission of the generator in a given run). Figure 4 shows the comparison of the Long Gate charge integral, as reported by the online analysis in the digitizer, for two samples: one dummy sample without uranium (CBNM000) and one uranium oxide powder sample of 200 grams and 36.2%  $^{235}\text{U}$  (UP362S). Notice that PSD analysis is not performed here. Data recording was in the full gate (50  $\mu\text{s}$  to 9 ms after the generator trigger).

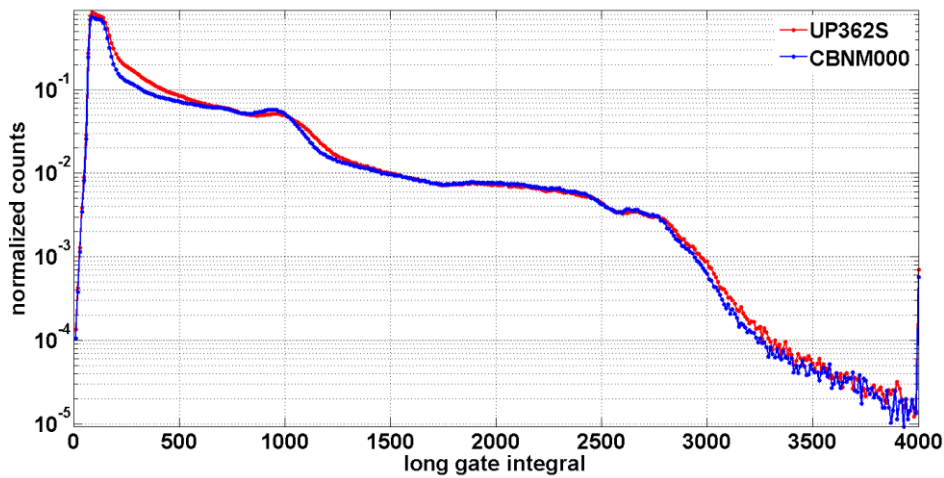


**Figure 4.** Comparison of Long Gate integral distribution for the samples CBNM000 and UP362S for detector #4.

The difference between the two samples is mainly observed in the low values of the Long Gate integral. This is expected as the signal from fission neutrons is generally smaller than the signal from  $\gamma$ -rays produced in these experiments. The graph also illustrates the small signal from fission neutrons to be sought after in a substantial background of  $\gamma$ -ray signals.

The PSD analysis of the same data (detector #4) is shown in Figure 5. The PSD values for  $\gamma$ -rays is centred on the value 0.15, the fast neutron PSD on 0.26. Notice also the small amount of fast neutron detections compared to  $\gamma$ -rays in this kind of experiments.

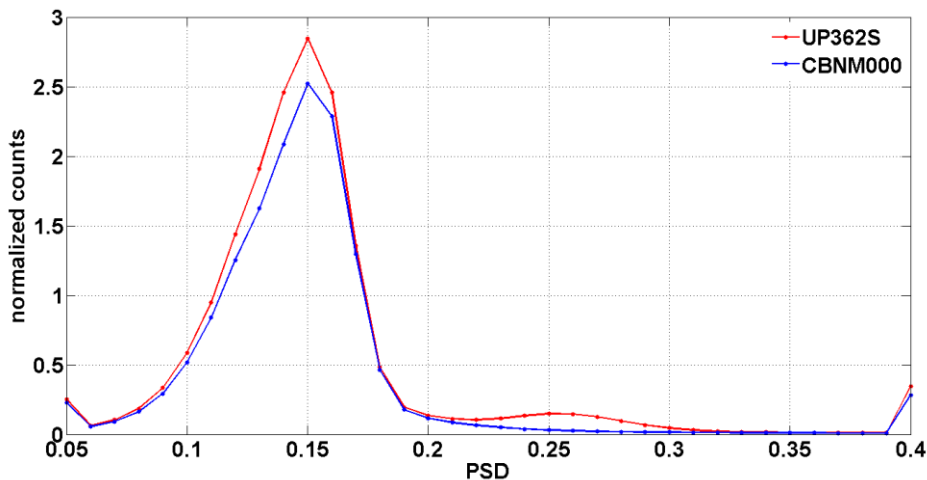


**Figure 5.** Comparison of PSD distribution for dummy sample (CBNM000) and a uranium powder sample (UP362S) for detector #4.

Figure 6 also shows the Long Gate integral observed for detector #4 for the two samples; dummy and uranium powder. In this case however only events with a PSD-value corresponding largely to fast neutron detections have been selected (PSD value in the range 0.2 to 0.35).

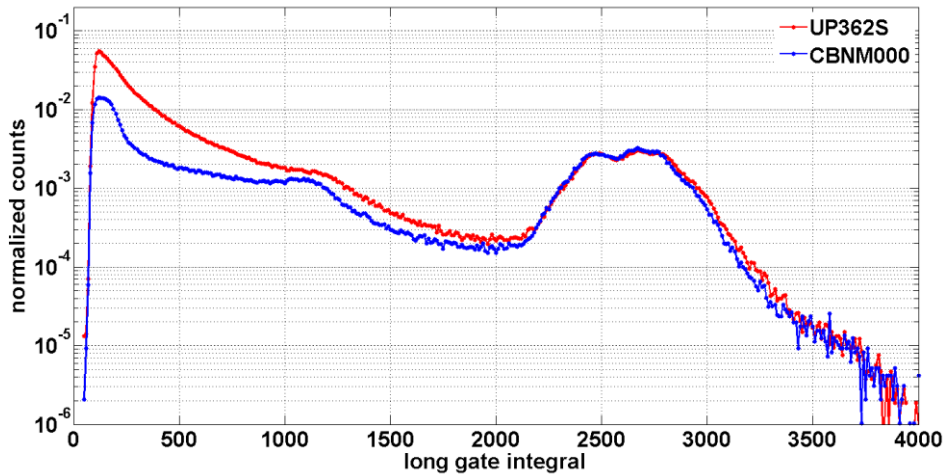


**Figure 6.** Comparison of distribution of neutron Long Gate integral for the dummy sample (CBNM000) and a uranium powder sample (UP362S) for detector #4.

Figure 6 shows two distinct energy regions; one of high value of the Long Gate integral (> 2000) which does not appear to include significant fission neutron detection event, and one of low integral values (to about 2000) which includes substantial fission neutron detection events. Again, in Figure 6 the entire time gate (from 50  $\mu$ s to 9 ms) is included, meaning fission event induced by both epi-thermal and thermal source neutrons. A significant part of the events with a Long Gate integral above 2000 are likely to be caused by  $\gamma$ -ray pile-up events.

Figure 7 shows the events in the neutron PSD range (see above), with a Long Gate integral less than 2000 for the two samples as of Figure 4 to 6, as function of the record event timestamp. Timestamp zero corresponds to the trigger signal from the neutron generator (i.e. 27  $\mu$ s prior to the 14-MeV neutron pulse). Again the event recording is gated to start at 50  $\mu$ s after the neutron pulse trigger.

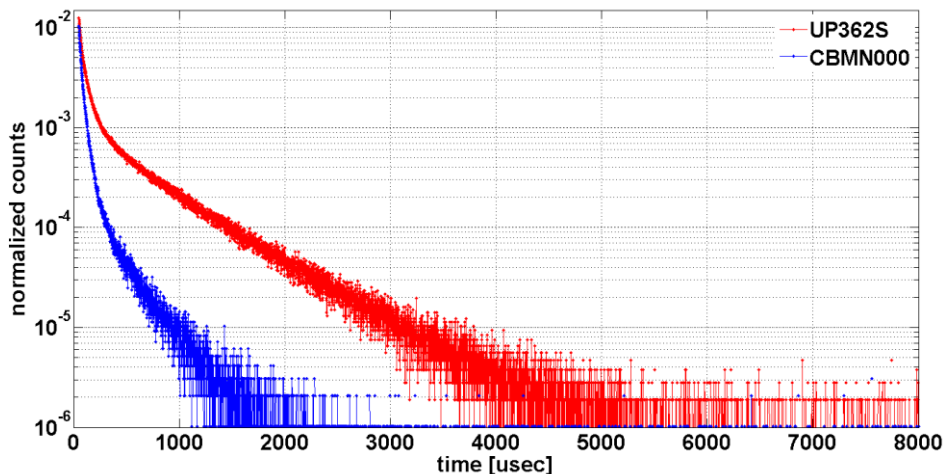


**Figure 7.** Time distribution of low values (less than 2000) of the Long Gate integral.

The difference between the red and blue curve is likely to be almost exclusively prompt fission neutrons produced mainly by epi-thermal neutron induced fission in the interval (50 – 200)  $\mu$ s, and by thermal neutron induced fission in the interval (300 – 4000)  $\mu$ s. The single exponential decay above 500  $\mu$ s of the prompt fission neutron detections (red curve) has the same decay constant as the known decay of the thermal neutron flux in the large graphite assembly of the PUNITA facility.

The most sensitive Long Gate integral range to fission neutrons is from 120 to 1100. This was also confirmed by a passive measurement (not shown in this paper) of  $^{252}\text{Cf}$ , a spontaneous fission neutron

source with high neutron to gamma emission ratio, where also the Long Gate integral, for events with a PSD values in the neutron range, peaks at 120 and has >90% of events with an integral value below 1100.

## 2.2. Detection of multiple neutrons from the same induced fission event

We used an ad hoc Python code for the analysis of the millions of events recorded in each experiment. This analysis aimed at selecting the neutron detection events along the lines of chapter 2.1. A further analysis consisted of analysing for multiple neutron detections from the same fission event. This was done by searching among the fission neutron detection events, as in Figure 7, for timestamps of events on all eight detector lines within a short range of time.

Figure 8 shows the time difference, in the interval 0 - 100 ns, between fast neutron detections originating from induced fission.

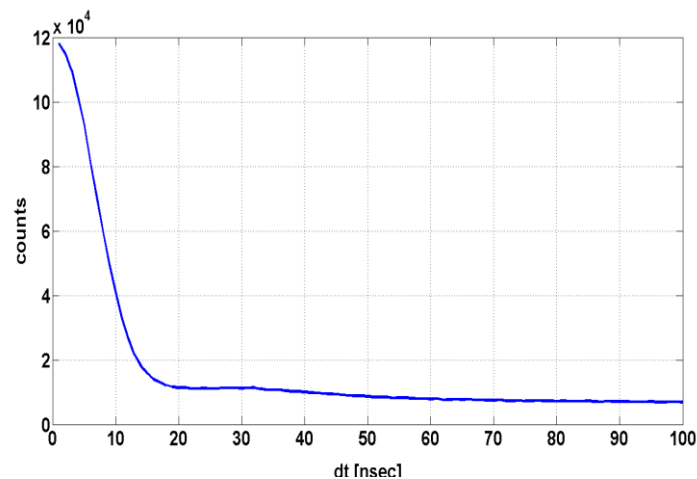


**Figure 8.** Time difference between fast neutron detections in the eight liquid scintillation detectors.

Based on Figure 8, a coincidence interval of 15 ns was selected for the observation of multiple neutron detections from the same fission event.

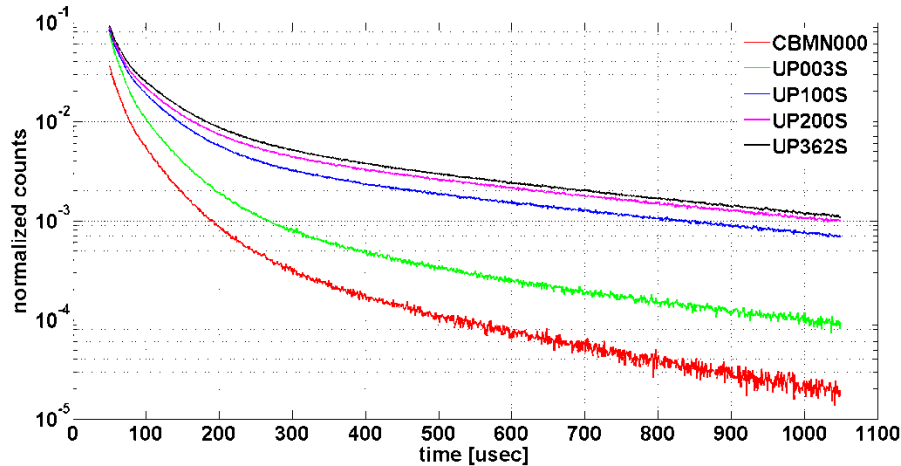
Finally, for the data analyses we used the following cuts: Long Gate integral value in the region of 120 to 2000, PSD value in the region of 0.2 to 0.35 and neutron coincidence time of 15 ns.

## 3. Results from measurements of uranium powder samples

We used a series of uranium oxide samples with the same container and total uranium mass, while varying only the  $^{235}\text{U}$  enrichment. All measurements were compared to the empty container called CBNM000. Each sample was measured both with and without a 2 mm cadmium (Cd) liner completely covering the sample. The purpose of the Cd-liner is to capture thermal source neutrons before reaching the uranium sample thus eliminating thermal neutron induced fission in the sample and allowing only epi-thermal neutron induced fission to take place.

### 3.1. Single neutron detection from induced fission

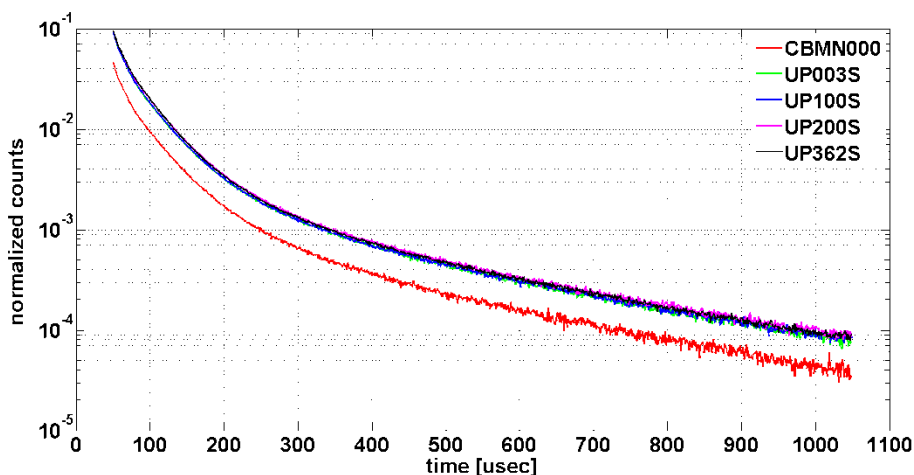
The neutron detection rate as function of time is shown in Figure 9 using the range of timestamps in the interval (50 - 1100)  $\mu\text{s}$ . The beginning of the range (near 50  $\mu\text{s}$ ) still sees neutrons from the generator pulse (27 - 36)  $\mu\text{s}$  in addition to the fast neutron induced fission neutrons from both  $^{235}\text{U}$  and  $^{238}\text{U}$ . The range (100 - 300)  $\mu\text{s}$  is dominated by  $^{235}\text{U}$  fission neutrons from the epi-thermal and (increasingly) thermal neutron source. Again, the decay above 500  $\mu\text{s}$  is directly proportional to the known thermal neutron flux in the sample cavity of PUNITA, perhaps with the exception of the response from the empty container CBNM000. Thus the neutron signal rate, above 500  $\mu\text{s}$ , can be assumed to originate largely from thermal neutron induced fission in  $^{235}\text{U}$ .



**Figure 9.** Time distribution of the single neutron count rate for the empty container, CBNM000, and uranium powder samples with increasing  $^{235}\text{U}$  concentration.

The fact that the empty container neutron response (red curve) is not zero, although significantly lower than the uranium samples, is attributed to  $\gamma$ -ray pile-up in the detectors. As stated earlier, the normalization refers to using the source monitor signal to relate each experiment to the same neutron emission from the 14-MeV neutron generator.

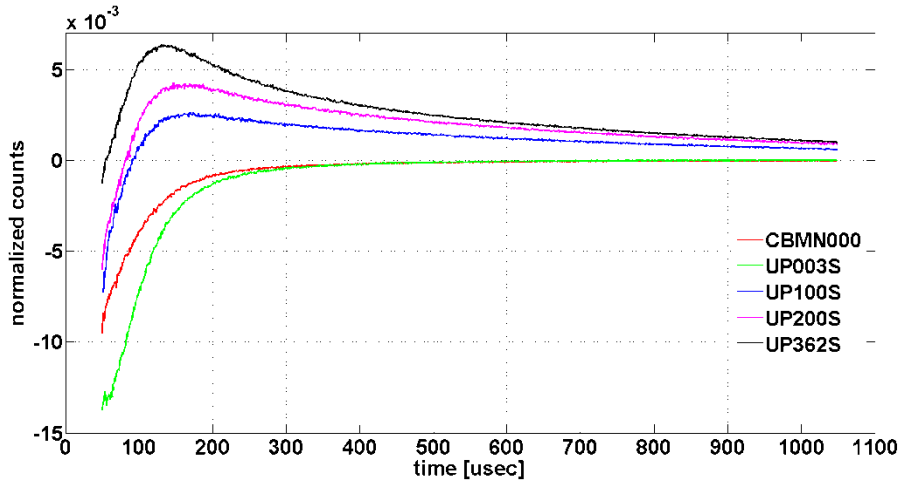
The measurements presented in Figure 9 were repetitions with a Cd-liner surrounding the samples. These results are shown in Figure 10.



**Figure 10.** Time distribution of the single neutron count rate for the empty container, CBNM000, and uranium powder samples with increasing  $^{235}\text{U}$  concentration with a 2 mm of Cd liner surrounding the container.

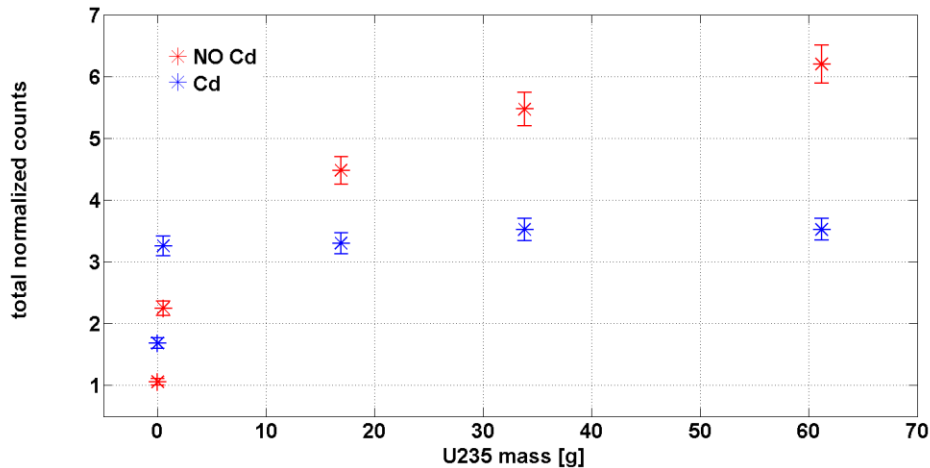
The fact that the uranium containing samples appear to collapse into one curve at least during thermal interrogation ( $>500 \mu\text{s}$ ) is reassuring. The thermal source neutrons are absorbed in Cd before reaching the sample so that thermal induced fission is eliminated. The sample curves however are significantly different from the empty container. This indicates that an additional contribution to the neutron PSD is at play, and appears to originate from  $^{238}\text{U}$ . This is assumed to be delayed neutrons from induced fission, or delayed  $\gamma$ -rays causing pile-up in the detectors.

Figure 11 shows the difference (subtraction) in neutron PSD events of the bare sample and the Cd covered sample as in figure 9 and 10, respectively. Clearly the Cd cover produces an addition amount of false neutron PSD events probably from  $\gamma$ -ray pile-up, dominating below approx.  $80 \mu\text{s}$  and yielding a negative net number of neutron events from the "cadmium difference" (sample – Cd-covered sample). After  $80 \mu\text{s}$  the real neutron detection events dominate at least for the three samples with the highest  $^{235}\text{U}$  content peaking at approx.  $120 \mu\text{s}$ . At this time the epi-thermal neutron flux induces fission events in  $^{235}\text{U}$ . The slow trailing off at times when only thermal source neutrons persist ( $> 500 \mu\text{s}$ ) cannot be understood as prompt fission neutrons.



**Figure 11.** Rate difference between the bare sample (Figure 9) and the Cd covered sample (Figure 10).

In Figure 12 the integral of events under the curves of Figure 9 and 10 are presented as function of  $^{235}\text{U}$  mass in the uranium powder samples. For the first two points (the dummy sample CBMN000, and the UP003S of only 0.5 grams of  $^{235}\text{U}$ ) the false neutron events caused by  $\gamma$ -ray pile-up in the Cd-covered sample dominate the induced fission by epi-thermal source neutrons.



**Figure 12.** Integrals of the distributions shown in Figures 9 and 10 as function of  $^{235}\text{U}$  mass of the sample.

### 3.1. Two-fold neutron coincidences from induced fission

We analysed the timestamps of the neutron detection events in a coincidence gate of 15 ns width, and recorded the two-fold neutron (neutron-neutron) detection events in the eight scintillation detectors. The operation presented in Figures 9, 10 and 11 was repeated for the two-fold neutron detection events. The graphs are presented in Figures 13, 14 and 15.

Unsurprisingly the results for the two-fold coincident neutrons show the same behaviour as the single neutron detection. The coincidences however are less prone to disturbances from  $\gamma$ -ray pile-up in the Cd cover than was the case for single neutron detections.

In Figure 15, the net neutron coincidence rate is dominated by real neutron-neutron coincident events in contrast to Figure 11 in the interval (50 - 80)  $\mu\text{s}$ . The two-fold coincidence rate peaks at roughly 90  $\mu\text{s}$  and is produced by epi-thermal neutron induced fission in  $^{235}\text{U}$ , with some likely false coincidences observed during the times where only thermal source neutrons persist (> 500  $\mu\text{s}$ ).

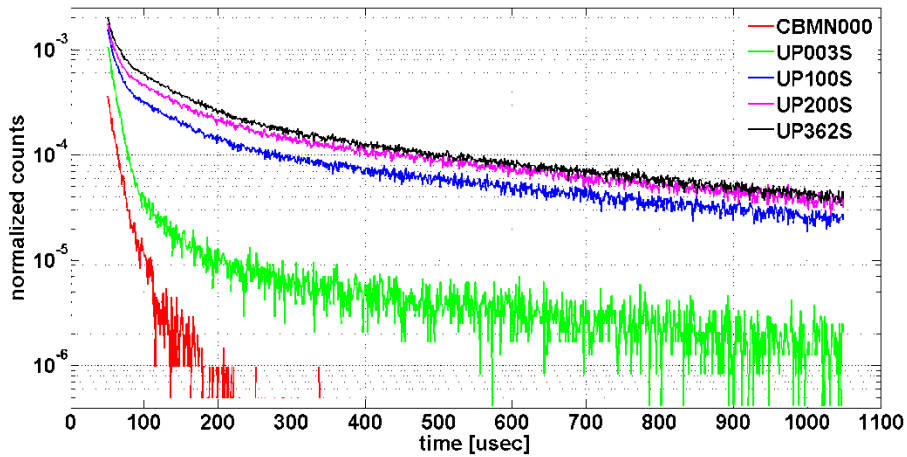


**Figure 13.** Time distribution of the two-fold neutron coincidence count rate for the empty container (CBMN000) and the UP uranium oxide samples.

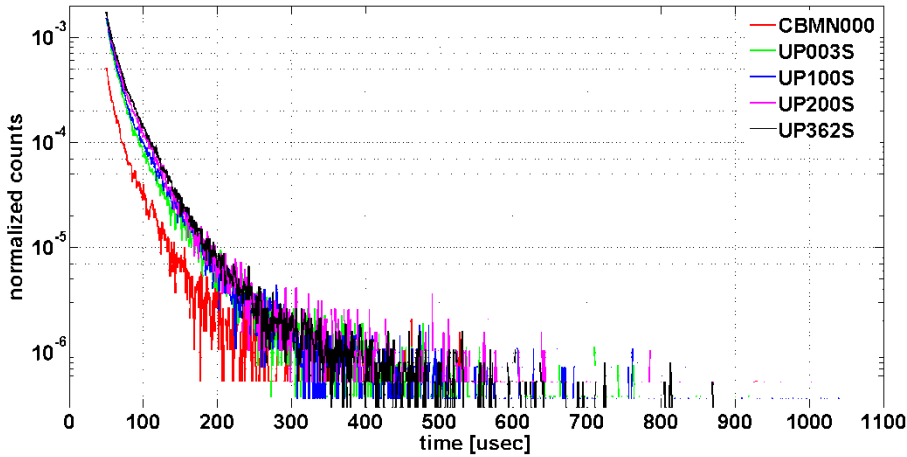


**Figure 14.1** Time distribution of the two-fold neutron coincidence count rate for the empty container (CBMN000) and the UP uranium oxide samples wrapped with 2 mm of Cadmium.

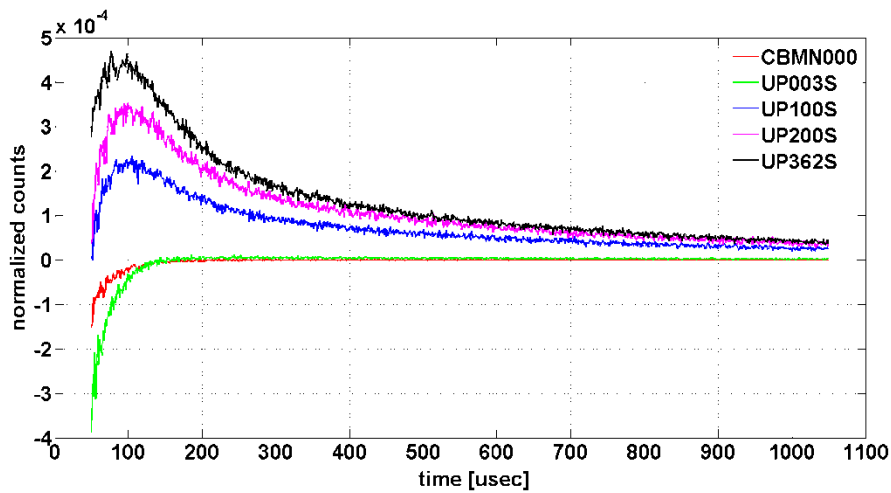


**Figure 15.** Rate difference between the bare sample (Figure 13) and the Cd covered sample (Figure 14).

Figure 16 shows the two-fold neutron coincidences as function of  $^{235}\text{U}$  mass similar to Figure 12 for single neutron count rates. The response, in terms of the neutron-neutron coincidence rate, appears to

be largely proportional to the  $^{235}\text{U}$  mass. Trailing off for higher  $^{235}\text{U}$  masses is expected due to the attenuation of the low-energy neutron flux in these (highly absorbing) samples. Importantly, the coincidence ratio of bare to Cd-covered samples is significantly higher than same ratio for single neutron counting indicating higher sensitivity in coincidence counting compared to single neutron counting although the number of events is significantly lower.

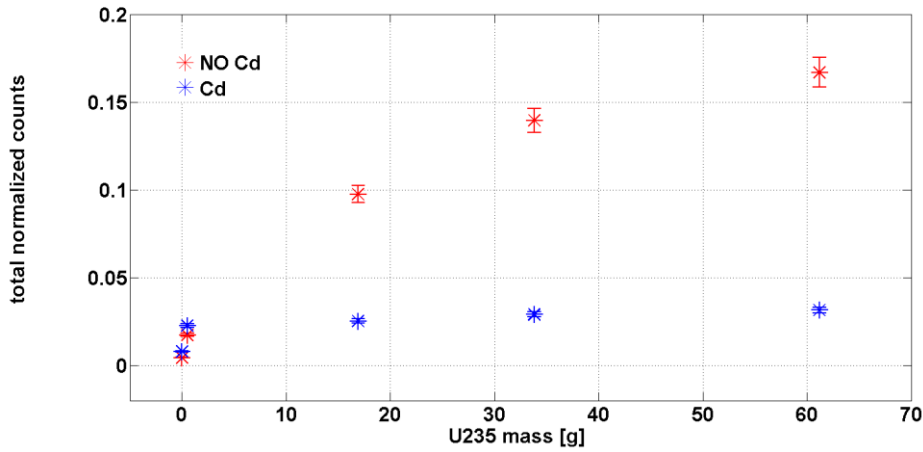


**Figure 16.** Integrals of the two-fold neutron coincidence distributions shown in Figures 13 and 14 as function of  $^{235}\text{U}$  mass of the sample.

### 3.2. Three-fold neutron coincidences from induced fission

The same pattern as for two-fold neutron coincidences is found to be true for three-fold neutron coincidences. The recorded data were analysed for neutron-neutron-neutron events present in the 15 ns coincidence interval. In this case the number of events is as expected significantly lower but the sensitivity to  $^{235}\text{U}$  mass even higher than the two-fold case.

The Figures 17 and 18 are similar to Figures 15 and 16 but for three-fold coincidences.

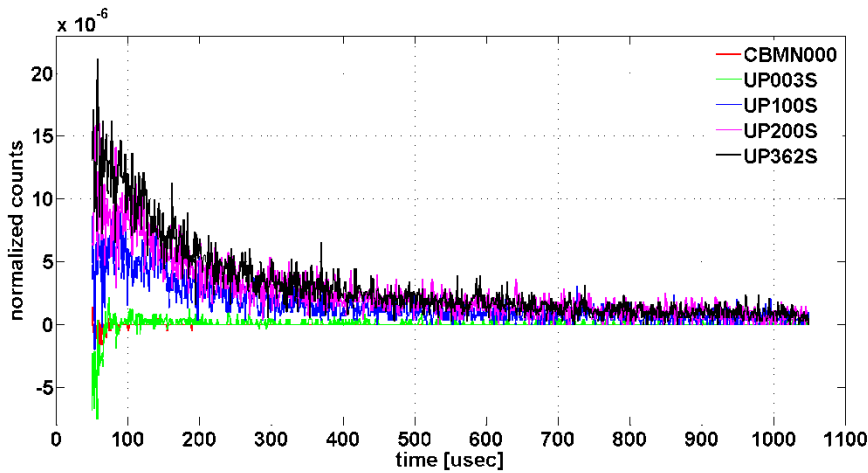


**Figure 17.** Rate difference of three-fold neutron coincidences between the bare sample and the Cd-covered sample.

Although the counting statistics is significantly lower for the three-fold coincidences the influence from false coincidences is further reduced. For the three largest samples in Figure 17 the epi-thermal neutron induced fission neutrons are clearly observed and the rate peaking at still earlier times (towards 50  $\mu\text{s}$ ) due to the absence of the false  $\gamma$ -ray pile-up coincidences in the Cd-covered experiments.

In Figure 18 a similar pattern as in Figure 16 is visible showing significantly lower number events but with still higher sensitivity to  $^{235}\text{U}$  mass. These coincidence events are clearly prompt neutrons caused by epi-thermal neutron induced fission.

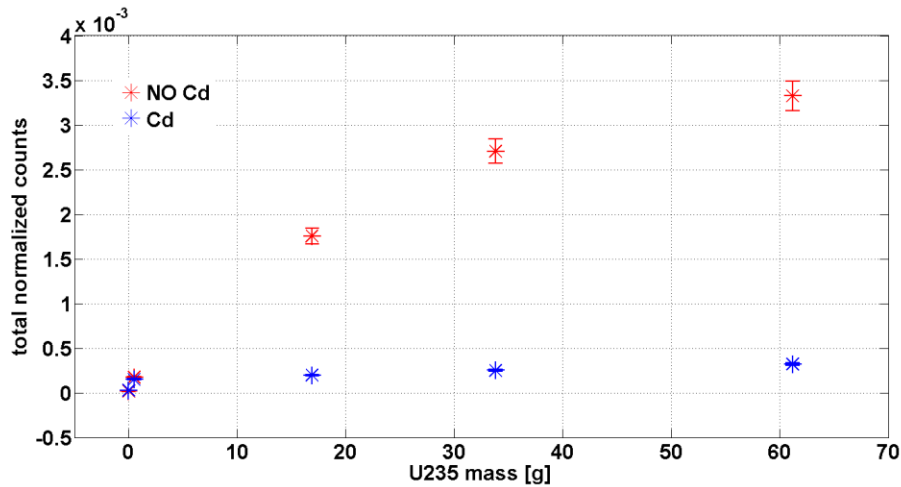


**Figure 18.** Integral number of events of the three-fold neutron coincidences for both bare and Cd-covered distributions (not shown) as function of  $^{235}\text{U}$  mass of the sample.

## 4. Conclusions

In the present work we have studied the detection of fast prompt neutrons in liquid scintillation detectors following fission events in  $^{235}\text{U}$  induced by an external source of epi-thermal and thermal neutrons. The motivation for this work is to verify that we can indeed see fission signatures induced by a neutron source above thermal energy for the purpose of detecting fissile materials in cargo which has been deliberately shielded by a thermal neutron absorber (e.g. cadmium liner).

We used a pulsed neutron generator with a short duty cycle to provide the periodic pulses of 14-MeV sources neutrons. A fast neutron source is less useful because of the difficulty to detect the fast fission neutrons in the (often high) background of source neutrons. By delaying the acquisition system for several tens of microseconds after the pulse so that only epi-thermal and thermal source neutrons persist, fast fission neutrons can be detected in the absence of fast source neutrons. When using liquid scintillation detectors this is particularly advantageous as the epi-thermal and thermal source neutrons do not appear in the neutron part of the detector response, thus providing a useful separation between the interrogating source neutrons from the fission neutrons.

The experiments clearly showed detection of prompt fission neutrons from  $^{235}\text{U}$  during the interrogation by low-energy source neutrons. For the purpose of studying the epi-thermal interrogation alone, experiments were repeated with the samples covered by a cadmium liner. This however introduced an additional problem in form of false neutron signals due to  $\gamma$ -ray pile-up making it difficult at times to interpret the "cadmium difference" results.

The response in form of two and three-fold neutron coincidences showed better sensitivity to fissile mass than single neutron counting. This may be however because of the relatively high neutron detection probability in the present experiments due to the short distance between sample and detectors. In a large-scale SNM detection facility, a lower neutron detection probability should be expected which would yield a significantly lower rate of neutron coincidences.

## 5. References

- [1] Ocherashvili A, Roesgen E, Beck A, Caspi E N, Mosconi M, Crochemore J-M, Pedersen B; *SNM detection by means of thermal neutron interrogation and a liquid scintillation detector*; JINST, 7 CO3037; 2012.
- [2] Ocherashvili A, Mosconi M, Crochemore J-M, Beck A, Roesgen E, V. Mayorov, Pedersen B; *Fast neutron coincidences from induced fission as a method for detection of SNM*; ESARDA Bulletin, Issue No 49, July 2013, p 42-51.

- [3] Ocherashvili A, Mayorov V, Beck A, Heger G, Roesgen E, Crochemore J-M, Mosconi M, Pedersen B; *Detection of fission signatures induced by a low-energy neutron source*, Proceedings ESARDA Symposium, 37<sup>th</sup> Annual meeting, Manchester, May 2015
- [4] Clarke S D, Flaska M, Pozzi S A, Peerani P; *Neutron and gamma-ray cross-correlation measurements of plutonium oxide powder*; Nucl. Instr. Meth. A; 604(3) 2009; p 618-623.
- [5] Pozzi S A, Clarke S D, Flaska M, Peerani P; *Pulse-height distributions of neutron and gamma rays from plutonium-oxide samples*; Nucl. Instr. Meth. A; 608(2); 2009; p 310-315.
- [6] Enqvist A, Flaska M, Dolan J L, Chichester D L, Pozzi S A; *A combined neutron and gamma-ray multiplicity counter based on liquid scintillation detectors*; Nucl. Instr. Meth. A; 652; 2011; p 48-51.

# Poster Session 2

# Evolving Technologies for Future Deep Geological Repositories: A Closer Look

Trinh Le

Stimson Center  
1211 Connecticut Avenue NW, 8<sup>th</sup> Floor,  
Washington DC 20036, USA  
E-mail: tle@stimson.org

## **Abstract:**

*The nuclear fuel cycle in the 21st century has been leaning toward the back-end of the fuel cycle. Recognizing that existing material stockpiles are continuing to grow; this study aims to advance the debate on back-end fuel cycle options to enhance the opportunity for the successful disposal of radioactive waste. Deep geological disposal is widely considered to be the best, safest option for long-term isolation and containment of radioactive waste minimizing the need for future maintenance. Nevertheless, deep geological repositories (DGRs) take decades to plan and many more to construct due to the intricate problem involving technical, legal, societal, economic and political aspects. Using an interdisciplinary approach, we recognize that current advancement in borehole drilling technology used intensively and extensively in the oil and gas industry might have potential application to DGRs. This working paper identifies several promising innovative drilling technologies that might be used in constructing and monitoring DGRs and provides safeguards recommendations for radioactive waste management and permanent disposal at DGRs.*

**Keywords:** safeguards; repository; geological disposal; emerging technology; spent nuclear fuel

## **1. Introduction**

As of 2018, there are 400,000 tonnes of heavy metal (tHM) in spent nuclear fuel existing globally [1]. A handful of states have started the process towards permanent disposal by R&D projects on deep geological disposal for high-level radioactive waste and spent nuclear fuel. Finland became the first country to issue a construction license for a DGR of spent nuclear fuel in 2015. Sweden and France are also moving forward with their DGRs design. During the 1980s, the Waste Isolation Pilot Plant repository was constructed for long-term disposal of defence-generated transuranic waste in the United States. For these DGRs, tunnelling method is used primarily for construction. Using an interdisciplinary approach, we recognize that current advancement in borehole drilling might have potential application to DGRs. Our working paper, therefore, is looking forward to an exploration of other drilling technologies and how they may be used in the future.

Geological repositories (GRs) typically have a depth greater than 1,000 feet (305 m) however their depths can vary based on host environmental characteristics, design and utilization purposes in each country. For examples, the DGR in Olkiluoto, Finland is at 1500 ft. (455 m) in the granite bedrock, Waste Isolation Pilot Plant (WIPP) has been constructed in an ancient salt bed at 2150 ft. (655 m) deep while a DGR in Canada anticipates being at a depth of about 1640 ft. (500 m), depending on rock characteristics at the site [2]. No matter how deep DGRs are, rock excavation and drilling would be primary methods used to construct them. Therefore, in our study of future DGRs, we focus on technical aspects of drilling and its potential implications for safeguards in perpetuity.

For many decades, drilling methods have been used intensively and extensively in the oil and gas industry. Current technology advancement resulted in reduced drilling and completion times, lower average well drilling and completion costs by 25-30% in the 2012-2015 period, and increased well performance [3]. Experiences in the oil and gas industry may have a potential application in designing,

constructing and monitoring the next generation of DGRs, enhancing faster construction time and lower the cost. We will examine some of the innovative technologies and explore how changes in technology side might affect the future geological repositories for spent nuclear fuel in the following sessions.

## **2. Technology Revolution and Implications**

Unconventional petroleum resources such as shale oil and gas, tight sandstone oil and gas, coal-bed methane, natural gas hydrates [4] have been gradually exploited due to exhausted conventional resources and the advance of directional drilling. On the ground, deep drilling can reach reserves at 15,000 ft. (4500 m) deep while ultra-deep drilling can go as far as 25,000 ft. (7500 m). When it comes to drilling under the seabed, it is more challenging. Yet, industry records show that operators can reach reserves in deep water at 1,000 ft. (300 meters) [5] and ultra-deep one at 11,156 feet (3,400 meters) [6]. To exploit ultra-deep petroleum resources, vertical drilling is needed, mainly due to the ability to reduce down-hole accidents. Unconventional petroleum resources, on the other hand, are exploited by mostly non-vertical wells, such as directional well, horizontal well, multilateral well, extended reach well [7]. In terms of geological disposal of spent nuclear fuel (SNF), both vertical and non-vertical boreholes drilling methods can be useful. By studying industrial use cases, we identify relevant technologies and make recommendations for geological disposal.

### **2.1. Vertical drilling for conventional boreholes**

Vertical boreholes are wells aimed at a target directly below its surface location. Vertical drilling is typically less than 20° deviation between the hole and the vertical, so the boreholes are almost straight down. In 1895, the first vertical well was drilled by the percussion drilling method or cable-tool drilling method to a depth of 65 ft. (20 m) at Titusville in the United States. It is still in use, particularly for shallow oil or gas wells in the Appalachian Basin [8],[9]. In this method, a heavy steel bit with a blunt chisel end repeatedly pounds the bottom hole by pulverizing the rock, or any other substances employed as power sources. Afterward, the steam engines take the wells the rest of the way as power sources. After monitoring the water flow, wells advance with casing by using primarily drive caps and switching to drive blocks when encountering large friction. However, the cable-tool drilling is not suitable for soft formations of the southern United States, i.e. sedimentary rocks such as sandstones, limestones, clays in Texas. Hence, a new approach was needed.

During the middle and late 20th century, rotary drilling became the preferred penetration method for improving the operation efficiency of oil and gas wells. In this method, including the power, hoisting [10], rotating, and circulation systems [11], the drilling rig rotates a long length of steel pipe (drill-string) with a sharp bit on the end to cut through even the most challenging and hardest formations. In contrast to the cable drill, the cuttings are lifted from the down-hole by drilling fluid which is continuously circulated down the inside of the drill-string through water nozzles in the bit, and upward into the annular space between the drill string and the borehole. Rotary drilling has demonstrated its efficiency among many technologies applied in the petroleum industry. As an example, after Shell [12] started applying rotary drilling in the Gulf of Mexico in 1907, other oil and gas companies followed suit, such as Standard Oil of California [13] to drill the hard formations of California. For an economic point of view, innovative rotary drilling started the bloom of oil and gas production with annual production exceeding one billion barrels in 1925 and two billion barrels in 1940. By the last decade of the 20th century, there were more than 20 billion barrels per year [14].

### **2.2. Directional drilling of unconventional boreholes**

Directional drilling is the method of drilling a borehole along a projected and controlled, non-vertical route to a favoured target. This method has transformed the oil and gas industry since the 1920s because of its efficiency in unfavourable surface configurations such as buildings, trees, water above, or a steeply inclined rock fault zone [15]. Several models of directional drilling include horizontal, multi-lateral, extended reach, which will be investigated in the next sections. These enable natural gas and oil businesses to work more expeditious, diminish waste, and reach more reserves. Directional drilling also has non-petroleum uses such as a potential application in building DGRs for permanent disposal of spent nuclear fuel. Deep Isolation [16] – a US-based waste company – has proposed to drill horizontal boreholes allowing countries to dispose of nuclear waste more quickly and at a much lower cost than traditional disposal approaches.

Directional drilling coupled with advanced drilling techniques [17] such as mud motors, rotary steerable systems (RSS), measurement-while-drilling (MWD) sensing and logging-while-drilling (LWD) has brought two-fold benefit: 1) overcoming prior disadvantages in slower rate of penetration and higher frequency of checking in the devices, and 2) increasing dramatically natural gas and oil production which helps balance the demand-supply relationship.

### **2.2.1. Mud motors and Rotary Steerable Systems**

Mud motors and RSS are helping directional drilling advance rapidly due to the ease of changing the drill bit's directions. While using mud motors, drilling fluid (or mud) is pumped through, making the drill bit to rotate continuously. This mud pressure pushes the bit into a different angle. On the other hand, RSS is 3D controlled from the surface using advanced communication techniques such as downlink drilling control system [18]. Therefore, RSS tools can either push the bit or point the bit in the required direction in real time. Mud motors, specifically high-performance motors, are more popular than RSS because they can result in daily cost savings of 50% or more, significantly low lost-in-hole cost (\$168,000 versus \$1 million) and be well-suit all bit types and sizes [19]. Yet, RSS can perform faster, deeper, and more precise. Mud motors and RSS offer petroleum operators with more drilling options, depending on target zones, precision, and time constraint. For future geological disposal, directional drilling coupled with RSS and mud motor can help construct DGRs in a faster, more secure, convenient and economical way, as compared with the traditional tunnelling method which is often required by a giant tunnel-boring machine.

### **2.2.2. LWD/MWD**

Logging-while-drilling (LWD) and measure-while-drilling (MWD) are well logging systems [20] used to acquire and collect wellbore information and transmit data to the surface in real time. While MWD is a type of LWD, they are not interchangeable due to their specific functions. LWD helps operators study composition, chemical and physical characteristics of the rocks. On the other hands, MWD records drilling mechanics data such as drillbit position, direction and downhole pressure.

In the construction of a DGR, the use of LWD will give operators up-to-the-minute updates to monitor canisters placement and avoid potential hazards. In the same manner, MWD allows operators to obtain information about the direction and drill steering. Being able to get real-time data of drilling measurements enables drillers to alter the direction of the wellbore for more accurate targeting the drill zone. For current and future DGRs, newest MWD sensors offer higher quality and accuracy data of the boreholes such as trajectory, rock properties, temperature, and pressure. In terms of international safeguards, the International Atomic Energy Agency (IAEA) requires all nuclear facilities to be verified in design, construction, and inventory. Therefore, IAEA inspectors perform Design Information Verification (DIV) activities while they are on-site. These activities include, but not limited to, auditing the facility's design and operation records to verify its information declaration to the Agency; verifying nuclear material balance; performing containment and surveillance techniques. If a future DGR is constructed by directional borehole method, inspectors cannot physically count and weigh waste canisters emplaced underground. Hence, a recent study of design verification of deep boreholes [21] addressed this challenge by evaluating LWD and MWD for a potential application to DIV inspections of DGRs. The study indicated that sharing some of technologies and tools between oil and gas industry and nuclear waste industry might not only leverage use of technologies but also help the Agency maintain Continuity of Knowledge of the entire borehole development process. IAEA-dedicated inspection tools coupled with drilling equipment enables inspectors to a broader spectrum of repository visualization without restrictions from ambient borehole environment (air or fluid).

## **2.3. Horizontal drilling**

Considered as one of the most successful models of directional drilling method, horizontal drilling has demonstrated its application since 1929 when first used in Texas. Since then, it has been rapidly adopted to drill wells in other locations in the United States, China and countries in the former Soviet Union [22]. Based on a U.S. patented concept [23] labelled as US459152 of non-straight line, relatively short-radius drilling, horizontal drilling distinguishes itself from traditional vertical drilling by deviating the wells until they orient horizontally. Once a target oil or gas resource is located, a well is first drilled vertically from the surface then bends its way just above the target along a curve to reach the reservoir

in the horizontal direction. If in case of vertical drilling, operators can only contact a certain amount of oil and gas within a specific hydrocarbon-bearing shale formation of about 200 ft. (61 m) thick on average [24]. However, horizontal drilling now allows these same operators to drill and contact for more than 5,000 ft. (1,500 m) of the formation. Thanks to the advancement and exactness of the technology, drillers today can approach a target with a drill string running 10,000 ft. (3,000 m) vertically, a mile-long horizontally, and is a few inches in diameter. For countries considering DGRs, the horizontal drilling technique can offer an alternative solution to lower footprints of their underground repositories while increasing the amount of disposed spent fuel along the horizontal section.

There are three popular patterns for horizontal drilling called short, medium and long. They can be distinguished using the angle-build rate, turn radius and horizontal extension. Table 1 shows the differences between these patterns.

Pattern name	Short	Medium	Long
Build rate	95–300 (°/100 ft.)	7.2–19.1 (°/100 ft.)	1.2–5.7 (°/100 ft.)
Turn radius	2–60 ft.	300–800 ft.	1000–3000 ft.
Horizontal extension	100–800 ft.	1500–3000 ft.	2000–5000 ft.

**Table 1:** Horizontal pattern classifications [25].

Canister specifications, including thickness, length and material may help determine the most effective drilling pattern. A typical DGR may benefit from the medium and long patterns of horizontal drilling because of the turn radius, horizontal extension, operational style, and cost. Larger turn radius helps avoid canisters from getting jammed; longer horizontal extension allows operators to emplace more spent fuels into the repository; conventional operation reduces man-hours on training and operating special devices; the cost is lower as the equipment and replacement parts are cheaper.

Constructing DGRs using horizontal drilling technique can also reduce the risk of a surface site having environmental sensitive or operational difficulty. It can also reduce the cost when drilling multiple boreholes in different horizontal directions from one location. For the environment, this means less land impact and society disturbance during the construction period.

## 2.4. Multilateral drilling

A multilateral borehole is a single borehole with one or more wellbore branches radiating from the main borehole. It may be as simple as a vertical wellbore with one sidetrack or as complex as a horizontal, extended-reach borehole with multiple lateral and sub-lateral branches. These types of boreholes serve several purposes such as exploration, infill development, or re-entry into an existing wellbore. Depending on the geological conditions of the drill zone, operators will make a decision on multilateral configurations [26]. In general, these boreholes represent two basic types: vertically staggered laterals and horizontally spread laterals, as shown in Figure 1 and 2.

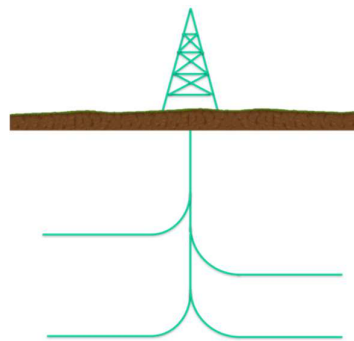


**Figure 1:** Vertically staggered laterals.

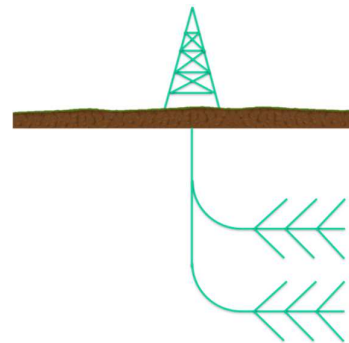


**Figure 2:** Horizontally spread laterals.

For DGRs, multilateral boreholes may yield advantages in storing more waste canisters. However, there is always a certain risk ranging from borehole instability, problems with too-close-distance between branches, stuck pipe and problems with over-pressured zones to the casing, cementing and branching problems [27].

## **2.5. Extended Reach Drilling (ERD)**

In oil and gas industry, this drilling technology allows operators to reach deposits that are great distances away from the drilling rig and tap oil and natural gas deposits under surface areas where a vertical well cannot be drilled, such as underdeveloped or environmentally sensitive areas. To date, the longest measured depth ERD well is the Chayvo Z-42 (Sakhalin Island, Russia) at 41,667 ft. (12.7 km) deep and 38,514 ft. (11.7 km) horizontally oriented [28]. Regarding the extreme distances, ERD requires the motor to be oriented and maintained in a particular direction while drilling to follow the desired path. Current technology advancement in Rotary Steerable System (RSS) allows operators to steer a hole continuously along a horizontal section of the wellbore. This technology is proven to be an asset for all directional drilling models.

## **3. Further Considerations**

### **3.1. Retrievability**

In industrial drilling dictionary, drilling retrieval or 'fishing' is a technique used to remove or retrieve a tool lost down a borehole or detached from the drill string. These obstructions are called 'fish'. Special tools are lowered into the borehole to retrieve specific types of 'fish', in which the fish can be speared, grasped, crushed into smaller piece, or destroyed using explosives. Fishing can be used all the way to 6000 meters (20,000 feet) and probably beyond [29], [30]. Big oil and gas companies such as Schlumberger, Weatherford, Halliburton all sell fishing tools and services, making the technique price-competitive and accessible to customers.

The IAEA considers all spent nuclear fuel as practically retrievable, even after emplacement and enclosure of a DGR [31] and therefore, safeguards remains in perpetuity. On January 2019, Deep Isolation demonstrated the ability to use wireline to successfully emplace and retrieve a prototype waste canister from a horizontal extension of an existing oil and gas borehole in Texas [32]. This is marked as the very first real-life application of oil and gas drilling technologies to nuclear waste disposal.

### **3.2. Long-term Borehole Monitoring**

A deep geological repository (DGR) is expected to take many decades to construct and permanently close due to legal, technical, and social issues. One aspect of a DGR worth considering is how to monitor and control DGR activities thoroughly before and after repository closure. As disposed spent fuel retrievability becomes technically feasible, long-term monitoring is highly recommended as a State moves forward with geological disposal. Examples of monitoring activities include seismic monitoring in case of undeclared excavations; documentation of underground openings in case of undeclared premises such as 3D laser imaging, photographs of the rock surface, geological mapping [33]. These technologies can assist safeguards management by creating a profile of undeclared borehole activities which might hinder proliferation pathways. This profile may be an essential resource as States develop acquisition path analysis to deter and prevent proliferation.

## **4. Acknowledgements**

This research is made possible by the generous financial and logistical support of the John D. and Catherine T. MacArthur Foundation to the Stimson Center's Back-end to the Future project.

## **5. Legal matters**

### **5.1. Privacy regulations and protection of personal data**

"I agree that ESARDA may print my name/contact data/photograph/article in the ESARDA Bulletin/Symposium proceedings or any other ESARDA publications and when necessary for any other purposes connected with ESARDA activities."

## 5.2. Copyright

The authors agree that submission of an article automatically authorises ESARDA to publish the work/article in whole or in part in all ESARDA publications – the bulletin, meeting proceedings, and on the website.

Once the article has been accepted for publication the copyright is reserved, but part of the publication may be reproduced, stored in a retrieval system, or transmitted in any form or by any means, mechanical, photocopy, recording, or otherwise, provided that the source is properly acknowledged.

The authors declare that their work/article is original and not a violation or infringement of any existing copyright.

## 6. References

- [1] IAEA; *Nuclear Technology Review*; GC (62)/INF/2; 2018;
- [2] Noronha J; *Deep Geological Repository Conceptual Design Report, Crystalline/Sedimentary Rock Environment*; APM-REP-00440-0015 R001; Nuclear Waste Management Organization; 2016.
- [3] U.S. Department of Energy, Energy Information Administration; *Trends in U.S. Oil and Natural Gas Upstream Costs*; 2016.
- [4] Zou C; *Unconventional Petroleum Geology 2<sup>nd</sup> ed*; ISBN-9780128122341; Elsevier; 2017; p 49-95.
- [5] OMV Group; *Horizontal Drilling: Lateral Approach to Straight Lines*; 2017.
- [6] Schuler M; *Maersk Drillship Spuds World's Deepest Well*; gCaptain; 2016.
- [7], [8] Ma T, Chen P, Zhao J; *Overview on vertical and directional drilling technologies for the exploration and exploitation of deep petroleum resources*; Volume 2, Issue 4; Geomechanics and Geophysics for Geo-Energy and Geo-Resources; 2016; p 365-395.
- [9] Pees S; *Cable-tool Drilling*; Oil History; 2004.
- [10] Term explanation: The *hoisting equipment* of the rotary system is used to raise and lower the tool in and out of the well or hole.
- [11] Term explanation: The *circulation system* is responsible for cooling and lubricating the drill bit to keep it at its optimal performance.
- [12] *Shell Oil Company* is the United States-based wholly owned subsidiary of Royal Dutch Shell, which is amongst the largest oil companies in the world. The U.S. headquarters are in Houston, Texas.
- [13] *Standard Oil of California* was part of the United States-based Standard Oil Corporation. Standard Oil of California acquired Standard Oil of Kentucky in 1961 and was renamed Chevron Corporation in 1984.
- [14] Caudle B; *Petroleum Production*; Encyclopedia Britannica; 2010.
- [15] In geology, a *fault* is a planar fracture or discontinuity in a volume of rock, across which there has been significant displacement as a result of rock-mass movement.
- [16] Muller R, Finsterle S, Grimsich J, Baltzer R, Muller E, Rector J, Payer J, Apps J; *Disposal of High-Level Nuclear Waste in Deep Horizontal Drillholes*; White paper.

- [17] Kinematicsmfg; *Advanced Drilling Techniques for Directional Drilling*; Blog; 2017.
- [18] Wang D, Finke M; *The New, Downlink Drilling Control System that Changes Conventional Drilling Operations*; AADE-03-NTCE-47; American Association of Drilling Engineers Technical Conference; 2003.
- [19] Drilling Contactor; *Reservoir Drives Choice of RSS vs Mud Motors*; 2012.
- [20] Wikipedia; *Well Logging Definition*.
- [21] Finch R, Smart H, Haddal R; *Design Verification of Deep Boreholes - A Scoping Study*; SAND2017-10586; Sandia National Laboratories Report; 2017.
- [22] Ma T, Chen P, Zhao J; *Overview on vertical and directional drilling technologies for the exploration and exploitation of deep petroleum resources*; Volume 2, Issue 4; Geomechanics and Geophysics for Geo-Energy and Geo-Resources; 2016; p 365-395.
- [23] Campbell J; *Flexible Driving-Shaft or Cable in Dental Engines*; U.S. Patent and Trademark Office; Patent number 459152A; 1891.
- [24] U.S. Department of Energy; *Shale Gas Glossary*; 2013. Penn State University, Marcellus Center for Outreach and Research; *Maps and Graphics – Thickness of Marcellus Shale*.
- [25] Ma T, Chen P, Zhao J; *Overview on vertical and directional drilling technologies for the exploration and exploitation of deep petroleum resources*; Volume 2, Issue 4; Geomechanics and Geophysics for Geo-Energy and Geo-Resources; 2016; p 365-395.
- [26] Term explanation: *Multilateral configurations* include multi-branched wells, forked wells, wells with several laterals branching from one horizontal main wellbore, wells with several laterals branching from one vertical main wellbore, wells with stacked laterals, and wells with dual-opposing laterals.
- [27] Bosworth S, El-Sayed H, Ismail G, Ohmer H, Stracke M, West C, Retnanto A; *Key Issues in Multilateral Technology*; Oilfield Review; Schlumberger; 1998.
- [28] Ma T, Chen P, Zhao J; *Overview on vertical and directional drilling technologies for the exploration and exploitation of deep petroleum resources*; Volume 2, Issue 4; Geomechanics and Geophysics for Geo-Energy and Geo-Resources; 2016; p 26.
- [29] Douglas C; *Fishing Techniques for Drilling Operations*; Cearley Technology; Texas.
- [30] Rigzone; *How Does Fishing Work?*
- [31] IAEA; *Developing multinational radioactive waste repositories: Infrastructural framework and scenarios of cooperation*; IAEA-TECDOC-1413; 2004.
- [32] Deep Isolation; *Technology Demonstration*; 2019.
- [33] Posiva; *Safeguards planning and implementation in the geological repository project*; 2018.

# **Synergy of robotized nondestructive testing methods: a key for safe, secure and reliable operation**

**Dmitry Sednev, Andrey Lider, Irina Bolotina, Daria Koneva**

National Research Tomsk Polytechnic University  
Russia, 634050, Tomsk, Lenina avenue, 30  
E-mail: sednev@tpu.ru

## **Abstract:**

*Last years a rapid grows of robotized equipment could be observed, i.e. manufacturing and quality control machines. It helps a lot in quality improvement, because a human factor could be minimised. Moreover, robust automatic operation allows to apply nondestructive testing (NDT) methods with use of CAD-model of tested object (TO). Thus, synergy could be achieved by means of data fusion (or comprehensive data analysis) of results of two or more NDT methods. Currently, scientists of Tomsk Polytechnic University (TPU) working on the project of combining three different robotized NDT methods: laser optical topography, X-ray tomography and ultrasonic tomography. All of these techniques supposed to be applied to large heavyweight parts. The system prototypes are already developed and currently are in manufacturing process. Since, a significant amount of data about the TO is collected it can be analyzed – the operator could gather a comprehensive information about the TO and make a TO's profile. First of all, it in use for safety reasons – we could precisely find all flaws and imperfections in TO's materials, but profile's information could be used for security check as well as for maintaining nonproliferation regime. TPU team had conduct successful first attempt to use an ultrasonic tomography as method for safety and nonproliferation synergy in 2012 [published in ESARDA Bulletin No 50] in interests of Rosatom. In this particular case, TO was a spent nuclear fuel cask. Increasing numbers of applied NDT methods and data fusion possibilities will allow to increase an accuracy of all procedures as well as broaden a types of TO.*

**Keywords:** *optics; x-ray; ultrasonic; nondestructive testing; synergy*

## **1. Introduction**

Taking into account growing manufacturing demands and industrial design complication the technological processes require constant improvement. One of such advances is considered to be automation of different technological stages. It is evident for different industries such as textile, automotive, chemical and others [1-3]. Most important automation is considered to be for the mechanical and metalworking manufacturing industries, which produce a lot of parts for nuclear application as well. Further to the increasing of the technological process efficiency by reducing number of the manufacturing stages, automation also allows to improve the quality of the final components via implementation of advanced testing techniques [4].

Metalworking manufacturing industry is a part of mechanical engineering complex which plays a crucial role in Russian manufacturing market. It includes fabrication of components for application in various industrial fields, including critical areas such as military industry, mining, nuclear energy, and others. This leads to the increased quality level requirements for the produced components.

At the same time, components with specific structure, such as large dimensions and complex shape, are often used in these critical areas, e.g. pipelines and related equipment of nuclear power plants or casks for spent nuclear fuel. It can not only affect the manufacturing process, but also complicate the following quality assessment performance.

Thus, a new concept of smart manufacturing was introduced for these purposes [5]. It provides a way for an industrial automation by implementation of advanced technological and information technology solutions that allow to optimize the manufacturing procedure.

One of the most important steps to ensure the effectiveness of the proposed automation of the manufacturing, is the initial determination of the factors that could lead to the quality reduction of the final components. For the mechanical manufacturing these components include: low initial quality of the workpiece; inaccurate settings of the final component characteristics; failures in the technological process.

In this paper we discuss manufacturing of the critical components with complex shape. The manufacturing of these products is primarily associated with the use of such metalworking equipment as milling machines. The object of study is made of steel by casting, and further complex geometry is achieved by milling.

## **2. The concept of smart manufacturing process**

When creating an automated system, it is necessary to take into account the existing features of technological processes to enable gradual automation, while developing a new smart manufacturing system starting not from zero but rather performing smooth step-by-step transformation. This approach is considered to be more realistic, rather than development of a new design, in which technological processes are developed entirely anew, and not on the basis of existing industrial facilities.

At that, as mentioned earlier, one of the main aspects is effective quality assessment of the components. Inspections are to be conducted at the final stage of the technological process as well as at the initial and early stages of the process to assess the quality of the workpieces thus enabling the quality monitoring during treatment to eliminate appearance of any possible defects caused by machining processing. Such approach requires structuring the entire process into several modules, while providing the option for interaction among them for further optimization and acceleration, at the same time minimizing human intervention and applying the principles of digitalization.

There are the following modules proposed:

- X-ray testing module;
- Ultrasonic testing module;
- Optical testing module;
- Automated machining module;
- Automated workplace for the operator (AWO).

The existing manufacturing cycle stages with the modules integrated are represented in Figure 1.

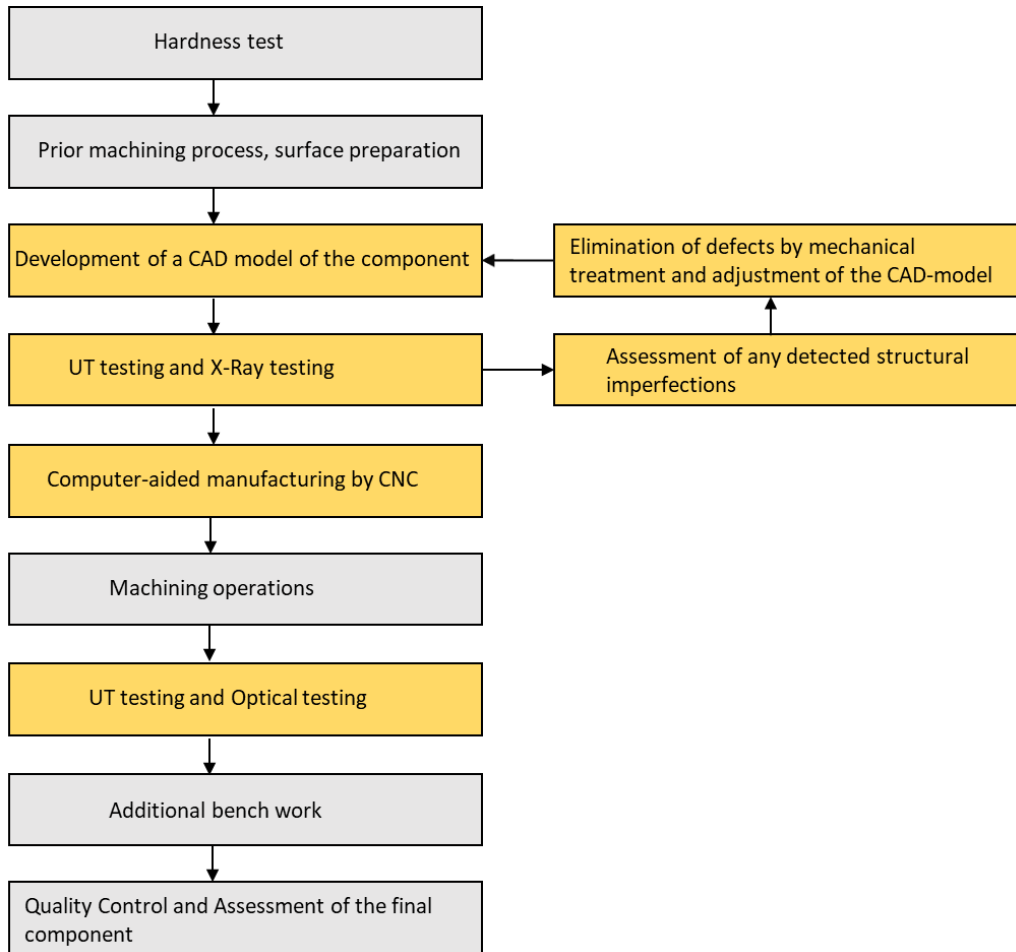


**Figure 1:** Modified manufacturing cycle diagram

Each block of the diagram requires direct human intervention which significantly increases labour costs and consequently the total production costs as well as the probability of defects occurrence. The first step to transition to smart manufacturing is development of an automated workplace for managing all manufacturing stages concurrently.

The X-ray and ultrasonic testing modules are designed to assess the component in terms of the presence of any defects in its internal structure. Moreover, the ultrasonic testing module allows to control the quality of the final component. The implementation of these two modules will enable to determine the size and location of a defect with very high accuracy. Further, this information will enable CNC parameters adjustment to provide better settings of the machining path for the efficient use of the workpiece while avoiding the detected structural defects. General concept of smart manufacturing process is presented on Figure 2.

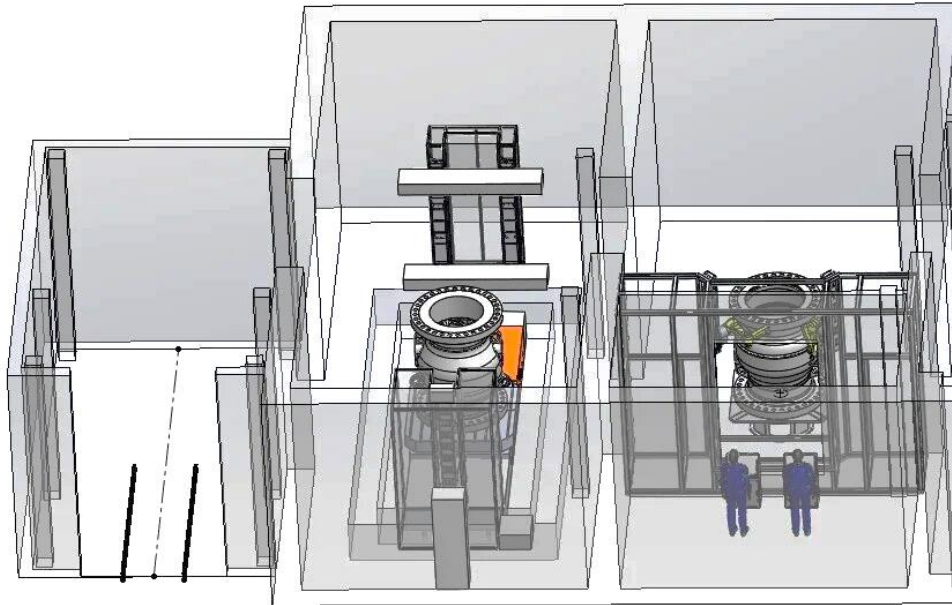


**Figure 2:** General view of quality assurance stage in smart manufacturing process

### 2.1. Automatized X-ray testing module

Industrial enterprises traditionally use film X-ray control methods. At the same time, there is a trend in the introduction of digital X-ray detectors. Digital detectors significantly increase the accuracy and reliability of the testing results. This allows you to optimize and reduce the cost of testing procedure and provide opportunities for solving reverse engineering tasks. The control results are provided in the form of a digital file, which can be used for further integration into a smart manufacturing lines; it also gives the possibility of carrying out qualitative and quantitative analysis, which is extremely important for the subsequent technological stages.

The testing results are compared with a given CAD model of the component for further calibration. This avoids the occurrence of defects in the course of further technological process. Moreover, in case of detection of any defects prior to the start of machining, it becomes possible to create a corrected machining program to avoid defective areas and use this blank in more efficient way.

The use of a betatron accelerator is proposed as a radiation source. This type of powerful X-ray sources is quite common, due to its simple design. Also, special attention should be paid to the choice of the detector for the proposed system. As previously discussed, film detectors are still quite widely used, but digital technologies offer a much wider range of possibilities. Authors propose to use a specialized digital linear detector as a detection device, information collection elements, as well as an image processing module.

For analysis purposes, it is necessary to obtain a data set consisting of a sequence of projections when scanning an object with respect to each angle during a rotation of  $360^\circ$ . In the future, this allows the use of projection data to create a 3D model of the TO. In addition to data on the sample surface, the proposed subsystem provides information about its internal structure in accordance with the density distribution. The most difficult is the development of the algorithm for the reconstruction of the received signals. One of the possible approaches is to use the reverse projection algorithm, often used as a reconstruction algorithm in computed tomography [6]. But the accuracy of the reconstruction is extremely dependent on the scanning method used. Traditionally, parallel scanning is considered the most appropriate way, and therefore certain methods of reconstruction exist for this method [7-8]. At the same time, for a considered TO and taking into account the betatron-type radiation source, the fan-type scan is more efficient. Thus, in order to further carry out the reconstruction of signals, the only approach currently available is to apply methods for transforming received signals to the type of signals obtained by parallel scanning. This leads to a significant increase in reconstruction errors due to the additional signal processing procedure. In this regard, within the framework of the model proposed in this paper, the development of a specialized reconstruction algorithm is proposed, which will allow the use of the initial

data set after the fan scan. The principles of the proposed algorithm are described in detail in [9]. General view of X-ray module is presented on Figure 3.

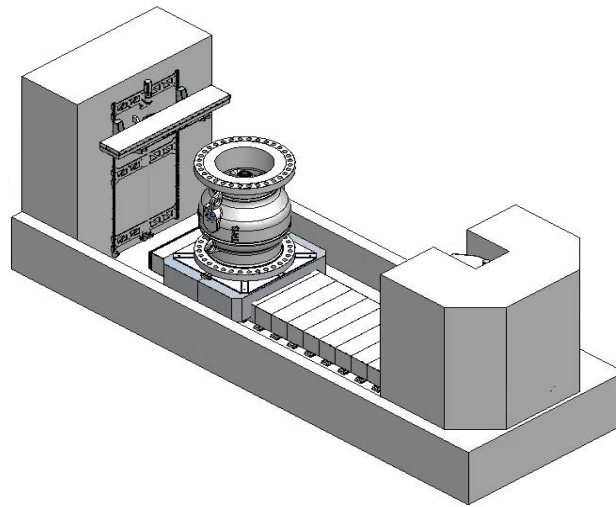


**Figure 3:** Automatized X-ray testing module

## 2.2. Robotized Optical and Ultrasonic testing modules

Deviations in the level of surface roughness can lead to a wide range of defects in the operation of the TO due to the characteristics of specified conditions of environment, such as high temperature, pressure or humidity level. In this regard, compliance with the requirements regarding the quality of a given surface is extremely important.

Currently, two types of methods, contact and non-contact, are used to control surface quality [10-11]. Contact methods involve the use of special tools, for example, when using stylus profilometers; and further surface analysis with a microscope. Due to the error that occurs when placing this instrument on the surface of the sample, the final results may have insufficient accuracy, and the time spent on conducting the inspection increases significantly. Non-contact methods serve as an alternative approach, providing data promptly and accurately. They may be based on the application of various physical principles such as optical scanning or acoustic methods [12], but the acoustic one is difficult to implement and requires large costs. In this connection, in the framework of this work it is proposed to use exactly the optical scan method.

Tacking into account the complex shape of the TO, the task of assessing the geometric parameters becomes rather important. For these purposes, it is proposed to create a three-dimensional model of the TO.

As a scanning technology is considered the use of laser triangulation methods. It is based on the principle of projecting a scanning beam onto the surface of a product and further recording deviations in the path of its propagation using a detector. In general, a detector is a digital camera with a sensitive matrix that can register the distribution of light [13]. Measuring the distance between the camera and the light source makes it possible to estimate the signal values at each point of the beam projection on the surface. As a result, a two-dimensional surface profile relative to the position of the laser can be built. But to assess the quality of the entire surface of a component of a two-dimensional model is not enough. Therefore, the project proposes the use of a robotic manipulator with 6 degrees of freedom, which will allow the measurement of the complex geometric shape of the surface for the entire object.

The laser source is mounted on the surface of the robotic manipulator. This allows the implementation of a sufficient set of data on the entire surface of the product. But in the case of objects with a complex geometry, the scanning process can be carried out along several scanning lines, which requires an accurate calibration of the manipulator's coordinate system and the object's coordinate system. The basic principle of calibration of the optical scanning system is given in more detail in [14]. In the future,

optical data are used to analyze technological deviation by comparing models obtained at the initial and final stages of the technological process, and thus further adjustment of incorrect technological parameters can be applied.

In addition to controlling the quality of the surface, you must also have information about the state of the internal structure of the object. For these purposes, the use of an ultrasonic tomography is proposed. Ultrasonic testing systems used in domestic industrial enterprises are based on the use of traditional equipment, using single-channel transducers, which does not allow obtaining results in the form of three-dimensional models. But given the significant technological progress in this area, using technologies for the reconstruction and visualization of data, innovative methods of ultrasound tomography are becoming more and more realistic for industrial applications [15].

The main feature in the case of control of complex-shaped products is the need to provide access from various scanning angles. The use of a six-axis robotic manipulator is proposed as a solution for this project. This includes the development of specialized software that allows the processing of acoustic signals and their further reconstruction using the technology of synthesized signal focusing (Synthetic aperture focusing technique, SAFT). This approach and the visualization algorithm are considered in [16].

General view of optical and ultrasonic modules is presented on Figure 4.

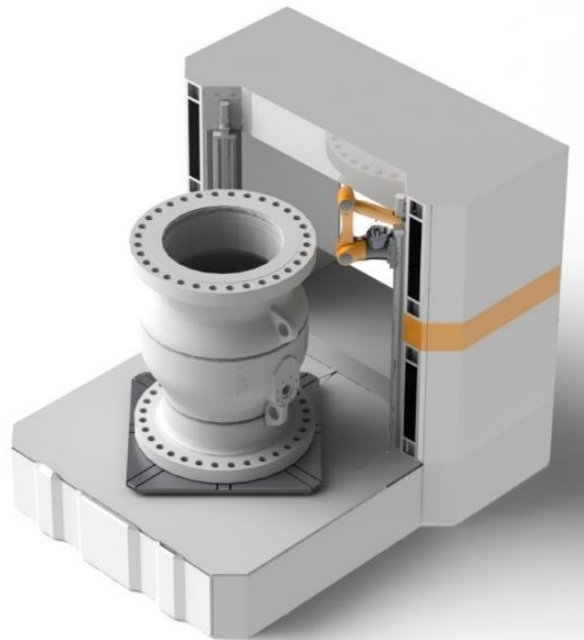


**Figure 4:** Robotized Optical and Ultrasonic testing modules

### **3. Synergetic effect of NDT methods for safety and nuclear nonproliferation**

Each of the considered methods of nondestructive testing allows to obtain data about the TO. At the same time, traditionally, these data are used to evaluate the quality of the structure of the TO and to decide on the possibility of its further safe operation. But at the same time, the authors proved that it is possible in principle to use an ultrasonic nondestructive testing method to obtain information for the nonproliferation of nuclear materials [17]. Within the framework of the development of the concept of using nondestructive testing methods for identifying nuclear power facilities, it is proposed to use the possibilities not only of the ultrasonic control method, but also of X-ray tomography and optical control. Experiments made it possible to obtain high-quality data on both the internal structure through tomography (Figure 5) and on the external surface through optical control (Figure 6).

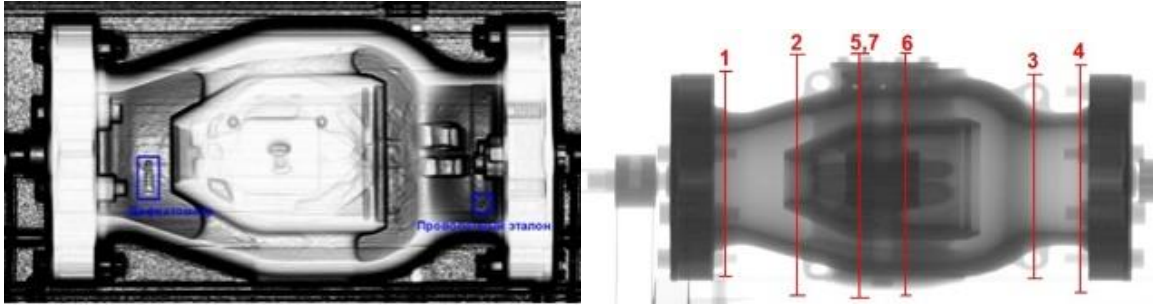


**Figure 5:** Examples of X-ray tomography results

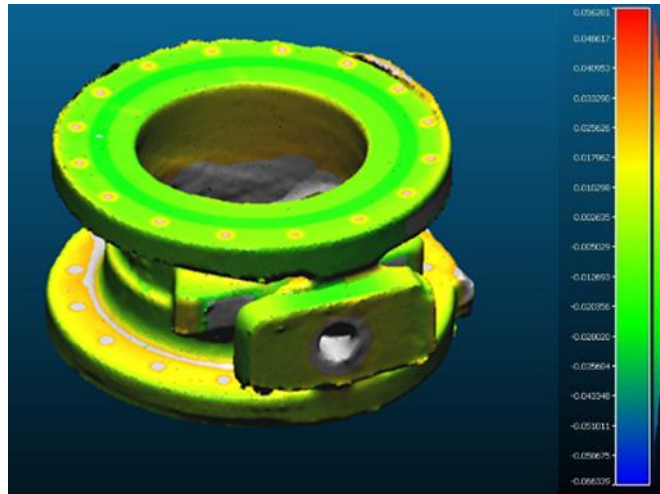


**Figure 6:** Example of optical testing results

In addition to these methods, it is proposed to use the already proven method of ultrasound tomography for the study of welded joints or other critical places of critical objects of nuclear energy (Figure 7).

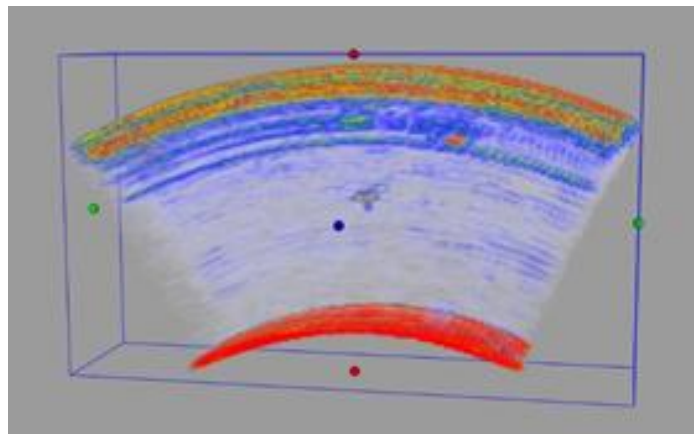


**Figure 7:** Example of ultrasonic tomography results

After receiving the initial data on the structure of the control object when transferring it to operation on the basis of the above methods, a digital passport for identifying the object will be generated, containing data on all features of the TO. These features in the further operation will be subject to regular verification to establish the identity of the object. The TO will be subject to re-inspection at the automated nondestructive testing site during regular maintenance and inventory procedures. Thus, a secondary digital passport of the object will be obtained, then using the mathematical correlation methods already used in [17], the identity of the secondary passport to the original one will be verified. In this case, the identity will be established both for each method separately and integrally for all three methods proposed

for use. Thus, the authors believe that the reliability of the obtained results will be improved and the number of false alarms of the proposed system will be reduced.

#### 4. Conclusion

The proposed decision on the development of a smart manufacturing system describes each individual module, including the features of the nondestructive testing systems using X-ray, optical and ultrasonic testing methods. This significantly optimizes the production process, improves the quality of manufactured products, and also reduces the cost of inspections. In addition, the use of a combination of nondestructive testing methods will allow a multivariate analysis of the TO and identify it in terms of nonproliferation of nuclear materials. The first stage will be the control and comparison of the internal structure by high-energy tomography, the second stage is the external surface being monitored by a robotic optical scanner and the third step allows obtaining data on the welded joint, thus forming a unique digital passport of the identification object based on the internal features of the object. Along with this, the quality control of the facility is carried out, which ensures safe and reliable operation. The next step, the authors consider the application of the data fusion algorithm to form a single digital twin of the identification object based on the three proposed methods, which, in view of the mutual overlapping of data, will reduce the number of artifacts in the results of nondestructive testing. Such an approach will improve both the identification process and the quality control process of an object.

#### 5. Acknowledgements

The study is financially supported by the Ministry of Science and Higher Education of the Russian Federation within the Federal Target Program entitled "R&D in Priority Areas of Development of Russia's Scientific and Technological Complex for 2014-2020" (unique project ID: RFMEFI57817X0251).

#### 6. References

- [1] Tsai W.; *Green production planning and control for the textile industry by using mathematical programming and industry 4.0 techniques*; Energies; Vol. 11(8); 2018; 24 p.
- [2] Peng T., Zhou B.; *Scheduling multiple servers to facilitate just-in-time part-supply in automobile assembly lines*; Assembly Automation; Vol. 38(3); p. 347-360.
- [3] Naghib S., Di Maio F., De Bartolo L. et al.; *Automation and control system for fluid dynamic stability in hollow-fiber membrane bioreactor for cell culture*; Journal of Chemical Technology & Biotechnology; Vol. 93(3); 2018; p. 710-719.
- [4] Schmidt M., Spieth H., Haubach C. et al.; *From manual work to series production—resource optimisation by coupling two CNC processing centres to an automated access pallet warehouse*; 100 Pioneers in Efficient Resource Management (Berlin, Heidelberg Springer Spektrum); 2019; p. 258-261.
- [5] Kang H., Lee J., Choi S. et al.; *Smart manufacturing: Past research, present findings, and future directions*; International Journal of Precision Engineering and Manufacturing-Green Technology; Vol. 3(1); 2016; p. 111-128.
- [6] Simonov E.N., Avramov D.V.; *On the issue of obtaining 3D images in X-ray computed tomography*; Vestn. South Ural State Univ. Ser. Komp. Tekhn. Upr. Radioelektron; Vol. 15(4); 2015; p. 50-57.
- [7] Cloetens P., Barrett R., Baruchel J., Guigay J. P., Schlenker M.; *Phase objects in synchrotron radiation hard x-ray imaging*; Journal of Physics D: Applied Physics; Vol. 29(1); 1996; p. 133.
- [8] Landron C., Maire E., Adrien J., Suhonen H., Cloetens P., Bouaziz O.; *Non-destructive 3-D reconstruction of the martensitic phase in a dual-phase steel using synchrotron holotomography*; Scripta Materialia 66(12); 2012; p. 1077-1080.
- [9] Ozdiev A.K, Kryuchkov Y.Y.; *Implementing a back-projection tomographic reconstruction algorithm using*

*a fan-shaped beam*; Russian Journal of Nondestructive Testing; Vol. 53(5); 2017; p. 387-392.

[10] Aulbach L., Salazar B.F, Lu M., Koch A. W.; *Non-Contact Surface Roughness Measurement by Implementation of a Spatial Light Modulator*; Sensors; Vol.17(3); 2017; p. 596.

[11] Li Z., Brand U., Ahbe T.; *Step height measurement of microscale thermoplastic polymer specimens using contact stylus profilometry*; Precision Engineering Vol. 45; 2016; p. 110-117.

[12] Sukmana D.D., Ikuo I.; *Quantitative Evaluation of Two Kinds of Surface Roughness Parameters Using Air-Coupled Ultrasound*; Japanese Journal of Applied Physics; Vol. 46; Part 1; Number 7B; 2017.

[13] Lu J.R., Huang Y.Q.; *Laser Triangulation Method for Surface Measurement*; Journal-Xiamen University Natural Science; Vol. 43(1); 2004; p. 50-53.

[14] Filippov G., Zhvyrblya V., Sharavina S., Salchak Y.; *Non-contact calibration technique of ultrasound tomography system for complex shaped objects*; MATEC Web of Conferences; Vol. 48; Article Number 03002; 2016.

[15] Bulavinov A., Pinchuk R., Pudovikov S., Reddy K. M., Walte F.; *Industrial Application of Real-Time 3D Imaging by Sampling Phased Array*; European Conference for Non-destructive Testing, Moscow; 2010; 9 p.

[16] Dolmatov D.O., Salchak Y.A., Pinchuk R.; *Frequency-domain imaging algorithm for ultrasonic testing by application of matrix phased arrays*; MATEC Web of Conferences; Vol. 102; Article Number 1015; 2017.

[17] Demyanuk D., Kroening M., Lider A., Chumak D., Sednev D.; *Intrinsic fingerprints inspection for identification of dry fuel storage casks*, ESARDA Bullitin 50; 2013; URL: [https://esarda.jrc.ec.europa.eu/images/Bulletin/Files/B\\_2013\\_50.pdf](https://esarda.jrc.ec.europa.eu/images/Bulletin/Files/B_2013_50.pdf).

## **7. Legal matters**

### **7.1. Privacy regulations and protection of personal data**

The authors agree that ESARDA may print my name/contact data/photograph/article in the ESARDA Bulletin/Symposium proceedings or any other ESARDA publications and when necessary for any other purposes connected with ESARDA activities.

### **7.2. Copyright**

The authors agree that submission of an article automatically authorises ESARDA to publish the work/article in whole or in part in all ESARDA publications – the bulletin, meeting proceedings, and on the website.

The authors declare that their work/article is original and not a violation or infringement of any existing copyright.

# Characterization of the Facility for the Storage of Radioactive Wastes

**Arturs Rozite**

European Commission Joint Research Centre  
Nuclear Safety and Security Directorate  
Nuclear Security Unit  
Via E. Fermi 2749, 21027 Ispra (VA), Italy  
E-mail: arturs.rozite@ec.europa.eu

## **Abstract**

*Modern gamma-ray imaging apparatus have been used for the characterization of the facility for the storage of radioactive wastes. Static measurements using Compton imager and dynamic measurements using a proximity imager having medium-resolution laser scanner used for spatial reconstruction of the imaging scene have been made.*

*In addition, detailed 3D model of the facility has been measured using portable high-resolution laser scanner. The combination of the gamma-ray imaging data and the results of the medium and high-resolution laser scanning form radiological maps. The maps allow seeing the radioactive hot spots and can be useful for the operators of the facility.*

*Another set of measurements at the facility was focused on the estimation of the migration of radionuclides in the tank filled with a radioactive solution before, during and after mixing. Analysis of the results of these measurements presented in the article improves understanding of the capabilities of the modern gamma-ray imagers and provides additional information essential for the improvement of nuclear safety and accountancy aspects of the facility.*

**Keywords:** gamma-ray imaging, Compton imaging, proximity imaging, CZT detector, laser scanning

## **1. Introduction**

In the frame of the EURATOM work program project called INSIDER [1], a measurement campaign on the characterization of the JRC liquid radioactive wastes storage facility using innovative tools that have recently become commercially available has been performed.

For the radiological and physical characterization of the facility, a Compton gamma-ray imager, a proximity gamma-ray imager with a laser scanner and a high-resolution laser scanner were used.

There were several goals of the measurement campaign:

- Study of the capabilities of the modern gamma-ray imagers;
- Perform radiological mapping that provides more complete picture compared to the traditional mapping based on the dose-rate measurements in the limited number of individual points
- Recommend possible improvements related to the personnel safety and radiological materials accountancy at the facility.

Prior characterization of the facility the measurements in the laboratory have been conducted.

The measurements made with a Compton gamma-ray imager, model Polaris-H were primary focused on the determination of its energy range of operation, field of view and angular resolution.

The measurements with a proximity gamma-ray imager, model N-Visage were aimed at understanding of its imaging and scanning capabilities. 2D dose-rate projection on the imaging scene of a gamma-ray source and 3D spatial scan of the lab have been obtained.

The measurement campaign at the facility was performed in 2018 and was divided into two stages: the first stage devoted to the physical and radiological mapping of the facility and the second stage devoted to the measurement of migration of radionuclides in the tank filled with liquid wastes during and after mixing.

## 2. Equipment

### 2.1. Gamma-ray imagers

The technical characteristics of the gamma-ray imagers are summarized in Table 1.

Table 1 – Technical characteristics of the gamma-ray imagers

#	Parameter	Polaris-H	N-Visage Recon
1.	Photograph		
2.	Principle of operation	Compton imager	Proximity imager
3.	Type of radiation detector	3D position sensitive CZT detector	CZT detector
4.	Detector sensitive volume	19 cm <sup>3</sup>	0.5 cm <sup>3</sup>
5.	Imaging energy range	240 keV – 3 MeV	20 keV – 3 MeV
6.	Energy resolution at 662 keV	Better than 1.1%	Better than 2.2%
7.	Imaging field of view	4π	4π
8.	Optical field of view	162° horizontal, 122° vertical	4π – 3D laser scanning
9.	Mode of operation	Static real time imaging	Dynamic real time imaging and spatial scanning
10.	Dimensions	24 cm x 9.5 cm x 18 cm	23 cm x 14 cm x 34 cm
11.	Weight	3.5 kg	3 kg
12.	User interface	Tablet with a touchscreen	Built-in pocket PC with a touchscreen

#### 2.1.1 Compton imager – Polaris-H

Polaris-H is a Compton imager based on a 3D position sensitive CZT detector having large sensitive volume of 19 cm<sup>3</sup> [2].

The Compton imaging is in principle possible when at least two scattering or one scattering followed by an absorption events occur in the detector. This along with the physical properties of the detector material (its mass number and density) defines bottom imaging energy threshold. The imaging energy threshold indicated by the manufacturer is 240-keV. Therefore, for example, events that correspond to the 185-keV peak of uranium or 208-keV peak of plutonium can't be imaged, but events that belong to the 662-keV peak of Cs-137 or 1174-keV and 1133-keV peaks of Co-60 can be.

We made several experiment in the lab with plutonium standards and industrial sources for better understanding of the imaging capabilities of the Polaris-H.

#### 2.1.2. Proximity imager – N-Visage Recon

N-Visage Recon is a proximity imager with an integrated laser scanner [3]. As a proximity imager, the system is designed to be used in a dynamic mode. Whilst walking an operator is measuring gamma-count rate (dose-rate) using radiation detector and physical position in space using laser scanner. The data – intensity of the radiation signal vs. detector position are plotted in the real time forming fused radiation and spatial map that is available to the operator via integrated processor with a touchscreen. The instrument contains CZT detector having sensitive volume of 0.5 cm<sup>3</sup>.

We have used the device for 2D mapping of the radioactive hot spots walking around the facility, around tanks filled with the liquid radioactive wastes and for a 3D imaging of the whole facility.

## 2.2. Technical characteristics of the 3D laser scanning system

A high-resolution laser scanner, model 3DLR for the measurement of detailed 3D model of the facility has been used [4]. The imaging results obtained with a Compton imager will be integrated into this model. Technical characteristics of the 3D laser scanner are shown in Table 2 below. The results will be available to the operator using the JRC software. The operator will be able to “walk” through the facility offline, see positions of the imager at which the measurements took place and access the imaging results (spectrum and gamma-ray images) selecting a corresponding bullet on the 3D map.

Table 2 – Technical characteristics of 3D laser scanner

#	Parameter	3DLR
1.	Photograph	
2.	Principle of operation	Laser scanner
3.	Type of sensor	Laser range finder
4.	Field of view	$4\pi$
5.	Time of scan	10 minute / 15 frames per second
6.	Number of scans made at the facility	5
7.	Spatial resolution	+/- 2 cm
8.	Mode of operation	Static real time scanning
9.	Dimensions	35 cm x 30 cm x 30 cm
10.	Weight	10 kg (without tripod)
11.	User interface	Tablet
12.	Post processing software	DIV tool

## 3. Measurements in the laboratory

In the laboratory, measurements with both imagers were made.

### 3.1. N-Visage Recon

A simple test with a point Cs-137 source located in the middle of the room has been made. The operator was walking in the room with the imager measuring radiation and laser signals simultaneously. The results of this dynamic measurement are shown in the Figure 1. 2D Imaging and scanning results are available to the operator in live mode. Resulting 3D spatial cloud (in white) and 2D projection of gamma-ray signal (in color) shown in the Figure 1 are obtained after reconstruction of the scan using open source software Cloud Compare.

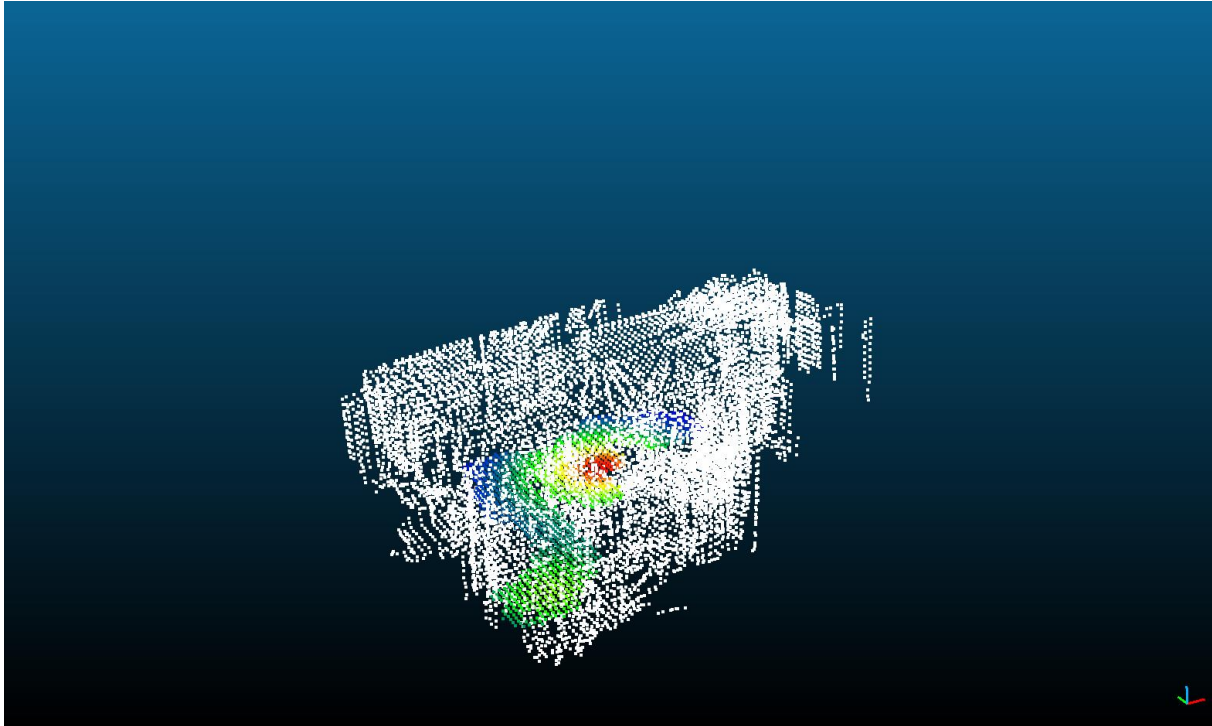


Figure 1 – Imaging results, N-Visage Recon, point gamma-ray source in the middle of the room.

### 3.2. Polaris-H

Tests in the laboratory were aimed at the understanding of imaging and spectroscopic capabilities of the Polaris-H. The following tests were made:

- a) Measurement with industrial radionuclides Ba-133, Cs-137 and Co-60 separated by 75 cm
- b) CBNM Pu70 and CBNM Pu61 standards separated by 150 cm
- c) A set of measurements with Co-60 sources of different activities:
  - Co-60 + Co-60 separated by 150 cm
  - Co-60 + Co-60 (shielded by 5 mm of lead), separated by 150 cm
  - Co-60 + Co-60 (shielded by 12 mm of steel), separated by 150 cm

All measurements were made at the distance of 150 cm between the imager and a virtual line that goes through the positions of all sources. The sources were put symmetrically along this line with reference to the imager.

### 3.1. Industrial radionuclides

A 15 minutes measurement with the following sources was made:

- Ba-133 point source with activity of 400 kBq,
- Cs-137 point source with activity of 700 kBq
- Co-60 point source with activity of 370 kBq

The sources were imaged based on the events that correspond to the full-energy absorption peaks. As it can be seen in the Figure 2, the instrument was able to image all radionuclides. Positions of all sources were correctly determined. Selecting corresponding full-energy peaks an operator can see an imaging result only for the radionuclides of interest.

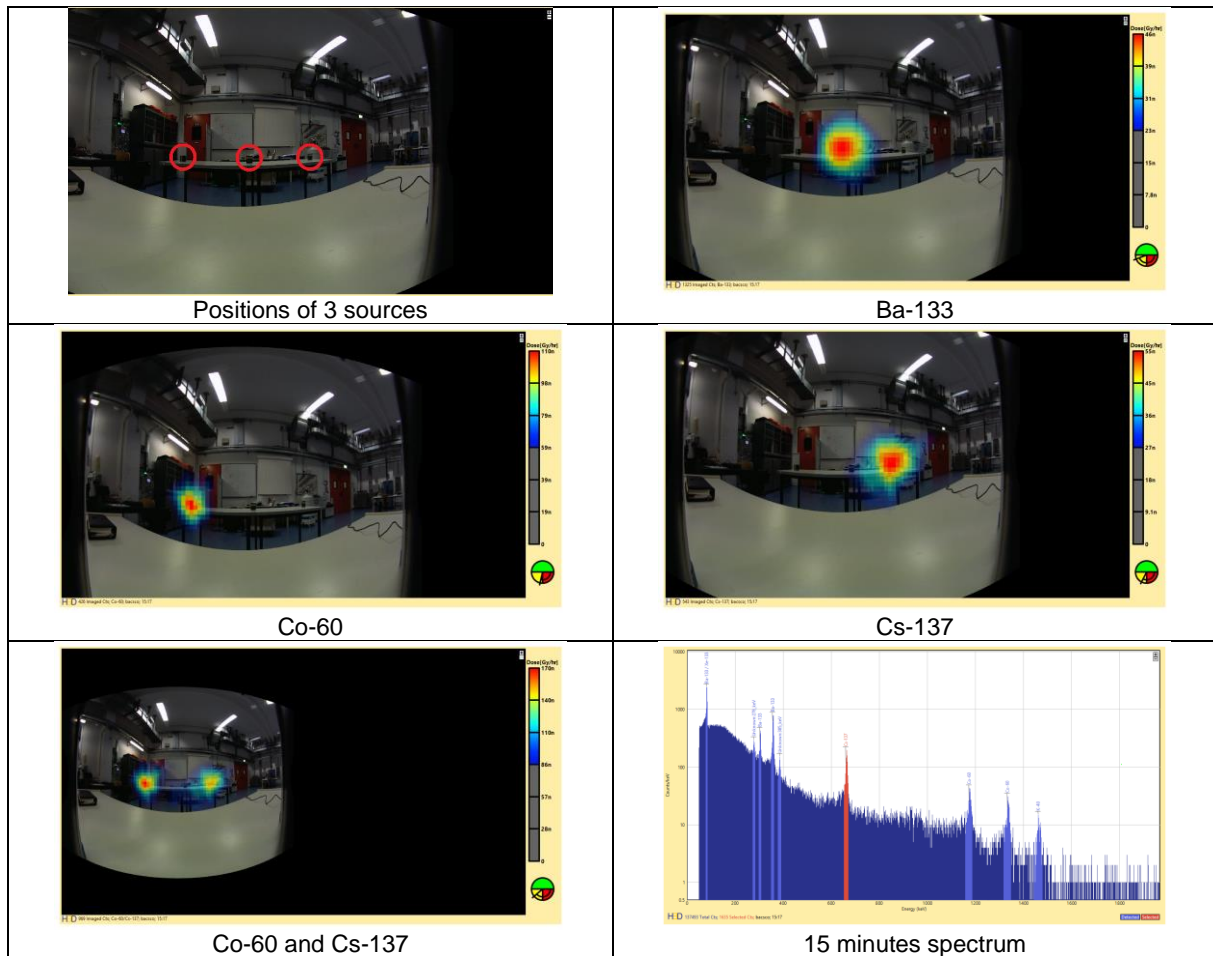


Figure 2 – Polaris-H, imaging results for different radionuclides

### 3.2. Plutonium standards

A 30 minutes measurement was made using CBNM Pu61 and CBNM Pu70 standards having Pu mass of 5.8 g each and Pu-239 content of 61 and 70%. The distance between the sources was 150 cm. Plutonium was imaged using events that correspond to the 336-keV, 375-keV and 415-keV spectral lines. These energies are above the imaging energy threshold. As it can be seen in Figure 3, the angular resolution of the imager allows separate the sources in space.

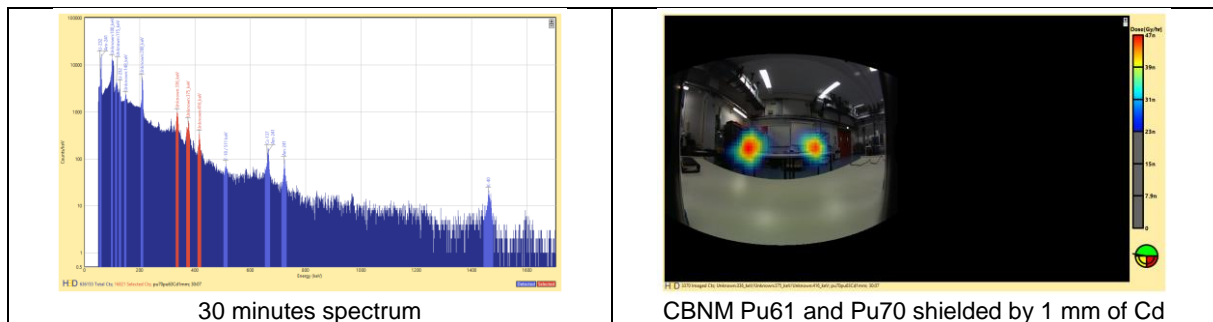


Figure 3 – Polaris-H, imaging of similar radionuclides

### 3.3. Co-60 sources with the shield

Three measurement were made with two point Co-60 sources. The results are shown in Figure 4. The imaging was made using interaction events in the detector that correspond to the full-energy absorption peaks. The first source had an activity of 370 kBq (the left one on the pictures) and the second source had an activity of 700 kBq (the right one on the pictures).

In the first measurement, the sources were unshielded and the gamma-ray image of the right source is much more prominent. The dose-rate at the imager position is 310 nGy/h.

In the second measurement the right source was shielded by 5 mm of lead, the dose-rate at the imager position dropped to 280 nGy/h and the left source became “visible” on the image.

In the third measurement the right source was shielded by 12 mm of steel, the dose-rate at the imager position raised to 290 nGy/h and the left source became more prominent on the image compared to the right one.

These examples illustrate the effects of the photons scattering and absorption on the imaging results.

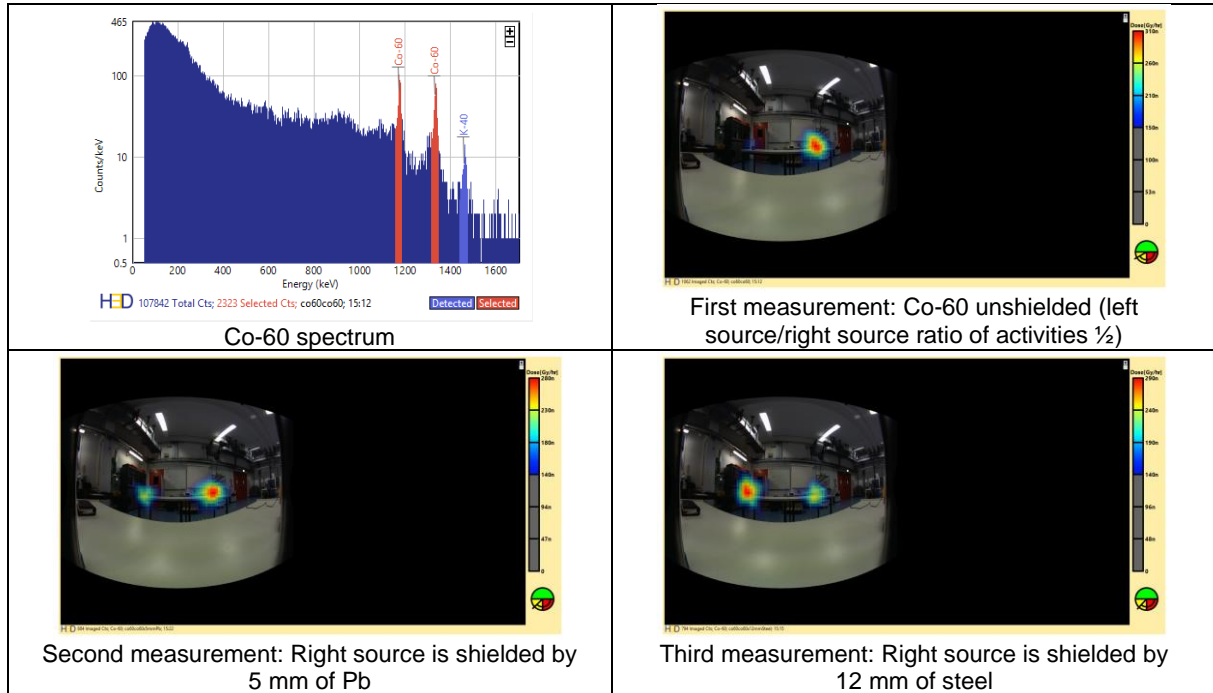


Figure 4 – Polaris-H, imaging of Co-60 radionuclides at different shielding conditions

## 4. Characterization of the facility

### 4.1. Radiological mapping of the facility

The facility for the storage of low-level radioactive wastes (Figure 5) contains three tanks (VA001, VA002 and VB-01) for the storage of liquid wastes. Two tanks of large volume (VA001 and VA002) are installed at a small angle (of 1 degree) in order to direct the radionuclides (by gravity) at one end of the tank. This end is shielded by 5 cm thick lead wall. The large tanks contain two mixers installed from the top at both ends of each tank for the mixing of radioactive solution.



Figure 5 – panoramic view of the facility

Initially a dose-rate mapping of the facility was made. The dose-rates were measured using ionization chamber survey meter Fluke 451P. The dose rates indicated in the Figure 6 in  $\mu\text{Sv/h}$  are in brackets. At position B4 two measurements (at the top (0.29  $\mu\text{Sv/h}$ ) and under the tank (21  $\mu\text{Sv/h}$ ) were done.

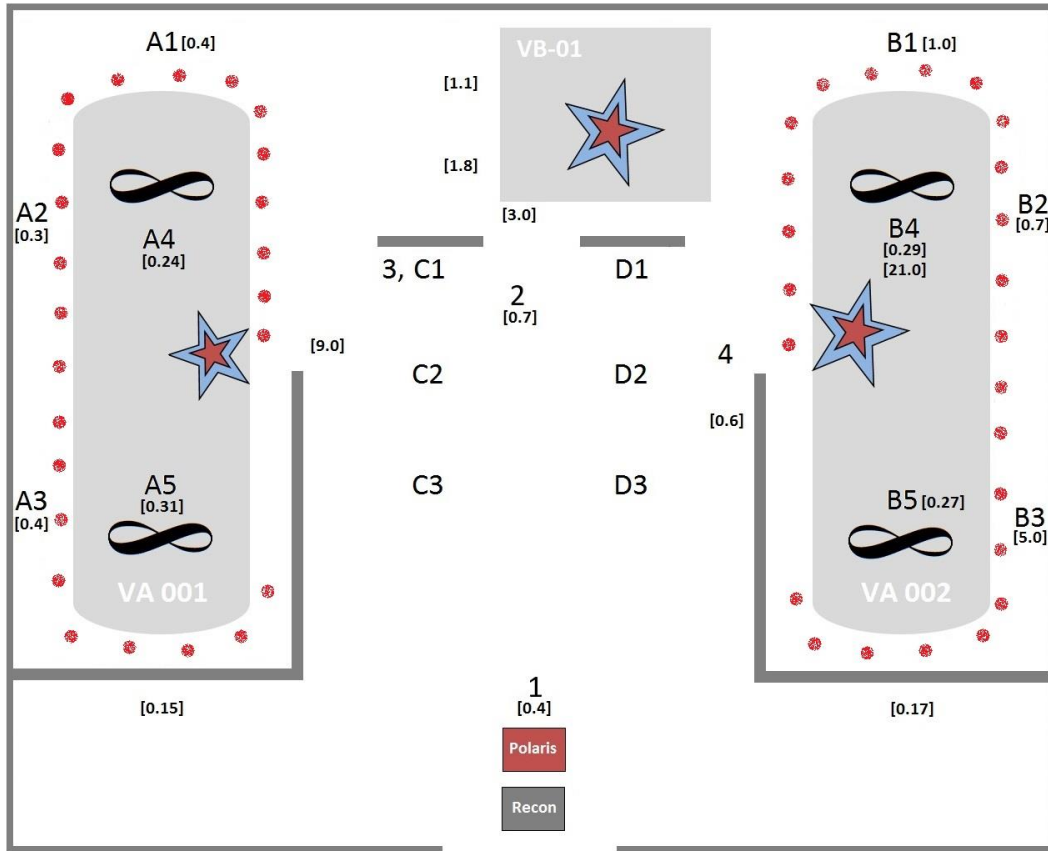


Figure 6 – Schematic map of the facility

## 4.2. Radiological imaging of the facility

For the imaging (radiological mapping) of the facility a set of static measurements with the Polaris-H and a number of dynamic measurements with the N-Visage Recon were made.

### 4.2.1. Polaris-H

All gamma-ray images were constructed based on the processing of the events that correspond to the 662-keV peak of Cs-137, which is the dominant radionuclide in all spectra (Figure 7).

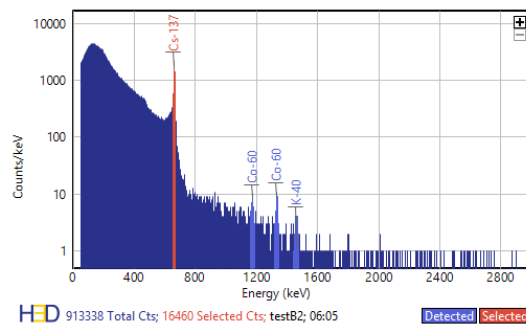


Figure 7 – typical spectrum measured with the Polaris-H at the facility

Two hours measurement with a coaxial high-purity germanium detector of a high-resolution spectrum at the position 4 in front of the hot spot of VA002 tank indicates presence of the Eu-154 in the tank in addition to Cs-137 and Co-60 radionuclides (Figure 8). Other tanks contain the same radionuclides.

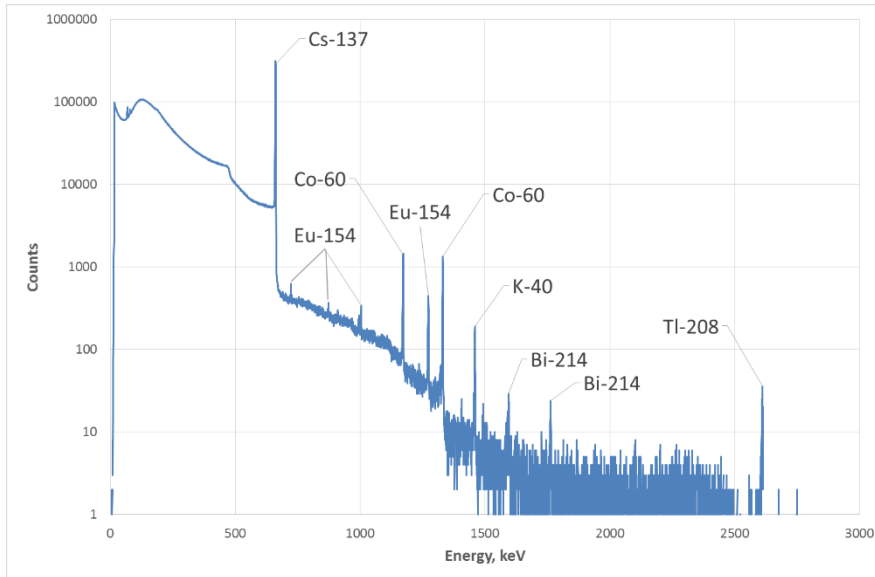


Figure 8 – spectrum measured with a HPGe detector at position 4

**4.2.1.1. Measurements at positions 1 to 4 across the facility**

From the measurement in positions 1, 3 and 4 (Figures 5 and 9), it can be concluded that there are three major hot spots at the facility. The hotspots correspond to the tank VB-01 (pos. 1), a middle of the tank VA001 (pos. 3) and a middle of the tank VA002 (pos. 4).

From the measurement in position 2 it can be concluded that the radioactivity in the tank VA002 is higher than in the tank VA001 because the hot spot is localised at the back of the imager and moreover the imager stays much closer to the VA001 tank than to the VA002 tank.

The black part of the main imaging screen corresponds to the scene behind the imager (with reference to the field of view of an optical camera).

It should be noted that the Compton imager is intrinsically a  $4\pi$  imager; however, the imaging efficiency from the back and from the front of the imager is not the same. It depends on the arrangement of electronics and batteries inside the device and is higher from the front.

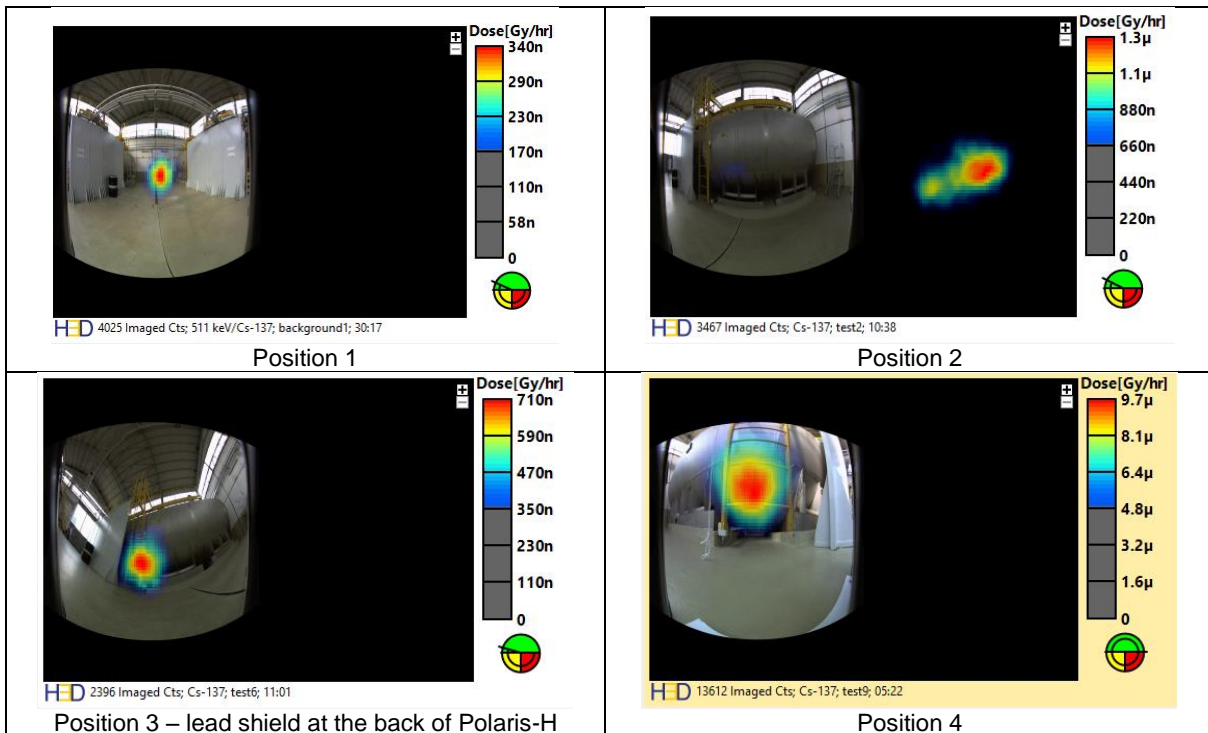


Figure 9 – Polaris-H imaging results at the facility

#### 4.2.1.2. Measurements at positions A and B around the VA tanks

From the comparison of the results of measurements (Figure 10) made around the tanks VA001 and VA002 it is evident that the radioactivity in the tank VA002 is higher. For example, the dose-rates for the measurements in positions A3 and B3 made from the side of the tanks is more than 20 times higher for the VA002 tank. For the measurements A4 and B4 made at the top of the tanks the difference is just 4 times, this can be explained by the self-shielding effect of gamma-rays in the water since as it can be seen from the gamm-ray images the radionuclides are basically localized at the bottom of the tanks. Almost the same dose-rates at positions A5 and B5 is difficult to explain.

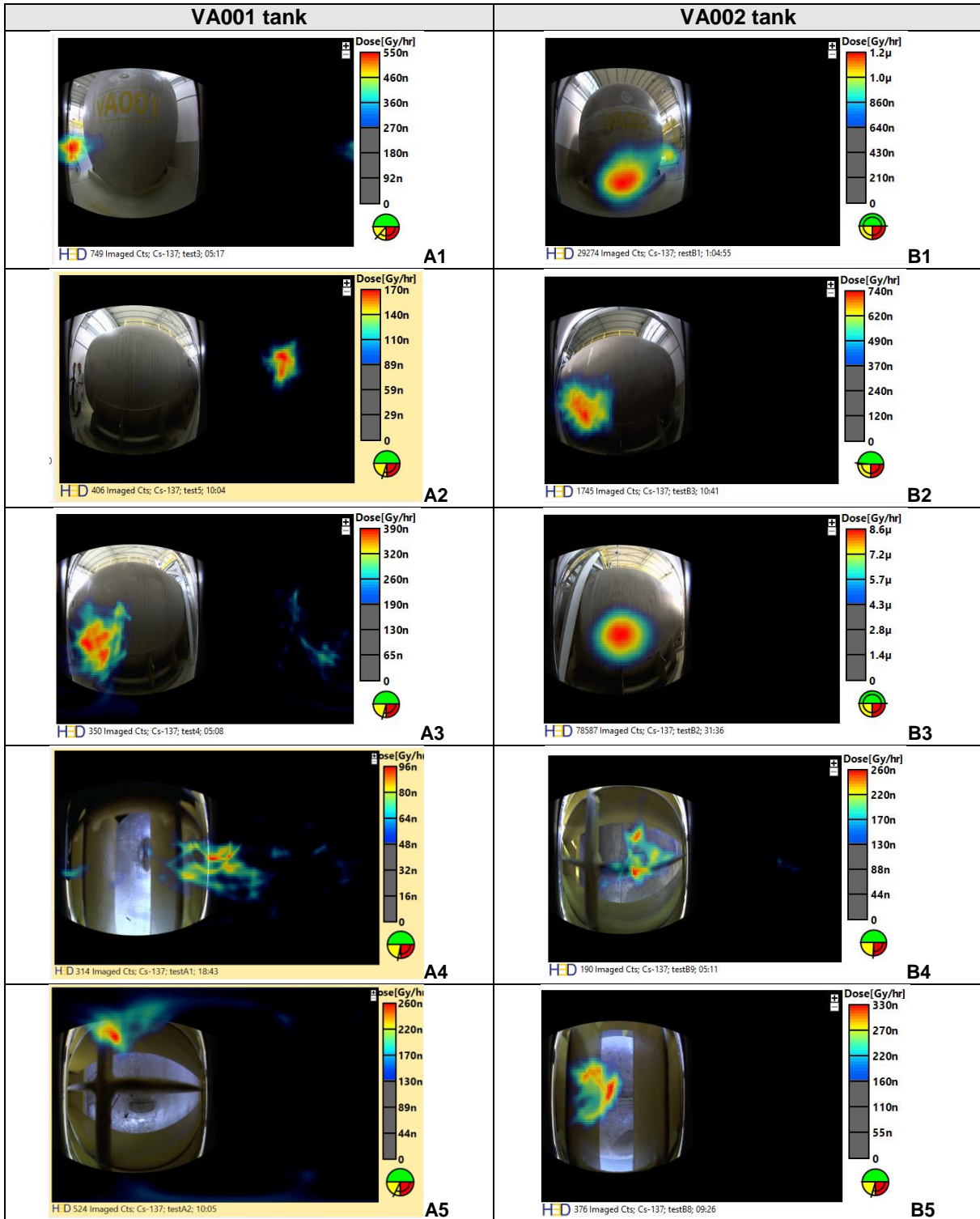


Figure 10 – Comparison of the results of measurements made around the VA tanks

### 4.2.1.3. Measurements at positions C and D

From the comparison of the results of measurements at positions C and D (Figure 11), it is clear that the radiation field coming from the unshielded part of the tank VA002 is approximately 2 times higher than the radiation field coming from the unshielded part of the tank VA001. The measurement were made shielding the side of the imager facing the tank VB-01 by lead bricks (as indicated in Figure 6 by grey right angles). A second measurement in the position D3 (D3.2) was made with the lead bricks shielding the imager also from the radiation coming from the unshielded part of the VA002 tank. This measurement indicates that the hot spot initially localized at the middle of the tank in fact is spread towards the end of the tank.

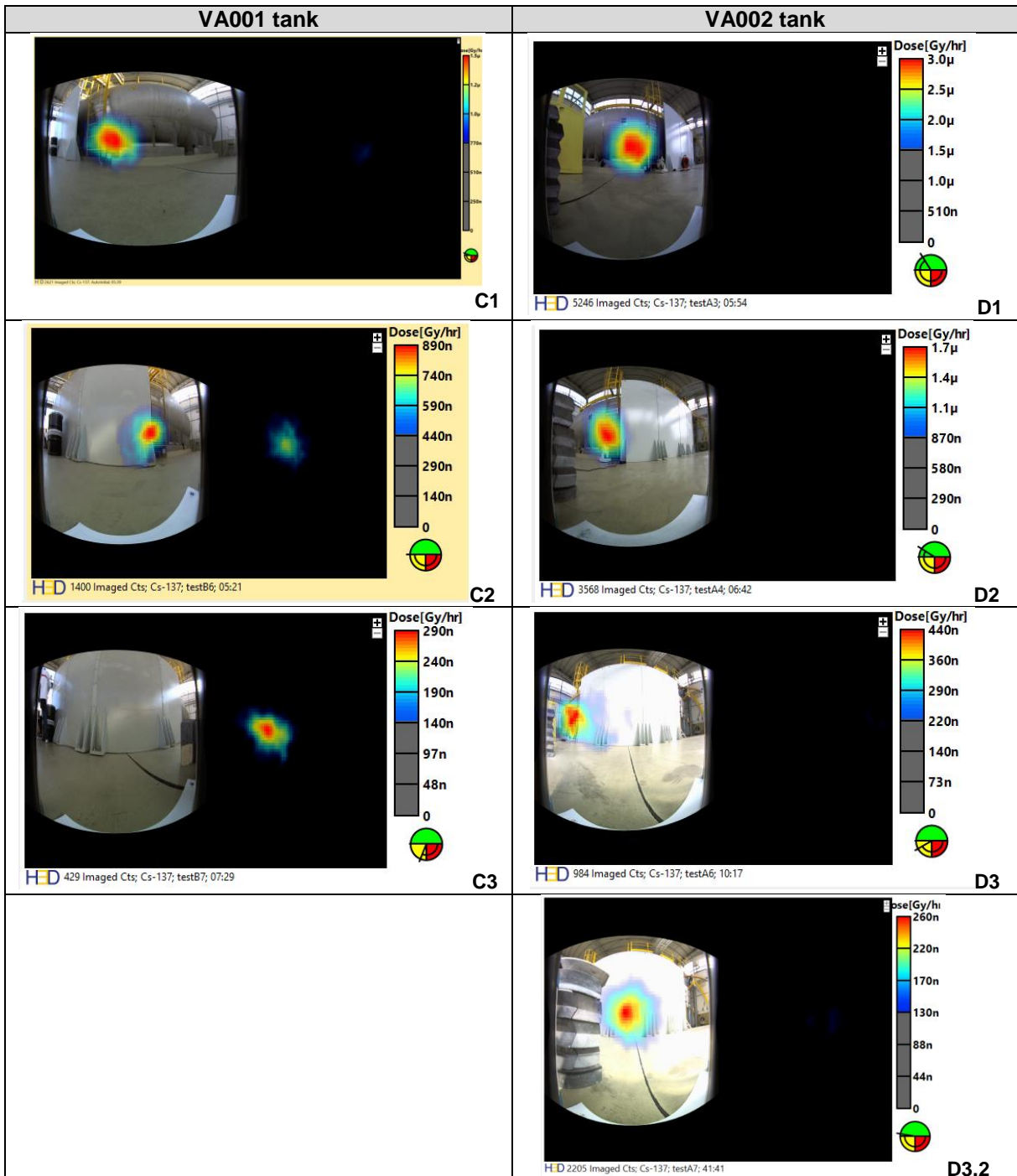


Figure 11 – Polaris-H, results of measurements at the position C and D

#### 4.2.2. N-Visage Recon

Dynamic measurements including scans of the facility and scans of the individual VA tanks have been made. The instrument was able to measure a physical 3D scenes and radiological 2D projections on these scenes.

##### 4.2.2.1. Scanning of the facility

The results of two scans of the facility are shown in the Figures 12 and 13. Physical 3D reconstruction of the facility is shown by the white cloud and radiological 2D projection is shown in the RGB color scheme. The duration of single scan was about 5 minutes.

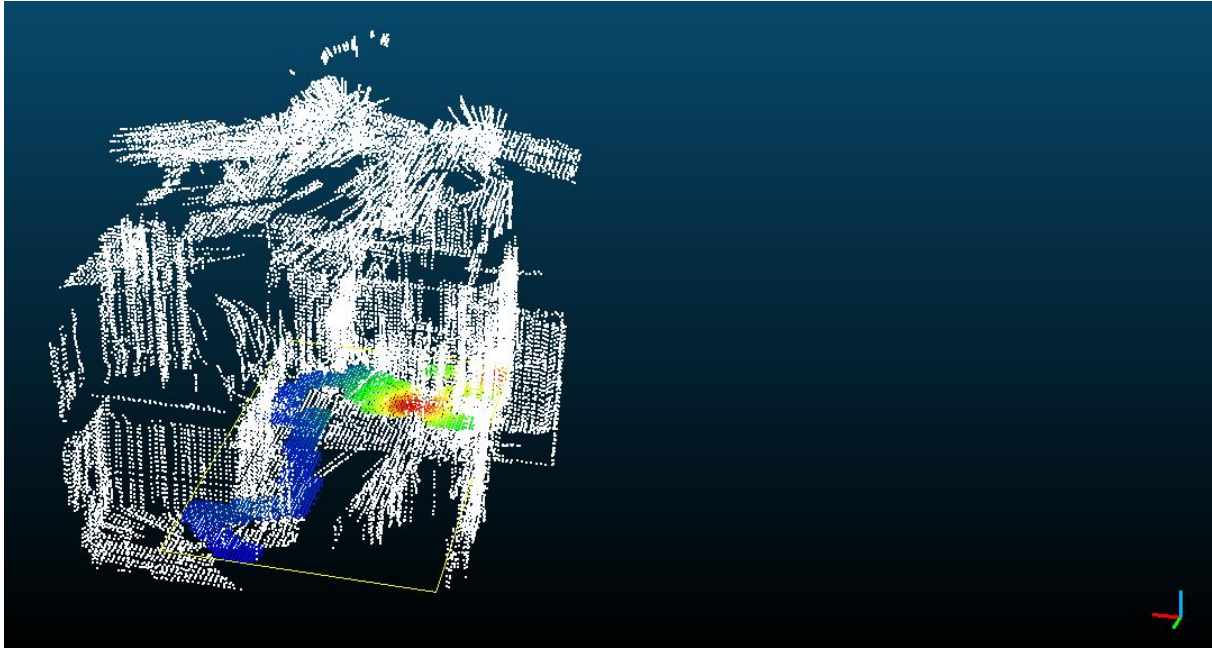


Figure 12 – N-Visage Recon, cloud computing of the first scan of the facility

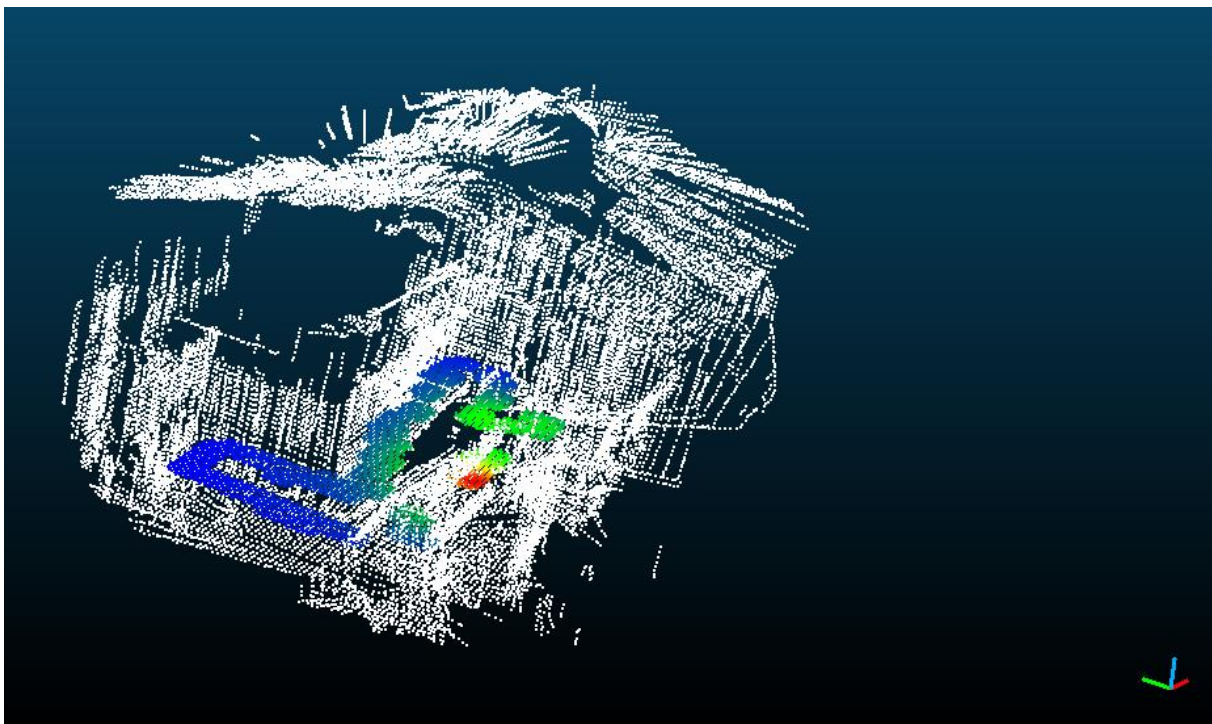


Figure 13 – N-Visage Recon, cloud computing of the second scan of the facility

#### 4.2.2.2 Scanning of the tanks

Scans of the VA001 and VA002 tanks were made walking the imager around the tanks following paths indicated by the red colour in Figure 6. The distance to the floor was approximately 1 m. The results of scanning are shown in Figures 14 and 15 below. The duration of a single scan was about 2 minutes.

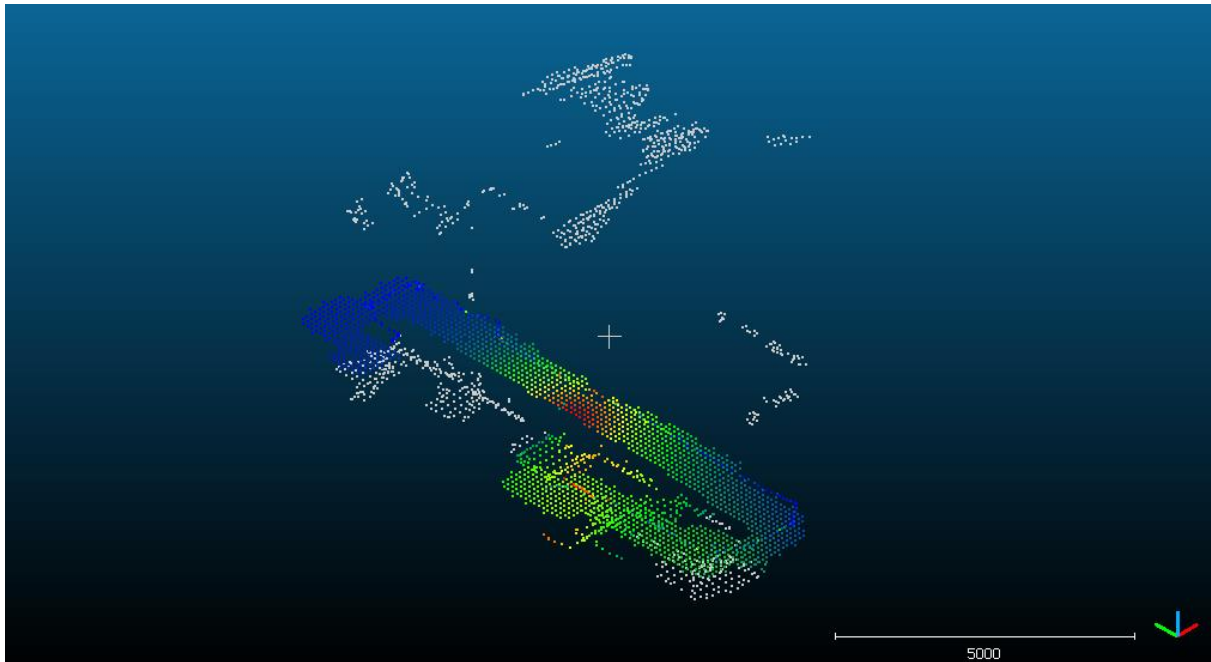


Figure 14 – Cloud computing of dose rates on tank VA001

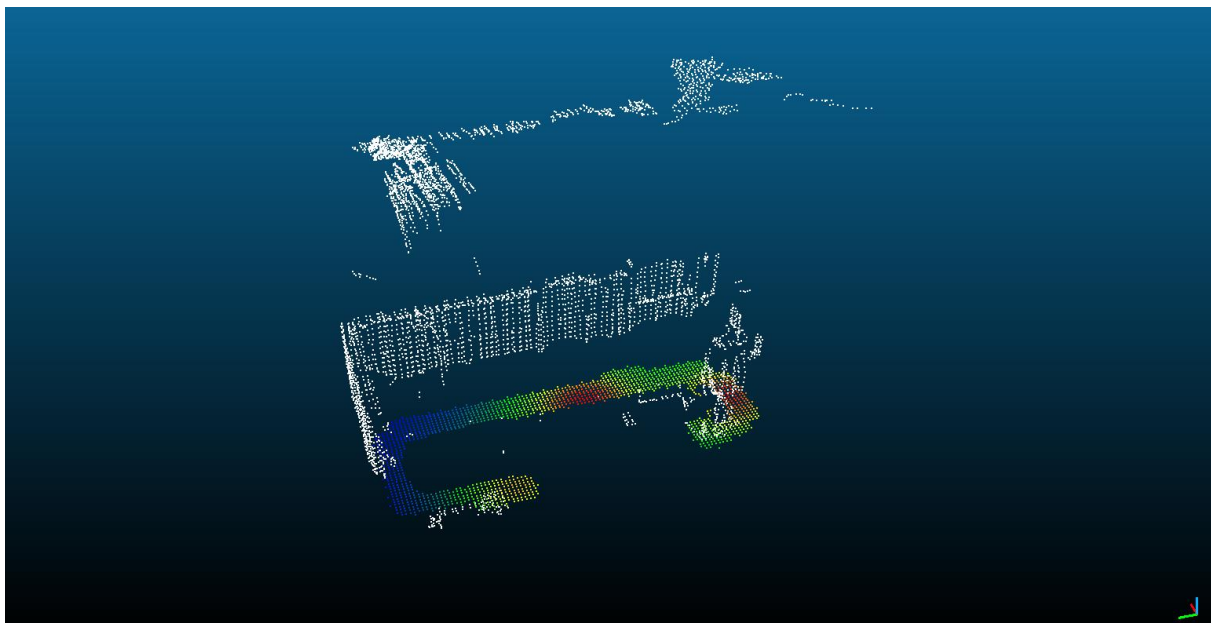


Figure 15 – Cloud computing of dose rates on tank VA002

## 5. Mixing

At both ends of the VA tanks mixers are installed, from the top of the tank (the mixers are indicated in Figure 6 by the infinity signs). The influence of mixing on the distribution of the radionuclides inside the VA002 tank was studied. The mixing with a frequency of 35 Hz was made. In principle, it was of interest if it is possible to achieve (and measure) a uniform distribution of the radionuclides inside the tank in the result of mixing or not. If it is possible than the total radioactivity in the tank can be easily measured and calculated.

### 5.1. Results of the measurements in position D1

The comparison of the results of gamma-ray imaging (Figure 16) shows that there is no significant influence of the mixing on the major hot spot or changes are simply not visible.

Indeed, before any mixing, the dose-rate at the imager position was  $2.9 \mu\text{Gy/h}$ , in the result of 30 minutes of mixing with one mixer the dose-rate went up a bit, up to  $3.1 \mu\text{Gy/h}$ . After 4h 30m of mixing the dose rate became  $3.2 \mu\text{Gy/h}$ . After the next 17 hours without mixing, the dose-rate went up to  $3.3 \mu\text{Gy/h}$ .

During the mixing with both mixers, the dose-rate went down to  $3.1 \mu\text{Gy/h}$ .

From the measurements focused on the major hot spot it was impossible to understand the effect of mixing and dynamics of migration of radionuclides inside the tank.

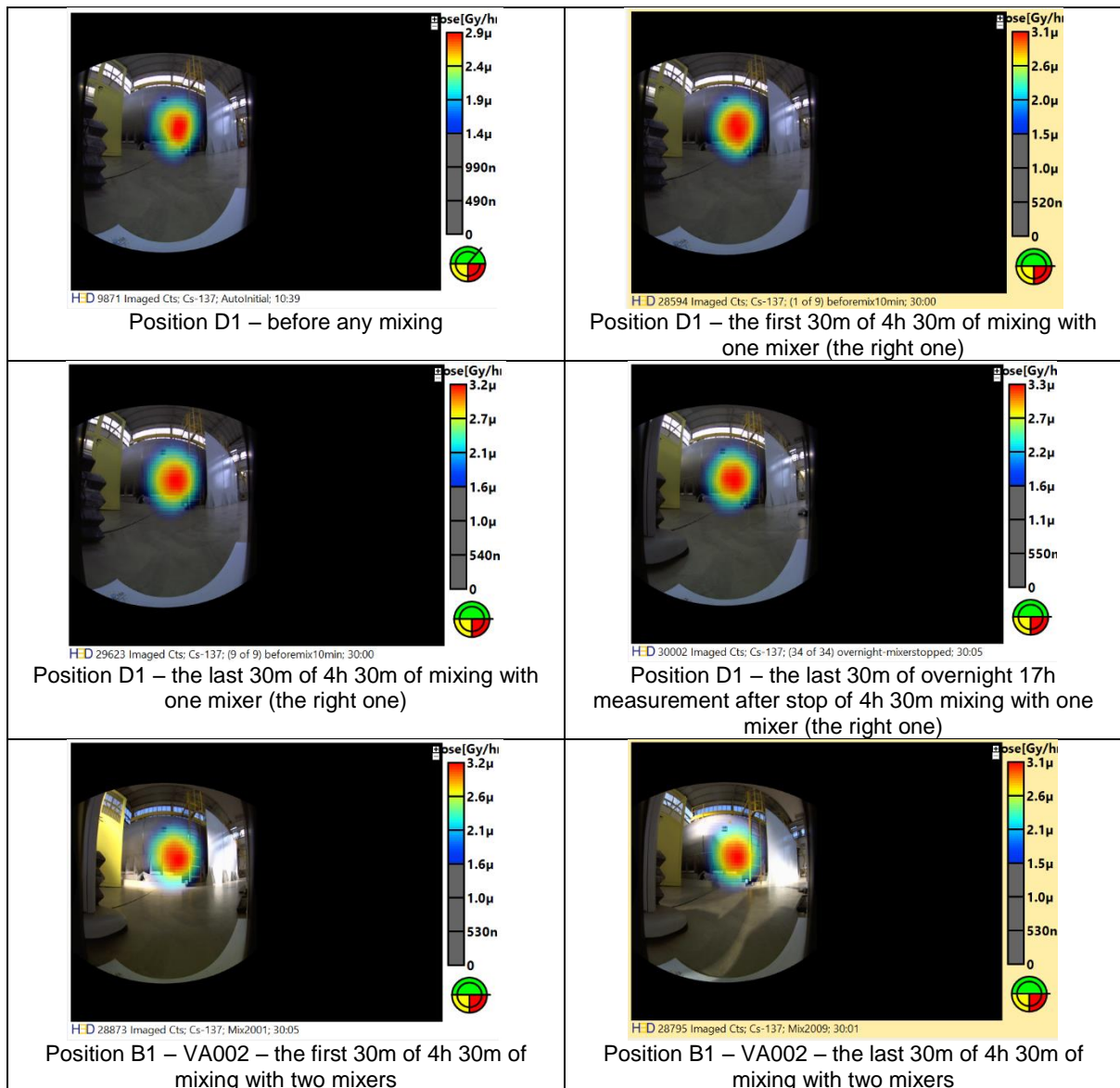


Figure 16 – influence of the mixing on the major hot spot

### 5.2. Results of measurements in the position B1

From the analysis of the results presented in Figure 17, the following conclusions can be made:

- Before any mixing (after long period of stability), the radionuclides are concentrated at the bottom of the tank and the dose-rate at the position B1 is the lowest – 1.2  $\mu\text{Gy/h}$ ;
- After 4h 30m of mixing with the right (far) mixer the radionuclides migrate to the left side of the tank and dose-rate at position B1 increases to 3.5  $\mu\text{Gy/h}$ , the radionuclides at the left side of the tank are tend to be at the bottom;
- After 17h of stability the dose-rate at B1 remains the same (3.5  $\mu\text{Gy/h}$ ) and distribution of the radionuclides is quite similar (tend to be at the bottom of the tank);
- After 4h 30m of mixing with both mixers the dose rate at B1 decreases to 2.0  $\mu\text{Gy/h}$  and the distribution of radionuclides becomes more homogeneous. Radionuclides go to the top of the tank. The dose-rate decreases because of the self-absorption in the water.

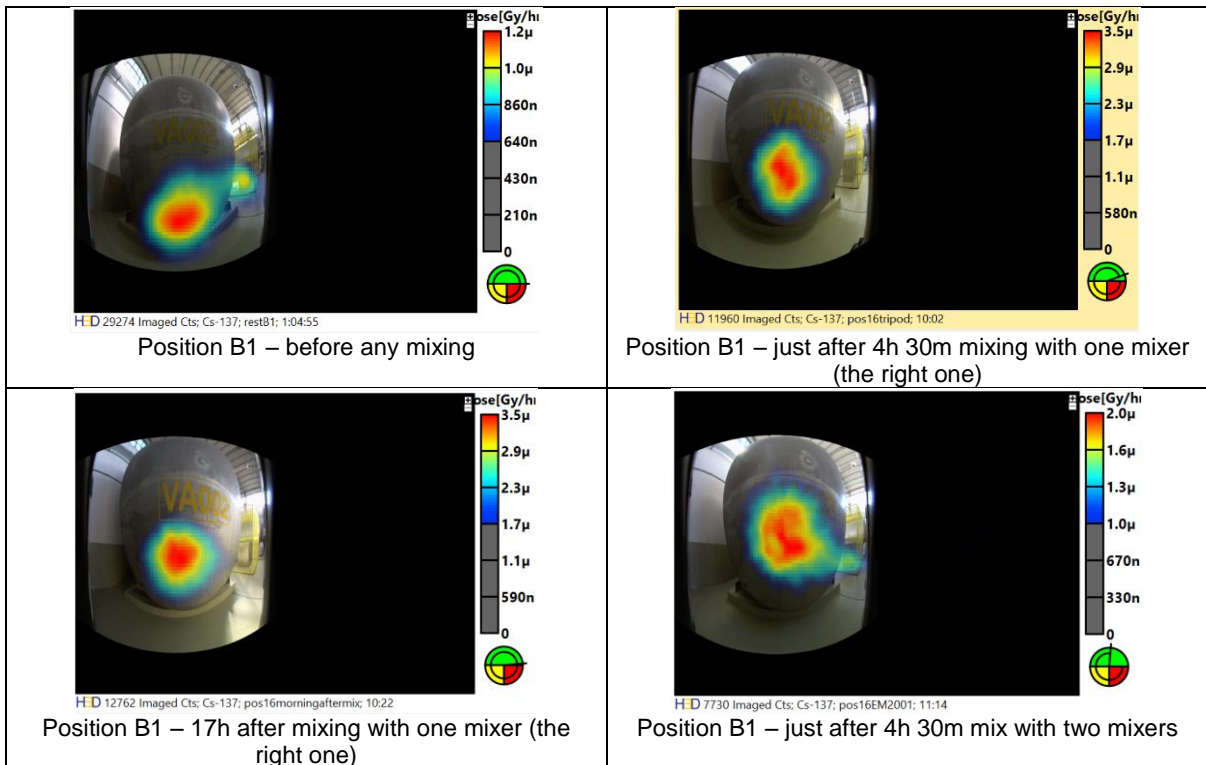


Figure 17 – influence of mixing on the distribution of the radionuclides in the tank, position B1

### 5.3. Results of measurements in the position B4

From the analysis of the results presented in Figure 18, it is evident that the radionuclides migrate readily from the bottom to the top of the tank during mixing.

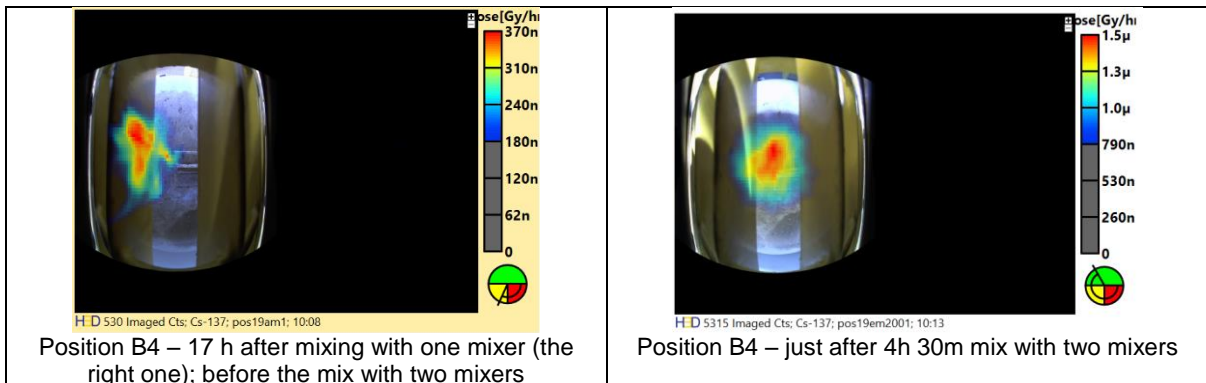


Figure 18 – influence of mixing on the distribution of the radionuclides in the tank, position B4

## 5.4. Results of measurements in the position B5

From the analysis of the results shown in Figure 19, the following observations can be made:

- The dose-rate at B5 (the imager is at the top of the tank) before any mixing and 17h after stop of 4h 30m of mixing is rather similar;
- The dose rate at B5 just after 4h 30m of mixing with both mixers is about 6 times higher than before any mixing;
- The radionuclides migrate readily from the bottom to the top of the tank during mixing and after stop of mixing fall down fast to the bottom of the tank.

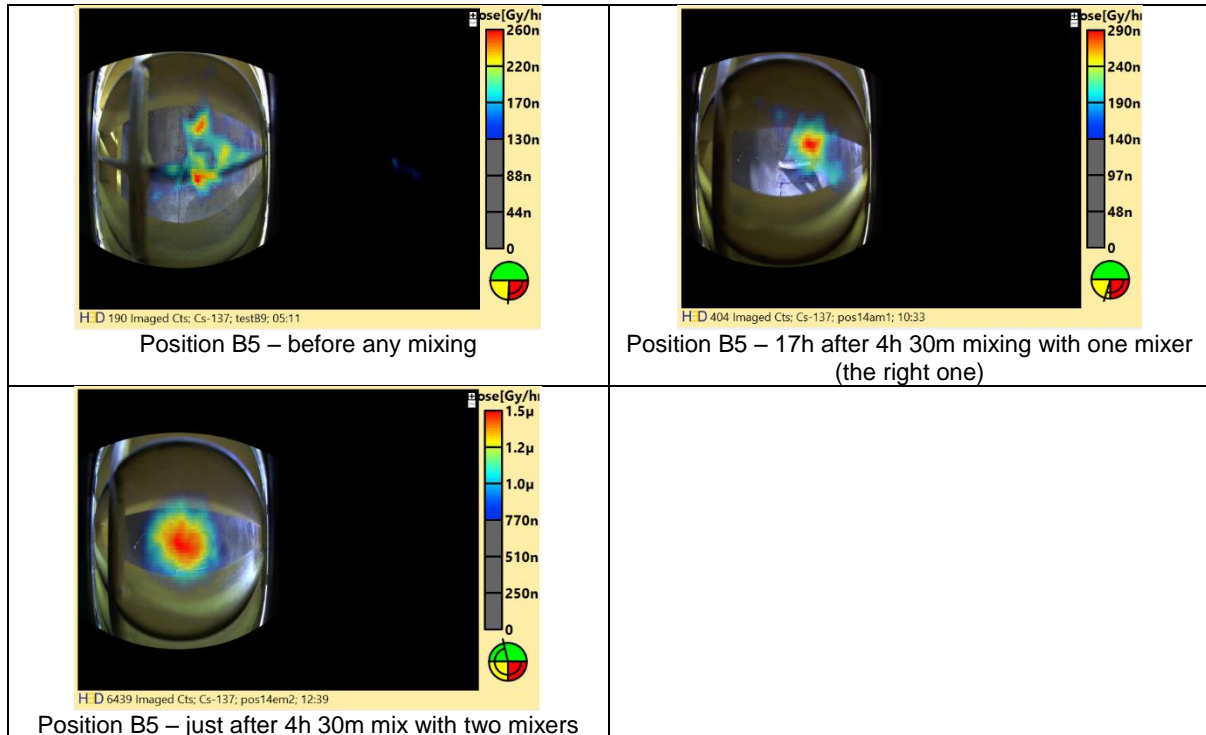


Figure 19 – influence of mixing on the distribution of the radionuclides in the tank, position B5

## 6. Conclusion

### 6.1. Radiological characterization

From the point of radiological characterisation of the facility, the following results have been achieved:

- Two types of radiological maps have been created;
- First type of the map gives continuous and overall picture of the distribution of the radionuclides at the facility and is based on the dynamic scans made with the N-Visage Recon;
- Second type of the map provides operator with more detailed information about the hot spots and is based on the static measurements made with the Polaris-H; the results of these measurements will be integrated into physical 3D model of the facility measured with the high-resolution laser scanner (3DLR);
- Gamma-ray imaging provides additional (to the dose-rate measurements) information essential for the correct radiological characterisation (mapping) of the facilities;
- Using the Polaris-H imager it was possible to identify three major hot spots that correspond to the middle of VA001, middle of VA002 and to the VB-01 tanks;
- The measurements with N-Visage Recon have provided more continuous, however less detailed picture and have confirmed that the major hot spot of VA002 is extended towards the end of the tank;
- Radioactivity of the wastes stored in the VB002 tank is at least 2 times higher compared to the VA001 tank;
- N-Visage Recon is probably most suitable for the fast radiological mapping of the facilities;
- Polaris-H is probably most suitable for the localization of the radioactive hot spots at the facilities and for their spectrometric characterization.

## 6.2. Dynamic behaviour of radionuclides during mixing

From the point of dynamic behaviour of radionuclides in the tank, the following conclusions are made:

- a) Before mixing most of the radioactivity comes from the bottom of the tanks;
- b) 4h 30m of mixing cause little migration of the radionuclides in the tank. Much longer period of mixing is required for achieving more uniform distribution of the radionuclides in the tank;
- c) The radionuclides migrate much more readily from the bottom to the top of the tank than from the left to the right;
- d) In addition, from the measurement it is visible that system comes rather fast to the previous state after stop of mixing, and in vertical direction (up and down) the velocity of migration of radionuclides before and after mixing is quite similar.

## 6.3. Recommendation

It could be beneficial from the points of radioprotection and radioactive materials accountancy to store radioactive solutions not in the horizontally oriented but in vertically oriented tanks (cylinders) having one mixer at the top of the tank. In this case, the radionuclides would stay at the bottom of the cylinder (which is easy to shield) for the most of the time and it would be easier to achieve uniform distribution of the radionuclides during mixing. Such uniform distribution is required for proper measurement of the activity of the radionuclides in the tank.

## 7. References

- [1] Peerani P. et al. *Identification of Needs for Innovative Technologies. Improved Nuclear Site Characterization for Waste Minimization in DD Operations under Constrained Environment (INSIDER)*. JRC Technical report JRC111575. 2018.
- [2] <https://h3dgamma.com/>
- [3] <https://www.createc.co.uk/>
- [4] Orpet Peixoto, Sílvia Almeida, Vítor Sequeira, João G.M. Gonçalves. *Joint Report on JRC Seminar: 3D Laser Range Finder (3DLR) for Design Information Verification*. JRC Technical report 54118. 2009.

# Characteristics of Site boundary monitoring systems for verifying future nuclear weapon arms control agreements

Ian Hayes  
Keir Allen

AWE plc, Aldermaston, Reading, RG18 3NH, UK  
E-mail: [ian.hayes@awe.co.uk](mailto:ian.hayes@awe.co.uk)  
©British Crown Owned Copyright 2019/AWE

## **Abstract:**

*Under the terms of a future nuclear weapons related arms control agreement, one might expect that several sites would be defined that contained treaty-controlled weapons or items. Accounting for the treaty-controlled items could be achieved via the creation of defined item balance areas for which inventories of controlled items are maintained. The total number of declared treaty-controlled items within the item balance area at any point should equal the number of declared items in the last inventory, plus declared shipments received from, and minus any declared transfers to, another area.*

*Setting up an item balance area poses a challenge. Accountable items could be considered unitary, yet they may contain internal sub-components that potentially could be diverted from the area, whilst the remainder of the original item continues to satisfy the definition of a unitary item. If the sub-components are considered treaty controllable then this situation could fundamentally undermine the accounting process. In addition, there should be no other objects within the item balance area that could be considered controllable items yet do not appear on the inventory. It may be important to ensure no such objects are removed from the item balance area without the monitoring agency being notified.*

*Item balance areas may therefore benefit from boundary monitoring systems. These could provide a monitoring agency with assurances that objects with critical characteristics cannot move into or out from the item balance area without the agency being made aware, whilst allowing declared shipments of inventory items across defined site boundaries. This paper considers the conditions that may be found at different sites declared to contain nuclear weapons or other potentially treaty accountable items and suggests desirable technical characteristics of boundary monitoring systems designed to monitor the movement of controllable items into and away from those sites.*

**Keywords:** Boundary, Monitoring, Treaty, Verification

## **1. Introduction**

Future nuclear weapon arms control agreements may include a requirement to monitor, control and account for various categories of nuclear weapons relevant item, termed Treaty Controlled, or Accountable, Items. For simplicity the term Treaty Accountable Items (TAI) is used as a general term in this paper.

TAIs might be found on any of multiple distinct and defined sites declared to be part of the nuclear weapon enterprise and likely spread across the territory of the nuclear weapon possessor state. Processes may occur on some sites that convert one category of TAI into another category of TAI and TAIs might be expected to periodically move between sites.

With a limited number of inspections per year, an inspectorate may not be present on sites for significant periods of time and almost certainly will not be able to monitor and inspect every TAI throughout its lifecycle, for instance, prior to it changing location or category.

If TAIs are considered as unitary items of account and the weapon possessing state keeps an accounting book of the TAIs on each site, then each site could be considered as an item balance area: the number of TAIs within each area at any point in time should equal the number of declared items in the last inventory, plus declared shipments received from, and minus any declared transfers to, another area. Newly created and registered TAIs or TAIs accountably destroyed may cause a further adjustment in the accounts for any given area. Complex or geographically extended sites could be split into multiple item balance areas of a more manageable scale. The accounts for any area could be verified through a physical inventory verification process, which could be considered as verifying the correctness of a site declaration.

The treatment of sites as Item balance areas is an attractive idea. Nevertheless, treating TAIs as unitary items introduces challenges.

## **2. Treating Treaty Accountable Items as Unitary Items: creating the potential for diversion**

One might consider the different potential categories of TAI. TAIs might be those that fall into categories of item where the total number of items is limited by the treaty: nuclear weapons may be considered one such category. On the other hand, categories of TAIs may not have a set limit on the number of items allowed, but each one might be subject to account and audit: nuclear weapon components, and containers of fissile material might all be considered as categories of this type. These categories are linked together by the processes that convert one to the other.

One might then consider that nuclear weapons be considered as unitary items of account – i.e. that a single weapon counts as one weapon for weapon accounting purposes. But the conversion of unitary weapons into a specific quantity of fissile material could be an accounting challenge when dealing with nuclear weapons. This is because the mass of fissile material contained within individual weapons might be considered as sensitive weapon design information: information that may not be disclosed or subjected to verification.

As a result, a weapon possessor state might not declare the quantity of fissile material used in the fissile components of weapons or in containers declared to contain fissile material (from a weapon stockpile) in any meaningfully verifiable way. If quantities of material were declared per container and this verified, then the monitoring and verification of the processes that change items from one category to another could lead to the inference of the quantity of material in the weapons themselves.

Herein lies the verification challenge, since the potential exists to divert fissile material away from a mass balance area undetected by physical inventory verification of the Site inventory, if the amount of fissile material contained within any one weapon or weapon component is unknown. In this situation, all items on the inventory could be verified to be in the correct location and correct status through a physical inventory inspection, but the total amount of material held within the mass balance area could not be verified completely.

## **3. Verifying completeness**

Any fissile material diverted from the declared inventory may be thought of as undeclared material. Perhaps more importantly one should not simply discount the existence of a stockpile of undeclared fissile material, components or weapons in the first place – a stock that has never been declared as part of the inventory. The process of verifying the absence of any such items from within a declared site could be considered important for verifying the completeness of a site declaration.

The challenge with verifying the absence of undeclared fissile materials, whether diverted from a declared inventory or contained with never-declared stocks of material, components or weapons, is the ability to ensure they do not exit a declared site or mass balance area undetected. Containers of fissile materials, components or weapons are small, mobile and concealable, potentially making the evasion of detection an easy task. Boundary monitoring systems might be considered as part of the solution if

they can be used to corral such items inside constrained geographic areas and prevent their undetected exit.

#### **4. Boundary monitoring systems**

To be effective, a boundary monitoring system should be capable of monitoring the boundary, or perimeter, of a site and detect any movement of undeclared items with characteristics of treaty accountable items across it, whilst enabling legitimate flow of declared TAIs and other objects to continue.

Boundary monitoring systems were implemented under the Intermediate-range Nuclear Forces (INF) Treaty and under the Strategic Arms Reduction Treaty, [1] to monitor the output of missile factories and ensure only treaty compliant products crossed the site boundary. Nevertheless, the characteristics of the system designed to ensure compliance under those treaties are unlikely to be enough for a system designed to detect the movement of undeclared (including diverted) accountable items in potential future nuclear weapon control agreements.

Many states today have installed radiation detecting, portal monitoring systems at their ports and borders to detect the illicit transport of a variety of radioactive materials, including fissile materials. The characteristics of these systems offer potential but need to be carefully considered within the context of an arms control agreement where quantities of material might not be declared. [2]

The development of a suitable system for such an arms control scenario could be a significant challenge, but the advances in technology that have taken place since last time boundary or perimeter monitoring systems were developed for arms control purposes have been significant to say the least, and so looking afresh at system characteristics could be beneficial.

#### **5. Characteristics of potential sites**

Many different types of site could exist across the weapons enterprise of a nuclear weapons possessing state. Some might be relatively small, declared to hold only one category of item, with little variety in the type of traffic observed crossing the site boundary. Others might cover very large geographical areas, potentially resulting in the need to monitor considerable perimeters but with very little traffic, again with only one category of item. For the purposes of this paper we will concentrate on a complex site – one which might ship and receive various categories of item to and from other sites, where various categories might be processed and stored, with a distributed supply chain, and extensive workforce.

On a complex site the traffic flow could consist of thousands of cars each day entering and leaving the site from multiple gates. The majority of which will cross the boundary in one direction during a period of a couple of hours in the morning, and cross again in the other direction over a period of a few hours in the evening. Hundreds of heavier goods vehicles with the capacity to carry TAI-sized objects may also cross the boundary through any one of multiple gates each day.

In addition, some vehicles could be carrying TAI scheduled to be moved from one site to another. The volume of this type of traffic might be just a small percentage of the total traffic flow and may only arrive or depart through one or a small number of gates. One characteristic of such sites might be an unwillingness to disclose in advance precisely when such movements are due to take place.

#### **6. Desirable operational capabilities of the boundary monitoring system**

Any boundary monitoring system must be capable of detecting movement of potential TAIs across the perimeter at any location along it, to prevent movements occurring through any point other than a designated gate.

At the gates, the boundary monitoring system must be capable of detecting attempts to cross the boundary with an object that may be considered treaty accountable but hasn't been declared (whether never declared or resulting from diversion away from the declared inventory) in either direction. The system must also be able to verify the items crossing it as part of a declared transfer, accurately reflecting the items declared on the site inventory and transfer manifest ensuring site inventory records remain correct.

The system should be capable of monitoring the traffic at a rate that does not overly burden the infrastructure and day-to-day operations of the site. Delaying commuter cars for more than a few minutes, for instance, could be challenging to accept for a facility operator. Though individual goods vehicles could potentially be delayed for longer times, capacity to deal with volumes of such traffic even in the low hundreds may rapidly become an issue.

## 7. Desirable detection capabilities

The emission of radiation by fissile material could be the most important characteristic for the detection of the movement of items across site boundaries, though the implementation of a system designed around the principle of radiation detection may not be straight forward in this case.

Over an extended perimeter potentially tens of kilometres long, it may be desirable to detect any physical breach of the perimeter and log the type of object that caused the breach. Should the object be theoretically capable of moving a quantity of fissile material, it could be useful to subject the object to monitoring for potential signatures of fissile materials. In practice this might be challenging, given that the object could take many forms, could pass the perimeter at any point and could travel at speed. In practice, the detection of a physical breach (and the object that caused it) might be enough, if treaty protocol insists that only designated gates or portals should be used to enter or leave the site.

The system should be capable of detecting small quantities of fissile material that may be well hidden and shielded, to ensure that the large volumes of traffic crossing the boundary are not used to systematically move undeclared quantities of material between sites.

The process of monitoring and verifying the number and identity of declared objects crossing a boundary as part of a declared shipment may take place within the site itself in practice, rather than at the site boundary. This would ensure progress of those items is not inhibited for significant periods of time in relatively vulnerable locations. In which case, the monitoring system should be capable of detecting any indicators of change to the contents of vehicle manifests since the verification of the manifest took place.

The potential lack of information declared by the weapon owner concerning quantities of fissile material (and locations of fissile material within an object) creates some challenges. For instance, what form might a 'change' to declared items take and how might it be identified?

If a manifest declared that five TAIs were being moved, five TAIs could be accounted and identified; but without a record of the quantity or location of fissile material within each of the TAIs, it might be difficult to ensure that each TAI was not carrying multiple undisclosed controllable items, or undeclared fissile materials. Such a situation would leave open a pathway for undeclared material or components to be shipped between sites undetected, co-located with declared inventory items. Perhaps somewhat counterintuitively, a desirable capability may be to detect if fissile material has been added to declared items, rather than removed.

A detection capability that focuses on comparing the configuration of accountable items against configuration data captured at an earlier point in time, and signifies any changes in configuration, might be a desirable capability in this situation. Templating [3], compares an object against a template of a class of objects to ensure the it meets the criteria to be considered one such object. It could be desirable to match the data of a declared individual object to a template of the individual object in question, this would aid in confirming the object remained unchanged.

## 8. Conclusion

This paper has begun to explore some of the issues associated with using boundary monitoring to aid in the verification of a nuclear weapon arms control agreement. The issues covered are not exhaustive, but the paper indicates how potential information constraints could impact the technical objective and technological architecture of any such boundary monitoring capability. There is reason to assume that nuclear weapons will be treated as individual or unitary items of account for arms control accountancy purposes in future arms control treaties or agreements; this could lead to uncertainty concerning the amount of fissile material in the weapon stockpile. Perhaps more importantly, stocks of undeclared materials may exist; it might be important to prevent such stocks from moving between sites. One of the key challenges could be how to detect the movement of undeclared materials co-located with declared inventory items.

## 9. Acknowledgements

The author would like to acknowledge all those who have reviewed this work.

I agree that ESARDA may print my article in the ESARDA Bulletin/Symposium proceedings.

The authors declare that their work is original and not a violation or infringement of any existing copyright.

## 10. References

- [1] *Treaty Between The United States Of America And The Union Of Soviet Socialist Republics On The Elimination Of Their Intermediate-Range And Shorter-Range Missiles (INF Treaty)*; <https://www.state.gov/t/avc/trty/102360.htm> Accessed 23/4/19
- [2] Downes R. J.; *Alarming Cargo: Regulation and control at the UK border; Terrorism and Political Violence*; 2019; DOI: 10.1080/09546553.2018.1557150
- [3] Seager K. D., Mitchell J. D., Laub T. W., Tolk, K.M, Lucero R. L., Insch K. W.; *Trusted Radiation Identification System*; [https://www.ipndv.org/wp-content/uploads/2017/10/SNL-12\\_SAND2001-1866C.pdf](https://www.ipndv.org/wp-content/uploads/2017/10/SNL-12_SAND2001-1866C.pdf) Accessed 23/4/19

# Opportunities for a graded approach in air sample assay and triage

**Robert B. Hayes, S. Joseph Cope**

North Carolina State University, Nuclear Engineering Department  
2500 Stinson Dr, Raleigh NC, 27695-7909  
rbhayes@ncsu.edu

## **Abstract:**

*Rather than waiting for radon progeny to decay prior to counting an air sample, scalar counts have been shown to provide useful information when appropriate technical interpretation is utilized. This work will review limits from the first frisk of an air sample to recent research showing how the initial decay profile can provide ever increasing discrimination capabilities if measured. Methods demonstrated in the literature along with future opportunities will be reviewed in this presentation. Applications for routine nuclear facility operation, radiological emergency response and treaty verification will also be considered.*

**Keywords:** Air monitoring; Triage; Routine sampling assay

## **1. Introduction**

Radiological aerosols have additional evolutionary size properties not found in typical organic materials. If these begin as a radioactive gas and have a charged particle decay mode, unique physics can change their subsequent behaviour. Specifically, when the airborne radioisotopes decay by charged particle emission, the resulting atom itself is left with a net charge. This can then induce polarization in any nearby aerosol such that the point charge and the induced dipole have a coulombic attraction allowing them to become attached causing the aerosol to evolve in shape as a function of time and subsequent decays.

Not all radioactive gases with charged particle decay modes will attach to aerosols. This results in an attached fraction and an unattached fraction of the subsequent decay progeny as occurs with radon progeny. The evolution of these radioaerosol particles are then generally sampled with an air filter which itself has particle size sampling efficiencies making precision air monitoring convoluted at best.

### **1.1. Natural sources and decay products from radium**

A primary difficulty in radiological air monitoring is due to the ubiquitous and dynamic properties of radon progeny. The crustal content of both  $^{226}\text{Ra}$  and  $^{224}\text{Ra}$  are from their respective  $^{238}\text{U}$  and  $^{232}\text{Th}$  parent primordial decay chains. All  $^{226}\text{Ra}$  and  $^{224}\text{Ra}$  decay into  $^{222}\text{Rn}$  and  $^{220}\text{Rn}$  respectively which are commonly referred to as radon and thoron accordingly. The radon and thoron then have their own decay chains eventually becoming isotopes of lead. These naturally occurring radioactive materials (NORM) have dynamic contributions arising from disparate decay rates, meteorology and regional geology.

The decay series of Radon and Thoron are shown in Figures 1 and 2 respectively

#### **1.1.1. Radon**

The relevant decay series for radon shown in Figure 1 includes maximum beta emission energies shown. Note that once  $^{210}\text{Pb}$  is formed, it's 21 year half-life effectively removes it from any atmospheric content as it is naturally scrubbed from the air into the soil. The subsequent decay series can be resuspended but generally has a negligible content in air samples.

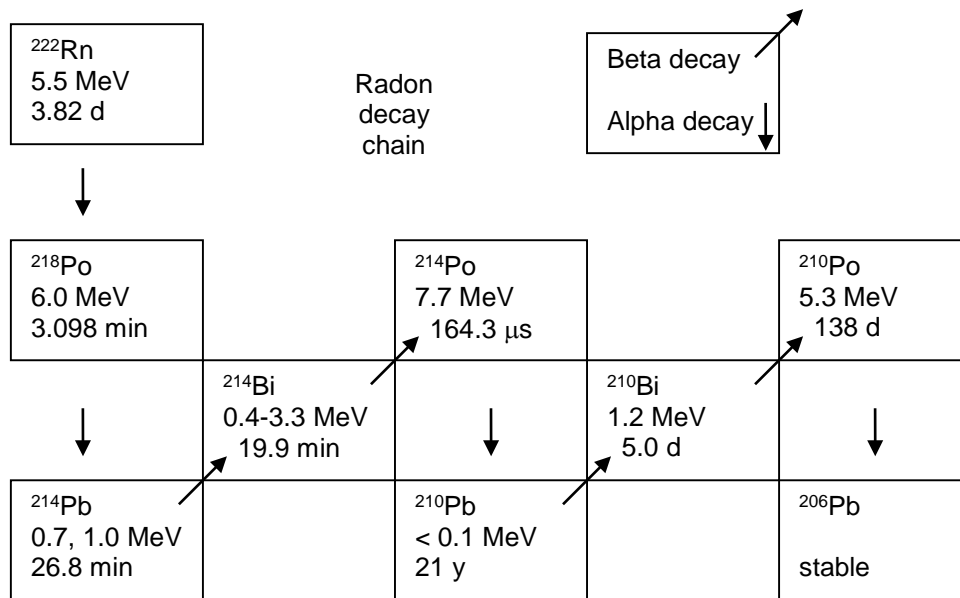


Figure 1:  $^{222}\text{Rn}$  decay series (from  $^{238}\text{U}$ ), half-lives shown below characteristic energies.

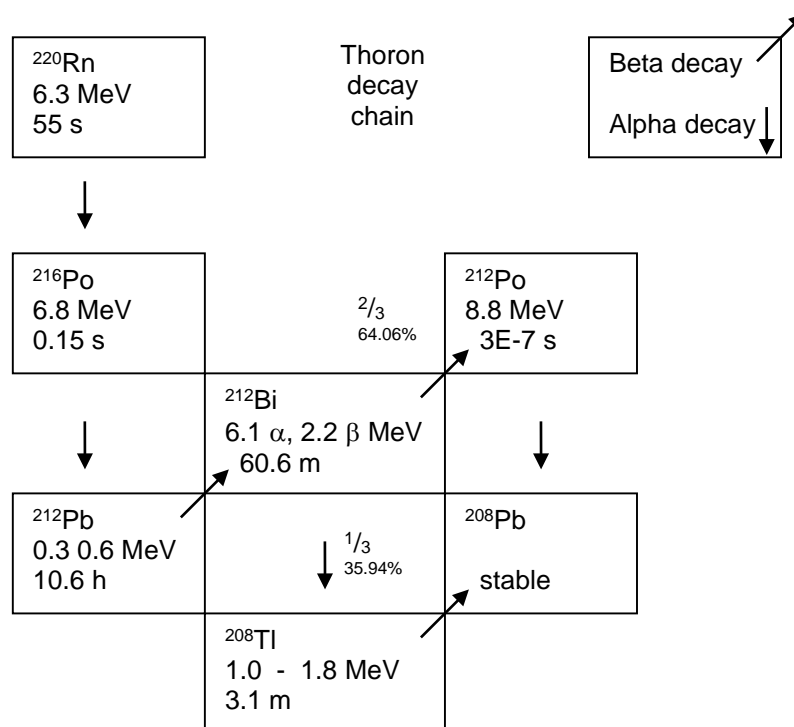


Figure 2:  $^{220}\text{Rn}$  decay series (from  $^{232}\text{Th}$ ), half-lives shown below characteristic decay energies.

As radon has a half-life of 3.8 days, it has some time to diffuse out of the host rock which contained its parent  $^{226}\text{Ra}$ . This does require that the noble gas can migrate to a grain boundary or other pathway out of the rock. Even being a noble gas, its generation in the radium inclusions of the host rock do not guarantee a simple diffusion path to the atmosphere. The alpha track damage from the radium decay accumulates over time around these radioactive inclusions and can create at least a portion of a viable path (particularly over time). Recoil from alpha decays of the  $^{226}\text{Ra}$  also cause shorter range local  $\mu\text{m}$  scale damage to the mineral matrix. The greater track length of an emitted alpha effectively punches a hole in its host matrix up to many 10's of  $\mu\text{m}$  which build up over time resulting in various radial starting

pathways for successive radon emanations to traverses when randomly attempting to find a grain boundary.

### 1.1.2. Thoron

The thoron decay series is shown in Figure 2 also includes maximum beta energies shown.

Thoron is a bit unique in that its parent  $^{224}\text{Ra}$  along with the primordial  $^{232}\text{Th}$  has a much higher crustal abundance compared to  $^{238}\text{U}$  and its progeny  $^{226}\text{Ra}$  but has a much lower atmospheric content. Although this converse relationship is not expected due to source terms (thoron having a lower air concentration than radon), the actual cause is the half-life of the noble gas  $^{220}\text{Rn}$  which is just under 1 minute. This means that if the thoron is not able to escape from the rock matrix into the atmosphere in less than a minute, it will decay back into a heavy metal and so the resultant decay chain is confined to the soil. As such, on average, radon will exceed thoron to around a 3 to 1 ratio even though their parent ratios are inversed.

The thoron decay series has a unique feature of interest in that the isotope  $^{212}\text{Bi}$  is able to decay by either beta or alpha decay with an approximate 2:1 split. This isotope will typically be in transient equilibrium with its longer lived parent  $^{212}\text{Pb}$  when left undisturbed over many hours.

#### 1.1.2.1 Thoron constancy

An additional unique aspect in thoron content is that with the parent having less than a 1 minute half-life, it cannot travel far prior to initiating its decay series. This because radioactivity by nature always has an independent probability of decay so that the portion which arises in gaseous form still has the same half-life as that which was retained in the soil mineral components.

Unlike radon which has a 4 day half-life and can travel great distances with the wind, the 1 minute half-life of thoron does not allow it to travel even nominal distances as it will decay into heavy metals very quickly (Figure 2). The  $^{212}\text{Pb}$  can travel nominal distances having an 11 hour half-life but it is not able to be fed by a continual  $^{220}\text{Rn}$  source as this thoron stays effectively right where it was generated (from  $^{224}\text{Ra}$  decay).

## 1.2. Temporal variations in radon progeny

There are many factors which give rise to variations in natural airborne radioactivity levels. The largest tends to be that of temperature inversions. A natural inversion typically occurs in the mornings due to the adiabatic lapse rates from the ground preventing any mixing of surface air with the upper atmosphere. This means that all radon which has escaped from the ground simply builds up near the surface until it can be diluted later in the morning due to convective currents which allow mixing with the upper atmosphere. These convective currents are initiated by ground heating from solar irradiance in the morning. This effect also has seasonal dependencies with winter typically having the largest inversion effects resulting in the largest ground radon concentrations.

Another very large effect in environmental radon and its progeny comes from precipitation. When rain falls through radon and its progeny it pushes these radionuclides to the ground cleaning the air but raising the terrestrial dose rate by many orders of magnitude [1]. Barometric pressure is another cause of changing radon levels. When a low pressure comes in, this can pull radon from the soil as a high pressure system can retard radon diffusion from the ground.

## 1.3. Alpha and beta spectra from environmental samples

The distribution of energies shown in Figures 1 and 2 result in spectra exemplified by Figure 3 where no TRU activity is present. Here, the peaks are labelled by their dominant contributing radionuclides. The peak location represents those occurrences when emitted alpha particles move normal to the filter and detector depositing a characteristic energy into the detector active volume. Spreading occurs from interstitial air, filter media and oblique paths to the detector from the source filter. In this sense, the majority of detected alpha particles is not at the maximum possible energy for a particle where minimum attenuation takes place in the filter, its sampled material, the air layer separating the detector and the detector dead layer.

The transuranic (TRU) region of interest (ROI) in Figure 3 represents where most of the transuranic isotopes will be present and so the large count rate present from tailing of the higher energy NORM alpha peaks creates considerable background in the TRU ROI (hence the desire to allow them to decay prior to assay).

The abscissa scale is based on only the three labelled NORM peaks so that the beta energies are overestimated in this scheme. This is because the ionization in the detector has a higher efficiency with beta particles than alphas for the same kinetic energy. Alpha particles lose a certain portion of their energy creating vacancies and interstitials due to recoiling nuclei whereas beta particles have a much higher threshold to displace an atom in the detector volume resulting in a larger fraction of their deposited energy going into ionization only.

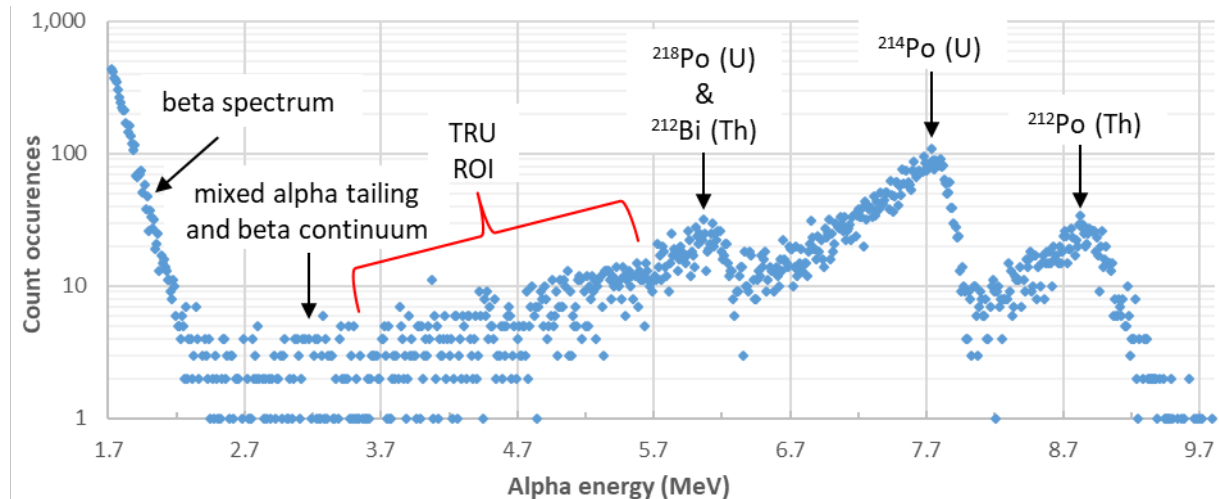


**Figure 3:** Example charged particle spectra (semi-log) measured from an environmental air sample with peaks and regions labelled associating primordial parents indicated as  $^{238}\text{U}=\text{U}$  and  $^{232}\text{Th}=\text{Th}$  from Figures 1 & 2.

### 1.3.1. Spectral manipulation options

Typical commercial options to mitigate these features involve curve fitting the shapes which is feasible when substantial particulate loading does not drastically degrade the spectra from self-attenuation effects. The more complicated options include Gaussian fits to the top of the peaks with exponential tails above and below these. Other options include simple region of interest (ROI) summing of the peak areas separated by their respective minima. Template shapes for each peak could be fit in amplitude as well but each of these options have potential issues with spectral degradation occurring as filter loading increases (due to dust build-up).

Peak shifting and tailing slope dependencies with filter loading could be mitigated by allowing peak locations to be variables along with exponential fitting portions (or template shapes). This would require sufficient knowledge of overlap dependencies in the TRU ROI for discrimination purposes.

#### 1.3.1.1. Limitations with spectral manipulation

When filter loading occurs, the peak locations shift to lower energies and the low energy tails from each peak will increase accordingly. The low energy tails seen in Figure 3 can be verified upon inspection that they would all match an exponential function well (due to the linear appearance in the semi-log format). The argument of the exponential in such a fit would then be functionally dependent on the filter loading in a potentially predictable manner with sample mass (assuming linear deposition rates). Similarly, the peak locations could also be functionally dependent on filter loading. In principle, dependencies such as these could be monitored and trended to estimate filter loading and so serve as a metric for when to change a filter and so optimize sample sensitivity overall.

It should be pointed out that there are some TRU isotopes having energies near the 6 MeV NORM peak, specifically, the californium and some of the curium isotopes such that these have peaks very near or

even indistinguishable from the 6 MeV NORM peak. Methods to mitigate this are discussed in a later section but invariably utilize the decay series (see section 1.3.2) in some fashion.

### 1.3.1.2. Potential benefits from spectral analysis

In principle, sensitivity could be increased over gross counting given that each alpha emitter has distinct ROIs which follow defined patterns which could be leveraged in the analysis using various means. If the contributions to the TRU ROI can be accurately estimated from the higher energy NORM peaks, then the background in this ROI can be substantially decreased and so concomitantly decrease the detection limit for anthropogenic activity. If spectral quality metrics are designed to indicate when the assumptions from the fit are being challenged, then additional rigor in the assay can be realized. Care should be utilized in any such approach as vendors have historically fallen short in properly testing and validating such systems prior to marketing.

### 1.3.2. Spectral and temporal coupling

The decay series given in Figures 1 & 2 all have to obey the Bateman equations represented by Equation 1. These are the governing equations for all radioactive decay series allowing for any length of a decay chain. Here each isotope activity  $A_j$  has an associated decay constant  $\lambda_j$  with an initial parent concentration  $N_1(0)$ .

$$A_j(t) = N_1(0) \sum_{m=1}^j C_m e^{-\lambda_m t} \text{ where the coefficients } C_m = \frac{\prod_{i=1}^j \lambda_i}{\prod_{i=1, i \neq m}^j (\lambda_i - \lambda_m)} \quad (1)$$

#### 1.3.2.1. Decay characteristics for thoron 6 MeV alpha contribution

This means that the standard decay rate of the  $^{212}\text{Bi}$  alpha peak at 6.1 MeV will be fed by the decaying  $^{212}\text{Pb}$  isotope which is easily discriminated by its associated isolated 8.8 MeV peak from the subsequent progeny  $^{212}\text{Po}$ . Due to the negligible half-life of  $^{212}\text{Po}$ , it is continually in transient equilibrium with its parent  $^{212}\text{Bi}$  scaled only by the appropriate beta branching ratio of the latter.

#### 1.3.2.2. Decay characteristics for the radon 6 MeV alpha contribution

Likewise, the radon progeny contribution to the 6 MeV peak from the  $^{218}\text{Po}$  initial activity is itself the source of contributing activity to the initial  $^{214}\text{Pb}$  activity which contributes to both of the initial  $^{214}\text{Bi}$  and  $^{214}\text{Po}$  activities with the latter emitting the readily discriminated 7.7 MeV peak. Specifically, due to the negligible half-life of  $^{214}\text{Po}$ , it is always in transient equilibrium with its parent  $^{214}\text{Bi}$ . From these, the Bateman equations (Eq. 1) could be used (explicitly or through some simplification) to correlate background in the TRU ROI (from  $^{218}\text{Po}$  contributions) to the readily discriminated count rates in the  $^{214}\text{Po}$  ROI (this would likely be a retrospective or delayed correction).

### 1.3.3. Beta spectral options

The beta portion of the spectrum can be folded into any desired use of the Bateman equations (Eq. 1). Typically, the radiological risk from beta activity is so much lower than that of TRU alphas that gross counting is adequate to provide desired detection sensitivity [2]. As such, the exact beta energy calibration is not considered of high importance given its added difficulty of only having a continuum source preventing a simple and precise means of scaling (particularly in the presence of alpha cross talk).

## 1.4. Mitigating radon progeny in air monitoring

Typical air monitoring techniques involve pulling a precisely measured volume of air through an air filter. The air filter is then assayed for radiological content such that the ratio of the assay to the volume is the resultant air concentration ascribed to the space sampled. The standard approach utilized in routine nuclear operations, radiological emergency response and even treaty verification is to allow the air sample to sit for multiple days to allow the entrained radon progeny to decay prior to characterizing any

anthropogenic content on the air filter. This is due to the array of alpha, beta and gamma disintegration energies present in any aged sample of ambient air due to all the radon progeny present (Figures 1, 2 and 3).

In principle, the air sample could be measured at any time while waiting for the radon progeny to decay away, but unless the anthropogenic component is large compared to the radon progeny, discrimination is haphazard at best. Vendors have claimed to produce algorithms which can discriminate anthropogenic activity based on alpha and beta spectrometry which have been shown to be unreliable [3,4].

#### **1.4.1. Initial frisk**

Based on the ratio of alpha to beta activity, some limits can be placed on the maximum anthropogenic which can be present and still attain these ratios [5]. Given that radiation cannot be sensed in any of the traditional observational modes (sight, smell and touch), it requires detectors and so airborne radioactivity, when present, requires similar infrastructure. The variability in alpha to beta ratios can vary dramatically due to all the dependencies on the contributing isotopes (see section 1.2). All that the initial frisk can determine is whether the ratio of alpha activity to beta activity could credibly have been obtained from the normal variability in NORM.

##### **1.4.1.1. Mitigation limitations**

Any initial frisk values will by definition be dynamic and so generally very insensitive in discriminating NORM from anthropogenic. The various combinations of attached and unattached fractions coupled with dynamic radon and thoron levels with size dependent filter efficiencies etc all couple into a difficult characterization at best.

This is problematic in that virtually all air samples have only trace quantities of the target isotopes unless only radon progeny itself is being assayed. This trace characteristic inherent to the isotopes of interest in an air sample arises from the nature and purpose of the sample. In normal operations, most air samples are intended to demonstrate either a zero release or at most a regulatory compliant result (which is always small).

In emergency response, field teams would have to dress out in full personnel protective equipment along with decontamination of vehicles if they were to sample in contaminated areas. As such, field teams typically sample on the penumbra of a plume so that the contamination levels are comparable to background already making detection difficult (where the bulk of any release or ground deposition characterization occurs from the air with large gamma detection arrays).

Treaty verification is generally very far down range again making concentrations almost vanishingly small. In all cases then, the radon progeny on an air sample is likely to be the dominant source of all ionizing radiation emissions.

### **1.5. Utility of the presented methodologies**

The research reviewed in this work demonstrates novel methods to characterize the anthropogenic activity in such a way as to utilize the interferent radon progeny signals to estimate the long lived activity on the filters. Rather than throw away these interferent signals, this work will review various means to use them in a graded approach to characterizing airborne radioactivity. In this way, rapid, yet quality, initial TRU estimates can be obtained in any air sample protocol from treaty monitoring to nuclear safety and even operational radiation safety applications.

## **2. Graded approach**

The graded approach itself means that improving levels of quality will scale with increasing effort or time permitting defence in depth towards the eventual goal. In this case, we are looking for a quality method to characterize anthropogenic radionuclide levels in the atmosphere despite the interfering radon progeny species. Quality being defined here as a measurement containing rigorous physics based characterization of the true dispersion inherent to the final assay results.

The current missing piece in air monitoring data is a quality assay technique which can be used to characterize air samples while the radon progeny is still relatively high. Provided that the uncertainty estimates are rigorous and accurately describe the dispersion in the measurements, high uncertainty values are entirely useful. This is because some quality information is always better than no information where quality is strictly defined as any assay having rigorous uncertainty estimators.

## **2.1. Quality convergence**

The intent for air monitoring is to properly characterize the risks associated with airborne materials. With radiological materials, this is typically the risk from inhalation which is measured in actual or potential dose. Potential dose being the dose a person would receive were they to actually be in a given location for a proscribed period of time (such as a theoretically maximally exposed individual). Consequences can also be in terms of land contamination which again is typically measured in terms of risk by the maximum potential dose an individual could credibly receive from all input vectors. With treaty compliance monitoring, the desired result is not just detection but discrimination from legitimate commercial sources.

### **2.1.1. Nuclear security**

In nuclear emergency response, treaty verification and even non-proliferation applications, quality may be measured in at least two ways. In some sense, characterization of any anomaly would be inherently useful enabling further investigation. In a more detailed example, quality may be expressed in terms of the rigor with which the anthropogenic portions of the air sample can be ascribed to adversary behaviour and discriminated from legitimate industrial or commercial endeavours. It is in the discrimination of adversary actions from those beneficial activities that is needed in nuclear security applications.

Current technology largely relies on chemical, nuclear and morphological assays from air sample particulate. As with all of the other air monitoring applications, the radiological characterization portion requires mitigation of the natural radon progeny inherent to all commercial air sampling technologies.

## **3. Using all the decay data**

When allowing the radon progeny to decay prior to the resultant air sample assay, it is inherently assumed that the progeny is purely an interferent and so does not contain useful information regarding the target assay of the anthropogenic activity. Our research has shown that there is useful information which can be extracted from the natural radon progeny when evaluated in a graded approach formalism. Specifically, starting with a quick handheld frisk for a very low quality assay (assuming a frisk has known efficiencies [5]), some information can be obtained. Additional measurements when continually applied (utilizing appropriate instrumentation and analysis) allows a continual improvement in the precision of assays (without compromising accuracy) until the eventual "gold standard" of destructive assay by radiochemistry can be applied some days or weeks later. The key is being able to use the physics of the interferent to help characterize it and so subtract or mitigate it in some useful way.

### **3.1. Decay curve fitting**

In principle, all radioactive decay chains adhere to the Bateman equations (Eq. 1) which can address only radioactive decay. If the initial conditions are known, then the Bateman equations can be solved to predict all isotopic abundances in the decay chain for all future times. Radon progeny has the inherent difficulty that the parent is continually changing (see section 1.2) and meteorological changes can also drastically bias progeny separate from the radon parent. This being partially due to the parent being a noble gas with the progeny being heavy metal (ions) either attached or unattached to ambient aerosols.

If the Bateman equations were utilized, their general form would follow that given in Equation 1 such that fitting to a measured series of counts (a decay curve) could result in an overdetermined system of equations. With radon having only 4 relevant radioactive progeny (Figure 1) and thoron having 5 (Figure 2), this would require at a minimum of 9 decay count measurements to obtain estimates for each isotope initial activity estimate. If only 9 counts were obtained, measurement scatter would prevent an exact fit

despite 9 fitting parameters attempting to model 9 data points as Equation 1 can only model continuous and smooth functions and so not noise.

### 3.1.1. Curve fitting statistics

Due to instrument uncertainty and statistical fluctuations in decay rates, at least a dozen or so measurements are desired for each degree of freedom to approximate a normal distribution in the fitted parameters convergent value. With this number of data points, a mean, its standard deviation along with a chi-squared test to evaluate the likelihood that the distribution was normal can all be estimated for any given parameter. When multiple parameters are being estimated in a curve fit, commensurately more data points would be desired. If only 2 parameters are to be estimated (an initial activity and a decay constant), then preferentially more than a dozen measurements would be the target.

This approximation assumes that around ten measurements are desired for a single mean, and a few dozen for a line and around 30 for a quadratic and so on. There is no hard limit or rule for such a generalization but the driver here is to get a quality  $t$ -test on each fitted parameter. A quality  $t$ -test is not dependent on sample number if the assumption of normality is valid. Estimating normality based on a small sample is largely untenable so this gross assumption is stated as a matter of opinion only.

### 3.1.2. Overdetermined curve fits

Technically, one can estimate the slope, intercept and their uncertainties along with a standard error of the fit and a correlation coefficient from just 3 points (even random points). In this extreme example, 5 values are obtained from 3 data points giving an apparent negative set of degrees of freedom. This really just means that multiple measures of the mean and distribution are redundant and do not convey independent information despite their typical interpretation being independent measures of central tendency.

One general goal in curve fitting is to increase your degrees of freedom as much as possible without excessively incurring scatter by splitting up your counting interval into ever decreasing intervals. Using the traditional definition of degrees of freedom ( $DoF$ ) being the difference between the number of fitted data points ( $N$ ) and that of the number of fitting parameters ( $M$ ), it is preferable to have this value ( $DoF=N-M$ ) as close to 30 as possible to enable an assumption of normal statistics. Otherwise, a  $t$ -distribution would be assumed incurring less certainty in distribution types (which can itself be tested).

## 3.2. Radon progeny decay curves

The two dominant isotopes driving the decay rates from radon progeny are the  $^{214}\text{Pb}$  and  $^{214}\text{Bi}$  isotopes having half-lives of 26.8 m and 19.9 m respectively (Figure 1). Combining these two in sequence via Equation 1 results in an approximately effective decay constant greater than either producing values ranging from 30 to 40 minutes (depending on initial conditions).

In order to get proper leverage in measuring the half-life of a radionuclide through a decay curve, ideally the measurement time should be long compared to the half-life. If a large section of the effective decay curve from radon progeny is to be sampled, then ideally at least 30 minutes of sampling time would be a minimum.

## 3.3. Long lived activity decay curves

If an operationally friendly time window for measuring an air sample is a few hours, then any activity having a half-life large compared to this would appear to be largely indistinguishable from a constant. Here, an isotope with constant activity does not actually exist but can be approximated by any radionuclide with a very long half-life compared to the count time.

With this, if thoron content is present in an air sample which only measures decay over a period of a few hours or less, the 10.6 hr half-life of  $^{212}\text{Pb}$  would cause it to look like constant (anthropogenic) activity like that of a transuranic (TRU) nuclide. If a decay curve fit modelling the radon progeny did not account for this thoron content in a short time window, this component would conservatively bias the long lived (approximately constant) activity to have a higher estimate.

### 3.4. Combined decay curves

If a decay curve is measured within a few hour window, the radon progeny would appear to go through multiple half-lives while the thoron progeny would appear largely constant. Any anthropogenic activity present will likely have decay constants comparable to <sup>137</sup>Cs, <sup>90</sup>Sr or any of the TRU nuclides which effectively would be modelled as a constant activity. Putting all this together in a decay curve fit model, Equation 2 presents the filter activity  $A(t)$  at any given time  $t$  following flow cessation. Here,  $m1$  is the initial short lived activity,  $m2$  is the effective short lived decay constant and  $m3$  is the long lived activity which will be biased high due to thoron progeny. If this function is then fit to a decay curve, the effective half-life is then  $\ln(2)/m2$ . All results used the Levenberg-Marquardt fitting algorithm to data.

$$A(t) = m1 * e^{-m2*t} + m3 \tag{2}$$

### 4. Historical results

When fitting actual filter decay data, the distribution seen in Figure 4 was obtained as described elsewhere [6]. The distribution shown represents the suite of resultant  $m3$  values and their uncertainties combined via a kernel density estimator. The results from plutonium superposition with environmental air samples is shown on the left with a similar thorium study shown on the right. In these works, the results from using Equation 2 on actual air filters both with and without anthropogenic activity are compared in their rapid assay capabilities.

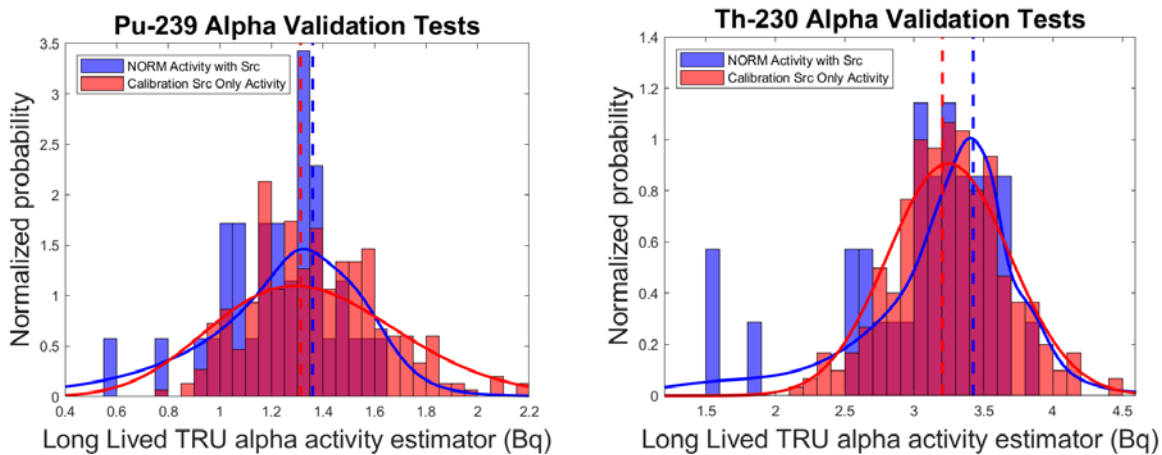


**Figure 4:** Decay curve fit results from effectively spiked air filters [6]. Blue values represent a used air filter superimposed with TRU activity. The red values represent blank (unused) filters superimposed on the same TRU activity used in making the blue results.

The histogram results shown in red are the calibration results obtained from filters not having any interferent NORM activity representing the correct values and their distribution which should be obtained from a proper use of Equation 2 on air filters having both interferent natural and anthropogenic activity.

The blue histogram results were obtained using Equation 2 on filter decay counts which had both the anthropogenic and natural radioactivity constituents. The two distributions (red and blue) are visually indistinguishable although the histogram results do not incorporate individual measurement errors from fitting Equation 2 to the decay curve data.

The red and blue dashed vertical lines represent the mean from each distribution. In this sense, the blue is the best estimate from the fitting approach of Equation 2 to environmental air samples with a TRU source superposition. The TRU source distribution without radon progeny activity is shown in red. What is evident from the blue data is that on average, use of Equation 2 provides conservative estimates of the known anthropogenic activity (indicated by the red data).

### 4.1. Kernel density estimator (KDE)

When histogramming data possessing individual uncertainties, the uncertainty portion of the data is simply discarded. This need not be the case when using a KDE which is represented by Equation 3. This effectively turns each data point used to construct the histogram into a normalized Gaussian so that the superposition of all these Gaussians becomes a continuous probability distribution function when Equation 3 is used to represent the data. This allows deconvolution of the resultant KDE into individual components or to conduct hypothesis testing on the resultant distribution. Note that the parameters used in Equation 3 are such that  $\mu_i$  are the individual measured values having unique uncertainty values of  $\sigma_i$  from  $n$  total measurements. The use of  $P(x)$  is intended to convey that when normalized in this way, the KDE is a proper probability density function sufficient for hypothesis testing.

$$KDE(x) = P(x) = \frac{1}{n} \sum_{i=1}^n \frac{e^{-0.5(\frac{x-\mu_i}{\sigma_i})^2}}{\sigma_i \sqrt{2\pi}} \tag{3}$$

The KDE values from the fitted  $m3$  distributions (Equation 2) are presented in Figure 3 as continuous lines which are color-coded in conjunction with the histograms.

### 4.2. Upper confidence limit of individual fits

The blue results seen in Figure 4 clearly have entries which are below the red dashed line. With the red vertical dashed line representing the correctly calibrated (best estimate) of the TRU content measured with the air filters, the lower blue occurrences would be underestimates and so not a conservative assay. As such, this might appear to give results which when using Equation 2 would underestimate the correct anthropogenic activity and so constitute a potential safety concern. This turns out not to be the case when individual measurement results are evaluated at their upper 95% confidence limit. When taking all the assayed results at their upper 95% CL, there were no underestimates of the characterized TRU source activity found demonstrating the savings offered from fitting decay curves using Equation 2 allowing for conservative upper bounds in all observed cases.

A histogram of all the measured assays of the TRU content using Equation 2 are shown in Figure 5. Here, the results shown are all of the  $m3 + 1.645\sigma_{m3}$  values obtained previously [6].

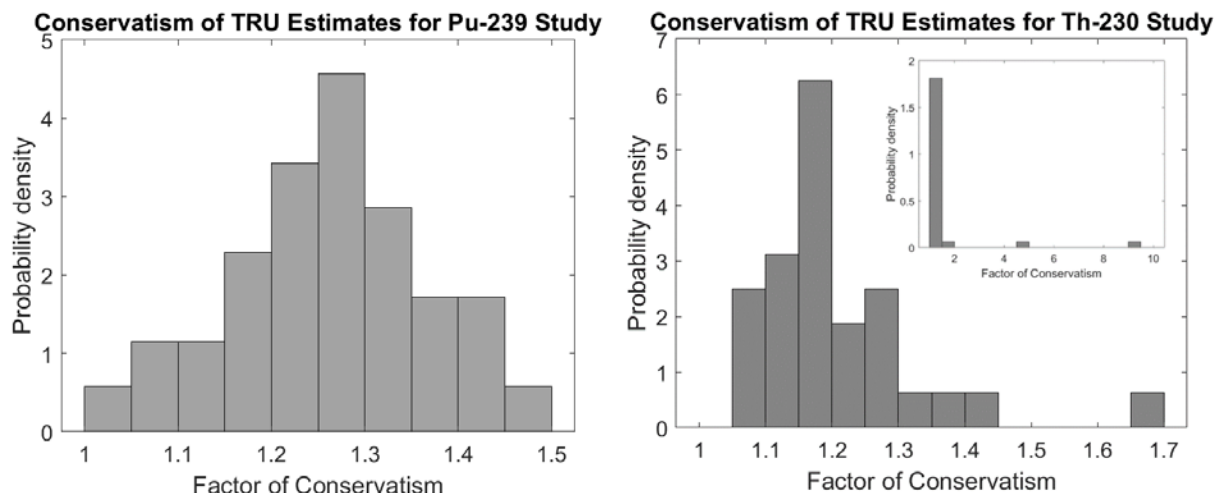


**Figure 5:** Upper 95% confidence level obtained from using Equation 2 to rapidly estimate anthropogenic content on air filters [6]. Values include thoron progeny bias from conducting only a 2 hour decay count.

Previous work has considered 30 min intervals within a 2 hr counting window to understand the uncertainty penalties associated with more rapid TRU activity estimation; again, the results can still be considered quality, even with a large uncertainty estimator, provided that it is rigorous and maintains a physical basis. Utilizing a weighted average of 35 filters for each TRU source study, the TRU estimate for each time study is given in Figure 6. The error bars noted in Figure 6 represent the standard error of

the mean at the 95% CL and should be interpreted as a potential “best estimate” scenario when conditions allow for a weighted average technique. What is truly profound is that this conservatism remains throughout the range of 30 minutes up to 2 hr measurement time with shorter measurement intervals incurring larger uncertainty (and so higher conservatism in the upper 95% CL) as reported elsewhere [7].

These results show that the asymptotic constant activity value at infinity from Equation 2 results in conservative estimates of the long lived activity whenever uncertainties are evaluated at the 95% CL. This is attributed to both the thoron progeny bias ( $^{212}\text{Pb}$  limiting the  $^{212}\text{Bi}$  activity change in rate) when measuring a short time interval and taking only the upper 95% CL. In this thoron progeny bias, the  $^{212}\text{Bi}$  alpha and beta decays approach a transient equilibrium with the parent  $^{212}\text{Pb}$  activity which has just under an 11 hour half-life.

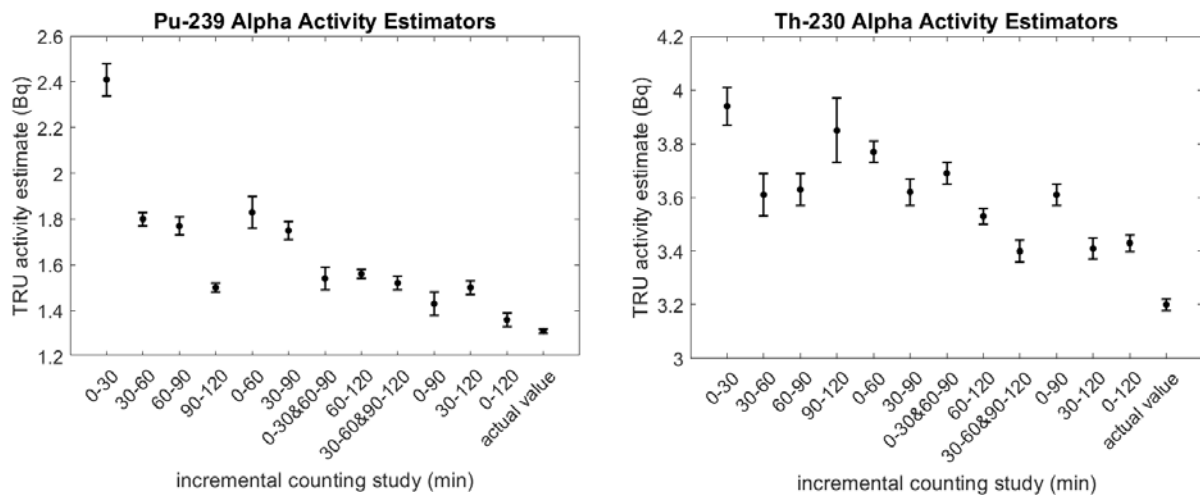


**Figure 6:** Incremental 30 min weighted average TRU alpha activity estimates from effectively spiked environmental air filters with uncertainties shown as standard error of the mean [7].

### 4.3 Summary of results

The decay curve fitting of sequential count data using the Levenberg-Marquardt algorithm can provide parameter estimates with their associated uncertainties to Equation 2. This enables novel applications involving kernel density estimators and their subsequent deconvolution [8]. More importantly, multiple options for using the information normally discarded in traditional air sampling assay has been shown to give quality low precision results quickly [7]. This in turn fills a high priority information gap typically occurring when air concentration data is desired rapidly from standard air samples.

#### 4.3.1 Alternative approaches to triage

Many other options for pursuing further graded approaches in air sample assay and triage have been identified beyond the results reported here [9,10]. These generally involve spectroscopy coupled with other methodologies but can even include additional gross assay techniques (such as longer count times). The spectral analysis methods could even include mass loading mitigation, temporal dependencies and assaying of TRU isotopes having the insidious alpha decay energies very near 6 MeV.

## 5. Discussion

The KDE results seen in Figure 4 would permit deconvolution into the respective error contributing sources. Previous results have been able to discriminate contributions from the instrument and those of radon and thoron [8]. The techniques described here demonstrate utility in the period of time while

samples are customarily being allowed to passively decay away to clear up the TRU ROI signals seen in Figure 3 and so allow low detection limits.

## 5.1 Emergency response applications

In emergency response scenarios, this could be accomplished when samples are being returned from the field. Having a small scalar or spectral counter in the transport vehicles would allow obtaining results prior to submitting samples to the lab. Starting with an initial frisk, the samples could be continually counted in a decreasing uncertainty manner allowing quality triage in determining which samples should be shipped off for formal radiochemical digestion, separation, electroplating and final vacuum alpha and beta spectroscopy (a high resolution version of Figure 3 with no radon progeny present).

## 5.2 Treaty verification applications

Modern CTBT monitoring based on the Radionuclide Aerosol Sampler/Analyzer (RASA) systems require a delay in assaying radioaerosols to allow radon progeny decay. If a large release just went past a monitoring station, it would have to wait for the decay period to elapse prior to even looking for the activity. The discussed approach involving decay curve fitting could be accomplished as a low sensitivity interim measurement enabling this early warning capability for any nominal plume passage prior to the customary wait periods.

## 5.3 Operational health physics applications

Nuclear facilities routinely allow air samples to lay dormant prior to measurement to remove radon progeny through decay. If early estimates were desired, fitting the decay curve would allow just such a graded approach to their defence in depth. Simply put, quality assays can be obtained rapidly if desired.

## 6. Conclusions

Many opportunities to improve standard air sample analysis have been explored with examples provided of some of those which already have experimental results. Utility of the decay curve fitting methodologies appear to have potential application in nuclear safeguards, non-proliferation, radiological emergency response and even routine health physics applications.

## 7. Acknowledgements

This material is based upon work supported by the Department of Energy National Nuclear Security Administration under Award Number(s) DE-NA0002576. Additional support of this work was through a joint faculty appointment between North Carolina State University and Oak Ridge National Laboratory in coordination with the Office of Defence Nuclear Nonproliferation R&D of the National Nuclear Security Administration sponsored Consortium for Nonproliferation Enabling Capabilities (CNEC) with additional support from the Nuclear Regulatory Commission grant NRC-HQ-84-14-G-0059.

## 8. References

- [1] Mercier JF, Tracy BL, d'Amours R, Chagnon F, Hoffman I, Korpach EP, Johnson S, Ungar RK; *Increased environmental gamma-ray dose rate during precipitation: a strong correlation with contributing air mass*; Journal of Environmental Radioactivity; **100**; p 527-533; 2009.
- [2] Code of Federal Regulations; *Derived Air Concentrations (DAC) for controlling radiation exposure to workers at DOE facilities*; 10 C.F.R. § 835 Appendix A; 2011.
- [3] Hayes RB; *False CAM Alarms from Radon Fluctuations*; Health Phys; **85**; p S81-84; 2003.
- [4] Hayes RB; *Problems found using a radon stripping algorithm for retrospective assessment of air filter samples*; Health Phys; **94**; p 366-372; 2008.

- [5] Justus AL; *Prompt Retrospective air sample analysis – A comparison of gross-alpha, beta-to-alpha ratio, and alpha spectroscopy techniques*; Health Phys; **100**-2; p 191-200; 2011.
- [6] Cope SJ, Hayes RB; *Validation of a Rapid, Conservative Transuranic Alpha Activity Estimation Method in Air Samples*; J Radiolog. Prot **39**, 749-765 doi.org/10.1088/1361-6498/ab1bfd.
- [7] Cope SJ, Hayes RB; *Incremental Gains in Transuranic Activity Analysis in Air Samples for Radiological Emergency Response*; Nuc Tech; . DOI: 10.1080/00295450.2019.1590074.
- [8] Cope SJ, Hayes RB; *Preliminary work toward a Transuranic Activity Estimation Method for Rapid Discrimination of Anthropogenic from Transuranic in Alpha Air Samples*; Health Phys; **114**-3; p 319-327; 2018.
- [9] Konzen K, Brey R; *A method of discriminating transuranic radionuclides from radon progeny using low-resolution alpha spectroscopy and curve-fitting techniques*; Health Phys; **102**; p S53-S59; 2012.
- [10] Pollanen R, Siiskonen T; *Minimum detectable activity concentration in direct alpha spectrometry from outdoor air samples: continuous monitoring versus separate sampling and counting*; Health Phys; **90**; p 167-175; 2006.

# On site evaluation of safeguards technical data in multi-cameras surveillance systems

Anibal Bonino<sup>(1)</sup>, Carlos Llacer<sup>(1)</sup>, Fábio Dias<sup>(1)</sup>, Horacio Lee<sup>(1)</sup>, Leonardo Dunley<sup>(1)</sup>, Luis Carlos Machado da Silva<sup>(1)</sup>, Marcos Moreira<sup>(1)</sup>, Max Facchinetti<sup>(1)</sup>, Sonia Moreno<sup>(1)</sup>

<sup>(1)</sup>Brazilian-Argentine Agency for Accounting and Control of Nuclear Materials (ABACC)

Avenida Rio Branco 123 5<sup>o</sup> Andar, Rio de Janeiro RJ. Brazil

[www.abacc.org.br](http://www.abacc.org.br)

## Abstract

During safeguards inspections inspectors normally analyze the safeguards data contained in the surveillance systems, including technical information related to the functioning of the systems, such as black images, authentication of the files, maximum interval between scenes, etc. However, the latest generation of cameras (NGSS) provide additional valuable information about the state of health (SoH) of the components, allowing early detection of failures in the system. This information contains data such as power outages, battery status, processor failures, communication errors, housing opening, temperature, humidity, movement, etc. Although this information is available on the server, it is unpracticable for the inspector, due to time constraints, to analyze this data for a system with multiple cameras.

This paper presents the conceptual program developed by ABACC that interrogates all cameras connected to the server, compares the values of certain parameters to define if they are within the acceptable range and informs the inspector in case of abnormal values.

Considering an adequate selection of variables, the program allows the identification of trends and early detection of technical failures in multi-camera surveillance systems based on NGSS technology. Since the system can operate in-situ, it is convenient for use in installations that do not allow the remote transmission of safeguards and/or state of health data.

Keywords: Nuclear Safeguards, NGSS Surveillance System, On site data evaluation.

## 1. Introduction

During safeguards inspections the agencies inspectors usually analyze the safeguards data contained in the surveillance systems, including some technical information related to the functioning of the systems, such as black images, authentication data, scenes gap, etc. However, the latest generation of cameras like Next Generation Surveillance Systems (NGSS) provide additional valuable information about the state of health (SoH) of components, allowing early detection of failures in the system. This information contains data such as power outages, battery status, memory failures, processor failures, communication errors, housing opening, temperature, humidity, movement, real time clock time and date, etc.

Although this information is available on the server it is unpracticable for the inspector, due to time constraints and file formats to analyze this data for a system with multiple cameras.

This paper presents the conceptual program developed by ABACC using the cameras and server communication possibility that interrogates all devices, compares the values of certain parameters to define if they are within the acceptable range and informs the inspector in case of abnormal figures.

Considering an adequate selection of variables, the program allows the identification of trends and early detection of technical failures in multi-camera surveillance systems based on NGSS technology. Since the system can operate on-site, it is applicable at installations that do not allow the remote transmission of safeguards or state of health data.

## 2. Program tasks description

### 2.1. Time verification and synchronization

One of the typical maintenance activities in a multi-camera surveillance system is to verify that the real-time clock of all cameras is synchronized. This issue is required because some cameras has a complementary image view of the others and for safeguards evaluation is relevant the image capture synchronization. In this sense, the program “time” makes a query with all the modules of the cameras and reports on a single screen each device time of. If higher differences at one minute among the cameras are found the real time clock should be corrected. As an additional issue in some facilities the camera time should be synchronized with the operator time so the figures showed by the software can be compared with operator time. As was mentioned before depending the facility if some differences were found an additional program to synchronize all the cameras clock with the remote review computer time should be run. After the synchronization the technician can check if everything worked successfully running again the “time” program. Figure 1 is showing the main screen of time program in an 18 NGSS system cameras.

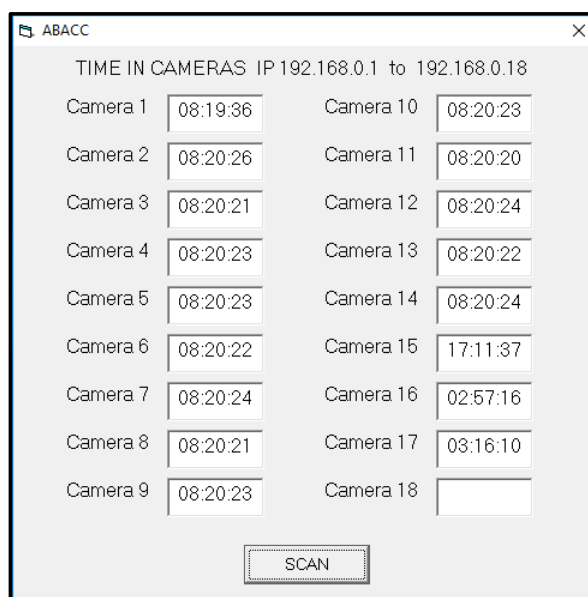


Figure 1

It is important to highlight that real time clock interrogation and synchronization is carried out without having to physically access the cameras. A configurable “.bat” file carries out the synchronization of all devices simultaneously.

### 2.2. Voltage supply check

Although the cameras are battery powered it is important to verify the status of the supply voltage and current consumption because in addition it charges the battery. In this sense, the program will display in only one screen the external supply voltage that depends on the camera power “A” or “B” source. “A” supply comes from the 24V power source from the server, in this condition the cameras reports 12 Volts supply. The “B” power supply comes from the grid 110VAC or 220VAC. When “A & B” power supply are connected the cameras reports 15 Volts. Another important issue related with power supply is the battery voltage which should be between 8.2V to 8.4V when battery is fully charged.

Finally related to voltage supplies is important to check the coin cell battery voltage and internal voltage which keeps the real time clock running and encryption certificates storage from keying process. These figures should be around 3.7Volts and 3.3Volts respectively. It is important to highlight that if the coin cell battery dies the camera erase the master key making it unusable.

### 2.3. Intensity supply check

As in the case of the voltage supply the intensity consumption is another important issue. In this case we have two figures; the external intensity which reports the total consumption (electronic & battery charge) and the internal electronic module consumption. In this condition we can identify that if both intensities values are similar there is not battery intensity for charging. It means that the battery fails or battery is not installed. This issue would be connected with battery voltage figures mentioned in item 2.2. on the other hand, if the external intensity is much higher than the internal intensity the battery is fully discharged or damaged.

For a system with fourteen cameras the voltage & intensity figures are shown in Figure 2.

	V	lint.	Vbat.	lext.	Coin.	Vint.
Dcm_stat_scan_01.txt	11.8 V	194 mA	0.0 V	183 mA	3.6 V	3.3 V
Dcm_stat_scan_02.txt	11.8 V	175 mA	7.5 V	171 mA	3.7 V	3.3 V
Dcm_stat_scan_03.txt	12.0 V	200 mA	0.0 V	187 mA	3.7 V	3.3 V
Dcm_stat_scan_04.txt	11.9 V	204 mA	8.3 V	175 mA	3.7 V	3.3 V
Dcm_stat_scan_05.txt	14.7 V	161 mA	8.2 V	136 mA	3.6 V	3.3 V
Dcm_stat_scan_06.txt	14.7 V	169 mA	8.2 V	134 mA	3.7 V	3.3 V
Dcm_stat_scan_07.txt	11.9 V	192 mA	8.2 V	161 mA	3.6 V	3.3 V
Dcm_stat_scan_08.txt	11.9 V	200 mA	8.2 V	177 mA	3.7 V	3.3 V
Dcm_stat_scan_09.txt	11.8 V	173 mA	8.2 V	144 mA	3.6 V	3.3 V
Dcm_stat_scan_11.txt	11.9 V	187 mA	8.2 V	161 mA	3.6 V	3.3 V
Dcm_stat_scan_12.txt	12.2 V	200 mA	8.4 V	175 mA	3.8 V	3.4 V
Dcm_stat_scan_13.txt	12.0 V	208 mA	8.3 V	173 mA	3.7 V	3.3 V
Dcm_stat_scan_14.txt	11.9 V	202 mA	8.3 V	161 mA	3.7 V	3.3 V
Fin de los archivos						

Figure 2

It can be seeing that the device 1,2 & 3 has not battery installed

### 2.4. Temperature and humidity report

Another important issue is the environmental report like temperature and humidity. During the camera's status scanning the program request the current temperature and humidity and report it in the main screen. Depending of the camera's location the expected temperature and humidity values would be about 30°C and 40% respectively. The request can be configured to get the maximum and minimum values from the cameras keying process.

### 2.5. Lid opening and closing report

Regarding the physical issues the camera stores the accumulative lid opening and closings. These numbers are valuable because they can provide information of improper access to the device by the facility operator during maintenance. In the main screen the program reports the accumulative lid opening and closings.

### 2.6. Memory errors

The surveillance systems implemented by NGSS technology have several cameras and one or more serves to concentrate the image data. Usually the inspectors remove the SD memory at the server which consolidate all facility surveillance cameras images. However, if the server fails the primary information is in the camera SD memory which stores the raw data. So, it is very important to know the memory errors and last error date reported by the main processor during the operational period. A number of several errors could indicate a memory damage or future memory malfunction. It is important that the number of errors would be close to zero from the camera setup date. In the main screen the program reports the accumulative memory errors and last error date. If the error value is zero the date shows the camera keying date.

## 2.6. Power cuts

Another important issue is number of power cuts and last power cut date. Notwithstanding that the cameras have battery supply the “A” and “B” external power interruption is considered a relevant information about facility power line quality. A number of few current cuts in a year it is acceptable. In the main screen the program reports the accumulative power cuts and last power cut date.

## 2.7. Server memory usage

As was mentioned before the surveillance systems implemented by NGSS technology have several cameras and one or more serves to concentrate the image data. In some facilities for cables layout it is used several intermediate camera interfaces to concentrate two or more cameras and finally all images are consolidated in a master interface. In a multi camera system just to concentrate al information in one memory it is divided in quotas. So, it is very important to know the memory usage each camera. In the main screen the program reports the accumulative memory usage. In order to avoid data lost this figures should be below 100%.

All this information is provided by the camera and server in “.XML” files that are converted in friendly view by the software and displayed in the Figure 3.

DCM-C5	V	Iint.	Vbat.	Iext.	Coin.	Vint.	Temp.	Hum%	Open	Clos.	Memory Error	Power Cuts		
Dcm_stat_scan_01.txt	11.8 V	192 mA	0.0 V	190 mA	3.6 V	3.3 V	33 C	35 %	9	9	6	2019-02-22	7	2019-02-20
Dcm_stat_scan_02.txt	11.8 V	175 mA	0.0 V	167 mA	3.7 V	3.3 V	32 C	37 %	8	8	2	2018-10-10	8	2019-01-25
Dcm_stat_scan_03.txt	11.9 V	185 mA	0.0 V	167 mA	3.7 V	3.3 V	31 C	40 %	3	3	1	2018-11-09	4	2019-01-08
Dcm_stat_scan_04.txt	11.9 V	204 mA	8.2 V	169 mA	3.7 V	3.3 V	32 C	37 %	5	5	1	2018-09-27	8	2019-01-31
Dcm_stat_scan_05.txt	14.7 V	161 mA	8.3 V	138 mA	3.7 V	3.3 V	34 C	35 %	8	8	1	2018-11-09	9	2019-01-23
Dcm_stat_scan_06.txt	14.7 V	167 mA	8.3 V	134 mA	3.7 V	3.3 V	35 C	32 %	7	8	2	2019-02-12	7	2019-01-23
Dcm_stat_scan_07.txt	11.9 V	192 mA	8.2 V	163 mA	3.6 V	3.3 V	36 C	34 %	7	8	0	2018-11-09	7	2019-01-23
Dcm_stat_scan_08.txt	11.9 V	190 mA	8.2 V	163 mA	3.7 V	3.3 V	35 C	34 %	5	7	1	2019-02-12	8	2019-01-23
Dcm_stat_scan_09.txt	11.9 V	167 mA	8.2 V	144 mA	3.6 V	3.3 V	34 C	35 %	8	8	0	2018-11-09	8	2019-02-12
Dcm_stat_scan_10.txt	11.8 V	181 mA	8.2 V	159 mA	3.7 V	3.3 V	35 C	35 %	6	7	2	2019-02-12	6	2019-01-23
Dcm_stat_scan_11.txt	11.9 V	194 mA	8.2 V	165 mA	3.6 V	3.3 V	35 C	35 %	7	7	0	2018-11-09	5	2019-01-23
Dcm_stat_scan_12.txt	12.3 V	185 mA	8.4 V	157 mA	3.8 V	3.4 V	35 C	37 %	6	7	0	2018-11-09	9	2019-01-23
Dcm_stat_scan_13.txt	11.9 V	200 mA	8.2 V	169 mA	3.7 V	3.3 V	36 C	34 %	7	7	1	2018-11-09	5	2019-01-23
Dcm_stat_scan_14.txt	11.9 V	202 mA	8.2 V	153 mA	3.7 V	3.3 V	35 C	34 %	5	7	0	2018-11-09	8	2019-01-23
Dcm_stat_scan_15.txt	11.8 V	181 mA	8.2 V	159 mA	3.7 V	3.3 V	35 C	35 %	6	7	2	2019-02-12	6	2019-01-23
Dcm_stat_scan_16.txt	14.7 V	167 mA	8.3 V	134 mA	3.7 V	3.3 V	35 C	32 %	7	8	2	2019-02-12	7	2019-01-23
Fin de los archivos														

DCI	M.Usage	M.Capacity
Dci_stat_scan_100.txt	89%	127827 MB
Dci_stat_scan_103.txt	29%	15923 MB
Fin de los archivos		

Figure 3

## 3. Conclusions

In this first phase the system has been tested only during maintenance activities in facilities with four cameras and others up to eighteen cameras and it has proven to be a powerful tool for the technical area to identify the surveillance devices status.

The real-time clock adjustment has proven to be one of the most valuable tools for multi-camera systems.

The objective of concentrating all information on a single screen has been satisfactorily fulfilled.

The variables selected for evaluation during this period indicate that the technical operational status of the devices is accurate.

The power cuts indicate that the system is able to recover properly of a power failure without any damage. In addition, it shows the usefulness of installing in the future a redundant power supply for the cameras which were already implemented in some facilities.

In conclusion the application of on-site evaluation software during the interim inspection, by the inspectors, is considered a future powerful tool to know the operational status of the surveillance devices at the facilities.

# Applying Knowledge Retention to Preserve a Core Safeguards Technical Area

Natacha L. Peter-Stein<sup>1</sup>, Heidi A. Smartt<sup>1</sup>, W. Cody Corbin<sup>1</sup>

<sup>1</sup>Sandia National Laboratories  
P.O. Box 5800  
Albuquerque, NM, USA  
E-mail: [npeters@sandia.gov](mailto:npeters@sandia.gov)

## **Abstract:**

*The international safeguards community is facing the significant challenge of accelerating loss of practical safeguards expertise due to retirement of established and knowledgeable experts. This loss of critical expertise is particularly evident in safeguards areas that traditionally receive less attention during inspector or safeguards staff training. One such area is Containment/Surveillance (C/S). Existing training for C/S is usually relegated to a small part of broader-scope training, where far more attention is devoted to accountancy measures, nondestructive assay, and other aspects of safeguards.*

*Sandia National Laboratories (SNL) has been key to designing, developing, and implementing C/S technologies and approaches since the 1970s. C/S is a key competency of SNL and of critical importance to all past and evolving international nuclear safeguards approaches. To counter the persisting issue of knowledge loss, SNL is currently engaging in a C/S knowledge retention program to provide opportunities for young professionals to work directly with mid-career safeguards practitioners as well as senior safeguards practitioners on safeguards C/S related topics. This initiative aims at capturing institutional knowledge on C/S and support knowledge retention and transmission bringing safeguards practitioners in close and constant collaboration.*

*This program has several pillars for knowledge transfer which include C/S history, C/S technologies (past, present, and future), vulnerability reviews/assessment, best practices for C/S technologies and approaches and finally, current and future technologies and issues.*

*This paper will describe efforts to allow for knowledge retention and transmission of one of SNL core safeguards technical areas. It will also highlight how new key contributors can be tied into the subject matter, not only from within the traditional safeguards field but from other technical areas like chemistry. The paper will further show how to broaden the C/S safeguards horizon by bringing in novel ideas from different industries and unlikely partners to redefine the future technological directions of C/S. SAND2019-0265 A.*

**Keywords:** International Safeguards; Containment/Surveillance; Knowledge Retention

## **1. Introduction**

Due to retirement of established and knowledgeable experts, the international safeguards community is facing the significant challenge of accelerating loss of practical safeguards expertise. This is part of a broader trend in the nuclear industry where staff that started work in the late 1970s and 1980s, when nuclear fleets were expanding in a number of countries world-wide, are starting to retire, leaving a gap as fewer newcomers enter the nuclear industry. A similar situation is visible in the area of international safeguards: long-standing experts that have guided safeguards implementation through the Comprehensive Safeguards Agreement (INFCIRC/153) and the Model Additional Protocol (INFCIRC/540) have to hand over the reins, but often without an appropriate transition plan or sufficient time to pass along a lifetime of expertise.

While the problem of knowledge retention is universal through the international safeguards and non-proliferation community, it is even more profound in smaller, technical areas that receive less attention during safeguards inspector and staff training which focus on accountancy measures and which are burdened with an ever-widening scope of activities related to the verification of the absence of undeclared activities under the Additional Protocol and State-Level safeguards. One such technical area is Containment and Surveillance (C/S).

C/S activities are indispensable for the safeguarding of declared nuclear facilities to establish Continuity of Knowledge (CoK) about the absence of diversion efforts in-between inspector visits. Instrumentation installed by the IAEA needs to be rugged, highly reliable, and the data generated tamper-indicating. Designing, operating, and maintaining such instruments (e.g., surveillance cameras and seals) requires not only specialized technical expertise, but also knowledge in other areas such as data encryption and authentication, secure storage, and tamper-indicating enclosures. The combination of skills needed is quite unique for international safeguards and as such the relevant technical staff has to be prepared and trained in-house over time.

Unexpected departure of knowledgeable staff and retirement without sufficient time to train replacement can lead to the loss of expertise that is difficult to replace. As such, knowledge retention efforts become an essential plan of human capital development in this area. This issue is by no means restricted to safeguards agencies such as IAEA or EURATOM alone, but also affects the numerous research and development laboratories that for decades have supported the development of C/S instrumentation, performed vulnerability assessments, and who have supplied expertise to the international safeguards community.

The following paper will outline the knowledge retention management effort at Sandia National Laboratories (SNL) and describe several pillars for knowledge transfer which include C/S history, C/S technologies (past, present, and future), vulnerability reviews/assessment, best practices for C/S technologies and approaches, and finally, current and future C/S technologies and issues. It will also highlight how new key contributors can be tied into the subject matter, not only from within the traditional safeguards field but from other technical areas like chemistry. The paper will further show how to broaden the C/S safeguards horizon by bringing in novel ideas from different industries and unlikely partners to redefine the future technological directions of C/S.

## **2. Sandia National Laboratories and C/S**

Traditional safeguarding of declared facilities includes a combination of inspections, analysis, and C/S measures. C/S methods ensure CoK about nuclear materials and stay at a facility between inspections. In the early days of the first rollout of C/S measures, the IAEA had some internal capabilities for technology development and built film camera systems as well as software-based systems using microprocessor technology in the 1970s. But quickly the design and development shifted from internal resources to outside parties, primarily to the laboratory community of the Treaty on the Non-Proliferation of Nuclear Weapons (NPT) Member States and the private sector.

SNL has been key to designing, developing, and implementing C/S technologies and approaches since the 1970s. During the early to mid 1980s, SNL was tasked to develop unattended monitoring systems, including surveillance and seals. In the early 1980s SNL developed the Cobra passive fiber optic loop seal [1]. The Cobra seal eventually became a standard tool for IAEA safeguards and EURATOM, and is – in an updated form – still a standard today.

In the mid 1980s, SNL developed a prototype surveillance system called the Modular Integrated Video System (MIVS) under DOE's program for international safeguards. Interestingly, even these early technologies included a tamper-indicating enclosure and tamper indication of the video and power line from the main unit to the camera unit, even though such measures were restricted in efficiency due to the analog nature of the data media. Requirements evolved from interactions between SNL and the IAEA's organization for system development and in the late 1980s MIVS was released for commercialization, involving the private sector for the first time [1].

Another effort beginning in the mid 1980s was for an active fiber optic loop seal for potential use by the IAEA. It was based on an earlier SNL developed RF seal that had been designed for domestic

safeguards at the Hanford site, but would require the addition of a tamper-indicating enclosure and other tamper-indicating features. It was called the Authenticated Item Monitoring System (AIMS). Included in AIMS, and all subsequent digital systems was the concept of data authentication. International safeguards rely on accurate assessments of nuclear material and activities. Data authentication ensures that safeguards authorities can trust the information they receive [1]. The associated data security R&D formed the basis for the cryptographic data authentication approaches still used today.

SNL's safeguards work in the 1990s was influenced by the policy development manifested in the 'Programme 93+2', the results of the NPT review conference in 1995, and the Model Additional Protocol in 1997 which changed the legal framework for international safeguards oversight and expanded activities beyond declared nuclear facilities and traditional safeguards. From the late 1990s to present, SNL has developed systems and technologies for both traditional safeguards and safeguards enhanced through the Additional Protocol and has provided analyses, vulnerability assessments, training and demonstrations throughout the safeguards community.

In the mid-2000s, SNL developed a new generation of RF-based active sealing technology supported by a standardized communications protocol: The Remotely Monitored Sealing Array (RMSA). Installed as a series of active loop seals at dry storage site of spent fuel, a large number of RMSA seals can constantly report data back to a data collection translator via authenticated and encrypted wireless transmission. The translator can alternatively store data locally for retrieval by an IAEA inspector or – when allowed – transmit it automatically to the remote monitoring data center at IAEA headquarters in Vienna, Austria [2].

Another instance of the development of creative solutions for C/S is SNL's collaboration with Savannah River National Laboratory (SRNL) on a tamper-indicating, ceramic seal. This seal consists of a ceramic body with fluorescent tamper-indicating coating, electronic monitoring of unauthorized opening or penetration, a self-securing wire, and in-situ verification with a handheld reader [2]. SNL continues its tradition of developing safeguards surveillance technologies with its recent Standoff Video project which offers options for the surveillance of objects in highly radioactive and difficult-to-access hazardous environments [2, 3].

SNL's rich history and deep expertise in the authentication of data and protecting instrumentation from tampering has made the laboratories a frequent provider of vulnerability assessments of solutions developed by other parties. Several decades of experience in independent and rigorous testing to take on the adversary's role and try to defeat a system have made SNL a key partner in the certification process of solutions for routine safeguards use [2].

### **3. Relevance of C/S in Future IAEA Safeguards**

With the shift from quantitative safeguards under the Comprehensive Safeguards agreement towards a more qualitative assessment of a State as a whole under State-Level safeguards, the question arises about the relevance of technical measures and C/S. If a state can be evaluated based on all available information from various sources, is CoK still a critical element or could such resources be of better use elsewhere in the analysis process?

While such a reallocation of resources might be tempting, the determination of compliance with safeguards agreements remains based on the verification of whether a diversion of nuclear material took place. Information analysis of a state as a whole is an extension of using all available data, but not a replacement for the usual verification methods applied at a facility. As such, C/S, along with the other disciplines such as material accountancy or sampling and analysis, will remain relevant [4].

This relevance underscores the dangers of the loss of critical expertise and the need for knowledge retention measures so much more immediate. C/S measures will need to continue to evolve to stay ahead of advancing methods to defeat older technologies, and a skilled workforce will be needed to develop new solutions, test new approaches, and train safeguards inspectors in their use [4].

## 4. Knowledge Retention at Sandia National Laboratories

SNL is currently engaging in a C/S knowledge retention program to provide opportunities for young professionals to work directly with mid-career safeguards practitioners as well as senior safeguards practitioners on safeguards C/S related topics. To support this program (and others), SNL has developed a Knowledge Transfer (KT) Process (Figure 1) for Subject Matter Experts (SME) in order to guide those who are involved in off-boarding activities (whether that be an internal move/transfer or other departure such as retirement) through a best-practice, step-by-step approach designed to support the successful transition of projects, work, and especially key knowledge [5].

The purpose of this process is also to stimulate conversations with regards to Knowledge Management and Knowledge Preservation by providing a basic structural framework to begin this work. Figure 1 depicts the flow of this process [5].



**Figure 1:** Knowledge Transfer Process for HR Business Partner (HRBP), Management and SMEs

Note: This process is designed to be used to meet urgent/emergent KT/Off-Boarding needs (Steps 1-9) as well as help support short and long-term Knowledge Management Process that enhance and build business/team/innovation capacities (Steps 4-12).

In the context of our C/S knowledge retention program we used the Steps 4-12 as describe below to guide our project goals and methodology:

**Step 4 – Identify Key/Critical Roles:** The purpose of this step is to identify the key/critical roles that are essential to fulfilling the C/S group’s mission. It is best practice to ensure there is bench strength within the key/critical roles.

**Step 5 – Identify Key SME’s:** Identification of the individuals who have the key/critical knowledge that is essential in fulfilling the group’s mission.

**Step 6 – Identify Key/Critical Tasks:** This step is designed to gain an understanding of what tasks are critical to a role or job.

**Step 7 – Identify Key/Critical Knowledge:** Once tasks have been identified and knowledge to do those tasks as been identified, this knowledge needs to be preserved and in a timely manner. As a tool, a

Knowledge Capture Decision Matrix could be used to determine what information is important to capture and when it needs to be captured.

**Step 8 – Set Knowledge Capture/Transfer Priorities:** The purpose of this step is to rank the importance of knowledge as it relates to ensuring the capabilities of the group are preserved. This priority list should drive the order of knowledge capture efforts in the next step.

**Step 9 – Create Knowledge Capture/Transfer Plan:** The purpose of this step is to create an actionable plan for both capturing and transferring essential knowledge and what methods will be used to do this work.

**Step 10 – Process Documentation:** In many cases, processes are all in people's heads (tacit knowledge) and it needs to be made explicit. Therefore, it is important for SMEs to capture essential processes that support their work, their ideas, their thinking, etc.

**Step 11 – Project Documentation:** Project documentation is very important for the continuity of many of the group's programs, especially those programs that have many projects associated with them and that extend over a broad period of time. This work is also essential when someone is vacating a position and others will be taking over where they left off. The sharing of the project documents is essential to the off-boarding/on-boarding process.

**Step 12 – Other Identified Knowledge Transfer Activities [5].**

## **5. C/S Knowledge Retention Program**

C/S is a key competency of SNL and of critical importance to all past and evolving international nuclear safeguards approaches, yet is greatly underrepresented in the existing training and as such particularly sensitive to knowledge loss. Existing training for C/S is usually relegated to a small part of broader-scope training, where far more attention is devoted to accountancy measures, nondestructive assay, and other aspects of safeguards.

The initiative of a C/S knowledge retention program at SNL aims at capturing institutional knowledge on C/S and support knowledge retention and transmission bringing young professionals and mid- to high-level career safeguards practitioners in close and constant collaboration, following the process outlined above.

This program was envisioned to comprehensively cover the subject area. To set the stage, it is covering all concepts of (dual) C/S, explain the concept of CoK, and outline the major elements that comprise C/S and also the following: tags, seals, tamper-indicating enclosures, data authentication and encryption, video surveillance, video review, unattended systems, remote systems, secure communication, vulnerability assessments, etc.

In addition to unfettered access to the accumulated expertise of mid- and high-level safeguards experts, young professionals are working hands-on with funded projects and actual devices, equipment and systems. The program also covers the legacy systems and the evolution of C/S over the years in reviewing safeguards knowledge left by recently retired safeguards experts. Understanding safeguards policy is critical for the appropriate placement of new research and development projects, as such, fundamental safeguards concepts (comprehensive safeguards agreement, model additional protocol, state-level concept, etc.) was covered, as well.

Consideration of candidates for the C/S knowledge retention program included SMEs with technical background, junior level experience at SNL, and high interest/enthusiasm for the field. SNL was initially unable to find a candidate with all three characteristics. However, a senior staff member had a new junior staffer (less than two years at SNL) on an NNSA project (NA-22 funded project "Tamper-Indicating Enclosures with Visually Obvious Tamper Response"). The young professional has a PhD in chemistry and works in the "Microsystem Packaging and Polymer Processing" department. While we did not initially consider a chemistry background for the candidate, he presented numerous ideas in the chemical field that could be relevant to C/S and tamper-indicating technologies. These ideas have the

potential to significantly contribute the technical aspects of C/S. Furthermore, he demonstrated an enthusiasm for the field, and thus was ultimately selected for the position.

## 6. C/S knowledge Retention Program: Work in Progress

This project has identified and is currently training the selected junior staff member with several pillars for knowledge transfer. These include:

- C/S history (including NNSA & ESARDA C/S course for background as well as SNL historical documents)
- C/S technologies (past, present, and future)
- Vulnerability reviews/assessments
- Best practices for C/S technologies and approaches
- Current and future C/S technologies and issues.

Once the individuals who have the key/critical knowledge that is essential in fulfilling the C/S knowledge retention program's mission were identified, the team identified and reviewed relevant literature and organized exchange with senior- and mid-level experts for the pillars mentioned above.

As part of the program, the Sandia Technology Training and Demonstration Area for equipment demonstration and hand-on learning was used (Figures 2 and 3).



**Figures 2 and 3:** Equipment demonstration during the C/S Knowledge Retention Program

Furthermore, SNL selected relevant training/workshop/conferences for the junior staff to attend and contribute, including:

- INMM Just Trust Me Workshop (March 2019): This workshop provided a professional development opportunity to learn from policy and technology experts involved in safeguards, security, and arms control around the theme of how we establish and authenticate trust. Its format combined presentations, and scenario-based table top exercises that integrate key themes from the presentations (Figures 4 and 5).
- 41<sup>st</sup> ESARDA Annual Meeting (May 2019): The 2019 Symposium marks the 50th anniversary of ESARDA, which provides a unique opportunity for research organizations, safeguards authorities and nuclear plant operators to exchange information on new aspects of international safeguards and non-proliferation, as well as recent developments in nuclear safeguards and non-proliferation related research activities and their implications for the safeguards community.
- DOE/NNSA's introductory course on nuclear nonproliferation and safeguards (June 2019): The purpose of the course is to provide participants with a fundamental understanding of the nuclear fuel cycle, the nuclear nonproliferation regime, international safeguards agreements and verification mechanisms including: nondestructive assay techniques and equipment, destructive assay techniques, environmental sampling, and C/S.



Figures 4 and 5: INMM Just Trust Me Workshop

## 7. Knowledge Retention and Cross-disciplinary Synergies

Exposing young professionals from other scientific fields to expertise transmitted during knowledge retention exercises can have an exciting side effect: it can inject novel ideas from different industries and unlikely partners into the original field. As an example, the young professional attended the 2018 Packaging Exposition (Pack Expo) in Chicago, IL. It provided an opportunity to evaluate unique techniques for tamper indication and unique identifiers for safeguard application purposes, from a field that is usually not connected to international safeguards in any way.

During this expo, there was a particular process that was identified that showed potential for application in C/S. A facile UV-curable ink was demonstrated on a small piece of plastic. The piece of plastic was placed on a conveyor belt that then went under an ink applicator followed by an UV light that instantly cured that ink into a solid. If the plastic was removed before the UV light then the ink easily wipes off. Upon closer examination of the cured ink it was seen that the ink application process is performed in lines and that the curing process causes patches of ink to come together. A second sample was requested from the company representative to compare the reproducibility of the ink patches upon curing. The optical images of the two samples is provided below (Figure 6) along with three particular areas in each.

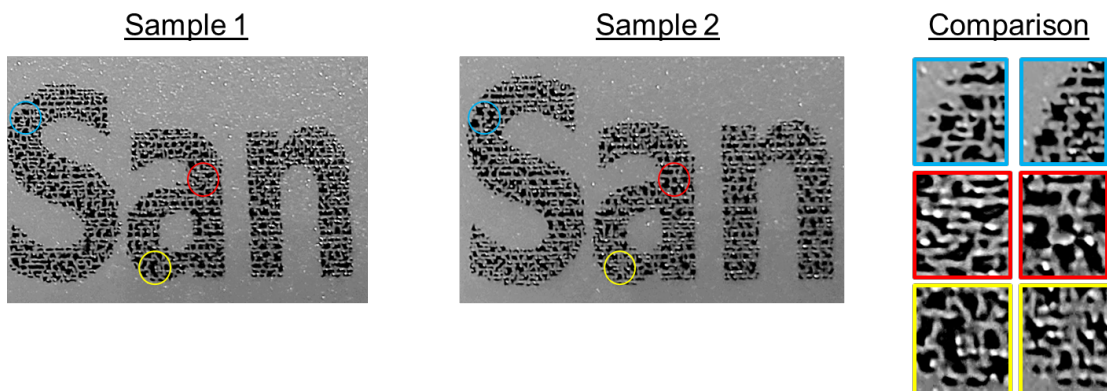


Figure 6: Two samples of UV-cured ink on a piece of plastic. Close-up comparisons of individual areas show drastically different patterns.

Due to the stochastic behavior of the curing process, every print and cure of ink is unique and could potentially be used as an efficiently-made identifier for safeguards applications. Furthermore, after discussions with printing subject matter experts, they suggested that the stochastic behavior and the minimum height of the ink would be very difficult to reproduce or counterfeit. Further investigation of this idea will follow.

## 8. Conclusion

Knowledge retention is a significant challenge in general and even more pronounced in smaller, niche applications of international safeguards, such as C/S. It can be addressed with foresight, planning, and the application of a standardized process to capture and preserve critical knowledge. Following the example of a young professional at SNL, benefits of such an effort become quickly visible.

With the understanding of the importance of the mentoring aspect, the young professional selected for the C/S knowledge retention program has in turn been encouraging his post-doctorate to join certain background sessions of the program to also get acquainted with not just the C/S application space itself, but also the very important role SNL has had in the past, present, and future in international safeguards. The post-doctorate is also significantly involved in the novel tamper-indicating enclosure project funded by NNSA. Together they bridge the gap between these applications spaces and the materials that are developed for them. Safeguards are constantly in need of updated or novel materials and mechanisms and utilizing materials scientists with application space knowledge retention is a promising avenue for the future of safeguards.

Finally, as a result of this program, a recent opportunity has presented itself for the involvement of the junior professional in areas related to vulnerability assessment. This topic is a key component of many areas of research, including those seen in C/S. If involvement is proven successful, additional experience will be obtained that will aid in the development of this retention program.

## 9. Acknowledgements

The authors are grateful to the National Nuclear Security Administration (NNSA) Office of International Nuclear Safeguards (NA-241), Safeguards Human Capital Development Program for support provided to Sandia National Laboratories. Sandia National Laboratories is a multi-mission laboratory managed and operated by National Technology and Engineering Solutions of Sandia, LLC., a wholly owned subsidiary of Honeywell International, Inc., for the U.S. Department of Energy's National Nuclear Security Administration under contract DE NA0003525. This paper is released as SAND2019-4332 C.

## 10. References

- [1] Tolk, K, Mangan, Glidewell, D, Matter, Whichello, J; *Safeguards Sensors and Systems: Past, Present, and Future*; Journal of Nuclear Material Management, vol. XXXV, no. 4, pp. 101 – 109, Summer 2007.
- [2] Haddal, R, Blair, D., Finch, R; *International Nuclear Safeguards and Sandia National Laboratories*; Proceedings of the 57<sup>th</sup> Annual Meeting of the Institute for Nuclear Materials Management, Atlanta, Georgia, July 2016.
- [3] Baldwin, G., Sweatt W., Thomas, M.; *Authentication Approaches for Standoff Video Surveillance*; Abstract for the IAEA Symposium on International Safeguards: Linking Strategy, Implementation and People, IAEA Headquarters, Vienna, Austria, October 2014.
- [4] Carlson, J.; *Future Directions in IAEA Safeguards*; Harvard Kennedy School, Belfer Center for Sciences and International Affairs, November 2018.
- [5] VanArsdale, A.; *Off-Boarding/Knowledge Transfer Toolkit*; Sandia National Laboratories; SAND2017-13443PE.

## 3D image recognition of nuclear fuel waste using tree-based classifiers

Stéphane Puydarrieux<sup>1</sup>, Mickaël Picq<sup>2</sup>, Sébastien Roman<sup>3</sup>,  
Yann Gallice<sup>3</sup>, Jean-Jacques Dupont<sup>4</sup>

1 Orano Cycle La Hague, 2 PICQ Consulting, 3 Siléane, 4 Orano Projets

[stephane.puydarrieux@orano.group](mailto:stephane.puydarrieux@orano.group)

### **Abstract:**

*In the context of nuclear waste management, ORANO must deal with old nuclear fuel waste from UNGG reactors in order to store them in specific barrels within optimal safeguard conditions. To prevent H<sub>2</sub> production within that kind of storage, Magnesium and Aluminum materials must be identified throughout the production, and quantified in each barrel.*

*Because of both the production line cell being hidden and the required production rate being one output per second, a human recognition of those materials would be difficult. Thus, an artificial intelligence approach, relying on tree-based classifiers, was developed. Knowing that each kind of material is associated with a specific geometry, the learning algorithm was built around a 3D reconstruction model where each material had to pass through a laser ray with a robotic handling help.*

*A selected range of samples was defined to let the algorithm learn to identify the materials. Firstly, methodic tests were conducted in order to minimize the material recognition error of the algorithm. Then, non-regression tests were required and performed consistently, from the R&D phase to the commissioning steps, to measure the impact of the working environment on the algorithm performance. Finally, additional developments of the learning algorithm were engaged to deal with issues related to the representativeness of the sample.*

**Keywords:** nuclear waste management, machine learning, 3D images

### **1. Context**

ORANO La Hague is a leader in nuclear materials recycling. The first facilities of ORANO La Hague site were designed to recycle the first generation of nuclear fuel burnt in French gas-cooled reactors (Uranium Naturel Graphite Gas, UNGG fuel). The structural parts of the fuel were separated from the Uranium inner parts by a mechanical process, and wastes were stored in silos.

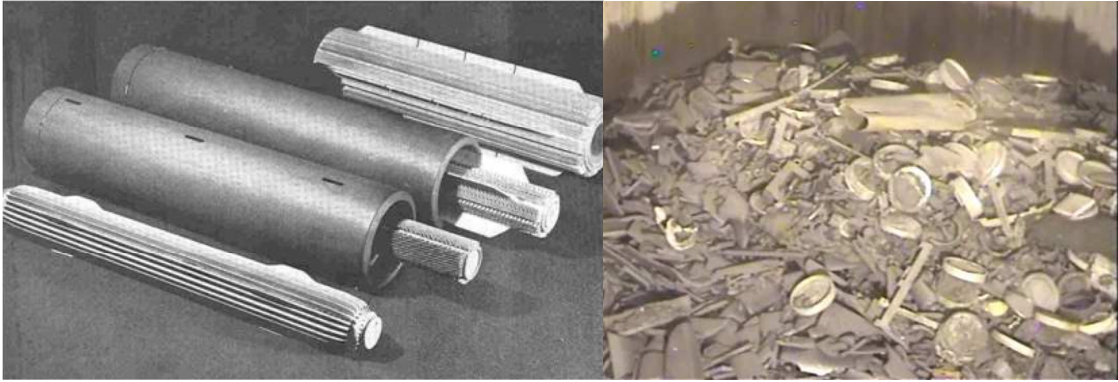


**Figure 1:** Original UNGG Fuel over view, and bulk waste in the silo

The silo 130 mainly contains UNGG structural parts, which are graphite (90%) magnesium and aluminum wastes. It received the first UNGG waste in 1976 until the end of the eighties. Because of safety standards evolution, the retrieval of such legacy waste is an important Group undertaking for Orano.

The difficulties inherent in retrieving and packaging waste stored in silo 130 are notably the imperfection of the data. Characterization prior to retrieval is based on records of its production and calculation. Due to a fire-accident in 1981, the storage in silo 130 can be divided in 3 main layers of wastes. As the lower layer is flooded since this fire-accident, the 2<sup>nd</sup> layer was temporally immersed, and the upper layer has never been on water contact. The corrosion kinetic of magnesium is quite different for each layer.

The aim of the retrieval program is to empty the silo 130 and store the waste in specific barrels within optimal safety conditions. The wastes would be flooded into the barrels, so H<sub>2</sub> production would be take place within the barrel and must be evacuated. The barrels are covered by a lid which carries gas exhaust orifices which have sintered metal porous filter PORAL®. In the accidental situation of a barrel falling down in the storage, the filter media would be flooded, thus the gas disposal requirements cannot be met until the barrel would be well stored and the filter media dried. To prevent accidental situation due to H<sub>2</sub> production, the safety requirements are laid down to limit the H<sub>2</sub> production rate within the barrels by limiting the quantity of magnesium and aluminum.

There are two ways of H<sub>2</sub> production: the radiolysis of water by radio-nuclides and the corrosion of magnesium and aluminum stored underwater. As the radiolysis of the water cannot be avoided, the magnesium materials must be identified throughout the production, and quantified in each barrel to reduce as low as possible the H<sub>2</sub> production rate. The aluminum material must be identified and taken off from the production line.

Regarding the high radiation dose rate, a human handle process cannot be considered. Each type of waste has specific geometric characteristics: magnesium parts are thin and long or with cylindrical portion; aluminum parts are plate-shaped; and graphite part have random geometry properties due to the grinding mechanism in the retrieval grapple. Thus, a machine learning approach, relying on tree-based classifiers, was developed based on geometry recognition.

An effective identification requires a process enable to pick out each piece individually throughout the production line. So that robotics arms took place upstream of the optical process of recognition which is programmed with "pick & place" artificial intelligence based proprietary algorithm by SILEANE. Each individual waste part is led under the optical AI based recognition process. As the piece pass through a laser ray, a combination of optical devices scans the laser ray deformation. A large range of geometrics parameters are drawn from the 3D reconstruction of each single piece and then data are analyzed by a tree-based classifier. The results are given as a recognition ratio for each kind of waste. The higher ratio corresponds to the most probability of recognized waste material family.

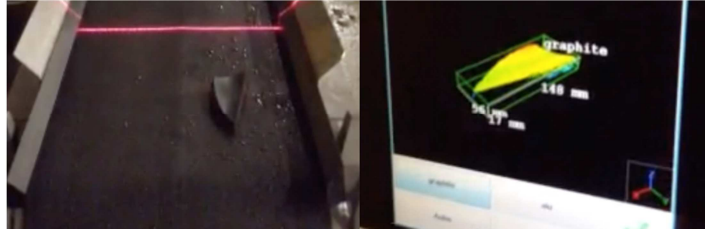


**Figure 2:** 3D reconstruction of a graphite piece after passing through the laser ray

The effectiveness of that kind of machine learning algorithm depends on a good representative range of waste sample taught to the classifier. A selected range of samples was defined to train the algorithm to identify the objects. These samples were defined by taking account all available information: production records, UNGG fuel fabrication data sheets, consequences of more than 30 years of underwater storage by analyzing the corrosion kinetic in laboratory ... Some sample were drawn from a similar silo.

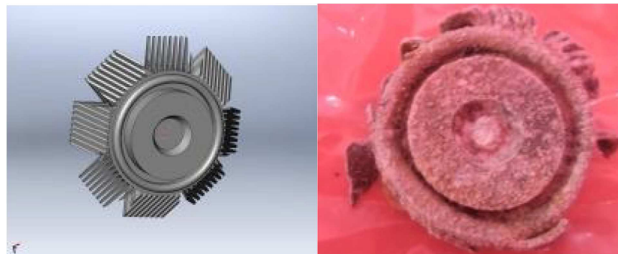


**Figure 3:** Magnesium queusot defined from fabrication date vs waste drawn from silo

Methodic tests were conducted in order to define a well calibrated classifier which is able to recognize magnesium parts, avoiding “false-negatives” (magnesium identified as graphite) and “false-positives” (graphite identified as magnesium).

## 2. Description of the chosen solution

### 2.1. Object picking

The first step towards objects identification is the extraction of objects one by one. Indeed, to obtain a good description of an object, it must be scanned alone.

Starting from a 3D reconstruction of the pick area obtained by a stereoscopic vision system, an algorithm detects areas that could be taken either by a suction cup or by a clamp without knowing the geometry of the objects to pick. Those instructions are sent to a robot, which can then pick up the objects and bring them to a conveyor for the scanning phase.

It can happen that the robot picks up several objects at once. However, most of the time, these objects are separated when they are dropped on the conveyor. For other cases (attached objects, objects in another object...) this can lead to misidentifications.

### 2.2. 3D reconstruction

In order to obtain an accurate 3D representation of an unknown object on the conveyor, 3D laser scanning is the best solution:

- Cameras can be far from the object
- The length of the object doesn't need to be known

- High resolution (less than 0.3 mm at 3 m)

Laser triangulation is based on the projection of a laser over an object and the image is captured by a digital camera. The 3D position of the laser line over the object can be calculated by trigonometry, if we know the distance between the laser source and the camera (called baseline) and the angle between the baseline and the laser beam.

Since the objects are placed on a conveyor, the system laser / cameras do not need to move to scan an object: an image of the laser line is acquired every time the conveyor advances one millimetre forward and when the end of the object is detected (i.e. when no more shifts are detected in the laser line), we sum the reconstruction of all the stored lines to obtain the 3D reconstruction of the whole object.

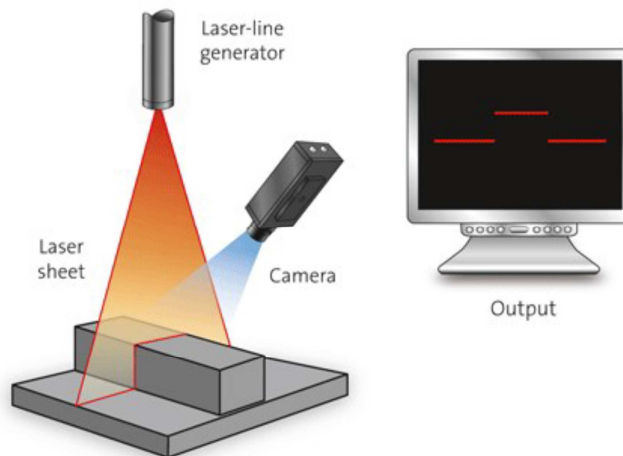


**Figure 4:** Principle of the laser triangulation

However, as a large range of shapes and compositions need to be detected, some issues had to be resolved.

In a single camera triangulation system, some areas may not be reconstructed due to the fact that the laser line may be hidden behind some parts of the objects. So a second camera was placed on the opposite side to fill in these shadow areas (Figure 5).

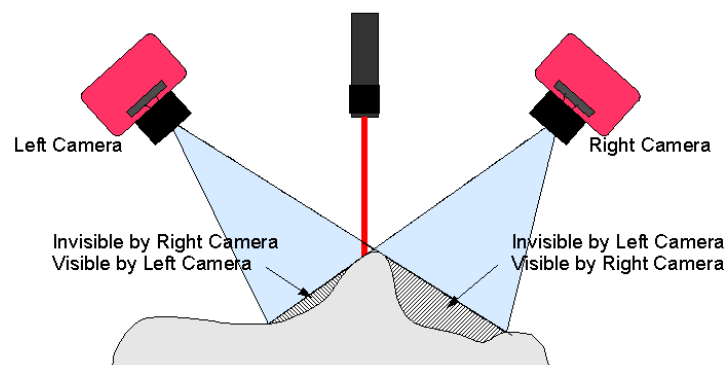


**Figure 5:** A two cameras triangulation system

Some objects are highly reflective (wide and bright laser line as on Figure 6) while others are highly absorptive (narrow and light laser line as on Figure 7).

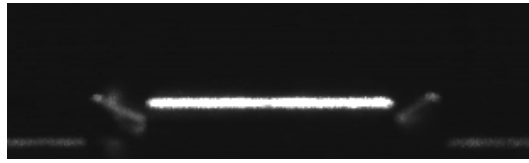


**Figure 6:** Laser on a highly reflective object

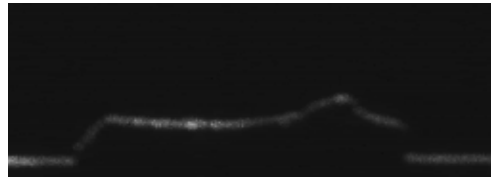


**Figure 7:** Laser on a highly absorbent object

If a low threshold is chosen, in order to be able to see a very light line, reflections can occur on reflective objects (Figure 8).

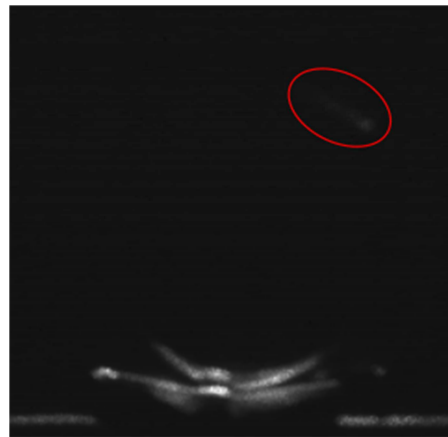


**Figure 8:** Reflection on a reflective object

To solve this issue, a multiple thresholds laser line detection was developed.

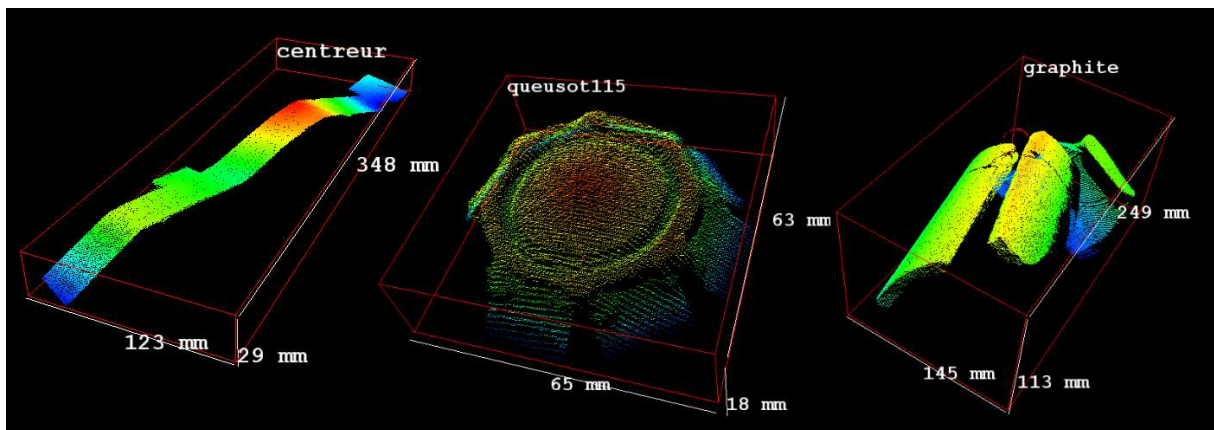


**Figure 9:** 3D reconstructions

### Points-cloud search

It can happen that two objects pass under the laser line side by side (due to a double grip, a jamming or if an object is long enough for the next object to be placed nearby). In this case, the 3D reconstruction will return one points-cloud containing all the objects. To retrieve the shape parameters of each object, it is necessary to dissociate the points-cloud of each object.

Then, an optimized points-cloud search algorithm was developed to quickly separate objects even if they are intertwined (as long as there is no contact between the two).

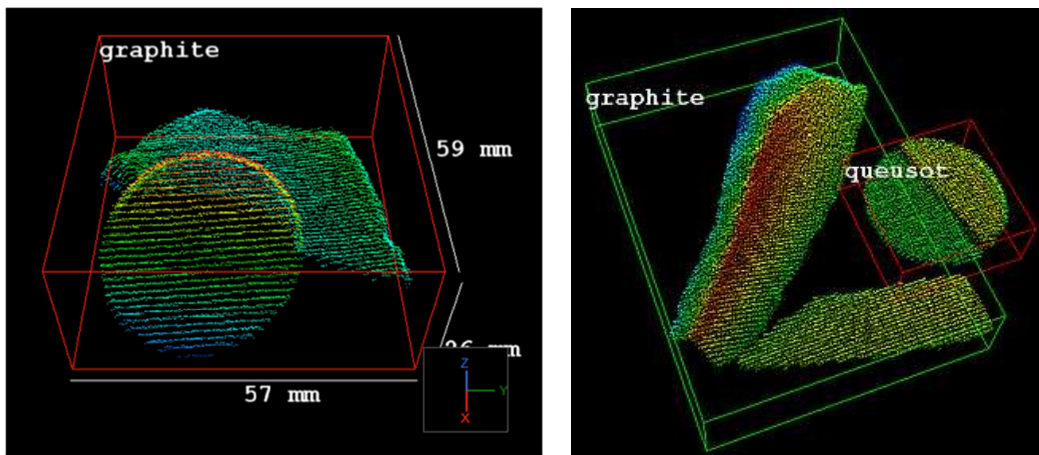


**Figure 10:** Examples of objects side by side

When there is no contact between two objects (like the queusot and the graphite on the right of Figure 10), the algorithm is able to separate the objects and the identification of both objects is possible. However, if two objects touch each other (like the two graphite parts), the choice was made not to try to separate them, which would have significantly increased the computation time and would have led to many separation errors for complex objects (such as the graphite object on the right of Figure 9). This may lead to misidentifications but during the testing phase, these cases were well below the acceptable tolerance.

But even if this algorithm is fast, it can take a significant amount of time when there are large objects and therefore many points to analyse. For this reason, the scanning of a large object requests the slowing down of the conveyor and its complete stop as soon as the end of the object is detected. This allows the points-cloud search algorithm to finish its treatment before the object falls into the cask.

## 3. Classification

In order to identify each object based on its shape, decision tree was used first.

### 3.1. First classifier and decision tree

A first classification algorithm had been designed to test the feasibility of the project. This algorithm was a simple decision tree only based on an estimation of the shape of an object (does it look more like a rectangle or a circle ? ) from a few shape parameters (width, height, area...) and empirically chosen threshold values.

As expected, this algorithm had correct results on the batch of samples that had been used to choose the threshold values, but it were not satisfactory when new objects were presented: 2% of "false positive" (graphite identified as magnesium) and 8% of "false negative" (magnesium identified as graphite) ... In order to improve these results, a random forest algorithm was implemented.

### 3.2. Random forest algorithm

It is necessary to train the classifier to determine the used parameters and the threshold values at each node: the classifier contains a set of known objects and each tree is trained only on a random part of these objects. Each tree will therefore be completely different, both in the order of the used parameters and the threshold values at each node.

Once the training is done, the execution of the random forest to identify an object is really fast (less than 200 milliseconds with 1000 trees in our forest).

### 3.3. Choice of characterization parameters

The random forest can't work directly on a points-cloud so it is necessary to extract data from this points-cloud. These data are the characterisation parameters and the performances of the random forest will depend essentially on the choice of these parameters.

Each parameter must represent a characteristic of the shape of the object and it must not be affected by the orientation of the object on the conveyor: the same object can be rotated (in the conveyor plane) and must have the same parameters values. Of course, these values will depend on the pose of the object on the conveyor: a queusot will not have the same shape if it is placed flat or if it is placed on its edge. These different poses of the same object must therefore be "learned" by the classifier.

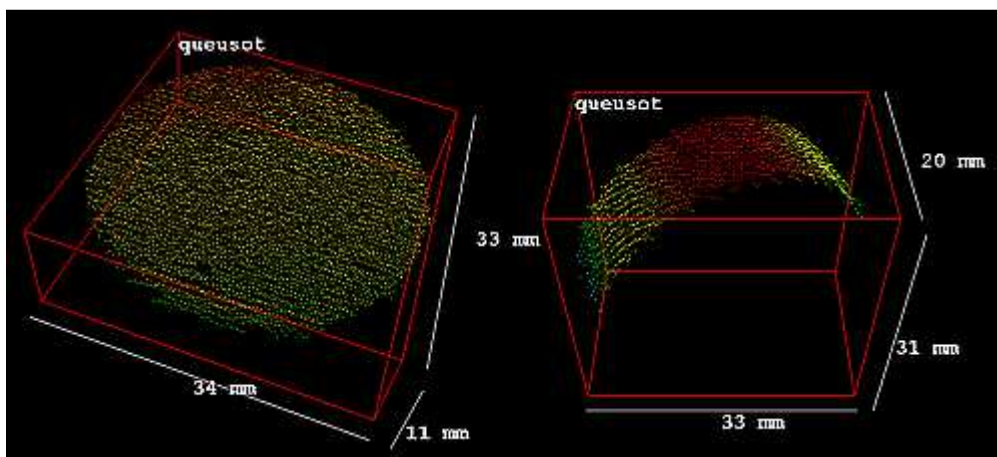


**Figure 11:** 3D reconstructions of a queusot flat on the conveyor (left) and on its edge (right)

Two types of parameters can be extracted from a 3D points-cloud:

- 2D parameters obtained by performing a projection of the reconstructed points in the plane (as seen from the top) and analysing the shape of the blob thus obtained
- 3D parameters obtained directly from the 3D points-cloud.

In order to be used in a random forest algorithm, all these parameters must have values between 0 and 1. Dimensional parameters (width, length, height and area) must then be normalized using a maximum value. And in order to be invariant regarding the orientation of the object, its length and width are the dimensions of the smallest enclosing oriented 2D rectangle, the length being always the largest of the two dimensions.

These are the chosen parameters:

- 2D parameters:
  - o WidthOverMaxWidth: width divided by the maximum width
  - o LengthOverMaxLength: length divided by the maximum length
  - o RatioWL: width divided by the length

- AreaOverMaxArea: area divided by the maximum area (the area of an object is the number of pixels in its 2D projection)
- AreaOverCircleArea: area divided by the area of the smallest enclosing circle
- AreaOverFeretArea: area divided by the area of the smallest enclosing oriented rectangle
- Roundness: area divided by the area of a circle with a radius equal to the major radius of the best fitting ellipse
- FormFactor: compactness of the object (area / perimeter length<sup>2</sup>) divided by the compactness of a circle ( $\frac{1}{4\pi}$ )
- Convexity: length of the convex hull divided by the perimeter of the object
- Solidity: area divided by the area of the convex hull
- 3D parameters:
  - Height: height divided by the maximum height
  - MeanHeight: mean height divided by the maximum height
  - StdHeight: standard deviation of the height divided by the maximum height
  - VolumeOverMaxVolume: volume divided by the maximum volume
  - VolumeOverFeretBox: volume divided by the volume of the smallest enclosing cuboid (area of the smallest enclosing 2D rectangle multiplied by the height of the object)
  - VolumeOverCylinder: volume divided by the volume of the smallest enclosing cylinder

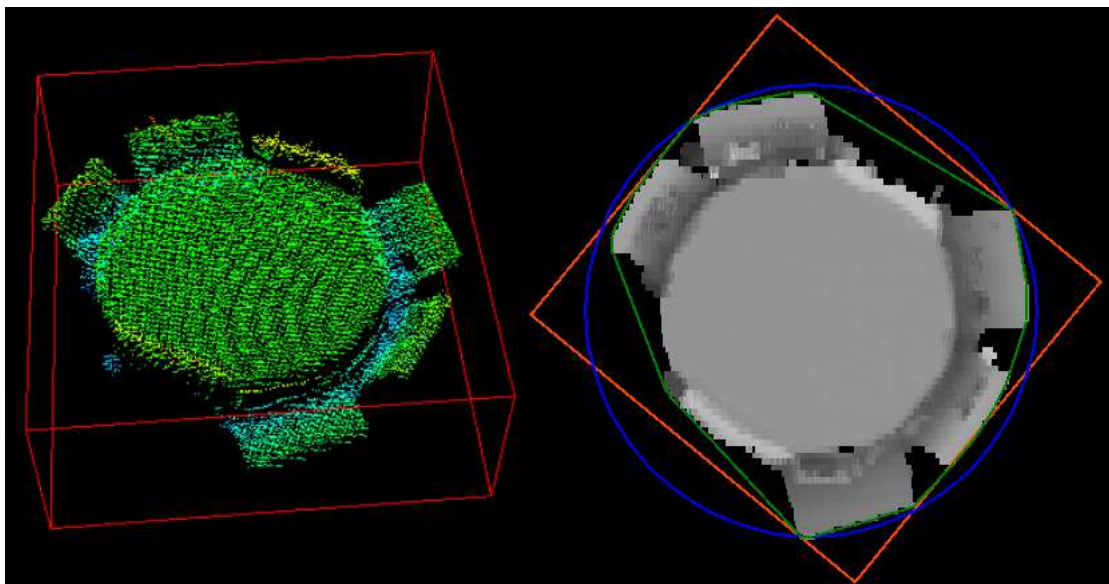


**Figure 12:** 3D reconstruction of an object and its 2D projection with the enclosing rectangle (red), the enclosing circle (blue) and the convex hull (green)

### 3.4. Training process

A first set of test runs were made with representative samples in order to build a large database of reconstructed objects. After each run, the results were analysed and some objects were added to the training set if they were misidentified. This selection was made manually in order to avoid the overfitting of the classifier and after each modification; the classifier was run on the objects of previous runs in order to check the relevance of these modifications.

Once a satisfactory classifier was obtained, its performances were checked during many other test runs and some observations were made.

For the majority of the misidentified objects, the score of the right class was really close under the score of the chosen class, i.e. nearly as many trees were choosing these two classes. Based on this

observation, the choice was made to implement an uncertainty threshold: each time the difference in score between the first two classes was under a threshold value, a validation from an operator is requested. Even if it decreased the cycle time, it greatly improved the performances of the system.

When large objects were scanned, the vision requests the slowing down of the conveyor and its complete stop as soon as the end of the object was detected. Once the cloud search algorithm had finished its task and if the object wasn't an aluminium one, the process was started again.

Here is the full description of one of the 1000 decision trees in the built random forest classifier:

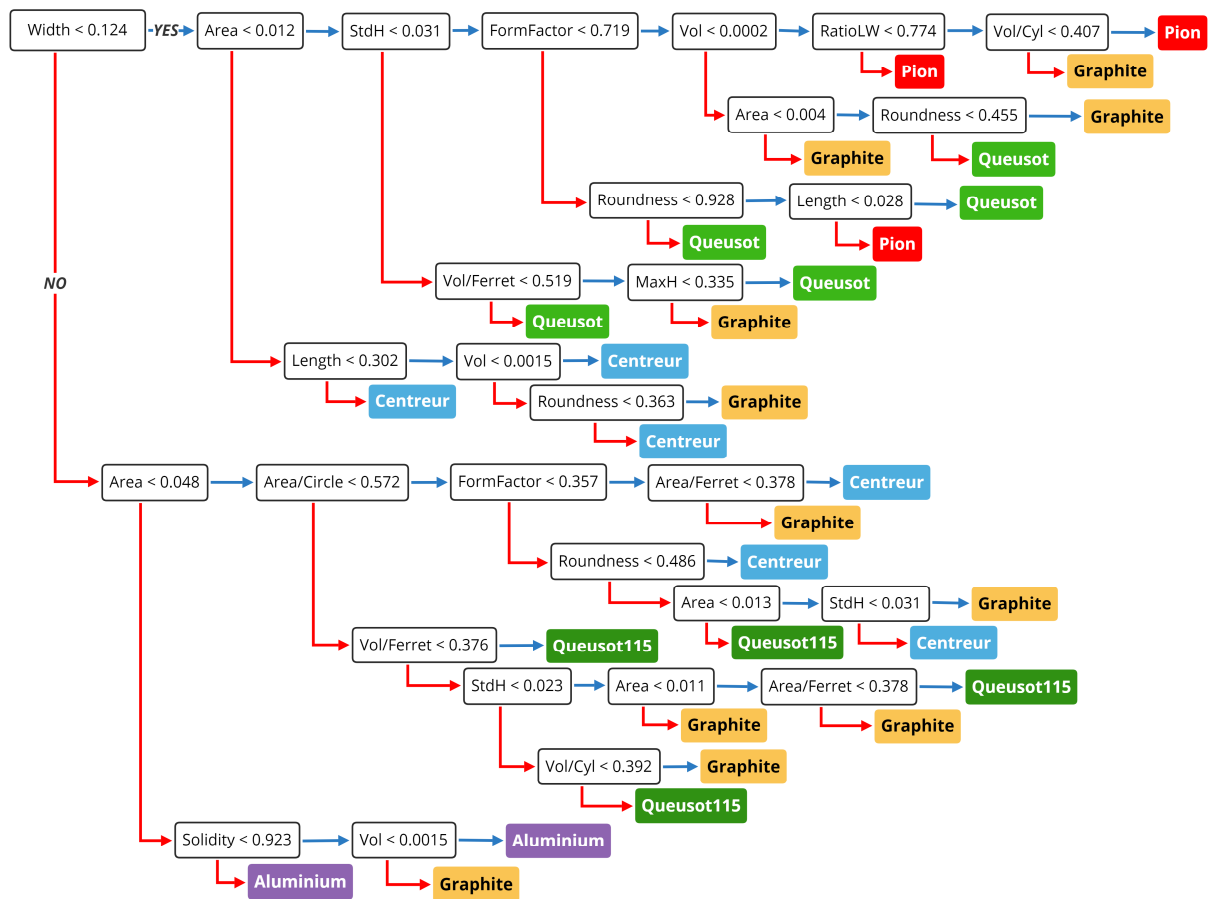


Figure 13: One of the 1000 trees of the classifier

## 4. Results

The main objective of this random forest classifier tool is to identify the magnesium part within the production flow. For each magnesium part, a predefined surface area value is recorded in the production software until the maximum authorized limit of cumulative area is reached.

### 4.1. Successful results

For each object, the output result coming from the random decision forest is basically a statistic result within a 0 to 1 range.

Even if some precautions have been taken to avoid all kind of misidentification, it could happen, because the random shape of the graphite parts could be very close to magnesium objects, and because the shape of magnesium parts could be different of the shape that have been trained in the classifier tool. That kind of difference could have several reasons: corrosion effects, several objects or

more in contact while passing through the laser ray, mechanical constraints have changed the predetermined global shape...

In order to declare the identification process is efficient, a threshold for acceptability was determined. It is required that at least 97% of the surface area of magnesium part put in the barrel has to be identified. That limit takes in account the increments due to “false positives” and the underestimate due to “false negatives”.

Two major kind of test have been performing to verify the effectiveness of the process:

- Test runs on the basis of mixed nature of waste batches (graphite, magnesium, aluminum...).
- Test runs on the basis of 100 % magnesium batches.

The mixed nature of waste batches enabled to determine the average rate of “false positive” and “false negative” within a representative selection of samples.

The 100% magnesium batches enabled to determine to pure effectiveness of the random forest decision software without any disturbance coming from the mechanical process.

Two test campaigns were engaged: the first took place in the supplier facilities in order to validate the conception. The second took place in the Orano facilities in order to verify the non-regression of the system after the final assembly of the process and all its interfaces.

Test configuration	Amount of simulation magnesium units	Amount of recognition errors “false-negatives”	Performance
100 % Mg (final facility)	7705	26	99,66 %
Average batch (final facility)	528	-5	100,95 %
100 % Mg (supplier facility)	10201	6	99,94 %
Average batch (supplier facility)	241	0	100 %

**Table 1:** Results

These results have been deemed satisfactory:

- Less than 0.5% of recognition errors,
- The cumulative surface area identified is above the safety threshold,
- The average markup of cumulative surface added in each barrel, due to “false positive” graphite parts, have an acceptable exploitation impact (10% barrel overproduction). A special attention would be payed during the real-wastes test to reduce as low as possible this amount of barrel overproduction by accurate training of the classifier.

## 4.2. Production phase

All the training was done with waste samples designed from production records, drawn samples and estimated effects of corrosion on magnesium parts. So even if these samples are as similar as possible to real wastes, it is not possible to be sure that the built random forest algorithm decision software will be able to correctly identify the wastes that will be extracted from the silo. Then it is necessary to anticipate the production launch and the possible problems that may arise.

The first phase will be a step by step production: all the results returned by the classifier must be manually validated one by one by an operator. This can be easily activated by raising the uncertainty threshold up to 1. This phase will be slow as it will sometime require a visual confirmation of the object but is essential as it will allow us to:

- Start the actual retrieval process and record the number of each part
- Build a database of 3D reconstructions of real wastes with their corresponding classes

- Check the performances of the classifier as its choices will be displayed and recorded for each object

During this phase, no new objects will be learnt by the classifier as the aim is to validate or not the classifier built during the training phase.

After this phase, three scenarios are possible:

- Performance is as good as in the tests with waste samples: this is the ideal possibility as no further learning will be necessary and the production can start immediately
- A majority of objects are correctly identified but the acceptable performance is not reached: the classifier need some further learning on misidentified objects
- Very few objects are correctly identified: this may happen if the real wastes are too different from the simulated ones. In this case, a new classifier will have to be learnt again.

Moreover, regardless of the scenario that may arise on the first layer of wastes, it will be essential to check the validity of the classifier as the silo is emptied as the shapes of the wastes may evolve as we go deeper.

No self-learning is planned as the classifier must be supervised at all time but all the tools are ready to learn a new classifier or improve an existing one with the possibility to check its results on a large database of 3D reconstructions.

## 5. Conclusion

The 3D image recognition of nuclear fuel waste using tree-based classifiers process was chosen for two main reasons.

- First, the required speed of the production flow imposes to have a reliable and reactive process which is able to identify quickly and with an error rate consistent with the safety threshold.
- Secondly, excluding time-wasting laboratory analysis, the only way to identify the material of each kind of every single piece of waste is based on geometrical parameters.

These two reasons lead the project team to innovate by using AI Machine Learning process and robots for the first time in that kind of process.

The speed production flow reached the treatment of one piece of waste every 2 seconds, for each production line. The process is equipped with two production lines.

The several tests, which the results were already approved by the French Nuclear Safety Authority, demonstrate that the performance criteria were reached. Such performance, less than 0.5% of recognition errors, could never be reach with traditional process of waste sorting with this rate of production.

As the nuclear waste sorting and conditioning is a real strategic and economic issue for the next decades, AI Machine Learning based process like this must be developed in nuclear facilities. This technology is mature, it allows to increase productivity and to reduce risks.

Even if this project focused on waste sorting applications, it is easy to imagine much kind of other doors that Machine Learning process can open. Many kind of material sorting could be concern by optical AI based recognition process: geometry of parts, colors of impurities, dimensions or grain size ... could match with Machine Learning decision tool for quantification, and could complete or replace laboratory analysis.

## Results of Data Matrix Barcode Testing for Field Applications

**Jim Garner, Logan Scott\***

Oak Ridge National Laboratory  
\*Oak Ridge Institute for Science and Education  
Oak Ridge, TN, USA  
\*Oak Ridge, TN, USA  
E-mail: GarnerJR@ornl.gov

### **Abstract:**

*For the last few years, researchers at Oak Ridge National Laboratory have been investigating direct-part-marking techniques and barcode specifications that may be applicable for UF<sub>6</sub> cylinders. Testing in 2016 and 2017 evaluated how the size of the barcode, read distance, read angle, surface finish of the material, and marking technique impacted barcode readability as measured by commercial off-the-shelf barcode readers. This work recommended a specific combination that was integrated into the 2017 World Nuclear Transport Institute "Standard for UF<sub>6</sub> Cylinder Identification." Parts of the recommendation, such as the suggestion to use laser etching with laser marking ink, were not previously systematically tested to ensure they would remain useful over a cylinder's entire lifespan. This paper discusses selected qualitative and quantitative results from accelerated environmental testing that tries to confirm that the marking ink and other characteristics of the recommendations would survive the environmental conditions UF<sub>6</sub> cylinders often experience.*

**Keywords:** global identifier; UF<sub>6</sub> cylinder; unique identifier

### **1. Introduction**

Staff at Oak Ridge National Laboratory (ORNL) have been evaluating machine-readable features to enhance safeguards for UF<sub>6</sub> cylinders for several years. As reported in the 2017 Institute of Nuclear Materials Management (INMM) paper by Garner et al. [1], the barcode size and marking technique can impact the range over which commercial off-the-shelf barcode readers can successfully decode barcodes. The 2017 INMM paper concluded that a 1.4 in. Data Matrix barcode laser etched with CerMark laser marking ink onto a ball blasted-stainless-steel plate would be very suitable for representative use cases involving a UF<sub>6</sub> cylinder global identifier. These recommendations were subsequently incorporated into the 2017 World Nuclear Transport Institute (WNTI) "Standard for UF<sub>6</sub> Cylinder Identification" [2].

This earlier work focused on Data Matrix two-dimensional (2D) barcodes. Data Matrix and QR (Quick Response) are two of the most widely used 2D barcode symbologies and can be printed on labels or directly marked on parts. The contrast and other characteristics these 2D barcodes are covered by several standards:

- ISO/IEC 16022, "Data Matrix bar code symbology specification"
- ISO/IEC 18004, "QR code bar code symbology specification"
- ISO/IEC 15415, "2-D bar code print quality standard," which incorporated and expanded upon marking quality definitions from ISO/IEC 16022 and ISO/IEC 18004
- AIM DPM-1-2006, verification standard for direct-part-marketing (DPM) 2D code image quality established by the Automatic Identification Manufacturers based on ISO/IEC 15415:2004
- ISO/IEC TR 29158, verification standard for DPM 2D code image quality adopted by International Organization for Standardization, which was based on AIM DPM-1-2006 and incorporated ISO/IEC 15415:2011

Figure 1 illustrates the relationship between the standards that govern 2D barcodes. Data Matrix barcodes are considered better than QR codes for industrial applications because they have higher error correction. Many 2D barcode symbologies include error correction. The 14 x 14 module Data Matrix barcodes as recommended by WNTI include 28 to 39% error correction [3]. QR codes have four error correction levels but top out at 30% error correction.

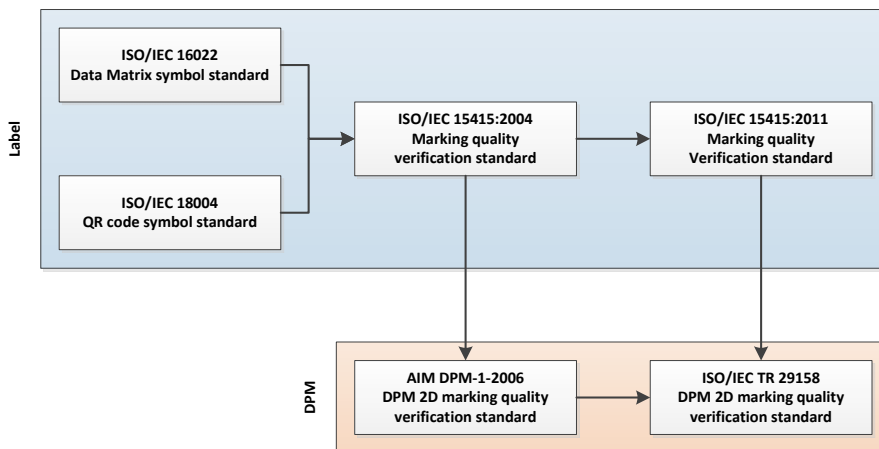


Figure 1: Multiple standards apply to 2D barcodes and barcode verification.

## 2. Samples for Accelerated Environmental Testing

In 2018 and early 2019 ORNL collected approximately 630 samples of the following types:

- Chemically etched stainless steel samples
- Laser-etched stainless steel samples
- CerMark-coated laser-etched stainless steel samples
- Laser-etched Tesa tape samples advertised to be as robust as metal once applied to a substrate
- Rebo premium vinyl labels
- Zebra Z-Ultimate 3000T
- Zebra Z-Endure 4000T advertised to offer 10-year outdoor durability

Most of these samples were welded, epoxied, or adhered to ½ in. thick A516 steel. This is the same alloy and thickness used to make model 30B UF<sub>6</sub> cylinders. The ORNL vendor supplied 4 ft x 8 ft A516 sheets with a mill finish. ORNL machinists laser-cut the large sheets to 3 in. x 6 in. coupons. The ORNL machinists then sandblasted the samples. Sandblasting did not sufficiently remove the mill finish for welding, so the coupons for the welded samples were all polished before welding.

Some of the stainless steel samples (chemically etched, laser etched, and CerMark-coated laser etched) were adhered to the A516 coupons using Arempco 517 epoxy. This epoxy has been used by other UF<sub>6</sub> industry members to adhere new placards to the skirt of cylinders. This type of epoxy may be an attractive alternative for industry compared to welding because it may be a permanent way to adhere the global identifier to the front face of UF<sub>6</sub> cylinders without requiring an R-stamp welder during the recertification process. Some of these samples were epoxied to sandblasted coupons, and some were epoxied to coupons that were sandblasted and polished. Some Tesa, Rebo, and Zebra

labels were affixed to sandblasted coupons, and some were affixed to coupons that had been sandblasted and polished.

The ORNL team then scanned the barcode samples using a Webscan TruCheck DPM Tower like the one shown in Figure 2. Barcode verifiers grade 2D barcodes printed on label material using ISO 15415 and grade 2D barcodes directly marked on metal using ISO 29158 (AIM-DPM).



Figure 2: Webscan TruCheck DPM Tower

### 3. Accelerated Environmental Tests

ORNL leased an environmental enclosure from Thermal Product Solutions to perform the temperature testing at ORNL and contracted with Q-lab and Global Testing Laboratories as third-party testing laboratories to perform 9 other tests. Q-Lab performed the following tests at their facilities: xenon arc lamp, UVA, UVB, combined UVA with salt fog. Global Testing Laboratories performed the cyclic corrosion and impact testing at their facilities and are scheduled to finish the corrosion, blowing sand/dust, and high pressure and temperature water jet testing at their facility. Each of these tests are further described in the following sections.

#### 3.1. Q-SUN xenon arc lamp testing

Q-Labs staff installed 22 samples into a Q-SUN Xe-3 xenon arc lamp tester as shown in Figure 3. Testing followed a cycle like ASTM G155 Cycle 1. Samples were exposed for 102 min of light at 63°C black panel temperature, then 18 min of light and water spray. These cycles were repeated for a total 500 h. An irradiance of 0.55 W/m<sup>2</sup> at 340 nm was used [4].



Figure 3: ORNL samples installed in Q-SUN Xe-3 Xenon arc test chamber.

### 3.2. QUV UVA testing

Q-Labs staff installed 24 samples into a QUV tester with UVA bulbs as shown in Figure 4 and Figure 5. Testing followed a cycle like ASTM G154 Cycle 1. Samples were exposed for 8 h of light at 60°C black panel temperature followed by 4 h of condensation at 50°C black panel temperature. These cycles were repeated for a total of 500 h. Fluorescent UVA-340 bulbs at 340 nm were used with an irradiance of 0.89 W/(m<sup>2</sup> • nm) [5].



**Figure 4:** ORNL samples installed in QUV chamber. Samples are shown facing out but were turned inward toward UV lamps for testing.



**Figure 5:** ORNL samples installed in QUV test chamber for UVA testing.

### 3.3. QUV UVB testing

Q-Labs staff installed 24 samples into a QUV tester with UVB bulbs similar to the setup shown in Figure 4 and Figure 5. Testing followed a cycle like ASTM G154 Cycle 2. Samples were exposed for 4 h of light at 60°C black panel temperature followed by 4 h of condensation at 50°C black panel temperature. These cycles were repeated for a total of 500 h. Fluorescent UVB-313 bulbs at 310 nm were used with an irradiance of 0.71 W/(m<sup>2</sup> • nm) [5].

### 3.4. QUV and Q-Fog testing

Testing followed ASTM D5894. Q-Labs staff exposed 24 samples to alternating weeks of one week in a fluorescent UV chamber followed by one week in a salt fog chamber. In the UV chamber, samples were set up similarly to what is shown in shown in Figure 4 and Figure 5. The samples were exposed for 4 h of light at 60°C black panel temperature followed by 4 h of condensation at 50°C black panel temperature. Fluorescent UVA-340 bulbs at 340 nm were used with an irradiance of 0.89 W/(m<sup>2</sup> • nm). In the salt fog chamber, samples were set up as shown in Figure 6 and exposed to 1 h of fog at

ambient temperature then a 1 h dry off at 35°C. The fog solution was 0.05% sodium chloride and 0.35% ammonium sulfate [6].



**Figure 6:** ORNL samples installed in Q-Fog test chamber.

### 3.5. Temperature testing

ORNL staff leased a Tenney TC20RC environmental enclosure from Thermal Product Solutions and had it installed at ORNL. ORNL staff then installed 61 samples as shown in Figure 7. All samples that were affixed to the ½ in. thick steel coupons were hung vertically. A few stainless samples that were not affixed to such coupons were laid flat on the stainless wire racks with their markings facing up. Samples were exposed to -40°C for 7 days then 113°C for 7 days. These cycles were repeated for a total of 6 weeks. Relative humidity was not controlled. The temperature ramp rate was not controlled such that the temperature changed as quickly as the chamber’s heating and cooling capacity permitted.



**Figure 7:** ORNL samples in Tenney TC20RC environmental enclosure.

### 3.6. Cyclic corrosion testing

Staff at Global Testing Laboratories installed 63 samples into a salt fog chamber as shown in Figure 8. Samples were exposed to five cycles that consisted of the following steps:

1. Ambient stage with stress: salt fog at ambient temperature for 8 h
2. Humid stage: 49–60°C at approximately 95% relative humidity for 8 h
3. Dry stage: 60°C at less than 30% relative humidity for 8 h

This testing is similar to that described by GM Cyclic Corrosion Laboratory Test (GMW 14872).[7]



**Figure 8:** ORNL samples installed in salt fog chamber

### **3.7. Corrosion testing**

Staff at Global Testing Laboratories are scheduled to test 57 samples in a salt fog chamber. The samples will be arranged similarly to those shown in Figure 8. The testing is planned to follow ASTM B117, "Standard Practice for Operating Salt Spray (Fog) Apparatus." [8]

### **3.8. Blowing sand/dust testing**

Staff at Global Testing Laboratories are scheduled to test 57 samples in a blowing sand/dust chamber. The testing is planned to follow MIL-STD 810G 510.6, "Sand and Dust 4.1 Procedure I – Blowing Dust," except temperature and humidity will not be controlled. [9]

### **3.9. Impact testing**

Staff at Global Testing Laboratories completed impact testing of 55 samples. Testing followed IEC 61010-1, Section 8.2.2, "Impact Test." A smooth steel sphere with a mass of 500 g was allowed to fall freely from a distance of 1000 mm onto each of the samples as shown in Figure 9. [10]



**Figure 9:** Impact testing allowed a 500 g smooth steel sphere to fall from 1000 mm onto each of the samples.

### **3.10. High pressure and temperature water jet**

Staff at Global Testing Laboratories are scheduled to subject 57 samples to high-pressure and -temperature water jets. Testing is planned to follow IEC 60529 CORR 1 IEC 60529 CORR 1 - Degrees of Protection Provided by Enclosures (IP Code) - Edition 2.2, Test 14.2.9 "Test for second characteristic numeral 9 with a spray nozzle" [11]

## 4. Qualitative Results

ORNL has received samples back from tests 1 through 5. Tests 7 and 9 have also been completed, but the samples have not yet been returned. The remaining tests are expected to be completed during the summer of 2019.

Many of the samples including stainless steel samples that were not affixed to A516 steel and nonmetallic labels appear rusty. While we expected the untreated surface of the A516 steel to rust, we were surprised how the rust spread over stainless and nonmetallic labels. This behavior was exceptionally apparent for the samples that underwent cyclic corrosion testing (test 6) and QUV & Q-Fog testing (test 4) but also to a lesser degree in the samples that were subjected to the UVA and UVB testing.

We observed that the Rebo labels subjected to temperature testing discolored. As shown in the side-by-side images in Figure 10 below, the Rebo labels discolored dramatically. We suspect the high temperatures caused the discoloration. We did not observe discoloring amongst the other nonmetallic labels nor with the other tests.



Figure 10: Image of selected samples after cyclic corrosion testing.

## 5. Selected Quantitative Results

As mentioned earlier, all samples were scanned before and after accelerated environmental testing. ORNL is still analyzing the data and plans a more comprehensive quantitative report later in 2019. ORNL configured the barcode verifier to produce a PDF report as well as a CSV summary file for each scan. The PDF report includes summary information at the top that provides the data, symbology, and grades for any tests selected. As shown in Figure 11, ORNL recorded results for both ISO 15415 and ISO 29158 for each sample; however, the ISO 15415 results are only meaningful for the label barcodes, and the ISO 29158 results are only meaningful for the DPMS. Figure 12 shows the ISO 29158 results for a laser-etched stainless steel sample that was part of test 4 (QUV and Q-Fog testing). As shown in Figure 11 and Figure 12, this sample received a C grade after environmental exposure. This same sample received an A grade before environmental exposure.



### Webscan TruCheck™ USB Verification Report

Software Version: 3.03.54, Unit Serial: TC-825-0318-121  
 Verified: Tue 16-Apr-2019 03:01:04 PM, Last Calibrated: Tue 16-Apr-2019 11:59:30 AM

Report Summary						
Data	YAGL123412					
Symbology	DataMatrix					
Verified By	ORNL_Admin					
Verification Grades						
Standard	Grade	Aperture	Wavelength	Lighting	Formal Grade	Notes
ISO15415	F (0.0)	20	660	45	0.0/20/660/45	
ISO29158 (AIM-DPM)	C (2.0)	81	660	45Q	DPM 2.0/81/660/45Q	[Warning]Symbol X-Dimension out of range

Figure 11: Top portion of Webscan Verification Report



### Webscan TruCheck™ USB Verification Report

Software Version: 3.03.54, Unit Serial: TC-825-0318-121  
 Verified: Tue 16-Apr-2019 03:01:04 PM, Last Calibrated: Tue 16-Apr-2019 11:59:30 AM

Image				General Characteristics	
				Matrix Size	14x14 (Data: 12x12)
				Horizontal BWG	10%
				Vertical BWG	-33%
				Encoded characters	10
				Total Codewords	18
				Data Codewords	8
				Error Correction Budget	10
				Errors Corrected	0
				Error Capacity Used	0
				Error Correction Type	ECC 200
				Image	Black on white
				Nominal X Dim	100.5 mil
				Contrast Uniformity	49 at module(5,1)
				Stability	98%
Data Matrix Codewords					
5A 42 4B 4D 8E A4 8E 81 2B B1 42 11 42 68 44 07 D3 9A					
* = Fixed by Error Correction					
ISO 29158 Quality Parameters				Modulation Values	
1. Unused Error Correction (UEC)	100%	A		41	50
2. Cell Contrast (CC)	58%	A	R/Rd (100/42)	50	99
3a. Cell Modulation (CMOD)		A		58	99
3b. Reflectance Margin (RM)		A		64	99
4. Axial Nonuniformity (ANU)	2%	A		50	99
5. Grid Nonuniformity (GNU)	15%	A		43	99
6. Fixed Pattern Damage (FPD)	2.0	C		47	99
7. Left 'L' Side (LLS)		A		39	99
8. Bottom 'L' Side (BLS)		A		37	99
9. Left Quiet Zone (LQZ)		C		69	99
10. Bottom Quiet Zone (BQZ)		A		75	99
11. Top Quiet Zone (TQZ)		A		94	99
12. Right Quiet Zone (RQZ)		A		90	99
13. Top Transition Ratio (TTR)	0%	A		92	99
14. Right Transition Ratio (RTR)	0%	A		69	99
15. Top Clock Track (TCT)		A		66	83
16. Right Clock Track (RCT)		B			
17. Distributed Damage Grade (DDG)	4.0	A			
18. DECODE		A			
19. Minimum Reflectance (MR)	41%	A			

Figure 12: Bottom portion of Webscan verification report showing ISO 29158 quality parameters related to DPMs.

Table 1 shows the before and after values for each of the metrics used as part of the ISO 29158 grading. We've highlighted several key metrics that changed dramatically between the before and after verification scans. Cell contrast refers to the relative contrast between the light and dark modules. Cell contrast is calculated as the difference between the mean of the light and dark areas divided by the mean of the light area. Cell contrast values greater than 30% will be graded as an A. RI/Rd is a ratio of the reflectance of the light modules to the reflectance of the dark modules. This parameter is not directly used for ISO 29158 grading. Fixed pattern damage is an overall grade for all the fixed pattern components and is equal to the lowest-grade fixed pattern components (left "L" side, bottom "L" side, left quiet zone, bottom quiet zone, top quiet zone, right quiet zone, top transition ratio, right transition ratio, top clock track, and right clock track). In this example, after environmental testing the right clock track grade fell from an A to a B, and the left quiet zone fell from an A to a C grade. The new left quiet zone grade was the lowest and caused the fixed pattern damage to fall from an A to a C.

ISO 29158 Quality Parameters	Before Testing			After Test 4 (QUV & Q-Fog)		
1. Unused Error Correction (UEC)	100%	A	PASS	100%	A	PASS
2. Cell Contrast (CC)	70%	A	RI/Rd (100/30)	58%	A	RI/Rd (100/42)
3a. Cell Modulation (CMOD)		A	PASS		A	PASS
3b. Reflectance Margin (RM)		A	PASS		A	PASS
4. Axial Nonuniformity (ANU)	1%	A	PASS	2%	A	PASS
5. Grid Nonuniformity (GNU)	3%	A	PASS	15%	A	PASS
6. Fixed Pattern Damage (FPD)	4.0	A	PASS	2.0	C	PASS
7. Left "L" Side (LLS)		A	PASS		A	PASS
8. Bottom "L" Side (BLS)		A	PASS		A	PASS
9. Left Quiet Zone (LQZ)		A	PASS		C	PASS
10. Bottom Quiet Zone (BQZ)		A	PASS		A	PASS
11. Top Quiet Zone (TQZ)		A	PASS		A	PASS
12. Right Quiet Zone (RQZ)		A	PASS		A	PASS
13. Top Transition Ratio (TTR)	0%	A	PASS	0%	A	PASS
14. Right Transition Ratio (RTR)	0%	A	PASS	0%	A	PASS
15. Top Clock Track (TCT)		A	PASS		A	PASS
16. Right Clock Track (RCT)		A	PASS		B	PASS
17. Distributed Damage Grade (DDG)	4.0	A	PASS	4.0	A	PASS
18. DECODE		A	PASS		A	PASS
19. Minimum Reflectance (MR)	37%	A	PASS	41%	A	PASS

Table 1: ISO 29158 metrics recorded before and after QUV and Q-Fog testing of YAGL123412.

## 6. Key Observations Conclusions, Lessons Learned and Next Steps

The analysis to date suggests that CerMark-coated laser-etched markings appears to be a good choice for global identifier markings. While anecdotal evidence suggests that chemically etched markings and epoxy adhesives may fail over time, the initial test data is inconclusive about these points. Preliminary qualitative assessments suggest that Zebra Ultimate, Zebra Endure, or Tesa labels can serve as a medium-term solutions to add a supplemental global identifier label to previously fabricated UF<sub>6</sub> cylinders in circulation before they are due for recertification. The limited quantitative data suggests laser-etched markings without CerMark should not be adopted for the global identifier.

The ORNL team was surprised to find the Rebo labels, but none of the other nonmetallic samples, subjected to temperature testing discolored. The barcode verifier also had trouble decoding several of the laser-etched (but not the CerMark-coated laser-etched) samples after environmental exposure.

The team was also surprised by the extensive rust on the nonmetallic and stainless portions of the samples. If similar testing is conducted in the future, it will be more representative to paint or otherwise treat the bare A516 portions of the samples before environmental exposure because bare A516 is typically not exposed after cylinder manufacture.

The ORNL team is working with Global Testing Laboratories to complete the remaining tests, at which point the ORNL team will prepare a more extensive quantitative analysis of the data.

## 7. Acknowledgments

Funding for this project was provided by the Department of Energy's NNSA Office of International Nuclear Safeguards (OINS). The authors would also like to thank Scott Palko for his assistance preparing samples for testing and Ed Wonder for his assistance refining the test plan.

This manuscript has been authored by UT-Battelle, LLC, under contract DE-AC05-00OR22725 with the US Department of Energy (DOE). The US government retains and the publisher, by accepting the article for publication, acknowledges that the US government retains a nonexclusive, paid-up, irrevocable, worldwide license to publish or reproduce the published form of this manuscript, or allow others to do so, for US government purposes. DOE will provide public access to these results of federally sponsored research in accordance with the DOE Public Access Plan (<http://energy.gov/downloads/doe-public-access-plan>).

## 8. References

1. Garner, J. and N. Pratt, *Design Specifications for a Machine-Readable Container Identifier*, in *58th Annual Meeting of the Institute of Nuclear Materials Management (INMM 2017)*. 2017, Curran Associates, Inc.: Indian Wells, California, USA. p. 370-379.
2. Institute, W.N.T., *UF6 Cylinder Identification*. 2017, WNTI: London, United Kingdom.
3. *ID CODE HANDBOOK: 2-D CODE BASIC GUIDE*. 2010, Keyence.
4. ASTM, *Standard Practice for Operating Xenon Arc Light Apparatus for Exposure of Non-Metallic Materials*. 2013.
5. ASTM, *Standard Practice for Operating Fluorescent Ultraviolet (UV) Lamp Apparatus for Exposure of Nonmetallic Materials*. 2016.
6. ASTM, *Standard Practice for Cyclic Salt Fog/UV Exposure of Painted Metal, (Alternating Exposures in a Fog/Dry Cabinet and a UV/Condensation Cabinet)*. 2016.
7. Motors, G.-G., *GMW14872 - Cyclic Corrosion Laboratory Test - Issue 4; English*. 2018, GMW - General Motors.
8. *Standard Practice for Operating Salt Spray (Fog) Apparatus*. 2019, ASTM.
9. *MIL-STD-810G W/CHANGE 1 - ENVIRONMENTAL ENGINEERING CONSIDERATIONS AND LABORATORY TESTS*, in 510.6. 2014, TE - Developmental Test Command (DTC).
10. IEC, *Safety requirements for electrical equipment for measurement, control, and laboratory use*, in *Impact Test*. 2017.
11. IEC, *Degrees of protection provided by enclosures (IP Code)*, in *Tests for protection against water indicated by the second characteristic numeral*. 2013.

# Hafnium Isotope Ratio Method for Enhanced Safeguards at Research Reactors

Jesse Johns  
Eirik Krogstad  
Steve Shen  
Dallas Reilly  
Bruce Reid

Pacific Northwest National Laboratory  
902 Battelle Ave  
Richland, WA 99354 USA  
E-mail: jesse.johns@pnnl.gov

## **Abstract:**

*Pacific Northwest National Laboratory (PNNL) is developing a Hafnium (Hf)-based, enhanced safeguards measure for the verification of total energy output in a research reactor. Historically, verification of nuclear reactor use has been based on extracting and measuring physical samples from non-fuel components of the reactor. The Hafnium Isotope Ratio Method for Enhanced Safeguards (HIRMES) provides a means of verifying reactor operation based upon measuring the changes in isotopic ratios in purpose-built coupons. The first activity is installing a purpose-built, integrated sample collection coupon containing hafnium which undergoes isotopic changes when irradiated in the reactor. The second activity is analysis of the isotopic changes of the irradiated coupon after removal of the coupon using the isotope ratio method (IRM). The total energy output or plutonium production, in a fission reactor, can be estimated using IRM by measuring and correlating stable isotope ratios in non-fuel reactor components using standard reactor modelling methods.*

*This paper presents HIRMES, a prototype technology intended to provide an inexpensive, accurate, and robust measurement capability for validating operator declarations at low-power research reactors. Deploying HIRMES in research reactors would provide the IAEA with an in-core reactor “odometer” on total energy output with higher accuracy than other methods. HIRMES could be integrated in new fuel or reactor core designs as part of a protocol that is simple to implement and minimises effort required of the operator or inspector.*

*This paper also discusses an early field test of the technology at U.S. research reactors to-date, which suggests HIRMES could be useful as a tool for independent verification of low-power research reactor utilisation. Specifically, the measurement uncertainty during an irradiation campaign of 39766 MWh was 22 MWh, representing two hours at a 10 MW reactor for a total irradiation campaign over the course of approximately six months.*

**Keywords:** research reactor safeguards, isotope ratio method, core utilisation verification

## **1. Introduction**

Current safeguards measures for research reactors include the examination of a State’s records and reports, physical and interim inventory verifications, random or unannounced inspections, design information verification and environmental sampling. Verification activities can include but are not limited to: fresh and spent fuel accountancy and verification, containment and surveillance on fresh and spent fuel, and unattended advanced thermalhydraulic power monitoring [1]. Attended verification activities are labour intensive, while the use of the acoustic-based advanced thermalhydraulic power monitor, allows for validating reactor power production declarations but can only be used on non-pool type research reactors. The advantages that Hafnium Isotope Ratio Method for Enhanced Safeguards

(HIRMES) could bring to the verification activities are: high accuracy for reactor power declarations verification (sufficient accuracy to detect a misdeclaration of reactor use to within an uncertainty of hours of reactor operation) for use in a wider range of research reactor types. This report details a technology that has the potential to significantly improve upon current IAEA verification approaches for low-power (<25MW) research reactors.

## 1.2 A Brief History of the Isotope Ratio Method

The Isotope Ratio Method (IRM) has been developed at Pacific Northwest National Laboratory (PNNL) to answer fundamental questions regarding the operating history of plutonium production reactors [2]. This section will provide a brief history of the development of this method, and in Section 2, the mathematical approach for IRM will be discussed in more detail.

At Hanford, Washington, during a period of 43 years starting in 1944, more than half of the weapons-grade plutonium in the United States was produced at nine graphite-moderated reactors. In the search of methods to verify reactor operations and total material production, the IRM was developed at the same time as analytical isotope ratio measurement capabilities matured to the point where minute changes in isotopics within graphite contaminants could be quantified. All Hanford production reactors were graphite-moderated, light-water cooled reactors; therefore, the graphite isotope ratio method (GIRM) was the first methodology developed for nuclear verification of plutonium production reactors. Initial proof-of-concept exercises were conducted on archive samples of Hanford's C reactor and the French G-2 reactor at Marcoule. PNNL's first full-scale demonstration of the GIRM for estimating Pu production was conducted at Trawsfynydd Unit II reactor in 1995-96 [3]. This was performed as a blind study with the operator, Nuclear Electric. The estimate from IRM was 3.633 metric tonnes (MT) Pu, and was found to be 0.3% from the declared value [4]. Detailed reports on GIRM, the methodology, and error analysis can be found in the following references [5]–[7].

While IRM was primarily developed for graphite reactors, the method was also developed for light water reactor (LWR) systems [8]–[10], including boiling water reactors [11]. A key conclusion of these works was that Hf, as an indicator element, provided many isotopic ratios that could be used to accurately determine a variety of reactor parameters, such as void fraction in the coolant. IRM was also applied to research reactors, such as the Ford reactor following its decommissioning [12]. Later, PNNL demonstrated that IRM can be conducted on research reactors without impacting continued operations (only requiring partial defueling) at the WWR-SM in Uzbekistan [13].

## 1.3 Overview of Hafnium Isotope Ratio Method for Enhanced Safeguards (HIRMES)

The process for IRM to date has been to remove material from the reactor, such as the moderator (graphite) in graphite-moderated reactors or core shrouds in the case of research reactors. The approach works very well as these components remain in the core for the life of the facility. It is, however, possible to develop removable components with specific indicator elements [14], [15]. Purposefully installed indicator elements on removable "coupons" provides the basis for the HIRMES technology. Due to the longevity of research reactor fuel for many facilities (up to multiple decades), it is optimal to have an alternative, independent measurement capability which does not require a redesign in the reactor fuel or removal of necessary reactor components. Though, ultimately a redesign in the fuel that includes a removable coupon, perhaps can be envisioned if this approach becomes more widely adopted.

HIRMES is intended to provide an inexpensive, accurate, and robust measurement capability for validating operator declarations at low-power research reactors. Installing a semi-permanent fixture would enable IAEA inspectors to easily insert and remove a hafnium coupon and perform accurate analysis of core utilisation without causing downtime in reactor operations beyond planned core maintenance. Deploying HIRMES in research reactors would provide the IAEA with an in-core, highly accurate reactor "odometer" on total reactor usage.

### 1.3.1 HIRMES Lifecycle

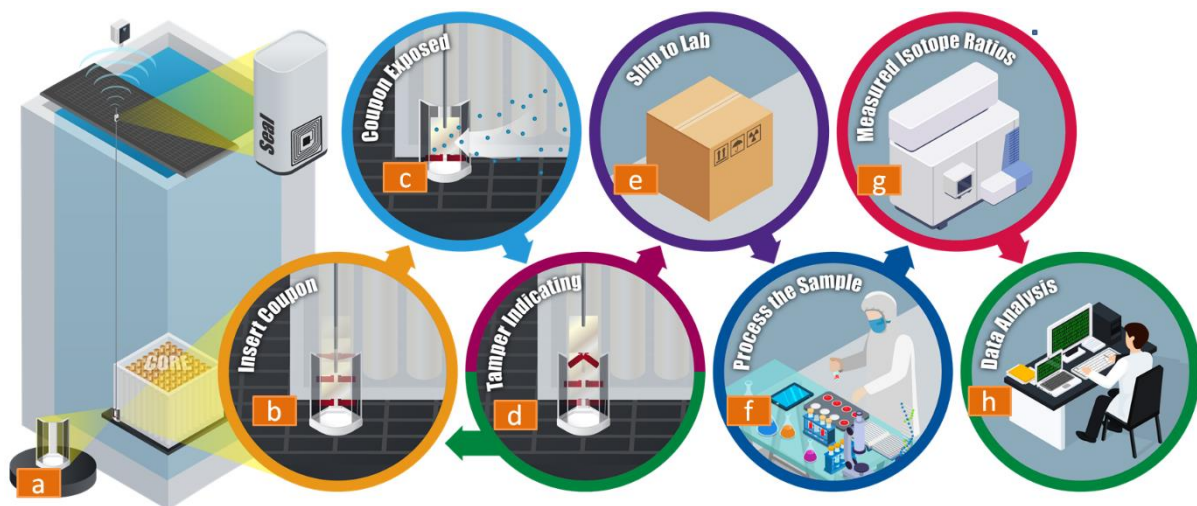
HIRMES is envisioned as a semi-permanent system that is assembled in two components on the research reactor shroud, support, or reflector, as illustrated in **Figure 1**. The lifecycle of HIRMES is as follows:

1. A permanent fixture (Figure 1.a) is attached to the core support or reflector region, the location of which is determined by neutronic and safety analyses to achieve a desirable accuracy without impacting reactor operations.

The mounting location of the fixture to the core will provide the only access to the irradiation location and provide sealing or other tamper indicator of the HIRMES coupon.

For Training, Research, Isotopes, General Atomics (TRIGA) reactors, as an example, the coupon can be attached to a rigid that allows tags and seals to be applied at the reactor bridge to support continuity of knowledge.

2. The HIRMES coupon is inserted into the fixture for irradiation (Figure 1.b).
3. The HIRMES coupon is exposed to the operating reactor's neutron flux (Figure 1.c), permanently recording total neutron exposure at the coupon location.
4. The coupon is removed from the reactor (Figure 1.d), based on a preset periodicity or when the IAEA determines that reactor operation declarations require verification, and is immediately replaced with a new unirradiated coupon.
5. The coupon is shipped to a laboratory for analysis (Figure 1.e) to determine the total exposure history of the HIRMES coupon. There is no inherent time sensitivity as the indicators in the coupon are stable; however, the HIRMES coupon is being designed to allow for shipping as soon as short-lived radioisotopes, such as  $^{24}\text{Na}$  from handling, have decayed.
6. Coupon processing in the laboratory (Figure 1.f) may include ashing and acid digestion (depending on final Hf coupon design) prior to dilution in preparation for analysis by an inductively coupled plasma mass spectrometer (ICP-MS) protocols are outlined in Section 3.2)
7. The measured isotope ratios (Figure 1.g) are used to evaluate the total energy production of the reactor during the coupon's residency. The analysis employs models (Figure 1.h) to back out the fluence using the ratios as the drivers for iterating to an acceptable average of core conditions (methods discussed in Section 2).



**Fixture Permanently Affixed to Core Support**

**Figure 1:** Anticipated lifecycle of HIRMES if implemented at a research reactor.

As of March 12<sup>th</sup>, 2019, 225 research reactors in 52 different countries, of which 34 are TRIGA type reactors with an additional 23 planned or under construction [16]. While many research reactors may be standardized, such as the TRIGA or Isseldovatel'sky Reaktor Teplovyy (IRT)-type reactors, notably, many research reactors are non-standard facilities, which pose their own unique challenges. The technology being developed takes these challenges into consideration by developing a generic concept

that can be suited to most research reactors without significant impact to reactor operations or added burden on IAEA inspectors charged with safeguarding these facilities. Currently, the HIRMES system is being designed for the most common IRT and TRIGA reactors. HIRMES is expected to be easily adapted to many non-common reactor designs (such as Missouri University Research Reactor (MURR) (USA), Open-Pool Australian Lightwater reactor (OPAL) (Australia), or SAFARI-1 (South Africa)).

## 2. Methodology of the Hafnium Isotope Ratio Method

The Hafnium isotopes ratio method is based on the IRM which relates the isotopes of specific indicator elements to reactor power. This methodology is discussed in detail in Section 2.1, and the application of this methodology to research reactor safeguards is discussed in Section 2.2.

### 2.1 Legacy IRM Approach

The irradiation of any material within a nuclear reactor will result in the transmutation of the constituent isotopes, which are described by the Bateman equations, represented in the following form:

$$\frac{dN(t)}{dt} = M(\phi(t))N(t), \quad \text{Eq. 1}$$

where  $N(t)$  is a matrix representing the nuclides as a function of time,  $t$ , and  $M(\phi(t))$  is the matrix operator that contains the physical information of the Bateman equations and is an explicit function of the neutron flux,  $\phi$ . The matrix operator is inherently dependent on many system variables, such as temperature, but a constant approximation is used in this work.

The first step of IRM is to analyse the material for known isotopic ratios of interest, which are usually elements with contaminants in the parts per billion level [8-13]. There are many characteristics of choosing these indicator elements which will not be described in this paper. The result of the physical measurement of the isotopes relays the following:

$$N(t_f) = \int_{t=0}^{t=t_f} M(\phi(t), T)N(t)dt, \quad \text{Eq. 2}$$

where  $t_f$  is the time at which the sample was extracted from the reactor and measured and  $t = 0$  is the time prior to irradiation within the reactor. Since neutron flux does vary with time, the matrix operator cannot simply be removed from the integral. Therefore, a detailed reactor physics analysis is used to determine the total neutron fluence from the physically-measured isotopic ratios,  $N(t_f)$ ,

$$\Phi = \int \phi(t)dt. \quad \text{Eq. 3}$$

Finally, the neutron fluence can be correlated to the total plutonium production, or reactor utilisation, depending on the application. Classically, IRM can be visualized as shown in Figure 2. The measured ratios are represented by the dotted lines, the reactor physics calculation of the ratios is depicted by the solid lines, and the total utilisation is determined where these two values intersect. Since the measured ratios come from the same section of extracted material, the neutron fluence must physically be the same for all of the measured ratios. Isotopic ratios within the region, therefore, must be self-consistent. Error arises from modelling approximation (unknowns in the system for example) and measurement uncertainties.

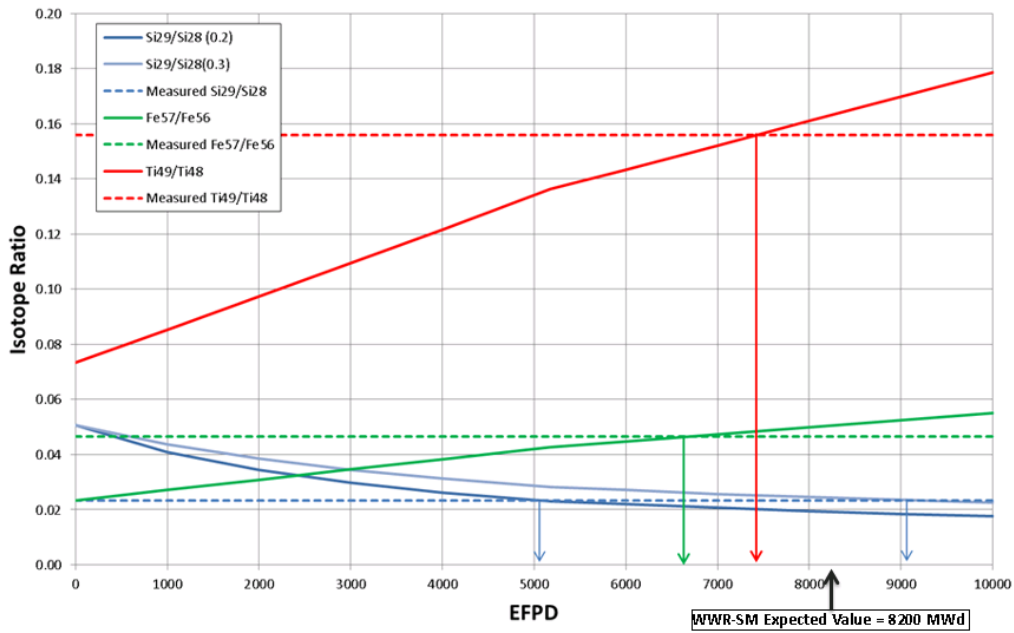


**Figure 2:** IRM analysis of a WWR-SM reactor which operated for 8200 megawatt-days (MWd). The dotted lines show the measured isotopic ratio, and the solid lines represent the reactor physical calculated isotopic ratios. Used with permission from [13].

## 2.2. IRM Applications to Research Reactors for Safeguards

Previous work has applied the IRM capability for the validation of plutonium production and total reactor utilisation in research reactors [8-13]. The approach for developing this for safeguards applications is similar. However, the differing aspect is that for this approach to be useful and adopted by the safeguards community, it must be robust with little dependence on detailed reactor physics modelling. To meet the need for a reactor physics independent methodology, PNNL is currently developing an approach which assumes that a suitable set of measured Hf isotopic ratios, combined with appropriate inverse-problem algorithms, can determine the neutron fluence without detailed operator-declared core parameters or explicit reactor-core modelling. This “declaration-free” analysis approach is described in the following sections.

### 2.2.1 Optimisation

The approach, which is currently under development, is an iterative analysis with the primary objective to converge on the multiple isotopic ratios of Hf to ensure self-consistency. Once the self-consistent ratios are determined, it is inferred that the final neutron fluence represents the averaged reactor conditions over the length of the irradiation period. This iterative approach requires an iterative optimisation on generic reactor parameters.

Let  $f$  be the response of isotopic ratios given an input of  $z_i$  model parameters for realisation  $i$  with measured isotopic ratios of  $\bar{x}$  (in this work, stable Hf isotopes) then the predicted fluence can be represented as:

$$y_i = f(\bar{x}, z_i) \tag{Eq. 4}$$

where the error of the average predicted fluence,  $Y$ :

$$Y = \frac{1}{N} \sum_i^N y_i$$

becomes:

$$e_i = \sum_i |Y - y_i| \tag{Eq. 5}$$

Therefore, the objective function is a minimisation on  $z_i$  such that:

$$\min_{z_i \in R} = \sum_i |Y - f(\bar{x}, z_i)| \tag{Eq. 6}$$

The optimisation technique used is that of differential evolution (DE) [17]. DE is a population-based, global optimisation algorithm technique that is useful for multimodal problems where gradient-based methods fail. DE is a class of evolutionary algorithms, which uses population selections to maintain diversity of the solution space in order to efficiently find globally minimised solutions.

Generally, the diversity is maintained, while simultaneously achieving improved fitness, by comparing candidate solutions with the current population of solutions and only survive (or continuing to the next iteration) if they possess higher fitness (or improve minimisation) than the current population. The candidate solutions are generated according to the current population. The starting population is generated by a uniform random distribution over some starting interval. Inputs into the modelling process include decisions such as fuel type, moderator, reflector, material temperature/density, and geometry thicknesses. These inputs need not come from the reactor operator, but open literature on the system. The simplicity of the approach allows for a 1D neutron transport code to be used; however, the preference is to use a continuous-energy Monte Carlo to reduce cross-section generation burdens. This approach only allows for the total fluence of the material to be determined, and additional modelling is necessary to relate fluence to energy production. The primary advantage of this approach is that no explicit reactor knowledge from the operators is necessary to arrive at an accurate fluence and neutron spectra.

The characteristic that allows this approach to be used is that the strong energy dependence of the Hf cross-sections will allow this genetic-algorithm method to implicitly account for reactor information (e.g., geometry, densities, and temperature) without the need for explicit values of those parameters from the operator. Final convergence will have some error due to modelling approximations (constant average neutron flux, for example) and nuclear data uncertainties.

The approach is illustrated in Figure 3. In each realisation, a new configuration is considered, which perturbs the impinging neutron spectrum on the Hf coupon. Only the representative spectrum will result in physically self-consistent Hf isotopic ratios (the minimisation of equation 3 – all fluences agree) due to the sensitivity of the many Hf isotopic ratios on the incident neutron spectrum. Preliminary studies suggest three isotopic ratios are necessary; however, more study is required to evaluate the uncertainties with this method. The self-consistency manifests itself in all measured ratios, using IRM, resulting in, ideally, the same predicted fluence for all isotopic ratios. Once the isotopic ratios become self-consistent, the “configuration” is used for subsequent analysis of the average neutron fluence on the Hf coupon. Once converged, the neutron spectrum and fluence are known.

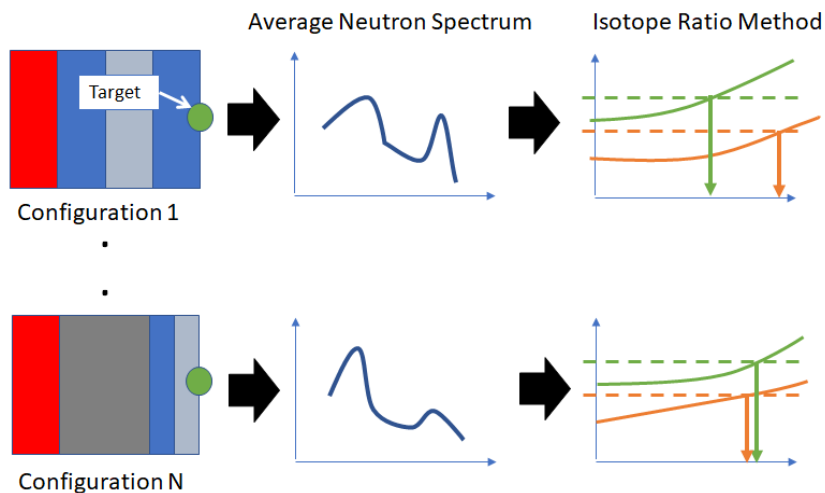


Figure 3: Illustration of declaration-free IRM approach.

### 2.2.1 Fluence-to-Energy

The next step in the analysis process is to translate one or more location-specific total fluence values (e.g., multiple Hf coupons located in and around the core) into the aggregate power produced by the research reactor during the coupon irradiation period. This neutron flux-to-power relationship is generally determined with detailed core modelling; however, potential approaches for performing these calibrations are currently being studied. These approaches, currently under investigation and out of scope for this paper, may reduce or completely negate the need for reactor modelling when performing total energy production verification estimates. If these analysis approaches can be successfully developed, the Hf-based IRM method could provide a completely independent research reactor verification method for the IAEA that does not require operator-declared operational values, nor explicit reactor core modelling.

## 3. Experimental Validation

This section describes the experimental validation conducted by irradiating and performing an end-to-end IRM analysis of a high-purity Hf wire in 2016-2017. This wire was irradiated in the US-based MURR reactor in a blind study. PNNL fabricated the irradiation capsule, MURR irradiated the target, PNNL measured and analysed the target for total neutron fluence with the method introduced in Section 2.2. Only once PNNL completed the analysis, did MURR provide their declaration of the neutron fluence.

### 3.1 Target Irradiation

A high-purity Hf (containing less than 3% Zr, see Table 1) wire was used for the primary irradiation target. The wire (0.25 mm diameter) was flattened to a thickness of approximately 0.1 mm to further reduce the potential for neutron self-shielding. Masses and elemental compositions were recorded for reactor irradiation calculations. Elemental analysis was performed on the stock material for all target materials using a Perkin Elmer 8300 inductively coupled plasma optical emission spectrometer, using external standards calibration.

**Table 1.** Elemental composition of irradiation target stock material, as determined by PNNL by inductively coupled plasma optical emission spectrometry

Hafnium	
Element	Weight Percent
Hf	95.94%
Mg	0.14%
Si	1.39%
Zr	2.53%

Two capsules were irradiated in a reflector location of the MURR reactor core for approximately 180 calendar days (MURR operates approximately five days per week). One capsule was irradiated at the bottom of the core reflector and the other capsule was irradiated in a location near the centreline of the reactor fuel (Figure 4). Neutron flux measurements taken by MURR in 2008 suggest a factor of two to three difference between these two irradiation locations. The total neutron flux in the sample irradiation location is predominantly thermal, so the neutron flux is used synonymously with thermal neutron flux in the rest of this report. A summary of the operator-declared information for the irradiation is provided in Table 2.

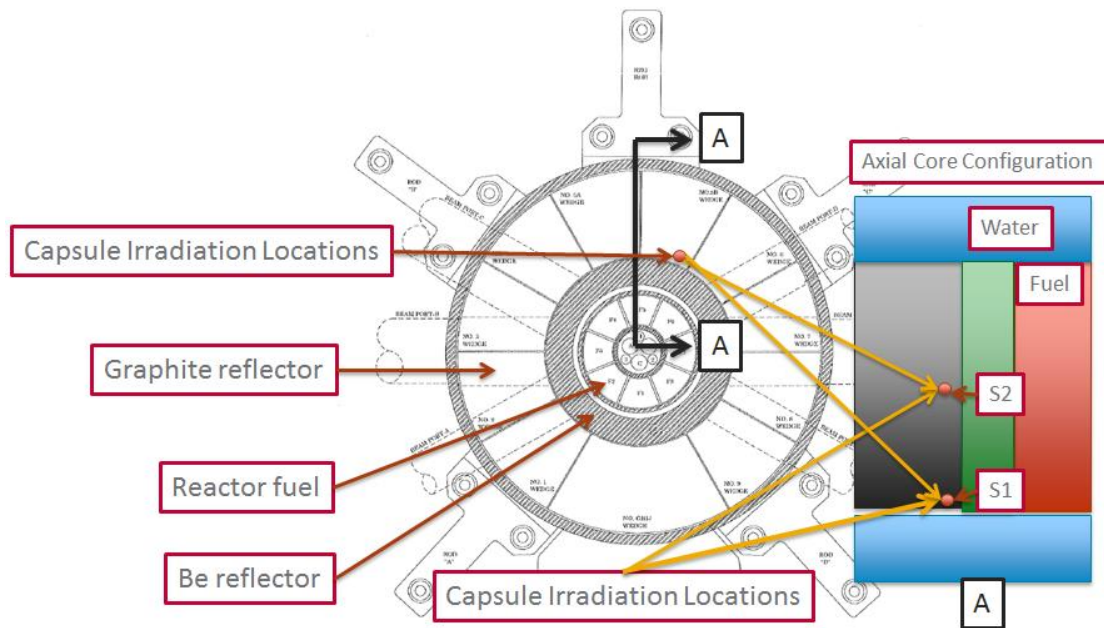


**Figure 4.** Shown is the approximate radial and axial core configuration. The relative sample locations in the reflector region are shown in the simplified, axial diagram on the right.

**Table 2.** Summary of operator-declared information for irradiation locations after IRM was performed on the samples received by PNNL.

Sample ID	Axial Height (cm)	Thermal Neutron Flux ( $10^{13} \text{ n/cm}^2/\text{s}$ )	Total Exposure (hrs at 10MW)
S1	1.27-3.81	2.38	3976.58
S2	39.4-41.9	5.35	3976.58

### 3.2 Measured Ratios

The samples were inserted into the reactor core June 14, 2016, removed December 12, 2016 and returned to PNNL on March 6, 2017. Laboratory measurements of the low and high fluence sample were performed by solution mass spectrometry using an ICP-MS. A section of Hf wire is cut from the primary sample and dissolved with a mixture of concentrated HF and concentrated HNO<sub>3</sub> (1:9) in a PFA Teflon vial. The solution is then diluted with 2% HNO<sub>3</sub> to a final strength of 4 ppb Hf in 2.7% HNO<sub>3</sub>/0.05% HF. This solution is introduced to the Nu Instruments NuPlasma HR MC-ICP-MS using an Apex Q desolvation nebulizer at about 200 microliters per minute. Five measurements were first made of the isotopic composition of an unirradiated high-purity Hf wire to control for mass fractionation in the plasma. The relative isotopic proportions of all Hf isotopes have been found to be fixed in nature, except for <sup>176</sup>Hf (produced by the decay of <sup>176</sup>Lu). Therefore, it is traditional to use the <sup>179</sup>Hf/<sup>177</sup>Hf ratio to correct for mass fractionation of the other ratios. This ratio has an accepted value of 0.7325. Due to the alteration of the isotopic composition of the irradiated sample, this within-run correction cannot be applied in the same way. Therefore, the deviation of the measured <sup>179</sup>Hf/<sup>177</sup>Hf from the accepted values in the Hf wire is used to correct for the current mass fractionation in the plasma. Finally, the natural Hf wire was analysed after the last irradiated sample to check for drift in the mass fractionation factor. All measurements were made in a static multi-collector mode with the ion beams being measured in Faraday cup detectors coupled to preamplifiers with 10<sup>11</sup> Ω resistors. Ion beams for <sup>180</sup>Hf (the most abundant isotope) averaged 9x10<sup>-11</sup> amperes (ca. 5.5x10<sup>8</sup> ions/sec). Results of these measurements are shown in Table 3.

**Table 3.** Results from measurement campaigns for each isotope ratio of interest with two standard deviation uncertainties reported in parentheses.

<b>Hf Ratio</b>	<b>Accepted [18]</b>	<b>Unirradiated</b>	<b>S1</b>	<b>S2</b>
174/177	0.008712	0.0086552(53)	0.0084861(23)	0.0081684(20)
176/177	NA*	0.282188(11)	0.342050(10)	0.441318(47)
178/177	1.4671	1.467187(28)	1.947864(82)	2.71319(10)
179/177	0.7325	NA**	0.948480(72)	1.32793(20)
180/177	1.8865	1.886804(15)	2.31329(21)	3.01572(30)

\*There is no accepted value as it varies in nature due to the decay of Lu176.

\*\*For natural Hf, the analysis of Hf 179/177 is monitored as a means to determine the current mass fractionation during that run.

### 3.2 IRM Analysis Results

The PNNL-calculated neutron energy spectra, computed with the approach outlined in Section 2.2, are shown in Figure 5 for the low and high fluence (S1 and S2, respectively) samples, noting that each sample is treated as an independent analysis. These two independent estimates of neutron energy spectrum reflect the different geometries and temperatures at each coupon irradiation location in the core. Systematic bias, likely resulting from temporal variations in the neutron flux and depletion simulation, were not taken into account in the analysis.

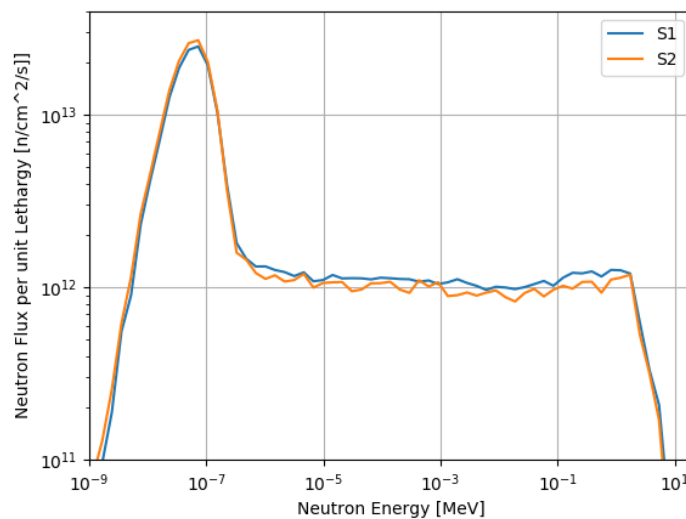


**Figure 5.** The neutron energy spectrum calculated for each sample location. S1 has a slightly higher fast-to-thermal ratio than S2.

The computed (from Eq. 1) and measured Hf ratios for S2 are shown in Figure 6. The predicted total energy production in megawatt-hours (MWh), based on each ratio is shown by a vertical line extending from the intersection of the measured (dotted line) and computed (solid curve) ratios (essentially solving Eq. 3). The energy-production estimates are performed by scaling the neutron fluence to the operator-declared neutron flux.

Systematic error of the energy-production estimates is noticed in Figure 6, specifically  $^{179}\text{Hf}/^{177}\text{Hf}$  predicts low and  $^{176}\text{Hf}/^{177}\text{Hf}$  and  $^{178}\text{Hf}/^{177}\text{Hf}$  track together. The systematic error is shared between the independent calculations of neutron energy spectra at two irradiation locations (numerical results are shown in Table 4). Initial investigations suggest this is not due to the optimisation techniques or the nuclear data (ENDF/B VII.0 and JEFF 3.1.1 generated similar behaviour), but this behaviour might arise from the core-average, constant neutron flux approximations mostly arising from not accounting for the cyclical operations of the reactor.

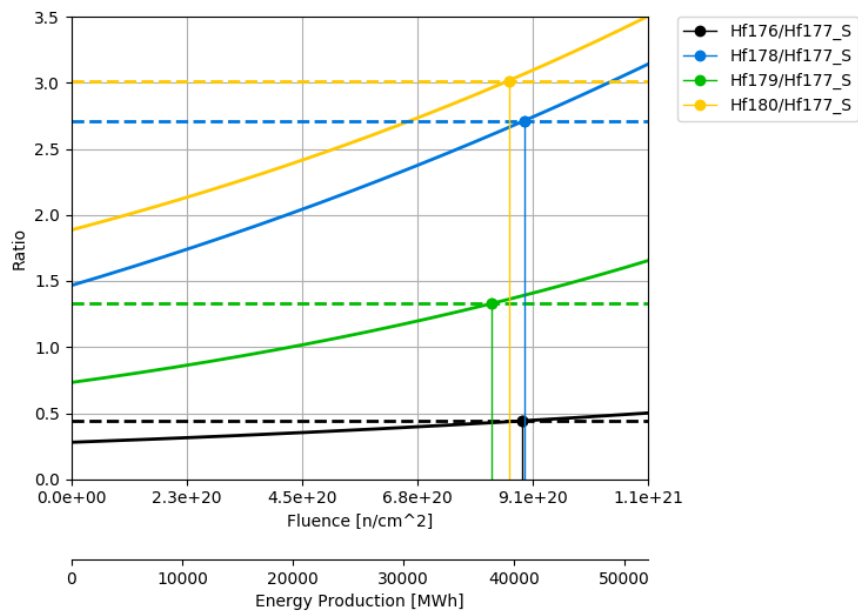


**Figure 6.** The IRM results for S2 showing ICP-MS measured ratios compared with the expected ratios during irradiation. The total fluence is where measured Hf ratios (dotted line) intersects with the calculated Hf ratios (solid curve).

Results of the IRM analysis are tabulated in Table 4, which shows the neutron fluence and energy production estimates for each of the isotope ratios, as well as an average across all ratios that represents the “independent verification value” using the Hf coupons.

**Table 4.** Results from the IRM analysis performed on the Hf samples irradiated in MURR, with uncertainty reported for two standard deviations resulting from the propagation of error from the measurements of the unirradiated Hf as well as the uncertainty of the irradiated measurements. The reported fluence is the operator declared exposure to the coupon.

	Neutron Fluence [ $10^{20}$ n/cm <sup>2</sup> ]	
	S1	S2
Hf176/177	3.69 +/- 0.00052	8.88 +/- 0.00215
Hf178/177	3.63 +/- 0.00068	8.93 +/- 0.00058
Hf179/177	3.37 +/- 0.00078	8.27 +/- 0.00162
Hf180/177	3.54 +/- 0.00187	8.62 +/- 0.00152
Average	3.55 +/- 0.0022	8.67 +/- 0.00315
Reported	3.41	7.66

The total neutron fluence is computed directly for each Hf irradiation target; reported neutron fluence values are determined using the neutron flux values provided by MURR (Table 5). Neutron flux measurements were performed by MURR in 2008 using a <sup>59</sup>Co target. These neutron flux values were calculated by MURR without Maxwellian correction and standard values were used for cross-sections. In the IRM analysis, neutron fluence values are computed to be comparable to the <sup>59</sup>Co neutron flux measurement to enable direct comparisons with MURR reported measurements.

The relative percent difference between the measured and reported neutron fluence values for S1 and S2 are 4.1% and 13.1%, respectively. These results are encouraging, given the preliminary nature of the measurement protocols and Hf-specific analysis methods, but further investigation is needed into

the sources of the discrepancies and the various terms (e.g., ratio measurement, fitting process, data uncertainties) in the overall uncertainty budget on the neutron fluence estimates.

**Table 5.** The neutron flux for experimental locations as reported by MURR based on measurements in 2008, and a comparison of the neutron fluence during the irradiation study, from MURR declaration and the IRM analysis.

	Neutron Flux ( $10^{13}$ n/cm <sup>2</sup> /s)	Neutron Fluence ( $10^{20}$ n/cm <sup>2</sup> )		
	MURR	MURR	IRM	Relative Percent Difference [%]
S1	2.38	3.41	3.55	4.1
S2	5.35	7.66	8.67	13.2

The calculated total energy production is the key verification parameter; however, understanding the uncertainty on that value is critical to understanding the potential value-added for IAEA safeguards verification activities. While a full uncertainty budget calculation was not performed in this scoping study, an initial assessment of how the ratio measurement uncertainties (likely the largest contributor in the uncertainty budget) translate to uncertainty in energy production and full-power operating time was performed. The following uncertainty study is exploring the potential precision of HIRMES as it relates to the IRM method, and not accounting for errors in the modelling. Therefore, the error report in Table 5 includes possible errors in MURR's neutron flux measurement, the variation in the neutron flux over a decade, and errors in modelling (knowledge of where the sample was in the irradiation channel compared to the reported flux, temperatures in the region, etc.). Therefore, the uncertainty analysed below is for the theoretical best-possible precision expected from the HIRMES concept.

This total uncertainty on energy production is summarized in Table 6 for the two samples, S1 and S2. For the S2 sample in the high neutron flux region, this uncertainty is approximately 16 MWh (approximately 0.04% of the total declared energy production) which is equivalent to 1.6 hours of operation. For the S1 sample in the lower neutron flux region, the uncertainty is 21.3 MWh (0.05%) using the solution analysis method, which translates to less than 3 hours of full power operation.

**Table 6.** The uncertainty on energy production estimates and full power operating time for MURR.

	Energy Production Uncertainty [MWh]	Full Power Operating Time	Percent of Total Declared Operations [%]
S1	21.3	2.1 hours	0.05
S2	15.9	1.6 hours	0.04

## 4. Concluding Remarks

This paper presents a preliminary study on a novel approach for high accuracy reactor utilisation measurements for low-power research reactors using the isotope ratio method. Preliminary studies indicate that this approach has promise as a safeguards technology; however, additional work is required to further develop the concepts of operation, extend the method to allow for declaration-free, total energy utilisation measurements, to quantify the uncertainty budgets, and to begin addressing practical implementation of such a technology.

## 5. Acknowledgements

This research was supported by the U.S. National Nuclear Security Administration (NNSA) Office of Nonproliferation and Arms Control (NA-24) under Contract DE-AC05-76RL01830 with the U.S. Department of Energy. Pacific Northwest National Laboratory is a multi-program national laboratory operated by Battelle for the U.S. Department of Energy.

## 6. Legal matters

### 6.1. Privacy regulations and protection of personal data

I agree that ESARDA may print my name/contact data/photograph/article in the ESARDA Bulletin/Symposium proceedings or any other ESARDA publications and when necessary for any other purposes connected with ESARDA activities.

### 6.2. Copyright

The authors agree that submission of an article automatically authorises ESARDA to publish the work/article in whole or in part in all ESARDA publications – the bulletin, meeting proceedings, and on the website.

Once the article has been accepted for publication the copyright is reserved, but part of the publication may be reproduced, stored in a retrieval system, or transmitted in any form or by any means, mechanical, photocopy, recording, or otherwise, provided that the source is properly acknowledged.

The authors declare that their work/article is original and not a violation or infringement of any existing copyright.

## 7. References

- [1] IAEA – International Atomic Energy Agency, “Safeguards Techniques and Equipment: 2011 Edition,” International Atomic Energy Agency, Vienna, Austria, International Nuclear Verification Series No. 1 (Rev. 2).
- [2] S. Fetter, “Nuclear Archaeology: Verifying Declaration of Fissile-Material Production,” *Sci. Glob. Secur.*, vol. Vol. 3, p. pg. 237-259, 1993.
- [3] B. Reid, P. Heasler, D. Gerlach, and J. Livingston, “Trawsfynydd Plutonium Estimate,” Pacific Northwest National Laboratory, Richland, WA, PNNL-13528, Nov. 2009.
- [4] T. W. Wood, B. D. Reid, J. L. Smoot, and J. L. Fuller, “Establishing confident accounting for Russian weapons plutonium,” *Nonproliferation Rev.*, vol. 9, no. 2, pp. 126–137, Jun. 2002.
- [5] C. Gesh, “A Graphite Isotope Ratio Method Primer - A Method for Estimating Plutonium Production in Graphite Moderated Reactors,” Pacific Northwest National Laboratory, Richland, WA, PNNL-14568, Feb. 2004.
- [6] J. McNeece, B. Reid, and T. Wood, “The Graphite Isotope Ratio Method (GIRM): A Plutonium Production Verification Tool,” Pacific Northwest National Laboratory, PNNL-12095, Jan. 1999.
- [7] P. G. Heasler, T. Burr, B. Reid, C. Gesh, and C. Bayne, “Estimation procedures and error analysis for inferring the total plutonium (Pu) produced by a graphite-moderated reactor,” *Reliab. Eng. Syst. Saf.*, vol. 91, no. 10, pp. 1406–1413, Oct. 2006.
- [8] D. Gerlach, C. Gesh, D. Hurley, M. Mitchell, G. Meriwether, and B. Reid, “Final Report on Isotope Ratio Techniques for Light Water Reactors,” Pacific Northwest National Laboratory, Richland, WA, PNNL-18573, Jul. 2009.
- [9] D. Gerlach, C. Gesh, M. Mitchell, D. Hurley, and B. Reid, “Proof-of-Principle Measurements on Unirradiated Zirconium Alloys,” Pacific Northwest National Laboratory, PNNL-16539, Apr. 2007.
- [10] D. Gerlach, M. Mitchell, B. Reid, C. Gesh, and D. Hurley, “Determination of Light Water Reactor Fuel Burnup with the Isotope Ratio Method,” Pacific Northwest National Laboratory, Richland, WA, PNNL-17053, Oct. 2007.
- [11] D. Frank *et al.*, “Application of the Isotope Ratio Method to a Boiling Water Reactor,” presented at the 51st Annual Meeting of the INMM, 2010.
- [12] J. Cliff *et al.*, “Isotope Ratio Method Analysis for the Ford Nuclear Reactor,” presented at the Test Research and Training Reactors, 2005.
- [13] B. Naes *et al.*, “Isotope ratio method analysis of the WWR-SM reactor,” presented at the INMM, 56th Annual Meeting, Atlanta, Georgia USA, 2015.
- [14] D. Gerlach, M. Mitchell, B. Reid, C. Gesh, and D. Hurley, “Selected Isotopes for Optimized Fuel Assembly Tags,” Pacific Northwest National Laboratory, Richland, WA, PNNL-17053 Vol. 2, Oct. 2008.
- [15] D. Gerlach, M. Mitchell, B. Reid, C. Gesh, and D. Hurley, “Measurement Protocols for Optimized Fuel Assembly Tags,” Pacific Northwest National Laboratory, Richland, WA, PNNL-17053 Vol. 3, Nov. 2008.

- [16] IAEA – International Atomic Energy Agency, “Research Reactor Database,” International Atomic Energy Agency, Vienna, Austria, <https://nucleus.iaea.org/Pages/rr-db.aspx>, 2012.
- [17] R. Storn and K. Price, “Differential Evolution – A Simple and Efficient Heuristic for Global Optimization over Continuous Spaces,” *J. Glob. Optim.*, vol. 11, no. 4, pp. 341–359, Dec. 1997.
- [18] M. Berglund and M. Wieser, “Isotopic compositions of the elements 2009 (IUPAC Technical Report),” *Pure Appl Chem*, vol. 83, no. 2, pp. 397–419, 2011.

# Application of the modified Small Quantities Protocol in French territories part of the Nuclear-Weapon-Free Zone in Latin America and the Caribbean

Louis Olivier

Institut de Radioprotection et de Sûreté Nucléaire (IRSN)  
Non-Proliferation and Nuclear Material Accountancy Department  
International Safeguards Unit  
B.P. 17 – 92262 Fontenay-aux-Roses Cedex, France  
E-mail: louis.olivier@irsn.fr

## Abstract:

*The Treaty of Tlatelolco, opened for signature in 1967, establishes the second Nuclear-Weapon-Free Zone (NWFZ) in the world. Its zone of application covers Latin America and the Caribbean and it has been ratified by all 33 countries concerned. Two Protocols are coupled to the treaty. Protocol I requires States that have territories in the zone of application to conclude a comprehensive safeguards agreement with the IAEA specifically for these territories. This is the case for France, which ratified the first protocol in 1992. All nuclear facilities and materials in the French territories there are thus subject to IAEA safeguards as is the case in a non-nuclear-weapon State. As these territories have very limited quantities of nuclear material, the corresponding safeguards agreement incorporates a Small Quantities Protocol (SQP) in its original form. Following the modified SQP established by the IAEA Board of Governors in 2005, French authorities have trained since 2014 to make declarations as if the modified SQP was in force. France ratified in 2018 this modified SQP and the first related official declaration was sent to the IAEA in March 2019. This article describes the French approach and the steps carried out by the national authorities for the application of the modified SQP, as well as the practical consequences for the concerned companies in the French territories located in the NWFZ of Latin America and the Caribbean.*

**Keywords:** Treaty of Tlatelolco; NWFZ; ModSQP

## 1. Introduction

The Treaty of Tlatelolco [1], named after a neighbourhood in Mexico City where the treaty opened for signature in 1967, created a Nuclear-Weapon-Free Zone (NWFZ) in Latin America and in the Caribbean, and has been ratified by all 33 concerned countries. Two Protocols are coupled to the treaty: Protocol I requires States that have territories lying within the zone of application to undertake to apply in these territories the statute of denuclearization in respect of warlike purposes, as defined in Articles 1, 3, 5 and 13 of the Treaty; Protocol II is directed to nuclear-weapon States that are asked to commit themselves not to contribute to the violation of the Treaty nor to threaten to use nuclear weapons against the contracting parties.

France ratified Protocol I to the Treaty of Tlatelolco in 1992, which implied to conclude a safeguards agreement with the IAEA for the French territories in the zone of application of the Treaty, namely French Guiana, Martinique, Guadeloupe, Clipperton Island, Saint Martin and Saint Barthélemy (see Figure 1). Consequently, the *Agreement between the French Republic, the European Atomic Energy Community and the International Atomic Energy Agency for the Application of Safeguards in Connection with the Treaty for the Prohibition of Nuclear Weapons in Latin America and the Caribbean*, known as INFCIRC/718, was signed in 2000 and entered into force on October 26, 2007. This agreement, unlike the France-Euratom-IAEA Voluntary Offer Agreement (INFCIRC/290), is similar to the comprehensive safeguards agreements in force in non-nuclear-weapon States: all

nuclear facilities and materials in the French territories part of the Tlatelolco NWFZ are subject to IAEA safeguards. Moreover, since these territories hold very limited quantities of nuclear material, the agreement incorporated a Small Quantities Protocol (SQP) in its original form: Protocol 1 of INFCIRC/718 corresponds to the SQP itself, while Protocol 2 defines the procedure to follow if the latter is suspended.



**Figure 1: French territories in the zone of application of the Tlatelolco Treaty.**

Most of the requirements of a comprehensive safeguards agreement are held in abeyance when an original SQP is associated, inducing several limitations. For example, the IAEA cannot perform verifications to ensure that SQP States meet the eligibility criteria. Due to proliferation concerns, the IAEA Board of Governors decided in 2005 to restore an important part of these requirements by establishing a modified SQP (ModSQP) [2]. States with an original SQP are since encouraged by the IAEA to adopt this ModSQP.

On September 17, 2017, France, Euratom and the IAEA signed an agreement [3] for amending the INFCIRC/718 SQP in order to apply the ModSQP in the French territories part of the Tlatelolco NWFZ. Following the ratification of this agreement by France in 2018, and the notification to the IAEA by France and the European Commission that internal legal requirements were in place, the ModSQP entered into force on February 25, 2019. Consequently, the first official declaration under the ModSQP was sent by the French authorities in March 2019.

## 2. The modified Small Quantities Protocol

Two criteria must be fulfilled to be eligible to the application of the INFCIRC/718 ModSQP. The first criterion is focused on the maximum quantities of nuclear material in the French territories part of the Tlatelolco NWFZ, which are the same as for the original SQP (see Figure 2). However, the second criterion of the ModSQP is significantly more restrictive than in the original SQP: whereas the original SQP is no longer available as soon as there is nuclear material in a facility (as defined in Article 96 of INFCIRC/718)<sup>1</sup>, the ModSQP is suspended as soon as France would take the decision to construct or to authorize the construction of a facility in the French territories concerned. If the abrogation of the ModSQP was to happen, Protocol 2 of INFCIRC/718 would apply, meaning that France, Euratom and the IAEA would have to agree on procedures for co-operation in the application of the full terms of the Comprehensive Safeguards Agreement in the aforementioned territories.

<sup>1</sup> A reactor, a critical facility, a conversion plant, a fabrication plant, a reprocessing plant, an isotope separation plant, a separate storage installation or any location where nuclear material in amounts greater than one effective kilogram is customarily used.

**Nuclear material quantities limit:**

- (a) One kilogram in total of special fissionable material, which may consist of one or more of the following:
  - (i) Plutonium;
  - (ii) Uranium with an enrichment of 0.2 (20%) and above, taken account of by multiplying its weight by its enrichment;
  - (iii) Uranium with an enrichment below 0.2 (20%) and above that of natural uranium, taken account of by multiplying its weight by five times the square of its enrichment;
- (b) Ten metric tons in total of natural uranium and depleted uranium with an enrichment above 0.005 (0.5%);
- (c) Twenty metric tons of depleted uranium with an enrichment of 0.005 (0.5%) or below;
- (d) Twenty metric tons of thorium.

**Figure 2:** Original and modified SQP quantities limits defined in Article 35 of INFCIRC/718.

As regards the requirements under the ModSQP, Part II of the INFCIRC/718 is held in abeyance, with the exception of Articles 31-37, 39, 47, 48, 58, 60, 66, 67, 69, 71-75, 81, 83-89, 93 and 94. As a reminder, the exception affected only Articles 31, 32, 37, 40 and 89 in the original SQP. In particular, the ModSQP restores the following measures and requirements:

- A general description of the use of the nuclear material and of the procedures for nuclear material accountancy and control (Article 47);
- An initial report on all nuclear material subject to safeguards under the Agreement within thirty days of the last day of the month in which the ModSQP has entered into force (Article 60);
- A special report if there is or may have been loss of nuclear material subject to safeguards under the Agreement (Article 66);
- IAEA ad hoc and special inspections (Articles 69 and 71);
- A notification for any expected import of nuclear material if the shipment exceeds one effective kilogram, or if, within a period of three months, the total of several separate shipments from the same State exceeds one effective kilogram (Article 93).

### 3. Practical implementation

The French CTE (Euratom Technical Committee), placed under the authority of the French Prime Minister, is in charge of monitoring the implementation of international controls on nuclear materials in France and is the French authorities' representative for Euratom and the IAEA. The CTE benefits from the technical support of IRSN Non-Proliferation and Nuclear Material Accountancy Department, among others for the collection and analysis of nuclear material data and the preparation of the international declarations.

As regards the implementation of the ModSQP, CTE and IRSN have trained since 2014 to establish declarations as if it was already in force.

#### 3.1. Regulations

Almost all information required by the ModSQP is already requested either by the national law or the Regulation (Euratom) No 302/2005. Therefore, no change was necessary in the French regulation to implement the ModSQP.

The French Code of Defence includes the regulation about the protection of nuclear material. It requires nuclear material holders to declare their physical inventory and the inventory changes (quantity, composition, destination), including for transfers within France, at least once a year, which is the minimum frequency for nuclear material reporting under the ModSQP. More details about the French national regulation can be found in reference [4].

As regards the Regulation (Euratom) No 302/2005, it states that nuclear material users must provide the basic technical characteristics (BTC) of their activity. Such a document provides, among other information, the general description required by Article 47 of INFCIRC/718. Furthermore, this Regulation foresees the transmission of a special report in similar circumstances to those described in Article 66 of the Safeguards Agreement and it can also be used for the notification of imports in the cases highlighted in Article 93.

### **3.2. Nuclear material holders involved**

Currently, there are two holders of nuclear material within the French territories under INFCIRC/718: one in Martinique and one in French Guiana. They have been identified thanks to the national regulation, for which they have sent annually declarations on nuclear material for several years. Both are considered as locations outside facilities (LOF) and possess only one category of nuclear material, namely depleted uranium shielding for industrial gamma radiography devices. In other words, these operators deal with 34c) nuclear material (as defined in INFCIRC/153). The quantities involved are far below the ModSQP limits quoted in Figure 2.

Considering the guidelines for the application of Regulation (Euratom) No 302/2005 [5], these two licensees are considered as non-nuclear LOF (not nuclear fuel cycle related). They are therefore eligible to be part of the catch-all material balance area (CAM) defined in the Annex I-G of the Euratom Regulation. Following the entry into force of the ModSQP, and upon request of the European Commission, a subcategory was created in the French CAM specifically for the holders under INFCIRC/718, in order to distinguish them from the LOF that are under INFCIRC/290. This separation was made for convenience, but the obligations of the LOF concerning the Euratom Regulation are of course the same, disregarding the Safeguards Agreement considered.

### **3.3. Guidance and advice to licensees**

An important task of IRSN, as a technical support to CTE, is to advise holders for the fulfilment of their international obligations in the event that they would have doubts about the procedure to follow. As an example, IRSN helped them to make their BTC in agreement with the Annex I-G of the Euratom Regulation and explained them what kind of information should be supplied in the general description requested by Article 47 of INFCIRC/718.

In August 2018, anticipating the impending entry into force of the ModSQP, an information meeting was organised by IRSN for the licensees concerned. The aim was to explain the history of the INFCIRC/718 and its differences with the French Voluntary Offer Agreement INFCIRC/290, as well as to detail the new obligations that the ModSQP will induce, in particular the possibility to undergo IAEA ad hoc and special inspections (Articles 69 and 71). This kind of training is of primary importance since most of the time users of nuclear material in non-nuclear industry, as is the case for the holders under INFCIRC/718, are not aware about IAEA safeguards and their differences with Euratom safeguards.

### **3.4. Report on nuclear material**

The initial report on nuclear material was prepared by the International Safeguards Unit of IRSN Non-Proliferation and Nuclear Material Accountancy Department, following the form given in the Appendix 2 of the IAEA guidance document for the implementation of the ModSQP [6]. The nuclear material data were based on the required national declaration the licensees sent to the Nuclear Material Accountancy Unit. The latter belongs to the same IRSN Department as the International Safeguards Unit and the cooperation between these two units was of great help for establishing such a report. As the initial report had to reflect the situation as of the last day of the month in which the ModSQP entered into force (namely February 2019) and as the two concerned holders are required to declare their inventory only once a year and as at December 31<sup>st</sup>, IRSN contacted them to know if any inventory change happened within the two first months of 2019. Each licensee is considered independently for the nuclear material reporting to IAEA, therefore two forms were filled, one for each holder. The global inventory of nuclear material under INFCIRC/718 safeguards is then simply obtained by summing the amounts held in each LOF. The initial report was approved by the CTE that sent the electronic version to the European Commission in March 2019 for a transmission to the IAEA within the same month, in compliance with Article 60 of the Safeguards Agreement.

An update of the nuclear material inventory will be established on an annual basis in order to take into account any change that occurred, such as imports/exports. As the two LOF are treated separately, any nuclear material transfer between them will also be reflected in this update, although such an operation does not affect the total amount of nuclear material that is covered by INFCIRC/718.

In addition to the inventory update, and also on an annual basis, a report of exports and imports of nuclear material from/into the French territories under INFCIRC/718 will be established, following the Appendix 3 of the IAEA guidance document [6]. As long as only 34c) nuclear material is involved, all transfers are reported, regardless of the end purpose. It should be stressed that exports/imports between the French territories under INFCIRC/718 and the rest of France, which is under the INFCIRC/290 Safeguards Agreement, are considered as foreign transfers and will therefore also be reported.

#### 4. Conclusion

On February 25, 2019, the ModSQP associated to the *Agreement between the French Republic, the European Atomic Energy Community and the International Atomic Energy Agency for the Application of Safeguards in Connection with the Treaty for the Prohibition of Nuclear Weapons in Latin America and the Caribbean* (INFCIRC/718) entered into force. The French authority for the implementation of international safeguards, the CTE, and its technical support, the IRSN, have trained since 2014 to make the related declarations. The holders concerned by INFCIRC/718 were closely associated to these exercises and a general information meeting was organised a few months before the entry into force of the ModSQP. Such a preparation allowed the timely transmission of the initial report on nuclear material.

#### 5. References

- [1] *Treaty for the Prohibition of Nuclear Weapons in Latin America and the Caribbean*; S/Inf. 652 Rev. 3; 2002. Available on [www.opanal.org](http://www.opanal.org)
- [2] IAEA Board of Governors; *Revision of the Standardized Text of the "Small Quantities Protocol"*; GOV/INF/276/Mod.1; 2006. Available on [www.iaea.org](http://www.iaea.org)
- [3] *An Agreement to amend Protocol 1 and Protocol 2 of the Agreement between the French Republic, the European Atomic Energy Community and the International Atomic Energy Agency for the Application of Safeguards in Connection with the Treaty for the Prohibition of Nuclear Weapons in Latin America and the Caribbean*; INFCIRC/718/Mod.1; 2019. Available on [www.iaea.org](http://www.iaea.org)
- [4] Lanave L.; *French system for accountancy and control*; Proceedings of the ESARDA 39th Annual Meeting; 2017; p 37-43. Available on [esarda.jrc.ec.europa.eu](http://esarda.jrc.ec.europa.eu)
- [5] European Commission; *Commission Recommendation of 15 December 2005 on guidelines for the application of Regulation (Euratom) No 302/2005 on the application of Euratom safeguards*; Official Journal of the European Union; L 28; 2006. Available on [eur-lex.europa.eu](http://eur-lex.europa.eu)
- [6] IAEA; *Safeguards Implementation Guide for States with Small Quantities Protocols*; Services Series 22; 2016. Available on [www.iaea.org](http://www.iaea.org)

# The algorithm for State-level concept software educational simulator

**Daria Koneva, Dmitry Sednev**

National Research Tomsk Polytechnic University  
Russia, 634050, Tomsk, Lenina avenue, 30  
E-mail: d.a.koneva@gmail.com

## **Abstract:**

*Renewal and advancing staff competences is one of the key issues for any industry, including a nuclear non-proliferation. A lack of qualified specialists should be overcoming by life-long learning concept. In Russia, the first step of professional education is a University, and Tomsk Polytechnic University (TPU) is the only one, that is giving a non-proliferation study as a major. In order to enhance educational environment in TPU by broad range of instruments, the development of State-level concept software educational simulator for course "Legal aspects of non-proliferation regime" was proposed.*

*State-Level Concept (SLC) along with Integrated Safeguards are most novel safeguard system developed and promoted by IAEA. The SLC includes State-Specific Factors (SSF), Acquisition Path Analysis (APA) and the development of State-Level Approaches (SLAs). Under the SLC, safeguards will be focused on understanding the entirety of the nuclear program in the State and developing a customized SLAs for the States. Within the proposed simulator student will start with a hypothetical State description by describing of its SSF, because it dedicated to provide the fundamental information for the further analysis. Since TPU by nature is technical University, the most detailed description should be given to SSF that corresponds to the nuclear fuel cycle and related technical capabilities of the State. Than student according to State's description will analyze a possible paths of proliferation, which could be taken from the presets or created by their own. After it the simulator provides a student with a quantitative information about results of APA and a student should develop a draft of SLAs. SLA's evaluation still requires a tutor, but we are searching for automatization possibilities.*

**Keywords:** State-Level Concept; educational simulator; non-proliferation regime; State-Specific Factor; State-Level Approach

## **1. Introduction**

One of the core and novel developments of IAEA regulation system is SLC, which contains the comprehensive consideration of the State nuclear program aspects. The main obstacle for wide implementation of SLC is lack of professionals with deep knowledge and understanding of concept itself. So far, in this paper proposed a development of Quantitative State-Level Simulation Tool or QSLSTool. As widely known, SLC is realized by three main steps: 1) determination of SSFs; 2) APA; 3) establishing of the effective safeguards measures. Further, in accordance with the results, SLAs are developed [1]. The developed QSLSTool implements the first two steps of concept. It is worth to mention, APA will be calculated automatically, based on State's nuclear fuel cycle description. The quantitative approach, that is described later in the paper, represents the basis of the Tool.

## **2. Algorithm of the QSLSTool**

The Tool helps go through several steps, corresponding to a separate SSFs. At each step, data is entered by operator, or he should make a selection from the presented list of options.

Step 1. The type of safeguards agreement in force for the State.

It is necessary to choose the type of signed agreement from the two proposed options: "Comprehensive Safeguards Agreement" or "Comprehensive Safeguards Agreement + Additional Protocol".

Step 2. The nuclear fuel cycle and related capabilities of the State.

This step includes several stages that allow characterization of the nuclear fuel cycle (NFC) of the state in accordance with the developed criteria (Heading 3.1). At the same time, the Tool collect the data necessary for analyzing the ways of acquiring NM, and automatically performs a full calculation according to the developed mathematical apparatus (Heading 3.2). To do this, at the first stage, it is necessary to select the types of NFC objects of the state and indicate their number:

- Ore mining;
- Milling of ore;
- Conversion;
- Enrichment;
- Fuel fabrication;
- Operation;
- Reactor spent nuclear fuel storage;
- Interim storage of spent nuclear fuel;
- Reprocessing;
- Final disposal.

It should be considered that the set of stages must have logic and be close to the real one. Some stages include the obligatory choice of additional parameters:

- Enrichment – "Gas diffusion" and/or "Gas centrifugation";
- Operation – "LWR" and/or "GCR" and/or "PHWR" and/or "FBR" and/or "Research reactor";
- Storage of spent nuclear fuel – "Dry" and/or "Wet".

After the selection of the type of NFC objects has been made and their number is defined, the Tool displays as the result of the first stage a preliminary graph, which shows all possible NM proliferation paths, and also highlighted with different colors the transactions. The second stage is to choose the type of NM on each NFC facility. Next, you need to select the values of the following parameters:

- Weapon grade nuclear material (meaning "no" or "yes");
- Presence of inseparable impurities (meaning "no" or "yes");
- Inherent security due to high radioactivity (meaning "no" or "yes");
- Chemical form (meaning "metal" or "ceramics" or "other compounds");
- Physical state of a matter (meaning "gaseous" or "solid" or "liquid").

At the third stage of Step 2, the amount of NM is selected at each stage of the nuclear fuel cycle, laterally, the mass of the fissile uranium/plutonium isotope. To perform this task, it is necessary to analyze each stage of the nuclear fuel cycle and, based on the obtained results, enter the numerical values of the following criteria:

- Uranium mass or Plutonium mass – depending on the stage of the NFC;
- Uranium enrichment – if uranium is used at the NFC stage.

At the fourth stage, it is necessary to determine at each stage of the nuclear fuel cycle "Technical capability for the theft of nuclear material": "Availability" or "Absence". And also choose the category of the theft process: "Switching", "Unreported Import", "Misusing", "Production of Undeclared Nuclear Material".

The fifth and final stage of Step 2 is the definition of "Availability" or "Absence" of "Import" and "Export" at each stage of the NFC.

The result of Step 2 is a constructed graph with prioritized ways of acquiring NM, based on an automatically conducted analysis of the ways of acquiring NM through the Tool.

Step 3. The technical capabilities of the State or regional system of accounting for and control of nuclear material.

To determine the technical capabilities, the following aspects should be described, choosing one of the proposed options, namely:

- 1) SSAC/RSAC and completeness of their compliance with the recommendations of the IAEA:
  - Implemented, full compliance with the recommendations; or
  - Implemented, partial compliance with the recommendations; or
  - Implemented, complete non-compliance with recommendations; or
  - Not Implemented.
  
- 2) The state or regional authority responsible for the implementation of the terms of the safeguards agreement in the state, and the fullness of its powers:
  - One SSAC and several RSAC exist. The state does not control and does not interfere in the activities of the SSAC. RSAC are fully subordinate to the SSAC; or
  - One SSAC and several RSAC exist. The state and the SSAC cooperate and perform coordinated joint activities. RSAC are fully subordinate to the SSAC; or
  - One SSAC exists. The state does not control and does not interfere in the activities of the SSAC; or
  - One SSAC exists. The state and the NRA cooperate and carry out coordinated joint activities; or
  - Several of the existing RSAC are subordinate to the state. The state and the RSAC carry out coordinated joint activities; or
  - No SSAC/RSAC. The state independently conducts activities to comply with the terms of the agreement on safeguards.

Step 4. The ability of the Agency to implement certain safeguards measures in the State.

At this step, it is necessary to determine the extent to which the state and the conditions for implementing the safeguards created in it enable the Agency to implement technical or inspection measures that can increase the effectiveness and efficiency of the safeguards. To do this, select one of the following options:

- Opportunities are not limited; or
- Possibilities are limited in part; or
- Opportunities are limited.

Step 5. The nature and scope of the cooperation between the State and the Agency in the implementation of safeguards.

To describe the cooperation from the state [2], it is proposed to evaluate nine possible options of the nature of cooperation presented below. To determine the scope of the cooperation from the state, each of the nine options, in turn, is assessed in the following grades: "Present" or "From case to case" or "None".

- Bringing into force or modifying Subsidiary Arrangements, General Part, that contain the latest revisions approved by the Board of Governors.
- Establishing and maintaining an effective SSAC/RSAC.
- Keeping appropriate records with respect to each material balance area and making arrangements for the examination of records by inspectors.
- Maintaining a system of measurements on which the records for the preparation of reports are based that shall be equivalent in quality to the latest international standards.
- Ensuring the timeliness, correctness, and completeness of State reports, declarations, design information, special reports, and notifications (e.g., exports and imports).

- Being responsive to addressing anomalies, questions, or inconsistencies and the Agency requests for information or clarifications to enhance the Agency understanding of nuclear activities of a State.
- Accepting inspector designations and issuing visas.
- Granting privileges and immunities to Agency inspectors and assets.
- Facilitating inspector access and activities during such access.

Step 6. The Agency's experience in implementing safeguards in the State.

Evaluation of the experience in the implementation of safeguards is carried out in four aspects, therefore this step is carried out in four stages. At the first stage, the conditions in the state and its facilities should be described by user, namely:

- National safety or security conditions that prohibit the Agency access to facilities.
- Conditions preventing the effective use of undeclared inspections.
- National laws restricting the removal or transfer of information.
- Existing or recurring conditions at facilities that affect the implementation of safeguards measures under the safeguards agreement.

At the second stage, the state's experience in fulfilling its safeguards obligations is described, where it is necessary to assess the state's influence on the SSAC/RSAC in the following categories:

- SSAC/RSAC under the full control of the state; or
- SSAC/RSAC is partly influenced by the state; or
- The SSAC/RSAC operates independently of the control and influence of the state.

The answer should not contradict the information chosen in Stage 2 of Step 3.

In the third stage, it is necessary to consider "Cases of potential non-compliance with the safeguards agreement" by selecting one of the following options:

- Absent; or
- Single; or
- Systematic.

At the fourth stage of Step 6, the "State action history beyond the requirements of the safeguards agreement" is described. This requires entering at least two agreements or treaties operating in a hypothetical state, which contribute to an increase in the transparency of nuclear activities in the State and the Agency knowledge of the State activities.

After completing the six steps, the Tools generates and offers to save the file, which is the legend of a hypothetical state. The legend includes user-created descriptions of all state specific factors and a graph with prioritized acquisition paths.

Figure 1 shows the flow chart of the Tool. Since the second step is rather sophisticated, it is presented in more detail in Figure 2.

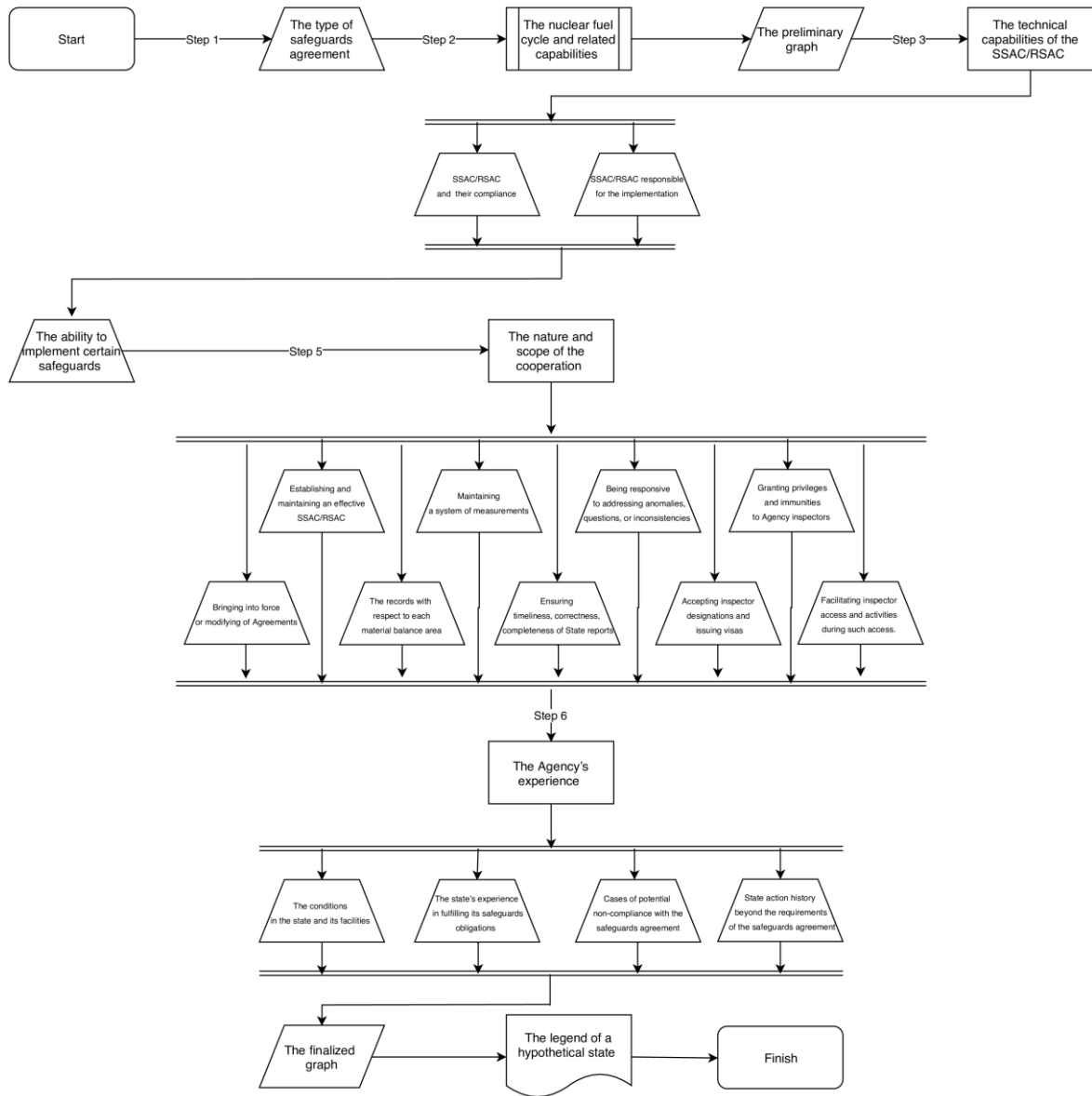


**Figure 1: General Flow Chart**

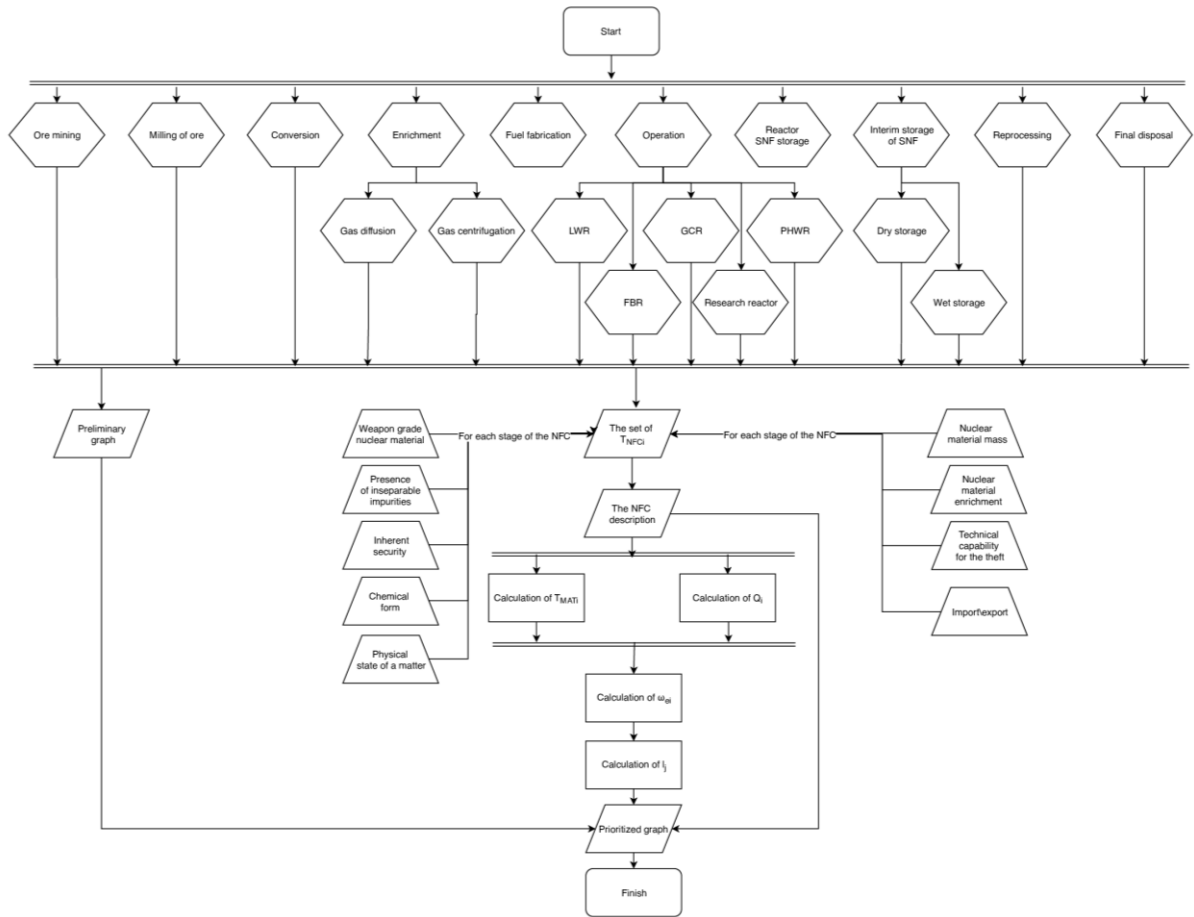


Figure 2: Flowchart in Step 2

### 3. Quantitative approach to Acquisition Path Analysis

In process of a quantitative analysis, two state specific factors are used, such as:

- The type of safeguards agreement in force for the State.
- The nuclear fuel cycle and related capabilities of the State.

The first factor cannot have a quantitative characteristic. Therefore, within the framework of the quantitative approach, a set of criteria characterizing the state NFC and having a numerical evaluation is proposed. On the basis of these criteria, an alternative approach to calculating the weight of the edge and the overall attractiveness of the path is carried out.

#### 3.1. The numerical evaluation of the nuclear fuel cycle of the state

The development of the specific characterization parameters of the nuclear fuel cycle of the state including establishment of the particular value for each of them is proposed (Table 1). The analysis of worldwide literature was carried out in order to prove the reliability of the created system [3-9].

#	Parameter	NFC of the State	Numerical value
1	N <sub>NFC</sub>	NFC stages number in edges chain	Pcs.
2	T <sub>NFC</sub>	The NFC facility type, weighting coefficient	Ore mining – 0 Milling of ore – 0 Conversion – 1,5 Enrichment: <ul style="list-style-type: none"> <li>• Gas diffusion – 3</li> <li>• Gas centrifugation – 4</li> </ul> Fuel fabrication – 1,5 Operation: <ul style="list-style-type: none"> <li>• LWR – 1</li> <li>• GCR – 1</li> <li>• PHWR – 1,5</li> <li>• FBR – 2</li> <li>• Research reactor – 2</li> </ul> Reactor SNF storage – 1 Interim storage of SNF – 1,5 Reprocessing – 2,5 Final disposal – 0
3	N <sub>TRAN</sub>	The number of ambient transactions	Pcs.
4	T <sub>MAT</sub>	Nuclear material type at a site	Unit of account
5	Q	Nuclear material quantity at a site	Unit of account
6	TP <sub>OUT</sub>	Principal possibility of theft capabilities at different stages of NFC, weighting coefficient	Presence – 1,25 Absence – 0,75
7	IE	Presence/absence of import/export of nuclear material and technologies at different stages of NFC, weighting coefficient	Import – 0,75 Export – 1,25 Absence – 1

**Table 1:** Characteristic parameters of the NFC

Each of the parameters is discussed in more detail below.

Parameters #1 and #3 correspond to the quantity of NFC facilities and nuclear material transactions between these facilities. The increase of these numbers will make safeguards administration more difficult. The growth of the facilities number included in NFC leads to the increase of the possibilities of the diversion. The transaction is considered as one of the most critical stages of the NFC, due to the lack of monitoring and security measures. Thus, the risk of undetected theft increases.

Parameter #2 is proposed taking into account technical difficulties and proliferation time of nuclear material for each particular spent nuclear fuel (SNF) stage that are required for the diversion to nuclear weapon production.

The first considered stage is U or Th ore mining. The materials in such form are not included into the Common System of Accounting and Control of Nuclear Materials, due to the fact that it is not valid for nuclear weapon production.

The ore milling stage comprises the extraction of U from the ore and its further conversion into the uranium oxide powder. In general, uranium ore consists of large amount of naturally occurring additional elements that are further removed by special physicochemical procedures. The final product in this process is U<sub>3</sub>O<sub>8</sub> – powder that contains 90% of naturally enriched uranium. At this stage material is suitable neither for nuclear weapon production nor for enrichment; both abovementioned processes require special conversion technologies [3].

Uranium conversion is the process in which natural uranium in the form of U<sub>3</sub>O<sub>8</sub> powder is converted to UF<sub>6</sub>, such form of uranium is appropriate for further isotope enrichment [4]. Despite the natural enrichment level of the nuclear material, the conversion stage is critical in terms of nuclear material proliferation due to the form of the final product.

Enrichment stage is the most sensitive and critical regarding to the production of nuclear weapon quality material, due to the fact that quality of nuclear material is determined by the percentage of the fissile isotope ( $U^{235}$  or  $Pu^{239}$ ). Each of the technologies enables increasing the percentage of the fissile isotope up to 90 %, which is sufficient for the production of nuclear weapons [3]. It was decided to compare and determine the coefficients for only two uranium enrichment technologies - gas diffusion and gas centrifugation, due to their use on an industrial scale. The technology of gas diffusion is a rather sophisticated process due to the fact that uranium must be pumped through a large number of porous barriers, since the separation coefficient is low (1,0043); and energy-consuming, because Compressors in such installations produce a lot of heat that needs to be removed. Gas centrifugation is more energy efficient due to the smaller number of stages, as well as a high separation factor (1,25-2,0). Despite the fact that centrifuges have significantly lower throughput than diffusion cascades, this allows you to increase production capacity in smaller steps. Modern centrifuges are able to rotate at a speed close to the speed of sound, therefore, it is extremely difficult to control this process. In addition, this degree of rotation makes it technically difficult to create such installation, as a centrifuge is to be perfectly stable and balanced and ready for operation in this form for many years without interruption for maintenance [5].

At the stage of the fuel fabrication the conversion of the enriched material to the form suitable for further exploitation in nuclear reactor is performed. The sensitivity of the stage mainly depends on the enrichment percentage, which is taken into account by corresponding weighting coefficients. The risk of the considered stage in terms of nuclear weapon production is related to the existence of the technology for conversion of the gaseous nuclear material into a solid that is sufficient for nuclear weapons [5].

The next stage of the NFC is the main process in nuclear power engineering. It is the operation of a nuclear reactor. The research is conducted within the framework of maintaining the international nuclear non-proliferation regime, thus the international classification of reactor types can be applied. The following types of reactors are discussed:

- Light-water reactor (LWR) type includes the pressurized water reactor (PWR), the boiling water reactor (BWR) and the supercritical water reactor (SCWR). When we consider nuclear nonproliferation issues, it has to be mentioned that LWR has two main features: low-enriched uranium (3-5%) fuel (LEU) and poor breeding capabilities. However, the reactor core has significant amount of fuel due to its low enrichment level. This fact makes LWR potentially capable for clandestine nuclear program [6].
- Gas-cooled reactor (GCR) type has the same characteristics as LWR in respect to proliferation application [6].
- Pressurized heavy water reactor (PHWR) has controversial properties: on the one hand, heavy water has low neutron absorption cross section, which makes it possible to use natural uranium as fuel and exclude the fuel enrichment stage from the NFC – all these facts significantly reduce proliferation risks. However, on the other hand, natural uranium has much better breeding potential due to conversion of  $U^{238}$  isotope to Pu as the result of neutron capture [6, 7].
- The main feature of Fast breeder reactor (FBR) is a breeding blanket of fertile material (usually, natural or depleted uranium) that surrounds the core. The blanket enables receiving significant amount of weapon or sub-weapon grade Pu. In addition to that, another proliferation challenge related to FRB is the possibility to use MOX-fuel as fissile material. MOX-fuel consists of U and Pu isotopes that potentially could lead to diversion of fuel itself for military applications [7].
- Majority of Research reactors (RR) use high-enriched uranium (HEU) as fuel. IAEA has initiated RR conversion from HEU to (LEU) [8]. Despite this fact, many of RR worldwide are still not engaged into this initiative.

The described classification of reactor types intentionally excludes industrial breeder reactors that were designed and tailored for weapon-grade plutonium breeding, because that type is operated in nuclear weapon states only.

Next stage of NFC is SNF reactor storage in a specialized pool at a reactor's site. This process has started immediately after a fuel load of a reactor is removed from the core and placed to a pool. Despite of SNF inherent security properties (due to high radiation hazard), it may have high percentage of Pu that can be used for military purposes [5]. Taking into account the fact that decision to diversify a material to a weapon program is to be made by government, the possibility of application of specialized equipment for handling high-radioactive SNF has to be considered. The radioactivity of SNF is

significantly decreasing after 3-5 years and, usually, spent fuel is transferred to dry or wet interim fuel storage facility. However, it has to be mentioned that inherent security level is decreasing as well. At the same time the Pu amount still remains the same [4]. So, proliferation risks on stage of interim storage are higher than during reactor storage.

The SNF reprocessing process could be used by a State for separation most valuable isotopes and further MOX-fuel production. Reprocessing stage is the most sensitive in respect to development of Pu-based nuclear weapon. Nevertheless, there are some limiting factors: high-radiation level, inseparable impurities etc. [9].

Any NFC has a back-end – disposal of radioactive wastes that has no valuable material and not supposed to have any use in further activities. So, wastes are useless in nuclear weapon production. Modern waste's immobilization technologies even more limit the possibilities of malicious use of wastes and prevent its' recovery [9].

Parameter #6 considers an increase of proliferation risks that is related to the theft capabilities of nuclear materials at different stages of NFC. Theft capabilities are understood as covered transfer of nuclear material from NFC for malicious purposes that cannot be identified during IAEA inspection.

Parameter #7 is dedicated to indicate presence/absence of import/export of nuclear material and technologies. Nuclear technologies import requires application of additional procedures of export control, thus decreasing the diversion attractiveness. Otherwise, an export of nuclear-related items highlights deep knowledge and know-how of a State and that significantly increases diversion possibilities.

"Nuclear material type at a site" ( $T_{MATi}$ ) and "Nuclear material quantity at a site" ( $Q_i$ ) are the units of account and described below by equation (1) and (2).

$T_{MATi}$  consists of five factors, describing the applicability of nuclear material for production of nuclear weapon. The parameter is based on multiplicative model (1) defined by the fact that the factors under consideration are interdependent and have strong mutual influence.

$$T_{MATi} = WG_i \cdot M_i \cdot R_i \cdot Ch_i \cdot Ph_i , \quad (1)$$

where  $WG_i$  – weapon grade nuclear material ("no" = 1, "yes" = 100);  
 $M_i$  – presence of inseparable impurities ("no" = 1, "yes" = 0,3);  
 $R_i$  – inherent security due to high radioactivity ("no" = 1, "yes" = 0,3);  
 $Ch_i$  – chemical form ("metal" = 1, "ceramics" = 0,9, "other composition" = 0,8);  
 $Ph_i$  – physical state of a matter ("gaseous" = 1, "solid" = 0,7, "liquid" = 0,3).

$WG_i$  is uranium with enrichment higher than 90% and plutonium that has in composition less than 20% of 238, 240, 241, 242 isotopes. Nuclear materials of such quality are called "direct use material" that allow to create a nuclear weapon without additional technological process.

The factor " $M_i$ " defines presence of impurities that are inseparable at state-of-art methods. The impurities taken into account should influence the possibility of military application of nuclear material via significant increase of its' critical mass.

The inherent security – " $R_i$ " is defined by quantity of short-lived isotopes.

" $Ph_i$ " demonstrates the possibility of application of the current state of nuclear material to a weapon program. It is important to mention, that the highest value belongs to a "gaseous" state. Despite its unsuitability for direct use in nuclear weapon production, it allows to perform material enrichment.

To define a relative number of nuclear explosive devices that is possible to create, the nuclear material quantity has to be taken into account:

$$Q_i = \frac{m_{FISi}}{SQ_{ISi}} , \quad (2)$$

where  $m_{FISi}$  – fissile isotope mass;  
 $SQ_{ISi}$  – IAEA Significant Quantity of the isotope.

Significant quantity is the approximate amount of nuclear material for which the possibility of manufacturing a nuclear explosive device cannot be excluded [10].

### 3.2. Mathematical instrument of quantitative approach to Acquisition Path Analysis

APA is performed in three stages: 1) path's net modelling; 2) analysis of all possible paths of the developed net; 3) state strategic evaluation.

Mathematically modelled net is calculated in accordance with the graph theory [11]. Analogy between APA elements and graph theory is provided in Table 2.

Graph theory	Acquisition path analysis
Node	Material form
Edge	Stage of nuclear fuel cycle
Path	Acquisition path
Edge weight	Attraction of an acquisition path

**Table 2:** Element analogy

The fundamentals of quantitative approach to APA is the set of parameters with appropriate numerical characteristics.

The multiplicative model is proposed for an edge weight calculation ( $\omega_e$ ). The model will depend on NFC stage and type and quantity of nuclear material at a facility:

$$\omega_{ei} = T_{NFCi} \cdot T_{MATi} \cdot Q_i . \quad (3)$$

Calculated value of  $\omega_e$  is the most fundamental to identifying the possibility of nuclear material diversion of the particular stage of NFC.

Within the quantitative approach the equation of the general attractiveness is the following:

$$I_j = \frac{(\sum \omega_{ei} \cdot \sum IE_i \cdot \sum TP_{OUTi}) \cdot (N_{NFCj} + N_{TRANj})}{n_e} , \quad (4)$$

where  $n_e$  – path's edge quantity.

Quantitative evaluation of the general attractiveness of potential acquisition path will be more objective in comparison with qualitative approach, because quantitative approach is based on the set of weight factors and numerical characteristics.

## 4. Conclusion

The quantitative approach proposed in this paper provides numerical evaluation of the potential paths of acquiring the nuclear material that enables making the impartiality of the choice of IAEA safeguards for further implementation. The developed and described algorithm is a basis for QSLSTool, that dedicated to help the Agency to promote SLC among safeguards professionals along with training a new one, e.g. at the University basis. The authors intended to implement the developed Tool at Tomsk polytechnic university.

## 5. Acknowledgements

The study is financially supported by the Ministry of Science and Higher Education of the Russian Federation within the Federal Target Program entitled "R&D in Priority Areas of Development of Russia's Scientific and Technological Complex for 2014-2020" (unique project ID: RFMEFI57817X0251).

## 6. References

- [1] *Supplementary Document to the Report on The Conceptualization and Development of Safeguards Implementation at the State Level (GOV/2013/38)*; IAEA; 2014; 65 p.
- [2] Cooley J.N., Moran B.W.; *Assessment and Use of State-Specific Factors in the Implementation of Safeguards*; 10 p.
- [3] *INPRO Collaborative Project: Proliferation Resistance: Acquisition/Diversions Pathway Analysis (PRADA)*; Vienna: IAEA; 2012; 62 p.
- [4] Zentner M.D.; *Nuclear proliferation technology trends analysis*; USA: Pacific northwest national laboratory; 2010; 130 p.
- [5] *Nuclear Fuel Cycle Information System IAEA-TECDOC-1613*; Vienna: IAEA; 2009; 82 p.
- [6] World Nuclear Association; *Nuclear Power Reactors* [Electronic resource]. – Access mode: <http://www.world-nuclear.org/information-library/nuclear-fuel-cycle/nuclear-power-reactors/nuclear-power-reactors.aspx>.
- [7] *Nuclear Reactor* [Electronic resource]. – Access mode: <http://www.nuclear-power.net/nuclear-power-plant/nuclear-reactor/>.
- [8] *The Reduced Enrichment for Research and Test Reactors (RERTR) Program* [Electronic resource]. – Access mode: <http://www.rertr.anl.gov>.
- [9] *Spent Fuel Reprocessing Options*; Vienna: IAEA; 2008; 151 p.
- [10] *IAEA safeguards glossary*; Vienna: IAEA; 2002; 230 p.
- [11] Listner C., Canty M.J., Stein G., Rezniczek A., Niemeyer I.; *Quantifying Detection Probabilities for Proliferation Activities in Undeclared Facilities*; 2014; 10 p.

## 7. Legal matters

### 7.1. Privacy regulations and protection of personal data

The authors agree that ESARDA may print my name/contact data/photograph/article in the ESARDA Bulletin/Symposium proceedings or any other ESARDA publications and when necessary for any other purposes connected with ESARDA activities.

### 7.2. Copyright

The authors agree that submission of an article automatically authorises ESARDA to publish the work/article in whole or in part in all ESARDA publications – the bulletin, meeting proceedings, and on the website.

The authors declare that their work/article is original and not a violation or infringement of any existing copyright.

# LATEST IMPROVEMENT ON FNCL FOR IAEA SAFEGUARDS

**Matteo Corbo, Massimo Morichi, Claudio Raffo, Francesco Pepe, Giovanni Cerretani**

CAEN SpA, Viareggio (LU), Italy

## **Abstract:**

*The Fast Neutron Collar (FNCL) is an NDA system for verification of fresh fuel assemblies using active interrogation and neutron coincidence counting. The FNCL has been developed by the IAEA to address the current issues in the fresh fuel assembly characterization: long measurement time and measurement biases due to the presence of Gadolinium. Tests have demonstrated verification of  $^{235}\text{U}$  enrichment in  $17\times 17$  PWR with statistical uncertainty on coincidence rates lower than 1% in about 15 minutes acquisition time. Moreover, the presence of Gd rods in  $17\times 17$  PWR assemblies causes a systematic bias lower than 3%, approximately half as much as alternatives.*

*CAEN S.p.A. is currently designing the upgrade of the FNCL system for IAEA with a revised mechanical layout with modular elements. The mechanics has been redesigned to be integrated in a rugged case with 19" rack frame, with independent 19" rack mounted units: KVM (keyboard-video-mouse), high performance multi-core computer and custom defined crate in industrial VME-64X standard. The whole collar detector has been designed to improve the mounting and the positioning of the detector panels, with dedicated source slabs for accommodating in the internal cavity BWR, PWR and WWER fuel bars. CAEN S.p.A. is producing the FNCL for the International Atomic Energy Agency (IAEA) according to user requirements defined by safeguards operational divisions. The detectors and data analysis were developed thank to the IAEA and Member States Support Programs.*

**Keywords:** NDA, Safeguards, Fuel Accountancy, Fuel Verification

## **1. Introduction**

Modern fuels commonly contain burnable neutron poisons, such as gadolinium oxide, to increase burn up and improve fuel economy. Such fuels present complications for verification by traditional NCC instruments due to high absorption of thermal neutrons by Gd.

This problem has been recently addressed following two approaches. The first is to apply a correction factor to the measurement which relies on a declaration of Gd content in the FFA. This cannot be independently verified and therefore presents a possibility that nuclear material could be diverted with a false declaration. The second is to use a cavity lining of Cd to remove thermal neutrons from the interrogation flux, thus significantly reducing the dependence of the measurement on Gd content [1]. The induced fission rate is suppressed and to compensate, the measurement times are extended to between two and three hours to achieve satisfactory statistics. Recent developments have aimed to reduce the measurement time by increasing the efficiency of a UNCL-type design by using high pressure  $^3\text{He}$  tubes [2] [3].

The FNCL utilises low-hazard liquid scintillation detectors and an integrated data acquisition system to measure coincident fast neutrons. When used in combination with a Cd cavity lining this leads to a minimal dependence on the FFA Gd content, removing the need for a correction. Additionally, no neutron thermalisation is required for detection thereby allowing the coincidence gate to be reduced from microseconds to nanoseconds. This virtually eliminates accidental neutron counts, the major source of measurement uncertainty in traditional NCC. Subsequently, measurement times for the same level of precision can be greatly reduced.

CAEN SpA provided the International Atomic Energy Agency (IAEA) with the first prototype of the FNCL in 2016. Since then few tests have been performed on field demonstrating the great advantages of the new methodology compared to the currently used measurement based on thermalized neutrons [4][5].

The potential advantages in the deployment of the FNCL by inspectors in fuel processing facilities generated a request for additional systems of the same kind with a renewed graphical user interface and improved the mechanical layout of the DAQ and of the neutron collar detector. CAEN SpA is currently involved in the production of the next generation of FNCL systems and the present paper describes the main features of those systems.

## 2. FNCL Detector Redesign

The FNCL detector has been redesigned mainly to improve the robustness of the detector panels and their fastening on the supporting plate. The new detector panels, integrating 4 liquid organic scintillator detectors, have approximately the same weight of the previous lateral panels, weighting only 3 kg more.

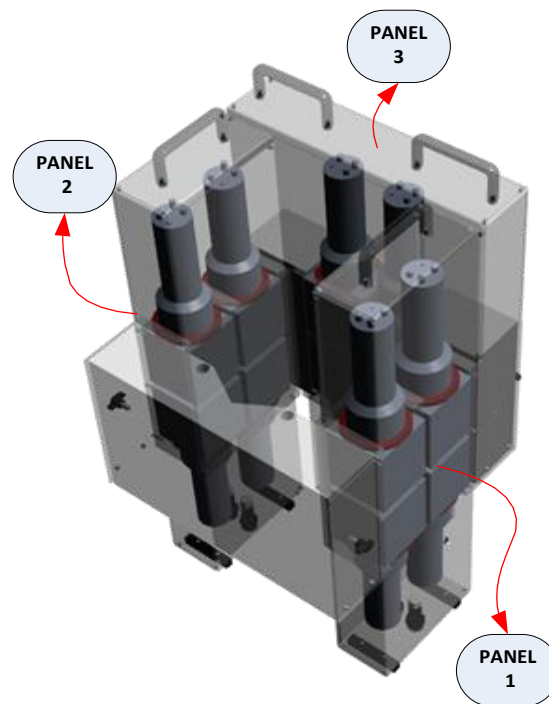


**Figure 1:** Current FNCL first design

The redesign of the panels makes them identical and independent from the mounting position, while in the previous version the 3<sup>rd</sup> panel was wider and weighting more, as shown in Figure 1. The new design imply that any panel can be exchanged with a spare part in case of need.

The detector panels are fastened a new supporting plate with increased thickness, to reduce to a negligible amount any incline of the panels respect to the perpendicular direction. Moreover, the support plate has an adjustable fixing for commercial forklifts meant to sustain the whole detector during the fuel verification.

The overall design of the collar is meant to accommodate BWR, PWR and WWER fuel bars, without any change in the mounting procedures of the detectors. Three different polyethylene slabs, housing the interrogation sources, can be used to optimize the fuel verification.

A provisional drawing of the next coning FNCL detector is showed in Figure 2. The drawing is related to the configuration for the PWR fuel verification.

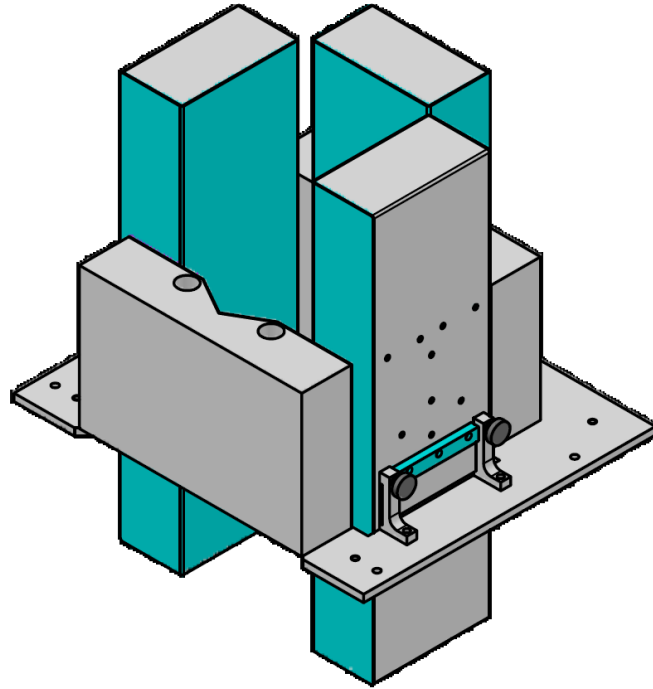


**Figure 2:** Provisional drawing of the next FNCL design for the verification of PWR fuel bars.

### 3. Data Acquisition System

The DAQ system is composed by independent modules rack mount for the 19" mechanical frame. This gives the flexibility of exchanging the building blocks independently and potentially guarantee a long-term maintenance capability of the system. The DAQ is embedded in a commercial rugged and transportable case with a 7 unit high 19" frame. The DAQ system is shown in the Figure 3.



**Figure 3:** New FNCL DAQ system

The core of the DAQ system is composed by CAEN waveform digitizers of the V1730 family. Those digitizers embed a flash ADC with 500 MHz sampling rate and 14-bit resolution, over a software selectable dynamic range of 2 or 0.5 Vpp. The waveform digitizers can transfer the digitized information through optical link, up to a total throughput of 80 MB/s. At the same time the digitizers can

process real time the information to provide time stamp and integrated charge of the scintillator detector signal.

Each waveform digitizer is connected to three detectors, for a total of 4 waveform digitizer per system. The total data throughput for waveform acquisition is 320 MB/s, transferred to quadruple optical link controller embedded in a multi-processor rack mount compact computer.

The DAQ includes independent high voltage power supplies for scintillator detector bias and electronics for the slow control of the high voltage condition.

The inspector or the technician can operate the FNCL system directly through the keyboard-video-mouse unit mounted in the rack. Figure 4 shows the DAQ system when in operation.



Figure 4: New FNCL DAQ system in operation.

#### 4. Software Redesign

The International Atomic Energy Agency has requested the upgrade of the analysis software interface and the implementation of additional features.

The major change in the FNCL software is the possibility to execute the calibration of the system and the fuel bar verification through a guided procedure, “inspector mode” (in Figure 5), which improves the usability and eliminate the chances of producing incorrect data by mistake. The system remains however opened to modifications and optimizations, which can be introduced in the interface of the “technician mode” (in figure 6). The user can login in the operating system of the DAQ system with technician or inspector access credentials; automatically, when the FNCL software is launched pressing on the icon in the tool bar, the relative interface for inspector or technician is showed.

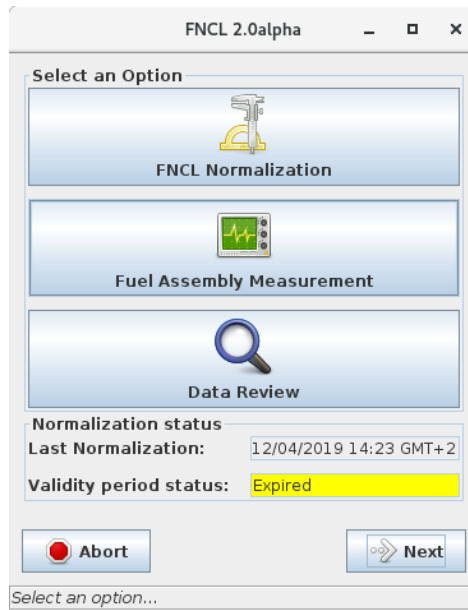


Figure 5: Main window of the software interface of the FNCL in inspector mode

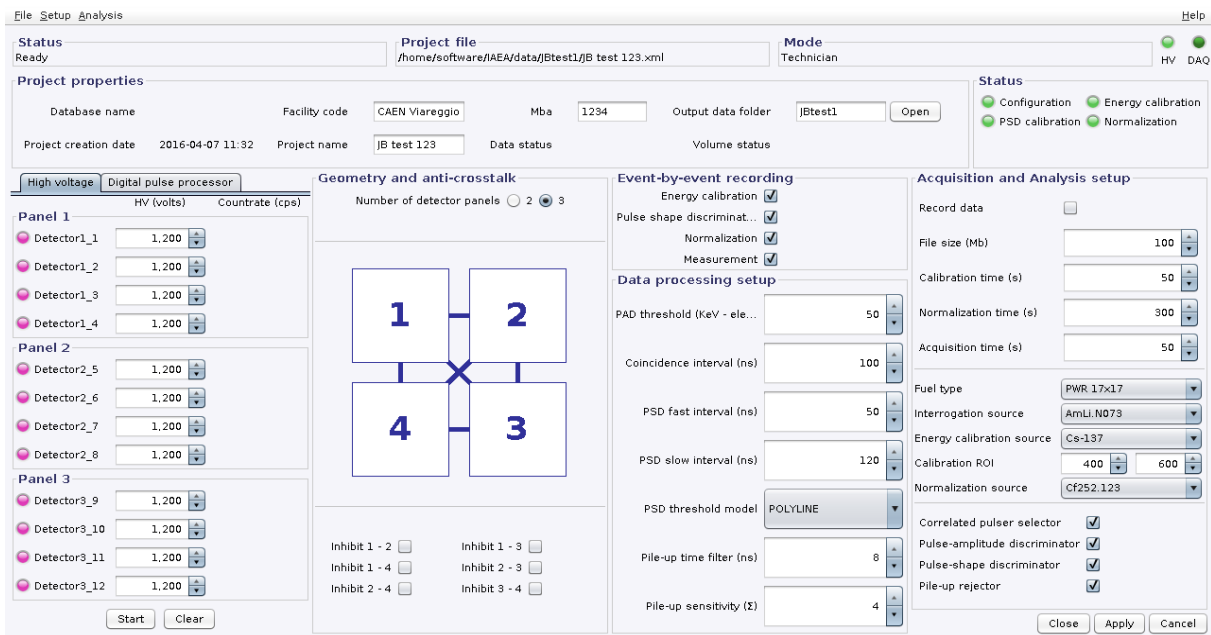


Figure 6: Main window of the software interface of the FNCL in technician mode

During the acquisition different quality check are executed. The software controls the counting rates of the acquisition channels:

- controls that all acquisition rates are above a fixed low level;
- controls if the current acquisition rates are consistent with the average acquisition rates in the run;
- controls if the independent acquisition rates are consistent with the average acquisition rates of the other detectors in the system.

Moreover, the energy calibration of the system is automatically processed in the inspector mode and the software monitors the good result of this calibration.

The software generates verification reports at the end of the measurements. The reports includes a series of summary plots, which ease the control of the results.

- [1] P. W. Henriksen et al. "Neutron collar calibration and evaluation for assay of LWR fuel assemblies containing burnable neutron absorbers," 1990.
- [2] H. Tagziria et al. "Calibration, characterisation and Monte Carlo modelling of a fast-UNCL," NIM A 687, pp. 82-91, 2012.
- [3] L. G. Evans et al. "A new fast neutron collar for safeguards inspection measurements of fresh low enriched uranium fuel assemblies containing burnable poison rods," NIM A 729, pp. 740-746, 2013.
- [4] M. Grund et al. "Fast Neutron Collar Tests at Nuclear Fuel Fabrication Plant in Brazil", IAEA Symposium on International Safeguards 2018.
- [5] J. Beaumont et al. "A fast-neutron coincidence collar using liquid scintillators for fresh fuel verification", J Radioanal Nucl Chem vol. 314, Issue 2, pp 803–812, 2017

# Data science in safeguards – opportunities and challenges

Irmgard Niemeyer

Forschungszentrum Jülich GmbH  
IEK-6: Nuclear Waste Management and Reactor Safety  
52425 Jülich, German  
E-mail: i.niemeyer@fz-juelich.de

## **Abstract:**

*Similar to 'big data' trends in other fields, also the data collected, processed, integrated, analysed and managed for safeguards purposes is not only increasing in volume, but also getting more heterogeneous, unstructured and complex in nature. While processing, integration and analysis of safeguards-relevant information is largely based on time consuming manual processes today, data science and modern data analytical tools can pave the way to a more effective exploitation of 'big data' in safeguards. Recently, applying data science in nuclear safeguards has been discussed in the context of, inter alia: automation of open source information collection and processing; natural language processing; supporting safeguards inspection activities and information analysis by machine learning; data integration using semantic graphs; improving reporting, matching, tracking and monitoring by block chain/shared ledger technologies. The aim of this paper is to present a recently started data science project and to introduce the first subproject on the opportunities of geospatial data science methods and techniques to be applied in safeguards.*

**Keywords:** data science, safeguards-relevant data, geospatial data

## **1. Introduction**

Similar to 'big data' trends in other fields, also the data collected, processed, integrated, analysed and managed for safeguards purposes is not only increasing in volume, but also getting more heterogeneous, unstructured and complex in nature. Safeguards-relevant information generally includes i) information provided by States, mainly reports and declarations, ii) information from IAEA safeguards activities such as in-field verification and the evaluation of nuclear material accounting information, including nuclear material measurements and environmental sampling and iii) information from open sources and third parties. While processing, integration and analysis of safeguards-relevant information is largely based on time consuming manual processes today, data science and modern data analytical tools can pave the way to a more effective exploitation of 'big data' in safeguards.

Recently, applying data science in nuclear safeguards was discussed in the context of, inter alia:

- Automation of open source information collection and processing [1,2]
- Natural language processing [3]
- Supporting safeguards inspection activities and information analysis by machine learning (convolutional neural networks and support vector machines) [4-7]
- Data integration using semantic graphs [8]
- Improving reporting, matching, tracking and monitoring by block chain/shared ledger technologies [9,10]

The aim of this paper is to present a recently started data science project and to introduce the first subproject on the opportunities of geospatial data science methods and techniques in safeguards.

## **2. Bringing forward the application of data science in nuclear safeguards**

A project recently started in Jülich is aimed at advancing and prioritizing the development and implementation of relevant data sciences methods and techniques, by taking the following approach:

- Based on the current state-of-the-art of data science in collecting and evaluating safeguards-relevant information, further complex data analysis problems in safeguards that may potentially be mitigated or solved by data science are being identified.
- At the same time, data science methods and techniques that were established in non-nuclear or non-safeguards sectors are being studied with regard to their potential suitability for nuclear safeguards.
- Following the analysis and prioritization of needs and objectives of promoting data science in nuclear safeguards, specific data science methods and techniques are further developed and evaluated.

Taking into consideration results and experiences from prior projects on geospatial information analysis and integration, the first subproject focuses on geospatial data science in nuclear safeguards and is described below. Further topics, possibly related to nuclear data or digitalisation challenges in safeguards, will be defined at a later stage.

## **3. Geospatial Data Science in Nuclear Safeguards – Extracting Safeguards relevant Information from Geospatial Big Data**

Geospatial data represents a key source of information for the implementation and verification of Nuclear Non-proliferation Treaty (NPT). In particular, satellite imagery, together with auxiliary data, can be used as a reference source to aid in field and inspection planning, to detect changes and monitor activities at nuclear facilities, to verify the completeness and correctness of information supplied by a member state as well as to investigate alleged illegal activities related to nuclear non-proliferation, arms control or disarmament.

Using geospatial data has become a part of the day-to-day operations at the IAEA Department of Safeguards, however, automated processing and integrated analyses of geospatial data with various metadata and different spatial temporal and, in case of satellite imagery, spectral resolutions is still a challenge. As an aside, this is also true for non-nuclear applications of geospatial data, where some procedures for subsets of all potentially relevant geospatial data or for only a few acquisition times exist, for instance for environmental monitoring or land-cover monitoring over time.

Therefore, this project aims at developing an automated procedure that allows for an effective integrated analysis of any number of geospatial data acquired over the same area of interest and providing a suitable visualisation of relevant trends, patterns and anomalies of safeguards-relevant information in the area of interest.

Three broad categories of safeguards-relevant geospatial information types are considered in this context: first, image data from earth observation satellites; second, information derived from satellite imagery; and third, supplementary geospatial datasets obtained from other open sources.

The proposed approach will include multiple steps in order to pre-process the data and information for processing, integrated analysis and extraction of safeguards-relevant information.

The first category includes multi-sensor satellite data (optical and radar) of different spatial, spectral and temporal resolution and different internal and external sensor geometries. While satellite imagery providers are launching new constellations of satellites, with the aim of images covering nearly all landmasses in the world on a daily basis, the quality and quantity of this data is increasing rapidly as are the methods to process and analyse the datasets. The resulting repositories of satellite imagery will offer analysts distinct insights into nuclear facilities and nuclear activities from space worldwide. The deluge of data, together with the variety of related metadata, however, will create new burdens on the analyst to use the datasets appropriately and in a timely manner. For this category, the steps in the procedure will consist of pre-processing methods in order to produce geometrically and spectrally corrected input imagery, including data file conversion to a model standard, orthorectification and co-registrations, radiometric normalization and screening for artefacts caused by clouds, cloud-shadow, snow, etc.

The second category contains datasets derived from the first category. By photogrammetric methods, digital elevation models can be automatically extracted from stereo pair and non-stereo-pair satellite images. Using interferometric methods, detailed information on surface elevation and can be generated from synthetic aperture radar (SAR) data. Moreover, various multivariate statistical approaches exist to extract information on land cover and land use, as well as spatial and semantic features of image objects. All methods have the potential to apply to a time series of images in order to generate information on anomalies, pattern or trends over time.

The third category consists of any other geospatial data potentially useful for nuclear verification, e.g. digital elevation models and vector datasets not derived from satellite imagery but from aerial photos or in-field activities. For this category, additional steps for geometric correction will be included.

While resulting image datasets in the second and third category can principally be of raster (image pixel) or vector (image objects) format, they will finally be all provided in object format. An image object can be described as “discrete region of a digital image that is internally coherent and different from its surroundings” [11]. An image object, in the optimum case, corresponds to a ‘real-world’ object, such as a building, a tree, a (part of a) road etc. Object extraction via specific segmentation methods will be performed at different steps, depending on whether the actual processing method requires pixel values (such as the extraction of digital elevation or the processing of SAR data) or object values (as beneficial for processing very high resolution satellite imagery).

For some processing step like object extraction and generating object correspondence, we may take advantage of methods developed in previous projects, such as the multiresolution segmentation for change detection (MRS4CD) and the object correspondence for change detection using intersecting objects (CDIO) [12]. These methods were developed for comparing bi-temporal datasets acquired over the same area of interest and need to be developed further for multi-temporal and multi-data use

For the integrated analysis of the available deep learning algorithms will be developed and implemented that will allow the user to conduct specific queries on the database. Previous studies investigated the potential of so-called ‘class dependent neural networks’ [13], including two layers of neural networks. This approach creates a neural network for each of the classes instead of usually one neural network for all classes). While neural networks in

general require a relatively large number of training sample for modelling the probability distributions of the classes accurately, the class dependent architecture works well even with a few training samples. The application of deep neural networks [14] will be part of the proposed study. While deep learning is a big trend in satellite imagery analysis, the potential for specific monitoring tasks such as nuclear verification still needs to be evaluated.

#### 4. References

- [1] Claude F et al (2017) Data Fusion at Scale: Strengthening Safeguards Conclusions Through Applied Analytics. Proc. INMM Annual Meeting, Indian Wells, CA
- [2] Stewart I et al (2018) Automated Processing of Open Source Information for Nonproliferation Purposes. Journal of Nuclear Materials Management 46(3):21-36
- [3] Diab JJ et al (2018) Using Machine Learning and Natural Language Processing to Enhance Uranium Mining and Milling Safeguards. Proc. IAEA Symposium on International Safeguards, Vienna
- [4] Gastelum Z et al (2018) Inferring the Operational Status of Nuclear Facilities with Convolutional Neural Networks to Support International Safeguards Verification. Journal of Nuclear Materials Management 46(3):37-47
- [5] Feldman Y (2018) Toward a Multimodal-Deep Learning Retrieval System for Monitoring Nuclear Proliferation Activities. Journal of Nuclear Materials Management 46(3):68-80
- [6] Kadner S et al (2017) Image Verification and Surveillance using Machine Learning. Proc. Workshop 'Novel Technologies, Techniques, and Methods for Safeguards and Arms Control Verification', Sandia National Laboratories
- [7] Haddad R et al (2018) Autonomous Systems, Artificial Intelligence and Safeguards. Proc. IAEA Symposium on International Safeguards, Vienna Cui Y et al (2018) Using Deep Machine Learning to Conduct Object-based Identification and Motion Detection on Safeguards Video Surveillance Proc. IAEA Symposium on International Safeguards, Vienna
- [8] Thomas MA et al (2018) Semantic Graphs for Safeguards Data Integration, Pattern Matching, and Event Classification. Proc. IAEA Symposium on International Safeguards, Vienna
- [9] Frazer SL et al (2017) Exploratory study on potential safeguards applications for shared ledger technology. Technical Report, PNNL-26229, Pacific Northwest National Laboratory
- [10] Frazer SL (2018) Identifying Safeguards Use Cases for Blockchain Technology. Proc. IAEA Symposium on International Safeguards, Vienna
- [11] Castilla G, Hay GJ (2008) Image Objects and Geographic Objects. In: Blaschke, T., Lang, S. & G.J. Hay (Eds.): Object-Based Image Analysis – Spatial Concepts for Knowledge-Driven Remote Sensing Applications. Springer, Berlin Heidelberg, 91-110
- [12] Listner C (2014) Änderungsdetektion digitaler Fernerkundungsdaten mittels objekt-basierter Bildanalyse. PhD Thesis, Technische Universität Bergakademie Freiberg. Schriften des Forschungszentrum Jülich, Reihe Energy & Umwelt, Band 242, <https://d-nb.info/107155543X>
- [13] Marpu PR (2009) Geographic Object-based Image Analysis. PhD Thesis, Technische Universität Bergakademie Freiberg, <https://d-nb.info/994521715/34>
- [14] Zhu XX, Tuia D, Mou L, Xia GS, Zhang L., Xu F, Fraundorfer F (2017) Deep Learning in Remote Sensing: A Comprehensive Review and List of Resources. IEEE Geoscience and Remote Sensing Magazine 5(4): 8-36 (doi: 10.1109/MGRS.2017.2762307)

# **Panel 1:**

# **Regional Safeguards Systems**

## Comparing Regional Proliferation Risks and Safeguards Systems

**Matteo Gerlini**

Sapienza University of Rome  
Special School for Archivists and Librarians  
Piazzale Aldo Moro, 5  
Rome, Italy  
E-mail: [matteo.gerlini@uniroma1.it](mailto:matteo.gerlini@uniroma1.it)

**Masako Ikegami**

Tokyo Institute of Technology  
Department of Innovation Sciences  
Ookayama 2-12-1-W9-42, Meguro  
Tokyo, Japan  
E-mail: [maike@valdes.titech.ac.jp](mailto:maike@valdes.titech.ac.jp)

### **Abstract:**

*The paper develop a comparison between Europe and East Asia as regional areas with analogies and differences on the international relations frame and international security paradigms. The analysis takes into account the strategic rims of conflict, the nuclear proliferation dynamics and the bilateral/multilateral answers to the elements of instability, mainly on the existing safeguards systems. It will compare the political interplay of the actors involved in the past and in the current times, with a forecast for the future. In the Post War we have in the areas: a) a defeated power (Germany/Japan) with a special tie with the United States; b) a nuclear-armed power ideologically antagonistic in the political, strategical struggle (USSR/PRC) with the other states of the area allied with the US; a group of states allied with the internal, nuclear power (the States of the Warsaw Pact/North Korea and South-East Asian communist states); an inner core of the US-allied states concerned both of the former defeated power and of the new nuclear power (France-Belgium/South Korea-Taiwan). By comparing the regional dynamics in Europe and East Asia, the theoretical approach proposed aims to identify with a qualitative method the game changers in the making of present times in the areas. We will demonstrate how Euratom prevented a nuclear cascade in Europe, as a regional safeguards system and inseparably an integrated frame of peaceful cooperation. Conversely to the NPT, EURATOM did not forbid military nuclear applications to its members, but it exerts a dissuasion through emphasising peaceful, safeguarded cooperation among the members. It limited the dual use of nuclear development because of its safeguards system, trusted by all its members' thanks to their direct participation, let say the right of self-inspection. To the contrary in East Asia, lacking such a regional cooperative framework as EURATOM, the NPT singly could not prevent North Korea's nuclearization. The paper will prove the significance of regional cooperation for successful safeguards.*

**Keywords:** EURATOM regional safeguards system; Nuclear Proliferation in Asia; Comparative analysis of international relations

## 1. Introduction

Is it the EURATOM safeguards system an exportable model? Moreover, why a cluster of countries should opt for a similar frame beside (or instead) of the existing IAEA non-proliferation regime? We focus on the unique features of EURATOM, whose make it different from the NPT and the IAEA: 1) the regional approach; 2) the supranational authority-steered cooperation in the nuclear domain; 3) the self-inspections system. These elements derived by comparing the political history of Post War in both the areas, a comparison which takes the parts 2 and 3 of this paper. In part 4 we analyse the EURATOM safeguard system, before and after the NPT.

In conclusion, we will try to advance possible political options for the East-Asian nuclear issues and the cooperation between East-Asian countries and the European Union in such a field.

## 2. Europe

After the end of World War II, the hard-political struggle for reconstruction between the superpowers crossed Europe. [1] This brought the division of the continent into two opposing camps tied to the Soviet Union and the United States. As it was the main Axis power in World War II, in the Cold War [2] Germany was the epicentre of the European political and ideological conflict. [3] On March 17, 1948, an Anglo-French treaty was signed, extended to the three Benelux countries known as the Pact of Brussels, aimed against the possible resurgence of a German threat. [4] The danger perceived by the Western governments of continental Europe, however, was twofold: one was coming from the communist bloc, and one from the rebirth of the German power. In 1949, two different States were established by the splitting of the German territory, according to the former occupation zones of the Allies.

### 2.1. Shaping solutions for the inner and outer problems

The problem for the framework of alliances that divided the continent was the German rearmament, as well as the presence, or absence, of the government of communist parties. In the Western field, a series of political initiatives were promoted - intended to bring European integration as a means to a future of peace and prosperity after centuries of wars. [5]

An integration based on the support of a significant part of American leadership engaged in an internal debate that would eventually see it victorious against the isolationists, a longstanding US policy element. [6] Similarly, Winston Churchill and the British Conservatives were convinced advocates of the need for a European integration, at the time limited to Western Europe because of the Soviet control over the Eastern part of the continent, which involved other European leaders as the Italian Alcide De Gasperi, the German Konrad Adenauer and the French Robert Schuman. [7] On the military level agreements, the North Atlantic Treaty - signed in Washington on April 4, 1949 - responded to the defence requirements of the Western European governments toward the perceived Soviet threat.

In August of that year, the US atomic monopoly ended: the Soviet Union had become a nuclear power. [8] This change was significant for the nature of the Atlantic alliance, which initiated the establishment of an organisational structure that allowed the creation in Europe of permanent deployment of armed forces, even in peacetime. Furthermore, the Atlantic organisation necessarily encouraged the integration of West Germany into the Western defence system. [9]

#### 2.1.1. Carbon and steel

Schuman proposed in 1950, the establishment of high authority for coal and steel that would have reconciled the needs of the French and the Germans on this strategic sector. [10] Actually, the control of the German mining areas was a problem that had marked the two world wars. The plan proposed by Schuman eliminated any element of subordination to foreign control of the German mining areas, in force of a principle of supranationality accorded to the participation in this community. The meaning of such concept was that the high authority would have full powers in the management of significant aspects of the coal and steel industries, thanks to the transfer of sovereignty of the acceding States to the authority itself. Konrad Adenauer responded very positively to the proposal, extended to other European countries. The negotiations were very long and challenging, both for relations with the industrial world and for the outbreak of the Korean War, which occurred on June 25 of that year (see below). The war increased the demand for steel and pushed the Americans to openly ask the participants in the negotiations for the rearmament of West Germany, as an ally in the conflict. The

head of the French government, René Pleven, responded with a plan for the creation of a European defence community, which would have followed the coal and steel community model: the Western governments eventually reached an agreement for the creation of European Steel and Coal Community (ECSC). The text of the Treaty establishing the community was approved April 18, 1951, and such supranational body came into effect on July 25, 1952, joining as member states France, Germany, Belgium, Italy, Luxembourg and the Netherlands. They were called the Six. Jean Monnet, the most significant contributor to Schuman's plan, was appointed President of the High Authority of the community. [11]

The treaty was a way to overcome historical rivalries that had bloodied Europe and established the superiority of diplomacy on the use of force. The politically important feature was that it established the principle of the transfer of sovereignty to a third party to solve or deter conflicts. It marked a significant step towards the reconciliation of France and Germany and addressed the joint development of resources, not only an overcoming of conflicts' roots. The community created a common market for the steel industry, which contrasted the trust and regulated the respective shares of production of various countries, as a framework for development and modernisation of the whole industry. The most important aspect was the creation of the High Authority of the Community, a body acting as the government of the entire community. The High Authority was composed of nine members with a maximum of two for each member state and did not respond to national governments. The other bodies were: an assembly of the community, elected by the Member States; a Council of Ministers, liaising the high authority and national governments; a court of justice, to resolve disputes arising under the Treaty. [12] The treaty entailed the possibility of verification of the peaceful use of the metallurgy industries supported by the community, through the visits of the authority officials. It was a guarantee for the member states that nobody could use the community resources to turn the ploughshares into swords.

### 2.1.2. Defense

The Korean War (June 25, 1950-July 27, 1953) pushed forward the integration of West Germany in the Western Europe defence frame. [13] The debate on the defense integration went on partially overlapping with the ECSC treaty discussion, but with a completely different outcome. The Korean conflict risked the exportation in Europe as a proxy war between the two superpowers, what had happened between North Korea and South Korea could occur between East Germany and West Germany. [14] As a result, the attitude of the European countries towards the establishment of an army in West Germany changed. The creation of armed forces of the Federal Republic of Germany would provide the first line before an invasion from the east, but the Europeans preferred a direct involvement of the US forces on the front, instead of German rearmament. The Atlantic allies debated the issue in September 1950 in New York. On the European side, it was required a commitment on the American field, as the secondment of permanent forces in times of peace in Europe: on this hypothesis, all Europeans agreed, hoping that the US commitment consistency was such as to avoid the formation of an army of Federal Germany. The Americans accepted the increased commitment in Europe, consistently increasing its military presence, forming an integrated allied force that would have taken the lead, but the Europeans had to accept the participation in the integrated forces of Federal Germany's ten divisions. [15]

The French head of government, René Pleven, launched the so-called Pleven plan, which transferred the ECSC model for European defence according to the same supranational principle. The European defence community (EDC), was the follow-up of the Pleven plan, but in August of 1954, after much procrastination, the French parliament did not ratify the treaty establishing the EDC. [16]

## 2.2. Towards EURATOM

The European Atomic Energy Community, already known as EURATOM by its makers, was thus created on the wave of success, and at the same time of failure. The ECSC had demonstrated the willingness to integrate a strategic sector such as coal and steel in a supranational way. The EDC had demonstrated the limits of this kind of integration instead when it involved a sensitive branch as a defence. Nevertheless, the failure of the EDC had given a new effort to the pact of Brussels mentioned above; the treaty placed in the background during the Atlantic alliance development, but in the new situation that has emerged after the failure of the EDC it was perceived as a point of resuming. A conference convened in London began its works on September 28, 1954, and an agreement was reached on 3 October to restore full sovereignty to Federal Germany. Over the following month, a commission drew the design of an organisation called the Western European Union (WEU) whose

ranks would collect the armed forces assigned by the member states. The WEU would have less supranational features than the EDC, but it was mainly planned to control armament plans of the member states so that they could not trigger weapons programs potentially dangerous for the allies. The governments of the Six plus the United Kingdom approved the project at a conference held in Paris on 20 to 23 October 1954. [17]

During that year, the United States government followed the spirit of the speech delivered by President Eisenhower during the United Nations general assembly in December 1953. The famous "Atoms for Peace" speech committed the United States to the peaceful uses of atomic energy, opening the world to bilateral cooperation with the American nuclear complex. The Atomic energy act of 1954 entailed the features of any future cooperation agreement with the United States. The basic assumption of the act was the peaceful task of the technology transfer. In order to do so, it forbid the transfer of any information related to weapon design or fabrication. However, to verify the compliance of the partner states with the peaceful uses of the transferred technology, the United States government subjected the transfer with the right to inspect the facilities of the partner state. This act was the frame of the agreement the US government proposed to the Europeans too. [18]

Horizontal proliferation was not yet the expression used to define the acquisition of nuclear weapons by other states than the three nuclear powers of those days, but in its substance, it was one of the main concerns of the government of the United States. The French ambitions to achieve nuclear weapons were on the top of the list. [19]

Meanwhile, Jean Monnet resigned from the post of High Commissioner of the ECSC. In the critical phase that the European integration was going through, he began to propose with conviction the creation of a European Community for Atomic Energy. A study promoted by Louis Armand, a prominent figure of the French nuclear sector, already referred to the advantages of an integrated entity for the management of nuclear development in Europe. Monnet then began to work on the project, illustrating a draft to the Belgian statesman Paul Henry Spaak. While sharing the emphasis on the need for resuming the integration process, he remained doubtful about the real possibilities of achieving integration in a field both so narrow and complex as nuclear energy was. [20] Even Johan Willem Beyen, Prime Minister of the Netherlands, harbored similar doubts, as he presented to Monnet and Spaak, on April 4, 1955, a proposal for a customs union between the two countries (Netherlands and Belgium), which would be followed in a short time by a real economic union. He perceived the path of an economic integration more viable than a nuclear one. On May 18, attracted by the new prospects that were emerging, Monnet and Spaak decided to merge the two memorandums in a single one that later became known as "Benelux Memorandum". It would become the basis for the negotiations held at the Messina Conference.

### **2.2.1. The first round of negotiations**

The governments of the six countries convened a conference from 1 to 3 June 1955 in Messina, Sicily. They disputed both the topics of the common market and the nuclear community. After a night of long debating, the French Foreign Minister Antoine Pinay agreed with the other delegates to create technical and politically mixed group that would run the negotiations.

Thus, an Intergovernmental Committee was established, better known as the Spaak Committee, as he chaired it. It worked throughout the summer of 1955, to bring together the negotiating positions of the Six, as they had been set out in Messina. The English economist Russell Frederick Bretherton, at the time undersecretary at the Ministry of Commerce of the British Government, participated as an observer, ensuring his presence in the early stages.

Bretherton left the works of the Spaak Committee on 7 November 1955. The concerns of the British were on the powerful supranational features of the Common Market project, as a rule for the integration in the atomic field. [21]

The Spaak committee produced a report presenting the EURATOM project. The first issue addressed was the thorniest: preventing risks of military diversion of fissile fuels distributed by the community to civilian purposes. The second question was related to the preferred modality to create a common supply system of fissile fuel, a request that had long been advocated and supported by the French delegation. Other points were the primacy of the community in the representativeness of the Six in the international nuclear forums, and the community's monopoly of nuclear materials supplies to the Six.

The plenary review of the work produced by the Spaak committee, however, had been useful because it had identified the most controversial points, emphasising the themes that were eliciting frictions among the Six. [22]

During these rounds of negotiations, the US government clearly and openly endorsed the project of a European atomic community. The reasons for the US to support EURATOM were clear: to make

Germany an organic element of the Western coalition, neutralising the Franco-German rivalry, fostering the spreading of nuclear technology in a peaceful direction and developing as quickly as possible a robust nuclear power industry in Europe. To achieve these goals, a supranational player was necessary. The US would accord to it the preferential treatment: the US could make vast resources available and ensure a privileged treatment not just to a single country through bilateral negotiations but also to a community of states to act multilaterally. [23]

### **2.2.2. The relations with the US and the Suez crisis as external drivers**

The Suez War of October 1956 placed France, the United Kingdom and Israel against Egypt. For the western powers, the war was a reaction against the decision of the Egyptian government to nationalise the Suez Canal. The superpowers and the United Nations called the opponents to a cease-fire, and the Soviet Union threatened the use of nuclear weapons to defend the attacked Egypt. The subsequent Canal blockade had had an immediate destabilising effect on the fuel market. The extensive import of Middle Eastern crude oil, which seemed free of any risk of interruption, based the reconstruction of the continent after the war. However, the Soviet menace had the effect of compelling the French government in pursuing an autonomous nuclear armament, to restore the international role of the French Republic after the Suez fiasco. [24]

After the Suez crisis, the attitude of the Europeans towards the Eisenhower administration and the US, in general, had become warier. France, Germany, Italy and the Benelux countries, appeared much more likely to give birth to forms of increasingly bland nuclear cooperation rather than to commit to fostering a real integration and its industry. The western European states asked for bilateral agreements for fissile materials, not endorsing the US position of the creation of a single continental supply agency in the frame of a European atomic energy community, committed to peaceful uses of such technology.

On September 20, 1956, the representatives of the Six agreed for the creation of a "Committee of Wise Persons" mandated to establish an emergency program to produce Atomic energy. It would reduce European dependency on foreign energy sources, and the Europeans would obtain support from the British and the US technological to do it. The Committee would include Louis Armand, Director General of Railways and member of the CEA, Franz Etzel, German Member of Parliament and vice president of the High Authority of the ECSC and Francesco Giordani, chemist and Chairman of the Italian National Research Council. [25] On December 21, the US government issued a press release officially inviting the three European experts to the US to have conversations with government officials and the CEOs of the major industrial corporations. On February 4, 1957, the three wise men arrived in Washington to collect the highest number of unclassified information technologies based on American peaceful programs, their costs and to discuss several research programs that were of interest to both sides.

The visit of the three wise men in the United States marked a turning point in the American attitude toward the nuclear military ambitions of the Europeans eventually. The State Department and the Atomic Energy Commission accepted the caveat of the national nuclear military to be run outside of the community cooperation, so dropping out any position calling for a renounce to nuclear weapons by the Europeans as a prerequisite for the participation in the community. Already in 1954, the Federal Germany Chancellor Konrad Adenauer had committed the German government to renounce to nuclear, chemical and biological weapons. Only the French government had the technical possibility to reach the nuclear threshold and, to cross it, to enter the nuclear weapons owner club. [26]

### **2.3. The Treaty and its Community**

The two Treaties of Rome of March 25, 1957, established the European Economic Community and the European Atomic Energy Community, already called EURATOM commonly. It came into force on January 1, 1958. The EURATOM treaty had a preamble and 225 articles in six titles, plus annexes and protocols.

Although following the letter of the Treaty, EURATOM was composed of seven organs directly related to his daily activities only two were, in fact, the institutional authority that drove the action: the Commission and the Council. The Commission was the executive body of the Community. Representatives of Member State governments formed the Council of Ministers. It has above all the task of ensuring the coordination of the actions of the Member States and the European Atomic Energy Community.

The development of a nuclear industry involved multiple aspects: it assumed the creation of a common continent-wide market of nuclear technologies, which would put no restrictions on the

circulation of knowledge, human resources and capital. So EURATOM should provide access to the necessary fissile fuels and technological components, encouraging and facilitating investment, research and sharing of technological information.

The Commission developed its activities in the nuclear research inside with the Joint Nuclear Research Center (JNRC), and outside with the allocation of research contracts.

The JNRC consisted of four research centres, each with a different speciality: Ispra (Italy), Petten (the Netherlands), Geel (Belgium) and Karlsruhe (Germany). It was the primary means of supporting research by the Community, and it absorbed a large proportion of the EURATOM budget, typically 50% of its total resources, at least until the second five-year plan. The allocation of research contracts, conversely, allowed EURATOM to attribute external research projects that were of common benefit to the Six.

Besides research, EURATOM's task it was to facilitate the growth of the nuclear industry in Europe: its main activity in this specific field consisted in ensuring the sharing of nuclear information among all actors, state and non, who were active in the sector. Another critical task was to facilitate the free and uninterrupted flow of capital, human resources and technologies; for this purpose, it was established the common market for goods and nuclear products on January 1, 1959. From that day, the Six have common external tariff and the freedom to exchange both technology and workforce. A similar measure was of fundamental importance: thanks to this industry could begin to negotiate purchases and sales of minerals, fuels and technologies with greater freedom than ever before and a significant reduction of the final price of traded goods.

All these tasks intertwined with a safeguard system ensuring the peacefulness of the community actions. [27]

### **2.3.1. From here to current times**

The EURATOM safeguard system crossed the various changes which brought the European integration up today outcome of a European Union. Focusing on this specific aspect, we let the other parts of the EURATOM history on the back, including the broader debate on the European integration in itself. This because the EURATOM safeguard system, once came into force, was never withdrawn or debased by the following treaties which made the EU. The system adapted itself to the international turns marked by the NPT or the implementation of the agreement with the US, as well as the enlargement of the number of member states. The safeguard system established with the treaty contained the spreading of nuclear weapons across Europe, limiting the number of nuclear weapon member states to two. The system safeguarded the nuclear materials for declared peaceful uses with the access of new member States, in particular after the end of the eastern block.

## **3. Asia**

As a stark contrast to Europe where EURATOM, the regional cooperation effectively prevented nuclear proliferation, in Asia so-called "Asian nuclear reaction chain" occurred being triggered by China's first nuclear test in 1964. [28] China had initiated research leading to the development of nuclear weapons in the 1950s and carried out 45 nuclear tests during 1964 and 1996. China's nuclear armament prompted India that had a border conflict with China in 1962 to go nuclear, first in the form of "peaceful nuclear explosion" in 1974, and later five nuclear tests in 1998. Pakistan established its nuclear weapons program in 1972 following the loss of East Pakistan in the 1971 war with India, and conducted nuclear tests in 1998 following the Indian nuclear test. North Korea established a large-scale atomic energy research complex in Yonbyon in the 1960s, and its nuclear weapons program can be traced back to the 1980s. North Korea conducted its first nuclear test in 2006. Even South Korea [29] and Taiwan [30] had attempted to go nuclear in the 1970s and 1980s respectively due to their severe senses of insecurity, but abandoned the efforts under strong pressures from the United States. Civilian nuclear activities of Japan, South Korea and Taiwan are tightly under control of their bilateral nuclear cooperation agreements with the United States as well as the IAEA respectively.

### **3.1. Networks of crises**

It is also noteworthy that India is not a member of the Treaty on the Non-Proliferation of Nuclear Weapons (NPT) or the Comprehensive Nuclear Test Ban Treaty (CTBT), though it is a state party to the Partial Test Ban Treaty (PTBT). Pakistan also refused to sign the NPT and CTBT, while it has blocked consensus at the Conference on Disarmament on starting negotiations for a Fissile Material Cutoff Treaty (FMCT). China joined the International Atomic Energy Agency (IAEA) in 1984 and the

NPT in 1992 as a nuclear weapon state, but supplied nuclear technology and reactors to several countries of proliferation concern in the 1980s and early 1990s; most notably, China supplied design information (including warhead design), and fissile material to the development of Pakistan's nuclear weapons program that were later transferred to Libya's program. Under international pressure, North Korea acceded to the NPT in 1985, but refused to sign a safeguards agreement with the IAEA until 1992, which triggered the first nuclear crisis. As regional efforts of the Six-Party Talks to stop North Korea's nuclear weapons program failed, North Korea declared to have withdrawn from the NPT in 2003.

In Asia, nuclear proliferation occurred under high military tensions of armed conflicts, and interlocking security complex among China, India and Pakistan triggered the so-called "Asian nuclear reaction chain". Both China and North Korea, in their declarations of their first nuclear tests, blamed that "U.S. nuclear black mail/threats" presumably being traced back to the Korean War. During the Korean War, the United States repeatedly threatened to use atomic bombs against North Korea and China as essential tools of conflict management throughout the war. [31] It is logical that both China and North Korea perceived the US nuclear threats as *the* decisive impediment to their ambition to unify the Korean Peninsula on their terms. Hence, Beijing's statement of its first nuclear test in October 1964 reads, "This is a major achievement to oppose the U.S. imperialist policy of nuclear blackmail and nuclear threats...in the face of the ever increasing nuclear threat posed by the United States. China is forced to conduct nuclear tests and develop nuclear weapons".[32] In October 2006, North Korea made a statement on its first nuclear test, which was basically a copy of the Beijing's 1964 statement with exactly the same logic; "The US extreme threat of a nuclear war and sanctions and pressure compel the DPRK to conduct a nuclear test, an essential process for bolstering nuclear deterrent...from the US threat of aggression". [33] The history of China and North Korea's nuclear armaments responding to the "US nuclear black mail" suggests that improved regional security settings are an essential condition to sustain a reliable nuclear non-proliferation regime.

### 3.2. Countering the cascade

The lack of regional confidence building measures (CBMs) or regional cooperation for security or energy worsened the situation. Nuclear non-proliferation was effectively implemented to Japan and South Korea through the bilateral nuclear cooperation with the United States respectively. In Southeast Asia, the Southeast Asian Nuclear-Weapon-Free Zone Treaty (SEANWFZ) or the Bangkok Treaty of 1995, a nuclear weapons moratorium treaty between 10 Southeast Asian member-states under the auspices of the Association of Southeast Asian Nations (ASEAN) effectively rooted out the cause of nuclear proliferation. The efforts for the SEANWFZ started already in 1971 when the 5 original members of ASEAN, Indonesia, Malaysia, Philippines, Singapore, and Thailand, signed the declaration on ASEAN's Zone of Peace, Freedom and Neutrality (ZOPFAN). In Central Asia, a Central Asian nuclear-weapon-free zone (CANWFZ) established in 2005 provides a vital platform for nuclear non-proliferation and effective nuclear material control among the five member states, Kazakhstan, Kyrgyzstan, Tajikistan, Turkmenistan, and Uzbekistan, as well as Mongolia that initiated and declared itself as a nuclear-weapon-free zone (NWFZ) in 1992. [34]

The overview of nuclear (non) proliferation dynamics in Asia — Northeast-, South- and Southeast Asia — suggests that regional cooperation entailed by security stability and CBMs is the key to successful implementation of nuclear non-proliferation. This tentative observation coincides with the successful outcome of ERATOM in Europe. In other words, establishment of regional cooperation and CBMs would be a necessary requirement to resolve the formidable nuclear crises in Northeast Asia over North Korea or the Middle East over Iran and Israel.

## 4. The Safeguard system

The EURATOM treaty limited the nuclear proliferation among its members by seclusion. The community extended the safeguards over all the peaceful uses of nuclear energy, severing the linkage between civilian and military development of the national nuclear complexes. So the military applications of nuclear energy were forced in a stand-alone status in the territory of the Community, with no legal possibility to receive nuclear materials from civilian facilities.

The core of the EURATOM safeguards system is in Title two, Chapter seven, of the Treaty. According to Howlett, it follows the frame of safeguards as the United States model of nuclear cooperation agreement stated, as well as the American concepts of international control of nuclear energy. [35, 90-1] The real difference is that the subject acting the safeguards was EURATOM, a supranational authority. The article 77 of the treaty states that "the Commission shall satisfy itself" on non-diversion

of ores, source materials and special fissile materials from their intended uses as declared by the users. In the category of users were gathered the member States users as well as third States or international organisations which had an agreement of cooperation with the EURATOM. In the following articles, the treaty perfected this principle. The nuclear players should provide to the Commission the basic technical characteristics of the installations, to the extent that knowledge of these characteristics is necessary for the attainment of the safeguards, and the Commission must approve the techniques to be used for the chemical processing of irradiated materials. The nuclear materials accountability is stated, as well as the control of any excess of nuclear materials. Article 81 defined the making of the inspections, taking the principle stated in the ECSC treaty, but applying it to a field hardly comparable to coal and steel, in theory, and practice.

The inspectors “shall at all times have access to all places and data and to all persons who, by reason of their occupation, deal with materials, equipment or installations subject to the safeguards [...], to the extent necessary in order to apply such safeguards to ores, source materials and special fissile materials and to ensure compliance with the provisions of Article 77”. The following articles described the implementation of the inspections, as well as the sanctions for the infringements of the treaty. The inspectors “shall be recruited by the Commission” among citizens of the member States, completing the self-inspection feature entailed in the EURATOM safeguard system. The sanctions ranged from a warning to the total withdrawal of source materials, with the role of the European court of justice in applying that.

The article 84 stated the sanctuary of the military facilities, a “defence clause” which excluded by the safeguards also the processing of nuclear materials outside from military areas but deemed to defence tasks. However, these materials cannot come by the Community supplies, because “in the application of the safeguards, no discrimination shall be made on grounds of the use for which ores, source materials and special fissile materials are intended”.

The safeguards may not extend to materials intended to meet defence requirements which are in the course of being specially processed for this purpose or which, after being so processed, are, following an operational plan, placed or stored in a military establishment. This is a central point of difference between the EURATOM safeguards system and the NPT regime because the association to the EURATOM treaty did not commit a non-nuclear weapon state member to the renunciation to pursuing a nuclear weapon program. However, if we drew a historical assessment on the effectiveness of the EURATOM safeguards, we can see that a member of the community has done no significant infringement. So we can advance that the system acted by enforcing a mutual trust among the members and not by moral suasion exerted by the supranational authority or by the harshness of the sanctions.

Promoting peaceful uses, and enforcing no diversion from civilian to military installations, the EURATOM treaty guaranteed the maximum control on the whole nuclear technology. It limited more than any other international agreement the uncontrolled spreading of dual-use nuclear technology. Thus, again Title two, Chapter six dealt with the supply of nuclear materials, special or other ones, while Chapter eight stated the property of the Community on the special fissile materials in the territories of the member states, enforcing the verification of the compliance by the authority. In this way, the EURATOM safeguards system was the only one covering the whole nuclear fuel cycle, from mining to final reprocessing [35, 93].

#### **4.1. The US-EURATOM agreement**

In 1958 the United States government prepared the agreement with EURATOM. It was a cornerstone for the effectiveness of the community’s action, and the nuclear policy of the United States as well. In the message delivered by Eisenhower to the Congress, pending for the approval of the agreement, he outlined for next five years in Europe about one million of kilowatts of installed nuclear capacity, from reactors developed in the United States. However, this would tie an active control on the technology transfer with the right of drawing back the spent fuel from Europe, as well a request of compatibility between the EURATOM safeguards system and the IAEA’s one.

The Congress of the United States eventually approved the agreement in the same 1958. The United States provided the Community with technology transfer and supply of U-235. EURATOM committed to refrain from using for military purposes the technology and the nuclear materials provided by the United States, directly or as a by-product. The Community did not transfer the same items to third parties without the authorisation of the government of the United States.

The requirements were strictly binding, to avoid any current or future diversion of the technology and the nuclear materials, for research or power production. However, it acknowledged the right of self-inspections for the Community, thus marking an exception in the frame of the United States nuclear

cooperation agreements, despite the disappointment of Sterling Cole, general director of the IAEA. He saw in this right of self-inspection by EURATOM, a limit to the authority of IAEA. [36] Actually, the less applied part of the agreement was the request of integration with the IAEA safeguards. The integration of the two safeguards systems was raised only with the debate on the Non-Proliferation Treaty.

In 1962, the agreement was amended on a very relevant point. The United States agreed to permit the reprocessing in the Community of the spent elements of the fuel provided.

The implementation of the treaty needed a legislative activity to allow the safeguards (and the inspections). The EURATOM commission enacted in 1959-1960 a slot of regulations (no 2, 7, 8 and 9) aimed to define the making of the safeguards. They were relevant to:

- the basic technical characteristics of each plant of which declaration should be communicated to the Commission;
- the nuclear materials accountability, which had to be periodically declared by the various enterprises having stocks or movements of ores, source materials and special fissile materials;
- the definition of the concentration of ores.

This consistent corpus of rules allowed to perform the first inspection, which took place in April 1960 at Mol, in Belgium. Its focus was more on material accountancy control than on-site inspection. However, with the growth of the nuclear industry in EURATOM countries, the inspections increased too. The amendment of the US-EURATOM agreement of 1962 put the Community in charge of the safeguarding of the reprocessing of spent fuel. This shifted the inspections features, introducing new procedures enabling them to control the reprocessing plants. As Howlett recalled, this expansion and improvement of the safeguards impelled increased recruitment of the inspectors. While the firstly recruited inspectors had a diplomatic or international legal background, the following levers came more from the technical and scientific careers in the nuclear sciences and technologies. [35, 114-6] In this respect, the personnel became more similar to today's staff.

From the first inspection to 1967, we had 411 inspections, mainly in research reactors (177) and in fuel fabrication plants (101); followed power reactors (53), research centres (50), irradiated fuel treatment facilities (20), and fuel stores (10). [37]

## 4.2. The Non Proliferation Treaty

The international nuclear situation was continuing to evolve, with the Popular Republic of China entering the nuclear club in 1964. This elicited the superpowers to promote a treaty aimed to limit the horizontal proliferation. [38]

The Non-proliferation treaty was open to signatures in 1968. The coming into force of the NPT marked a significant milestone in the history of the safeguard systems. It renewed the conflict between an international organisation as the IAEA with its international safeguard system and a supranational authority as EURATOM with its regional safeguard system. As in 1957, the EURATOM authority overwhelmed the IAEA one, the NPT gave the IAEA a new role in the incoming nonproliferation regime, so the EURATOM member states found themselves in the middle of two overlapping safeguard systems.

However, from 1957 many things had changed. The proponents of NPT called all the Nations of the world to adhere, but not all the Nations signed the treaty. Among the Six EURATOM members, the French Republic did not sign the treaty, while the Federal Republic of Germany and the Italian Republic signed in 1969 but waited up to 1975 to ratify the treaty. So, when the non-proliferation regime came into force, the only nuclear weapon state of EURATOM did not adhere, and the other two EURATOM states did not ratify. [39] In this frame, the coalition to keep in force the EURATOM safeguards system was strong enough to enforce the Commission to open a negotiate with the Agency. The first round of negotiations occurred during the writing of the text of the treaty. EURATOM and the European States backing it had recognised its right to exist interpreting article 8 of the NPT which stated the right of any group of States to conclude regional treaties. However, this was in order to assure the total absence of nuclear weapons in their respective territories, and it was not the case of EURATOM.

So in the aftermath of the treaty is coming into force, the nature of the relations between EURATOM and the IAEA was the new field of confrontation. The pressure of the Six and the superpowers contributed in the making of an agreement between the Agency and the Community, in a very complicated diplomatic process. From our perspective, it is worth following the point of negotiations between the supranational authority and the international organization.

The INFCIRC/153 enacted by the IAEA board of governors in June 1971 described the agreement between the agency and the adherent states. Articles 78-82 mentioned the concept of third safeguarding agents functionally independent by the member states nuclear material accounting

system. It seemed that the agreement proposed a proxy role for EURATOM, passing to IAEA the data of the inspections ran by EURATOM. However, this met France's opposition, because the Republic of France was not part of the NPT but was the most inspected EURATOM state. The final negotiation took form in the IAEA INFCIRC/193, in September 1973, providing guarantees in order to solve such problem, recognising the EURATOM safeguard system and avoiding overlapping with it to the maximum extent.

EURATOM committed to enacting subsidiary agreements with the IAEA, to implement INFCIRC/193. This was Regulation 3227/76 of October 1976, which outlined the technical aspects of the making of safeguards according to the agreement. It was Regulation 3227/76 which renewed the right of safeguards exemption for defence facilities, without any ambiguity.

This special status accorded to EURATOM raised some criticism in other NNWS, particularly Japan, which saw a preferential treatment for the members of the Community. However, we have to take into account also the uniqueness of EURATOM: the world did not have, and still does not, another similar Community which has adopted a regional safeguard system. Therefore, the case could not automatically extend elsewhere. Nevertheless, the Government of Japan successfully negotiated an agreement with the IAEA entailing some features of INFCIRC/193, appeasing this quarrelsome issue.

### 4.3 The completion of the system

The Regulation 3227/76 came after a relevant turning point in European history, that is, the first enlargement of the European Communities with the entering of the United Kingdom in EURATOM. French president Charles De Gaulle formerly opposed the process of association of Great Britain, but after De Gaulle's resignation, British and Continental supporters of such option renewed it. When the deal was drawn up with the IAEA, the United Kingdom was already a member of the European community, as it formally entered it on January 1, 1973.

The British nuclear complex was co-processing the nuclear materials aimed to defence or civilian use, not having a real distinction between the two tracks in some relevant nuclear facilities of the Country. Being the United Kingdom an NWS not belonging to any safeguard system before the coming into force of NPT, there was no need to separate the nuclear fuel cycle management as required by EURATOM safeguards.

The UK-EURATOM-IAEA verification Agreement of August 1978 was a "voluntary offer" of the UK Government to put under safeguards some nuclear facilities, so splitting the civilian track and the military one. The hosting of nuclear materials transferred in the United Kingdom based on bilateral agreements subjected to safeguards identified the facilities.

## 5. Conclusions

The value of the self-inspection system is its slowing down of a possible nuclear cascade. Keeping the right of defence related nuclear applications, it brought NWS to sever military and civilian nuclear sites. Before their joining the NPT as NNWS, all the EURATOM states could undertake a military program. They did not for a complex of reasons, but it is relevant to identify what role had had the EURATOM safeguard system in this long during situation. The main achievement of the self-inspection system was a mutual trust it enforces among its members. It non forbids any possibility of realising nuclear weapons, but it limited the reasons why a state should look for the integration of a nuclear capability in defence against its neighbours. The French nuclear capability not primarily aims at France's European partners, but to rescue France's role among the world powers, and among its allies too. That is the difference with Israel or Pakistan nuclear capability.

In East Asia we had

- 1) People Republic of China (PRC): full status NWS, member of the NPT, with global projection and secondarily regional fewer intensity conflicts;
- 2) Democratic Popular Republic of Korea (DPRK): new NWS with a weak nuclear capability but not more NPT member;
- 3) Japan, Republic of Korea, Republic of China (Taiwan): three states with the industrial strength to develop a nuclear capability, but only Japan and Republic of Korea are a member of the NPT.

In such a landscape the main achievement will be the avoiding of both vertical and horizontal proliferation, let say: the increasing of PRC nuclear weapons stocks, the strengthening of DPRK nuclear capability, the turning of the three to NWS status.

A safeguard agreement based on self-inspection of the recognised civilian sites will be a game changer in a situation in which the perceived threat by the neighbour will be the trigger of a nuclear cascade and a nuclear confrontation. Not bound to a renunciation to the nuclear option for NNWS, as

well not bound to denuclearisation for NWS, a self-inspection system will act on the expected shared part of security concerns, smoothing the climate and ensuring the visit of inspectors by the neighbours in the territory of the states.

## 6. Acknowledgements

The authors would like to acknowledge all those who have reviewed these guidelines and contributed to their completion.

## 7 Legal matters

### 7.1. Privacy regulations and protection of personal data

We agree that ESARDA may print our name/contact data/photograph/article in the ESARDA Bulletin/Symposium proceedings or any other ESARDA publications and when necessary for any other purposes connected with ESARDA activities.

### 7.2. Copyright

The authors agree that submission of an article automatically authorises ESARDA to publish the work/article in whole or in part in all ESARDA publications – the bulletin, meeting proceedings, and on the website.

Once the article has been accepted for publication the copyright is reserved, but part of the publication may be reproduced, stored in a retrieval system, or transmitted in any form or by any means, mechanical, photocopy, recording, or otherwise, provided that the source is properly acknowledged.

The authors declare that their work/article is original and not a violation or infringement of any existing copyright.

## 8. References

[1] Trachtenberg M; *A constructed peace: the making of the European Settlement (1945- 1963)*; Princeton: Princeton University Press; 1999

[2] Gaddis JL; *The Cold War. A new History*; New York: Penguin Book Press; 2005

[3] Wurm C; *Western Europe and Germany: the beginnings of European Integration, 1945-1960*; Oxford: Berg Publishers; 1995

[4] Bossuat G; *Les fondateurs de l'Europe*; Paris: Belin Sup; 1994

[5] Bitsch M-T (Ed.); *Le couple France–Allemagne et les institutions européennes*; Brussels: Bruylant; 2001.

[6] Dobbs M; *Six months in 1945: FDR, Stalin, Churchill, Truman, and the birth of the modern world*; New York: Alfred A. Knopf; 2012

[7] Milward A; *The reconstruction of Western Europe 1945-51*; Berkeley-Los Angeles: University of California Press; 1984

[8] Holloway D; *Stalin and the bomb. The Soviet Union and Atomic Energy (1939-1956)*; New Haven: Yale University Press; 1994

[9] Osgood R; *NATO: the Entangling Alliance*; Chicago: University of Chicago Press; 1962

[10] Girault R; Bossuat G (Ed.); *Europe brisée, Europe retrouvée. Nouvelles réflexions sur l'unité européenne au XXe siècle*; Paris: Publications de la Sorbonne; 1994

- [11] Spierenburg D; Poidevin R; *The History of High Authority of the European Coal and Steel Community: supranationality in operation*; London: Weinfeld and Nicholson; 1994
- [12] Gillingham J; *European Integration 1950-2003: Superstate or new market economy?*; Cambridge: Cambridge University Press; 2003
- [13] Haruki W; *The Korean War. An International History*; Lanham: Rowman and Littlefield; 2013
- [14] Schwarz H-P; *The division of Germany, 1945–1949*. In Leffler M; Westad O (Eds.); *The Cambridge History of the Cold War*; Cambridge: Cambridge University Press; 2010
- [15] Leffler M; *The emergence of an American grand strategy, 1945–1952*; In Leffler M; Westad O (Eds.); *The Cambridge History of the Cold War*; Cambridge: Cambridge University Press; 2010
- [16] Ruane K; *The Rise and Fall of the European Defence Community: Anglo-American Relations and the Crisis of European Defence (1950-1955)*; New York: St. Martin Press; 2000
- [17] Rohan S; *The Western European Union: International Politics between Alliance and Integration*; London: Routledge; 2014
- [18] Pilat J; Pendley R; Ebinger CK (Eds.); *Atoms for Peace: An Analysis After Thirty Years*; Boulder: Westview Press; 1985
- [19] Mongin D; *La bombe atomique française 1945-1958*; Bruxelles: Bruylant; 1997
- [20] Duchene F; *Jean Monnet: the first statesman of interdependence*; New York: Norton; 1994
- [21] Young JW; *Britain and European Unity, 1945-1992*; London: The Macmillan Press LTD; 1993
- [22] Dumoulin M; *Spaak*; Bruxelles: Editions Racine; 1999
- [23] Skogmar G; *The United States and the nuclear dimension of European Integration*; Basingstoke: Palgrave and Macmillan; 2004
- [24] Smith SC (ed.); *Reassessing Suez 1956. New Perspectives on the crisis and its aftermath*; Aldershot: Ashgate Publishing Ltd; 2008
- [25] Teissier du Cros H; *Louis Armand, visionnaire de la modernité*; Paris: Odile Jacob; 1987
- [26] Scheinman L; *Atomic Energy Policy in France under the Fourth Republic*; Princeton: Princeton University Press; 1965
- [27] Pirotte O; Girerd P; Marsal P; Morson S; *Trente ans d'expérience EURATOM. La naissance d'une Europe nucléaire*; Brussels: Bruylant; 1988
- [28] Cirincione J; *Asian Nuclear Reaction Chain*; Carnegie Endowment for International Peace; March 2000; <<https://carnegieendowment.org/2000/03/02/asian-nuclear-reaction-chain-pub-76>>
- [29] *South Korea special weapons*; Global Security; <<https://www.globalsecurity.org/wmd/world/rok/index.html>>
- [30] Albright D; Gay C; *Taiwan: Nuclear nightmare averted*; "Bulletin of the Atomic Scientists"; 54/1: January 1998
- [31] Dingman R; *Atomic Diplomacy during the Korean War*; "International Security", 13/3: 1988
- [32] "Statement of the Government of the People's Republic of China", 16 October 1964 <<https://digitalarchive.wilsoncenter.org/document/134359>>

[33] 'North Korea Statement on Nuclear Test' released by the North Korean Foreign Ministry, 3 October 2006 (Korean Central News Agency).

[34] "Central Asian nuclear-weapon-free zone (CANWFZ)", *Nuclear Threat Initiative*, <<https://www.nti.org/learn/treaties-and-regimes/central-asia-nuclear-weapon-free-zone-canwz/>>

[35] Howlett D; *EURATOM and Nuclear Safeguards*; Basingstoke: MacMillan; 1990

[36] Krige J; *Euratom and the IAEA: the problem of self-inspection*; "Cold War History"; Vol. 15: 3/2015

[37] Bharat P; Chare P; *Fifty Years of Safeguards under the EURATOM Treaty – A regulatory Review by the EURATOM inspectorate*; in Janssens-Maenhout G (ed.) *Nuclear Safeguards and Non-Proliferation. Syllabus of the ESARDA course*; Brussels: Publication Office of the European Union; 2008

[38] Goldschmit B; *Le complexe atomique. Histoire politique de l'énergie nucléaire*; Paris: Fayard; 1980

[39] Popp R; Horowitz L; Wenger A; *Negotiating the Nuclear Non-Proliferation Treaty: Origins of the Nuclear Order*; London: Routledge; 2016

## **Euratom safeguards: sixty years of implementation in France**

**François Bonino, Julie Oddou**

Comité technique Euratom (CTE)  
B. 447 (Head Office) – PC n° 212  
91191 Gif-sur-Yvette cedex  
France

[Francois.bonino@cte.gouv.fr](mailto:Francois.bonino@cte.gouv.fr), [Julie.oddou@cte.gouv.fr](mailto:Julie.oddou@cte.gouv.fr)

### **Abstract:**

*France being a member of the European Union and party to the Euratom treaty since 1957, all its civil nuclear activities have been submitted, for more than sixty years, to international safeguards applied by the European Commission. In 2017, around 1399 (1521 with IAEA inspections) Person Days Inspection (PDI) were used during 326 (345) inspections in French nuclear facilities (representing about 37% of the total inspection effort in the European Union). This puts France among the group of states welcoming the largest number of international safeguards inspections (with Canada, Japan, Argentina, Germany, ROK...) and will make it, after Brexit, the most heavily controlled nuclear weapon state (NWS) in the world. After briefly describing the scope of Euratom safeguards in France and how the application of the controls translates in practical terms for French authorities and operators, the paper will aim at taking stock of six decades of implementation from an EU member state perspective: benefits and constraints. While underlining the fact that controls in France are identical to those carried out in EU non-nuclear weapon states, specificities related to France's NWS status will be explained. In particular, the paper will focus on how nuclear materials of foreign origins are followed, thanks to Euratom and domestic nuclear materials accountancies, and will try to restore the truth about the management of connections between civil and defense cycles.*

### **1. Introduction**

France has been a founding member of the European Union and party to the Euratom treaty since 1957. Therefore, all its civil nuclear activities have been subject, for more than sixty years, to international safeguards applied by the European Commission (EC) in accordance with chapter VII of the Euratom Treaty.

This paper is intended to describe what are the benefits or added value for the French authorities and operators, and for the international community, of the implementation of Euratom safeguards in France, taking into account the fact that IAEA safeguards are applied under a voluntary offer safeguards agreement in accordance with France's nuclear weapon state (NWS) status under the Non Proliferation Treaty (NPT).

### **2. Euratom safeguards: a full-scope and robust control**

While IAEA safeguards are considered to be a "finality control", Euratom safeguards are generally characterized as a "conformity control" which aims at checking that nuclear materials "are not diverted

*from their intended uses as declared by the users” and that “the provisions relating to supply and any particular safeguarding obligations assumed by the Community under an agreement concluded with a third State or an international organisation are complied with” (article 77 of the treaty).*

They are based on Euratom treaty whose section VII provides for the enforcement of controls on nuclear materials, and following a Commission regulation (N°302/2005) on the application of Euratom safeguards<sup>1</sup>. The European Commission is in charge of the Regional System of Accounting and Control of Nuclear Material (RSAC) on which the IAEA safeguards system can rely.

For each material balance area (MBA), nuclear operators must produce and transmit a series of documents and reports to the European Commission: initial inventory, design information (or Basic Technical Characteristics), outline programme of activities (annually), inventory change reports (monthly), physical inventory listing (annually), material balance report (annually), import/export notifications...

The definition of nuclear materials subject to Euratom control is the same as for IAEA safeguards but the scope for Euratom is larger as nuclear material contained in ore, source material and waste is covered. It is worth noting that this facilitates the implementation of the Additional Protocol which requires EU Member States to declare information regarding mines and source material production, and some intermediate or high-level waste or installations for the treatment, storage and disposal of waste.

Article 81 gives to the European Commission the same rights of on-site inspection in all EU member states: *“inspectors shall at all times have access to all places and data and to all persons who, by reason of their occupation, deal with materials, equipment or installations subject to the safeguards...”*

The treaty (article 83) also gives strong sanction power to the Commission ranging from a formal warning, withdrawal of technical or financial assistance, placing the undertaking under administration or withdrawal of the source materials and the Commission has actually imposed sanctions on several occasions in the past.

This ability to apply enforcement action on the operator or the Member State and the fact that the Commission is the only party to inspect all the civil facilities in the EU Member States, including UK and France, in a comprehensive and nondiscriminatory manner, make the Euratom safeguards system unique.

### **3. Euratom safeguards in France: a comprehensive control on all civil nuclear materials**

Nuclear materials in France are subject to several layers of controls exercised by the operators, the French SSAC (State System for Accounting and Control), the European Commission and the IAEA.

Even if the on-site application of IAEA safeguards in French facilities is limited to facilities selected by the Agency, as in any other nuclear weapon state, it is worth noting that Article XI of France’s safeguards agreement (INFCIRC/290) provides that *“account shall be taken of the inspection effort carried out by the Community in the framework of its multinational system of safeguards”*. The agreement also states that the European Commission shall, in applying Euratom safeguards, cooperate with the IAEA with a view to ascertaining that IAEA obligated nuclear material in France is not withdrawn from civil activities.

This acknowledges the value of Euratom safeguards and how they can contribute to help the IAEA implementing its non-proliferation mandate within all the EU member states.

France being a founding member of the Treaty, Euratom safeguards have been applied by the European Commission for 60 years over **all its civil nuclear materials**. The Euratom safeguards mandate is identical across France, UK and the 26 non-nuclear weapons states of the EU. French operators sent the first monthly declarations of nuclear material movements in mid-1959 and regular on-site inspections started in May 1960.

---

<sup>1</sup> which entered into force in 2005 and replaced the previous regulation n° 3227/76

Verification on-site is carried out through, inter alia, routine inspections, physical inventory verification inspections, short notice random inspections (in one fuel fabrication plant in France) and unannounced inspections (in all 58 French power reactors).

In 2018 :

- 45 French nuclear facilities representing 176 Material Balance Areas (MBA) were subject to Euratom safeguards ;
- 322 inspections were carried out representing 1405 man.days of inspection ;
- Around 260 000 inventory changes accountability lines were declared under Euratom regulation ;
- 768 nuclear material international transfers were notified (through 1339 notifications).

This makes France the most heavily controlled country in the European Union (around 37% of global EC inspection effort), followed by the United Kingdom (around 25%) and Germany (around 10%).

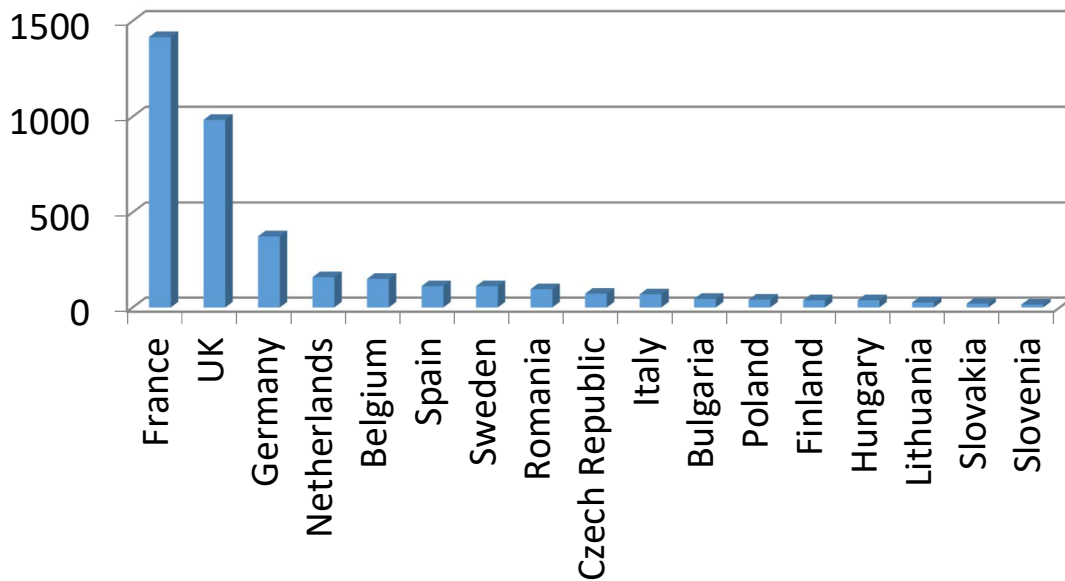


Figure 1: Euratom inspection effort in EU member states (> 10 man-days) (EC data 2016)

Taking into account the excellent quality record of Euratom safeguards over 60 years, as a multinational safeguards authority, and the fact that its basic principles, methods and equipment are very much the same as for IAEA safeguards, one can consider that France is de facto under international safeguards for all its civil nuclear activities.

On this basis, the following comparison was made between some States subject to international safeguards (IAEA, Euratom, ABACC):

States	Number of facilities open to international safeguards	Number of facilities inspected	Total number of inspections	Person-days of inspection	Numbers of ICR reporting units	Numbers of MBR reporting units	PDI/open facility
Canada	34	34	241	853	6370	50	25,1
Brazil	26	26	91	629 <sup>2</sup>	1627	28	24,2
Argentina	51	51	93	1157 <sup>3</sup>	1770	46	22,7
United Kingdom	62	62 <sup>4</sup>	219 <sup>5</sup>	1183 <sup>6</sup>	360567	78	19
Germany	70	70	223 <sup>7</sup>	1114 <sup>8</sup>	54000	123	15,9
France	104 <sup>9</sup>	104 <sup>10</sup>	328 <sup>11</sup>	1521 <sup>12</sup>	260172	178	14,4
Japan	125	125	269	1337	14800	317	10,7
Republic of Korea	46	46	56	346	7180	43	7,5
China	25	3	10	76	985	3	3,04
Russian Federation	22	1	1	4	0	2	0,18
United States of America	292	1	5	19	40592	6	0,065

**Table 1 : International verification activities in 2017**

<sup>2</sup> 457 for ABACC – ABACC report 2017

<sup>3</sup> 752 for ABACC – ABACC report 2017

<sup>4</sup> 3 for IAEA

<sup>5</sup> 36 for IAEA, 33 joint, Euratom figures for 2014

<sup>6</sup> 200 for IAEA, Euratom figures for 2014

<sup>7</sup> 208 for IAEA, 166 joint inspections, 181 for Euratom (figures for 2014)

<sup>8</sup> 740 for IAEA, Euratom figures for 2014

<sup>9</sup> 17 for IAEA

<sup>10</sup> 2 for IAEA

<sup>11</sup> 19 for IAEA, 17 joint inspections

<sup>12</sup> 122 for IAEA



Figure 2: International inspections in 2017

## 4. Specificities of Euratom safeguards implementation in France

### 4.1 Nuclear material transfers between civil and defense fields

Article 84 of the Euratom treaty provides that “*The safeguards may not extend to materials intended to meet defence requirements which are in the course of being specially processed for this purpose or which, after being so processed, are, in accordance with an operational plan, placed or stored in a military establishment.*”

Consequently, France being a nuclear weapon state under the NPT, some nuclear materials can be withdrawn from Euratom safeguards (and vice versa) following accountancy procedures defined in Euratom regulation 302/2005. Those requests for withdrawal (or submission) are declared to both the European Commission and the French domestic accountancy system (SSAC) which check if the movement can be authorized. In addition, the strict application of EU and national regulations allows the French authorities to ensure that **NO transfer out of Euratom safeguards occurs for nuclear material under a peaceful use commitment**. This exclusion applies to nuclear material:

- Supplied by a third country in the frame of a nuclear cooperation agreement with Euratom (e.g. USA, Canada, Australia, Japan...);
- Supplied by a third country in the frame of a French bilateral nuclear cooperation agreement;
- Subject to IAEA safeguards in France<sup>13</sup>.

**In any case, the French authorities, in particular the Comité Technique Euratom (CTE), ensure that no nuclear material is withdrawn from IAEA safeguards.**

Transfers of nuclear material under or out of Euratom safeguards are very limited in numbers and only possible for a particular type of material identified by a specific national accountancy code. In 2017, the vast majority (80%) of requests granted by the French authorities concerned transfers of nuclear material under Euratom safeguards.

<sup>13</sup> In accordance with article 1 (a) of INFCIRC/290. Those nuclear materials correspond mostly to those imported in France under Euratom or bilateral agreements.

The share of nuclear material withdrawn from Euratom safeguards in 2017, by category, compared to the total inventory of nuclear material under Euratom safeguards in France as of 31 December 2017, is nil (0) when rounded to the nearest  $10^{-6}$ .

As stated above, only non-obligated nuclear material can be transferred out of Euratom safeguards.

#### **4.2 Third country and/or IAEA obligated nuclear material follow up**

Obligations taken by the Euratom Community or by France, towards a third country and/or the IAEA, are tracked using specific codes mentioned in all accountancy lines declared by the operators.

When foreign nuclear materials under IAEA safeguards enter French facilities, they keep their “flag”, whether country specific or implying a peaceful use through a submission to IAEA safeguards. In other words, Euratom and national controls are designed to **prevent the direct or indirect use of foreign nuclear material in the French defense programs** and to ensure that they remain in civil activities, subject to IAEA safeguards.

### **5. Taking stock after 60 years**

After 60 years of Euratom safeguards implementation in France, its benefits can be identified at several levels.

First, the **credibility of the Euratom safeguards system** as a robust Regional System of Accounting and Control (RSAC) has been proved over the years. Being founded on the principle of the Euratom Treaty and with staff coming from all the EU Member States, the European Commission is a regulatory authority whose integrity, effectiveness and independence is widely recognized both within the EU and internationally.

French authorities and nuclear operators have been used for decades to deal with very demanding and time consuming but effective international controls, in more than 100 facilities, made of timely reporting and inspections. The safeguards approaches implemented by the European Commission have evolved over time: Low Frequency Unannounced Accesses were introduced in GB II (Gas Centrifuge Enrichment Plant), Short Notice Random Inspections are implemented in a fuel fabrication plant, and unannounced inspections are now carried out routinely in French nuclear power plants...

From the operators' perspective, Euratom Safeguards have shown their value by encouraging them to improve their nuclear material accountancy procedures and measurement capabilities. Indeed, the provisions of the Euratom Treaty and of its secondary legislation impose on nuclear operators to establish, implement and maintain a **high-quality nuclear material management system**. They are required, in particular, to monitor at any time the location and state of all the nuclear material in their facilities. The implementation of safeguards verification activities allows the European Commission to evaluate continuously if the nuclear operators (or holders) meet this crucial requirement. Those verifications can be seen as an audit of the operators practices to identify deficiencies, and when needed to enforce strict application of the rules.

This evaluation is carried out through the monitoring of nuclear material flows and inventories, including direct verifications at all nuclear facilities, while taking into account the operational and technical constraints on-site. Euratom inspections proved their capacity to detect discrepancies in operators' records or declarations. These anomalies are subject to investigation and, in general, are due to isolated mistakes or cases of poor practice rather than generic problems.

The implementation of Euratom safeguards has also contributed to facilitate nuclear material transfers, and nuclear trade as a whole, within the EU. France being a major nuclear supplier country, the existence of this system is recognized to be of great value by the French nuclear industry. In addition, Euratom safeguards not only provide a guaranty of the nuclear material peaceful use but also constitute the only international oversight on nuclear installations in Nuclear Weapon States, and consequently **avoid distortion of competition within the EU**.

Finally, the Euratom safeguards system has provided reassurance to governments, members of parliaments and the public opinion that within the EU nuclear materials are strictly controlled, that operators are being carefully regulated and that obligations are being met.

In 2007, the European Parliament noted that *“these safeguards also provide a real guarantee for countries that supply nuclear materials as to the use of those materials, complementing the non-proliferation controls of the International Atomic Energy Agency (IAEA)”*.

# Bringing IAEA Safeguards in the United States into the 21<sup>st</sup> Century

David H. Hanks, Eduardo Sastre

U.S. Nuclear Regulatory Commission  
Washington, DC USA

[David.hanks@nrc.gov](mailto:David.hanks@nrc.gov), [Eduardo.sastre@nrc.gov](mailto:Eduardo.sastre@nrc.gov)

## **Abstract:**

The United States (U.S.) has allowed the International Atomic Energy Agency (IAEA) to apply safeguards to its civil nuclear facilities since 1980 through its Voluntary Offer Agreement (VOA), and before that through INFCIRC/66 type safeguards., by which time the U.S. had established the necessary infrastructure to support IAEA safeguards implementation. The State System of Accounting for and Control of Nuclear Material (SSAC) included developing the necessary procedures, system of records and reports, equipment, experts and organizational structure to meet IAEA safeguarding requirements. After nearly four decades following initial implementation, the U.S. is engaged in multiple efforts to bring the SSAC infrastructure into the 21<sup>st</sup> Century. Beginning in 2011, the U.S. Nuclear Regulatory Commission has worked with its licensees to update all the required IAEA Design Information Questionnaires (DIQ) and Transitional Facility Attachments (TFA) for selected licensed facilities under the Reporting Protocol to the US-IAEA Voluntary Offer Safeguards Agreement INFCIRC/288. This activity, now nearly complete, entailed extensive revisions as some of the DIQs and TFAs had not been updated in more than three decades. In 2016, the U.S. and the IAEA agreed to apply an amendment to modify the Small Quantities Protocol to the U.S.-IAEA Agreement for the Application of Safeguards in Connection with The Treaty for the Prohibition of Nuclear Weapons in Latin America, i.e., the "Tlatelolco Safeguards Agreement." Bringing this amendment into force in July 2018 required changes in the U.S. regulations for possessors of nuclear material in the US Caribbean Territories. Other improvements to U.S. reporting to the IAEA have been made by the Department of Commerce under the Additional Protocol and Department of Energy using the national nuclear material accountancy database with the goal of enhancing its tracking and reporting capabilities. The expected combined outcome of all these projects is a more efficient and modern infrastructure that will facilitate the implementation of safeguards in the U.S. This paper will address the development of these projects, including the challenges encountered and the expected future ones.

**Keywords:** Safeguards, NRC, Licensees

## **1. Introduction**

The Energy Reorganization Act of 1974 provides the United States of America (U.S.) Nuclear Regulatory Commission (NRC) with the authority to issue regulations implementing *The Agreement between the U.S. and the International Atomic Energy Agency (IAEA) for the applications of Safeguards in the U.S.* (Voluntary Offer Agreement INFCIRC/288), *the Protocol Additional to the US-IAEA Safeguards Agreement* (US Additional Protocol), and *The Agreement between the U.S. and the IAEA for the Application of Safeguards in Connection with the Treaty for the Prohibition of Nuclear Weapons in Latin America* (US-IAEA Caribbean Territories Safeguards Agreement) (INFCIRC/366) and its Small Quantities Protocol at NRC licensed facilities, locations, sites, applicants, licensees, any certificate holder, or possessor of nuclear material. Acting as the U.S.'s national regulatory authority for the commercial nuclear industry, the NRC is charged with providing oversight for implementation of procedures and practices necessary to facilitate information gathering, timely reporting, and in-field verification.

In an effort to allay concerns during the negotiation of the Treaty on the Non-Proliferation of Nuclear Weapons (NPT),<sup>1</sup> President Johnson stated that the United States was not asking any country to accept safeguards that it was unwilling to accept, and that, "...when such safeguards are applied under the

<sup>1</sup> The NPT Is reproduced in IAEA INFCIRC/140; 22 April 1970, Vienna (1970).

Treaty, the United States will permit the IAEA to apply its safeguards to all nuclear activities in the U.S. -- excluding only those with direct national security significance."<sup>2</sup> Guided by this policy, the U.S. concluded the Voluntary Offer Agreement (INFCIRC/288) with the IAEA as a separate, formal agreement. The VOA provides the IAEA the right, but not obligation, to apply international safeguards on source and special nuclear material (SNM) within the U.S., excluding facilities associated with activities of direct national security significance. Periodically, the U.S. provides the IAEA with an updated list of facilities eligible for the application of IAEA safeguards, adding or removing facilities from that list as necessary (Art. 2(b)). Revisions to this eligible facilities list (EFL) by the NRC and Department of Energy are submitted for a 60-day Congressional review before they are submitted to the IAEA.

The U.S. Additional Protocol (AP), was brought into force in January 2009 and has marked a significant shift in the way safeguards are handled in the United States. The U.S. signed an AP in 1998 and after the necessary implementing legislation was passed by Congress, the U.S. AP entered into force on January 6, 2009. The U.S. AP is identical to the model AP (INFCIRC/540) in all ways, except for the inclusion of a national security exclusion.

The US-IAEA Caribbean Territories Safeguard Agreement (INFCIRC/366), unlike the U.S.-IAEA Safeguards Agreement (INFCIRC/288), is not a VOA and does not have a national security exclusion currently exercised by all the NWS. INFCIRC/366 and its small quantities protocol entered into force in 1989. The original INFCIRC/366 small quantities protocol that held most of Part II of the Agreement in abeyance was amended by the IAEA in July 2018. The modified SQP (ModSQP), which still holds many requirements in abeyance, also applies to articles in Part II of the US-IAEA Caribbean Territories Agreement. The model SQP for States with only small quantities was amended in 2005 by the IAEA to address proliferation concerns, resulting in removal of abeyance from Articles in Part II of INFCIRC/366; 31-37, 39, 47, 48, 58, 60, 66, 67, 69, 71-75, 81, 83-89, 93, and 94 (slight variation from model). All paragraphs in Part I of the Agreement are in effect for the U.S. territories in the zone of application of the Tlatelolco Treaty.

## 2. Assessment of IAEA Documents

The U.S.'s agreement to the VOA in 1979 led to Senate Hearings to discuss NRC activities and facility burden associated with the implementation of the VOA. At hearings before the Senate Committee on Foreign Relations, the Director of the NRC Office of International Programs (OIP) made a statement to the described how NRC regulations and oversight activities for nuclear material and other radioactive material at licensed facilities would ensure the U.S. meets its obligations under the U.S.-IAEA Safeguards Agreements. Since those early discussions of the possible burden to facilities, the U.S. Government and its nuclear industry have experienced the impact of implementation of these Agreements.

Each licensed facilities selected from the EFL for IAEA safeguards under the VOA is required to provide a completed IAEA design information questionnaire (DIQ) to the NRC, in accordance with Title 10 of the Code of Federal Regulations Part 75 (10 CFR Part 75). Subsidiary Arrangements describing details of the IAEA safeguards approach for each facility are established in a Facility Attachment (FA) or, in the case of selection under the U.S. Reporting Protocol, a Transitional Facility Attachment (TFA). These documents are negotiated by the U.S. Government with the IAEA for each facility selected. The NRC works with the selected facilities to ensure complete and accurate information is provided to the IAEA in both the DIQ and FA/TFA, while evaluating the burden to the facility itself.

Currently there are three NRC licensed low enriched uranium (LEU) fuel fabrication facilities and one gas centrifuge enrichment plant (GCEP) selected for reporting to the IAEA under the U.S. Reporting Protocol, utilizing a TFA for guidance and a completed IAEA DIQ describing essential equipment and routine operations of the facility. These facilities, however, are not subject to IAEA inspections. Considerations for facility selection in the U.S. by the IAEA usually include opportunities for the IAEA to evaluate performance of a particular safeguards approach or new instrumentation used in strengthening a safeguards approach. Historically, the IAEA has implemented and subsequently withdrew traditional safeguards at several facilities under the U.S.-IAEA Safeguards Agreement. In past years, The list of 13 NRC licensed facilities that have been selected and inspected at various times between 1980 and 2005

<sup>2</sup> *Remarks of Lyndon B. Johnson to Ceremonies Marking the 25th Anniversary of the First Nuclear Reactor*, December 2, 1967, <http://www.presidency.ucsb.edu/ws/index.php?pid=28578&st=&st1=>.

includes: 6 commercial power reactors, 5 LEU fuel fabrication facilities (one additional selected but not inspected), and two HEU down-blending projects. Several other U.S. facilities have been selected to further a nonproliferation objective (e.g., safeguarding plutonium or high enriched uranium declared in excess to U.S. defense needs).

Fuel fabrication facilities selected for IAEA safeguards soon after the VOA came into force in 1980 utilized technology of the time to provide drafters' drawings, rudimentary charts and simple graphs to answer the complicated questions posed by the IAEA in the DIQ forms. Technological advancements designed into various stages of the process have greatly improved SNM handling procedures and practices at these facilities. Many of the original SNM process streams once considered to be very efficient have been replaced with continuously improving state-of-the-art equipment and controls. Along with these conversions of advanced design essential systems, some outdated processes are actually abandoned in place—leaving caches of legacy equipment to be declared in the DIQ.

Although DIQs describing SNM handling and storage at the fuel fabrication facilities have been amended from time-to-time since the early days of providing design information to the IAEA, it became increasingly apparent that continuing to “patch” the old DIQs is too time consuming and difficult. Advanced software programs being used at each of the three currently selected fuel fabrication facilities could be utilized in order to bring the DIQ/TFA information into the 21<sup>st</sup> Century. Thus, the NRC commenced working with these facilities in 2011 to anew their DIQs to ensure they contained a holistic and modern description of SNM handling and storage. The process for this endeavor is further discussed in Section 2.2 of this report.

Subsidiary Arrangements were not negotiated for the U.S.-IAEA Caribbean Territories Safeguards Agreement of 1989, but were brought into force in conjunction with the ModSQP to support NRC's implementation of the requirements. Prior to implementation of the ModSQP, federal regulations outlined in 10 CFR Part 75 did not include any conditions related to INFCIRC/366 and needed to be updated to reflect obligations agreed to in the Agreement's newly negotiated Subsidiary Arrangements. The U.S. Government developed and negotiated both a Subsidiary Arrangement document including typical Codes 1-10, in addition to a Locations Outside Facilities Attachment (LOFA) for the overall material balance area that included all nuclear material locations in the U.S. Caribbean Territories. These documents were used to support the required regulation changes to 10 CFR Part 75. On May 4, 2018, the final 10 CFR Part 75 rule was published in the *United States Government Federal Register* (83 FR 19603). The rule became effective June 3, 2018, 30 days after the publication of the Federal Register Notice. Licensee compliance with the final rule was required by July 3, 2018, 60 days after the publication of the Federal Register Notice. It should be noted here that shipments and receipts between US Caribbean Territories and any of the 50 U.S. states or other U.S. territories outside of the zone of application of the Treaty of Tlatelolco are considered foreign shipments/receipts.

## 2.2 Updating Existing IAEA Documents

The U.S. experienced great success when developing the DIQ and TFA for the most recent gas centrifuge uranium enrichment facility built in Eunice, New Mexico, by Louisiana Energy Services/URENCO USA (LES/UUSA). The IAEA selected the LES/UUSA facility under the Reporting Protocol in 2013. Prior to selection, the NRC helped inform the facility's operators, engineers and designers about the needs and expectations of the IAEA for a completed DIQ and TFA that would be acceptable for submission. In 2011-2012, experienced staff from required disciplines at LES/UUSA worked to bring together the information needed. Enhanced software programs were used in 2012-2014 while building process, handling and storage area drawings, applicable charts, and cross-reference tables for required attachments. The plan and schedule designed for the initial declarations of the LES/UUSA GCEP were used in updating the DIQ/TFA submissions for the selected fuel fabrication facilities.

The three licensed LEU fuel fabrication facilities currently selected for IAEA safeguards under the Reporting Protocol include: Global Nuclear Fuel Americas (GNF-A) Fuel Fabrication Facility, Columbia Fuel Fabrication Facility (CFFF), and FRAMATOME Fuel Fabrication Facility. The NRC staff held workshops at each of these sites during 2014-2015, using the following training modules and a simulated IAEA design information verification (DIV) visit by a mock IAEA inspector.

On-Site training was provided to improve facility understanding of IAEA Safeguards in these key areas:

- Overview of IAEA Safeguards
- U.S. Voluntary Offer Agreement (INFCIRC/288)

- U.S. Additional Protocol
- Facility Type Safeguards
- Site Specific Safeguards
- Mock DIV

Subsequent to the workshop at each site, a plan for revising all the DIQ/TFA documents at the three fuel fabrication facilities was provided to the Subgroup on IAEA Safeguards in the U.S. (SISUS). This U.S. interagency subcommittee agreed with the NRC proposal to work with operators to provide the IAEA an updated DIQ/TFA for each facility utilizing the latest available software tools. Priority would be based on availability of knowledgeable staff at each facility and the number of iterations with NRC staff during DIQ/TFA drafting.

### 3. Outreach to NRC Licensees

In order to determine conditions related to the implementation burden at facilities, the NRC staff reached out to facility operators or possessors of nuclear material to determine what issues were most challenging for meeting obligations of the applicable articles of the VOA, AP and US-IAEA Caribbean Territories Agreement. Subsidiary Arrangements for INFCIRC/288 have been in place for over 30 years, but a new Subsidiary Arrangement- had to be negotiated for INFCIRC/366. This in turn required changes to the federal regulations and modifications to the nuclear material management and safeguards system (NMMSS) IAEA reporting modules. Communication with licensees on a routine basis was necessary for achieving a near seamless transition, providing significantly updated information and new reporting regimes while utilizing 21<sup>st</sup> Century practices and technology.

One good example of modernizing ideas is how outreach to the fuel fabrication facilities led to improved reporting. Upon completion of each workshop provided to the fuel fabrication facilities, discussions were held with the licensees on the status of their specific DIQ and TFA. An effort at each facility site determined what site expertise would be needed to answer the more complex questions of the IAEA DIQ. The NRC worked closely with the facilities to provide feedback on various iterations of the draft DIQ and to request clarification from the IAEA Country Officer for the U.S. and its territories, when needed.

The current IAEA DIQs for all licensed facility types are posted on the NRC public website so that each selected facility is able to read and download the appropriate blank DIQ form. When notified by the NRC, a selected facility is required to submit an initial completed IAEA DIQ for NRC review and final submission to the IAEA. Revisions of the DIQ are cleared through SISUS in order to maintain consistency in declarations from the U.S. Government. Subsidiary Arrangements, FA/TFAs, dictate when the DIQ must be updated or a revision is required. Voluntary revisions to the DIQ are submitted to the IAEA when the facility and U.S. Government mutually agree that a revision would improve clarity of the DIQ.

Licensed fuel fabrications facilities are required to revise their TFAs in order to update IAEA material description codes originally introduced into the early TFAs. Material description codes (MDC) are used in reporting nuclear material inventory and flow, in accordance with specifications of the TFA (Code 4). A limited number of 4-digit codes were used in the early material control and accounting (MC&A) reports to the IAEA: Physical Inventory Reports, Inventory Change Reports, and Material Balance Reports. However, as business models for all three currently selected fuel fabrication plants began to change, and new handling methods continue to develop, new MDCs were reported using concise notes to the reports. Tracking of these multiple concise notes became difficult and prone to error.

Feedback from fuel fabrication facilities provided other insights, as well. NMMSS is used by the U.S. to track all domestic SNM movements and facility inventories; subsequently NMMSS captures all transaction data related to IAEA selected facilities for reporting. Alignment of the IAEA 4-digit MDC is modified in the new TFAs, allowing each possible combination of MDCs to be grouped using 4 columns: physical, chemical, containment, and irradiation. This format expands the possibilities for unique MDCs to be used outside the normal routine transactions during the material balance period—minimizing the need for tracking concise notes.

Communication with all the IAEA selected facilities is vital to ensuring declarations to the IAEA are up-to-date, complete and accurate. The annual NMMSS Users Meeting, attended by operators from licensed facilities, allows the NRC to circulate any new information concerning IAEA safeguards and acquire information about challenges in implementation at the sites. Presentations are usually provided to the participants of the meetings regarding MC&A reporting issues and IAEA nuclear material transit error messages received by the U.S. Government. The Users Meeting also provides one-on-one

opportunities for facilities to raise questions or concerns regarding their reporting, often leading to on-the-spot resolution or encouraging collaborative ongoing discussion with other selected facilities.

Another good example of modernizing ideas is the information outreach to the possessors of nuclear material in the US Caribbean Territories. The NRC's first outreach trip to the US Caribbean Territories, in 2016, was conducted by NRC staff responsible for safeguards implementation in the U.S. and regional NRC inspectors who have inspection oversight of the possessors of nuclear material. The outreach team visited each of the licensees identified as potentially possessing nuclear material. After documenting the quantities and types of nuclear material present during each site visit, staff provided guidance on the upcoming reporting and IAEA inspection access requirements. NRC staff also provided the IAEA Service Series 22 (Safeguards Implementation Guide for States with Small Quantities Protocols). Staff found it especially helpful to provide the Service Series in English and Spanish (the native language used in Puerto Rico). Of vital importance when presenting this new information was the recognition that licensees in the U.S. Caribbean Territories had little knowledge of IAEA international safeguards. To compensate for this, the NRC created a high-level summary guide, in English and Spanish, to explain the concept of the modified SQP and the requirements that must be met by NRC licensees. This guide was also shared with the IAEA.

NRC staff conducted a second outreach visit in 2017 to provide more in-depth instruction on how to complete the domestic nuclear material accountancy forms, which are already used by licensees in the U.S. mainland. The outreach included a workshop that provided an overview of the history of the agreement between the U.S. and the IAEA for the application of safeguards in the U.S. Caribbean Territories. The workshop also provided instructions and examples on completing the forms used to comply with the proposed reporting requirements, such as the initial inventory report, material balance reports, and nuclear material transaction reports. All accountancy forms are submitted by licensees to NMMSS. Staff from the Department of Energy, Office of Nuclear Materials Integration, which operates NMMSS, supported the workshop.

#### 4. Continuous Improvement

After more than four decades of continuous improvements in implementation of the VOA, the U.S. is engaged in multiple efforts to bring the U.S. State System of Accounting for and Control of Nuclear Material (SSAC) infrastructure into the 21<sup>st</sup> Century. Albeit in the past, the SSAC has included developing the necessary procedures, system of records and reports, equipment, experts and organizational structure to meet IAEA safeguarding requirements, significant progress has been made in recent years to rejuvenate the SSAC.

Continuous improvement includes knowledge management within the NRC international safeguards team. Recent efforts have been made to strengthen the training and qualification program of the NRC International Safeguards Analysts, Import and Export Analysts, and NMMSS Analysts. The new program provides for well-informed technical support and expertise in the national safeguards implementation infrastructure. Individuals selected for analyst positions are asked to design, develop, and evaluate international safeguards systems and programs in order to improve organizational performance with the goal of achieving mission and performance goals of the NRC. These goals include licensing and regulation of the U.S. civilian use of radioactive material to protect the public health and safety, promote the common defense and security, and protect the environment.

Analysts assigned to the US NRC Office of Nuclear Material Safety and Safeguards need the knowledge and expertise to analyze international safeguards issues and other generic studies related to commercial fuel cycle facilities, and recommend NRC positions and policies as they relate to nuclear nonproliferation. Additionally, analysts assess complex safeguards and threat information and evaluate the safeguards significance associated with threats to nuclear facilities, materials, or the transportation of licensed material. Each category of analysts requires a slightly different focus in order to fulfill the position, which requires the qualification program to be flexible. When a new analyst becomes part of the team, the trainee's supervisor will decide what parts of the *Training Requirements and Qualification Journal for International Safeguards Analysts, Nuclear Materials Management and Safeguards System (NMMSS) Analysts, and Import/Export Analysts* must be completed for a particular analyst. The journal includes goals and objectives that are broken down into two main parts: 1) training and 2) qualification cards.

Recurring training at IAEA selected facilities is used to continue to improve knowledge of U. S. obligations under the VOA and AP throughout the U.S. nuclear industry. Modules of the workshops provided to selected NRC licensees prior to the DIQ updates are routinely updated to include changes

in federal regulations and/or reporting requirements to the IAEA. The NRC provides follow-on workshops to some facilities when requested in an effort to maintain continuity of knowledge of U.S. obligations under the US Safeguards Agreements when new employees are moved into affected positions of responsibility at each site. Sessions are also provided at national meetings like the annual NMMSS Users Meeting jointly hosted by the US NRC and Department of Energy to improve licensee knowledge of reporting requirements.

## 5. Technological Advancements on Reporting and Tracking

Other U.S. government agencies are also conducting their own improvements. The U.S. Department of Commerce is planning to roll-out in the near future an advanced domestic web portal to facilitate Additional Protocol reporting by U.S. companies. This online portal would streamline the reporting by letting U.S. companies report their exports and annual declaration through the U.S. Department of Commerce website. The software is being designed with the same specifications as the IAEA Protocol Reporter 3 which will improve the internal process for the U.S. in meeting its international reporting requirements. The online reporting capabilities are expected to be functioning sometime in 2020, and testing and outreach have already started.

With the goal of enhancing U.S. tracking and reporting capabilities, the U. S. Department of Energy's National Nuclear Security Administration is working on a substantial upgrade to the U.S. national nuclear material accountancy database. These improvements are focused on upgrading infrastructure, developing new software, and refining the user interface as to facilitate data analysis and accessibility. Another core aspect of the upgrade is automating the development of reports required under the U.S.-IAEA Safeguards Agreements, with the analysts concentrating in the quality control functions instead of spending time developing the reports. This would also facilitate the change in reporting scheme to "xml" format. Furthermore, these enhancements will allow more automated and efficient development of the required notification under the U.S. bilateral Nuclear Cooperation Agreements.

The expected combined outcome of all these projects is a more efficient and modern SSAC that will facilitate the implementation of safeguards in the U.S.

## 6. Summary

When the U.S.-IAEA Safeguards Agreement came into force in 1980, the IAEA applied safeguards to certain U.S. civil nuclear facilities in support of IAEA infrastructure and safeguards implementation. The U.S. SSAC includes the necessary procedures, system of records and reports, equipment, experts and organizational structure to meet IAEA safeguarding requirements. After nearly four decades following initial implementation, the U.S. is engaged in multiple efforts to bring the SSAC infrastructure into the 21<sup>st</sup> Century. Beginning in 2011, the U.S. Nuclear Regulatory Commission has worked with its licensees to update all the required IAEA Design Information Questionnaires (DIQ) and Transitional Facility Attachments (TFA) for selected licensed facilities under the Reporting Protocol to the U.S.-IAEA Voluntary Offer Safeguards Agreement INFCIRC/288. In 2016, the U.S. and the IAEA agreed to apply an amendment to modify the Small Quantities Protocol to the U.S.-IAEA Agreement for the Application of Safeguards in Connection with The Treaty for the Prohibition of Nuclear Weapons in Latin America, i.e., the "Tlatelolco Safeguards Agreement." The expected combined outcome of all these projects and others has produced a modern infrastructure that will facilitate the implementation of safeguards in the U.S.

<sup>i</sup>U.S. Nuclear Regulatory Commission; *Training Requirements and Qualification Journal for International Safeguards Analysts, Nuclear Materials Management and Safeguards System (NMMSS) Analysts, and Import/Export Analysts*; <http://www.nrc.gov/docs/ML1603/ML16035A147.pdf>; 2016.

# Experience with maintaining the SSAC in the Czech Republic

Adam Pavlik, Karolina Janatkova, Ondrej Stastny

Department of Non-Proliferation, State Office for Nuclear Safety, Czech Republic

## Abstract:

*Effective State System of Accounting for and Control of Nuclear Material (SSAC) is a key measure for implementation of the provisions of the Treaty on the Non-Proliferation of Nuclear Weapons and requirements of the comprehensive safeguards agreement. Establishing solid national legislation is an essential starting point for implementation of all the commitments related to the non-proliferation. State Office for Nuclear Safety (SONS) was appointed to the role of the State Responsible Authority (SRA) in the Czech Republic. National legislation is represented by the atomic law, recently updated to address all the new challenges, and completed by the corresponding new decrees covering requirements for the SSAC and export control. Comprehensive training of the SRA staff responsible for safeguards implementation is critical element for capacity building. Qualified SONS employees share the knowledge and train other key players within the Nuclear Material Accountancy and Control (NMAC) system to avoid a risk of incorrect and uncomplete reporting, especially with the respect to the new legislation. Long-term training for SONS inspectors includes suitable inspection skills and precise verification techniques together with internal system for data evaluation representing fundamental measures for verification of safeguards implementation on the Material Balance Area (MBA) level. One of the challenges for the SONS was correct and complete reporting for two Locations Outside Facilities (LOFs) MBAs. Sophisticated software also plays an important role for successful creation of the SSAC. SONS has recently developed new, modern and innovative software to reflect legislation changes and software evolution. One of the main perpetual issues for long-term maintaining of the SSAC in the Czech Republic is an employee retention closely connected with continuity of knowledge at the SONS or LOFs side. Responding to this issue is challenging for the SONS senior management.*

**Keywords:** LOFs, Non-Proliferation, Nuclear Material, SRA, SSAC

## 1. Introduction

In accordance with the Article III of the Treaty on the Non-Proliferation of Nuclear Weapons (NPT), each Non-nuclear-weapon state party to the NPT undertakes to accept safeguards, as set forth in an agreement to be negotiated and concluded with the International Atomic Energy Agency (IAEA) in accordance with the Statute of the IAEA and the Agency's safeguards system, for the exclusive purpose of verification of the fulfilment of its obligations assumed under the NPT with a view to preventing diversion of nuclear energy from peaceful uses to nuclear weapons or other nuclear explosive devices [1]. Based on this, the state should develop a State System of Accounting for and Control of Nuclear Material (SSAC) to ensure that all the relevant safeguards requirements are fulfilled. The SSAC, built by the state, should have two main objectives. Firstly, national objective aiming to account for and control nuclear material within the state and to contribute to the detection of possible losses, or unauthorized use or removal of nuclear material. Secondly, international objective providing the essential basis for the application of IAEA safeguards pursuant to the provisions of Safeguards Agreement between the state and the IAEA [2]. Creation of and subsequent successful maintaining the SSAC on the state level is a crucial area of implementation of the provisions of the NPT and requirements of the Safeguards Agreement represented by the Article 7 of this agreement [3]. To achieve effective and efficient implementation of the requirements mentioned above, the state must establish and develop a State Responsible Authority (SRA), which will be exclusively responsible for safeguards implementation. As defined by the IAEA guide "Safeguards Implementation Practices Guide on Provision of Information to the IAEA" the State authority with responsibility for safeguards

*implementation is the authority established at the national level to ensure and facilitate the implementation of safeguards. In addition to its safeguards functions, the SRA (if established within a broader nuclear authority) may have additional responsibilities associated with nuclear safety, security, radiation protection and export/import controls. One of the primary responsibilities of an SRA is to establish (initially) and maintain (continuously) an SSAC [4]. The same IAEA guide also defines the SSAC as a system comprised of all of the elements that enable the State to fulfil its nuclear material accounting, control and reporting responsibilities. These elements include information systems (computerized or paper-based); operators of facilities and other locations and their nuclear material accounting systems that produce accounting data; various processes, procedures and administrative controls (such as for import and export reporting; collection and submittal of design information); quality checks; and the SRA itself and its oversight activities to ensure all safeguards obligations are effectively met [4]. As it will be discussed further within this article, establishing the SRA with an effective and efficient SSAC is the initial step towards successful safeguards implementation in the state. Knowledge preservation, either human or artificial, is another key aspect of the SSAC, and comprehensive safeguards implementation cannot be fulfilled without addressing this issue as well.*

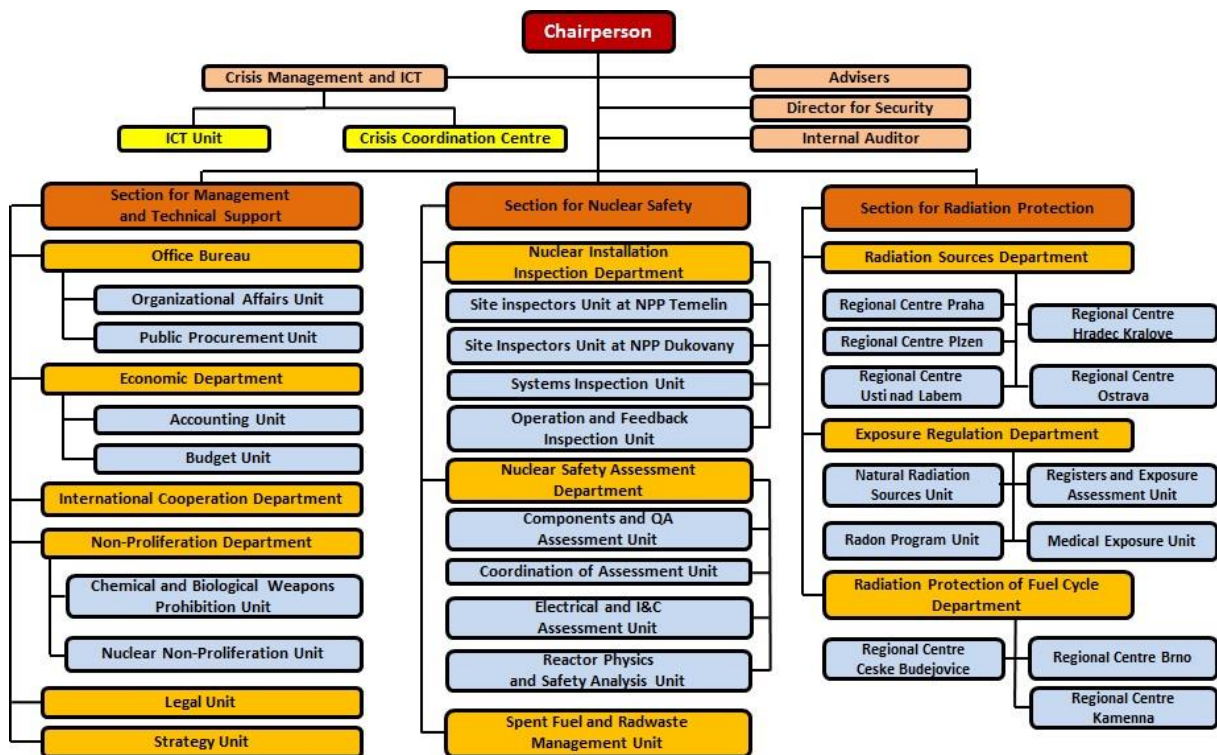
## **2. State Responsible Authority**

The IAEA recommends that all the safeguards responsibilities arising from the Safeguards Agreement and from the Additional Protocol should be assigned to the same organization so called the SRA. The Government of the Czech Republic has therefore decided that only one institution will be responsible for all the important matters related to the “nuclear area”, and essential for smooth operation of nuclear facilities such as nuclear security and safety, radiation protection, non-proliferation and emergency preparedness. The SRA executes control over these fields primarily to meet its national needs and objectives. However, there is also the area related to the nuclear non-proliferation, where the SRA should fulfil the international obligations on behalf of the state. Following the government’s decision, the State Office for Nuclear Safety (SONS) was given the role of the SRA in the Czech Republic in 1993 as a direct successor of the Czechoslovak Atomic Energy Commission, which was responsible for safeguards implementation in the former Czechoslovakia from 1972. After the accession of the Czech Republic to the European Union in 2004, the SONS became responsible for implementation of provisions of Chapter VII of the Treaty establishing the European Atomic Energy Community (Euratom Treaty) [5] and for control and coordination of fulfilment of the relevant regulations issued by the European Commission (EC) as of October 2009.

### **2.1. State Office for Nuclear Safety**

The SONS is mainly responsible for a state supervision on nuclear safety at nuclear facilities, physical protection of nuclear facilities, radiation protection, and emergency preparedness of nuclear facilities and workplaces handling ionizing radiation sources. By the decision of the government, the coordination and information role towards the SONS is fulfilled by the Prime Minister of the Czech Republic. Roles and responsibilities of the SONS are, as a governmental body, on the level of ministry with dedicated chapter within the state budget to ensure its independence. The SONS is divided into three main sections: Section for Management and Technical Support, Sections for Nuclear Safety and Section for Radiation Protection. The whole structure of each section within the SONS is shown in the Picture 1. The work of the SONS in the field of non-proliferation is targeted on the area of state control over the so-called nuclear items representing nuclear material, trigger list items and nuclear related dual-use items through the licensing approach. Fulfilling the international obligations of the Czech Republic in accordance with the NPT, the trilateral Safeguards Agreement between the IAEA, EC and Czech Republic, and the trilateral Additional Protocol to this agreement is one the most important areas of the SONS in the field of nuclear non-proliferation. Special section called Nuclear Non-Proliferation Unit (Unit) has been established within the SONS structure to supervise this matter related to the safeguards implementation. This Unit is solely responsible for implementation of the State Level Approach in the Czech Republic. The integrated safeguards system of the IAEA, as being implemented in the Czech Republic since 2007, established the highest standards of safeguards for the IAEA and integrated an optimal set of measures to enhance the IAEA’s capability to verify correctness through the Nuclear Material Accountancy and Control (NMAC). These measures are complemented by containment and surveillance measures to verify completeness through the broader information access and provisions of the Additional Protocol in the Czech Republic. Export control, as

another important aspect of the non-proliferation, is also fulfilled by the Unit. A licence is issued upon a review and in cooperation with other special state agencies by the SONS for import or export of nuclear items as defined above. As a special competency, quite unusual for nuclear authority, the SONS received responsibility to regulate governmental administration in the whole CBRN area from the year 2002. The SONS is a regulatory body responsible for governmental administration and supervision in the field of chemical weapons prohibition resulting from the Chemical Weapons Convention and, as well, the national authority responsible for the fulfilment of the Biological Weapons Convention. Both conventions are implemented into the Czech legal system by several measures. The main principles of the conventions are covered by two individual Acts and corresponding decrees.



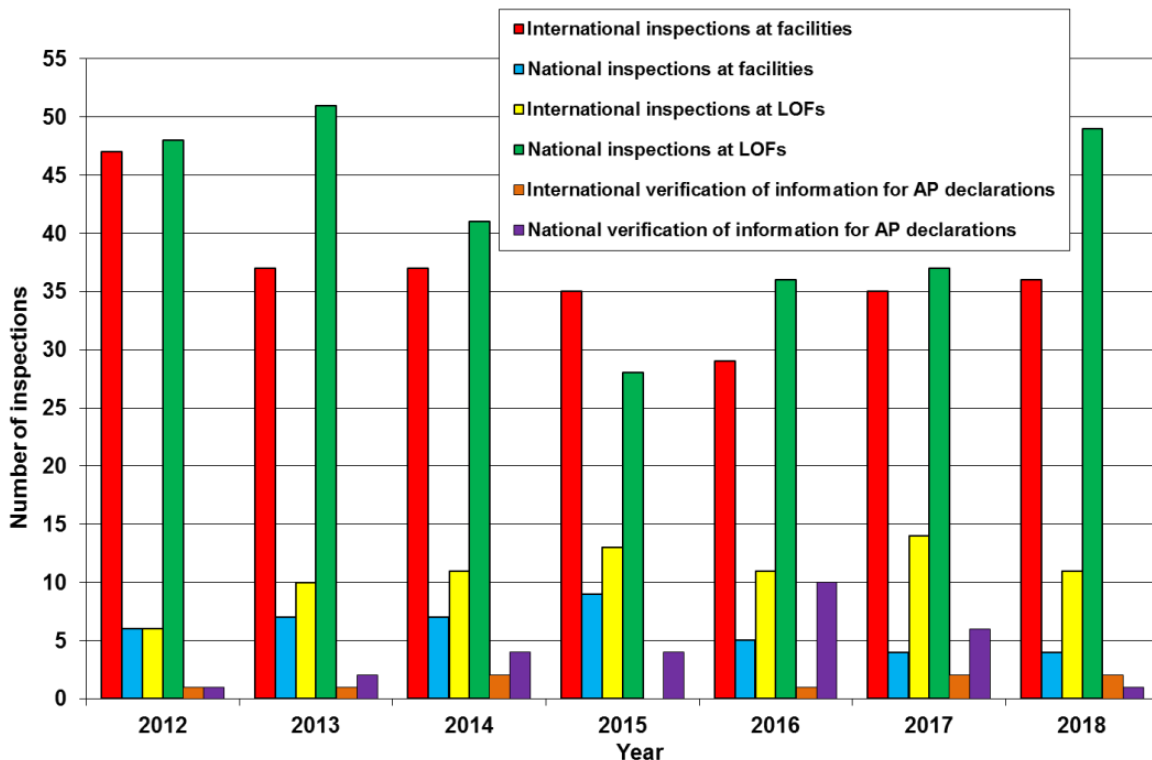
Picture 1: Organizational structure of SONS

## 2.2. Legal framework

The authority and responsibilities of the SONS, including the responsibility for safeguards implementation within the state, had been set out in 1997 by the Act. No. 18/1997 Coll. on Peaceful Utilisation of Nuclear Energy and Ionising Radiation (the Atomic Act). Main requirements of the NPT, Safeguards Agreement and Additional protocol were solely implemented to the national legislation through this act. The Atomic Act requires licensees to maintain the SSAC at the licensee level and to report to the SONS all the relevant information as required by the international commitments. The Atomic Act also established appropriate security level of physical protection for nuclear material in possession and limited access to nuclear material for authorized personnel only, including such special condition for rejecting access to the nuclear material if the criminal investigation related to nuclear material is discovered. Broader requirements of the above-mentioned non-proliferation obligations of the country were implemented through decrees related to the NMAC and export control. National legislation covering the whole nuclear field as represented by the Atomic Act was entirely updated in 2017 to address all the new challenges in the nuclear area, new security threats to this field and to implement new strict requirements for safeguards implementation arising from the EC commitments. Newly issued Act No. 263/2016 Coll., the Atomic Act, was subsequently completed by the corresponding new decrees covering requirements for the NMAC and export control. The SONS performed number of outreach sessions for all the main stakeholders to support implementation of the new legislation. Furthermore, two years of transitional period were given to the licensees to fully implement conditions of the new act and decrees.

### 3. Management of Czech SSAC

The SSAC structure within the Czech Republic follows the recommended approach of the IAEA and is divided into the Material Balance Areas (MBAs), including determination of Key Measurements Points (KMPs) within the MBA [6]. Main aim of the SSAC is to ensure that all the nuclear material located in the state remain in use only for the peaceful purposes. The overall system is supervised by the SONS and supported with corresponding local NMAC systems created within each facility or location outside facilities (LOF). This structure assures that the SSAC system within the Czech Republic is independent from any facility operator or the LOFs. In accordance with current domestic and EU legislation, all the facility operators report directly to EC and send copies of each accounting report or any other major safeguards related communication to the SONS. Contrary, the LOF operators send all the accounting reports or other submissions related to the NMAC only to the SONS. A system of unique IDs for each nuclear material batch has been created by the SONS. These unique batch IDs are not used just on the MBA level, but they must be used within the whole SSAC. This approach avoids any misleading batch duplication and enables easier and faster batch follow-up in the case of any potential issue. Currently, the SSAC consist of 17 MBAs possessing the amount of nuclear material equal to almost 2967 Significant Quantities. SSAC of the Czech Republic is constituted from nuclear power plants and spent fuel storages, research and training reactors, closed down uranium mines, radioactive waste repositories, manufacturer of shielding containers and irradiators and the LOFs. All these installations are divided into the structure of MBAs, including two special LOFs MBAs for small holders of nuclear material. MBA WCZA is covering approximately 130 LOFs, in which the users are handling depleted uranium in a form of shielding containers and MBA WCZZ contains almost 40 LOFs managing a variety of nuclear materials including small amount of highly enriched uranium and plutonium used mainly for research purposes. Safeguards implementation at the facility MBA is mostly verified by the SONS inspectors during the international inspections performed by the IAEA and EC. Separated national safeguards inspections at the facilities are performed by the SONS inspectors only for the reactor core loading verification at the nuclear power plants, inspections at the former uranium mines or in the case of identified non-compliance. On the other hand, the national safeguards inspections are regularly performed to verify NMAC system at the LOFs side, and frequency of these inspections is set by nuclear material balance at the given LOF. The overall statistics of the national and international inspections performed in the Czech Republic within last 7 years is shown in the Graph 1.



Graph 1: Inspection activities in Czech Republic

The minimum inspection period for single LOF is at least once in three years. The inspection frequency also strongly depends on the LOF overall performance and fulfilment of the legislation conditions. If the LOF is recognized due to its low performance or follow up on the previous finding is required, then the inspection frequency is not driven by the time but rather by the need. The SONS safeguards inspectors also focus on the verification of the information gathered for preparation of the annual update of the declarations prepared under the obligations of the Additional Protocol. National inspections related to the verification of exports and imports of the nuclear items are triggered in cooperation with other special state agencies.

### **3.1. Software evolution**

Sophisticated software plays an important role for successful creation of the SSAC. Our NMAC software was intended to be used as a national nuclear material accounting system and database. This software has been developed since the 90's to serve as a reporting tool just for IAEA safeguards. It was designed to meet the necessary functionality and capabilities to support accounting and reporting requirements. The accounting component of the system was created to meet generally accepted accounting practices and the forms and formats defined in the IAEA Code 10, labelled format, of the Subsidiary Arrangements (General Part). The software was also developed to be compatible with the software used for management of NMAC at the nuclear power plants. Later on, due to the accession to the European Union, the software was rebuilt to be compatible with the EC software called ENMAS. The SONS has recently developed new, modern and innovative software to reflect legislation changes and software evolution. New features, based on users' experience over the many years of usage, were implemented into the updated software. This software is built on modern platform enabling its direct use during in-field verification activities just using mobile device. Two different software versions were created. One version is capable to report under the requirements of the EC safeguards and the other is built for traditional IAEA safeguards. Both versions could be offered to other IAEA member states for their use in their national NMAC databases.

### **3.2. Managing the Location Outside Facilities Material Balance Area**

Correct and complete reporting for the LOFs MBA is challenging aspect of routine work within the Unit. Two LOFs MBAs covering almost 170 locations are currently created within the SSAC structure of the Czech Republic. Due to the fact that there is not any IAEA or EC system or guidance for creation of the LOF codes, SONS had developed its own naming convention for the LOFs. Each LOF is assigned with unique ID consisting of 4 characters. First character represents a code for KMP inventory, and it is also used to define type of institution and purpose of nuclear material use. Second character represents first number in post code related to the address system in the Czech Republic. Third character states an area of work and fourth character is used for alphabetical order to distinguish the LOFs with the same area of work and location. This assembled code is assigned to LOF during licensing process. Despite the fact that MBA WCZA, representing almost 130 LOFs, is exempted from the IAEA safeguards, the Unit must still oversee the both MBAs in full scale and this large number represents enormous effort for the whole Unit to keep system running without any major issues. Strict inspection system together with precise reports and records review plays key factor of the successful work. An Inventory Change Document is filled out on the LOF side, sent in pdf or hardcopy format to the SONS within 5 days, where it is reviewed and recorded into the NMAC software. An Inventory Change Report, prepared on monthly basis for each MBA, is submitted to the EC within 15 days of the following month. In accordance with existing legislation, each operator of the MBA is responsible for preparation and submission of the accounting reports. The SONS, as an operator of the LOFs MBAs, is solely responsible for reporting on behalf of the both MBAs. Reports on inventory changes for transfers between locations within the LOFs MBA are not required for the state to be reported to the IAEA or EC, however and in accordance with our robust legislation system, such transfers must be reported on domestic level from the LOF to the SONS and recorded into the SSAC for the corresponding LOFs MBA. Significant number of the LOFs within MBA WCZZ use depleted uranium for colouring of glass, which leads to the termination of nuclear material from the safeguards. This inventory change brings another challenge for correct and complete reporting for the LOFs MBA. Each termination request is validated and subsequently verified in the field during the national inspection activities. To support accurate reporting, each location must have designated chief accountancy officer and his/her deputy. These so called NMAC officers are trained by the SONS and those NMAC officers responsible for accountancy at the MBA or larger LOF are usually trained through the NMAC training courses provided by the IAEA or EC. Their knowledge and NMAC skills are always verified during

national inspections by the SONS safeguards inspectors. The SONS requires annual update of their contacts and information about statutory body. The LOFs are required to have a NMAC procedure document concerning safeguards and physical protection of nuclear material. This QA/QC document is reviewed during license application review. Implementation of this document is also verified during inspection activities. Major safeguards areas like nuclear material accountancy, operating records or physical verification of nuclear material are not the only inspection goals. Fundamental aspects of physical protection of nuclear material are also verified during safeguards inspections by the SONS inspectors. Any major non-compliance is usually addressed through improvement either skills of the NMAC officers or quality of the NMAC procedure implemented within the licensee's NMAC system.

## **4. Staff**

Nuclear Non-Proliferation Unit currently consists of 10 employees. These employees are solely responsible for implementation of safeguards. Therefore, their knowledge and understanding of the daily work is critical aspect of correct and complete reporting to the IAEA and EC. Over the past years, this Unit has never faced any abnormal staff losses due to career change or retirement. Common training practice for the newly hired staff at that time was, due to the small numbers of new employees, just the basic approach when the qualified senior employees shared their knowledge of NMAC system to avoid a risk of incorrect and uncomplete reporting with the new employee in the Unit. However, in 2017 and mainly in 2018 almost 80 % of experienced staff left the Unit and were suddenly replaced by the new unexperienced junior employees. As the training of the SRA staff responsible for safeguards implementation is fundamental element for capacity building, this massive staff change brought in to attention of the senior management of the SONS an immediate need of development of robust and long-term training plan for newly recruited employees. Long-term training for new SONS inspectors was formed to include acceptable knowledge of the IAEA and EC safeguards systems, suitable inspection skills and precise verification techniques together with internal system for data evaluation representing necessary measures for verification of safeguards implementation on the MBA level.

### **4.1. Training**

Development of the long-term training plan at the SONS was inspired with already prepared safeguards qualification plan for new safeguards inspectors at the SRA of a different state. The training plan, used at the other SRA, was created in cooperation among the formal IAEA inspectors, international safeguards experts and the IAEA training section, and represents preferred golden standards for employees working at the safeguards section. Graduate of this training will be able to implement gained knowledge of cooperation between the SRA and the IAEA in the field of nuclear safeguards and international control regimes. Principles of safeguards (e.g. SSAC management and verification activities according to a structure of MBAs or containment & surveillance systems) should be trained to ease implementation on the SRA level. Participant will also be able to use gained knowledge to the implementation of the safeguards principles in the nuclear fuel cycle of the state (nuclear power plant, LOFs) and principles of new safeguards approaches with main focus on strengthening of safeguards and Additional Protocol requirements. Inspection skills focused on the verification of nuclear material located at the nuclear facilities and small holders of nuclear materials (LOFs) are important part of the training including use of new verification technologies (measurements and instrumentation), analytical techniques (non-destructive assay), examples of sealing, surveillance and monitoring techniques used by the IAEA or EC. Training prepared at the SONS includes 6 main training modules. Each module covers several topics introduced to the new staff during numerous training sessions. All the modules are further described within Table 1. Duration of the whole training was intended to be minimally one year. The training is finished with an official oral exam in front of experts' panel.

Module	Name	Topics
Module 1	State Office for Nuclear Safety	<ul style="list-style-type: none"> <li>• Framework of SRA</li> <li>• Roles and competencies</li> <li>• Legislation</li> </ul>
Module 2	Nuclear Energy	<ul style="list-style-type: none"> <li>• Ionising radiation</li> <li>• Nuclear material</li> <li>• Nuclear fuel cycle</li> <li>• NPPs</li> <li>• Nuclear weapons</li> </ul>
Module 3	Non-Proliferation	<ul style="list-style-type: none"> <li>• History</li> <li>• Legislation</li> <li>• Non-proliferation regime</li> <li>• Export control regimes</li> </ul>
Module 4	IAEA and European Commission safeguards	<ul style="list-style-type: none"> <li>• History</li> <li>• IAEA framework</li> <li>• European Commission framework</li> <li>• Safeguards implementation</li> </ul>
Module 5	SSAC	<ul style="list-style-type: none"> <li>• MBA and KMP structure</li> <li>• NMAC</li> <li>• Reporting</li> <li>• Additional Protocol</li> <li>• Exercises</li> </ul>
Module 6	Verification activities	<ul style="list-style-type: none"> <li>• National inspections</li> <li>• International inspections</li> <li>• Verification techniques</li> <li>• Non-Destructive Assay</li> <li>• Containment &amp; Surveillance measures</li> <li>• Radiation protection</li> </ul>

**Table 1:** Training plan

## 4.2. Retention

One of the main perpetual issues for long-term maintaining the SSAC in the Czech Republic is employee retention closely connected with continuity of knowledge at the SONS or LOFs side. Employee fluctuation is a key issue not just on the SRA level, but also occurs on the licensee side. Nuclear facilities always preserve more experienced employees and potential loss of one NMAC officer due to retirement or career change is usually substituted without any major issue. On the other hand, a loss of NMAC officer at the LOF side could be challenging and might transform well performing LOF into a company with reporting issues and unsafeguarded nuclear material. The SONS provides ad hoc trainings in such cases or performs outreach during inspection activities. As mentioned in the previous chapter, the SONS has developed comprehensive internal training plan to avoid any unexpected problems with staff replacement.

## 5. Conclusion

Maintaining the SSAC represents a key aspect for non-proliferation effort of the Czech Republic. Implementation of the NPT obligations together with requirements of the Safeguards Agreement and Additional Protocol are the main parts of the regular work for the SONS. Fully trained and qualified staff is crucial for management and reporting for the SSAC. The SONS recently had to take an action to preserve the continuity of knowledge within the safeguards Unit due to massive employees push back. A comprehensive training plan for the Unit's newcomers has been created to effectively address staff fluctuation. Transition and successful implementation of the new legislation has been done within

the last two years. The legal changes were accompanied by the complete modernization of the existing NMAC software, which became operational in 2018. Staff changes and their safeguards training will be completed within the second half of 2019. Further improvements and optimization of the SSAC has been performed to guarantee an effective, reliable and credible safeguards system. Verification activities of the IAEA and EC inspectors conclude every year that correct and complete safeguards implementation of the NPT provisions and Chapter VII of the Euratom Treaty within the framework of the SSAC has been done in the Czech Republic. Integrated safeguards approach of the IAEA implemented in the Czech Republic seeks to benefit from the synergy resulting from the combination of “correctness and completeness” measures to achieve overall effectiveness and cost efficiency. Safeguards conclusions of the IAEA always underline that all nuclear material remained in peaceful activities in the Czech Republic. With respect to the overall conclusions made by the both “nuclear watchdogs”, we strongly believe that our SSAC organisation is maintained with the highest standards and prepared for future challenges.

## 6. REFERENCES

- [1] International Atomic Energy Agency; *Treaty on the Non-Proliferation of Nuclear Weapons*; INFCIRC/140; IAEA; 1970.
- [2] International Atomic Energy Agency; *Nuclear Material Accounting Handbook*; IAEA Service Series 15; 2008; p 5.
- [3] International Atomic Energy Agency; *The Structure and Content of Agreements between the IAEA and States required in Connection with the Treaty on the Non-Proliferation of Nuclear Weapons*; INFCIRC/153 (Corrected); IAEA; 1972.
- [4] International Atomic Energy Agency; *Safeguards Implementation Practices Guide on Provision of Information to the IAEA*; IAEA Services Series 33; 2016; p 3.
- [5] European Union; *Consolidated version of the Treaty establishing the European Atomic Energy Community (Euratom)*; 2012/C 327/01; Official Journal of the European Union; 2012.
- [6] International Atomic Energy Agency; *Guidelines for States' Systems of Accounting for and Control of Nuclear Materials*; IAEA; 1980; p 10.

## **Web-Portals complementing the NMAC centralised accountancy: the French experience**

**LANAVE François**

IRSN Institut de Radioprotection et Sûreté Nucléaire  
31, Av de la division Leclerc Fontenay-aux-Roses, FRANCE  
francois.lanave@irsn.fr

### **Abstract:**

In the second half of the twentieth century, France developed a nuclear program of great magnitude. This program currently covers the full nuclear fuel cycle as well as many research and testing facilities. In 1965, a national centralised accounting system was already set up, making it the oldest one in the world. In the 1980 's, with the implementation of a national regulation on security, this centralised accountancy became part of an integrated NMAC system. It integrated, later on, the various safeguards commitments. Old computer technology has been gradually replaced with a centralised CFT network and a dedicated Java application. This system has been processing for 35 years, under various and upgraded versions, all of the national daily data for security purposes and also, at a later stage, most of the monthly data for safeguards purposes. However, new safeguards requirements appeared in the mid 2000's (Import/Export notifications, Additional Protocol declaration) which were, on the one hand decorrelated from data collected for security purposes and on the other hand, involved new industry players. This prompted the need for new IT networks, complementing the existing one. Two Web-Portals were designed: PIMENT/CENTIME is dedicated for the input of Import/Export notifications and PASTEL for the input of specific data under the Additional Protocol, both at the facility level, with many benefits. By means of a customized interface, PIMENT/CENTIME addresses in a personalized and more accurate manner the specificities of three of the national major players. A new Web-Portal, PATIO, has recently been designed for the input, at the facility level, of the identity of the accounting and operational staff. These data feed into the existing central system. Compliance and encryption of data for a secure transmission and efficient processing are of course crucial issues.

**Keywords:** NMAC centralised accountancy, Web-portal, IT network, encryption.

### **1. Introduction**

IRSN – the French Institute for radiological protection and nuclear safety - is the French Technical Support Organization in nuclear and radiation risks. It provides technical support to all the government authorities involved in the safety and security of nuclear facilities, nuclear material, transportation and protection of the population. Among these many activities, IRSN carries out the centralised accountancy of nuclear materials as part of NMAC for national security purposes. It also collects, analyses and processes data as part of the French obligations towards international non-proliferation agreements.

The purpose of this paper is to illustrate:

- How the activities of the centralised accountancy for NMAC purposes naturally link and complement with those of data collecting and processing for specific Safeguards purposes;
- How the available tool of the Centralised Accountancy system needed to be complemented and scaled with Web-Portals in order to achieve the objective of compliance with the growing needs of international safeguards agreements.

Constraints and benefits of these additional Web-Portals will be addressed in a feedback approach as well as the technical requirements in a context of a general technological development.

## **2. Historical background and context**

In the second half of the twentieth century, France developed a nuclear program of great magnitude. This program currently covers the full nuclear fuel cycle, a major part of the electrical production with 58 power reactors, many research and testing facilities as well as the treatment and storage of wastes. For a long time however, a public state institution known as the CEA had been the sole owner of the nuclear materials present on French soil. As far back as 1945, an accountancy system was already set up within this public state institution, first on a manual mode and then in 1965 on a computerized process at a national scale, making it the oldest centralized accountancy in the world. The transition to the industrial stage has led to the multiplication of private stakeholders in the civil nuclear fuel cycle. This has resulted in the need to create in the early eighties a national legislative and regulatory framework for nuclear materials with a national security perspective. This framework, more recently updated in 2011, includes physical monitoring and accountancy measures designed to track with accuracy the quantities of nuclear material present at facilities and its location. It also establishes a centralized accountancy of all nuclear material used for civil purposes in France which is nowadays managed by IRSN.

### **2.1. General principles of the national accounting system for NMAC**

For the maintaining of a license, any operator shall demonstrate the following:

- Accurate knowledge of any variation such as shipment, receipt, conversion, processing, blending operation, irradiation, etc ... with full description of the type, characteristics and quantity of each nuclear material;
- Accurate knowledge for each nuclear material of the particular obligation code as well as, for safeguarded zones, of the key measurement point, measurement code and material container code;
- Daily recording of the identified variation in the accounting ledger;
- Communication of the recorded variations on a daily basis to the centralized accountancy;
- Production, systematically at the end of each month of a complete accounting closure;
- Verification on a monthly basis of the local accounting balance in comparison with the existing balance of the centralized accountancy in order to identify any discrepancy;
- In case a discrepancy is identified by the operator, communication within twelve working days in a report called Reconciliation Report to the centralized accountancy and obligation to resolve the issue in a timely manner.

The efficiency of the accounting system is thus mainly based on:

- A daily information flow between facilities and the centralized accountancy;
- An ongoing verification of the transmitted data and of their consistency.

## 2.2. The centralised accountancy technology

All the French authorized facilities daily transmit their variation reports to the centralized accountancy through a VPN (Virtual Private Network) connection. CFT is the secure computer file transfer program and protocol used for transmission in both ways (input and output). This software is used extensively in finance and banking sectors in Europe. National data (daily variation reports) come in as txt files. They are processed by an internally developed accounting software (LCCMN) under C Sharp application. It is run on a heavyweight server. The data base is SQL server 2016. This current architecture is the last one resulting of a continuous improvement in technological equipment, from the early age in 1945, when processing was manual.

## 2.3. Leveraging the NMAC data for safeguards purposes

France had so far lived up to its various international obligations by fully collecting, exploiting or transcoding the data from the NMAC system (excepted the import/export notifications). The various commitments to Safeguards agreements are as follows:

- Commission Regulation n° 3227/1976 [1], Commission Regulation n° 302/2005 [2];
- IAEA agreements : INFCIRC/290 [3], INFCIRC/207 add.1 [4], INFIRC/415 [5], INFIRC549 [6]
- Bilateral agreements concluded by France (Australia, Japan, Switzerland,...);
- European Commission agreements with specific provisions and administrative arrangements.

The scope of these agreements covers the provision of various data and reporting about import/export, enriched uranium, plutonium, thorium, ore production, etc. Data are basically extracted from the NMAC database and transcoded and/or reprocessed by peripheral application softwares. Only Import/export notifications had for a long period been provided on hard copies by operators before processing by an application software.

## 3. New Safeguards requirements

On the 22nd of September 1998, in order to participate in the strengthening of IAEA safeguards, France signed an additional protocol (INFCIRC/290/add.1 [7]) to its safeguards agreement (INFCIRC/290). The protocol entered into force at the same time as those of the other Member States of the European Union, on the 30th of April 2004. Pursuant to this protocol, France commits to supply additional information to the IAEA on activities carried out in cooperation with non-nuclear-weapon States (NNWS). It appeared that the data required as part of the additional protocol where on the one hand decorrelated from data collected for security purposes and on the other hand, involved numerous new industry players.

### 3.1. Introduction of Web-Portals

These new entities had in addition no connection to our centralized accountancy network and were often medium-sized. These new context and needs led to the introduction in 2012 of a double Web-portal, PIMENT/CENTIME dedicated to the input of data relating to import/export notifications. Shortly afterwards in 2015, PASTEL another Web-portal has been launched. Benefiting from technological advances, in both cases, the following aims were pursued:

- Accessibility and ease of use at facility level;
- Customization in order to address in a personalized and more accurate manner the specificities of the major players;

- Possibility for the entities to reuse previously registered information;
- Reduction of the rewriting work done by IRSN in order to focus on the content assessment;
- Direct and explicit attention to content and format suggestions from Euratom and the Agency.

A new Web-Portal, PATIO, has recently been designed for the input, at facility level, of the identity of the accounting and operational staff. In the case of PATIO, the data feed into the existing centralized accountancy system.

### **3.2. Technical challenges**

Special attention is paid to these crucial key issues:

- Security
- Formats

#### **3.2.1. Security**

The implementation of these new IT networks, complementing the long-running VPN one, is subjected to security requirements. Restricted access and encrypted connection with two-factor authentication ensures that only authenticated users are authorized to remote access for the input of data. An unidirectional gateway insures the transfer via a secure network to an internal server. Disjoint data bases provide additional security.

The output of reprocessed data to be transmitted to Euratom and the Agency in the future in a fully digital way requires compatibility of international security systems : combined use of encryption, pgg keys, secured access to SDP portal.

#### **3.2.2. Formats**

Compliance and compatibility of data formats between IRSN, Euratom and the Agency are still a major issue. Formats which were not defined with directive instructions are likely to evolve and will require adjustments toward homogeneity.

## **4. Feedback**

The centralized accountancy system intended for NMAC, complemented with peripheral web-portals, has greatly succeeded so far insuring both the national accounting for security purposes since 1945 and later on the international safeguards requirements. However, the technical evolution has been established stepwise, following the entries into force of successive new international requirements and commitments. The time lag between two international commitments has required new successive developments not allowing an overall concept. Instead of a unified central system, several input networks feeding disjoint databases and various peripheral software have to be managed and maintained. A break in regulatory regimes, international as well as national, should allow a consolidation and homogenization in an increasingly overwhelmed system.

## **5. References**

- [1] Commission Regulation (Euratom) n°3227/1976, Luxemburg (1976)
- [2] Commission Regulation (Euratom) n°302/2005, Luxemburg (2005)
- [3] International Atomic Energy Agency, Information Circular, INFCIRC/290, Vienna (1981)
- [4] International Atomic Energy Agency, Information Circular, INFCIRC/207/Add1, Vienna (1984)
- [5] International Atomic Energy Agency, Information Circular, INFCIRC/415, Vienna (1992)
- [6] International Atomic Energy Agency, Information Circular, INFCIRC/549, Vienna (1998)
- [7] International Atomic Energy Agency, Information Circular, INFCIRC/290/Add1, Vienna (2004)

# Nuclear Material Measurements at ABACC: Status Update and Future Steps

Aníbal Bonino, Fábio Dias, Horacio Lee, Luis Machado da Silva, Marcos Moreira, Max Facchinetti, Sonia Fernandez Moreno

Brazilian-Argentine Agency for Accounting and Control of Nuclear Materials (ABACC), Av. Rio Branco 123, Gr 515, 20040-005, Rio de Janeiro, Brazil.

[www.abacc.org.br](http://www.abacc.org.br)

## **Abstract:**

The Brazilian-Argentine Agency for Accounting and Control of Nuclear Material (ABACC) is a bilateral organization created in 1991 by Argentina and Brazil to verify the peaceful use of nuclear materials and installations in both countries. Among several responsibilities, ABACC has to perform quantitative verification of the declared nuclear material inventories and transactions by independent measurements that must meet internationally recognized quality levels.

In this paper we present and discuss some of the most relevant measurement results obtained by ABACC inspectors during on-site activities, as well as data resulting from destructive analysis of samples performed by the network of Argentinean and Brazilian analytical laboratories that support ABACC. Data obtained during recent past years are compiled and evaluated according applicable international standards.

Finally, we discuss the future actions that will be essential for ABACC to maintain the capacity to accomplish its mission, in accordance with the agreement established by Argentina and Brazil.

**Keywords:** nuclear safeguards, non-destructive and destructive analysis, measurements systems.

## **1. Introduction**

Argentina and Brazil decided to establish a common system of accounting and control of all nuclear materials (SCCC) and create ABACC in 1991, as an independent organization responsible for verifying the appropriate implementation of the SCCC in both countries [1]. The countries took another decision, in the scope of the international safeguards regime implemented by the IAEA, with the decision to move from separate and limited bilateral safeguards agreements to a multilateral comprehensive safeguards agreement fully consistent with the international non-proliferation regime [2].

In order to avoid unnecessary duplication of efforts, most of the verification activities are jointly performed by ABACC and IAEA inspectors, but the agencies draw independent conclusions. In most inspections, measurements of uranium are jointly performed by the inspectors using non-destructive systems. The agencies establish joint use procedures and ensure that appropriate measurement capabilities are always available. On the other hand, since destructive analysis techniques are not yet submitted to this scheme, samples are collected in duplicate during inspections for independent analysis at laboratories that provide analytical support to ABACC or the IAEA.

Data obtained during recent past years are compiled and evaluated according applicable international standards [3] and statistical historical values.

## **2. Non-destructive measurements**



The relative standard deviation of the data plotted in Fig. 1 is 2.4%, which is significantly lower than the ITV for low resolution (5.8%). This indicates that medium resolution systems have been able to perform much better than low resolution and then a specific ITV should be available.

Results obtained from verification of LEU UF<sub>6</sub> cylinders are plotted in Figure 2.

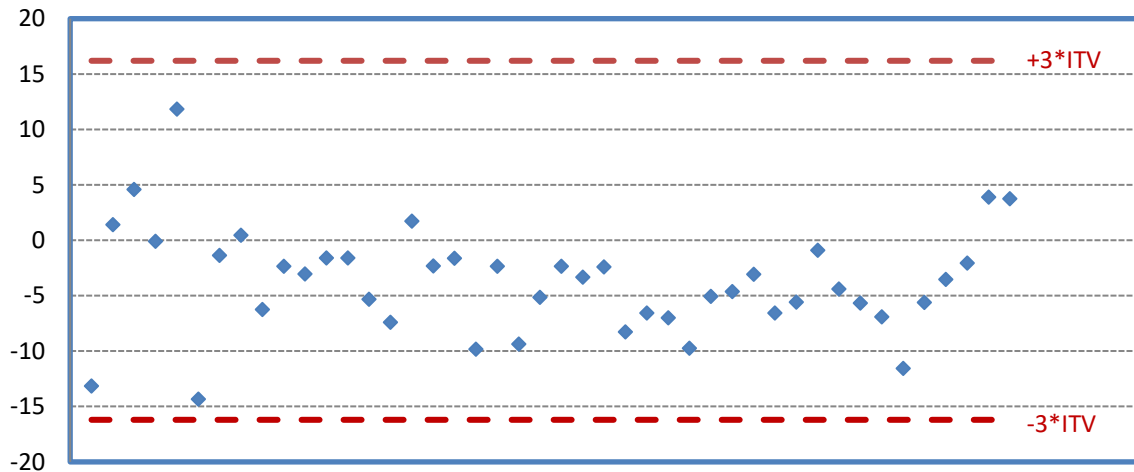


**Figure 2: Declared to Measured % deviation in enrichment measurements of LEU UF<sub>6</sub> cylinders with high resolution gamma spectrometry.**

The relative standard deviation of the data plotted in Fig. 2 is 4.9%, which is consistent with the corresponding ITV (5.4%). Although all data points are well within the indicated limits, the plot indicates a negative bias of about 3.7%. Since most data points refer to measurements of 30B cylinders, such a bias may be due to inaccurate correction of the attenuation caused the thick and dense wall of the cylinder (0.5 in. carbon steel). Improvements on it could be implemented for example by minimizing wall attenuation variations between calibration and item measurements, i.e. material type and thickness.

Low enriched fresh fuel assemblies produced at two commercial fuel fabrication plants are verified by active and passive neutron measurements using the uranium neutron coincidence collar (UNCL). A simple hand-held gamma monitor is used to determine the active length of the fuel assembly, which is used as one of the input values for the analysis software. Figure 3 shows results jointly obtained by ABACC and the IAEA during the last five years.

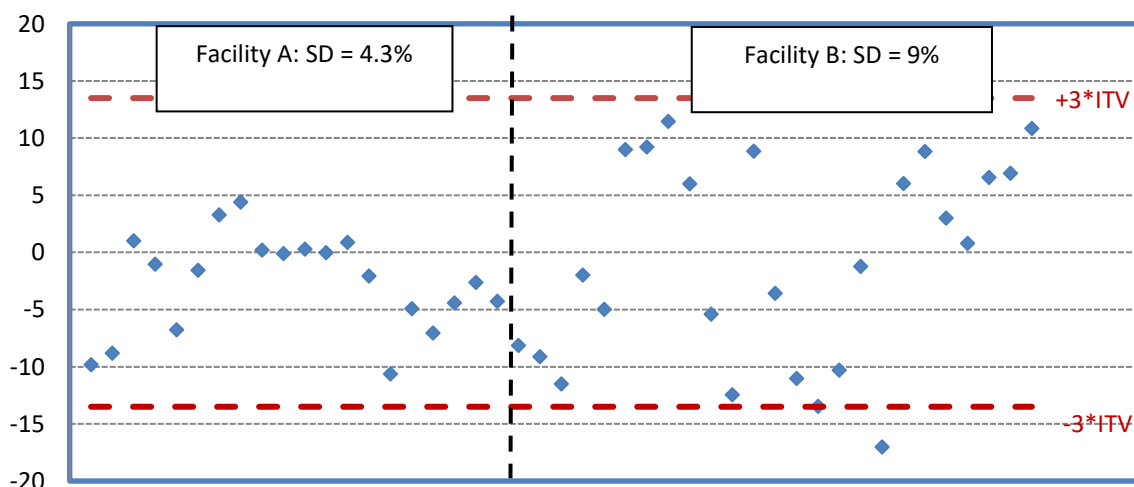


**Figure 3: Declared to Measured % deviation in <sup>235</sup>U mass content resulting from verification of fresh fuel with the UNCL system.**

At facility A (left side of Figure 3), the measured fuel assemblies are all of the same design, same enrichment and without burnable poison. The observed RSD is 4.3%, which is in good agreement with the corresponding ITV (4.5%). At facility B (right side), fuel assemblies of different designs are measured: geometry, enrichment and burnable poison content. This explains why the observed RSD (9%) is significantly higher. Although in both cases the results are well within  $\pm 3 \cdot \text{ITV}$  (only one is out), the enlarged data variation for this facility indicates that the measurement technique is very sensitive to the fuel design. It should be noted that the currently available ITV does not consider the influence of burnable poison.

### 3. Destructive measurements

Destructive assay techniques can provide improved measurement accuracy and precision in comparison with NDA. They may be used for the evaluation of other NDA or DA measurement techniques used by facility operators or detection of small discrepancies on declared values. Differently from NDA, uranium samples are always taken by ABACC and IAEA inspectors in duplicate, allowing for independent elemental and/or isotopic analysis. Due to the higher strategic value, samples are more frequently taken from LEU materials than DU and NU. The number of samples is limited to the minimum necessary due to the high associated cost and large time associated with the process: sample collection at the facility, international transportation arrangements, sample treatment and analysis, and final issue of the analysis report. The process may take approximately 3 months to be completed. In case of  $\text{UF}_6$  samples, this time can be longer due to more severe transportation requirements.

The uranium materials submitted to sampling are typically the same as for NDA. Pure nitrate solutions found in NU conversion plants is one of the exceptions, but with reduced sampling frequency. The analysis techniques used by the laboratories are Davies & Gray titration for element fraction and thermal ionization mass spectrometry (TIMS) for isotopic analysis. Traceable uranium reference materials are used for quality control and calibration of the analytical instruments.

Results obtained during the last five years are shown in the next Figures. Figure 4 shows the relative deviations between declared and measured uranium concentration values for powders. The dashed lines indicate three times the combined ITV resulting from propagation of sampling and D&G measurements performed by both operator and ABACC. The plot indicates good consistence between actual performance (RSD = 0.39%) and the propagated ITV (0.35%).

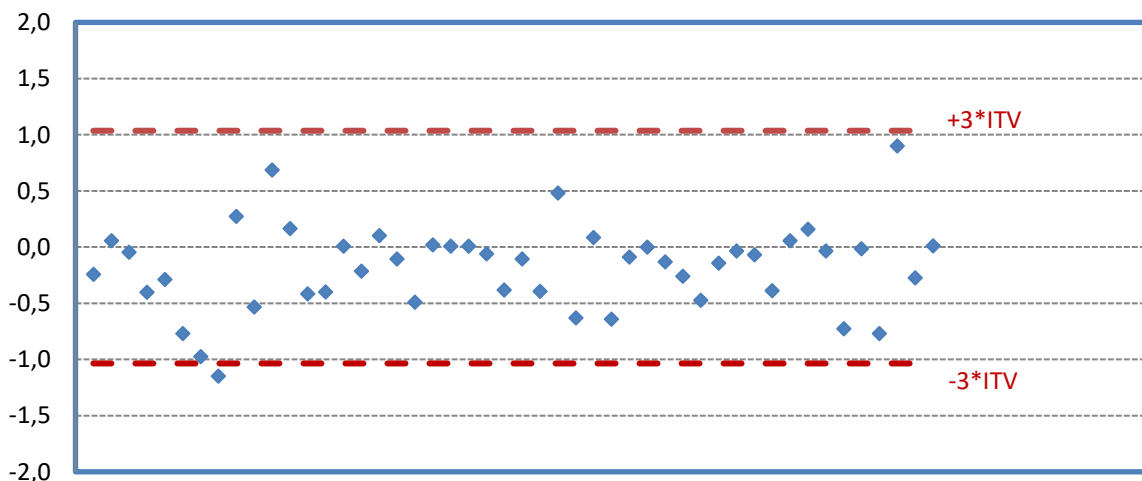


**Figure 4: Declared to Measured % deviation in uranium concentration measurements of powders by D&G Titration.**

In regards to  $\text{UO}_2$  sintered pellets, as shown in Figure 5, actual RSD is 0.11%. This is because pellets are more stable and less susceptible to the presence of undesirable components (i.e. humidity) than powders.

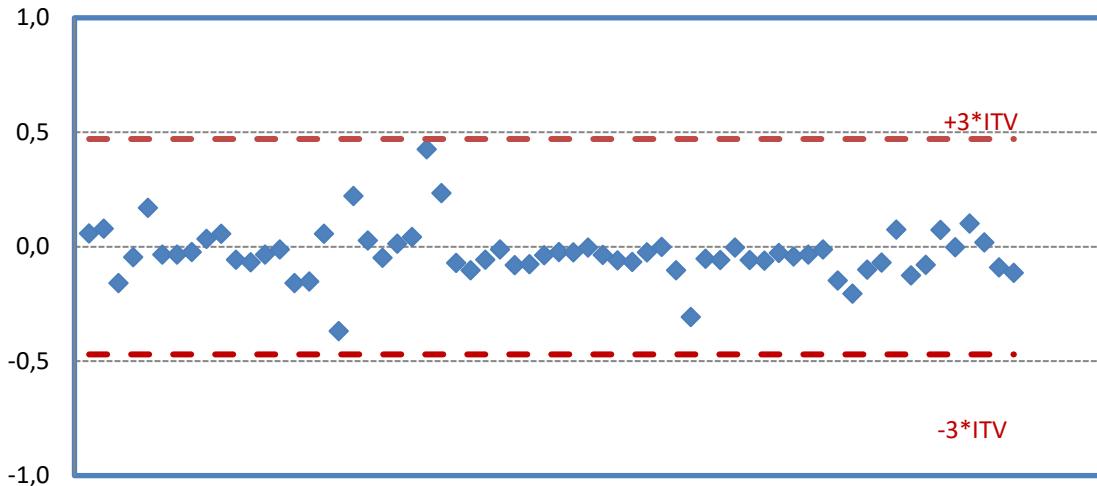


**Figure 5: Declared to Measured % deviation in uranium concentration measurements of UO<sub>2</sub> pellets by D&G Titration.**

Determination of <sup>235</sup>U/<sup>238</sup>U ratio is performed by the laboratories using TIMS for all samples. For NU and LEU materials with enrichment below 1%, as shown in Figure 6 and 7, the actual performance data is quite consistent with the propagated ITV (0.41%) considering two independent measurements.

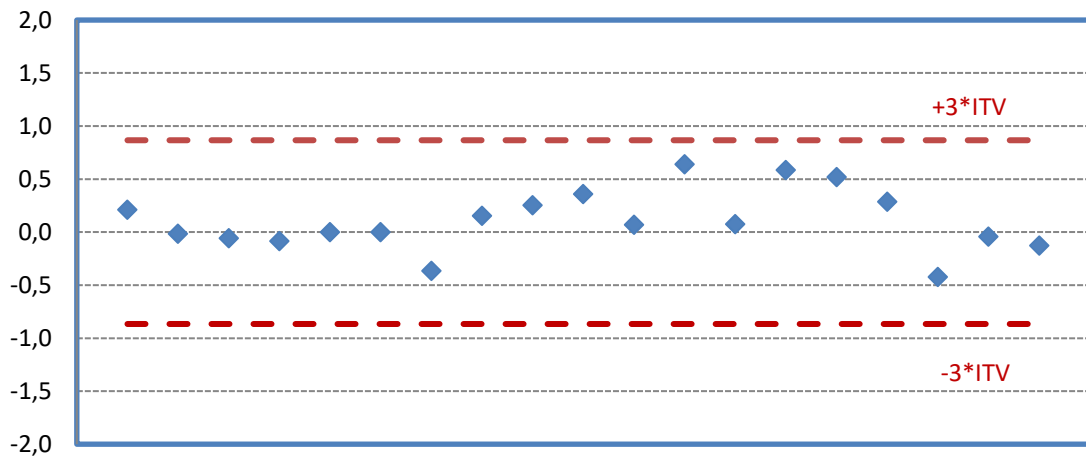


**Figure 6: Declared to Measured % deviation in <sup>235</sup>U/<sup>238</sup>U ratio of natural UO<sub>2</sub> pellets by TIMS**

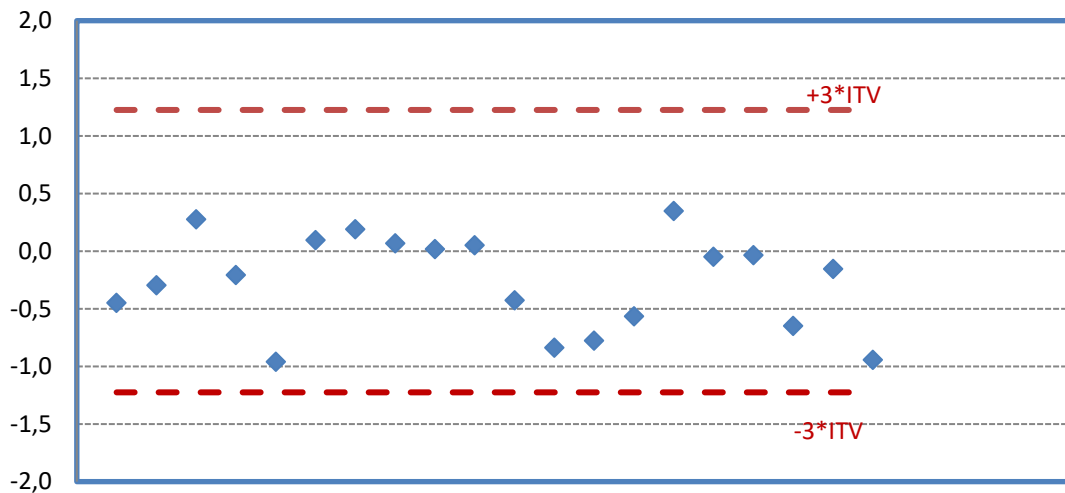


**Figure 7: Declared to Measured % deviation in <sup>235</sup>U/<sup>238</sup>U ratio of LEU (< 1%) materials by TIMS**

However, for LEU samples enriched above 1%, as presented in the Figure 8, the actual performance (RSD = 0.46%) is affected by important sampling uncertainties associated with sampling of gaseous UF<sub>6</sub> from feed and withdraw lines at enrichment plants.

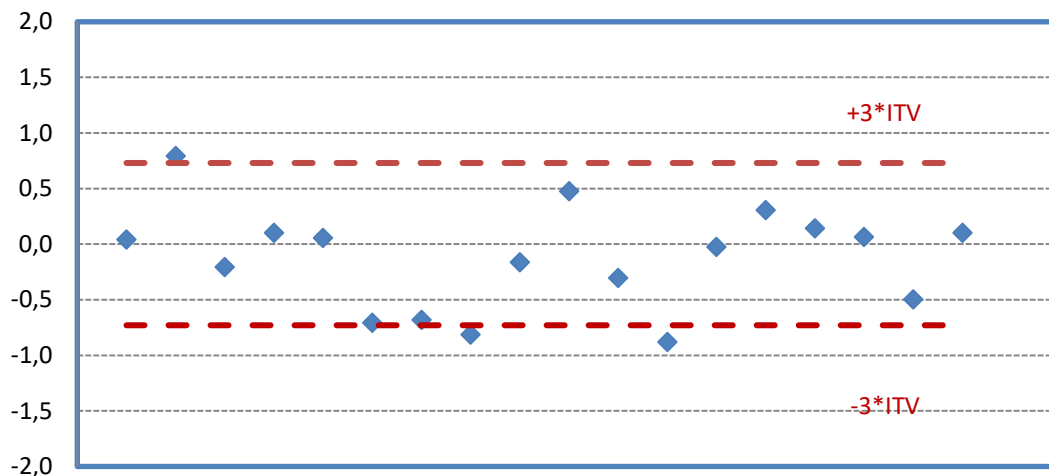


Figure 8: Declared to Measured % deviation in <sup>235</sup>U/<sup>238</sup>U ratio of LEU (> 1%) materials by TIMS

#### 4. Measurement Evaluation Programs

The routine assessment of the quality of the analytical measurements is very important for the laboratories, in particular when a formal QA/QC program is in place. In this context, ABACC supports the participation of the laboratories of its analytical network in safeguards Measurement Evaluation Programs (MEP) promoted by internationally recognized organizations such as the New Brunswick Program Office (NBL) in the USA and the Institute for Reference Materials and Measurements (IRMM) in Europe.

ABACC coordinated the participation of its network laboratories in the Nuclear Material Round Robin (NMRoRo) promoted by the IAEA as a MEP in 2017, which offered the following sample for analysis: one gram-sized low enriched UO<sub>2</sub> pellets for determination of atom ratios ( $n_{235}/n_{238}$ ,  $n_{234}/n_{238}$  and  $n_{236}/n_{238}$ ) and/or uranium mass fraction. The following laboratories from Argentina and Brazil participated in this MEP:

- Development of Uranium Compounds Laboratory (LADCU/CNEA – Argentina)
- Physical and Chemical Control Laboratory (CNEA – Argentina)
- Mass Spectrometry Laboratory (LEM/CNEA – Argentina)
- Uranium Characterization Laboratory (LCU/CTMSP – Brazil)
- Safeguards Laboratory (LASAL/CNEN – Brazil)

ITV values were also used as reference in establishing acceptance levels.

Uranium mass fraction: four laboratories (two from each country) provided results obtained by Davies & Gray titration. All reported results were within expected performance levels.

Uranium atom ratios: two laboratories (one from each country) provided results obtained by total evaporation thermal ionization mass spectrometry (TE-TIMS). All  $n_{235}/n_{238}$  reported results were consistent with the expected performance levels.

Although minor isotope ratios  $n_{234}/n_{238}$  and  $n_{236}/n_{238}$  have no available ITV, reported results were consistent with the corresponding reference values at 95% (two-sigma) confidence level.

#### 5. Conclusions

The performance for the most relevant NDA and DA measurements routinely performed by ABACC has been summarized. In the area of NDA, the full migration from low to medium resolution gamma spectrometry systems based on LaBr<sub>3</sub>(Ce) scintillation detectors represented a remarkable step for improved enrichment measurements of powders in particular. The need for a specific ITV for this technique seems to be evident and the experience of ABACC may be useful

in this regard. Enrichment measurements of UF<sub>6</sub> cylinders by high resolution gamma spectrometry is still a valuable tool, but special attention to the calibration procedure is required since the size and wall thickness of the measured cylinders may vary significantly.

Total <sup>235</sup>U mass measurements in modern PWR fresh fuel assemblies using the UNCL system may be subject to enlarged uncertainties, in particular for fuel designs that include different enrichment layers in the same fuel rod and/or gadolinium as burnable poison. These additional uncertainties are probably of systematic nature, caused by limitations on the calibration procedure. As an attempt to mitigate those limitations, advanced neutron counting systems and calibration techniques are under development at the international level. In this regard, ABACC, Brazil and the IAEA are working together to test a new NDA system based on fast neutron coincidence counting. Since there is currently a single ITV available for fresh fuel measurements, a future revision should consider the possibility to differentiate uniform and single enrichment from complex fuel designs.

In regards to DA analysis of the samples collected during inspections by D&G titration for uranium concentration determination, the operator versus ABACC data comparison has indicated good agreement with international practices. As for enrichment measurements, uncertainties associated with sampling of powders and gaseous UF<sub>6</sub> may be relevant for the evaluation process.

The performance achieved in the 2017-NMRORO program indicates that laboratories currently supporting ABACC are performing reliable uranium mass fraction and isotopic determinations. ABACC continues to support the participation of the laboratories in different MEPs that are currently being promoted by the IAEA and NBL during the biennium 2018/2019.

## 6. References

- [1] *Agreement between the Republic of Argentina and the Federative Republic of Brazil for the Exclusively Peaceful Use of Nuclear Energy*, The Bilateral Agreement (1991).
- [2] *Agreement between the Republic of Argentina, the Federative Republic of Brazil, The Brazilian-Argentine Agency for Accounting and Control of Nuclear Materials and the International Atomic Energy Agency for the Application of Safeguards*, IAEA INFCIRC/435 (1994).
- [3] K. Zhao, et al., *International Target Values 2010 for Measurement Uncertainties in Safeguarding Nuclear Materials*, IAEA STR-368 (2010).
- [4] P. Matussek, *Accurate Determination of the <sup>235</sup>U Isotope Abundance by Gamma Spectrometry*, KfK 3752 (1985).

# Back-end to the Future: Safeguards Considerations for Multinational Geological Repositories

Cindy Vestergaard

Stimson Center  
1211 Connecticut Ave NW, 8<sup>th</sup> Floor  
Washington, D.C., 20036  
E-mail: [cvestergaard@stimson.org](mailto:cvestergaard@stimson.org)

## **Abstract:**

*The responsibility of countries to manage and dispose of their own spent fuel and radioactive waste does not preclude a collaborative approach. The economies of scale of multinational geological repositories (MGRs) would benefit not only countries without suitable geological conditions or those with small waste volumes but also the nuclear non-proliferation regime given material would be consolidated at fewer sites. Safeguards agreements for MGRs would have to be negotiated among participants in line with international, multilateral and bilateral safeguards obligations while addressing complexities specific to shared geological facilities such as transport and transfer of ownership. The long timelines of underground disposal also require the forecasting of several “what ifs” regarding the future global political landscape and its nuclear risks. Raising more questions than answers, this working paper is the first in a series considering safeguards for MGRs. It will particularly focus on potential scenarios where safeguards agreements may no longer apply, but also how they may be shifted, and the potential for the current (and future) nuclear non-proliferation regime to respond.*

**Keywords:** safeguards; waste disposal; geological repository; nuclear cooperation agreements

## **1. Introduction**

Geological repositories have long been considered the safest option for long-term isolation and permanent disposal of nuclear waste. Although it is recognized that states are responsible for their own waste management and disposal, the principle does not preclude multilateral collaboration, particularly, for countries without suitable geological conditions or those with waste volumes too small for national repositories to be practical. Over the past forty years, a variety of models for multinational geological repositories (MGRs) have emerged, each underscoring how consolidating nuclear waste at fewer sites globally would benefit not only economies of scale and size, but also non-proliferation and international security. At the same time, there has been little study on the safeguards obligations that would accompany MGRs, particularly the network of bilateral nuclear cooperation agreements (NCAs) that have evolved alongside international treaty requirements to shape global nuclear trade. These treaty-level mechanisms are additional to IAEA safeguards and provide further assurances of peaceful uses and could have wide-ranging implications for a multinational repository.

This working paper is a part of the Stimson Center’s ‘Back-end to the Future’ project and the first in a series considering multilateral and bilateral safeguards considerations relevant to MGRs. The long timelines of underground disposal require the forecasting of several “what ifs” regarding the future global political landscape and its nuclear risks. It will particularly focus on potential scenarios where safeguards agreements may no longer apply, but also how they may be shifted, and the potential for the current (and future) nuclear non-proliferation regime to respond.

## 2. Multinational Geological Repositories

Over the past forty years, various scenarios for shared repositories have been put forward by a number of studies and initiatives, whether international, multinational or national [1], [2]. In each, repositories could be located on national territory or in an extraterritorial area, but they diverge in management and ownership structures. Multinational geological repositories (MGRs) could be characterised by participating (partner) countries that jointly develop a repository framework with or without a host country [2]. Whether a host would be identified at an early or later stage, all financial and administrative responsibilities could be placed in a multinational group with participation restricted to a select group of states or on a commercial basis from other countries [3]. Alternatively, an ‘add-on scenario’ could be envisioned where a host country developing its own national repository accepts foreign radioactive waste at a later stage. In this case, the host country would drive the process and would require a national framework to receive nuclear waste from abroad [2].

Whether nationally or multilaterally driven, MGRs would allow for the sharing of expertise and technology and may provide greater degree of supply assurances. At the same time, they would reduce proliferation and security risks by consolidating nuclear material at fewer sites and harmonising approaches to waste management. MGRs would also offer benefits in economies of scale (both capital and operating costs) and would provide more transparency than their national counterparts, but they also face greater administrative challenges, thus taking longer to establish [3].

It could be assumed any host country for a MGR would need to have exemplary nuclear non-proliferation, nuclear security, nuclear safety and environmental protection credentials. This would provide a degree of assurance to the participating countries and to the broader international community and may also help to address some of the societal concerns with respect to the MGR concept. MGRs could also be specifically designed, sited and constructed to create high levels of security that would benefit the host country, partner countries, and international security. One of the challenges however will be the harmonisation of bilateral safeguards requirements and how they relate to material subject to bilateral nuclear cooperation agreements (NCAs)

## 3. Nuclear Cooperation Agreements

Nuclear Cooperation Agreements (NCAs) are bilaterally negotiated agreements that are additional to IAEA safeguards to provide further assurances of peaceful uses. Given IAEA safeguards are generally not concerned with origin attribution, several suppliers employ NCAs to account for, and add controls to, the use of all the nuclear material they export, including on any material generated through its use. Although not all suppliers have legal or policy requirements for NCAs (such as EURATOM), countries such as Australia, Canada, Japan and the United States require them to be in place before nuclear trade is permitted.

NCAs include information-sharing measures to track material, essentially attaching reporting obligations or ‘flags’ to material as it moves globally through the nuclear supply chain. These obligations begin from the export of yellow cake to material reprocessed or stored as nuclear waste as well as to plutonium, which is in the spent fuel or recovered from it. This has led to a system of multiple flagging, where obligations from multiple suppliers can apply to the same item. Natural uranium originating in one country, for example, may acquire additional obligations as it is subsequently processed in other countries. With progress slow in the development of final disposal facilities, it is perhaps not surprising that spent nuclear fuel is treated like any other item subject to NCAs. As noted by Jim Casterton: “There are no special or additional requirements that must be met – whether the spent fuel is located in a spent fuel bay at the reactor site, in a dry storage facility above ground or in a deep geological repository” [4].

Features common to all NCAs generally include:

- a peaceful, non-explosive use commitment;
- IAEA safeguards on items subject to the agreement;
- fallback safeguards in the event that a situation arises where the IAEA is unable to administer its safeguards functions;
- controls on retransfers of items subject to the agreement;

- controls on reprocessing and enrichment; and
- assurances of adequate physical protection.

The establishment of MGRs would not likely require a revision of these provisions, but it could be expected that they would need to be more expressly clarified and strengthened, particularly when considering the following scenarios:

### 3.1. Scenario 1: The IAEA is unable to implement safeguards

In this scenario, the IAEA may be unable to implement safeguards in the event: 1) a State withdraws from the NPT; 2) the NPT falls into disrepute or; 3) the IAEA ceases to exist. The commitment to the peaceful uses of nuclear energy would remain in effect for countries with NCAs in force, but the removal of international oversight may undermine confidence that the commitment is upheld. NCAs address this potential scenario by including the provision for the continuity of safeguards, or 'fallback safeguards.'

Currently, the provision for fallback safeguards generally requires parties to promptly conclude an agreement equivalent to Agency safeguards in the event the IAEA is not able to carry through its mandate. Australia's NCAs require "other safeguards arrangements" that will replace those applied by the Agency to "provide safeguards equivalent in scope and effect to those provided by a NPT safeguards agreement" [5], [6]. Japan and the United States stipulate fallback arrangements "which conform to the Agency's safeguards principles and procedures [7] [8]. Similarly, Canada's agreements with Kazakhstan [9], Mexico [10] and the UAE [11] apply equivalency if the IAEA is not administering safeguards "for any reason or at any time." These agreements state that the parties shall conclude an agreement equivalent in scope and effect to IAEA safeguards being replaced or a safeguards system conforming to the principles and procedures set out in the IAEA document INFCIRC/66 (and its subsequent amendments) [9].

India, a country that also requires NCAs before nuclear trade but is not party to the NPT, is less concerned with equivalency. Its agreements with Australia, Canada, Japan and the United States all state that if the IAEA decides the application of its safeguards are no longer possible, the parties "should" (or "shall" in the case of the agreements with Japan and Australia) "consult and agree on appropriate verification measures" [12] [13] [14].

While a separate study would be needed on the framework and risks associated with MGRs in states that possess nuclear weapons, the current system of NCAs demonstrates how provisions for fallback safeguards should be negotiated and clarified once a decision has been taken to create an MGR.

Negotiations could involve the host state, the multinational body administering the MGR and stakeholder countries. One could imagine provisions that would allow for inspections by a State attaching obligations to nuclear material in the repository, by the multinational body, and/or by other countries participating in the MGR [15]. If fallback safeguards were left unclarified until after a situation led to the IAEA being unable to implement safeguards, the host state (and/or MGR administrative body) would have to undertake parallel and lengthy negotiations with partners and potentially with several other States that have obligated material in the host country. This complex scenario would create room for disagreement and lack of consensus that could result in safeguards coverage at the lowest common denominator (and therefore not likely considered equivalent to IAEA safeguards). It could also result in a mixed safeguards regime for the repository where negotiations with one country results in explicit measures and higher assurances for peaceful uses on its nuclear material than those that apply to another country's nuclear material.

Accordingly, the legal framework for an MGR would be strengthened by including a commitment by the host country and the partner countries to undertake measures at the facility designed to verify the peaceful use commitment and to provide credible assurance of non- diversion and absence of any undeclared activities. These measures could be supported financially and logistically by the host country and all partner countries. The host country, particularly if it is a NWS, may undertake to bear a disproportionate share of the costs involved. Such measures would be in addition to those undertaken by the IAEA as part of the requirements between the host country and the Agency. They could involve cost sharing with the Agency to purchase, use and maintain safeguards equipment required by the IAEA pursuant to its safeguards approach for the MGR and also relevant to the MGR's independent verification programme. However, they could also include measures additional to those required by a

safeguards agreement designed to give enhanced assurance on the location of the nuclear material in the repository and on the continued non-proliferation, security, safety and environment aspects after the repository has been completely back-filled and closed. These measures could include ongoing geophysical, radiological and environmental monitoring.

### **3.2. Scenario 2: What if the host state withdraws from the NPT?**

Like the first scenario, a host State withdrawing from the NPT would lead to the IAEA being unable to implement safeguards. It would remove the host State's international commitment to the peaceful, non-explosive use of nuclear energy, leaving only the peaceful use commitment vested in various bilateral NCAs. NPT withdrawal would negatively impact relations between the host country, the multinational body administering the MGR and/or participating countries. Even if the previous safeguards regime remained in place on items subject to an NCA in the host country, it may no longer be considered effective given the lack of peaceful non-explosive use commitment vested in the NPT. Furthermore, political and public pressures would likely preclude any further cooperative endeavours with the host country, including the continued participation in the MGR.

If either of these scenarios play out as suggested above the overall non-proliferation framework provided by a NCA would be weakened. It could result in a less desirable commitment to nuclear non-proliferation by the host country and less safeguards coverage on the items transferred to the repository.

It should also be noted that NCAs stipulate that inventories of obligated nuclear material be maintained and agreed in the countries in which the nuclear material resides. However, items can be removed from the inventory if both parties agree with the IAEA determination that safeguards should be terminated or if the parties otherwise agree. Existing IAEA safeguards policy considers that safeguards will continue to be applied when the repository is backfilled and closed; i.e., safeguards will not be terminated. This means that the only way to remove the material from the inventory would be if both Parties could agree to the terms and conditions for such removal. Although maintaining inventories of obligated nuclear material in a closed repository may be seen as having little value, the agreement to remove the material from the inventory would certainly have to take account of public concerns in each country party to the agreement. The question is how could those concerns be addressed in whole or in part?

In establishing the institutional, legal and financial framework necessary to support the MGR, provisions in the legal documentation could include a commitment to peaceful, non-explosive use for the facility and the nuclear material consigned to the facility. The commitment would pertain most particularly to the host country (whether a possessor of nuclear weapons or not) and to all MGR partners. The commitment would cover the lifetime of the repository, including after it had been backfilled and closed.

The existence of commitments with respect to the peaceful, non-explosive use of nuclear material at the repository and to measures at the facility designed to verify the peaceful use commitment and to provide credible assurance of non-diversion and absence of any undeclared activities in the legal framework establishing the MGR would be significant in addressing the requirements of NCAs pertaining to: (1) the peaceful, non-explosive use of items consigned to the repository; and (2) the agreement for a fallback safeguards regime should the IAEA be unable to implement safeguards at the facility. This MGR legal framework may also be useful for justifying the removal of material from NCA obligations when the repository is closed.

It should be noted that some NCAs have a provision that could require the return of obligated items to the originating country if certain scenarios develop, including the inability to agree on appropriate fallback safeguards. While this option, subject to other international legal obligations, could be applicable to spent fuel that has not yet been emplaced in the repository, it would seem impossible to implement if emplacement has taken place, let alone if the repository had been backfilled and closed.

## **4. For Further Consideration**

The long timelines of MGRs present a higher risk for disposal facilities outliving international treaties and institutions than for other nuclear facilities. Assuming MGRs are built during the non-proliferation regime in place today and in a host state with a strong record on non-proliferation, the continuity and

equivalency of IAEA safeguards would remain a priority – even more so when considering that IAEA policy has long considered spent fuel as ‘inherently retrievable’, even after emplacement in a geological repository [16].

The development of MGRs are therefore complex in their need for foresight of potential political and proliferation risks that may arise. This draft outlines two potential scenarios which raise further questions and scenarios such as: what types of safeguards requirements should be applied to transit/transshipment states? What are the different considerations for safeguards if an MGR is located in a nuclear weapons state (NWS) or a non-nuclear-weapon state (NNWS)?

## 5. Acknowledgements

This research is made possible by the generous financial and logistical support of the John D. and Catherine T. MacArthur Foundation to the Stimson Center’s Back-end to the Future project. The author is also grateful to James Casterton, Nonresident Fellow, Stimson Center, for his insights, laughs and partnership in thinking through the scenarios presented. I look forward to many more conversations as the project moves forward.

## 6 Legal matters

### 6.1. Privacy regulations and protection of personal data

"I agree that ESARDA may print my name/contact data/photograph/article in the ESARDA Bulletin/Symposium proceedings or any other ESARDA publications and when necessary for any other purposes connected with ESARDA activities."

### 6.2. Copyright

The authors agree that submission of an article automatically authorises ESARDA to publish the work/article in whole or in part in all ESARDA publications – the bulletin, meeting proceedings, and on the website.

The author declares that the draft is original and not a violation or infringement of any existing copyright.

### 6.3. Disclaimer

This draft is a working paper that will be further developed through a series of roundtables and discussions, including at ESARDA, at the Stimson Center and at the INMM annual meeting.

## 7. References

[1] International Atomic Energy Agency, *Framework and Challenges for Initiating Multinational Cooperation for the Development of a Radioactive Waste Repository*, IAEA Nuclear Energy Series, No. NW-T-1.5, Vienna, 2016.

[2], International Atomic Energy Agency, *Developing multinational radioactive waste repositories: Infrastructural framework and scenarios of cooperation*, IAEA-TECDOC-1413, October 2004.

[3] International Atomic Energy Agency, *Waste Management and Disposal: Report of INFCE Working Group 7*, International Fuel Cycle Evaluation (INFCE), Vienna, 1980, p. 112.

[4] James Casterton, *Multinational Geological Repositories and Nuclear Cooperation Agreements: Some Considerations*, Working Paper DRAFT, April 2019, p. 6.

- [5] Article VI of the *Agreement between the Government of Australia and the Government of the Czech Republic on Cooperation in Peaceful Uses of Nuclear Energy and the Transfer of Nuclear Material*, Prague 27 July 2001 (Entry into force 17 May 2002).
- [6] Article V of the *Agreement between the Government of Australia and the Government of Canada Concerning the Peaceful Uses of Nuclear Energy*, Ottawa, 9 March 1981 (Entry into force 9 March 1981).
- [7] Article XI of the *Agreement for Cooperation Concerning Civil Uses of Atomic Energy Between the Government of the United States of America and the Government of Canada*, 21 July 1955/1 January 2030 (with rolling 5 years extensions).
- [8] Article 8 (3), *Agreement Between the Government of Japan and the European Atomic Energy Community for co-operation in the peaceful uses of nuclear energy*, L 32/65, 6/2/2007.
- [9] Article 7 (3), *Agreement Between the Government of Canada and the Government of the Republic of Kazakhstan for Co-operation in the Peaceful Uses of Nuclear Energy*, E105212 (Entry into force 14 August 2014).
- [10] Article VI (3) (b) of the *Agreement Between the Government of Canada and the Government of the United Mexican States for Co-operation in the Peaceful Uses of Nuclear Energy*, E101761 – CTS 1995 No. 9, (Entry into force 24 February 1995).
- [11] Article 9 (3), *Agreement Between the Government of Canada and the Government of the United Arab Emirates for Cooperation in the Peaceful Uses of Nuclear Energy*, E105360, (Entry into Force 10 June 2013).
- [12] Article 8 (6), *Agreement between the Government of Canada and the Government of the Republic of India for Co-operation in the Peaceful Uses of Nuclear Energy*, E105192, (Entry into Force 20 September 2013).
- [13] Article 4 (3), *Agreement Between the Government of Japan and the Government of the Republic of India for Cooperation in the Peaceful Uses of Nuclear Energy*, (Entry into Force 20 July 2017).
- [14] Article VII (5), *Agreement between the Government of Australia and the Government of India on Cooperation in the Peaceful Uses of Nuclear Energy*, (Entry into Force 13 November 2015).
- [15] It was common for NCAs to include bilateral inspections before the NPT was established. For example, Canada's Atomic Energy Control Board (AECB) carried out inspections in the late 1960s in France, Federal Republic of Germany, India, Japan, Pakistan, Switzerland, United States and United Kingdom to verify that materials of Canadian origin supplied abroad were used for peaceful purposes only. See: Cindy Vestergaard, *Governing Uranium in Canada*, DIIS Report 2015:12, p. 41.
- [16] Permanent SNF disposal therefore means the permanence of IAEA safeguards for as long as the safeguards agreement with a State is in force.

# The CWC and its verification regime, a tool against the non-proliferation and reemergence of chemical weapons: a parallel with the nuclear treaty

**Noémie Balistreri**

Institute of radioprotection and nuclear safety (IRSN)  
31 avenue de la Division Leclerc, Fontenay-aux-Rose  
E-mail: nnoemie.balistreri@irsn.fr

## **Abstract:**

*The Convention against Chemical Weapons (CWC), established in 1993, is the most universal treaty in the world, gathering 193 member states. Like the treaty on the non-proliferation of nuclear weapons (NPT), the CWC is a non-proliferation treaty; however there are no state specificities in its implementation. As well as the NPT, the CWC presents a strong verification system based on annual national declarations from chemical industries concerned by the Convention and plant site inspections. The activities linked to the CWC are really similar as those of the NPT. Thus, at the entry into force of the Convention, because IRSN had already a such know-how, it was designated as a stakeholder, acting on behalf of the French Ministry of Industry, to ensure the correct application of CWC on the French territory as it is done for the nuclear treaty.*

*In terms of verification activities, the French Ministry of Industry has delegated to IRSN the census of the concerned chemical industries, the gathering of the annual declarations and the escort of the inspections of plant sites. Thus, France developed important skills concerning the application of the CWC on its territory thanks to a robust method involving the outreach and the follow-up of chemical industrial operators by a group of technical experts from the IRSN. Moreover, as the NPT permits to compare imports and exports of nuclear material, the tracking of chemical materials is also done by comparing imports and exports between member countries in order to prevent reemergence of chemical warfare agents. In this context, a data cross is performed by the IRSN.*

*The article will present how the synergy between nuclear and chemical activities has facilitated the implementation of the CWC. It will also discuss of the present synergies and the possible way of improvement.*

**Keywords:** Destruction and non-proliferation treaty, verification, similarities, know-how

## **1. Introduction**

The Organization of prohibition of the chemical weapons (OPCW) defines a chemical weapon as being “a chemical used to cause intentional death or harm through its toxic properties. Munitions, devices and other equipment specifically designed to weaponise toxic chemicals also fall under the definition of chemical weapons” [1]. The Convention against chemical weapons (CWC) is the world's first multilateral disarmament agreement to provide for the elimination of an entire category of weapons of mass destruction within a fixed time frame [2]. The implementation of the convention stems from a long process leading to a verification regime in the same way as the nuclear non-proliferation treaty. National declarations and international inspections of production facilities are the bedrock of the latter and France defined a robust method based on the transposition of OPCW decisions in its national regulation in order to fulfill its obligations. The creation of a common office for nuclear and chemical treaties is a force for their good application. Synergy between these two units could be reinforced in favor of each field.

## 2. History

Contrary to the treaty on the non-proliferation of nuclear weapons (NPT) whose beginnings coming from the Second World War with the use of the nuclear bomb in Hiroshima and Nagasaki, the Chemical Weapons Convention comes from farther back in time. Indeed, toxic chemicals had been employed during wars for thousands of years (like poisoned arrows, arsenic smoke and noxious fumes...) but it is during the First World War that the world witnessed the use of toxic chemicals in first large scale attacks with chemical weapons and condemned this unnecessary cruelty. The biggest one took place at Ieper, in Belgium, on the 22<sup>th</sup> of April 1915 with the release of 124,200 tons of chlorine, mustard gas and other chemical agents leading to more than 90,000 soldiers deaths in suffered painful and close to a million more men left battlefields blind, disfigured or with debilitating injuries [1]. Because of this, international efforts to ban chemical weapons took a prominent position in many early disarmament agreements.

The first important step corresponds to the Protocol for the Prohibition of the Use of Asphyxiating, Poisonous or Other Gases, and of Bacteriological Methods of Warfare, commonly known as the 1925 Geneva Protocol. However, in the 1920s and 1930s, a lot of developed countries still worked on chemical weapons and the discovery of powerful nerve gases in the late 1930s renewed interest in the field [3]. Surprisingly, all the major powers involved in the Second World War had anticipated the use of large-scale chemical on European battlefields that fortunately did not happen. During the Cold War, even if chemical weapons were overshadowed by concerns about nuclear war, the United States and the Soviet Union maintained enormous stockpiles of tens of thousands of tons of chemical weapons [3]. One of limitations that slowed down the establishment of the Convention was the refusal of the Soviet Union of any control over their territory until 1986 [4]. The CWC stems from a long process (*cf.* Table 1 below)[1]. During the Iran-Irak conflict between 1982 and 1986, chemical war was publicized and public opinion morally opposed to the use of chemical weapons. Finally, in 1991, the announcement of a bilateral United States–Soviet Union agreement to destroy most of their chemical weapon stockpiles and to refrain from further chemical weapon production intensified the Convention negotiations [1][3][4].

Thus, after many years of painstaking negotiations in the Conference on Disarmament and Preparatory Commission, a CWC project was adopted in Geneva on the 3<sup>rd</sup> of September 1992. After that, the United Nations Secretary-General opened the CWC for signature on the 13<sup>th</sup> of January 1993 in Paris and the Convention entered into force on the 29<sup>th</sup> of April 1997 [1][3][4]. The resulting international chemical weapons disarmament regime was headed by the Organization for the Prohibition of Chemical Weapons, located at The Hague in Netherland. The first challenge of the OPCW was therefore to ensure the elimination of chemical weapons stockpiles and their manufacturing facilities. This aim is now almost completed and so the second step is enforcing a verification regime that prevents the re-emergence of such weapons. So, in 2013, in recognition of its extensive efforts to eliminate chemical weapons, the OPCW was awarded the Nobel Peace Prize [5]. Currently, 193 State Parties signed and ratified the CWC, making it the most universal convention.

Major Developments in the Use and Prohibition of Chemical Weapons		
1675	The Strasbourg Agreement	The first international agreement limiting the use of chemical weapons, in this case, poison bullets.
1874	The Brussels Convention on the Law and Customs of War	Prohibited the employment of poison or poisoned weapons, and the use of arms, projectiles or material to cause unnecessary suffering.
1899/1907	Hague Peace Conferences	Bans on use of poisoned weapons, 'asphyxiating or deleterious gases'.
1915-1918	Europe, World War I	1.3 million casualties, 90,000 fatalities from chemical weapons; first large-scale use of CW at Ieper, Belgium.
1920s	Morocco	Use of chemical weapons in Morocco.
1925	Geneva Protocol	Ban on CW use, but no prohibition on development, etc.
1930s	China and Abyssinia	Use of chemical weapons in China and Abyssinia.
1972	Biological Weapons Convention	Comprehensive BW prohibition - 170 parties, 10 signatories by 2014, but no verification mechanism; commitment to negotiate on CW.
1980s	Iran-Iraq War	Including use by Iraq of CW against civilian populations.
1993	Chemical Weapons Convention	Signing of the CWC in Paris, 13 January.
1997	OPCW, The Hague	CWC enters into force and the OPCW commences its operations.
2007	Tenth Anniversary of the CWC	182 Member States 25,000 metric tons of chemical weapons certified by the OPCW as destroyed, 3,000 inspections carried out.
2013	Syrian Civil War	The Ghouta and Khan al-Assal chemical attacks deadliest.
2013	Nobel Peace Prize	OPCW receives the Nobel Peace Prize for its efforts to eliminate CW.

**Table 1** : Major developments in the use and prohibition of chemical weapons [1]

### 3. The verification regime of the CWC

The CWC prohibits the development, production, stockpiling, acquisition and use of chemical weapons and requires States Parties to destroy, within specific time frames, any chemical weapons and related production facilities they may possess [6]. One of the engagements of the CWC is the global disarmament with a specific deadline, on the 29<sup>th</sup> April 2012 [7]. Otherwise, the Article VI of the NPT quotes that *"Each of the Parties to the Treaty undertakes to pursue negotiations in good faith on effective measures relating to cessation of the nuclear arms race at an early date and to nuclear disarmament, and on a treaty on general and complete disarmament under strict and effective international control"* [8], and so the disarmament of nuclear weapons is not planned in a specific calendar yet.

Military activities are not the only ones concerned and the Convention contains several provisions particularly related to the industrial activities. The aim of the Convention is not only to make sure of the destruction of chemical weapons and related facilities declared, but also to provide for restrictions on international trade in toxic chemicals and their precursors that could be used for weapon purposes. The main tools to achieve these missions are the submission of the national declarations by each State Party and the inspections by the OPCW of corresponding facilities, where the declared chemicals are manufactured, processed or consumed.

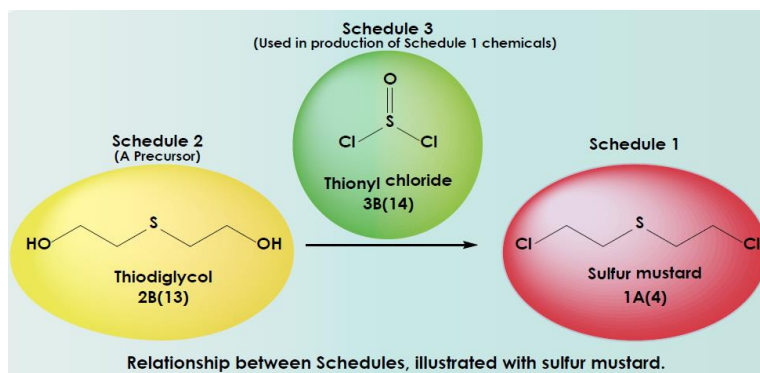
#### 3.1. National declarations

In one of the CWC Annexes, chemicals are classified in three schedules according to their degree of dangerousness. Each of the three schedules are subdivided in two parts, A and B, and so contains lists of toxic chemicals (part A) and precursors (part B) with their CAS number (Chemical Abstracts Service) permitting to identify the product. Depending of these schedules, the measures of verification are different. Guidelines specify the criteria to be applied to classify the products in the three schedules. The table 2 below shows this classification.

CWC Schedules of Chemicals			
Schedule	General Criteria for Inclusion	Examples	
		Toxic Chemicals	Precursors
<b>Schedule 1</b>	<ul style="list-style-type: none"> <li>Has been developed, produced, stockpiled or used as a chemical weapon</li> <li>Poses a high risk to the object and purpose of the Convention because of its toxicity or similarity to other Schedule 1 toxic chemicals</li> <li>Used in the final stage of formation of any Schedule 1 toxic chemical</li> <li>Has little or no use for purposes not prohibited</li> </ul>	<ul style="list-style-type: none"> <li>Sarin</li> <li>VX</li> <li>Mustard agents</li> <li>Ricin</li> </ul>	<ul style="list-style-type: none"> <li>DF</li> <li>QL</li> <li>Chlorosarin</li> </ul>
<b>Schedule 2</b>	<ul style="list-style-type: none"> <li>Poses a significant risk to the object and purpose of the Convention because of lethal or incapacitating properties</li> <li>Used in the final stage of formation, or important for the production, of any of the chemicals listed in Schedule 1 or Schedule 2, part A</li> <li>Is not produced in large commercial quantities for purposes not prohibited</li> </ul>	<ul style="list-style-type: none"> <li>Amiton</li> <li>BZ</li> </ul>	<ul style="list-style-type: none"> <li>Thiodiglycol</li> <li>Quinuclidin-3-ol</li> </ul>
<b>Schedule 3</b>	<ul style="list-style-type: none"> <li>Has been produced, stockpiled or used as a chemical weapon</li> <li>Poses a risk to the object and purpose of the Convention because of lethal or incapacitating properties</li> <li>Important in the production of one or more chemicals listed in Schedule 1 or Schedule 2, part B</li> <li>May be produced in large commercial quantities for purposes not prohibited</li> </ul>	<ul style="list-style-type: none"> <li>Phosgene</li> <li>Hydrogen cyanide</li> </ul>	<ul style="list-style-type: none"> <li>Phosphorus oxychloride</li> </ul>

**Table 2 :** The classification of CWC chemicals [9]

It is possible to see that the dangerousness of the products contained in each schedules increases from schedule 3 to 1. The scheme below, illustrates the linked between the chemicals of the different schedules with the example of sulfur mustard.



**Scheme 1 :** Relationship between Schedules, illustrated with sulfur mustard [10]

Initial declarations are required for these three kinds of products. Aggregate national data on the amounts of each chemical produced, processed, consumed, imported and exported during the previous year is to be submitted to the OPCW within 30 days of entry into force for the State Party and, following entry into force, annually no later than 90 days from the end of each calendar year.

The organic chemicals that are not expressly listed in tables or elsewhere in the Convention, excluding the exceptions specified in the Convention, are included in defined organic chemicals (DOC). The

Verification Annex defines the DOC as "any chemical belonging to the class of chemical compounds that includes all carbon compounds, with the exception of oxides and carbon sulphides as well as carbonates of metals, identifiable by its chemical name, its formula developed, if known, and its number CAS file, if assigned". Among these DOCs, products containing a sulfur, phosphorus or fluorine atom belong to the PSF sub-category. The presence of these atoms increases the relevance of these products to the object and the purpose of the Convention, since many chemical weapons are organophosphorus compounds.

According to the schedule of the product, different rules are applied concerning the declarations or inspections. Indeed, as shown in the table 3, according to the nature of the chemical product, different thresholds, particularly mass, define the rules associated to the verification process.

Declaration and Inspection Thresholds		
Chemical Category	Declaration Threshold	Inspection Threshold
<b>Schedule 1</b>	Single small-scale facility / Facility for protective purposes: any amount Other facilities: 100g	Single small-scale facility / Facility for protective purposes: any amount Other facilities: 100g
<b>Schedule 2</b>	2A* (BZ): 1kg 2A (other toxic chemicals): 100kg 2B (precursors): 1 metric tonne	2A* (BZ): 10kg 2A (other toxic chemicals): 1 metric tonne 2B (precursors): 10 metric tonnes
<b>Schedule 3</b>	30 metric tonnes	200 metric tonnes
<b>Unscheduled DOCs</b>	200 metric tonnes (aggregate)	200 metric tonnes (aggregate)
<b>PSF Chemicals</b>	30 metric tonnes	200 metric tonnes

**Table 3 :** Declaration an inspection thresholds [9]

For the schedule 1, the declaration threshold deals only with production and transfers activities. The targeted activities for the schedule 2 are production, consumption, treatment and transfers. The schedule 3 is only concerned by production and transfers and for DOC, only the production is followed.

The chemicals included in schedule 1, 2, 3 and the DOCs must be declared in an annual declaration concerning the past year activities and called the annual declaration of past activities (ADPA). This declaration concerns all the possible activities (production, consumption, treatment, transfers). For the chemicals of the schedule 1, 2 and 3, another declaration is required: the annual declaration of the anticipated activities for the next year (ADAA). However, this declaration does not include the transfer activities.

### 3.2. Inspections

The national declarations are the basis of the verification regime. Based on ADPA and ADAA, on-site inspections with data monitoring are planned by the OPCW in order to verify that activities within States Parties are consistent with the objectives of the Convention and the contents of declarations submitted to the OPCW. Three types of inspections are described in the CWC: routine inspections, challenge inspections and investigations of alleged use.

Routine inspections are cooperation between OPCW and State parties. They are based on the national declaration data of each State party. The particular installation to be inspected is selected from the list of declared facilities and a confidential inspection program is established on a yearly basis. Warning orders are issued to the inspectors chosen for the mission. The selection of the plant site is based on several criteria depending on the relevance of the site to the purpose and object of the Convention. Moreover, the rules of inspections in chemical industry facilities (annual inspection rate, notification, duration or inspector access) depend on the chemicals that these facilities produce, *i.e.* chemical weapons, schedule 1, 2, 3 chemicals or DOC (see table 4 and 5 below).

Article IV and V of the CWC [4] concern the inspections dealing with chemical weapons facilities. They allow OPCW inspectors access to all stockpiles of weapons and all facilities for the production, stockpiling and destruction of chemical weapons.

	Routine Inspections of Chemical Weapons Facilities		
	Production Facilities	Storage Facilities	Destruction Facilities
<b>Annual Inspection Rate</b>	Maximum 4 per year	Determined by Secretariat after initial inspection	Determined by Secretariat after initial inspection
<b>Notification Prior to Inspection</b>	At least 24 hours	At least 24 hours	At least 24 hours
<b>Duration of Inspection</b>	Determined by Secretariat	Determined by Secretariat	Determined by Secretariat
<b>Inspector Access</b>	Unimpeded	Unimpeded	Unimpeded

**Table 4 :** Routine inspection characteristics for chemical weapons facilities [6]

Article VI [4] of the CWC governs the inspections linked to the not prohibited activities (research, medical, pharmaceutical or protective purposes) concerning schedules 1, 2, 3 and DOC and so particularly chemical industries. Namely, States Parties are obliged to accept inspections at sites and facilities that produce or are in other ways related to such chemicals, provided facilities meet the criteria for inspectability (cf. the thresholds Table 3). The objective of these inspections is mainly the non-proliferation by guaranteeing that chemicals with proliferation potential and used for legitimate business purposes are not hijacked for prohibited activities related to chemical weapons. It is important to note that the inspection teams can not under any circumstances adopt an investigative approach but only check that the activities are in line with those declared. The table 5 shows the differences between inspections according to the nature of the targeted product and so the increased inspection constraint as the product's relevance to the CWC increases.

	Routine Inspections of Chemical Production Facilities			
	Schedule I Facilities	Schedule 2 Facilities	Schedule 3 Facilities	Other Chemical Production Facilities
<b>Annual Inspection Rate</b>	Single Small-Scale Facility: twice per year on average; Other Facilities: on average once a year	Based on risk assessment after initial inspection and facility agreement; no more than two per year per site	Based on random selection, equitable geographical distribution and information available to the Secretariat; no more than two per year at any one site  Combined number of Schedule 3 and other chemical production facility inspections in any State Party per year not to exceed three plus 5% of total number of declared Schedule 3 and other chemical production sites in the State Party, or 20, whichever is lower	Based on random selection, equitable geographical distribution, information available to the Secretariat and proposals by States Parties; no more than two per year at any one site
<b>Notification Prior To Inspection</b>	At least 24 hours	At least 48 hours	At least 120 hours	At least 120 hours
<b>Duration of Inspection</b>	Determined by Secretariat	96 hours (extension possible)	24 hours (extension possible)	24 hours (extension possible)
<b>Inspector Access</b>	Unimpeded to plant and unit but no access to wider plant site	Unimpeded to plant and within plant site; access to other plant areas guided by clarification and facility agreement rules or, if no facility agreement, managed access rules	Unimpeded to plant and within plant site; access to other plant areas guided by clarification rules	Unimpeded to plant and within plant site; ISP can apply managed access to protect confidential information; for other plant areas, request for access based on ambiguity rule or granted by ISP

**Table 5 :** Routine inspection characteristics for chemical production facilities [6]

Unlike complementary accesses defined by the additional protocols and permitting to the International Atomic Energy Agency (IAEA) to visit non declared sites are not provided in the CWC, OPCW can carry out inspections only on declared sites.

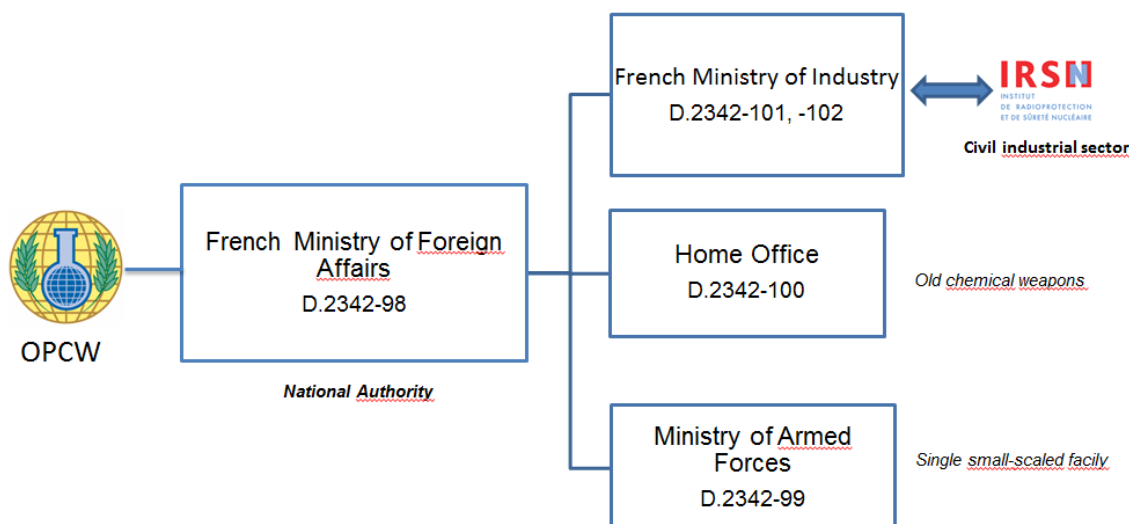
Challenge inspections are defined by Article IX of the Convention [4] and permits to any State Party to request the Secretariat in order to conduct an on-site challenge inspection anywhere in the territory (or

under the jurisdiction or control) of any other State Party. Prior to trigger this kind of inspection, the requesting State Party has to present an inspection request to the Executive Council and to the Director-General at the same time. If the inspection is accepted, the targeted State Party cannot refuse this kind of inspections even if the concerned facility is not declared. After the reception of the inspection demand by a state party, the OPCW has 12 hours to decide whether or not to carry out the inspection. This effectiveness of this kind of inspection depends on the speed of execution and so the Convention provides that the inspection team is to arrive at the point of entry not earlier than 12 hours after the ISP has been notified. Until now, no challenge inspections have been requested even in Syria.

The last tool provided by the verification regime is the investigations of alleged use. The OPCW is the only international organization with a legal requirement to maintain on standby a fully trained and equipped capability to investigate allegations of use of chemical weapons [6]. They are two ways to trigger this kind of investigations, either with submission of challenge inspection or by a request for assistance to the Director- General, in accordance with Article X [4] in which chemical weapons are alleged to have been used against the requesting State Party. The OPCW is also to respond in cases of alleged use of chemical weapons either involving non-States Parties or taking place in territory not controlled by States Parties. In this case, the Organization cooperates closely with the Secretary-General of the United Nations. Such a situation occurred in 2013, when the OPCW participated in United Nations investigations into the use of chemical weapons in the Syrian Arab Republic, which was not a State Party to the Convention at this period [6]. After that and under international pressure, Syria ratified the Convention the 13<sup>th</sup> of September 2013 [7]. Moreover, after several cases of alleged use of chemical weapons in Syria and recently at Salisbury in Great Britain, a decision (C-SS-4/DEC.3) [11] was adopted in June 2018 and permits the OPCW to attribute the responsibilities of the use of chemical weapons. This tool does not permit OPCW to decide on any sanctions to impose on a State Party, but only to transmit its conclusions to the General Council of the United Nations.

#### 4. Tools introduced in France

The French organization for the implementation of the CWC is shown below in Scheme 2. The national authority directly dealing with the OPCW is the French ministry of foreign affairs. According to the nature of the activity linked with the CWC, three different ministries manage and monitor the application of the Convention. The French ministry of Industry deals with activities related to the civil industrial sector.



**Scheme 2 :** French organization for the implementation of the CWC on the French territory

#### **4.1. The Institute of radioprotection and nuclear safety as expert for the CWC implementation**

On behalf of the French Ministry of Industry, the Institute of radioprotection and nuclear safety (IRSN) is responsible for the implementation of the CWC in the civil industrial sector. IRSN is the technical support of the French authorities, particularly for the application of international treaties to combat the proliferation of weapons of mass destruction in the civilian sector. When the Convention has been ratified, IRSN already had the know-how in the management of international nuclear treaties. So it has been designated to monitor the technical part concerning the implementation of the Convention. The activities of the CWC unit are various: census of concerned industries, management of French international declarations (centralization analysis, processing, aggregation and preservation); preparation, assisting and following of international inspections, preparation of technical support to Authorities (analyze and provide advice on technical documents...); assistance, advice and training for industrial operators and authorities and the participation in national and international working groups, specifically for the industry clusters at the OPCW (technical meetings in order to discuss about the application of the CWC in industrial facilities).

#### **4.2. Tools for national declarations**

In order to meet the dual objective of an accurate and complete national declaration, France defined a robust method based on the transposition of OPCW decisions in the national regulation and direct data collection from industrial operators. The cooperation with stakeholders, such as the Customs Services and trade associations from the chemical industry, also contributes to improve the national declaration. The CWC-dedicated French documentation also includes supporting material to the declarations (such as tools to exchange data with industrial operators and good practices guides) and dedicated web site. Moreover, the set-up of a documentary watch and information exchanges with some French entities (chemistry federations, National agency for health and medicine, etc.) permits to raise awareness of chemical operators who are not yet aware of the convention and improves the identification of plant sites.

#### **4.3. Tools for routine inspections**

The IRSN escorts all of the inspections, in the civil sector, approximately ten inspections per year. In order to ensure the smoothest possible running of these verifications, the IRSN trains industrial operators on a regular basis and helps them to prepare on-site inspections as soon as the inspection notification has been received. Once the verifications have started, the escort team's role is to ensure they take place in a satisfactory manner thus allowing France to demonstrate full compliance with its obligations whilst ensuring the protection of the French scientific heritage. Finally, the IRSN makes sure that industrial operators implement OPCW inspectors' recommendations, fully in line with France's objective to file an accurate national declaration, in compliance with the OPCW requirements.

#### **4.4. Tools to outreach the operators**

Several tools are used to outreach the chemical operators about the CWC, like the collaboration with the chemical federations to which they belong. Indeed, each year IRSN and the most important one, France Chimie, organize a specific training course for the chemical industry to explain the CWC declaration criteria, how to declare, the inspection process, regulation on importations and exportations etc. Moreover, since 2017, a booklet "Preventing the misappropriation of chemical products or facilities" was created and published in French and in English (*cf.* Figure 1 below). This educational guide is a self-diagnosis tool on the CWC obligations in France. It comes from a reflection between the Ministry of Industry, IRSN and the French professional federations of chemistry and textiles.

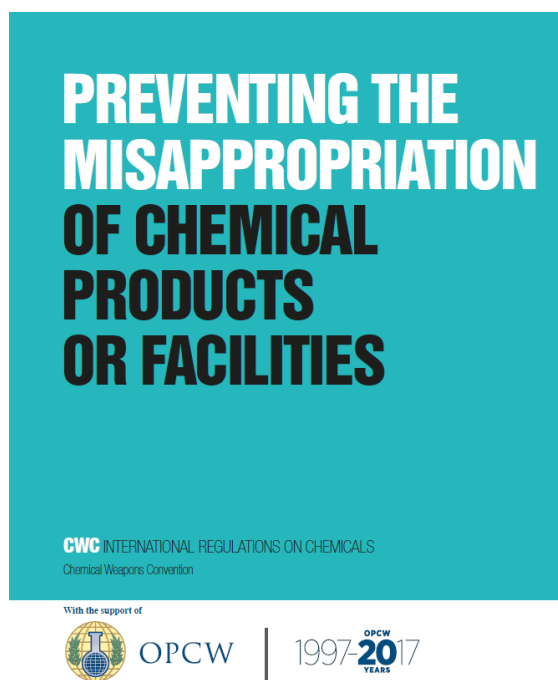


**Figure 1:** The outreach booklet elaborates by IRSN and chemical federations

The publication of this booklet leads to a seminar with around 150 people and various speakers like the General Director of the OPCW, the permanent representation of France at the OPCW, the Ministry of the Industry, federations, IRSN and some chemical operators to speak about their inspection feedback. This event has been welcomed by the international professional federations of chemistry and the OPCW.

## 5. Synergies between French nuclear and chemical offices of the IRSN

Within the IRSN, the nuclear and chemical offices have similar activities, namely the monitoring of the different declarations in each field and escort team during OPCW or IAEA international inspections. Moreover, in the case where a challenge inspection would be launched in France, any members of the units in charge of CWC and nuclear non-proliferation treaties can legally belong to the escort team of an OPCW inspection.

In addition, after the ratification of the CWC, one of the first steps for IRSN was to identify the chemical plant sites that were concerned by the Convention and its obligations. For that, the CWC unit capitalized on the census method that had been developed by the nuclear non-proliferation unit several years before. The inspiration of the working techniques also concerns the building of computer tools used for nuclear and chemical declarations. Indeed, each unit has web declaration portals to make easier the declaration of industrial operators. Chemical operators can use the IODA portal for CWC declaration and for nuclear operators there are several portals. PIMENT and CENTIME permit them to declare importations and exportations of nuclear materials and PASTEL is aimed at the information linked to the additional protocol. In order to deal with the received information, two softwares have been developed, SGI for the CWC declarations and GENIE for the nuclear ones. Thus, for the development of IODA and the associated software SGI, the CWC unit was inspired by the work that had been done before for the nuclear tools.

Moreover, some cross inspections took place, which means that a CWC implementation officer went to a Euratom or IAEA inspection and vice versa. The aim of these exchanges is to observe the work method of each unit. In a near future, it is envisaged to develop transversality between the two units, particularly to improve the distribution of the workload during rush periods. It would also allow the officers to get a global vision concerning these international treaties.

Since a few years, some events in Syria or Salisbury in UK showed the need to strengthen the OPCW verification regime and to go further in transversality. Indeed, the OPCW needs to adapt its verification capabilities in order to move from being mainly geared as a “disarmament verification” structure to a “counter-proliferation and deterrence towards use” institution. For that reason, the reinforcement initiatives implemented in other regimes, like those of IAEA, should also be taken into account, as their logic can be transferred to chemical weapons. The current setting does not allow the OPCW to have visibility on activities that may contribute to the proliferation or re-emergence of the use of chemical weapons beyond the declared industrial sites of States Parties, even on the field of civil installations. While entrusting the OPCW unlimited scope for inspections seem somewhat unrealistic and that challenge inspections are not actually implemented, options could be explored on the basis of the experience of IAEA, an additional control tool that would allow OPCW to cover facilities or locations that are not declared would be of great relevance.

In the context of the IAEA's complementary access tool, the Agency may verify the absence of nuclear material and / or undeclared nuclear activities. The State provides information on ongoing activities related to a civilian nuclear program (such as research and development, imports and exports of equipment, etc.) and gives IAEA inspectors access to the relevant facilities, even when they do not use nuclear material. Thus, the possibility of a similar tool under the OPCW, through a gradual and voluntary membership such as that of the IAEA, could help to complete the OPCW's verification regime, in the same way as the additional protocol did it for the non-proliferation treaty.

## 6. Conclusion

Finally, despite the CWC being one of the most universal Treaties and having a well-structured verification regime, the recent events showed that several gaps remain. The Convention could be enriched on the basis of experience in the nuclear field, which for example led to the need to put in place the additional protocol to overcome proliferation in the years 1980-1990. Be that as it may, in addition to being a non-proliferation treaty, this Convention guarantees the global disarmament of chemical weapons, thereby promoting global security.

## 7. Acknowledgements

The author would like to acknowledge all those who have reviewed this article and contributed to its completion.

## 8. References

- [1] OPCW; *What is a chemical weapon* [online]. 2019. 5 March 2019. <https://www.opcw.org/our-work/what-chemical-weapon>
- [2] OPCW; *Origins of the Chemical weapon convention and the OPCW*. 2016. 5 p. Available on: <https://20years.opcw.org/resources/posters-fact-sheets/>
- [3] OPCW; *History - Looking back helps us look forward* [Online]. 2019. 5 March 2019. <<https://www.opcw.org/about-us/history>>
- [4] IRSN; *Convention on the prohibition of the development, production, stockpiling and use of chemical weapons and on their destruction*. September 2014. 144 p.
- [5] *Organization for the Prohibition of Chemical Weapons (OPCW) – Facts* [Online]. NobelPrize.org. Nobel Media AB 2019. 3 April 2019. <<https://www.nobelprize.org/prizes/peace/2013/opcw/facts/>>
- [6] OPCW; *Three Types of Inspections*. 2016. <https://20years.opcw.org/resources/posters-fact-sheets/>

- [7] Executive council. *Note by the Director-general, Status of implementation of the final extended deadline of 29 April 2012*. EC-68/DG.7, 1 May 2012.
- [8] IRSN. *Treaty on the non-proliferation of nuclear weapons*. In *Référentiel réglementaire et technique abrégé – Textes AIEA*. December 2014. pp 4-8.
- [9] OPCW. *Monitoring Chemicals with Possible Chemical Weapons Applications*. 2016. 4 p. Available on: <https://20years.opcw.org/resources/posters-fact-sheets/>
- [10] OPCW. *Scheduled Chemicals under the Chemical Weapons Convention (CWC)*. 1 p. < <https://20years.opcw.org/resources/posters-fact-sheets/>>
- [11] Conference of the States Parties. *Report of the fourth special session of the conference of the States parties*. C-SS-4/DEC.3, 27 June 2018.
- [12] OPCW; *Member states – Syria* [Online]. 2019. 5 March 2019. <<https://www.opcw.org/about-us/member-states/syria>>

# **Panel 2:**

# **Safeguards by Design**

## Progress in SBD for Pyroprocessing Facilities by KAERI

**Ho-Dong Kim, Se-Hwan Park, Seong-Kyu Ahn, Byung-Hee Won, Chae-Hoon Lee, Dae-Yong Song, and Hee-Seong Shin**

Korea Atomic Energy Research Institute

111, Daedeok-daero 989 beon-gil, Yuseong-gu, Daejeon, Republic of Korea,  
34057

[khd@kaeri.re.kr](mailto:khd@kaeri.re.kr)

### **Abstract:**

Pyroprocess is being studied as a promising strategy for the sustainable development of nuclear energy production and management of spent fuel. KAERI (Korea Atomic Energy Research Institute) has been developing pyroprocessing technology to resolve the issue of PWR spent fuel accumulation and produce metal-based fuel for future fast reactors. There have been no cases of IAEA (International Atomic Energy Agency) safeguards applied to actual pyroprocessing facilities except R&D activities. In particular, the absence of experience of a general safeguards approach has motivated the IAEA to pursue preparations for this. Since the late 2000s, KAERI has been developing a safeguards approach for REPF (Reference Engineering-scale Pyroprocessing Facility) and provided it to the IAEA through an MSSP (Member State Support Program). The SBD (Safeguards by Design) activities related to the development of safeguards approaches for the REPF+ model facility are being performed under IAEA MSSP. This paper will address the role and progress of KAERI, which has been carrying out SBD of pyroprocessing facilities for more than 10 years, explore the application of the SBD concept to virtual facilities, and propose future technical methods to strengthen the facility system's response to threats.

Keywords: SBD; Safeguards Approach; Nuclear Fuel Cycle; Pyroprocessing

### **1. Introduction**

The application of a Safeguards-by-Design (SBD) concept is now widely acknowledged as a fundamental consideration for the effective and efficient implementation of safeguards. KAERI has implemented the SBD concept in nuclear fuel cycle facilities for research activities since the early 1990s. Such facilities include the DUPIC Fuel Development Facility (DFDF), the Advanced spent fuel Conditioning Process Facility (ACPF), and the Pyroprocessing Integrated inactive DEMonstration facility (PRIDE). The experience of applying the SBD concept to such facilities has resulted in a successful outcome, and the implementation of the safeguards of facilities by this concept is now well underway [1].

A Member State Supporting Program for Agency Safeguards (MSSP) for the 'Support for

Development of a Safeguards Approach for a Pyroprocessing Plant' was contracted between the IAEA and the ROK in 2008. Six pyroprocessing facility concepts suggested by the US, Japan, and the ROK were analyzed, and the Reference Engineering-scale Pyroprocessing Facility (REPF) concept was developed. The input material for the REPF is PWR spent fuel, and the output materials are U ingot and U/TRU ingot. The size of the process batch is 50 kgHM, the throughput per campaign is 500 kgHM, and the throughput per year is 10 MTHM. While the SBD concept of REPF primarily was an application of a virtual facility that did not complete the design from a safeguards standpoint, the efforts to design a reference facility and develop a safeguards approach for pyroprocessing have been helpful in establishing the SBD concept for pyroprocessing facilities [2].

At present, KAERI is developing a safeguards approach of an intermediate-sized facility named Reference Engineering-scale Pyroprocessing Facility plus (REPF+) as a MSSP task.

## **2. Experience in Developing Safeguards Technology for Pyroprocessing Facilities**

Starting in 2004, KAERI designed and manufactured remotely operable electrolytic reduction equipment capable of handling 20 kgU/batch PWR spent fuel and installed it in the ACPF hot cell for a hot demonstration of the pyroprocess. The ACPF construction was completed in July 2005. Since then, several campaigns for cold tests using fresh U and simulated fuels have been completed. The ACPF can provide a valuable opportunity to test various types of safeguards equipment for nuclear material accountancy, containment and surveillance, as well as for process monitoring. At present, there are two types of safeguards equipment at the ACPF, i.e., ASNC (ACP Safeguards Neutron Counter) and ALIM (ACP LIBS Monitoring system).

KAERI has been developing a passive-mode neutron coincidence counter for material accounting of the ACP. This well-type neutron counter, the so-called ASNC, is used for conducting an NDA of the materials that exist during the ACP process [3]. The operator's overall material balance is quantified by a  $^{244}\text{Cm}$  measurement using the ASNC. The ASNC was upgraded to improve its remote-handling and maintenance capabilities. Based on the results of the previous design study, the neutron counter was completely rebuilt, and various detector parameters for neutron coincidence counting (i.e., high-voltage plateau, efficiency profile, dead time, die-away time, gate length, doubles gate fraction, and stability) were experimentally determined. The measurement data showed good agreement with the MCNP simulation results. The ASNC is the only safeguards neutron coincidence counter in the world that is installed and operated in a hot-cell. The final goals to be achieved are (1) to evaluate the uncertainty level of the ASNC in nuclear material accountancy of the process materials of the oxide-reduction process for spent fuels and (2) to evaluate the applicability of the neutron coincidence counting technique within a strong radiation field [4].

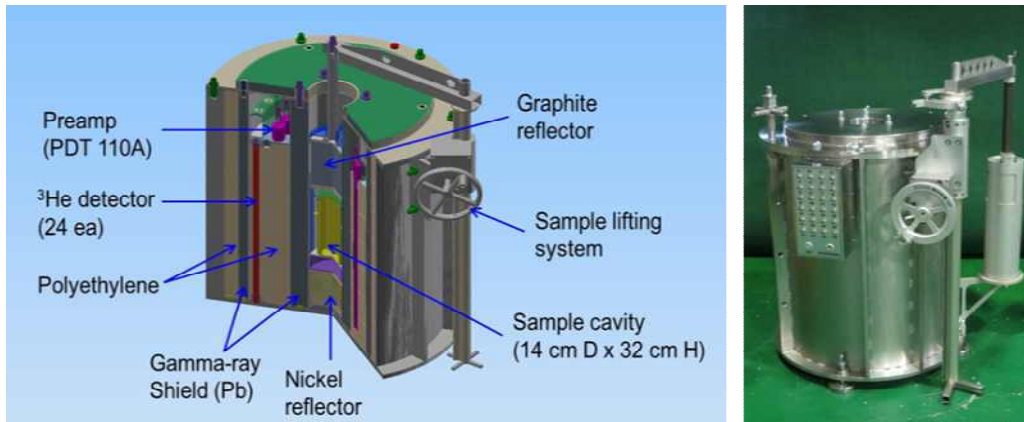


Figure 1. ASNC installed in the ACPF

LIBS (Laser Induced Breakdown Spectroscopy) was recognized as a promising technique because the material can be analysed without careful sample preparation. The use of LIBS based on fibre optics is a beneficial applications in a hot cell environment, delivering laser energy to the target and collecting the plasma light. The Fiber-Optic LIBS (FO-LIBS) system used to measure the Pu/U ratio of the process material of ACPF was installed in an air cell of ACPF, and the performance will be tested as the spent fuels are introduced to ACPF [5].

PRIDE (PyRoprocess Integrated inactive Demonstration facility) has been constructed as an engineering-scale demonstration facility for pyroprocessing studies. The process material of PRIDE is depleted uranium, and spent fuel is not processed in PRIDE. The unit process in PRIDE consists of voloxidation, oxide reduction, electrorefining, electrowinning, and waste treatment processes. Most of these processes are carried out in the argon cell of the second floor, and air-atmosphere processes are carried out on the first floor. The expected throughput of PRIDE is 10 tonU/yr [6].

One of the purposes of PRIDE is to test the safeguards technology for the pyroprocessing facility, and a safeguards system of PRIDE has been designed. The demand for robust safeguards applied to pyroprocessing facilities requires the IAEA to develop new measures and techniques to complement the more traditional safeguards systems. The bus bar system, together with portal radiation monitors, was selected and installed in the PRIDE facility to support the IAEA safeguards implementation in this facility [7]. The unified NDA (UNDA) is the integration of three measurement parts, neutron counting for the measurement of  $^{238}\text{U}$  quantity, gamma-ray spectroscopy to measure the  $^{238}\text{U}/^{235}\text{U}$  ratio, and a balance to measure the total mass of the processed material. Process parameters such as the voltage, current, temperature, and humidity are collected from the processing equipment. All parameters relevant to the PRIDE safeguards are collected, and are displayed and provided to the IAEA [8].

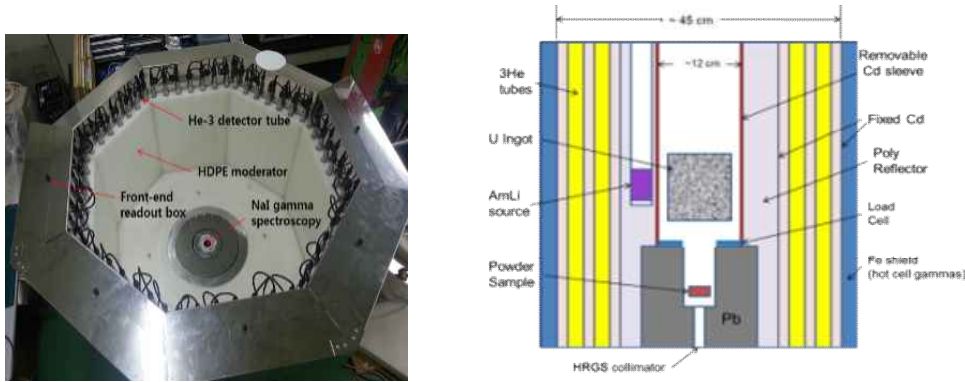


Figure 2. UNDA installed in the PRIDE facility

The PRIDE facility is used for testing a way to develop the safeguards signature of the process monitoring data and the containment and surveillance (C&S) device as well as for the training of IAEA inspectors on an engineering-scale pyroprocessing facility.

### 3. SBD for REPF

As part of a cooperative effort with the IAEA to find a safeguards approach for the pyroprocessing facility, KAERI developed the safeguards approach of a reference facility named Reference Engineering-scale Pyroprocessing Facility (REPF) in collaboration with Korea Institute of Nuclear Nonproliferation and Control (KINAC) from 2008 to 2011 as an IAEA MSSP [9].

The main processes performed in the REPF consist of the receipt and storage of spent fuels, the head-end process, the electrolytic reduction process, the electro-refining process, the electro-winning process, and waste salt regeneration and solidification. The head-end process has five steps: disassembling and rod extraction, chopping, decladding, homogenization, and pretreatment of the oxide fuel. In the electrolytic reduction process, the oxide fuel is converted into a metallic form. The electro-refining system, which is composed of an electro-refiner, a salt distiller, and a melting furnace, recovers pure uranium from the electrolytically reduced fuel. The electro-winning system is able to recover actinides from salt after the electro-refining operation. The waste salts are fabricated into durable waste forms in the waste salt regeneration and solidification process.

Three Material Balance Areas (MBAs) were identified for the REPF, which consists of the spent fuel receiving area, the storage and head-end process area (MBA-1), the main pyroprocessing area (MBA-2), and the product and waste storage area (MBA-3). Key Measurement Points (KMPs) at which the nuclear materials are present should be identified to make it possible to measure them and determine the material flow or inventory. This is necessary because the main nuclear materials that should be accounted for are uranium and plutonium in the REPF, and the most important KMPs for accounting

for these materials are the points before the main pyroprocessing, and two points where the final U ingot and U/TRU ingot products of the pyroprocessing are placed.

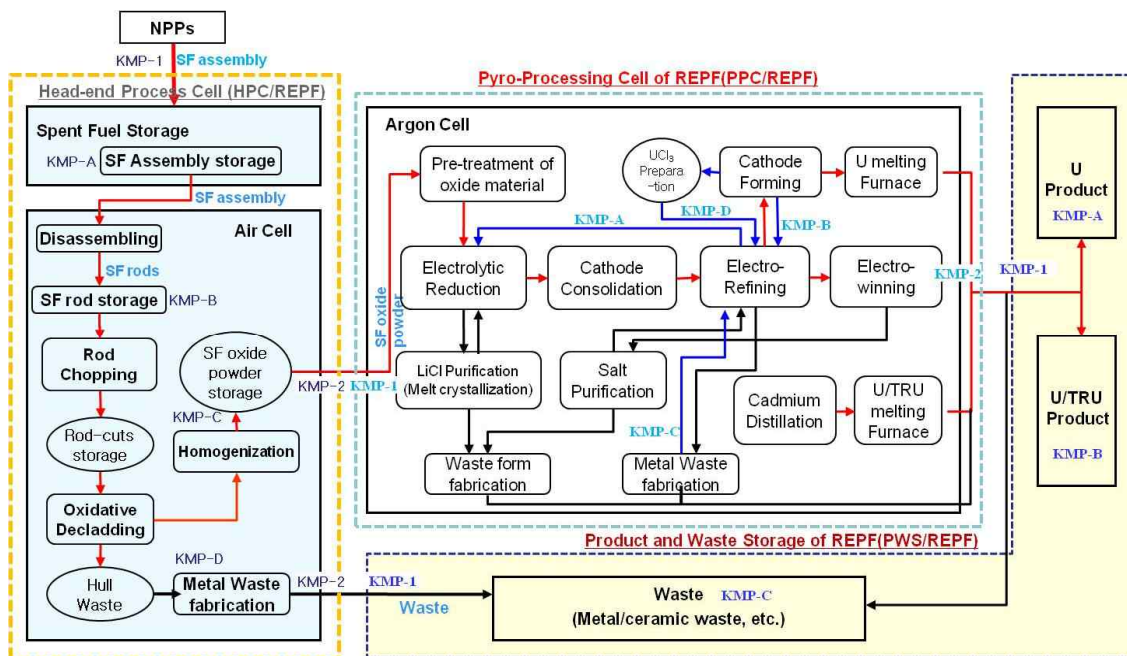


Figure 3. MBA and KMP structure of the REPF

A simulation program called a Pyroprocessing Material flow and Material unaccounted for Uncertainty Simulation (PYMUS) has been developed to analyze the nuclear material flow in the REPF and to calculate the MUF uncertainty [10]. DA-based material accounting in the REPF can give accurate information for the necessary accountability, and the NDA-based accounting can also yield useful accounting information in a timely manner. The REPF's NRTA system's NDA methods are based mainly on neutron balance using the Pu/Cm ratio. From a Sigma-MUF evaluation of the NMA system it was concluded that the overall REPF safeguards system meets the IAEA's detection goal.

Although REPF modeling was mainly based on safeguards concerns, and an analysis under these conditions gave limited results, the efforts to design a reference facility and develop a safeguards approach for pyroprocessing were helpful in implementing the Safeguard-by-Design concept.

#### 4. SBD for REPF+

The REPF is presently being upgraded to the REPF+, a 30 MTHM-throughput facility, in order to investigate the scale-up effect on the safeguards. One of the key features of the REPF+ is its allowance for unlimited nuclear-material mixing between campaigns, which was limited in the REPF.

The REPF+ is a conceptually designed pyroprocessing facility. The SFR fuel fabrication process as well as the pyroprocessing process is included in the REPF+. The input material of the REPF+ is PWR

spent fuel, and the output materials are the SFR fuel assembly and U ingot. The annual throughput is 30 MTH and the total operation days are roughly 200.

The facility is divided into four Material Balance Areas (MBAs). Inventory Key Measurement Points (IKMPs) are identified mainly based on the material type. Flow Key Measurement Points (FKMPs) are also identified to verify the nuclear material streams across the MBA boundaries. Other Strategic Points (OSPs) are defined for the verification of nuclear material flow within the MBA.

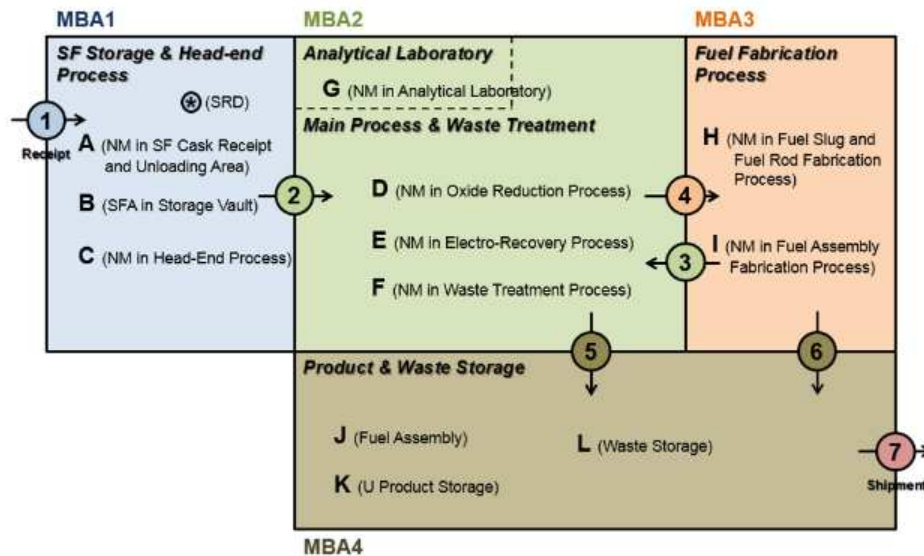


Figure 4. Draft MBA and KMP structure of the REPF+

MBA1 consists of a spent fuel receipt and storage area and an air-filled hot cell named the Head End Process (HE) cell. The spent fuel assembly is converted into feed material of an oxide reduction process such as in the form of fragments and porous pellets. The Shipper Receiver Difference (SRD) is evaluated in the MBA1. The containment/surveillance plays an important role before determining the receiver value in the MBA1. Near Real Time Accountancy (NRTA) is not applied to the MBA1.

MBA2 consists of an Oxide Reduction process (OR) cell, an Electro Recovery (ER) cell, a Waste Treatment (WT) cell, and Analytical Laboratory (AL). Most of the material in the MBA2 is in bulk form. The NRTA is applied to the OR cell, the ER cell, and WT cell, but the NRTA is not applied to the AL.

The MBA3 consists of a Fuel Slug Fabrication/Fuel rod Welding Process (FF) cell and Fuel Assembly Fabrication (FA) cell. The input materials of the MBA3 are the U/TRU product, and the U product, and the output material of the MBA3 is the fuel assembly. Process materials in the FF cell are contained in a container, upon which an ID is attached. The NRTA is only applied to the FF cell, and the NRTA is not applied to the FA cell.

MBA4 consists of a fuel assembly storage, and a U product & waste storage. The input material of the

MBA4 is fuel assembly, U product and waste form. They can be shipped to an outside facility. The material in the MBA4 is in item form, and the MUF is not evaluated in the MBA4. The NRTA is not applied to the MBA4.

Physical Inventory Verification (PIV) is carried out once per year. Facility operators should arrange a process plan to complete the last campaign prior to the PIT. The Interim Inventory Verification (IIV) is carried out once a month or every three months, and Short Notice Random Inspection (SNRI) and unannounced inspection can be included. Inventory change verification methods at each FKMP are specified.

Joint use of the operator's DA/NDA system and automatic sampling system are included in the verification methods in the REPF+ safeguards approach. For analysis of nuclear-material flow and calculation of MUF uncertainty, a simulation program, PYMUS was upgraded for evaluation of detection probability based on statistical testing for various diversion scenarios.

The NRTA systems are introduced in the MBA2 and the MBA3 to timely detect 8 kg of plutonium, which is a Significant Quantity (SQ). In the MBA2, Material Balance Period (MBP) for NRTA is set at about 30 days, during which 10 spent fuel assemblies are handled. MBP of the MBA3 is considered to be shorter than the MBA2. DA systems are mainly applied in the major measurement points where large amounts of nuclear material are present such as input, output, and ER vessels and NDA systems are considered in the other measurement points having small amount of nuclear material. The study to evaluate performance of REPF+ NRTA system are being performed using the PYMUS+ code [11].

## 5. Conclusions

KAERI has studied the Safeguard-by-Design concept at several nuclear fuel cycle facilities for research activities on spent fuel treatment. Such facilities include the ACPF and PRIDE. As part of a cooperative effort with the IAEA to find a safeguards approach for a pyroprocessing facility, the ROK designed the REPF model through an IAEA MSSP, and developed a safeguards system for the REPF that was reviewed by the IAEA. At present, KAEI is developing a safeguards approach of an intermediate-sized facility named Reference Engineering-scale Pyroprocessing Facility plus (REPF+) as an IAEA MSSP task. The safeguards measures in the safeguards approach are based on the current IAEA equipment and the safeguards technology under development. The NRTA is applied to the specified area of the REPF+. KAERI's effort for SBD will help implementation of effective and efficient safeguards in future pyroprocessing facilities.

## References

- [1] H.D. Kim et al., "Application of safeguards-by-design for the pyroprocessing facilities in the ROK", JNMM, Vol. XL(4), 24 (2012)
- [2] H.D. Kim et al., "Status of safeguards R&D on pyroprocessing related facilities at KAERI", ESARDA Bulletin, No.55, 59-63 (2017)
- [3] T.H. Lee, H.O. Menlove, S.Y. Lee, and H.D. Kim, "Development of the ACP safeguards neutron counter for PWR spent fuel rods", Nuclear instruments and methods in physics research A 589, (2008)
- [4] H. Seo et al., "ASNC upgrade for nuclear material accountancy of ACPF", Nuclear Inst. And Methods in Physics Research, A 880, 58-66 (2018)
- [5] B.Y. Han et al., "Feasibility study for on-line monitoring of process materials in LiCl-KCl molten salt using FO-LIBS", 8th Euro Symposium on LIBS (2015)
- [6] I.J. Cho et al., "Development of engineering scale pyroprocessing facility - PRIDE", HOTLAB 2015 (2015)
- [7] W. Bekiert et al., "Safeguarding Pyro. Related Facilities in the ROK", Proceedings of IAEA Safeguards Symposium (2014)
- [8] H. Seo et al., "Development of PRIDE UNDA for safeguards application," J. of Nuclear Science and Technology, Vol. 53, 6 (2015)
- [9] S.H. Park et al., "Status of development pf pyroprocessing safeguards at KAERI", J. of Nuclear Fuel Cycle and Waste Technology, Vol. 15, 3 (2017)
- [10] H.S. Shin, B.Y. Han, S.K. Ahn, J.S. Seo, and H.D. Kim, "Development of a Simulation Program for the Pyroprocessing Material Flow and MUF Uncertainty", Proc. of INMM 52th, California, USA (2011)
- [11] B.H. Won et al., "Development of PYMUS+ Code for Quantitative Evaluation of Nuclear Material Accountancy (NMA) System", Science and Technology of Nuclear Installations, Vol. 2019 (2019)

# 15 Years of Safeguards-by-Design in Finland

**Marko Hämäläinen  
Tapani Honkamaa  
Elina Martikka  
Mikael Moring  
Olli Okko**

STUK- Radiation and Nuclear Safety Authority

## **Abstract:**

*The need to have good communication between the facility designers and the safeguards authorities was realised in Finland in early 2000's when new nuclear construction projects were authorised. Since then the experiences obtained from different construction projects clearly point out the need to bring in the safeguards requirements by the licensing body at an early stage of facility design.*

*Early preliminary design information is generated when the applicant is preparing the licensing documentation before the construction of a facility begins. However, the Finnish experience showed that the applicants/licensees were not able to submit formal design information to the safeguards authorities for economic and contractual reasons. The need to have safeguards equipment and infrastructure included in the design process throughout the facility development was not understood by the applicants or licensees nor by the facility vendors or designers. On the other hand the safeguards inspectorates were sometimes reluctant to accept the long design process and commit themselves to continuous communication during the facility development instead of the tradition of fitting safeguards to ready-built facilities. These shortcomings were avoided when authorising the new nuclear installations in the 2010's.*

*It became obvious that strong national involvement is needed to launch early communication between the IAEA and the licensee and other stakeholders. This was enforced in Finland when the nuclear safety regulations were updated in 2013 with the requirement to submit preliminary design information shortly after the initial authorisation of a new construction project. The need of an early adaptation of safeguards arrangements within the applicant's organisation is essential also for the control of sensitive information already before the contracted design process; and, for newcomer countries the whole SSAC shall be established to facilitate the nuclear programme. Thus, raising awareness at old and new stakeholders is an essential educational task within safeguards.*

**Keywords:** safeguards-by-design; new nuclear installations; safeguards regulations; communication; raising awareness

## **1. Introduction**

The experiences obtained from the three construction projects at Olkiluoto in early 2000's clearly pointed out the need to bring in the safeguards requirement at an early stage of facility design. The early Design Information is generated, in principle, before the construction, but when planning the installation of containment and surveillance and non-destructive assay equipment and their cabling, some of the desired precautions were missing in the nuclear safety documentation and thus in design of facilities both at the Olkiluoto 3 reactor unit and the geological repository, because of missing of common understanding about the needs and formalities. The third construction project described by Okko et al 2011 [1] was the enlargement of the existing spent fuel storage. This project was communicated by updating the BTC-documents and informing the interested parties. The enlargement

was finalised in 2018 and the updated C/S systems were installed accordingly by the IAEA and European Commission. At the reactor site the Safeguards-by-Design (SbD) process was not included from the start, and therefore the retrofitting of C/S equipment became difficult and costly. However, the C/S systems are now installed for the commissioning of the reactor unit. At the repository site, the construction of the encapsulation plant is scheduled to begin with casting first concrete in summer 2019 and in a successful cooperation between the IAEA, European commission, national regulator, operator and designers, the safeguards equipment has been included and updated in the facility design and the safeguards requirements will be included in the construction process. This experience shows the importance of continuous communication between the stakeholders.

The same SbD process is also initiated with the management and safeguards staff members of the new operator that was licensed in 2011 to construct a new nuclear power plant at a new site in Finland and the requirements of safeguards is now a part of their bidding process. The first task is to raise awareness about safeguards need in the nuclear industry. In this paper experiences from the current projects is presented.

## 2. Safeguards-by-Design is communication and cooperation

The design of any nuclear facility is subject to many economic, technical, legal, security, safety, environmental and other constraints; and thus, it is the function of the design team to find solutions which are optimal within these constraints. Safeguards implementation is an additional factor which shall be taken into account, preferably during the design stage at latest. This was indicated by the IAEA already in 1998 [2]. However, there is no clear requirement for the SbD process, and thus the operators may not be willing to provide the IAEA with additional early official information e.g. because of contractual reasons in the contracted design process as recognised in Finland in the early 2000's. It became obvious that the mutual benefits have to be communicated to the stakeholders.

Owing to the international treaties and current IAEA practices, the planning and implementation of safeguards measures at a new facility begins often after the design and construction phase when the formal Design Information is available at the IAEA. The timeline based on INFCIRC/153 and specified in Subsidiary Arrangements is "as early as possible but not later than 180 days before nuclear material is introduced to the facility". Therefore, the operator typically submits the "final" information when the design is presented in the nuclear licence application. In order to find means to have safeguards involved in the facility design phase, the IAEA organised a work shop in 2008. As a result of the work shop more than 60 proposals were presented in the STR-360 report [3], called the Safeguards-by-Design (SbD) initiative, but no exact mechanism to adopt these was specifically addressed. The workshop participants emphasised that the IAEA should continue to cooperate with other stakeholders. The communication and cooperation can be most easily facilitated by an experienced national regulator.

In Finland, the basis for the Safeguards-by-Design is set in the nuclear energy act, and especially in the nuclear energy decree that states "the planning, construction and operation of a nuclear facility shall be implemented so that the obligations concerning the control of nuclear material, as provided and defined in the Nuclear Energy Act and provisions issued thereunder, and in the Euratom Treaty and provisions issued thereunder, are met". As a result these requirements are included and described in more detail in STUK's regulatory guide on regulatory control of nuclear materials, revised in 2013 [4]. This includes early provision of design information within 60 days from the decision to construct a new nuclear facility is made. In Finland this decision is considered as the decision-in-principle made by the Parliament.

Safeguards-by-Design is a part of the national Finnish 3S approach which aims at fulfilling international and national requirements. Any use of nuclear energy shall be planned and implemented so as to satisfy the requirements pertaining to nuclear safeguards and to ensure that the use is safe and secured. Safeguards is a prerequisite for use of nuclear energy in Finland and it shall be implemented in such a way that the nuclear security and safety of the facility are not compromised, the objective is to combine safeguards, security and safety in an optimal manner. As a result, a Safeguards-by-Design approach is employed to facilitate an efficient way to ensure effective safeguards implementation in all phases of use of nuclear energy.

## 2.1. Geological repository – a new type of facility

The final disposal of the nuclear material shall introduce new safeguards approaches which have not been applied previously in the IAEA's safeguards measures for spent fuel. The encapsulation plant to be built at the site will be the final opportunity for verification of spent fuel assemblies prior to their transfer to the geological repository, where no direct verification of the fuel assemblies can be performed after the fuel is encapsulated in the welded disposal canisters. There will be no access to fuel once it is transfer to the repository and canisters are emplaced in the bedrock, and the tunnels are backfilled. Within the framework of the IAEA support programme SAGOR and later ASTOR the concepts have been discussed and generic approaches were developed in the 1990's. The approaches begin in the "pre-operational phase", i.e. with the site investigations for a selected site. This can be considered as one of the earliest calls for Safeguards-by-Design [5].

The decision to construct an underground repository for spent nuclear fuel in Finland was made already in 1983. This final disposal of spent nuclear fuel in geological formations is expected to serve the overall good of the Finnish society. In order to follow those national requirements the geological repository has been developed in several phases to start the emplacement of spent fuel around 2025. The site selection phase took 15 years and owing to information from geological site investigations and geoscientific monitoring programme the application to locate the preliminary designed repository near the Olkiluoto nuclear power plant was endorsed in 2001 by the Finnish Parliament. In this context, the national safeguards approach [6] of applying long-term monitoring data collected for the safety case to support safeguards reporting in the preoperational phase in a cost-effective and non-intrusive manner was developed and launched in 2003. The approach follows the SAGOR recommendations [5]. The main focus has been on the generation of credible regulations for documenting construction and adjoining geoscientific monitoring records and State findings that have to survive over the more than 100-year disposal project. The proposal to submit geoscientific findings to the IAEA was published in 2006 [6]. Even data from site investigations was submitted to the IAEA, but no formal communication was initiated.

The Safeguards-by-Design process was launched after the submission of the nuclear construction licence application for the final disposal facility; and, the submission of separate design information for the two future MBAs, the encapsulation plant and geological repository to the EC/IAEA in 2012. The current SbD-process is presented by Murtezi et al 2018 [7]. The focus has been on the safeguards equipment and infrastructure to be installed at the encapsulation plant. The plant design has been revised twice after the licence application, thus the detailed plan for safeguards equipment has been modified after communication with the operator and according to the facility's needs. The mutual benefits can be achieved only through good communication and cooperation. The casting of first concrete is foreseen to take place in summer 2019, and during the construction it is essential to communicate the timing of installation of the safeguards equipment within the project's schedule.

## 2.3. New reactor – awareness to be raised in the contracts

The Olkiluoto 3 unit was ordered in 2003 by the operator of the Olkiluoto power station on a turnkey basis with a rapid time schedule to start nuclear energy production by 2009. It became obvious that at the bidding phase the detailed design was considered only as the basis for a cost estimate. After the contract, the supply organisation, designers and manufacturing companies etc. were selected. The project coordination and management was developed at the operator for the purpose, but the project has been delayed for several reasons. One of the major reasons is the lack of current experience in designing, constructing and licensing nuclear facility in any western country. According to the national requirements and company level quality assurance policies and practices the design has to be approved independently within the design organisation, the ordering company and according to the nuclear safety relevance at the nuclear authority. The safeguards-related organisation was in place in the operator's organisation, but the comprehensive safeguards requirements on a new reactor were not communicated properly during the bidding or early construction phase and thus the safeguards C/S equipment had to be incorporated in the late phases of the construction process.

The plant owner informed the nuclear authorities about the development and prepared a draft for Design Information in 2007, much before the time lines in safeguards agreements and regional

safeguards regulations. In this documentation some details describing the fuel handling systems were still missing owing to the fact that the design was not yet accepted in the contracted chain and the confidential information had not reached the owner. The need to have space and electricity for safeguards instrumentation and penetrations for cables was not obvious in the design phase. Owing to traditional safeguards approach the search for locations of surveillance cameras and seals started after the draft documentation when the casting of the containment was already going on. It became obvious that this caused additional costs in design and installation of safeguards equipment [7]. For contractual reasons the installation was agreed to take place in a later phase before the commissioning of the facility. The surveillance was installed and commissioned in 2017-2018 in order to have safeguards surveillance in place before receiving nuclear fuel in 2018. Thus, the need for proper Safeguards-by-Design process was acknowledged in Finland in late 2000's; and, since then STUK has actively been participating in supporting the early communication and cooperation, needed for all new facilities. The proliferation resistant structures in the facility should also be a common interest for those dealing with the safeguards and security precautions.

As an conclusion of the Olkiluoto 3 project, the owner noticed that putting the safeguards requirements already into any future the bid specifications is essential, already for commercial reasons. This way it can be ensured that there is no need to argue about the costs with the supplier during the construction phase, when all the details are agreed beforehand. Another reason is technical. When the safeguards requirements are already acknowledged in the plant contract, it is easier to take them into account in the documentation and plans concerning the whole unit. Plant designers can reserve some extra space and penetrations for the safeguards equipment and especially the remote data transmission will be much easier to implement. However, in the Olkiluoto 3 case this probably would not have helped much, because the plans and designs of the unit were at such a preliminary stage when the construction began. Thus it was seen important that safeguards measures and applying necessary safeguards methods in must be taken into account in the planning and design of nuclear projects. This demands that requirements are well understood and clearly described and included already from the beginning and taken into account already in preparing requests for tenders.

### **2.3. New operator – awareness to be raised by new personnel**

A new company, Fennovoima, was founded in 2007 to become a new nuclear power operator in Finland. After preliminary site investigations and a licence application the Finnish Government approved a decision-in-principle in 2010 for the new operator to construct a new nuclear power plant at one of the new candidate sites. The preliminary Basic Technical Characteristics (BTC) were submitted to the European Commission in summer 2013, once the selection of the future Hanhikivi site at Pyhäjoki was decided. Fennovoima submitted the construction licence application to the Government in June 2015. Provision of the necessary information to STUK, required for construction licence as per Nuclear Energy Decree has been delayed. Fennovoima expects the construction licence to be granted in 2021. The first Hanhikivi site declaration (according to the Additional Protocol) will be submitted once the construction licence has been granted.

Taking into account the lessons learned in the Olkiluoto projects, understanding the requirements for safeguards and combination of safeguards with security and safety, it is especially important with a completely new operator to start a dialogue on safeguards matters and measures as early as possible. In Finland, this is underlined with the requirement presented in [4] to provide preliminary design information within 60 days from the decision-in-principle. The preliminary design information includes information about the owner of the facility, operator of the facility, purpose, location, type, foreseen power output (in reactor facilities) and expected commissioning date (preliminary time table for the project). This information shall be provided to STUK and to international inspectorates (in Finland, to Euratom and via Euratom to the IAEA) to create the material balance area and to enable the supervision of the project and start of the SbD process.

The need to have a safeguards manual as a part of the applicant's quality management system at an early phase is seen necessary in Finland. It is a valuable tool for the regulatory authority to ensure that the operator (user of nuclear energy) understands its duties and is able to provide necessary information for the planning and implementation of safeguards thereafter. Dedicated persons responsible for safeguards at the operator are necessary in conducting practical measures and to be contact points towards the authorities. The duties of the responsible persons involves to inform their

superiors about necessary safeguards demands and requirements: One task is to ensure that safeguards measures are included in the bids and in evaluating of tenders. These persons need good contacts with plant designers too.

As the requirements will vary from state to state and from facility to facility, it is necessary to arrange localised training and workshops to discuss about the safeguards requirements and how to include them in all phases of a nuclear project. STUK has organised a few workshops with Fennovoima, where requirements were clarified to the Fennovoima staff as well as management. Safeguards-relevant documentation has been reviewed also as a part of the licensing process. In addition to this national oversight, workshops on SbD and international requirements were organised with the IAEA and European Commission. In these workshops, also other stakeholders, i.e., vendors and staff from subcontracted organisations have been participating. As the safeguards methods and equipment are not familiar to newcomers, a visit to the IAEA safeguards labs was organised in 2017. Workshops and informal meetings on development of the design and the whole project will be organised as often as seen necessary, by the operator or by the any other stakeholder. The experience gathered by the new operator was presented at the IAEA Safeguards Symposium 2018 [8]. This continuous interaction shows, how awareness about safeguards need has raised at all of the nuclear stakeholders.

### 3. Conclusions

Safeguards-by-Design requirements for operators are included into recent IAEA guidelines and Finnish regulations. According to these, operators of new and operating facilities in Finland are fulfilling their obligations accordingly. Effective national and international co-operation is required in facilitating effective safeguards and especially Safeguards-by-Design at all levels. This applies to experienced operators, but especially to applicants and new operators who have much less experiences or knowledge of safeguards or combining safeguards, security and safety.

The objective of SbD is to ensure that safeguards can be applied at a new facility by the operator in a manner that provides a firm basis for granting the construction licence and later the operating licence as well as to enable the effective safeguards implementation by STUK, the IAEA and the European Commission in all phases. This requires continuous communication and cooperation between all parties throughout the planning, designing, construction, operation and even decommissioning of a nuclear installation.

In conclusion, efficiently utilising multilateral opportunities including all relevant regimes and parties is necessary to enhance the SbD process and the implementation of safeguards. The experience and knowledge to identify the safeguards requirements and bring them into attention is vital. The need of exchange of information and sharing the output is not only enabling the effective implementation of safeguards but is also promoting the safe use of nuclear energy.

Experience gained in Finland during more than 15 years from Olkiluoto repository and reactor projects, as well as from a totally new company's NPP project, shows that Safeguards-by-Design offers a transparent and efficient approach for implementation of safeguards at all stages of use of nuclear energy.

### 4. References

- [1] Okko O, Honkamaa T, Kuusi A, Hämäläinen M.; *New nuclear power reactors to Finland: safeguards, security and safety considerations in design*. In: Abstracts – 33rd ESARDA Annual Meeting. Symposium on safeguards and nuclear material management. 2011 May 16–20; Budapest, Hungary. Budapest: 2011.
- [2] IAEA *Design Measures to Facilitate Implementation of Safeguards at Future Water Cooled Nuclear Power Plants*; Technical Report Series No. 392, IAEA 1998.

- [3] IAEA, *Facility Design and Plant Operation Features that Facilitate the Implementation of IAEA Safeguards*, STR-360 February 2009.
- [4] STUK; *YVL D.1 Regulatory control of nuclear safeguards*; issued 15.11.2013
- [5] IAEA *Safeguards for the Final Disposal of Spent Fuel in Geological Repositories*, STR-312, 5 Volumes, 1997.
- [6] Okko, O., Rautjärvi, J.; *Evaluation of monitoring methods available for safeguards use at Olkiluoto geological repository*” STUK-YTO-TR-216, 2006.
- [7] Hämäläinen, M.; Lamminpää, T.; Rintala, P.; Martikka, E.; Honkamaa, T.; Wiander, T.; *Safeguards by Design: Finnish Experiences and Views*; IAEA Symposium on International Safeguards, Linking Strategy, Implementation and People, IAEA-CN-220, 2015.
- [8] Murtezi, M., Zein, A., Canadell-Bofarull V., Koutsoyannopoulos, C., Martikka, E., Pekkarinen, J., Lahti, M., Moring, M., Okko, O., Schwalbach, P., Klumpp, P., Mustonen, S., Vaccaro, S., Honkamaa, T.; *Getting Ready for Final Disposal of Spent Fuel in Finland – Lessons Learned down the path of the Safeguards-by-Design Cooperation*; IAEA Symposium on International Safeguards, 5-8 November 2018, Book of Abstracts, CN267-083, p. 161.
- [9] Pellinen, K., Virlander, H.; *Starting from Scratch – Safeguards by Design work in the Hanhikivi-1 NPP Project*; IAEA Symposium on International Safeguards, 5-8 November 2018, Book of Abstracts, IAEA CN267-194, page 164

## Safeguards Regulatory Review for Small Modular Reactor Designs in Canada

**Henry Gao, Stephanie Herstead, Marcel de Vos, David Moroz**

Canadian Nuclear Safety Commission

Ottawa, ON K1P 5S9, Canada

Email: [henry.gao@canada.ca](mailto:henry.gao@canada.ca), [Stephanie.herstead@canada.ca](mailto:Stephanie.herstead@canada.ca),  
[marcel.devos@canada.ca](mailto:marcel.devos@canada.ca), [david.moroz@canada.ca](mailto:david.moroz@canada.ca)

### **Abstract:**

*In recent years, several organizations have demonstrated interest in Small Modular Reactor (SMR) technology and various designs have been proposed with the potential to be deployed at remote, off-grid areas in Canada. Natural Resources Canada engaged stakeholders across Canada to develop a roadmap on the future of SMRs in Canada. The Canadian Nuclear Safety Commission (CNSC) issued a discussion paper on SMRs in 2016 that helped to enhance regulatory clarity. The CNSC also offers a cost-recovered pre-licensing vendor design review (VDR) as an optional service. Currently, eleven vendors have applied to have a VDR of their new SMR designs. Applying the safeguards by design principle, the CNSC is engaging the IAEA and vendors to ensure that safeguards requirements can be met. This paper discusses the pre-licensing VDR, potential safeguards challenges, and general SMR developments in Canada.*

**Keywords:** Nuclear reactor; Small Modular Reactor (SMR); safeguards challenges; safeguards by design

### **1. Introduction**

In recent years, novel reactor technologies have emerged to potentially supply power to smaller electrical grids or to remote, off-grid areas. A reactor based on these novel technologies is commonly called a small modular reactor (SMR) which is viewed by many as the potential way of the future in nuclear technology, and therefore there has been a global renewed interest in developing and deploying reactor technology in the form of SMR.

The term SMR has no legal meaning in Canada but is generally understood to mean a nuclear reactor facility (single or multiple units) that has a smaller output than a traditional nuclear power plant. SMR concepts may employ alternative fuels and coolant approaches as well as other design features and may differ from conventionally operating reactors in deployment strategy. As a guide, the International Atomic Energy Agency (IAEA) defines SMRs as nuclear reactors producing less than 300 MW of electricity [1] but there is no legal power threshold in Canada. CNSC has noted that SMR technologies being discussed in Canada can range from a few megawatts to several hundred megawatts electrical and may also be used for production of process heat for industrial use. Developers of the technologies are promoting greater simplicity of design, use of passive and inherent safety features, economy of series production largely in factories, short construction times, and reduced siting costs. The use of security-by-design and safeguards-by-design is also being promoted as a means to maintain a high state of plant robustness. This approach is being used to make a case for lower plant staff complements but also to permit siting of these facilities in locations not previously considered for larger nuclear power plants.

Examples of alternative locations may include remote regions of the country to sites in close proximity to industrial facilities or high population centres.

In 2009 [2], the IAEA performed an assessment on SMR under its Innovative Nuclear Power Reactors & Fuel Cycle (INPRO) program, and concluded that there could be 96 small modular reactors (SMRs) in operation around the world by 2030 in its 'high' case, and 43 units in the 'low' case. The IAEA further noted in 2018 that, according to the IAEA Department of Nuclear Energy, there are at least 50 small modular reactor (SMR) designs being considered for potential development.

The World Nuclear Association recently provided an update on SMR development and technologies, and concluded that there is strong interest in small and simpler SMRs and their development [2]:

- Three small reactors are operating.
- Six very small reactor designs are being developed (up to 25 MWe).
- Five small reactor designs are under construction.
- Nine small reactors for near-term deployment – development well advanced.
- Twenty-four small reactor designs at earlier stages.

Stakeholder interest in SMRs has increased in recent years in Canada. Three major areas of application are being considered:

- On-grid power generation, especially in provinces phasing out coal in the near future. Larger SMRs may align to this application.
- On- and off-grid combined heat and power for heavy industry. For example, remote mines could benefit from load following medium-sized higher temperature reactor options for bulk heat and power.
- Off-grid power, district heating, and desalination in remote communities. Smaller simpler SMR concepts could potentially be used to supplement or even replace the use of fossil fuels such as diesel which is traditionally subsidized due to high cost of production and delivery. Waste heat from such facilities could also potentially be further utilized for other uses including agriculture and local industry.

Based on market studies Natural Resources Canada, who oversees national energy policy, established a partnership with interested provinces, territories and power utilities, Natural Resources Canada to convene a roadmap to engage stakeholders on the future of small modular reactors in Canada. Through a series of expert working groups, and workshops held across Canada, the roadmap gathered feedback on the direction for the possible development and deployment of SMRs in Canada. CNSC provided regulatory information to the stakeholders to help them further understand the regulatory landscape. The SMR Roadmap Steering Committee recommended [3]:

**Demonstration** Governments, utilities, industry, and the national laboratory support demonstration of SMR technologies, preferably more than one, at appropriate sites in Canada.

**Risk Sharing** A risk sharing mechanism between governments, utilities, and industry to support early deployment in Canada by off-setting first of a kind risk through appropriate financial and funding mechanisms.

**Legislation and Regulation:** Canada's regulatory framework and waste management regime are well positioned to respond to the SMR paradigm shift, but some modernization will be necessary to reflect the reality of the smaller size of an SMR. Governments should work with partners to modernize legislative and regulatory requirements to ensure an economically viable and timely pathway for SMRs, while maintaining high safety and security requirements.

**Capacity Building and Engagement** Governments, utilities and industry support capacity building initiatives to develop a robust knowledge base related to SMRs in Canada, and commit to open and proactive engagement with public and Indigenous groups on SMRs.

As the regulator of nuclear activities in Canada, the Canadian Nuclear Safety Commission (CNSC) is maintaining a state of readiness for regulatory reviews of licence applications for SMR projects in Canada using an objective based safety framework that can be applied to different reactor technologies. The CNSC is actively working to further enhance the existing regulatory framework as experience is gained from new technologies. The CNSC has also engaged with the public through the publication of discussion paper DIS-16-04, *Small Modular Reactors: Regulatory Strategy, Approaches and Challenges* in 2016. Recently, CNSC developed a supplementary information document, REGDOC-1.1.5, *Licence Application Guide: Small Modular Reactor Facilities* to further clarify SMR implications on safety and control measures expected in a licence application. As part of the CNSC's overall regulatory framework planning and periodic review cycle, regulatory documents applicable to nuclear power plants are being reviewed for SMR specific considerations and clarified as needed to reflect emerging operating experience. However, changes to regulatory requirements cannot be implemented based on claims of future safety performance. A sound regulatory framework implements change based on proposals justified by sound science and sufficient technical evidence including relevant operational experience.

There are two stakeholder groups seeking to engage early with the CNSC regarding the potential deployment of SMRs:

- *Potential Applicants for a licence:* The companies have traditionally been power utilities who will oversee the construction and operation of the facility – these stakeholders participate in the licensing and Environmental Assessment processes and are responsible for demonstrating to the CNSC that they will conduct their activities in accordance with regulatory requirements. This stakeholder procures the SMR technology and therefore specifies to their supply chain (vendors) how they expect the supplies will meet regulatory requirements. Potential applicants approach the CNSC to understand the licensing process and the requirements that will apply in specific cases.
- *Technology developers (Vendors):* These companies provide design and safety analysis information to potential applicants and are generally responsible for specific technology design activities. Potential applicants are expecting vendors to demonstrate a strong understanding and application of Canadian regulatory requirements in their design activities. As a result, vendors approach the CNSC early for feedback on how well they are demonstrating their understanding and application of requirements in their activities.

This paper focuses on the CNSC process used to provide regulatory feedback to the technology developers. Vendors have the ability to leverage this feedback to address design issues (either on their own or in consultation with end-users) before an application for a licence to build or operate a SMR or other nuclear power plant is initiated.

## 2. Pre-Licensing Vendor Design Review (VDR)

CNSC is currently engaged in a number of [pre-licensing vendor design reviews](#) (VDR) for SMRs.

A VDR is a structured and optional process that enables CNSC staff to provide feedback early in the design process based on a vendor's reactor technology. An application by a vendor for a review is **not** an application for a licence to prepare a site or to construct or operate a nuclear power facility, and is not an indication of intent to proceed with a project. This review does not certify a reactor design or involve the issuance of a licence under the *Nuclear Safety and Control Act*, and it is not required as part of the

licensing process for a new nuclear power plant. The conclusions of any design review do not bind or otherwise influence decisions made by the Commission.

The primary purpose of a vendor design review is to provide feedback to the vendor about how the vendor is addressing Canadian regulatory requirements and CNSC expectations in its design activities and outcomes. The CNSC enters into a service agreement with the vendor that is based on a fixed scope of work. Because the generic design of a reactor is not yet adapted to a specific site, the level of design completion does not permit CNSC to make conclusions about whether the design is fully in compliance with regulatory requirements. However, this process provides for the early identification and resolution of potential regulatory or technical issues in the design process, particularly those that could result in potential fundamental barriers in a future licensing process. VDR outcomes provide the vendor with information to resolve issues in a timely manner.

When an applicant submits an application for a licence for a project to construct and/or operate a facility referencing the vendor's design, the CNSC then initiates the licensing process with the applicant and the vendor is considered part of the applicant's supply chain. Licensing will conduct a detailed project specific review of the applicant's safety case which would typically reference the vendor's design information as adapted for the site specific conditions. If the applicant utilizes the vendor's information from the VDR process, CNSC staff can leverage that information in the conduct of licensing activities.

## 2.1 General Review Criteria

All review criteria originate from the CNSC regulatory framework. VDR submissions are assessed using CNSC [regulatory documents](#) pertinent to design and safety analysis activities.

Some key overarching regulatory documents include:

- REGDOC 2.5.2, *Design of Reactor Facilities: Nuclear Power Plants and/or* CNSC RD-367, *Design of Small Reactor Facilities*. (CNSC decides which is applicable)
- REGDOC 2.4.1, *Deterministic Safety Analysis*
- REGDOC 2.4.2, *Probabilistic Safety Assessment (PSA) for Nuclear Power Plants*

These documents in turn may point to other more specific regulatory documents such as

- REGDOC-2.4.3, *Nuclear Criticality Safety*
- REGDOC-2.13.1, *Safeguards and Nuclear Material Accountancy*.

These regulatory documents in turn provide information about any codes and standards that may be useful in addressing requirements and guidance. The vendor may propose alternative approaches to address requirements; however, it must provide information that outlines the basis of how the alternate meet or exceed Canadian requirements. This justification approach, which typically involves a gap analysis, is integral to the vendor demonstrating its understanding of Canadian requirements. Initial consideration is also given to the extent to which generic or outstanding safety issues have been resolved, and to whether the knowledge base for new or innovative features in the design has been established.

The VDR process is composed of three distinct phases, corresponding with the level of design detail normally available:

**Phase 1 review** – Demonstration of intent to comply with regulatory requirements in vendor processes and conceptual level design outcomes: CNSC staff assess the information submitted in support of the vendor's design and determine if, at a general level, the vendor design and design processes are

demonstrating implementation of CNSC design requirements. Design outcomes are used to illustrate effective use of design processes and that requirements are being addressed. The duration of a review is estimated based on the vendor's proposed schedule but a Phase 1 review typically takes 12–18 months.

**Phase 2 review** – Typically initiated once a design has achieved system design completion (e.g. system performance specifications being established and supported by credible information). CNSC revisits corrective actions from Phase 1 and then reviews system level design outcomes, including progress on substantiating design claims with a focus on identifying if any potential fundamental barriers to licensing exist or are emerging with respect to the reactor's design. The duration of a review is estimated based on the vendor's proposed schedule but a Phase 2 review typically takes 24 months.

**Phase 3 review** – In this phase, the vendor can choose to follow up on one or more focus areas covered in phases 1 and 2 against CNSC requirements pertaining to a licence to construct. For those areas, the vendor's anticipated goal is to demonstrate and receive feedback from CNSC that issues are being resolved in a timely and effective manner.

Phase 1 and 2 reviews have 19 review focus areas, which represent, based on global experience, key long lead areas of importance to nuclear safety that have presented issues in a construction and operating licence. The Phase 3 review is tailored on a case-by-case basis.

Because a pre-licensing vendor design review does not lead to a regulatory decision, CNSC staff must strike a balance between, on the one hand, protecting a vendor's sensitive commercial information and, on the other hand, securing CNSC staff access to this information for the purposes of performing an effective review and communicating the CNSC's activities to the public transparently, to the extent practicable. As a result, the overall conclusions and key findings of a pre-licensing vendor design review are posted by the CNSC in an executive summary for public information. However, release of detailed discussions and review results are at the discretion of the vendor. For the purposes of regulatory cooperation between countries, CNSC may share the results of the detailed report with the permission of the vendor.

The results of a VDR, if used by an applicant for a licence, can be taken into account for the Construction Licence Application review and is likely to result in increased efficiencies of technical reviews. For more Information on the CNSC's Pre-licensing Vendor Design Review, please refer to [REGDOC-3.5.4, Pre-Licensing Review of a Vendor's Reactor Design](#).

## 2.2 Status of Pre-licensing Vendor Design Reviews

Current participating SMR vendors and their review completion dates are outlined below. Table 1 presents an overview of vendors who have established service agreements with the CNSC for pre-licensing engagement using the vendor design review process for their new reactor designs. The status of each project at time of publication of this paper is provided.

Vendor	Name of design and cooling type	Approximate electrical capacity (MW electrical)	Type	Applied for	Review start date	Status
Terrestrial Energy Inc. (Canada)	IMSR Integral Molten Salt Reactor	200	MSR	Phase 1	April 2016	Complete
				Phase 2	December 2018	Assessment in progress
Ultra Safe Nuclear Corporation (USA)	MMR-5 and MMR-10 High-temperature gas	5-10	HTR	Phase 1	December 2016	Complete
				Phase 2	Pending	Project start pending
LeadCold Nuclear Inc. (Sweden)	SEALER Molten Lead	3	Lead FNR	Phase 1	January 2017	On hold at vendor's request
Advanced Reactor Concepts Ltd. (USA)	ARC-100 Liquid Sodium	100	Sodium FNR	Phase 1	September 2017	Assessment in progress
Moltex Energy (UK)	Moltex Energy Stable Salt Reactor Molten Salt	300	MSR FNR	Series Phase 1 and 2	December 2017	Phase 1 assessment in progress
SMR, LLC. (A Holtec International Company: USA and Canada)	SMR-160 Pressurized Light Water	160	PWR	Phase 1	July 2018	Assessment in progress
NuScale Power, LLC (USA)	NuScale Integral pressurized water reactor	60	Integral PWR	Phase 2*	Pending 2019	Project start pending

\*Phase 1 objectives will be addressed within the Phase 2 scope of work. PWR: Integral pressurized water reactors; MSR: Molten salt reactors; HTR: High-temperature gas reactors.

**Table 1: Vendor design review service agreements in force between vendors and the CNSC**

Table 2 presents an overview of vendors who have applied for but have not yet signed service agreements with the CNSC to conduct a vendor design review for their new reactor designs. Although it typically takes a few months for the CNSC to establish and sign a service agreement, this time period can vary, depending on:

- The organizational and technical readiness of the vendor.
- Sufficient completeness of the vendor's design activities for the Phase of VDR applied for.
- The vendor's financial readiness to undertake the vendor design review.
- Other legal, timing or business aspects that may influence a vendor's decision to proceed.

Vendor	Name of design and cooling type	Approximate electrical capacity (MW electrical)	Type	Application received	Applied for
StarCore Nuclear (Canada)	StarCore Module High-temperature gas	10	HTR	October 2016	Series Phase 1 and 2
URENCO (UK)	U-Battery High-temperature gas	4	HTR	February 2017	Phase 1
Westinghouse Electric Company, LLC (USA)	eVinci Micro Reactor solid core and heat pipes	Various outputs up to 25 MWe		February 2018	Phase 2*
GE-Hitachi Nuclear Energy (USA)	BWRX-300 boiling water reactor	300	BWR	March 2019	Phase 2*

\*Phase 1 objectives will be addressed within the Phase 2 scope of work.

**Table 2: Vendor design review service agreement between vendors and the CNSC under development**

The CNSC Executive Summaries of phase I VDR reports for TEI and USNC can be found with the

following link:

- [Phase 1 Pre-Licensing Vendor Design Review Executive Summary: Ultra Safe Nuclear Corporation](#) (USNC) (February 2019)
- [Phase 1 Executive Summary: Pre-Project Review of Terrestrial Energy's 400-thermal-megawatt integral molten salt reactor \(IMSR400\)](#) (PDF, November 2017)

### 3. Canada's First New Build SMR Project

In March 2019, a new Canadian company, Global First Power (GFP), submitted an application for a licence to prepare a site for a small modular reactor on Atomic Energy of Canada Limited's property at the Chalk River Laboratories location. GFP has partnered with existing Canadian utility Ontario Power Generation and SMR vendor, Ultra Safe Nuclear Corporation (USNC) on a proposed 5 MWe high-temperature gas reactor full-scale demonstration project. One of the objectives of the project includes demonstration of Safeguards By Design (SBD) for the purposes of informing future fleet deployment of this design in Canada. The CNSC licensing process to be used for this project will be consistent with the process described in CNSC Regulatory Document [REGDOC 3.5.1, Licensing Process for Class I Nuclear Facilities and Uranium Mines and Mills, version 2](#). In accordance with safeguards agreements and arrangements, this information has been provided to the IAEA.

### 4. Safeguards by Design and regulatory review

As part of Canada's commitments under *Treaty on the Non-Proliferation of Nuclear Weapons*, Canada has concluded a comprehensive safeguards agreement and an Additional Protocol to that agreement with the IAEA (INFCIRC/164, *Agreement between Canada and the Agency for the Application of Safeguards in Connection with the Treaty on the Non-Proliferation of Nuclear Weapons; and INFCIRC/164 Add.1*). These agreements form the basis for implementing safeguards in Canada, which in turn provides confidence to Canadians and the international community that all nuclear material in Canada is in peaceful use and that there are no undeclared nuclear materials or activities in Canada.

To facilitate safeguards implementation at Canadian nuclear facilities, CNSC published a regulatory document REGDOC-2.13.1, *Safeguards and Nuclear Material Accountancy* in 2018. This document sets out requirements and guidance for safeguards programs for applicants and licensees who possess nuclear material, carry out specified types of nuclear fuel-cycle related research and development work, or carry out specified types of nuclear-related manufacturing activities, including provision of support IAEA inspection and equipment as well as nuclear material accountancy and reporting.

Safeguards and non-Proliferation is one of the safety and control areas in CNSC's regulatory framework. The CNSC also recommends the application of SBD principle to integrate safeguards considerations into the early design phase of a new nuclear facility. The VDR process considers the areas of design that relate to reactor safety, security, and safeguards. As part of the CNSC's SMR VDR process, safeguards is assessed under item 15 *Robustness, safeguards and security*.

The objective of Safeguards regulatory review is to confirm that the vendor, through its design documentation, understands Canadian requirements and CNSC expectations regarding the implementation of safeguards in the design, with the focus on the vendor's description of the general design approach and strategy for safeguards in the design. The general review criteria used in the review include the following:

- *International Safeguards in the Design of Nuclear Reactors* (IAEA Nuclear Energy Series NP-T-2.9).
- *International Safeguards in Nuclear Facility Design and Construction* (IAEA (IAEA Nuclear Energy Series NP-T-2.8).
- REGDOC 2.5.2, *Design of Reactor Facilities: Nuclear Power Plants*.
- CNSC RD-367, *Design of Small Reactor Facilities*.
- REGDOC-2.13.1, *Safeguards and Nuclear Material Accountancy*.

Generally speaking, the vendor design documents should:

- Outline safeguards design considerations and design methodologies in the design.
- Propose methods by which the IAEA can maintain continuity of knowledge over the nuclear material flows at the facility when considering the need for the permanent installation of safeguards equipment and the provision of services required for ongoing operation of that equipment.
- Proposes methods to minimize the number of locations with nuclear material and the ability to accurately control and account for such material to meet Canada's safeguards requirements for recording and reporting accountancy data, and for monitoring flows and inventories of nuclear material.

The VDR process is an opportunity to propose a SBD approach, to ensure that safeguards are being considered in the initial design stages, and can be implemented readily when SMRs will be deployed. In many cases, vendors originate in states that have different safeguards agreements than those where they wish to do business. This engagement initiates or raises the vendor's awareness of safeguards requirements in the State.

In general, vendors have been expressing their intent to comply with Canadian requirements through the VDR process including nuclear safeguards requirements in Canada. To date, the CNSC has found that the vendors actively understand and learn Canadian safeguards requirements, specifically for those vendors originating outside of Canada. In addition, there is a very limited amount of preliminary design information made available by the vendor and their deployment strategy may introduce safeguards challenges (i.e. remote locations in Canada's North). From a logistics perspective, facilitating IAEA in-field verification and equipment maintenance activities at a remote location introduces travel complexities for personnel from both the IAEA and the State, and the technological challenges due to extreme climate. In this deployment scenario, it might be more practical to rely more heavily on unattended monitoring systems.

Specific SMR technology may also presents unique challenges to safeguards. For example, for molten salt fuel the fuel is not a distinguishable as a unique item such as in traditional solid-fuel reactors and its composition will change with time as well as with changing reactor operating conditions. Therefore, nuclear materials accountancy is not as straightforward as traditional power reactors. Much of the equipment needed to support safeguards verification of this form of fuel does not exist yet, and needs to be developed.

As development of SMRs mature and projects come to the point of realization where vendor engagement on safeguards is feasible, the IAEA has recently requested a support task to address these potential safeguards challenges from the member States including Canada. As described in the task proposal, this task will identify the key technical challenges for safeguards implementation involving SMRs, and steps that can be taken to support incorporating SBD principles into SMR designs.

The CNSC accepted this task under the Canadian Safeguards Support Program in January 2019. In the following two years, the CNSC will work closely with the IAEA and vendors to provide information and expertise necessary for evaluating aspects of the SMR design that could impact safeguards, investigating safeguards implementation strategies, and identifying ways in which the SMR may be modified to facilitate safeguards implementation. The CNSC will identify the appropriate SMR design to bring forward to the IAEA currently undergoing licensing or a Phase 2 VDR. By applying SBD principle, CNSC, IAEA, and vendors will work together to address key technical areas including safeguards measures and the possibility of implementation to ensure that safeguards are being considered in the early stages of the design and deployment of SMRs, and to enable the IAEA to be adequately prepared to safeguard these facilities.

## 5. Conclusion

There is strong interest in SMRs in Canada and a number of SMR vendors have applied for pre-licensing vendor design reviews from the CNSC. The CNSC regulatory framework has been developed using a technology neutral objective based approach based on operational experience. The framework is ready to perform regulatory review of pre-licensing VDR and licence application for SMRs. The CNSC recommends a SBD approach, and will work closely with the IAEA and vendors to develop safeguards approaches, measures, and implementation strategies to ensure that safeguards are properly implemented in SMRs.

## 6. References

[1] Small and Medium Sized Reactors (SMRs) Development, Assessment and Deployment, 2013.

<http://www.iaea.org/NuclearPower/SMR/>.

[2] <http://www.world-nuclear.org/information-library/nuclear-fuel-cycle/nuclear-power-reactors/small-nuclear-power-reactors.aspx>.

[3] <https://www.nrcan.gc.ca/energy/uranium-nuclear/21183>.

# Safeguards Information Assurance by Design

**Dianna S. Blair  
F. Mitch McCrory**

Sandia National Laboratories  
PO Box 5800  
Albuquerque, NM, USA 87185  
dsblair@sandia.gov  
fmmccro@sandia.gov

## **Abstract:**

*The assurance of Safeguards Information is crucial to meet IAEA obligations. Information can be potentially at risk for alteration when it is generated, stored, transmitted, or manipulated (such as in a calculation). Where, when, and how information is assured can vary depending on where in the information lifecycle it exists. Often, information protection measures are not considered until after a system is architected and built or are only applied to a portion of the information system. This typically limits the effectiveness of information assurance, can increase the cost of assuring the information, and can reduce the trust in the information received. Designing information assurance into the architecture of a system can significantly reduce information vulnerability at an affordable cost while improving the trust of the information. This paper discusses safeguards information assurance by design and architectural approaches from a lifecycle perspective including potential tools that can be utilized to help define information assurance requirements and help validate the effectiveness of these requirements as the system transitions through the lifecycle. The tools discussed include risk management tools, architectural approaches, modeling approaches, and red teaming benefits.*

**Keywords:** safeguards, information assurance, design, risk

## **1. Introduction**

To support informed choices while working to optimize economic, operational, safety, security, and safeguard factors in the design of nuclear facilities, the International Atomic Energy Agency (IAEA) has been promoting Safeguards by Design (SBD) for more than 10 years. "Defined as the consideration of safeguards throughout the lifetime of the facility from preliminary conceptual design to decommissioning" [1] it encourages the consideration of continual integration of safeguards obligations throughout the facility lifecycle. A U.S. DOE National Laboratory project team developed a SBD framework that was dependent upon three pillars: requirements definition (for safeguards performance), design processes, and design toolkit. It was recognized that "successful implementation of SBD is a project management and coordination challenge," articulating the need for continued integration between the key elements [2].

Similar to integration into the design process of objectives for safety [3] to reduce accidents and security to minimize the risk of malicious acts [4], SBD brings a systems-level perspective to the problem. However, most of the SBD open literature focuses on the integration of safeguards hardware into nuclear facilities and not the protection of digital assets, information, and data collection systems critical to safeguards systems. This paper will focus on approaches designed to address the need to protect information from compromise in these complex systems.

## 2. Safeguards Information Assurance by Design (SIAD)

IAEA safeguards are those technical measures used to independently verify that nuclear materials and activities are not diverted from peaceful purposes or misused. It is an essential component of the international nuclear security regime. The independent verification relies on a large volume of data/information from a variety of sources that is collected, stored, integrated, transmitted, and analyzed. The quality of conclusions and decisions that the IAEA can make is based on the timeliness, relevancy, and accuracy of data/information it collects. The timeliness detection goals are well understood and are determined based on nuclear material categories such as: one month for uneradicated direct use material, three months for irradiated direct use material, and one year for indirect use material when no additional protocol is in force [5]. Relevancy of data/information is determined by the IAEA based on objectives and conditions [6]. However, accuracy for data/information is not well understood.

Accuracy is commonly viewed for data as the quality or state of being correct. For physical measurements this is understood to be how close the results come to a true value and is typically addressed through calibration measures, traceable standards [7], chain of custody of samples, etc. Present in this definition is the underlying assumption that the instruments or data streams have not been modified by an adversary. There are also other characteristics that describe the data that need to be considered by the IAEA based on how the data/information will be used such as its confidentiality, integrity, or availability. The term that is often used to describe those measures that protect and defend data/information and data/information systems by ensuring their availability, integrity, authentication, confidentiality, and non-repudiation, is Information Assurance (IA) [8]. Integrating risk identification and assessment methods early in the design process to eliminate data/information compromise throughout the life of the system is information assurance by design (IAD). For Safeguards systems we will refer to this as Safeguards Information Assurance by Design (SIAD).

### 2.1. SIAD is a Lifecycle Challenge

It is never too early in the lifecycle of a system to begin thinking about IA. As early as the conceptualization phase, maintaining IA as a key system objective could influence what approaches and options are available to the IAEA (i.e. joint use equipment versus IAEA owned and operated). This could help eliminate wasting resources researching and developing approaches that could never provide the information confidence needed by the system.

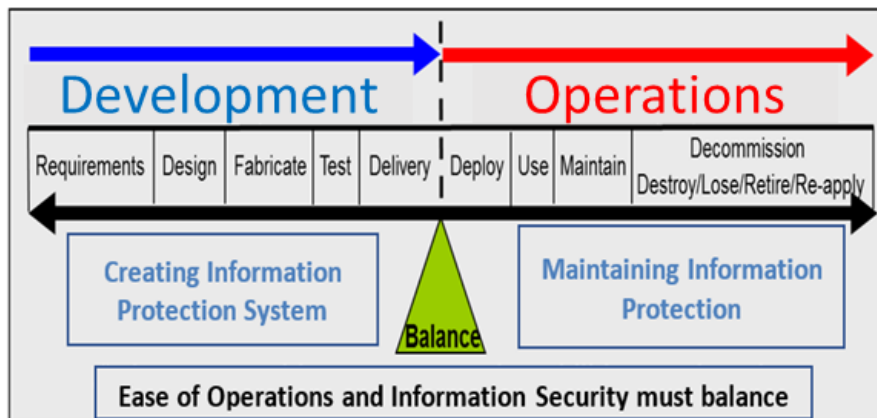


Figure 1 – Technology/system lifecycle with focus on information protection

As shown in Figure 1, the lifecycle of technology can be viewed as a series of discrete steps. Each step presents unique challenges and opportunities for the system or equipment to possess strong IA characteristics and features. During the Development Phase the system is designed and fabricated. This is the best time to establish and implement data/information security requirements due to the design flexibility of the systems and components. Effective communication of requirements with vendors and other stakeholders establishes the expectations that data/information security is a key element of the system. This is extremely important. From a vulnerability standpoint the Development Phase is a prime time for inserting birth defects or attack vectors so strong protections of data/information and supply chain should be used.

In Operations Phase, SIAD is tested against requirements based on intentional attacks or system failures. Being aware of the new attack vendors that can be introduced during the Use and Maintain stages through communications and system updates contributes to the overall system design. In the Operations Phase, upgrades and modifications to a facility that has not previously used a SIAD phase could initiate a SIAD process for any upgrades/modifications.

High security systems can be the most cumbersome to use with passwords, biometrics, processes and procedures designed with one end in mind: security for data/information and the system. Unfortunately, there is still a job that must be done and workers have been known to disable features or disregard rules if they find the security systems burdensome [9]. The balancing of requirements, costs, and performance of systems where IA is needed should be focused on throughout its lifecycle and is supported by SIAD.

## 2.2. Safeguards Information Risks

The types of risks that should be taken into consideration for safeguards information are implied in the pillars of IA and include but are not limited to:

- Confidentiality (compromise of data)
- Integrity (alteration of data)
- Availability (interruption of critical IAEA equipment/services)

Understanding risk related to safeguards system failure is a key component of the SIAD concept. While there are many types of failures to the system that need to be evaluated, such as reliability of components and other non-malicious failure mechanisms, this paper primarily focuses on the intentional intervention into the safeguards system by an actor with malicious intent. This has significant implications in how risk is evaluated. Risk is generally defined as the product of Likelihood and Consequence ( $Risk = Likelihood \cdot Consequences$ ) with Likelihood generally treated as a probability function related to failure of a system or component. When dealing with an intentional act, the probabilistic nature of an event typically is considered 1.0 and, as such, the risk equation doesn't provide useful information. There have been many papers that have described Risk related to an intentional event and it is often described as Risk is the product of Threat, Vulnerability, and Consequences ( $Risk = Threat \cdot Vulnerability \cdot Consequences$ ) [10]. In this representation, the earlier Likelihood variable is replaced with the product of Threat and Vulnerability. This representation assumes Threat and Vulnerability are independent variables but the relationship between them can be complex due to potential inter-dependencies. Wyss, et al., [11] discusses many of the complexities of determining malicious risk to information enterprise systems. Wyss introduces the concept of Difficulty to the risk determination process. Using Difficulty to execute an attack as a surrogate for Likelihood of an attack for an adversary, Wyss postulates the difficulty (work effort) can be approximated and provide some level of quantification for likelihood of an attack.

To adequately determine the risks from a malicious actor, there are several approaches and tools that can be applied to better address the malicious risk to a system and inform design requirements.

### 2.2.1. Threat Model

Threat models are an important part of any SIAD process as it is a key driver for the types of IA design features that need to be implemented into a system. A common approach used for designing a secure system is to bind the threat variable by creating a design basis threat (DBT). IAEA Nuclear Security Series 13 [12] encourages States to develop a DBT for protection of nuclear facilities and IAEA Nuclear Security Series 17 (NSS17) [13] further uses the DBT in guiding computer security for nuclear facility data/information systems. The State DBT's as well as IAEA processes can be used to create a set of adversary metrics for use by the designer of safeguards in their threat model. For example, F. McCrory, et al., [14] combined the generic IDART™ [15] Threat Matrix with the NSS17's attacker profile to create a table on attacker profiles and reproduced it here.

Table 1 shows the NSS17 attacker profiles in the first column and the assigned the generic IDART™ threat model (GTM) level to each profile in column two. Columns three thru eleven combine the two sources' metrics with the result giving a more detailed set of metrics for potential adversary profiles. From this table, a determination of which adversary profiles the system is to be designed to be defended against can be made and the metrics used as inputs to the SIAD requirements.

Table 1 Potential NSS Attacker Profiles Adversary Threat Matrix [14]

		Commitment Category			Resources Category					
NSS Name	GTM #	Intensity	Stealth	Time	Technical Personnel	Computer Knowledge	Physical Security Knowledge	Nuclear Engineering Knowledge	Access	Motivation
Covert Agent	6	Medium	Medium	Weeks to Months	Ones	Medium	Medium	Medium	Medium	Theft of business information, technology secrets, personal information. Economic gain (information selling to competitors). Blackmail.
Disgruntled employee /user	6-	Low	Low	Weeks to Months	Ones	Medium	Medium	Medium	Medium	Revenge, havoc, chaos. Theft of business information. Embarrass employer/other employee. Degrade public image or confidence.
Recreational hacker	8	Low	Low	Days to Weeks	Ones	Low	Low	Low	Low	Fun, status. Target of opportunity. Exploitation of 'low hanging fruits'.
Militant opponent to nuclear power	3 to 7	Medium	Low	Months to Years	Tens	Medium	Medium	Medium	Low	Conviction of saving the world. Sway public opinion on specific issues. Impede business operations.
Disgruntled ex-employee /user	7+	Low	Low	Weeks to Months	Ones	Medium	Medium	Medium	Low	Revenge, havoc, chaos. Theft of business information. Embarrass employer/other employee. Degrade public image or confidence.
Organized Crime	4-5	Medium	Medium	Months to Years	Tens of Tens	Medium	Medium	Medium	Medium	Blackmail. Theft of nuclear material. Extortion (financial gain). Play upon financial and perception fears of business. Information for sale (technical, business or personal).
Nation State	1 or 2	High	High	Years to Decades	Hundreds	High	High	High	High	Intelligence collection. Building access points for later actions. Technology theft.
Terrorist	2 or 3	High	Medium	Months to Years	Tens of Tens	Medium	Medium	Medium	Medium	Intelligence collection. Building access points for later actions. Chaos. Revenge. Impact public opinion (fear).

**2.2.2. System characteristics**

If an adversary has knowledge of the information system, it enables them to tailor and focus their attacks on vulnerable elements. Control of system information is often an underappreciated aspect of IA and is a key component of the SIAD process. If an adversary has no information about the system, it is nearly impossible to craft a successful attack. Turner, et al., [16] discusses three essential elements that an adversary needs to plan a successful attack: Information, Access (Vulnerabilities), and Technology (Adversary Capabilities). This can be represented as a simplified Venn diagram, Figure 2. The overlap of the Venn diagram is where an adversary needs to get to be confident in a successful attack and can be considered the attack surface for implementing the attack. If information is limited as part of the SIAD, then the complexity of the work effort (difficulty) needed to achieve a successful attack increases and the risk of an attack decreases.

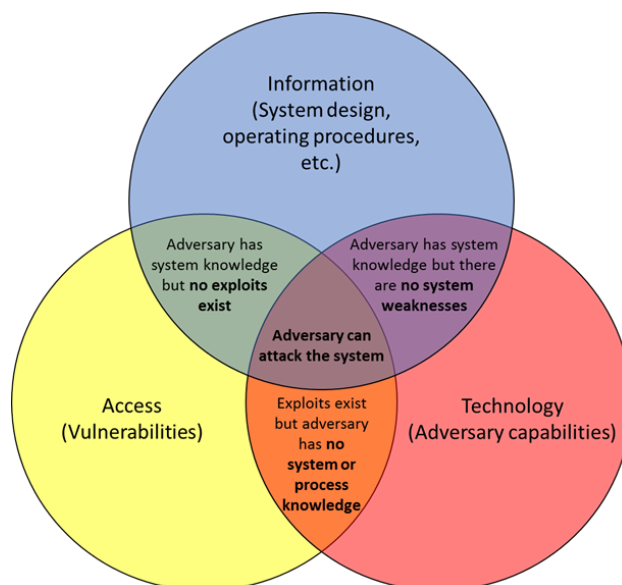


Figure 2 Elements Needed for a Successful Cyber Attack [16]

### 2.2.3. Vulnerabilities and Access

Vulnerabilities and Access (physical and logical) of IA systems is a widely studied area with multiple state generated documents on how to protect these systems. As such, this paper does not discuss the generalities of this related to SIAD.

## 3. SIAD Approaches, Methods, and Tools

Information assurance for IAEA Safeguards data/information is particularly challenging due to the limited community where the instruments are manufactured and deployed, increasing cyber skills of the adversary, growing reliance on digital systems, globalization of digital components and systems, and the growing safety and security responsibilities and concerns for plant operators.

### 3.1. Supply Chain Risk Management

Supply Chain Risk Management (SCRM) is a recognized critical element of any comprehensive cybersecurity systems [17] and has been addressed in detail by the authors [18]. The increased reliance on digital systems, subsystems, and components compounded with the increased functionality of hardware, complexity of software, and globalization of the digital supply chain has created a nexus of IA security concerns.

A particularly challenging aspect of securing the supply chain for IAEA technologies is the small number of equipment suppliers available and the unique equipment they deploy. Blind buys often are not an option for this community, equipment numbers are relatively limited, and they are expected to have long design life. These factors make IA particularly challenging and highlight the need for SIAD sharing information security requirements and objectives throughout the system lifecycle.

Creating a comprehensive SCRM program can be very cost intensive. A SCRM policy for safeguards should be created early in the SIAD process. Edwards [19] provides a high-level presentation on supply chain decision analytics and can be the basis for a SCRM program and includes a Decision Analytics Framework with the following attributes:

- Decision Analytics Framework
- Supply Chain Mapping
- Vulnerability & Mitigation Modeling
- Risk Assessment
- Optimization

### 3.2. Risk Management

Identifying, assessing, and controlling threats and vulnerabilities are a key part of any SIAD program and like SIAD should be addressed over the lifecycle of the safeguards systems. A risk management program, to address these threats and vulnerabilities, should evolve over time as threats advance and vulnerabilities become known. There are many risk management methods and frameworks that can be utilized with varying utility for data/information systems. The Electric Power Research Institute has published a technical assessment methodology [20] that provides a detailed method for assessing risk related to nuclear power plant critical digital assets. This method could be adapted to safeguards systems. Additionally, Clark, et al., [21] has published a paper on hazard and consequence analysis for digital systems that provides a risk method that leverages traditional Probabilistic Risk Assessments, Systems-Theoretic Process Analysis, and Fault Tree Analysis methods. These methods in conjunction with methods related to Table 1 provide some methodologies to support a rigorous risk management program.

### 3.3. Modeling and Simulation

Modeling and simulation (M&S) is used throughout engineering to provide insight to system design features, explore design space without physically building systems, evaluate various architectures to explore system resiliency to threats, perform optimization studies, explore impacts to current systems from modifications and upgrades, and many other purposes. As SIAD is a lifecycle problem, a Modeling framework that explores the M&S space from threat to consequence and recovery is needed.

#### 3.3.1 Modeling Framework

A Modeling framework, that connects multiple types of Modeling domains, developed by Sandia National Laboratories to explore the impact of an event and the threat that could initiate it in the cyber and/or physical realms has been reported [22]. The framework, Integrated Cyber Physical Impact Analysis (ICPIA™), was first developed to explore cyber impact to critical infrastructures. This resulted from the many questions being asked regarding the possible impact of cyber events and the threats that could create particular consequences. This modeling framework covers the event from the threat capability needed to initiate the event and to recovery from the event.



Figure 3 Integrated Cyber/Physical Impact Analysis Framework

A framework such as ICPIA™ can help a design process make architectural decisions and explore the impacts that various threats have on a system through their potential consequences.

Threat modeling, discussed in Section 2.2.1, is helpful in determining the types of vulnerabilities that the adversary could exploit and the resultant potential consequences (Event Model). For data/information systems this modeling of an exploit could have a physical or logical impact on a component within the system. This often requires its own component (sub-system) model (e.g. a field-programmable gate-array or programmable logic device). The exploited component behaviour would then result in a system response that would create a consequence of concern such as data interruption, alteration, substitution, theft, etc. After a consequence has been achieved, recovery from the consequence is another set of modeling tools.

For SIAD network modeling, there are many open source and for-purchase software packages that can be used to develop a relatively high-fidelity model of the network and often the vendors of various components, such as routers or switches, will provide a model of their component. Models of various operating systems can often be utilized directly using the software of concern or can be modeled with various fidelity for many end users within the overall model. For operational technology systems (OT) (control systems), modeling tools are relatively limited. Additionally, modeling of IT and OT systems impact on physical systems is even limited further. SCEPTRE [23] [24] is a modeling tool that couples digital systems to physical environments. Tools like SCEPTRE are useful in the transition modeling between a cyber event and an actual physical impact.

### 3.4. Architectural Approaches

Utilizing the SIAD approach for data/information systems could result in reduction of the overall lifecycle cost of implementing safeguards in a nuclear facility.

Understanding the likely threat that a system could face supports in the identification of threat vectors into the system. This then allows for designing an architecture not susceptible to the threat vector, identifying type and location of intrusion sensors needed to promptly identify when compromise occurs, developing redundant or diverse ways of providing the needed data/information should one channel be compromised, or other approaches based on the threats and their capabilities that are identified. Evaluation of the necessity to isolate the safeguards data/information system from business networks and/or internet potentially can have a significant impact to the overall security of the system. A system isolated from business networks and the internet remove certain classes of attack but can still be vulnerable from other classes of attacks such as the supply chain or insiders.

Designing the safeguards IA system in a tiered manner so that the most critical data/information, determined through risk-informed analysis and M&S, has layered protections, often called defense-in-depth. The IAEA recently published NP-T-2.11 [25] which focuses on architectural approaches for nuclear power plants and has many best practices that can benefit SIAD. These include discussions around defense-in-depth, independence, categorization of system functions, computer security zones, elimination of unnecessary complexity, etc.

### 3.5. Red Teaming

Red teaming has many definitions. For the purposes of this paper, we use the Sandia National Laboratories definition from their Information Design Assurance Red Teaming (IDART™) [15] method. This states that red teaming is an “authorized, adversary-based assessment for defensive purposes.” IDART™ defines eight different types of red teaming: design assurance, hypothesis testing, benchmarking, behavioral red teaming, gaming, operational red teaming, penetration testing, and analytical red teaming. For SIAD, we will briefly discuss the most applicable red teaming types: design assurance, analytical, and penetration testing. It should be recognized that the other types of red teaming have potential value to SIAD depending on the questions that need to be answered.

#### 3.5.1 Design Assurance Red Teaming

Design Assurance red teaming is conducted early in the lifecycle to provide an adversary’s perspective. It is typically applied as soon as a preliminary architecture of the system is defined. It is useful if the design basis threat or the threat actor is defined to ensure that the red team only simulates the adversary capability of concern. If the adversary level emulated is too high, then the red team may provide unnecessary suggestions that would increase the cost of the system. If the adversary is defined as too low of a level, the red team might not provide enough feedback and potentially leave the system inadequately protected. Design Assurance red teaming should be performed during lifecycle processes that include development of designs.

#### 3.5.2 Analytical Red Teaming

Analytical red teaming performs a detailed adversary-based assessment of the system and uses threat-based M&S tools to help identify how an attacker would approach exploiting the safeguards system. Typically, the red team generates attack graphs that can be analysed for their difficulty in exploitation generating risk-informed information identifying the weakest components with an architecture. The red team starts with the consequences of concerns on the right side of the graph and access points on the

left side of the graphs. Working with the system designers and subject matter experts, attack paths between access points are identified that lead to a consequence of concern. The various attack paths are then rank ordered based on execution difficulty, providing critical information to designers. Often multiple attack paths go through a single node that once identified can be rearchitected to remove that series of attack paths. This method can result in large numbers of attack paths depending on the complexity of the system. This method should also be performed in the design stage before the final design is set.

### 3.5.3 Penetration Red Teaming

Penetration red teaming is performed once a design has been built, but before fielding if possible. Penetration testing uses a host of tools that looks for vulnerabilities within an information system and then attempts to exploit those vulnerabilities. Penetration testing should be performed periodically throughout the lifecycle on a system since new vulnerabilities to various IT systems are continuously being discovered that might be exploited by an adversary or the design basis threat could evolve.

## 4. Conclusions

Designing information assurance into the architecture of a safeguards system can significantly reduce data/information vulnerability cost effectively while improving the trust of the data/information. SIAD is the integration of risk identification and assessment methods early in the design process to eliminate data/information compromise throughout the life of the safeguards systems. Some approaches used in physical security can be adopted or leveraged for cyber security but there are critical differences when evaluating risk. Due to the evolving capabilities of adversaries and insertion of possible vulnerabilities throughout its lifecycle, continual risk identification and assessment methods for data/information systems is required to ensure data/information is not compromised.

It is important to remember:

- Data/information systems present vulnerabilities and risks throughout their lifecycle. These do not end when design is finalized, built, deployed or even decommissioned.
- It is necessary to control distribution of details regarding information system operations or vulnerabilities. Knowledge of the system arms an adversary.
- Adversaries evolve over time and continual reexamination of the data/information system vulnerabilities and risks is critical to ensuring its dependable performance.
- There is no such thing as a standalone or isolated system. Protection is needed for all sensitive digital assets with a graded approach applied.

## 5. Acknowledgements

Sandia National Laboratories is a multimission laboratory managed and operated by National Technology & Engineering Solutions of Sandia, LLC, a wholly owned subsidiary of Honeywell International Inc., for the U.S. Department of Energy's National Nuclear Security Administration under contract DE-NA0003525. SAND2019-5166 R

## 6. References

- [1] International Atomic Energy Agency, «IAEA Nuclear Energy Series, NP-T-2.8, International Safeguards in Nuclear Facility Design and Constructionq,» IAEA, Vienna, 2013.
- [2] T. Bjornard, R. Bean, P. C. Durst, J. Hockert e J. Morgan, «Implementing Safeguards-by-Design, INL/EXT-09-17085,» Idaho National Laboratory, Idaho Falls, 2010.
- [3] DOE-STD-1189-2016, «Integration of Safety into the Design Process,» U.S. DOE AU Office of Environment, Health, Safety and Security, Washington, 2016.
- [4] C. J. S. J. a. C. S. M.K. Snell, «Security-by-Design Handbook,» SAND2013-0038, Sandia National Laboratories, 2013.

- [5] IAEA, «IAEA Safeguards Glossary, 2001 Edition, International Nuclear Verification Series No. 3,» International Atomic Energy Agency, Vienna, 2002.
- [6] IAEA, «Safeguards Implementation Practices Guide on Provision of Information to the IAEA, IAEA Services Series 33,» International Atomic Energy Agency, Vienna, 2016.
- [7] Chemicool Dictionary, «Definition of Accuracy,» 2017. [Online]. Available: <https://www.chemicool.com/definition/accuracy.html>. [Consultato il giorno 23 04 2019].
- [8] National Institute of Standards and Technology, U.S. Department of Commerce, «Information Technology Laboratory, Computer Security Resource Center (CSRC), Glossary, information assurance (IA),» [Online]. Available: <https://csrc.nist.gov/glossary/term/information-assurance>. [Consultato il giorno 23 04 2019].
- [9] Kaspersky Lab Daily, «The Human Factor in IT Security: How Employees are Making Businesses Vulnerable from Within,» Kaspersky Lab, 2019. [Online]. Available: <https://www.kaspersky.com/blog/the-human-factor-in-it-security/>. [Consultato il giorno 05 05 2019].
- [10] U.S. Department of Homeland Security Risk Steering Committee, «Risk Lexicon,» U.S. Department of Homeland Security, Washington, D.C., September 2008.
- [11] G. Wyss e et al., «A Method for Risk-Informed Management of Enterprise Security (RIMES), SAND2013-9218,» Sandia National Laboratories, Albuquerque, 2013.
- [12] International Atomic Energy Agency, «IAEA Nuclear Security Series No. 13, Nuclear Security Recommendations on Physical Protection of Nuclear Material and Nuclear Facilities (INFCIRC/225/Revision),» IAEA, Vienna, 2011.
- [13] International Atomic Energy Agency, «IAEA Nuclear Security Series No. 17, Computer Security at Nuclear Facilities,» IAEA, Vienna, 2011.
- [14] F. Mitch McCrory, R. Parks e R. Hutchinson, «An Adversary's View of Your Digital System,» in *IAEA-CN-228-54*, Vienna, 2015.
- [15] Sandia National Laboratories, «Information Design Assurance Red Team,» [Online]. Available: <https://idart.sandia.gov/>. [Consultato il giorno 02 05 2019].
- [16] P. L. Turner, F. M. McCrory e L. A. Dawson, «Nuclear Power Plant Instrumentation and Control Cyber Security High Value Access Points Leading to Relational Common Cause Failure,» in *10th International Topical Meeting on Nuclear Power Plant Instrumentation, Control, and Human Machine Interface Technologies*, San Francisco, 2017.
- [17] S. R. Chabinsky, «Cybersecurity Strategy: A Primer for Policy Makers and Those on the Front Line,» *Journal of National Security Law & Policy*, vol. 4, p. 27, 2010.
- [18] F. M. McCrory, G. K. Kao e D. S. Blair, «Supply Chain Risk Management: The Challenge in a Digital World,» in *International Conference on Computer Security in a Nuclear World: Expert Discussion and Exchange*, Vienna, 2015.
- [19] N. J. Edwards, «Supply Chain Decision Analytics: Application & Case Study for Critical Infrastructure Security,» 2016. [Online]. Available: <https://www.osti.gov/servlets/purl/1347081>. [Consultato il giorno 02 05 2019].
- [20] Electric Power Research Institute, «Cyber Security Technical Assessment Methodology: Risk Informed Exploit Sequence Identification and Mitigation, Revision 1,» EPRI, Charlotte, 2018.
- [21] A. J. Clark, A. D. Williams, A. Muna e M. Gibson, «Hazard and Consequence Analysis for Digital Systems - A New Approach to Risk Analysis in the Digital Era for Nuclear Power Plants,» in *Transactions of the American Nuclear Society, Vol. 119*, Orlando, 2018.
- [22] L. A. Dawson e F. M. McCrory, «ICPIA and Red Teaming,» in *ESARDA Symposium 2019, 41st Annual Meeting*, Stresa, 2019.
- [23] Sandia National Laboratories, «SCEPTRE,» SNL, 2019. [Online]. Available: <https://www.osti.gov/servlets/purl/1376989>.
- [24] Sandia National Laboratories, «SCEPTRE Demonstration,» Vimeo, <https://vimeo.com/178492617>, Albuquerque, 2017.
- [25] International Atomic Energy Agency, «Approaches for Overall Instrumentation and Control architectures of Nuclear Power Plants, IAEA Nuclear Energy Series, NP-T-2.11,» IAEA, Vienna, 2018.

# The GIF Proliferation Resistance and Physical Protection Methodology Applied to GEN IV System Designs: An Update

L.Y. Cheng<sup>1</sup>, G.G.M Cojazzi<sup>2</sup>, G. Renda<sup>2</sup>, B. Cipiti<sup>3</sup>, B. Boyer<sup>4</sup>, G. Edwards<sup>5</sup>,  
E. Hervieu<sup>6</sup>, K. Hori<sup>7</sup>, H. Kim<sup>8</sup>, P. Peterson<sup>9</sup>

<sup>1</sup> Brookhaven National Laboratory, Upton, NY 11973-5000, USA

<sup>2</sup> European Commission, Joint Research Centre (JRC), Ispra, Italy

<sup>3</sup> Sandia National Laboratories, Albuquerque, NM, USA

<sup>4</sup> International Atomic Energy Agency, Austria

<sup>5</sup> Canadian Nuclear Laboratories, Canada

<sup>6</sup> Commissariat à l'énergie atomique et aux énergies alternatives, Paris, France

<sup>7</sup> Japan Atomic Energy Agency, Vienna office, Vienna, Austria

<sup>8</sup> Korea Atomic Energy Research Institute, Daejeon, Republic of Korea

<sup>9</sup> University of California Berkeley, CA, United States of America

E-mail: <sup>1</sup> [cheng@bnl.gov](mailto:cheng@bnl.gov), <sup>2</sup> [giacomo.cojazzi@ec.europa.eu](mailto:giacomo.cojazzi@ec.europa.eu), [guido.renda@ec.europa.eu](mailto:guido.renda@ec.europa.eu),  
<sup>3</sup> [bbcipit@sandia.gov](mailto:bbcipit@sandia.gov), <sup>4</sup> [b.boyer@iaea.org](mailto:b.boyer@iaea.org), <sup>5</sup> [geoffrey.edwards@cnl.ca](mailto:geoffrey.edwards@cnl.ca), <sup>6</sup> [eric.hervieu@cea.fr](mailto:eric.hervieu@cea.fr),  
<sup>7</sup> [hori.keiichiro@jaea.go.jp](mailto:hori.keiichiro@jaea.go.jp), <sup>8</sup> [khd@kaeri.re.kr](mailto:khd@kaeri.re.kr), <sup>9</sup> [peter@nuc.berkeley.edu](mailto:peter@nuc.berkeley.edu)

## Abstract:

*The Generation IV International Forum (GIF) formed a proliferation resistance and physical protection (PR&PP) Working Group (PRPPWG) to develop a methodology to evaluate the six GIF reactor technologies. The PRPPWG developed the methodology through a series of development and demonstration case studies and many insights were gained from the process. The PRPPWG, in collaboration with representatives of the GIF System Steering Committees/provisional Steering Committees (SSCs/pSSCs) for each of the six GIF reactor technologies, analyzed and evaluated the PR&PP aspects of the six reactor technologies. The outcome of this activity is documented in a joint PRPPWG and SSCs/pSSCs report made publicly available in 2011, highlighting the analysis performed and its main outcomes. Currently, the PRPPWG and the six GIF SSCs/pSSCs are in the process of repeating the exercise, based on the status of the six GIF system design concepts, considering the designs' evolution since 2011. In line with the PR&PP by Design concept, whilst during the first exercise the level of detail of the design options enabled only a high-level evaluation of the systems' proliferation resistance, the early design stage allowed designers to introduce modifications for improving the systems' performance. With the designs' current level of development, the opportunity for proposing modifications diminishes, whilst at the same time increasing the opportunity to inform the safeguards R&D community on potential R&D needs to meet safeguardability issues. The paper will first summarize the main concepts behind the PR&PP evaluation methodology. It will then present the main outcomes and lessons learned as in the current white papers on the PR aspects of the six GIF design concepts and will finally describe the ongoing activity to update them within a PR&PP-by-Design context.*

**Keywords:** GIF; Generation IV reactors; proliferation resistance; safeguardability

## 1. Introduction

The Generation IV International Forum (GIF) Proliferation Resistance & Physical Protection Working Group (PRPPWG) was formed in 2002 to investigate tools and measures to analyse the proliferation resistance and physical protection robustness of the six GIF reactor technologies and support the GIF designers in meeting the PR&PP goal set out in the 2002 GIF Roadmap ("Generation IV nuclear energy systems will increase the assurance that they are a very unattractive and the least desirable route for diversion or theft of weapons usable materials, and provide increased physical protection

against acts of terrorism” [1]). The group developed a Proliferation Resistance & Physical Protection Evaluation Methodology (PRPPEM) that was refined over the years through selected case studies documented in reports (see e.g. [2]) and articles (see e.g. [3]). The PRPPEM is currently in its sixth revision [4].

Since 2007 the PRPPWG and the GIF System Steering Committees (SSCs/pSSCs) interacted regularly to discuss the status of each system design with respect to PR&PP. These interactions resulted in the publication of a PRPPWG and GIF SSCs/pSSCs joint report including white papers delineating the main PR&PP features of the six GIF reactor technologies [5]. The report addresses also a number of crosscutting issues common to the GIF technologies.

The PRPPEM undertakes a holistic approach to evaluate the proliferation resistance and physical protection characteristics of nuclear systems. In evaluating the response of a nuclear system against PR&PP threats, the methodology considers not only intrinsic features (by nature of the design) but also extrinsic features (per institutional and regulatory requirement) that account for existing nuclear safeguards and security measures and techniques. The PRPPEM provides a tool for various stakeholders to evaluate potential modifications in design and safeguards approaches to enhance the safeguardability [6] of nuclear systems in terms of efficiency and effectiveness. This resulted in a widespread involvement of many PRPPWG members in other international initiatives and concepts like those of the IAEA on Safeguards by Design (SbD) and INPRO. These efforts facilitated synergies and cross-fertilization between the various initiatives and gained a larger audience in the nuclear reactor design community. Many national programmes applied –directly or through adaptations– the PRPPEM in their studies and activities (see e.g. [7-14]). To keep track and cognizance of the use of the PRPPEM inside and outside GIF, the group maintains and updates annually a bibliography collecting articles, papers and reports. This bibliography is available on the GIF PR&PP external website [15].

Building on previous publications [16, 17], the paper first summarizes the main concepts behind the PR&PP evaluation methodology [4]. It then summarizes the main outcomes and lessons learned focusing in the current white papers looking at the PR aspects of the six GIF reactor technologies [5]. It describes the ongoing activity to update them, and presents some reflections to support the PR&PP by design concept.

## 2. The GIF PR&PP Evaluation Methodology

Starting in 2002, the GIF PRPPWG investigated the possibility to analyse and evaluate the proliferation resistance and physical protection robustness of an innovative nuclear energy system design, aiming at developing a methodology that could be used inter alia by GIF system designers to evaluate the designs under consideration against the GIF PR&PP goal. The activity led to the definition of an overall framework inspired by the risk & safety domain, and after a series of revisions and case studies, GIF PRPPWG produced its sixth revision [4] which was approved by GIF for open publication. Figure 1 illustrates the methodology’s paradigm (top) and its framework main evaluation steps (bottom).

The evaluation framework, via a pathway analysis, assesses the response of the system to different challenges, i.e. the threats. Pathways are potential sequences of events/actions followed by a proliferant state or adversary to achieve its objective (proliferation, theft, or sabotage). A pathway is composed of segments, where each segment is characterized by an action, target, and system element. The results of the system response are expressed in terms of PR&PP measures. Measures are the high-level characteristics of a pathway that affect the likely decisions and actions of an actor and therefore are used to evaluate the actor’s likely behaviour and the outcomes. For PR, the measures are [4]: proliferation technical difficulty (TD), proliferation cost (PC), proliferation time (PT), fissile material type (MT), detection probability (DP) and detection resource efficiency (DE). Each PR measure represents major system characteristics that would be important impediments to the strategy of a proliferant nation attempting diversion, misuse or breakout. For PP, the measures are [4]: probability of adversary success (PAS), consequences (PPC) and PP resources (PPR). Each PP measure assesses major system characteristics that would be important impediments to the strategy of a non-host-state group attempting theft of material or sabotage of a facility.

The GIF PRPPWG created a case study [2] to develop, test, improve and demonstrate the PRPEM after its initial rollout. The case study report [2] highlighted the importance and the potential of starting the analysis with a qualitative approach. By following the PRPEM evaluation framework, a qualitative estimation of the PR measures associated with the identified pathways is often informative enough to provide valuable feedback to system designers even at the very early design stages. A qualitative analysis, on the other hand, needs detailed guidance for use in the framework of the PRPEM and requires the availability of experienced domain experts who can work in synergy with PR&PP experts.

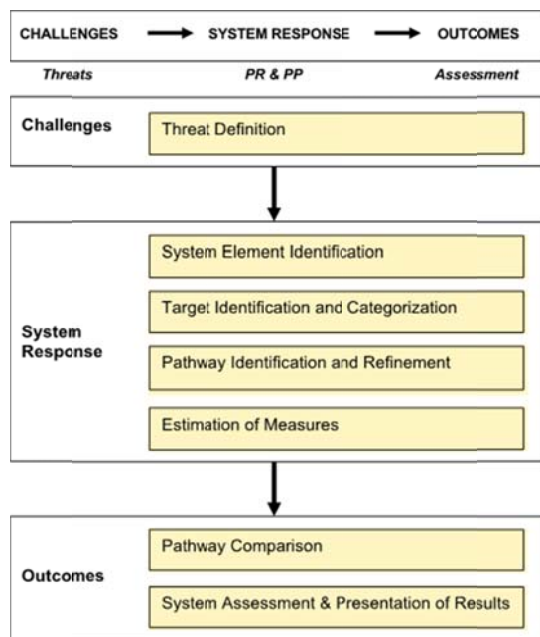


**Figure 1:** Basic paradigm (top) and evaluation framework for the PR&PP Evaluation Methodology (bottom). (Image: PRPPWG [4])

### 3. Interactions with the GIF Systems Steering Committees

Since 2007 the PRPPWG and the six SSCs/pSSCs held several workshops to discuss the PR&PP characteristics of the considered systems designs and to identify where R&D was needed to ensure that each design could reach the desired PR aims. The collaborating groups systematically collected the design information needed to investigate the PR&PP of the concept under consideration, and their analysis culminated in a series of internal reports, referred to as “white papers” inside GIF. These “white papers” were the outcome of the joint effort of the PRPPWG and the six GIF SSCs/pSSCs and represented the first comprehensive effort to highlight the PR&PP strength of the GIF systems. The “white papers” also recommended practicable ways to optimize their PR&PP performance where weaknesses existed in the designs. The “white papers” were a key part of an overall public report made available in 2011 [5]. Table 1 reports the six GIF reactor technologies and the main system design options discussed in the report, together with a mention of the analysis performed.

In addition to the description and evaluation of the GIF design options, the report identified crosscutting aspects (such as the fuel type and refuelling modes, coolants, moderators, fuel cycle architectures, safeguards, safety, economics [5]) common to all six reactor technologies that could be the subject of ad hoc studies. The report also identified the importance of considering not only the reactor but also the fuel cycle needed by the reactor. The fuel cycle might not always require an in-depth PR&PP analysis, but the context might help in identifying potential PR&PP sensitivities in the front-end or the back-end of the fuel cycle as required by the GIF options under consideration.

In April 2017 the PRPPWG organized a joint workshop in Paris with the participation of representatives of all six SSCs/pSSCs, representatives of the GIF Senior Industry Advisory Group Panel (SIAP) and the IAEA. The Paris workshop provided a forum to refresh the main aspects of the

PRPEM and the corresponding “PR&PP by Design” concept, and to update the PRPPWG on the evolutions and current status of the six GIF reactor technologies. In addition, the workshop indicated possible aspects for further interaction and collaboration between the PRPPWG and the SSCs/pSSCs to increase the use of the PR&PP Evaluation Methodology among system designers.

GIF System	System Options considered in [5]	Design Tracks considered in [5]	PR&PP Evaluation
GFR	Reference Concept	2400MWt GFR <sup>1</sup>	Used reference GFR in the evaluation
LFR	Large System	ELSY	Discussed special features of the two design tracks in the evaluation
	Small Transportable	SSTAR	
MSR	Liquid Fuel	MSFR MOSART <sup>2</sup>	Only used the MSFR design based on the Th fuel cycle (breeder option) in the evaluation
	Solid Fuel	AHTR <sup>3</sup>	
SCWR	Pressure Vessel	Thermal core (HPLWR)	Used generic system elements based on BWR and fuel reprocessing facility in the evaluation
		Fast core (Super Fast Reactor)	
SFR	Pressure Tube Loop Configuration	Thermal core (CANDU) JSFR	Used generic SFR system elements in the evaluation
	Pool Configuration	KALIMER	
	Small Modular	SMFR	
VHTR	Prismatic Fuel Block	AREVA Modular HTR (ANTARES)	Used generic VHTR system elements in the evaluation
		General Atomics GT-MHR Russian OKBM GT-MHR JAEA GTHTR300C KAERI NHDD	
	Pebble Bed	Westinghouse/South African PBMR HTR-PM (China)	

<sup>1</sup> UPuC or UPuN ceramic fuel.

<sup>2</sup> Not considered in detail, only mentioned in a footnote.

<sup>3</sup> Not considered in detail, only mentioned in a footnote.

**Table 1:** System designs considered by the 2011 GIF PRPPWG & SSC/pSSC “white papers”.

The workshop highlighted that in most cases the design options under consideration either significantly evolved or changed since the 2011 joint report. The participants acknowledged the opportunity to update the existing PR&PP “white papers” to reflect the current systems under consideration and their evolution in recent years. In the aftermath of the workshop, the PRPPWG produced an updated white paper template to be used as guideline for the type of information and structure of the new documents. Table 2 reports the high-level structure of the updated template, together with some of the information requested for each section.

While sections 1 and 2 of the template should be compiled by the SSCs/pSSCs, sections 3 to 6 of the template should be compiled jointly by the PRPPWG (providing the knowledge of the PR&PP domain) and the SSCs/pSSCs (providing the detailed knowledge of the system designs under consideration).

In characterizing the PR&PP features of a design, the analyst evaluates the design against potential threats using the technical design information to gauge the response of the system. Figure 2 provides a sample of typical PR questions that facilitate the evaluation of a design against the diversion of material or the misuse of a facility to manufacture material covertly. In the White Papers update, the response is analysed by discussing qualitatively the system’s response to the four identified PR

strategies (diversion, misuse, breakout, replication of technology in clandestine facilities) and the two PP strategies (theft, sabotage).

Section	Type of Information Requested
1. Overview of Technology	Description of the various design options in terms of their major reactor parameters, such as: core configuration, fuel form and composition, operating scheme and refueling mode, fresh/spent fuel storage and shipment, safety approach and vital equipment, physical layout and segregation of components, etc.
2. Overview of Fuel Cycle(s)	High level description of the type, or types, of fuel cycles that are unique to this Gen IV system and its major design options. Information such as recycle approach, recycle technology, recycle efficiency, waste form(s)
3. PR&PP Relevant System Elements and Potential Adversary Targets	For each design option, identification and description of the relevant System Elements and their potential Adversary Targets, Safeguards and Physical Security Approaches
4. Proliferation Resistance Features	High-level, qualitative overview developed jointly by the SSC and the PR&PP working group, to identify and discuss the features of the system reference designs that create potential benefits or issues for each of the representative proliferation threats. Ideally the section should highlight the response of the system to a) the concealed diversion or b) production of material, c) the use of the system in a breakout strategy, and d) the replication of the technology in clandestine facilities
5. Physical Protection Features	High-level, qualitative overview developed jointly by the SSC and the PR&PP working group, to discuss those elements of the system design that create potential benefits or issues for potential subnational threats, with specific discussion on the general categories of PP threats (a) theft of material for nuclear explosives or dispersal device and b) radiological sabotage)
6. PR&PP Issues, Concerns and Benefits	Review of the outstanding issues related to PR&PP for the concepts and their fuel cycles, the areas of known strength in the concept, and plans for integration and assessment of PR&PP for the concept. This section would ideally terminate with a bullet list of identified PR&PP R&D needs for the system concept.

Table 2: High level structure of the updated PR&PP white paper template.

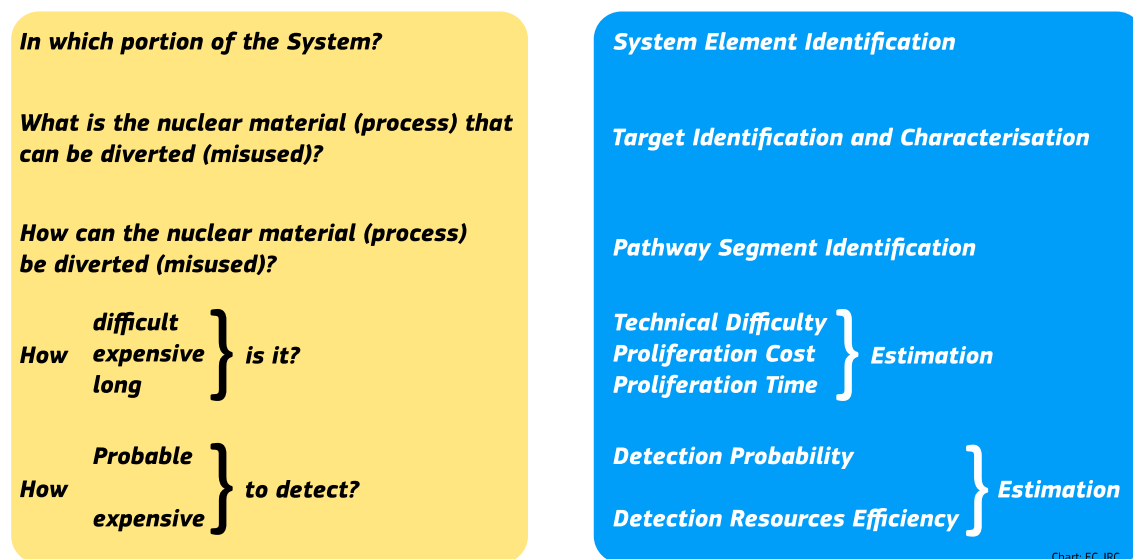


Figure 2: Some key questions for diversion and misuse scenarios.

Table 3 illustrates the relevance of the technical information supplied by sections 1 and 2 of the white papers to the PR&PP evaluation. A key feature of the analysis is that the impact of the technical parameters on each of the PR and PP measures is highly scenario or pathway dependent. The analysis characterizes the system-wide response to a threat or challenge by aggregating the PR & PP measures of the intervening segments along each pathway.

Parameter	Main PR Relevance	Main Affected Measures (PR)
<b>SECTION 1</b>		
Fuel Form	Diversions/Misuse	MT, TD
Main Fertile Material	Misuse	TD, PT
Fissile Material	Diversions	MT, DP
Weight of Assembly	Diversions	TD, DP
Dimensions of Fuel Assembly	Diversions	TD, DP
Fuel Enrichment	Diversions	MT
Source of Fissile Material	Diversions	
Fuel Inventory	Diversions	PT, DP
Presence and Type of Fertile Blanket	Misuse	TD
Presence and Type of Transmutation Targets	Misuse	MT, DP
Number of Assemblies to Make 1 SQ	Diversions	TD, PT, DP
Irradiation Scheme	Diversions/Misuse	MT, TD, PT
Composition and Burnup of Spent Fuel Elements	Diversions	MT, TD, PT, PC, DP
Composition of Fresh Fuel Elements	Diversions/Misuse	MT, TD, PT, DP
Fuel Storage and Intra-Site Transport Methods	Diversions	TD, PT, DP
Safety Approach and Vital Equipment	(PP)	
Physical Arrangement (layout, segregation, etc)	Diversions/(PP)	TD, PT, DP
<b>SECTION 2</b>		
Recycle Approach	Diversions/Misuse	ALL
Recycle Technology	Diversions/Misuse	ALL
Recycle Efficiency	Diversions/Misuse	ALL
Waste Form(s)	Diversions/Misuse	ALL

**Table 3:** Relevance of technical design information.

Application of safeguards is a requirement where the energy system is in a non-nuclear weapon state (NNWS) and is as a premise of the PR evaluation. The probability of detecting a proliferation act is contingent on the effectiveness of safeguards approaches implemented on the nuclear system. In general, different material protection, control and accounting (MPCA) measures apply to system elements that store or manufacture special nuclear materials (SNM). Figure 3 shows an example of the system elements for a VHTR. The PR&PP evaluation will assess the effectiveness or robustness of the safeguards and physical protection of the targets within the system elements.

The updating of the former white papers is an ongoing activity. Table 4 summarizes the system options and design tracks candidates for inclusion in the white paper updates. The current roadmap foresees the completion of the activity in the later part of the year.

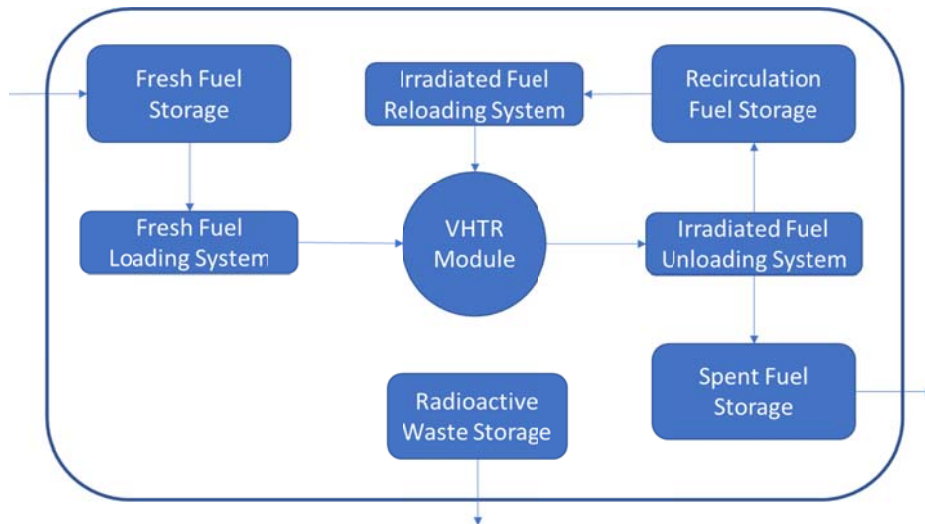


Figure 3. Example of system elements for a notional VHTR.

GIF System	System Options considered in update	Design Tracks considered in update	Comment
GFR	Reference Concept	2400MWt GFR Mentions ALLEGRO as a GFR demonstrator	Other GEN IV designs include: EM2 (GA) ALLEGRO (V4G4) HEN MHR (High Energy Neutron Modular Helium Reactor) (CEA-ANL and GA-AREVA)
LFR	Large System	600 MWe (ELFR)	These are the three reference design configurations discussed in the GIF LFR System Research Plan
	Intermediate System	300 MWe (BREST-OD-300)	
	Small Transportable	20 MWe (SSTAR)	
MSR	Circulating Fuel	MSFR, MOSART, MCFR, etc. Dual Fluid Reactor	There is a wide variety of MSR technologies, encompassing thermal/fast spectrum reactors, solid/fluid fuel, burner/breeder modes, Th/Pu fuel cycles, and onsite/offsite fissile separation.
	Fixed Fuel	Fuel in tubes: Stable Salt Reactor Solid Fuel: TMSR-SF1, Kairos	
	Replaceable Core	IMSR	
SCWR	Pressure Vessel	Thermal core (HPLWR) (EU) Super Fast Reactor (Japan) Thermal core (Japan) Thermal core (China) Mixed spectrum (China) Thermal core (EU) Fast core (RF)	Most concepts are based on "familiar" technology, such as, light-water coolant, solid fuel assemblies, and batch refuelling. Implementation of Th and Pu fuel cycles creates additional special nuclear materials of concern.
		Pressure Tube	
SFR	Loop Configuration	JSFR	Expect key PRPP issues to be tied to fuel handling, TRU inventory and fuel cycle options.
	Pool Configuration	ESFR, BN-1200, KALIMER-600	
	Small Modular	AFR-100	

GIF System	System Options considered in update	Design Tracks considered in update	Comment
VHTR	Prismatic Fuel Block	AREVA Modular HTR (ANTARES)	SC-HTGR is a follow on of the ANTARES and the GA GT-MHR development. Expect some PR&PP differences between the prismatic block and pebble bed design.
		Framatome SC-HTGR	
		General Atomics GT-MHR	
		OKBM GT-MHR	
		JAEA GTHTR300C	
		KAERI NHDD	
	Pebble Bed	X-Energy Xe-100 HTR-PM (China)	

**Table 4:** System designs considered in the white paper updates.

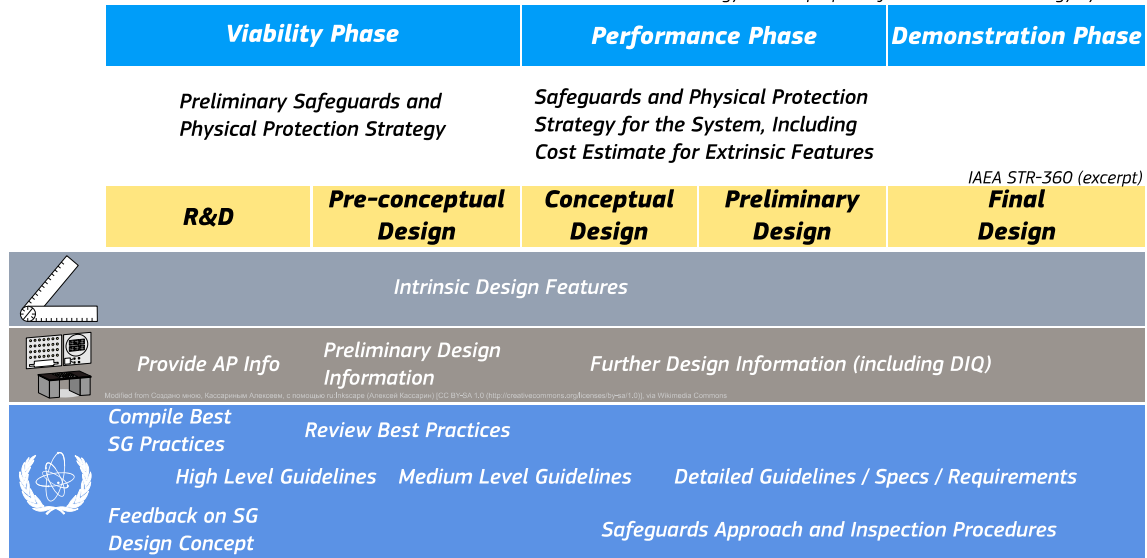
#### 4. The GIF White Papers update and the PRPP-by-Design concept

The update of the six GIF Reactor Technologies “white papers” is a *de facto* example of the application of the PRPP-by-Design concept to the GIF reactor designs, adopting the PR&PP Evaluation Methodology as a PRPP-by-Design main enabling tool. PRPP-by-Design can be described as the process performed by systems designers (eventually supported by PR&PP experts) to identify what might cause proliferation concerns (e.g., those design aspects that would result being attractive to a potential proliferation) by applying the PRPP Evaluation Methodology in a graded way, appropriate to each design stage. When done properly, PR&PP by Design would achieve the technical objectives of having a system that has better PR&PP *intrinsic features* (e.g., system engineering and process features that naturally make a proliferation/nuclear material theft/sabotage effort unattractive). The system would also exhibit a better *safeguardability* (here defined as “*the degree of ease with which a nuclear system can be effectively and efficiently put under international nuclear safeguards*” [6]).

The PRPP-by-Design approach has the potential to provide benefits to several stakeholders. For instance, from a proliferation resistance point of view:

- *Nuclear system designers* would encounter less design changes and adaptation requests from the safeguards inspectorates at a design stage where accommodating them would result in higher design costs and substantial delays in the overall project execution.
- *Nuclear operators* would be able to set up and operate easier and more efficient *Nuclear Material Accounting and Control* (NMA/C) systems, which would ensure a higher quality of the nuclear safeguards reporting. In addition, the nuclear system would ensure a smoother hosting of nuclear safeguards inspections, resulting in faster and cheaper onsite activities.
- *Safeguards inspectorates* would face easier nuclear safeguards design and implementation, resulting in a higher non-proliferation assurance obtain through more effective and cost-efficient verification activities.
- *The general public* would not perceive the nuclear system to be built in their own territory as a potential nuclear proliferation threat, leading to a better public acceptance for the deployment of nuclear technology.

There is no internationally codified breakdown of what PRPP-by-Design activities should take place at each design stage. Figure 4 shows a possible, high-level break down of PR by design-related activities for designers, operators and an international safeguards inspectorate when an innovative reactor technology is considered.



Legenda. AP: Additional Protocol; DIQ: Design Information Questionnaire; SG: Safeguards.

**Figure 4.** Example of possible PR by Design activities at various design stages for system designers (grey), operators (brown) and safeguards inspectorates (azure). The two possible design stages paradigms are taken from [18] (azure) and [19] (yellow).

The approach proposed by the GIF PRPPWG foresees the use of the PR&PP Evaluation Methodology framework as the starting point for a PRPP-by-design analysis by a nuclear system design. Being the methodology proposed as an evaluation tool for the entire nuclear system, with use principally by PR&PP experts, the standard evaluation framework presented in [4] and reported in Figure 1 – originally built for a full system application – needs to be partially adapted to the analysis of a particular design aspect. Figure 5 proposes such adaptation for the PR part, through the identification of a set of relevant questions (actions) the system designer should answer (perform), for the *challenges*, *system response* and *outcomes* phases foreseen by the methodology.

**PR Evaluation Framework for Full System**

**PR Analysis on Particular Design Aspect**

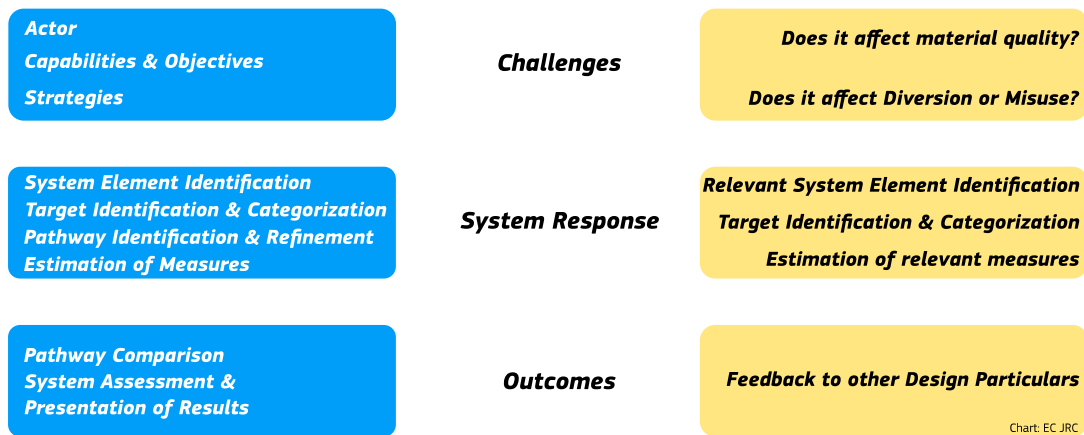
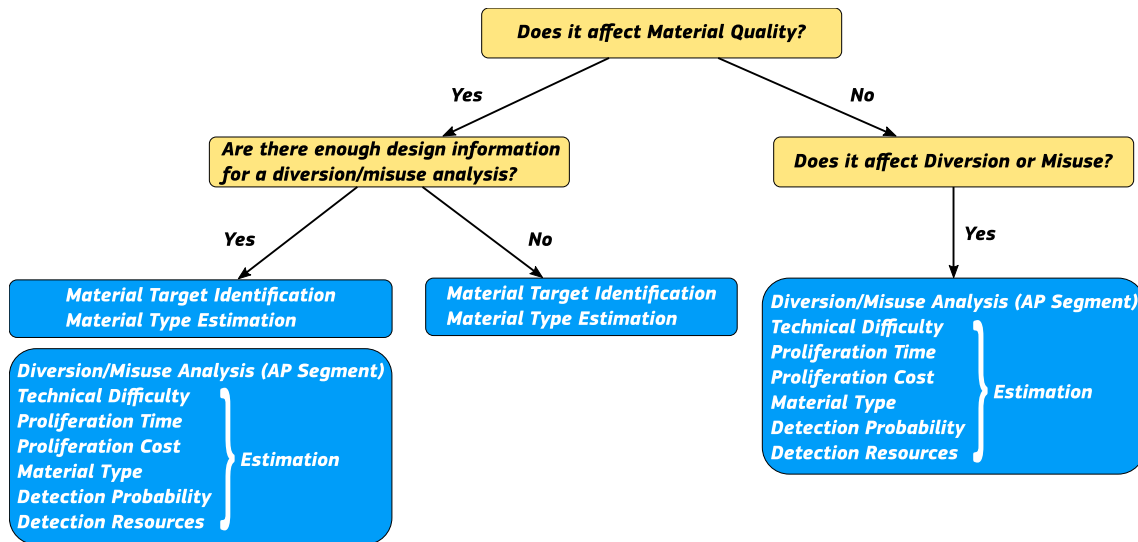


Chart: EC JRC

**Figure 5:** PR&PP evaluation informs system designers.

Figure 6 proposes a possible practical procedure for the PR analysis on a single design particular by a system designer. The level of detail of the analysis would need calibration on the level of design maturity and detail. In the early design stages, the estimation of the six measures would result in a coarse qualitative estimation.



Legenda. AP: Acquisition-Pathway.

Figure 6: Possible practical approach to the PR analysis of a single design particular.

Intrinsic PR features and safeguardability are two intertwined main technical outcomes of a PR by design analysis. Better intrinsic features would mean that the nuclear material would be more difficult to divert/misuse, requiring more time and more resources. Better safeguardability would make proliferation activities easier and cheaper to detect. Similarly, safeguardability and safeguards by design are non-coincident and related aspects:

- *Safeguardability* facilitates the design of nuclear safeguards; designers perform it during the design stages [6, 20-22].
- *Safeguards by Design* supports the design of nuclear safeguards at early design stages; the Safeguards inspectorate drives it and designers will perform it across all the project life cycle of the nuclear system [23, 24].

High safeguardability naturally leads to an easier Safeguards by Design process, with benefits to all the major players involving in the nuclear system’s life cycle.

As the design progresses, the room for major design modifications dictated by PR&PP requirements will shrink considerably. With time, the analysis will shift its focus from design modification suggestions to highlighting the safeguards challenges that the designs entail, so that the safeguards inspectorates could be better informed on future safeguards R&D needs.

The design options under consideration within the GIF SSCs are seldom real reactor designs that will see a commercial life as documented today. More often, they are paradigmatic concepts of potential nuclear systems that could be commercially deployed in the future. The application of a PRPP-by-Design approach to the six GIF reactor technologies within the update of the PR&PP “white papers” can highlight the general PR&PP strengths and weaknesses intrinsic to the various paradigms, ideally providing guidance on which technical option among the various ones considered to achieve a specific goal might be better suited from a PR&PP point of view.

The growth of venture capital vendors developing advanced nuclear reactor designs presents both challenges and opportunities for PRPP-by-design. These companies tend to focus on safety and economic viability in the reactor design process and push off PR and PP concerns for a later date,

usually due to limited resources. However, these companies are typically very open to support from national laboratories or other research groups to examine PRPP issues and provide input to their designs. The updated GIF PRPP “white papers” could serve as both an analysis paradigm and a source of potential suggestions for these analysts.

PRPP-by-design should not be limited to being aware of PR and PP concerns early in the design process. It also should mean making significant design decisions that balance PR and PP with operational considerations. For example, an MSR designer may need to examine the trade-offs of on-site salt processing (that may require more accountancy measures) as compared to salt processing at a centralized facility (which will have its own accountancy and economics challenges). The white paper updates should help designers with these types of trade-offs specifically for the PRPP aspects.

## 5. Conclusions

The PRPPWG developed an evaluation methodology that proved to be one of the most comprehensive publicly available PR&PP tools to inform the design process of any nuclear technology. The experience gained in the process of developing and testing the PRPPWG formed the basis for a close interaction with the GIF SSCs/pSSCs that in 2011 created a joint document highlighting the PR&PP characteristics of the six GIF reactor technologies.

Currently, the PRPPWG and the six SSCs/pSSCs are collaborating to update that document in view of the design evolutions and changes that have occurred in recent years. This activity will not only shed light on the PR&PP advancements of the current system designs, but will also inform designers, operators and regulators of future activities to enhance the robustness and efficiency of the safeguards and physical protection of nuclear systems.

The six white papers will all have some cross-cutting topics that may be common across different designs. Examples include fuel type, refuelling, the fuel cycle, safety and economics, PP siting, transportation, and cyber-security. The 2011 white papers identified some of these cross-cutting areas, but others will be identified in the course of the update.

## 6. Acknowledgements

The efforts and ideas of the many members and observers of the PR&PP working group over the past dozen years are the foundation of this status paper. The full list of authors and contributors to the PR&PP methodology appears in its rev. 6 report [4]. The corresponding authors would like to thank all the other PRPPWG members and observers.

The collaboration with the GIF SSCs and pSSCs in issuing the six GIF white papers and the compendium study was essential and the result was only possible with a strong support by them. The GIF SSCs and pSSCs efforts so far devoted to start the updating of the six GIF white papers are acknowledged. Their continuous support for successfully completing the update will be essential as well.

## 7. References

- [1] Generation IV International Forum (GIF). *A Technology Roadmap for Generation IV Nuclear Energy Systems*. Technical report, Generation IV International Forum (GIF), 2002.
- [2] GIF PRPPWG. *PR&PP Evaluation: ESFR Full System Case Study Final Report*. Technical Report GIF/PRPPWG/2009/002, Generation IV International Forum (GIF), 2009.
- [3] American Nuclear Society. Special Issue on Safeguards. *Nuclear Technology*, volume 179, no. 1:pp. 1–168, 2012.
- [4] PRPP Working Group. *Evaluation Methodology for Proliferation Resistance and Physical Protection of Generation IV Nuclear Energy Systems — Revision 6*. Technical report, Generation IV International Forum (GIF), 2011.
- [5] PRPP Working Group and System Steering Committees of the Generation IV International Forum. *Proliferation Resistance and Physical Protection of the Six Generation IV Nuclear*

- Energy Systems*. Technical Report GIF/PRPPWG/2011/002, Generation IV International Forum (GIF), 2011.
- [6] PRPP Working Group. *Evaluation Methodology for Proliferation Resistance and Physical Protection of Generation IV Nuclear Energy Systems, Technical Addendum to Revision 5*. Technical Report GIF/PRPPWG/2006/005-A, Generation IV International Forum, 2007.
- [7] Bari, R.A., Phillips, J., Pilat, J., Rochau, G., Therios, I., Wigeland, R., Wonder, E., and Zentner, M. Proliferation Risk Reduction Study of Alternative Spent Fuel Processing. In *Institute of Nuclear Materials Management (INMM) 50th Annual Meeting, Tucson, Arizona, USA, July 12-16, 2009*. 2009.
- [8] Zentner, M.D., Therios, I., Bari, R.A., Cheng, L., Yue, M., Wigeland, R., Hassberger, J., Boyer, B., and Pilat, J. An expert elicitation based study of the proliferation resistance of a suite of nuclear power plants. In *Proceedings of the 51st Annual Meeting of the Institute of Nuclear Materials Management, July 11-15, 2010, Baltimore, Maryland*. 2010.
- [9] Yue, M., Cheng, L.Y., and Bari, R.A. Relative proliferation risks for different fuel cycle arrangements. *Nuclear Technology*, volume 165, no. 1:pp. 1–17, 2009.
- [10] Whitlock, J. Incorporating the GIF-PRPP Proliferation Resistance Methodology in Reactor Design. In *Proceedings of the 51st Annual Institute for Nuclear Material Management Meeting, Baltimore*. 2010.
- [11] Rossi, F. Application of the GIF PR&PP Methodology to a Fast Reactor System for a Diversion Scenario. In *Symposium on International Safeguards: Linking Strategy, Implementation and People; Vienna (Austria), 20-24 Oct 2014*. 2014.
- [12] Renda, G., Alim, F., and Cojazzi, G.G.M. Proliferation Resistance and Material type considerations within the collaborative project for a European Sodium Fast Reactor. *ESARDA Bulletin*, no. 52:pp. 124–143, 2015.
- [13] Rossa, R., Van der Meer, K., and Borella, A. Application of the PR and PP Methodology to the MYRRHA research facility. *ESARDA Bulletin*, volume 49:pp. 82–94, 2013.
- [14] Ahn, S., Kwon, E., Chang, H., and Kim, H. A Proliferation Resistance Evaluation for a Pyroprocessing Facility Design. In *Proceedings of the INMM 55th Annual Meeting, Atlanta, GA, USA*. 2014.
- [15] PRPP Working Group. Bibliography. [https://www.gen-4.org/gif/upload/docs/application/pdf/2018-08/gif\\_prppwg\\_bibliography\\_rev06\\_-\\_2018-07-18-final.pdf](https://www.gen-4.org/gif/upload/docs/application/pdf/2018-08/gif_prppwg_bibliography_rev06_-_2018-07-18-final.pdf)
- [16] Cojazzi, G., Renda, G., Cheng, L., Peterson, P., Bari, R., Boyer, B., Chebeskov, A., Edwards, G., Henderson, D., Hervieu, E., Hori, K., Kim, D., and Padoani, F. The GIF Proliferation Resistance and Physical Protection working group (PRPPWG): achievements and perspectives. In *Atoms for the Future 2018 and GIF Symposium 2018, 16-17 October 2018, UIC Paris*. 2018.
- [17] Cojazzi, G., Renda, G., Cheng, L., Peterson, P., Bari, R., Henderson, D., Boyer, B., Chebeskov, A., Choe, K., Cipiti, B., Edwards, G., Hervieu, E., Hori, K., Kim, H., and Padoani, F. The GIF Proliferation Resistance and Physical Protection methodology applied to GEN IV system designs: some reflections. In *Building Future Safeguards Capabilities (IAEA-CN-127), 05-08 November 2018, Vienna*. 2018.
- [18] Generation IV International Forum (GIF). *Technology Roadmap Update for Generation IV Nuclear Energy Systems*. Technical report, Generation IV International Forum (GIF), 2014.
- [19] International Atomic Energy Agency. *Facility designs and plant operating features that facilitate the Implementation of the IAEA Safeguards*. Technical Report STR-360, IAEA, 2009.
- [20] Bjornard, T., Schanfein, M., Hebditch, D., Bari, R., and Peterson, P. Improving the safeguardability of nuclear facilities. *Journal of Nuclear Materials Management*, volume 37, no. 4:p. 74, 2009.
- [21] Cojazzi, G.G.M., Renda, G., and Sevini, F. Proliferation Resistance Characteristics of Advanced Nuclear Energy Systems: a Safeguardability Point of View. *ESARDA Bulletin*, volume 39:pp. 31–40, 2008.
- [22] Sevini, F., Renda, G., and Sidlova, V. A Safeguardability Check-List for Safeguards by Design. *ESARDA Bulletin*, volume 46:pp. 79–84, 2011.
- [23] International Atomic Energy Agency. *International Safeguards in Nuclear Facility Design and Construction*. Technical Report NP-T-2.8, 2013.
- [24] International Atomic Energy Agency. *International Safeguards in the Design of Nuclear Reactors*. Technical Report NP-T-2.9, IAEA, 2014.

# Regulatory Experience with the Safeguards by Design Project of Planned New Nuclear Power Reactors in Hungary

András Jezeri, Árpád Vincze, Erzsébet Földesi

Hungarian Atomic Energy Authority, Budapest, Hungary  
[jezeria; vincze; szollosi]@haea.gov.hu

## **Abstract:**

*The Agreement between the Government of Hungary and the Government of Russian Federation for co-operation in the field of peaceful uses of nuclear energy was promulgated in 2014. The scope of cooperation contains the capacity upgrade and development of the Paks Nuclear Power Plant in operation as well as planning, construction, commissioning and decommissioning of two new units (units 5 and 6).*

*The planned new units will be generation III+ pressurized water reactors of type V-527 WWER-1200. Gross nominal electrical output of the planned nuclear power plant is 1,200 MWe per unit. The planned newly build nuclear power reactors triggered several regulatory activities in Hungary and amendment of the relevant national legislation, including safeguards requirements, was necessary. A guideline on how to fulfil the new national requirements on the implementation of safeguards in case of the new power plant was issued by HAEA. The guideline gives recommendation on how to provide early design information of new facilities, provide advance notification of the imports of the fuel, how to meet design and installation requirements for newly build reactors to ensure its safeguardsability.*

*A taskforce to facilitate 'safeguards by design' for the new nuclear power plant has been set up in Hungary. HAEA facilitates the tasks between the stakeholders in order to ensure that international, European and national requirements in this field are met. The details of the safeguards specific requirements and guidance for new built NPPs as well as the regulatory experiences gained so far will be described in our paper.*

**Keywords:** new NPP, Safeguards by Design, national legislation

## **1. Introduction**

The beginning of the planning of the new power plant units can be traced back to 30 March 2009, when the Hungarian Parliament granted its consent in principle to the preparation of the new NPP project in its Resolution No. 25/2009 (IV.2.) OGY. The next step was the establishment of the Paks II Nuclear Power Plant Private Company Limited by Shares as the operator company of the new power plant. In April, 2014 this new company submitted the site survey and assessment license to the Hungarian Atomic Energy Authority (HAEA). In November 2014 the site survey and assessment license, and in March 2017 the license for the site for the new NPP were issued by the HAEA. Currently the project is in the designing phase and HAEA is waiting for the construction license application to be submitted.

In order to facilitate the inclusion of the 'safeguards by design' concept into the project well in advance, HAEA identified several tasks: (1) update of the national safeguards related requirements; (2) preparation of a guideline on how to fulfil the new national requirements and (3) set up taskforce to facilitate the 'safeguards by design' with the involvement of all stakeholders.

In general Safeguards by design means an approach whereby international as well as domestic safeguards requirements and objectives are fully integrated into the design process of a nuclear facility, from initial planning through design, construction, operation, and decommissioning. By including awareness of all regulatory issues, including international agreements that concern international

safeguards, project management can schedule consideration at the appropriate time and level of detail and subsequently reduce the project risk.

In this article, the new national regulations related to the safeguards by design topic and its development history, the related guidance as well as the efforts and achievements of the stakeholders participating in the safeguards by design task force will be discussed.

## **2. The legal background of the safeguards by design in Hungary**

### **2.1. The relevant national decree**

In Hungary the relevant legislation on the implementation of safeguards, the Ministerial decree 7/2007. (III. 6.) IRM on the rules of accountancy and control of nuclear material had to be extended to natural and legal person which install a facility or location outside facility. The decree says that "The scope of this decree covers: each natural and legal person which, in the territory of Hungary or under its jurisdiction or control, possesses nuclear material or performs any nuclear material related peaceful activity including the installation of a facility or location outside of a facility serving for manufacturing, separating, reprocessing, storing of nuclear material or for using it any other way (organization possessing nuclear material);

The decree above stipulates the phases when basic technical design data (called as Basic Technical Characteristics – BTC in EURATOM term or Design Information Questionnaire – DIQ for IAEA) for new facilities shall be submitted to the Hungarian Atomic Energy Authority. These phases are the following:

- a) when the decision on construction is made or when the authorization for launching the construction is granted, whichever is earlier, and in case of activity requiring environmental effect analysis when the environmental protection license becomes effective;
- b) when the application for construction license is submitted;
- c) when the application for commissioning license is submitted;
- d) when the application for first safeguards license is submitted;
- e) when the application for modification safeguards license is submitted due to the changes in the basic technical characteristics as submitted in the first safeguards license.

### **2.2. Guideline on safeguards requirements in new NPPs**

To facilitate the understandings of safeguards obligations on local, facility level the Director General of the HAEA issued guidelines. They contain the rationale behind safeguards obligations and give methods on how the requirements determined in relevant regulations shall be complied with. Though guidelines are not obligatory, they encourage the licensees to take into account the recommendations of the guidelines to the extent possible.

One of these guidelines, the 'SG-2 Guideline' was already issued specifically on safeguards requirements in new NPPs in June, 2015, after the bilateral agreement on co-operation in the field of peaceful use of nuclear energy between the Government of Hungary and the Government Russian Federation.

The guideline gives recommendations on how to fulfil national legislation when implementing safeguards in new nuclear power plants. Details of obligations to provide advance information to meet design and installation requirements in case of a new NPP to ensure its safeguardsability are described. The guideline does not cover safeguards obligations for the NPP which is already operating. Requirements detailed in the guideline include obligations undertaken under IAEA and EURATOM safeguards system as well as the relevant IAEA documents in the field of safeguards by design.

The guideline briefly introduces the basic objectives of safeguards and gives on how to basic objectives of facility level. It advises on use proliferation resistance technical solutions, to maintain strict nuclear material accountancy, to put into effect data provision obligations, and to ensure timely detection of diversion and/or misuse and deterrence through risk of early detection.

In its chapter on Safeguards by design (SbD) the guideline describes what measures are called safeguards by design and says that „Design of safeguards measures/safeguards in course of design (safeguards by design) is the process whereby – through all phases of the lifecycle of a nuclear facility- from initial planning through design, construction, operation to decommissioning international safeguards requirements are taken into account. Safeguards by design do not raise new requirements, however do create the opportunity to implement the existing requirements cost effectively.

The guideline calls for the early and effective dialogue on SbD among stakeholders: IAEA, EURATOM, national authority, investors, designers, constructors, suppliers and representatives of future operators. It also advises to identify the tasks and responsibilities in course of design, installation, commissioning and operation with the aim to effectively support the design of safeguards measures.

The Guideline calls for update of the BTC as soon as new design data are available and recommends data provision additional to those included in the BTC format to enhance that power plant design from its onset to the final stage can support future safeguards measures. Information beyond BTC may include e.g. any other nuclear fuel cycle facility nearby, possibility of diversion in that facility, hidden routes suitable for uncontrolled shipment from the site, accidental contamination due to previous use of the site that may later covert undeclared activities, etc.

Requirements of the following IAEA documents were also taken into account in the Guideline:

- IAEA Nuclear Energy Series no. NP-T-2.8 on International Safeguards in Nuclear Facility Design and Construction, IAEA, Vienna, 2013
- IAEA Nuclear Energy Series no. NP-T-2.9 on International Safeguards in the Design of Nuclear Reactors, IAEA, Vienna, 2014

### **3. Safeguards by design workshop at the HAEA**

In September, 2018 a workshop was initiated by the Hungarian Atomic Energy Authority. The main objectives of the workshop were that all Stakeholders (Vendor, Operator, HAEA, European Commission and the IAEA) understand the importance of ‘safeguards by design’ and identify the tasks of each stakeholder to meet the international, European and national requirements. The workshop was also planned to share national experience in SbD by the Finnish Radiation and Nuclear Safety Authority (STUK), related experience and initial expectations by EURATOM and the International Atomic Energy Agency to that greatly facilitated the understanding of the Vendor and the Hungarian stakeholders. Therefore all relevant stakeholders were present at the workshop, i.e.: representatives of the International Atomic Energy Agency (IAEA), European Commission Directorate-General for Energy Directorate E - EURATOM Safeguards (EURATOM), Hungarian Atomic Energy Authority (HAEA), representatives of Paks II Nuclear Power Plant Private Company Limited by Shares (Paks II Ltd) as the licensee, as well as designers of the new NPP from the Russian vendor (ASE). The STUK took also part at the workshop to assist the Hungarian stakeholders with their valuable practical experience in this field.

#### **3.1. Main statements and conclusions of the workshop**

One of the most important benefits of the workshop was to bring together all the stakeholders concerning the safeguards by design. The main conclusions of the workshop are as follows:

- Safeguards by design is the integration of features to support IAEA safeguards into the design process for a new nuclear facility, from the initial planning through design, construction, operation, and decommissioning.
- As a result of applying ‘Safeguards by design’ costly and time-consuming redesign work or retrofits of new nuclear facilities to implement nuclear safeguards can be avoided. Effectiveness and efficiency of IAEA safeguards can be improved and workload on the operator and State authority can be reduced. Safeguards measures intrude to the operation to the lowest extent possible.

- Nuclear facilities shall be designed with safeguards measures, surveillance and containment in mind. Early communication between designers and safeguards inspectorate is essential. The knowledge on the basic technical characteristics of the facility lies with the designers.
- To reach an effective 'safeguards by design' communication between the stakeholders is very important, therefore 'safeguards by design' responsible persons for each stakeholder have to be nominated.
- Preliminary basic technical characteristic data shall be sent to the EURATOM as early as possible, technical requirements for 'safeguards by design' will be set up afterwards as an outcome of further expert level meetings.
- International inspectorates first get acquainted with the design data of the facilities and then make proposals on potential safeguards equipment.
- Representatives of international, European and national inspectors have to provide the designers with exact details of the technical characteristics of the safeguards equipment (dimensions of the equipment, power requirements, data transfer protocols, etc.).
- It is the designers' task to incorporate safeguards "needs" into plant design in the most effective way to accommodate to international safeguards approaches. This may change at different stages of facility development/operation. 'Safeguards by design' should offer flexibility for differing international safeguards approaches over plant design life.
- Inspectorates shall be proactive and think about not only equipment and tools which are already in safeguards use but also on those, which can be approved for safeguards verification use in the future, e.g. they are under development.
- After the BTC of the newly built facility has been sent to the EURATOM, one or more MBA codes are attributed to the facility. This allows the EURATOM to create budgetary provisions and start to work on possible safeguards measures for the new facility.
- BTC is analysed by the stakeholders of 'safeguards by design', i.e. EURATOM, IAEA, designers, licensees and HAEA. The more technical data stakeholders know on the new nuclear facility, the more effectively 'safeguards by design' can be realized instead of safeguards catching up after the design. Therefore, information beyond the obligatory BTC data will give more support to establish the safeguards system of the new facility (access to drawings, etc.)
- Not only the design is important but also the description of nuclear material flow and the understanding of normal operations and also emergency operations, or possible other operations that can result in extra safeguards verifications. This can result in the need of redundancy of the equipment, uninterruptable surveillance, etc. Inspectors may propose more equipment if needed to avoid the need for retrofit later.
- The updated version of the BTC is to be submitted to the EURATOM as soon as possible. In this case, recommendations of the EURATOM for potential equipment for safeguards measurements, surveillance and containment systems can be incorporated into the design before its final stage.

### **3.2. Further formulated activities of the stakeholders**

After the determination of the main statements and conclusions of the safeguards by design as described above, the participants specified the further activities necessary for each stakeholder. Here is a list of these activities and tasks in chronological order:

- The taskforce to facilitate 'safeguards by design' for the new nuclear power plant has been set up. HAEA is ready to facilitate the tasks between the stakeholders in order to ensure that international, European and national requirements in this field are met.
- HAEA promotes 'safeguards by design' among stakeholders.
- The licensee submits the updated BTC as early as possible to the EURATOM and parallel to the HAEA.
- The licensee provides EURATOM, IAEA and HAEA with the timeline of the project, including the schedules of the forthcoming licences as well as the subsequent design stage including the date for freezing of the design.
- The EURATOM together with IAEA analyses the BTC and attach one or more MBA codes to the new nuclear facility.

- The EURATOM in cooperation with IAEA and HAEA organizes technical meetings involving safety, security and safeguards experts of the new NPP to highlight the importance of 'safeguards by design'.
- The EURATOM works together with the IAEA on the BTC and on the possible safeguards measures of the new nuclear facility.
- EURATOM and IAEA provides the designer/operator with the technical specifications of the potential safeguards equipment.
- Technical meetings are to be organised, if possible, in conjunction inspections planned in Hungary.
- Designers make proposals on possible ways to include safeguard measures into the design.
- Designers and the licensee document the need for safeguards requirements in all stages of the design.
- Designers promote the knowledge on the 'safeguards by design' among their designer partners.
- As soon as the MBA code is assigned to the new facility, the HAEA yearly informs the EU about the status of the construction of the new NPP and the next key steps will be identified.
- Stakeholders meet several times to analyse the possible safeguards measures for the new nuclear facility and to include them into the design.
- IAEA defines the key DIV inspections in course of the construction.
- STUK is ready to share its expertise gained in this field.
- STUK and HAEA will make joint efforts to distribute their experience in this field to the international safeguards community.

#### **4. The current situation of SbD in Hungary**

At the September SbD Workshop, it was determined that the next step of the safeguards by design of the new nuclear power plant units would be the submission of the updated BTC to EURATOM. The finalisation and approval of the BTC is still pending.

In order to keep the information up-to-date, the HAEA regularly organizes meetings with operators who report on the outcome of their discussions with designers and also on possible changes to the BTC. Our last meeting was held in May, 2019.

#### **5. Summary**

One of the key objectives of the HAEA is to take into account the requirements and recommendations of the safeguards at all stages of the design of the newly built nuclear power plant units, which could be best met by the initiation of the safeguards by design project. This is not only in the interest of the licensing authority but in the interest of all stakeholders.

The HAEA is making considerable efforts to achieve this goal. These results include the creation of a guideline specifically covering the requirements and recommendations of the safeguards of the to be built nuclear reactors. In addition, a start-up workshop was held where all relevant stakeholders were involved to understand the concept of the safeguards by design and to meet all the safeguards requirements that arise, thus facilitating the smooth running of the project.

Here, it should be emphasized that while these results are already significant, we are only at the beginning of achieving the objectives mentioned in the third chapter. Further experiences with the SbD project for the implementation of the safeguards by design for new nuclear power plant units built in Hungary will be discussed in our subsequent paper.

#### **6. References**

[1] Ministry of Justice; *Ministerial decree 7/2007. (III. 6.) IRM on the rules of accountancy and control of nuclear material; 2007.*

- [2] International Atomic Energy Agency; *IAEA Nuclear Energy Series no. NP-T-2.8 on International Safeguards in Nuclear Facility Design and Construction*, IAEA, Vienna, 2013.
- [3] International Atomic Energy Agency; *IAEA Nuclear Energy Series no. NP-T-2.9 on International Safeguards in the Design of Nuclear Reactors*, IAEA, Vienna, 2014.
- [4] Hungarian Atomic Energy Authority; *SG-2 Guideline on safeguards requirements in new NPPs*; HAEA, Budapest, 2015.

# **Panel 3:**

# **Education and Training**

## Collaboration for Development of Comprehensive NDA Course in SSAC Training

Megumi Sekine<sup>1</sup>, Yoko Kawakubo<sup>1</sup>, Perpetua Rodriguez<sup>1</sup>, Naoko Noro<sup>1</sup>,  
Francesco Raiola<sup>2</sup>, Jean-Michel Crochemore<sup>2</sup>, Arturs Rozite<sup>2</sup>, Kamel Abbas<sup>2</sup>

<sup>1</sup>Japan Atomic Energy Agency, Integrated Support Center for Nuclear Nonproliferation and Nuclear Security (JAEA/ISCN)

<sup>2</sup> European Commission, Joint Research Center (EC/JRC)

<sup>1</sup> 765-1, Funaishikawa, Tokai, Ibaraki, Japan, 319-1118

<sup>2</sup> Via E. Fermi, 2749, TP 800, I-21027 Ispra (VA), Italy  
sekine.megumi@jaea.go.jp

### Abstract:

*The JAEA has been conducting the International/Regional Training Course on the State Systems of Accounting for and Control of Nuclear Material (SSAC) since 1996. A majority of the course participants have expressed the need to learn Non-destructive assay (NDA) techniques to augment their knowledge on nuclear material accountancy. At the SSAC Training Course, JAEA has provided a short session dedicated for NDA demonstration with the use of some detectors and equipment. In addition, since 2016, for selected participants, JAEA has developed and provided in collaboration with the European Commission, Joint Research Centre (EC/JRC), a 5-day follow-up NDA course at JRC Ispra (Italy). This collaboration has been performed under "the Agreement between the JAEA and the EURATOM in the Field of Nuclear Material Safeguards Research and Development". The JAEA has a plan to develop its own Comprehensive NDA course in Japan in the future. The JAEA sends its NDA experts as lecturers to present NDA techniques used in various nuclear fuel cycle facilities in JAEA. On the other hand, JAEA staffs have had the opportunity to learn the use of NDA techniques and effective teaching methods from EC/JRC. This paper summarizes "the Follow-up Course on NDA of Nuclear Materials" conducted by the EC/JRC and JAEA from 2016 to 2019. In these courses, in addition to lectures, hands-on training on gamma and neutron measurements, as well as visits to NDA laboratories were provided to promote a better understanding of NDA techniques. Furthermore, this paper assesses the requirements and resources to develop the future Comprehensive NDA course for the SSAC, and formulate the scheme of effective training methodology to implement the NDA course in Japan.*

**Keywords:** Non-destructive assay techniques, gamma measurements, neutron measurements, SSAC training, safeguards, capacity-building

## 1. Background

The Japan Atomic Energy Agency (JAEA) has been conducting in collaboration with the International Atomic Energy Agency (IAEA) the International/Regional Training Course on the State Systems of Accounting for and Control of Nuclear Material (SSAC) since 1996. The two-week SSAC course takes place in Tokai, (Japan) annually, in the second semester. As part of the SSAC training course curriculum, lectures on the concept and a short demonstration on the use of non-destructive assay (NDA) techniques are provided. One of the feedback received from the SSAC participants is the importance of the analytical techniques used for the characterization of nuclear material. The participants often express their interests to learn more on the NDA techniques and ask for possibilities of a follow-up training in order to acquire a broader understanding and knowledge on how the technique is being used for nuclear material verification. Since 2016, the JAEA, Integrated Support Center for Nuclear Nonproliferation and Nuclear Security (ISCN), in collaboration with the European Commission, Joint Research Centre (EC/JRC), has developed and provided a 5-day NDA course (Follow-up NDA Course) at JRC Ispra, Italy as a follow-up to the ISCN's SSAC training course for the selected participants. This activity is covered under "the Agreement between the JAEA and the EURATOM in the Field of Nuclear

Material Safeguards Research and Development”. The 4<sup>th</sup> Follow-up NDA Course was successfully conducted from 28 January to 1 February 2019 in EC/JRC Ispra, Italy with participants from Armenia, Malaysia, Thailand, Vietnam, and Japan.

## 2. Training content and structure

The follow-up training on NDA techniques is based on decades of experience from those training provided by the JRC Nuclear Security Unit in Ispra to the EURATOM nuclear safeguards inspectors. This one-week follow-up training in Ispra provides the selected participants of the SSAC, hands-on experience on gamma spectrometry and neutron counting as applied in the nuclear safeguards verification system. The topics covered by the NDA training provided to EURATOM inspectors are uranium enrichment verification, plutonium isotopic composition, and nuclear material mass determination. Each one of these topics corresponds to a one-week training. However, for the follow-up NDA course for the SSAC, the three topics are combined in one week. Most of the trainers are from EC/JRC in view of their knowledge of equipment and instrumentation; on the other hand, one of the objectives is to have JAEA/ISCN trainers as well and the plan to organize such follow-up NDA course in Tokai, Japan in the near future, provided that the NDA training infrastructures are available at JAEA.

The Follow-up course on NDA includes classroom lectures and exercises as a refresher to several laboratory sessions, which also include practical (hands-on) exercises and case studies. In addition to the lectures, the Follow-up NDA course provides a half-day session dedicated to laboratory visits on Tank Calibration techniques, Laser 3D system and containment (seals) systems as applied to nuclear safeguards. The course agenda is shown in Table 1. For the 4<sup>th</sup> edition of the follow-up course on NDA techniques, two days were dedicated to verification using gamma-ray spectrometry, two days for neutron counting, and a half-day was dedicated to additional lectures delivered by JAEA trainers on the application of NDA techniques in reprocessing and MOX fuel fabrication facilities. The last day of the course was utilized for laboratory visits.

Table 1: Agenda of Follow-up NDA course (January 28 - February 1, 2019)

	Monday, 28 Jan.	Tuesday, 29 Jan.	Wednesday, 30 Jan.	Thursday, 31 Jan.	Friday, 1 Feb.
09:00-09:30	Opening Ceremony	Part I presented by JRC ESSOR Bldg. 82A		Part II presented by JRC ESSOR Bldg. 82A	
	Part I presented by JRC ESSOR Bldg. 82A				Part III presented by JRC and JAEA Bldg. 18
09:30-12:00	<ul style="list-style-type: none"> <li>Physics background of the gamma-ray spectrometry Detectors, electronics and signal analysis</li> <li>Introduction of U enrichment</li> </ul>	Practical Exercises: U enrichment determination with a HPGe detector  Introduction to Pu isotopic composition determination	Introduction to neutron counting for safeguards: <ul style="list-style-type: none"> <li>Sources of neutrons in actinides</li> <li>Neutron interactions with matter</li> <li>Neutron detectors for safeguards</li> <li>Signal processing from neutron measurements</li> </ul>	Interpretation model for neutron counting: <ul style="list-style-type: none"> <li>Demonstration of neutron counters</li> <li>The neutron signal pulse train</li> <li>The Shift Register analyzer</li> <li>The interpretation model for neutron measurements</li> <li>Introduction to inspector software for neutrons</li> </ul>	Tank calibration  NDA Application in Reprocessing Facility/Waste Drum Assay  NDA Application in MOX Fabrication Facility
12:00-13:30	Lunch	Lunch	Lunch	Lunch	Lunch
	Visit to ESSOR Laboratories	Visit to ESSOR Laboratories	Visit to ESSOR Laboratories	Visit to ESSOR Laboratories	Visit to AS3ML & SILab Laboratories
13:30-17:00	Practical Exercises - Gamma-ray spectrometry: <ul style="list-style-type: none"> <li>Set-up of the gamma-ray spectrometry chain</li> <li>Calibration and resolution determination</li> </ul> Practical Exercises: U enrichment determination with a NaI detector	Practical Exercises: Pu isotopic composition verification with HPGe and use of calculation code MGA	Experiments with neutron detectors and analysers	Experiments with neutron detectors and analysers	Visit to AS3ML and SILab Laboratories  Course evaluation and distribution of attendance certificates  Closing ceremony

### 3. NDA measurement techniques

#### 3-1. Gamma-ray measurements

##### 3-1-1. Lectures and hands-on exercises (28-29 January 2019)

The EC/JRC lecturers (Fig. 1) explained the principle of gamma-ray measurements with NDA systems using the High Purity Ge (HPGe) and NaI(Tl) scintillator detectors. The provided lectures are indicated in Table 2.

Table 2 Lectures on Gamma-ray Measurements

Lecture 1: Basics of radiation physics for NDA of nuclear material	Lecture 2: Gamma-ray detection techniques
<ul style="list-style-type: none"> <li>➤ Introduction to nuclear material verification with NDA methods                             <ul style="list-style-type: none"> <li>· Gamma-ray spectrometry</li> <li>· Neutron counting</li> <li>· Calorimetry</li> </ul> </li> <li>➤ Basics of radiation properties for NDA verification of nuclear material                             <ul style="list-style-type: none"> <li>· Chemical elements</li> <li>· Nuclides</li> <li>· Uranium</li> <li>· Plutonium</li> </ul> </li> <li>➤ Radiation properties and radioactivity decay</li> <li>➤ Others safeguards techniques – spent nuclear fuel verification</li> <li>➤ DA methods</li> </ul>	<ul style="list-style-type: none"> <li>➤ Introduction to gamma radiation detectors                             <ul style="list-style-type: none"> <li>· Scintillator based detector</li> <li>· Semi-conductor</li> </ul> </li> <li>➤ Electronic chain of a Gamma-ray spectrometry system                             <ul style="list-style-type: none"> <li>· Detector crystal</li> <li>· Signal pre/amplification</li> <li>· ADC and MCA</li> </ul> </li> <li>➤ Gamma-ray spectrometry quality control                             <ul style="list-style-type: none"> <li>· Gamma-ray spectrum optimization</li> <li>· Energy resolution and efficiency</li> <li>· Hands-on exercise</li> </ul> </li> </ul>
Lecture 3: Uranium Enrichment verification	Lecture 4: Plutonium isotopic composition determination
<ul style="list-style-type: none"> <li>➤ Use of gamma-ray spectrometry for nuclear safeguards</li> <li>➤ Methods for uranium enrichment verification                             <ul style="list-style-type: none"> <li>· Use of standards</li> <li>· Use of calculation codes</li> </ul> </li> <li>➤ Methods for plutonium isotopic composition verification</li> </ul>	<ul style="list-style-type: none"> <li>➤ Introduction to plutonium</li> <li>➤ Isotopic composition of plutonium with gamma-ray spectrometry:</li> <li>➤ Plutonium mass determination (Pu-240 eff)</li> </ul>



Fig. 1 Gamma-ray lecture

### 3-1-2. Hands-on exercises with the HM-5 and HPGe

The participants and JAEA lecturers formed 3 groups (2~3 members/group). The enrichment of the uranium standard source was measured with the HM-5 (Fig. 2). This exercise has provided the participants not only with the knowledge on the operation but also with the understanding of the measurement concepts of the equipment. In addition, the enrichment and isotopic ratios of the uranium and plutonium standard sources were measured with the HPGe (Fig. 3). After the known energy range (i.e., 186 keV, 60 to 208 keV) was measured, the enrichment and isotopic ratios were analyzed with the MGAU and MGA software. For the plutonium source which emits spontaneous neutrons, measurements were made with variations on the thickness of the cadmium plates and the distances between the detector and the source.



Fig. 2 HM-5



Fig. 3 HPGe

## 3-2. Neutron measurements

### 3-2-1. Lectures and hands-on exercises (30 -31 January 2019)

The EC/JRC lecturer (Fig. 4) explained the principle of neutron measurements with the use of the neutron coincidence counting techniques.

Table 3 Lectures on Neutron Measurements

Lecture 5: Verification of Plutonium mass by neutron coincidence counting 1 <sup>st</sup> module	Lecture 6: Verification of Plutonium mass by neutron coincidence counting 2 <sup>nd</sup> module
<ul style="list-style-type: none"> <li>➤ Properties of Pu isotopes and other neutron sources</li> <li>➤ Neutron detector heads</li> <li>➤ Rossi- alpha curve and the shift register</li> </ul>	<ul style="list-style-type: none"> <li>➤ Pairs of signals: reals and accidentals</li> <li>➤ Relationship between measurement and physics quantities</li> <li>➤ Calibration curve</li> <li>➤ Dead-time correction</li> </ul>

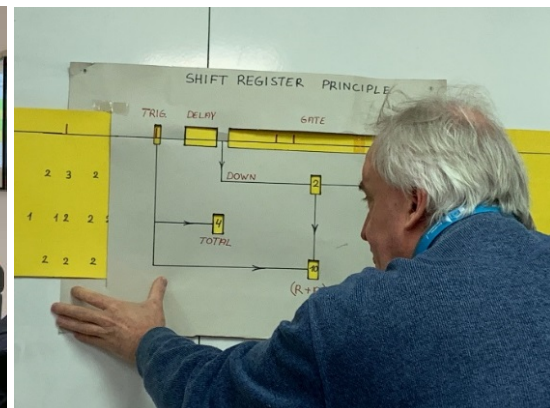


Fig. 4 Neutron lecture

### 3-2-2. Hands-on exercises with the High Level Neutron Coincidence Counter (HLNCC-II):

The EC/JRC lecturer demonstrated the measurement of the neutron die-away time with a single channel analyzer. This demonstration helped participants to understand the effects of the moderator (polyethylene). Standard plutonium sources for the verification of Pu-mass using the “calibration method” was demonstrated with the HLNCC-II (Fig. 5). The HLNCC is a typical measurement device used for nuclear safeguards verification purposes.

The JAEA neutron NDA experts supported the participants in the learning process (e.g., providing advice on the use of three different neutron sources such as Pu, Cf-252, Am-Li).



Fig. 5 High Level Neutron Coincidence Counter (HLNCC-II).

## 4. NDA application in reprocessing and MOX fabrication facilities

In the morning of the last day, additional lectures on how NDA techniques are applied in the actual facility were provided by JAEA, focusing on NDA techniques used in the back end of the nuclear fuel cycle, specifically reprocessing. The scope of the JAEA's nuclear fuel cycle facility (reprocessing and MOX fuel fabrication facilities) and the applied NDA techniques were introduced by the JAEA lecturers. The JAEA lectures were supported with images/pictures in consideration with the background knowledge of the participants. This facilitated an easy understanding among the participants, as well as the EC/JRC's lecturers. For the reprocessing facility, the NDA for nuclear waste measurement and the nuclear material flow during operation were described using a video. For the MOX fuel fabrication facilities, NDA systems to check nuclear materials which are stored in different forms and the optimum evaluation according to the characteristics of the measurements were introduced. The importance of safeguards by design was also mentioned.

## 5. Laboratory visit

The participants visited three research laboratories during the course:

### (1) Tank calibration facilities

The EC/JRC lecturer explained and demonstrated the calibration method and error evaluation of the Tank Monitoring System (Solution Measurement and Monitoring System - SMMS) using the solution storage tanks (Slab type: about 2m width, Annular type: about 4m height, etc.) of a reprocessing facility. These facilities are also used for EURATOM inspectors' training.

### (2) Advanced Safeguards Measurement, Monitoring and Modelling Laboratory (AS3ML)

The EC/JRC lecturer demonstrated the portable 3D scanning technology for the purpose of comparing building information received from the facility with the as-built and the verification of possible undeclared

building modifications. The laser 3D image reconstruction is one of the important safeguards verification techniques.

### (3) Sealing and Identification Laboratory (SILab)

The EC/JRC lecturers explained the ultrasonic (US) bolt seals and the Electronic Optical Sealing System (EOSS) with mock-up configurations to demonstrate the seals' application concepts.

## 6. Training Materials

The training materials were printed and distributed to the participants. These materials were also distributed in electronic format as well. The training materials included the following:

- Course agenda,
- Lecture materials,
- Lab sessions contents and schedule, and
- Standard operating procedures for different equipment.

## 7. Course evaluation by the participants

At the end of the course, EC/JRC and JAEA/ISCN conducted the course evaluation and received feedback from the participants. It covered the evaluation of the course content and the substance of each of the lectures delivered and the laboratory sessions provided; it also covers assessment on the conduct and delivery of the training and the content of the training materials. The participants found the course highly satisfactory (i.e. very good or outstanding). The positive feedback contains comments such as the following:

- The lectures and exercises were well organized;
- JAEA's lecturer explained training materials using images and pictures as much as possible, so the contents are very easy to understand and
- To consider increasing the time for hands-on exercises.

However, the lecture materials used during the course were specifically developed for the EURATOM inspectors. As a result, some parts of the lectures on neutron counting has taken time for the participants to understand the technical terms and the principles of neutron measurements.

## 8. Course reviews and recommendations

The SSAC follow-up NDA courses conducted from 2016 to 2019 were successfully delivered and implemented through the collaborative efforts between EC/JRC and JAEA/ISCN (Fig. 6). The course has provided a valuable opportunity for the selected participants in augmenting their understanding of NDA techniques as applied in nuclear safeguards. It is expected that the cooperation between EC/JRC and JAEA/ISCN would continue with the Follow-up NDA courses in the coming years.

For the next Follow-up NDA course, the following recommendations should be considered:

- Since this course is more focused on hands-on exercises, for the participant's selection process, JAEA/ISCN staff will assess the participant's technical background and knowledge during the SSAC course.
- Based on the comments provided in the course evaluation, JAEA/ISCN and EC/JRC will work together to improve the general arrangements (e.g., agenda, lunch location, etc.). Special attention will be given to lecture materials on the neutron measurements which were developed for EURATOM inspectors (having advanced-level and had studied nuclear physics); the material seems to be too difficult for the participants in this course. EC/JRC and JAEA/ISCN will work together to modify the training materials considering the technical level of the participants.



Fig. 6 Group photo after the graduation ceremony

## 9. Future JAEA NDA courses

NDA is one of the key technologies in nuclear material verification activities implemented by IAEA safeguards. A majority of the SSAC course participants have expressed the need to learn NDA techniques to augment their knowledge on nuclear material accountancy. Having the knowledge and the understanding of the NDA techniques is beneficial to the inspectors and the staffs of the SSAC.

Based on this premise, JAEA/ISCN will plan to develop an NDA course for the staffs of the SSAC, mainly involved in nuclear material verification activities and the nuclear material management from newcomer countries of nuclear energy in the Asian region. It is the objective of this course to improve the quality of the State's domestic (national) nuclear material management system by providing the following:

- A better understanding of the basic principles of NDA technology;
- Getting familiar with and learning the operating methods of NDA equipment;
- Expand one's knowledge of NDA technology through hands-on experience from real facilities;
- Creating a long-term network among NDA practitioners.

First and foremost, JAEA/ISCN will develop a course targeting participants who are involved in safeguards and nuclear material management from (Newcomer countries) nuclear power countries mainly coming from the Asian region. These will include the following:

- Staffs in charge of safeguards and nuclear material management of existing nuclear facilities (practitioners and researchers of nuclear fuel cycle-related facilities, etc.);
- Staffs from the State's Regulatory Authority, Domestic (National) inspectors;
- JAEA Young officers in charge of safeguards and nuclear material management; and
- Students whose field of study are related to the nuclear fuel cycle may also be considered.

## 10. Summary

The collaboration between JAEA/ISCN and EC/JRC is assured to continue for the delivery and conduct of the follow-up NDA courses. The efforts made during the 4 years from 2016 to 2019 have proven the success of enhancing the knowledge of the selected SSAC participants in the NDA techniques.

The JAEA/ISCN has a plan to develop its own Comprehensive NDA course in Japan in the near future. This paper has achieved to evaluate the essential requirements and resources to develop the future Comprehensive NDA course for the SSAC and to formulate the scheme of effective training methodology to implement the NDA course in Japan. Supporting the effective and efficient implementation of the IAEA safeguards activities and enhancing its credibility is extremely important for maintaining and strengthening the nuclear non-proliferation regime. Above all, in addition to the cooperation of strengthening the IAEA safeguards implementation, addressing the efforts in the capacity building of human resources involved in the nuclear material management system, mainly coming from

the Asian region, has become an important issue. These are among the defined objectives of the JAEA's NDA future training courses.

JAEA/ISCN, together with EC/JRC, will develop a curriculum addressing the specific needs of the staffs of the SSAC and considering their technical background, knowledge, and experience. The training materials will be further improved and specifically developed to provide the participants with a better understanding of the concepts of gamma measurements and neutron counting. The time element and scheduling of the course will ensure adequate hands-on exercises are provided. Participation of EC/JRC lecturers will provide excellent technical support in the conduct of the course. In addition, JAEA/ISCN will consider a visit to nuclear fuel cycle-related facilities. Improvements will be implemented gradually based on lessons learned, feedback from the participants and the experience following the delivery and conduct of the course. It is foreseen that the follow-up NDA course will continue to support and enhance the capacity-building efforts of the SSAC training activities.

# Strengthening of the French training and qualification activities on nuclear safeguards

**Decroocq Camille, Humbert-Brun Margot**

Institut de Radioprotection et de Sûreté Nucléaire (IRSN)  
Nuclear Defense and Security Expertise Division  
Non-Proliferation and Nuclear Material Accountancy Department  
International Safeguards Unit  
31 avenue de la Division Leclerc  
B.P.17 92262 Fontenay-aux-Roses, France  
E-mail: [camille.decroocq@irsn.fr](mailto:camille.decroocq@irsn.fr), [margot.humbertbrun@irsn.fr](mailto:margot.humbertbrun@irsn.fr)

## **Abstract:**

Training on nuclear safeguards and non-proliferation of Nuclear Weapons is essential to ensure the effective application of safeguards. France supports non-proliferation instruments, signed the Euratom treaty and, has concluded Voluntary Offer safeguards Agreement complemented by an Additional Protocol. In accordance with these commitments and given the well-developed civil nuclear industry, the management of the training on nuclear safeguards is considered since a long time of key importance by France. For these specific competencies, there is currently no offer of university courses leading to qualification. In France, an internal training system is in place allowing authorities and their technical support or nuclear industries staff to acquire the necessary skills (for example frequent training sessions for operators or state officers...). Among the challenges of the management of training, knowledge continuity and the upholding of an up-to-date high level of competency are most important.

The CTE (Euratom Technical Committee), the French authority representative, in charge of the implementation of international nuclear non-proliferation controls and its technical support, IRSN (Institute for Radioprotection and Nuclear Safety) are currently working on strengthening the French training system on nuclear safeguards to enhance its performance. This strengthening program consists first in establishing a comprehensive inventory of the current training system including sources and materials available for the trainings, the actors and, the programs of the courses available in France. It further consists in a global reflection allowing the identification of areas of improvement, as examples: the setting up of a quality approach for the management of trainings or the reinforcement of the French program with the integration of approaches developed by international or foreign entities.

**Keywords:** safeguards, non-proliferation, training, skills, qualification.

## **1. Introduction**

France has a well-developed nuclear energy industry composed of 58 electronuclear reactors and a whole nuclear fuel cycle going from the conversion of yellow cake, to the reprocessing of irradiated fuel, and the production of recycled fuel (MOX fuel or Recovered Uranium fuel).

Therefore, France stands as one of the major world actors in the field of nuclear energy production. With more than 60 years of experience in nuclear industry, French training offer is large.[1] It includes education and training programs at several university levels as well as continuing education to train personnel for the industry and the research and development activities. The French expertise allows thereby to build highly skilled professionals.

During last NPT conference in 2015, France highlighted the importance of training in the field of electronuclear civil energy [2] and its wish for a cooperative response to the growing international

demand in order to increase the international training mainly for countries accessing to nuclear energy.

The technical training offer has to go along with trainings on nuclear non-proliferation treaties and nuclear safeguards. Indeed, the knowledge of nuclear safeguards in the nuclear industry is essential to fulfill the objectives of safeguards against the spread of nuclear weapons and for the early detection of clandestine nuclear activities. The verification measures of IAEA include declarations, on-site inspections, monitoring and evaluations that involve various people from the industry, the research area and the authorities. At different levels depending on the responsibilities of the professionals, the training on nuclear safeguards is necessary to comply with obligations linked to safeguards agreements.

France is engaged in non-proliferation agreements and developed a training system on safeguards. Indeed, France signed the Treaty on Non-Proliferation of Nuclear Weapons (NPT) in 1992, yet respecting its provisions since 1968. As a Nuclear Weapon States (NWS), France signed a voluntary offer safeguards agreement (VOA) in 1978 and an additional protocol (AP) in 2004. Since 35 years France contributes to IAEA safeguards with a French program that supports financially and brings expertise to IAEA safeguards department. Part of the European Atomic Energy Community (EAEC), France signed the Euratom treaty in 1957. Euratom security control and IAEA safeguards are thus in place in France. To support the commitments of France to its international obligations and contribute to the objectives of these treaties, the various stakeholders of the nuclear industry, the authorities and their technical support are trained to safeguards. The French organization and the training system in place are described in this article as well as the actions that are implemented to develop and strengthen this system.

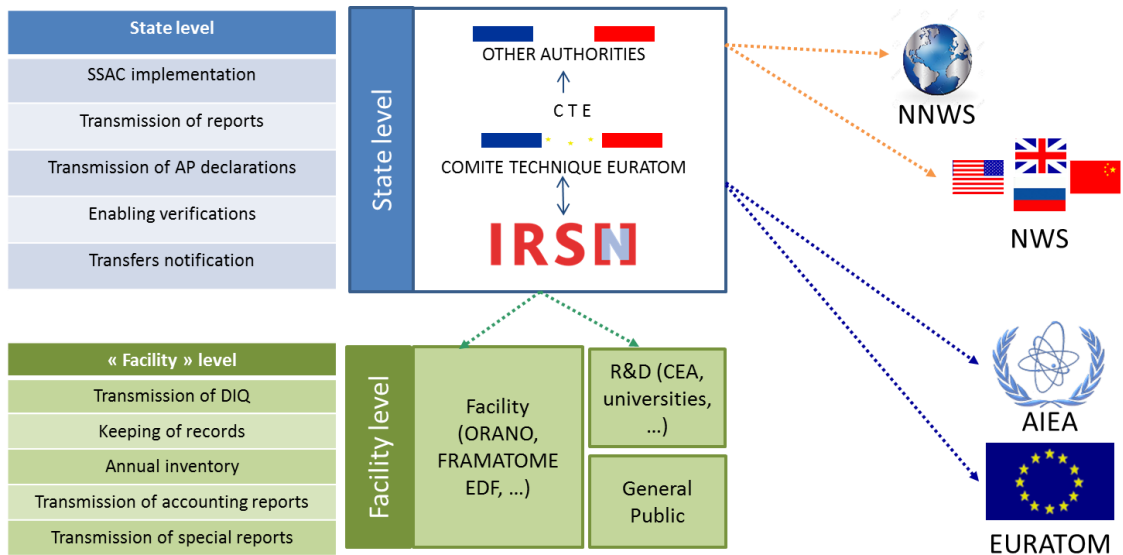
## **2. French organization, description and performance of actual safeguards training system**

### **2.1. French organization and challenges**

As featured on the following scheme, the nuclear domain in France includes many people with various functions that require different levels of knowledge regarding safeguards and their practical application. The level of required skills can be separated in two categories: the state level and the "facility" level. The French training network is adapted to that scheme. It is centralized around the CTE (Euratom Technical Committee), the French authority in charge of the monitoring of the implementation of international treaties of non-proliferation, and its technical support IRSN (Institute for Radioprotection and Nuclear Safety). These two entities are French experts on safeguards and contribute as members to different international working groups on the topics related to safeguards. Communication with international organizations and other states on the best practices or returns of experience is handled by CTE and IRSN and is beneficial for all parties. Thus, CTE and IRSN take part in both the transmission of the knowledge and the sustaining and improvement of the expertise.

The nuclear industry and R&D players are trained to be able to comply with their obligations regarding the non-proliferation controls. Education in the field of safeguards is necessary for them because of the nature of their activities subject to safeguards.

As well, France views that awareness-raising is needed for the public in general to communicate on its international commitments on nuclear non-proliferation.



In this framework, the challenges in safeguards training rely on the variety of protagonists in the nuclear field. France shall ensure knowledge continuity with a large offer for French institutions representatives, industry managers and operators, research and development sector and possibly the general public.

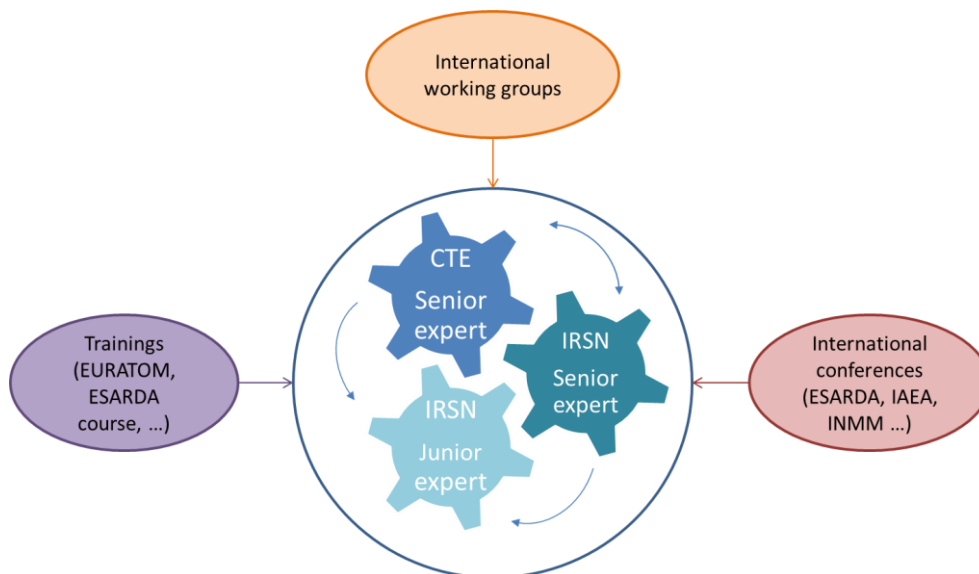
## 2.2. Source of knowledge

The expertise of IRSN and CTE relies on extensive knowledge shared by staff of various levels of seniority on the international agreements, the regulatory documents and other application documents. This knowledge is based on initial training, independent learning, field experience and continuous improvement.

For the initial training of newcomers in the non-proliferation department of IRSN, an internal process of training is in place with a mentoring period managed by a senior expert of the department. This process is composed of training units of 1 to 4 hours provided progressively over a year punctuated by milestones and covers the extensive general knowledge on safeguards. Some specific job tasks allow the trainee to go into more details for particular topics. This process ensures to address the workforce renewal challenges and knowledge continuity.

In addition to this internal training program, newcomers from the CTE or IRSN are encouraged to attend the ESARDA course on nuclear safeguards or the training of the European Commission entitled "Member State Training" specifically on Euratom safeguards. These courses give the opportunity of exchanging knowledge with other institutions and the attendees can share with their colleagues current topics when coming back from the class.

CTE and IRSN are also taking part to international working groups such as Esarda Implementation of Safeguards, Esarda Export Control or Esarda Verification Technologies and Methodologies. Through these working groups, new practices and directions are shared for the implementation of safeguards. This is a valuable way of keeping a high level of knowledge on the latest novelties related to safeguards. The same approach is applied when CTE and/or IRSN attend international conferences such as IAEA symposium, Esarda symposium, INMM annual meeting. Meetings with experts are an effective tool for continuous learning and worldwide technology watch on safeguards.



### 2.3. Training programs

The knowledge gathered, enriched and sustained as mentioned above is then used for different external trainings in France. Different types of training are provided depending on audience and level of details needed. Beyond the technical part of the training at the facility level, the goal is also to give meaning to the work of people that are involved in safeguards implementation and to motivate them in their daily job to guarantee a better quality.

#### Trainings covering general aspects of safeguards

These short trainings are generally part of a global training for professionals given by a continuing education center. The expertise of CTE or IRSN is solicited by the training organization for ½ day to 1 day course on non-proliferation and safeguards. For example, contributions are given in the following courses:

- Training “Management of nuclear materials” offered by INSTN (National Institute for Nuclear Science and Technology), a public higher education institution administered by the CEA (French Atomic Energy and Alternative Energies Commission). The targeted audience is people from the CEA involved in the management of nuclear materials such as, for example, professionals responsible for accountancy or for physical inventory;
- Training “nuclear materials protection, nuclear safeguards and interface with nuclear safety” offered by ENSTTI (organism in charge of training program and organization for IRSN) to professionals involved in nuclear security activities employed in National Regulatory Authorities (NRA) and Technical Support Organizations (TSO);
- Orano training addressed to Orano employees involved in the management of nuclear materials. The training was completely rebuilt in 2019 and the participation of IRSN is now concentrated in a tutorial.

#### Training for French institutions representatives

One-time general presentations on safeguards are regularly given for French institutions representatives such as SGDSN (the General Secretariat for Defense and National Security), MEAE (the Ministry for Europe and Foreign Affairs), MTES (the Ministry for the Ecological and Solidary Transition) for examples. These presentations give the necessary knowledge on the regulatory obligations that apply in France and an overview on the contribution of the different stakeholders (state or facility level) to authorities that are not directly involved in the implementation of international agreements on non-proliferation.

#### Specific trainings

Training can be organized for specific purposes. For example, an annual training is organized on the French additional protocol. The objectives are to strengthen the awareness of declarants to the declaration requirements linked to the additional protocol and to improve their declarations. Such training includes practical exercises that aim to reinforce the knowledge of the attendees. As a positive

result, we observe an improvement in their declaration. This is emphasized by the timing of the training that takes place just ahead of the declaration period.

#### Technical assistance

Upon request of facilities for specific needs linked to compliance with obligations regarding safeguards, CTE and/or IRSN can provide specific tailor-made training. For instance, CTE and IRSN take part yearly to a meeting with accountants from EDF (the French electric utility company).

#### International trainings

In response to a call to tender, IRSN can organize a more detailed training on safeguards and their implementation. For instance, IRSN responded through a consortium driven by RISKAUDIT to the demand of Moroccan nuclear regulatory authority (AMSSNuR) in assisting for capacity building and for enhancing the regulatory framework for nuclear and radiation safety, nuclear safeguards as well as radioactive waste management in Morocco.

### **3. Evolutions foreseen**

#### **3.1. Objectives definition**

Many projects have been conducted with the objective of strengthening the institutional capacity of the states' regulatory authorities by means of international conferences (IAEA Symposium), workshops (ESARDA), training courses (Facility training courses) and field exercises. A specific working group has been set up with participants from CTE and IRSN to address the challenge in France: The first step consisted in building an exhaustive map of the French training system and training possibilities described above. The second step consisted in identifying development and improvement tracks. With an emphasis on continuous improvement, 6 priority objectives for the safeguards training and qualification were identified.

- Improve continuously the current training system (a)
- Ensure French authorities and French operators comply with international agreements (b)
- Sustain and update the expertise of people in charge of safeguards implementation on safeguards related topics (c)
- Complete the training offer by identifying work on innovation possibilities of the training system (d)
- Effectively represent French interests (e)
- Enhance French ability to deliver its safeguards expertise to foreign states (f)

#### **3.2. Implementation**

The proposed implementation of the objectives is described in the following table. One of the first actions linked with objective (a) was the creation of an internal working group. The actions specified in the table for the other objectives constituted the first discussion of this working group. Introducing performance metric as a quality measurement of the training system will help to find out the possibilities for continuous improvement. Feedback form is usually distributed at the end of the training sessions, never the less trainings are given by different organisms and collecting data relative to safeguards would be very interesting. The e-learning could help reaching a larger audience and reduce for some part the training workload.

An analysis could be carried out in order to verify the match between the training offer and the knowledge of the relevant actors to comply with international agreements (b). The knowledge on safeguards should be maintained at its best level (c) and technology intelligence through sharing of information from international discussions and workshops is therefore important. When a suggested improvement is identified (d), the training offer should be adapted. For example, it appeared recently, that a new training gathering information on international agreements, rules for imports/exports could be proposed specifically to nuclear industry sales and marketing departments in order to reinforce their knowledge on safeguards necessary for negotiation of international contracts and nuclear transactions. One more global consideration would be to enlarge the safeguards training offer to some technical university degrees, as it is only little developed yet. This would require a detailed analysis to evaluate the interest of this proposition and the means necessary to implement it. An additional benefit would be to attract students to this sector that is not well known to the general public.

As well, visibility of French knowledge and expertise on safeguards topics could be enhanced by effective communication during the international workshops (e). Concerning the training skills and the

cooperation between states, IRSN responded recently to a call to tender from the European Commission for 6 one-week-courses on safeguards over 3 years.

Objective	Implementation
<b>a. Improve continuously the current training system</b>	<ul style="list-style-type: none"> <li>➤ Build an internal working group</li> <li>➤ Consider participation to ESARDA TKM working group [3]</li> <li>➤ Brainstorm to identify the topics and information needed by occupation</li> <li>➤ Introduce E-learning and performance metric</li> <li>➤ Build network between the training organisms</li> </ul>
<b>b. Ensure French authorities and French operators comply with international agreements</b>	<ul style="list-style-type: none"> <li>➤ Knowledge and understanding of all relevant actors roles and responsibilities</li> <li>➤ Knowledge of the international agreements (IAEA, EURATOM; bilateral agreements).</li> <li>➤ Knowledge of the France-IAEA safeguards agreement and protocols</li> <li>➤ Ability to provide acknowledged technical expertise to discussions</li> </ul>
<b>c. Sustain and update the expertise of people in charge of safeguards implementation on safeguards related topics</b>	<ul style="list-style-type: none"> <li>➤ Presentation of topics colleagues after participation to workshops, training or working groups</li> <li>➤ Create and maintain a documentary base ordered by safeguards related topics</li> </ul>
<b>d. Complete the offer by identifying work on innovation possibilities of the training system</b>	<ul style="list-style-type: none"> <li>➤ Work and respond to immediate identified needs (for example short training to industry sales and marketing department)</li> <li>➤ Propose safeguards introduction courses to some university degrees</li> </ul>
<b>e. Effectively represent French interests</b>	<ul style="list-style-type: none"> <li>➤ Representation and visibility in international meetings on non-proliferation issues (AIEA Symposium, ESARDA, INMM)</li> <li>➤ Study the possibility to inform general public through conferences on the French commitments regarding non-proliferation</li> </ul>
<b>f. Enhance French ability to deliver its safeguards expertise to foreign states</b>	<ul style="list-style-type: none"> <li>➤ Benefit from international experience, for example ANNETTE course on safeguards [4]</li> <li>➤ Ability to understand other countries motivations and interests</li> <li>➤ IRSN/ENSTTI training courses 2019-2021</li> </ul>

#### 4. Conclusion

As described in this paper, the French training offer regarding safeguards is large to respond to the need of multiple relevant actors of the civil nuclear industry and the research and development sector. An internal working group was built to engage an approach of continuous improvement. The objective is to maintain a high level of skills in France to effectively implement the international agreements and therefore contribute to the goals of safeguards in the world. Among the possible outcomes of the working group, the key perspectives are the improvement of the current training system and the strengthening of the French support and cooperation to the international training offer in particular for states that are developing a civil nuclear industry for energy.

## 6. References

[1] <https://i2en.fr/en/> visited on April 9<sup>th</sup> 2019

[2] Review Conference of the Parties to the Treaty on the Non-Proliferation of Nuclear Weapons; New York; April 27<sup>th</sup>- May 22<sup>nd</sup> 2015

- NPT/CONF.2015/10 - Report submitted by France under actions 5, 20 and 21 of the Final Document of the 2010 Review Conference of the Parties to the Treaty on the Non-Proliferation of Nuclear Weapons
- Statement during General Debate H.E. Mr. Jean-Hugues Simon-Michel, Permanent Representative to the Conference on Disarmament, April 28<sup>th</sup> 2015.
- NPT/CONF.2015/WP.35 - Capacity-Building Initiative: An informal group to support capacity-building networking, in the frame of the International Atomic Energy Agency: Working paper submitted by France and Romania.

[3] [https://esarda.jrc.ec.europa.eu/index.php?option=com\\_content&view=article&id=69&Itemid=218](https://esarda.jrc.ec.europa.eu/index.php?option=com_content&view=article&id=69&Itemid=218) and <http://www.nusaset.org/> visited on April 8<sup>th</sup> 2019

[4] Rossa, R *et al.*; *The education and training offer in nuclear safeguards within the Euratom research and training project "ANNETTE"*; IAEA Symposium on International Safeguards 2018

## EURATOM safeguards inspector training capabilities of the JRC-Ispra

F. Raiola<sup>1a</sup>, J. M. Crochemore<sup>1</sup>, T. Bogucarska<sup>1</sup>, A. Rozite<sup>1</sup>, B. Pedersen<sup>1</sup> and K. Abbas<sup>1</sup>

<sup>1</sup>European Commission, Joint Research Centre, Nuclear Safety and Security Directorate G, Nuclear Security Unit G.II.7, Ispra (Italy)  
E-mail : francesco.raiola@ec.europa.eu

### **Abstract:**

*The Nuclear Security Unit of the Joint Research Centre based in Ispra (Italy) has a long experience in providing trainings to a large variety of customers and audience in several fields such as nuclear safeguards, security including non-proliferation and export control of dual use commodities. With regard to safeguards, for over thirty years, the Nuclear Security Unit has provided training to nuclear safeguards inspectors of DG ENER and the IAEA which is essential to the proper implementation of the international safeguards and in line with the JRC mandate to support DG ENER under the EURATOM treaty. In addition to those trainings fully organised by JRC, the unit is also support other internal organisations such as JAEA and US DoE/DoS to implement their training programmes. This paper reports the implementation experience on nuclear material Non Destructive Assay's trainings that are provided to EURATOM inspectors on uranium enrichment verification and plutonium isotopic composition with gamma-ray spectrometry and also plutonium mass determination by passive neutron coincidences. These training courses deliver both the theoretical understanding of methods and the practical use of the instrumentation starting from the detection principles, analysis methods, to hands-on exercises using nuclear materials and explain the adaptation of advanced analysis codes for the extraction of information. They generally last a single week including not only classroom lectures and exercises but also cases studies and practical exercises in the laboratory, and they fit well the needs of EURATOM inspectors. A recent focus in these courses has been evaluation of the error estimate in measurements and the understanding of possible sources of measurement errors with regard to metrology and conformity assessment.*

*Further use of modern educational techniques and methods is described to highlight also the importance of "the right teaching method for the right audience" to achieve the best possible transfer of knowledge.*

**Keywords:** EURATOM Safeguards; NDA measurement techniques; Education;

<sup>a</sup> Contact: [francesco.raiola@ec.europa.eu](mailto:francesco.raiola@ec.europa.eu)

---

## 1. Introduction

EURATOM Safeguards are an important cornerstone of global non-proliferation of nuclear materials and verification of their civil use [1]. As stated in EURATOM treaty establishing the European Atomic Energy Community (E.A.E.C. - EURATOM), title two - provisions for the encouragement of progress in the field of nuclear energy, chapter vii: safeguards:

### ARTICLE 77:

"In accordance with the provisions of this chapter, the commission shall satisfy itself that, in the territories of member states,

- A. ores, source materials and special fissile materials are not diverted from their intended uses as declared by the users;
- B. the provisions relating to supply and any particular safeguarding obligations assumed by the

community under an agreement concluded with a third state or an international organisation are complied with.” (ndr. obligations under the Non-Proliferation Treaty)

Besides the importance of the EURATOM training and its continuity is reflected on the Council adopted regulation [2] extending the EURATOM Programme for 2019-2020.

The European Commission has developed a well consolidated safeguards system in the last 60 years from when the EURATOM Treaty was signed in Rome 60 years ago, in 1957. This system, which in the sixties was only controlling 29 mines in operation and approximately 140 installations, currently monitors around 700 installations and more the 1,500 small holders of nuclear materials with about 130 inspectors and 1167 on-site inspections.

The Nuclear Security Unit of the Joint Research Centre based on the Ispra site has provided for more than 30 years training to nuclear safeguards inspectors of DG ENER and the IAEA. This is also an opportunity for sharing information between inspectors of both organization considering most importantly that about 60% of inspections in European Union Member States are performed jointly between EURATOM and the IAEA. The support of JRC in terms of R&D and this training is in the mandate of JRC of EURATOM treaty towards DG ENER.

The safeguards training at the JRC Ispra covers three of the four main categories of activities of nuclear safeguards: non-destructive analysis (gamma spectrometry and neutron counting), process monitoring and containment & surveillance.

## 2. Aim of the EURATOM training course

Each nuclear facility of EU must declare every month all movements of nuclear materials in and out of their installation to the European Commission. Once a year they must record all stocks of nuclear material they ownership. In order to guarantee and verify that nuclear materials would not be diverted to purposes other than those for which they were originally declared, the EURATOM inspectors shall:

- Make measurements to ensure that declarations refer to the correct type and quantities of nuclear materials;
- Use video surveillance systems to establish the correctness of declarations of receipts or shipments of nuclear materials;
- Put on seals to hold nuclear materials that will not be used immediately;
- Conduct annual verifications of inventories made at nuclear installations.

All these activities are strictly dependent on the effectiveness of the procedure utilized by the inspectors and in order to make a smoother nuclear facility operation they must be well structured. Thus the EURATOM training course needs to aim at the successful application of those procedure and it is worth to mention that it is enhanced by the R&D activities in the JRC laboratories that focus on new technical solutions and methodologies to be applied to the routine work on the EURATOM inspectors. In the three main categories of activities of nuclear safeguards mentioned above (NDA, process monitoring and containment & surveillance) the JRC sites will perform a Safeguards training plan 2019 for DG ENER with the following courses:

1. Mass/Volume Methodology and tank Calibration at the PML (Process Monitoring Laboratory) part of AS3ML (Advanced Safeguards Measurement, Monitoring and Modelling Laboratory): the course provide training on volume measurements in tanks and vessels used in reprocessing facilities; calibration exercises with particular attention on various on most the technical boundaries; a didactical software tool is used by the inspectors to learn on-line the results of those effects, geometrical design and choice of the right instrument to be used.
  - AS3ML, Ispra (April 08/12)
2. Passive neutron assay and active neutron interrogation at PERLA (Performance Laboratory for Non-destructive assay) and PUNITA (Pulsed Neutron Interrogation Test Assembly): the course provides the participants with theoretical and practical sessions to use the passive neutron correlation technique (coincidence counting) to determine the Pu mass in a sample. A particular emphasis is devoted to hands-on exercise with standard hardware and software tools to familiarize and be proficient in the use of the instrumentation for neutron counting. In the Active Neutron Interrogation course presented by the Nuclear Security Unit at Karlsruhe site is

focused on non-destructive active neutron interrogation techniques for the measurement of the mass of U-235 in U samples. The course focuses on: familiarisation of the instrument and its calibration, the verification measurements and the data processing. Hands-on exercises are spent on practical examples of LEU and HEU.

- PERLA Lab, Ispra (Feb 18/22 - Oct 21/25)
  - JRC Karlsruhe, AWCC: Nov 18/22
3. JRC ultrasonic seals for underwater and dry storage: the Seals and Identification Techniques Laboratory (SILab) conduct training courses on the use of JRC CANDU sealing system: theoretical class on the principle of ultrasound technique for sealing; practical sessions on the software management and mechanical seal installation procedure at the spent fuel mock-up realized in the laboratory.
    - AS3ML Laboratory, Ispra (Apr 16/17 - Oct 15/16)
  4. Uranium enrichment and plutonium isotopic composition verifications: this non-destructive analysis course will be described in detail in the following below sections.
    - PERLA Lab, Ispra (Mar 25/29 - Sep 23/27)
  5. 3D Laser-based Design Information Verification: course include operation of the 3 Dimensional Laser Range system (3DLR) and associated DIV tool software with preparation of the database; acquisition of the scans; performing registration and 3D model construction; comparison with later scans: verification activities. The participants will acquire the necessary skills to identify where and under which conditions to use the tool for best results.
    - Laser Lab, Ispra (Mar 12/14)
  6. In JRC Karlsruhe site: training on integrated automated nuclear measurements, data collection and data handling and evaluation on advanced hands-on RADAR/CRISP/XSEAT course. The course focuses on unattended monitoring of plutonium at Pu-handling facilities with the use of remote acquisition software RADAR and the related evaluation software CRISP.
    - in JRC Karlsruhe:
      - i. RADAR: Mar 18/22
      - ii. APEX, for IAEA, Mar 18/22 (at IAEA premises) & Mar 25/29 (at JRC site)
      - iii. NDA refresher course for IAEA (ENER invited), Sep 16/20
      - iv. APEX: Nov 4/8 (at IAEA premises) & Nov 11/15 (at JRC site)

This paper will focus on those trainings performed in JRC Ispra in PERLA laboratory namely on nuclear verification with gamma spectrometry and neutron counting.

### 3. Training modules

The course contents must fit with the knowledge level of the trainees in nuclear physics and engineer for the NDA. In this context, the first session on any training is dedicated to discussion and interaction with the trainees to best understand their technical backgrounds and objectives in order to organise the training for their best expectations although the over whole objectives are set. This requires a high grade of flexibility of the trainers. In particular for the NDA course in gamma spectrometry and neutron counting [3] shall adopt a balance combination of theoretical sessions (mostly in a form of classical slide presentation) and a practical sessions (hands-on experience on the instruments/procedures used in field by the inspectors).

Usually the NDA EURATOM training course in JRC Ispra develops in the arc of three weeks thus distribute between U enrichment verification and Pu isotopic composition in the first two weeks on gamma spectrometry:

One week	One week
<ul style="list-style-type: none"> <li>• Physics background of the gamma-ray spectrometry</li> <li>• Detectors, electronics and signal analysis</li> <li>• Introduction of <i>U enrichment verification</i></li> </ul>	<ul style="list-style-type: none"> <li>• Physics background of the gamma-ray spectrometry</li> <li>• Detectors, electronics and signal analysis</li> <li>• <i>Pu isotopic composition</i> determination</li> </ul>

and on the third week, the Passive neutron Assay sessions will include:

- Properties of Pu isotopes and other neutron sources,
- Neutron detector heads
- Rossi- $\alpha$  curve and the Shift Register
- Demonstration of passive neutron instrumentation
- Elements of neutron correlation counting, analysis methods, calibration curves
- Pu mass determination by “hand calculations”
- Calibration and verification measurement of Pu sources using INCC and the passive neutron detectors: PSMC, INVS and HEPC
- Setup of INCC software for passive neutron measurements, calibration and verification exercises using measured data from large PuO<sub>2</sub> samples

The JRC team can also offer ad-hoc trainings in those topics if requested by the DG ENER. The number of the participants during a NDA training course is usually 6-8 people and that assures a complete (as will be explained in the sections below Sec.3) integration of all of them in the discussion during each theoretical/practical sessions. It also guarantees the possibility to cover all possible questions raised during the courses.

### 3.1. Theoretical session

In order to give the basic understanding of the physical process that involve gamma spectrometry and neutron counting determination, a set of theoretical sessions have been optimized over the last 30 years through the use of the high experience of the JRC team. They have been also adjusted in complexity in relation to the knowledge level of the trainees in the nuclear physics field and enriched by the R&D activities at the JRC laboratories (e.g. testing comparison MCA-166 and MCA-527, analysis performance HPGe planar and coaxial, etc.). The main focus of the first part of the theoretical module sessions for the gamma spectrometry course is thus structured in detail:

- Overview on basic nuclear physics:
  - Characteristics of atom and nuclei
  - Radioactivity
  - Interactions of radiation with matter
  - Attenuation law
  - Decay law
- Detectors and electronics
  - Overview on scintillation based and semiconductor devices
  - Signal chain electronics: pre-amplifier, amplifier, ADC, MCA

After theoretical sessions, the trainees carry hand-on experience on the described nuclear devices and perform few exercises in the laboratory (below described in the Sec.3.2) to improve their knowledge on their functionality and their related signal chain electronics/software combined in order to be ready for the second part of the theoretical sessions. This second part is thus structured:

- U enrichment determination by gamma spectrometry
  - U-235 enrichment determination by intrinsic calibration
  - U-235 enrichment determination with the enrichment meter principle
- Pu isotopic composition determination by gamma spectrometry
  - Measurement principle
  - Gamma spectra evaluation

A typical training course for EURATOM inspectors last full 5 days where 30% of the time is devolved to the theoretical modules with the topics described above and the rest of the time to the hands-on experience in PERLA laboratory on the electronic instrumentation that will be used on field by the inspectors.

The theoretical sessions shall create the right background and the path to understand the meaning of the different procedure used for either gamma spectrometry course (U enrichment or Pu isotopic composition determination) or Pu neutron assay course (neutron counting determination) but with the starting lessons on basic elements of gamma spectroscopy and neutron counting to pave the path for a smooth learning curve to the final mentioned topics (see sec.3). The aim must also be that the

principles of the methods are completely understood by the participants before going to the hands-on exercises.

In the gamma spectrometry course extra effort is also devolved to the gamma-ray multi-group analysis code (MGA) developed at Lawrence Livermore National Laboratory [4]. This code has been widely used in the area of gamma-ray NDA plutonium assay essentially but also in the U enrichment determination because of the possibility to use no calibration standard/s for it. Calibration of the detector efficiency is not required, but is determined intrinsically from the measured spectra. Through the peak unfolding on certain energy regions (e.g. mostly 59-300 keV) the code is able to determine the net peak area and calculates the Pu isotopic ratios at the day of the measurement. From the side of setting the measurement, the JRC team explained the critical conditions (i.e. energy resolution, peak/channel positioning) and consequently the procedure to be used by the inspectors at which the code will perform correctly and with a reasonable accuracy due to just the statistics of the counts.

Even if for the Uranium enrichment determination other analysis could be used (U235, WinUF6, NaIGEM) and they are also currently used, a strong emphasis is put on the MGA/U for its simplicity from the procedural point of view but rather complexity from the code analysis. Lately due to the increasing of interest from several experienced inspectors, some extra time has been devoted to understand the way the MGAU code does the analysis and possible further improvement will be also put in the explanation of the physics behind it (e.g. methods and algorithms).

The same approach has been used to the course on Pu neutron assay course. It evolves in a full week with 20% on theoretical sessions and the rest on hands-on the procedure and instrumentation exercises. The typical structure of the theoretical session on Pu neutron assay course is:

- The physics principles of neutron sources and neutron counting
- Composition/design of detectors and analysers
- The neutron coincidence counting analysis method

### 3.2. Hands-on session

Most of the time of the training course is devote to the practical exercise in order for the trainees to get familiar with the equipment as used by inspectors in field, to understand the set-up of equipment before measurements and to explore many measurements in a wide range of situations that are linked to the place in the nuclear fuel cycle in which they will be performed. As in their real duty job the inspectors will faced different instrument and methods to analyze the U enrichment and Pu isotopic composition. This training has to provide inspectors with the practical skills for those methods. The mentioned number of participants permit us to take advantage on the division of the inspectors in group of two (typical configuration at a nuclear facility during an inspection) in order to make them able to perform the measurement (U enrichment or Pu isotopic composition determination) with a total control of the parameters of the electronic setting. By also exchange the operator between the software at the dedicated PC and the electronic configuration assure the full understanding of the procedure.

For this purpose the inspectors are instructed in the PERLA in which we have advanced nuclear instrumentation and nuclear materials standards (CBNM - Central Bureau for Nuclear Measurements). In the specific the hands-on exercise is structured as following:

- Set-up of the gamma-ray spectrometry chain using HPGe and NaI
- Calibration and resolution determination using HPGe and NaI
- U enrichment determination
  - with NaI and the calculation code NaIGEM
  - with HM-5 handheld equipment HM-5
  - with HPGe and the calculation code WinUF6
  - with HPGe planar and the calculation code MGAU
- Pu isotopic composition determination
  - with a Planar HPGe and the calculation code WinMGA

The important at this point of the training is ensure that the trainees have the enough information to process from the theoretical sessions and with the right labs configuration (i.e. nuclear instrumentation, PC, electronics chain available and so on), as well as at least one instructor at their complete disposal to be able to be comfortable with the procedures and methods for the U-enrichment and the Pu isotopic composition determination. The actual learning configuration assure also an active communication between the instructor and the trainees with, at the best of their knowledge, the JRC team available to answer any questions that it come along the practical exercise sessions. Besides in this way there is the possibility to create ad-hoc practical exercises and explain specific detector configuration (i.e. Cd filter, Pb collimator etc.) and methods that has been or not explained during the theoretical sessions. In



**Figure 1:** Practical exercise on U and Pu CBNM samples at the PERLA laboratory for EURATOM inspectors.

the below pictures (see **Figure 3**) it showed the different type of nuclear device (NaI, HPGe planar and coaxial, CdZnTe) used during the laboratory exercises, the signal electronic chains (power supply, cable connections and Multi-Channel Analyzer – MCA 527) and the software for the analysis (WinSpec and MGA/MGAU code windows).

In a similar way the Passive Neutron Assay course is intended for nuclear inspectors and the main objective is to teach how to perform mass determination of bulk Pu samples by means of the so-called neutron coincidence counting method. The course form is a mixture of lecture sessions, practical sessions with guided experiments with nuclear samples and standard detectors, and calculation exercises. The practical sessions take place in the PERLA laboratory. They include the following main aspects:

- hands-on exercises with standard neutron detectors and analysers
- familiarization with the standard safeguards neutron software package INCC
- calibration of a standard neutron well-counter using INCC and nuclear samples
- INCC verification procedure of standard bulk samples
- troubleshooting in instrumentation and data analysis

The purpose of the course is to prepare the inspector for the task of verification measurements of plutonium under field conditions. The complete analysis procedure from acquiring data with the neutron counter and the INCC software to the final comparison of operator's mass declarations with the analysis result is examined. Also the performance of different analysis methods and routinely used algorithms is discussed. The course includes a number of practical sessions to familiarize the course participant with the handling of the instrumentation (like showed on the bottom right neutron device on **Figure 3**), the INCC software, and the operational procedures. Finally the course uses practical examples of real measurement data for analysis, interpretation and troubleshooting.

Other courses in neutron counting are also offered to EURATOM. This includes specialised course on specific instrumentation such as the passive neutron Drum Monitor for measurement of Pu in waste (PUNITA laboratory). Also training in neutron detection methodologies such as basic neutron counting

instrumentation, or specific training in neutron multiplicity counting can be given. JRC also has capabilities for hands-on training in active neutron counting in techniques such as the differential die-away (DDA) although such a course has not been given yet.

At the end of the day the inspector will need to answer a question like this: Can you confirm that the enrichment of this item is 3.6% as declared by the operator? Is the measured isotopic composition in agreement with the declared one (e.g.  $^{240}\text{Pu}_{\text{eff}}$  value agrees within  $\pm 3\sigma$ )?



**Figure 2:** Plutonium isotopic composition training course on September '18 for EURATOM inspectors.

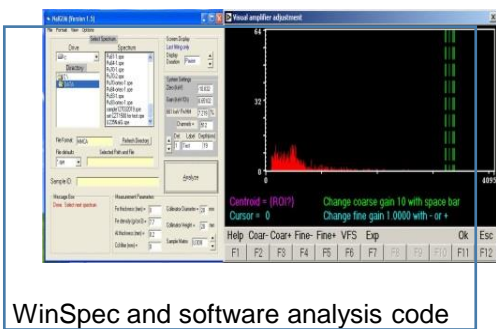
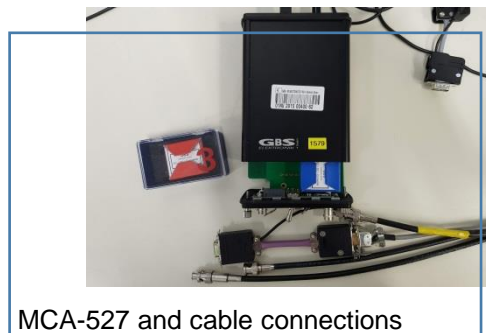
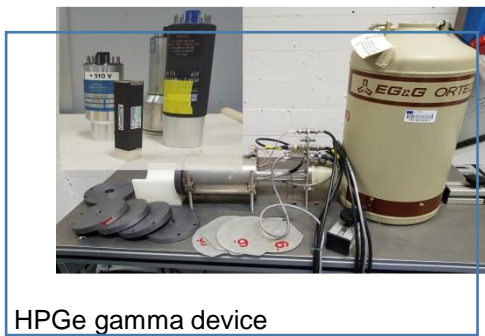


**Figure 3:** PERLA laboratory instrumentations.

#### 4. Educational technique and methods

Educational techniques and methods require the perfect understating of the audience at which a specific course it is addressed, that can be reached by long experience on the subject matter (NDA experience from theoretical as experimental point of view), in order to be able to use the correct language (not in the specific language context but on the level of terminology to be used) to connect with the audience as well as by the use of learning tools (i.e. flip chart, active white board, virtual reality,

simulation tools and etc.). The outstanding experience of the JRC team on the NDA and related fields has enormously helped in the past years to fulfill the first condition and the future

It was very important for the NDA experts to have a very good balance between theory and practice and to focusing on the learning objectives of the EURATOM inspectors attending the course.

During the training we make also aware the participants about dedicated web tools (i.e Nucleonica, the leading nuclear science applications platform for web-based calculations, Nuclide chart app, etc.).

Interactive method of learning experience to the use of new media has active screen representation (tablet, mobile phone and similar) or even the use of Augmented reality that produce a better interaction with the trainees and increase the level of attention during a theoretical sessions. During the hands-on module the JRC team frequently tests the comprehension of the specific topic (i.e. energy calibration, energy resolution, U-235 enrichment determination, hardware and software chain, INCC software, neutron counting) through the use of practical exercises and examples adequate to the specific knowledge level of the trainees.

Beside the final questionnaire it is used to promote the discussion between the participants and as input for the lectures to understand if the main message has been correctly transmitted, while the feedback form it has been proposed has the starting point for improvement and modification on the arguments and teaching method/tools used during the training. For example is worth to mention the following DG ENER participant's feedback (after the "Uranium enrichment determination by gamma ray spectroscopy training course" - JRC ISPRA, 20-24 March 2017): "The most valuable thing the participants learned was all applicable gamma spectroscopy methods for the determination of Uranium content in samples." In that circumstance the EURATOM inspectors gave an overall rating of the course: 4.9 (out of 5). Another good input that was taken from one other of the participants' feedback: "will be beneficial to introduce a small statistics module, where uncertainty of measurements is discussed, as to raise awareness of the distinction between uncertainty of a measurement and standard deviation provided by the software".

## 5. Collaboration with different entities

Established in 1981, the European Commission Cooperative Support Programme (EC-SP) provides a framework for the technical support to the IAEA in the field of nuclear safeguards. The EC-SP was involved in numerous tasks (134 in the late 2015) with currently 40 tasks ongoing (see **Figure 4** on the right graph). The JRC operates the EC-SP in close cooperation with the EC DG ENER. One of these activities is training of inspectors: jointly with EURATOM inspectors or targeted to IAEA needs.

EU and the US have a long standing tradition to cooperate towards nuclear material is managed worldwide in the most secure way. During the IAEA Safeguards Symposium, on 2.11.2010 a new „Agreement in the field of nuclear material safeguards and security research and development“ was signed.

Since 2016, the JAEA, Integrated Support Center for Nuclear Non-proliferation and Nuclear Security (ISCN), in collaboration with the European Commission, Joint Research Centre (EC/JRC), has developed and provided a 5-day NDA course (Follow-up NDA Course) at JRC Ispra, Italy as a follow-up to the ISCN's SSAC training course for the selected participants. This activity is covered under "the Agreement between the JAEA and the EURATOM in the Field of Nuclear Material Safeguards Research and Development". The 4<sup>th</sup> Follow-up NDA Course was successfully conducted from 28 January to 1 February 2019 in EC/JRC Ispra, Italy with participants from Armenia, Malaysia, Thailand, Vietnam, and Japan (see **Figure 4**). This fruitful collaboration was an exchange from JAEA NDA experts (use of NDA techniques in various nuclear fuel cycle facilities at JAEA) and the JRC experts (use of NDA techniques and effective teaching methods from EC/JRC) as extensive described in Ref. [5].

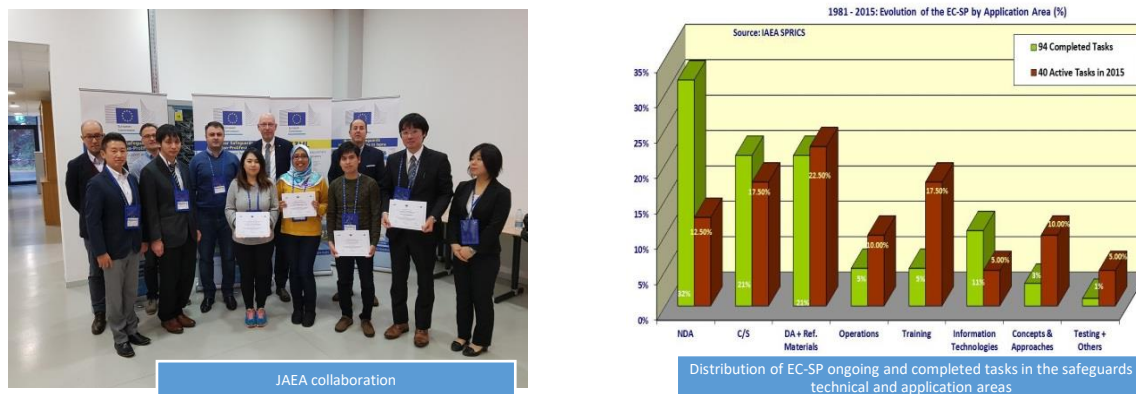


**Figure 4:** EU collaboration for training with external actors in nuclear safeguards.

The collaborative work with different entities has a tremendous value for the JRC because it allows return-of-experience from users, understanding different reality, strengthened contacts, exchange of different ideas and suggestions and not least higher visibility for our organization.

## 6. Summary and Conclusions

A full review of the feedback forms from the participants and from the organisational entities has been put as one of the main source to improve the current training courses. The classroom discussion and interactive exercises have been evaluated constantly by the team and improvements have been put in place to have a better learning curve. In the specific the final Quiz session at the end of the training course has been tailored to the specific knowledge of the participants as well to the open questions that the participants has brought up during the hands-on exercise. In this way the JRC team has used a more practical approach to a stand-alone multi choice questionnaire. A particular attention will be put in place in the future to the understanding of the error determination from the software point of view (MGA/U code) and the requirements form the EURATOM. Besides an in depth review of the used algorithms will be in the future implemented.

Particular attention has been enlightened in the last 2-3 years to some generational change. The JRC Ispra team has been so far successful undertake this change (acknowledgment of the teaching experience of the predecessors [3]) and it is on the improvement path for the future training course sessions.

Besides EURATOM continuously enhances and modernises its tools. The internal procedures are currently being updated, addressing how to deal, inter alia, with occasional measurement uncertainties and inconclusive results. Also new challenges for nuclear safeguards inspectors:

- Emphasis to the back-end of the nuclear fuel cycle;
- New types of nuclear installations (long term and final repository);
- Tomography technology for verification;
- Cybersecurity threats by the use of digital tools in safeguards.

A particular mention must be devoted to the new infrastructure, Ispra Nuclear Safeguards, Security and Standardisation Laboratory (INS3L). It has been conceived as a user-laboratory for client DGs of the European Commission, EU member state authorities and national laboratories, international research partners and international organisations. This new facility will be a more versatile NDA infrastructure than the present, and will be able to accommodate a larger range of R&D and training projects in a more agreeable environment. The expectation is that a construction contract will be allocated by the end of 2019, followed by the construction phase of little more than one year, completion of the licensing phase, and taking into service expected by end of 2021.

In the international safeguards regime, the IAEA director, Yukiya Amano (Challenges in Nuclear Verification – Washington, DC, USA) 5.April '19 (statement at Center for Strategic and International Studies), said: "Our safeguards budget last year was around 142 million euros. Since 2010, it has

increased by only 6.3 percent in real terms". However, in the same period, the number of nuclear facilities under safeguards rose by 12 percent to just over 1,300, while the number of so-called significant quantities of nuclear material under safeguards grew by 24% to 213,000. The number of nuclear material accounting reports from Member States which IAEA inspectors' process has gone up by more than a third since 2010 to 880,000. Then an ever-increasing burden is being placed on IAEA nuclear safeguards inspectors and analytical staff. They have responded by doing their best to work as efficiently as possible and find more cost-effective ways of doing things (increased the number of surveillance cameras and number of unattended monitoring systems). Is EURATOM facing the same problem with their HR?

## 7. Bibliography

- [1] L. S. Ciccarello S., "International Cooperation for Enhancing Nuclear Safety, Security, Safeguards and Non-proliferation—60 Years of IAEA and EURATOM," Heidelberg, 2018.
- [2] Council of the European Union, "Council Regulation (Euratom) 2018/1563 of 15 October 2018 on the Research and Training Programme of the European Atomic Energy Community (2019–2020) complementing the Horizon 2020 Framework Programme for Research and Innovation, and repealing Regulation," vol. 61, no. L262/1, 2018.
- [3] P. Mortreau, and R. Berndt, Handbook of gamma spectrometry for Non-destructive Assay of Nuclear Materials, Luxembourg:: Office for Official Publications of the European Communities, 2006.
- [4] R. Gunnink and W. Ruhter, MGA: A Gamma-Ray Spectrum Analysis Code for, vol. I & II, Livermore, UCRL-LR-103220, CA: Lawrence Livermore National Laboratory, 1990.
- [5] M. Sekine, Y. Kawakubo, P. Rodriguez, N. Noro, F. Raiola, J.-M. Crochemore, A. Rozite and K. Abbas, "Collaboration for Development of Comprehensive NDA Course in SSAC Training," 2019.

## Current training activities at IRSN and ENSTTI on Safeguards

Pierre Funk – Didier Louvat

IRSN Institut de Radioprotection et Sûreté Nucléaire  
ENSTTI European Nuclear Safety Training and Tutoring Institute  
31, Av de la division Leclerc, 92260 Fontenay-aux-Roses, France  
12 rue de la Redoute, 92260 Fontenay-aux-Roses, France  
pierre.funk@irsn.fr  
didier.louvat@enstti.eu

### **Abstract:**

*This paper presents the two new training courses on Safeguards that are proposed in 2019 by IRSN and ENSTTI. ENSTTI (European Nuclear Safety Training and Tutoring Institute) is an initiative of European Technical Support Organizations, created in 2010, to optimize the training of their professionals, with the provision of training and tutoring on nuclear related issues. IRSN is the French Technical Support Organization set up in 2001, with expertise covering all nuclear related scientific and technical issues.*

*The two following training are designed by IRSN and will be managed by ENSTTI. The first one is a 5-day training course. The objective is to improve the competences and the level of understanding of the participants in the field of nuclear safeguards. The course focuses on the implementation of IAEA and EURATOM Safeguards, with detailed lectures on the different techniques used for Safeguards. Several practical exercises are proposed during these 5 days. The second one specifically focuses on Nuclear Material Accounting and Control (NMAC) from the operator point of view. It is a 2-day tabletop exercise that addresses organizational and technical aspects of NMAC.*

**Keywords:** Safeguards, training, NMAC, tabletop exercise

### **1. Introduction**

This paper presents two new training courses on Safeguards that are proposed in 2019 by IRSN and ENSTTI. They are designed by IRSN and managed by ENSTTI. The first one is a 5-day training course. The objective is to improve the competences and the level of understanding of the participants in the field of nuclear safeguards. The course focuses on the implementation of IAEA and EURATOM Safeguards, with detailed lectures on the different techniques used for Safeguards. Several practical exercises are proposed during these 5 days. The second one specifically focuses on the Nuclear Material Control and Accountancy (NMAC) from the operator point of view. It is a 2-day tabletop exercise that addresses organizational and technical aspects of NMAC.

ENSTTI, European Nuclear Safety Training and Tutoring Institute, is an initiative of European Technical Support Organizations, created in 2010, to optimize the training of their professionals, with the provision of training and tutoring on assessment in nuclear safety, nuclear security, nuclear Safeguards and radiation protection. ENSTTI calls on European TSOs' expertise to maximize the transmission of knowledge, practical experience and culture. ENSTTI's ultimate goal is to ensure that personnel at European Nuclear Regulatory Authorities and Technical Support Organizations can maintain skills in their current positions and remain prepared to take on emerging tasks or advancements.

IRSN, the French Institute for radiological protection and nuclear safety; is the French Technical Support Organization in nuclear and radiation risks. It provides technical support to all the government authorities involved in nuclear safety, security and safeguards, as well as radioprotection.

## 2. Training course: “Implementing Nuclear Safeguards in practice”

This training course will be proposed in the framework of the Instrument for Nuclear Safety Cooperation of the European Commission (INSC MC3.01/18) which is managed by the Directorate-General for Development and Co-operation (DEVCO). The course is expected to be held at least six times during the period 2019-2021.

The objective of this course is to strengthen the capabilities of regulatory authorities and technical support organisations in charge of nuclear safeguards in fulfilling their countries' international safeguards obligations by providing adequate training.

### 2.1 Training objectives and learning outcomes

The structure of this training course follows the ENSTTI's pedagogical approach. The training course will be structured around presentations by IRSN's experts as well as other recognized international experts. Presentations will be complemented by a well-balanced mix of case studies and exercises derived from the actual work experience of the experts.

The training objectives are to increase the knowledge of the participants on:

- the importance of implementing fully safeguards obligations to facilitate the effective and efficient application of safeguards for the country;
- the continued evolvement of safeguards through modern technology and newly developed concepts, such as the broader use of information analysis to confirm the absence of undeclared activities, the possibility for States to submit declarations electronically with the IAEA State Declarations Portal, and the use of State-level safeguards approaches under CSAs with APs.

In terms of training learning outcomes, after the attendance to the course, the participants will:

- understand the international and EURATOM safeguards agreements including the Additional Protocols and the Small Quantity Protocols;
- be able to contribute to the practical implementation of safeguards in their country in applying the principles of nuclear material accountancy and control;
- understand differences and interfaces between nuclear safeguards and nuclear security;
- be able to describe safeguards techniques and to practically use some of them.

### 2.2 Detailed course content

Training modules will have a standard duration of one week. The detailed course content and plan are as follows:

#### Day 1 and 2. Application of safeguards

The course starts with introductory lectures on non-proliferation history with the objective to explain safeguards evolution regarding NPT, IAEA safeguards system as well as EURATOM treaty:

- INFCIRC 153 obligation and Comprehensive Safeguards Agreement (CSA)
- INFCIRC/540, conclusion of Additional Protocols (AP)
- Small Quantity Protocol (SQP)
- Item-specific safeguards agreements under document INFCIRC/66/Rev.2
- Voluntary offers.
- Integrated Safeguards approaches.
- State level approach

#### Day 3. Verification activities

The course continues with lectures on verification activities

- EURATOM and IAEA inspections, complementary access
- Non-destructive measurement techniques for various nuclear material types; gamma-ray measurements and neutron measurements;
- Containment and surveillance systems and unattended monitoring systems.

These lectures are complemented by hands-on demonstration of the relevant equipment.

#### **Day 4. Case study**

A case study is then proposed to the participants, in order to demonstrate the practical implementation of safeguards in a country with CSA and AP in force, emphasising

- principles of nuclear material accountancy and control;
- measures taken by country's Nuclear Regulatory Authorities for establishing safeguards infrastructure and providing operational support for verification activities

#### **Day 5. Differences between nuclear safeguards and nuclear security**

A specific session explains differences between nuclear safeguards and nuclear security:

- Information on the legal framework for nuclear security
- Categorization of nuclear material for nuclear security purposes, and
- Principal differences and possible synergies between nuclear safeguards and nuclear security measures applied.

At the end of the module, a roundtable discussion session addresses issues identified by participants. It is followed by an evaluation session: knowledge testing of the participants, correction and discussion, and course evaluation by participants.

### **3. Tabletop exercise on NMAC**

#### **Training objectives and learning outcomes**

States must put in place a system of Nuclear Material Accounting and Control (NMAC) also referred as a State System for Accounting and Control (SSAC). They are indeed defined both for security application and for safeguards. In any case, within a nuclear facility, there is only one single accounting and control system for both safeguards and security. This is well explained in reference [1].

France has a long experience on that topic with a strong nuclear security architecture in place for NMAC with the objective to protect nuclear material from adversaries having authorized access (insiders) and to fulfill safeguards commitments. With regards to that topic, IRSN has developed a tabletop exercise that addresses the following key ideas:

- Organizational and human separation between follow-up, accountancy, physical protection, management of transport;
- Daily information flow of nuclear material associated with an ongoing cross-checking of accounting and transportation data at central level;
- Separated databases deterring malicious action.
- Practical implementation in order to fulfill both security and safeguards commitments.

Participants may be facility operators as well as regulators and technical support organization.

The tabletop exercise has a standard duration of two days. It is a role-playing game where the missions of the main actors in the management of nuclear material are attributed to the participants. The purpose is to provide each participant with the information necessary to a global understanding of the principles of nuclear material management as requested by the French regulation (decree and order on "physical follow-up and accountancy of nuclear material") as well as in the EURATOM Regulation No 302/2005 of 8 February 2005.

To this end, a facility that handles and processes nuclear material is considered. Participants have to carry out all physical follow-up and accountancy activities of nuclear material by *simulating* the physical operations to be carried out on such materials. It concerns for instance the receipt of nuclear material, its transformation, followed by its internal and external transfer. At the end of these operations, a physical inventory should be carried out at the facility as well as a Material Unaccounted For (MUF) calculation.

The training is divided into several sequences that starts with the establishment of an organization, to continue with the breaking down the facility into Material Balance Area, with Key Measurement Points

at the various stages of the process. Each sequence ends with recalls of the regulatory requirements from national and international framework as well as good practices.

### **Detailed course content**

The different sequences of the tabletop exercise are the following:

- Management of nuclear material in the facility: attribution of the different roles
- Material Balance Area
- Key measurement Point
- Receipt
- Transfer
- Control
- Transformation
- Transfer
- Management of an anomaly
- Sealing
- Shipment
- Physical inventory
- MUF calculation

## **4. References**

[1] J. Vidaurre-Henry, K. A. Robertson and M. Hirai, "The Meaning of "Control" in "SSAC", " in INMM 58th Annual Meeting, 2017.

## **The Need to Establish Certified Professional Development Programmes for Nuclear Safeguards**

**Daniel Johnson**

World Institute for Nuclear Security  
Landstrasser Hauptstrasse 1/18  
AT-1030 Vienna, Austria  
E-mail: dan.johnson@wins.org

**Jeffrey Chapman**

National Nuclear Security Administration  
NA-84 Office of Nuclear Incident Response  
1000 Independence Ave. S.W., Washington D.C., 20585, USA  
E-mail: Jeffrey.Chapman@nnsa.doe.gov

**Cary Crawford**

Oak Ridge National Laboratory  
Nuclear Security and Isotopes Technology Division  
1 Bethel Valley Rd, Oak Ridge, TN, 37830, USA  
Email: crawfordce@ornl.gov

**Rhonda Evans**

World Institute for Nuclear Security  
Landstrasser Hauptstrasse 1/18  
AT-1030 Vienna, Austria  
E-mail: rhonda.evans@wins.org

### **Abstract:**

At the 2018 Institute for Nuclear Materials Management (INMM) Annual Meeting, William Tobey, Chair of the World Institute for Nuclear Security (WINS), proposed a challenge to the INMM Membership: "That every member of INMM will have the opportunity to take certified, professional development courses relevant to their professional discipline by 2025." WINS proposed this challenge based on its experience establishing the WINS Academy, a nuclear security management certification programme supported by international commitments from 15 countries (IAEA INFCIRC/901) and over 1,000 participants from 92 countries. The objective in launching the challenge was to draw attention to the presently poor opportunities for structured professional development in the various nuclear materials management professions and to supplement on-the-job and awareness training with certified programmes that support statements of professional competence. As a result of this challenge, WINS is encouraging INMM members to undertake an analysis of their own training and professional development needs and determine if there is a market for establishing a certifying body for their profession. As a first step, INMM members have begun to explore the feasibility of establishing a certification programme for Non-Destructive Assay (NDA). The proposed certification would build on lessons learned from the WINS Academy, as well as the American Nuclear Society's Professional Engineering Licensure and the Certified Health Physicist certification programme. Ultimately, the goal of the challenge is to develop a dedicated group of committed practitioners—in safeguards and other nuclear materials management fields—who have invested the time to become

certified in their professional field and who in turn promote certification and continuous professional development amongst their peers. ESARDA and its members could play a key role in promoting this objective, resulting in a global network of trained professionals that receive higher professional respect and are better able to implement effective and sustainable nuclear materials management programmes.

**Keywords:** NDA; certification; training; education;

## 1. Introduction

At the 2005 Institute for Nuclear Materials Management (INMM) annual meeting, Charlie Curtis, then President and COO of the Nuclear Threat Initiative, put forward a challenge to the INMM membership to establish a new international organisation to share international best practices on nuclear security. There followed a three-year planning effort undertaken with the leadership of INMM, and subsequently, the World Institute for Nuclear Security (WINS) was launched in 2008 at the 52<sup>nd</sup> IAEA General Conference in Vienna, Austria. Since its foundation ten years ago, WINS has achieved many important milestones, including the launch of the WINS Academy nuclear security management certification programme. The WINS Academy is now supported by international commitments from 15 countries (published as IAEA INFCIRC/901),<sup>1</sup> a growing body of over 1,200 participants from 92 countries, and strategic partnerships with like-minded national training organisations who also support the development of certified training programmes based on quality management standards.

Ten years after the launch of WINS, the Chairman of the WINS Board, Will Tobey, proposed a new challenge to the INMM membership:

“That every member of INMM will have the opportunity to take certified, professional development courses relevant to their professional discipline by 2025.”

WINS issued this challenge to draw attention to the presently poor opportunities for structured professional development in nuclear materials management professions; along with the need to replace on-the-job and awareness training with certified programmes that support statements of professional competence. The inspiration for the challenge comes from other technical professions (nuclear and otherwise) which have developed professional development programmes for their practitioners, often connected to professional certifications that indicate if a person possesses qualifications in a key subject area. In some professions, certification can form the primary formal basis for gaining entry to and practicing within the profession.

Following the WINS challenge, members of INMM have already begun to explore the possibility of establishing certification programmes for safeguards, with an initial focus on a specialisation for non-destructive assay (NDA). This paper will review the proposed NDA certification, the benefits of such programmes, examples from other nuclear professions, and how the certification might integrate with existing safeguards training initiatives.

## 2. Licensure or Certification in other Professions that Support Nuclear Safeguards and Security

A review of a wide variety of technical professions demonstrates that certification and accreditation programmes are common and often associated with professional societies.<sup>2 3</sup> Whether it is the certification of individuals, products or services, the credentialing of professionals, or the accreditation of programmes, services or institutions, these programmes confer an array of valuable benefits not only to certified individuals and professional societies, but also to industry, government, and the general public. Certification requirements in nearly every professional field demonstrate that practitioners meet the necessary educational and vocational standards required by their professional bodies to perform their jobs.

Furthermore, employers seek out credentialed professionals. It is not uncommon for tenders to include a provision requiring that the bidder include at least one licensed or certified person to be included on the key staffing plan. Additional benefits of being certified include:<sup>4</sup>

- Mastery of principles and best practices
- Demonstration of credibility and competence
- Demonstration of growth and professional development
- Improved job performance
- Recognition by peers, employers and recruiters
- Professional networking opportunities
- Improved salary and employment opportunities

While it is recognised that employers will not likely require a license or certification immediately following a new programme, the authors believe that such a programme will drive the change that leads to this behaviour. With the proper planning and support from the most influential international organisations, such a programme will gain traction and become standard practice and possibly even a requirement in many organisations.

In the nuclear industry, safety professionals, many of whom are nuclear engineers, undergo extensive training in their specific areas. Furthermore, they have numerous opportunities to obtain ongoing continuing education, to not only facilitate the advancement of their trade but also to maintain credentials for those who are certified/licensed.

For example, the American Nuclear Society (ANS) facilitates, through the Professional Engineering Examination Committee (PEEC), the development of a question bank for use in the administration of the *exam for licensure*, known as the Professional Engineering Exam, Nuclear. The Certification exam in Health Physics (CHP) is administered completely by the American Academy of Health Physics (AAHP), and, unlike the PE-licensing process, is not a legal qualification to practice health physics. The professional engineer's license and the certification in health physics processes are described separately below.

## 2.1. Professional Engineering Licensure (Nuclear)

ANS members, who are licensed as professional engineers (nuclear) may join the ANS' Professional Engineering Examination Committee (PEEC) to write exam questions, develop training materials and study guides, and teach continuing education courses offered during the annual and winter meetings. The American Nuclear Society (ANS) has a professional development coordination committee responsible for the development and delivery of special seminars and courses which result in a service to the membership as well as income to the Society. Under this committee ANS administers computer-based examinations for the Professional Engineering Licensure for Nuclear Engineers, along with an exam preparation workshop during its annual meeting and a 900 page study guide. ANS also awards Professional Development Hours (PDHs) to licensed members who attend technical sessions at conferences or who author papers, articles, or books that are published by the ANS.

The first step to licensure as a professional engineer (nuclear) is to take and pass the 6-hour-long, 110-question, Fundamentals of Engineering (FE) exam.<sup>5</sup> Most nuclear engineers take the FE "Other Disciplines" exam which consists of fifteen topic/knowledge areas:

- 1) Mathematics and Advanced Engineering Mathematics
- 2) Probability and Statistics
- 3) Chemistry
- 4) Instrumentation and Data Acquisition
- 5) Ethics and Professional Practice
- 6) Safety, Health, and Environment
- 7) Engineering Economics
- 8) Statics
- 9) Dynamics
- 10) Strength of Materials
- 11) Materials Science
- 12) Fluid Mechanics and Dynamics of Liquids
- 13) Fluid Mechanics and Dynamics of Gases
- 14) Electricity, Power, and Magnetism

## 15) Heat, Mass, and Energy Transfer

The FE Exam is administered by the National Council of Examiners for Engineering and Surveying® (NCEES). The pass rate for this exam varies between 65% and 80%; the pass-rate decreases if candidates delay taking the exam after graduation, as would be expected.<sup>6</sup>

Once the candidate successfully completes the FE exam and has practiced the trade of nuclear engineering for at least four years, the candidate is eligible to take the professional engineer's (PE) exam.<sup>7</sup> The PE Nuclear exam is 9.5 hours in length and consists of 85 multiple-choice questions.<sup>8</sup> There are four functional areas: 1) Nuclear Power Systems (Design and Analysis; Components and Systems; Regulations Codes and Standards), 2) Nuclear Fuel Cycle (Fuel Design and Analysis; Handling, Shipping, and Storage), 3) Interaction of Radiation with Matter (Analysis; Protection), and 4) a broad category of Nuclear, Criticality, Kinetics, and Neutronics.

Upon passing the PE-Nuclear exam, the candidate is awarded a license to practice nuclear engineering in the state of his or her choice.<sup>9</sup> Many commercial bids for services will mandate that a professional engineer be a key staff engineer. The benefit to the ANS is that continuing education classes are held concurrent to meetings, and there is a great sense that membership who take these courses are advancing their own capability, furthering the quality of services for the company which they service.

## 2.2. Certification in Health Physics

Another example of certification comes from the profession of Health Physics. Every year during the Health Physics Society (HPS) annual meeting, the American Academy of Health Physics (AAHP)<sup>10</sup> offers the Part 1 CHP examination world-wide at testing centres. The AAHP also administers the Part 2 CHP examination to become a Certified Health Physicist during the annual HPS meeting both at the location of the HPS meeting and other locations selected based on need. A separate but affiliated body called the American Board of Health Physics (ABHP), develops both parts of the examination, grades part 2, and validates and approves the passing scores of both examinations. The certification is not a license to practice and does not confer any legal qualification to practice health physics. However, the certification is well respected in the field and indicates a high level of achievement by those who obtain it.

The process for becoming a Certified Health Physicist is similar to that of the PE-nuclear process. Immediately after a four-year degree in Health Physics, a candidate may apply to take the Part I exam. The Part I exam is a three-hour exam consisting of 150 multiple-choice questions. The breakdown by subject matter follows the five Domains of Practice:<sup>11</sup>

- 1) Measurements and Instrumentation;
- 2) Standards and Requirements;
- 3) Hazards Analysis and Controls;
- 4) Operations and Procedures; and
- 5) Fundamentals and Education.

Once the candidate passes the Part I exam and has at least 6-years' experience in health physics, the candidate is eligible to take the Part II exam. The Part II exam is 6-hours in length, and consists of two sections, each with a long-form solution format, rather than multiple choice as in Part I.<sup>12</sup> The two sections of the exam include:

- 1) Six core topical questions in health physics, each question designed to be completely solved in 10-15 minutes; and
- 2) Eight questions, of which four must be selected and answered.

The first set of six core question topics are: personnel dosimetry (internal and external), shielding and activation, measurements and instrumentation, and biological effects of radiation risk. The second set of eight question topic areas are: accelerators, environmental, fuel cycle (mining, milling, fuel fabrication and fuel reprocessing) and waste management, medical, research and power reactors, university, general (can include emergency response, meteorology, standards and regulations, and topical subjects) and nonionizing radiation.

The “specialty area” set of eight questions are designed for candidates to focus on specific areas of expertise that will require greater knowledge and experience to answer satisfactorily. The topical areas are the same for the specialty area questions, but the questions are more integral to the complete health physics practices for a given operation involving radioactive material or radiation-producing machines. When considering a certification in safeguards, it may be prudent to consider “specialty areas” such as non-destructive assay; sampling and analytical analysis; forensics; or statistics for nuclear material control and accountability.

Once conferred the CHP is not a legally binding license to practice. However, the ABHP is a specialty board recognised by the U.S. Nuclear Regulatory Commission under part 10 CFR§ 35.50, Training for Radiation Safety Officer (RSO), when the RSO oversees or is responsible for the “medical use of byproduct material.”<sup>13</sup> This job specification is the only known job function as an RSO where the regulator recognises CHPs after a certain date to automatically be qualified to be a medical RSO.

For completeness, it is important to note that for health physicists whose job function is in line with a radiation protection technologist (or technician), the National Registry of Radiation Protection Technologists (NRRPT) credentials this job classification through administration of a separate examination process.<sup>14</sup> This credential has been highly successful.

In addition, both the AAHP and HPS have very active Continuing Education and Professional Development Committees. AAHP offers two or three 8-hour equivalent classes at the HPS midyear and annual meetings. HPS also offers a wide variety of professional development opportunities for its membership, including several courses held before and during its annual meeting. Courses include an annual Professional Development School (PDS) which provides 20 hours (12 lecture and 8 hands-on) of training to different disciplines within the community. This course is accredited for 20 hours of continuing education credits. For example, a recent PDS was held on Medical Health Physics.<sup>15</sup>

A summary table, comparing the relevant distinctions between the Professional Engineering (Nuclear) license and the Certified Health Physicist is presented below.

	<b>Professional Engineer (PE) License, Nuclear</b>	<b>Certified Health Physicist (CHP)</b>
Administrating Body	National Council of Examiners for Engineering and Surveying (NCEES)	<ul style="list-style-type: none"> <li>American Board of Health Physics (ABHP)</li> <li>Administrative services subcontracted to the Secretariat</li> </ul>
First Part Exam	Fundamentals of Engineering (FE) <ul style="list-style-type: none"> <li>eligible to take <u>during</u> senior year of engineering college, or immediately thereafter</li> </ul> <i>(generally, candidates have an engineering degree)</i>	Part I, eligibility: <ul style="list-style-type: none"> <li><u>after</u> senior year of a B.S. in Health Physics and 1-year experience</li> <li><u>after</u> M.S. in Health Physics</li> <li><u>after</u> “acceptable” B.S. degree and 2-years’ experience</li> </ul> <i>(generally, it is not uncommon for eligible candidates to transition from a non-HP degree into HP)</i>
Second Part Exam	Professional Engineering (PE) <ul style="list-style-type: none"> <li>Eligible candidates must have passed the FE exam and have at least four-year’s experience in nuclear engineering.</li> </ul>	Part II <ul style="list-style-type: none"> <li>Parts I and II can be taken in same year, but eligibility for Part II requires at least six years’ experience in the field.</li> <li>It is most typical for candidates to take Part I early in career, and then take Part II after six years’ experience has been reached.</li> <li>Both Parts must be passed within 7 years of each other.</li> <li>Candidate application includes reference letters from existing CHPs</li> </ul>

Licensure vs. Certification	<ul style="list-style-type: none"> <li>• States license the candidate to practice nuclear engineering in that specific State.<sup>16</sup></li> <li>• PE is <u>legally binding</u> and allows the licensed engineer to bid on contracts and sell services.</li> <li>• State-to-State reciprocity</li> </ul>	<ul style="list-style-type: none"> <li>• CHPs are eligible for membership in the American Academy of Health Physics (AAHP)</li> <li>• The CHP is <u>not</u> legally binding</li> <li>• The CHP is recognised internationally</li> </ul>
Renewals and Fees	<ul style="list-style-type: none"> <li>• State of CA: \$115.00/ 2 years</li> <li>• Continuing Education Credits                         <ul style="list-style-type: none"> <li>• <u>Not</u> required in CA.</li> <li>• Many other states, required</li> </ul> </li> </ul>	<ul style="list-style-type: none"> <li>• CHPs are eligible for membership in the American Academy of Health Physics (AAHP), maintenance fees: \$100/year</li> <li>• Continued Education Credits are required (80 CECs per recert period)<sup>17</sup></li> </ul>

**Table 1:** Comparison of PE and CHP certification and licensure

### 3. Proposed Certification in Nuclear Safeguards, with a Specialty in Nondestructive Assay (NDA)

Building from the already existing certification programmes in nuclear engineering, health physics, and security, INMM members have begun to explore the feasibility of establishing a certification programme for nuclear safeguards, beginning with a specialty area in Nondestructive Assay (NDA). The preliminary vision is a two-part exam, similar in scope and style to that administered by the ABHP for the American Academy of Health Physics. Similar to the CHP exam, the certification body would ensure that questions are written and selected that test the ability of each candidate to apply their knowledge, as well as certification-specific courses that will emerge through INMM or by private engagement and support from ESARDA, for example.

The first part of the exam might be 4-6 hours in length and could include the general topical areas covered by the Texas A&M University certificate programme in the fundamentals of nuclear safeguards. This existing robust programme of courses consists of several online, self-paced courses equivalent to approximately 25 hours of coursework and 2.5 continuing education units (CEUs)<sup>18</sup> in the fundamentals of nuclear safeguards. The modules for this programme include:<sup>19</sup>

- Introduction to Nuclear Security and Safeguards
- Introduction to Commercial Nuclear Fuel Cycle
- Introduction to Statistics
- Nuclear material Accountancy
- Containment and Surveillance
- Spent Nuclear Fuel Safeguards
- Uranium Enrichment Safeguards
- Applied Statistics for Nuclear Safeguards

The second part of the exam could take on various shapes and will evolve through stakeholder discussions. The current proposal is to require the candidate to select a specialty topic, for example:

- 1) Policy-Safeguards;
- 2) NMC&A;
- 3) DA; and
- 4) NDA.

The pilot NDA specialty could include the core competency areas outlined in Table 2.

<b>Gamma-ray/X-ray Techniques</b>	<b>Neutron Counting Techniques</b>
Nuclear Decay Processes <ul style="list-style-type: none"> <li>• Beta Decay</li> <li>• Gamma-ray Signatures</li> </ul>	Nuclear Decay Processes <ul style="list-style-type: none"> <li>• Alpha Decay</li> <li>• Spontaneous Fission</li> <li>• muons and anti-neutrinos</li> <li>• Gamma-ray Signatures</li> </ul>
Origin of Gamma Rays and X-rays	Origin of Neutrons

<ul style="list-style-type: none"> <li>• Gamma-ray Production</li> <li>• X-ray Production (Bremsstrahlung)</li> <li>• Characteristic x-ray spectra</li> </ul>	<ul style="list-style-type: none"> <li>• Spontaneous and Induced Fission</li> <li>• (alpha,n) reactions</li> <li>• Cosmic-ray Spallation</li> </ul>
<b>Interactions</b> <ul style="list-style-type: none"> <li>• Photoelectric Effect</li> <li>• Compton Scattering</li> <li>• Photo Pair Production and Annihilation</li> <li>• Transport Models</li> </ul>	<b>Interactions</b> <ul style="list-style-type: none"> <li>• Inelastic Scattering</li> <li>• Elastic Scattering</li> <li>• Moderation and Absorption</li> <li>• Transport Models</li> </ul>
<b>Gamma-Ray Detectors</b> <ul style="list-style-type: none"> <li>• Gas-Filled Detectors</li> <li>• Scintillation Detectors</li> <li>• Detector Response Characteristics and Specifications</li> </ul>	<b>Neutron Detectors</b> <ul style="list-style-type: none"> <li>• Gas-Filled Detectors</li> <li>• Scintillation Detectors</li> </ul>
<b>Instrumentation</b> <ul style="list-style-type: none"> <li>• Electronics</li> <li>• Data Reduction and Analysis Algorithms</li> </ul>	<b>Instrumentation</b> <ul style="list-style-type: none"> <li>• Electronics</li> <li>• Data Reduction and Analysis Algorithms</li> </ul>
<b>Methods</b> <ul style="list-style-type: none"> <li>• Isotopics – Uranium Plutonium MOX</li> <li>• Far-field, Attenuation Correction</li> <li>• Segmented Gamma-ray Scan</li> <li>• Tomographic Gamma-ray Scan</li> <li>• In-situ (holdup)</li> <li>• Densitometry</li> <li>• X-ray Fluorescence</li> </ul>	<b>Methods</b> <ul style="list-style-type: none"> <li>• Total Neutron Counting</li> <li>• Coincidence Counting</li> <li>• Multiplicity Counting</li> </ul>
<b>Miscellaneous</b> : Calorimetry, Spent Nuclear Fuel Assay	

**Table 2:** Core competency areas of pilot NDA specialisation

## 4. Interface with Existing Safeguards Training Programmes

In addition to the aforementioned Texas A&M safeguards certificate, there are a wide variety of safeguards courses available for practitioners. Following is a sample of the major courses and programmes, all of which could be reviewed for their contribution to the safeguards certification.

### 4.1. ESARDA

The objective of the ESARDA safeguards course is to provide modules to an internationally recognised reference standard.<sup>20</sup> The course is open to master's degree students, in particular nuclear engineering students, but also to young professionals and international relations and law students. It aims at complementing nuclear engineering studies by including nuclear safeguards in the academic curriculum. The course addresses aspects of the efforts to create a global nuclear nonproliferation system and how this system works in practice: the Treaty on Nonproliferation of Nuclear Weapons (NPT), safeguards technology, and export control. Also regional settings, such as the Euratom Treaty, are presented and discussed. The course deals in particular with technical aspects and application of safeguards; i.e. how to implement the safeguards principles and methodology within the different nuclear facilities.

### 4.2. IAEA

The IAEA offers training programmes that covers a wide variety of topics related to the management of nuclear materials. The Safeguards Training Section is responsible for the development, coordination and provision of safeguards related training for the Department and for personnel of Member States in relation to their obligations under safeguards agreements with the IAEA. To meet these needs, the Safeguards Training Unit was formed in February 1980. The function of the Training

Unit is to analyse the requirements of the operational sections in the Safeguards Department, to assess the qualifications and needs of each trainee, and to decide, in consultation with the operational sections, the skills and knowledge each will need to carry out their work. With this knowledge, the Unit can plan its courses to fit its students for their work in the operational sections.<sup>21</sup>

The IAEA also works with partners to host international training events. For example, in collaboration with the U.S. National Nuclear Security Administration (NNSA), the IAEA holds an International Training Course (ITC) on State Systems of Accounting for and Control of Nuclear Material (SSACs). NNSA and the IAEA co-sponsor the ITC to educate and train technical experts from around the world on how to properly account for nuclear materials used in their home countries. The first SSAC ITC in the United States was held in Richland, Washington in 1979. Since then, over 500 participants from 50 countries have completed the training. The ITC supports U.S. obligations under the U.S. Nuclear Nonproliferation Act of 1978.

### **4.3. United States Support Program<sup>22</sup>**

The United States Support Program (USSP) was established in January 1977 to respond to urgent needs of the IAEA Department of Safeguards more quickly than could be met through the IAEA's administrative procedures. The requests have included nondestructive and destructive analysis instrumentation and techniques, procedures and training, system studies, information technology, containment and surveillance, and management support. The USSP has traditionally provided significant support in enhancing the NDA and containment/surveillance capabilities of the IAEA and works with a network of 16 national laboratories and numerous companies to provide training amongst other support.

### **4.4. International Nuclear Safeguards Engagement Program (INSEP)<sup>23</sup>**

INSEP's mission is to work with international partners to support and enhance nuclear safeguards implementation at all stages of civil nuclear development. INSEP cooperates with more than 25 bilateral and regional partners on more than 100 technical projects to strengthen the international safeguards system. A number of countries require legislative and technical support to prepare the infrastructure and procedures necessary to provide timely, correct, and complete declarations pursuant to the Additional Protocol (AP), and INSEP cooperates with nearly a dozen partner countries to strengthen their AP implementation. In total, INSEP trains more than 500 foreign practitioners each year on international and domestic safeguards.

### **4.5. Next Generation Safeguards Initiative (NGSI)**

The Human Capital Development (HCD) subprogramme of NGSI is developing sustainable academic and technical programmes that support the recruitment, education, training, and retention of the next generation of international safeguards professionals to help meet the needs of both the United States and the IAEA for decades to come.<sup>24</sup> Focus areas include:

- University engagement through curriculum development, guest lectures, and textbook development;
- Safeguards policy and technology courses to strengthen young and mid-career professional development;
- Ongoing analysis of workforce needs of safeguards-relevant staff at DOE National Laboratories.

### **4.6. US National Laboratories**

Nearly all of the U.S. National Laboratory support U.S. government support to IAEA safeguards activities. For example, over the last 15 years Brookhaven National Laboratory (BNL) has become a safeguards training centre, presenting courses for IAEA inspectors and Member States. BNL delivers a course on Design Information Verification of Research Reactors, as well as a course on Additional Protocol / Complementary Access for IAEA inspectors. This training has been redesigned for delivery to IAEA Member States to teach them their responsibilities under the Additional Protocol. In addition, under the NGSI programme, Brookhaven has offered a course that is intended to encourage qualified American and international students to enter the fields of safeguards and nonproliferation. The three-week course "Nuclear Non-proliferation, Safeguards and Security in the 21<sup>st</sup> Century," is designed to

give students a sound understanding of the foundations of the nuclear nonproliferation regime, the IAEA safeguards system, and U.S. efforts to meet emerging nuclear proliferation threats.

Los Alamos National Laboratory (LANL) also runs a safeguards School for Inspectors. IAEA inspectors initially learn to wield their instruments at IAEA headquarters in the Agency’s Introductory Course for Agency Safeguards (ICAS). New inspectors complete ICAS and additional training at a light-water reactor, then finish out their first year on real inspections in the company of more-experienced colleagues. At the end of that year, they are ready to learn even more, and so they attend the LANL NDA Inspector Training course, specially developed for IAEA inspectors. Los Alamos started teaching the special IAEA course in 1980, and since then, all IAEA inspectors have been trained at Los Alamos.<sup>25</sup>

#### 4.7. Academia

In addition to the Texas A&M safeguards certificate, a number of US universities offer nuclear safeguards and security-related courses, as outlined in Table 3 below.

University/Organization	Scope
Texas A&M (nuclear engineering)	<ul style="list-style-type: none"> <li>● Professional Certification in Nuclear Safeguards Fundamentals</li> <li>● Masters of Science Concentration in Nuclear Nonproliferation</li> <li>● Graduate Certificate in Nuclear Security</li> </ul>
Middlebury Institute of International Studies at Monterey	<ul style="list-style-type: none"> <li>● International Safeguards Policy and Information Analysis-Intensive Summer Course</li> </ul>
University of Tennessee, Knoxville (nuclear engineering)	<ul style="list-style-type: none"> <li>● Graduate Certificate in Nuclear Science and Analysis</li> </ul>
University of Nevada, Reno (mechanical engineering)	<ul style="list-style-type: none"> <li>● Graduate Certificate in Packaging and Transportation</li> <li>● Graduate Certificate in Nuclear Safeguards and Security (under development)</li> </ul>
Purdue University (multi-disciplinary)	<ul style="list-style-type: none"> <li>● Nuclear Security Graduate Program (under development)</li> </ul>
Multiple universities offer individual nuclear security related courses	<ul style="list-style-type: none"> <li>● Pennsylvania State University (e.g., nuclear security threat analysis and assessments)</li> <li>● University of Georgia</li> <li>● Massachusetts Institute of Technology (e.g., principles of nuclear radiation measurement and protection)</li> </ul>

**Table 3:** Representative set of US universities offering degree/certificates in nuclear safeguards and security<sup>26</sup>

## 5. Conclusion

Nearly every professional field, such as medicine or engineering, has its practitioners demonstrate their experience and competence through belonging to professional associations that certify members. This certification in turn provides recognition and is respected by peers in their industry. The basis for the WINS Challenge is the opinion is that attitudes to nuclear materials management have fallen behind the more progressive approaches taken in other professions, and that we need to support professional development that results in new and more integrated approaches to safeguards to make it more effective.

That said, there needs to be a measured approach for addressing the challenge. All too often the development of training is taken in response to a perceived need to “do something.” A better and more strategic approach is to identify a group of like-minded stakeholders who can clearly articulate a vision and roadmap that leads to a well-defined career path. To be effective, stakeholders within safeguards will need to conduct a “bottom up” analysis of their own training and professional development needs and then decide if there is a market for establishing a certifying body, which can either be a certification board or a new professional society.

As a first step, ESARDA leadership could join a new INMM committee that is being established to explore the efficacy of developing a certification programmes for nuclear safeguards. This committee will be in a position to provide the framework for the discussions and a road map, appoint committee members with a passion for this to be achieved, gather existing data on opportunities, formulate focus groups on curriculum development, and establish which institutes would be interested in providing certifications.

Ultimately, the goal is to develop a dedicated group of committed practitioners who have taken the time to become certified in safeguards professions, who will in turn promote certification and continuous professional development among their peers. The result will be a network of trained professionals who are implementing meaningful and sustainable changes that will translate into greater employment opportunities and benefits, including increased salaries and managerial responsibilities.

## 6. Acknowledgements

This paper has previously been submitted for publication in ESARDA Bulletin n.58 – June 2019.

## 7. References

<sup>1</sup> IAEA INFCIRC/901; *Communication dated 1 December 2016 received from the permanent Mission of Canada concerning Certified Training for Nuclear Security Management: Joint Statement on Certified Training for Nuclear Security Management*; 2016; <https://www.iaea.org/sites/default/files/publications/documents/infcircs/2016/infcirc901.pdf>

<sup>2</sup> The American Academy of Health Physics (AAHP) advances the profession of Health Physics and encourages the highest standards of ethics and integrity in its members. The AAHP offers membership to all individuals who have been granted certification in Comprehensive Health Physics by the American Board of Health Physics (ABHP). Certification in the practice of Health Physics is granted by the ABHP upon successful completion of a two-part examination. While the AAHP is completely independent from the Health Physics Society (HPS) – Certified Health Physicists who are members of the Academy are not required to become members of the HPS – the large majority of continuing educational courses sponsored and provided by certified members of the AAHP are provided concurrent with the HPS midyear and annual meetings.

<sup>3</sup> The American Nuclear Society (ANS), through the Professional Engineering Examination Committee (PEEC), develops materials and conducts workshops to prepare individuals for the nuclear professional engineering exam, which is developed, administered, and scored by the National Council of Examiners for Engineering and Surveying (NCEES). During the ANS winter and annual meetings, continuing education courses are offered to PE-licensed members so that Continuing Professional Competency-credits are accumulated to maintain the PE license.

<sup>4</sup> Pearson VUE; *Pearson VUE 2017 Value of IT Certification Survey: Results Summary*; 2017.

<sup>5</sup> American Nuclear Society; *The Fundamentals of Engineering Exam for Nuclear Engineers*; <http://www.ans.org/pe/fe/>

---

<sup>6</sup> A joint ANS/NCEES PowerPoint presentation on the FE exam is available at <http://cdn.ans.org/pe/docs/the-fundamentals-of-engineering-exam-presentation.ppt>

<sup>7</sup> *PE Nuclear Exam*. National Council of Examiners for Engineering and Surveying; <https://ncees.org/engineering/pe/nuclear/>

<sup>8</sup> When one of the authors of this paper took the exam in 1989, the exam format was long-form rather than multiple choice. However, to make the exam easier to grade and more uniform, the multiple-choice format was adopted.

<sup>9</sup> One of the authors of this paper also notes that he took the exam in California and has since maintained licensure in the State of California and opted out of seeking a license to practice in the state of Tennessee. The State of Tennessee requires a \$140.00 biennial fee as well as 24 hours of continuing professional education, whereas California does not require the continuing education credits.

<sup>10</sup> The American Academy of Health Physics; *Prospectus*; <https://www.aahp-abhp.org/abhp/prospectus>

<sup>11</sup> The American Academy of Health Physics; *Exam Preparation Guide*; <https://www.aahp-abhp.org/abhp/pg>

<sup>12</sup> Ibid.

<sup>13</sup> For additional information see: <https://www.nrc.gov/reading-rm/doc-collections/cfr/part035/part035-0050.html>

<sup>14</sup> The National Registry of Radiation Protection Technologists (NRRPT), separate from the ABHP was established in 1976 to credential personnel whose function is at the Technologist level. More information on this credentialing exam can be found at <http://www.nrrpt.org/>

<sup>15</sup> Health Physics Society; *Hands-on Medical Health Physics: Emerging Technologies and Challenges*; <http://hps.org/meetings/pds.html>

<sup>16</sup> Each State implements, in part and in accordance with their own specific laws to practice engineering in that State, the guidance and formalism maintained within the National Society of Professional Engineers. See: <https://www.nspe.org/resources/licensure/what-pe>. One of the authors is registered in the State of California, for example.

<sup>17</sup> Interested parties can refer to the AAHP Recertification Policy at <https://www.aahp-abhp.org/ce-policy>.

<sup>18</sup> University coursework hours and continuing education credit systems will vary worldwide. It should be noted that other universities offer certificate programmes and courses in safeguards.

<sup>19</sup> Texas A&M; *NSPI1101- Professional Certification in Nuclear Safeguards Fundamentals*; <http://teesedgecourses.tamu.edu/modules/shop/index.html?action=section&OfferingID=159>

<sup>20</sup> ESARDA; *18<sup>th</sup> ESARDA Course 2019*; [https://esarda.jrc.ec.europa.eu/index.php?option=com\\_content&view=article&id=352&Itemid=443](https://esarda.jrc.ec.europa.eu/index.php?option=com_content&view=article&id=352&Itemid=443)

<sup>21</sup> Pontes B, Bates G, Dixon G; *Training the Agency's Inspectors*; IAEA Bulletin Vol 23, No 4; IAEA; p 26-29; <https://www.iaea.org/sites/default/files/23403252629.pdf>

<sup>22</sup> Queirolo A; *The U.S. Support Program to IAEA Safeguards Priority of Training and Human Resources*; Brookhaven National Laboratory; 2008; <https://www.bnl.gov/isd/documents/43169.pdf>

<sup>23</sup> National Nuclear Security Administration; *International Nuclear Safeguards Engagement Program*; 2014; <https://www.energy.gov/sites/prod/files/2017/10/f37/2014-06-25%2520NIS%2520insep-booklet%5B1%5D.pdf>

<sup>24</sup> National Nuclear Security Administration; *Next Generation Safeguards Initiative*; 2017;  
[https://www.energy.gov/sites/prod/files/2017/10/f37/Next%20Generations%20Safeguards%20Initiative\\_0%5B1%5D.pdf](https://www.energy.gov/sites/prod/files/2017/10/f37/Next%20Generations%20Safeguards%20Initiative_0%5B1%5D.pdf)

<sup>25</sup> Patterson E; *National Security Science*; Los Alamos National Laboratory;  
[https://www.lanl.gov/science/NSS/issue2\\_2012/story3full.shtml](https://www.lanl.gov/science/NSS/issue2_2012/story3full.shtml)

<sup>26</sup> The table is adapted from a research paper by Crawford C and Williams A; *Human Capacity Building in Nuclear Security*; IAEA Conference on Nuclear Security; 2016.

# Evolution of ESARDA Course: Outreach Contribution of ESARDA Course on Nuclear Safeguards and Non-Proliferation

**K. Abbas, W. Janssens, F. Raiola, G. Cojazzi and P. Richir**

European Commission, Joint Research Centre, Nuclear Safety and Security  
Directorate, Nuclear Security and Safeguards Department, Nuclear Security Unit,  
Ispra (VA), Italy

kamel.abbas@ec.europa.eu

## **Abstract:**

*Education and training (E&T) programmes in nuclear safeguards are generally missing from curricula of Universities or other E&T organisations active in nuclear science and engineering. In order to fill this gap, ESARDA developed a dedicated course on Nuclear Safeguards and Non-Proliferation, the so-called "ESARDA Course". Since almost two decades, the Nuclear Security Unit of the Department of Nuclear Security and safeguards of the Joint Research Centre of the European Commission in close collaboration with the Training and Knowledge Management Working Group of ESARDA is providing yearly a one-week well-established specialized course on Safeguards and Non-Proliferation; the so-called "ESARDA Course". The course is organized in Ispra (Italy) and attended by an audience around fifty participants not only students but also professionals from nuclear inspectorates (IAEA and Euratom), national nuclear regulators, nuclear operators and research centres. ESARDA Course includes lectures, practical exercises, case studies, laboratory visits and its content is continuously improved or completed such as including new topics that have emerged to be of interest of nuclear safeguards and non-proliferation.*

*In the recent years ESARDA evolved to be reached out in some regions worldwide. In fact, EC DG DEVCO has funded outreach ESARDA Courses that are organized by European Commission, Joint Research Centre Directorate General (EC JRC). The two first courses of this kind were successfully organised by EC JRC in 2013 in Kuala Lumpur (Malaysia) in partnership with Atomic Energy Licensing Board and the Royal Malaysian University and in 2014 in Bangkok in partnership with the University of Chulalongkorn.*

*In 2017 in China, in collaboration with Tsinghua University of Beijing, an ESARDA course was organized with EU-EC-IAEA-US lecturers with participants from 18 Chinese Universities and 6 external companies. This paper reports the feedback of this China ESARDA 2017 Course, and of the two outreach ESARDA courses organized in 2018, the first in Pretoria (South Africa) for thirteen South African countries of South African region (February 2018) and the second in Algiers (Algeria) for Eight North African and Sahel countries (October 2018).*

*The way these courses were tailored with respect to the original content of ESARDA Course to best fit needs of the region and the intention to make it a sustainable initiative in the region is also reported.*

**Keywords:** Training, Education, Safeguards, Non-proliferation

## **1. Introduction**

Over the last almost two decades, the Nuclear Security Unit of the Joint Research Centre of the European Commission in close collaboration with the Training and Knowledge Management Working Group of the European Safeguards Research and Development Association (ESARDA) provides a yearly one-week well-established specialized course on safeguards and non-proliferation, which takes place in Ispra (Italy) [1,2,3]. The course is open to an average of 50 participants either students such as

master students or professionals in relation to nuclear safeguards, Security and no proliferation such as legal, political, regulatory, international relations etc. The lecturers to this course are well-established experts from the IAEA, US DoE, JAEA, EC ENER (EURATOM inspectors) and EC JRC.

The course is addressed to master degree students, in particular nuclear engineering students, but also to young professionals in nuclear regulations or operations and International Relations.

The course aims at complementing not only nuclear engineering study programs by including nuclear safeguards and non-proliferation in the academic curriculum in Europe but also to contribute to efforts of international and national organizations such as IAEA, INMM, JAEA, etc. to enhance and harmonize safeguards and non-proliferation approaches. Moreover, the course presents an overview on inspections techniques, ranging from non-destructive assay (NDA) to destructive assay (DA) techniques, containment and surveillance, information verification, satellite imaging, environmental sampling, etc. The course also addresses aspects of how to create the global and regional settings of nuclear non-proliferation systems, such as the Treaty on Non-proliferation of Nuclear Weapons (NPT) and the EURATOM Treaty, and how they work in practice.

Over years, the content and the programme of the ESARDA Course have been yearly fine-tuned and enriched thanks to the expertise of the organisers and lecturers that contributed build a well-established international course on nuclear safeguards and non-proliferation with a participation of all regions of the world.

To support capacity building worldwide on nuclear safeguards and non-proliferation, ESARDA Course was outreach thanks to the initiative of the European Commission Directorate for Development Cooperation (DG DEVCO). The European Commission through its Nuclear Safety Cooperation funding instrument covered cost of these outreach courses.

Two first courses of this kind were successfully organised by EC JRC in 2013 in Kuala Lumpur (Malaysia) in partnership with Atomic Energy Licensing Board and the Royal Malaysian University and in 2014 in Bangkok in partnership with the University of Chulalongkorn.

Then in 2017 in China, in collaboration with Tsinghua University of Beijing, an ESARDA course was organized with EU-EC-IAEA-US lecturers with participants from 18 Chinese Universities and 6 external companies.

This paper reports on the course held in China as well as two others, which were organised in Africa in 2018. The first was organised in Pretoria (South Africa) for thirteen South African countries of south African region (February 2018) and the second in Algiers (Algeria) for ten North African and Sahel countries (October 2018). The way these courses were tailored with respect to the original content of ESARDA Course to best fit needs of the region and the intention to make it a sustainable initiative in the region is also reported.

## **2. Delivered outreach regional ESARDA courses**

With respect to the classical ESARDA course held yearly in Ispra (Italy), these courses targeted towards the academic world to attempt sustainability of the initiative in the sense that the course or part of it could be integrated in the cursus and education programmes of the participating countries. In this respect, the key objective is to motivate university professors, of the participating countries to embed one or more modules of the course provided by the EC in their teaching whether for nuclear engineers, political scientists of law faculty students. These outreach courses targeted also nuclear regulatory authorities such as safety, security or safeguards and non-proliferation.

The content of the course was tailored with respect to original content of ESARDA Course to best fit needs of the participating countries.

### **2.1. Course for China**

By the participation to conferences dealing with uranium enrichment, JRC was informed that the Department of Engineering Physics of the Tsinghua University in Beijing was seeking cooperation in the safeguards field to, eventually; introduce this topics in the curriculum of their students. In 2016, JRC representatives met people in charge of this department in China. Rapidly the interest of setting up an ESARDA course at Tsinghua University was seen and the cooperation between JRC, under the auspices of DG DEVCO, was concretized by the signature of a letter of commitment.

In order to cope with the availability of the speakers and the planning of the students, the ESARDA course was planned in September 2017. The agenda (Figure 1) was reviewed by both parties and it was decided that the session devoted to the technical subjects related to gamma and neutron



Two to three trainees from each of thirteen countries, most of them from south African region attended the course. These countries are (Figure 3): South Africa, Namibia, Zimbabwe, Botswana, Mozambique, Zambia, Malawi, Angola, Tanzania, Angola, Congo (D.R), Kenya, Ghana and Nigeria.

教育部高等院校核工程类专业教学指导委员会  
2017年全国核不扩散与核安保课程建设暑期研讨会 2017.9.4



Figure 2: Picture of the participants to the ESARDA course and lecturers.

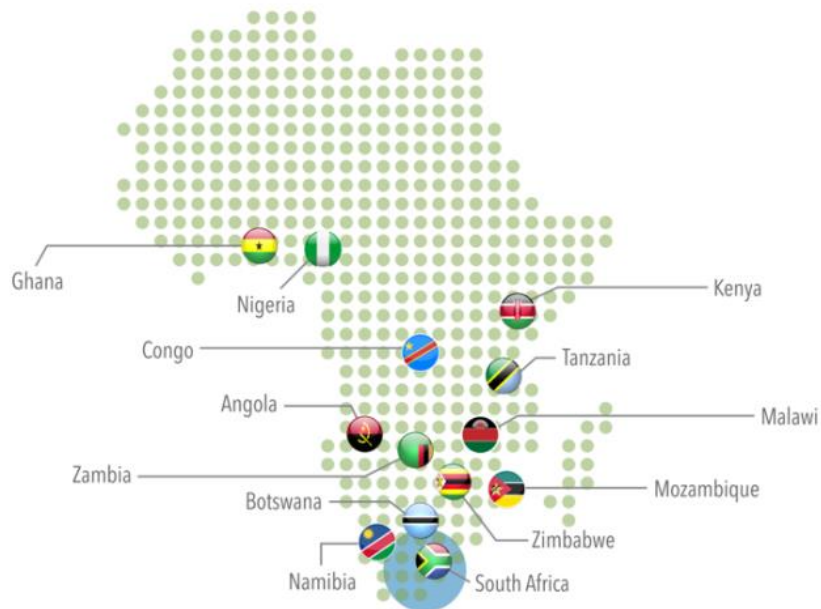


Figure 3: Participating countries of the outreach ESARDA course for the South African Region

High level South Africa Officials together with those of the European Union Delegation to South Africa addressed the audience during the opening ceremony of the course. The course delivered clear messages on nuclear safeguards and non-proliferation in different sections during the week course such as:

### **Basics of Nuclear Fuel Cycle and Safeguards:**

Description of the nuclear fuel cycle from mining to final repository, focussing on enrichment in the front-end and reprocessing in the back-end. The evolution of the Non Proliferation Treaty-regime, safeguards, international control regimes in theory and practice, and present trends in the nuclear nonproliferation efforts.

### **Material to be safeguarded:**

Definition of nuclear material that is subject to nuclear safeguards and related safeguards goals (significant quantity, timeliness and detection probabilities).

### **Legal Framework:**

Which legal protection means exist, Overview on international and regional Non-Proliferation Treaties and established Institutions and Organisations.

### **Instrumentation and methodologies for verifications and inspection:**

Nuclear material accountancy principles and statistics of auditing. What is the methodology to verify? Overview on inspector tools and their use to verify the nuclear activities as declared under the safeguards agreements (Non Destructive Assay, Monitoring, Containment/ Surveillance); additional safeguards measures under the Additional Protocol (complementary access, satellite imagery, environmental sampling) and how they are applied in field (storage facility, process facility, enrichment facility, research institute, spent fuel transfer).

### **How to control Import/ Export:**

Guidelines of the Nuclear Suppliers Group, trigger list and dual-use list. Means to combat illicit trafficking, including nuclear forensics.

### **What additional information offers:**

Collection of open source data and demonstration of some case studies.

As shown in the programme (Figure 4) the courses included lectures, group exercises and a questionnaire session (Quiz based of MCQ from each of the lectures of the course). An evaluation of the course by the trainees are gathered at the closing ceremony.

Considering the specificity of the participating countries to this regional safeguards and non-proliferation course, it was deemed important to include few other topics in the programme such as security and safety aspects related to radioactive sources, uranium mining and transportation related topic and also nuclear research reactors safeguards regime capacity building.

A whole afternoon was fully dedicated to the technical visit to nuclear research center of Pelindaba (NECSA) located in about two hours drive from Pretoria. NECSA (The South African Nuclear Energy Corporation) is in charge to undertake and promote research and development in nuclear energy and radiation sciences. The nuclear research reactor SARARI-I and a waste management facility were visited.

In addition to the international experts in their specific years that have lectured with a high motivation in this outreach initiative on nuclear safeguards capacity building, two lectures for the South African Regions were given. The first lecture was presented by the Atomic Energy Commissioner of Democratic Republic of Congo who showed his experience in safeguards aspect regarding of a research reactor. The second lecture regarded the experience of South Africa in the field of export control of sensitive commodities.

## **2.3. Course for North Africa and Sahel**

In Africa and in 2018, a second Regional Training Course on Nuclear Safeguards and Non-Proliferation was organised in Algiers (Algeria) on 21-25 October 2018, in a same format of the one that took place in South Africa. EC JRC in collaboration with the Algerian Atomic Energy Commission (Commissariat à l'Energie Atomique, COMENA) organised the event. Ten countries of North Africa and Sahel (Morocco, Algeria, Tunisia, Libya, Egypt, Senegal, Niger, Chad) participated in addition to international lecturers. The preparation of the course started with collaborative contacts between the high level officials of EC JRC and the Algerian Ministry of Foreign Affairs that conducted to the successful organisation of the regional course.

Representatives of high level authorities have attended the opening ceremony such as:

- The EU Delegation to Algeria represented by his Excellency the EU Ambassador in Algeria and his
- The Algerian MFAs represented by the Director of Multilateral affairs.
- The Algerian Atomic Energy Commission (COMENA).
- The African Atomic Energy Commission (AFCONE) represented by its executive secretary.
- and obviously the EC JRC.

The course included lectures, practical exercises and case studies. All lecturers physically presented their topics except a lecture on "Implementation experience of Non Proliferation Treaty" which was successfully presented from New York by video conference. This topic included a case study exercise. A demonstration of radiation detection equipment was organised by COMENA which was very well received by the audience.

The schedule of the course is shown in Figure 5. In addition to the specific topics that were added with respect the ESARDA course of Ispra in the course in South Africa (Security of radioactive course, uranium mining, safeguards experience on nuclear research reactors, the IAEA Small Quantities Material Protocol was presented to fulfil an expressed wish of the participating countries.



EUROPEAN COMMISSION  
JOINT RESEARCH CENTRE  
Directorate Nuclear Safety & Security  
Department Nuclear Security & Safeguards

**Regional Training Course on Nuclear Safeguards  
and Non-Proliferation for South African region  
Centurion (Pretoria), 12-16 February 2018**



UNIVERSITY OF THE  
WITWATERSRAND  
JOHANNESBURG

	Mon., Feb. 12th	Tue., Feb. 13th	Wed., Feb. 14th	Thu., Feb. 15th	Fri., Feb. 16th
09:00	<b>Opening Ceremony</b> (JL, WJ, KA)	History of Non-Proliferation (QM)	Implementing NPT (QM)	Inspection on Site (SP)	Uranium Mining Group Exercise (CV)
10:00	Nuclear Fuel Cycle (JL)	NDA II (neutron counting) & DA introduction (KA)	Group Exercise (QM)	Information Collection & Analysis (JB)	Inspection of a Research Reactor (VL)
11:00					
11:20	<b>Break/Group Picture</b>	<b>Break</b>	<b>Break</b>	<b>Break</b>	<b>Break</b>
11:20	Material & Facilities Subject to Safeguards (WJ)	NPT (QM)	Case Study (JL)	Uranium Mining Safeguards Requirements (CV)	Questionnaire, Assessment
12:20					
13:45	<b>Lunch</b>	<b>Lunch</b>	<b>Lunch and Technical Visit (12:20-17:00)</b>	<b>Lunch</b>	<b>Lunch</b>
13:45	Physical Protection (AH)	NM Account and Control Principles (SP)		Satellite Imagery (JB)	Certificate Delivery Debriefing and Way Forward
14:45	NDA I (gamma spec.) (KA)	Practical Exercise (SP)		Combating R/N Illicit Trafficking (WJ)	<b>Group Picture Closing</b>
15:45					
16:05	<b>Break</b>	<b>Break</b>		<b>Break</b>	
16:05	Safeguards and Nuclear Export Arrangements (JK)	Nuclear Trade Regulation (MR)		Safety/Security of R. Sources (KA)	
17:05					
	<b>Cocktail 18:00-19:30</b>			<b>Social Diner, 19:30-22:00</b>	

KA: Kamel ABBAS, EC  
JL: James LARKIN, South Africa (SA)  
SP: Susan PICKET, IAEA  
JK: Johann KELLERMAN, SA

WJ: Willem JANSSENS, EC  
QM: Quentin MICHEL, Belgium  
CV: Cindy VESTERGAARD, USA  
MR: Melanie Reddiar, SA

VL: Vincent LUKANDA, R.D. Congo  
JB: Jacques BAUTE, IAEA  
AH: Anne HARRINGTON, USA

Figure 4: Programme of the outreach ESARDA Course organized for the South African Region in February 2018 in Pretoria.

The executive secretary of AFCONE presented the main features of the organization and its action plan aiming at playing an important role in Africa. In fact, the PELINDABA treaty (the nuclear free zone treaty signed in Pelindaba) is the basis of AFCONE. Unfortunately, so far neither Morocco nor Egypt are active members, so some creativity will be required in organising regional events in collaboration with AFCONE.

As in the course of South Africa, international experts have lectured, this included as well African lecturers. In fact, in order to use the knowledge already available in Africa, two topics of the course were dealt by African experts. The first on Nuclear Material Accounting for and Control (NMAC) topic was lectured by an expert from COMENA. The topic on the experience on research reactor safeguards was given by the Egyptian Atomic Energy Agency for their long experience on operating a research reactor. On the last day, the course evaluation (by the trainees) was collected from the audience and a Quiz was organized which is composed by 2 to 4 questions out from each of the lectures of the course.




**PROGRAMME**  
**Regional Training Course on Nuclear Safeguards and Non-Proliferation**  
**for North Africa and Sahel**  
 21-25 October 2018, Hotel Mercure, Bab Ezzouar, Algiers, Algeria

	Sun., Oct. 21st	Mon., Oct. 22 <sup>nd</sup>	Tue., Oct. 23 <sup>rd</sup>	Wed., Oct. 24 <sup>th</sup>	Thu., Oct. 25 <sup>th</sup>
08:15-09:00	Registration				
09:00-09:30	Opening Ceremony with Algerian and EU Authorities	Non-Destructive Assay I (gamma spec.), (KA)	Group Exercise Cont. Legal Instruments Implementing NPT, (IV/KA/IMC)	On Site Safeguards Inspection, (IMC)	Satellite Imagery, (JB)
09:30-10:15	Introduction of the participants and Presentation of the course	Group Exercise Cont. Nuclear Fuel Cycle, (LV)	NM Account and Control Principles (IMC)	IAEA safeguards an effective nuclear non-proliferation means, Case Study, (IV/IMC)	Experience on a Research Reactor Safeguards, (HIK)
10:15-10:45	Break/Group Picture	Break	Break	Break	Break
10:45-11:30	History of Non-Proliferation, (JV)		Safeguards and SSAC, (SK)	IAEA safeguards an effective nuclear non-proliferation means Cont. Case Study, (JV)	Implementing Small Quantities Protocols, (JV)
11:30-12:15	Nuclear Fuel Cycle, (LV)	Non-Destructive Assay II (neutron counting) (KA)	Uranium Mining Safeguards Requirements, (QM)	Safeguards Efforts of AFCONE, (MB)	Sustainability of the RTC NSNP, Course Analysis, Discussion & Way forward (WI/KA)
12:15-13:45	Lunch	Lunch	Lunch	Lunch	Lunch
13:45-14:30	Material & Facilities Subject to Safeguards, (WJ)	Safeguards and Nuclear Export Arrangements (QM)	Demonstration and Discussion on Radiation Detection Instrumentation used in Nuclear Safeguards, (COMENA/IRC)	Information Collection & Analysis, (JB)	Quiz, Course Evaluation
14:30-15:30	Group Exercise Nuclear Fuel Cycle, (LV)	Legal Instruments Implementing NPT (LR via VC)		Safety and Security of Radioactive Sources, (KA)	Certificate Delivery, Group Picture, Closing Ceremony
15:30-16:00	Break	Break		Break	End of the RTC NSNP
16:00-16:45	Physical Protection, (CI)	Group Exercise. Legal Instruments Implementing NPT (LR via VC)		Implementation of Nuclear Safeguards and Non-Proliferation Best Practices in South Africa, (IL)	
18:30-19:30	Evening Lecture (R&D and E&T in EC-JRC (WJ)) followed by a Cocktail	Group Exercise Safeguards and Nuclear Export Arrangements (QM)		Social Diner	

Registration on Saturday 16:00 - 19:00 and on Sunday 08:15- 09:00



EUROPEAN COMMISSION  
 JOINT RESEARCH CENTRE  
 Directorate Nuclear Safety & Security  
 Department Nuclear Security & Safeguards



Algerian Atomic Energy Commission

Figure 5: Programme of the outreach ESARDA Course organized for the North African and Sahel in October 2018 in Algiers.

### 3. General observations and perspectives

The audience of these outreach safeguards and non-proliferations courses, which was quiet spread and composed of university teachers, regulatory authorities, representatives of ministries, research centers, has shown and demonstrated a high interest and motivation to the courses. A high interaction with the lecturers thus have strongly contributed the success of these outreach education and training initiatives. The participants from the education and training organisations were encouraged to use as much as they see fit all the course material that was distributed such as even including some the lectures in their own education programmes in their respective organisations. In fact, the course material was distributed not only in prints but in electronic format as well.

As mentioned, most of the lectures are experts from international organisations such as from ESARDA lecturers pool or IAEA. IAEA has strongly contributed to these regional courses by the availability of several IAEA lecturers. Several African experts have successfully contributed to these course with their lectures.

### 4. Conclusion

For capacity building worldwide on nuclear safeguards and non-proliferation, the EU is contributing significantly either through R&D or E&T programmes that are in place under various collaborations and networks. This paper presented an example of three outreach courses, two regionals and one national, which were successfully organised in 2017 and 2018 by EC JRC in collaboration with the hosting countries, here South Africa, Algeria and China. Beside the content of the course substance (lecturer, programme, selected topics), which delivered clear messages and for which the participants expressed full satisfaction, other different logistics arrangements, venue location and facilities, accommodations, transportations, were also well organised for all the three courses.

The objective of these outreach training course in safeguards and non-proliferation is not only the organisation of these training courses. The other objective is to attempt to make such initiatives sustainable in the region or country. This would be possible if follow-ups of such course are undertaken

that could be repetition of such courses as such or with other specific and targeted activities. As it is clear that a week training or awareness course organised once has limited chance to be sustained specially in those regions where nuclear safeguards and non-proliferation are deemed with low priorities. Consequently, the plan for the reorganisation of these course in those regions are under way to be set in agreement with EC DG DEVCO in view of stimulating sustainability of this nuclear safeguards capacity building initiative. Moreover, the identification of next regions to target with this initiative is under discussion.

## 5. References

- [1] Janssens W., Scholz M., Jonter T., Marin Ferrer M., De Luca A, Nuclear Safeguards and Non Proliferation Education and Training, initiatives by ESARDA, INMM and JRC. Brugge, Belgium : s.n., 27-30 May 2013. ESARDA Symposium 2017
- [2] Janssens W., Abousahl S., Luetzenkirchen L, Mondelaers W European Commission Safeguards and Non-Proliferation R&D, 60 years of experience. J. Indian Wells, California USA : s.n., 16-20 July, 2017. 58th INMM Annual Meeting
- [3] Janssens W., Nuclear Safeguards Challenges From a JRC Perspective, XX Edoardo Amaldi Conference, 9 - 10 October 2017, Rome
- [4] Abbas K., Janssens W., Irmgard Niemeyer I. and Raiola F. Educational efforts in Nuclear Safeguards and Non-Proliferation in the European Commission, Joint Research Centre, in collaboration with the European Safeguards Research and Development Association, INMM, 59th Annual Meeting, July 22-26, 2018, Baltimore
- [5] Janssens W., Abbas K. and Raiola F., Outreach Education and Training in Nuclear Safeguards and Non-Proliferation of the European Commission, Joint Research Centre, IAEA SAFEGUARDS 2018 Symposium, 6-9 Nov, Vienna

# **Panel 4:**

# **Digital Transformation**

# The Role of Maps in Site Knowledge and Wayfinding: A Human Performance Evaluation for International Nuclear Safeguards Inspections

Zoe N. Gastelum,<sup>a</sup> Mallory C. Stites,<sup>b</sup> Laura M. Matzen<sup>b</sup>

- a. International Safeguards & Engagements
- b. Applied Cognitive Science  
Sandia National Laboratories<sup>1</sup>  
Albuquerque, NM, USA  
Email: [zgastel@sandia.gov](mailto:zgastel@sandia.gov)

## **Abstract:**

*International Atomic Energy Agency (IAEA) safeguards inspectors conducting in-field activities are responsible for taking a variety of samples, measurements, and observations, as well as being aware of their environment to notice any unusual activities that might indicate undeclared activities or materials. The data collected by safeguards inspectors are highly dependent on location (i.e., they should pertain directly to a material balance area, facility, site, location outside facilities, etc.), thus an inspector's ability to confidently confirm their location within a facility, the route they accessed to traverse a facility, and the location within a facility where they observed specific phenomena is highly relevant.*

*The cognitive science community has extensively studied wayfinding across multiple navigation environments (indoors, outdoors, over multiple stories indoors) and modalities (paper maps, electronic maps, step-by-step instructions, landmarks, etc.) yet the unique nuances of wayfinding for international nuclear safeguards inspections (indoors, in an industrial environment, escorted, and with the potential for deceit or manipulation) offer exciting research opportunities. We approach this opportunity via the use and interaction with facility map information for international nuclear safeguards inspectors working in the field. In this paper we will describe research within the cognitive science community that is relevant for wayfinding applications for in-field safeguards activities, our experimental design for testing human performance on indoor, escorted wayfinding activities in a multi-story industrial facility across multiple map-based conditions, our results to-date, and recommendations for safeguards inspectors on their use of maps in the field.*

**Keywords:** safeguards inspection; wayfinding; cognitive science; situational awareness; maps

<sup>1</sup> Sandia National Laboratories is a multimission laboratory managed and operated by National Technology & Engineering Solutions of Sandia, LLC, a wholly owned subsidiary of Honeywell International Inc., for the U.S. Department of Energy's National Nuclear Security Administration under contract DE-NA0003525. SAND2019-4560 C.

## 1. Introduction

International Atomic Energy Agency (IAEA) safeguards inspectors carry out highly visible and important tasks for international security under environments of cognitive duress. They may be jet-lagged from travelling across the globe to reach the facility they will inspect, are working in industrial and potentially hazardous environments, their movements are constrained by protective attire, and they may be working in a language other than their mother tongue. Furthermore, some inspectors may be completing activities under the stress of their presence being unwanted by the facility operator—every day that an inspector interrupts normal facility operations represents a financial loss for the operator.

More information is available to help inspectors complete their tasks than at any other time in history: open source data, overhead imagery, the state's declarations, inspector observations or notes from prior visits, and results from previous sampling activities at the facility. Cognitive science research shows us that providing too much information may be detrimental to performance, and can cause confusion, frustration, errors, or other signs of information overload. We must consider how to best provide information to safeguards inspectors so they are most able to benefit from it and act upon it.

In 2017, our research team conducted an extensive literature review within the cognitive science domain and a safeguards prioritization activity in which we identified safeguards tasks that pose challenges to inspectors that also represent new or emerging research domains within the field of cognitive science [1, 2]. From those activities, we identified three safeguards activities on which to focus our research:

1. Visual list comparisons, in which inspectors compare long lists of items such as inventory lists to operator records [3, 4];
2. Knowledge transfer, in which inspectors record their observations and findings in the field for their future use, for briefing to management, or for use by a future inspection team [5, 6]; and
3. Wayfinding, in which inspectors are escorted through complex, multi-story, industrial facilities and must maintain their awareness of their surroundings and location.

Wayfinding has been studied extensively in the cognitive science community, especially as it relates to outdoor navigation, different navigational support tools (maps, step-by-step directions, landmark cues, and GPS), differences in travel modalities (e.g. walking or by car), etc. [7, 8]. Indoor wayfinding has been studied far less, and the combination of indoor navigation with escorted access posed a new research opportunity. In this paper, we will describe our human performance testing which examined the impact of the provision and format of maps for inspector wayfinding and provide recommendations for enhanced safeguards practice and future research.

## 2. Research Question

IAEA safeguards inspectors are constantly required to find their way—through new cities, nuclear sites, and facilities. Their ability to know their current and historical locations, follow their routes on maps, and recall locations of observations throughout a facility is crucial to their work. Good navigators can tell if they are being led in circles by an adversarial operator/escort, if they have avoided specific areas of a facility through indirect routing, and can recall specific observations according to locations on a map so that they can communicate that information for follow-up in future visits.

In this research, we used a battery of tests to explore how map information impacted an individual's ability to understand their location and surroundings following escorted (guided) access in a multi-story former nuclear facility. Our human performance studies included three map conditions: studying a map but not carrying it through a facility; studying and carrying a map through the facility; or having no map at all. We are currently conducting additional experiments to test the impact of the level of detail provided in a map, so that we may compare human performance on wayfinding tasks between having access to a simple map typical of what might be posted for fire escape routes or staff navigation, a complex CAD drawing, and a three-dimensional rendering.

### 3. Method

#### 3.1 Participants

Our test population included sixty self-selected staff members of Sandia National Laboratories. The average participant age was 37 years, and our sample included 20 females and 40 males. The females were reasonably distributed among the three test conditions (map study, map study + carry, no map). 50 of the 60 participants had at least a university degree, with 35 reporting advanced degrees (Masters or PhD). None of the participants had prior experience in our test facility.

Participants were asked to self-assess their sense of direction using the Santa Barbara Sense of Direction Scale (SBSOD) [9] after they completed the experiment. To avoid biasing individuals based on their self-evaluations (i.e., stereotype threat; Steele & Aronson [10]), we opted to administer the SBSOD survey post-experiment. Most questions on the SBSOD are different enough from our experimental conditions that we did not anticipate participants degrading their score based on the challenging nature of our experimental tasks.

#### 3.2 Materials

The experiment used two different paper maps. The map used for participant study and carry throughout the facility was a simplified computer-aided drafting (CAD) drawing of the facility showing upstairs and downstairs of the facility. The map included color-coded arrows marking the connections between stairways to help participants identify how the ground floor and mezzanine levels aligned since the mezzanine level only covered a fraction of the ground floor. The participant study/carry map is provided in Figure 1. The map used for testing was a line drawing of the facility, with some of the CAD markers removed to minimize perceptual overlap with the studied map but retaining the color-coded arrows to facilitate stairway matching between stories (see Section 3.3).

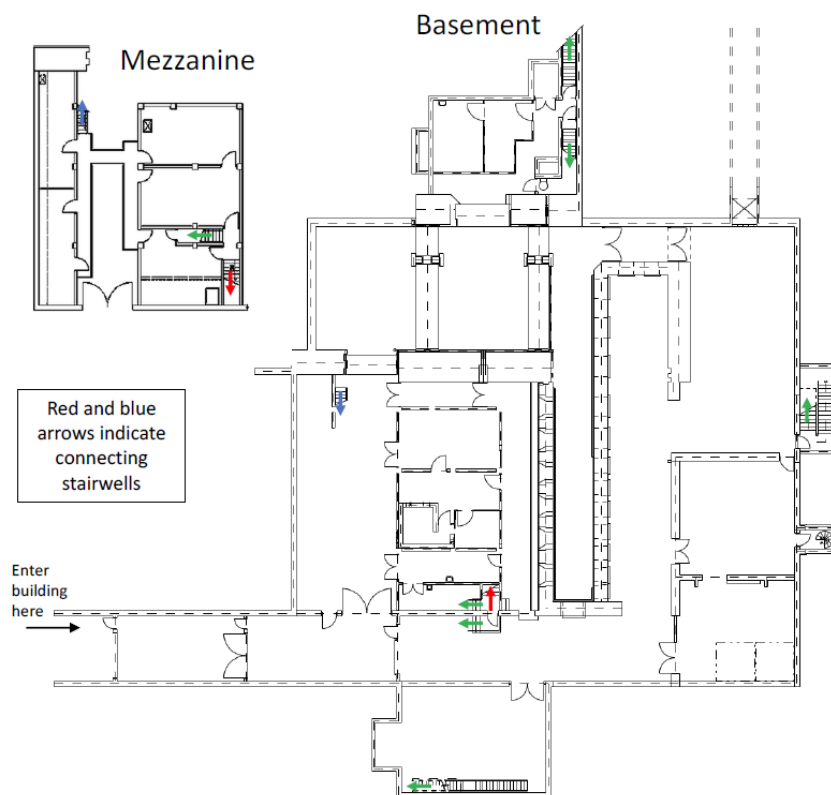


Figure 1 Participant Study/Carry Map

### 3.3 Procedure

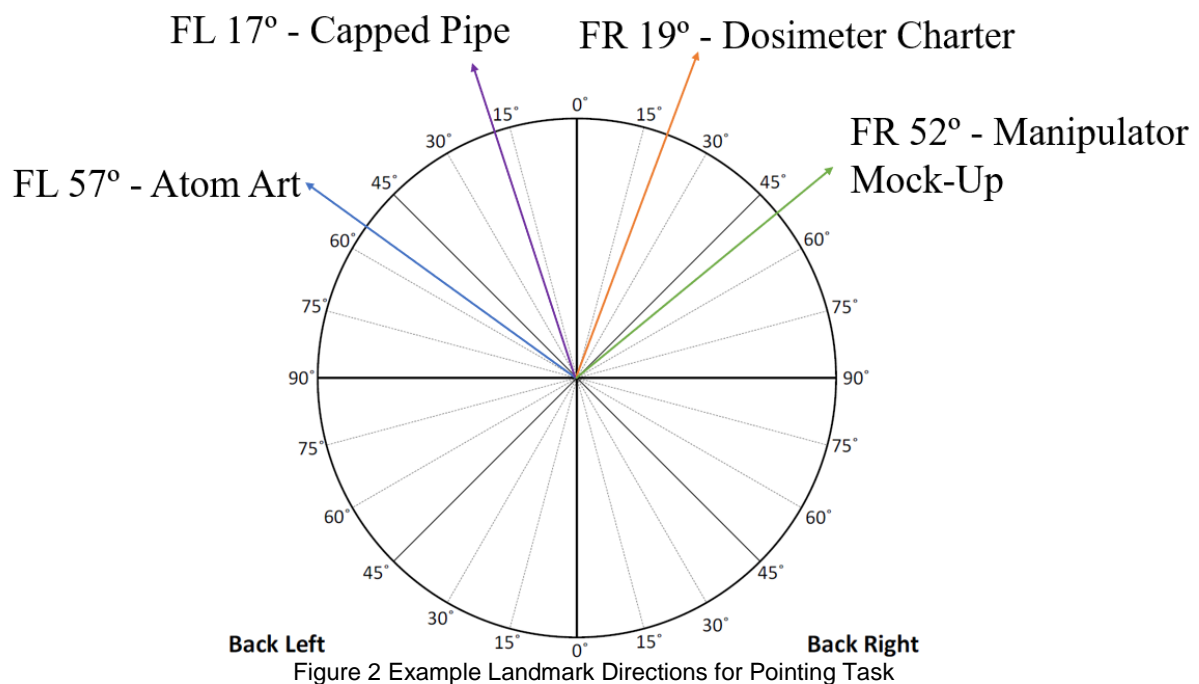
All participants participated in a five-minute study period, in which they were allowed to study either the participant study/carry map or a one-page document about international nuclear safeguards. The participants were provided an approximately three-minute tour of the test facility, which included a three-second pause at each of eight "landmarks" throughout the facility such as a dosimeter charger, a set of remote manipulators, or a water meter that the participants were requested to remember. The starting point of the tour stayed constant, and half of the participants completed the tour in a clockwise manner, the other half counter-clockwise.

Following the tour, the participants completed a battery of four tasks: a pointing task, a shortcut task, a map drawing task, and a memory task. As previously noted, they completed the SBSOD survey at the conclusion of the experiment.

### 3.4 Tasks

After completing a guided facility tour, participants completed four tasks, in a set order.

The first task was a directional pointing task (adapted from Rand et al. [11]). The participants returned to the starting position of their tour and were faced half-way between the two route directions (so that all participants were facing the same way, and none were facing their exact route). Then they were asked to indicate which direction, according to degrees on a printed circle, each of the eight landmarks were. This included landmarks that were on their current (ground) level and the mezzanine. A compass with four of the landmark directions is shown in Figure 2.



Then, participants completed a shortcut task (adapted from Labate et al [12]). In this task, participants were taken to one of the eight landmarks, and asked to find the shortest possible route to another landmark in the facility. In all cases, the shortest route involved the participant traversing a part of the facility they had not previously entered. Three shortcuts were requested, which were the same for all participants regardless of route direction. If the participants got too far off-course during this task, the experimenter would stop and re-direct the participant at pre-defined points.

For the third task, participants traced their route and marked the name and location of the eight landmarks on a copy of the test map, which was a simplified line drawing of the participant study/carry map.

The final task was a landmark recognition task, in which the participants were shown a series of images taken in the facility, including photographs of the landmarks that they had been tasked with remembering, incidental landmarks that were visible along their route, and distractor images of objects from within the facility that the participants would not have seen during the experiment. The landmark recognition task was administered in E-Prime software so that we could track accuracy and response time to different types of stimuli. The participants were requested to say if they had seen the object in the image as part of their tour (which they called an “old” item) or if they had not previously seen the object (a “new” object). Example photographs are shown in Figure 3.



Figure 3 Example Photographs from the Memory Test

## 4. Results

Results were analyzed by map condition, by SBSOD self-assessment score (under the assumption that people with better sense of direction will perform better regardless of map condition), and by gender. SBSOD scores were not independent from gender: females in our sample had a mean SBSOD score of 61.6 (SD 18.5) and males 75.5 (SD 15) out of a possible 105, which was a significant difference. This scoring difference by gender was reflective of the general population [13].

However, we found anecdotally from our experiment proctors that several male participants in the experiment expressed that they had signed up for the study because they were interested in testing their “superior” navigational skills, a story that was not generally expressed by our female participants. Also anecdotally, we observed that female participants who performed well on the task still did not give themselves the highest ratings on the SBSOD, but many of the male participants gave themselves high ratings that did not necessarily correlate with their performance level.

### 4.1 Directional Pointing Task Results

The directional pointing task was scored by degrees error, from 0 to 360. Degrees error was determined by calculating the degrees of error between the direction the participant pointed and the actual direction, going both clockwise and counter-clockwise. The smaller error (either based on clockwise or counter-clockwise measurement) was used as the metric.

The no map condition showed the highest overall error, followed by the map study and then map carry conditions, though the difference between all three conditions was not statistically significant. However, planned comparisons with the no map baseline condition showed a statistically significant difference in which the no map condition performed worse on pointing tasks than the map carry condition. See Figure 4 for the pointing error results.

Participants who self-assessed as having better sense of direction on the SBSOD survey performed better on the pointing task and this effect did not interact with the map condition effect.

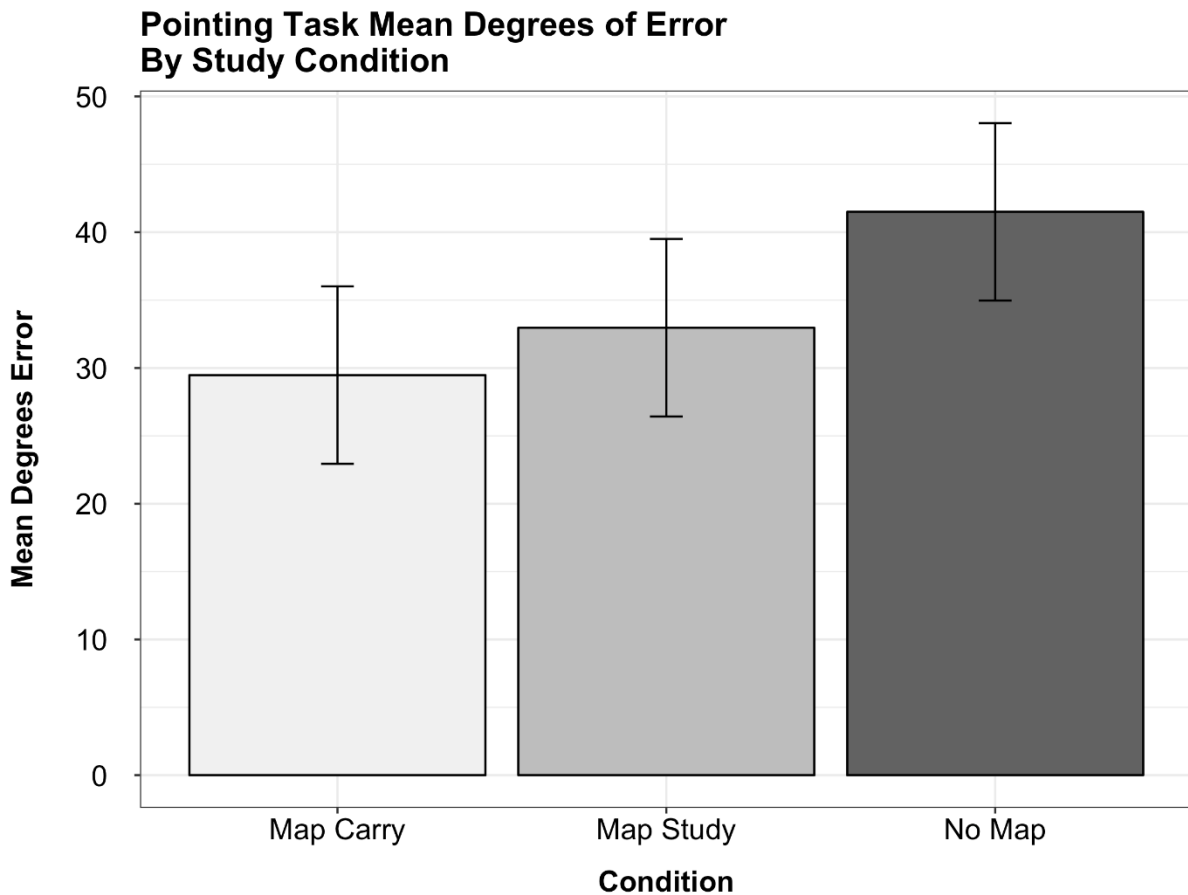


Figure 4 Pointing Error Across Conditions

#### 4.2 Shortcut Task Results

There were no significant effects of map condition on either the shortcut distance or the participants' overall ability to find any shortcut. However, SBSOD scores showed a significant negative correlation with shortcut error when considered separately from map condition, in which people with better sense of direction took shorter shortcuts.

#### 4.3 Map Completion Task Results

Our results showed no difference in map completion scores based on map conditions, including when the route was scored separately from the landmark portion of the task. SBSOD had a primary effect on the overall map completion scores, meaning people with better self-assessed sense of direction were more accurate in tracing their route and marking landmark locations.

#### 4.4 Landmark Recognition Test Results

Performance on the landmark recognition test was assessed in two ways—accuracy, and reaction time. As we expected, participants were better able to identify landmarks than the incidental targets, and had an easier time discriminating between target landmarks and distractor items than incidentals and distractors. The map carry group had the lowest accuracy rate for incidental objects, but the effect was not statistically significant. When SBSOD was included as a covariate, it had a highly significant effect on accurately recognizing target landmarks.

Participant reaction time for incidental landmarks was longer than for target landmarks. This effect was more pronounced in the map carry condition, with an average three seconds longer response time to incidental targets than the no map condition. This marked difference in reaction time is significant and suggests that the map carry participants were less efficient at creating and retrieving memories of incidental landmarks. Participants in the map study condition also showed a longer

reaction time, though not as severe. For the map study participants, the mental effort of trying to mentally compare their location to their previously learned map seems to have lowered their outward attention, compared to the no map participants who were likely also trying to remember their locations but had not previously seen a map of the facility. See Figure 5 for response time results. SBSOD did not have a significant effect on response times.

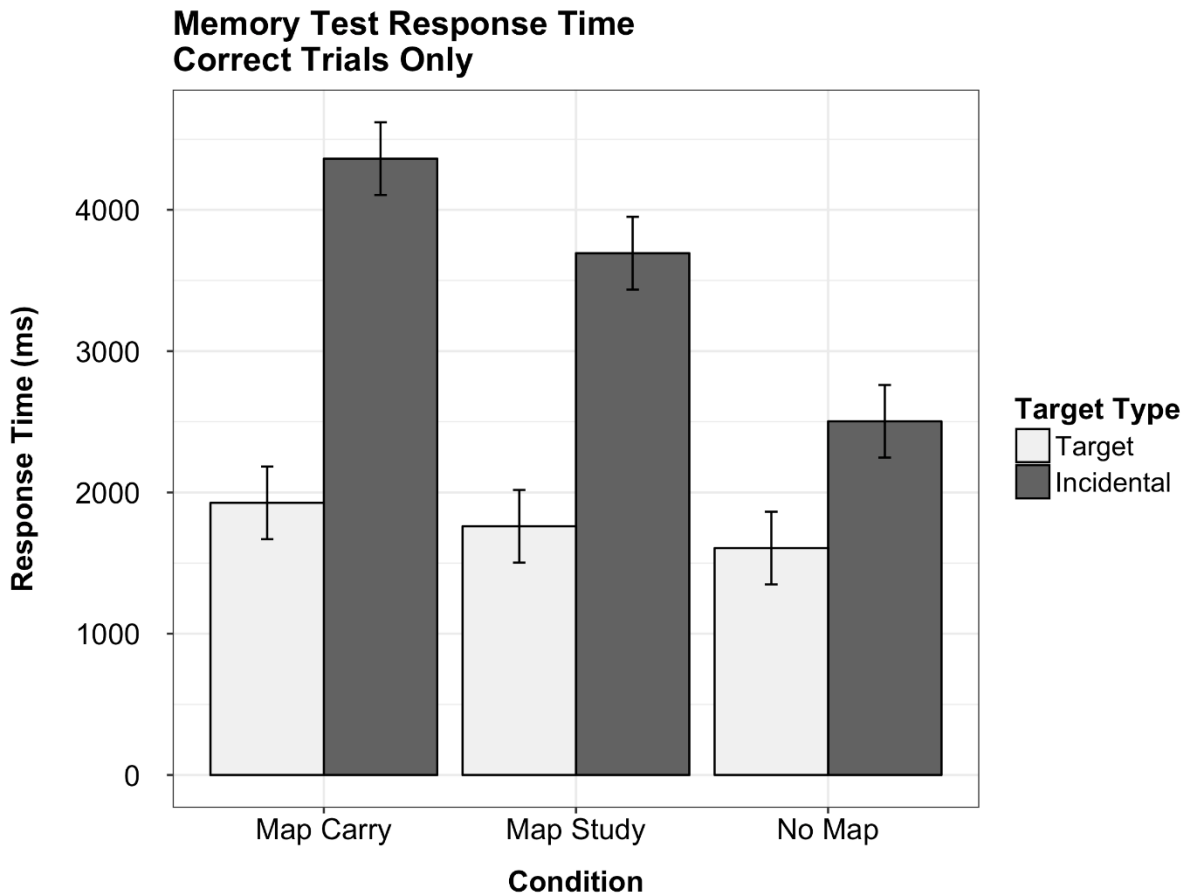


Figure 5 Memory Test Response Time for Correct Trials

#### 4.5 Demographic Impacts

We also investigated the impact of gender on our results. When included as a covariate in the pointing task, gender had a significant effect. When including gender as a covariate on the shortcut task, we observed a marginal effect of gender, in which males took marginally shorter shortcuts than females. Gender also had a significant effect on memory task accuracy, specifically with males showing lower false positive identifications of landmarks than females. There was no effect of gender on map completion accuracy. These findings are consistent with other patterns of gender differences in the literature.

Our findings suggest that the provision of a map may eliminate or mitigate gender or SBSOD-based deficits in spatial learning. This confirms other studies in showing gender differences in spatial tasks that involve needing to know survey knowledge, like the pointing task, but not seeing gender differences in tasks that can rely on route knowledge, like the map completion task.

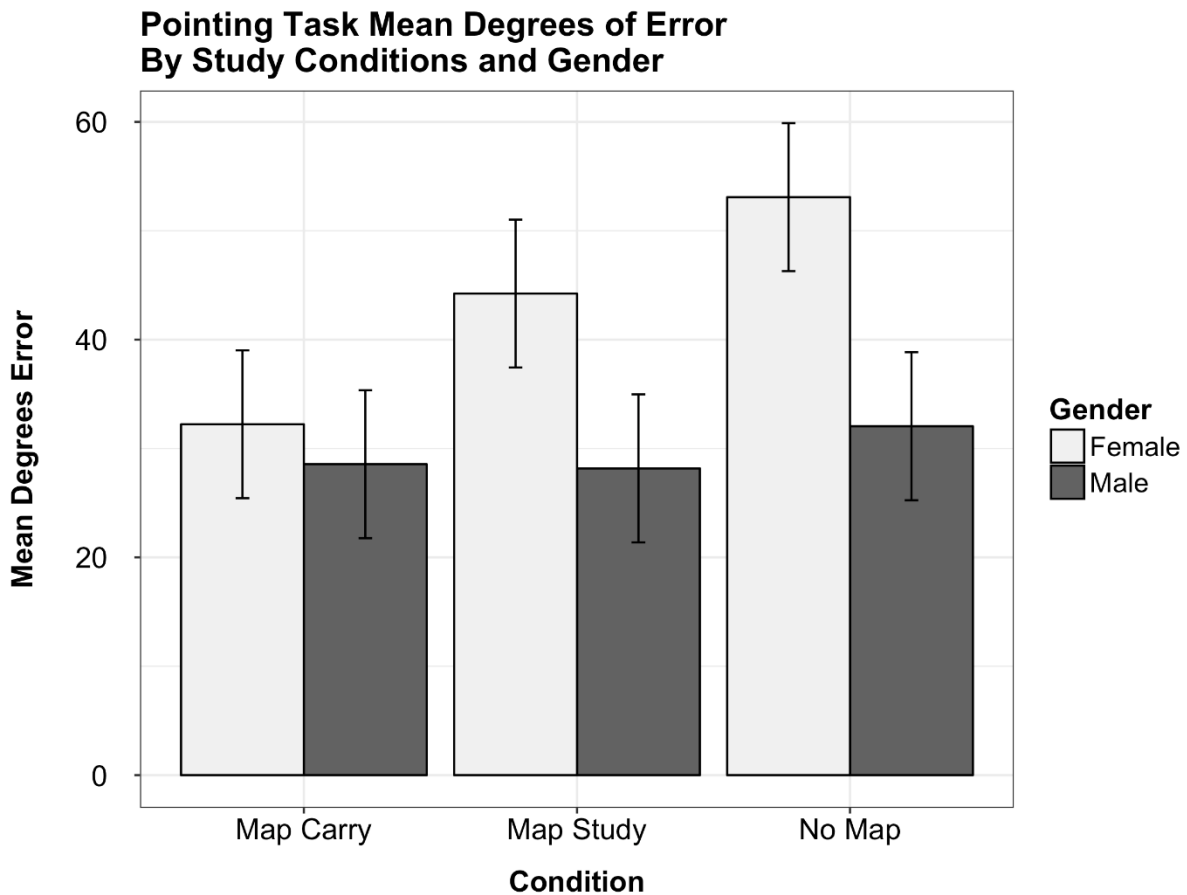


Figure 6 Gender Differences for Pointing Task by Map Condition

## 5. Discussion

Many of the tasks our participants completed were correlated with an individual's sense of direction. This self-assessed measure of individual difference, which also correlated with gender, shows that in general our participants were able to accurately predict their performance on these tasks, specifically the pointing task and map completion task. This may facilitate task self-selection among inspector teams working in the field.

Participants who had access to maps—either for map study or map carry—did perform better on the directional pointing task than participants who had not been exposed to a map of the facility prior to the test. This is important because the pointing task results represent the development of survey knowledge, or the ability to recognize straight-line directions between two locations. Survey knowledge could help support such inspector tasks as noticing when circuitous routes were used between two landmarks. The superior results of the map study and map carry groups on the pointing task indicate that there is a significant role for maps in supporting inspector survey and route knowledge of a facility, but that map study might be sufficient, especially in cases where portable maps are unavailable or infeasible to use.

For the landmark recognition task, the impact of map condition could indicate that participants not carrying physical maps focused on facility surroundings rather than the map during inactive periods of the facility tour, which allowed them to have higher landmark recognition accuracy and faster response times. Participant responses to the incidental landmarks represented general awareness of surroundings, and so we interpreted lower response times as representing better situational awareness. These results indicate that maps do and should play a role in inspection teams' ability to recount and locate their activities. Due to the impact of maps for reduced situational awareness, however, we recommend that inspectors either divide duties so that one member of the inspection team is responsible for the map while others focus on the facility environment, or that the team use the map only to study before a facility visit.

While we intend the findings of this research to inform international nuclear safeguards inspection activities, it is critical to remember that participants were not real inspectors, and it's possible that inspectors may have developed strategies over their years of experience that novices in our studies did not have. Furthermore, inspectors might return to same facility many times over career, and we did not capture interactions with facility familiarity here. We would also assume that expert knowledge in the nuclear fuel cycle may help direct attention during inspections (i.e., attention to incidental things along the route may be heightened in real inspectors if they show a deviation from the normal fuel cycle).

## 6. Future Work

The map used in the first part of this study is not broadly representative of map-type information available to inspectors, which may vary significantly by facility, site, or state. In a second iteration of wayfinding experiments currently being conducted at Sandia National Laboratories, we are testing two more map presentations to determine how the level of detail of the map impacts performance.

In this new research, we are running identical experiments as described above using a highly detailed CAD drawing of the facility and a three-dimensional representation created using the SketchUp software package (see Figure 7). Results will allow direct comparisons between maps with different levels of detail and orientations, to better understand which features directly support safeguards-relevant aspects of spatial knowledge.

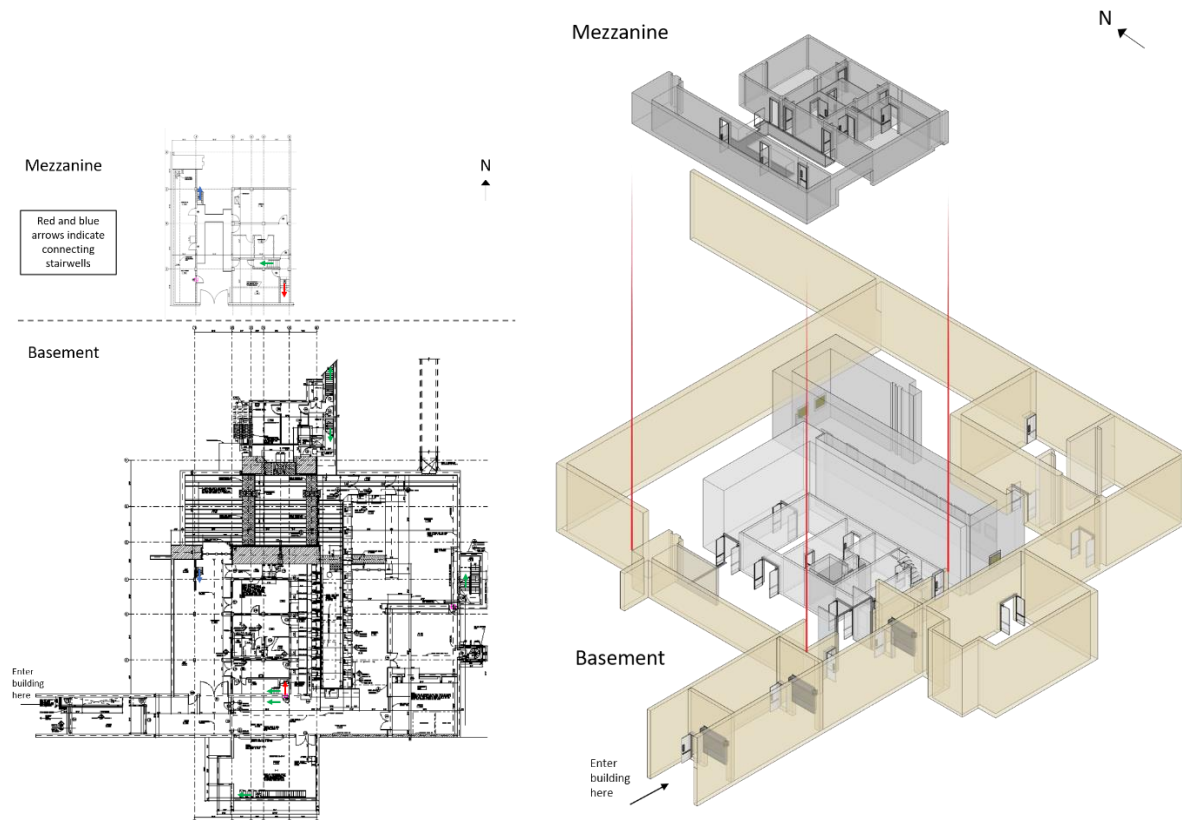


Figure 7 New Map Representations: Highly Detailed CAD (left) and 3D SketchUp (right)

## 7. Acknowledgements

This work was funded by Sandia National Laboratories' Laboratory-Directed Research and Development (LDRD) program, through the Global Security Investment Area. The research team wishes to thank Michael Trumbo for his experimental support, Heidi Smartt for her safeguards contributions to our experimental design, and Greg Baum for his facility engagement support.

## 8. References

- [1] Gastelum, Z.N., Matzen, L.E., Smartt, H.A., Horak, K.E., Moyer, E.M., St. Pierre, M.E.; *Brain Science and International Nuclear Safeguards: Implications from Cognitive Science and Human Factors Research on the Provision and Use of Safeguards-Relevant Information in the Field*; *ESARDA Bulletin*; N. 54. June 2017.
- [2] Gastelum, Z.N., Matzen, L.E., Smartt, H.A., Horak, K.E., Solodov, A.A., Moyer, E.M., St. Pierre, M.E.; *Testing Human Performance in Simulated In-Field Safeguards Information Environment*; *Proceedings of the Institute of Nuclear Materials Management Annual Meeting*; 2017.
- [3] Gastelum, Z.N., Matzen, L.E., Stites, M.C., Smartt, H.A.; *Cognitive Science Evaluation of Safeguards Inspector List Comparison Activities using Human Performance Testing*; *Proceedings of the Institute of Nuclear Materials Management Annual Meeting*; 2018.
- [4] Matzen, L.E., Stites, M.C., Smartt, H.A., Gastelum, Z.N.; *The Impact of Information Presentation on Visual Inspection Performance in the International Nuclear Safeguards Domain*; *Proceedings of Human Computer-Interaction International*; (forthcoming) 2019.
- [5] Gastelum, Z.N., Matzen, L.E., Stites, M.C., Smartt, H.A.; *Human Performance Testing on Observation Capture Methods for International Nuclear Safeguards Inspections: Transferring Knowledge from the Field to Headquarters and Back*; *Proceedings of the Institute of Nuclear Materials Management Annual Meeting*; (forthcoming) 2019.
- [6] Stites, M.C., Matzen, L.E., Smartt, H.A., Gastelum, Z.N.; *Effects of Note-Taking Method on Knowledge Transfer in Inspection Tasks*; *Proceedings of Human Computer-Interaction International*; (forthcoming) 2019.
- [7] Wiener, J.M., Buchner, S.J., Holscher, C.; *Taxonomy of Human Wayfinding Tasks: A Knowledge-Based Approach*; *Spatial Cognition & Computation*; 9. 2009. 152-165.
- [8] Chrastil, E.R., Warren, W.H.; *Active and Passive Contributions to Spatial Learning*; *Psychonomic Bulletin and Review*, 19. 2012. 1-23.
- [9] Hegarty, M., Richardson, A.E., Montello, D.R., Lovelace, K., Subbiah, I.; *Development of a Self-Report Measure of Environmental Spatial Ability*; *Intelligence*; 30. 2002. 425-447.
- [10] Steele, C.M., Aronson, J.; *Stereotype threat and the intellectual test performance of African Americans*; *Journal of Personality and Social Psychology*; 69. 1995. 797-811.
- [11] Rand, K., Creem-Regehr, S.H., Thompson, W.B.; *Spatial Learning While Navigating With Severely Degraded Viewing: The Role of Attention and Mobility Monitoring*; *Journal of Experimental Psychology: Human Perception and Performance*; 41(3). 2015. 649-664.
- [12] Labate, E., Pazzaglia, F., Hegarty, M.; *What Working Memory Subcomponents Are Needed in the Acquisition of Survey Knowledge? Evidence from Direction Estimation and Shortcut Tasks*; *Journal of Environmental Psychology*; 37. 2014. 73-79.
- [13] Hegarty, M., Montello, D. R., Richardson, A. E., Ishikawa, T., Lovelace, K.; *Spatial Abilities at Different Scales: Individual Differences in Aptitude-Test Performance and Spatial-Layout Learning*; *Intelligence*; 34. 2006. 151-176.

## Digital Declaration Site Maps of Additional Protocol are Digitalization at State Level

Tapani Honkamaa  
Timo Ansaranta  
Marko Hämäläinen  
Jussi Heinonen  
Tarja Ilander  
Elina Martikka  
Mikael Moring  
STUK-  
Radiation and Nuclear Safety Authority  
Po-BOX 14  
00881 Helsinki FINLAND  
Tapani.Honkamaa@stuk.fi

### **Abstract:**

*STUK, the regulatory authority in Finland, has established a strategy for 2018–2022. Digital services, tools and automation are becoming more common in everyday work. STUK will identify opportunities for carrying out its regulatory work in new ways and with new tools.*

*One example of digitalization are DDSM (Digital Declarations Site Maps). The Additional Protocol (INFCIRC/540 (Corrected)) stipulates that the member states shall provide the IAEA a declaration including a map of the site. Site maps have been provided to the IAEA in various formats. In the past years the IAEA has developed DDSM guidelines for the submission of the maps in digital format which simplifies and accelerates the ingestion process into the IAEA's Geographic Information Systems. Finland and IAEA have tested these guidelines in practice; in 2018 Finland provided DDSM from one NPP site to the IAEA as a test declaration.*

*DDSM benefits the regulatory work of STUK. They enable digital links between the maps and declaration entries. This will result in improved information exchange with the operators and improved data consistency reducing errors. DDSM are also an important part of the overall digitalization effort of Additional Protocol declarations alongside with Protocol Reporter 3 and State Declaration Portal.*

*The goal is that Finland declares maps from all major sites in DDSM format in 2020. This requires development of tools and practices in close cooperation with operators, the European Commission and the IAEA.*

*This paper describes the development work done and experience obtained in STUK. Future development needs and ideas will be presented.*

**Keywords:** Digital Declarations Site Maps, Digitalization, Additional Protocol, Safeguards Agreement, Integrated Safeguards, Safeguards declarations

## 1. Introduction

STUK, Radiation and Nuclear Safety Authority in Finland has established its strategy for 2018-2020. One of the strategic goals is to develop digitalization to enhance efficiency.

States with comprehensive safeguards agreements (CSA) and an additional protocols (AP) in force shall submit to the IAEA under Article 2.a.(iii) of the AP declaration, a general description of each building and a map for each site [1]. IAEA has introduced a concept of Digital Declaration Site Maps (DDSM) [2,3]. The development of DDSMs has been done under the auspices of Member State's support programmes. The Finnish Support Programme to the IAEA safeguards has participated in the development work in the past four years.

The current AP guidelines [1] do not specify a uniform format for the preparation of declarations and attached site maps and states submits maps to the IAEA in a variety of formats (including electronic and hardcopies), originating from different reporting and mapping software, as well as different standards used in states [3]. Paper copies are scanned, digitized and stored into the IAEA GIS systems, before they can be utilized. This part of the work is labour intensive. These work stages add another possibility for inaccuracies and errors. On the other hand site operators create their maps using digital tools. Conversion of these maps to hard copies or PDF printouts will remove all geographic metadata, which must be created again in the IAEA headquarters. DDSM will maintain this data from the operator to the IAEA, which greatly enhances the correctness and effectiveness.

### **Development and status of the DDSM process in Finland.**

The development of a DDSM process in Finland has taken place under Finnish Support Programme Task D 1996 "Digital Declaration Site Maps (DDSM)"[4]. The task started in 2015 and Finland agreed to provide DDSMs from one Finnish pilot site, Loviisa NPP. The first maps were submitted to the IAEA in January 2016. Based on the experiences collected in 2016-2018 the IAEA developed reporting guidelines and a framework for DDSMs. These guidelines were finalised in fall 2018. In 2019 Loviisa NPP operator Fortum prepared a DDMS package, which will be a part of the official declaration submission from Finland.

The official declaration also has traditional maps in PDF format. However, the principle is that the map in PDF format shall be a direct printout from GIS software handling the DDSM data. Therefore, the PDF map cannot contradict the DDSM. Finland is an EU member state and the declarations are submitted via the European Commission to the IAEA. Currently EC has no capabilities to utilize DDSMs. Therefore PDF printouts are needed for EC.

STUK has prepared a tool to view the site declaration information from the PR3-database (Protocol Reporter 3) together with the digital maps of the site in GIS software. ESRI ArcMap™, open source QGIS and other GIS software can be used to review the DDSM. The preferred file formats for the site map data are shapefiles or ESRI geodatabases.

The PR3 data contains detailed information of the site declaration and general description for the buildings on the site. The data is exported from PR3 in XML-format. We have created a Python tool to convert the XML-data to CSV format file. When the data is in CSV format it can be uploaded to the GIS software. A join is then created between the PR3 data file and the shapefile containing building information using the BuildingID field. Then the information from the site declaration and the maps can be easily reviewed by the inspector.

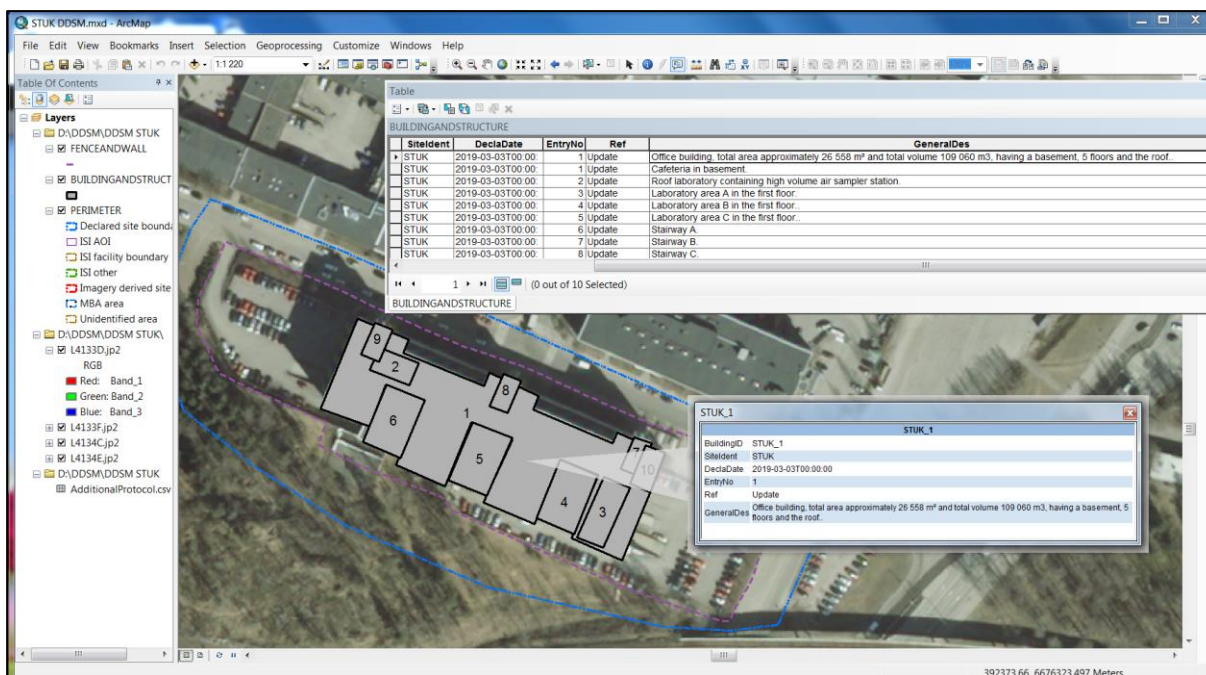


Figure 1. A layout of an imaginary declaration site in STUK premises.

## DDSM benefits in regulatory work.

For the IAEA the benefits of DDSM are paramount. The IAEA is able to automatically ingest DDSM data into the Geospatial Exploitation System (GES) and to seamlessly integrate and exploit DDSM data with the IAEA's other safeguards-relevant datasets [4].

DDSM can also bring in benefits for the work of STUK and the Finnish SSAC.

- In accordance with comprehensive safeguards agreement one of the primary SSAC duties is to facilitate IAEA safeguards. Implementation of DDSMs in a State clearly is a step in this direction.
- STUK is moving rapidly towards a paperless office and our way of work is changing. STUK will move into new premises in 2022, which encourages us to minimise the use of paper and exploit digital tools as much as possible.
- With the developed DDSM tool we can directly link the buildings on the DDSM with their respective entries in IAEA AP declaration software Protocol Reporter 3 (PR3). This will improve the quality of inspection work and diminish the risk of human errors.
- Traceability of changes and updates is enhanced, when DDSMs are used. Changes can be displayed automatically when reviewing the site declaration provided by the operator. New kinds of visual aids can be developed in a digital environment.
- STUK will inspect declarations provided by the operator on the site. A DDSM package can be stored on the laptop and used on the site inspection. All linking tools are available and consistency of the declaration can be checked on site. Amendments can be directly made into digital form.

## Future Steps

Finland has another major nuclear site in Olkiluoto with 3 NPP reactors and geological repository of spent nuclear fuel. We will discover possibilities to extend DDSMs to Olkiluoto for 2020 declarations, provided in early 2021. Guidelines prepared by the IAEA provide a good basis for a new site to start using DDSM for site declarations. Fennovoima, a new nuclear operator in construction licence phase will start using DDSM from the beginning. The first declaration will be submitted when the construction licence is obtained. This is expected to take place in 2021 at the earliest.

In STUK currently all the phases of loading the data to the GIS software are done manually. We are planning to automate the steps in the future to make using the tool easier. It can be rather difficult to use the tool if you are not a GIS expert or you don't use the software regularly. We are also going to install the server based ArcGIS Enterprise which will improve capabilities of customizing the user interface without the need of a desktop software installation. Maybe in the future also mobile devices can be used during site inspections.

One of the main obstacles of more widespread use of DDSMs is that SSACs do not have the necessary expertise and tools to review the contents of DDSM packages. Nuclear operators usually have GIS specialists who maintain the maps, so generation of DDSM is not a problem for them. STUK is open to share its experiences with other regulators, but provision of a necessary toolbox and support would be a bigger task and subject to separate discussion. Our view is that the IAEA should take a central role for developing necessary capabilities in member states. However, STUK is willing to provide necessary support to the EC so they can review the contents of Finnish DDSMs packages before submission. ESARDA provides a good network to spread the experiences.

## Conclusions

Digital Declaration Site Maps (DDSMs) have been taken in official use in Finland this year. Loviisa NPP provided a DDSM of its site, compatible with the framework document provided by the IAEA. This achievement is a result of 4 year of development work of the IAEA, Finnish Support Programme to the IAEA and Loviisa NPP.

DDSM is clearly a good practise. DDSMs provide benefits for the IAEA but also for STUK. Digitalisation is a strategic goal of STUK and DDSM is one step in that direction. STUK is open to share its experiences with a wider community.

## 8. References

- [1] INTERNATIONAL ATOMIC ENERGY AGENCY, Guidelines and Format for Preparation and Submission of Declarations Pursuant to Articles 2 and 3 of the Model Protocol Additional to Safeguards Agreements, Services Series 11, May 2004, Vienna.
- [2] Rutkowski J, Keskinen A, Balter E, Steinmaus K, Rialhe A, Idinger J, Nussbaum S; "Digital Declarations: The Provision of Site Maps Under INFCIRC/540 Article 2.a.(iii)", Symposium on International Safeguards: Linking Strategy, Implementation and People, 20-24 October 2014, Vienna.
- [3] Rutkowski J, Keskinen A, Idinger J, Niemeyer I, Rialhe A, Rezniczek A; "Digital Declaration Site Map Submissions for Additional Protocol Article 2.a.(iii)", JRC Conference and Workshop Reports, ESARDA 39th Annual Meeting, 2017 Symposium, 16-18 May 2017, Düsseldorf, Germany, (2018).
- [4] Keskinen A, Idinger J, Honkamaa T, Martikka E, Ilander T, Ansaranta T, Nissinen T, Preparation of Additional Protocol (AP) Declarations Using Protocol Reporter 3 and Attached Digital Declaration Site Maps for an Article 2.A.(III) – Experiences from Finland; Symposium on International Safeguards: Building Future Safeguards Capabilities, 5-8 November 2018, Vienna.

# Trusting Embedded Hardware and Software in Treaty Verification Systems

Jay Brotz

Sandia National Laboratories  
PO Box 5800  
Albuquerque, NM, USA 87112  
E-mail: jay.brotz@sandia.gov

## **Abstract:**

*Treaty verification equipment in bilateral or multilateral disarmament verification treaties has unique and challenging requirements for trust. With more intrusive verification concepts utilizing a wider variety of measurements and chain of custody technologies, more complex and custom equipment will be needed. Each treaty partner must have confidence that the verification equipment is behaving as expected and the host nation, in particular, must have confidence that sensitive nuclear information is not released to the inspectors. Many tools have been and continue to be created to support such verification concepts, and the process of trusting those tools, referred to as certification and authentication, have emerged as a primary challenge. We present a conceptual framework for trusting the electronics and software that control such equipment. This paper discusses a framework for trusting these programmable logic elements by a series of inspections to gain trust throughout the development cycle.*

**Keywords:** treaty; certification; authentication; verification

## **1. Introduction**

Trust is a key requirement in any treaty verification activity. Verification activities have several key components: an agreement between parties, a series of measurements, analysis of the results of those measurements, and a judgement<sup>1</sup>. The agreement, to maintain, reduce, or otherwise restrict key assets, such as nuclear weapons, drives the verification measurements, which include the procedures and the equipment to be used. Measurements, in this usage, are any on-site data collection, which can mean anything from sophisticated and time-consuming radiation spectrum collection to an inspector viewing an object. The analysis of those measurements, leading to the judgement of the agreement, is only useful to each party if the measurements themselves are trusted. While trust is often framed as a personal willingness to accept another party's declarations, far more important is the trust that each party has in the measurements that are intended to verify their agreement<sup>2</sup>.

In bilateral or multilateral nuclear disarmament agreements, trust in the equipment and procedures of verification measurements takes on a few dimensions that pose similarities and differences to those measurements taken for physical security or international nuclear safeguards. All three domains have a similar need for trust in equipment and personnel to provide correct data and for a verification system to provide complete data. In addition, all three domains have needs for protecting sensitive information. Disarmament treaties, however, have two (or more) parties that have different needs, unlike physical security, in which one party is protecting assets and information from a broad array of adversaries, and international nuclear safeguards, in which a central authority representing a highly multilateral treaty confirms declarations of each of its member states. In a bilateral nuclear weapons limitation treaty, the limitations have historically been (and in many cases will be in the future) reciprocal, so that each party is both limiting their own stockpile and verifying that the other party has done the same. This creates the need for on-site inspections for each party in the other's territory, during which each party plays the role of host and monitor. The host is concerned primarily with convincing the monitor of their compliance with the agreement and in protecting sensitive information

that is not part of the agreement. The monitor is concerned primarily with receiving sufficient evidence – collected data that can be effectively analysed – to make a compliance judgement. In a multilateral treaty, there is the potential for a party to be monitor without the reciprocal role of being host; however, in this case the concern of the monitor is the same as in the reciprocal situation – to gather sufficient evidence to make a compliance determination.

New verification concepts will require greater functionality in verification systems in the future, leading to greater complexity<sup>3</sup>. This complexity, enabled by general advances in private industry, is often embodied in the hardware and software of programmable logic elements. Sensors remain important, but software can extend the functionality of a sensor or a group of sensors beyond what has been produced in the past, and often at a lower cost than sensor improvements. A key question is how the host and monitor can trust more functional and complex verification equipment in which the complexity is allocated to programmable logic elements, such as software or firmware running on a processor<sup>4</sup>, or a programmed logic device, such as a field programmable gate array (FPGA)<sup>5</sup>. Whereas trust may be gained on a simpler, less functional system by visual inspection (or other means to verify the physical construction of a piece of equipment, such as radiography), the verification of programmable elements cannot simply be visual. Trust in these elements must be proven in other ways.

## 2. Certification and authentication

The community of developers of treaty verification systems use the terms certification and authentication to describe how parties to an agreement gain trust in equipment<sup>6,7</sup>. Certification is the process by which the host gains confidence that the equipment used for treaty measurements is safe for use in their facilities and will not reveal sensitive information that is not part of the agreement. Authentication is the process by which the monitor gains confidence that the equipment used for treaty measurements is correct and complete. These processes may be similar but have different requirements. Certification involves multiple stakeholders in the host party that represent facility safety, physical security, and information security. The host is concerned about limiting the information given to the monitor to that which is necessary for compliance and no more. Authentication gives the monitor confidence that equipment is providing true, correct data, and has not been tampered to give a false impression of compliance.

The effort involved in certification and authentication processes are dependent on whether equipment is host-provided or monitor-provided. Other models are possible, such as the host providing some components and the monitor others and assembling the equipment in a joint fashion prior to use. Another model is the use of third-party or commercial-off-the-shelf (COTS) equipment, though even in this case, “host-provided” or “monitor-provided” should be defined as the last party to have sole control of the equipment. If the host procures COTS equipment and has it ready prior to an inspection by the monitor, it must be considered host-provided.

The effort by the monitor to assess *completeness* in measurements is a system-level task. The effort by the monitor to assess *correctness* and the effort by the host to protect sensitive information are equipment-level tasks. The host uses equipment certification to gain confidence that the equipment has no exploited vulnerabilities that could reveal sensitive information to the monitor. The monitor uses equipment authentication to gain confidence that the equipment is designed to give correct data and that it has not been modified to give incorrect data that would support a compliance determination. In each case, the activities can be summarized as ensuring that the equipment exhibits the agreed functionality and has no additional functionality.

## 3. A framework for trust in new hardware and software development

While there are cost benefits to using COTS measurement equipment, treaties may have such unique sets of requirements that no COTS equipment is suitable, and therefore new equipment must be designed and built. This section describes a framework for certifying and authenticating custom treaty equipment from the requirements through to system operation, moving through the development cycle stage by stage to ensure the major objectives of confirming that the system exhibits the agreed functionality and that it has no additional functionality.

This agreed functionality can be captured as well-defined requirements that specify the allowed functions. If these functional requirements are specific and complete, any function in a system or system design that is not described in the requirements is disallowed by the agreement. Therefore, the requirements become the functional reference that is used to trust the system design, and then the built system. The requirements serve as the functional reference for trusting the rest of the development flow, as seen in Figure 1.

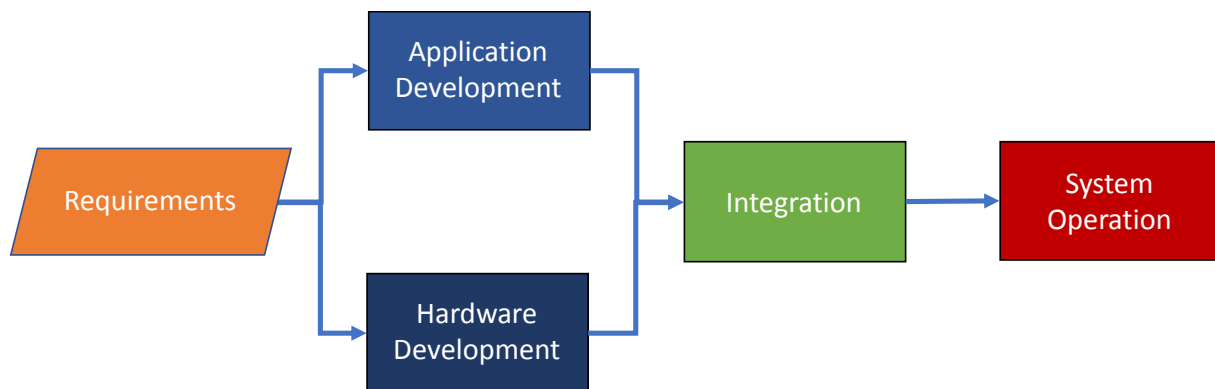


**Figure 1:** A generic system development flow

Once the requirements are developed and agreed to by all parties to the treaty, they can be used to authenticate or certify the system design, regardless of the party that creates the design. As seen in Figure 1, design can be divided into hardware design and application design (the outputs of the hardware development and application development processes, respectively)<sup>8</sup>. These design outputs can be verified by physical inspection (by visual means including radiography, thermal imaging, etc.) or digital inspection.

In each step of the development cycle, the output of the design or build process is compared to a reference to confirm the inspection objectives. That reference is the trusted output of the previous process. For example, within the Hardware Development stage in Figure 1 could be the creation of an electronic circuit on a printed circuit board (PCB). The stages of developing that PCB could include the definition of the circuit that results in a graphical schematic, the synthesis of that schematic into a netlist, and the layout of that netlist in the physical space of the PCB, as indicated in Figure 2.

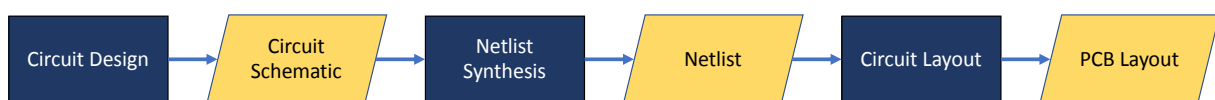


**Figure 2:** An example development flow for a printed circuit board

In Figure 2, the rectangles are development processes and the rhombuses are development outputs. During each inspection, a process output is compared to a reference that is the previous trusted process output in order to confirm that it still exhibits all agreed functionality with no additional functionality. As an example, the circuit schematic output of the circuit design process is compared against the requirements for this hardware component. When the circuit schematic is found to have the required functionality with no additional functionality, it becomes a trusted reference for the next inspection, in which the synthesized netlist is inspected, as shown in Figure 3.

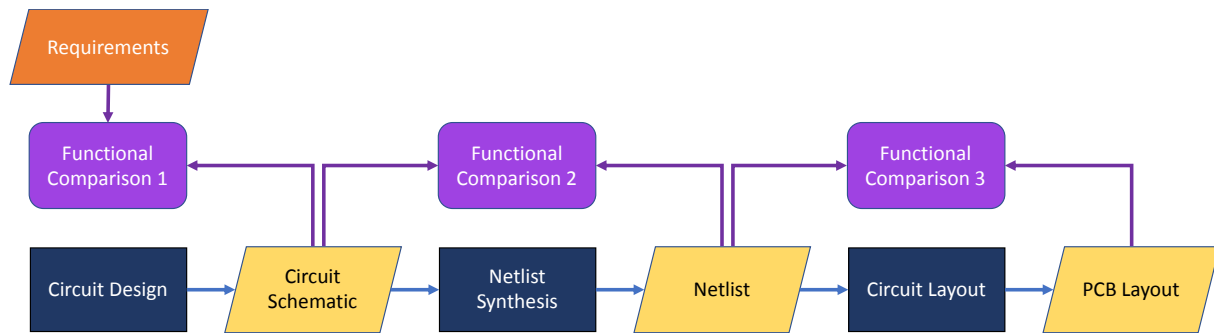


**Figure 3:** Functional comparisons of outputs in the example development flow of a printed circuit board

Most of these inspections against a reference work in one of two ways: reference comparisons can be exact or functional. In an exact comparison, the known output is already trusted, and the specific output is compared against it. For example, compiled software that resides on a piece of equipment can be compared to a golden copy of that compiled software (either in its entirety or by using a hash) and if any bit is not the same, it will fail. A functional comparison, on the other hand, can be used when a known, trusted output does not exist yet, or that output can vary in form depending on the specifics of the process used to create it (for example, compiled software varying by the compiler used and the compiler's settings). In a functional comparison, the output is analysed for its functionality and then compared to the reference list of functions (potentially going backward in the development flow all the way to the requirements). For example, in Figure 2, the output netlist can be functionally compared (with the right tools) to the circuit schematic, or to the requirements themselves, to understand whether it exhibits the agreed functionality and has no additional functionality. That netlist then becomes a trusted output.

The entire system development flow for a particular equipment design can be constructed as a flowchart that begins with requirements agreed to by the treaty partners and ends in system operation. It would be like the flowchart in Figure 1 with each process stage expanded to the level of detail in Figure 2. This flowchart will be a directional graph with no loops; that is, despite the number of parallel processes that occur, every process will have inputs that are closer to the requirements and outputs that are closer to the final system operation than the process itself. As such, every system development flow can be trusted by functional or exact reference comparisons starting from requirements and moving, process by process (and output by output) toward the system operation. A logical way to utilize these inspections is to use functional comparisons throughout the development process to authenticate or certify a system as it is being designed and built. A system could be designed and built entirely by one partner and presented as a complete system, which could then be authenticated or certified by functional comparison of the built system with the requirements, though the inspections involved may be more difficult to perform and have greater uncertainties in that case. Once a functional comparison has resulted in a trusted output, that output can then be used as a reference for exact comparisons. An example of this use is with compiled firmware: the firmware machine code could be compared to the trusted source code through a functional comparison, and when found to be in accordance with the agreed objectives, be used as a reference for an exact comparison of the loaded firmware the next time the system is used.

While exact comparisons can be designed to have very small uncertainties, functional comparisons are likely to leave some room for doubt when yielding a positive ("matching" the trusted reference) result, and functional comparisons will require different tools and procedures for different development flow processes. In many cases, the functional comparison tools are themselves an area of research or non-existent and must be created or adapted from other tools for a specific equipment authentication or certification. There are classes of functional comparison tools that could be used in many situations for different pieces of equipment. These include:

- Comparing software source code to requirements
- Comparing compiled software to source code
- Comparing FPGA hardware description code to requirements
- Comparing FPGA synthesized netlists to hardware description code
- Comparing FPGA bitfiles to synthesized netlists

- Comparing hardware circuit schematics to requirements
- Comparing hardware circuit designs (such as PCB layout) to schematics
- Comparing fabricated and populated PCBs to PCB layouts

#### 4. Evaluating functional comparison methods

Functional comparisons for certification and authentication inspections are a research need, and this research would benefit from a common evaluation method. Each of these inspections compares a development output to a trusted reference output from a previous process to verify that the functionality is the same, and that there is no additional functionality in the new output. Effectiveness of that comparison can be measured with the metrics of sensitivity (true positive rate) and specificity (true negative rate).

The sensitivity of the comparison method measures the proportion of positive results (or functional matches) that were correctly identified as such. The true positive test can be conducted with a number of different designs undergoing the same development process and applying the comparison method to the outputs of that process, as shown in Figure 4. Since the output should functionally match the reference, each positive result from the comparison method would contribute to the true positive rate.

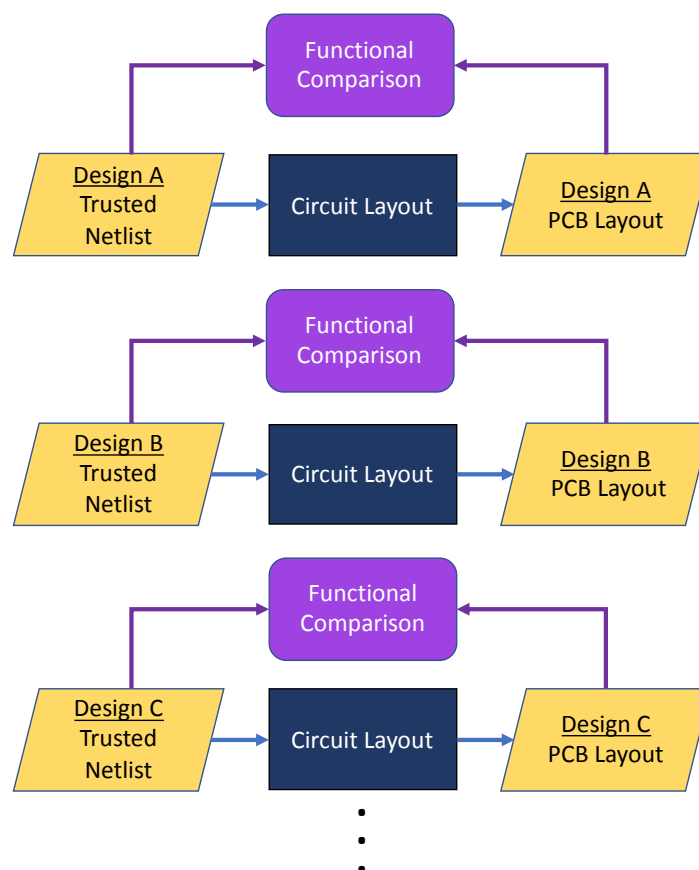


**Figure 4:** Sensitivity tests of a functional comparison method with three separate designs in the same development process

The specificity of the comparison method measures the proportion of the negative results (or cases with functional differences) that were correctly identified as such. The true negative rate test can be conducted with a set of modified inputs to a development process that create a functionally modified output and comparing that modified output to the trusted (unmodified) input, as shown in Figure 5. For example (seen in Figure 5), for a PCB layout process, a trusted netlist could be modified by adding or removing functions in the form of circuit branches and elements, and then used to create a layout with

an autoroute tool followed by manual finishing. A functional comparison method could be evaluated by comparing a range of various modifications in the circuit layout to the trusted netlist. Since the output is functionally different than the input in this comparison, each negative result would contribute to the true negative rate.

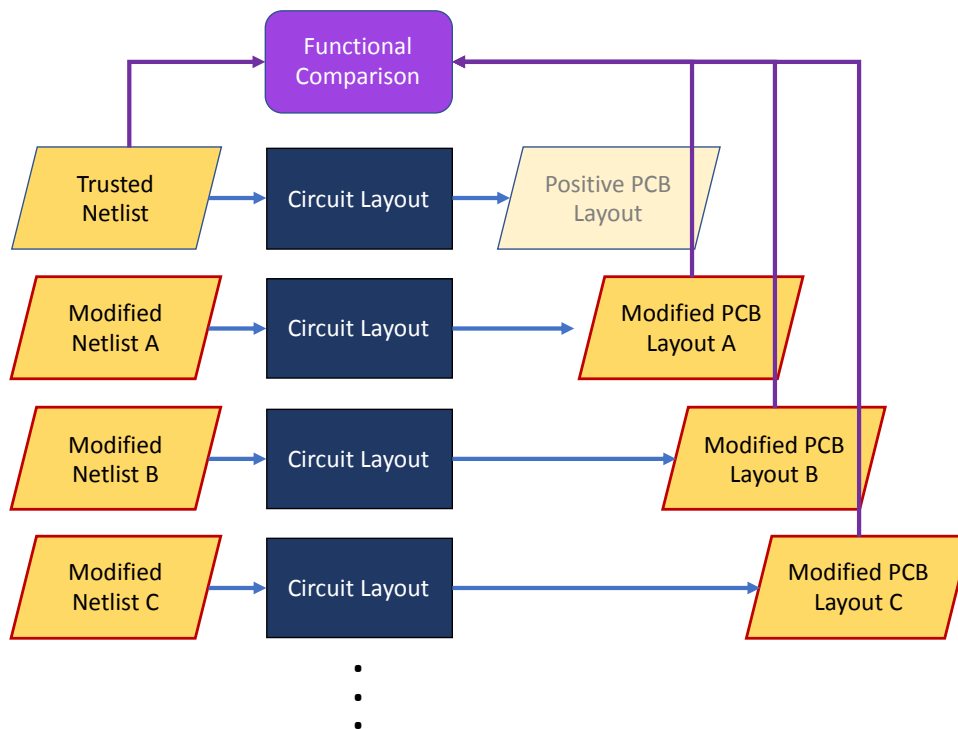


**Figure 5:** Specificity tests of a functional comparison method with three modifications of the same design compared to the trusted input

Maximizing the volume of data from these tests will improve the evaluation of a functional comparison method for sensitivity and specificity. In addition, the complexity of the designs and the nature of the modifications may have an impact on the ability of the functional comparison method to exhibit a high sensitivity and specificity.

## 5. Recommendations for a path forward

A broad array of inspection techniques could be useful for certification and authentication throughout the development cycle of custom treaty verification equipment. These techniques that perform functional comparisons, especially for design outputs for the programmable elements of a system, should continue to be developed. These inspection techniques should be developed in parallel to the development of the treaty verification tools themselves, to produce custom treaty verification equipment that is more inspectable and, in the eventual case of use in a treaty or agreement, more trustable by all parties.

The development of the verification tools and the inspection techniques are neatly separable into activities that can be performed by two different organizations in collaboration, where one organization conducts “blind” tests of the other’s development outputs. This can serve as a model for international collaboration on nuclear verification in a number of fora.

Finally, tools for functional comparisons in related industries, such as integrated circuit verification used for error prevention by chip manufacturers, or software verification tools used for high consequence software applications, should be analysed for their utility in this framework.

## 6. References

- [1] Avenhaus, R., Kyriakopoulos, N., Richard, M., and Stein, G., (Eds.); *Verifying Treaty Compliance: Limiting Weapons of Mass Destruction and Monitoring Kyoto Protocol Provisions*; Springer-Verlag; Berlin and Heidelberg, Germany; 2006.
- [2] Wuest, C. R.; *The Challenge for Arms Control Verification in the Post-New START World*; Lawrence Livermore National Laboratory, Livermore, CA; 2012.
- [3] Woolf, A.; *Monitoring and Verification in Arms Control*; Congressional Research Service; 2011.
- [4] Kütt, M., Götsche, M., and Glaser, A.; *Disarmament Hacking 2.0: Toward a Trusted, Open-Hardware Computing Platform for Nuclear Warhead Verification*; Proceedings of the Institute for Nuclear Materials Management Annual Meeting, 2016.
- [5] Brotz, J., et. al.; *FPGA Authentication Methods: US-UK Collaboration for Treaty Verification*; Sandia National Laboratories and AWE; Albuquerque, NM, USA and Reading, UK; 2017.
- [6] MacArthur, D., Hauck, D., and Thron, J.; *Simultaneous Authentication and Certification of Arms-Control Measurement Systems*; Proceedings of the Institute for Nuclear Materials Management Annual Meeting, 2012.
- [7] Tolk, K. and Benz, J.; *An Architectural Approach to Authentication and Certification of Arms Control Equipment*; Proceedings of the Institute for Nuclear Materials Management Annual Meeting, 2018.
- [8] Brotz, J. and Hymel, R.; *Framework for Evaluating Authentication Methods for Treaty-Related Processor Systems*; Proceedings of the Institute for Nuclear Materials Management Annual Meeting, 2016.

SAND2019-5077 C

*This paper describes objective technical results and analysis. Any subjective views or opinions that might be expressed in the paper do not necessarily represent the views of the U.S. Department of Energy or the United States Government. Sandia National Laboratories is a multimission laboratory managed and operated by National Technology & Engineering Solutions of Sandia, LLC, a wholly owned subsidiary of Honeywell International Inc., for the U.S. Department of Energy's National Nuclear Security Administration under contract DE-NA0003525.*

# ICPIA Modeling and Red Teaming

**Lon Dawson, Fredrick McCrory**

Sandia National Laboratories  
PO Box 5800 MS 0748  
Albuquerque, NM 87185-0748  
E-mail: [ladawso@sandia.gov](mailto:ladawso@sandia.gov), [fmmccro@sandia.gov](mailto:fmmccro@sandia.gov)

## ***Abstract:***

At the heart of international safeguards activities are agreements between many organizations supported by complex monitoring and verification activities. Such activities involve precise testing, monitoring, and evaluation of complex systems which generate data that must be proven free from compromise and protected. Sandia National Laboratories has developed the Integrated Cyber-Physical Impact Analysis (ICPIA) modeling framework to facilitate high-fidelity analysis for understanding the impact of a cyber attack on complex evolutions or systems such as nuclear treaty verification systems or critical infrastructure. The intention was to model the event with enough fidelity that decision makers could make security, operational, or other investment decisions based on the results. Such analysis is spread across multiple domains. For example, in nuclear treaty verification, testing relies on measuring system parameters that are indicative of treaty compliance; generates analytical data for analysis that is free from compromise and ensures it remains free of compromise as it is transmitted, stored and shared with stakeholders. It quickly became clear that organizing the problem into distinct modeling domains facilitated the complex analysis scope. The researchers separated the modeling into six distinct domains: threat analysis, cyber and/or physical event, component impacts, system behavior/response, consequence, and recovery. The threat portion of the ICPIA framework is conducive to using red teaming methods to help model the threat and the potential consequences that adversaries might want to achieve. This modeling framework has similarities to how many formal red teaming methodologies work such as Sandia's Information Design Assurance Red Teaming (IDART) [1]. In planning for a red team analysis, IDART members typically start their attack analysis with determining the set of consequences they desire, they identify adversary access points, and then determine the type of components within a system that need to be overcome to get the desired system response and consequences. This paper is going to introduce ICPIA, its uses, and how red teams can better inform the process.

**Keywords:** cyber-physical, ICPIA, IDART, Modeling and Simulation, SAND2019-4889 C

# 1. Introduction

## 1.1 The Opportunity

Nuclear safeguards monitoring is reliant on advanced information, communications and digital control technologies. These “system-of-systems” are complex and difficult to defend. Many domains are well-characterized with accurate computer modeling, but the integrated effects from an isolated event to the associated system-level impacts that potentially involve other systems represents an opportunity for deeper analysis and better management. Multiple national organizations are trying to understand exactly how the use of increasingly complex digital technologies might impact critical operations and data security. Much of the publicly available information available today describes cyber-attacks in a hypothetical way without identifying how the cyber vulnerability *propagates to system failure or impacts important system interactions*. Additionally, the consequences of a publicized cyber-attack are not typically founded in scientific analysis but rather in generalized events. Because the systems are extremely complex, it takes a richer analysis to not only understand the potential impact of exploited cyber vulnerabilities within their component or subsystem, but also how the exploited vulnerabilities may *propagate to physical or socioeconomic impacts*. For example, STUXNET [2] leveraged multiple digital vulnerabilities for it to persist in an isolated control system, propagate and ultimately impact its target. Additionally, the ability to model digital systems, at the appropriate fidelity, opens up the ability to do other high-end system engineering.

## 1.2 An organizing framework

The ICPIA framework [3] shown below was developed using internal Sandia National Laboratories (SNL) funding with an objective to develop and demonstrate the cross-mission ability to model complex events to our energy infrastructure and manage the resulting risks. The framework has been shown repeatedly to help organize the framing and solutions for such complex events (such as cyber-attacks) on critical evolutions or systems. The six domains are: 1) Threat modeling, 2) Event, 3) Component including network and control system emulation, simulation and analysis, 4) System including physical system modeling and simulation, 5) Consequences including impacted systems modeling and 6) system Recovery analysis.

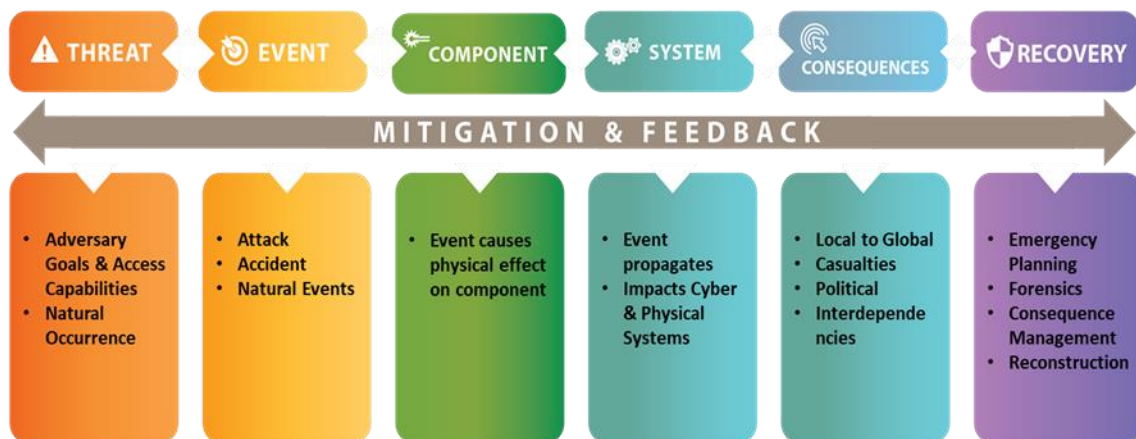


Figure 1: ICPIA framework

## 1.3 An example scenario

The framework was vetted by analysing potentially significant impacts to national critical infrastructures from cyber events. For example, Sandia partnered with a photovoltaic (PV) manufacturing company to help identify and eliminate potential security concerns with their infrastructure for system maintenance and upgrades. This work was informed by the consequences the vendor was trying to avoid. The same capability that helps the manufacturer monitor and update their products was shown to be vulnerable to certain classes of attack, allowing a potential adversary the ability to subvert their system and impact the correct operations of their energy systems. This

example while not specific to nuclear safeguards processes shows the important intersection between digital communications and real-world physical equipment.

To understand the physical consequences of a successful attack the Sandia team referenced previous studies to deliver the impact on electric grid stability as a function of renewable penetration. This information fed an additional economic analysis of disruption due to degraded inverter performance with a focus on the loss of power due to system failures and the resulting short-and long-term impacts on investor confidence in renewables. The economic analysis concluded wide-scale disruption of inverters leading to system outages will cause economic losses and reduce investor confidence. In a similar sense, nuclear safeguards relationships are based on trust so even a rumor of corruption in verification data could have rippling impacts to the related organizations.

The results of this distribution scenario included enabling conditions and assumptions, such as the attacker technical expertise, resources and knowledge of relevant systems and networks. Such information allows threat analysis to determine the feasibility of such an attack as well as developing mitigations that could be put in place to improve the resilience of the simulated system. The project also developed roadmaps to further enhance the analysis capability which ultimately will help manage national security.

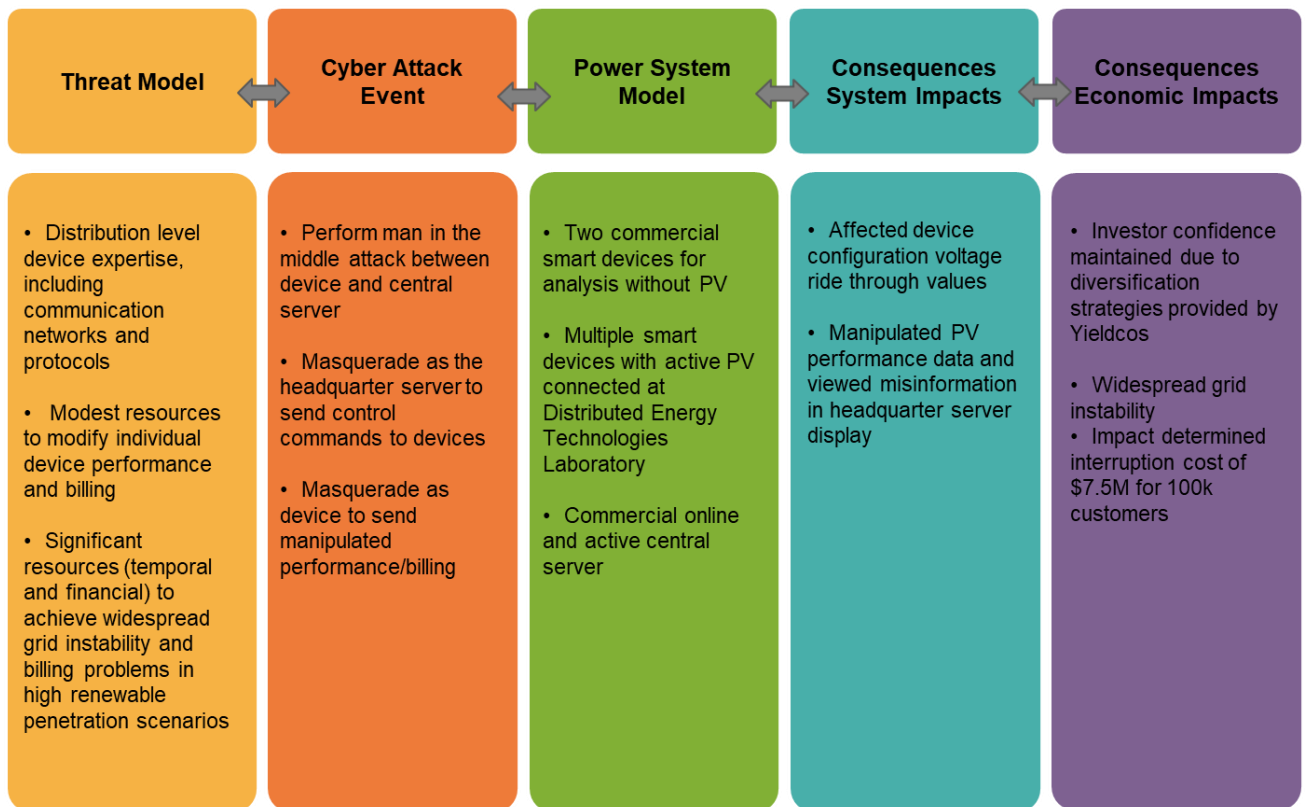


Figure 2: Hypothetical Distribution Cyber Attack Scenario – Mapped to ICPIA Framework

## 2. Information Design Assurance Red Teaming (IDART™)

Red teaming has strong ties to both network vulnerability assessment and penetration testing. Many different groups perform red teaming and use differing terminology, techniques, and processes: commercial security firms, various military units and government agencies, and National Labs. Sandia National Laboratories' IDART™ defines red teaming to be "authorized, adversary-based assessment for defensive purposes." [1]

Red team assessments can be performed throughout the system lifecycle, but often have the highest impact during the design and development phase where cooperative red team assessments cost less, and potential critical vulnerabilities can be uncovered and mitigated more easily. The IDART

assessment methodology (Figure 3) is a flexible tool that program managers and sponsors use to identify critical vulnerabilities, understand threat, deliver effective and secure components, systems, and plans, and consider alternative strategies and courses of action.

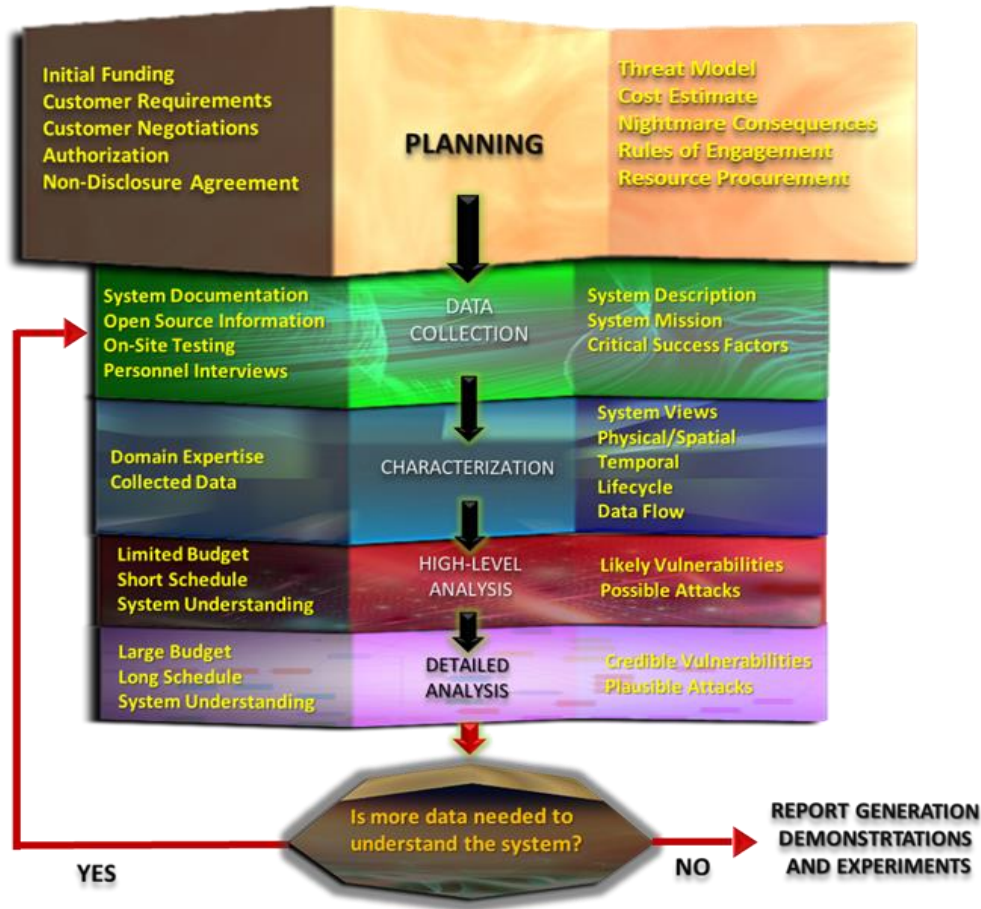


Figure 3: IDART™ Methodology

IDART utilizes a multi-disciplinary assessment team to improve the security of critical systems through systematic analysis from an adversary perspective. By using a wide range of security expertise in a variety of operational contexts it can be integrated into IDART types of assessments to assist in the characterization and analysis of target systems.

These focused assessments are performed in partnership with system stakeholders and include such tasks as:

- Identify nightmare consequences,
- Characterize target systems,
- Identify potential vulnerabilities whose exploitation will result in nightmare consequences, and
- Provide prioritized mitigation strategies so owners can make informed choices.

This approach supports having the red team work cooperatively with system developers, owners, and operators through the entire process to allow for a more in-depth understanding of the system and to save time and resources. This approach allows the red team to find as many attack paths as possible and to prioritize attacks on difficulty and consequences.

Understanding the capabilities adversaries possess is necessary for building systems capable of withstanding cyber or kinetic attacks. Formal red teaming methodologies utilize adversary models that include a spectrum of outsider and insider threats characterized by both measurable capabilities, such as knowledge, access, and resources, as well as intangibles such as risk tolerance and motivation.

These models are used to screen attack possibilities and assist in threat-based prioritization of protection strategies. The principal advantage of these models is an adversary perspective that yields a view of information systems different from that of defenders and yields critical insights into the system’s security.

### 3. IDART informing ICPIA

A fully developed ICPIA framework and the associated modeling and simulation capabilities can be informed with IDART and support the following use cases:

Use Case	IDART Deliverables	ICPIA Modeling and Simulation
New Threat Analysis	New Threat models / capabilities Possible Vulnerabilities Evolving Attack Methods Nightmare consequences	Network Emulation – penetration evaluation, network response, cyber/physical interactions, system impacts, extended consequences
System Integration Testing	System Documentation System Mission Plausible Attacks Nightmare consequences Known Vulnerabilities	Evaluate protective measures (detection, deter, respond)
Designing secure architectures	New system design features Evolving operational requirements	Evaluate protective measures – e.g. an Intrusion Detection System (IDS) is added to the network emulation
Training	Threat Model Evolving operational requirements Possible attacks	Plant operators and network administrators are presented real life attack scenarios  Red Team attackers can evaluate attack effectiveness
Integrated Risk Management	Hazardous events including cyber and physical attacks, attack difficulty metrics	Impact and consequence analysis

**Table 1:** IDART informs ICPIA

ICPIA is a modelling framework that breaks a complex analysis into distinctive domains that helps decision makers both understand the areas that need to be modeled to get to a complete answer (dependent on the questions being asked) related to cyber and/or physical events and to help understand the complexities related to simple questions. Questions such as: how secure is my nuclear material monitoring system to a cyber-attack; what information could be altered, omitted, erased, or corrupted and what are the potential consequences? Red teaming methodologies such as IDART help to better model the threat to add realism to inform the other physical models.

Using a methodology such as ICPIA and IDART early in the design phase of a system (physical and safeguards monitoring) can provide a significantly more secure architecture that can potentially increase the trust and confidence in the system and the data it collects for monitoring functions. Additionally, the rigor of formal red teaming as well as using a modeling framework such as ICPIA give decision makers far more information to help them make trade-off decisions and justify those decisions to other stakeholders.

## **4. Acknowledgements**

Sandia National Laboratories is a multimission laboratory managed and operated by National Technology & Engineering Solutions of Sandia, LLC, a wholly owned subsidiary of Honeywell International Inc., for the U.S. Department of Energy's National Nuclear Security Administration under contract DE-NA0003525.

## **5. References**

- [1] Sandia National Laboratories, "Information Design Assurance Red Team," 21 March 2019. [Online]. Available: <http://idart.sandia.gov/>.
- [2] Symantec, "W32.Stuxnet Dossier Version 1.4 February 2011," 22 04 2019. [Online]. Available: [https://www.symantec.com/content/en/us/enterprise/media/security\\_response/whitepapers/w32\\_stuxnet\\_dossier.pdf](https://www.symantec.com/content/en/us/enterprise/media/security_response/whitepapers/w32_stuxnet_dossier.pdf).
- [3] Sandia National Laboratories, "Integrated Cyber/Physical Impact Analysis to secure US Critical Infrastructure," 9 Sep 2016. [Online]. Available: <https://www.osti.gov/servlets/purl/1378066>.
- [4] Eastern Interconnection Planning Collaborative, "Phase 2 Report," July 2, 2015.

# Defense Nuclear Nonproliferation Research and Development Initiatives in Data Science for Safeguards

**Christopher Ramos<sup>1</sup>, Chris A. Pickett<sup>2</sup>**

<sup>1</sup>National Nuclear Security Administration

<sup>2</sup>Oak Ridge National Laboratory

E-mail: [christopher.ramos@nnsa.doe.gov](mailto:christopher.ramos@nnsa.doe.gov); [chris.pickett@nnsa.doe.gov](mailto:chris.pickett@nnsa.doe.gov)

## **Abstract:**

*The Defense Nuclear Nonproliferation Research and Development (DNN R&D) program has made recent investments at three national laboratories to research the use of data science methods for improving the detection of diverted material, facility misuse, or any undeclared activity of concern. This multi-lab effort will utilize actual data obtained from an operating nuclear facility at the Oak Ridge National Laboratory (ORNL) for most functional evaluations. The projects will investigate the use of common and new data science methods; with the goal of developing safeguards-specific algorithms and methodologies that may require the utilization of new datasets, not currently used by domestic or international safeguards programs. Initial efforts will focus on developing methods that examine facility behavioural patterns, improve anomaly detection, rapidly handle and analyse large datasets, and examine existing datasets to determine if commonly collected safeguards data can be utilized more efficiently and effectively. This paper will discuss the data sources being utilized for these evaluations, plus provide basic details on the efforts of each lab to date.*

**Keywords:** Data Science; Safeguards, Data Analytics, Machine Learning

## **1. Introduction**

The primary objective of safeguards is to deter the spread of nuclear weapons by the early detection of the misuse of nuclear material or technology through the legal framework outlined in the Nuclear Nonproliferation Treaty (NPT). Safeguards methods are designed to verify the correctness and completeness of declarations made by states about the use of their nuclear materials and their fuel cycle activities. The US Department of Energy's National Nuclear Security Administration, Office Defense Nuclear Nonproliferation Research and Development (DNN R&D) will make investments in fundamental science that support next generation tools and technologies to support this vision of safeguards to ensure that safeguards techniques remain effective for detecting proliferant activity for both domestic and international needs. Nuclear safeguards is a data-rich field that is ideal for the application of modern data science techniques. The DNN R&D Safeguards Basic R&D portfolio has invested in three projects that are investigating new data science methods to determine the effectiveness and efficiency of these tools for detecting material diversion or facility misuse. Each project will be using datasets collected from both traditional and non-traditional sources. The datasets are being collected from a DNN R&D testbed facility, Multi Informatics for Nuclear Operations (MINOS) that includes materials processing, reactor operations and a domestic safeguards program at Oak Ridge National Laboratory (ORNL). The three projects are Data Analytics for Verifying Nuclear Facility Operations being worked on at ORNL, Disparate Data Integration for Improved Safeguards Verification at Los Alamos National Laboratory (LANL), and Anomaly Detection and Surety for Safeguards Data at Sandia National Laboratories (SNL). The projects will investigate the use of common and new data science methods; with the goal of developing safeguards-specific algorithms and methodologies that may require the utilization of new datasets, not currently used by either domestic or international safeguards programs. Initial efforts will focus on developing methods that examine facility behavioural patterns, improve anomaly detection, rapidly handle and analyse large datasets, and examine existing datasets to determine if commonly

collected safeguards data can be utilized more efficiently and effectively. This paper will discuss the data sources being utilized for these evaluations, plus provide basic details on the efforts of each lab to date.

## 2. Goals

The following section of this paper describes the goals of each of the laboratories participating in the DNN R&D Safeguards Elements' basic research and development into the application of data science to safeguards. The projects have been designed to be complementary efforts with each national laboratory investigating unique tools and data sets. The overarching goal is to provide the safeguards community with a set of innovative analytical tools that can determine efficiencies and provide a trusted data use and data sharing environment. Multidisciplinary teams at three national laboratories are working together to advance the suite of data analytic capabilities to support safeguards activities at declared facilities.

### 2.1. A hierarchical problem decomposition approach to safeguards questions

ORNL is developing a hierarchical problem decomposition approach that can be used to understand how well data analytic techniques can answer specific safeguards questions and can be used to objectively compare the performance of different data analytic techniques in answering those questions. ORNL will also deliver a mature set of data analytics algorithms that can be used to understand how important individual safeguards data streams are to answering safeguards questions and where additional data streams might be warranted to improve the conclusions drawn at a facility.

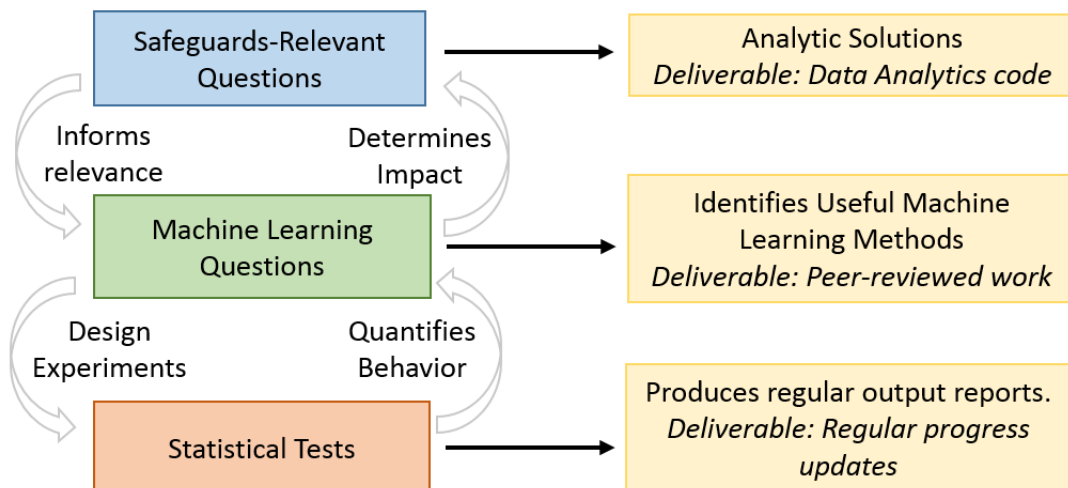


Figure 1. Hierarchical Problem Decomposition Enabling Test-Driven Development

A testing framework will drive development of data analytics models in two stages: (1) data triage and (2) methods to study the decisions made by analytic models. The testing framework will identify gaps in the team's analysis methods that should be addressed to answer safeguards questions. This framework will be created using a hierarchical problem decomposition approach that translates safeguards questions that a safeguards expert may develop for a facility or process within a facility into statistical tests that can be used to evaluate algorithm performance. This testing framework combined with capabilities of novel analytics currently under development at ORNL will allow the team to evaluate which data streams provided the most value for providing data input to help draw safeguards conclusions.

ORNL will use the relevance vector machine (RVM) with integrated feature selection and the multivariate quantile-quantile comparator (QQC) to apply this framework. The RVM is a general function estimation method that uses a sparse basis expansion constructed with Bayesian inference. This approach accounts for uncertainty in the input testing data, modelling error, test data error, and gives a rigorous statistical interpretation to the results. The RVM has demonstrated the ability to produce models that can make accurate predictions even with noisy data inputs, identify the most important variables for

distinguishing between data classes, and generate metrics for analysts to use when characterizing each data class. The QQC leverages the work of Chaudhuri and Dhar [1, 2], who generalized the notion of quantiles to multivariate data, to compare the unknown distributions that generate the known (library/training) and unknown (testing) data. ORNL will use QQC to optimize data libraries and class definitions used for classification and to improve performance. Conclusions drawn about the known data (e.g., insufficient data for a particular class leading to a lack of uniquely identifying information) can be used to prioritize future data collection. These conclusions may also indicate a new data stream is needed (thus a new measurement modality should be developed and deployed) or improvements in accuracy or precision of existing detection systems are needed. The key contribution of this work is providing a standardized, overarching methodology, in which new data analytics tools can be applied to safeguards questions.

## **2.2. Disparate data integration for improved safeguards verification**

LANL is investigating the use of data analytics for improving efficiency and effectiveness of safeguards verification. LANL is evaluating supervised machine learning methods for automatically integrating disparate data streams representative of safeguards information. This project will test and evaluate methods on real data generated at a dedicated testbed at the LANL Safeguards Training Facility (TA-66 testbed), a CAT III nuclear facility. The expected outcome of this work will be demonstrated data analytic methods that will be tested on data collected under the MINOS venture. It is expected that this work will provide decision support tools to increase both the productivity and the probability of detecting material diversion or misuse of a safeguarded facility.

This work is envisioned to support safeguards activities at nuclear facilities that typically exceed operations at TA-66 testbed in scale and complexity, the main advantage of this experimental setup is its flexibility and direct access that allows an iterative type of research. LANL can analyse, in detail, performance as well as directly compare failure modes of different data analytical approaches reflecting standard as well as atypical or artificially staged operations. LANL can reconfigure sensors settings or change their locations to test assumptions about usefulness of strategically placed sensors that require operator's approval and cooperation versus more restricted access type of information more typical for industrial settings with some degree of security protections. If an anomaly that defies standard classification criteria is detected, different detection and data analytics scenarios can be tested when recreating such an anomaly thus improving efficiency and confidence levels. At the later stages of the project, the validity of this approach, together with its confidence levels and predictive power will be tested on data streams from the MINOS venture that focuses on collecting signatures from an active and rather complex nuclear facility hosting a research reactor and hot cells with isotope producing activities.

The use of established methods in supervised and unsupervised machine learning applied to the data will aid in rapid development and attainment of technical progress goals. LANL will investigate the use of regularized regression (e.g., lasso or ridge regression [3]) and Bayesian nonparametric clustering [4] for automatically identifying and classifying the various operational modes at the facility. Once a baseline capability is established for predicting the state of operations with these methods, a combination of statistically-designed experiments and simulated data to validate models and evaluate the robustness of the approach to previously unobserved anomalies will be implemented. If successful, the team will work to identify a transition partner in the final year of the project for field evaluation at, for example, a research reactor or commercial nuclear facility.

The key contribution of this work will be integrating disparate data streams to provide decision support tools for the safeguards community. Combining multisource information to develop an automated method for characterizing activity patterns, producing alert reports or identifying anomalies and irregularities. This new approach to facility data analysis will increase both productivity as well the ability to detect undeclared materials and activities at safeguarded facilities.

## **2.3. Anomaly detection and surety for safeguards data**

SNL will engage in work that focuses on ensuring continuity of knowledge through data surety, anomaly detection, and timely diversion detection. SNL is studying Grammar Compression techniques, distributed ledger technology, and multiparty computation (garbled circuits). The current verification methodology uses authentication and encryption of the data to be transmitted and stored at a centralized location. The SNL team is evaluating a new safeguards data paradigm by developing and testing a novel safeguards data authentication, integration, and analysis workflow.

SNL is developing a practical method for effective and efficient detection of anomalies in multivariate time-series data obtained from fielded safeguards-like equipment. When rare events occur during a series of “normal” repetitive activities, these events manifest themselves as so-called *anomalies* (or outliers). These anomalies can be discovered through the analysis of recorded data such as that from monitoring equipment to uncover abnormal events. The key component of the approach is the cutting-edge method of unsupervised anomaly detection based on Grammar Compression (GC) [5-10]. The method: (1) scales linearly with data size, enabling fast analysis of large datasets and facilitating the discovery of possible issues immediately after they occur; (2) detects sub-dimensional (correlated) anomalies in multivariate data from heterogeneous sensors (video cameras, electronic seals, radiation detectors, etc.); (3) detects multiple anomalies at once, and ranks them; (4) includes additional capabilities for in-depth analysis of data subsets that contain suspected anomalies. The GC method of anomaly detection adapted to the analysis of safeguards-like data, will produce a powerful tool for automated discovery of potential abnormalities in fuel cycle activity, such as material diversion or facility misuse. The successful development of this method and associated data visualization will provide an array of new data analytic tools to support the Safeguards community.

The current safeguards data authentication regime relies on data authentication at the point of creation of the data, through the data transmission and arrival to a secure facility where authenticity can be verified. Current mechanisms using private keys have challenges of key management, and eventually the underlying algorithms could be broken. Public-private keys have been proposed to ameliorate this issue, but their use is computationally expensive. Modern provenance tracking technology in other domains have impressively addressed similar challenges (e.g., the 1.6 million diamonds whose metadata are on Everledger) [11] by strengthening authenticity, provenance, and custody across their entire and complicated supply chain. The SNL team is designing and prototyping a pilot safeguards data tracking system that will take advantage of recent advances in provenance tracking based on the distributed ledger technology (DLT) [12-15]. This work will result in rigorous and realistic lab bench demonstrations of new methods for tracking safeguards data provenance, technical solutions that are well postured for transition into field evaluations by users, and metrics that quantitatively compare the effectiveness of this pilot system versus the current system.

Privacy-preserving data sharing, such as multi-party computation (MPC), also known as “garbled circuits,” can significantly enhance data analytic assessments of civilian fuel cycle activities to provide better confidence that materials are not being diverted and facilities are not misused for weapon programs [16-18]. The key take-away and developments for this work from SNL will be developing and provisionally applying privacy-preserving MPC to allow sensitive-sharing of otherwise proprietary safeguards-relevant data, combined with an auditable DLT, to enhance data analytical methods for providing improved verification of fuel cycle activity. The data made available through MPC will complement traditional safeguards data, resulting in a much larger body of data to use in safeguards-focused data analytics.

### 3. Conclusions

In an effort to apply new data analytic tools to the safeguards problem set, the DNN R&D Safeguards portfolio has invested in the development of a paradigm for translating safeguards questions into testable metrics that will provide tools for verification. Within this paradigm techniques such as supervised learning, unsupervised learning, and data fusion are being explored for their utility in verification of declarations of nuclear activity. Techniques that include multiparty computation, grammar compression, and distributed ledger technology are being explored for their utility in detection of anomalies and data surety for the Safeguards community. Research teams from ORNL, LANL, and SNL are collaborating using data sets obtained at their own facilities and from MINOS. The results of this work will produce insight into the best practices for applying data science to a variety of questions in the safeguards problem set and provide analytic tools for investigating those questions further.

### 4. Acknowledgements

The authors would like to acknowledge the U.S. Department of Energy, National Nuclear Security Administration, Office of Defense Nuclear Nonproliferation Research and Development for funding these efforts.

Thank you to Scott L. Stewart, Ken Dayman, Mark Adams, Louise Worrall of ORNL; Vlad Henzl, Kendra Van Buren, Emily Casleton, Janette Frigo, Paul Mendoza, Karen Miller, Rosalyn Rael, Jonathan

Woodring of LANL; and Alexander Solodov, Tina Hernandez of SNL, and Jessica Lin of George Mason University for the program contributions described in this paper.

## 5 Legal matters

### 5.1. Privacy regulations and protection of personal data

I agree that ESARDA may print my name/contact data/photograph/article in the ESARDA Bulletin/Symposium proceedings or any other ESARDA publications and when necessary for any other purposes connected with ESARDA activities.

### 5.2. Copyright

The authors agree that submission of an article automatically authorises ESARDA to publish the work/article in whole or in part in all ESARDA publications – the bulletin, meeting proceedings, and on the website.

Once the article has been accepted for publication the copyright is reserved, but part of the publication may be reproduced, stored in a retrieval system, or transmitted in any form or by any means, mechanical, photocopy, recording, or otherwise, provided that the source is properly acknowledged.

The authors declare that their work/article is original and not a violation or infringement of any existing copyright.

### 5.3 Disclaimer

This paper was prepared as an account of work sponsored by an agency of the United States Government. Neither the United States Government nor any agency thereof, nor any of their employees, makes any warranty, express or limited, or assumes any legal liability or responsibility for the accuracy, completeness, or usefulness of any information, apparatus, product, or process disclosed, or represents that its use would not infringe privately owned rights. Reference herein to any specific commercial product, process, or service by trade name, trademark, manufacturer, or otherwise does not necessarily constitute or imply its endorsement, recommendation, or favoring by the United States Government or any agency thereof. The views and opinions of authors expressed herein do not necessarily state or reflect those of the United States Government or any agency thereof.

## 6. References

[1] Chaudhuri, P., "On a Geometric Notion of Quantiles for Multivariate Data," *Journal of the American Statistical Association*, 91: 434, pp. 862–872, 2013.

[2] Dhar, S.S., Chakraborty, B., Chaudhuri, P. "Comparison of multivariate distributions using quantile-quantile plots and related tests," *Bernoulli* 20: 3, pp. 1484–1506, 2014.

[3] G. James, et al., *An Introduction to Statistical Learning*, New York: Springer-Verlag, 2013.

[4] S.J. Gershman and D.M. Blei, "A Tutorial on Bayesian Nonparametric Models", <https://arxiv.org/pdf/1106.2697.pdf>, 2011.

[5] V. Chandola, A. Banerjee, and V. Kumar, "Anomaly detection: A survey", *ACM Computing Surveys*, 41 (3), 1–58 (2009). doi:10.1145/1541880.1541882.

[6] A. Zimek, E. Schubert, and H. P. Kriegel, "A survey on unsupervised outlier detection in high-dimensional numerical data", *Statistical Analysis and Data Mining*, 5 (5), 363–387 (2012). doi:10.1002/sam.11161.

[7] E. Schubert, A. Zimek, and H. P. Kriegel, "Local outlier detection reconsidered: a generalized view on locality with applications to spatial, video, and network outlier detection", *Data Mining and Knowledge Discovery*, 28 (1), 190–237 (2014). DOI:10.1007/s10618-012-0300-z.

- [8] M. Gupta, J. Gao, C. C. Aggarwal, and J. Han, "Outlier detection for temporal data: A survey", *IEEE Transactions on Knowledge and Data Engineering*, 26 (9), 2250–2267 (2014). doi:10.1109/TKDE.2013.184.
- [9] C. C. Aggarwal, "Outlier analysis", in *Data Mining*, pp. 237–263 (Springer, Berlin, 2015). DOI: 10.1007/978-3-319-14142-8\_8.
- [10] L. Akoglu, H. Tong, and D. Koutra, "Graph-based anomaly detection and description: a survey", *Data Mining and Knowledge Discovery*, 29 (3), 626–688 (2015). DOI:10.1007/s10618-014-0365-y.] G. James, et al., *An Introduction to Statistical Learning*, New York: Springer-Verlag, 2013.
- [11] N. Joshi, "Blockchain: Diamond Industry's New Hope" (2017), SysTweak. [Online]. Available: <https://blogs.systweak.com/blockchain-diamond-industrys-new-hope/>
- [12] "Blockchain: the solution for transparency in product supply chains" (2015). [Online]. Available: <https://www.provenance.org/whitepaper>.
- [13] J. Palfreyman, "Proving Provenance with Blockchain" (2016). [Online]. Available: <https://www.ibm.com/blogs/insights-on-business/government/proving-provenance-with-blockchain/>.
- [14] X. Liang, S. Shetty, D. Tosh, C. Kamhoua, K. Kwiat, and L. Njilla, "ProvChain: A Blockchain-Based Data Provenance Architecture in Cloud Environment with Enhanced Privacy and Availability," in 17th IEEE/ACM International Symposium on Cluster, Cloud and Grid Computing (CCGRID) (2017). doi:10.1109/CCGRID.2017.8.
- [15] D. Galvin, "IBM and Walmart: Blockchain for Food Safety" (2017). 3] G. James, et al., *An Introduction to Statistical Learning*, New York: Springer-Verlag, 2013.
- [16] A. C.-C. Yao, "Protocols for secure computations." In *FOCS*, Volume 82, pages 160–164, 1982.
- [17] A. C.-C. Yao, "How to generate and exchange secrets." *Foundations of Computer Science*, 1986, 27<sup>th</sup> Annual Symposium on, pages 162–167. IEEE, 1986.
- [18] V. T. Hoang, "The Foundations of Garbled Circuits". Ph.D. Thesis, University California, Davis, 2013.

# **Panel 5:**

# **Strategic Trade Control**

## Export control and nuclear safeguards

**Filippo Sevini, Guido Renda, Simone Cagno,  
Xavier Arnes Novau, Christos Charatsis, Willem Janssens**

European Commission Joint Research Centre  
Directorate Nuclear Safety and Safeguards  
Via Enrico Fermi, 2749  
21027 Ispra, Italy  
E-mail: [filippo.sevini@ec.europa.eu](mailto:filippo.sevini@ec.europa.eu)

### **Abstract:**

*The control of strategic trade has been set up along various decades as a barrier against the diffusion of sensitive materials, components and technologies, which could be used for the proliferation of nuclear, biological and chemical weapons of mass destruction and their means of delivery.*

*The result has been a continuously evolving multi-layered regime which comprises Treaties, International Agreements, UN Security Council Resolutions, embargo measures and national laws. In particular, nuclear export controls and international safeguards have developed in parallel in various phases triggered by major international events, which showed how the insufficient scope of the controls existing at that time, as well as how the legal framework's loopholes could be exploited to acquire sensitive goods. Although not implementing export controls, IAEA benefits from their existence and from the inclusion of Model Additional Protocol's requirements related to its Annexes I and II that could also provide indicators for IAEA's verification activities.*

*The paper reviews the background and key aspects of strategic export controls, developing on contents and relevance to countering the proliferation of weapons of mass destruction as well as the synergies with nuclear safeguards, describing challenges and open issues.*

**Keywords:** export control; nuclear safeguards; non-proliferation; dual-use; strategic trade

## **1. Strategic export control and nuclear safeguards**

Strategic export control is a barrier against proliferation called for by United Nations Security Council Resolution 1540 [1], aiming to limit the unauthorized access to strategic technology and goods.

Export control and nuclear safeguards developed in parallel, as two intimately linked elements of the non-proliferation framework. This link is evident in both the Non Proliferation Treaty [2] and the Nuclear Suppliers Group (NSG) Trigger List guidelines [4]:

- The Non Proliferation Treaty's Art. III.2. conditions the export of nuclear items to international safeguards
- Safeguards are a condition of supply for nuclear goods also clearly stated by the Nuclear Suppliers Group's Trigger List guidelines[4, Art. 4].

### **1.1 The Non-Proliferation Treaty (NPT)**

The close relationship between export control and nuclear Safeguards is clearly visible in the NPT Article III.2's requirement for safeguards as a principal condition of the supply of nuclear items:

*Each State Party to the Treaty undertakes not to provide: (a) source or special fissionable material, or (b) equipment or material especially designed or prepared for the processing, use or production of special fissionable material, to any non-nuclear-weapon State for peaceful purposes, unless the source or special fissionable material shall be subject to the safeguards required by this Article.*

The need to interpret the term “especially designed or prepared for” components led to the formation of the NPT Exporters’ (or Zangger) Committee, which could not come up with a definition but instead identified a list of key nuclear fuel cycle items. The resulting “Trigger List” (i.e. a list of equipment and facilities “triggering” the need for safeguards) and guidelines for the supply were communicated to Member States by the IAEA in INFCIRC/209 whose latest revision is reported in [6].

## 1.2 The Nuclear Suppliers Group (NSG)

In line with the NPT provisions, many steps were undertaken for the development of international nuclear safeguards, with the objective of “*preventing diversion of nuclear energy from peaceful uses to nuclear weapons or other nuclear explosive devices. [...] The safeguards [...] shall be applied on all source or special fissionable material in all peaceful nuclear activities within the territory of such State, under its jurisdiction, or carried out under its control anywhere.*” (NPT, art. III.1).

The effort led to the definition of a Comprehensive Safeguards Agreement (CSA – INFCIRC/153) defining how IAEA safeguards would be implemented in NPT States in compliance to the NPT Article III.1

The Indian “peaceful nuclear explosion”, in 1974 showed that, notwithstanding the entry into force of the Non Proliferation Treaty, various countries had anyway exported nuclear technology to India, a non-signatory to the Treaty.

To address this gap, the nuclear supplier states decided to form the “Nuclear Suppliers Group (NSG)” [3] which, like the Zangger Committee, also issued additional Guidelines in 1978, published as INFCIRC/254/Part 1 and including an extended Trigger List [4].

The NSG has been quite active since its establishment, growing its membership to the current 48 Participating Governments, plus the European Commission as Observer.

The results of its work are two distinct NSG guidelines, respectively the:

- “Guidelines for nuclear transfers” setting the conditions for transfers of nuclear items (i.a. nuclear safeguards and physical protection requirements) and containing two annexes, where Annex B contains the Trigger List (TL)
- “Guidelines for transfers of nuclear-related dual-use equipment, materials, software and related technology”, containing in annex the Dual-Use List (DUL) [5]

The creation of the second set of guidelines covering dual-use equipment was decided in 1992, after the discovery of the covert Iraqi nuclear programme, supported also by the illicit import of non-Trigger List goods and technology.

## 2. International Safeguards framework

The discovery of undeclared proliferation activities in Iraq in 1991 was also a turning point for what concerns the international safeguards framework.

After having implemented Comprehensive Safeguards Agreements (CSA) with a focus on the single nuclear facilities for decades, the discovery of the Iraqi military nuclear programme in the 1990s made the IAEA and its Member States to start a paradigm shift for the implementation of NPT safeguards,

from both a legal and practical point of view. From a legal point of view, the introduction in 1997 of the “Model Protocol Additional to the Agreement(s) between State(s) and the International Atomic Energy Agency for the Application of Safeguards” (AP - INFCIRC/540) [7] expanded the set of information the State transmits to the Agency under their reporting obligations and expanded the verification toolkit at the IAEA disposal to exclude the presence of possible undeclared nuclear and nuclear-related activities in a State.

## 2.1 Model Additional Protocol

The Additional Protocol’s Article 2.a. requires that States:

*..... shall provide the Agency with a declaration containing:  
(i) A general description of and information specifying the location of nuclear fuel cycle-related research and development activities not involving nuclear material...*

and

*...  
(iv) A description of the scale of operations for each location engaged in the activities specified in Annex I to this Protocol.*

Annex I lists fifteen key nuclear fuel cycle related activities:

- i. The manufacture of *centrifuge rotor tubes* or the assembly of *gas centrifuges*.
- ii. The manufacture of *diffusion barriers*.
- iii. The manufacture or assembly of *laser-based systems*.
- iv. The manufacture or assembly of electromagnetic isotope separators.
- v. The manufacture or assembly of *columns* or *extraction equipment*.
- vi. The manufacture of aerodynamic separation nozzles or vortex tubes.
- vii. The manufacture or assembly of uranium plasma generation systems.
- viii. The manufacture of *zirconium tubes*.
- ix. The manufacture or upgrading of *heavy water* or *deuterium*.
- x. The manufacture of nuclear grade graphite.
- xi. The manufacture of flasks for irradiated fuel.
- xii. The manufacture of *reactor control rods*.
- xiii. The manufacture of criticality safe tanks and vessels.
- xiv. The manufacture of irradiated fuel element chopping machines.
- xv. The construction of *hot cells*.

The AP also requires export declarations of “Trigger list” items (see above NSG) listed in its Annex II, related to nuclear activities listed in Annex I.

Art. 2.a.(ix) of the AP requires that States:

*...shall provide the Agency with a declaration containing the following information regarding specified equipment and non-nuclear material listed in Annex II:*

*For each export: the identity, quantity, location of intended use in the receiving State and date ... of export;*

*Upon specific request, confirmation as importing State of information provided by another State concerning the export of such equipment and material*

Annex II lists the items contained in the NSG Trigger List (INFCIRC 254/Part 1) available in 1995 (Rev. 2). Unfortunately, the AP Annex II’ list has not been amended thereafter with respect to the

NSG's TL, amended already several times (the current version being Rev. 13 of 2016). This fact creates discrepancies to exporters and authorities which is addressed in various practical ways as outlined in [8,9].

Annex B item	Title	Since	Year
1.8	Nuclear reactor internals	Rev. 3	1997
1.9	Heat exchangers	Rev. 3	1997
1.1	Neutron detectors	Rev. 3	1997
1.11	External thermal shields	Rev. 12	2013
3.5	Neutron measurement systems for process control	Rev. 12	2013
5.2.1.c	Solidification or liquefaction stations	Rev. 12	2013
5.2.3	Special shut-off and control valves	Rev. 9	2007
6.8	Complete heavy water upgrade systems or columns therefor	Rev. 3	1997
6.9	NH <sub>3</sub> synthesis converters or synthesis units	Rev. 12	2013
7.1.9	Especially designed or prepared systems for the conversion of UO <sub>2</sub> to UCl <sub>4</sub>	Rev. 4	2000

**Table 1: Items part of the NSG Trigger List (as of Revision 13 of 2016), which are not listed in Annex II of the Additional Protocol, with their year of appearance in the Trigger List**

The States or other organizations depending on the countries' attribution of competences (e.g. EURATOM for some European Union Member States), are responsible for retrieving AP-related information and provide it to the IAEA along with the CSA-related and other required declarations. The experience of some ESARDA members with the export control provisions of the AP is summarised in [10].

## 2.2 State Level [safeguards] Approaches\

From a practical point of view, building on both CSAs and the AP, the current IAEA nuclear safeguards framework (the so-called State Level Concept –SLC) foresees the application of “State Level [safeguards] Approaches” (SLA), uniquely tailored to each State, with the objective to detect any NPT non-compliance, spanning from detection of diversion of declared nuclear material to the detection of undeclared nuclear activities on undeclared sites.

For the design and conception of a SLA (Figure 1), the IAEA evaluates all the possible routes to achieve weapons-useable material in a given State through the application of Acquisition Paths Analysis. In order to assess the plausibility of each proliferation path, the Agency evaluates its potential time to completion, which in turn depends, *inter alia*, on the State's technical and industrial capability.

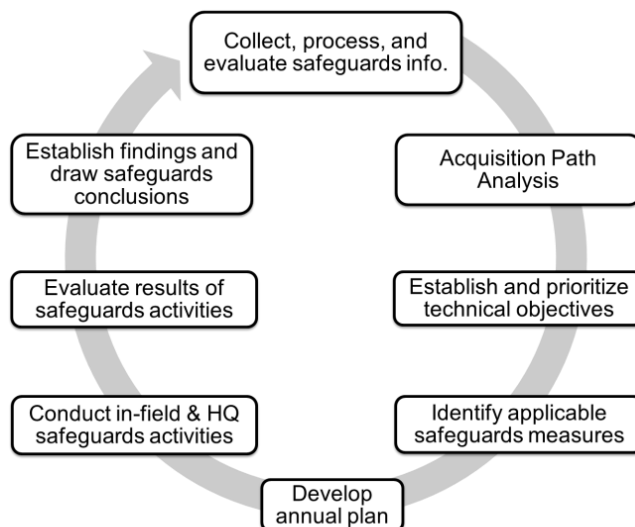


Figure 1 - Flow chart of processes supporting State-level safeguards implementation, adapted from [11].

### 2.3 SLA Acquisition Path Analysis

An acquisition path (AP) is defined as a sequence of activities which a State could consider in order to acquire a Significant Quantity of weapons usable material. APA is a key element of the SLC. By considering the State's nuclear profile, the APA generates a list of acquisition paths ranked by their attractiveness for the State. The acquisition path analysis (APA) analyses all conceivable APs, retaining only those that could be completed within a short period), aiming to optimise the design of sets of safeguards measures focusing on the critical (more plausible) paths, while maintaining the desired efficiency and effectiveness standards. Currently, this process is mainly based on expert judgment. However, comprehensive guidance is/is becoming available, since the IAEA's requirements state that APA must be objective, reproducible, transparent, standardized, documented and as a result non-discriminatory [12].

Within the APA, the information and insights coming from the export control regime and the trade analysis of dual-use and non-dual-use goods and equipment has the potential to play a very important role in understanding the technical and industrial capability of a State and the direction in which it is evolving. Together with all the other information and analyses performed by the IAEA, these insights enable a more effective acquisition pathway analysis and therefore a more efficient design of the SLA.

A central tool at the IAEA's disposal to support the identification and the characterization of APs in a State's nuclear fuel cycle is the Physical Model [13]. The Physical Model is a full description of the nuclear fuel cycle, internal to the IAEA's Department of Safeguards, subdivided into several volumes. It contains indicators (materials, equipment, technology, observables) of nuclear activities with different degrees of strength. Such indicators are linked to with explicit references in the text to controlled items and respective codes.

Whereas the detection of exports of Trigger List's items would clearly point at an illicit development of nuclear activities, the export of dual-use items is more difficult to put in relation to undeclared activities. Nevertheless dual-use items derived from the nuclear suppliers group's guidelines are part of, and referenced in the IAEA's Physical Model. Tracing transactions based on customs commodities is one of the detection activities performed by IAEA as part of their verification process and dedicated tools were/are developed by JRC to facilitate this [14].

### 3. Strategic Trade Control Sources of Information

The IAEA does not implement export controls, but benefits from their existence.

Besides the data formally due by States and collected during regular inspection activities, the IAEA makes wide use of various sources of information to detect potential indicators of undeclared nuclear material and activities, and for States with an AP in force, be able to derive broader conclusions on the absence of undeclared nuclear material and activities.

Apart from regular open-source information, these include trade data analysis, based on customs data, together with the analyses of actual and attempted covert procurement for nuclear-related goods (both single and dual-use) – information which is received from States and their companies on a voluntary basis [15]. Cross-matching the declarations with data sources used in verification may provide red flags that require further assessment.

The strategic export control framework not only provides an important barrier to proliferation, it also helps generating data instrumental to the verification process. The following paragraphs describe some of the potential sources of information within the strategic export control's framework.

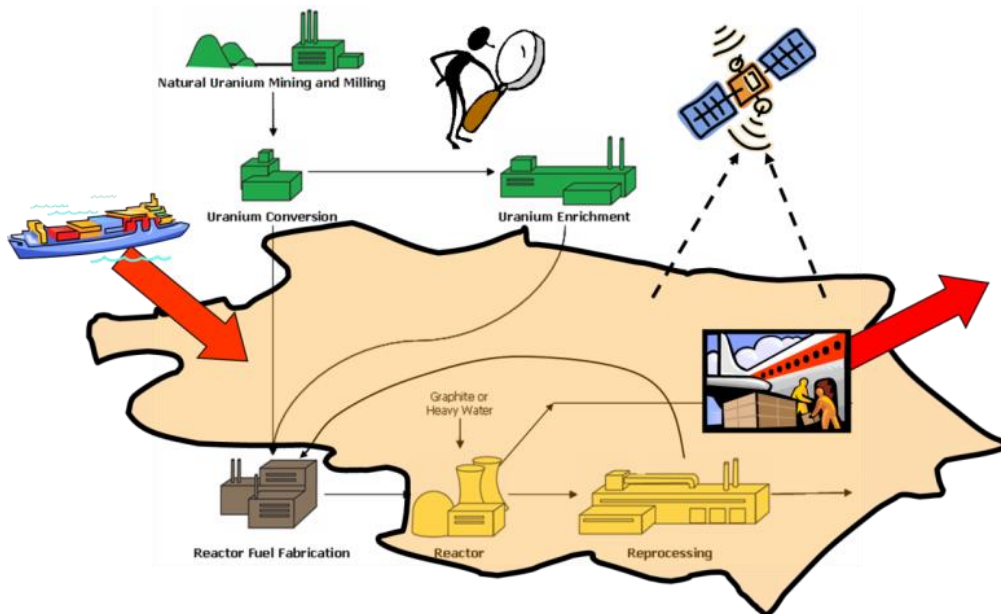


Figure 2 – Matching State's declarations and verification activities

### 3.1 Strategic Trade Data

For the analysis of strategic trade data, analysts can use international trade databases, which are provided by several web services. Export-controlled items listed in regulatory documents represent a limited amount of the international trade volume covered by trade databases, which include all commodities.

As previously seen, Trigger List or dual-use items can be associated to specific parts of the nuclear fuel cycle. In order to acquire additional information on a State's nuclear-related trade, the selected items' Harmonized System codes can then be obtained, by which trade data can be retrieved from data providers [14].

The process is complicated by the fact that the commodities' categorisations used by licensing (e.g. the EU dual-use control list [16, 17]) and customs (Harmonized System) differ and the correlation between the two datasets is not one-to-one.

### 3.2 Denied export authorisations

Although the members of the regimes and the EU member states among them, exchange information about denied export authorisations, these are not directly available to the IAEA. The associated

information may be relevant to verification activities, also for dual-use items not directly nuclear-related, including catch-all clauses on non-listed items.

### **3.3 Intangible Technology Transfers**

Technology according to the NSG guidelines is the knowledge needed to perform an activity. Like items, components and materials, also software and technologies are subject to export authorisations and may be a proof of illicit transfers and undeclared activities. However, software and technology's export declarations are not included in AP's Annex II.

Although the availability of technology (and software to model, assist the processes) may be described in association to AP Annex I's list of activities, their transfer to third country's entities is therefore not due to be declared to IAEA. We have therefore an inconsistency and distortion with respect to the national export control systems and NSG guidelines.

Linked to this, also the on-site provision of technical assistance and associated technology transfer is subject to national authorisation, although for the time being the EU export control framework still has it as a Joint action process separate from the dual-use export control requirements.

Technical assistance is also an activity performed by the IAEA itself and can constitute an additional source of indicators for third countries.

## **4. Compliance and procurement outreach**

The implementation of strategic trade controls and nuclear safeguards can be effective only relying on informed, aware, collaborative and complaint suppliers and exporters. For this reason also, the IAEA encourages suppliers to provide information on procurement attempts for nuclear-related (dual and single use) goods, what constitutes a valuable source of information to enable the early detection of potential undeclared nuclear activities.

Export compliance is a two way process and public authorities should promote an engaging and trusted relationship with the exporters that can be facilitated by an effective outreach strategy and open contacts and communication with the exporters. Industry can apply due diligence procedures and develop Internal Compliance Programmes (ICPs) as one of the most effective ways in addressing proliferation risks and ethical sensitivities, also besides those foreseen in the law.

The supply chain's diversity presents threats and complexities. Nuclear exporters are willing to comply but challenges like the illustrative character of the TL may create interpretation issues. Some States interpret it as an indicative list while others consider that TL export controls only apply to the items specifically mentioned on the list.

More broadly, interpretation issues and "catch-all" controls relate not only to dual-use items originating from the Nuclear Suppliers Group, but also from all the international export control regimes [18,19,20,21], included for the EU in the dual-use control list published every year as Delegated Act [16], amendment to the EU Dual-use Regulation's Annex I [17], and adopted also by several non-EU countries.

Governments should strive to apply controls consistently without interfering with legitimate business or distort competition. This needs to take into account complex supply chains involving actors including several actors (suppliers, clients, brokers, shippers, sub-contractors, banks, research, consultancy and others).

Certain emerging technologies may also provide opportunities with regards to export compliance. Modern approaches like Distributed Ledger and Blockchain could facilitate the logistics and document access all along the supply chain thus improving the processes and speeding up shipments across the controls [22].

Increased and smarter awareness is a key to a successful control of possible sensitivities, save the need to not unduly hinder research and development, besides licit trade.

## 5. Conclusions

The paper revisited the parallel evolution of international nuclear safeguards and export controls, underlying once more their close and complementary relationship which should be continuously reinforced in order to strive for a more efficient strive against nuclear proliferation in violation to the NPT.

The various components of the safeguards and export control framework all contribute to the prevention and verification of the absence of undeclared nuclear activities potentially aiming at the development of nuclear weapons and means of delivery.

Various declarations are due to IAEA and EURATOM, and sources of independent information can help identifying anomalies and inconsistencies, whenever made available.

In the framework of the Additional Protocol (AP), information is exchanged with the IAEA about real exports of nuclear technology. Additionally the IAEA has agreements with some States to exchange information about refused export control licenses. This provides the IAEA with the possibility to detect at an earlier stage illicit trafficking networks. However, monitoring technology transfers by intangible means poses its own set of problems.

Countries with an Additional Protocol in force are inherently more safeguarded and thus having an AP in force minimizes proliferation risk, making positive export licensing decisions easier to make. The existence of an AP is also a key instrument for the IAEA to use to derive State Level conclusions.

The reporting requirements to IAEA do not cover supply of Trigger List's technology, as there are no physical exports, nor customs declarations to complete. States may anyway report also such transfers, where they are known, on a voluntary basis.

The role of suppliers and exporters is crucial to the success of the system, at the same time safeguarding licit trading activities from unnecessary burden and delays. Collaboration and exchanges with suppliers is key to defining complete and workable guideline and procedures.

The ESARDA Working Group bringing together various stakeholders, including representatives of larger nuclear industries, authorities, universities, research institutes and NGOs provides a multi-disciplinary open forum to exchange views for the potential benefit of safeguards and export controls. Exchanges on this subject are also taking place with INMM, supported by discussions at symposia and joint meetings that could hopefully intensify further in the future.

## References

1. United Nations Security Council. Resolution 1540 Adopted by the Security Council at its 4956th Meeting, on 28 April 2004, S/RES/1540, 2004
2. IAEA INFCIRC/140 - TREATY ON THE NON-PROLIFERATION OF NUCLEAR WEAPONS (1970)
3. Nuclear Suppliers Group, NSG, [www.nuclearsuppliersgroup.org](http://www.nuclearsuppliersgroup.org)
4. IAEA INFCIRC/254/Rev.13/Part 1, GUIDELINES FOR NUCLEAR material, equipment and technology, available at [www.nuclearsuppliersgroup.org](http://www.nuclearsuppliersgroup.org)
5. IAEA INFCIRC/254/Rev.10/Part 2 GUIDELINES FOR TRANSFERS OF NUCLEAR-RELATED DUAL-USE EQUIPMENT, MATERIALS, SOFTWARE, AND RELATED TECHNOLOGY, available at [www.nuclearsuppliersgroup.org](http://www.nuclearsuppliersgroup.org)
6. Zangger Committee, [www.zanggercommittee.org](http://www.zanggercommittee.org)

7. IAEA INFCIRC/540 (Corrected). Model Protocol Additional to the Agreement(S) Between State(S) and the International Atomic Energy Agency for the Application of Safeguards, (1997).
8. Filippo Sevini, Renaud Chatelus, Malin Ardhammar, Jacqueline Idinger, Peter Heine, States' reporting of Annex II exports (AP) and the significance for safeguards evaluation, IAEA SG2014
9. F. Sevini, Nuclear export controls update, paper presented at the 55th INMM annual meeting, 2014, Atlanta, USA
10. F. Sevini et al., Some ESARDA Parties' experience with Additional Protocol export control declarations, paper presented at the 33<sup>rd</sup> ESARDA Symposium, Budapest 2011, available at <https://esarda.jrc.ec.europa.eu/>
11. "The Conceptualization and Development of Safeguards Implementation at the State Level," International Atomic Energy Agency, Available at: <http://www.isisnucleariran.org/assets/pdf/GOV201338.pdf>, GOV/2013/38, Aug. 2013
12. C. Listner et al.: "Approaching Acquisition Path Analysis formally – a comparison between AP- and Non-AP States", ESARDA Symposium 2013, 27-30 May, Bruges, Belgium
13. Z. Liu, S. Morsy, Development of the Physical Model, Proceedings of the IAEA Safeguards Symposium, vol. 29, IAEA, Vienna, 2007.
14. C. Versino, A. El Gebaly, E. Marinova, C. Pasterczyk, G.G.M. Cojazzi, Integrating IAEA's Physical Model with JRC's The Big Table Document Search Tool, JRC Scientific and Policy Report, 2013, EUR26215 EN.
15. M. Ardhammar, "Trade and procurement analysis in the context of IAEA safeguards", Presentation at ESARDA Joint meeting on „IAEA State Level Concept“, Nov 12, 2013, Ispra ,12 November 2013
16. COMMISSION DELEGATED REGULATION (EU) 2018/1922 of 10 October 2018
17. Council Regulation No 428/2009 of 5 May 2009 setting up a Community regime for the control of exports, transfer, brokering and transit of dual-use items (Recast), (2009).
18. Missile Technology Control Regime, [www.mtcr.info](http://www.mtcr.info)
19. Australia Group, [www.australiagroup.net](http://www.australiagroup.net)
20. Wassenaar Arrangement [www.wassenaar.org](http://www.wassenaar.org)
21. Organisation for the Prohibition of Chemical Weapons, OPCW, <http://www.opcw.org/>
22. F. Sevini, C. Charatsis, X. Arnes Novau, E. Stringa, J. Barrero, A.S. Lequarre, P. Colpo, D. Gilliland, W. Janssens, Emerging Dual-use Technologies and Global Supply Chain Compliance, IAEA Safeguards Symposium 2018

## **Export controls and safeguards: inseparable elements of the non-proliferation regime?**

**Ian Stewart**

King's College London

### **Abstract:**

*This paper examines why it is that there appears to be divisions between the nuclear export control and nuclear safeguards practitioner community. The paper argues that export controls and safeguards are the two inseparable elements of the non-proliferation control regime. It is thus argued that efforts should be undertaken to reconcile these communities. In making this argument, the paper briefly examines the closely interrelated evolution of both sets of instruments. The paper then explores why it is that despite the interrelation between the two, two separate communities of practice have formed around each. The paper finishes by identifying a number of ways in which closer integration between the communities can be realised in order to strengthen the non-proliferation regime into the future.*

### **Introduction**

Nuclear non-proliferation controls which includes primarily export controls and safeguards are a vital tool of international peace and security. Instances in which non-proliferation controls break down – or are perceived to have broken down – are often taken up by the UN Security Council in accordance with its mandate under Chapter VII of the UN Charter to address such security challenges. And successive failures of non-proliferation controls since the beginning of the nuclear age have seen periodic concerted efforts to strengthen non-proliferation controls.

Despite this, it is apparent that there is division between the safeguards and nuclear export control communities. This division is no more apparent than in Vienna which is both the home of nuclear export controls and the home of International Atomic Energy Agency (IAEA) safeguards. A gulf has arisen in Vienna between these two communities which results in a lack of formal communications between safeguards and export control communities.

The purpose of this paper is to examine why it is that these two communities has grown apart and what might be done to bring the communities back together. The paper begins by charting the mutual development of nuclear export controls and safeguards. It then examines why it is that a gulf has developed. Finally, it considers what might be done to overcome this division in the practitioner community.

## **The Evolution of Nuclear Controls**

Before turning to the current state of affairs, it is useful first to examine the history of the development of nuclear export controls and safeguards. Both sets of measures developed hand in hand over the second half of the 20<sup>th</sup> century. Non-proliferation controls have improved markedly since the early nuclear age. Lessons began to be learned following the first examples of nuclear cooperation in which, for example, Canada supplied India a nuclear reactor without any form of safeguards.<sup>1</sup> Also in the 1950s, early efforts took place to establish common rules of supply for nuclear exports including around when an export might trigger a requirement for safeguards. Both safeguards and export controls were strengthened in the 1970s first following the NPT which saw development of a comprehensive system of safeguards then with the creation of the Nuclear Suppliers Group (NSG) following India's so-called peaceful nuclear explosion, which resulted in agreement on common rules of supply in relation to when safeguards would be triggered. Export control and safeguards have developed in parallel and become intertwined. For example, as the NPT requires transfers to be subject to safeguards, safeguards have become one of the key criteria used for considering export licenses. This joint development continued in the 1990s following the first Gulf War first with agreement through the NSG on extending the coverage and conditions associated with nuclear export controls then the development of the IAEA's additional protocol (AP).

## **Safeguards vs Export Controls?**

Despite the intermingled development of nuclear controls, this paper argues that there is a gulf between the nuclear export control and safeguards practitioner communities. In this section, the existence of this gulf is examined and explained. It is argued that this gulf exists because of the increasingly political environment surrounding the topic of non-proliferation controls.

The gulf that exists between the export control and safeguards communities has not been well documented in existing literature and is, to some extent, an issue visible mainly to insiders who have visibility of how the NSG and the IAEA operate. However, during the 2018 IAEA safeguards symposium, an opportunity arose to discuss these issues in a session entitled, which the author co-chaired with an official from the IAEA. This session was notable in part because it included in its speakers a representative of the NSG. Indeed, polling of audience members showed a strong preference for the NSG as the organization in the strategic trade community that is most appropriate for the IAEA to

engage in dialogue with.<sup>2</sup> in the course of the discussion at this session, a number of areas where better cooperation between safeguards and export controls were identified. These are captured below.

- Denial notifications: presently, while NSG members are required to share information on denied exports with other members of the group through a platform established for this purpose<sup>3</sup>, there is no similar requirement to share such information with the IAEA. At the session, the utility of denial notifications to the work of the IAEA was highlighted; it was pointed out, for example, that a blocked export licence could reveal information on an attempt to acquire equipment for an undeclared nuclear activity. Under its mandate of verifying the correctness and completeness of a state's declaration, the IAEA would investigate such cases if the information was shared.
- Industry outreach: at the session, it was highlighted that the IAEA operates a procurement outreach program intended to build links with the private sector such that any suspicious enquiries, which do not make it to the export licence stage, can be fed into the IAEA for analysis. Export control authorities should also be conducting such outreach as an aspect of their own implementation of export controls.<sup>4</sup> However, presently, there is no requirement for states to cooperate with the procurement outreach program and the agency can thus engage with companies only in countries that voluntarily engage with the program. While statistics are not available on which countries participate in this voluntary program, it was clear from the discussion that at present the program does not benefit from universal adherence and that valuable information could be missed as a result.
- Mandatory reporting: a third topic discussed at the session related to updating the reporting obligations under the IAEA AP to reflect developments in the NSG's trigger list. The AP incorporates a 1990s version of the NSG trigger list and requires states to report the export of these technologies. The NSG has undertaken substantial updates to this list including through its 'comprehensive review', which concluded in 2013. However, to date, there has been no move to update the model AP perhaps on the assumption that the political environment in Vienna is not conducive to changes to the AP.

This paper argues that the current limited cooperation in relation to the above-mentioned points is a result of divisions between the two communities which itself is a result of the politicisation of safeguards.

### **What are the implications of this gap? Less effective controls**

The session at the IAEA safeguards symposium highlighted areas where cooperation between export control authorities and safeguards could be improved. Before examining the barriers to such cooperation and possible paths forward, it is useful to briefly consider the implications of this gap from a non-proliferation perspective. When considering the effect of the gap, it is useful to recall the mandate and purpose of both the IAEA and export controls.

The IAEA's mandate with regards to safeguards is to ensure the correctness and completeness of state's declarations. There are relatively few sources of data that can be used in pursuit of the second

part of this mandate – ensuring the completeness of state's declarations. Perhaps the only comprehensive source available to the IAEA is trade information given that all states are reliant to a greater or lesser extent on imports to build and sustain their nuclear fuel cycle. Other sources such as intelligence information and academic publications can reveal the presence of undeclared activity but there is no guarantee that undeclared activity will show up in either of these two sources.

The purpose of export controls is to prevent transfers that would contribute to the proliferation of nuclear weapons and explosive devices. Detecting undeclared weapons of mass destruction programs is not a declared goal of export controls in most jurisdictions and, from the author's experience, is at best a secondary benefit when analysts have the time to step back from assessing individual licences to look at trends across the board. Closer cooperation between the communities would be beneficial as it would spur joint efforts to detect and prevent nuclear proliferation and render the system of controls more responsive to emerging trends and technologies.

There have been cases in which the disconnect between export controls and safeguards have resulted in unchecked proliferation. Perhaps the prime instance of this related to the AQ Khan proliferation network through which several countries received nuclear technology outside of safeguards equipment for uranium enrichment.<sup>5</sup> The author is not aware of cases from the last decade in which the disconnect between safeguards and export controls has resulted in unchecked proliferation. However, it is clearly possible that there are proliferation networks still at work or that there are states that are clandestinely acquiring nuclear technology without declaring this to the IAEA. As such, the ultimately risk associated with inadequate integration of export controls and safeguards remains that it could result in missed opportunities to detect clandestine nuclear programs.

Even beyond this important risk that proliferation could be missed, there are other consequences of this lack of integration between export controls and safeguards. Perhaps principle among these is resource optimisation. It can be argued that the closer the integration between export controls and safeguards the fewer resources that the IAEA need to put into verifying the correctness and completeness of state's declaration. This argument is predicated on the fact that safeguards should inform licensing decisions and licensing decisions should inform safeguards. Given that both safeguards and export control analysts also examine the same topics from different perspectives, better cooperation would help in building human capacity as well as new tools and techniques across both communities.

## **Why Is there A Gap? The Politicisation of Safeguards**

Having now examined whether there is a gap and what the consequences of this gap are for the non-proliferation regime, it is useful to briefly examine why it might be that such a gap has emerged. This analysis is somewhat complex as in recent years there have been a number of intransigent safeguards issues in Vienna some of which have persisted since the 1990s.

The first of these relates to the AP. While coverage of the AP has expanded since the 1990s to more than 130 states, the AP continues to be viewed as a discriminatory instrument by some states. One reason for this is that there continues to be a view that the AP was adopted as an extra non-proliferation

commitment over and above those set out in the Nuclear Non-proliferation Treaty (NPT) without parallel advancements in the NPT's other provisions including in relation to nuclear disarmament.<sup>6</sup>

The second relates to the State Level Concept (SLC). The history of the SLC is beyond the scope of this paper. It is perhaps sufficient to note that the IAEA secretariat has attempted to move the IAEA toward looking at the state as a whole rather than focusing only on safeguarding known nuclear facilities and following up on information about potential nuclear activity outside nuclear sites.<sup>7</sup> Some states have expressed concern about how the agency would decide where to invest verification resource under the SLC which is attributed by some as the reason that the SLC has become a contentious issue in Vienna.

The third relates to the use of third-party information and the case of Iraq in 2003. The question of how flawed and mis-characterised intelligence led the US and UK to war with Iraq has been well documented.<sup>8</sup> Of relevance to this paper is the fact that this intelligence was used first to pressure the IAEA and second to dismiss the IAEA's assessment that Iraq had not resumed its nuclear program.<sup>9</sup> Thus, while the IAEA performed well in the case of Iraq, the case led to concerns that intelligence information could negatively influence the independence of the IAEA. The net result is that the agency must take a very cautious approach to any third-party information.<sup>10</sup>

The collective effect of these issues is that the safeguards environment in Vienna has become very politicised. While states might have genuine concerns or grievances around specific issues, the result is that the expression of concern about any one of the above-mentioned issues is viewed through a political lens. For example, some believe that Russia's supposed obstinance over the SLC is motivated by broader geostrategic interests rather than a limited and specific concern about the SLC itself. It seems likely that Russian officials would similarly accuse US officials of politicising safeguards in relation to Iran particularly given the withdrawal of the US from the Joint Comprehensive Plan of Action (JCPOA) with Iran.

While this section has focused on examining issues around safeguards, it should also be born in mind that export controls are a politicised instrument in their own right. This has manifest itself clearly in relation to the question of whether the non-NPT countries of India and Pakistan should be admitted to the NSG. This question has taken up much of the NSG's efforts in recent years and highlights the fact that the question of membership has an important effect in setting what's feasible within a regime. Thus finally, it should be born in mind that the membership of the NSG and the IAEA are not the same and that the IAEA and NSG are fundamentally different instruments.

How do these issues affect cooperation between export controls? In both the NSG and the IAEA, much of the energy of the policy making apparatus – i.e. the plenary of the NSG and the board of governors of the IAEA – has been consumed by issues other than the optimisation of controls. Second, the politicisation of both lends itself to a risk-adverse approach of limiting interactions between regimes until the political climate is more open to novel ways of cooperating.

## **A path Forward**

This paper has argued that a gulf has emerged between two closely related communities who work to common purpose. In this context, it is important to ask what might be done to bridge this divide. Evidently it would be beneficial for the topics of safeguards and export controls to become less political in Vienna so that the focus could switch toward comprehensively improving the holistic set of non-proliferation controls. However, such a de-politicisation cannot be achieved by any one state on its own or by either the NSG or IAEA without the support of its member states.

Given this, is there scope for more limited areas of progress? Two particular areas are apparent. First, it appears that there is scope for more technical cooperation between the IAEA and the NSG to share information without violating any confidences. The participation of an NSG official in the Safeguards symposium was an example of the type of official-level exchange that should be encouraged. Further exchanges on topics of common interest are necessary. One area identified at the symposium relates to emerging technology where it is necessary for both export control and safeguards practitioners to build understanding of the implications of technology for the design of controls. The value of civil society organised workshops on technical aspects of non-proliferation analysis was also recognised.

Second, a number of areas in which the voluntary action of individual states was highlighted above as being beneficial. For example, participation in the IAEA's procurement outreach program and the sharing of denial notifications with the NSG.<sup>11</sup> There is a need for more states to undertake such voluntary measures even in the absence systematic agreement for all states to enter into such cooperation.

## Conclusions

This paper has examined the existence and effect of an apparent gulf between the safeguards and export control community. Both communities work in different but complementary ways to prevent the proliferation of nuclear weapons. Closer cooperation could increase effectiveness by reducing the risk of undeclared nuclear activity while also potentially utilising less resource. A number of specific areas where closer cooperation would be beneficial have been identified including in relation to the sharing of denial notifications, coordination with regards to industry outreach, and updating mandatory reporting requirements under the IAEA AP. However, it was argued that a key priority should be in developing informal opportunities for exchange around topics of mutual interest such as emerging technology.

The reasons for the gulf were also examined with it being argued that the gap between the communities is in part a result of the politicisation of safeguards in Vienna. While safeguards are and should continue to be viewed as a technical subject, this paper also argued that there is a need to carve a path for improvements in safeguards even in this more politicised environment. It was argued that at least two approaches can help bridge the gap: increased technical-level interaction between export control and safeguards officials to discuss topics of mutual interest and increased voluntary action by states even when formal and multinational agreement cannot be reached.

## Acknowledgements

The research on which this article is based was funded in part by Carnegie Corporation of New York and the UK Support Program to the IAEA. The author would also like to acknowledge those who contributed to session CHA-S4 of the 2018 IAEA safeguards symposium.

<sup>1</sup> For a history of the Canadian export, see R. Bothwell, *Nucleus: the history of Atomic Energy of Canada Limited*. University of Toronto Press.

<sup>2</sup> Audience Polling Results, CHA-S4, IAEA Safeguards Symposium, 2018.

<sup>3</sup> Nuclear Suppliers Group FAQ. Available online at: <http://www.nuclearsuppliersgroup.org/en/about-nsg/nsg-faq> (Accessed 5 May 2019)

<sup>4</sup> The author saw first-hand the value of such outreach when responsible for dual-use goods technical and intelligence assessment in the UK Ministry of Defence.

<sup>5</sup> On the history of the AQ Khan network, see David Albright, *Peddling Peril: How the Secret Nuclear Trade Arms America's Enemies*, Free Press.

<sup>6</sup> Leonardo Bandarra, Brazilian nuclear policy under Bolsonaro: no nuclear weapons, but a nuclear submarine, the *Bulletin of the Atomic Scientists*. Available online at: <https://thebulletin.org/2019/04/brazilian-nuclear-policy-under-bolsonaro/> 12 April 2019.

<sup>7</sup> For background on the SLC, see Laura Rockwood, "The IAEA's State-Level Concept and the Law of Unintended Consequences". Available online at: [https://www.armscontrol.org/act/2014\\_09/Features/The-IAEAs-State-Level-Concept-and-the-Law-of-Unintended-Consequences](https://www.armscontrol.org/act/2014_09/Features/The-IAEAs-State-Level-Concept-and-the-Law-of-Unintended-Consequences) (Accessed 6 May 2019)

<sup>8</sup> For example, in the UK the misuse of intelligence was investigated by the Lord Butler Review of Intelligence on Weapons of Mass Destruction. See for example, *The Guardian*: "Iraq intelligence 'seriously flawed'", available online at: <https://www.theguardian.com/politics/2004/jul/14/butler.iraq1> (accessed 5 May 2019)

<sup>9</sup> U.N. weapons inspector Hans Blix faults Bush administration for lack of "critical thinking" in Iraq

<sup>10</sup> IAEA, Information collection and evaluation. Available online at: <https://www.iaea.org/topics/information-collection-and-evaluation> (Accessed 5 May 2019)

<sup>11</sup> Nuclear Suppliers Group FAQ. Available online at: <http://www.nuclearsuppliersgroup.org/en/about-nsg/nsg-faq> (Accessed 5 May 2019)

# The NSG Part 1 Guidelines and the mutually reinforcing role of nuclear safeguards and in the non-proliferation regime.

**Diego Cándano Laris**  
**Nuclear Suppliers Group**  
**Chair of the Consultative Group**  
[dcandano@sre.gob.mx](mailto:dcandano@sre.gob.mx)

## **Abstract**

*At the 2018 ESARDA Annual Meeting in Luxembourg, participants raised the importance to reinforce the link between nuclear safeguards and nuclear export controls and to create avenues for stronger dialogue between the two communities.*

*The Nuclear Suppliers Group (NSG) seeks to contribute to the non-proliferation of nuclear weapons and the peaceful use of nuclear energy through the implementation of two sets of Guidelines that regulate their nuclear and nuclear-related exports. The Guidelines are increasingly recognised as the global standard of nuclear export controls.*

*The NSG Trigger List is the meeting point of nuclear safeguards and export controls. A correct understanding of the nature and evolution of the Part 1 Guidelines and their Trigger List will contribute to the development and implementation of effective non-proliferation policies and can be the foundation of stronger engagement between the safeguards and the export control communities.*

*The paper will elucidate fundamental aspects of the NSG Part 1 Guidelines and Trigger List, which is unique when compared to the rest of the control lists of the other multilateral export control regimes. These aspects include the single use and illustrative nature of the Trigger List, as opposed to the dual-use and indicative nature of the Part 2 Guidelines and Dual-Use List; and issues related to their implementation by adhering governments.*

*The paper will also evaluate ways in which the Part 1 Guidelines and the Trigger List have evolved since their publication in 1978, particularly during the fundamental review that concluded in 2013, and point to practical implications that this review could have for the effective implementation of safeguards.*

**Keywords:** nuclear export controls, safeguards, NPT Review Conference, NSG, 1540

## **1. Introduction**

Article III of the Non-Proliferation Treaty (NPT) requires that Treaty members do not supply nuclear items (especially designed or prepared items) to non-nuclear-weapon States unless these accept the safeguards required by the Article. Nuclear export controls thus originate in the NPT and constitute an important element of the non-proliferation regime [1].

It is worth noting that while the Treaty leaves in the hands of individual States the responsibility of controlling and authorizing such transfers, it tasks International Atomic Energy Agency (IAEA) safeguards with their verification [2]. From this point of view, it is evident that the effective implementation of nuclear export controls contributes to fulfilling the goals of the NPT and should be seen as mutually reinforcing with the verification role of nuclear safeguards.

Moreover, there is close interdependence between the controls in the Nuclear Suppliers Group (NSG) Part 1 Guidelines [3] and the effective implementation of comprehensive IAEA safeguards. A full-scope safeguards agreement with the IAEA is an NSG condition for the future supply of Trigger List items to any non-nuclear-weapon State. The title itself is indicative of this interdependence: these items are known as Trigger List Items as the transfer of an item “triggers” safeguards.

This interdependence with the NPT and with the safeguards regime, creates a unique situation for nuclear export controls; they differ from other multilateral regimes, where the commitments of regime members may not necessarily be tied to multilateral Treaties. A correct understanding of this relationship should enable a better implementation of nuclear export controls, justify stronger engagement with the rest of the non-proliferation regime and address future challenges in the nuclear fuel cycle in a responsible and efficient manner.

## 2. The NSG and the Non-proliferation regime

It is well known that soon after the NPT entered into force, several countries engaged in multilateral consultation with the aim of developing common understandings on the implementation of Article III.2 of the Treaty:

*Each State Party to the Treaty undertakes not to provide: (a) source or special fissionable material, or (b) equipment or material especially designed or prepared for the processing, use or production of special fissionable material, to any non-nuclear-weapon State for peaceful purposes, unless the source or special fissionable material shall be subject to the safeguards required by this Article.*

These consultations led to the establishment of the two nuclear export controls mechanisms: the Zangger Committee, also known as the NPT Exporters Committee, and the NSG.

The members of the Zangger Committee limited their mandate to interpreting the meaning of Article III.2. The NSG has decided to go beyond to include technology controls, dual-use controls and physical security standards. For example, the export of a nuclear reactor falls within the NPT, but the design information that would explain how to build it would not, and neither would the items for weaponization of the special fissionable material [4].

While the NSG may go beyond some NPT provisions, its interdependence with Article III of the Treaty is undeniable and the spirit behind the article underlines the NSG Guidelines. It must be pointed out that when Participating Governments (PGs) of the NSG implement their NSG policy commitments, they do so as a means to comply with their obligations under the NPT.

The NSG Guidelines are sets of conditions of supply that are applied equally by members to nuclear transfers for peaceful purposes to help ensure that such transfers will not be diverted to unsafeguarded nuclear fuel cycle or nuclear explosive activities. Although NSG Guidelines are not legally-binding, NSG PGs commit to apply those Guidelines via their national legislation.

The NSG comprises major suppliers of nuclear and nuclear-related dual use goods who have adopted a common commitment to uphold these high non-proliferation standards for transfers and seeks to develop common approaches and conditions of supply to ensure the consistency of articles III and IV of the NPT, that is, to make sure that broad nuclear programs do not lead to diversion. Thus, the NSG creates a set of responsible policies and commitments that enable nuclear trade, and not, as is often thought, a list of items and technologies that cannot be traded.

## 3. Safeguards and Part 1 Guidelines

The non-proliferation regime may be seen as a “network of global, regional and bilateral agreements in which States commit themselves not to manufacture or possess nuclear weapons” [5]. The respect for these commitments is verified by the system of international safeguards and the different policy commitments that regulate nuclear and nuclear-related trade incorporated in the NSG Guidelines are a further element of the regime. Indeed, there is a close interdependence between the controls in the NSG Part 1 Guidelines and the effective implementation of comprehensive IAEA safeguards.

The NSG has stated that it fully supports international efforts to strengthen safeguards to detect undeclared activities as well as to monitor declared nuclear activities to ensure that they continue to

meet vital nuclear non-proliferation requirements and to provide the assurances needed for the continuation of international nuclear trade. Of particular relevance is the fact that a full-scope safeguards agreement with the IAEA is an NSG condition for the future supply of Trigger List items to non-nuclear-weapon States. The Part 1 Guidelines also stipulate repercussions in the case of violations of the supplier-recipient agreements, including verification measures in the case of termination of safeguards.

Controls on the transfer of items and technologies listed on the NSG Control Lists provide essential support for the implementation of the NPT and other international legally binding non-proliferation instruments. They facilitate the safe expansion of access to the peaceful uses of nuclear energy consistent with the highest non-proliferation standards.

Adhering to the NSG Guidelines represents a commitment to the highest standards across the whole nuclear cycle. Part 1 Guidelines include a prohibition on nuclear explosives; commitment to physical protection levels; comprehensive safeguards as condition of supply, including provisions in case of the termination of such agreements, such as verification measures; an agreement to exercise particular caution in the transfer of sensitive facilities (i.e. enrichment and reprocessing facilities, including equipment and technology); controls on retransfers; a commitment to the “non-proliferation principle” which indicates that suppliers should only transfer Trigger List items or technology when satisfied that the transfers will not contribute to the proliferation of nuclear weapons or other explosive devices or be diverted to acts of nuclear terrorism; as well as implementation and supporting commitments related to the promotion of international cooperation on the exchange of physical security information, protection of nuclear materials in transit, and recovery of stolen nuclear materials and equipment.

Part 1 Guidelines also seek to support effective IAEA safeguards, physical security and implementation in member states, including the Agency’s efforts to help states in accounting and control; physical security standards including the convention on the physical protection of nuclear material and the IAEA Recommendations for the Physical Protection of Nuclear Material; and support for effective IAEA safeguards including the improvement of national systems of accounting and control. They indicate that suppliers should encourage designers and makers of sensitive equipment to construct it to facilitate IAEA safeguards, enhance physical protection, consider risk of nuclear terrorist attacks, protect information, and include safety and non-proliferation features in designing and constructing of Trigger List facilities. Suppliers should also encourage recipients to develop effective export controls and, as already stated, Part 1 Guidelines stipulate repercussions in the case of violations of the supplier-recipient agreements, particularly in the case of testing and explosions of a nuclear device, as well as termination of safeguards.

The NSG Guidelines are a full integrator of non-proliferation principles in the nuclear fuel cycle and perhaps the strongest comprehensive amalgamation of responsible nuclear policies and the NSG Part 1 Guidelines and their associated Trigger List can be seen as a meeting point between the nuclear safeguards and export controls.

#### **4. The Illustrative Nature of the Trigger List**

One of the guiding questions in the initial consultations on NPT implementation was the definition of what constituted “equipment or material especially designed or prepared for the processing, use or production of special fissionable material”. According to Carlton E. Thorne, since 1971, the Zangger Committee has interpreted “the condition and procedures that would govern exports of such equipment or material in order to meet obligations of Article III.2 on a basis of fair commercial competition” [6].

The Zangger Committee developed a memorandum which has been known as Trigger List (INFCIRC/209, Memorandum B). It lists the equipment or material especially designed or prepared for the processing, use or production of special fissionable material. The memorandum opens the door for NPT Parties to interpret for themselves that “any equipment or material which was especially designed or prepared for use in any of the activities listed in Paragraph 2 of Memorandum B, would require safeguards as required by the Treaty”.

Already at that early stage, the Committee acknowledged the difficulty of defining in practice the types of equipment and materials which were especially designed or prepared. It therefore developed an

attachment to the Trigger List, an Annex to INFCIRC/209. The Annex provided examples of such items and was not meant to be a definitive or exhaustive list of items. It is important to stress that this same philosophy underlines the NSG Part 1 [7].

As already indicated, the NSG Part 1 Guidelines govern the export of items that are especially designed or prepared for nuclear use. These items are also known as Trigger List Items as the transfer of an item triggers safeguards. The Trigger List covers EDP equipment, components, materials, subsystems and facilities for processing, use and production of special fissionable material.

The Trigger List is a control list and technical annex to the NSG Part 1 Guidelines, listing the specific types of material and equipment to which the conditions of supply described in the NSG Part 1 Guidelines apply. The Trigger List covers fuel cycle items, technology and software.

The NSG Trigger List is found in INFCIRC/254/Part 1/Annex A and the clarification of items are found in Annex B of the same document. Annex B is often taken as the NSG Trigger List, although it clearly states its role as “clarification of items on the Trigger List as designated in section 2 of material and equipment of Annex A”.

For this reason, the list is derived from the definition of especially designed or prepared in the NPT and is written in an illustrative way with technical descriptions providing examples that are sufficiently broad to cover all usable items of that type. Furthermore, they avoid offering proliferators a “shopping list”. It is worth noting that, among other things, the NSG Trigger List is distinguished from other multilateral control lists by this characteristic. This includes the NSG Dual-Use List which is indicative in nature.

## **5. Evolution of the NSG Trigger List**

The illustrative nature of the Trigger List does not impede the NSG from undertaking updates and further clarifications. The NSG and the Zangger Committee have always sought to ensure harmonization in the evolution of their Lists. For example, the NSG undertook a comprehensive review of the enrichment section of the Annex in the early 1990s.

Of note is the fact that in 2013 the NSG finalised a careful evaluation of its Control Lists. The so-called Dedicated Meeting of Technical Experts (DMTE) met several times to deliberate on thematic areas such as reprocessing, fuel fabrication, isotope separation, and reactors, agreeing to more than 50 updates in both lists (around 20 in the Trigger List).

As a result of this process, the NSG also established a formal Technical Experts Group, which meets regularly and is tasked with keeping the Control Lists technologically relevant and up-to-date.

The guiding question for listing items has been and will continue to be “do the items meet the ‘especially designed or prepared’ (EDP) criteria for the processing, use, or production of special fissionable material?” as it originates from Article III.2 of the NPT.

The first NSG Guidelines were published in 1978 by the IAEA (INFCIRC/254). On November 2016, the NSG Chairperson forwarded to the IAEA for publication in the INFCIRC series the latest version of the Part 1 Guidelines and Trigger List, which is revision 13 of the document INFCIRC/254.

Future challenges such as emerging technological trends and new generation reactors will pose questions for both the nuclear export control and safeguards communities. The strong interdependence between both elements of the non-proliferation regime seems to argue for stronger engagement and better understanding between both communities.

## **6. Conclusions**

This paper argues that the NSG promotes policies that ensure consistency between Articles III and IV of the NPT. Support for safeguards is an essential component of the responsible policies and commitments that the NSG supports in order to enable nuclear trade.

The NSG Control Lists, annexed to the NSG Guidelines, are not, as is often thought, merely a list of items and technologies that cannot be traded and are controlled by a few. Rather the controls should be understood as an international gold standard, dependent on responsible policy commitments, that allow governments to support a principled position on nuclear non-proliferation and help ensure that nuclear transfers are made for peaceful purposes. Conditions of supply are written in a way that stipulates how transfers can be approved and not how transfers can be denied. From this conceptual point of view, the role of nuclear export controls and safeguards mutually reinforce each other.

The NSG Trigger List is a meeting point of nuclear safeguards and export controls. A correct understanding of the nature and evolution of the Part 1 Guidelines and their Trigger List will contribute to the development and implementation of effective non-proliferation policies and can be the foundation of stronger engagement between the safeguards and the export control communities. This is particularly relevant as the Trigger List is not only implemented by NSG PGs. Governments are encouraged to unilaterally adhere to the NSG Guidelines and implementation of them may help countries fulfil international commitments, including under United Nations Security Council Resolution 1540.

It is worth noting that the NSG PG's agree on the Guidelines and the associated Control Lists but that implementation of the Guidelines is done on a national basis. As already indicated, it is the sovereign responsibility of a country to take decisions regarding the licensing of an export. Nevertheless, a correct understanding of the origins and philosophy of Trigger List should enable more uniform and responsible implementation of the NSG commitments in light of the obligations under the NPT.

As the international community prepares for the 2020 Review Conference of the NPT, it is worth remembering that complying with NSG Part 1 Guidelines represents a policy commitment that strengthens both the safeguards regime and the NPT as a whole, ensuring the consistency of the pillars of non-proliferation and promotion of peaceful use of nuclear energy.

## 7. References

The present paper incorporates some ideas originally presented by the author in the IAEA Safeguards Symposium in November 2018.

[1] *The Nuclear Suppliers Group: its origins, role and activities* (INFCIRC/539/Rev. 6, 22 January 2015): <https://www.iaea.org/sites/default/files/infirc539r6.pdf>

[2] Schmidt, Franz W. *The Role of the IAEA in Nuclear Export Controls*

[3] The NSG Part 1 Guidelines govern the export of items that are especially designed or prepared for nuclear use. These include: (i) nuclear material; (ii) nuclear reactors and equipment therefor; (iii) non-nuclear material for reactors; (iv) plants and equipment for the reprocessing, enrichment and conversion of nuclear material and for fuel fabrication and heavy water production; and (v) technology (including software) associated with each of the above items.

[4] Thorne, Carlton E. *Multilateral Nuclear Export Controls: Past, Present and Future*

[5] Blix, Hans, *Keynote Speech in International Seminar on the Role of Export Controls in Nuclear Non-Proliferation* (October 1997)

[6] Thorne, Carlton E. *The Illustrative Nature of the Trigger List*

[7] *Ibid*

# Nuclear Export Control System of the Czech Republic

Alois Tichy, Martin Kafka, Ondrej Stastny

State Office for Nuclear Safety  
Department of Non-Proliferation  
Senovazne namesti 9  
1100 00 Prague 1 CZ  
E-mail: alois.tichy@sujb.cz

## **Abstract**

*The Czech Republic, thanks to its significant nuclear components production capability and high volume of nuclear and dual-use exports, is in excellent position to share its experience with implementation of export control system for nuclear related items.*

*This paper examines the efforts of the Department of Non-Proliferation of the State Office for Nuclear Safety in implementing obligations under Article 3.2. of the Treaty on the Non-Proliferation of Nuclear Weapons and requirements of relevant International Control Regimes. The paper focuses on introduction of the Czech export control system for nuclear and dual-use items and describes in particular various procedures applied to license applications during their assessment. The paper will also address some of the lessons learned and best practices relating to the Czech Republic's decades long experience with the licensing process with over 200 licenses issued every year.*

*The goal of this paper is to provide a valuable insight in the Czech Republic's dual-use licensing process, mechanics behind it and to share its experience.*

**Keywords:** Non-Proliferation, Licensing, Nuclear, Export Control, Dual-Use

## **1. Introduction**

This paper addresses the export control system for dual-use nuclear items in the Czech Republic. It focuses on details of the licensing process and also deals with the issue of intangible transfers of technology. Next, the paper presents statistical data for exports and imports of controlled nuclear items for the last five years. Finally the paper concludes with a brief description of the role of Czech Customs Administration in export control in the Czech Republic.

## **2. International Control Regimes and Intangible Transfers of Technology**

The Czech Republic is an active member of following international control regimes focusing on trade with strategic goods: Nuclear Suppliers Group (NSG), Missile Technology Control Regime, Australia Group and the Wassenaar Arrangement. The reason for existence of these regimes and the Czech membership in them is based on the global effort to curb the proliferation of weapons of mass destruction (WMD) and their delivery vehicles. Each international control regime has a specific list of controlled items and Guidelines for exports of these items, which are implemented in national legislation of participating governments. The subject of control of these regimes is so-called dual-use items. These dual-use items can be products of the chemical, biological, nuclear or engineering industry produced for civilian purposes, but can be due to their nature and properties, misused for

WMD related purposes. One example of such item can be a high-precision machining centre. Such equipment has an irreplaceable role in the automotive industry, but can be also misused for machining of various components for nuclear weapons programmes. It is also important to note that dual-use items are not always physical palpable items, but are nowadays increasingly taking the form of so-called intangible technology. Such items are best described as information required for the production or use of any item contained in the respective control lists. Intangible transfers of technology (ITT) can have many forms – it can be provision of technical data and know-how (in form of blueprints, designs or instructions) or technical assistance (in form of training, consulting services or collaboration). ITT can be realized via electronic transmissions or can be recorded on electronic media. Such transfers can pose significant challenges for licensing and export control. Although the same conditions apply for licensing of both tangible and intangible items in the Czech Republic, significant effort had to be developed in order to raise awareness among licensees and applicants about licensing requirements for transfers of intangible items. SONS therefore conducted several seminars and included section dedicated to ITT on the SONS website.

### **3. Characterization of the Czech Export Control System for Nuclear Items**

The Czech Republic has a double stage licensing process for both dual-use and trigger-list items. For the first licensing stage the competent authority is State Office for Nuclear Safety (SONS), Czech nuclear regulator, which is also responsible for implementation of Safeguards. The designated body in the SONS is Department of Non-Proliferation, which performs its assessment of export applications strictly from technical and non-proliferation perspective. Every application is evaluated on case by case basis. During this process NSG Handbooks are consulted and NSG Information Sharing System is checked for any existing export denials or other relevant information. Attention is also paid to the End-User entity, credibility of stated use and EUC of given dual-use items and potential for diversion or misuse. It is the usual practice that the applicant is repeatedly consulted and asked to submit all information which SONS during the evaluation may consider as substantial. License issued by the SONS is required for import or export of nuclear items and transit of nuclear materials or Trigger list items. Since 2017 for intra-Community transfers, only so-called advance notification is required.

Most applications for exports of dual-use items can be evaluated with SONS in-house capacity. If not, SONS can request an expert opinion from cooperating advisory organizations (agreements with Nuclear Research Institute Řež, Association of Mechanical Engineers and the Academy of Sciences of the Czech Republic). In special cases, SONS inspectors also carry out an in-field inspection at the applicant's location with focus on verification of information declared in the application. During such inspection experts from advisory organizations can also be present.

The competent authority for the second stage of the licensing process is Licensing Office of Ministry of Industry and Trade (LO MIT). LO MIT is responsible for the execution and management of Czech exporting policy and restrictive measures in economic relations with foreign countries. It licenses military items, dual-use items that are controlled by any international control regime (including NSG and ZC) and civil firearms. The LO MIT takes into consideration Czech foreign policy, political situation in target countries and international sanctions. LO MIT also has the authority to issue so-called Catch-All denial for goods that are not on any control lists, but where exists a credible indication that such items might be misused for prohibited purposes (production of weapons of mass destruction). This Catch-All denial can be also issued by the LO MIT on request of the SONS. Both licensing authorities in the Czech Republic also cooperate with other supporting authorities, which provide additional information for the application evaluation process. Among the most important ones belong Ministry of Foreign Affairs of the Czech Republic, Ministry of Finance, Financial Analytical Office and Czech Intelligence Services.

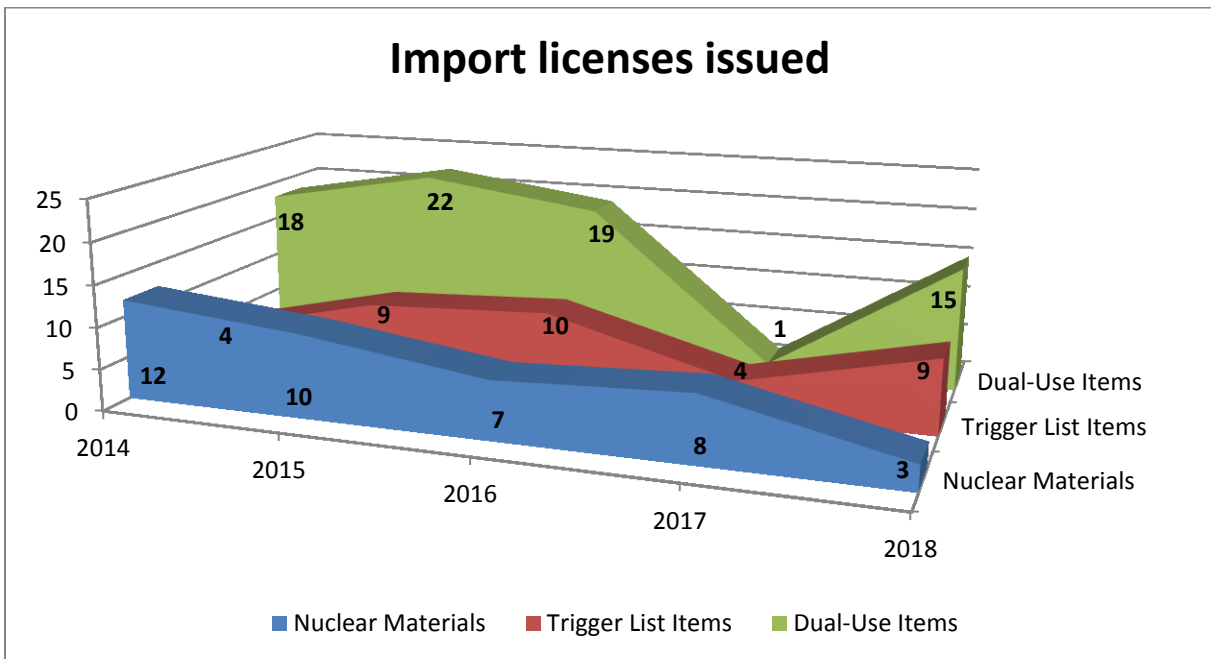
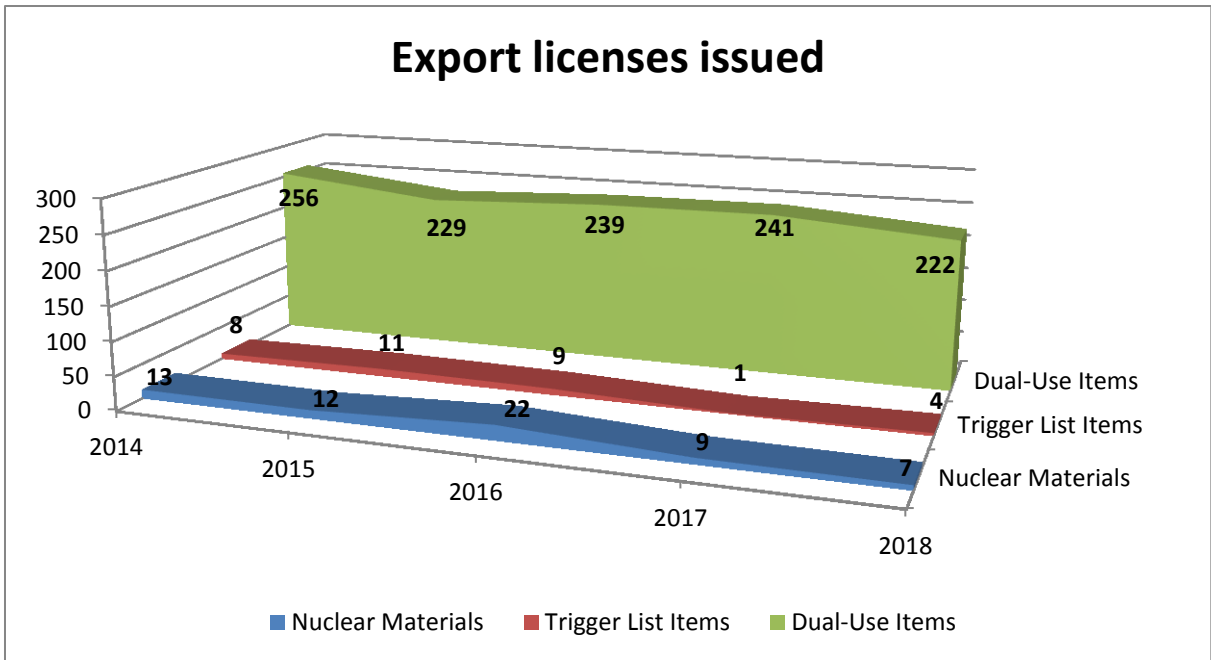
Licensing conditions for trade with controlled nuclear items are based on the Czech Republic's membership in the Nuclear Suppliers Group and Zangger Committee. Control lists and guidelines of these international control regimes are implemented in the Czech legislation, which consists of following laws: act No. 263/2016 Coll., Atomic Act, Law No. 594/2004 Coll. implementing the European Community Regime for the Control of Exports, Transfer, Brokering and Transit of Dual-use Items. There are also two implementing regulations No. 375/2016 Coll. and No. 376/2016 Coll. which deal exclusively with controlled nuclear items and material. The Czech legislation clearly states that nuclear energy and nuclear items can be used only for peaceful purposes and their misuse is strictly prohibited.

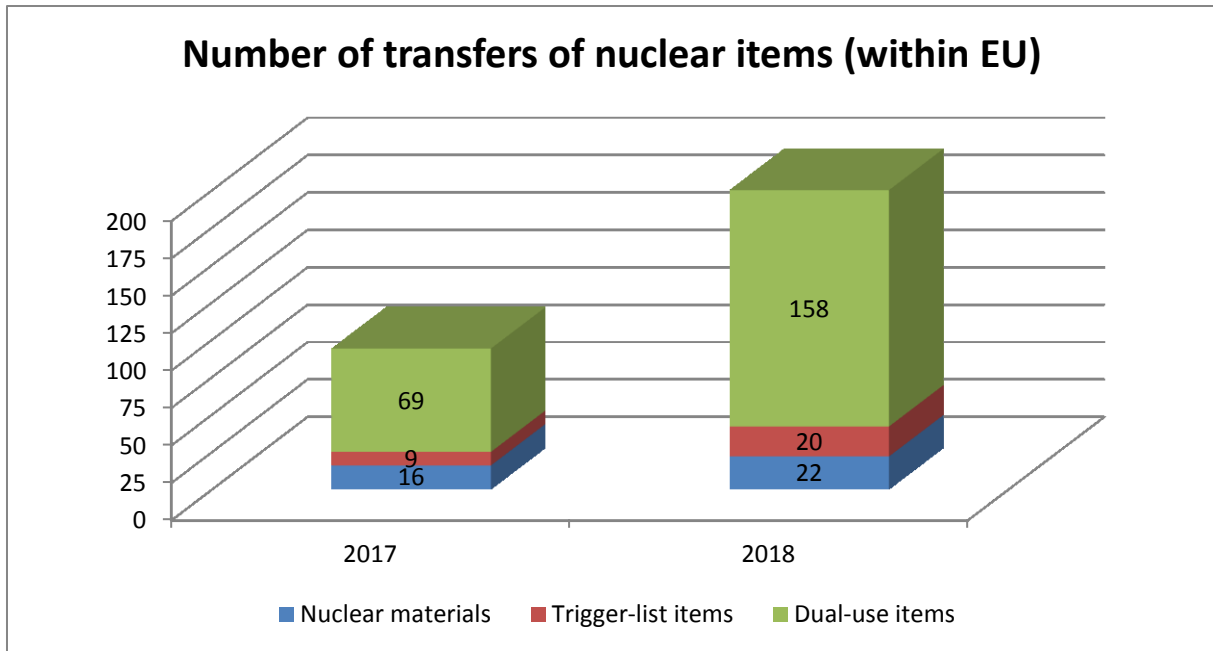
#### **4. Most Frequently Exported Nuclear Items**

The Czech Republic mostly exports dual-use items such as lathe machines, machining centres, grinding and milling machines (i. e. items that fall under category of Machine Tools). Most common target countries for these exports are Peoples Republic of China, Russian Federation and many EU Member States. Second most common dual-use items exported from the Czech Republic are pulse discharge capacitors. These are mostly exported to Peoples Republic of China and USA. While several thousand of pulse discharge capacitors are exported per year, there are only few companies exporting them as compared to number of companies exporting dual-use Machine Tools. Other commonly exported items comprise of high explosive substances, usually for training purposes for army or police forces in various countries, beryllium as a part of americium-beryllium neutron sources, carbon or aramid fibrous or filamentary materials.

#### **5. Controlled Nuclear Items Trade Statistics**

For better clarity, following two graphs illustrate the numbers of licenses issued by the Department of Non-Proliferation for import and export of dual-use items, trigger list items and nuclear materials in the last five years. There is a slight decrease in number of issued licenses, which is most apparent in issued export licenses for dual-use items in 2018 and in issued export licenses for trigger list items and nuclear materials in 2017 and 2018. Number of issued import licenses is also impacted by this, but on a lower scale since Czech industry is primarily export oriented. This effect was caused by the introduction of new Atomic Act, which removed the requirement for intra-Community transfers to apply for a license. Since 2017 only an advance notification is sufficient for such transfers to take place. The number of intracommunity transfers is illustrated in a third graph, which shows combined numbers of import and export notifications for 2017 and 2018 (before 2017 all transfers were required to have a license).





Since 2014 SONS issued only two denials of export license for controlled nuclear items in 2017 and one in 2018. In all cases the items were dual-use and the reason for issuing these denials was unacceptable risk of diversion to weapons of mass destruction programmes.

## 6. Conclusion

The SONS also cooperates with Czech Customs Administration, which applies various checks to exported items during customs procedure, with the purpose to prevent unauthorized exports or imports of controlled nuclear items. During the customs procedure several parameters and conditions are evaluated and it is also possible to identify controlled items even if the item is incorrectly declared by the exporter. This system recognizes not only nuclear items, but also controlled items which belong to other controlled areas. In cases of misidentified or otherwise suspicious nuclear items, SONS cooperates with the Czech Customs Administration on proper identification of such items and subsequent investigation, because any export control system is only good as the customs administration and mechanisms for enforcement of compliance.

# Export control and Additional Protocol working in synergy to strengthen nuclear non-proliferation: implementation in France

Eugénie Vial<sup>1</sup> and Louis Olivier<sup>2</sup>

<sup>1</sup>Comité Technique Euratom (CTE)  
Bâtiment 447 (Siège)  
Point courrier n°212  
91191 Gif-sur-Yvette Cedex, France  
E-mail: eugenie.vial@cte.gouv.fr

<sup>2</sup>Institut de Radioprotection et de Sûreté Nucléaire (IRSN)  
Non-Proliferation and Nuclear Material Accountancy Department  
International Safeguards Unit  
B.P. 17 – 92262 Fontenay-aux-Roses Cedex, France  
E-mail: louis.olivier@irsn.fr

## Abstract:

*Export control and Additional Protocol are two sides of the same coin. While the first falls within the jurisdiction of States and focuses on governing the movements of strategic goods and technologies outside the national territory, the second comes under international safeguards and helps IAEA to detect attempts of State-level nuclear proliferation. There can be important benefits of making use of their complementarity in favour of nuclear non-proliferation, especially since most of the items described in the Additional Protocol fall under the dual-use goods licensing system. In France, two separate agencies are in charge of carrying out export control and Additional Protocol. This article depicts the path that led to their cooperation, which started six years ago and has been reinforced in the last two years, following the incorporation of the French Additional Protocol in the national law. This joint effort already gave promising results in terms of potential declarants' detection and the first feedbacks are discussed in the paper, leading to different ideas of enhancement that will be implemented in a near future.*

**Keywords:** export control, Additional Protocol, dual-use items

## 1. Introduction

A major tool of nuclear non-proliferation is the surveillance of the dual-use items spread within the world. Indeed, non-nuclear-weapon States that tried to or developed a military nuclear programme did so mainly using dual-use goods and technologies rather than benefiting from direct support from nuclear-weapon States [1]. In order to respond to these attempts of proliferation, two regimes were set up over the past decades: export control and the Additional Protocol.

Historically, the control of exports is one of the pillars upon which the sovereignty of States rests; it governs the movements of strategic goods and technologies, including dual-use items, outside the national territory. For its part, the Additional Protocol is a legal framework related to international safeguards, designed and used by the IAEA to detect attempt of State-level nuclear proliferation. This complementarity is of primary importance for nuclear non-proliferation.

In France, two different authorities are in charge of carrying out the export control of dual-use items and the implementation of the Additional Protocol. A few years ago, they started to cooperate on a more regular basis for strengthening their efficiency and this joint effort gave promising results. The first feedbacks of such cooperation are discussed in this paper as well as the enhancement that should be implemented in the next few years.

## 2. Two complementary regimes

Albeit governed by different legislations, export control and Additional Protocol are complementary regimes that work toward a common objective: non-proliferation. In France, two separate State services are in charge of carrying them out.

### 2.1 Export control

After the end of the Second World War and the rise of the weapon of mass destruction (WMD) proliferation risk, different multilateral export control regimes were created to limit the spread of dual-use items. The Non-Proliferation Treaty (NPT) itself implies to control the exports, in order to fulfil the obligation set forth in Article III.2). Thereupon, the Zangger Committee was set up in 1971 with the purpose to interpret the Article III.2) of the NPT; it established in 1974 a list of items whose export to non-nuclear-weapon States not party to the NPT would trigger IAEA safeguards.

Following the first Indian nuclear weapon test in May 1974, the Nuclear Suppliers Group (NSG) was founded. The NSG completed the Zangger Committee's work and published its own trigger list in 1978, including guidelines for nuclear transfers (physical protection, safeguards, etc.). This did not prevent Iraq, a country party to the NPT, to develop a clandestine military nuclear programme through the use of dual-use items not covered by the trigger list [2]. After the discovery of this programme in 1991, the NSG adopted guidelines for transfers of nuclear-related dual-use equipment, material, software and technology (in other words, items that have both nuclear and non-nuclear applications).

An important step in export control was taken with the adoption of the United Nations Security Council Resolution 1540, in 2004. It requires all States to implement national measures in favour of the control of exports, in order to prevent illicit trafficking of dual-use items and fight against non-governmental actors' involvement in proliferation of WMD, in particular terrorist groups. This Resolution was a response to the 11 September 2001 terrorist attacks and the discovery, in 2003, of the A. Q. Khan's nuclear trafficking network [3].

In the European Union, the *Council Regulation (EC) No 3381/94 of 19 December 1994 setting up a Community regime for the control of exports of dual-use goods* is the first regulation about the dual-use items concern. It ordered EU Member States to implement an export control system with a set of common rules for the Community, like the delivery of export licenses, and focused only on the export of tangible goods. In 2000, a new regulation included intangible items like software and technology. It has been followed by the Regulation (EC) No 428/2009 that also takes into account brokering and transit of dual-use items. The latter regulation is currently in force and the list of items concerned is regularly updated. It includes the trigger list and the nuclear-related dual-use items list of the NSG.

As any EU regulation, the Regulation (EC) No 428/2009 is directly applicable in all Member States, without transposition. In France, the Dual-Use Goods Department (SBDU, Service des Biens à Double Usage) of the Ministry of Industry is the authority in charge of the delivery of export licenses for dual-use items. For the most sensitive cases, the examination of the exporter's application is performed by the Interministerial Commission for dual-use goods, composed of one representative for each strategical Ministry (Foreign Affairs, Industry, Defence, Interior, Energy, Customs, etc.).

### 2.2 Additional Protocol

In the early 1990s, with the discovery of Iraq's clandestine military nuclear programme and the refusal by DPRK of an IAEA special inspection, it became clear that the provisions of the Comprehensive Safeguards Agreements (CSA) were not sufficient to guarantee the IAEA's ability to detect undeclared nuclear activities. Consequently, the Agency started to work on a plan of actions, called the "Programme 93+2"<sup>1</sup>, in order to fill the identified gaps [4].

This programme was made of two parts. Part 1 consisted in emergency measures that could be implemented without modifying the existing legal framework defined by the CSA, such as the early provision of design information, environmental sampling or unannounced inspections within a declared

<sup>1</sup> The programme started in 1993 and was planned to be finished two years later, in 1995, for the NPT Review Conference. The plan of action was finally completed in 1997.

facility. Part 2 included further measures, like enlarging the scope of verifications anywhere on the territory of a State, which required the extension of the IAEA's legal authority. For this purpose, the addition of a protocol to the CSA was proposed. In May, 1997, the IAEA Board of Governors approved the Model Protocol Additional to the CSA (INFCIRC/540), containing all measures that must be accepted by States with a CSA and willing to conclude an additional protocol.

This Model Additional Protocol provides that States shall declare, inter alia, to the IAEA the following activities:

- All their nuclear fuel cycle research and development activities;
- All parts of their nuclear fuel cycle (from uranium mines to nuclear wastes);
- Manufacturing and export of sensitive nuclear-related equipment and material.

It should be noted that among others, States shall declare information about each export of specified equipment and non-nuclear material listed in Annex II, which is a copy of the NSG's trigger list in force when the Model Additional Protocol was approved [5].

In addition to these declarations, the Model Additional Protocol gives the IAEA a broader access for its verification activities, with a short notice (2 or 24 hours). With this so-called complementary access, the Agency can perform verifications in any building on a nuclear site and any declared location related to the nuclear fuel cycle, and can collect environmental samples in any other locations within a State. This last possibility clearly strengthens the ability of the Agency to detect a potential clandestine nuclear activity.

France signed a Protocol Additional to its Voluntary Offer Agreement (INFCIRC/290) on September 22, 1998 (INFCIRC/290/Add1). Its main difference with the Model Additional Protocol is that the activities mentioned above have to be declared only if they are carried out in collaboration with a non-nuclear-weapon State. As for all Member States of the European Union, the French Additional Protocol entered into force on April 30, 2004.

The French Parliament transposed and supplemented the provisions of the Protocol Additional to the INFCIRC/290 Safeguards Agreement into a national law in 2016 [6]. This law makes compulsory the declaration of the concerned activities and envisages criminal penalties in case of non-declaration or voluntary obstruction of a complementary access. The Euratom Technical Committee (CTE, Comité Technique Euratom) is the French administrative authority in charge of monitoring the implementation of the French Additional Protocol. The CTE benefits from the technical support of IRSN Non-Proliferation and Nuclear Material Accountancy Department, particularly for the collection and analysis of data and the preparation of the French declarations to the IAEA.

### 3. Cooperation between SBDU and CTE

#### 3.1 Legal framework

The second title of the French *Law n° 2016-113 of 5 February 2016, in respect of the Protocol Additional to the Agreement between France, the European Atomic Energy Community and the International Atomic Energy Agency for the Application of Safeguards in France signed in Vienna on 22 September 1998* [6], is devoted to the reporting obligations. It brings into the national legal framework the declarations set forth in the French Additional Protocol and positions the economic or research actors at the very heart of the reporting system: while the Additional Protocol provides that the French State shall provide the IAEA with the relevant information, the law imposes this obligation on the people involved. The CTE can also ask, at any moment, for any additional information that it feels useful in order to establish the French declaration for the IAEA.

This reporting obligation has also been penalized: for not transmitting to the CTE the relevant information, the maximum penalty prescribed by law is two years' imprisonment and a fine of € 75,000 (increased to € 375,000 for companies).

The Decree [7] adopted in 2018 by the Government for the application of the Law goes a little further considering the link between the dual-use goods and non-proliferation. Indeed, the Article 7 states that each year, the Minister responsible for Industry (through the SBDU) shall make available to the CTE a

list with the identity of any person having obtained an export or transfer license for the goods falling under category 0 (“Nuclear materials, facilities and equipment”) of Regulation (EC) No 428/2009, as well as the designation and description of these goods. This list considered in category 0 of the EC Regulation implements internationally agreed dual-use controls, including the NSG’s trigger list.

### 3.2 Implementation and interactions

Before the 2016 Law [6] and since the entry into force of the French Additional Protocol in 2004, the CTE was already in touch with the SBDU to validate the French declarations to the IAEA. Before each French declaration requested by the Additional Protocol, IRSN prepares the information and data it has collected from the operators. It submits a draft declaration to the CTE, which makes it circulate and validate among the ministries concerned (Defence, Foreign Affairs, Ecology, Interior, etc.), to be sure of the accuracy and completeness of the information.

The 2018 Decree [7] gave a new impulse to the cooperation between the CTE and the SBDU. Now, before preparing the French declaration for the IAEA, the SBDU gives to the CTE, before the end of February, an updated list of the license holders allowed to export dual-use goods related to nuclear material, facilities and equipment. The CTE and its technical support, the IRSN, are then in a position to check that these license holders have yet transmitted information according to the 2016 Law.

If they have not, CTE or IRSN analyses the description of the dual-use goods considered in the license to understand if the operator shall declare under the Additional Protocol. If they consider that the goods are listed in the Additional Protocol, they contact each license holder to make them aware of their legal reporting obligation.

As the Regulation (EC) No 428/2009 is often modified, among others to reflect the work done by the NSG, the category 0 considered in the SBDU communication may be more up to date than the Annex II of the Additional Protocol, unchanged since 1997. Hence the SBDU potentially communicates to the CTE a list with license holders that are not in the scope of the Additional Protocol. Nevertheless, it is of common interest to have a contact with these operators to inform them about the Additional Protocol and the non-proliferation concerns.

The communication from the SBDU to the CTE is of great help to enable the potential identification of exporters and manufacturers that should give the CTE information to prepare the French declaration for the Additional Protocol. It is a new complementary tool to ensure the completeness of the national declaration.

Otherwise, even if there is no legal requirement for the CTE to give information to the SBDU, the exchange of information is reciprocal and also benefits to the dual-use goods management: the list of declarants to the Additional Protocol helps to check any potential person that should have asked for a dual-use license. Moreover, each declarant to the Additional Protocol must name its French partners, in particular for research and development activities and programs. Considering especially intangible goods, it can also be a useful tool to identify new and/or small companies that should ask for a dual-use license in case of export.

## 4. Conclusion

The 2016 French Law has been a first step to inscribe in the national legal framework the cooperation between the CTE, in charge of the implementation of the Additional Protocol and the relevant declarations to the IAEA, and the SBDU, in charge of the delivery and monitoring of the licences for the export of the dual-use goods. More than a simple communication of an annual list of license holders, the Law and the Decree have given a legal basis to a long cooperation for the mutual benefit of these two concerns. This first step shall be followed by others, such as a formalization of the use made by the CTE of the SBDU’s list. It is also planned to strengthen the information and the training of the license holders, especially the smaller ones, to make them aware of their reporting obligations for the Additional Protocol; it should, in the coming years, go through common trainings or awareness. To be continued.

## 5. References

- [1] Windt A., *Success and failures of the Non-Proliferation Treaty demonstrated in history*, ESARDA Bulletin No. 54, 2017, pp 108-121
- [2] Nuclear Threat Initiative (NTI), [www.nti.org/learn/treaties-and-regimes/nuclear-suppliers-group-nsg](http://www.nti.org/learn/treaties-and-regimes/nuclear-suppliers-group-nsg), visited on April 6, 2019
- [3] Dill C. B. and Stewart I. J., *Defining Effective Strategic Trade Controls at the National Level*, Strategic Trade Review, Volume 1, Issue 1, 2015, pp 4-17
- [4] International Atomic Energy Agency (IAEA), [www.iaea.org/topics/additional-protocol](http://www.iaea.org/topics/additional-protocol), visited on April 5, 2019
- [5] The NSG's trigger list considered here is given in the Annex B of the *Guidelines for nuclear transfers*; INFCIRC/254/Rev.2/Part.1; 1995.
- [6] *French Law n° 2016-113 of 5 February 2016, in respect of the Protocol Additional to the Agreement between France, the European Atomic Energy Community and the International Atomic Energy Agency for the Application of Safeguards in France, signed in Vienna on 22 September 1998*. Available on [www.legifrance.gouv.fr/jo\\_pdf.do?id=JORFTEXT000031983198](http://www.legifrance.gouv.fr/jo_pdf.do?id=JORFTEXT000031983198) (in French)
- [7] *French Decree n° 2018-885 of 12 October 2018, for the application of the law n° 2016-113 of 5 February 2016, in respect of the Protocol Additional to the Agreement between France, the European Atomic Energy Community and the International Atomic Energy Agency for the Application of Safeguards in France, signed in Vienna on 22 September 1998 and onto the procedures of accreditation of international inspectors carrying the controls on nuclear materials*. Available on [www.legifrance.gouv.fr/jo\\_pdf.do?id=JORFTEXT000037493086](http://www.legifrance.gouv.fr/jo_pdf.do?id=JORFTEXT000037493086) (in French)

# Development and Examination of a Proliferation Trade Risk Metric

Adam Attarian  
Peter Heine  
Amanda Sayre

Pacific Northwest National Laboratory  
1100 Dexter Ave N Seattle, WA 98148  
E-mail: peter.heine@pnnl.gov  
PNNL-SA-143116

## **Abstract:**

*A Proliferation Trade Risk metric has been calculated for each country represented in a publicly-available global trade dataset. This metric, comprising both direct and indirect proliferation trade risk components, represents the risk that each country's proliferation-relevant exports will go to a designated set of proliferation threat countries. This metric can serve to prioritize nonproliferation export control capacity building engagement. Further, within such engagement, the decomposition of the proliferation trade risk metric can identify specific industrial sectors and trade relationships of greatest importance for outreach and enforcement measures. Finally, these supply-side perspectives can be complemented by threat-based profiles identifying the most important suppliers to each threat country.*

**Keywords:** export controls; trade analysis

## **1. Introduction**

In 2018, the U.S. National Nuclear Security Administration's International Nonproliferation Export Control Program (INECP) replaced the qualitative trade-based metrics used in its engagement planning process using the publicly available trade data that underlies the Strategic Trade Atlas developed jointly with the European Commission's Joint Research Centre.<sup>1</sup> [1] [2] A Proliferation Trade Risk metric was developed which can be calculated from the BACI data given a set of proliferation threat countries and a set of proliferation-relevant goods. Proliferation Trade Risk was calculated using six countries identified as WMD threats by the 2019 National Intelligence Strategy [3], the 2017 National Security Strategy [4], and the 2018 Nuclear Posture Review [5]. Specifically, these were China, Iran, North Korea, Pakistan, Russia, and Syria, but the methodology can be used for other sets of countries or goods of concern as appropriate for various threat assessments. At the time this metric was developed, it was computed using BACI data for the year 2016 but has since been computed for each year between 1995 and 2016 inclusive.

The Proliferation Trade Risk metric is demand-driven, meaning that trade flows are scored based on their importance to the recipient of the trade rather than the supplier, as will be shown in the Methodology section of this paper below. This can have surprising results, where trade flows seeming small to a supplier may represent significant proliferation trade risk because they constitute a large fraction of a threat country's imports of that commodity, or a large fraction of the imports into an intermediary which is also an important direct supplier of that commodity to one or more threat countries. Once computed,

<sup>1</sup> This BACI dataset, which is used extensively in academic trade analyses, is a statistical elaboration of UN COMTRADE that reconciles import and export declarations to enhance the completeness and reliability of the data. [http://www.cepii.fr/cepii/en/bdd\\_modele/presentation.asp?id=1](http://www.cepii.fr/cepii/en/bdd_modele/presentation.asp?id=1)

the analysis can support engagement prioritization decisions, and deconstructing the components of the metric can suggest highest risk trade flows and industrial sectors on which to focus risk reduction efforts.

## 2. Methodology

Given a set of designated proliferation threat countries of concern, a Proliferation Trade Risk (PTR) score can be computed for each country in the BACI dataset. The Proliferation Trade Risk score for each country is a measure of the risk that the country's proliferation-relevant exports<sup>2</sup> will go to a threat country, directly or indirectly. As such, it comprises two terms: Direct Proliferation Trade Risk (D) and Indirect Proliferation Trade Risk (I). Note that proliferation-relevant trade represents the types of goods most likely to include export-controlled items, but it does not necessarily indicate trade in controlled items. For example, trade in commodities classified as pumps is most likely to include export-controlled pumps, but most pumps are not export controlled. The intent is not to identify specific trade flows of proliferation interest, but to identify the regular trading relationships with the greatest proliferation risk.

### 2.1 Direct Proliferation Trade Risk (D)

The Direct Proliferation Trade Risk posed by a supplier country is a measure of the risk that the country's proliferation-relevant exports will go directly to a threat country. It is a demand-driven metric calculated as the sum of the fraction of each threat country's proliferation-relevant imports that come from the supplier.

$$D_{supplier} = \sum_{threat\ countries} \frac{v_{supplier,threat\ country}}{V_{threat\ country}} \quad (1)$$

where

$v_{supplier,threat\ country}$  is the value of proliferation relevant trade exported from the supplier to the threat country and  $V_{threat\ country}$  is the total value of proliferation relevant trade imported by the threat country.

### 2.2 Indirect Proliferation Trade Risk (I)

The Indirect Proliferation Trade Risk posed by a supplier country is a measure of the risk that the country's proliferation-relevant exports will go indirectly to a threat country via one or more intermediary countries. It is calculated as the sum of the fraction of each intermediary country's proliferation-relevant imports coming from the supplier multiplied by the intermediary country's Direct Proliferation Trade Risk (D), which captures the risk that proliferation-relevant goods exported by that country would go to a threat country.

$$I_{supplier} = \sum_{intermediary\ countries} \frac{v_{supplier,intermediary}}{V_{intermediary}} D_{intermediary} \quad (2)$$

Thus, exports from a supplier to an intermediary only contribute to Indirect Proliferation Trade Risk if that intermediary also exports proliferation-relevant trade directly to threat countries, and the contribution is proportional to the fraction of the intermediary's imports coming from the supplier and the threat countries' imports coming from the intermediary.

### 2.3 Computation

<sup>2</sup> Proliferation-relevant trade excludes goods classified under Harmonized System (HS) chapters unlikely to correspond to proliferation-relevant commodities, such as agricultural products, wood products, fossil fuels, apparel, etc. While proliferation trade risk can be calculated using any basket of goods, this analysis used trade classified under HS Chapters 28 and 29 (chemicals), 75 (aluminum), 76 (nickel), 81 (other/exotic base metals), 84 (machinery), 85 (electronics), and 90 (measurement and test equipment). These selections are configurable and easily modified as needed.

The Direct and Indirect Proliferation Trade Risks can quickly and efficiently be calculated using matrix algebra with the BACI dataset. To facilitate computation, we construct a matrix  $v_{ij}$  with column  $i$  and row  $j$  where each entry is the total value of proliferation relevant trade from export country  $i$  to import country  $j$ . The total value of proliferation relevant trade  $V$  for a given threat country is simply the sum of that country's column in the trade matrix and is represented by a column vector with  $N$  entries. Using matrix index notation, equations (1) and (2) become

$$D = v[:, coc] \times (1/V[coc])^T, \quad (3)$$

$$I = (v \times (1/V))D, \quad (4)$$

where  $\times$  denotes element-wise multiplication and  $coc$  denotes the column indices corresponding to the countries of concern. The direct trade risk vector  $D$  is then zero for all countries except countries of concern, whereas  $I$  is fully populated for each country assuming relevant trade. The PTR is given as the sum of  $I$  and  $D$ .

## 2.4 Known Issues

While BACI attempts to reconcile incomplete or missing trade reports, the data is inherently noisy. Some countries report many thousands of import and export records per year, while other countries provide only sporadic and sparse reporting. This methodology becomes very sensitive when total reported proliferation-relevant imports into a country are small. Because the total value of proliferation relevant trade is in the denominator, when this value is small, relatively small trade flows can generate large proliferation trade risk scores. In general, this appears to be a strength of the methodology, as it successfully highlights small but unusual trade flows that may indicate import and re-export to threat countries via intermediaries. In addition, trade with intermediary countries with zero Direct Proliferation Trade Risk ( $D = 0$ ) offers no additional Indirect Trade Risk, even though those intermediary countries may have non-zero indirect trade risk. This "second-order risk" (i.e., the risk of trade flows to threat countries via multiple intermediaries) is currently ignored, but preliminary investigation indicates this has only small impacts on the results.

## 3. Results

Figure 1 shows the computed Proliferation Trade Risk scores over time, and Figure 2 shows normalized Direct and Indirect Proliferation Trade Risk scores for each country in the BACI dataset for the year 2016. China (CN) had the highest Direct and Indirect Proliferation Trade Risk by far. A cluster of four countries, Germany (DE), South Korea (KR), Japan (JP), and the United States (US), represented the next level of Proliferation Trade Risk.

Excluding these top 5 risks, Figure 2 shows more clearly the raw Direct and Indirect Proliferation Trade Risk scores for the remaining countries for 2016. Of these, the United Arab Emirates (AE), Italy (IT), Turkey (TR), and India (IN) were the top Direct Proliferation Trade Risks, while Malaysia (MY), Singapore (SG), Vietnam (VN), Italy (IT), France (FR), Thailand (TH), the Netherlands (NL), the United Kingdom (UK), and the Philippines (PH) had the highest Indirect Proliferation Trade Risks. Italy (IT) was high on both measures.

In Figure 3, a third cluster of countries found to have elevated Proliferation Trade Risk includes Russia (RU), Belgium (BE), Switzerland (CH), Czech Republic (CZ), Austria (AT), Poland (PL), Hong Kong (HK), Spain (ES), Sweden (SE), Saudi Arabia (SA), Canada (CA), Finland (FI), Indonesia (ID), Denmark (DK), Belarus (BY), and Lebanon (LB).

PTR over time

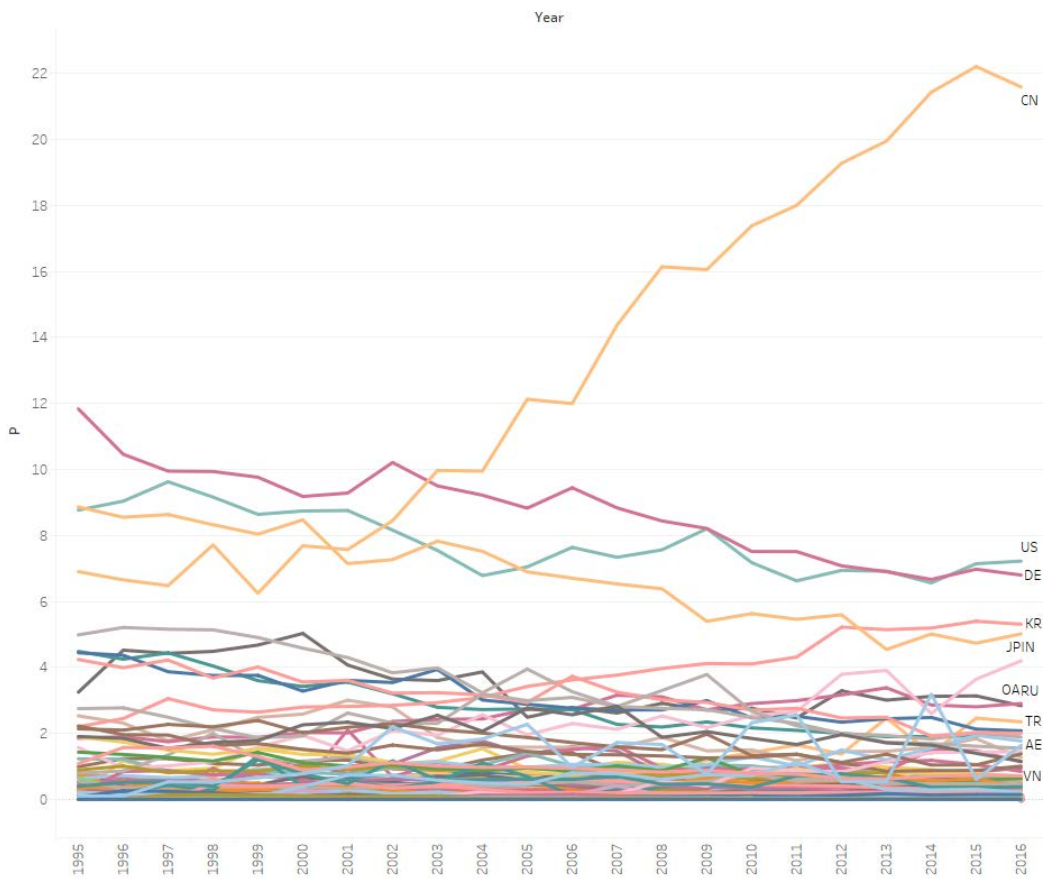


Figure 1 – Proliferation Trade Risk Over Time

Direct and Indirect Proliferation Trade Risks

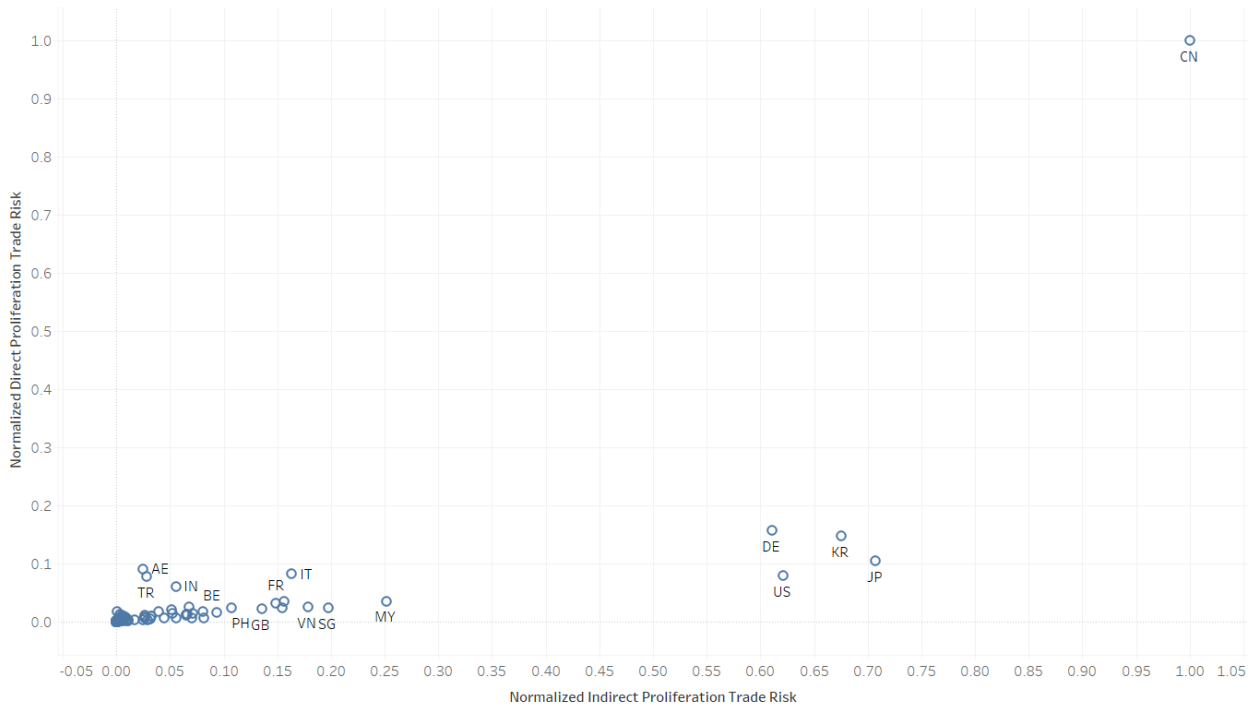
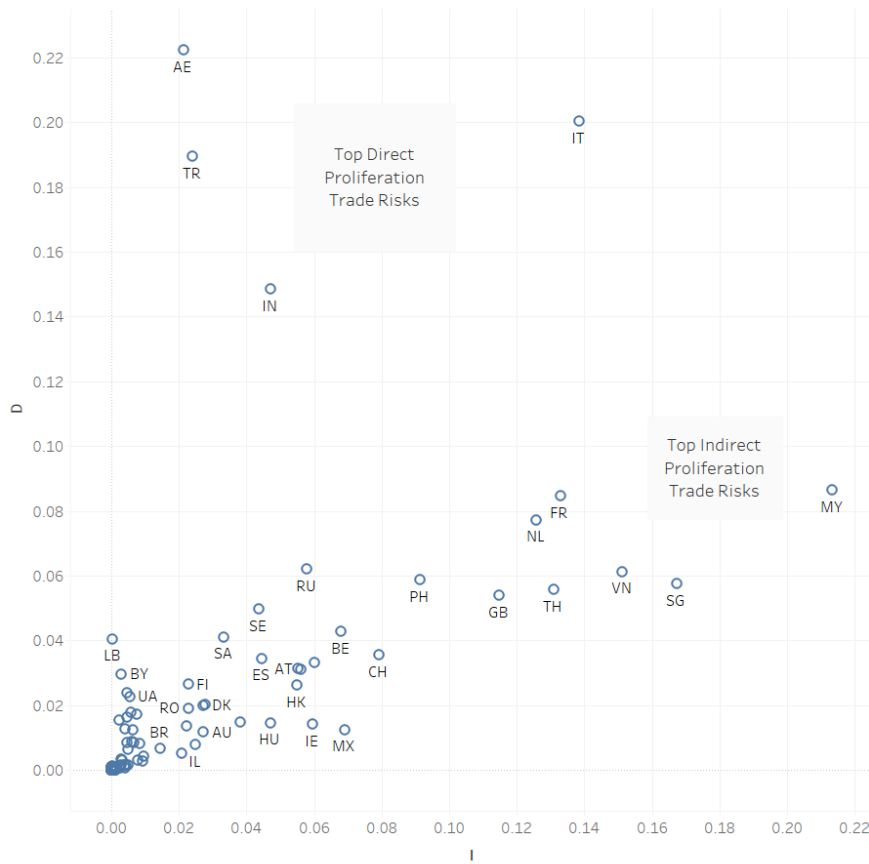


Figure 2 – Normalized Direct and Indirect Proliferation Trade Risks for 2016

Direct and Indirect Trade Risks **excluding CN, DE, KR, JP, and US**



Sum of I vs. sum of D. The marks are labeled by Country Of Interest. The view is filtered on Country Of Interest, which keeps 214 of 220 members.

**Figure 3 – Direct and Indirect Proliferation Trade Risks for 2016, excluding China, South Korea, Germany, Japan, and the United States**

#### 4. Decomposition of Proliferation Trade Risk for Individual Countries

In addition to providing an overall scoring mechanism for ranking and comparing countries, these computations also provide a means for better understanding the specific proliferation risks faced by individual supplier or intermediary countries. For example, the Proliferation Trade Risk for Jordan (JO) can be broken down as shown in Figure 4, which shows the contributions of each export destination to Jordan’s Proliferation Trade Risk score. It shows that Jordan’s Proliferation Trade Risk derives primarily from direct exports of proliferation-relevant goods to Syria (SY) and Pakistan (PK), followed by indirect trade risk from proliferation-relevant exports to India. Syrian imports from Jordan make a large contribution to Jordan’s Proliferation Trade Risk score not because they represent a large share of Jordan’s exports, but because they represent an important share of Syria’s proliferation-relevant imports (see **Figure 10**). Such decompositions of Proliferation Trade Risk can be generated for any country of interest.

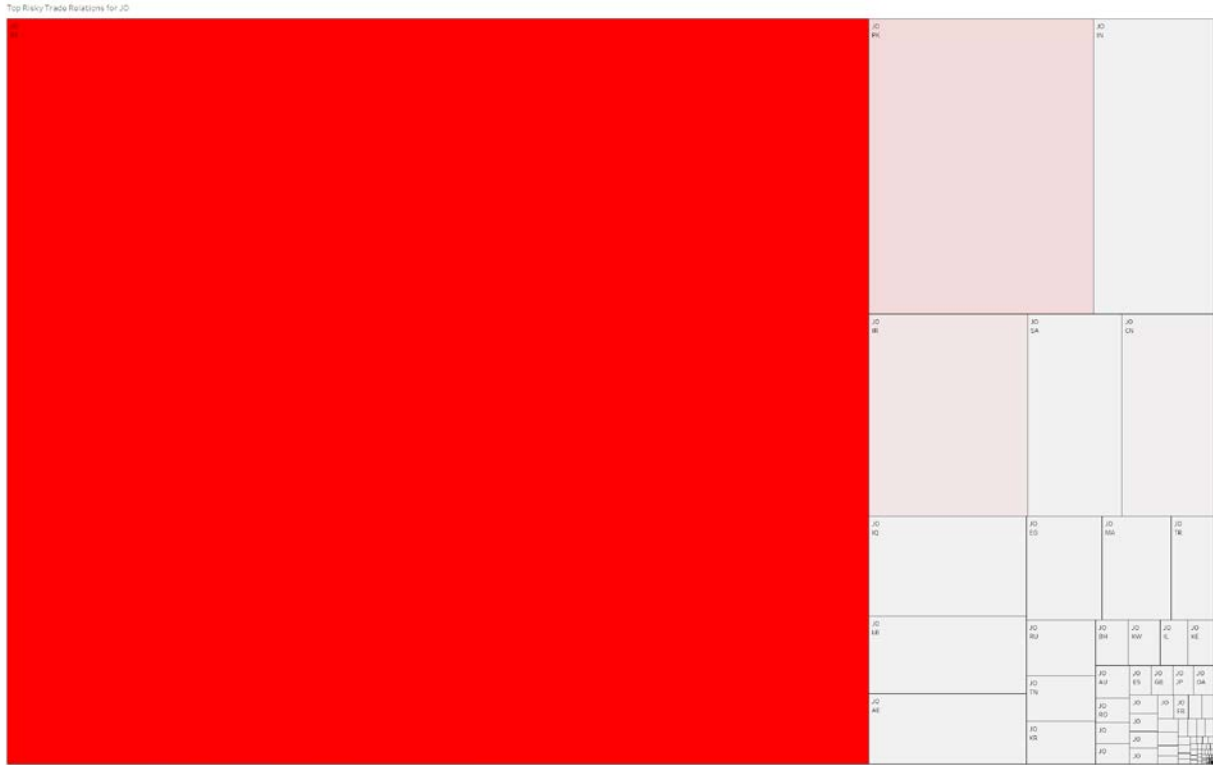


**Figure 4 – Treemap Representing Jordan’s Proliferation Trade Risk by Trading Partner**

In addition, the data supports further decomposition of these proliferation trade risks by commodity type. The breakdown of Jordan's proliferation trade risk by industrial sector, depicted in Figure 5, shows that risk comes predominantly from metals exports (to Syria and Pakistan), accounting for approximately 70% of Jordan's proliferation trade risk. Chemicals represent approximately 25% of proliferation trade risk from exports to China, India, Syria, and Iran. Equipment exports account for a minor share of proliferation trade risk, primarily from equipment exports to Syria.

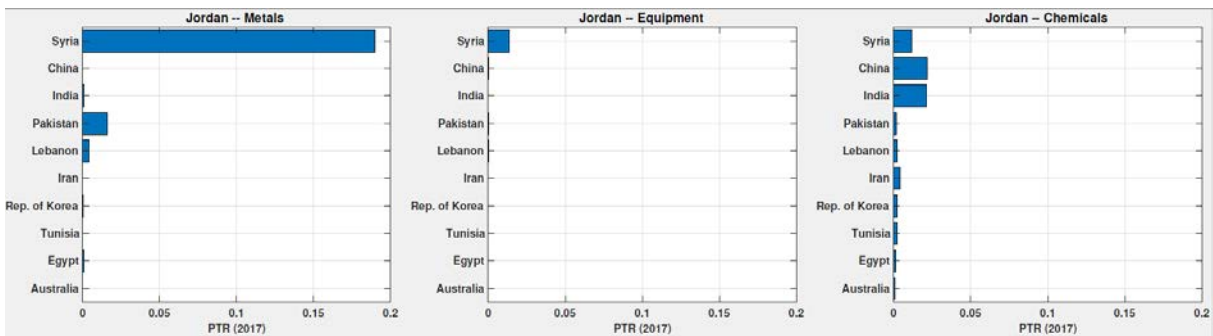
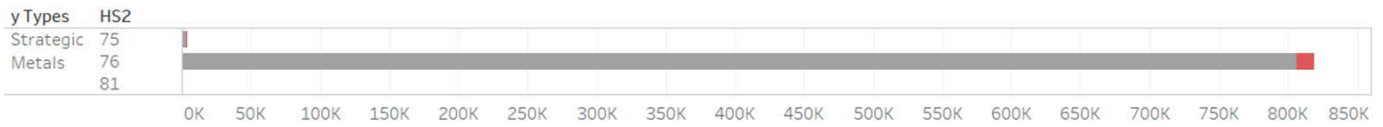


**Figure 5 – Jordan’s Proliferation Trade Risk Profile by Industrial Sector**

Figure 6 digs deeper into Jordan's metal trade to Syria. The top portion shows that Jordan's major metal export is aluminum (HS Chapter 76). Of this, less than 2% is exported to threat countries (shown in red). However, looking at the bottom portion of Figure 6, Jordan's exports represents a significant fraction of Syria's imports; Jordan is Syria's 4<sup>th</sup> largest supplier of Aluminum (shown in blue). This is a small trade flow for Jordan, but an important one for Syria, which is what the Proliferation Trade Risk metric measures.

Exports from Jordan to All for 2015, 2016, 2017



Imports to Syria from All for 2015, 2016, 2017

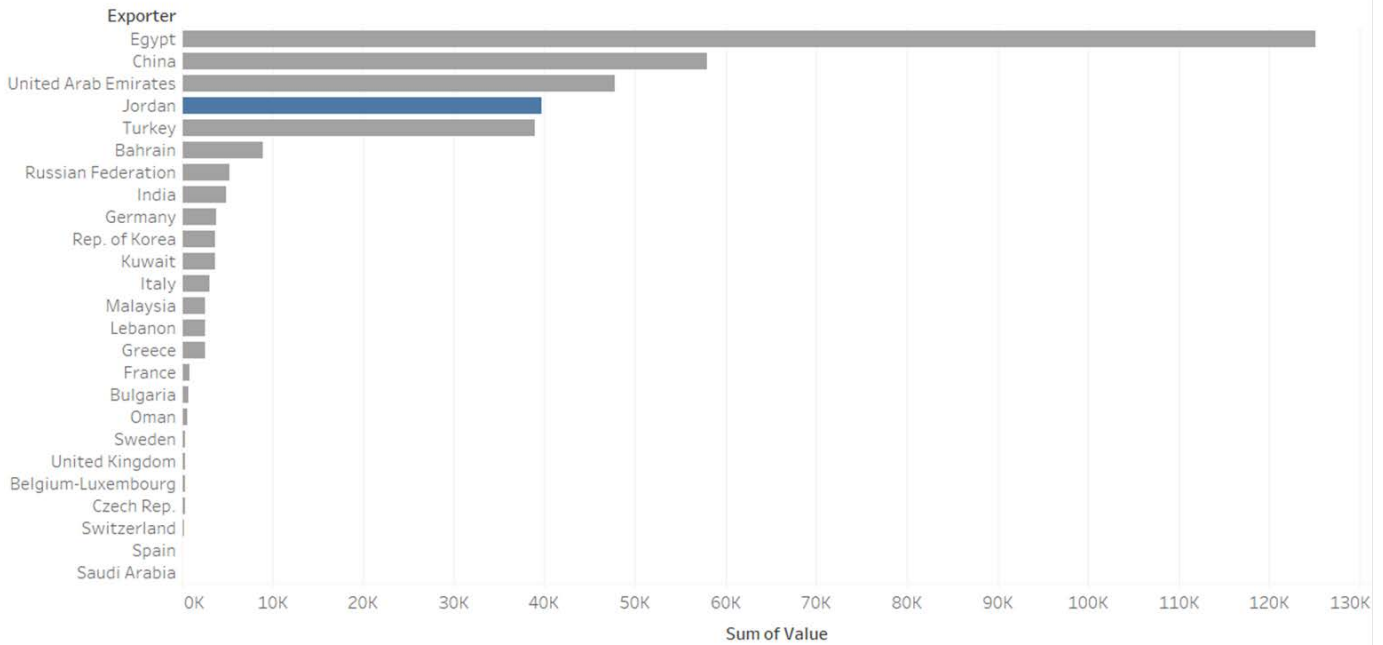


Figure 6 – Jordan’s Exports of Metals to Syria and Syria’s Imports of Metals from All Suppliers

Threat PTR decomposition for Jordan

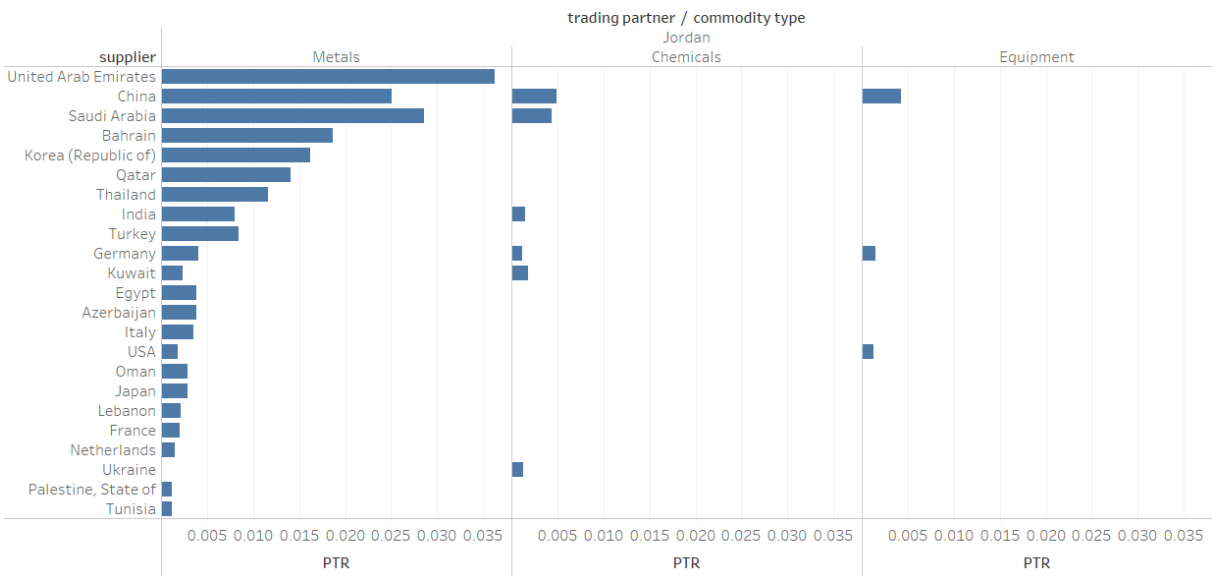


Figure 7 – Import Risk Profile for Jordan

It is also possible to use this methodology to rank the proliferation trade risk of imports to an intermediary country, and to decompose that trade risk by supplier and commodity type. Figure 7 shows the highest Proliferation Trade Risk scores arising from exports to Jordan based on their potential for re-export to threat countries. This suggests, for example, focusing transshipment control

efforts on shipments of metals from United Arab Emirates, China, Saudi Arabia, Bahrain, South Korea, and Qatar; shipments of chemicals and equipment from China and chemicals from Saudi Arabia.

## 5. The Big Picture

Figure 8 brings together the overall ranking and comparison among countries with the breakdown of each country's risky trade relationships all on the same scale. The first block at the top left represents China's Proliferation Trade Risk and is subdivided to show the relative contributions arising from China's export destinations. The block at the lower left similarly represents South Korea's Proliferation Trade Risks, and so on. The color scale indicates the relative magnitude of Direct Proliferation Trade Risk while the size of each area represents the total Proliferation Trade Risk (Direct plus Indirect).

top risky trade relations

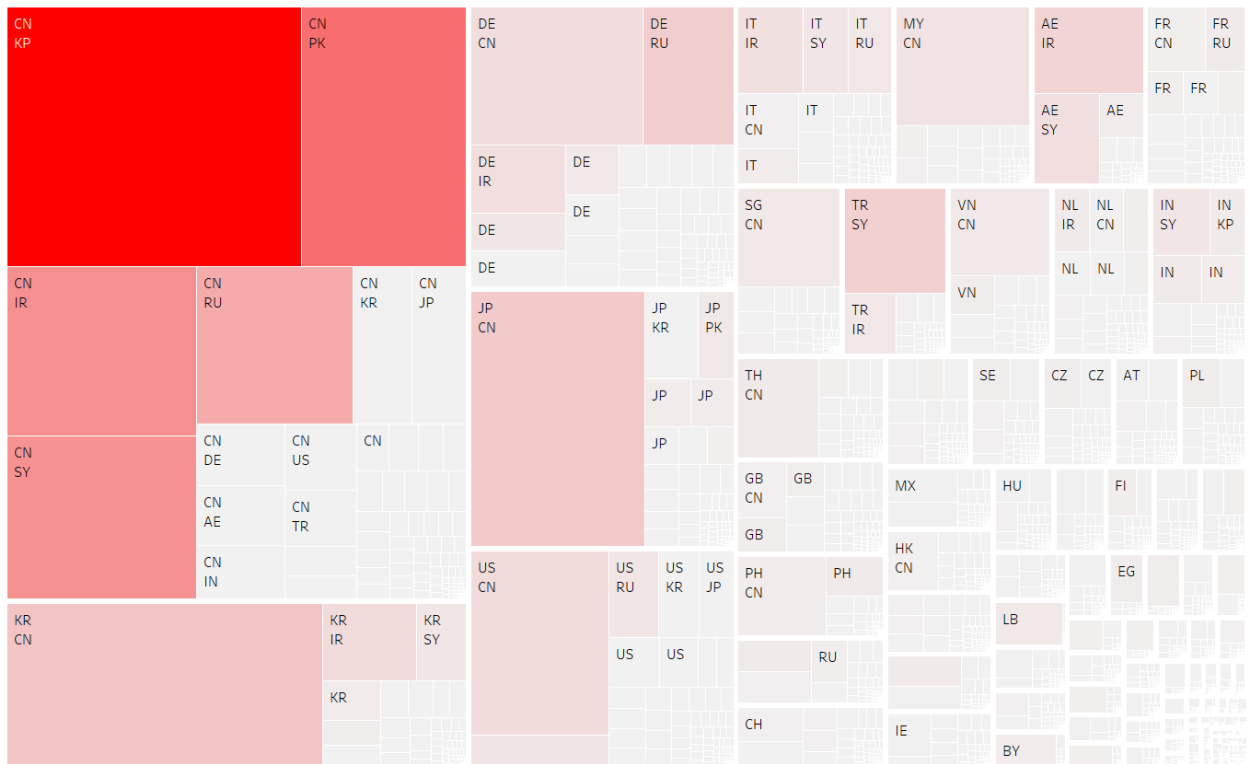


**Figure 8 – Global Proliferation Trade Risks**

As was done in Figure 3, Figure 9 repeats the previous figure but excludes the top 5 Proliferation Trade Risks to show the remaining countries more clearly.

top risky trade relations\* excluding CN, KR, DE, JP, US

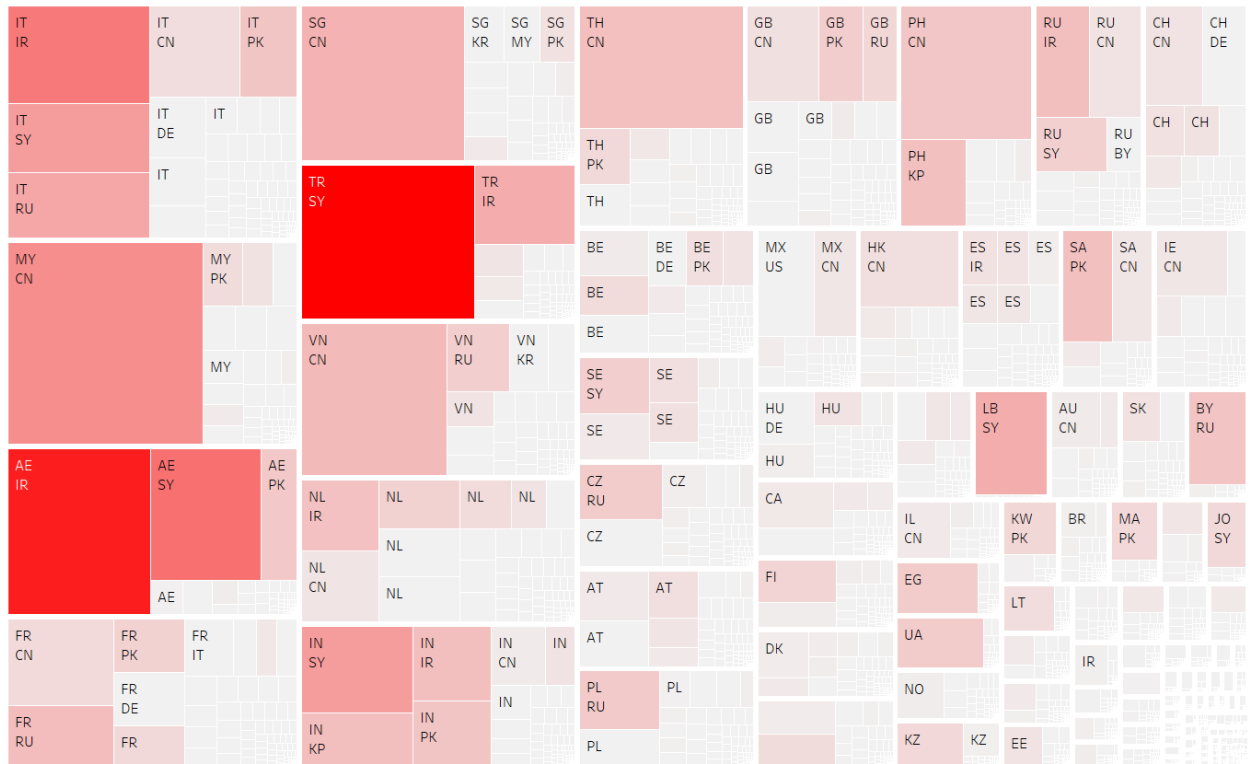


**Figure 9 – Global Proliferation Trade Risks excluding China (CN), South Korea (KR), Germany (DE), Japan (JP), and the United States (US)**

## 6. Threat Perspective

The calculations can also be used to view proliferation-relevant trade from the perspective of the designated threat countries. Based on the original PNNL study, the figures that follow show top suppliers of proliferation-relevant trade to each of the designated proliferation threat countries [1].

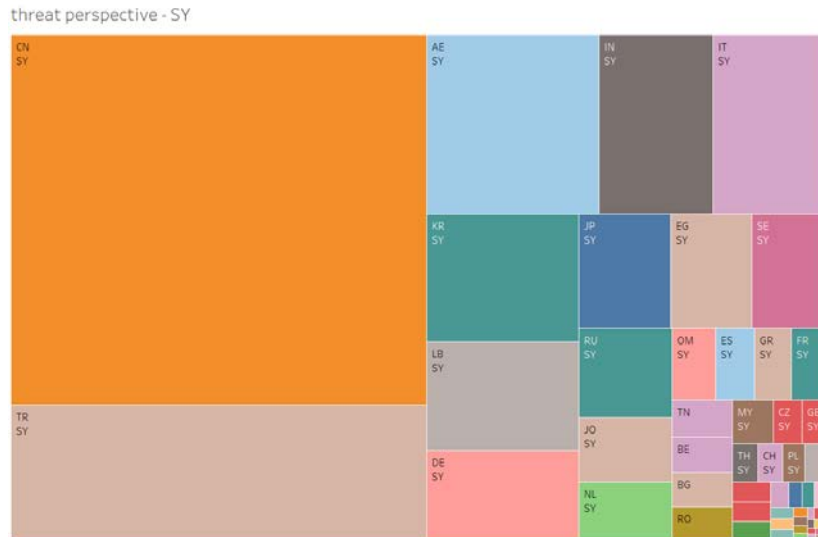


Figure 10 – Top suppliers of proliferation-relevant exports to Syria (SY) in 2016

Syria's (SY) most important suppliers based on Proliferation Trade Risk were China (CN), Turkey (TR), United Arab Emirates (AE), India (IN), Italy (IT), South Korea (KR), Lebanon (LB), and Germany (DE).



Figure 11 – Top suppliers of proliferation-relevant exports to Iran (IR) in 2016

Iran's (IR) most important suppliers based on Proliferation Trade Risk were China (CN), United Arab Emirates (AE), South Korea (KR), Germany (DE), Italy (IT), Turkey (TR), Russia (RU), and India (IN).



**Figure 12 – Top suppliers of proliferation-relevant exports to Pakistan (PK) in 2016**

Pakistan’s (PK) most important suppliers based on Proliferation Trade Risk were China (CN), the United States (US), Germany (DE), Japan (JP), Saudi Arabia (SA), Italy (IT), India (IN), United Arab Emirates (AE), and the United Kingdom (GB).



**Figure 13 – Top suppliers of proliferation-relevant exports to DPRK (KP) in 2016**

DPRK’s most important suppliers based on Proliferation Trade Risk were China (CN), India (IN), and the Philippines (PH).



**Figure 14 – Top suppliers of proliferation-relevant exports to China (CN) in 2016**

China’s (CN) most important suppliers based on Proliferation Trade Risk were South Korea (KR), Japan (JP), the United States (US), Germany (DE), Malaysia (MY), Singapore (SG), Vietnam (VN), and Thailand (TH).



**Figure 15 – Top suppliers of proliferation-relevant exports to Russia (RU) in 2016**

Russia’s most important suppliers based on Proliferation Trade Risk were China (CN), Germany (DE), the United States (US), Italy (IT), France (FR), South Korea (KR), Belarus (BY), Japan (JP), Poland (PL), Czech Republic (CZ), and Ukraine (UA).

## **7. Conclusion**

The Proliferation Trade Risk metric was developed to help prioritize nonproliferation export control capacity building engagement and to tailor that engagement to maximize risk reduction. Beyond this purpose, the metric can help inform any country's export control efforts. The decomposition of the proliferation trade risk metric can identify specific industrial sectors and trade relationships of greatest importance for outreach and enforcement measures. These supply-side perspectives can also be complemented by threat-based profiles identifying the most important suppliers to each threat country.

## 8. References

[1] Heine, P., Blackburn, T., Attarian, A., *TradeRisk: INECP's Development and Examinations of a Proliferation Trade Metric*; Pacific Northwest National Laboratory; 2018. PNNL-28455

[2] Versino, C., Heine, P., Carrera, C.; *Strategic Trade Atlas: Country-Based Views; 2018*. Retrieved from: <https://ec.europa.eu/jrc/en/publication/strategic-trade-atlas-country-based-views-0>

[3] *The National Intelligence Strategy of the United States of America*; Office of the Director of National Intelligence; 2019. Retrieved from: [https://www.dni.gov/files/ODNI/documents/National\\_Intelligence\\_Strategy\\_2019.pdf](https://www.dni.gov/files/ODNI/documents/National_Intelligence_Strategy_2019.pdf)

[4] *U.S. National Security Strategy*; White House; 2017. Retrieved from: <https://www.whitehouse.gov/wp-content/uploads/2017/12/NSS-Final-12-18-2017-0905-2.pdf>

[5] *Nuclear Posture Review*; U.S. Department of Defense Office of the Secretary of Defense; 2018. Retrieved from: <https://dod.defense.gov/News/SpecialReports/2018NuclearPostureReview.aspx>

## **GETTING IN TOUCH WITH THE EU**

### **In person**

All over the European Union there are hundreds of Europe Direct information centres. You can find the address of the centre nearest you at: [https://europa.eu/european-union/contact\\_en](https://europa.eu/european-union/contact_en)

### **On the phone or by email**

Europe Direct is a service that answers your questions about the European Union. You can contact this service:

- by freephone: 00 800 6 7 8 9 10 11 (certain operators may charge for these calls),
- at the following standard number: +32 22999696, or
- by electronic mail via: [https://europa.eu/european-union/contact\\_en](https://europa.eu/european-union/contact_en)

## **FINDING INFORMATION ABOUT THE EU**

### **Online**

Information about the European Union in all the official languages of the EU is available on the Europa website at: [https://europa.eu/european-union/index\\_en](https://europa.eu/european-union/index_en)

### **EU publications**

You can download or order free and priced EU publications from EU Bookshop at: <https://publications.europa.eu/en/publications>. Multiple copies of free publications may be obtained by contacting Europe Direct or your local information centre (see [https://europa.eu/european-union/contact\\_en](https://europa.eu/european-union/contact_en)).

## The European Commission's science and knowledge service

Joint Research Centre

### JRC Mission

As the science and knowledge service of the European Commission, the Joint Research Centre's mission is to support EU policies with independent evidence throughout the whole policy cycle.



**EU Science Hub**

[ec.europa.eu/jrc](https://ec.europa.eu/jrc)



@EU\_ScienceHub



EU Science Hub - Joint Research Centre



Joint Research Centre



EU Science Hub



Publications Office

doi:10.2760/159550

ISBN 978-92-76-08679-6